THE IMPACT OF TUMOR EXTRACELLULAR MATRIX CROSS-TALK ON CANCER HALLMARKS

EDITED BY: Hamid Morjani, Fawzi Aoudjit, Nils Cordes, Monique Dontenwill, Rafael Fridman, Erik Maquoi, Frederic Saltel and Sophie Tartare-Deckert

PUBLISHED IN: Frontiers in Oncology and Frontiers in Cell and Developmental Biology

frontiers Research Topics

frontiers

Frontiers eBook Copyright Statement

The copyright in the text of individual articles in this eBook is the property of their respective authors or their respective institutions or funders. The copyright in graphics and images within each article may be subject to copyright of other parties. In both cases this is subject to a license granted to Frontiers.

The compilation of articles constituting this eBook is the property of Frontiers.

Each article within this eBook, and the eBook itself, are published under the most recent version of the Creative Commons CC-BY licence. The version current at the date of publication of this eBook is CC-BY 4.0. If the CC-BY licence is updated, the licence granted by Frontiers is automatically updated to the new version.

When exercising any right under the CC-BY licence, Frontiers must be attributed as the original publisher of the article or eBook, as applicable.

Authors have the responsibility of ensuring that any graphics or other materials which are the property of others may be included in the CC-BY licence, but this should be checked before relying on the CC-BY licence to reproduce those materials. Any copyright notices relating to those materials must be complied with.

Copyright and source acknowledgement notices may not be removed and must be displayed in any copy, derivative work or partial copy which includes the elements in question.

All copyright, and all rights therein, are protected by national and international copyright laws. The above represents a summary only. For further information please read Frontiers' Conditions for Website Use and Copyright Statement, and the applicable CC-BY licence.

ISSN 1664-8714
ISBN 978-2-88966-659-1
DOI 10.3389/978-2-88966-659-1

About Frontiers

Frontiers is more than just an open-access publisher of scholarly articles: it is a pioneering approach to the world of academia, radically improving the way scholarly research is managed. The grand vision of Frontiers is a world where all people have an equal opportunity to seek, share and generate knowledge. Frontiers provides immediate and permanent online open access to all its publications, but this alone is not enough to realize our grand goals.

Frontiers Journal Series

The Frontiers Journal Series is a multi-tier and interdisciplinary set of open-access, online journals, promising a paradigm shift from the current review, selection and dissemination processes in academic publishing. All Frontiers journals are driven by researchers for researchers; therefore, they constitute a service to the scholarly community. At the same time, the Frontiers Journal Series operates on a revolutionary invention, the tiered publishing system, initially addressing specific communities of scholars, and gradually climbing up to broader public understanding, thus serving the interests of the lay society, too.

Dedication to Quality

Each Frontiers article is a landmark of the highest quality, thanks to genuinely collaborative interactions between authors and review editors, who include some of the world's best academicians. Research must be certified by peers before entering a stream of knowledge that may eventually reach the public - and shape society; therefore, Frontiers only applies the most rigorous and unbiased reviews.
Frontiers revolutionizes research publishing by freely delivering the most outstanding research, evaluated with no bias from both the academic and social point of view. By applying the most advanced information technologies, Frontiers is catapulting scholarly publishing into a new generation.

What are Frontiers Research Topics?

Frontiers Research Topics are very popular trademarks of the Frontiers Journals Series: they are collections of at least ten articles, all centered on a particular subject. With their unique mix of varied contributions from Original Research to Review Articles, Frontiers Research Topics unify the most influential researchers, the latest key findings and historical advances in a hot research area! Find out more on how to host your own Frontiers Research Topic or contribute to one as an author by contacting the Frontiers Editorial Office: frontiersin.org/about/contact

THE IMPACT OF TUMOR EXTRACELLULAR MATRIX CROSS-TALK ON CANCER HALLMARKS

Topic Editors:
Hamid Morjani, Université de Reims Champagne-Ardenne, France
Fawzi Aoudjit, Laval University, Canada
Nils Cordes, Technische Universität Dresden, Germany
Monique Dontenwill, UMR7213 CNRS
Rafael Fridman, Wayne State University, United States
Erik Maquoi, University of Liège, Belgium
Frederic Saltel, INSERM U1053 Bordeaux Recherche en Oncologie Translationnelle, France
Sophie Tartare-Deckert, INSERM U1065 Centre Méditerranéen de Médecine Moléculaire, France

Citation: Morjani, H., Aoudjit, F., Cordes, N., Dontenwill, M., Fridman, R., Maquoi, E., Saltel, F., Tartare-Deckert, S., eds. (2021). The Impact of Tumor Extracellular Matrix Cross-Talk on Cancer Hallmarks. Lausanne: Frontiers Media SA. doi: 10.3389/978-2-88966-659-1

Table of Contents

05 ***CAGE-miR-140-5p-Wnt1 Axis Regulates Autophagic Flux, Tumorigenic Potential of Mouse Colon Cancer Cells and Cellular Interactions Mediated by Exosomes***

Minjeong Yeon, Seungheon Lee, Joo-Eun Lee, Hyun Suk Jung, Youngmi Kim and Dooil Jeoung

25 ***Collagen Kinase Receptors as Potential Therapeutic Targets in Metastatic Colon Cancer***

Marie Lafitte, Audrey Sirvent and Serge Roche

33 ***Transmembrane Peptides as Inhibitors of Protein-Protein Interactions: An Efficient Strategy to Target Cancer Cells?***

Camille Albrecht, Aline Appert-Collin, Dominique Bagnard, Sébastien Blaise, Béatrice Romier-Crouzet, Roman G. Efremov, Hervé Sartelet, Laurent Duca, Pascal Maurice and Amar Bennasroune

41 ***Tumor Microenvironment: Extracellular Matrix Alterations Influence Tumor Progression***

Sylvie Brassart-Pasco, Stéphane Brézillon, Bertrand Brassart, Laurent Ramont, Jean-Baptiste Oudart and Jean Claude Monboisse

54 ***Impact of Extracellular Matrix Components to Renal Cell Carcinoma Behavior***

Sandra Majo, Sarah Courtois, Wilfried Souleyreau, Andreas Bikfalvi and Patrick Auguste

66 ***Shaping Up the Tumor Microenvironment With Cellular Fibronectin***

Georgios Efthymiou, Angélique Saint, Michaël Ruff, Zeinab Rekad, Delphine Ciais and Ellen Van Obberghen-Schilling

84 ***Functional Interplay Between Collagen Network and Cell Behavior Within Tumor Microenvironment in Colorectal Cancer***

Cuong Cao Le, Amar Bennasroune, Benoit Langlois, Stéphanie Salesse, Camille Boulagnon-Rombi, Hamid Morjani, Stéphane Dedieu and Aline Appert-Collin

92 ***Label-Free Infrared Spectral Histology of Skin Tissue Part I: Impact of Lumican on Extracellular Matrix Integrity***

Lise Nannan, Valérie Untereiner, Isabelle Proult, Camille Boulagnon-Rombi, Charlie Colin-Pierre, Ganesh D. Sockalingum and Stéphane Brézillon

101 ***Syndecan-1-Dependent Regulation of Heparanase Affects Invasiveness, Stem Cell Properties, and Therapeutic Resistance of Caco2 Colon Cancer Cells***

Sampath Kumar Katakam, Paride Pelucchi, Cinzia Cocola, Rolland Reinbold, Israel Vlodavsky, Burkhard Greve and Martin Götte

112 ***Label-Free Infrared Spectral Histology of Skin Tissue Part II: Impact of a Lumican-Derived Peptide on Melanoma Growth***

Stéphane Brézillon, Valérie Untereiner, Hossam Taha Mohamed, Estelle Ahallal, Isabelle Proult, Pierre Nizet, Camille Boulagnon-Rombi and Ganesh. D. Sockalingum

123 ***LRP-1 Promotes Colon Cancer Cell Proliferation in 3D Collagen Matrices by Mediating DDR1 Endocytosis***
Cao Cuong Le, Amar Bennasroune, Guillaume Collin, Cathy Hachet, Véronique Lehrter, Damien Rioult, Stéphane Dedieu, Hamid Morjani and Aline Appert-Collin

138 ***Cell Derived Matrix Fibulin-1 Associates With Epidermal Growth Factor Receptor to Inhibit Its Activation, Localization and Function in Lung Cancer Calu-1 Cells***
Keerthi Harikrishnan, Omkar Joshi, Saili Madangirikar and Nagaraj Balasubramanian

156 ***TRPM7/RPSA Complex Regulates Pancreatic Cancer Cell Migration***
Thibaut Lefebvre, Pierre Rybarczyk, Clara Bretaudeau, Alison Vanlaeys, Rémi Cousin, Sylvie Brassart-Pasco, Denis Chatelain, Isabelle Dhennin-Duthille, Halima Ouadid-Ahidouch, Bertrand Brassart and Mathieu Gautier

166 ***Targeting the Extra-Cellular Matrix—Tumor Cell Crosstalk for Anti-Cancer Therapy: Emerging Alternatives to Integrin Inhibitors***
Girieca Lorusso, Curzio Rüegg and François Kuonen

183 ***Contribution of the Low-Density Lipoprotein Receptor Family to Breast Cancer Progression***
Océane Campion, Tesnim Al Khalifa, Benoit Langlois, Jessica Thevenard-Devy, Stéphanie Salesse, Katia Savary, Christophe Schneider, Nicolas Etique, Stéphane Dedieu and Jérôme Devy

192 ***Reciprocal Interplay Between Fibrillar Collagens and Collagen-Binding Integrins: Implications in Cancer Progression and Metastasis***
Isabelle Bourgot, Irina Primac, Thomas Louis, Agnès Noël and Erik Maquoi

220 ***Extracellular Vesicle-Dependent Cross-Talk in Cancer—Focus on Pancreatic Cancer***
Lise Nannan, Jean-Baptiste Oudart, Jean Claude Monboisse, Laurent Ramont, Sylvie Brassart-Pasco and Bertrand Brassart

229 ***A Complex and Evolutive Character: Two Face Aspects of ECM in Tumor Progression***
Margaux Sala, Manon Ros and Frédéric Saltel

254 ***Type I Collagen Aging Increases Expression and Activation of EGFR and Induces Resistance to Erlotinib in Lung Carcinoma in 3D Matrix Model***
Thomas Sarazin, Guillaume Collin, Emilie Buache, Laurence Van Gulick, Céline Charpentier, Christine Terryn, Hamid Morjani and Charles Saby

262 ***Discoidin Domain Receptors in Melanoma: Potential Therapeutic Targets to Overcome MAPK Inhibitor Resistance***
Coralie Reger de Moura, Marco Prunotto, Anjum Sohail, Maxime Battistella, Fanelie Jouenne, Daniel Marbach, Celeste Lebbé, Rafael Fridman and Samia Mourah

268 ***Crosstalk Between Cancer Associated Fibroblasts and Cancer Cells in Scirrhous Type Gastric Cancer***
Yuichiro Miki, Masakazu Yashiro, Lidia Moyano-Galceran, Atsushi Sugimoto, Masaichi Ohira and Kaisa Lehti

281 ***Thrombospondin-1 Receptor CD47 Overexpression Contributes to P-Glycoprotein-Mediated Multidrug Resistance Against Doxorubicin in Thyroid Carcinoma FTC-133 Cells***
Marie-Pierre Courageot, Laurent Duca, Laurent Martiny, Emmanuelle Devarenne-Charpentier, Hamid Morjani and Hassan El Btaouri

frontiers in Oncology

ORIGINAL RESEARCH
published: 14 November 2019
doi: 10.3389/fonc.2019.01240

CAGE-miR-140-5p-Wnt1 Axis Regulates Autophagic Flux, Tumorigenic Potential of Mouse Colon Cancer Cells and Cellular Interactions Mediated by Exosomes

Minjeong Yeon[1], *Seungheon Lee*[1], *Joo-Eun Lee*[1], *Hyun Suk Jung*[1], *Youngmi Kim*[2] *and Dooil Jeoung*[1]*

[1] Department of Biochemistry, Kangwon National University, Chuncheon-si, South Korea, [2] College of Medicine, Institute of New Frontier Research, Hallym University, Chuncheon-si, South Korea

OPEN ACCESS

Edited by:
Rafael Fridman,
Wayne State University, United States

Reviewed by:
Guang-Chao Chen,
Academia Sinica, Taiwan
Priyanka Gupta,
University of Alabama at Birmingham, United States

***Correspondence:**
Dooil Jeoung
jeoungd@kangwon.ac.kr

Specialty section:
This article was submitted to Molecular and Cellular Oncology, a section of the journal Frontiers in Oncology

Received: *08 August 2019*
Accepted: *28 October 2019*
Published: *14 November 2019*

Citation:
Yeon M, Lee S, Lee J-E, Jung HS, Kim Y and Jeoung D (2019) CAGE-miR-140-5p-Wnt1 Axis Regulates Autophagic Flux, Tumorigenic Potential of Mouse Colon Cancer Cells and Cellular Interactions Mediated by Exosomes. Front. Oncol. 9:1240. doi: 10.3389/fonc.2019.01240

Although the cancer/testis antigen CAGE has been implicated in tumorigenesis, the molecular mechanisms of CAGE-promoted tumorigenesis remain largely unknown. $CT26^{Flag-CAGE}$ cells, CT26 (mouse colon cancer cells) cells stably expressing CAGE, were established to investigate CAGE-promoted tumorigenesis. Down-regulation of CAGE led to decreased autophagic flux in $CT26^{Flag-CAGE}$ cells. CAGE interacted with Beclin1, a mediator of autophagy. The $CT26^{Flag-CAGE}$ cells showed enhanced autophagosome formation and displayed greater tumor spheroid-forming potential than CT26 cells. MicroRNA array analysis revealed that CAGE decreased the expression of various microRNAs, including miR-140-5p, in CT26 cells. CAGE was shown to bind to the promoter sequences of miR-140-5p. MiR-140-5p inhibition increased the tumorigenic potential of and autophagic flux in CT26 cells. A miR-140-5p mimic exerted negative effects on the tumorigenic potential of $CT26^{Flag-CAGE}$ cells and autophagic flux in $CT26^{Flag-CAGE}$ cells. MiR-140-5p was predicted to bind to the 3′-UTR of Wnt1. $CT26^{Flag-CAGE}$ cells showed higher expression of Wnt1 than CT26 cells. Down-regulation of Wnt1 decreased autophagic flux. Luciferase activity assays showed the direct regulation of wnt1 by miR-140-5p. Tumor tissue derived from the $CT26^{Flag-CAGE}$ cells revealed higher expressions of factors associated with activated mast cells and tumor-associated macrophages than tumor tissue derived from CT26 cells. Culture medium from the $CT26^{Flag-CAGE}$ cells increased autophagic flux in CT26 cells, mast cells and macrophages. Culture medium from the $CT26^{Flag-CAGE}$ cells increased CD163 and autophagic flux in CT26 cells, mast cells, and macrophages in a Wnt1-dependent manner. Exosomes from $CT26^{Flag-CAGE}$ cells increased autophagc flux in CT26 cells, mast cells, and macrophages. Exosomes from $CT26^{Flag-CAGE}$ cells increased the tumorigenic potential of CT26 cells. Wnt1 was shown to be present within the exosomes.

Recombinant Wnt1 protein increased autophagic flux in CT26, mast cells, and macrophages. Recombinant wnt1 protein mediated interactions between the CT26 cells, mast cells, and macrophages. Our results showed novel roles for the CAGE-miR-140-5p-Wnt1 axis in autophagic flux and cellular interactions mediated by exosomes.

Keywords: cancer associated gene CAGE, cellular interactions, exosomes, micro RNA-140-5p, tumor microenvironment, wnt1

INTRODUCTION

CAGE, a cancer/testis antigen, is present in the sera of patients with various cancers (1, 2). Furthermore, CAGE predominantly reacts with sera from cancer patients, but not with healthy control (3).

CAGE displays tumor-promoting potential and promotes cell cycle progression by inducing expression of cyclin D1 and E in AP-1 and E2F-dependent manner (4). CAGE stimulates angiogenesis (5, 6) and interacts with HDAC2 and confers resistance to anti-cancer drugs (7). The CAGE-miR-200b negative feedback loop regulates anti-cancer drug-resistance and tumorigenic potential (5).

Phthalate enhances cancer cell metastasis and anti-drug resistance by increasing cancer cell stemness (8). Autophagy promotes cancer stem cell (CSC) characteristics such as self-renewal, tumor initiation, and drug resistance (9). The prosurvival autophagy pathway is critical for CSC maintenance (10). The inhibition of autophagic flux enhances apoptosis and anti-cancer effects in hepatocellular carcinoma cells (11). Autophagic flux is closely related to multiple myeloma stem cell-like properties (12). Cisplatin resistance results from the inhibition of apoptosis and autophagy (13). These reports suggest that CAGE may regulate autophagy and CSC-like properties.

CSCs educate monocytes/macrophages toward tumor associated macrophages (TAMs) and the CSCs and TAMs interact and reciprocally promote stem cell-like properties of CSCs such as self-renewal and anti-cancer drug-resistance (9). TLR2 stimulation of human mast cells promotes the growth of colon cancer spheroids (14). Mast cell-derived mediators activate STAT3 signaling via the down-regulation of GSK3β expression, which in turn inhibits glioma cell proliferation and migration (15). Exosomes from bone marrow stromal macrophages regulate CSC-like properties, by either inducing or reversing dormancy (16). These reports suggest role for exosomes in mediating cellular interactions involving cancer cells and stromal cells within the tumor microenvironment.

We investigated the mechanisms of CAGE-promoted tumorigenesis in detail. We identified miR-140-5p as a direct target of CAGE. We present evidence that the CAGE-miR-140-5p axis regulates autophagic flux, CSC-like properties, and tumorigenic potential. MiR-140-5p acted as a negative regulator of Wnt1. Wnt1 was present within exosomes derived from mouse colon cancer cells expressing CAGE. We present evidence that the CAGE-miR-140-5p-Wnt1 axis regulated cellular interactions within the tumor microenvironment mediated by exosomes. We suggest that CAGE can serve as a target for the development of anti-cancer drugs.

MATERIALS AND METHODS

Materials

An enhanced chemiluminescence (ECL) kit was purchased from Amersham Biosciences. Lipofectamine and Plus™ reagent were purchased from Invitrogen. SiRNAs, miRNA inhibitors, and miRNA mimics were purchased from Bioneer Company (Daejeon, Korea). Goat anti-rabbit IgG (conjugated with HRP) was purchased from Enzo Company (ADI-SAB-300-J), Goat anti-mouse IgG (conjugated with HRP) was purchased from Thermo Fisher Company (31430), and Donkey anti-goat IgG (conjugated with HRP) was purchased from Thermo Fisher Company (A15999). Recombinant wnt1 protein was purchased from R&D systems.

Cell Lines and Cell Culture

Cancer cell lines used in this study were cultured in Dulbecco's modified minimal essential medium (Invitrogen) supplemented with heat-inactivated 10% fetal bovine serum (Invitrogen) and antibiotics at 37°C in a humidified incubator with a mixture of 95% air and 5% CO_2. Mouse $CT26^{Flag-CAGE}$ cells that stably express CAGE were established by selection in medium containing G418 (400 μg /ml). $CT26^{Flag-CAGE}1$ cells and $CT26^{Flag-CAGE}2$ cells stably express CAGE. These cells are separate independent clone. CT26 cells were purchased from Korea Cell Line Bank (KCLB 80009). Lung mast cells and lung macrophages were isolated according to standard procedures (17).

Immunoblot

For PAGE and Western blot, cell or tissues lysates were prepared using lysis buffer (62.5 mm Tris-HCl, pH 6.8, 2% (w/v) SDS, 10% (v/v) glycerol, 50 mm dithiothreitol, 0.01% (w/v) bromphenol blue, 10 mm NaF, 1% (v/v) protease inhibitor mixture, 1 mm sodium orthovanadate). The samples were boiled for 5 min, and equal amounts of protein (20 μg/well) were analyzed on a 10% SDS-PAGE. After electrophoresis, proteins were transferred onto a PVDF membrane (Amersham, Cat.10600023) and subjected to immunoblotting. The membranes are blocked with 2% BSA (Gendepot, Cat.A0100-050) in Tris buffered saline with 0.1% Tween-20 (TBS-T) for 30 min. The membranes were incubated with each primary antibody on a shaker at 4°C overnight. The dilution of each primary antibody was empirically determined. After extensive washing, blots were further incubated with an anti-mouse or anti-rabbit IgG-horseradish peroxidase-conjugated antibody at a 1:3,000 dilution for 1 h at room temperature and were developed using an enhanced chemiluminescence kit (ELPIS, 1073).

Immunoprecipitation

Cells (1×10^7) were lysed in immunoprecipitation buffer (50 mmol/l HEPES, pH 7.6, 150 mmol/l NaCl, 5 mmol/l EDTA, 0.1% Nonidet P-40). After centrifugation (10 min at 15,000× g) to remove particulate material, the supernatant was incubated with each antibody (2 μg/ml) with constant agitation at 4°C. The immunocomplexes were precipitated with protein A/G-Sepharose (Santa Cruz, sc-2003) and analyzed by Western blot. Two hundred microgram of cell lysates or tissue lysates were subjected to immunoprecipitation.

Immunofluorescence Staining

Cells were fixed with 4% paraformaldehyde (v/v) and then permeabilized with 0.4% Triton X-100. Cells were incubated with primary antibody specific to LC3 (Cell Signaling, 12741, 1:200), CD163 (AbCam, Ab 182422, 1:100), iNOS (Cell Signaling, 13120, 1:100) or Flag (Sigma, sc-398254, 1:500) for 2 h. Anti-rabbit Alexa Fluor 488 (for detection of LC3 and CD163, 1:500) or anti-goat Alexa Fluor 546 (for detection of iNOS) secondary antibody (Molecular Probes, 1:500) was added to cells and incubated for 1 h. For immunofluorescence staining of exosomes, Exosomes in PBS were applied to fibronectin-coated chamber slides (10 μg/ml) for 24 h at 4°C to allow binding exosomes to the slide surface. Immunofluorescence staining employing anti-TSG101 antibody (Santa Cruz Biotechnology, sc-7964, 1:100) or CD63 (Cusabio, CSB-PA259468, 1:100) was performed as previously described.

Chemo Invasion and Migration Assays

Invasion and migration potential of cancer cells were determined according to the standard procedures employing transwell chamber system (5, 18). Results were analyzed for statistical significance using the Student's *t*-test. Differences were considered significant when $p < 0.05$.

MicroRNA Array

MicroRNA array analysis was performed according to the protocols provided by the manufacturer (Koma Biotech).

RNA Extraction and Quantitative Real Time PCR

Total miRNA was isolated using the *mir*Vana miRNA isolation kit (Ambion). CDNA was synthesized from miRNA with poly (A) tail using a poly (T) adaptor primer and qScript™ reverse transcriptase (Quanta Biogenesis). Expression levels of miR-140-5p was quantified with a SYBR Green qRT-PCR kit (Ambion) using a miRNA-specific forward primer and a universal poly (T) adaptor reverse primer.

Transfection

Transfections were performed according to the manufacturer's instructions (Invitogen). For miR-140-5p knockdown, cells were transfected with 10 nM oligonucleotide (inhibitor) with Lipofectamine 2000 (Invitrogen), according to the manufacturer's protocol. The sequences used were 5′-CAG UGGUUUUACCCUAUGGUAG-3′ (miR-140-5p inhibitor) and 5′-TAACACGTCTATACGCCCA-3′ (control inhibitor).

In vivo Tumorigenic Potential

Cancer cells (1×10^6) were injected subcutaneously into the dorsal flank area of the BALB/c mice to induce formation of tumors. After tumors reach certain size, control mimic or miR-140-5p mimic (each at 100 nM) was injected five times to determine the effect of miR-140-5p on the tumorigenic potential of $CT26^{Flag-CAGE}$ cells. Control inhibitor or miR-140-5p inhibitor (each at 100 nM) was also injected five times to determine the effect of miR-140-5p on the tumorigenic potential of CT26. To examine whether exosomes would affect the tumorigenic potential, CT26 cells (5×10^6) in 1:1 ratio of exosomes:Matrigel (Growth Factor Reduced; BD Biosciences) were injected subcutaneously in flanks of 8-week-old male nude mice. All animal experiments were performed according to the guide lines of the Korean Council for the Care and Use of Animals in Research and approved by the Institutional Animal Care and Use Committee (IACUC) of Kangwon National University (KIACUC-160329-2).

Immunohistochemical Staining

The immunohistochemical staining was performed according to the protocols provided by the manufacturer (Vector Laboratories Inc., Burlingame, CA). Tissues were fixed in 10% (v/v) buffered formalin, embedded in paraffin, sectioned at 4–6 μm, Immunohistochemistry staining of tissues was performed by using the avidin-biotin detection method (Vectastain ABC kit, Vector Laboratories Inc., Burlingame, CA). Briefly, 4–6-μm-thick sections of the paraffin-embedded tissue blocks were cut, mounted on positively charged glass slides, and dried in an oven at 56°C for 30 min. The sections were deparaffinized in xylene and then rehydrated in graded ethanol and water. Endogenous peroxidase was blocked by incubation in 3% (v/v) hydrogen peroxide for 15 min. Antigen retrieval was accomplished by pretreatment of the sections with citrate buffer at pH 6.0 for 20 min at 56°C in a microwave oven and then allowing the sections to cool for 30 min at room temperature. Non-specific endogenous protein binding was blocked using 2.5% normal horse serum (Vector, S-2012). The sections were then incubated with primary antibodies overnight at 4°C. The following primary antibodies were used: Flag (Sigma, F31645, 1: 1,000), $pAMPK^{Thr172}$ (R&D Systems, 2535, 1:200), p62 (Santa Cruz, sc-25575, 1:500), tryptase (Santa Cruz, sc-59587,1:100), chymase (Santa Cruz, sc-25575, sc-59586, 1:200), Wnt1 (Abcam, ab-15251, 1:500), β-catenin (Santa Cruz, sc-59737, 1:100), cyclin D1(Santa Cruz, sc-20044, 1:200), or ATG7 (Cell Signaling, 8558. 1:200). After washing, sections were treated with biotinylated secondary antibodies (Vector, MP-7500). The color was developed with diaminobenzidine (Vector, Cat.SK-4100). Sections were counterstained with Mayer's hematoxylin(Dako, S3309).

Chromatin Immunoprecipitation (ChIP) Assays

ChIP assays were performed according to the standard procedures (19). Mouse miR140-5p promoter-1 [5′-GGTTGT CCTTGGCTACGTG-3′ (forward) and 5′-TAGAAGGAAAGCC AGGGG-3′ (reverse)], miR-140-5p promoter-2 [5′-TATGTGA

TGCAGCCAGAGCA-3′ (forward) and 5′-CCAGCAAGCAG GGTCAGA-3′ (reverse)] were used.

Tumor Sphere-Forming Potential Assay

For tumor spheroid forming assay, cells were plated (5×10^4 cells/well) in ultralow attachment plates (Corning Inc.) in DMEM/F12 stem cell medium. Cells were maintained at 37°C in a humidified 5% CO_2 incubator and fed with 0.2 ml of fresh stem cell medium on days 2, 4, and 6. The total number of spheres was counted after 7 days by inverted microscopy (Olympus).

Matrigel Plug Assays

Matrigel plug assays employing culture medium were performed according to the standard procedures (5, 20). All animal experiments were performed according to the guide lines of the Korean Council for the Care and Use of Animals in Research and approved by the Institutional Animal Care and Use Committee (IACUC) of Kangwon National University (KIACUC-160329-2).

Luciferase Activity Assays

A 343-bp mouse wnt1 gene segment encompassing 3′-UTR of wnt1 was PCR-amplified and subcloned into the (XbaI) site of pGL3 luciferase plasmid. The mutant pGL3-3′-UTR-wnt1 construct was made with the QuikChange site-directed mutagenesis kit (Stratagene). Luciferase activity assay was performed according to the standard procedures (19).

Electron Microscopic Observation of Autophagosomes

Electron microscopic observation of autophagosomes was performed according to the standard procedures (19). Briefly, the cells were dehydrated with a graded acetone series, and embedded into Spurr medium (Electron Microscopy System). The samples were sectioned (60 nm) with an ultra-microtome (RMC MTXL, Arizona, USA), and double-stained with 2% uranyl acetate for 20 min and lead citrate for 10 min. The sections were then viewed under a Tecnai G2 (FEI, USA) TEM at 200 kV.

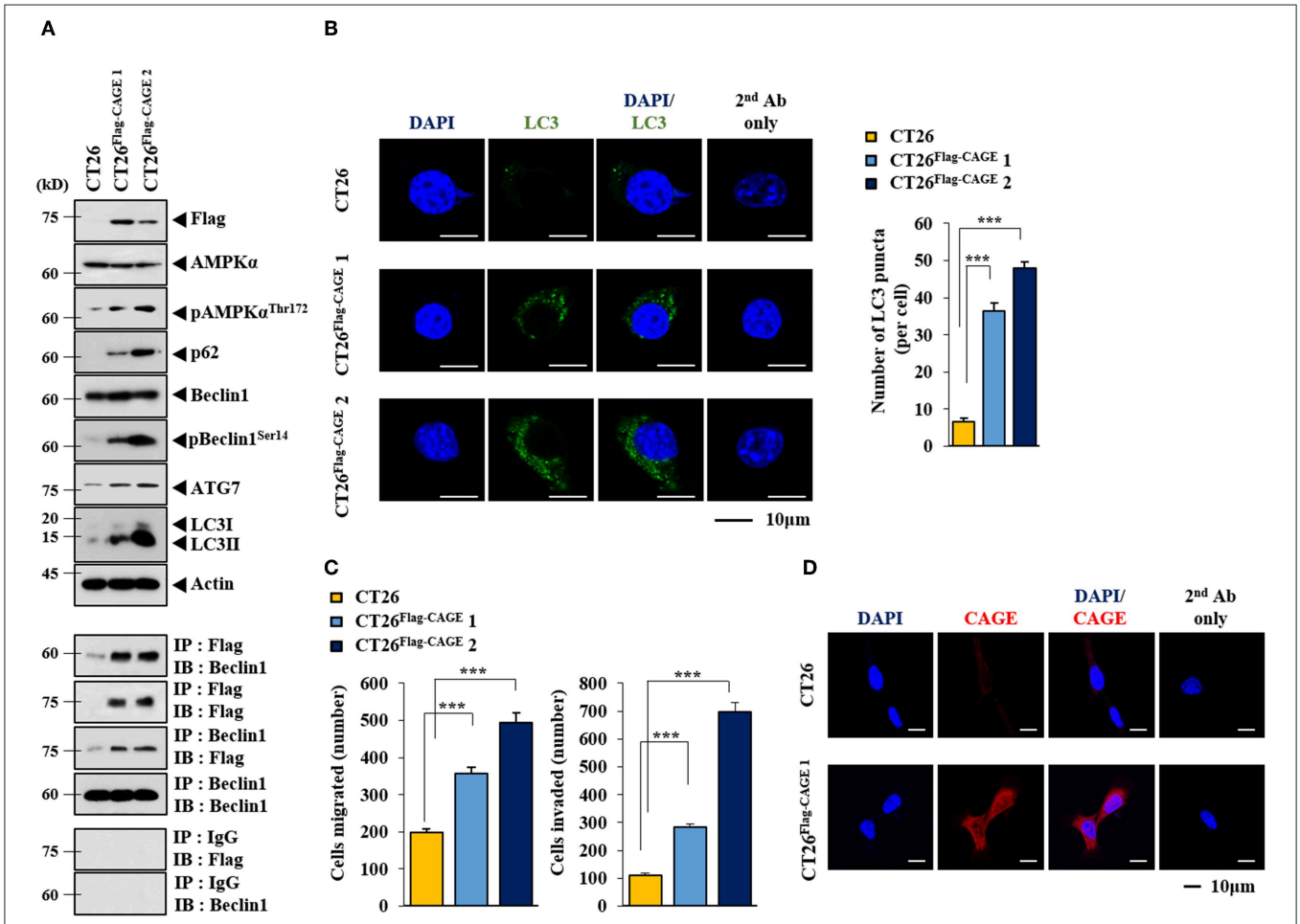

FIGURE 1 | CAGE increases the expression of autophagic flux. **(A)** Cell lysates from the indicated cancer cells were subjected to immunoblot (upper panel) and immunoprecipitation (lower panel). Each blot is a representative of three independent experiments. **(B)** LC3 puncta expression was determined as described. ***$p <$ 0.0005. **(C)** The indicated cancer cells were subjected to migration and invasion assays. ***$p < 0.0005$. **(D)** Immunofluorescence staining was performed to examine the localization of CAGE.

Isolation and Characterization of Exosomes

Isolation of the exosomes was performed according to the manufacturer's instructions (System Biosciences, Mountain View, CA). Exosomes were observed under a Tecnai T10 transmission electron microscope (FEI, USA).

Labeling and Internalization of Exosomes

Exosomes from CT26$^{Flag-CAGE}$1 cells were labeled using PKH67 Fluorescent Cell Linker kits (Sigma-Aldrich, St. Louis, MO). Uptake of exosomes was determined according to the standard procedures (19). Cells were visualized under a confocal laser scanning microscope LX70 FV300 05-LPG-193 (Olympus).

The Presence of wnt1 in the Exosomes of CT26$^{Flag-CAGE}$ Cells

In order to precipitate exosomes, exosomes extractions purified from CT26$^{Flag-CAGE}$ cells were subjected to centrifugation at 60,000 g for 30 min. Precipitated exosomes were collected and cross-linked by 0.1% glutaraldehyde and 2% paraformaldehyde in phosphate buffer (pH 7.4) for 1 h (4°C), then post-fixed in 2% osmium tetroxide for 30 min (4°C). They were dehydrated with a graded series of ethanol and embedded into epoxy resin (PELCO, USA). Ultrathin sections (~80 nm) were prepared from Ultracut UCT (Leica, Germany) and the sections were mounted on copper grids. Followed to the sectioning, it has stained with 1% uranyl acetate for 20 min, and lead citrate for 10 min for the subsequent TEM observations. For immune-gold labeling electron microscopy, ultrathin sections on the grids were treated with 3% sodium (meta) periodate for 30 min for etching and it was treated with 0.02 M glycine (10 min) for quenching the reaction of free aldehyde group. Sections were then washed in deionized water, floated for 1 h in PBS containing 1% BSA. Etching specimens were incubated directly in the primary rabbit or/and mouse antibodies (Anti-Wnt1 or/and Anti-TSG101 antibodies) at 1:20 dilutions for overnight at 4°C.

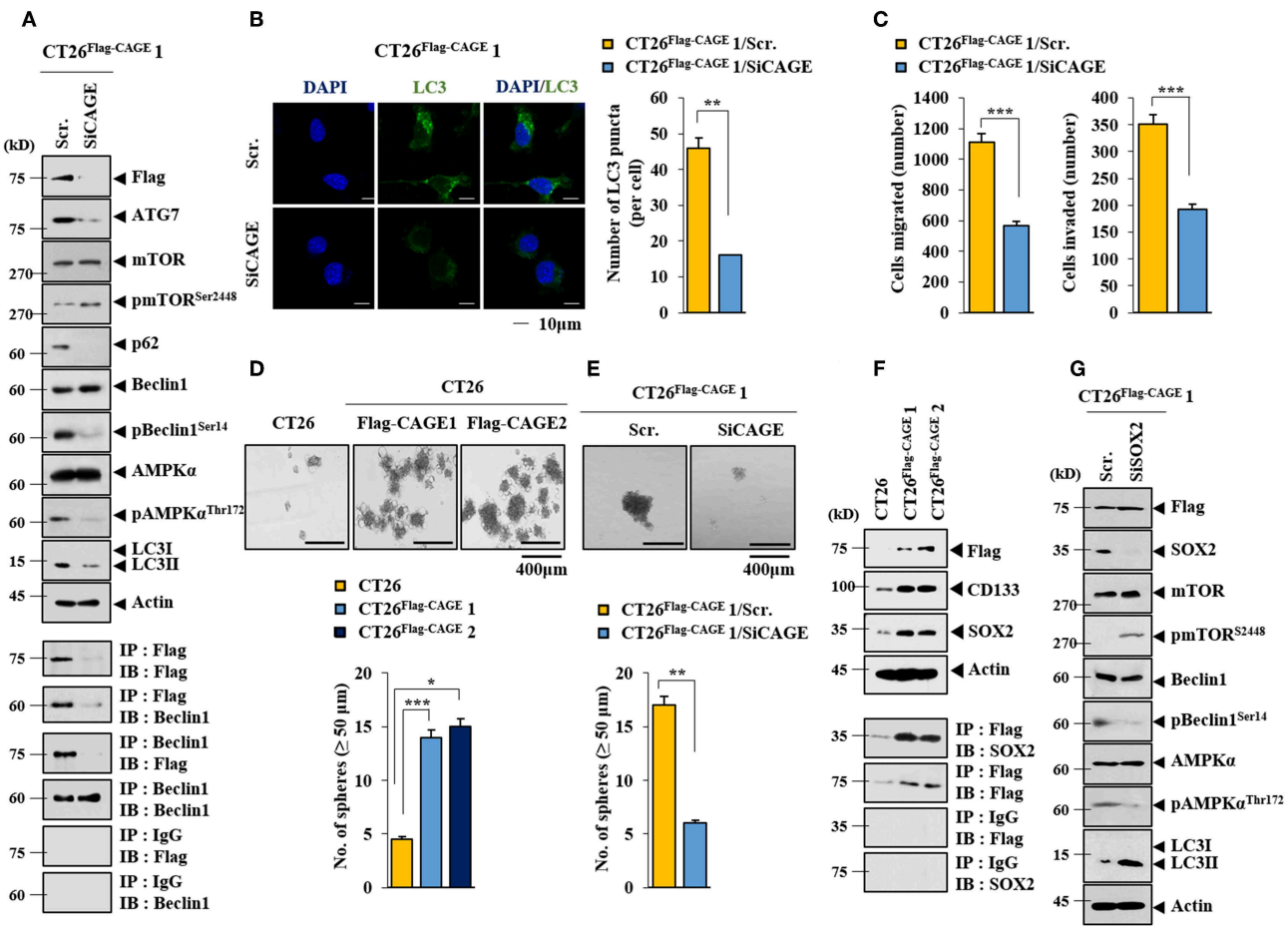

FIGURE 2 | Down-regulation of CAGE decreases autophagic flux, and CSC-like properties. **(A)** The indicated cancer cells were transfected with the indicated siRNA (each at 10 nM) for 48 h, followed by immunoblot (upper) and immunoprecipitation (lower). **(B)** Same as A except that LC3 puncta expression was determined. $^{**}p < 0.005$. **(C)** The indicated cancer cells were transfected with the indicated siRNA (each at 10 nM) for 48 h, followed by migration and invasion potential assays. $^{***}p < 0.0005$. **(D)** Tumor spheroid forming potentials of the indicated cancer cells were determined as described. $^{*}p < 0.05$; $^{**}p < 0.005$; $^{***}p < 0.0005$. **(E)** Cells were transiently transfected with the indicated siRNA (each at 10 nM) for 48 h. Cells were then subjected to tumor spheroid forming potential assays. $^{**}p < 0.005$. **(F)** Cell lysates from the indicated cancer cells were subjected to immunoblot (upper) and immunoprecipitation (lower). **(G)** The indicated cancer cells were transiently transfected with the indicated siRNA (each at 10 nM) for 48 h, followed by immunoblot.

The grid were washed five time with 0.1% BSA in PBS, incubated in secondary antibodies, anti- Rabbit IgG conjugated to 10 nm and anti-mouse IgG conjugated to 25 nm (AURION, Holland) diluted 1:20 in 0.1% BSA-PBS. The sample grids were stained with uranyl acetate and lead citrate. The sectioned and immune-gold labeled grids were examined using a Tecnai T10 (FEI, USA) operated at 100 kV and JEOL-2100F (JEOL, USA) operated at 200 KV.

Statistical Analysis

Data were analyzed and graphed using GraphPad Prism statistics program (GraphPad Prism software). Results are presented as means ± S.E. Statistical analysis was performed using one way *t*-tests with differences between means considered significant when $p < 0.05$.

RESULTS

CAGE Regulates Autophagic Flux and Cancer Stem Cell-Like Properties

Anti-cancer drug-resistance is closely related to autophagy (18, 21). The effect of CAGE on autophagic flux was investigated. For this, we established mouse colon cancer cells stably expressing CAGE. $CT26^{Flag-CAGE}1$ and $CT26^{Flag-CAGE}2$ cells showed higher autophagic flux, such as p62, $pBeclin1^{Ser14}$, LC3II, ATG7, and $pAMPK\alpha^{T172}$ than the parental CT26 cells (**Figure 1A**). CAGE displayed binding to Beclin1, a mediator of autophagy, in the $CT26^{Flag-CAGE}1$ and $CT26^{Flag-CAGE}2$ cells (**Figure 1A**). These cells also displayed higher expression of LC3 puncta than the CT26 cells (**Figure 1B**). The $CT26^{Flag-CAGE}1$ and $CT26^{Flag-CAGE}2$ cells showed higher migration and invasion potential than the parental CT26 cells (**Figure 1C**). CAGE showed both cytoplasmic and nuclear localization (**Figure 1D**). CAGE increased autophagosomes formation in the CT26 cells (**Supplementary Figure 1**). Down-regulation of CAGE led to decreased autophagic flux in the $CT26^{Flag-CAGE}1$ and $CT26^{Flag-CAGE}2$ cells (**Figure 2A**). Down-regulation of CAGE led to decreased expression of LC3 puncta (**Figure 2B**) and decreased the migration and invasion potentials of the $CT26^{Flag-CAGE}1$ cells (**Figure 2C**). Autophagy regulates the expression of pluripotency-associated proteins (PA), such as SOX2, in cervical CSCs (10). Calpain-6 promotes autophagy and maintains the tumor-initiating cell population in sarcoma

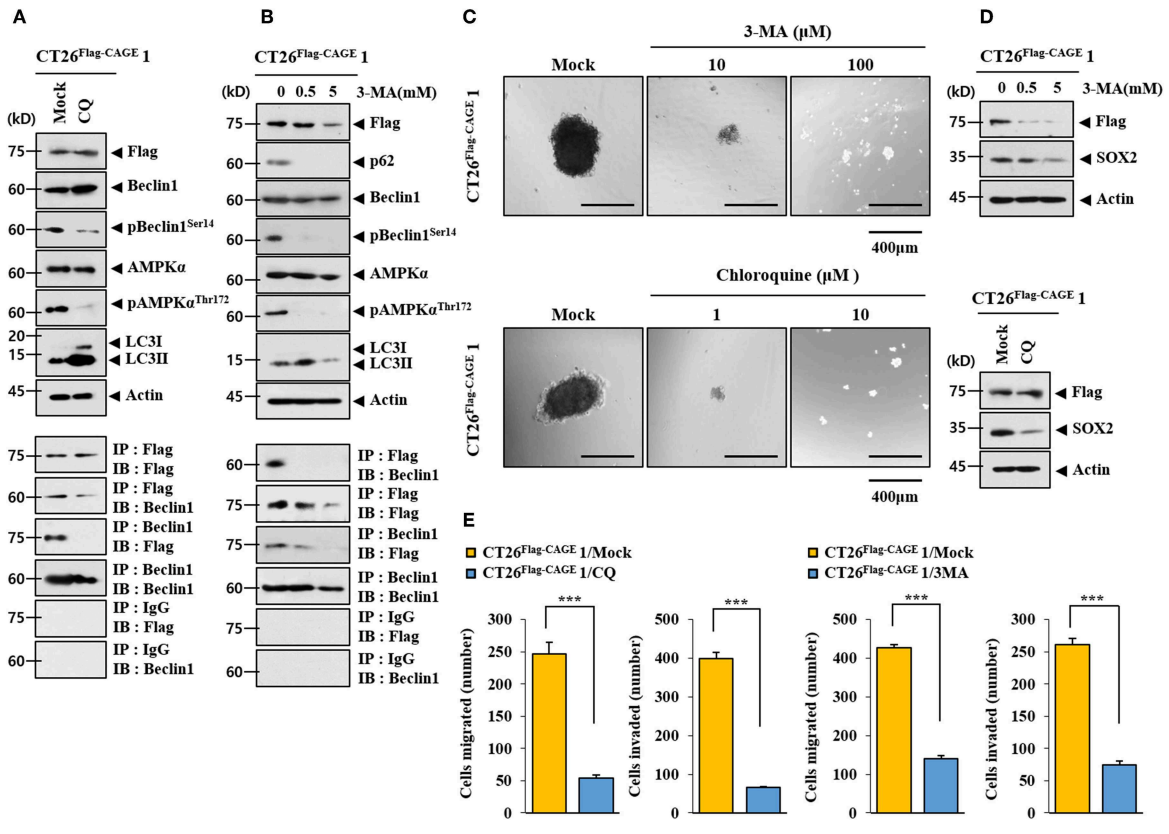

FIGURE 3 | CAGE-Beclin1 interaction is necessary for autophagy. **(A)** The indicated cancer cells were treated with CQ (50 μM) for 12 h, followed by immunoblot and immunoprecipitation. **(B)** The indicated cancer cells were treated with various concentrations of 3-MA for 12 h, followed by immunoblot and immunoprecipitation. **(C)** The indicated cancer cells were treated with CQ or 3-MA at the indicated concentration, followed by tumor spheroid forming potential assays. **(D)** The indicated cancer cells were treated with 3-MA at the indicated concentration for 12 h or treated with CQ (50 μM) for 12 h, followed by immunoblot. **(E)** The indicated cancer cells were treated with CQ (50 μM) for 12 h or with 3-MA (0.5 mM) for 12 h, followed by invasion and migration potential assays. ***$p < 0.0005$.

stem cells (22). We examined the effect of CAGE on CSC-like properties. The CT26$^{Flag-CAGE}$1 and CT26$^{Flag-CAGE}$2 cells showed higher tumor spheroid-forming potential than the CT26 cells (**Figure 2D**). CAGE was necessary for the tumor spheroid forming potential of CT26$^{Flag-CAGE}$1 cells (**Figure 2E**). The CT26$^{Flag-CAGE}$1 and CT26$^{Flag-CAGE}$2 cells showed higher expression of CD133 and SOX2, markers of cancer stemness (23), than CT26 (**Figure 2F**). CAGE interacted with SOX2 (**Figure 2F**). SOX2 did not affect the expression of CAGE, but decreased autophagic flux in CT26$^{Flag-CAGE}$1 cells (**Figure 2G**). Thus, CAGE regulates autophagic flux and CSC-like properties.

CAGE-Beclin1 Interaction Is Necessary for Autophagy

CQ (**Figure 3A**) and 3-MA (**Figure 3B**), inhibitors of autophagy, decreased autophagic flux and inhibited the interaction between CAGE and Beclin1 in CT26$^{Flag-CAGE}$1 cells. CQ and 3-MA decreased the tumor spheroid-forming potential (**Figure 3C**) and the expression of SOX2 in CT26$^{Flag-CAGE}$1 cells (**Figure 3D**). CQ and 3-MA negatively regulated the migration and invasion potential of CT26$^{Flag-CAGE}$1 cells (**Figure 3E**). These results suggest that CAGE-Beclin1 interaction is necessary for autophagic flux.

CAGE Enhances the Tumorigenic Potential of CT26

CT26$^{Flag-CAGE}$1 and CT26$^{Flag-CAGE}$2 cells showed higher tumorigenic potential than the CT26 cells (**Figure 4A**). Immunoblots of tumor tissue lysates showed that CAGE increased autophagic flux and demonstrated binding to Beclin1 (**Figure 4B**). Immunohistochemical staining showed that CAGE increased autophagic flux (**Figure 4C**). Thus, CAGE enhances the tumorigenic potential of CT26 by increasing autophagic flux.

Identification of miRNAs Regulated by CAGE

To identify the miRNAs regulated by CAGE, miRNA array analysis was performed. The CT26$^{Flag-CAGE}$1 and CT26$^{Flag-CAGE}$2 cells showed lower expressions of miRNAs, such as miR-140-5p, than the CT26 cells (**Figure 5A**). QRT-PCR analysis confirmed the microRNA analysis (**Figure 5B**). CAGE

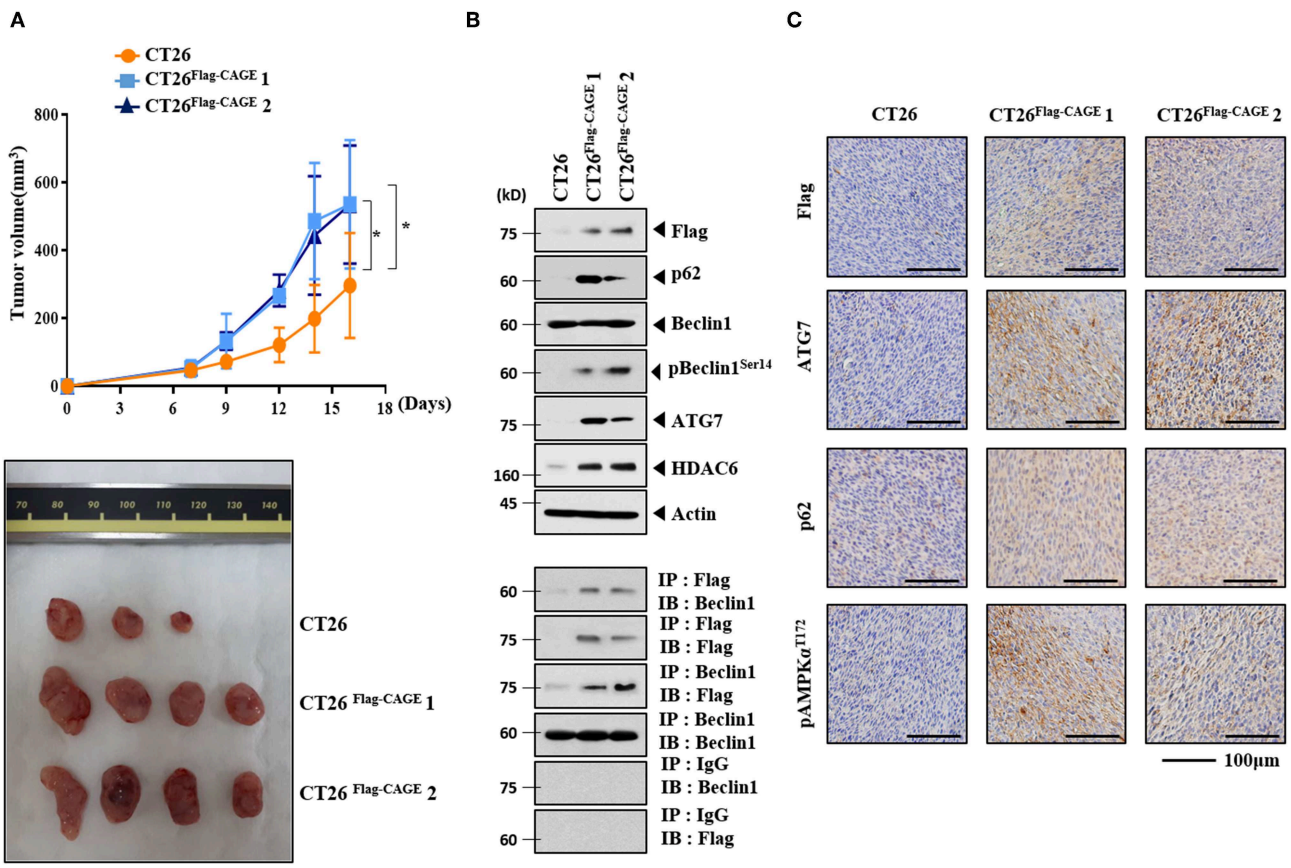

FIGURE 4 | CAGE enhances the tumorigenic potential of CT26 cells. **(A)** The indicated cancer cells (each at 1 × 10^6) were injected into the dorsal flanks of BALB/C mice. Each value represents an average obtained from BALB/C mice of each group. Data are expressed as a mean ± S.D. Tumor volumes were measured as described. *$p < 0.05$. Each experimental group consisted of four BALB/C mice. **(B)** Lysates from the indicated tumor tissues were subjected to immunoblot and immunoprecipitation. **(C)** Immunohistochemical staining of tumor tissue employing the indicated antibody (2 μg/ml) was performed. Scale bar represents 100 μm.

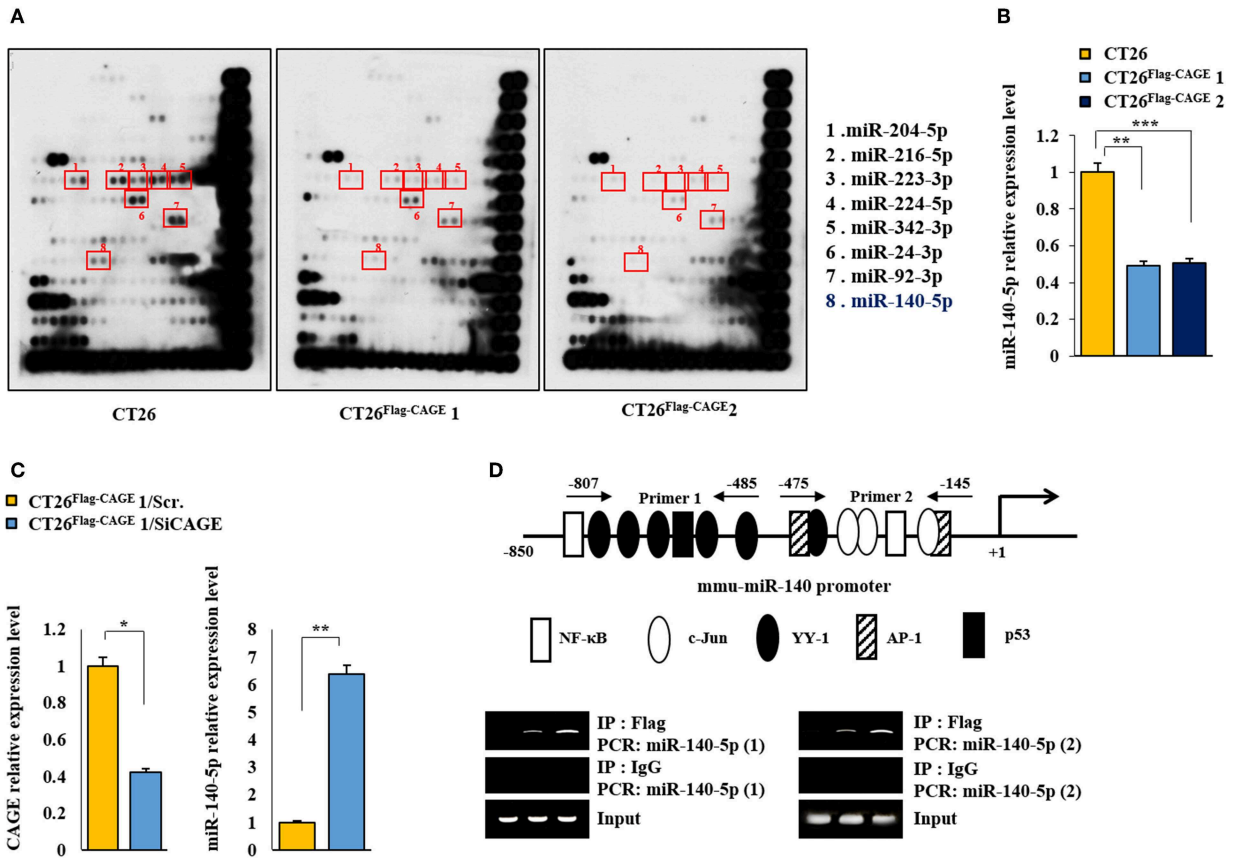

FIGURE 5 | MiR-140-5p serves as a target of CAGE. **(A)** MicroRNA array analysis was performed as described. **(B)** QRT-PCR analysis of the indicated cancer cells was performed. $^{**}p < 0.005$; $^{***}p < 0.0005$. **(C)** CT26 $^{Flag-CAGE}1$ cells were transfected with the indicated siRNA (each at 10 nM). At 48 h after transfection, cells were subjected to qRT-PCR analysis. $^{*}p < 0.05$; $^{**}p < 0.005$. **(D)** Shows potential binding sites for various transcriptional factors in the promoter sequences of miR-140-5p (upper). ChIP assays employing the indicated antibody (2 μg/ml) was performed as described (lower panel).

negatively regulated the expression of miR-140-5p (**Figure 5C**). The miR-140-5p promoter sequences served as binding sites for transcription factors (**Figure 5D**, upper). CAGE displayed binding to the promoter sequences of miR-140-5p (**Figure 5D**, lower). This indicates direct regulation of miR-140-5p by CAGE. Thus, miR-140-5p, a direct target of CAGE, may inhibit autophagic flux.

MiR-140-5p Regulates Autophagic Flux

The miR-140-5p inhibitor increased autophagic flux while decreasing the expression of $pmTOR^{Ser2448}$, an inhibitor of autophagy, in CT26 cells (**Figure 6A**). The miR-140-5p mimic exerted the opposite effects on autophagic flux and the interaction between CAGE and Beclin1 in $CT26^{Flag-CAGE}1$ cells (**Figure 6B**). The miR-140-5p inhibitor increased LC3 puncta expression (**Figure 6C**) and enhanced the migration and invasion potential of the CT26 cells **Figure 6D**). The miR-140-5p mimic decreased the expression of LC3 puncta in $CT26^{Flag-CAGE}1$ cells (**Figure 6E**). MiR-140-5p mimic decreased the migration and invasion potentials of the $CT26^{Flag-CAGE}1$ cells (**Figure 6F**). Thus, miR-140-5p regulates autophagic fluxes.

MiR-140-5p Regulates the Tumorigenic Potential of CT26

The effect of the miR-140-5p inhibitor on the tumorigenic potential of the CT26 cells was examined. The miR-140-5p inhibitor enhanced the tumorigenic potential of the CT26 cells (**Figure 7A**). MiR-140-5p inhibitor increased autophagic flux while decreasing the expression of $pmTOR^{Ser2448}$ in the CT26 cells (**Figure 7B**). The miR-140-5p mimic decreased the tumorigenic potential of the $CT26^{Flag-CAGE}1$ cells (**Figure 7C**). QRT-PCR showed the expression of miR-140-5p in tumor tissue lysates (**Figure 7C**). The miR-140-5p mimic decreased autophagic flux and inhibited the interaction between CAGE and Beclin1 (**Figure 7D**). Thus, miR-140-5p regulates tumorigenic potential and autophagic flux.

MiR-140-5p Directly Targets Wnt1

TargetScan analysis predicted that Wnt1 would be a target of miR-140-5p (**Figure 8A**). It is reasonable that miR-140-5p may directly regulate Wnt1 expression level. Both the wild type and mutant 3′-UTR of Wnt1 showed luciferase

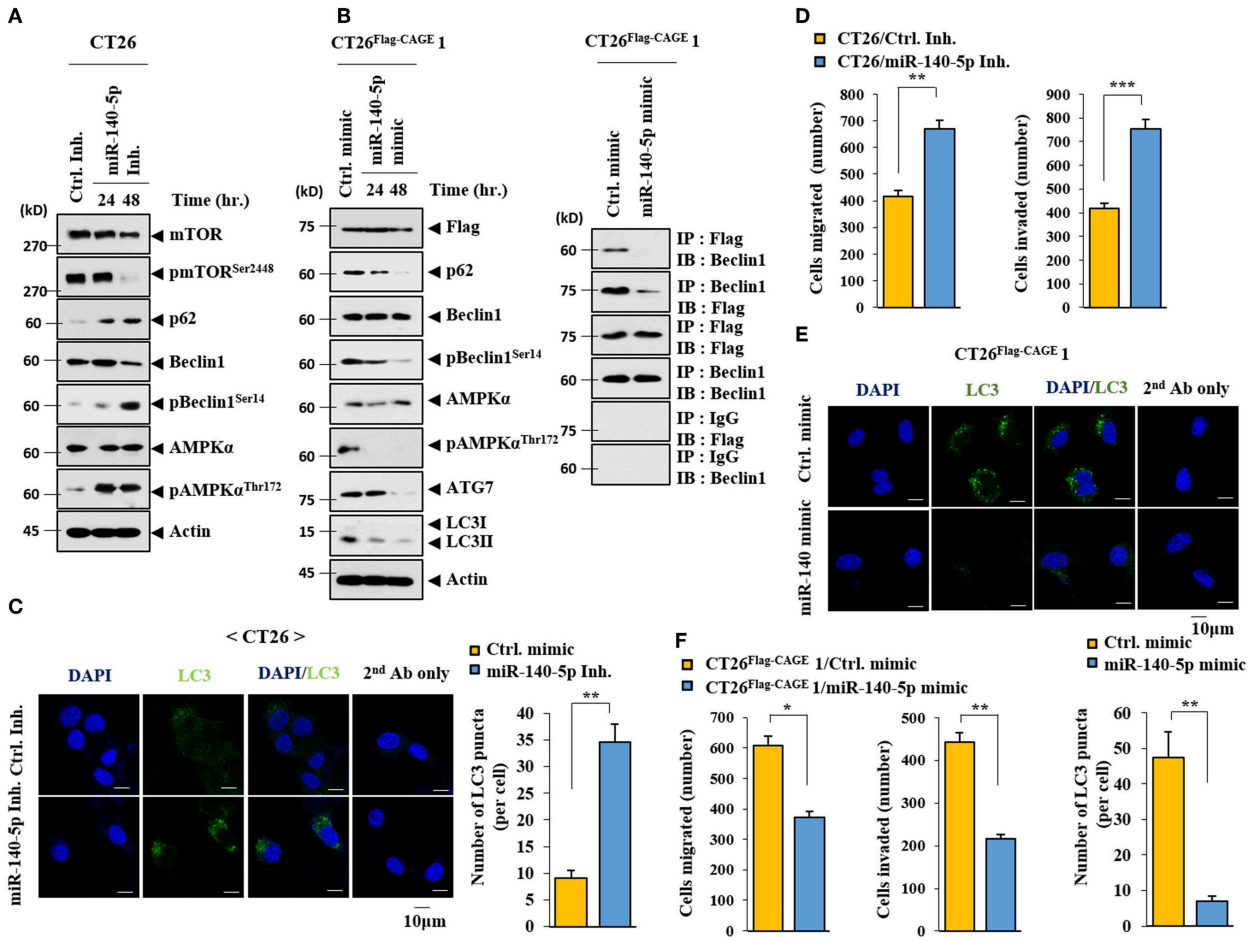

FIGURE 6 | MiR-140-5p regulates autophagic flux. **(A)** CT26 cells were transfected with control inhibitor (10 nM) for 48 h or with miR-140-5p inhibitor (10 nM) for various time intervals. Immunoblot was performed. **(B)** The indicated cancer cells were transfected with control mimic (10 nM) for 48 h or with miR-140-5p mimic (10 nM) for various time intervals, followed by immunoblot (left). The indicated cancer cells were transfected with the indicated mimic (each at 10 nM) for 48 h, followed by immunoprecipitation. **(C)** CT26 cells were transfected with control inhibitor (10 nM) or with miR-140-5p inhibitor (10 nM) for 48 h. LC3 puncta expression was determined. $^{**}p < 0.005$. **(D)** CT26 cells were transfected with the indicated inhibitor (each at 10 nM) for 48 h, followed by migration or invasion potential assay. $^{**}p < 0.005$; $^{***}p < 0.0005$. **(E)** The indicated cancer cells were transfected with control mimic (10 nM) or with miR-140-5p mimic (10 nM) for 48 h intervals. LC3 puncta expression was determined. $^{**}p < 0.005$. **(F)** Same as E except that CT26 cells were subjected to migration and invasion assays. $^{*}p < 0.05$; $^{***}p < 0.005$.

activities in CT26$^{Flag-CAGE}$1 cells (**Figure 8B**). The miR-140-5p mimic inhibited the luciferase activity associated with the Luc-3′-wild type UTR of wnt1, but not the luciferase activity associated with the Luc-3′-mutant UTR of Wnt1 (**Figure 8B**). Wnt 1 may act as a direct target of miR-140-5p to regulate autophagic flux. CAGE increases the expression of cyclinD1 in an AP1-dependent manner (4). Prodigiosin decreases the tumorigenic potential and expression of cyclin D1 in breast cancer cells by inhibiting the Wnt/β-catenin pathway (24). The CT26$^{Flag-CAGE}$1 cells and CT26$^{Flag-CAGE}$2 cells showed higher expression of Wnt1 mRNA than the CT26 cells (**Figure 8C**). CT26$^{Flag-CAGE}$1 cells showed higher expressions of Wnt1, pGSK3β^{Ser9} (an inactive form of GSK3β), and cyclinD1 than the CT26 cells (**Figure 8D**). Inhibition of Wnt1 prevents leptin-stimulated GSK3β phosphorylation (25). Down-regulation of CAGE led to the decreased expression of Wnt1, pGSK3β^{Ser9}, and cyclinD1 in the CT26$^{Flag-CAGE}$1 cells (**Figure 8E**). CAGE also regulated the expression of Wnt1 at the transcription level (**Figure 8F**). The miR-140-5p inhibitor increased the expression of Wnt1, pGSK3β^{Ser9}, and cyclinD1 in the CT26 cells (**Figure 8G**) while the miR-140-5p mimic exerted the opposite effect on the expression of these proteins in the CT26$^{Flag-CAGE}$1 cells (**Figure 8H**). The down-regulation of Wnt1 decreased autophagic flux, pGSK3β^{Ser9}, and cyclinD1 in the CT26$^{Flag-CAGE}$1 cells (**Figure 8I**). Tumor tissue lysates of the CT26$^{Flag-CAGE}$1 cells showed higher expression of Wnt1, β-catenin, pGSK3β^{Ser9}, and cyclin D1 than the tumor tissue lysates of the CT26 cells (**Supplementary Figure 2A**). The autophagic degradation of β-catenin by p62 led to a

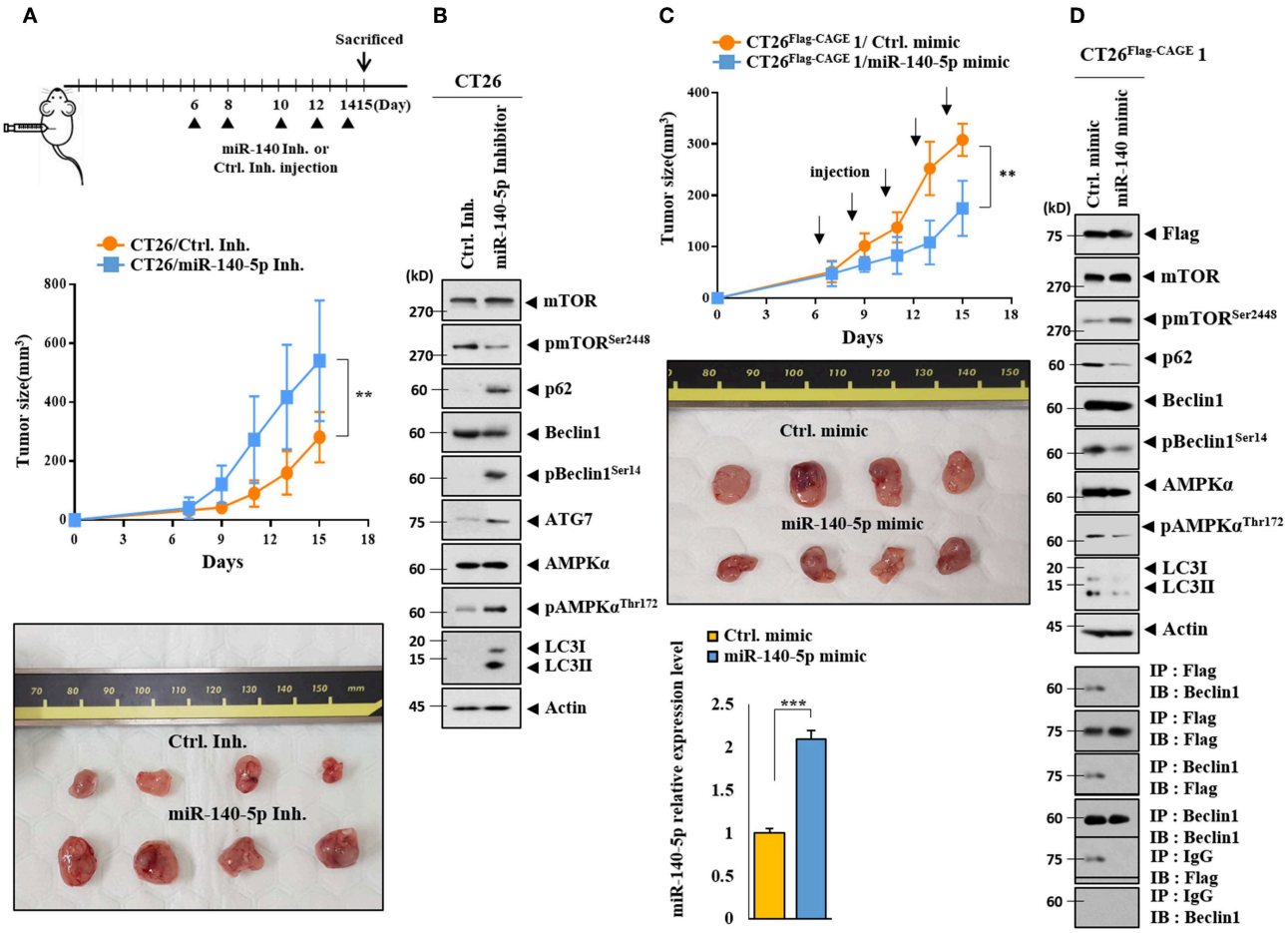

FIGURE 7 | MiR-140-5p regulates the tumorigenic potential. **(A)** CT26 cells (1×10^6) were injected into the dorsal flanks of BALB/C mice. Following the establishment of sizeable tumor, the indicated inhibitor (each at 100 nM) was injected at the indicated day. Each value represents an average obtained from BALB/C mice of each group. Data are expressed as a mean ± S.D. $^{**}p < 0.005$. Each experimental group consisted of four BALB/C mice. **(B)** Tumor tissue lysates were subjected to immunoblot. **(C)** CT26 $^{Flag-CAGE}1$ cells (1×10^6) were injected into the dorsal flanks of BALB/C mice. Following the establishment of sizeable tumor, the indicated mimic (each at 100 nM) was intravenously injected five times in a total of 15 days. Tumor tissue lysates were subjected to qRT-PCR analysis (lower). $^{**}p < 0.005$; $^{***}p < 0.0005$. Each experimental group consisted of four BALB/C mice. **(D)** Tumor tissue lysates were subjected to immunoblot (upper) and immunoprecipitation (lower).

decreased self-renewal capacity of the colonospheres (26). Immunohistochemical staining showed the same results as the immunoblot (**Supplementary Figure 2B**). Thus, CAGE and miR-140-5p exerted opposite effects on the expression of Wnt1 to regulate autophagic flux.

CAGE May Mediate Cellular Interactions Within the Tumor Microenvironment

Cancer cells interact with various stromal cells, such as mast cells, within the tumor microenvironment (27). Thus, we examined whether CAGE would affect cellular interactions within the tumor microenvironment. Tumor tissue derived from CT26$^{Flag-CAGE}$1 cells showed higher expression of CD163, tryptase, and chymase but lower expression of iNOS than the tumor tissue derived from the CT26 cells (**Figure 9A**). CD163 and iNOS are makers of TAM and M1 macrophages, respectively. Tryptase and chymase are hallmarks of allergic inflammation. Tumor tissue lysates of the CT26$^{Flag-CAGE}$1 cells showed higher expression of autophagic flux, tryptase, chymase, and CD163 but lower expression of iNOS than CT26 tumor tissue lysates (**Figure 9B**). Tumor tissue lysates of the CT26$^{Flag-CAGE}$1 cells showed the interaction of FcεRIβ with HDAC3 and SOCS1 (**Figure 9B**). Tumor tissue lysates of the CT26$^{Flag-CAGE}$1 cells showed more activated mast cells than the tumor tissue lysates of CT26 cells (**Figure 9C**). Thus, CAGE may mediate cellular interactions within the tumor microenvironment.

Exosomes Mediate Cellular Interactions

We examined whether CAGE would mediate cellular interactions. Culture medium from the CT26$^{Flag-CAGE}$1 and CT26$^{Flag-CAGE}$2 cells increased autophagic flux in

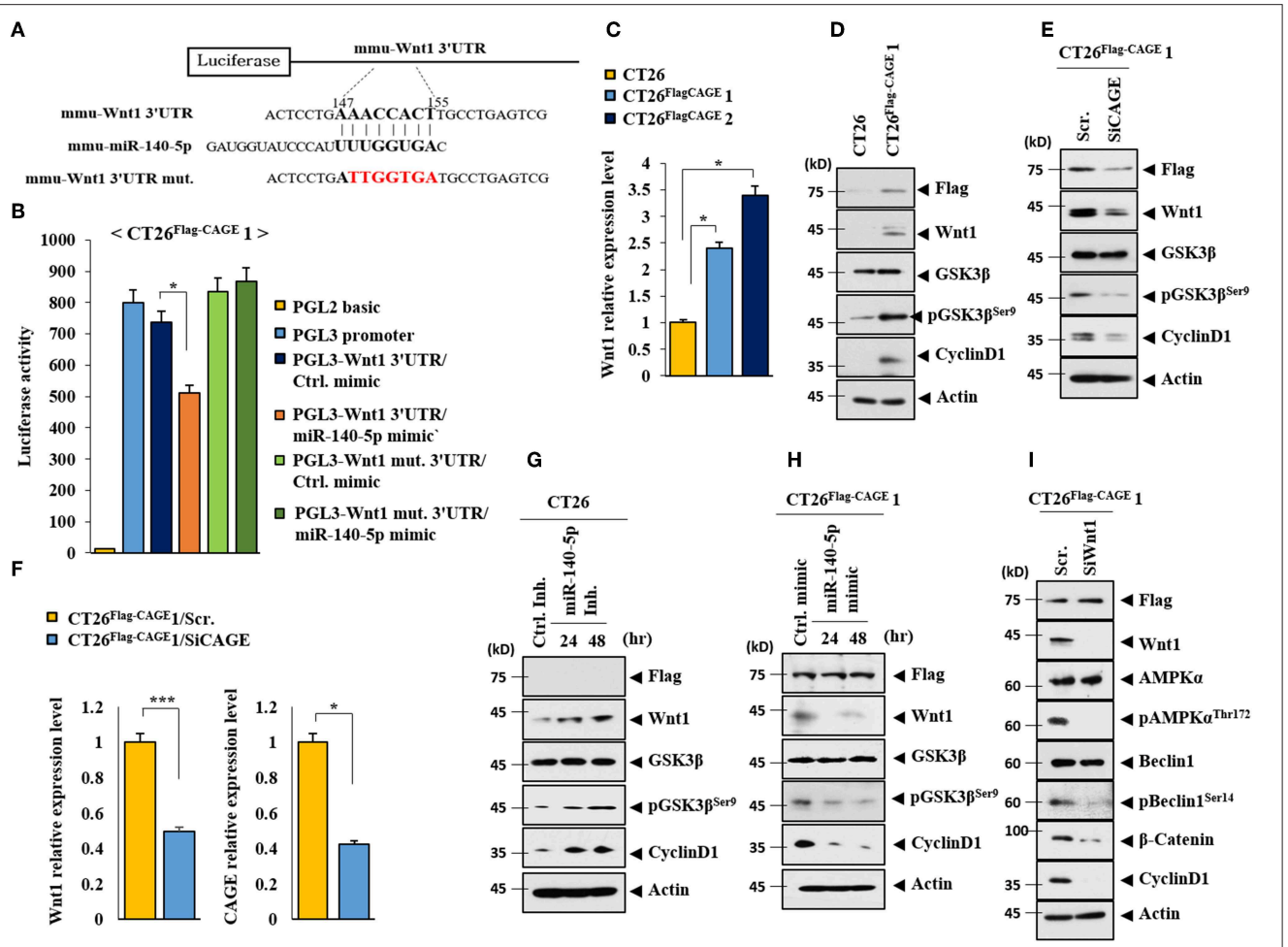

FIGURE 8 | CAGE and miR-140-5p regulate the expression of wnt1. **(A)** Potential binding of miR-140-5p to 3′-UTR of wnt1. **(B)** Wild type Luc-p62-3′-UTR or mutant Luc-p62-3′-UTR was transfected along with control mimic or miR-135-5p mimic (each at 10 nM) into the indicated cell line. At 48 h after transfection, luciferase activity assays were performed. *$p < 0.05$. **(C)** Cell lysates from the indicated cancer cells were subjected to qRT-PCR analysis. *$p < 0.05$. **(D)** Cell lysates from the indicated cancer cells were subjected to immunoblot. **(E)** The indicated cancer cells were transfected with the indicated siRNA (each at 10 nM) for 48 h, followed by immunoblot. **(F)** Same as E except that qRT-PCR analysis was performed. *$p < 0.05$; ***$p < 0.0005$. **(G)** The indicated cancer cells were transfected with control inhibitor (10 nM) for 48 h or miR-140-5p inhibitor (10 nM) for various time intervals. **(H)** The indicated cancer cells were transfected with control mimic (10 nM) for 48 h or miR-140-5p mimic (10 nM) for various time intervals, followed by immunoblot. **(I)** The indicated cancer cells were transfected with the indicated siRNA (each at 10 nM) for 48 h, followed by immunoblot analysis.

the CT26 cells (**Figure 10A**). Culture medium from the $CT26^{Flag-CAGE}1$ cells treated with GW4869, an inhibitor of exosomes formation, did not increase autophagic flux in the CT26 cells (**Figure 10B**). It is probable that exosomes from the $CT26^{Flag-CAGE}1$ cells may have increased autophagic flux in the CT26 cells. Culture medium from the $CT26^{Flag-CAGE}1$ cells increased LC3 puncta expression in the CT26 cells (**Figure 10C**). Immunofluorescence staining of the exosomes showed the co-localization of Wnt1 with TSG101, an exosomal marker (**Supplementary Figure 3A**). Wnt1 was detected in the lumen of the exosomes, whereas TSG101, a known membrane marker of exosomes, was detected in the outer membrane of the exosomes based on immunogold staining of Wnt1 (as shown by 10 nm golds located in the inner of the vesicles) and TSG101 (as shown by 25 nm golds located in the outer membrane of the vesicles) (**Supplementary Figure 3B**). Exosomes from the $CT26^{Flag-CAGE}1$ cells enhanced the migration and invasion potential of the CT26 cells (**Figure 10D**). Immunofluorescence staining showed that the PKH67-labeled exososmes from $CT26^{Flag-CAGE}1$ cells could be transferred to the CT26 cells (**Figure 10E**). Immunoblot showed the expression of Wnt1 within exosomes from the $CT26^{Flag-CAGE}1$ cells (**Figure 10F**). Exosomes from the $CT26^{Flag-CAGE}1$ cells also showed the presence of CXCL10 and IL-27 (**Figure 10F**). Rapamycin, an inducer of autophagy, enhanced the cytotoxic effect of NK cells by increasing the expression of IL-27 in uterine endometrial cancer cells (28). Exosomes from the $CT26^{Flag-CAGE}1$ cells also increased autophagic flux in lung mast cells (**Figure 10G**). It is probable that the exosomes mediate the effects of CAGE

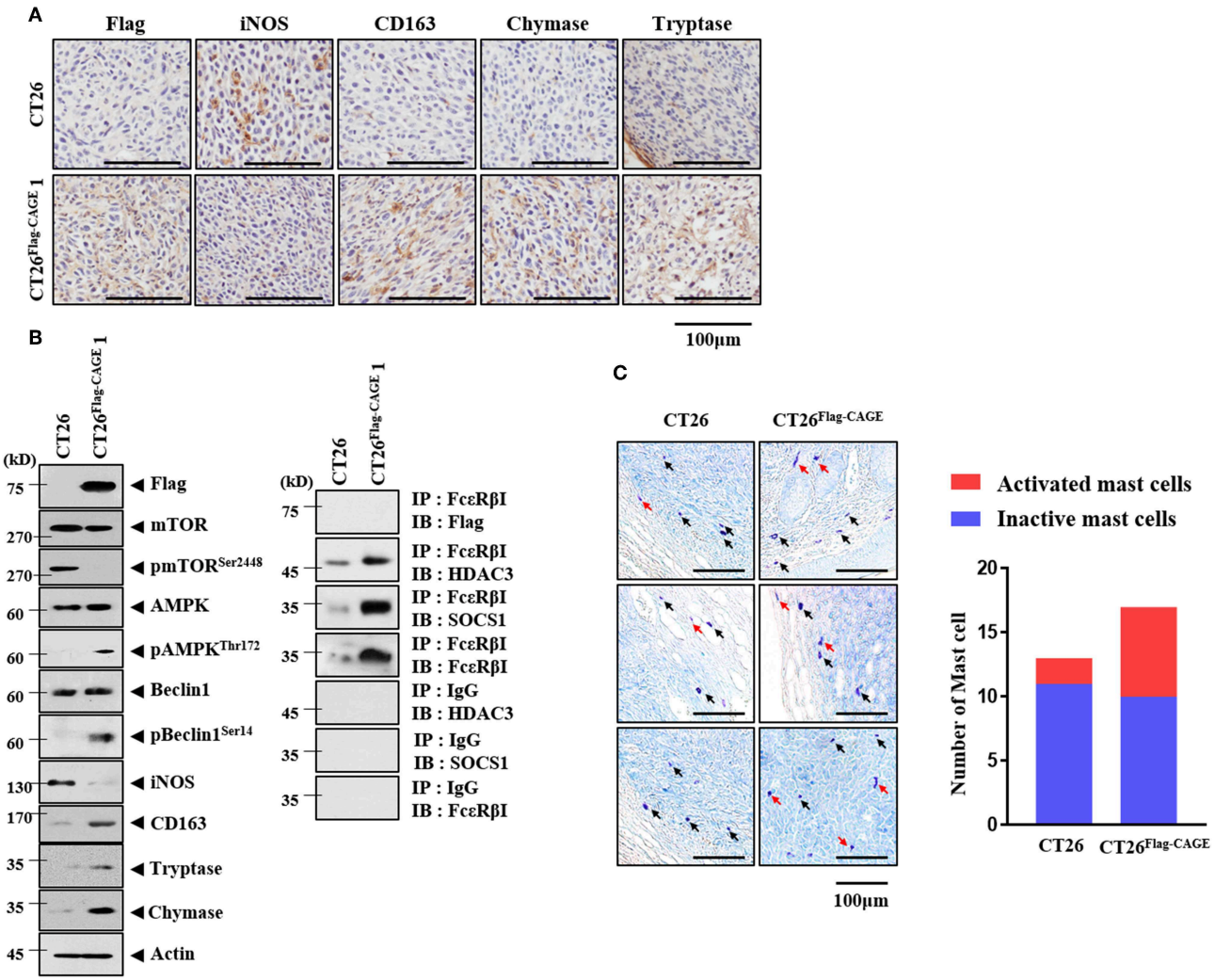

FIGURE 9 | CAGE may promote activation of macrophages and mast cells. **(A)** Tumor tissues were subjected to immunohistochemical staining as described. **(B)** Tumor tissue lysates were subjected to immunoblot (left) and immunoprecipitation (right). **(C)** Tumor tissues were subjected to toluidine blue staining. Red arrows represent activated mast cells. Black arrows represent mast cells.

on autophagic flux and cellular interactions. These results suggest that Wnt1 may mediate cellular interactions within the tumor microenvironment.

Exosomes From CT26$^{Flag\text{-}CAGE}$ Cells Activate Macrophages

Exosomes form the CT26$^{Flag-CAGE}$1 cells increased the expression of CD163, but decreased the expression of iNOS in lung macrophages (**Figure 11A**). Exosomes from the CT26$^{FlagG-CAGE}$ 1 cells also increased the expression of autophagic flux in macrophages (**Figure 11A**). Immunofluorescence staining showed that exosomes from the CT26$^{Flag-CAGE}$1 cells increased the expression of CD163 (**Figure 11B**) and LC3 (**Figure 11C**) and decreased the expression of iNOS (**Figure 11B**). PKH67-labedled exosomes from the CT26$^{Flag-CAGE}$1 cells were transferred to the lung macrophages (**Figure 11D**). Thus, exosomes mediated the activation of macrophages by CT26$^{Flag-CAGE}$1 cells.

Exosomes From CT26$^{Flag\text{-}CAGE}$ Cells Enhance the Tumorigenic Potential of CT26 Cells

Exosomes from the CT26$^{Flag-CAGE}$1 cells enhanced the tumorigenic potential of CT26 cells (**Figure 12A**), but those of the CT26 cells did not affect the tumorigenic potential of CT26. Tumor tissue lysates of CT26 cells that received exosomes from the CT26$^{Flag-CAGE}$1 cells displayed higher expressions of Wnt1, β-catenin, cycinD1, pGSK3β^{Ser9}, and autophagic flux than tumor tissue lysates from the CT26 cells that received CT26 exosomes (**Figure 12B**). Tumor tissue

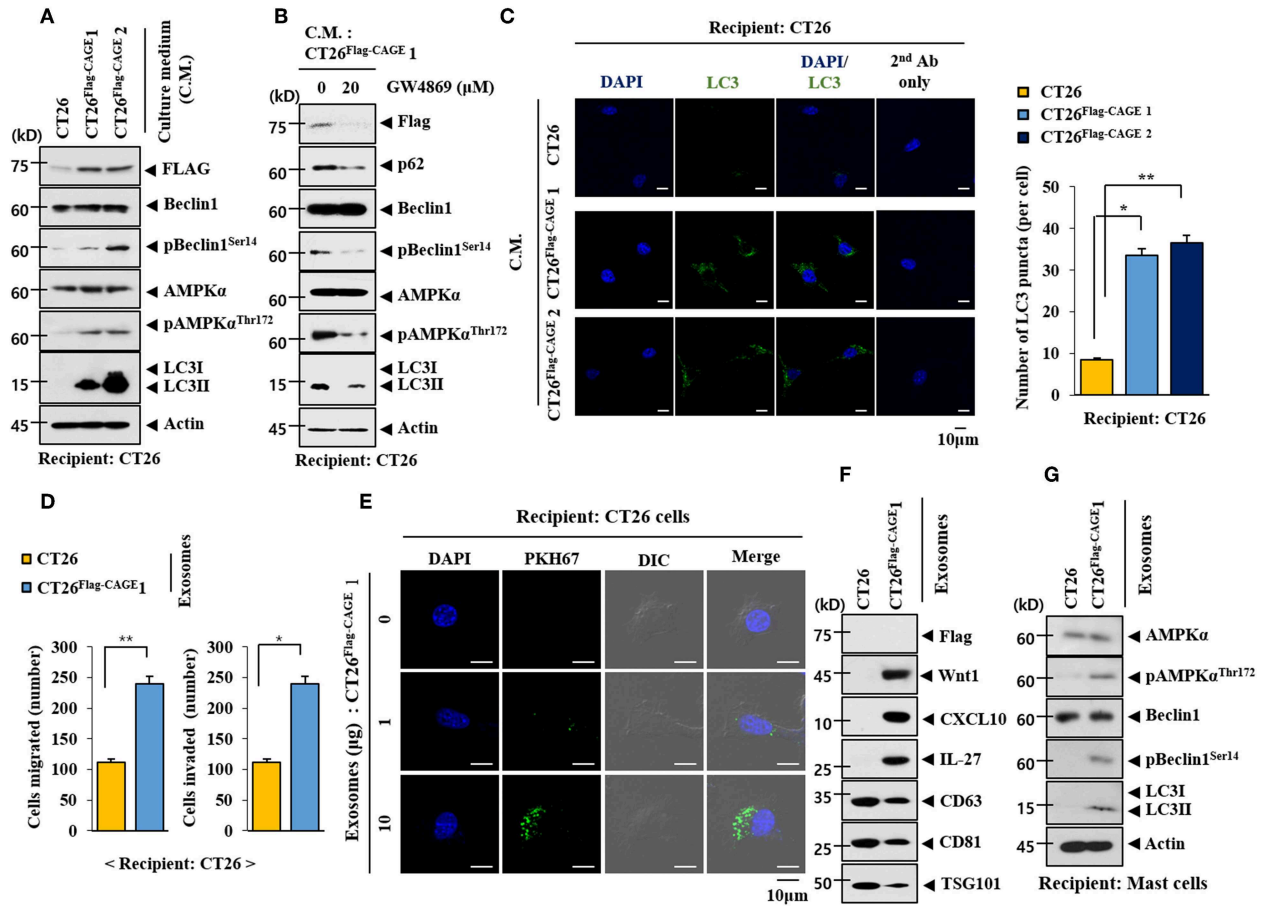

FIGURE 10 | Exosomes of CT26$^{Flag-CAGE}$1 cells increase autophagic flux. **(A)** Culture medium of the indicated cancer cells was added to CT26 cells for 24 h, followed by immunoblot. **(B)** CT26$^{Flag-CAGE}$1 cells were treated without or with GW4869 (10 μM) for 24 h. Culture medium was then added to CT26 cells for 24 h, followed by immunoblot. **(C)** Same as A except that LC3 puncta expression was determined. *$p < 0.05$; **$p < 0.005$. **(D)** Exosomes (10 μg) from the indicated cancer cells were added to CT26 cells for 24 h, followed by invasion and migration potential assays. *$p < 0.05$; **$p < 0.005$. **(E)** Exosomes (10 μg) from CT26$^{Flag-CAGE}$1 cells were labeled with PKH67 and added to CT26 for 24 h. Cells were visualized under a confocal laser scanning microscope. **(F)** Exosomes (10 μg) from the indicated cancer cells were subjected to immunoblot. **(G)** Exosomes (10 μg) from the indicated cancer cells were added to lung mast cells for 24 h, followed by immunoblot.

lysates from CT26 cells that received exosomes from the CT26$^{Flag-CAGE}$1 cells displayed increased FcεRIβ expression, and interactions of FcεRIβ with SOCS1 and Lyn (**Figure 12B**) compared to the tumor tissue lysates of CT26 cells that received CT26 exosomes. Immunohistochemical staining confirmed the immunoblot results (**Supplementary Figure 4**). The CT26 tumor that received exosomes from the CT26$^{Flag-CAGE}$1 cells showed more activated mast cells than the CT26 tumor tissue that received CT26 exosomes (**Supplementary Figure 4**). Matrigel plug assays employing culture medium showed that Wnt1 was necessary for the angiogenic potential of the CT26$^{Flag-CAGE}$1 cells (**Supplementary Figure 5**). MiR-140-5p negatively regulated the angiogenic potential of CT26$^{Flag-CAGE}$1 cells (**Supplementary Figure 5**). This suggests that the culture medium of CT26$^{Flag-CAGE}$1 cells may promote the tumorigenic potential of CT26 cells. Thus, the exosomes from the CT26$^{Flag-CAGE}$1 cells enhanced the tumorigenic potential of the CT26 cells by increasing autophagic flux and promoting cellular interactions.

MiR-140-5p-Wnt 1 Regulates Cellular Interactions

Wnt1 was necessary for the increased autophagic flux, Wnt1, β-catenin, and cyclin D1 in CT26 cells induced by the culture medium from CT26$^{Flag-CAGE}$1 cells (**Figure 13A**). Wnt1 was necessary for the increased autophagic flux and CD163 in lung macrophages activated by the culture medium from the CT26$^{Flag-CAGE}$1 cells (**Figure 13A**). Down-regulation of Wnt1 exerted a negative effect on the increased autophagic flux, and SOCS1, and COX2 in lung mast cell activated by the culture medium from the CT26$^{Flag-CAGE}$1 cells (**Figure 13A**). MiR-140-5p prevented the CT26$^{Flag-CAGE}$1 cell culture medium from increasing autophagic flux in the CT26 cells (**Figure 13B**). The overexpression of miR-140-5p

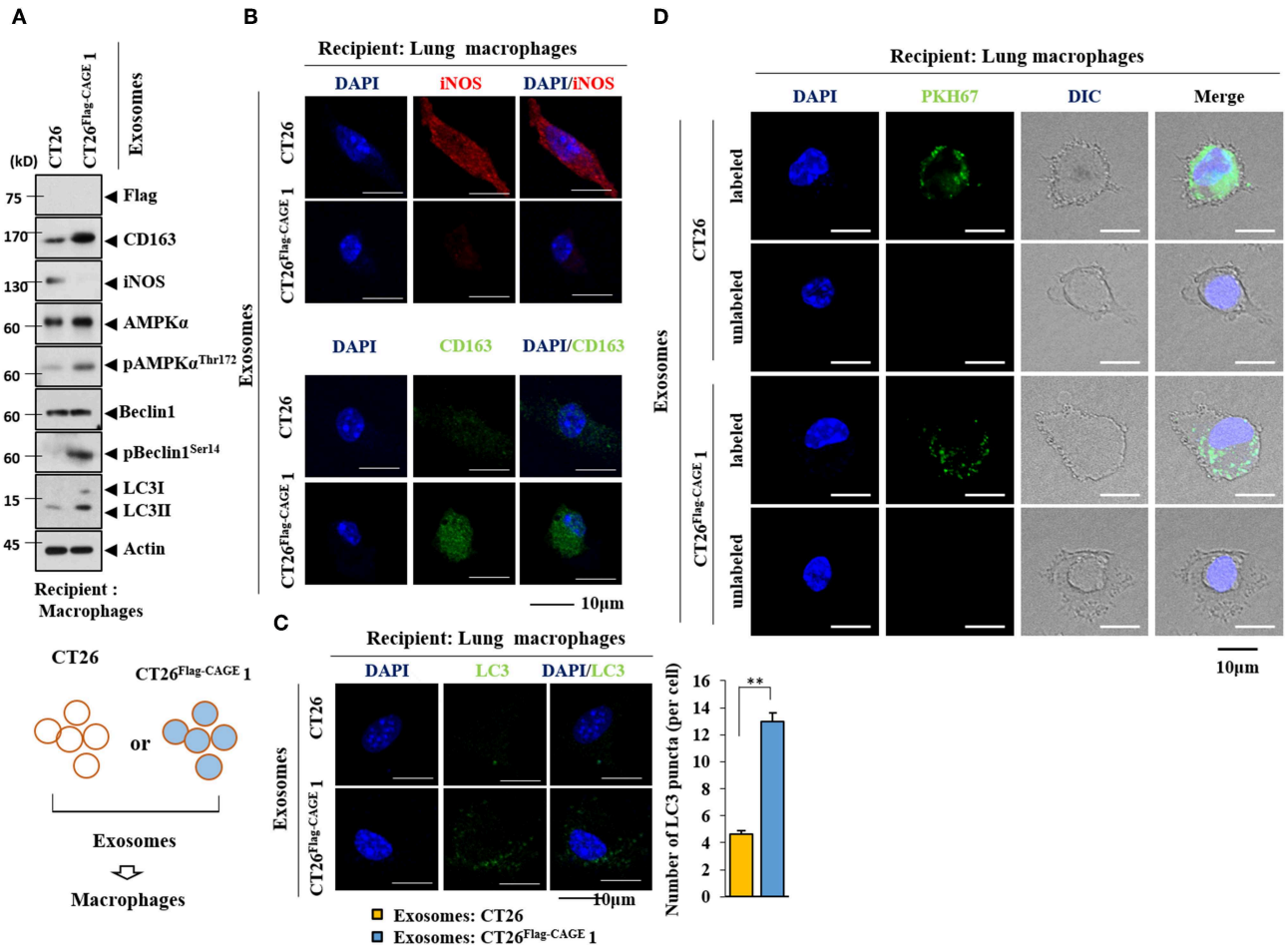

FIGURE 11 | Exosomes mediate the effect of CAGE on the activation of macrophages. **(A)** Exosomes (10 μg) from the indicated cancer cells were added to lung macrophages for 24 h, followed by immunoblot. **(B,C)** Same as A except that immunofluorescence staining employing the indicated antibodies (2 μg/ml) was performed. $^{**}p < 0.005$. **(D)** Exosomes (10 μg) from the indicated cancer cells were labeled with PKH67 and added to lung macrophages for 24 h. Cells were visualized under a confocal laser scanning microscope.

prevented culture medium from the CT26$^{Flag-CAGE}$1 cells from increasing autophagic flux and CD163 in lung macrophages (**Figure 13B**). MiR-140-5p exerted negative effects on the increased autophagic flux and hallmarks of allergic inflammation in lung mast cells activated by CT26$^{Flag-CAGE}$1 cell culture medium (**Figure 13B**). Immunofluorescence staining showed that Wnt1 was necessary for the effects of CT26$^{Flag-CAGE}$1 cell culture medium on the expression of CD163, LC3, and iNOS in macrophages (**Supplementary Figure 6A**). MiR-140-5p mimic or Wnt1 siRNA prevented the CT26$^{Flag-CAGE}$1 cell culture medium from regulating the expression of CD163, LC3, and iNOS in lung macrophages (**Supplementary Figure 6B**). Thus, the miR-140-5p-Wnt1 axis regulates cellular interactions.

Wnt1 Mediates Cellular Interactions

Because Wnt1 was present within the exosomes from the CT26$^{Flag-CAGE}$1 cells (**Figure 10D**), the direct effects of Wnt1 on cellular interactions were investigated. Recombinant Wnt1 protein (rWnt1) increased autophagic flux, Wnt1, β-catenin, and cyclin D1 in CT26 cells (**Figure 14A**). Culture medium from CT26 cells treated with rWnt1 increased autophagic flux and CD163, but decreased iNOS expression in macrophages (**Figure 14B**). Culture medium from CT26 cells treated with rWnt1 increased autophagic flux, SOCS1, and COX2 in lung mast cells (**Figure 14B**). Recombinant Wnt1 protein increased autophagic flux and CD163, but decreased the expression of iNOS in macrophages (**Figure 14C**). Culture medium from macrophages treated with rWnt1 increased autophagic flux, Wnt1, β-catenin, and cyclin D1 in CT26 cells (**Figure 14D**). Culture medium of macrophages treated with rWnt1 increased autophagic flux, SOCS1, and COX2 in mast cells (**Figure 14D**). Immunofluorescence staining showed that culture medium from CT26 cells treated with rWnt1 protein increased the expression of CD163 and LC3, but decreased the expression of iNOS in macrophages (**Supplementary Figure 7A**). Recombinant Wnt1 protein increased the expression of CD163 and LC3, but decreased the expression of iNOS in macrophages

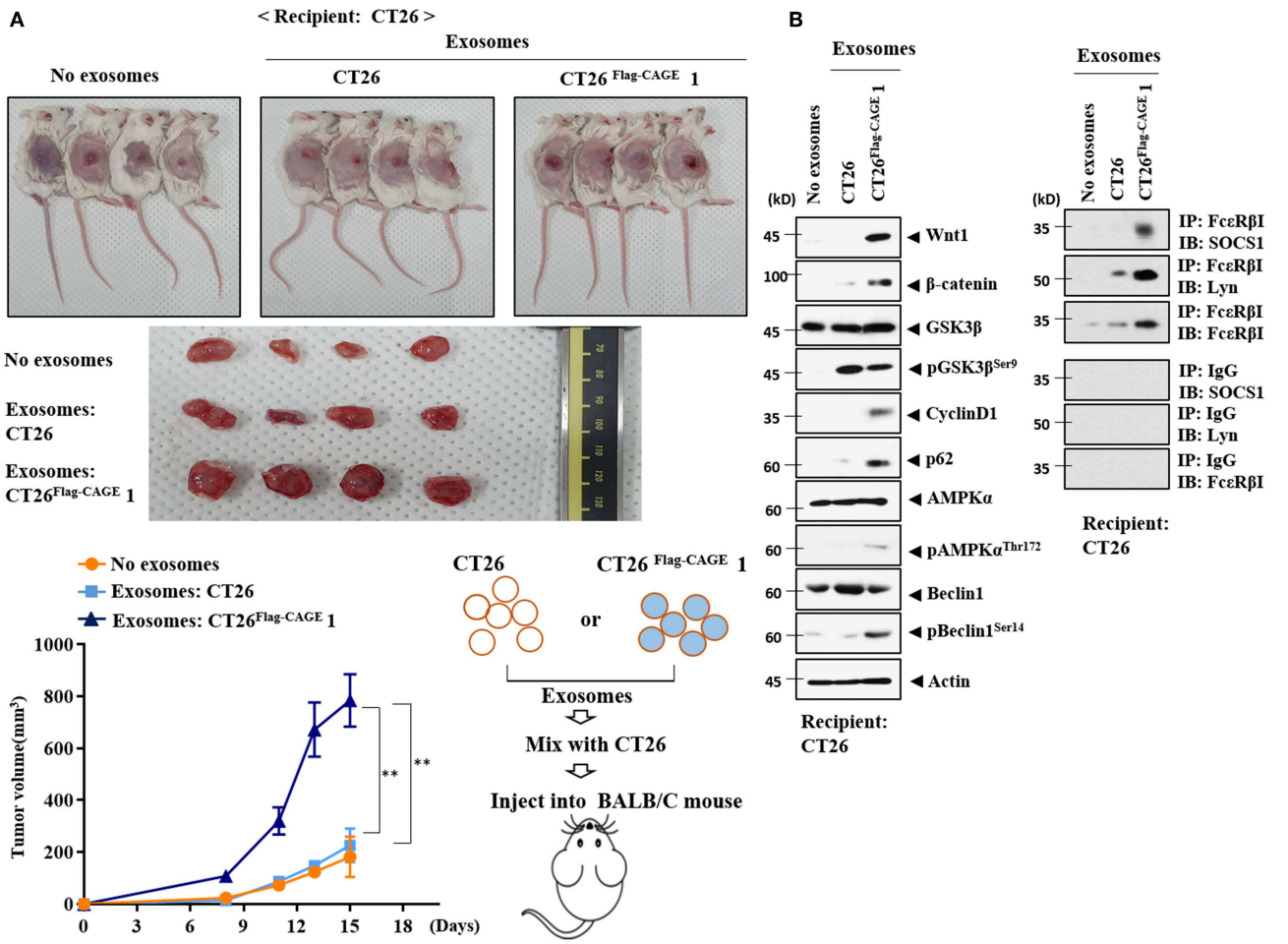

FIGURE 12 | Exosomes of CT26$^{Flag-CAGE}$1 cells enhance the tumorigenic potential of CT26 cells. **(A)** CT26 cells (1×10^6) mixed without or with the exosomes (10 μg) of the indicated cancer cells were injected into the dorsal flanks of BALB/C mice. Each value represents an average obtained from BALB/C mice of each group. Data are expressed as a mean ± S.D. Tumor volumes were measured as described. Each experimental group consisted of four BALB/C mice. **(B)** Lysates from the indicated tumor tissues were subjected to immunoblot and immunoprecipitation.

(**Supplementary Figure 7B**). This suggests that Wnt1 may directly mediate cellular interactions.

In summary, we have shown that the CAGE-miR-140-5p-Wnt1 axis regulates autophagic flux, CSC-like properties, and tumorigenic potential. By employing culture medium, we demonstrated interactions between CT26$^{Flag-CAGE}$ cells, mast cells, and macrophages. We also show that exosomes containing Wnt1 mediated these cellular interactions.

DISCUSSION

EGFR signaling is necessary for the initiation and progression of the autophagic process (29). The decreased expression of HER2 by the downregualtion of Beclin1 confers sensitivity to anti-cancer drugs such as tamoxifen (30). CAGE interacts with EGFR and HER2 in human melanoma cells (31). We, therefore, hypothesized that CAGE would regulate autophagic flux. We found that the overexpression of CAGE in CT26 cells increased autophagic flux and induced an interaction between CAGE and Beclin1. The overexpression of CAGE in CT26 cells also enhanced the formation of autophagosomes. These results suggest the role of CAGE in autophagy. The identification of the CAGE domain necessary for Beclin1 interaction will provide valuable information for the development of CAGE-targeting anti-cancer drugs.

The phosphorylation of ULK1 by AMPK, a mediator of autophagy, is essential for self-renewal and pluripotency in embryonal stem cells (32). Autophagy-related gene 7 (ATG7) induces the binding of β-catenin to the promoter sequences of OCT4 to increase the expression of OCT4, which promotes self-renewal, tumor initiation, and drug resistance (9). Inhibition of NANOG decreases autophagy in tumor cells (9). We showed that the inhibition of autophagy negatively regulated CSC-like properties. CAGE increased the expression of markers of cancer stemness, such as, SOX2, and showed an interaction with SOX2

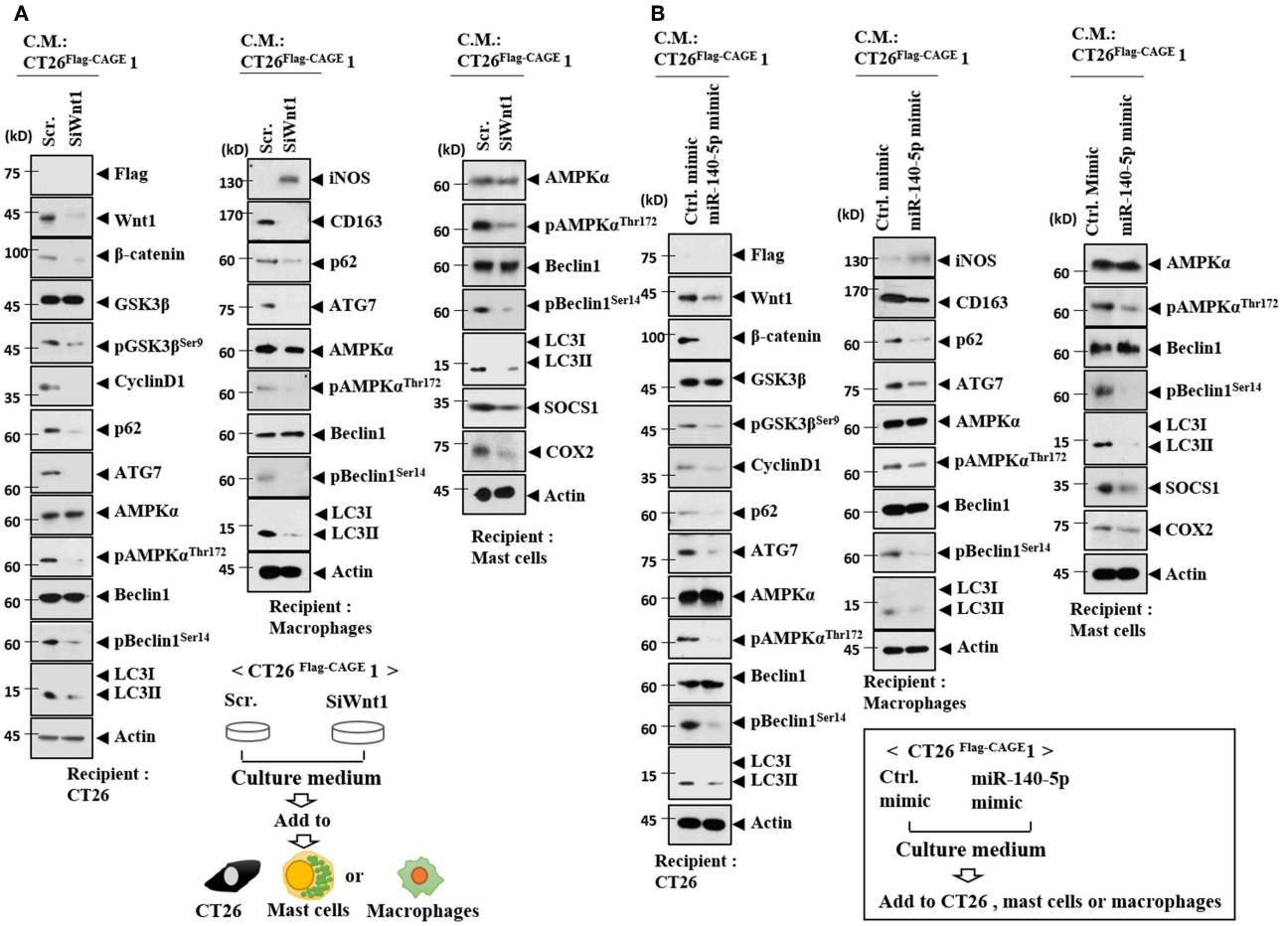

FIGURE 13 | MiR-140-5p and wnt1 regulate cellular interactions. **(A)** The indicated cancer cells were transfected with the indicated siRNA (each at 10 nM) for 48 h. Culture medium was added to CT26 cells, mast cells or lung macrophages for 24 h, followed by immunoblot. **(B)** The indicated cancer cells were transfected with the indicated mimic (each at 10 nM) for 48 h. Culture medium was added to CT26 cells or lung macrophages for 24 h, followed by immunoblot.

(33). Identification of the CAGE domain necessary for SOX2 interaction is necessary to better understand CAGE-prompted CSC-like properties. HDAC6 regulates the expression of pluripotency factors, such as POU5F1, NANOG, and SOX2, and is necessary for the pluripotency of CSCs (34). P62 binds to HDAC6 and regulates the deacetylase activity of HDAC6 (35). Thus, it is reasonable that HDAC6 may mediate the effects of CAGE on autophagic flux and tumorigenesis.

MicroRNA array analysis revealed that CAGE decreased the expression of miR-140-5p. MiR-140-5p/miR-140-3p-null mouse shows an increased number of Leydig cells in the developing XY gonad (36). This suggests a regulatory role for miR-140-5p/miR-140-3p in testis differentiation. CAGE, like other cancer/testis antigens, is assumed to be involved in testis development. ChIP assays revealed the direct regulation of miR-140-5p by CAGE. Vitamin D receptor increases the expression of miR-140-5p, which in turn inhibits MAPK signaling in osteoblasts (37). It is reasonable that CAGE may affect MAPK signaling in CT26.

MiR-140 regulates the parathyroid hormone (PTH)-related peptide (PTHrP)-HDAC4 pathway to control chondrocyte differentiation (38). HDAC4 is necessary for autophagy and vascular inflammation through its effect on FoxO3a (39). HDAC4 promotes autophagy and anti-apoptosis and confers resistance to cisplatin (13). Therefore, it would be interesting to examine the effect of CAGE on the expression of HDAC4.

We showed the binding of miR-140-5p to the 3′UTR of Wnt1. SOX2 regulates the expression of Wnt1 in lung cancer cells (40). Wnt1 promotes mammary tumorigenesis (41) and CSC activity by increasing mitochondrial mass (42). Downregualtion of Wnt1 inhibits the growth of hepatic cancer cells by inducing cellular apoptosis (43). Luciferase activity assays showed the direct regulation of Wnt1by miR-140-5p. We showed that CAGE increased the expression of Wnt1 in CT26 cells and the downregulation of Wnt1 led to decreased autophagic flux in $CT26^{Flag-CAGE}1$ cells. Wnt1-inducible signaling pathway protein-3 (WISP-3, also termed CCN6) regulates cell proliferation, differentiation, and migration

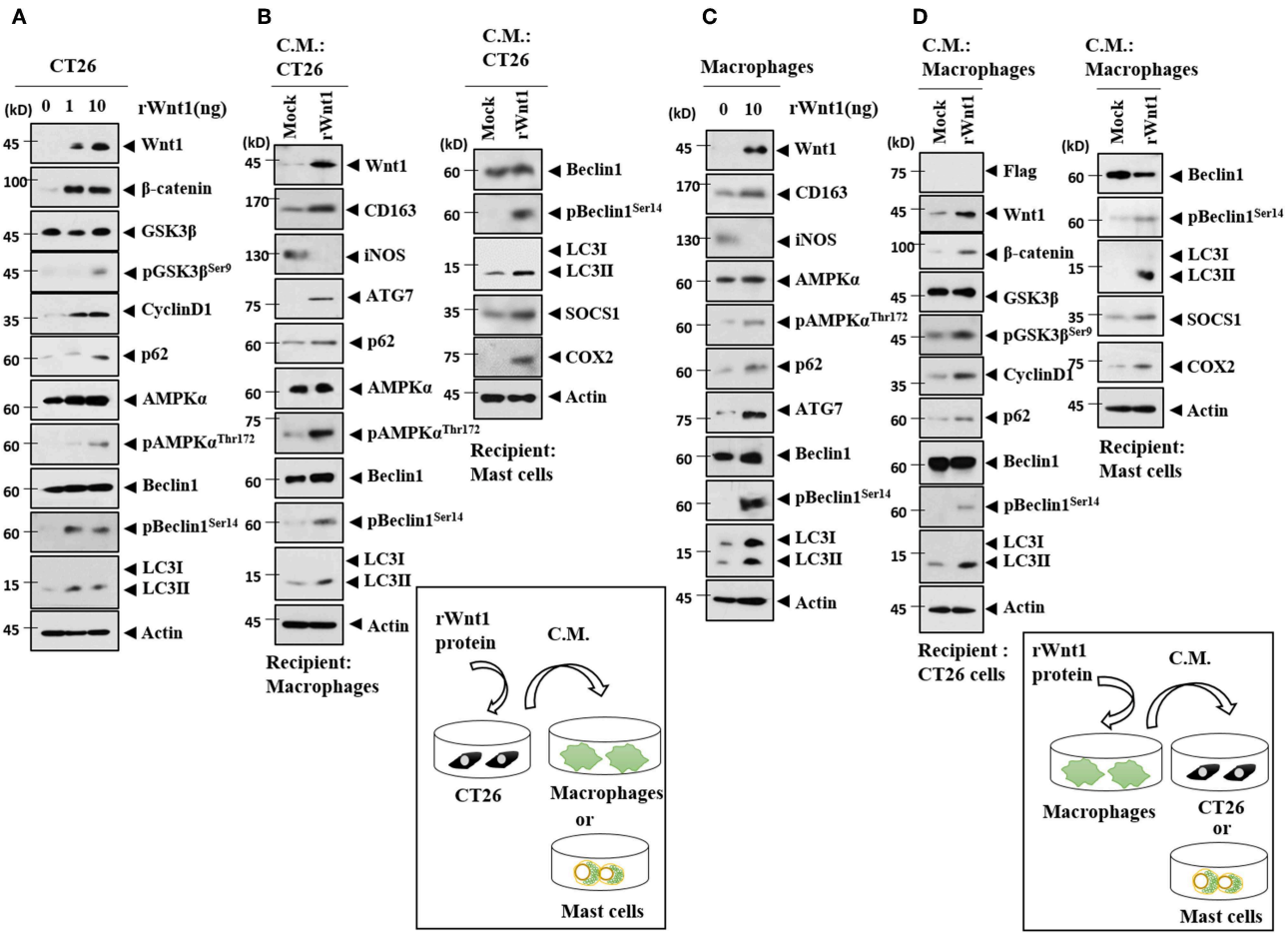

FIGURE 14 | Wnt1 mediates cellular interactions. **(A)** Recombinant wnt1 protein at the indicated concentration was added to CT26 cells for 24 h, followed by immunoblot. **(B)** CT26 cells were treated with recombinant wnt1 protein (10 ng/ml) for 24 h. Culture medium was then added to lung macrophages or lung mast cells for 24 h, followed by immunoblot. **(C)** Recombinant wnt1 protein (10 ng/ml) was added to macrophages for 24 h, followed by immunoblot. **(D)** Macrophages were treated with recombinant wnt1 protein (10 ng/ml) for 24 h. Culture medium was then added to CT26 cells for 24 h, followed by immunoblot.

(44). It is probable that CAGE may regulate the expression of WISP-3.

MiRNA array analysis revealed that CAGE decreased the expression of miR-24-3p. MiR-24-3p was predicted to be a negative regulator of TCF7. TCF7 activates the WNT/β-catenin signaling pathway (45). MiR-24-3p and miR-92-3p, decreased by CAGE, were predicted to target WNT8B. It would be interesting to examine the effects of these miRNAs on autophagic flux in $CT26^{Flag-CAGE}$ cells. MiR-342-3p, decreased by CAGE, was predicted to target RICTOR. RICTOR promotes autophagy and tumor angiogenesis (46). MiR-216-5p, decreased by CAGE, was predicted to target ATG12. The knockdown of ATG12 impairs the effects of miR-1265 inhibition on gastric cancer progression and oncogenic autophagy (47).

Tumor-stromal interaction is critical for the progression of cancers (27). The conditioned medium of human mast cells increased anti-cancer drug-resistance by reducing apoptosis in human pancreatic ductal adenocarcinoma cells (27). Pancreatic cancer cells have been shown to induce mast cell migration and the culture medium of mast cells enhanced cancer cell invasion and proliferation (48). Mast cells were reported to accumulate in colorectal cancer tissues and their density was correlated with cancer progression. The interaction between mast cells and human colon cancer cells is mediated by CCL15 or SCF (14). Mast cells promote colon cancer cell growth by inducing the production of multiple cytokines from cancer cells (14). The tumor tissue lysates of $CT26^{Flag-CAGE}1$ cells revealed the activation of mast cells based on the induction of interactions of FcεRIβ with HDAC3 and SOCS1.

The tumor tissue lysates of $CT26^{Flag-CAGE}1$ cells revealed the activated macrophages based on the higher expression of CD163 than in CT26 tumor lysates. This suggests interactions between $CT26^{Flag-CAGE}1$ cells and macrophages. Tumor-infiltrating macrophages promote glioma cell survival and stimulate angiogenesis by secreted phospho protein 1 (SPP1) (49). Alternatively activated macrophages (AAM)-derived factors utilize a JAK/STAT signaling pathway to induce ovarian cancer metastasis (50). IL-32γ has been known to

mediate the effect of multiple myeloma cells on enhancing immunosuppressive function of macrophages (51). These reports suggest cancer cell-macrophage interactions lead to tumor growth.

The inhibition of phosphoinositide kinase PIKfyve increases the secretion of exosomes containing autophagy-related proteins and induces autophagy (52). Exosomes from the gefitinib-treated PC9 cells (Exo-GF) increase autophagic activity and confer resistance to cisplatin (53). Exosomes from pigment epithelium-derived factor (PEDF)-modified adipocyte-derived stem cells (ADSCs) attenuate cerebral injury by activating autophagy and modulating apoptosis (9). Thus, exosomes mediate cellular interactions by regulating autophagy.

Exosomes from AsPC-1, an ascites-derived human pancreatic ductal carcinoma (PDAC) cell line, increase the levels of M2 macrophages markers, such as CD163 (54). Macrophages treated with AsPC-1 exosomes increased the secretion of pro-tumoral, bioactive molecules including VEGF, MCP-1, IL-6, and MMP-9 (54). Exosomes from human mast cells activate KIT-SCF signal transduction and accelerate the proliferation of human lung adenocarcinoma cells (55). Exosomes from miR181-5p-adipose-derived stem cells (ADSCs) activate autophagy by decreasing the expression of Stat3 and Bcl-2 in mouse hepatic stellate (HST-T6) cells (56). These reports suggest that exosomes may mediate cellular interactions. We found that exosomes from $CT26^{Flag-CAGE}1$ cells increased autophagic flux in mast cells and macrophages. Identification of exosomal cytokines and miRNAs that mediate these cellular interactions will facilitates the understanding of tumor-stroma interactions within the tumor microenvironment.

M2 macrophages, but not M1 macrophages, activate the Wnt signaling pathway in epithelial cells (57). IL-10 derived from macrophages activates cAMP response element-binding protein (CREB) and induces the secretion of the pro-repair WNT1-inducible signaling protein 1 (WISP-1) (58). These reports suggest that Wnt1 may mediate cellular interactions. We showed the presence of Wnt1 protein in the exosomes of $CT26^{Flag-CAGE}1$ cells. Culture medium from CT26 cells treated with recombinant Wnt1 protein increased the expression of CD163 in lung macrophages. We showed that recombinant Wnt1 protein increased the expression of CD163 in lung macrophages. Culture medium of macrophages treated with recombinant wnt1 protein increased the expression of autophagic flux in CT26 cells. It is, therefore, probable that Wnt1 mediates cellular interactions within the tumor microenvironment. Exosomal Wnt1 protein enhances the proliferation and migration of colorectal cancer by activating non-canonicial Wnt signaling (59). Identification of cytokines and miRNAs that are regulated by exosomes is necessary for understanding of exosomal-mediated cellular interactions.

CAGE acts as an upstream direct regulator of miR-140-5p and enhances autophagic flux and tumorigenic potential. MiR-140-5p negatively regulates the expression of Wnt1, autophagic flux and tumorigenic potential. Tumor tissue derived from CAGE-expressing cancer cells shows the activation of mast cells and macrophages. We presented evidence that CAGE mediated interactions between cancer cells, mast cells, and macrophages. Wnt1 is present within the exosomes of CAGE-expressing cancer cells and we show that exosomes and Wnt1 mediate these cellular interactions. Our results suggest CAGE as a target for the development of anti-cancer drugs.

DATA AVAILABILITY STATEMENT

All datasets generated for this study are included in the article/**Supplementary Material**.

ETHICS STATEMENT

The animal study was reviewed and approved by Institutional Animal Care and Use Committee (IACUC) of Kangwon National University (KIACUC-160329-2).

AUTHOR CONTRIBUTIONS

DJ, YK, and HJ designed the study and provided conceptual guidance. MY and SL performed functional assays concerning CAGE-miR-140-5p-wnt1 axis. J-EL performed experiments concerning immune EM and observations of autophagosomes. DJ wrote the manuscript.

FUNDING

This work was supported by National Research Foundation Grants (2017R1A2A2A05001029, 2017M3A9G7072417, 2018R1D1A1B07043498), a grant from the BK21 plus Program. This work was also supported by Korea Foundation for Cancer Research (KFCR-2018-002).

SUPPLEMENTARY MATERIAL

The Supplementary Material for this article can be found online at: https://www.frontiersin.org/articles/10.3389/fonc.2019.01240/full#supplementary-material

REFERENCES

1. Cho B, Lim Y, Lee DY, Park SY, Lee H, Kim WH, et al. Identification and characterization of a novel cancer/testis antigen gene CAGE. *Biochem Biophys Res Commun.* (2002) 292:715–26. doi: 10.1006/bbrc.2002.6701
2. Cho B, Lee H, Jeong S, Bang YJ, Lee HJ, Hwang KS, et al. Promoter hypomethylation of a novel cancer/testis antigen gene CAGE is correlated with its aberrant expression and is seen in premalignant stage of gastric carcinoma. *Biochem Biophys Res Commun.* (2003) 307:52–63. doi: 10.1016/S0006-291X(03)01121-5
3. Iwata T, Fujita T, Hirao N, Matsuzaki Y, Okada T, Mochimaru H, et al. Frequent immune responses to a cancer/testis antigen, CAGE, in patients with microsatellite instability-positive endometrial cancer. *Clin Cancer Res.* (2005) 11:3949–57. doi: 10.1158/1078-0432.CCR-04-1702
4. Por E, Byun HJ, Lee EJ, Lim JH, Jung SY, Park I, et al. The cancer/testis antigen CAGE with oncogenic potential stimulates cell proliferation by up-regulating cyclins D1 and E in an AP-1- and E2F-dependent

manner. *J Biol Chem.* (2010) 285:14475–85. doi: 10.1074/jbc.M109.084400
5. Kim Y, Park D, Kim H, Choi M, Lee H, Lee YS, et al. miR-200b and cancer/testis antigen CAGE form a feedback loop to regulate the invasion and tumorigenic and angiogenic responses of a cancer cell line to microtubule-targeting drugs. *J Biol Chem.* (2013) 288:36502–18. doi: 10.1074/jbc.M113.502047
6. Park D, Park H, Kim Y, Kim H, Jeoung D. HDAC3 acts as a negative regulator of angiogenesis. *BMB Rep.* (2014) 47:227–32. doi: 10.5483/BMBRep.2014.47.4.128
7. Kim Y, Park H, Park D, Lee YS, Choe J, Hahn JH, et al. Cancer/testis antigen CAGE exerts negative regulation on p53 expression through HDAC2 and confers resistance to anti-cancer drugs. *J Biol Chem.* (2010) 285:25957–68. doi: 10.1074/jbc.M109.095950
8. Chen HP, Lee YK, Huang SY, Shi PC, Hsu PC, Chang CF. Phthalate exposure promotes chemotherapeutic drug resistance in colon cancer cells. *Oncotarget.* (2018) 9:13167–80. doi: 10.18632/oncotarget.23481
9. Huang X, Ding J, Li Y, Liu W, Ji J, Wang H, et al. Exosomes derived from PEDF modified adipose-derived mesenchymal stem cells ameliorate cerebral ischemia-reperfusion injury by regulation of autophagy and apoptosis. *Exp Cell Res.* (2018) 371:269–77. doi: 10.1016/j.yexcr.2018.08.021
10. Yang Y, Yu L, Li J, Yuan YH, Wang XL, Yan SR, et al. Autophagy regulates the stemness of cervical cancer stem cells. *Biologics.* (2017) 11:71–9. doi: 10.2147/BTT.S134920
11. Klose J, Stankov MV, Kleine M, Ramackers W, Panayotova-Dimitrova D, Jager MD, et al. Inhibition of autophagic flux by salinomycin results in anti-cancer effect in hepatocellular carcinoma cells. *PLoS ONE.* 9:e95970. doi: 10.1371/journal.pone.0095970
12. Du J, Liu S, He J, Liu X, Qu Y, Yan W, et al. MicroRNA-451 regulates stemness of side population cells via PI3K/Akt/mTOR signaling pathway in multiple myeloma. *Oncotarget.* (2015) 6:14993–5007. doi: 10.18632/oncotarget.3802
13. Zhang X, Qi Z, Yin H, Yang G. Interaction between p53 and Ras signaling controls cisplatin resistance via HDAC4- and HIF-1alpha-mediated regulation of apoptosis and autophagy. *Theranostics.* (2019) 9:1096–114. doi: 10.7150/thno.29673
14. Yu Y, Blokhuis B, Derks Y, Kumari S, Garssen J, Redegeld F. Human mast cells promote colon cancer growth via bidirectional crosstalk: studies in 2D and 3D coculture models. *Oncoimmunology.* (2018) 7:e1504729. doi: 10.1080/2162402X.2018.1504729
15. Attarha S, Roy A, Westermark B, Tchougounova E. Mast cells modulate proliferation, migration and stemness of glioma cells through downregulation of GSK3beta expression and inhibition of STAT3 activation. *Cell Signal.* (2017) 37:81–92. doi: 10.1016/j.cellsig.2017.06.004
16. Walker ND, Elias M, Guiro K, Bhatia R, Greco SJ, Bryan M, et al. Exosomes from differentially activated macrophages influence dormancy or resurgence of breast cancer cells within bone marrow stroma. *Cell Death Dis.* 10:59. doi: 10.1038/s41419-019-1304-z
17. Noh K, Kim M, Kim Y, Kim H, Kim H, Byun J, et al. miR-122-SOCS1-JAK2 axis regulates allergic inflammation and allergic inflammation-promoted cellular interactions. *Oncotarget.* (2017) 8:63155–76. doi: 10.18632/oncotarget.19149
18. Yeon M, Byun J, Kim H, Kim M, Jung HS, Jeon D, et al. CAGE binds to Beclin1, regulates autophagic flux and CAGE-derived peptide confers sensitivity to anti-cancer drugs in non-small cell lung cancer cells. *Front Oncol.* (2018) 8:599. doi: 10.3389/fonc.2018.00599
19. Kim M, Park Y, Kwon Y, Kim Y, Byun J, Jeong MS, et al. MiR-135–5p-p62 axis regulates autophagic flux, tumorigenic potential, and cellular interactions mediated by extracellular vesicles during allergic inflammation. *Front Immunol.* (2019) 10:738. doi: 10.3389/fimmu.2019.00738
20. Kim Y, Kim H, Park H, Park D, Lee H, Lee YS, et al. miR-326-histone deacetylase-3 feedback loop regulates the invasion and tumorigenic and angiogenic response to anti-cancer drugs. *J Biol Chem.* (2014) 289:28019–39. doi: 10.1074/jbc.M114.578229
21. Tan Q, Joshua AM, Wang M, Bristow RG, Wouters BG, Allen CJ, et al. Up-regulation of autophagy is a mechanism of resistance to chemotherapy and can be inhibited by pantoprazole to increase drug sensitivity. *Cancer Chemother Pharmacol.* (2017) 79:959–69. doi: 10.1007/s00280-017-3298-5
22. Andrique C, Morardet L, Linares LK, Cisse MY, Merle C, Chibon F, et al. Calpain-6 controls the fate of sarcoma stem cells by promoting autophagy and preventing senescence. *JCI Insight.* (2018) 3:e121225. doi: 10.1172/jci.insight.121225
23. Chien CS, Wang ML, Chu PY, Chang YL, Liu WH, Yu CC, et al. Lin28B/Let-7 regulates expression of Oct4 and Sox2 and reprograms oral squamous cell carcinoma cells to a stem-like state. *Cancer Res.* (2015) 75:2553–65. doi: 10.1158/0008-5472.CAN-14-2215
24. Wang Z, Li B, Zhou L, Yu S, Su Z, Song J, et al. Prodigiosin inhibits Wnt/beta-catenin signaling and exerts anticancer activity in breast cancer cells. *Proc Natl Acad Sci USA.* (2016) 113:13150–5. doi: 10.1073/pnas.1616336113
25. Yan D, Avtanski D, Saxena NK, Sharma D. Leptin-induced epithelial-mesenchymal transition in breast cancer cells requires beta-catenin activation via Akt/GSK3- and MTA1/Wnt1 protein-dependent pathways. *J Biol Chem.* (2012) 287:8598–612. doi: 10.1074/jbc.M111.322800
26. Panda PK, Naik PP, Praharaj PP, Meher BR, Gupta PK, Verma RS, et al. Abrus agglutinin stimulates BMP-2-dependent differentiation through autophagic degradation of beta-catenin in colon cancer stem cells. *Mol Carcinog.* (2018) 57:664–77. doi: 10.1002/mc.22791
27. Porcelli L, Iacobazzi RM, Di Fonte R, Serrati S, Intini A, Solimando AG, et al. CAFs and TGF-beta signaling activation by mast cells contribute to resistance to gemcitabine/nabpaclitaxel in pancreatic cancer. *Cancers.* (2019) 11:E330. doi: 10.3390/cancers11030330
28. Zhou WJ, Chang KK, Wu K, Yang HL, Mei J, Xie F, et al. Rapamycin synergizes with cisplatin in antiendometrial cancer activation by improving IL-27-stimulated cytotoxicity of NK cells. *Neoplasia.* (2018) 20:69–79. doi: 10.1016/j.neo.2017.11.003
29. De Iuliis V, Marino A, Caruso M, Capodifoglio S, Flati V, Marynuk A, et al. Autophagy processes are dependent on EGF receptor signaling. *Oncotarget.* (2018) 9:30289–303. doi: 10.18632/oncotarget.25708
30. Gu Y, Chen T, Li G, Xu C, Xu Z, Zhang J, et al. Lower Beclin 1 downregulates HER2 expression to enhance tamoxifen sensitivity and predicts a favorable outcome for ER positive breast cancer. *Oncotarget.* (2017) 8:52156–77. doi: 10.18632/oncotarget.11044
31. Kim H, Kim Y, Goh H, Jeoung D. Histone Deacetylase-3/CAGE axis targets EGFR signaling and regulates the response to anti-cancer drugs. *Mol Cells.* (2016) 39:229–41. doi: 10.14348/molcells.2016.2244
32. Gong J, Gu H, Zhao L, Wang L, Liu P, Wang F, et al. Phosphorylation of ULK1 by AMPK is essential for mouse embryonic stem cell self-renewal and pluripotency. *Cell Death Dis.* (2018) 9:38. doi: 10.1038/s41419-017-0054-z
33. Kim Y, Yeon M, Jeoung D. DDX53 Regulates cancer stem cell-like properties by binding to SOX-2. *Mol Cells.* (2017) 40:322–30. doi: 10.14348/molcells.2017.0001
34. Sharif T, Martell E, Dai C, Ghassemi-Rad MS, Hanes MR, Murphy PJ, et al. HDAC6 differentially regulates autophagy in stem-like versus differentiated cancer cells. *Autophagy.* (2019) 15:686–706. doi: 10.1080/15548627.2018.1548547
35. Yan J, Seibenhener ML, Calderilla-Barbosa L, Diaz-Meco MT, Moscat J, Jiang J, et al. SQSTM1/p62 interacts with HDAC6 and regulates deacetylase activity. *PLoS ONE.* 8:e76016. doi: 10.1371/journal.pone.0076016
36. Rakoczy J, Fernandez-Valverde SL, Glazov EA, Wainwright EN, Sato T, Takada S, et al. MicroRNAs-140–5p/140–3p modulate Leydig cell numbers in the developing mouse testis. *Biol Reprod.* (2013) 88:143. doi: 10.1095/biolreprod.113.107607
37. Luo W, Liu L, Yang L, Dong Y, Liu T, Wei X, et al. The vitamin D receptor regulates miR-140–5p and targets the MAPK pathway in bone development. *Metabolism.* (2018) 85:139–50. doi: 10.1016/j.metabol.2018.03.018
38. Papaioannou G, Mirzamohammadi F, Lisse TS, Nishimori S, Wein MN, Kobayashi T. MicroRNA-140 provides robustness to the regulation of hypertrophic chondrocyte differentiation by the PTHrP-HDAC4 pathway. *J Bone Miner Res.* (2015) 30:1044–52. doi: 10.1002/jbmr.2438
39. Yang D, Xiao C, Long F, Su Z, Jia W, Qin M, et al. HDAC4 regulates vascular inflammation via activation of autophagy. *Cardiovasc Res.* (2018) 114:1016–28. doi: 10.1093/cvr/cvy051
40. Chen S, Xu Y, Chen Y, Li X, Mou W, Wang L, et al. SOX2 gene regulates the transcriptional network of oncogenes and affects

tumorigenesis of human lung cancer cells. *PLoS ONE.* (2012) 7:e36326. doi: 10.1371/journal.pone.0036326
41. Cicchini M, Chakrabarti R, Kongara S, Price S, Nahar R, Lozy F, et al. Autophagy regulator BECN1 suppresses mammary tumorigenesis driven by WNT1 activation and following parity. *Autophagy.* (2014) 10:2036–52. doi: 10.4161/auto.34398
42. Lamb R, Bonuccelli G, Ozsvari B, Peiris-Pages M, Fiorillo M, Smith DL, et al. Mitochondrial mass, a new metabolic biomarker for stem-like cancer cells: understanding WNT/FGF-driven anabolic signaling. *Oncotarget.* (2015) 6:30453–71. doi: 10.18632/oncotarget.5852
43. Zhang JG, Shi Y, Hong DF, Song M, Huang D, Wang CY, et al. MiR-148b suppresses cell proliferation and invasion in hepatocellular carcinoma by targeting WNT1/beta-catenin pathway. *Sci Rep.* (2015) 5:8087. doi: 10.1038/srep08087
44. Tzeng HE, Tang CH, Wu SH, Chen HT, Fong YC, Lu YC, et al. CCN6-mediated MMP-9 activation enhances metastatic potential of human chondrosarcoma. *Cell Death Dis.* (2018) 9:955. doi: 10.1038/s41419-018-1008-9
45. Park YL, Kim HP, Cho YW, Min DW, Cheon SK, Lim YJ, et al. Activation of WNT/beta-catenin signaling results in resistance to a dual PI3K/mTOR inhibitor in colorectal cancer cells harboring PIK3CA mutations. *Int J Cancer.* (2019) 144:389–401. doi: 10.1002/ijc.31662
46. Lamanuzzi A, Saltarella I, Desantis V, Frassanito MA, Leone P, Racanelli V, et al. Inhibition of mTOR complex 2 restrains tumor angiogenesis in multiple myeloma. *Oncotarget.* (2018) 9:20563–77. doi: 10.18632/oncotarget.25003
47. Xu Z, Li Z, Wang W, Xia Y, He Z, Li B, et al. MIR-1265 regulates cellular proliferation and apoptosis by targeting calcium binding protein 39 in gastric cancer and, thereby, impairing oncogenic autophagy. *Cancer Lett.* (2019) 449:226–36. doi: 10.1016/j.canlet.2019.02.026
48. Strouch MJ, Cheon EC, Salabat MR, Krantz SB, Gounaris E, Melstrom LG, et al. Crosstalk between mast cells and pancreatic cancer cells contributes to pancreatic tumor progression. *Clin Cancer Res.* (2010) 16:2257–65. doi: 10.1158/1078-0432.CCR-09-1230
49. Chen P, Zhao D, Li J, Liang X, Li J, Chang A, et al. Symbiotic macrophage-glioma cell interactions reveal synthetic lethality in PTEN-null glioma. *Cancer Cell.* (2019) 35:868–84 e866. doi: 10.1016/j.ccell.2019.05.003
50. Fogg KC, Olson WR, Miller JN, Khan A, Renner C, Hale I, et al. Alternatively activated macrophage-derived secretome stimulates ovarian cancer spheroid spreading through a JAK2/STAT3 pathway. *Cancer Lett.* (2019) 458:92–101. doi: 10.1016/j.canlet.2019.05.029
51. Yan H, Dong M, Liu X, Shen Q, He D, Huang X, et al. Multiple myeloma cell-derived IL-32gamma increases the immunosuppressive function of macrophages by promoting indoleamine 2,3-dioxygenase (IDO) expression. *Cancer Lett.* (2019) 446:38–48. doi: 10.1016/j.canlet.2019.01.012
52. Hessvik NP, Overbye A, Brech A, Torgersen ML, Jakobsen IS, Sandvig K, et al. PIKfyve inhibition increases exosome release and induces secretory autophagy. *Cell Mol Life Sci.* (2016) 73:4717–37. doi: 10.1007/s00018-016-2309-8
53. Li XQ, Liu JT, Fan LL, Liu Y, Cheng L, Wang F, et al. Exosomes derived from gefitinib-treated EGFR-mutant lung cancer cells alter cisplatin sensitivity via up-regulating autophagy. *Oncotarget.* (2016) 7:24585–95. doi: 10.18632/oncotarget.8358
54. Linton SS, Abraham T, Liao J, Clawson GA, Butler PJ, Fox T, et al. Tumor-promoting effects of pancreatic cancer cell exosomes on THP-1-derived macrophages. *PLoS ONE.* 13:e0206759. doi: 10.1371/journal.pone.0206759
55. Xiao H, Lasser C, Shelke GV, Wang J, Radinger M, Lunavat TR, et al. Mast cell exosomes promote lung adenocarcinoma cell proliferation - role of KIT-stem cell factor signaling. *Cell Commun Signal.* (2014) 12:64. doi: 10.1186/PREACCEPT-1817458803126023
56. Qu Y, Zhang Q, Cai X, Li F, Ma Z, Xu M, et al. Exosomes derived from miR-181–5p-modified adipose-derived mesenchymal stem cells prevent liver fibrosis via autophagy activation. *J Cell Mol Med.* (2017) 21:2491–502. doi: 10.1111/jcmm.13170
57. Cosin-Roger J, Ortiz-Masia D, Calatayud S, Hernandez C, Alvarez A, Hinojosa J, et al. M2 macrophages activate WNT signaling pathway in epithelial cells: relevance in ulcerative colitis. *PLoS ONE.* (2013) 8:e78128. doi: 10.1371/journal.pone.0078128
58. Quiros M, Nishio H, Neumann PA, Siuda D, Brazil JC, Azcutia V, et al. Macrophage-derived IL-10 mediates mucosal repair by epithelial WISP-1 signaling. *J Clin Invest.* (2017) 127:3510–20. doi: 10.1172/JCI90229
59. Wang FW, Cao CH, Han K, Zhao YX, Cai MY, Xiang ZC, et al. APC-activated long noncoding RNA inhibits colorectal carcinoma pathogenesis through reduction of exosome production. *J Clin Invest.* (2019) 129:727–43. doi: 10.1172/JCI122478

Conflict of Interest: The authors declare that the research was conducted in the absence of any commercial or financial relationships that could be construed as a potential conflict of interest.

Copyright © 2019 Yeon, Lee, Lee, Jung, Kim and Jeoung. This is an open-access article distributed under the terms of the Creative Commons Attribution License (CC BY). The use, distribution or reproduction in other forums is permitted, provided the original author(s) and the copyright owner(s) are credited and that the original publication in this journal is cited, in accordance with accepted academic practice. No use, distribution or reproduction is permitted which does not comply with these terms.

frontiers in Oncology

MINI REVIEW
published: 12 February 2020
doi: 10.3389/fonc.2020.00125

Collagen Kinase Receptors as Potential Therapeutic Targets in Metastatic Colon Cancer

Marie Lafitte, Audrey Sirvent and Serge Roche**

CRBM, CNRS, Univ. Montpellier, Montpellier, France

Colorectal cancer (CRC) is one of the leading causes of tumor-related death worldwide. While surgery can cure patients with early stage CRC, the 5-year survival rate is only 10% for patients with metastatic disease. Therefore, new anti-metastatic therapies are needed for this cancer. Metastatic spread defines the dissemination of cancer cells with tumor-initiating capacities from the primary tumor and their colonization of distinct organs, mainly the liver, for secondary tumor formation. Although the underlying mechanisms are not fully understood, components of the tumor microenvironment have gained strong interest. Among the known metastatic-promoting factors, collagens are extracellular matrix components that are deposited within the tumor, the tumor microenvironment, and at metastatic site(s), and are recognized to play essential roles during metastasis development. Here, we review recent findings on the metastatic role of the collagen receptors Discoidin Domain Receptors 1 and 2 (DDR1 and DDR2) in CRC and discuss the therapeutic value of targeting these receptor tyrosine kinases in this cancer.

Keywords: collagen, extracellular matrix, tumor microenvironment, receptor, tyrosine kinase, colorectal cancer, metastasis, targeted therapy

OPEN ACCESS

Edited by:
Erik Maquoi,
University of Liège, Belgium

Reviewed by:
Birgit Leitinger,
Imperial College London, United Kingdom
Jose Javier Bravo-Cordero,
Icahn School of Medicine at Mount Sinai, United States

****Correspondence:***
Audrey Sirvent
audrey.sirvent@crbm.cnrs.fr
Serge Roche
serge.roche@crbm.cnrs.fr

Specialty section:
This article was submitted to Molecular and Cellular Oncology, a section of the journal Frontiers in Oncology

Received: *10 December 2019*
Accepted: *23 January 2020*
Published: *12 February 2020*

Citation:
Lafitte M, Sirvent A and Roche S (2020) Collagen Kinase Receptors as Potential Therapeutic Targets in Metastatic Colon Cancer. Front. Oncol. 10:125. doi: 10.3389/fonc.2020.00125

INTRODUCTION

Colorectal cancer (CRC) remains one of the leading causes of malignancy-related death worldwide. While early-stage tumors have good prognosis, the 5-year survival rate is lower than 10% for patients with metastatic CRC (1). CRCs are heterogeneous in nature and their development is influenced by specific genetic, epigenetic, and environmental factors (1). The molecular characterization of CRC for therapeutic decision-making has identified four consensus molecular subtypes (CMS 1-4) (2). CMS1 represents hyper-mutated, microsatellite instable (MSI+) tumors with strong immune activation; CMS2 are WNT/MYC-dependent proliferative tumors; CMS3 include KRAS-mutated tumors and tumors with dysregulated metabolism; and CMS4 tumors are characterized by strong stromal infiltration. Targeted therapies have been developed for metastatic CRC (mCRC), but they display moderate clinical effects. For instance, anti-EGFR or -VEGFR agents prolong patient survival by only few months. Moreover, anti-EGFR therapies cannot be used for KRAS-mutated CRC because of systematic innate resistance (3, 4). Similarly, the results obtained with immune checkpoint inhibitors, such as anti-Programmed cell Death 1 (PD1) antibodies, are variable due to poor immune infiltration, except in the CMS1 subtype (5, 6). Currently, effective therapies for mCRC remain a challenge.

COLLAGENS IN CRC METASTASES

CRC metastatic spread is characterized by dissemination of specific tumor cell clones with tumor-initiating properties primarily to the liver due to venous drainage (7). The underlying molecular causes are not well-known, but they might not involve additional genetic alterations (7). Indeed, CRC dissemination seems to be an early event (i.e., metastatic clones have disseminated before the tumor clinical detection) (8, 9). Metastasis development may be mainly influenced by aberrant tumor cell communication with specific components of the tumor microenvironment, the immune system, the blood circulation, or the metastatic niche, in line with the seed and soil theory originally formulated by Paget (7, 10). Among the metastatic factors involved in this process, extracellular matrix (ECM) components have gained strong interest. Specifically, collagens, which are the most abundant ECM components, have been involved in tumor progression (7, 10). Aberrant collagen I, IV, and XVII protein levels in CRC samples have been associated with worse prognosis and metastasis development (11, 12). Collagens are produced by cancer-associated fibroblasts (CAF), tumor-associated macrophages (TAM) and tumor cells, and are deposited within or around the tumor or at the metastatic niche, mostly via cancer exosomes, and TAMs (13, 14). Collagen deposition induces tumor stiffness, resulting in enhanced tumor growth, reduced immune infiltration, and metastatic colonization (12, 15). Besides their type, the level of collagen architecture (i.e., polymerization, fiber alignment, and distribution) also might influence metastatic progression. Mounting evidences indicate that dense and aligned collagen fibers favor cancer cell invasion (16, 17). Enzymatic remodeling of collagen polymers also is involved in this malignant process. Specifically, well-known collagen modifiers expressed by tumor or stromal cells, such as metalloproteases, collagenases and lysine oxidases, influence collagen architecture by promoting cross-linkage and stabilization of insoluble collagen deposited in tumor tissues, thus enabling CRC progression (11, 12, 18). Mechanistically, accumulation of collagen fibers induces an integrin-dependent mechanotransduction pathway that involves actin cytoskeleton contraction (19, 20). Other post-translational modifications of the collagen matrix might contribute to their metastasis-promoting effect, as recently evidenced for Peptidyl Arginine Deaminase 4 (PAD4) (21). Specifically, PAD packed in tumor-derived exosomes increases the stiffness of collagen fibers deposited in the liver pre-metastatic niche, through conversion of arginine residues into citrullin residues. Stiffened collagen matrix increases the adhesion of CRC cells at the metastatic site, promoting mesenchymal to epithelial transition, and enabling liver metastasis growth.

THE COLLAGEN RECEPTORS DDR1 AND DDR2

The many different collagen entities detected in the tumor microenvironment suggest the existence of complex, not-yet fully characterized mechanisms that influence tumor progression. For instance, it was suggested that integrins mediate tumor signaling induced by highly cross-linked collagen fibers (22), while the tumor-promoting effects of soluble fibrillar collagens are independent from integrin engagement (23). This tumor-promoting activity might be mediated by a poorly characterized class of collagen receptors called Discoidin Domain Receptors (DDR) (24, 25). DDRs include DDR1 and DDR2 and belong to the receptor tyrosine kinase family (RTK) (24, 25). They are evolutionarily conserved, but they are distinct from the other RTKs due to their capacity to bind to ECM components (26, 27). DDR1 and DDR2 share highly conserved sequences and a similar modular structure (i.e., extracellular domain with binding affinities to collagens, short transmembrane domain, and large cytoplasmic tail containing a kinase domain), but they differ in collagen binding, tissue expression, and signaling. Indeed, DDR1 is activated by most collagen types, including I and IV, which is abundant in the basement membrane. Conversely, DDR2 is only activated by fibrillary collagens, specifically collagen I, III, and X (24, 25). DDR1 is preferentially expressed in epithelial tissues, whereas DDR2 is expressed in mesenchymal tissues (24, 25). Unlike other RTKs, DDR activation kinetic is slow (detected after 1 h of collagen stimulation), but sustained over time (more than 1 day). Although the underlying mechanism is not fully understood, it has been proposed that collagen induces the lateral association of DDR1 dimers (i.e., receptor clustering) and phosphorylation between dimers (28–30). Whether DDR2 is activated through a similar mechanism remains unclear (30). Indeed, it was reported that DDR2 activation can be mediated by Src-induced phosphorylation of its activation loop (31, 32). DDRs act as a cellular sensor of the ECM microenvironment and can cross-talk with several transmembrane receptors, such as Notch, TGF-β and adhesive receptors, and influence their signaling activity upon collagen deposition (23, 33). In physiological conditions, DDRs regulate cell polarity, adhesion, migration, and proliferation. Knock-out mice showed that DDR1 has a role in mouse mammary gland development, specifically in stromal-epithelial interaction during ductal morphogenesis (34), and that DDR2 acts as an ECM sensor to modulate cell proliferation, required for bone formation (35). However, it is not known whether DDRs have a role in intestinal epithelium development and homeostasis.

DDR1 IN CRC METASTASES

DDR1 oncogenic role in human cancers was first highlighted by global phospho-tyrosine profiling in lung cancer (36). Since then, many evidences of an important DDR1 tumor-promoting role in metastasis development have been reported, although this activity may depend on the tumor type and the collagen microenvironment nature. For instance, DDR1 has been involved in the collective migration of squamous cell carcinoma (37) and breast tumor cells (38), metastatic reactivation in breast cancer (23), homing and colonization of lung and bones (23, 39), and peritoneal metastases from gastric carcinoma (40).

Moreover, in lung cancer, KRAS mutations induce DDR1 expression to sustain tumorigenesis (40). We and others (41, 42) recently showed that DDR1 promotes CRC cell invasion and metastatic behavior in nude mice, and that its overexpression potentiates these properties. DDR1 also regulates invasiveness of patient-derived cell lines from mCRC and circulating CRC cells, which are at the origin of metastasis development (42). These studies also suggest that DDR1 acts at different steps of CRC liver metastasis formation (**Figure 1**). First, *in vitro* evidence support DDR1 role in local invasion by primary tumor cells and in the invasive properties of disseminated CRC cells, which is essential for metastasis formation. DDR1 activity may then promote CRC cell homing in the liver upon collagen deposition (**Figure 1**). Finally, DDR1 inhibition displays anti-tumor activity in mice that have already developed DDR1-dependent metastatic nodules, revealing an additional important DDR1 role in metastatic growth (42). Consistently, DDR1 expression level is associated with shorter overall survival in patients with mCRC, and DDR1 phosphorylation is strongly increased in the corresponding metastatic lesions (42, 43). Interestingly, DDR1 upregulation is an independent marker of poor prognosis in patients with stage IV CRC, and is not correlated with any CMS subtype (42). How DDR1 oncogenic activity is induced in human cancer is not clear, because DDR1 is not frequently mutated. DDR1 upregulation has been linked to oncogenic activation, such as KRAS mutations (44), a collagen-dependent amplification loop mechanism, and epigenetic mechanisms. Although all these mechanisms may contribute to DDR1 aberrant expression in CRC, a miRNA-dependent epigenetic mechanism was recently documented in this cancer (41, 45).

Several kinase-dependent and kinase-independent mechanisms by which DDR1 promotes metastatic progression have been reported, depending on the tumor type and/or the stage of metastasis development. For instance, DDR1 activates, via a kinase-independent mechanism, Tuba and CDC42 to induce early proteolysis-based invasion of breast tumor cells (38). By interacting with the tetraspanin TM4SF1, DDR1 recruits PKC alpha to activate JAK2, leading to STAT3 activation for metastatic reactivation (23). Conversely, bladder tumor cells colonize airway smooth muscle cells, a rich source of collagen III in lung, via a DDR1 kinase-dependent mechanism, leading to STAT3 transcriptional activation (46). Similarly, DDR1 kinase activity is required for K-RAS-driven lung cancer and Notch tumor signaling (44). In CRC, we established the central role of DDR1 kinase activity in metastatic progression, as indicated by the loss of such function upon introduction of a kinase-inactive mutation or pharmacological

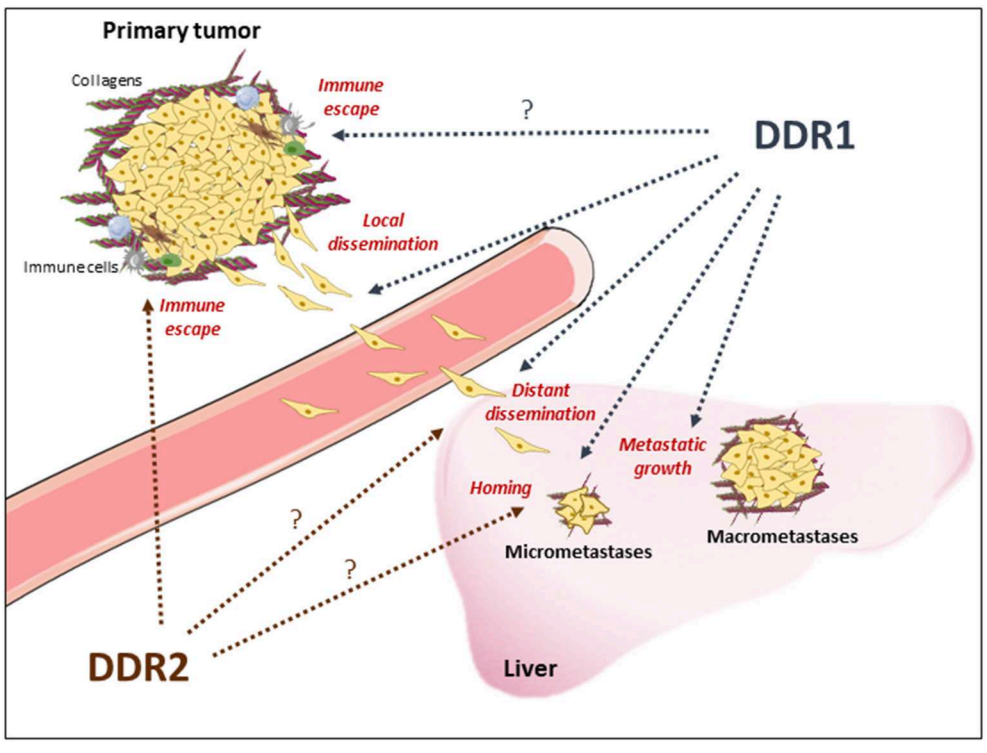

FIGURE 1 | Proposed DDR1 and DDR2 functions during metastasis development of CRC. DDR1 and DDR2 activation upon collagen deposition may promote local CRC cell invasion from the primary tumor, through invadosomes formation and epithelial cell migration, and immune evasion enabling cell dissemination; CRC cells lending at the metastatic site for CRC cells survival; metastatic reactivation (micrometastases) and development (macrometastases). Note that DDRs functions reported in other tumor-types and to be confirmed in CRC are indicated with a question-mark. Immune cells and collagens deposition around the tumor or at the metastatic niche are indicated.

inhibition (42). By phospho-proteomic analysis of tyrosine phosphorylation, we then revealed that DDR1 acts through a Wnt/β-catenin-dependent and RAS-independent mechanism. Specifically, we identified two unsuspected DDR1 substrates involved in this oncogenic process: the signaling protein Breakpoint Cluster Region (BCR) and the pseudo-kinase PEAK1 of the Pragmin family (42, 47). Mechanistically, DDR1 phosphorylation of BCR on tyrosine 177 alleviates a negative regulatory loop on β-catenin signaling to sustain its oncogenic activity, resulting in the induction of genes that are important for tumor cell dissemination and metastasis development, such as *MYC, CYCD1,* and *LGR5* (42, 48). Although not investigated in this study, DDR1 may also induce PEAK1 invasive activity (49, 50), possibly via a YAP1-dependent mechanism, as recently suggested (51). As nuclear YAP1 can form a β-catenin transcription complex that is essential for the transformation and survival of β-catenin-driven cancer (52), we propose that DDR1 supports metastatic development in a collagen-rich environment via a BCR- and PEAK1-dependent mechanism.

DDR2 IN CRC METASTASES

The first evidence of DDR2 oncogenic role in human cancer came from its alteration in squamous lung cancer (53). Afterwards, DDR2 was found to be upregulated in many epithelial malignancies, including breast (54) and ovarian tumors (55), and plays a major role in epithelial to mesenchyme transition (EMT) and metastasis development (54, 55). Mechanistically, DDR2 activity stabilizes the transcription factor and EMT inducer SNA1 (54). DDR2 upregulation in the stroma also may participate in this malignant process by promoting tumor stiffness through integrin-mediated mechanotransduction in CAFs and by promoting stromal-breast cancer cell interaction for metastatic colonization (56–58). Interestingly, these DDR2 oncogenic activities require a Src-dependent kinase activation mechanism (54). In CRC, evidence for similar DDR2 tumor-promoting functions is lacking. Nevertheless, a recent report suggested that epithelial DDR2 could participate in metastatic progression (**Figure 1**). Specifically, in a small cohort of patients with CRC, DDR2 level in tumors was associated with high frequency of peritoneal dissemination and poor prognosis (59). It is unclear whether stromal DDR2 has a similar metastatic role in CRC as in breast tumors. A mouse study suggested that stromal DDR2 deficiency predisposes the hepatic tissue to CRC metastases (60) by fostering trans-differentiation of hepatic stellate cells into myo-fibroblasts for metastatic niche development (60). Whether a similar mechanism operates in human CRC is unknown. Finally, an *in vivo* functional genomic study using isogenic mouse cancer models to identify genes the inhibition of which potentiates the response to anti-PD1 immunotherapy showed that tumor DDR2 is an essential regulator of MSI+ CRC cell immune evasion (**Figure 1**) (61). Whether DDR2 has a similar role in microsatellite-stable CRC cells remains to be tested. Similarly, it was suggested that DDR1 promotes breast tumor growth by suppressing the anti-tumor immunity (62). How exactly and in which circumstances DDR1 and DDR2 may regulate human tumor evasion, particularly in CRC, deserve further investigation.

TABLE 1 | Anti-tumor activity of DDRs inhibitors/antibodies in CRC.

	molecule	IC_{50} DDR1 (nM)	IC_{50} DDR2 (nM)	Biological effects in CRC	References
Multi-kinase inhibitor	Dasatinib (BMS-354825)	0.5	1.4	Enhances the anti-tumor response of anti-PD1 in a CRC mouse model	(61, 63)
	Imatinib (STI571)	337	675	Inhibits CRC cell growth and stromal-induced growth stimulation	(63, 64)
	Nilotinib (AMN107)	43	55	Inhibits CRC cells invasion and metastatic development in nude mice	(42, 63)
	Ponatinib (AP24534)	9	9	Inhibits CRC cell migration Inhibits CRC tumor growth in nude mice	(65, 66)
	Bafetinib (INNO-406)	n/a	220	n/a	(67)
	Sitravatinib (MGCD516)	29	0,5	n/a	(68)
DDRs kinase inhibitor	Compound 1	10	234	n/a	(69)
	Compound 2	21	76	n/a	(69)
	Compound 4	279	162	n/a	(69)
	WRG-28	–	230	n/a	(70)
	DDR1-IN-1	105	413	Inhibits CRC cells growth	(71)
	DDR1-IN-2	47	143	Inhibits CRC cells growth	(71)
	7rh	6,8	101,4	n/a	(72)
	7rj	7	93,6	n/a	(72)
DDR1 antibody	T4H11-DM4 antibody	n/a	–	Inhibits CRC tumor growth in nude mice	(43)
	mAb 3E3	n/a	–	n/a	(73)
	Neutralizing DDR1 antibody	n/a	–	n/a	(62)

TARGETING DDR TUMOR ACTIVITY IN METASTATIC CRC

All these results suggest that DDR1 and possibly DDR2 are attractive therapeutic targets in mCRC. DDR inhibition could reduce metastasis dissemination or reactivation, and prevent disease relapse (**Figure 1**). This therapeutic strategy may be particularly relevant for tumors that disseminate at an early stage, as recently suggested for CRC. Moreover, DDR inhibition could reduce metastatic growth, thus facilitating metastatic nodule resection, and also sensitize "cold" tumors to immune checkpoint-based therapies. The fact that DDR1 expression level is not restricted to any specific CMS subclass and that its tumor-promoting function is KRAS mutation-independent suggests that DDR1 inhibitors could be active in all CRC subtypes, including CMS3 tumors for which the therapeutic options are limited. As DDR1 tumor-promoting function in CRC requires its kinase activity, small DDR1 kinase inhibitors might be of therapeutic value. Interestingly, chemical proteomic profiling of several clinical TK inhibitors, including those targeting oncogenic Src or ABL activities, identified DDRs as additional major targets. For instance, DDR1 and DDR2 are inhibited by the anti-leukemic agents nilotinib, bosutinib, and dasatinib (IC_{50} in the nM range) (**Table 1**) (67, 74, 75). This important observation suggests that DDR inhibition may contribute to the clinical effects of these compounds, and that these inhibitors could be used to target DDR-dependent tumors, including mCRC. We validated this second hypothesis in a preclinical model by showing a strong anti-metastatic activity of nilotinib in DDR1-dependent mCRC cells (42). The major DDR1 role in this response was demonstrated by the lack of nilotinib activity in CRC cells that express a kinase-dead DDR1 mutant. Similarly, targeting DDR2 activity with dasatinib enhanced the tumor response to anti-PD1 immunotherapy in a CRC mouse model (**Table 1**) (61). Overall, these results predict that these anti-leukemic agents have also an anti-CRC effect. They could be combined with immune checkpoint inhibitors, particularly in tumors with high DDR level/activity. More recently, several ATP-site inhibitors have been developed to specifically inhibit DDR1 and/or DDR2 activity, and they display significant anti-tumor activities in several cancer models, including CRC cells (**Table 1**) (69, 71, 76). As these receptors can also signal through kinase-independent mechanisms, non-kinase inhibitors have been developed to target these tumor-promoting activities. For instance, anti-DDR1 antibodies can interfere with DDR1 binding to collagens, by sterically blocking the extracellular association of DDR1 subunits (**Table 1**) (73). Similarly, a neutralizing antibody against DDR1 inhibits breast tumor growth in a mouse model by suppressing the anti-tumor immunity (62). Due to DDR1 aberrant expression in CRC, an anti-DDR1 antibody-drug conjugate was recently developed for CRC treatment. This agent displayed significant anti-tumor activity in a preclinical model of CRC, without overt toxicity in control animals (**Table 1**) (43). Finally, small-molecule allosteric inhibitors of DDR2 extracellular domain inhibit the tumor–microenvironment interaction and breast tumor invasion (70). Whether such inhibitor displays similar anti-invasive effect in CRC was not reported.

CONCLUSION AND FUTURE DIRECTIONS

Since their discovery more than 20 years ago, the DDR1 and DDR2 collagen receptors are considered critical regulators of cancer invasion. Specifically, they may promote important cancer functions in collagen-rich microenvironments (i.e., cell survival, invasion, cancer stem cell traits, and immune evasion) that are required for mCRC development. As a result, these receptors are becoming attractive therapeutic targets in CRC (77). However, many important questions remain to be addressed to better understand their roles in CRC and to successfully develop anti-metastatic therapies targeting DDR signaling. First, it will be important to clarify DDR1 and DDR2 respective roles in CRC, specifically in the stromal and tumor compartments. Moreover, as development pathways are often reactivated in cancer, it would be important to address their physiological roles in intestinal homeostasis and regeneration. Due to the complexity of DDR signaling, any kinase-independent function in CRC should be explored because it could have important therapeutic consequence. Similarly, much research is needed to describe the largely unknown DDR1 and DDR2 kinase regulation, and its deregulation in CRC. Although DDR1 upregulation and aberrant tumor collagen deposition are obvious mechanisms, additional mechanisms may be expected. How DDRs induce cancer signaling is another critical question, although we established an important connection between DDR1 signaling and the β-catenin pathway (42). Last, but not least, recent reports uncovered unsuspected DDR roles in CRC immune evasion (61, 62). How these receptors contribute to this cancer hallmark is a basic and clinical question because DDR signaling inhibition could define a therapeutic strategy to reduce metastatic development and sensitize CRC to immune checkpoint inhibitors.

AUTHOR CONTRIBUTIONS

SR drafted the first version of the manuscript. ML and AS contributed towards the figure and the table. All authors have critically reviewed and approved the manuscript.

FUNDING

This work was supported by the Association pour la Recherché contre le Cancer ARC, Montpellier SIRIC Grant ≪INCa-DGOS-Inserm 6045≫, CNRS, and the University of Montpellier. ML was supported by the Fondation pour la Recherche Médicale (FRM) and the Fondation de France. SR is an INSERM investigator.

REFERENCES

1. Brenner H, Kloor M, Pox CP. Colorectal cancer. *Lancet Lond Engl.* (2014) 383:1490–502. doi: 10.1016/S0140-6736(13)61649-9
2. Guinney J, Dienstmann R, Wang X, de Reyniès A, Schlicker A, Soneson C, et al. The consensus molecular subtypes of colorectal cancer. *Nat Med.* (2015) 21:1350–6. doi: 10.1038/nm.3967
3. Lièvre A, Laurent-Puig P. Genetics: predictive value of KRAS mutations in chemoresistant CRC. *Nat Rev Clin Oncol.* (2009) 6:306–7. doi: 10.1038/nrclinonc.2009.69
4. Pohl M, Schmiegel W. Therapeutic strategies in diseases of the digestive tract - 2015 and beyond targeted therapies in colon cancer today and tomorrow. *Dig Dis Basel Switz.* (2016) 34:574–9. doi: 10.1159/000445267
5. Le DT, Durham JN, Smith KN, Wang H, Bartlett BR, Aulakh LK, et al. Mismatch repair deficiency predicts response of solid tumors to PD-1 blockade. *Science.* (2017) 357:409–13. doi: 10.1126/science.aan6733
6. Ciardiello D, Vitiello PP, Cardone C, Martini G, Troiani T, Martinelli E, et al. Immunotherapy of colorectal cancer: challenges for therapeutic efficacy. *Cancer Treat Rev.* (2019) 76:22–32. doi: 10.1016/j.ctrv.2019.04.003
7. Vanharanta S, Massagué J. Origins of metastatic traits. *Cancer Cell.* (2013) 24:410–21. doi: 10.1016/j.ccr.2013.09.007
8. Alves JM, Prado-López S, Cameselle-Teijeiro JM, Posada D. Rapid evolution and biogeographic spread in a colorectal cancer. *Nat. Commun.* (2019) 10:5139. doi: 10.1038/s41467-019-12926-8
9. Hu Z, Ding J, Ma Z, Sun R, Seoane JA, Scott Shaffer J, et al. Quantitative evidence for early metastatic seeding in colorectal cancer. *Nat Genet.* (2019) 51:1113–22. doi: 10.1038/s41588-019-0423-x
10. Hanahan D, Weinberg RA. Hallmarks of cancer: the next generation. *Cell.* (2011) 144:646–74. doi: 10.1016/j.cell.2011.02.013
11. Wei B, Zhou X, Liang C, Zheng X, Lei P, Fang J, et al. Human colorectal cancer progression correlates with LOX-induced ECM stiffening. *Int J Biol Sci.* (2017) 13:1450–7. doi: 10.7150/ijbs.21230
12. Xu S, Xu H, Wang W, Li S, Li H, Li T, et al. The role of collagen in cancer: from bench to bedside. *J Transl Med.* (2019) 17:309. doi: 10.1186/s12967-019-2058-1
13. Afik R, Zigmond E, Vugman M, Klepfish M, Shimshoni E, Pasmanik-Chor M, et al. Tumor macrophages are pivotal constructors of tumor collagenous matrix. *J Exp Med.* (2016) 213:2315–31. doi: 10.1084/jem.20151193
14. Lafitte M, Lecointre C, Roche S. Roles of exosomes in metastatic colorectal cancer. *Am J Physiol Cell Physiol.* (2019) 317:C869–80. doi: 10.1152/ajpcell.00218.2019
15. Brauchle E, Kasper J, Daum R, Schierbaum N, Falch C, Kirschniak A, et al. Biomechanical and biomolecular characterization of extracellular matrix structures in human colon carcinomas. *Matrix Biol. J. Int. Soc. Matrix Biol.* (2018) 68–69:180–93. doi: 10.1016/j.matbio.2018.03.016
16. Friedl P, Wolf K. Tumour-cell invasion and migration: diversity and escape mechanisms. *Nat Rev Cancer.* (2003) 3:362–74. doi: 10.1038/nrc1075
17. Lu P, Weaver VM, Werb Z. The extracellular matrix: a dynamic niche in cancer progression. *J Cell Biol.* (2012) 196:395–406. doi: 10.1083/jcb.201102147
18. Baker A-M, Bird D, Lang G, Cox TR, Erler JT. Lysyl oxidase enzymatic function increases stiffness to drive colorectal cancer progression through FAK. *Oncogene.* (2013) 32:1863–8. doi: 10.1038/onc.2012.202
19. Paszek MJ, Zahir N, Johnson KR, Lakins JN, Rozenberg GI, Gefen A, et al. Tensional homeostasis and the malignant phenotype. *Cancer Cell.* (2005) 8:241–54. doi: 10.1016/j.ccr.2005.08.010
20. Levental KR, Yu H, Kass L, Lakins JN, Egeblad M, Erler JT, et al. Matrix crosslinking forces tumor progression by enhancing integrin signaling. *Cell.* (2009) 139:891–906. doi: 10.1016/j.cell.2009.10.027
21. Yuzhalin AE, Gordon-Weeks AN, Tognoli ML, Jones K, Markelc B, Konietzny R, et al. Colorectal cancer liver metastatic growth depends on PAD4-driven citrullination of the extracellular matrix. *Nat Commun.* (2018) 9:4783. doi: 10.1038/s41467-018-07306-7
22. Hamidi H, Ivaska J. Every step of the way: integrins in cancer progression and metastasis. *Nat Rev Cancer.* (2018) 18:533–48. doi: 10.1038/s41568-018-0038-z
23. Gao H, Chakraborty G, Zhang Z, Akalay I, Gadiya M, Gao Y, et al. Multi-organ site metastatic reactivation mediated by non-canonical discoidin domain receptor 1 signaling. *Cell.* (2016) 166:47–62. doi: 10.1016/j.cell.2016.06.009
24. Valiathan RR, Marco M, Leitinger B, Kleer CG, Fridman R. Discoidin domain receptor tyrosine kinases: new players in cancer progression. *Cancer Metastasis Rev.* (2012) 31:295–321. doi: 10.1007/s10555-012-9346-z
25. Leitinger B. Discoidin domain receptor functions in physiological and pathological conditions. *Int Rev Cell Mol Biol.* (2014) 310:39–87. doi: 10.1016/B978-0-12-800180-6.00002-5
26. Shrivastava A, Radziejewski C, Campbell E, Kovac L, McGlynn M, Ryan TE, et al. An orphan receptor tyrosine kinase family whose members serve as nonintegrin collagen receptors. *Mol Cell.* (1997) 1:25–34. doi: 10.1016/S1097-2765(00)80004-0
27. Vogel W, Gish GD, Alves F, Pawson T. The discoidin domain receptor tyrosine kinases are activated by collagen. *Mol Cell.* (1997) 1:13–23. doi: 10.1016/S1097-2765(00)80003-9
28. Coelho NM, Arora PD, van Putten S, Boo S, Petrovic P, Lin AX, et al. Discoidin domain receptor 1 mediates myosin-dependent collagen contraction. *Cell Rep.* (2017) 18:1774–90. doi: 10.1016/j.celrep.2017.01.061
29. Juskaite V, Corcoran DS, Leitinger B. Collagen induces activation of DDR1 through lateral dimer association and phosphorylation between dimers. *eLife.* (2017) 6:e25716. doi: 10.7554/eLife.25716.023
30. Yeung DA, Shanker N, Sohail A, Weiss BA, Wang C, Wellmerling J, et al. Clustering, spatial distribution, and phosphorylation of discoidin domain receptors 1 and 2 in response to soluble collagen I. *J Mol Biol.* (2019) 431:368–90. doi: 10.1016/j.jmb.2018.11.015
31. Ikeda K, Wang L-H, Torres R, Zhao H, Olaso E, Eng FJ, et al. Discoidin domain receptor 2 interacts with Src and Shc following its activation by type I collagen. *J Biol Chem.* (2002) 277:19206–12. doi: 10.1074/jbc.M201078200
32. Yang K, Kim JH, Kim HJ, Park I-S, Kim IY, Yang B-S. Tyrosine 740 phosphorylation of discoidin domain receptor 2 by Src stimulates intramolecular autophosphorylation and Shc signaling complex formation. *J Biol Chem.* (2005) 280:39058–66. doi: 10.1074/jbc.M506921200
33. Vogel W, Brakebusch C, Fässler R, Alves F, Ruggiero F, Pawson T. Discoidin domain receptor 1 is activated independently of beta(1) integrin. *J Biol Chem.* (2000) 275:5779–84. doi: 10.1074/jbc.275.8.5779
34. Vogel WF, Aszódi A, Alves F, Pawson T. Discoidin domain receptor 1 tyrosine kinase has an essential role in mammary gland development. *Mol Cell Biol.* (2001) 21:2906–17. doi: 10.1128/MCB.21.8.2906-2917.2001
35. Labrador JP, Azcoitia V, Tuckermann J, Lin C, Olaso E, Mañes S, et al. The collagen receptor DDR2 regulates proliferation and its elimination leads to dwarfism. *EMBO Rep.* (2001) 2:446–52. doi: 10.1093/embo-reports/kve094
36. Rikova K, Guo A, Zeng Q, Possemato A, Yu J, Haack H, et al. Global survey of phosphotyrosine signaling identifies oncogenic kinases in lung cancer. *Cell.* (2007) 131:1190–203. doi: 10.1016/j.cell.2007.11.025
37. Hidalgo-Carcedo C, Hooper S, Chaudhry SI, Williamson P, Harrington K, Leitinger B, et al. Collective cell migration requires suppression of actomyosin at cell-cell contacts mediated by DDR1 and the cell polarity regulators Par3 and Par6. *Nat Cell Biol.* (2011) 13:49–58. doi: 10.1038/ncb2133
38. Juin A, Di Martino J, Leitinger B, Henriet E, Gary A-S, Paysan L, et al. Discoidin domain receptor 1 controls linear invadosome formation via a Cdc42-Tuba pathway. *J Cell Biol.* (2014) 207:517–33. doi: 10.1083/jcb.201404079
39. Valencia K, Ormazábal C, Zandueta C, Luis-Ravelo D, Antón I, Pajares MJ, et al. Inhibition of collagen receptor discoidin domain receptor-1 (DDR1) reduces cell survival, homing, and colonization in lung cancer bone metastasis. *Clin Cancer Res.* (2012) 18:969–80. doi: 10.1158/1078-0432.CCR-11-1686
40. Jin H, Ham I-H, Oh HJ, Bae CA, Lee D, Kim Y-B, et al. Inhibition of discoidin domain receptor 1 prevents stroma-induced peritoneal

metastasis in gastric carcinoma. *Mol Cancer Res MCR.* (2018) 16:1590–600. doi: 10.1158/1541-7786.MCR-17-0710
41. Hu Y, Liu J, Jiang B, Chen J, Fu Z, Bai F, et al. MiR-199a-5p loss up-regulated DDR1 aggravated colorectal cancer by activating epithelial-to-mesenchymal transition related signaling. *Dig Dis Sci.* (2014) 59:2163–72. doi: 10.1007/s10620-014-3136-0
42. Jeitany M, Leroy C, Tosti P, Lafitte M, Guet JL, Simon V, et al. Inhibition of DDR1-BCR signalling by nilotinib as a new therapeutic strategy for metastatic colorectal cancer. *EMBO Mol Med.* (2018) 10:e7918. doi: 10.15252/emmm.201707918
43. Tao Y, Wang R, Lai Q, Wu M, Wang Y, Jiang X, et al. Targeting of DDR1 with antibody-drug conjugates has antitumor effects in a mouse model of colon carcinoma. *Mol Oncol.* (2019) 13:1855–73. doi: 10.1002/1878-0261.12520
44. Ambrogio C, Gómez-López G, Falcone M, Vidal A, Nadal E, Crosetto N, et al. Combined inhibition of DDR1 and Notch signaling is a therapeutic strategy for KRAS-driven lung adenocarcinoma. *Nat Med.* (2016) 22:270–7. doi: 10.1038/nm.4041
45. Chen L-Y, Zhi Z, Wang L, Zhao Y-Y, Deng M, Liu Y-H, et al. NSD2 circular RNA promotes metastasis of colorectal cancer by targeting miR-199b-5p-mediated DDR1 and JAG1 signalling. *J Pathol.* (2019) 248:103–15. doi: 10.1002/path.5238
46. Lee Y-C, Kurtova AV, Xiao J, Nikolos F, Hayashi K, Tramel Z, et al. Collagen-rich airway smooth muscle cells are a metastatic niche for tumor colonization in the lung. *Nat Commun.* (2019) 10:2131. doi: 10.1038/s41467-019-09878-4
47. Roche S, Lecointre C, Simon V, Labesse G. SHEDding light on the role of Pragmin pseudo-kinases in cancer. *Am J Cancer Res.* (2019) 9:449–54.
48. Ress A, Moelling K. Bcr is a negative regulator of the Wnt signalling pathway. *EMBO Rep.* (2005) 6:1095–100. doi: 10.1038/sj.embor.7400536
49. Wang Y, Kelber JA, Tran Cao HS, Cantin GT, Lin R, Wang W, et al. Pseudopodium-enriched atypical kinase 1 regulates the cytoskeleton and cancer progression [corrected]. *Proc Natl Acad Sci USA.* (2010) 107:10920–5. doi: 10.1073/pnas.0914776107
50. Huang L, Wen C, Yang X, Lou Q, Wang X, Che J, et al. PEAK1, acting as a tumor promoter in colorectal cancer, is regulated by the EGFR/KRas signaling axis and miR-181d. *Cell Death Dis.* (2018) 9:271. doi: 10.1038/s41419-018-0320-8
51. Strnadel J, Choi S, Fujimura K, Wang H, Zhang W, Wyse M, et al. eIF5A-PEAK1 signaling regulates YAP1/TAZ protein expression and pancreatic cancer cell growth. *Cancer Res.* (2017) 77:1997–2007. doi: 10.1158/0008-5472.CAN-16-2594
52. Rosenbluh J, Nijhawan D, Cox AG, Li X, Neal JT, Schafer EJ, et al. β-Catenin-driven cancers require a YAP1 transcriptional complex for survival and tumorigenesis. *Cell.* (2012) 151:1457–73. doi: 10.1016/j.cell.2012.11.026
53. Hammerman PS, Sos ML, Ramos AH, Xu C, Dutt A, Zhou W, et al. Mutations in the DDR2 kinase gene identify a novel therapeutic target in squamous cell lung cancer. *Cancer Discov.* (2011) 1:78–89. doi: 10.1158/2159-8274.CD-11-0005
54. Zhang K, Corsa CA, Ponik SM, Prior JL, Piwnica-Worms D, Eliceiri KW, et al. The collagen receptor discoidin domain receptor 2 stabilizes SNAIL1 to facilitate breast cancer metastasis. *Nat Cell Biol.* (2013) 15:677–87. doi: 10.1038/ncb2743
55. Grither WR, Divine LM, Meller EH, Wilke DJ, Desai RA, Loza AJ, et al. TWIST1 induces expression of discoidin domain receptor 2 to promote ovarian cancer metastasis. *Oncogene.* (2018) 37:1714–29. doi: 10.1038/s41388-017-0043-9
56. Corsa CAS, Brenot A, Grither WR, Van Hove S, Loza AJ, Zhang K, et al. The action of discoidin domain receptor 2 in basal tumor cells and stromal cancer-associated fibroblasts is critical for breast cancer metastasis. *Cell Rep.* (2016) 15:2510–23. doi: 10.1016/j.celrep.2016.05.033
57. Gonzalez ME, Martin EE, Anwar T, Arellano-Garcia C, Medhora N, Lama A, et al. Mesenchymal stem cell-induced DDR2 mediates stromal-breast cancer interactions and metastasis growth. *Cell Rep.* (2017) 18:1215–28. doi: 10.1016/j.celrep.2016.12.079
58. Bayer SV, Grither WR, Brenot A, Hwang PY, Barcus CE, Ernst M, et al. DDR2 controls breast tumor stiffness and metastasis by regulating integrin mediated mechanotransduction in CAFs. *eLife.* (2019) 8:e45508. doi: 10.7554/eLife.45508.023
59. Sasaki S, Ueda M, Iguchi T, Kaneko M, Nakayama H, Watanabe T, et al. DDR2 expression is associated with a high frequency of peritoneal dissemination and poor prognosis in colorectal cancer. *Anticancer Res.* (2017) 37:2587–91. doi: 10.21873/anticanres.11603
60. Badiola I, Olaso E, Crende O, Friedman SL, Vidal-Vanaclocha F. Discoidin domain receptor 2 deficiency predisposes hepatic tissue to colon carcinoma metastasis. *Gut.* (2012) 61:1465–72. doi: 10.1136/gutjnl-2011-300810
61. Tu MM, Lee FYF, Jones RT, Kimball AK, Saravia E, Graziano RF, et al. Targeting DDR2 enhances tumor response to anti-PD-1 immunotherapy. *Sci. Adv.* (2019) 5:eaav2437. doi: 10.1126/sciadv.aav2437
62. Zhong X, Zhang W, Sun T. DDR1 promotes breast tumor growth by suppressing antitumor immunity. *Oncol Rep.* (2019) 42:2844–54. doi: 10.3892/or.2019.7338
63. Day E, Waters B, Spiegel K, Alnadaf T, Manley PW, Buchdunger E, et al. Inhibition of collagen-induced discoidin domain receptor 1 and 2 activation by imatinib, nilotinib and dasatinib. *Eur J Pharmacol.* (2008) 599:44–53. doi: 10.1016/j.ejphar.2008.10.014
64. Stahtea XN, Roussidis AE, Kanakis I, Tzanakakis GN, Chalkiadakis G, Mavroudis D, et al. Imatinib inhibits colorectal cancer cell growth and suppresses stromal-induced growth stimulation, MT1-MMP expression and pro-MMP2 activation. *Int J Cancer.* (2007) 121:2808–14. doi: 10.1002/ijc.23029
65. Canning P, Tan L, Chu K, Lee SW, Gray NS, Bullock AN. Structural mechanisms determining inhibition of the collagen receptor DDR1 by selective and multi-targeted type II kinase inhibitors. *J Mol Biol.* (2014) 426:2457–70. doi: 10.1016/j.jmb.2014.04.014
66. Tan FH, Putoczki TL, Lou J, Hinde E, Hollande F, Giraud J, et al. Ponatinib inhibits multiple signaling pathways involved in STAT3 signaling and attenuates colorectal tumor growth. *Cancers.* (2018) 10:E526. doi: 10.3390/cancers10120526
67. Rix U, Remsing Rix LL, Terker AS, Fernbach NV, Hantschel O, Planyavsky M, et al. A comprehensive target selectivity survey of the BCR-ABL kinase inhibitor INNO-406 by kinase profiling and chemical proteomics in chronic myeloid leukemia cells. *Leukemia.* (2010) 24:44–50. doi: 10.1038/leu.2009.228
68. Patwardhan PP, Ivy KS, Musi E, de Stanchina E, Schwartz GK. Significant blockade of multiple receptor tyrosine kinases by MGCD516 (Sitravatinib), a novel small molecule inhibitor, shows potent anti-tumor activity in preclinical models of sarcoma. *Oncotarget.* (2016) 7:4093–109. doi: 10.18632/oncotarget.6547
69. Zhavoronkov A, Ivanenkov YA, Aliper A, Veselov MS, Aladinskiy VA, Aladinskaya AV, et al. Deep learning enables rapid identification of potent DDR1 kinase inhibitors. *Nat Biotechnol.* (2019) 37:1038–40. doi: 10.1038/s41587-019-0224-x
70. Grither WR, Longmore GD. Inhibition of tumor-microenvironment interaction and tumor invasion by small-molecule allosteric inhibitor of DDR2 extracellular domain. *Proc Natl Acad Sci USA.* (2018) 115:E7786–94. doi: 10.1073/pnas.1805020115
71. Kim H-G, Tan L, Weisberg EL, Liu F, Canning P, Choi HG, et al. Discovery of a potent and selective DDR1 receptor tyrosine kinase inhibitor. *ACS Chem Biol.* (2013) 8:2145–50. doi: 10.1021/cb400430t
72. Gao M, Duan L, Luo J, Zhang L, Lu X, Zhang Y, et al. Discovery and optimization of 3-(2-(Pyrazolo[1,5-a]pyrimidin-6-yl)ethynyl)benzamides as novel selective and orally bioavailable discoidin domain receptor 1 (DDR1) inhibitors. *J Med Chem.* (2013) 56:3281–95. doi: 10.1021/jm301824k
73. Carafoli F, Mayer MC, Shiraishi K, Pecheva MA, Chan LY, Nan R, et al. Structure of the discoidin domain receptor 1 extracellular region bound to an inhibitory Fab fragment reveals features important for signaling. *Struct. Lond. Engl.* (2012) 20:688–97. doi: 10.1016/j.str.2012.02.011
74. Bantscheff M, Eberhard D, Abraham Y, Bastuck S, Boesche M, Hobson S, et al. Quantitative chemical proteomics reveals mechanisms of action of clinical ABL kinase inhibitors. *Nat Biotechnol.* (2007) 25:1035–44. doi: 10.1038/nbt1328

75. Rix U, Hantschel O, Dürnberger G, Rix LLR, Planyavsky M, Fernbach NV, et al. Chemical proteomic profiles of the BCR-ABL inhibitors imatinib, nilotinib, and dasatinib reveal novel kinase and nonkinase targets. *Blood.* (2007) 110:4055–63. doi: 10.1182/blood-2007-07-102061
76. Rammal H, Saby C, Magnien K, Van-Gulick L, Garnotel R, Buache E, et al. Discoidin Domain Receptors: Potential Actors and Targets in Cancer. *Front Pharmacol.* (2016) 7:55. doi: 10.3389/fphar.2016.00055
77. Sirvent A, Lafitte M, Roche S. DDR1 inhibition as a new therapeutic strategy for colorectal cancer. *Mol Cell Oncol.* (2018) 5:e1465882. doi: 10.1080/23723556.2018.1465882

Conflict of Interest: The authors declare that the research was conducted in the absence of any commercial or financial relationships that could be construed as a potential conflict of interest.

Copyright © 2020 Lafitte, Sirvent and Roche. This is an open-access article distributed under the terms of the Creative Commons Attribution License (CC BY). The use, distribution or reproduction in other forums is permitted, provided the original author(s) and the copyright owner(s) are credited and that the original publication in this journal is cited, in accordance with accepted academic practice. No use, distribution or reproduction is permitted which does not comply with these terms.

frontiers in Oncology

MINI REVIEW
published: 15 April 2020
doi: 10.3389/fonc.2020.00519

Transmembrane Peptides as Inhibitors of Protein-Protein Interactions: An Efficient Strategy to Target Cancer Cells?

Camille Albrecht[1,2], *Aline Appert-Collin*[1,2], *Dominique Bagnard*[3,4], *Sébastien Blaise*[1,2], *Béatrice Romier-Crouzet*[1,2], *Roman G. Efremov*[5,6], *Hervé Sartelet*[1,2], *Laurent Duca*[1,2], *Pascal Maurice*[1,2] *and Amar Bennasroune*[1,2]*

[1] Université de Reims Champagne-Ardenne, Reims, France, [2] CNRS UMR 7369, Matrice Extracellulaire et Dynamique Cellulaire, MEDyC, Reims, France, [3] Université de Strasbourg, Strasbourg, France, [4] INSERM U1119 Biopathologie de la Myéline, Neuroprotection et Stratégies Thérapeutiques, Labex Medalis, Fédération de Médecine Translationnelle de Strasbourg, Strasbourg, France, [5] M. M. Shemyakin and Yu. A. Ovchinnikov Institute of Bioorganic Chemistry, Russian Academy of Sciences, Moscow, Russia, [6] Higher School of Economics, Moscow, Russia

OPEN ACCESS

Edited by:
Rafael Fridman,
Wayne State University, United States

Reviewed by:
Gunjan Agarwal,
The Ohio State University,
United States
Chris Allan McCulloch,
University of Toronto, Canada

***Correspondence:**
Amar Bennasroune
amar.bennasroune@univ-reims.fr

Specialty section:
This article was submitted to Molecular and Cellular Oncology, a section of the journal Frontiers in Oncology

Received: 14 January 2020
Accepted: 23 March 2020
Published: 15 April 2020

Citation:
Albrecht C, Appert-Collin A, Bagnard D, Blaise S, Romier-Crouzet B, Efremov RG, Sartelet H, Duca L, Maurice P and Bennasroune A (2020) Transmembrane Peptides as Inhibitors of Protein-Protein Interactions: An Efficient Strategy to Target Cancer Cells? Front. Oncol. 10:519. doi: 10.3389/fonc.2020.00519

Cellular functions are regulated by extracellular signals such as hormones, neurotransmitters, matrix ligands, and other chemical or physical stimuli. Ligand binding on its transmembrane receptor induced cell signaling and the recruitment of several interacting partners to the plasma membrane. Nowadays, it is well-established that the transmembrane domain is not only an anchor of these receptors to the membrane, but it also plays a key role in receptor dimerization and activation. Indeed, interactions between transmembrane helices are associated with specific biological activity of the proteins as cell migration, proliferation, or differentiation. Overexpression or constitutive dimerization (due notably to mutations) of these transmembrane receptors are involved in several physiopathological contexts as cancers. The transmembrane domain of tyrosine kinase receptors as ErbB family proteins (implicated in several cancers as HER2 in breast cancer) or other receptors as Neuropilins has been described these last years as a target to inhibit their dimerization/activation using several strategies. In this review, we will focus on the strategy which consists in using peptides to disturb in a specific manner the interactions between transmembrane domains and the signaling pathways (induced by ligand binding) of these receptors involved in cancer. This approach can be extended to inhibit other transmembrane protein dimerization as neuraminidase-1 (the catalytic subunit of elastin receptor complex), Discoidin Domain Receptor 1 (a tyrosine kinase receptor activated by type I collagen) or G-protein coupled receptors (GPCRs) which are involved in cancer processes.

Keywords: transmembrane peptides, protein-protein interaction, transmembrane protein dimerization inhibition, cancers, peptide delivery strategy

INTRODUCTION

Membrane proteins are defined as proteins found in cell membrane either at the surface or on intracellular organelles and represent around 30% of all eukaryotes and prokaryotes proteins. Membrane proteins are classified as transmembrane (TM) or peripheral proteins. Their membrane-spanning domains are described to be structured as β-sheets in bacteria and mitochondria or essentially as α-helices (1, 2). The TM proteins (single or multi-pass membrane proteins) are involved in several cellular processes such as cell signaling, cell-cell communication, transport, energy transduction, and activation of enzymes which induce several functions like cell proliferation, migration, and differentiation. These cellular responses are induced by external stimuli and mediated by signaling pathways activated by membrane receptors associated with a large panel of proteins constituting complex signal networks (3, 4). Their role in cellular and physiological responses, and consequently in pathologies associated with their dysfunctions, lead researchers to develop several strategies to target these membrane proteins.

Activation of membrane receptors occurs most of the time by dimerization or oligomerization of these single-pass proteins in cell membranes and cumulative data underline the role of TM/TM domain interactions during the formation of these receptor complexes (5–8). Nowadays, it is well-established that the TM domain plays a key role in receptor dimerization and activation (9). Indeed, interactions between TM helices are associated with specific biological activity of these proteins. Overexpression or constitutive dimerization (due notably to mutations) of these TM receptors are involved in several physiopathological contexts as cancers. The TM domain of receptor tyrosine kinase (RTK) as ErbB family proteins (associated with several cancers) or other receptors as Neuropilin and G-protein coupled receptors (GPCRs) has been described these last years as putative targets to inhibit their dimerization/activation using several strategies. In this review, we will focus on the history of a strategy which consists of using peptides to disturb in a specific manner the interactions between TM domains and the signaling pathways induced by ligand binding of ErbB receptors and Neuropilins. This approach can be extended to inhibit other TM protein dimerization such as neuraminidase-1 (Neu-1, the catalytic subunit of elastin receptor complex), DDR1 (Discoidin Domain Receptor 1, a RTK activated by type I collagen) and GPCRs which are involved in cancer processes.

Abbreviations: A2AR, A2A adenosine receptor; D2R, D2 dopamine receptor; DDR, Discoidin Domain Receptor; EBP, Elastin-binding protein; EDP, elastin-derived peptides; ERC, Elastin receptor complex; EGFR, Epidermal Growth Factor Receptor; GPCRs, G-protein coupled receptors; HER, Human epidermal growth factor receptor; MMP, Matrix metalloproteases; Neu-1, Neuraminidase-1; NRP1, Neuropilin; PPCA, Protective protein/cathepsin A; RTK, Receptor tyrosine kinase; TM, Transmembrane; VEGF, Vascular endothelial growth factor.

TARGET RECEPTOR TRANSMEMBRANE DOMAIN: TM PEPTIDES STRATEGY

Most of the membrane receptors involved in cancer are single pass membrane receptors including RTKs, the integrins and the cytokine receptors. From HER2/ErbB2 (10), being the origin of one of the first targeted therapy, to for example VEGFR (11), RTKs are crucial players controlling abnormal cell proliferation, migration, or tumor angiogenesis. Consistently, several approaches had been developed to block them in order to fight cancer progression. Classical strategies using small molecules or blocking function antibodies showed tremendous therapeutic effects that contributed to significant increase of patient survival or remission in many different types of cancer. However, these targeted strategies still suffer from major hurdles such as resistance or compensatory mechanisms as exemplified for EGFR inhibitors (12) adding to often severe side effects of the drugs (13). Facing the need of developing new drugs potentially addressing these challenges, conceptual studies moved from extracellular or intracellular domains of membrane receptors to explore whether the TM domain could be an alternative solution to current drug design. Indeed, TM domains contribute in the dimerization of membrane receptors and their role in multimerization to form dynamic receptor platforms ensures complex biological functions in response to the diversity of ligands. Involvement of TM domains in these processes thus defines a totally virgin territory to design new drugs which may meets the eyes for more efficient and less toxic therapeutic compounds. As the TM domains of a multitude of membrane proteins are directly involved in receptor dimerization and activation, several strategies using short hydrophobic peptides have been developed as tools to target specifically the corresponding receptor activation (**Figure 1**). This part will describe the main results concerning the targeting of several membrane proteins involved in cancers by TM hydrophobic peptides which mimic the TM segments of these receptors.

ErbB Receptor TM Domains as Targets in Cancer

Concerning receptors activated by dimerization, the case of RTKs, notably ErbB receptors, is among the more described. The ErbB family receptors include epidermal growth factor receptor (EGFR/ErbB1), ErbB2, ErbB3, and ErbB4 which are expressed ubiquitously in epithelial, mesenchymal, cardiac and neuronal cells. These receptors are associated with several cellular processes—as proliferation, survival, and angiogenesis—and are often dysregulated in cancers (14). In most cases, the binding of growth factors to the extracellular region of these receptors provokes their dimerization and their activation (14–16).

Several studies have highlighted a major role for interactions between TM domains and their importance in membrane protein structure, function and assembly. Furthermore, mutations in these TM domains are often associated with numerous pathological contexts (5–8, 17). Although it was initially thought

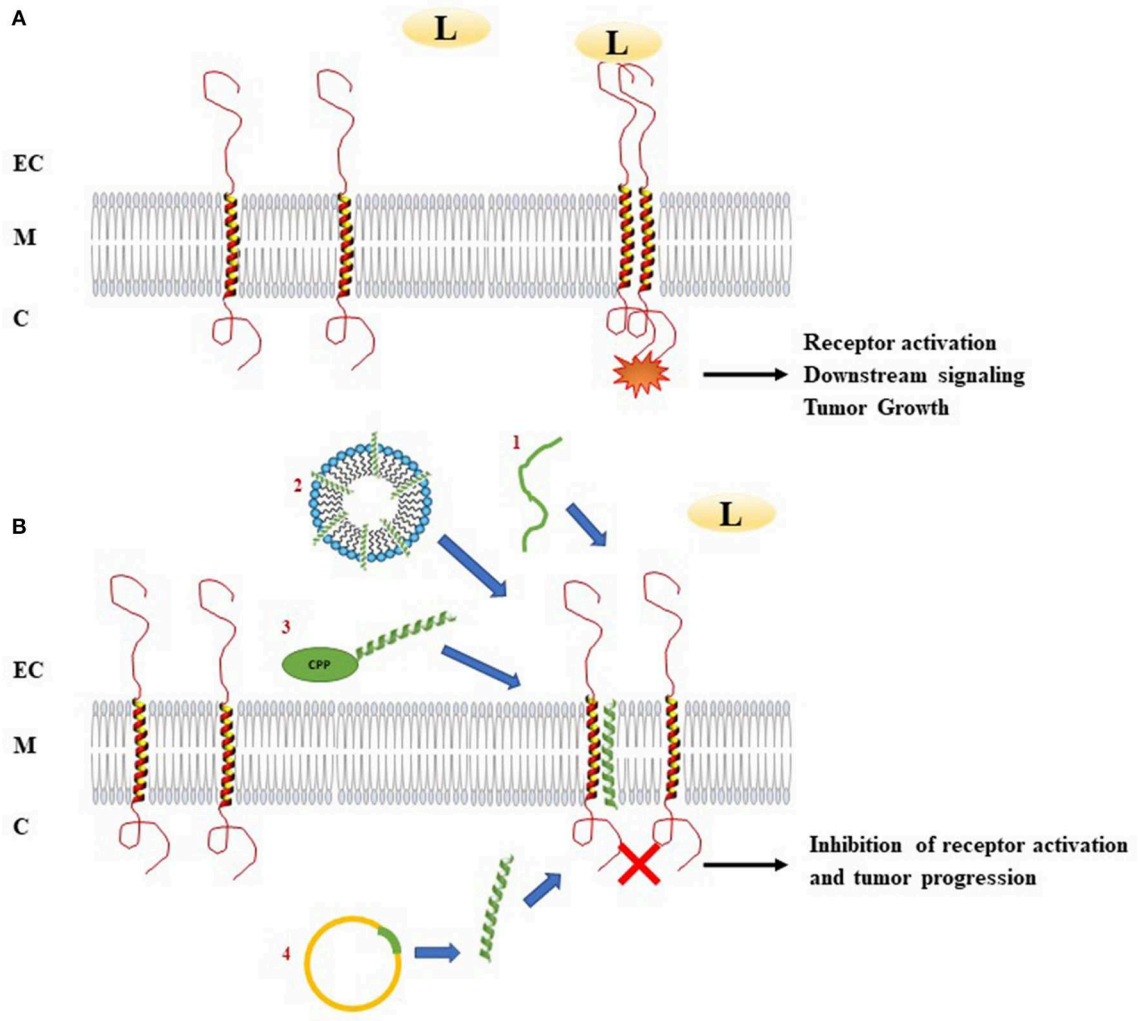

FIGURE 1 | Mechanism of action of transmembrane peptides to inhibit receptor dimerization. **(A)** Ligand binding induces dimerization and activation of receptors. This activation leads to downstream signaling activation. In the case of abnormal activation, receptor dimerization can be associated with pathological processes as tumor growth. **(B)** Introduction of TM hydrophobic peptides which mimic the TM segments of membrane proteins involved in cancers can disturb the dimerization of these receptors. In order to deliver TM peptides, several methods could be used: (1) acidity-Triggered Rational Membrane (ATRAM) peptide, (2) delivery of the peptide by detergent micelles, (3) delivery of the peptide using cell penetrating peptide, (4) plasmid encoding TM peptide. C, Cytoplasm; CPP, Cell penetrating peptide; EC, Extracellular environment; L, Ligand; M, Membrane; TM peptide, Transmembrane peptide.

that the TM domain of RTKs as ErbB receptors was a passive anchor to the membrane, it is now well-established that it plays a key role in protein dimerization. Indeed, previous studies have shown that TM domain of these proteins are able to self-assembly and induce biological activity. For instance, Val^{644} to Glu mutation within the TM domain of ErbB2/Neu is associated with an uncontrolled activation of this RTK leading to glioblastomas in rats (18). Moreover, Gardin et al. (19) showed that changing the TM domain of the insulin receptor (IR) with the highly dimerizing TM domain of glycophorin A is associated with an inhibition of insulin-induced receptor kinase activity. Other works have shown that homodimerization of EGFR/ErbB1 receptors is linked to interactions between their TM domains (20) and that TM domains of ErbB receptor family members can spontaneously homodimerize in cell membranes (21–23). Furthermore, sequence motifs have been reported to mediate TM domain interactions: the GxxxG motifs (x = any amino acid) or GxxxG-like motifs (a consensus sequence that has been extended to SmallxxxSmall sequences where small amino acids are glycine, alanine, or serine). These sequences are very frequent in TM helix and represent the core of dimerization interface (5, 24).

As interactions between TM segments occur during receptor dimerization, several studies have been carried out to evaluate if introduction in the membrane of peptides with homologous sequences—corresponding to the TM domain—could act as competitors of the dimerization and thus disturb the cancer

involved RTK activity. Lofts et al. (25) showed for the first time that expression of TM sequence of the rat neu/ErbB2 receptor could inhibit cell growth of mutant-transformed NIH3T3 cells. As this work did not include characterization of receptor activation, several subsequent studies demonstrated that TM domain-derived peptides are able to interfere with dimerization of ErbB2 receptors in whole cells. Indeed, Bennasroune et al. (26) demonstrated in human cancer cells which overexpress EGF or ErbB2 receptors that TM peptides are able to specifically inhibit the autophosphorylation and the signaling pathway of their cognate receptor. These results were obtained using two strategies: the first one consisted of using expression vectors encoding fusion TM peptides and the second one consisted of incubating cells with chemically synthesized peptides. This study was extended and confirmed by the same research group who demonstrated that in cells overexpressing chimeric IR (where the TM domain has been replaced by that of EGFR or a mutated ErbB2 domain), TM peptides can inhibit specifically the autophosphorylation and the signaling pathway of IR with the corresponding domain (27).

Thereafter, few studies using TM peptide as tools to target specifically protein dimerization have been realized *in vivo*. Concerning RTK, Arpel et al. (28) showed that small peptides interfering with the TM domain of ErbB2 inhibit breast tumor growth and metastasis when used at micromolar concentrations in a mouse model of breast cancer. Thus, even if there was a disdain toward the use of peptides as a strategy to inhibit protein-protein interaction, this technique has been extended to target other membrane proteins involved in cancers.

Neuropilin and Plexin TM Domain as Targets in Cancers

Other membrane receptors such as Neuropilins (NRP1) or Plexins are also important regulators of cancer progression through signaling pathways involving actin cytoskeleton remodeling (29). NRP1 TM domain which contributes to the dimerization of the receptor was shown mandatory to trigger Sema3A-dependent cancer cell migration (30). It turns out to be an efficient strategy to limit glioblastoma (31) or breast cancer (32) growth *in vivo*. These studies used a peptide mimicking the TM domain of NRP1 to interfere with the dimerization by direct competition for binding with the natural TM domain of the membrane receptor. To circumvent the hydrophobic nature of the peptides which may preclude their use, the decoy peptides were solubilized in micelles of Lithium Dodecyl Sulfate favoring delivery to the membrane both *in vitro* or *in vivo*. Biological or therapeutic effects were observed with low dose of the peptide (in the range of 1 μg/kg *in vivo*, three times per week after intraperitoneal injection) and showed remarkable tolerance. The same strategy of mimetic peptide was also used to target HER2 (ErB2) in the context of metastatic breast cancer as described above (28). In the same line, the interference of Plexin-A1 heterodimerization with a peptide mimicking the natural sequence of this Rho-GTPase activating receptor exhibited anti-angiogenic effects in models of brain tumors and glioblastoma cancer stem cells growth (33). More recently the same Plexin-A1 targeting peptide was shown as an efficient tool to circumvent the Sema3A molecular barrier blocking the remyelination process in the context of demyelinating diseases (34). Because TM peptides interact with intra-membrane targets, they do not have the capacity to be used to selectively reach the cancer cells expressing the target. Rather, they exert their function as small molecules by a widespread distribution in the body. However, TM domain peptides can be combined with targeting moieties attached to nanocarriers to address this point and produce drugs with a more selective action on a given cell type (35). While the development of formulations compatible with a clinical use remains to be fully achieved, the recent development in the production of TM domain peptides with pH sensitive membrane interaction is opening interesting opportunities both in term of solubility or activity. The so-called acidity-triggered rational membrane (ATRAM) peptides demonstrated preferential membrane insertion in breast cancer cells and exhibited prolonged circulating time in the blood thanks to a reversible binding to serum albumin (36).

TRANSMEMBRANE PEPTIDE STRATEGY EXTENDED TO INHIBIT OTHER TRANSMEMBRANE PROTEIN DIMERIZATION: NEU-1, DDR-1, AND GPCRs AS PUTATIVE TARGETS

The transmembrane peptide strategy can be extended to inhibit other TM protein dimerization. Even if several membrane proteins can be targeted by this approach, three examples will be described in this section: Neu-1, DDR1, and GPCRs which are involved in several cancer processes.

Neu-1 TM Domain as a Potential Target in Cancers

Elastin degradation contributes to cancer progression (37). The interaction of cancer cells with elastin-derived peptides (EDP) induces mitogenic signals and a release of elastases that enhance further elastin degradation (38). Most of the biological effects of elastin degradation and EDP rely on the catalytic activity of Neu-1 activated upon the binding of EDP on the elastin receptor complex (ERC). This membrane heterotrimeric complex is composed of the elastin-binding protein (EBP), a spliced variant of the lysosomal β-galactosidase which interacts with EDP and tropoelastin, PPCA/Cathepsin A ensuring the integrity of the complex, and Neu-1 harboring a sialidase/neuraminidase activity (39). Neu-1 is a member of the sialidase family composed also of Neu-2, Neu-3, and Neu-4 (40). These exoglycosidases, widely distributed amongst species (41), remove terminal sialic acid residues from glycoproteins, glycolipids, and oligosaccharides.

Neu-1 regulates breast cancer cell proliferation and invasion. EDP enhance invasiveness of MDA-MB-231 cells by enhancing matrix metalloproteases (MMP) 2 and 14 activities (42). Moreover, an increase of elastolysis is correlated with severity of the disease. Clinical studies show that level of EDP in serum of patients is higher in patients with large tumor size (43). Blocking Neu-1 with oseltamivir phosphate (Tamiflu®) or a

Neu-1 siRNA in mammary carcinoma cells, MCF-7, and MDA-MB-231 cell lines, inhibits cell growth (44). Additional studies also point out an inhibition of tumor neovascularization growth and metastasis under oseltamivir phosphate treatment in mouse model of breast cancer that mimics human triple-negative breast cancer (45). Furthermore, EDP induce an enhanced invasion of melanoma cells (46–48). Implication of EDP and Neu-1 in other cancer types has also been shown: Neu-1 is involved in the development of hepatocellular carcinoma (49) and ovarian cancer (50). Altogether, these data indicate that Neu-1 plays a key role in the development and the amplification of several cancers and can constitute a new target to slow down cancer progression.

Recent studies have identified two potential TM domains in the sequence of human Neu-1 protein (51). Dynamic molecular simulation studies underline that the TM domain 2 (TM2) is able to preserve a stable helical conformation and homodimerizes in membrane-mimicking environments. Further, molecular biology experiments show that Neu-1 sialidase activity is linked to its ability to homodimerize. Point mutations in the TM2 region of Neu-1 are able to inhibit homodimerization and its associated sialidase activity. Indeed, when EDP bind on EBP, two Neu-1 subunits homodimerize and generate a sialidase activity. Knowing that dimerization is required for its activity, interfering peptides targeting specifically TM2 domain of Neu-1 constitute novel key tools to selectively block Neu-1 activity and its linked biological effects in cancer.

DDR-1 TM Domain as a Potential Target in Cancers

The DDR belongs to RTKs family and consists of two members, DDR1 and DDR2. They possess an extracellular discoidin homology domain and are activated by the most abundant component of tumor extracellular matrix, native triple-helical collagen (52, 53). The expression of DDR1 in several different types of human cancer including human esophageal (54), gastric cancer (55), glioma (56), breast cancer (57), lung cancer (58), suggests a function in tumor progression. After activation by collagen, DDRs play a role in cell adhesion, proliferation, migration, invasion, and DDR1/myosin dependent extracellular matrix remodeling (59, 60).

Both DDRs have the same domain architecture containing a conserved discoidin I domain in their N-terminal extracellular part which is responsible for collagen binding, a single-span TM domain, an unusually large cytosolic juxtamembrane domain, and a C-terminal tyrosine kinase domain. After collagen binding, conformational modifications of the receptors are associated with a slow but sustained self-phosphorylation compared to other RTKs whose activation is rapid after ligand binding (52, 53). DDR1 activation induces transphosphorylation at the juxtamembrane and kinase domains of adjacent dimers. Moreover, this phosphorylation requires specific contacts within the TM domains but not in the extracellular domain (61).

One of the notable features is that in the absence of ligand, the DDRs form stable, non-covalent dimers kept in an inactivated state via N-glycosylation at highly conserved N211 residue (62–64). Contacts between extracellular domains, cytoplasmic domains, and TM regions contribute to the dimerization process. However, interaction between the extracellular and cytoplasmic regions is not critical for dimerization. Nevertheless, a mutation in the leucine zipper motif of the TM segment results in dimerization disruption highlighting the importance of TM region in ligand independent dimerization of DDR1 (63). The isolated DDR1 and DDR2 TM helices interact very robustly, as detected in a bacterial TOXCAT reporter assay (63). In fact, the comparison by a systematic study of the self-interaction potential of all RTK TM domains shows that the DDR1 and DDR2 TM domains gave the strongest signal of all RTKs in this assay (65). Activation of DDR is induced by forming lateral clusters in the presence of collagen thereby phosphorylating the DDR dimers leading to activation thanks to specific TM domain interactions. These data strengthen a key role for the DDR1 TM domain in signaling. TM domain contacts may also be necessary for DDR1 clustering, with direct receptor-receptor interactions or another membrane protein domain (61). These data suggest that TM peptides could be an adequate strategy to target the TM domain of DDR and in particular the leucine zipper motif to inhibit DDR activation and then receptor autophosphorylation at multiple residues on its tyrosine kinase intracellular domain. This inhibition could have an important role considering the involvement of these receptors in cancer progression but also in collagen processing events that contribute to fibrosis.

GPCR TM Domain as a Putative Target in Cancers

GPCRs are the largest class of membrane receptors and play crucial roles in virtually every physiological process. Over the past few decades, the idea that these seven TM helical domain receptors function as isolated monomeric receptors has been challenged by the accumulation of evidence for the formation of homo- and hetero-dimers, and higher order oligomers. Combined with x-ray structures, computational molecular modeling, and bioinformatic approaches, synthetic TM peptides targeting the TM domains of GPCRs have been shown to be powerful tools to help in identifying the dimer interface of GPCRs and to examine the functional importance of GPCR dimerization both *in vitro* and *in vivo*. For instance, receptor homodimerization and agonist-dependent signaling can be inhibited by a synthetic TM peptide targeting the TM domain VI for the β2-adrenergic (66), IV for the secretin (67), and V for the A2A adenosine (68) receptors. Interestingly, TM peptides are also able to disrupt heterodimerization. A prototypical GPCR heterodimer is the one formed by the A2A adenosine receptor (A2AR) and D2 dopamine receptor (D2R). In a recent study by Borroto-Escuela et al. (69), TM peptides corresponding to the TM domain IV and V of the A2AR were shown to block heterodimer interactions and to disrupt the allosteric effect of A2AR activation on D2R agonist binding. Thus, the use of TM peptides permitted to identify the dimer interface of GPCRs and to understand the functional role of their dimerization. As in recent years, several studies have shown the involvement of these receptors in different cancer

types, as breast and prostate cancers, using TM peptides could also be a very interesting strategy to target GPCRs in these pathologies (70).

CONCLUSION

Overall, it is now well-established that interactions between TM domains are specific and play a crucial role in many membrane receptor activations. Consequently, this observation has been exploited to develop TM peptides as specific inhibitors of dimerization/activation of several receptors involved in cancers as RTKs and Neuropilins. However, as TM peptides interact with intra-membrane receptors, they do not have the capacity to selectively target the cancer cells expressing the target. Indeed, they exert their function as small molecules by a widespread distribution in the organism. That's why the next step will be to combine TM peptides with targeting moieties attached to nanocarriers to ensure specific delivery and to produce anti-cancer drugs with a more selective action on a given cancer cell type.

AUTHOR CONTRIBUTIONS

CA, AA-C, DB, PM, and AB participated in writing the manuscript. SB, BR-C, RE, HS, and LD realized a careful reading of the manuscript (and corrections).

FUNDING

Financial support was received from CNRS, URCA, Région Champagne-Ardenne, Ligue Nationale Contre le Cancer (Projet de Recherches Interrégional), ANR (ANR-18-CE44-0017-01), Programme de Recherche Conjoint (PRC 2017 CNRS/RFBR n° PRC 1967), and RFBR (grant 18-54-15007).

REFERENCES

1. Fagerberg L, Jonasson, K, von Heijne G, Uhlen M, Berglund L. Prediction of the human membrane proteome. *Proteomics.* (2010) 10:1141–9. doi: 10.1002/pmic.200900258
2. Stevens TJ, Arkin IT, Do more complex organisms have a greater proportion of membrane proteins in their genomes? *Proteins.* (2000) 39:417–20. doi: 10.1002/(SICI)1097-0134(20000601)39:4<417::AID-PROT140>3.0.CO;2-Y
3. Wu H, Higher-order assemblies in a new paradigm of signal transduction. *Cell.* (2013) 153:287–92. doi: 10.1016/j.cell.2013.03.013
4. Moore DT, Berger BW, DeGrado WF. Protein-protein interactions in the membrane: sequence, structural, biological motifs. *Structure.* (2008) 16:991–1001. doi: 10.1016/j.str.2008.05.007
5. Matthews EE, Zoonens M, Engelman DM. Dynamic helix interactions in transmembrane signaling. *Cell.* (2006) 127:447–50. doi: 10.1016/j.cell.2006.10.016
6. Hubert P, Sawma P, Duneau JP, Khao J, Henin J, Bagnard, et al. Single-spanning transmembrane domains in cell growth and cell-cell interactions: more than meets the eye? *Cell Adh Migr.* (2010) 4:313–24. doi: 10.4161/cam.4.2.12430
7. Sawma P, Roth L, Blanchard C, Bagnard D, Cremel G, Bouveret E, et al. Evidence for new homotypic and heterotypic interactions between transmembrane helices of proteins involved in receptor tyrosine kinase and neuropilin signaling. *J Mol Biol.* (2014) 426:4099–111. doi: 10.1016/j.jmb.2014.10.007
8. Westerfield JM, Barrera FN, Membrane receptor activation mechanisms and transmembrane peptide tools to elucidate them. *J Biol Chem.* (2019) 295:1792–814. doi: 10.1074/jbc.REV119.009457
9. Ahmed S, Sami A, Xiang J. HER2-directed therapy: current treatment options for HER2-positive breast cancer. *Breast Cancer.* (2015) 22:101–16. doi: 10.1007/s12282-015-0587-x
10. Lacal PM, Graziani G, Therapeutic implication of vascular endothelial growth factor receptor-1 (VEGFR-1) targeting in cancer cells and tumor microenvironment by competitive and non-competitive inhibitors. *Pharmacol Res.* (2018) 136:97–107. doi: 10.1016/j.phrs.2018.08.023
11. Karachaliou N, Codony-Servat J, Bracht JWP, Ito M, Filipska M, Pedraz C, et al. Characterising acquired resistance to erlotinib in non-small cell lung cancer patients. *Expert Rev Respir Med.* (2019) 13:1019–28. doi: 10.1080/17476348.2019.1656068
12. Rhea IB, Oliveira GH, Cardiotoxicity of novel targeted chemotherapeutic agents. *Curr Treat Options Cardiovasc Med.* (2018) 20:53. doi: 10.1007/s11936-018-0649-4
13. Appert-Collin A, Hubert P, Cremel G, Bennasroune A. Role of ErbB receptors in cancer cell migration and invasion. *Front Pharmacol.* (2015) 6:283. doi: 10.3389/fphar.2015.00283
14. Ullrich A, Schlessinger J, Signal transduction by receptors with tyrosine kinase activity. *Cell.* (1990). 61:203–12. doi: 10.1016/0092-867490801-K
15. Tsai CJ, Nussinov R, Emerging allosteric mechanism of EGFR activation in physiological and pathological contexts. *Biophys J.* (2019) 117:5–13. doi: 10.1016/j.bpj.2019.05.021
16. Bordag N, Keller S. Alpha-helical transmembrane peptides: a "divide and conquer" approach to membrane proteins. *Chem Phys Lipids.* (2010) 163:1–26. doi: 10.1016/j.chemphyslip.2009.07.009
17. Bargmann CI, Hung MC, Weinberg RA. Multiple independent activations of the neu oncogene by a point mutation altering the transmembrane domain of p185. *Cell.* (1986) 45:649–57. doi: 10.1016/0092-867490779-8
18. Gardin A, Auzan C, Clauser E, Malherbe T, Aunis D, Cremel G, et al. Substitution of the insulin receptor transmembrane domain with that of glycophorin A inhibits insulin action. *FASEB J.* (1999) 13:1347–57. doi: 10.1096/fasebj.13.11.1347
19. Tanner KG, Kyte J. Dimerization of the extracellular domain of the receptor for epidermal growth factor containing the membrane-spanning segment in response to treatment with epidermal growth factor. *J Biol Chem.* (1999) 274:35985–90. doi: 10.1074/jbc.274.50.35985
20. Gerber D, Sal-Man N, Shai Y. Structural adaptation of the glycophorin A transmembrane homodimer to D-amino acid modifications. *J Mol Biol.* (2004) 339:243–50. doi: 10.1016/j.jmb.2004.03.004
21. Mendrola JM, Berger MB, King MC, Lemmon MA. The single transmembrane domains of ErbB receptors self-associate in cell membranes. *J Biol Chem.* (2002) 277:4704–12. doi: 10.1074/jbc.M108681200
22. Cymer F, Schneider D. A single glutamate residue controls the oligomerization, function, and stability of the aquaglyceroporin GlpF. *Biochemistry.* (2010) 49:279–86. doi: 10.1021/bi901660t
23. Russ WP, Engelman DM. The GxxxG motif: a framework for transmembrane helix-helix association. *J Mol Biol.* (2000) 296:911–9. doi: 10.1006/jmbi.1999.3489
24. Lofts FJ, Hurst HC, Sternberg MJ, Gullick WJ. Specific short transmembrane sequences can inhibit transformation by the mutant neu growth factor receptor *in vitro* and *in vivo*. *Oncogene.* (1993) 8:2813–20.
25. Bennasroune A, Fickova M, Gardin A, Dirrig-Grosch S, Aunis D, Cremel G, et al. Transmembrane peptides as inhibitors of ErbB receptor signaling. *Mol Biol Cell.* (2004) 15:3464–74. doi: 10.1091/mbc.e03-10-0753
26. Bennasroune A, Gardin A, Auzan C, Clauser E, Dirrig-Grosch S, Meira M, et al. Inhibition by transmembrane peptides of chimeric insulin receptors. *Cell Mol Life Sci.* (2005) 62:2124–31. doi: 10.1007/s00018-005-5226-9

27. Arpel A, Sawma P, Spenle C, Fritz J, Meyer L, Garnier N, et al. Transmembrane domain targeting peptide antagonizing ErbB2/Neu inhibits breast tumor growth and metastasis. *Cell Rep*. (2014) 8:1714–21. doi: 10.1016/j.celrep.2014.07.044
28. Neufeld G, Mumblat Y, Smolkin T, Toledano S, Nir-Zvi I, Ziv K, et al. The semaphorins and their receptors as modulators of tumor progression. *Drug Resist Updat*. (2016) 29:1–12. doi: 10.1016/j.drup.2016.08.001
29. Roth L, Nasarre C, Dirrig-Grosch S, Aunis D, Cremel G, Hubert P, et al. Transmembrane domain interactions control biological functions of neuropilin-1. *Mol Biol Cell*. (2008) 19:646–54. doi: 10.1091/mbc.e07-06-0625
30. Nasarre C, Roth M, Jacob L, Roth L, Koncina E, Thien A, et al. Peptide-based interference of the transmembrane domain of neuropilin-1 inhibits glioma growth *in vivo*. *Oncogene*. (2010) 29:2381–92. doi: 10.1038/onc.2010.9
31. Arpel A, Gamper C, Spenle C, Fernandez A, Jacob L, Baumlin N, et al. Inhibition of primary breast tumor growth and metastasis using a neuropilin-1 transmembrane domain interfering peptide. *Oncotarget*. (2016) 7:54723–32. doi: 10.18632/oncotarget.10101
32. Jacob L, Sawma P, Garnier N, Meyer LA, Fritz J, Hussenet T, et al. Inhibition of PlexA1-mediated brain tumor growth and tumor-associated angiogenesis using a transmembrane domain targeting peptide. *Oncotarget*. (2016) 7:57851–65. doi: 10.18632/oncotarget.11072
33. Biname F, Pham-Van LD, Spenle C, Jolivel V, Birmpili D, Meyer LA, et al. Disruption of Sema3A/Plexin-A1 inhibitory signalling in oligodendrocytes as a therapeutic strategy to promote remyelination. *EMBO Mol Med*. (2019) 11:e10378. doi: 10.15252/emmm.201910378
34. Gamper C, Spenle C, Bosca S, van der Heyden M, Erhardt M, Orend G, et al. Functionalized tobacco mosaic virus coat protein monomers and oligomers as nanocarriers for anti-cancer peptides. *Cancers*. (2019) 11:1609. doi: 10.3390/cancers11101609
35. Nguyen VP, Palanikumar L, Kennel SJ, Alves DS, Ye Y, Wall JS, et al. Mechanistic insights into the pH-dependent membrane peptide ATRAM. *J Control Release*. (2019) 298:142–153. doi: 10.1016/j.jconrel.2019.02.010
36. Duca L, Lambert E, Debret R, Rothhut B, Blanchevoye C, Delacoux F, et al. Elastin peptides activate extracellular signal-regulated kinase 1/2 via a Ras-independent mechanism requiring both p110gamma/Raf-1 and protein kinase A/B-Raf signaling in human skin fibroblasts. *Mol Pharmacol*. (2005) 67:1315–24. doi: 10.1124/mol.104.002725
37. Lapis K, Timar J. Role of elastin-matrix interactions in tumor progression. *Semin Cancer Biol*. (2002) 12:209–17. doi: 10.1016/S1044-579X00024-X
38. Hinek A, Pshezhetsky AV, von Itzstein M, Starcher B. Lysosomal sialidase (neuraminidase-1) is targeted to the cell surface in a multiprotein complex that facilitates elastic fiber assembly. *J Biol Chem*. (2006) 281:3698–710. doi: 10.1074/jbc.M508736200
39. Monti E, Bonten E, D'Azzo A, Bresciani R, Venerando B, Borsani G, et al. Sialidases in vertebrates: a family of enzymes tailored for several cell functions. *Adv Carbohydr Chem Biochem*. (2010) 64:403–79. doi: 10.1016/S0065-231864007-3
40. Giacopuzzi E, Bresciani R, Schauer R, Monti E, Borsani G. New insights on the sialidase protein family revealed by a phylogenetic analysis in metazoa. *PLoS One*. (2012) 7:e44193. doi: 10.1371/journal.pone.0044193
41. Salesse S, Odoul L, Chazee L, Garbar C, Duca L, Martiny L, et al. Elastin molecular aging promotes MDA-MB-231 breast cancer cell invasiveness. *FEBS Open Bio*. (2018) 8:1395–404. doi: 10.1002/2211-5463.12455
42. Nicoloff G, Deliiyski T, Nikolov A, Detection of serum collagen collagen type IV and elastin derived peptides in patients with breast cancers. *Diabetol Croatica*. (2010) 39:83–93.
43. Thulasiraman P, Kerr K, McAlister K, Hardisty S, Wistner A, McCullough I. Neuraminidase 1 regulates proliferation, apoptosis and the expression of Cadherins in mammary carcinoma cells. *Mol Cell Biochem*. (2019) 462:207–15. doi: 10.1007/s11010-019-03623-7
44. Haxho F, Allison S, Alghamdi F, Brodhagen L, Kuta VE, Abdulkhalek S, et al. Oseltamivir phosphate monotherapy ablates tumor neovascularization, growth, and metastasis in mouse model of human triple-negative breast adenocarcinoma. *Breast Cancer (Dove Med Press)*. (2014) 6:191–203. doi: 10.2147/BCTT.S74663
45. Pocza P, Suli-Vargha H, Darvas Z, Falus A. Locally generated VGVAPG and VAPG elastin-derived peptides amplify melanoma invasion via the galectin-3 receptor. *Int J Cancer*. (2008) 122:1972–80. doi: 10.1002/ijc.23296
46. Ntayi C, Labrousse AL, Debret R, Birembaut P, Bellon G, Antonicelli F, et al. Elastin-derived peptides upregulate matrix metalloproteinase-2-mediated melanoma cell invasion through elastin-binding protein. *J Invest Dermatol*. (2004) 122:256–65. doi: 10.1046/j.0022-202X.2004.22228.x
47. Hornebeck W, Robinet A, Duca L, Antonicelli F, Wallach J, Bellon G. The elastin connection and melanoma progression. *Anticancer Res*. (2005) 25:2617–25.
48. Hou G, Liu G, Yang Y, Li Y, Yuan S, Zhao L, et al. Neuraminidase 1 (NEU1) promotes proliferation and migration as a diagnostic and prognostic biomarker of hepatocellular carcinoma. *Oncotarget*. (2016) 7:64957–66. doi: 10.18632/oncotarget.11778
49. Ren LR, Zhang LP, Huang SY, Zhu YF, Li WJ, Fang SY, et al. Effects of sialidase NEU1 siRNA on proliferation, apoptosis, and invasion in human ovarian cancer. *Mol Cell Biochem*. (2016) 411:213–9. doi: 10.1007/s11010-015-2583-z
50. Maurice P, Baud S, Bocharova OV, Bocharov EV, Kuznetsov AS, Kawecki C, et al. New insights into molecular organization of human neuraminidase-1: transmembrane topology and dimerization ability. *Sci Rep*. (2016) 6:38363. doi: 10.1038/srep38363
51. Shrivastava A, Radziejewski C, Campbell E, Kovac L, McGlynn M, Ryan TE, et al. An orphan receptor tyrosine kinase family whose members serve as nonintegrin collagen receptors. *Mol Cell*. (1997) 1:25–34. doi: 10.1016/S1097-276580004-0
52. Vogel W, Gish GD, Alves F, Pawson T. The discoidin domain receptor tyrosine kinases are activated by collagen. *Mol Cell*. (1997) 1:13–23. doi: 10.1016/S1097-276580003-9
53. Nemoto T, Ohashi K, Akashi T, Johnson JD, Hirokawa K. Overexpression of protein tyrosine kinases in human esophageal cancer. *Pathobiology*. (1997) 65:195–203. doi: 10.1159/000164123
54. Xie R, Wang X, Qi G, Wu Z, Wei R, Li P, et al. DDR1 enhances invasion and metastasis of gastric cancer via epithelial-mesenchymal transition. *Tumour Biol*. (2016) 37:12049–59. doi: 10.1007/s13277-016-5070-6
55. Yamanaka R, Arao T, Yajima N, Tsuchiya N, Homma J, Tanaka R, et al. Identification of expressed genes characterizing long-term survival in malignant glioma patients. *Oncogene*. (2006) 25:5994–6002. doi: 10.1038/sj.onc.1209585
56. Malaguarnera R, Nicolosi ML, Sacco A, Morcavallo A, Vella V, Voci C, et al. Novel cross talk between IGF-IR and DDR1 regulates IGF-IR trafficking, signaling and biological responses. *Oncotarget*. (2015) 6:16084–105. doi: 10.18632/oncotarget.3177
57. Xiao Q, Jiang Y, Liu Q, Yue J, Liu C, Zhao X, et al. Minor type IV collagen α5 chain promotes cancer progression through discoidin domain receptor-1. *PLoS Genet*. (2015) 11:e1005249. doi: 10.1371/journal.pgen.1005249
58. Agarwal G, Smith AW, Jones B. Discoidin domain receptors: micro insights into macro assemblies. *Biochim Biophys Acta Mol Cell Res*. (2019) 1866:118496. doi: 10.1016/j.bbamcr.2019.06.010
59. Coelho NM, Wang A, McCulloch CA. Discoidin domain receptor 1 interactions with myosin motors contribute to collagen remodeling and tissue fibrosis. *Biochim Biophys Acta Mol Cell Res*. (2019) 1866:118510. doi: 10.1016/j.bbamcr.2019.07.005
60. Juskaite V, Corcoran DS, Leitinger B. Collagen induces activation of DDR1 through lateral dimer association and phosphorylation between dimers. *Elife*. (2017) 6:e25716. doi: 10.7554/eLife.25716
61. Mihai C, Chotani M, Elton TS, Agarwal G. Mapping of DDR1 distribution and oligomerization on the cell surface by FRET microscopy. *J Mol Biol*. (2009) 385:432–45. doi: 10.1016/j.jmb.2008.10.067
62. Noordeen NA, Carafoli F, Hohenester E, Horton MA, Leitinger B. A transmembrane leucine zipper is required for activation of the dimeric receptor tyrosine kinase DDR1. *J Biol Chem*. (2006) 281:22744–51. doi: 10.1074/jbc.M603233200
63. Xu H, Abe T, Liu JK, Zalivina I, Hohenester E, Leitinger B. Normal activation of discoidin domain receptor 1 mutants with disulfide cross-links, insertions, or deletions in the extracellular juxtamembrane region: mechanistic implications. *J Biol Chem*. (2014) 289:13565–74. doi: 10.1074/jbc.M113.536144
64. Finger C, Escher C, Schneider D. The single transmembrane domains of human receptor tyrosine kinases encode self-interactions. *Sci Signal*. (2009) 2:ra56. doi: 10.1126/scisignal.2000547

65. Hebert TE, Moffett S, Morello JP, Loisel TP, Bichet DG, Barret C, et al. A peptide derived from a β2-adrenergic receptor transmembrane domain inhibits both receptor dimerization and activation. *J Biol Chem.* (1996) 271:16384–92. doi: 10.1074/jbc.271.27.16384
66. Harikumar KG, Pinon DI, Miller LJ. Transmembrane segment IV contributes a functionally important interface for oligomerization of the Class II G protein-coupled secretin receptor. *J Biol Chem.* (2007) 282:30363–72. doi: 10.1074/jbc.M702325200
67. Gallo M, Navarro G, Franco R, Andreu D. A2A Receptor homodimer-disrupting sequence efficiently delivered by a protease-resistant, cyclic CPP vector. *Int J Mol Sci.* (2019) 20:4937. doi: 10.3390/ijms20194937
68. Borroto-Escuela DO, Rodriguez D, Romero-Fernandez W, Kapla J, Jaiteh M, Ranganathan A, et al. Mapping the interface of a GPCR dimer: a structural model of the A2A adenosine and D2 dopamine receptor heteromer. *Front Pharmacol.* (2018) 9:829. doi: 10.3389/fphar.2018.00829
69. Bhat RR, Yadav P, Sahay D, Bhargava DK, Creighton CJ, Yazdanfard S, et al. GPCRs profiling and identification of GPR110 as a potential new target in HER2+ breast cancer. *Breast Cancer Res Treat.* (2018) 170:279–92. doi: 10.1007/s10549-018-4751-9
70. Sawada Y, Kikugawa T, Iio H, Sakakibara I, Yoshida S, Ikedo A, et al. GPRC5A facilitates cell proliferation through cell cycle regulation and correlates with bone metastasis in prostate cancer. *Int J Cancer.* (2020) 46:1369–82. doi: 10.1002/ijc.32554

Conflict of Interest: The authors declare that the research was conducted in the absence of any commercial or financial relationships that could be construed as a potential conflict of interest.

Copyright © 2020 Albrecht, Appert-Collin, Bagnard, Blaise, Romier-Crouzet, Efremov, Sartelet, Duca, Maurice and Bennasroune. This is an open-access article distributed under the terms of the Creative Commons Attribution License (CC BY). The use, distribution or reproduction in other forums is permitted, provided the original author(s) and the copyright owner(s) are credited and that the original publication in this journal is cited, in accordance with accepted academic practice. No use, distribution or reproduction is permitted which does not comply with these terms.

frontiers in Oncology

MINI REVIEW
published: 15 April 2020
doi: 10.3389/fonc.2020.00397

Tumor Microenvironment: Extracellular Matrix Alterations Influence Tumor Progression

Sylvie Brassart-Pasco [1,2], Stéphane Brézillon [1,2], Bertrand Brassart [1,2], Laurent Ramont [1,2,3], Jean-Baptiste Oudart [1,2,3] and Jean Claude Monboisse [1,2,3]*

[1] Université de Reims Champagne Ardenne, SFR CAP-Santé (FED 4231), Laboratoire de Biochimie Médicale et Biologie Moléculaire, Reims, France, [2] CNRS UMR 7369, Matrice Extracellulaire et Dynamique Cellulaire - MEDyC, Reims, France, [3] CHU Reims, Service Biochimie-Pharmacologie-Toxicologie, Reims, France

The tumor microenvironment (TME) is composed of various cell types embedded in an altered extracellular matrix (ECM). ECM not only serves as a support for tumor cell but also regulates cell–cell or cell–matrix cross-talks. Alterations in ECM may be induced by hypoxia and acidosis, by oxygen free radicals generated by infiltrating inflammatory cells or by tumor- or stromal cell-secreted proteases. A poorer diagnosis for patients is often associated with ECM alterations. Tumor ECM proteome, also named cancer matrisome, is strongly altered, and different ECM protein signatures may be defined to serve as prognostic biomarkers. Collagen network reorganization facilitates tumor cell invasion. Proteoglycan expression and location are modified in the TME and affect cell invasion and metastatic dissemination. ECM macromolecule degradation by proteases may induce the release of angiogenic growth factors but also the release of proteoglycan-derived or ECM protein fragments, named matrikines or matricryptins. This review will focus on current knowledge and new insights in ECM alterations, degradation, and reticulation through cross-linking enzymes and on the role of ECM fragments in the control of cancer progression and their potential use as biomarkers in cancer diagnosis and prognosis.

Keywords: cancer, microenvironment, extracellular matrix, matrikines, integrins, proteases

OPEN ACCESS

Edited by:
Erik Maquoi,
University of Liège, Belgium

Reviewed by:
Achilleas D. Theocharis,
University of Patras, Greece
Christian Stock,
University of Münster, Germany

****Correspondence:***
Sylvie Brassart-Pasco
sylvie.brassart-pasco@univ-reims.fr

Specialty section:
This article was submitted to Molecular and Cellular Oncology, a section of the journal Frontiers in Oncology

Received: *16 January 2020*
Accepted: *05 March 2020*
Published: *15 April 2020*

Citation:
Brassart-Pasco S, Brézillon S, Brassart B, Ramont L, Oudart J-B and Monboisse JC (2020) Tumor Microenvironment: Extracellular Matrix Alterations Influence Tumor Progression. Front. Oncol. 10:397. doi: 10.3389/fonc.2020.00397

INTRODUCTION

The tumor microenvironment (TME) is a complex structure composed of a large variety of cell types embedded in a modified extracellular matrix (ECM), with bidirectional communication between cells and ECM macromolecules to determine tumor progression and metastatic dissemination. The communication may involve cell–cell contacts but may also be controlled by intact ECM macromolecules or by several of their domains released by limited proteolysis and called matrikines or matricryptins. In this review, we will focus on ECM alterations occurring in TME, on the role of released matrikines in the control of cancer progression, and on the potential use of ECM fragments as biomarkers for cancer diagnosis and prognosis.

TUMOR MICROENVIRONMENT: AN ACTIVE PLAYER IN CANCER PROGRESSION

Tumors are diverse by the nature of their TME composition, stromal cell proportion, and activation states. TME undergoes transformations during tumor progression as a result of tissue remodeling. TME comprises a wide variety of cell types such as fibroblasts, endothelial cells, pericytes, and immune and inflammatory cells. These different cells elicit cross-talks leading to cell activation and differentiation and alterations in ECM structural and biological properties facilitating tumor cell proliferation, invasion, and metastatic dissemination. Within the TME, different T cell and B cell populations infiltrate invasive tumors and draining lymphoid organs (1). Tumor-associated macrophages (TAMs) are either tissue-resident or derived from bone marrow or spleen and play an important role in tumorigenesis regulation by facilitating cell migration, invasion, and metastasis (2). Tumor cells lead to the recruitment of neutrophils in tumorigenesis sites by secreting chemokines and interleukin (IL)-8. Infiltration by neutrophils appears to confer a poor prognosis (3). A dominant cellular component is fibroblasts that exert a key role in cancer progression and metastasis. Fibroblasts are usually quiescent and become activated to differentiate into myofibroblasts, also called cancer-associated fibroblasts (CAFs) (4). The main progenitors of CAFs come from resident fibroblasts, but CAFs can also come from smooth muscle cells, pericytes, or from bone marrow-derived mesenchymal cells leading to a heterogeneous cell population (5–7). Growth factors, secreted by tumor cells and infiltrating immune cells, largely govern stromal fibroblast recruitment. Transforming growth factor (TGF)β, platelet-derived growth factor (PDGF), and fibroblast growth factor (FGF)2 are key mediators of fibroblast activation. CAFs become synthetic machines that produce TME components creating an ECM structure as well as metabolic and immune reprogramming of TME. CAF secretome includes growth factors [epidermal growth factor (EGF), bone morphogenetic protein (BMP), FGF, or TGFβ] and some chemokines such as C-X-C motif ligand (CXCL)12 or stroma-derived factor (SDF)-1, which recruit circulating endothelial progenitor cells (4). These soluble factors, in conjunction with the angiogenic switch and several miRNAs, stimulate endothelial cells and their associated pericytes to develop tumor angiogenesis or lymphangiogenesis (2).

Abbreviations: ADAMTS, a disintegrin and metalloproteinase with thrombospondin motifs; BMP, bone morphogenetic protein; CAF, cancer-associated fibroblast; ECM, extracellular matrix; ERC, elastin receptor complex; FGF, fibroblast growth factor; 4E-BP1 protein, eukaryotic initiation factor 4E-binding protein 1; HER2, human epidermal growth factor receptor-2; LN, laminin; LOX, lysyl oxidase; MMP, matrix metalloproteinase; mTOR, mammalian target of rapamycin; PDGF, platelet-derived growth factor; ROS, reactive oxygen species; SDF 1, stroma-derived factor 1; SSTN, synstatin; sVEGFR1, soluble VEGF tyrosine kinase receptor 1; TAM, tumor-associated macrophage; TGFβ, transforming growth factor β; TME, tumor microenvironment.

METABOLIC ALTERATIONS IN THE TUMOR MICROENVIRONMENT

During the local growth of tumor, the surrounding vessels fail to meet the high demand of oxygen leading to hypoxic areas within the tumor and TME (8). Prolyl-hydroxylases are responsible for the labeling of hypoxia-inducible factors (HIFs) to be degraded by 26S proteasome. Under hypoxic conditions, prolyl-hydroxylases are inhibited, leading to the stabilization of HIFs that induces the expression of various genes implicated in tumor progression. Moreover, hypoxic responses include the unfolded protein response (UPR) and mammalian target of rapamycin (mTOR) signaling (9). mTOR signaling, through the phosphoinositide 3-kinase (PI3K)/Akt pathway, largely contributes to the regulation of cell survival, growth, and metabolism through phosphorylation of the eukaryotic initiation factor 4E-binding protein 1 (4E-BP1 protein) and ribosomal protein S6 kinase (10). HIF-1 is also a key regulator of the metabolic switch. By inducing specific gene expression, it alters the cellular metabolism, increasing glycolysis and lactate production (11, 12). Lactate arises from glycolysis which takes place under hypoxic conditions, but in tumors, glycolysis can also take place in oxygenated areas (8).

Nicotinamide adenine dinucleotide phosphate (NADPH) oxidase of inflammatory cells generates oxidative stress. Superoxide ions are converted into hypochlorous acid (HOCl) by myeloperoxidase and into $OH^{\bullet}$ radicals. Tumor cells with a high metabolism also release reactive oxygen species (ROS) and promoted ROS production in CAFs. ROS induce oxidative stress in TME and activate HIF-1 and nuclear factor (NF)-κB pathways, leading to an increase in autophagy (7). ROS also induce strong alterations in DNA, cell membrane, and ECM components. For example, collagen I is partially degraded by ROS and becomes more susceptible to proteolytic cleavage (13). Among proteases, neutrophils or TAMs secrete matrix metalloproteinase (MMP)-8 and-9 as well as neutrophil elastase that collaborates with CAF-secreted proteases to degrade ECM.

Main metabolic alterations of TME are summarized in **Figure 1**.

EXTRACELLULAR MATRIX ALTERATIONS IN THE TUMOR MICROENVIRONMENT

Another important feature of TME is the composition and organization of ECM, whose mechanical properties affect cell behavior. The ECM is mainly secreted by CAFs which produce more ECM proteins than normal fibroblasts. It is composed of various macromolecules including collagens, glycoproteins (fibronectin and laminins), proteoglycans, and polysaccharides with different physical and biological properties. Interstitial matrix, primarily synthesized by stromal cells, is rich in fibrillar collagens and proteoglycans. CAF secretome analyses show an increased secretion of bone morphogenetic protein (BMP)1, thrombospondin-1, and elastin interface 2 (7, 14). Several splice variants of fibronectin ED-A and ED-B and tenascins C and W may be secreted by CAFs (15). Interstitial ECM is highly

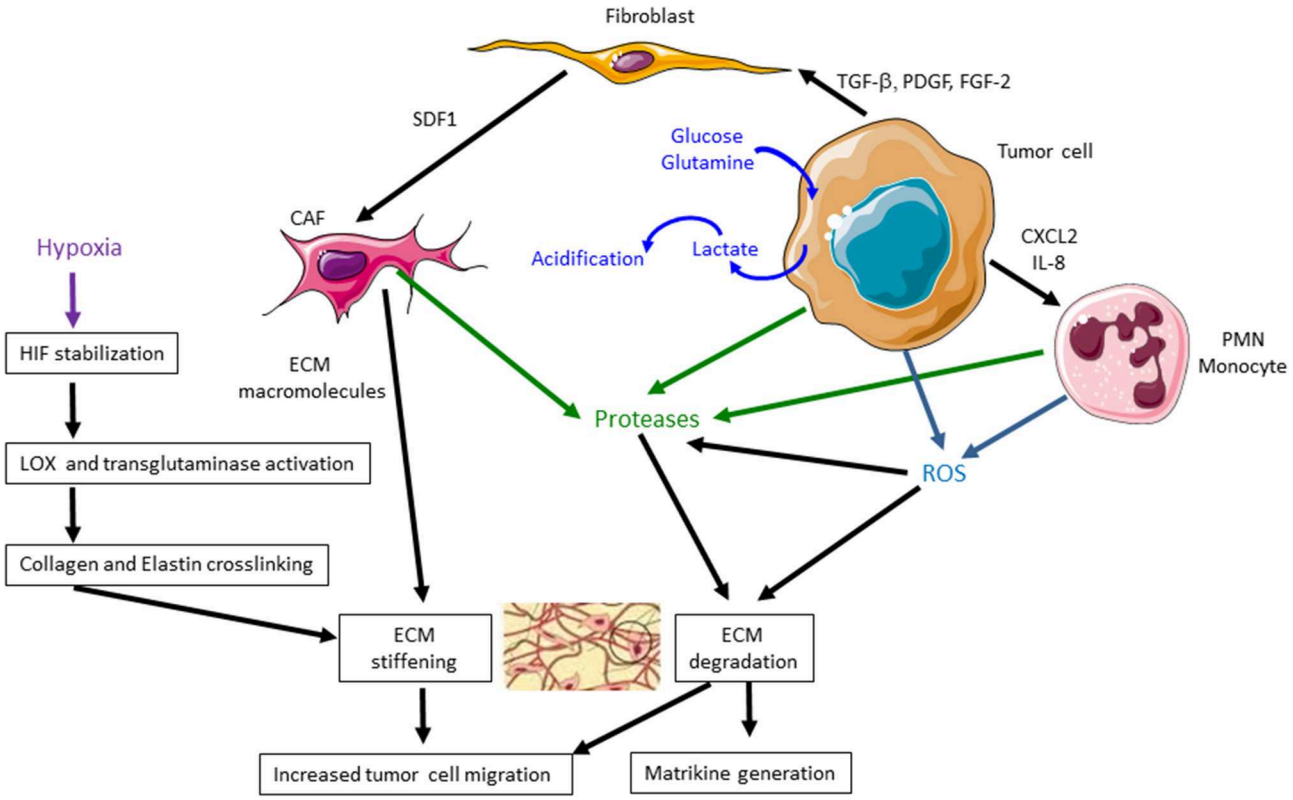

FIGURE 1 | Main metabolic and extracellular matrix (ECM) alterations in the tumor microenvironment (TME) during tumor progression. During cancer progression, tumor cells increase lactate production, leading to an acidification of TME. Tumor cells, cancer-associated fibroblasts (CAFs), polymorphonuclear leukocytes (PMNs), and monocytes secrete proteases, such as matrix metalloproteinases (MMPs), that degrade ECM and release matrikines. CAFs induce a higher secretion of ECM macromolecules that leads to an excessive deposition of ECM components. Tumor cells, PMNs, and monocytes produce reactive oxygen species (ROS) that degrade ECM components and particularly collagen I, facilitating tumor cell migration. They also stimulate the production of MMPs. Hypoxia also induces hypoxia-inducible factor (HIF) stabilization, lysyl oxidase (LOX) and transglutaminase activation, collagen and elastin cross-linking leading to ECM stiffening. These events favor tumor cell migration and cancer progression.

charged and hydrated and greatly participates in the tensile strength of tissues. Stiffness of neoplastic tumors is strongly higher than adjacent normal tissues. Cancer cells, CAFs, and TAMs, stimulated by hypoxia, modulate together ECM within the TME through an excessive deposition of structural components such as collagens, as well as cross-linking enzymes of the lysyl oxidase (LOX) and transglutaminase families, particularly LOX-1, LOXL-2, and transglutaminase-2 (16, 17). Collagen and elastin fibers are reoriented and cross-linked by LOX and transglutaminase, resulting in larger and more rigid fibrils that facilitate cell migration (18, 19). **Figure 1** summarizes the main ECM alterations in TME.

EXTRACELLULAR MATRIX BREAKDOWN BY MIGRATING CANCER CELLS

A decisive hallmark in cancer progression is the crossing of ECM and basement membrane (BM) by cancer cells. To penetrate the ECM, cancer cells secrete a number of proteolytic enzymes of the MMP family. BMs are specialized ECMs which are more compact and less porous. They present a distinct composition with collagen IV and laminin interconnected networks and proteoglycans such as perlecan. Several other types of collagen are associated to the BM, collagens XV, XVIII, and XIX. During ECM-barrier crossing, proteases release soluble and active fragments referenced in **Table 1**, called matrikines or matricryptins which may control cancer progression.

EXTRACELLULAR MATRIX-DERIVED FRAGMENTS INFLUENCE TUMOR PROGRESSION

The different matrikines derived from ECM macromolecules, collagens, glycoproteins, or proteoglycans may exert either pro- or anti-tumorigenic properties in various cancer models (**Table 1**). We and others demonstrated that collagen IV-derived matrikines (canstatin, tumstatin, and tetrastatin) and collagen XIX-derived matrikine act through binding to α3β1, α5β1, or αVβ3 integrins. The binding elicits an inhibition of

TABLE 1 | ECM fragments affect the main hallmarks of cancer progression.

ECM bioactive fragments	Parent molecule	Generating enzymes	Receptors	Biological activity
Collagen fragments				
Type IIB procollagen NH2 propeptide	Type IIB collagen	ADAMTS-3 (20)	αvβ3, αvβ5 integrins (21)	↗ EC and tumor cell death (chondrosarcoma, cervical and breast cancer) (21) through programmed cell necrosis (22)
Arresten (α1 chain NC1 domain)	Type IV collagen	Cathepsin S (23) MT1-MMP, MT2-MMP (24)	α1β1 integrin (25, 26)	↘ Angiogenesis and tumor growth (melanoma, glioblastoma, colorectal and lung cancer, squamous cell carcinomas) (25) ↘ FAK/c-Raf/MEK-1/2/ERK-1/2/p38 MAPK pathways in EC ↗ EC apoptosis through bcl-xl/bax ratio modulation (25)
Canstatin (α2 chain NC1 domain)	Type IV collagen	Cathepsin S (23) MT1-MMP, MT2-MMP (24)	α1β1, αvβ3, αvβ5 integrins (27)	↘ Angiogenesis and tumor growth (ocular, lung, breast, oral squamous cell, esophageal carcinoma, gastric, ovarian, pancreatic, prostate, and colorectal cancer (28) ↘ VEGF-A/VEGFR-1-2 signaling pathway in squamous cell carcinoma (29) ↗ Apoptosis in cancer cell and EC through bcl-2bcl-xl/bax ratio modulation (30) ↘ Caspase 8 and 9 activation in EC (27)
Tumstatin (α3 chain NC1 domain)	Type IV collagen	MMP-9 (31)	αvβ3, αvβ5 integrins (32)	↘ Angiogenesis and tumor growth (melanoma, glioma, osteosarcoma, breast, colon, prostate and lung cancer, gastric, hepatocellular, and squamous cell carcinoma (33, 34)
54–132 amino-acid sequence				54–132 amino-acid sequence:↗ G1 arrest, ↗ caspase-3 activation and ↘ FAK/PI3K/Akt/mTOR pathway in ECs (35)
185–203 amino-acid sequence				185–203 amino-acid sequence :↘ melanoma and EC migration through a decrease in MMP-2, uPA, t-PA (36)
Tetrastatin (α4 chain NC1 domain)	Type IV collagen		αvβ3 integrin (37)	↘ Tumor growth (melanoma, glioma, osteosarcoma, breast, colon, prostate and lung cancer, gastric, hepatocellular and squamous cell carcinoma (37–40) ↘ FAK/PI3K/Akt pathway and ↘ MMP-2 in tumor cells (37, 38)
Lamstatin (α5 chain NC1 domain)	Type IV collagen			↘ Angiogenesis (41) and lung cancer growth (42, 43) Unknown molecular mechanism
Hexastatin (α6 chain NC1 domain)	Type IV collagen			↘ Angiogenesis and tumor growth (Lewis lung carcinoma and spontaneous pancreatic insulinoma) (44) Unknown molecular mechanism
Vastatin (NC1 domain of collagen VIII alpha 1 chain)	Type VIII collagen			↘ EC proliferation and tumor growth and metastasis in murine hepatocellular carcinoma models (45) ↘ PcK1, JAG2, and c-Fos, ↘ Notch/AP-1 pathway (46)
Restin (NC10 domain of collagen XV)	Type XV collagen			↘ EC migration, renal carcinoma growth (47) and breast cancer metastasis (48) ↘ ATF3 activity by direct interaction (49) ↘ EMT through p-73 binding, mir-200a/b increase and ZEB1/2 inhibition in breast cancer cells (48)
Endostatin (20-kDa C-terminal fragment of collagen XVIII)	Type XVIII collagen		α5β1 integrin; caveolin-1 (50)	↘ Angiogenesis, lymphangiogenesis and tumor growth (51) ↗ Src-kinase pathway, ↘ RhoA GTPase activity; ↘ Ras/c-Raf/p38/Erk-1 pathway in EC (52, 53)

(Continued)

TABLE 1 | Continued

ECM bioactive fragments	Parent molecule	Generating enzymes	Receptors	Biological activity
				Frizzled domain (FZC18): ↘ Wnt/β-catenin pathway (54)
NC1 XIX	Type XIX collagen	Plasmin (55)	αvβ3 integrin (56)	↘ Melanoma cell migration, invasion, tumor growth and angiogenesis (56, 57) ↘ MMP-14 (57) in melanoma ↘ FAK/PI3K/Akt/mTOR pathway in melanoma cells (57)
Elastin fragments				
VG-6 (VGVAPG)	Elastin	Proteinase 3, cathepsin G (58), MMP-7,9,12 (59), neprilysin (60)	ERC, αvβ3 and αvβ5 integrins, galactin-3 (61), RPSA (62)	↗ Angiogenesis (63) and tumor growth in melanoma models (62, 64, 65) ↗ MT1-MMP, ↗ PI3K/Akt/NO synthase, ↗ NO/cGMP/Erk1/2 pathways in EC (66) ↗ IL-1β through NF-κB pathway in melanoma cell (67) ↗ MMP and plasminogen activation cascades in cancer cells
AG-9 (AGVPGLGVG)	Elastin	Proteinase 3, cathepsin G (58), MMP-7,9,12 (59), neprilysin (60)	RPSA (62)	↗ Tumor growth in a melanoma model (62) ↗ Tumor cell migration, invasion through MMP and plasminogen activation cascades
Laminin fragments				
IKVAV (α1 chain fragment)	Laminin-111		α3β1 and α6β1 integrins (68)	↗ Angiogenesis, tumor growth, and metastasis (68) ↗ bone marrow mesenchymal stem cell proliferation by activating MAPK/ERK1/2 and PI3K/Akt signaling pathways (69) ↗ t-PA in melanoma cells (68)
AG73 (RKRLQVQLSIRT from α1 chain)	Laminin-111		Syndecans 1, 2, and 4 (68)	↗ Angiogenesis and tumor growth (68) ↗ Rac1 and ERK1/2 signaling pathways (70)
YIGSR (β1 chain fragment)	Laminin-111		67 KD receptor (68)	↘ Tumor growth and metastasis (68) Unknown mechanism
C16 (KAFDITYVRLKF from γ1 chain)	Laminin-111		αvβ3 and α5β1 integrins (68)	↗ Tumor growth (68) ↗ MMP-9 production in melanoma cells (68)
γ2 chain N-terminal fragment	Laminin 332	MMP-2, cathepsin S, MT1-MMP (71)	α3β1 integrin, CD-44 (71)	↗ Angiogenesis, tumor growth and metastasis (71) Unknown mechanism
α3 chain C-terminal fragment	Laminin 332	Plasmin, MMP-2, MT1-MMP, C-proteinase, mTLD, BMP-1 (71)	α3β1 and α6β1 integrins (71)	↗ Angiogenesis, tumor growth (71) Unknown mechanism
A5G27 (RLVSYNGIIFFLK from α5 chain)	Laminin 511		Cell surface glycans (72)	↘ Breast tumor cell proliferation ↗ 4T1.2 experimental pulmonary metastasis (72) Unknown mechanism
Fibronectin fragments				
Anastellin (type III module)	Fibronectin			↘ Angiogenesis, tumor growth and metastasis (73) ↗ p38 MAPK activation in EC (74)
Proteoglycans fragments				
Metastatin	Aggrecan	ADAMTS (75)		↘ Growth, migration, angiogenesis of melanoma and prostate cancer (76) Unknown mechanism
Endorepellin LG3 fragment (C-terminal fragment of Endorepellin)	Perlecan	MMP-7 (77) Cathepsin L and BMP-1-Tolloid-like proteases (78)	α2β1 integrin (79)	↘ EC proliferation and migration, angiogenesis, tumor growth (78–84) ↘ VEGF-A/VEGFR pathway in EC (79) ↗ autophagy through Peg3 activation in EC (79, 85)

(Continued)

TABLE 1 | Continued

ECM bioactive fragments	Parent molecule	Generating enzymes	Receptors	Biological activity
Versikine	Versican	ADAMTS (86)	TLR2 (34)	↗ Immunogenicity in myeloma (87, 88) ↗ IL-1β, IL-6 expression by myeloma-associated macrophages through both Ppl2 kinase-dependent or -independent pathways (88)
Lumcorin (SSLVELDLSYNKLKNIP) L9M (ELDLSYNKLK) Lumikine/LumC13 (YEALRVANEVTLN)	Lumican		α2β1 integrin (89), MMP-14 (90, 91), ALK5/TGFβR1 (92)	↘ Growth, migration, angiogenesis in melanoma and breast cancer (93–96) ↘ FAK/Akt/ERK pathway ↘ MMP-14 proteolytic activity (90, 97) ↗ keratocytes migration (92, 98)
Synstatins				
SSTN 92-119, SSTN 82-130, SSTN 210-240	Syndecan-1		αvβ3, αvβ5 and α3β1 integrins, HER2, VEGFR2 (co-receptors of ectodomain) (34, 99–103)	↘ Angiogenesis in breast cancer (104–106) Depend on HER2- and EGFR-coupled mechanism (104)
SSTN87-131	Syndecan-4		EGFR, α3β1 integrin (co-receptors of ectodomain) (34)	↘ Cell motility (104) Depend on HER2- and EGFR-coupled mechanism (104)
Glypican fragments				
Glypican-3 derived peptide	Glypican-3		Wnt	↗ Cell proliferation, migration and invasion in hepatocellular carcinoma (107) ↗ Wnt/β-catenin, Hedgehog, and YAP pathway (108–110) ↗ Macrophage recruitments in tumor (108) ↗ EMT (108)
Has				
HA oligosaccharides	HA		CD44 (111)	Alters tumor growth, metastatic potential, and progression in prostate, colon, breast, and endometrial cancers (112, 113, 165) LMW HA promotes angiogenesis (114) HMW HA decreases angiogenesis, induces EMT (114)

4E-BP1 protein, eukaryotic initiation factor 4E-binding protein 1; ADAMTS, a disintegrin and metalloproteinase with thrombospondin motifs; AP-1, activator protein 1; ATF, activating transcription factor; ALK5, TGFβ type I receptor kinase; BMP, bone morphogenetic protein; cGMP, cyclic guanosine monophosphate; EC, endothelial cell; ECM, extracellular matrix; EGFR, epidermal growth factor receptor; EMT, epithelial–mesenchymal transition; ERC, elastin receptor complex; ERK, extracellular signal-regulated kinase; FAK, focal adhesion kinase; HA, hyaluronan; HER2, human epidermal growth factor receptor-2; HMW-HA, high-molecular-weight HA; IL, interleukin; JAG2, jagged canonical Notch ligand 2; LMW-HA, low-molecular-weight HA; MAPK, mitogen-activated protein kinase; MEK, MAPK/ERK kinase; MMP, matrix metalloproteinase; mTLD, mammalian Tolloid; mTOR, mammalian target of rapamycin; NF, nuclear factor; NO, nitric oxide; PI3K, phosphoinositide 3-kinase; RPSA, ribosomal protein SA; TLR, Toll-like receptor; t-PA, tissue-type plasminogen activator; uPA, urokinase-type plasminogen activator; VEGF, vascular endothelial growth factor; VEGFR, vascular endothelial growth factor tyrosine kinase receptor; TGFβ, transforming growth factor β.

the focal adhesion kinase (FAK)/PI3K/Akt/mTORC1 pathway, which is one of the main intracellular pathways involved in TME metabolic alterations. The inhibition leads to a decrease in the proliferative and invasive properties of tumor cells in various cancer models (27, 33, 38, 56). The main receptors, biological activities, and molecular mechanisms identified for ECM bioactive fragments are reported in **Table 1** and are illustrated in **Figure 2**.

EXTRACELLULAR MATRIX FRAGMENTS AS TUMOR BIOMARKERS

During cancer progression, an excessive ECM remodeling by proteinases, especially MMPs, is observed, and small ECM fragments are released into the circulation. The levels of these fragments may represent a measure of tumor activity and invasiveness and could be proposed as biomarkers (115). Serum and biofluid biomarkers are easy to collect, noninvasive, low cost, and can be followed over the course of the disease. Identification of new biofluid biomarkers may help in early detection, diagnosis, disease monitoring, and in individual treatment selection and thus on patient outcome. However, the low concentrations of ECM-derived fragments in body fluids remain a limitation to the development of these biomarkers in daily practice.

Collagens

Type I collagen is a major ECM component susceptible to proteinase degradation during cancer progression. Type I collagen cross-linked carboxyterminal telopeptide (ICTP) measurement in patient sera appears to be useful for bone metastasis screening in lung cancer patients, including stage III–IV non-small-cell lung cancer (NSCLC) or extensive disease (ED) small-cell lung cancer (SCLC) (116). ICTP

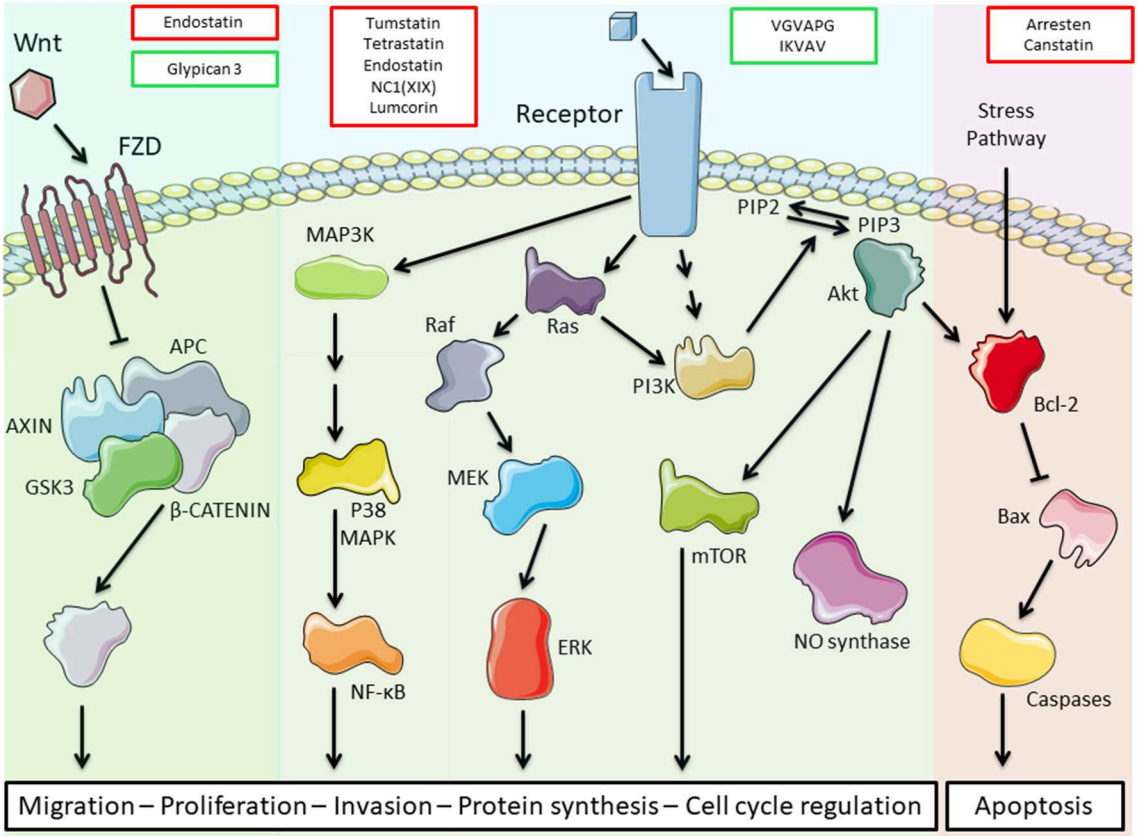

FIGURE 2 | Schematic representation of the main transduction pathways altered by extracellular matrix (ECM) bioactive fragments. Bioactive fragments stimulating the pathway are outlined in green, and fragments with inhibitory activity are outlined in red. Endostatin inhibits the Wnt/β-catenin pathway, while glypican-3 triggers this pathway. Tumstatin, tetrastatin, endostatin, NC1(XIX), and lumcorin inhibit the phosphoinositide 3-kinase (PI3K)/Akt/mammalian target of rapamycin (mTOR) pathway through integrin binding while VGVAPG and IKVAV activate this pathway through elastin receptor complex (ERC) and integrin binding, respectively. VGVAPG and IKVAV also activate the mitogen-activated protein kinase (MAPK) pathways. Arresten and canstatin activate the Bcl-2 pro-apoptotic pathway through integrin binding.

level in serum from patients with esophageal squamous cell carcinoma significantly correlates with tumor progression variables, including TNM stages (≥T2, N1, and M1), TNM stage ≥II, and maximal tumor length greater than 50 mm (117). A high level of ICTP in preoperated patient serum appears to be an important marker of better prognosis in triple-negative breast cancer and luminal-B-like [human epidermal growth factor receptor (HER)2-negative] subtypes (118). The elevation of the cross-linked N-telopeptide of type I collagen (NTx) appears positively related with the development and progression of bone metastasis in lung cancer (119). NTx serum concentration may also have a prognostic value in patients with prostate cancer at diagnosis (120). A high level of serum NTx (>22 nmol BCE/L) is correlated with a reduction in overall survival (OS) in patients with NSCLC (121).

In the follow-up of patients with radical resection of colorectal carcinoma, the N-terminal peptide of type III procollagen (marker of ECM synthesis) was reported as an early prognostic indicator of recurrence (122).

The serum level of tumstatin is significantly higher in patients with NSCLC compared to healthy patients (123).

The levels of markers reflecting type I (C1M), type III (C3M), and type IV (C4M, C4M12) collagen degradation by MMPs were significantly elevated in serum of ovarian or breast cancer patients compared to healthy controls (124).

Type VI collagen expression is correlated with various pro-tumorigenic events. Levels of type VI collagen α1 and α3 chain fragments, derived from MMP proteolysis, appear higher in serum from cancer patients (breast, colon, gastric, ovarian, pancreas, prostate cancer, NSCLC, SCLC, melanoma) compared to healthy patients and have promising diagnostic accuracy (125). Type VI collagen α3 chain circulating fragment levels were significantly higher in the serum of pancreatic ductal adenocarcinoma patients compared to healthy patients or patients with benign lesions (126).

Elevated serum endostatin levels were found in various human cancers including colorectal cancer (127), soft tissue sarcoma (128), and advanced-stage nasopharyngeal carcinoma (129). They are correlated with a favorable outcome in acute myeloid leukemia (130). On the contrary, high serum endostatin levels are associated with enhanced ECM degradation and poor patient outcome in patients with bladder cancer (131) and with non-Hodgkin lymphoma (132). Determination of soluble vascular

endothelial growth factor tyrosine kinase receptor (sVEGFR)-1 and endostatin levels may be useful in the diagnosis of malignant pleural effusions in patients with lung cancer (133). Preoperative serum VEGF and endostatin levels may be used for evaluating the biological behavior, invasion, and metastasis of gastric, hepatocellular, and colorectal carcinoma (134).

Elastin

Elastin fragments, released by proteases, are increased in the serum of stage I–IV NSCLC patients compared to healthy controls. These results suggest the use of elastin fragments as potential biomarkers (135), but further validations in clinical trials are needed.

Laminins

Laminins were reported to promote tumor progression. The serum level of LNγ2 fragments increases according to the T classification of head and neck squamous cell carcinoma (HNSCC) and decreases after the use of curative treatments. The level of LNγ2 fragments in serum may be useful to predict response to treatment of patients with HNSCC (136). The presence of soluble laminin fragments (ULN) corresponding to the N-terminal domain of the β2 chain was measured in urine of healthy subjects and patients with tumor. Mean level of ULN in lung tumor patients is significantly higher than that in healthy subjects (137). Serum laminin P1 fragment was studied in patients with SCLC and NSCLC and in normal subjects. The serum concentration of laminin P1 was elevated in 58.9% of SCLC and in 11.5% of NSCLC patients compared to healthy subjects. Median value in SCLC patients was significantly higher than that in NSCLC patients and in normal subjects (138). Urine laminin P1 measurement allows to discriminate between invasive and noninvasive urothelial cell carcinoma of the bladder (139).

Proteoglycans

The cleavage of proteoglycans like aggrecan and versican by a disintegrin and metalloproteinase with thrombospondin motifs (ADAMTS) in epithelial ovarian cancer has been demonstrated and is considered of prognostic value (75).

Perlecan fragments in the serum of prostate cancer patients were correlated with overall MMP-7 staining levels in prostate cancer tissues. Domain IV fragments of perlecan were highlighted in stage IV patient sera, but not detected in normal patient sera, suggesting that perlecan is degraded during metastasis. The association of perlecan fragments in sera and MMP-7 expression in tissues reflects prostate cancer invasivity (77). In breast cancer, the level of the endorepellin LG3 fragment in serum was significantly lower in breast cancer patients compared to healthy subjects. This suggests the endorepellin LG3 fragment as a new potential serological biomarker in breast cancer (140).

NSCLC patients presenting tumors with a low concentration of sulfated glycosaminoglycans (GAG) and high proteoglycan (PGs) levels presented better overall survival compared to patients with a high concentration of sulfated GAG and low expression of proteoglycans. These data suggest that matrix PGs could be considered as biomarkers in lung cancer (141).

Versican has been shown to be a potential biomarker in different cancers such as hepatocellular carcinoma (142), colon cancer (143), and recently in ovarian cancer (144). Hope et al. (145) provide a rational for testing versican proteolysis as a predictive and/or prognostic immune biomarker.

Lumcorin, a lumican-derived peptide mimics the inhibitory effect of lumican in melanoma progression (97). Lumikine, another lumican-derived peptide, promotes the healing of corneal epithelium debridement (92). These peptides might be putative cancer biomarkers but, to our knowledge, there are up to now no data in the literature describing lumican-derived peptides as biological markers in cancer.

Syndecan-1 was reported to play an immunomodulatory function in the polarization of $CD4^+$ T helper (Th) cells that were isolated from the TME of inflammatory breast cancer (IBC) and non-IBC patients (99). These results suggest that syndecan-1 expression in tumor could offer therapeutic potential in breast cancer. Remarkably, syndecan-1 seems to be overexpressed in inflammatory breast cancer, making it a potential biomarker.

New biomarkers such as syndecan-2 gene methylation (with improved detection sensitivity and specificity at lower costs) should lead to a great improvement in colorectal cancer screening. Syndecan-2 gene methylation was reported as a frequent event in precancerous lesions and appears detectable in bowel lavage fluid to identify patients with colorectal cancer (146, 147).

Syndecan-3- and aggrecan-peptides were recently described as novel biomarkers for the detection of epithelial ovarian cancer (144).

Syndecan-1 and syndecan-4 are described as independent indicators in breast carcinomas (148). Peptides based on interaction motifs in syndecan-1 and syndecan-4, named synstatins or SSTN peptides, are potential therapeutic agents for carcinomas depending on the HER2 and epidermal growth factor receptor (EGFR) pathway for their invasion and survival (104).

Glypican-1 detected in exosomes was suggested as a putative biomarker for early detection of pancreatic (149–154) and colorectal cancer (155, 156).

Glypican-3 is an important player in the Wnt, Hedgehog, and YAP signaling cascades involved in cancer cell proliferation and migration (108, 109). It is overexpressed in hepatocarcinoma and lung carcinoma and was reported as a poor prognosis marker in hepatocarcinoma. Glypican-3 represents a promising immunotherapeutic target. Different GPC3-targeting therapies have been developed: the use of humanized anti-GPC3 cytotoxic antibodies, the treatment with peptide/DNA vaccines, immunotoxin therapies, and genetic therapies (107, 157–162).

The involvement of CD44 and hyaluronan (HA) and the interaction of both molecules were demonstrated in numerous cancers (**Table 1**) and suggest their potential as biomarkers. HA molecules may exert distinct effects depending on their size and concentration. High-molecular-weight HAs (HMW HAs) are involved in cell proliferation and tissue development, whereas low-molecular-weight HAs (LMW HAs) enhance angiogenesis. Serum level of LMW HA in patients with breast cancer was correlated with lymph node metastasis, and LMW HA was suggested as a cancer biomarker (114). An increase in HA levels

induces tumor growth in mice and is associated with poor prognosis in pancreatic ductal adenocarcinoma (PDAC) patients. The inhibition of HA synthesis/signaling or the depletion of HA in tumor stroma may be a promising therapeutic approach to fight against PDAC progression (112). HA was also reported to facilitate cell proliferation and invasiveness in malignant pleural mesothelioma (163) and in melanoma (164) and may be used as a biomarker for early diagnosis and management of these diseases (163–165).

CONCLUSION

ECM fragments evidenced peripheral tissue proteolysis by cancer cells and could control cancer progression by exerting both anti-angiogenic and anti-tumorigenic properties. We showed that ECM-derived bioactive fragments are able to inhibit major transduction pathways involved in TME alterations, such as the FAK/PI3K/Akt/mTORC1 pathway (**Figure 2**). They represent potent antitumor agents that might be useful in combination with conventional chemo-, immune-, and targeted therapies as part of personalized medicine. Moreover, they diffuse into the body and are easy to measure in the blood or body fluids and thus can represent valuable markers for the diagnosis and prognosis of numerous cancers.

AUTHOR CONTRIBUTIONS

SB-P, SB, BB, and JM contributed to manuscript writing. LR and J-BO contributed to manuscript revision. J-BO designed **Figure 2**. All authors approved the final version of the manuscript.

FUNDING

This work was supported by the Centre National de la Recherche Scientifique (UMR 7369), the University of Reims Champagne-Ardenne, and the Region Grand-Est.

ACKNOWLEDGMENTS

The authors thank R. Rivet for his helpful contribution in bibliography.

REFERENCES

1. Joyce JA, Pollard JW. Microenvironmental regulation of metastasis. *Nat Rev Cancer.* (2009) 9:239–52. doi: 10.1038/nrc2618
2. Quail DF, Joyce JA. Microenvironmental regulation of tumor progression and metastasis. *Nat Med.* (2013) 19:1423–37. doi: 10.1038/nm.3394
3. Gregory AD, Houghton AM. Tumor-associated neutrophils: new targets for cancer therapy. *Cancer Res.* (2011) 71:2411–6. doi: 10.1158/0008-5472.CAN-10-2583
4. Kalluri R. The biology and function of fibroblasts in cancer. *Nat Rev Cancer.* (2016) 16:582–98. doi: 10.1038/nrc.2016.73
5. Martin M, Wei H, Lu T. Targeting microenvironment in cancer therapeutics. *Oncotarget.* (2016) 7:52575–83. doi: 10.18632/oncotarget.9824
6. Joyce JA. Therapeutic targeting of the tumor microenvironment. *Cancer Cell.* (2005) 7:513–20. doi: 10.1016/j.ccr.2005.05.024
7. Santi A, Kugeratski FG, Zanivan S. Cancer associated fibroblasts: the architects of stroma remodeling. *Proteomics.* (2018) 18:e1700167. doi: 10.1002/pmic.201700167
8. Saggar JK, Yu M, Tan Q, Tannock IF. The tumor microenvironment and strategies to improve drug distribution. *Front Oncol.* (2013) 3:154. doi: 10.3389/fonc.2013.00154
9. Laitala A, Erler JT. Hypoxic signalling in tumour stroma. *Front Oncol.* (2018) 8:189. doi: 10.3389/fonc.2018.00189
10. Griselda de la Cruz Lopezi K, Esperanza Toledo Guzman M, Ortiz Sanchez E, Garcia Carranca A. mTORC1 as regulator of mitochondrial functions and a therapeutic target in cancer. *Front Oncol.* (2019) 9:1373. doi: 10.3389/fonc.2019.01373
11. Escoté X, Fajas L. Metabolic adaptation to cancer growth: From the cell to the organism. *Cancer Lett.* (2015) 356:171–5. doi: 10.1016/j.canlet.2014.03.034
12. Lyssiotis CA, Kimmelman AC. Metabolic interactions in the tumor microenvironment. *Trends Cell Biol.* (2017) 27:863–75. doi: 10.1016/j.tcb.2017.06.003
13. Monboisse JC, Gardès-Albert M, Randoux A, Borel JP, Ferradini C. Collagen degradation by superoxide anion in pulse and gamma radiolysis. *BBA Gen Subj.* (1988) 965:29–35. doi: 10.1016/0304-4165(88)90147-X
14. Socovich AM, Naba A. The cancer matrisome: From comprehensive characterization to biomarker discovery. *Semin Cell Dev Biol.* (2019) 89:157–66. doi: 10.1016/j.semcdb.2018.06.005
15. Grahovac J, Wells A. Matrikine and matricellular regulators of EGF receptor signaling on cancer cell migration and invasion. *Lab Investig.* (2014) 94:31–40. doi: 10.1038/labinvest.2013.132
16. Emon B, Bauer J, Jain Y, Jung B, Saif T. Biophysics of tumor microenvironment and cancer metastasis - a mini review. *Comput Struct Biotechnol J.* (2018) 16:279–87. doi: 10.1016/j.csbj.2018.07.003
17. Eble JA, Niland S. The extracellular matrix in tumor progression and metastasis. *Clin Exp Metastasis.* (2019) 36:171–98. doi: 10.1007/s10585-019-09966-1
18. Balkwill FR, Capasso M, Hagemann T. The tumor microenvironment at a glance. *J Cell Sci.* (2012) 125:5591–6. doi: 10.1242/jcs.116392
19. Levental KR, Yu H, Kass L, Lakins JN, Egeblad M, Erler JT, et al. Matrix crosslinking forces tumor progression by enhancing integrin signaling. *Cell.* (2009) 139:891–906. doi: 10.1016/j.cell.2009.10.027
20. Fernandes RJ, Hirohata S, Engle JM, Colige A, Cohn DH, Eyre DR, et al. Procollagen II amino propeptide processing by ADAMTS-3. *J Biol Chem.* (2001) 120:453–65. doi: 10.1074/jbc.M103466200
21. Wang Z, Bryan J, Franz C, Havlioglu N, Sandell LJ. Type IIB procollagen NH2-propeptide induces death of tumor cells via interaction with integrins αvβ3 and αvβ5. *J Biol Chem.* (2010) 285:20806–17. doi: 10.1074/jbc.M110.118521
22. Sandell LJ. Novel functions for Type II procollagen. *Connect Tissue Res.* (2014) 55:20–5. doi: 10.3109/03008207.2013.867340
23. Sugiyama A, Mitsui A, Okada M, Yamawaki H. Cathepsin S degrades arresten and canstatin in infarcted area after myocardial infarction in rats. *J Vet Med Sci.* (2019) 103:1562–70. doi: 10.1292/jvms.18-0674
24. Rebustini IT, Myers C, Lassiter KS, Surmak A, Szabova L, Holmbeck K, et al. MT2-MMP-dependent release of collagen IV NC1 domains regulates submandibular gland branching morphogenesis. *Dev Cell.* (2009) 40:1581–96. doi: 10.1016/j.devcel.2009.07.016
25. Aikio M, Alahuhta I, Nurmenniemi S, Suojanen J, Palovuori R, Teppo S, et al. Arresten, a collagen-derived angiogenesis inhibitor, suppresses invasion of squamous cell carcinoma. *PLoS ONE.* (2012) 7:e51044. doi: 10.1371/journal.pone.0051044
26. Sudhakar A, Nyberg P, Keshamouni VG, Mannam AP, Li J, Sugimoto H, et al. Human α1 type IV collagen NC1 domain exhibits distinct antiangiogenic activity mediated by α1β1 integrin. *J Clin Invest.* (2005) 317:2562–72. doi: 10.1172/JCI24813

27. Magnon C, Galaup A, Mullan B, Rouffiac V, Bidart JM, Griscelli F, et al. Canstatin acts on endothelial and tumor cells via mitochondrial damage initiated through interaction with αvβ3 and αvβ5 integrins. *Cancer Res.* (2005) 8:9837. doi: 10.1158/0008-5472.CAN-04-3536
28. Okada M, Yamawaki H. A current perspective of canstatin, a fragment of type IV collagen alpha 2 chain. *J Pharmacol Sci.* (2019) 7:122–34. doi: 10.1016/j.jphs.2018.12.001
29. Hwang-Bo J, Park JH, Bae MG, Chung IS. Recombinant canstatin inhibits VEGF-A-induced lymphangiogenesis and metastasis in an oral squamous cell carcinoma SCC-VII animal model. *Cancer Med.* (2016) 5:2977–88. doi: 10.1002/cam4.866
30. Xing YN, Deng P, Xu HM. Canstatin induces apoptosis in gastric cancer xenograft growth in mice through the mitochondrial apoptotic pathway. *Biosci Rep.* (2014) 7:255–65. doi: 10.1042/BSR20140012
31. Hamano Y, Zeisberg M, Sugimoto H, Lively JC, Maeshima Y, Yang C, et al. Physiological levels of tumstatin, a fragment of collagen IV α3 chain, are generated by MMP-9 proteolysis and suppress angiogenesis via αVβ3 integrin. *Cancer Cell.* (2003) 28:101–9. doi: 10.1016/S1535-6108(03)00133-8
32. Pedchenko V, Zent R, Hudson BG. α v β 3 and α v β 5 integrins bind both the proximal RGD site and non-RGD motifs within noncollagenous (NC1) domain of the α3 chain of type IV collagen: Implication for the mechanism of endothelial cell adhesion. *J Biol Chem.* (2004) 61:1022–8. doi: 10.1074/jbc.M311901200
33. Monboisse JC, Oudart JB, Ramont L, Brassart-Pasco S, Maquart FX. Matrikines from basement membrane collagens: a new anti-cancer strategy. *Biochim Biophys Acta Gen Subj.* (2014) 1840:2589–98. doi: 10.1016/j.bbagen.2013.12.029
34. Ricard-Blum S, Vallet SD. Fragments generated upon extracellular matrix remodeling: Biological regulators and potential drugs. *Matrix Biol.* (2019) 57–8:285–98. doi: 10.1016/j.matbio.2017.11.005
35. Maeshima Y, Colorado PC, Kalluri R. Two RGD-independent α(v)β3 integrin binding sites on tumstatin regulate distinct anti-tumor properties. *J Biol Chem.* (2000) 56:381–91. doi: 10.1074/jbc.C000186200
36. Floquet N, Pasco S, Ramont L, Derreumaux P, Laronze JY, Nuzillard JM, et al. The antitumor properties of the α3(IV)-(185-203) peptide from the NC1 domain of type IV collagen (Tumstatin) are conformation-dependent. *J Biol Chem.* (2004) 278:4238–49. doi: 10.1074/jbc.M307736200
37. Brassart-Pasco S, Sénéchal K, Thevenard J, Ramont L, Devy J, Di Stefano L, et al. Tetrastatin, the NC1 domain of the α4(IV) collagen chain: A novel potent anti-tumor matrikine. *PLoS ONE.* (2012) 7:e29587. doi: 10.1371/journal.pone.0029587
38. Lambert E, Fuselier E, Ramont L, Brassart B, Dukic S, Oudart JB, et al. Conformation-dependent binding of a Tetrastatin peptide to αvβ3 integrin decreases melanoma progression through FAK/PI3K/Akt pathway inhibition. *Sci Rep.* (2018) 6:30599. doi: 10.1038/s41598-018-28003-x
39. Pasco S, Ramont L, Venteo L, Pluot M, Maquart FX, Monboisse JC. *In vivo* overexpression of tumstatin domains by tumor cells inhibits their invasive properties in a mouse melanoma model. *Exp Cell Res.* (2004) 301:251–65. doi: 10.1016/j.yexcr.2004.07.036
40. Thevenard J, Floquet N, Ramont L, Prost E, Nuzillard JM, Dauchez M, et al. Structural and antitumor properties of the YSNSG cyclopeptide derived from tumstatin. *Chem Biol.* (2006) 13:1307–15. doi: 10.1016/j.chembiol.2006.10.007
41. Karagiannis ED, Popel AS. Identification of novel short peptides derived from the α4, α5, and α6 fibrils of type IV collagen with anti-angiogenic properties. *Biochem Biophys Res Commun.* (2007) 17:687–98. doi: 10.1016/j.bbrc.2006.12.231
42. Weckmann M, Moir LM, Heckman CA, Black JL, Oliver BG, Burgess JK. Lamstatin - a novel inhibitor of lymphangiogenesis derived from collagen IV. *J Cell Mol Med.* (2012) 35:34–41. doi: 10.1111/j.1582-4934.2012.01648.x
43. Koskimaki JE, Karagiannis ED, Tang BC, Hammers H, Watkins DN, Pili R, et al. Pentastatin-1, a collagen IV derived 20-mer peptide, suppresses tumor growth in a small cell lung cancer xenograft model. *BMC Cancer.* (2010) 128:680–5. doi: 10.1186/1471-2407-10-29
44. Mundel TM, Yliniemi AM, Maeshima Y, Sugimoto H, Kieran M, Kalluri R. Type IV collagen α6 chain-derived noncollagenous domain 1 (α6(IV)NC1) inhibits angiogenesis and tumor growth. *Int J Cancer.* (2008) 122:1738–44. doi: 10.1002/ijc.23269
45. Li Y, Li J, Woo YM, Shen Z, Yao H, Cai Y, et al. Enhanced expression of Vastatin inhibits angiogenesis and prolongs survival in murine orthotopic glioblastoma model. *BMC Cancer.* (2017) 588:4319–24. doi: 10.1186/s12885-017-3125-8
46. Shen Z, Yao C, Wang Z, Yue L, Fang Z, Yao H, et al. Vastatin, an endogenous antiangiogenesis polypeptide that is lost in hepatocellular carcinoma, effectively inhibits tumor metastasis. *Mol Ther.* (2016) 75–6:271–85. doi: 10.1038/mt.2016.56
47. Ramchandran R, Dhanabal M, Volk R, Waterman MJF, Segal M, Lu H, et al. Antiangiogenic activity of restin, NC10 domain of human collagen XV: Comparison to endostatin. *Biochem Biophys Res Commun.* (1999) 118:9152–232. doi: 10.1006/bbrc.1999.0248
48. Lu Z, Jiao D, Qiao J, Yang S, Yan M, Cui S, et al. Restin suppressed epithelial-mesenchymal transition and tumor metastasis in breast cancer cells through upregulating mir-200a/b expression via association with p73. *Mol Cancer.* (2015) 62:125–33. doi: 10.1186/s12943-015-0370-9
49. Wu Y, Lu F, Qi Y, Wang R, Zhang J, Lu Z, et al. Interaction of Restin with transcription factors. *Sci China Ser C Life Sci.* (2005) 8:e82730. doi: 10.1360/04yc0073
50. Wickström SA, Alitalo K, Keski-Oja J. Endostatin associates with integrin alpha5beta1 and caveolin-1, and activates Src via a tyrosyl phosphatase-dependent pathway in human endothelial cells. *Cancer Res.* (2002) 62:5580–9.
51. Walia A, Yang JF, Huang YH, Rosenblatt MI, Chang JH, Azar DT. Endostatin's emerging roles in angiogenesis, lymphangiogenesis, disease, and clinical applications. *Biochim Biophys Acta Gen Subj.* (2015) 280:2194–206. doi: 10.1016/j.bbagen.2015.09.007
52. Digtyar AV, Pozdnyakova NV, Feldman NB, Lutsenko SV, Severin SE. Endostatin: current concepts about its biological role and mechanisms of action. *Biochem.* (2007) 132:235–246. doi: 10.1134/S00062979070 30017
53. Hamano Y, Kalluri R. Tumstatin, the NC1 domain of α3 chain of type IV collagen, is an endogenous inhibitor of pathological angiogenesis and suppresses tumor growth. *Biochem Biophys Res Commun.* (2005) 652:50–8. doi: 10.1016/j.bbrc.2005.05.130
54. Hendaoui I, Lavergne E, Lee HS, Hong SH, Kim HZ, Parent C, et al. Inhibition of Wnt/β-Catenin signaling by a soluble Collagen-Derived frizzled domain interacting with Wnt3a and the receptors frizzled 1 and 8. *PLoS ONE.* (2012) 7:e30601. doi: 10.1371/journal.pone.0030601
55. Oudart JB, Brassart-Pasco S, Vautrin A, Sellier C, Machado C, Dupont-Deshorgue A, et al. Plasmin releases the anti-tumor peptide from the NC1 domain of collagen XIX. *Oncotarget.* (2015) 5:e202. doi: 10.18632/oncotarget.2849
56. Oudart JB, Doué M, Vautrin A, Brassart B, Sellier C, Dupont-Deshorgue A, et al. The anti-tumor NC1 domain of collagen XIX inhibits the FAK/PI3K/Akt/mTOR signaling pathway through αvβ3 integrin interaction. *Oncotarget.* (2016) 41:1010428319847081. doi: 10.18632/oncotarget.6399
57. Oudart JB, Monboisse JC, Maquart FX, Brassart B, Brassart-Pasco S, Ramont L. Type XIX collagen: a new partner in the interactions between tumor cells and their microenvironment. *Matrix Biol.* (2017) 13:347–61. doi: 10.1016/j.matbio.2016.07.010
58. Heinz A, Jung MC, Jahreis G, Rusciani A, Duca L, Debelle L, et al. The action of neutrophil serine proteases on elastin and its precursor. *Biochimie.* (2012) 2015:563818. doi: 10.1016/j.biochi.2011.10.006
59. Heinz A, Jung MC, Duca L, Sippl W, Taddese S, Ihling C, et al. Degradation of tropoelastin by matrix metalloproteinases - Cleavage site specificities and release of matrikines. *FEBS J.* (2010) 277:1939–56. doi: 10.1111/j.1742-4658.2010.07616.x
60. Mora Huertas AC, Schmelzer CEH, Luise C, Sippl W, Pietzsch M, Hoehenwarter W, et al. Degradation of tropoelastin and skin elastin by neprilysin. *Biochimie.* (2018) 146:73–8. doi: 10.1016/j.biochi.2017.11.018
61. Pocza P, Süli-Vargha H, Darvas Z, Falus A. Locally generated VGVAPG and VAPG elastin-derived peptides amplify melanoma invasion via the galectin-3 receptor. *Int J Cancer.* (2008) 122:1972–80. doi: 10.1002/ijc.23296
62. Brassart B, Da Silva J, Donet M, Seurat E, Hague F, Terryn C, et al. Tumour cell blebbing and extracellular vesicle shedding: key role of matrikines and ribosomal protein SA. *Br J Cancer.* (2019) 120:453–65. doi: 10.1038/s41416-019-0382-0

63. Robinet A, Fahem A, Cauchard J-H, Huet E, Vincent L, Lorimier S, et al. Elastin-derived peptides enhance angiogenesis by promoting endothelial cell migration and tubulogenesis through upregulation of MT1-MMP. *J Cell Sci.* (2005) 118:343–56. doi: 10.1242/jcs.01613
64. Ntayi C, Labrousse AL, Debret R, Birembaut P, Bellon G, Antonicelli F, et al. Elastin-derived peptides upregulate matrix metalloproteinase-2-ediated melanoma cell invasion through elastin-binding protein. *J Invest Dermatol.* (2004) 122:256–65. doi: 10.1046/j.0022-202X.2004.22228.x
65. Devy J, Duca L, Cantarelli B, Joseph-Pietras D, Scandolera A, Rusciani A, et al. Elastin-derived peptides enhance melanoma growth *in vivo* by upregulating the activation of Mcol-A (MMP-1) collagenase. *Br J Cancer.* (2010) 103:1562–70. doi: 10.1038/sj.bjc.6605926
66. Fahem A, Robinet A, Cauchard JH, Duca L, Soula-Rothhut M, Rothhut B, et al. Elastokine-mediated up-regulation of MT1-MMP is triggered by nitric oxide in endothelial cells. *Int J Biochem Cell Biol.* (2008) 40:1581–96. doi: 10.1016/j.biocel.2007.11.022
67. Debret R, Le Naour RR, Sallenave JM, Deshorgue A, Hornebeck WG, Guenounou M, et al. Elastin fragments induce IL-1β upregulation via NF-κB pathway in melanoma cells. *J Invest Dermatol.* (2006) 126:1860–8. doi: 10.1038/sj.jid.5700337
68. Kikkawa Y, Hozumi K, Katagiri F, Nomizu M, Kleinman HK, Koblinski JE. Laminin-111-derived peptides and cancer. *Cell Adhes Migr.* (2013) 7:150–9. doi: 10.4161/cam.22827
69. Li B, Qiu T, Zhang P, Wang X, Yin Y, Li S. IKVAV regulates ERK1/2 and Akt signalling pathways in BMMSC population growth and proliferation. *Cell Prolif.* (2014) 47:133–45. doi: 10.1111/cpr.12094
70. Nascimento CF, de Siqueira AS, Pinheiro JJV, Freitas VM, Jaeger RG. Laminin-111 derived peptides AG73 and C16 regulate invadopodia activity of a human adenoid cystic carcinoma cell line. *Exp Cell Res.* (2011) 317:2562–72. doi: 10.1016/j.yexcr.2011.08.022
71. Rousselle P, Beck K. Laminin 332 processing impacts cellular behavior. *Cell Adhes Migr.* (2013) 7:122–34. doi: 10.4161/cam.23132
72. Kusuma N, Anderson RL, Pouliot N. Laminin α5-derived peptides modulate the properties of metastatic breast tumour cells. *Clin Exp Metastasis.* (2011) 28:909–21. doi: 10.1007/s10585-011-9422-8
73. Ambesi A, McKeown-Longo PJ. Anastellin, the angiostatic fibronectin peptide, is a selective inhibitor of lysophospholipid signaling. *Mol Cancer Res.* (2009) 7:255–65. doi: 10.1158/1541-7786.MCR-08-0195
74. You R, Klein RM, Zheng M, McKeown-Longo PJ. Regulation of p38 MAP kinase by anastellin is independent of anastellin's effect on matrix fibronectin. *Matrix Biol.* (2009) 28:101–9. doi: 10.1016/j.matbio.2009.01.003
75. Lima MA, Dos Santos L, Turri JA, Nonogaki S, Buim M, Lima JF, et al. Prognostic value of ADAMTS proteases and their substrates in epithelial ovarian cancer. *Pathobiology.* (2016) 12:508–15. doi: 10.1159/000446244
76. Liu N, Lapcevich RK, Underhill CB, Han Z, Gao F, Swartz G, et al. Metastatin: a hyaluronan-binding complex from cartilage that inhibits tumor growth. *Cancer Res.* (2001) 61:1022–8.
77. Grindel B, Li Q, Arnold R, Petros J, Zayzafoon M, Muldoon M, et al. Perlecan/HSPG2 and matrilysin/MMP-7 as indices of tissue invasion: Tissue localization and circulating perlecan fragments in a cohort of 288 radical prostatectomy patients. *Oncotarget.* (2016) 59:615–29. doi: 10.18632/oncotarget.11976
78. Gubbiotti MA, Neill T, Iozzo RV. A current view of perlecan in physiology and pathology: a mosaic of functions. *Matrix Biol.* (2017) 57–8:285–98. doi: 10.1016/j.matbio.2016.09.003
79. Douglass S, Goyal A, Iozzo RV. The role of perlecan and endorepellin in the control of tumor angiogenesis and endothelial cell autophagy. *Connect Tissue Res.* (2015) 56:381–91. doi: 10.3109/03008207.2015.1045297
80. Mongiat M, Sweeney SM, San Antonio JD, Fu J, Iozzo RV. Endorepellin, a novel inhibitor of angiogenesis derived from the C terminus of perlecan. *J Biol Chem.* (2003) 278:4238–49. doi: 10.1074/jbc.M210445200
81. Le BV, Kim H, Choi J, Kim JH, Hahn MJ, Lee C, et al. Crystal structure of the LG3 domain of endorepellin, an angiogenesis inhibitor. *J Mol Biol.* (2011) 414:231–42. doi: 10.1016/j.jmb.2011.09.048
82. Goyal A, Gubbiotti MA, Chery DR, Han L, Iozzo RV. Endorepellin-evoked autophagy contributes to angiostasis. *J Biol Chem.* (2016) 291:19245–56. doi: 10.1074/jbc.M116.740266
83. Poluzzi C, Iozzo RV, Schaefer L. Endostatin and endorepellin: a common route of action for similar angiostatic cancer avengers. *Adv Drug Deliv Rev.* (2016) 97:156–73. doi: 10.1016/j.addr.2015.10.012
84. Gubbiotti MA, Iozzo RV. Proteoglycans regulate autophagy via outside-in signaling: an emerging new concept. *Matrix Biol.* (2015) 48:6–13. doi: 10.1016/j.matbio.2015.10.002
85. Neill T, Andreuzzi E, Wang ZX, Peiper SC, Mongiat M, Iozzo RV. Endorepellin remodels the endothelial transcriptome toward a pro-autophagic and pro-mitophagic gene signature. *J Biol Chem.* (2018) 293:12137–48. doi: 10.1074/jbc.RA118.002934
86. McCulloch DR, Nelson CM, Dixon LJ, Silver DL, Wylie JD, Lindner V, et al. ADAMTS metalloproteases generate active versican fragments that regulate interdigital web regression. *Dev Cell.* (2009) 17:687–98. doi: 10.1016/j.devcel.2009.09.008
87. Nandadasa S, Foulcer S, Apte SS. The multiple, complex roles of versican and its proteolytic turnover by ADAMTS proteases during embryogenesis. *Matrix Biol.* (2014) 35:34–41. doi: 10.1016/j.matbio.2014.01.005
88. Hope C, Foulcer S, Jagodinsky J, Chen SX, Jensen JL, Patel S, et al. Immunoregulatory roles of versican proteolysis in the myeloma microenvironment. *Blood.* (2016) 128:680–5. doi: 10.1182/blood-2016-03-705780
89. Zeltz C, Brézillon S, Käpylä J, Eble JA, Bobichon H, Terryn C, et al. Lumican inhibits cell migration through α2?1 integrin. *Exp Cell Res.* (2010) 316:2922–31. doi: 10.1016/j.yexcr.2010.08.002
90. Pietraszek K, Chatron-Colliet A, Brézillon S, Perreau C, Jakubiak-Augustyn A, Krotkiewski H, et al. Lumican: a new inhibitor of matrix metalloproteinase-14 activity. *FEBS Lett.* (2014) 588:4319–24. doi: 10.1016/j.febslet.2014.09.040
91. Pietraszek-Gremplewicz K, Karamanou K, Niang A, Dauchez M, Belloy N, Maquart FX, et al. Small leucine-rich proteoglycans and matrix metalloproteinase-14: key partners? *Matrix Biol.* (2019) 75–6:271–85. doi: 10.1016/j.matbio.2017.12.006
92. Gesteira TF, Coulson-Thomas VJ, Yuan Y, Zhang J, Nader HB, Kao WWY. Lumican peptides: rational design targeting ALK5/TGFBRI. *Sci Rep.* (2017) 5:e1238542. doi: 10.1038/srep42057
93. Brézillon S, Pietraszek K, Maquart FX, Wegrowski Y. Lumican effects in the control of tumour progression and their links with metalloproteinases and integrins. *FEBS J.* (2013) 280:2369–81. doi: 10.1111/febs.12210
94. Pietraszek K, Brézillon S, Perreau C, Malicka-Błaszkiewicz M, Maquart FX, Wegrowski Y. Lumican - derived peptides inhibit melanoma cell growth and migration. *PLoS ONE.* (2013) 8:e76232. doi: 10.1371/journal.pone.0076232
95. Karamanos NK, Piperigkou Z, Theocharis AD, Watanabe H, Franchi M, Baud S, et al. Proteoglycan chemical diversity drives multifunctional cell regulation and therapeutics. *Chem Rev.* (2018) 118:9152–232. doi: 10.1021/acs.chemrev.8b00354
96. Karamanou K, Franchi M, Vynios D, Brézillon S. Epithelial-to-mesenchymal transition and invadopodia markers in breast cancer: Lumican a key regulator. *Semin Cancer Biol.* (2019) 62:125–33. doi: 10.1016/j.semcancer.2019.08.003
97. Zeltz C, Brézillon S, Perreau C, Ramont L, Maquart FX, Wegrowski Y. Lumcorin: a leucine-rich repeat 9-derived peptide from human lumican inhibiting melanoma cell migration. *FEBS Lett.* (2009) 62:639–52. doi: 10.1016/j.febslet.2009.08.012
98. Yamanaka O, Yuan Y, Coulson-Thomas VJ, Gesteira TF, Call MK, Zhang Y, et al. Lumican binds ALK5 to promote epithelium wound healing. *PLoS ONE.* (2013) 8:e82730. doi: 10.1371/journal.pone.0082730
99. Saleh ME, Gadalla R, Hassan H, Afifi A, Götte M, El-Shinawi M, et al. The immunomodulatory role of tumor Syndecan-1 (CD138) on *ex vivo* tumor microenvironmental CD4+ T cell polarization in inflammatory and non-inflammatory breast cancer patients. *PLoS ONE.* (2019) 18:3686–3696. doi: 10.1371/journal.pone.0217550
100. Rapraeger AC. Synstatin: a selective inhibitor of the syndecan-1-coupled IGF1R-αvβ3 integrin complex in tumorigenesis and angiogenesis. *FEBS J.* (2013) 280:2207–15. doi: 10.1111/febs.12160
101. Rapraeger AC, Ell BJ, Roy M, Li X, Morrison OR, Thomas GM, et al. Vascular endothelial-cadherin stimulates syndecan-1-coupled insulin-like growth factor-1 receptor and cross-talk between αvβ3 integrin

and vascular endothelial growth factor receptor 2 at the onset of endothelial cell dissemination during angiogenesis. *FEBS J.* (2013) 280:2194–206. doi: 10.1111/febs.12134

102. Jung O, Beauvais DLM, Adams KM, Rapraeger AC. VLA-4 phosphorylation during tumor and immune cell migration relies on its coupling to VEGFR2 and CXCR4 by syndecan-1. *J Cell Sci.* (2019) 132:jcs232645. doi: 10.1242/jcs.232645
103. Metwaly HA, El-Gayar AM, El-Shishtawy MM. Inhibition of the signaling pathway of syndecan-1 by synstatin: a promising anti-integrin inhibitor of angiogenesis and proliferation in HCC in rats. *Arch Biochem Biophys.* (2018) 652:50–8. doi: 10.1016/j.abb.2018.06.007
104. Wang H, Jin H, Rapraeger AC. Syndecan-1 and syndecan-4 capture epidermal growth factor receptor family members and the α3β1 integrin via binding sites in their ectodomains: novel synstatins prevent kinase capture and inhibitα6β4-integrindependent epithelial cell motility. *J Biol Chem.* (2015) 18:58. doi: 10.1074/jbc.M115.679084
105. Beauvais DM, Ell BJ, McWhorter AR, Rapraeger AC. Syndecan-1 regulates α vβ 3 and α vβ 5 integrin activation during angiogenesis and is blocked by synstatin, a novel peptide inhibitor. *J Exp Med.* (2009) 206:691–705. doi: 10.1084/jem.20081278
106. Jung O, Trapp-Stamborski V, Purushothaman A, Jin H, Wang H, Sanderson RD, et al. Heparanase-induced shedding of syndecan-1/CD138 in myeloma and endothelial cells activates VEGFR2 and an invasive phenotype: prevention by novel synstatins. *Oncogenesis.* (2016) 5:e202. doi: 10.1038/oncsis.2016.5
107. Shimizu Y, Suzuki T, Yoshikawa T, Endo I, Nakatsura T. Next-generation cancer immunotherapy targeting glypican-3. *Front Oncol.* (2019) 57–8:169–77. doi: 10.3389/fonc.2019.00248
108. Zhou F, Shang W, Yu X, Tian J. Glypican-3: a promising biomarker for hepatocellular carcinoma diagnosis and treatment. *Med Res Rev.* (2018) 13:1307–15. doi: 10.1002/med.21455
109. Li N, Wei L, Liu X, Bai H, Ye Y, Li D, et al. A frizzled-like cysteine-rich domain in glypican-3 mediates Wnt binding and regulates hepatocellular carcinoma tumor growth in mice. *Hepatology.* (2019) 70:1231–45. doi: 10.1002/hep.30646
110. Kolluri A, Ho M. The role of glypican-3 in regulating Wnt, YAP, and Hedgehog in liver cancer. *Front Oncol.* (2019) 9:708. doi: 10.3389/fonc.2019.00708
111. Yang C, Cao M, Liu H, He Y, Xu J, Du Y, et al. The high and low molecular weight forms of hyaluronan have distinct effects on CD44 clustering. *J Biol Chem.* (2012) 287:43094–107. doi: 10.1074/jbc.M112.349209
112. Sato N, Kohi S, Hirata K, Goggins M. Role of hyaluronan in pancreatic cancer biology and therapy: once again in the spotlight. *Cancer Sci.* (2016) 277:1939–56. doi: 10.1111/cas.12913
113. Adamia S, Pilarski PM, Belch AR, Pilarski LM. Aberrant splicing, Hyaluronan synthases and intracellular Hyaluronan as drivers of oncogenesis and potential drug targets. *Curr Cancer Drug Targets.* (2013) 13:347–61. doi: 10.2174/1568009611313040001
114. Karousou E, Misra S, Ghatak S, Dobra K, Götte M, Vigetti D, et al. Roles and targeting of the HAS/hyaluronan/CD44 molecular system in cancer. *Matrix Biol.* (2017) 94:192–202. doi: 10.1016/j.matbio.2016.10.001
115. Kehlet SN, Sanz-Pamplona R, Brix S, Leeming DJ, Karsdal MA, Moreno V. Excessive collagen turnover products are released during colorectal cancer progression and elevated in serum from metastatic colorectal cancer patients. *Sci Rep.* (2016) 12:e0187860. doi: 10.1038/srep30599
116. Tang C, Liu Y, Qin H, Li X, Guo W, Li J, et al. Clinical significance of serum BAP, TRACP 5b and ICTP as bone metabolic markers for bone metastasis screening in lung cancer patients. *Clin Chim Acta.* (2013) 436:316–18. doi: 10.1016/j.cca.2013.09.011
117. Nabeya Y, Shimada H, Okazumi S, Matsubara H, Gunji Y, Suzuki T, et al. Serum cross-linked carboxyterminal telopeptide of type I collagen (ICTP) as a prognostic tumor marker in patients with esophageal squamous cell carcinoma. *Cancer.* (2002) 94:940–9. doi: 10.1002/cncr.10267
118. Jääskeläinen A, Jukkola A, Risteli J, Haapasaari KM, Karihtala P. Elevated preoperative serum levels of collagen I carboxyterminal telopeptide predict better outcome in early-stage luminal-B-like (HER2-negative) and triple-negative subtypes of breast cancer. *Tumor Biol.* (2019) 13:554. doi: 10.1177/1010428319847081
119. Liu B, Zhao Y, Yuan J, Zeng L, Sun R, Meng X, et al. Elevated N-telopeptide as a potential diagnostic marker for bone metastasis in lung cancer: A meta-analysis. *PLoS ONE.* (2017) 12:693–8. doi: 10.1371/journal.pone.0187860
120. Jablonka F, Alves B da CA, de Oliveira CGB, Wroclawski ML, Szwarc M, Vitória W de O, et al. Serum crosslinked-N-terminal telopeptide of type I collagen (NTx) has prognostic implications for patients with initial prostate carcinoma (PCa): A pilot study. *Clin Chim Acta.* (2014) 18:7–15. doi: 10.1016/j.cca.2014.06.025
121. Tamiya M, Kobayashi M, Morimura O, Yasue T, Nakasuji T, Satomu M, et al. Clinical significance of the serum crosslinked N-telopeptide of type i collagen as a prognostic marker for non-small-cell lung cancer. *Clin Lung Cancer.* (2013) 111:1605–13. doi: 10.1016/j.cllc.2012.03.012
122. Plebani M, Basso D, Roveroni G, De Paoli M, Galeotti F, Corsini A. N-terminal peptide of type III procollagen: a possible predictor of colorectal carcinoma recurrence. *Cancer.* (1997) 79:1299–303. doi: 10.1002/(SICI)1097-0142(19970401)79:7<1299::AID-CNCR5>3.0.CO;2-C
123. Nielsen SH, Willumsen N, Brix S, Sun S, Manon-Jensen T, Karsdal M, et al. Tumstatin, a matrikine derived from collagen type IVα3, is elevated in serum from patients with non-small cell lung cancer. *Transl Oncol.* (2018) 130:2922–9. doi: 10.1016/j.tranon.2018.02.005
124. Willumsen N, Bager CL, Leeming DJ, Smith V, Karsdal MA, Dornan D, et al. Extracellular matrix specific protein fingerprints measured in serum can separate pancreatic cancer patients from healthy controls. *BMC Cancer.* (2013) 97:2767–75. doi: 10.1186/1471-2407-13-554
125. Willumsen N, Bager C, Karsdal MA. Matrix metalloprotease generated fragments of type VI collagen have serum biomarker potential in cancer - a proof of concept study. *Transl Oncol.* (2019) 63:1371–8. doi: 10.1016/j.tranon.2019.02.004
126. Kang CY, Wang J, Axell-House D, Soni P, Chu ML, Chipitsyna G, et al. Clinical significance of serum COL6A3 in pancreatic ductal adenocarcinoma. *J Gastrointest Surg.* (2014) 59:1865–8. doi: 10.1007/s11605-013-2326-y
127. Kantola T, Väyrynen JP, Klintrup K, Mäkelä J, Karppinen SM, Pihlajaniemi T, et al. Serum endostatin levels are elevated in colorectal cancer and correlate with invasion and systemic inflammatory markers. *Br J Cancer.* (2014) 65:509–14. doi: 10.1038/bjc.2014.456
128. Feldman AL, Pak H, Yang JC, Richard Alexander H, Libutti SK. Serum endostatin levels are elevated in patients with soft tissue sarcoma. *Cancer.* (2001) 65:608–12. doi: 10.1002/1097-0142(20010415)91:8<1525::AID-CNCR1161>3.0.CO;2-P
129. Mo HY, Luo DH, Qiu HZ, Liu H, Chen QY, Tang LQ, et al. Elevated serum endostatin levels are associated with poor survival in patients with advanced-stage nasopharyngeal carcinoma. *Clin Oncol.* (2013) 25:308–17. doi: 10.1016/j.clon.2012.11.009
130. Aref S, El-Sherbiny M, Azmy E, Goda T, Selim T, El-Refaie M, et al. Elevated serum endostatin levels are associated with favorable outcome in acute myeloid leukemia. *Hematology.* (2008) 2:23–32. doi: 10.1179/102453308X315898
131. Szarvas T, László V, Vom Dorp F, Reis H, Szendröi A, Romics I, et al. Serum endostatin levels correlate with enhanced extracellular matrix degradation and poor patients' prognosis in bladder cancer. *Int J Cancer.* (2012) 35:233–42. doi: 10.1002/ijc.26343
132. Bono P, Teerenhovi L, Joensuu H. Elevated serum endostatin is associated with poor outcome in patients with non-Hodgkin lymphoma. *Cancer.* (2003) 15:38–47. doi: 10.1002/cncr.11399
133. Zhu YY, Wu HM, Liu RY. Diagnostic values of sVEGFR-1 and endostatin in malignant pleural effusions in patients with lung cancer. *Clin Lab.* (2017) 37:878–87. doi: 10.7754/Clin.Lab.2017.170217
134. Li M, Liu FG, Sun P, Gao YJ, Chen HY, Liu HY, et al. Correlations between serum levels of vascular endothelial growth factor and endostatin with clinical pathological characteristics of patients with gastrointestinal cancers. *Hepatogastroenterology.* (2012) 59:1865–8. doi: 10.5754/hge10602

135. Thorlacius-Ussing J, Kehlet SN, Rønnow SR, Karsdal MA, Willumsen N. Non-invasive profiling of protease-specific elastin turnover in lung cancer: biomarker potential. *J Cancer Res Clin Oncol.* (2019) 199:1933–941. doi: 10.1007/s00432-018-2799-x
136. Kuratomi Y, Sato S, Monji M, Shimazu R, Tanaka G, Yokogawa K, et al. Serum concentrations of laminin γ2 fragments in patients with head and neck squamous cell carcinoma. *Head Neck.* (2008) 583:3027–32. doi: 10.1002/hed.20838
137. Katayama M, Kamihagi K, Hirai S, Kurome T, Murakami K, Hino F, et al. Urinary laminin fragments as a tumour marker potentially reflecting basement membrane destruction. *Br J Cancer.* (1992) 7:42057. doi: 10.1038/bjc.1992.105
138. Nakano T, Iwahashi N, Maeda J, Hada T, Higashino K. Serum laminin P1 in small cell lung cancer: a valuable indicator of distant metastasis? *Br J Cancer.* (1992) 14:e0217550. doi: 10.1038/bjc.1992.123
139. Abou Farha KMM, Menheere PPCA, Nieman FHM, Janknegt RA, Arends JW. Urine laminin p1 assessment discriminates between invasive and noninvasive urothelial cell carcinoma of the bladder. *Urol Int.* (1993) 12:479–80. doi: 10.1159/000282545
140. Chang JW, Kang UB, Kim DH, Yi JK, Lee JW, Noh DY, et al. Identification of circulating endorepellin LG3 fragment: Potential use as a serological biomarker for breast cancer. *Proteomics Clin Appl.* (2008) 290:26103–13. doi: 10.1002/prca.200780049
141. Rangel MP, de Sá VK, Prieto T, Martins JRM, Olivieri ER, Carraro D, et al. Biomolecular analysis of matrix proteoglycans as biomarkers in non small cell lung cancer. *Glycoconj J.* (2018) 35:233–42. doi: 10.1007/s10719-018-9815-x
142. Naboulsi W, Megger DA, Bracht T, Kohl M, Turewicz M, Eisenacher M, et al. Quantitative tissue proteomics analysis reveals versican as potential biomarker for early-stage hepatocellular carcinoma. *J Proteome Res.* (2016) 4:64. doi: 10.1021/acs.jproteome.5b00420
143. Chida S, Okayama H, Noda M, Saito K, Nakajima T, Aoto K, et al. Stromal VCAN expression as a potential prognostic biomarker for disease recurrence in stage II-III colon cancer. *Carcinogenesis.* (2016) 9:19006–13. doi: 10.1093/carcin/bgw069
144. Kulbe H, Otto R, Darb-Esfahani S, Lammert H, Abobaker S, Welsch G, et al. Discovery and validation of novel biomarkers for detection of epithelial ovarian cancer. *Cells.* (2019) 21:838–47. doi: 10.1136/ijgc-2019-ESGO.197
145. Hope C, Emmerich PB, Papadas A, Pagenkopf A, Matkowskyj KA, Van De Hey DR, et al. Versican-derived matrikines regulate Batf3-dendritic cell differentiation and promote T cell infiltration in colorectal cancer. *J Immunol.* (2017) 38:741–67. doi: 10.4049/jimmunol.1700529
146. Kim JH, Park SC. Syndecan-2 methylation as a new biomarker for early detection of colorectal neoplasm. *Gut Liver.* (2018) 5:e1129483. doi: 10.5009/gnl18286
147. Park YS, Kim DS, Cho SW, Park JW, Jeon SJ, Moon TJ, et al. Analysis of syndecan-2 methylation in bowel lavage fluid for the detection of colorectal neoplasm. *Gut Liver.* (2018) 10:85–91. doi: 10.5009/gnl17357
148. Lendorf ME, Manon-Jensen T, Kronqvist P, Multhaupt HAB, Couchman JR. Syndecan-1 and syndecan-4 are independent indicators in breast carcinoma. *J Histochem Cytochem.* (2011) 107:569–75. doi: 10.1369/0022155411405057
149. Melo SA, Luecke LB, Kahlert C, Fernandez AF, Gammon ST, Kaye J, et al. Glypican-1 identifies cancer exosomes and detects early pancreatic cancer. *Nature.* (2015) 523:177–82. doi: 10.1038/nature14581
150. Herreros-Villanueva M, Bujanda L. Glypican-1 in exosomes as biomarker for early detection of pancreatic cancer. *Ann Transl Med.* (2016) 55:20–5. doi: 10.3978/j.issn.2305-5839.2015.10.39
151. Lai X, Wang M, McElyea SD, Sherman S, House M, Korc M. A microRNA signature in circulating exosomes is superior to exosomal glypican-1 levels for diagnosing pancreatic cancer. *Cancer Lett.* (2017) 81:522–31. doi: 10.1016/j.canlet.2017.02.019
152. Zhou X, Yan T, Huang C, Xu Z, Wang L, Jiang E, et al. Melanoma cell-secreted exosomal miR-155-5p induce proangiogenic switch of cancer-associated fibroblasts via SOCS1/JAK2/STAT3 signaling pathway. *J Exp Clin Cancer Res.* (2018) 17:482–93. doi: 10.1186/s13046-018-0911-3
153. Frampton AE, Prado MM, López-Jiménez E, Fajardo-Puerta AB, Jawad ZAR, Lawton P, et al. Glypican-1 is enriched in circulating-exosomes in pancreatic cancer and correlates with tumor burden. *Oncotarget.* (2018) 139:59–64. doi: 10.18632/oncotarget.24873
154. Lu H, Niu F, Liu F, Gao J, Sun Y, Zhao X. Elevated glypican-1 expression is associated with an unfavorable prognosis in pancreatic ductal adenocarcinoma. *Cancer Med.* (2017) 6:1181–91. doi: 10.1002/cam4.1064
155. Li J, Li B, Ren C, Chen Y, Guo X, Zhou L, et al. The clinical significance of circulating GPC1 positive exosomes and its regulative miRNAs in colon cancer patients. *Oncotarget.* (2017) 8:101189–202. doi: 10.18632/oncotarget.20516
156. Li J, Chen Y, Guo X, Zhou L, Jia Z, Peng Z, et al. GPC1 exosome and its regulatory miRNAs are specific markers for the detection and target therapy of colorectal cancer. *J Cell Mol Med.* (2017) 21:838–47. doi: 10.1111/jcmm.12941
157. Iwama T, Horie K, Yoshikawa T, Nobuoka D, Shimomura M, Sawada Y, et al. Identification of an H2-Kb or H2-Db restricted and glypican-3-derived cytotoxic T-lymphocyte epitope peptide. *Int J Oncol.* (2013) 42:831–8. doi: 10.3892/ijo.2013.1793
158. Nobuoka D, Yoshikawa T, Takahashi M, Iwama T, Horie K, Shimomura M, et al. Intratumoral peptide injection enhances tumor cell antigenicity recognized by cytotoxic T lymphocytes: A potential option for improvement in antigen-specific cancer immunotherapy. *Cancer Immunol Immunother.* (2013) 17:126. doi: 10.1007/s00262-012-1366-6
159. Suzuki S, Sakata J, Utsumi F, Sekiya R, Kajiyama H, Shibata K, et al. Efficacy of glypican-3-derived peptide vaccine therapy on the survival of patients with refractory ovarian clear cell carcinoma. *Oncoimmunology.* (2016) 14:102. doi: 10.1080/2162402X.2016.1238542
160. Sawada Y, Yoshikawa T, Nobuoka D, Shirakawa H, Kuronuma T, Motomura Y, et al. Phase I trial of a glypican-3-derived peptide vaccine for advanced hepatocellular carcinoma: Immunologic evidence and potential for improving overall survival. *Clin Cancer Res.* (2012) 48:256–62. doi: 10.1158/1078-0432.CCR-11-3044
161. Sawada Y, Yoshikawa T, Ofuji K, Yoshimura M, Tsuchiya N, Takahashi M, et al. Phase II study of the GPC3-derived peptide vaccine as an adjuvant therapy for hepatocellular carcinoma patients. *Oncoimmunology.* (2016) 5:e1129483. doi: 10.1080/2162402X.2015.1129483
162. Sun Z, Zhu Y, Xia J, Sawakami T, Kokudo N, Zhang N. Status of and prospects for cancer vaccines against hepatocellular carcinoma in clinical trials. *Biosci Trends.* (2016) 6:3656–68. doi: 10.5582/bst.2015.01128
163. Cortes-Dericks L, Schmid RA. CD44 and its ligand hyaluronan as potential biomarkers in malignant pleural mesothelioma: evidence and perspectives. *Respir Res.* (2017) 18:58. doi: 10.1186/s12931-017-0546-5
164. Wu RL, Sedlmeier G, Kyjacova L, Schmaus A, Philipp J, Thiele W, et al. Hyaluronic acid-CD44 interactions promote BMP4/7-dependent Id1/3 expression in melanoma cells. *Sci Rep.* (2018) 122:1972–80. doi: 10.1038/s41598-018-33337-7
165. Cyphert JM, Trempus CS, Garantziotis S. Size matters: molecular weight specificity of hyaluronan effects in cell biology. *Int J Cell Biol.* (2015) 2015:563818. doi: 10.1155/2015/563818

Conflict of Interest: The authors declare that the research was conducted in the absence of any commercial or financial relationships that could be construed as a potential conflict of interest.

The handling Editor declared a past co-authorship with one of the authors BB.

Copyright © 2020 Brassart-Pasco, Brézillon, Brassart, Ramont, Oudart and Monboisse. This is an open-access article distributed under the terms of the Creative Commons Attribution License (CC BY). The use, distribution or reproduction in other forums is permitted, provided the original author(s) and the copyright owner(s) are credited and that the original publication in this journal is cited, in accordance with accepted academic practice. No use, distribution or reproduction is permitted which does not comply with these terms.

frontiers in Oncology

ORIGINAL RESEARCH
published: 28 April 2020
doi: 10.3389/fonc.2020.00625

Impact of Extracellular Matrix Components to Renal Cell Carcinoma Behavior

Sandra Majo[1,2], *Sarah Courtois*[3], *Wilfried Souleyreau*[1,4], *Andreas Bikfalvi*[1,4] *and Patrick Auguste*[1,2]*

[1] Université de Bordeaux, Bordeaux, France, [2] INSERM, U1035, Bordeaux, France, [3] IIS Aragon, Hospital Universitario Miguel Servet, Zaragoza, Spain, [4] INSERM, U1029, Pessac, France

Renal cell carcinoma (RCC) represents the main renal tumors and are highly metastatic. They are heterogeneous tumors and are subdivided in 12 different subtypes where clear cell RCC (ccRCC) represents the main subtype. Tumor extracellular matrix (ECM) is composed, in RCC, mainly of different fibrillar collagens, fibronectin, and components of the basement membrane such as laminin, collagen IV, and heparan sulfate proteoglycan. Little is known about the role of these ECM components on RCC cell behavior. Analysis from The Human Protein Atlas dataset shows that high collagen 1 or 4A2, fibronectin, entactin, or syndecan 3 expression is associated with poor prognosis whereas high collagen 4A3, syndecan 4, or glypican 4 expression is associated with increased patient survival. We then analyzed the impact of collagen 1, fibronectin 1 or Matrigel on three different RCC cell lines (Renca, 786-O and Caki-2) *in vitro*. We found that all the different matrices have little effect on RCC cell proliferation. The three cell lines adhere differently on the three matrices, suggesting the involvement of a different set of integrins. Among the 3 matrices tested, collagen 1 is the only component able to increase migration in the three cell lines as well as MMP-2 and 9 activity. Moreover, collagen 1 induces MMP-2 mRNA expression and is implicated in the epithelial to mesenchymal transition of two RCC cell lines via Zeb2 (Renca) or Snail 2 (Caki-2) mRNA expression. Taken together, our results show that collagen 1 is the main component of the ECM that enhances tumor cell invasion in RCC, which is important for the metastasic process.

Keywords: renal cell carcinoma, extracellular matrix, migration, invasion, metalloproteinases

OPEN ACCESS

Edited by:
Hamid Morjani, Université de Reims Champagne-Ardenne, France

Reviewed by:
Miguel Ángel Medina, University of Malaga, Spain
Eswari Dodagatta-Marri, University of California, San Francisco, United States

***Correspondence:**
Patrick Auguste
patrick.auguste@inserm.fr

Specialty section:
This article was submitted to Molecular and Cellular Oncology, a section of the journal Frontiers in Oncology

Received: *12 January 2020*
Accepted: *03 April 2020*
Published: *28 April 2020*

Citation:
Majo S, Courtois S, Souleyreau W, Bikfalvi A and Auguste P (2020) Impact of Extracellular Matrix Components to Renal Cell Carcinoma Behavior. Front. Oncol. 10:625. doi: 10.3389/fonc.2020.00625

INTRODUCTION

Renal cell carcinoma (RCC) represents about 2% of all adult malignancies and 90% of all kidney tumors (1, 2). It is the most lethal urological tumor with ∼40% of patient's dead due to disease progression (3). Most of RCCs are sporadic and only 4–5% are inherited. Moreover, RCCs are highly metastatic and 25–30% of patients have metastasis at the time of diagnosis. According to the 2004 WHO classification, 12 histological subtypes are recognized with 3 main represented by clear cell renal cell carcinoma, papillary renal cell carcinoma and chromophobe renal cell carcinoma (4).

Clear cell RCC (ccRCC), the most frequent subtype with a 75% incidence, originates from proximal tubule epithelium. Cells are characterized by a clear or, occasionally eosinophil granular cytoplasm (3, 4). In the majority of the ccRCC, the Von Hippel-Lindau (VHL) gene is inactivated.

This inactivation includes gene mutation, promoter hypermethylation, loss of heterozygosity by allele deletion and concomitant alteration of the second gene. Loss of VHL deregulates and constitutively activates hypoxia-inducible factor HIF1α and HIF2α. The two transcription factors play a role in ccRCC, but seem to have opposite effects, HIF1α is acting as a tumor suppressor with an expression lost in 30–40% of tumors whereas HIF2α is acting as an oncoprotein. HIF1α and HIF2α are both implicated in angiogenesis, cell proliferation, metastasis, resistance against endoplamic reticulum (ER) and oxydative stresses (5). Nevertheless, a recent meta-analysis study from Kim and colleagues found no correlation between VHL inactivation and patient survival in ccRCC (6).

Papillary renal cell carcinoma (pRCC) is a less aggressive tumor, accounting for 10% of all RCC. They derived from distal tubule epithelium (3) and are organized in papillae with small cells arranged in a single layer (type 1 or basophilic) or with cells of higher nuclear grade, eosinophilic cytoplasm and pseudostratified nuclei (type 2 or eosinophilic) (4). Type 2 is considered as more aggressive than type 1 (7).

Chromophobe renal cell carcinoma is derived from intercalated cells of the collecting duct and represents 5% of all RCC. The tumor is composed of large cells with a clear reticulated cytoplasm and perinuclear halos, but in some variants the cytoplasm is eosinophilic. It is the less aggressive RCC subtype unless a sarcomatoid transformation occurs (3, 4).

The other RCC subtypes, such as the medullary subtype, represent <5% of all RCC and are rare.

In 1982, Fuhrman and al proposed a RCC grading system based on nuclear size and shape and on nucleolar prominence. The Fuhrman tumor grade (I–IV) is directly correlated to patient survival (8) and to metastasis (9). Nevertheless, in several studies on chromophobe RCC, no correlation between the Fuhrman nuclear grade and patient survival was found (10). Beyond the Fuhrman grade, some RCCs with extreme dedifferentiation called sarcomatoid RCC, undergo epithelial to mesenchymal transformation (EMT) and exhibit spindle cells. This sarcomatoid morphology is associated with very poor prognosis and a survival rate of 15–22% at 5 years (10).

In low grade RCC, treatment consists in partial or radical nephrectomy. Targeted- and immuno-therapies are the treatments of choice for inoperable metastatic RCC (11). Hanahan and Weinberg have proposed 10 organizing principles, called hallmarks, which are causative for tumor development and spread. Targeting one or, better, several hallmarks is thought to increase efficacy of anti-tumor therapies (12).

The tumor stroma is composed of cells (fibroblasts, mesenchymal stroma cells, pericytes, immune cells, vascular and lymphatic endothelial cells…) and extracellular matrix (ECM) (13). In RCC, several filamentous collagens are expressed and include type I (Col 1) and type III (Col 3) collagen. These are present in about half of the tumors, the remaining are represented by type V, VI, and XI collagen (14–16). The organization of the collagen fibers depends on the RCC grade. In high grade (Fuhrman grade IV) tumors fibers are aligned and the density is greater than in low grade tumors (17). Fibronectin 1 (FN1) or its alternative splicing variant EDA-FN are widely distributed in the RCC stroma (14, 16). RCC cells expressed FN1 and silencing its expression inhibits cell proliferation and invasion *in vitro* (18). Other components are derived from the basement membrane and include laminins (LNα1, β1-2, and γ1), collagen type IV (α1-2 chains), entactin (nidogen-1), tenascin-C, periostin and heparin-sulfate proteoglycans (HSPG) (14, 15, 19–21). ECM remodeling involves metalloproteinases (MMPs, mainly MMP-2, and 9) and cleavage of HSPGs by heparanase. All of these enzymes are increased in many metastatic cancers (22, 23).

In the present study, we analyzed the role of different ECM molecules (i.e., Col 1, FN1) and a mixed basement membrane components (Matrigel) in the phenotypic modulation of RCC cells.

MATERIALS AND METHODS

In silico Analysis of RCC Patient Survival in The Human Protein Atlas

The impact of high protein expression on the survival of RCC patients was analyzed using the Pathology Atlas from The Human Protein Atlas (24). The Human Protein Atlas used transcriptomic data from TCGA. For RCC, data were available for 877 patients, 528 ccRCC patients and 285 pRCC patients. Overall survival was analyzed using Kaplan-Myer plots.

RCC Cell Lines and ECM Used

The human 786-O cell line is derived from ccRCC mutated on the VHL gene (25). The human Caki-2 cell line was first classified as a ccRCC cell line. The VHL gene mutation status of this cell line is not well-defined but HIF1α and HIF2α are expressed (26). Caki-2 cells injected in mouse immunodeficient kidney develop in tumors resembling more pRCC (27). The Renca cell is a non VHL mutated ccRCC cell line derived from a spontaneous tumor in a BalbC mouse (28).

Rat tail Col 1 was obtained from Corning, bovine FN1 from Sigma Aldrich and Matrigel from Corning. Matrigel is a soluble basement membrane extract of murine Engelbreth-Holms-Swarm sarcoma tumor composed of LN, collagen IV, entactin, and HSPG where growth factors can be bind.

Cell Culture

The mouse Renca and the human 786-O and Caki-2 cell lines were cultured in complete medium (RPMI complemented with 10% Fetal Bovine Serum (FBS); 100 U/ml penicillin and 100 μg/ml streptomycin) at 37°C and 5% CO_2 in a humidified incubator.

For cell stimulation, dishes were coated with 400 μg/ml of Col 1, 5 μg/ml of FN1, or 33 μg/ml of Matrigel for 1 h at 37°C. Dishes were washes 3 times with PBS (Phosphate Buffer Saline) and used immediately.

Cell Immunolabeling

RCC cells were cultured for 24 h on glass coverslips coated or not with the different ECMs, then fixed 10 min with 4% paraformaldehyde. Coverslips were blocked 1 h with 5% BSA (Bovine Serum Albumin) and 0.3% Triton X100 in PBS and

incubated overnight at 4°C with mouse anti-β-catenin antibody diluted 1/800 (Cell Signaling Technology) in incubation buffer (1% BSA and 0.3% Triton X100 in PBS). After 3 washes in PBS, coverslips were incubated 1 h with appropriate FITC-conjugated secondary antibody, Alexa 556-conjugated Phalloïdin (1/500 dilution, FluoProbes) and DAPI (1 μg/ml, FluoProbes) in incubation buffer. After 3 washes in PBS, coverslips were mounted for microscope observation using Fluoromount G (Interchim). Cells were observed and pictures taken under a Nikon microscope.

Cell Proliferation

Ten thousand (786-O and Caki-2) or 20,000 (Renca) cells in 500 μl of complete medium were cultured for 72 h in a 24 well plate coated or not with the different ECMs. Cells were trypsinized and counted using a Coulter Particle Counter (Beckman Coulter France).

Cell Adhesion

Cell adhesion assay was performed as previously described with minor modifications (29). Briefly, cells were quickly trypsinized and washed 5 times in adhesion buffer (RPMI containing 0.1% BSA). Cells were counted, the concentration adjusted to 50,000 cells in 500 μl of adhesion buffer and leave 1 h at 37°C. Five hundred microliter of cells were deposed in a 24 well plate previously coated and blocked 30 min with 500 μl of adhesion buffer. After 1 h of incubation, dishes were washed 3 times with RPMI. Adherent cells were fixed with 4% paraformaldehyde for 10 min and nuclei were labeled 10 min with DAPI (2 μg/ml). Five pictures per dish were taken using a Zoe Fluorescent Cell Imager (Biorad). Nuclei were counted using Image J software.

TABLE 1 | Primers used in q-PCR analysis.

Target	Human sequences	Mouse sequences
MMP-2	GGAGACAAGTTCTGGAGATAC AATG	GGAGACAAGTTCTGGAGATAC AATG
	TTTGGTTCTCCAGCTTCAGGTA	TTTGGTTCTCCAGCTTCAGGTA
MMP-9	GTTCCCGGAGTGAGTTGAAC	CGTGTCTGGAGATTCGACTTGA
	TTTACATGGCACTGCCAAAGC	TGGAAACTCACACGCCAGAA
MMP-14	ACTGCCAAGCCACCCTAAGA	GCCCTCTGTCCCAGATAAGC
	CTGAGCAACGAAGACCCTCTCT	CCAGAACCATCGCTCCTTGA
Heparanase	ACTTCTTCACCCAGGAGCCG	AGTTTTACACCAAGCGGCCGC
	AGGTACGCAGGAGACAAGCC	GTATGCAGGAGATAAGCCTCTAG
Zeb1	TTACACCTTTGCATACAGAACCC	GCTGGCAAGACAACGTGAAAG
	TTTACGATTACACCCAGACTGC	GCCTCAGGATAAATGACGGC
Zeb2	GGAGACGAGTCCAGCTAGTGT	ATTGCACATCAGACTTTGAGGAA
	CCACTCCACCCTCCCTTATTTC	ATAATGGCCGTGTCGCTTCG
Snail 1	TCGGAAGCCTAACTACAGCGA	CACACGCTGCCTTGTGTCT
	AGATGAGCATTGGCAGCGAG	GGTCAGCAAAAGCACGGTT
Snail 2	CGAACTGGACACACATACAGTG	TGGTCAAGAAACATTTCAACGCC
	CTGAGGATCTCTGGTTGTGGT	GGTGAGGATCTCTGGTTTTGGTA
GAPDH	CAAGGAGTAAGACCCCTGGA	TGCCCCCATGTTTGTGATG
	AGGGGAGATTCAGTGTGGTG	TGTGGTCATGAGCCCTTCC

Cell Migration/Invasion Assays

Cell migration was assessed in two different assays, a scratch-wound assay and a Transwell assay.

For the scratch-wound assay 60,000 cells in 100 μl of complete medium were cultivated in 96-well plate ImageLock dishes coated or not with the different ECMs. When cells were at confluence the wound was performed using a Wound Maker (Essen BioScience), the cells were washed with PBS and 100 μl of complete medium were added. Cell migration was followed for 24 h using an IncuCyte system (Essen BioScience).

In the Transwell assay, 8 μm pore diameter inserts in 24-well plates (BD Falcon) were used and coated or not with the different ECMs. Twenty five thousand RCC cells in 500 μl of RPMI medium were put inside the insert. One milliliter of complete medium was used as chemoattractant. After 16 h at 37°C, cells were fixed with 4% paraformaldehyde for 20 min. After intensive PBS washes, non-migrating cells were removed. Nuclei from migrating cells were labeled with 1 μg/ml of DAPI for 20 min. After three washes, 5 photos/insert were taken and migrated cells counted with Image J software.

Gelatin Zymography

The effect of ECMs on MMP-2 and MMP-9 activity was assessed by gelatin zymography on Renca, 786-O and Caki-2 cell lines.

TABLE 2 | Kidney extracellular matrix and 5 years patient survival.

	All renal cancer	Kidney renal clear cell carcinoma: ccRCC	Kidney renal papillary cell carcinoma: pRCC
Col 1A1	− P ($7.2.10^{-12}$)	− (4.10^{-4})	− ($8.1.10^{-10}$)
Col 1A2	− P ($1.5.10^{-9}$)	− (0.0078)	− ($1.7.10^{-7}$)
FN1	− P ($3.4.10^{-8}$)	− (0.0044)	− ($1.4.10^{-7}$)
LNα1	NS (0.19)	+ (0.02)	− (0.026)
LNβ1	+ (0.029)	− (0.0021)	NS (0.27)
LNγ1	− (0.0019)	+ (0.0038)	− ($2.5.10^{-5}$)
LNβ2	+ (0.0012)	+ ($1.4.10^{-7}$)	N/A
Col 4A2	− P ($3.5.10^{-5}$)	+ (0.004)	− (0.0036)
Col 4A3	+ P ($2.5.10^{-7}$)	+ ($1.3.10^{-5}$)	NS (0.31)
Entactin (Nid1)	− P ($5.4.10^{-8}$)	+ (0.006)	− ($5.5.10^{-7}$)
HSPG2 (Perlecan)	+ (0.0012)	+ ($3.5.10^{-9}$)	− ($5.2.10^{-4}$)
Syndecan 1	NS (0.16)	NS (0.2)	NS (0.44)
Syndecan 2	+ (0.016)	+ (0.0014)	NS (0.54)
Syndecan 3	− P ($1.7.10^{-4}$)	− (0.0036)	NS (0.15)
Syndecan 4	+ P ($2.4.10^{-7}$)	NS (0.29)	+ (0.0024)
Glypican 1	NS (0.19)	− ($3.3.10^{-6}$)	− (0.02)
Glypican 2	− ($1.7.10^{-4}$)	− ($2.9.10^{-10}$)	+ (0.041)
Glypican 3	− (0.0038)	− (0.008)	− ($6.2.10^{-4}$)
Glypican 4	+ P ($1.2.10^{-5}$)	+ ($1.4.10^{-5}$)	N/A
Glypican 5	− ($1.8.10^{-6}$)	− (0.0062)	− (0.0091)
Glypican 6	+ (0.0025)	+ ($1.3.10^{-6}$)	+ (0.018)

Data were obtained from The Human Protein Atlas dataset (https://www.proteinatlas.org) for the different ECM components in RCC, ccRCC, or in pRCC. +, high expression is favorable in renal cancer; -, high expression is unfavorable in renal cancer; NS, high expression has no specific effect on patient survival; in parentheses is found the P score 5 year survival value. N/A, non applicable; P, the ECM molecule is a pronostic factor for RCC.

For this, 400,000 cells (Renca) or 300,000 cells (786-O and Caki-2) were cultured in complete medium for 24 h in 6 cm diameter petri dish coated or not with the different ECMs. Then, cells were cultured in fresh RPMI media without FBS for 24 h. Supernatants were harvested and centrifuged 10 min at 13,000 rpm. Thirty microliter of each sample in non-reducing loading buffer were loaded in 10% SDS-PAGE containing 0, 2% porcine gelatin (Sigma) and run at 100 V. Subsequently, the gel was rinsed with 2,5% Triton X-100 before being washed 4 times 15 min in 2,5% Triton X-100 at room temperature. After, the gel was rinsed with a revealing solution allowing enzymatic activity (50 mM Tris-HCl pH 7.4, 0.2 M NaCl, 10 mM $CaCl_2$) before being incubated in this solution during 48 h at 37°C under agitation. Finally, the gel was stained with 0.5% Coomassie blue solution (0.5% Coomassie blue, 5% methanol, 10% acetic acid) and treated with destaining solution (30% ethanol, 10% acetic acid) until the appearance of clear bands. The gel was photographed and active MMP-2 and MMP-9 were quantified with image J software.

RT-qPCR

Four thousand (Renca) or 300,000 (786-O and Caki-2) cells were cultivated in a 6 cm diameter dish coated or not with the different ECMs for 24 h. Total RNA was extracted using TRI Reagent (Molecular Research Center) following the manufacturer's instructions and quantified by spectrophotometry (Nanodrop, DS-11 DeNovix). Complementary DNA (cDNA) was synthesized with random primers from 500 ng of total RNA using reverse transcription kit (ThermoFisher Scientific) according to the manufacturer's instructions. The quantitative PCR was performed in duplicate on a CFX96 Real-Time System (C1000 Touch Thermal Cycler, Biorad) using TB Green Premix Ex Taq, Bulk (TaKaRa). The cycling parameters included 39 cycles of denaturation at 95°C for 30 s and annealing-elongation at 60°C for 30 s. Sequence specific primers (eurofins) designed and/or used to assess the mRNA expression of target genes are summarized in **Table 1**, and GAPDH was used as a housekeeping gene standard.

Sensibility to Drugs-MTS Cell Viability Assay

Two thousand Renca, 1,500 786-O or 1,000 Caki-2 cells in 100 µl of complete medium were cultured for 24 h on 96-well plates coated or not with the different ECMs. After removing the media, 100 µl of new media containing increasing concentrations of Pazopanib and Sorafenib [0.03 to 30 µM and 0.01 to 10 µM, respectively, for Pazopanib and Sorafenib (Enzo Life Sciences)] were added. After 24 h of treatment, 10 µL/well of MTS (Promega) were added to the cells for 2 h at 37°C. Finally, the optical density was read at 490 nm using a microplate reader (CLARIOstar^{Plus}). The results are expressed as (OD experiment—OD blank) where OD blank represent the optical density of the wells with media alone.

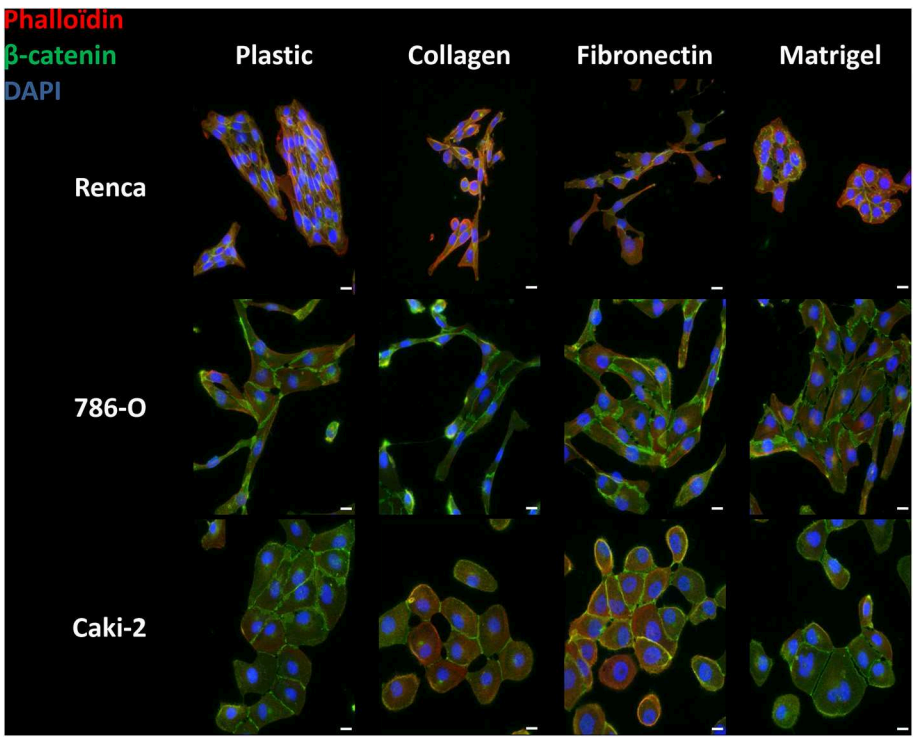

FIGURE 1 | Effect of the different ECM components on the phenotype of RCC cells. Cells were cultured for 24 h on uncoated (Plastic) or Col 1, FN1 or Matrigel glass coverslips, fixed and stained with β-catenin antibody (green), with phalloïdin (filamentous actin, red), and with DAPI (nucleus, blue). Images were captured using a Nikon microscope. Bar: 20 µm. $N = 3$.

Statistical Analysis

Statistical analysis was performed using the GraphPad Prism 5 software. Comparisons were performed with One Way ANOVA analysis of variance, followed by Dunnett's Multiple Comparison Test. ★, $P < 0.05$; ★★, $P < 0.01$; ★★★, $P < 0.001$.

RESULTS

Kidney Extracellular Matrix and 5 Years Patient Survival

We first investigated whether expression of the main components of the ECM is correlated to kidney cancer aggressiveness in The Protein Atlas dataset and analyzed the 5-years survival of kidney cancer patients. Col 1 (1A1 or 1A2) or FN1 expressions correlated with reduced survival of ccRCC and pRCC patients (**Table 2**). In contrast, ccRCC patients with higher expression of LNα1, LNγ1, Col 4A2, or entactin (Nidogen 1) have a better survival rate However for pRCC, survival was reduced in this case (**Table 2**). In addition, LNβ1, expression is correlated with reduced survival in ccRCC. Furthermore, patients with high Col 4A3 expression have better survival rate in ccRCC (**Table 2**). For HSPG, high expression of transmembrane receptors of perlecan or syndecan 2, is correlated with better survival in ccRCC patients (**Table 2**). For GPI anchored HSPG, ccRCC patients with high expression of glypican 1, 2, 3, and 5 have lower survival rate, whereas patients with high expression of glypican 4 and 6 have higher survival rate (**Table 2**).

Some highly expressed ECM components (including Col 1A1, 1A2, 4A2, FN1, entactin, syndecan 3) are of bad prognosis. However, high Col 4A3, syndecan 4, and glypican 4 expression is of good prognosis in RCC (**Table 2**).

Altogether these results suggest a negative correlation between the expression of ECM components, that are not part of the basal lamina, and 5-years survival of ccRCC and pRCC patients. On the contrary, a positive correlation was observed between several basal lamina ECM components and ccRCC patient survival. For pRCC a negative correlation was observed in this case.

Effect of the Different ECM Components on the Phenotype of RCC Cells

RCC cells were cultured for 24 h on the different ECM molecules and immunolabeled with anti-β-catenin antibody for visualization of cell-cell junctions and with phalloïdin for actin filament remodeling (**Figure 1**, **Supplementary Figures 1–3**).

On plastic and without any stimulation, Renca cells grew in clusters and exhibited cell to cell junctions. On Col 1 or FN1, Renca cell were more dissociated and fusiform with numerous

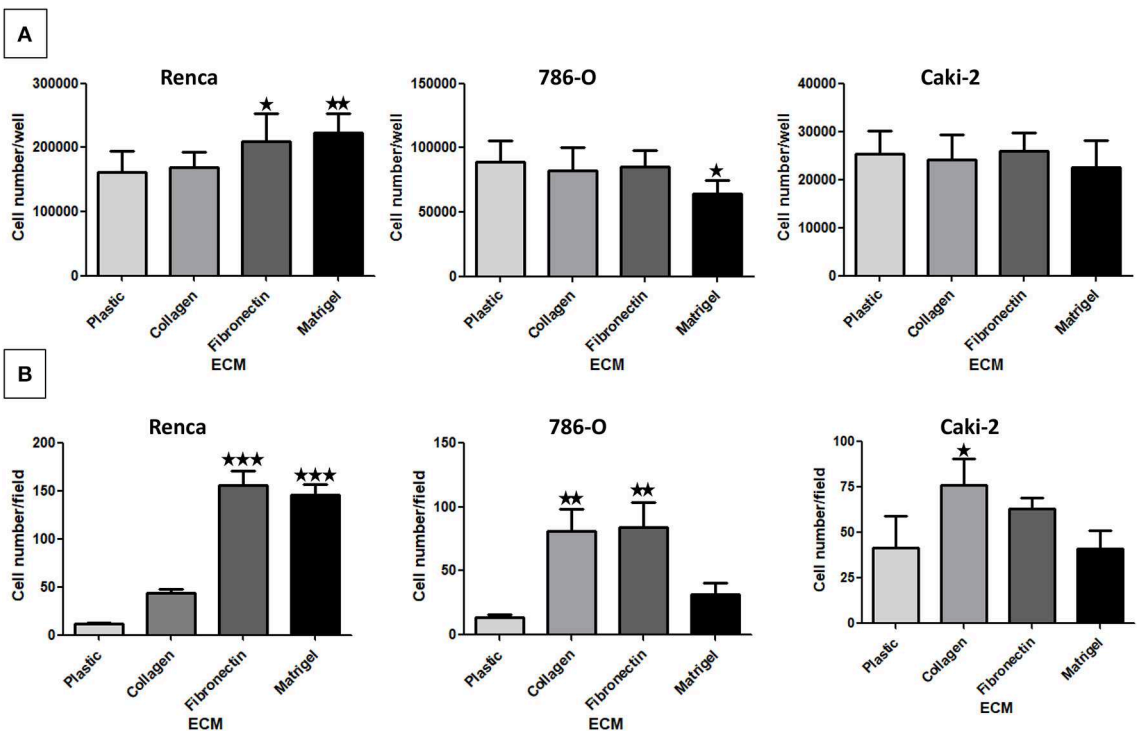

FIGURE 2 | Effect of the different ECM components on RCC cell proliferation **(A)** and adhesion **(B)**. **(A)** Renca, 786-O, and Caki-2 cells were cultured on uncoated (Plastic) or Col 1, FN1 or Matrigel coated dishes for 72 h. Then cells were detached and counted. Renca, $N = 4$; 786-O and Caki-2, $N = 3$. **(B)** Renca, 786-O, and Caki-2 cells were allowed to adhere on plastic, Col 1, FN1, or Matrigel for 1 h, fixed and nuclei labeled. Five photos per well were taken and nuclei counted using ImageJ software. $N = 3$. ★$P < 0.05$; ★★$P < 0.01$; ★★★$P < 0.001$.

membrane extensions. On Matrigel, cells grew in clusters and arrange themselves as acini. Cortical actin was not modified.

The Human RCC 786-O cell line cultured on plastic, Col 1 or FN1, acquired an elongated shape with cell-cell junctions. On Matrigel, cells were not elongated and grew in clusters. On all ECM components, only sparse cortical actin is observed. Furthermore, on Col 1, cortical actin was found at membrane extensions.

The Caki-2 RCC cell line was also tested. Caki-2 cells had a round shape and grew in clusters with β-catenin at cell-cell junctions but with little cortical actin, excepted when grown on FN1.

Taken together, different RCC cells adopted various phenotypic changes when cultured in the different ECMs.

Effect of the Different ECM Components on RCC Cell Proliferation

The impact of the ECM components on RCC cell proliferation was analyzed after 72 h (**Figure 2A**). We observed only a small increase in proliferation when Renca cells were cultured on FN1 or on Matrigel. On the other end, proliferation of 786-O cells was decreased to some extent when grown on Matrigel. No effect of the ECMs on Caki-2 proliferation was observed. Thus, ECM components had only a minor impact on the proliferation of RCC cells.

Effect of the Different ECM Components on RCC Cell Adhesion

Cell adhesion to ECM is mainly mediated by integrins (30). Cell adhesion assays were performed on the different ECMs (**Figure 2B**). Renca cell adhesion was greatly increased on FN1 and on Matrigel. Adhesion of 786-O cells was increased on Col 1 and on FN1. On the contrary, adhesion of Caki-2 cells to Col 1 was only increased to a small extent. These results show that these RCC cell types present different adhesion profiles when cultured in the different ECMs.

Effect of the Different ECM Components on RCC Cell Migration

We next performed a scratch wound assay. In this case, no significant difference in cell migration was observed for 786-O and Caki-2 cells when cultured on the different ECMs. Renca cells did not migrate efficiently in this assay (**Figure 3A**).

In the Transwell assay, cells are attracted to the lower side of the insert by serum present in the lower chamber. From the 3 cell lines, 786-O cells had a higher migrating capacity in absence of

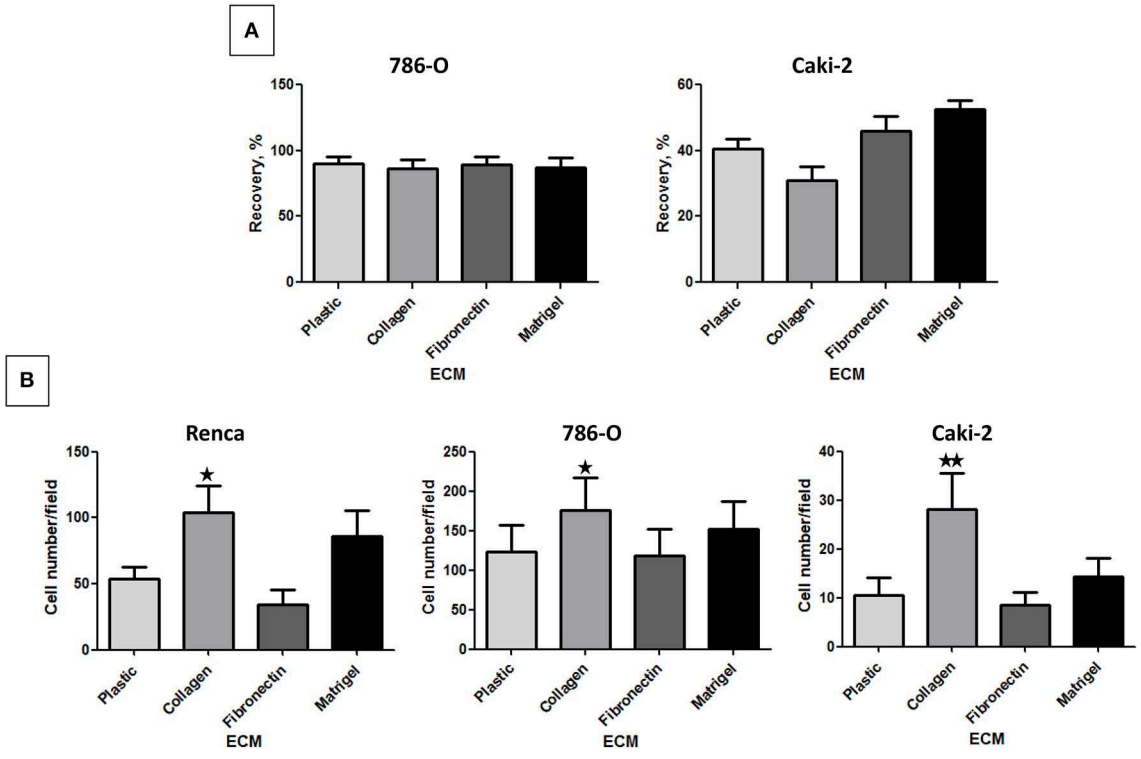

FIGURE 3 | Effect of the different ECM components on RCC cell migration. **(A)** 786-O or Caki-2 cell migration was assessed in a scratch-wound assay with cells cultured on plastic, Col 1, FN1, or Matrigel. The kinetic of the cell migration into the wound was followed using an IncuCyte system (Essen BioScience). The percentage of wound closure was obtained after 24 h of cell migration, $N = 4$. **(B)** Renca, 786-O, or Caki-2 cell migration was assessed in a Transwell assay. Filters were uncoated (Plastic) or previously coated with Col 1, FN1, or Matrigel and FBS was used as chemoattractant. After 16 h, migrated cells were fixed and nuclei labeled. Five photos per well were taken and nuclei counted using ImageJ software. Renca: $N = 4$; 786-O: $N = 5$; Caki-2: $N = 6$. ★$P < 0.05$; ★★$P < 0.01$; ★★★$P < 0.001$.

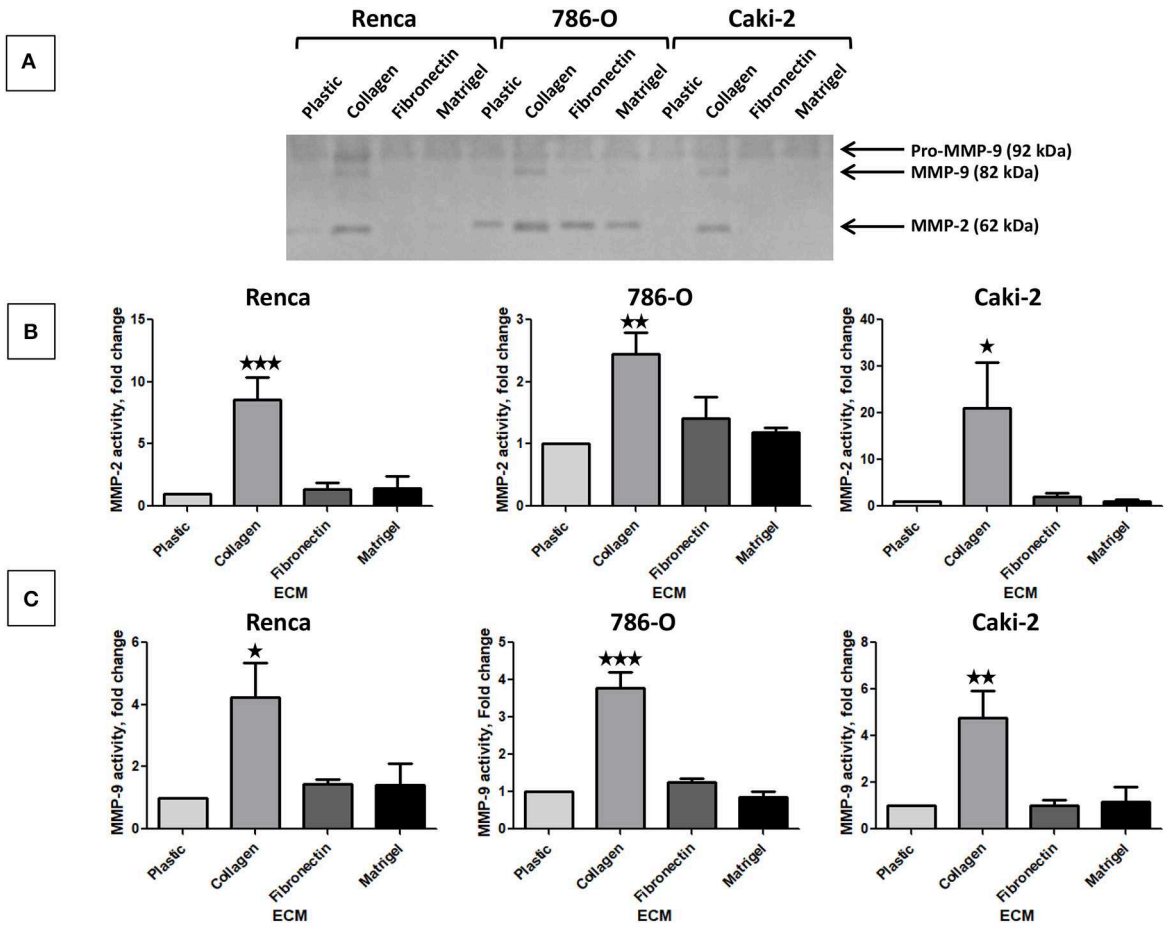

FIGURE 4 | Effect of the different ECM components on active MMP-2 and MMP-9. **(A)** gelatin zymography was assessed on supernatants of RCC cells cultured on plastic, Col 1, FN1, or Matrigel for 24 h as indicated in materiel and methods. $N = 4$, a representative gel is presented. **(B)** quantification of active MMP-2 normalized to cell grown on plastic, $N = 4$. **(C)** quantification of active MMP-9 normalized to cell grown on plastic, $N = 4$. ★$P < 0.05$; ★★$P < 0.01$; ★★★$P < 0.001$.

ECM. Col 1 was the only ECM, which significantly increased the migration of all 3 cell lines (**Figure 3B**).

Effect of the Different ECM Components on Active Proteases and on Protease Expression

The activity of secreted MMP-2 and MMP-9 was assessed by gelatin zymography using cell culture supernatants. In absence of ECM, the 3 cell lines expressed Pro-MMP-9 but active MMP-9 or MMP-2 were only detected in 786-O supernatant (**Figure 4A**). Col 1 was the only ECM molecule that increased MMP-9 and MMP-2 activity in the three cell lines. FN1 and Matrigel had no effect on MMP-9 or 2 activity (**Figures 4A–C**).

We next investigated MMP-2 and 9 mRNA by RT-qPCR analysis of RNA in RCC cells stimulated or not by the different ECM components. Because it is well-known that the activation of MMP-2 and, in some instance, of MMP-9 is MMP-14 (MT1-MMP)-dependent, we also measured MMP-14 mRNA expression (31, 32). Renca cells cultured on Col 1 exhibited an increase in MMP-2 and MMP-9 mRNA but not in MMP-14 mRNA expression (**Figure 5A**). This indicates that the increase MMP activity is mediated, at least in part, by an increase in MMP-2 or MMP-9 mRNA. 786-O and Caki-2 cells grown on the different ECMs did not showed changes in MMP mRNA expression, excepted for MMP-2 in 786-O cultured on Matrigel (**Figures 5B,C**).

Heparanase mRNA expression was quantified by RT-qPCR in RCC cells stimulated or not by the different ECM molecules. Using 2 different sets of primers, no heparanase expression was found in Renca cells. In contrast, heparanase mRNA was expressed in 786-O and Caki-2 cells but no modulation by the different ECMs was observed (**Supplementary Figure 4**).

Effect of the Different ECM Components on the Expression of Transcription Factors Implicated in EMT

We next measured the expression of mRNA of several transcription factors associated with EMT. No difference in Zeb1, 2 or Snail 1, 2 mRNA was observed in 786-O cells cultured on the different ECMs (**Supplementary Figures 5**, **6**). In contrast,

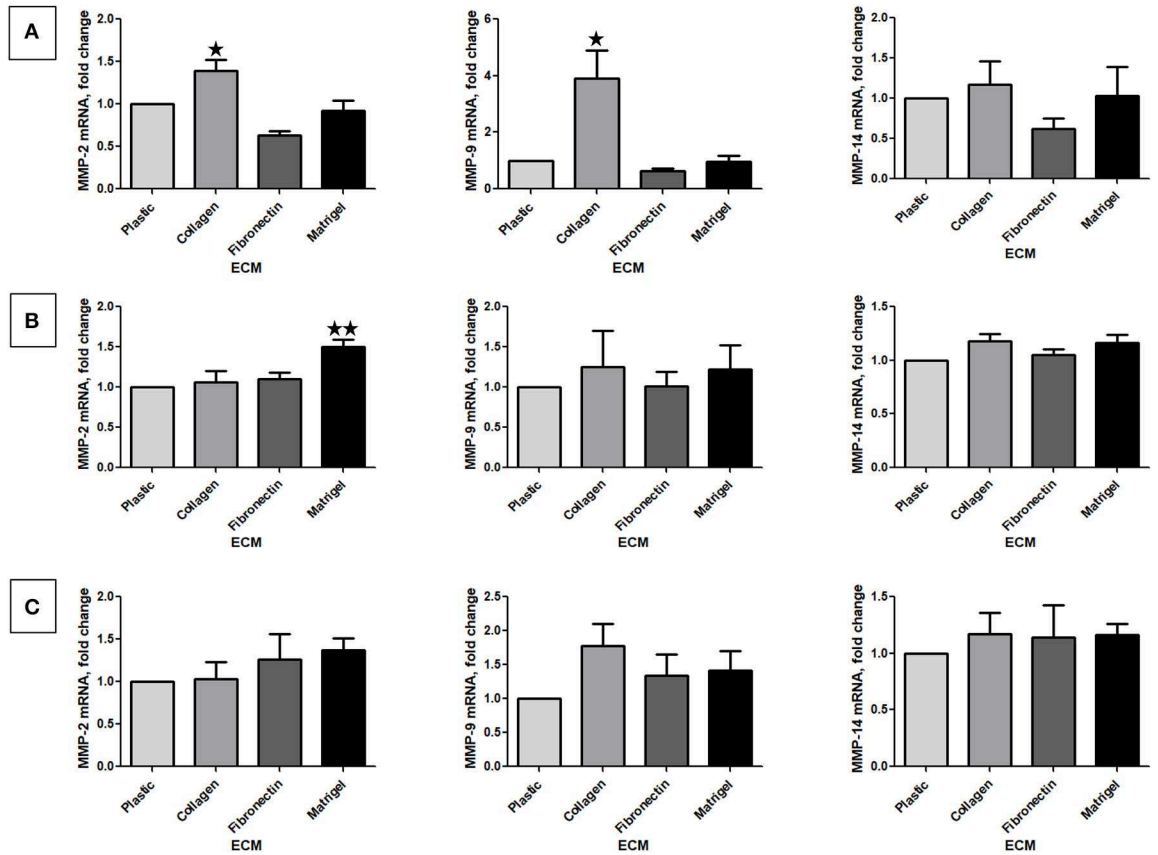

FIGURE 5 | Effect of the different ECM components on MMP-2, 9, and 14 mRNA expression. Relative mRNA levels for MMP-2, 9, and 14 were assessed by RT-qPCR after 24 h of RCC cells cultured on plastic, Col 1, FN1, or Matrigel. **(A)** Renca cells, $N = 3$. **(B)** 786-O cells, $N = 4$. **(C)** Caki-2 cells, $N = 4$. ★$P < 0.05$; ★★$P < 0.01$; ★★★$P < 0.001$.

in Renca cells, Zeb1 and Zeb2 mRNAs were upregulated, respectively, when cells were seeded on Matrigel or Col 1 (**Figure 6**). In Caki-2, Col 1 increased Snail 2 mRNA expression. In opposite, when cells were seeded on FN1 a small but significant downregulation of Snail 1 mRNA was observed (**Figure 6**). These results indicate that EMT-associated transcription factors are modulated by ECM components.

Effect of ECM on Drug Sensitivity

We next investigated whether the different ECMs may have a protective effect when cells are exposed to tyrosine-kinase inhibitors (TKI) such as Sorafenib or Pazopanib, two TKI used in clinic. Cells, seeded on the different matrices for 24 h, were incubated with increasing concentrations of Sorafenib or Pazopanib for another 24 h and cell survival was measured with MTS. As shown in **Figure 7**, ECM components had no effect on the chemosensitivity of the three RCC cell lines to this two TKI.

DISCUSSION

Analysis of the 5-year patient survival in the The Human Protein Atlas reveals a negative correlation between ccRCC and pRCC and high Col 1 expression. This is in agreement with other cancers where collagens are factors of bad prognosis, e.g., Col A1 in colorectal and breast cancers (33).

The different RCC cells adopted various phenotypic changes when cultured in the different ECMs. Cell morphology is mainly dependent on cell signaling and on ECM stiffness (34). The tumor cells, used in this study are genetically different (VHL/HIF2α) and expressed different integrins and ECM receptors. Consequently, these cells respond differently to different ECM.

In most cancers, collagen expression is related to cell migration, invasion and metastasis. Col 1 increases migration of three RCC cell lines and stimulate MMP-2 and 9 activity, two metalloproteinases implicated in cancer cell invasion and metastasis formation (22). Moreover, Col 1 increases the expression of Zeb2 in Renca cells or Snail 2 in Caki-2 cells, two transcription factors implicated in EMT. However, in 786-O cells, no increase in EMT-related transcription factors was observed. VHL is implicated in the inhibition of EMT (25) and 786-O is a VHL negative cell line. In the Renca cell line, CRISPR inactivation of VHL induced EMT (28). We postulate that, in the VHL negative 786-O, the amount of the transcription factors implicated in EMT is already too high to be regulated by Col 1.

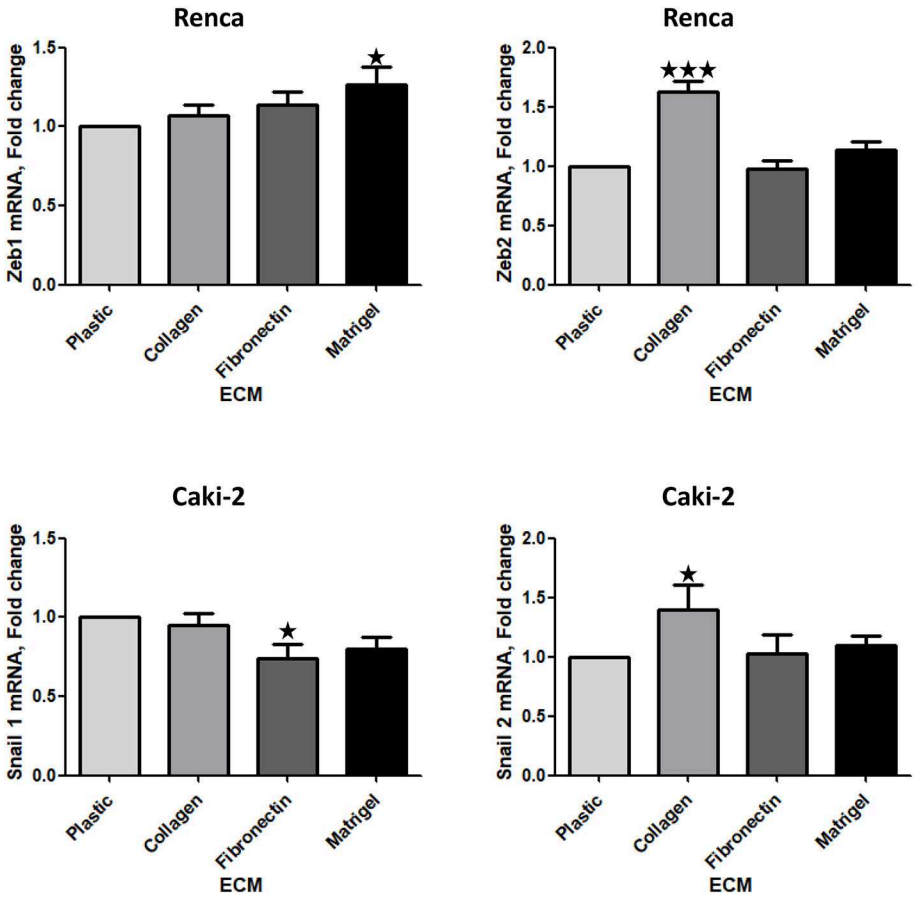

FIGURE 6 | Effect of the different ECM components on the expression of transcription factors implicated in EMT. Relative mRNA levels for Zeb1, Zeb2, Snail 1, and Snail 2 were assessed by RT-qPCR after 24 h of RCC cells cultured on plastic, Col 1, FN1, or Matrigel. Upper panels, Renca cells, $N = 7$. Lower panels, Caki-2 cells, $N = 5$. ★$P < 0.05$; ★★$P < 0.01$; ★★★$P < 0.001$.

Alternatively in this cell line, Col 1 increases the expression of other transcription factors such as Sox4 or Twist 1 (35).

Col 1 binding to their membrane receptors can directly activate EMT. Col 1 can bind to at least two types of receptors, integrins and the discoidin domain receptors, DDR1 and DDR2. Integrins and DDRs are potent EMT inducers. Col 1 binding to integrins can activate AKT and GSK3β and, in turn, directly EMT (36). DDRs exhibit tyrosine kinase activity and are implicated in cell proliferation, migration, invasion and EMT (37). Alternatively, as in lung cancer, the role of Col 1 in EMT is indirect and can be mediated via TGFβ3 expression (38). The role of DDRs in RCC development and EMT is under investigation.

High FN1 concentration correlated with poor survival in RCC patients. RCC cells exhibited increased adhesion on FN1 compare to plastic, suggesting that integrins such as αvβ3 or α5β1 are implicated (39). However, we did not evidence an effect on RCC cell migration and MMP activity. Poor survival may be alternatively related to a role of FN1 in the tumor microenvironment. It is well-known that FN1 is an RGD-motif containing protein able to bind the αvβ3 integrins present at the cell surface of endothelial cells and induces angiogenesis. Targeting angiogenesis by inhibiting FN1 binding to αvβ3 inhibits tumor angiogenesis and tumor growth in teratocarcinoma and in the ccRCC cell line 786-O (40).

With the exception of LNβ1 and glypican 1-3, 5, all the other basement membrane proteins found in RCC, e.g., LNα1, γ1, β2, Col IV, entactin, syndecan, glypican 4, and 6 and perlecan, are good prognostic factors for ccRCC but bad prognostic factors for pRCC. Matrigel, a basement membrane matrix derived from a Engelbreth-Holms-Swarm sarcoma which contains LN, Col IV, entactin and HSPG, had no significant effect on the phenotype of 786-O and Caki-2 cells. In Renca cells, Matrigel stimulated slightly cell proliferation, as well as MMP-2 and Zeb1 mRNA expression but without interfering significantly with cell migration.

Heparanase, an enzyme implicated in the degradation of HSPG is found upregulated in many cancers (23) such as in advanced-stage RCC (2, 41). Little is known about heparanase's transcription regulation, only estrogen receptor activity or inflammatory mediators TNFα or IFNα were found to increase heparanase mRNA (42). In our study, Col 1, FN1 or other

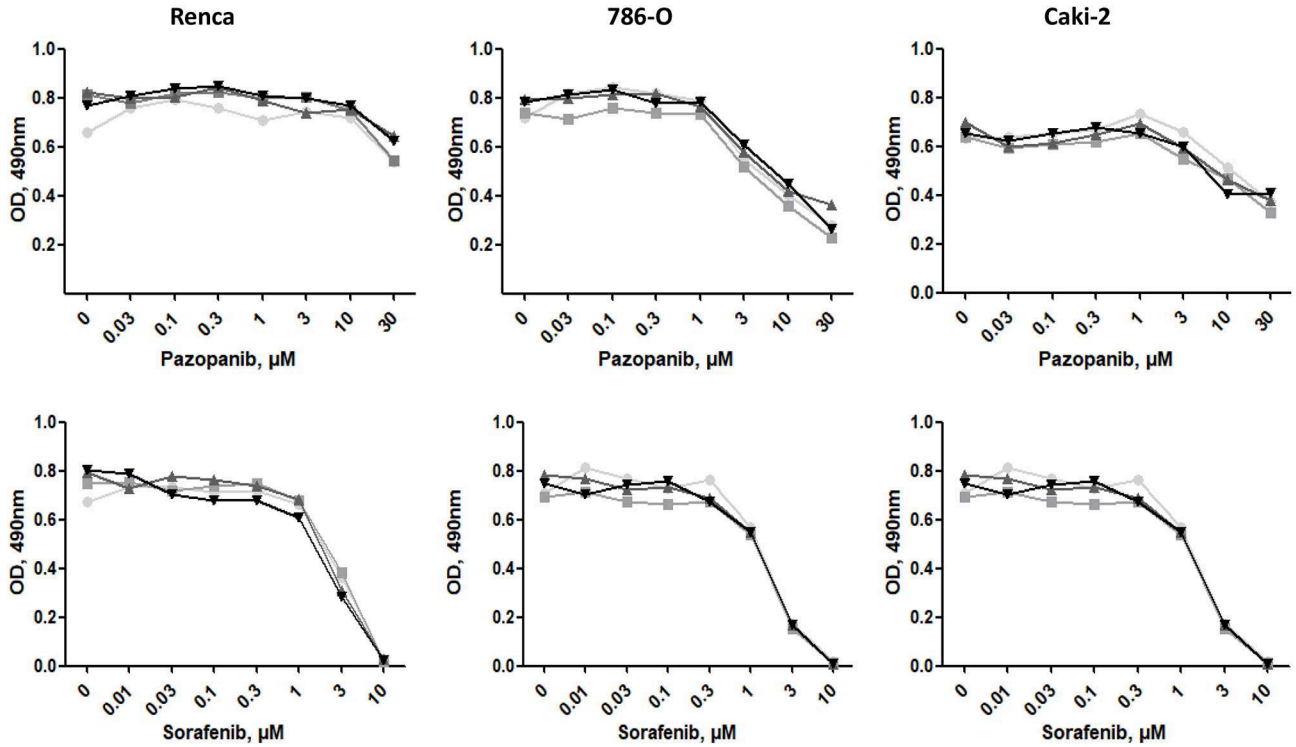

FIGURE 7 | Effect of ECM on drug sensitivity. RCC cells were cultured on plastic ●, Col 1 ■, FN1 ▲, or Matrigel ▼ for 24 h. Then, cells were treated with increasing concentrations of Pazopanib or Sorafenib for 24 h. Cell viabilities were assessed with MTS.

main components of the basement membranes, were unable to modulate heparanase expression.

It is well-known that the ECM is able to modulate the sensitivity of cells to anti-cancer drugs and that density and stiffness can inhibit accessibility of drugs to the tumor. This was particularly well-study in breast cancers (43) but little is known in RCC. *In vitro* experiments did not reveal an effect of ECM components on the sensitivity to Pazopanib and Sorafenib, two TKI commonly used in clinic. In breast cancers, ECM stiffness creates a protective barrier that reduces the accessibility to TKI (43). In our experiments, low ECM concentrations were used, which results in insufficient stiffness to create a barrier to drug accessibility.

Tumor cells adhered differently on the ECMs, indicating that different RCC cell lines do not express the same integrins. Renca cell adhesion to Col 1 is low, suggesting that α1, 2, 10, or 11/β1 are expressed at low level. On the contrary, 786-O and Caki-2 are likely to express high level of these integrins. All RCC cells adhered to FN1 suggesting a strong expression of FN1- specific integrins, such as αvβ5. Only Renca cells adhere well to Matrigel, which is in favor of high expression of LN-specific integrins such as α6β1 (39).

Taken together, we show in this study that the effect of ECM components on various RCC cell lines is heterogenous varying according to RCC cell type and matrix with Col 1 being the main enhancer of tumor cell invasion, of MMP-2 and 9 activity and consequently to metastasis.

DATA AVAILABILITY STATEMENT

All datasets generated for this study are included in the article/**Supplementary Material**.

AUTHOR CONTRIBUTIONS

SM, SC, and WS contributed to data acquisition and statistical analysis. SM prepared the manuscript. AB and PA drafted this manuscript. PA supervised the study. All authors read and approved the final manuscript.

FUNDING

This work was supported by grants from Inserm and Bordeaux University and from La Ligue Contre Le Cancer, region Aquitaine et Charentes to PA and grants from The Plan Cancer (Inserm) to AB. SM was supported by Région Nouvelle Aquitaine and by Fondation Groupama.

SUPPLEMENTARY MATERIAL

The Supplementary Material for this article can be found online at: https://www.frontiersin.org/articles/10.3389/fonc.2020.00625/full#supplementary-material

Supplementary Figure 1 | Effect of the different ECM components on the phenotype of Renca cells. Cells were cultured for 24 h on uncoated (Plastic) or Col

1, FN1, or Matrigel glass coverslips, fixed and stained with β-catenin antibody or with phalloïdin (filamentous actin). Bar: 20 μm. $N = 3$.

Supplementary Figure 2 | Effect of the different ECM components on the phenotype of 786-O cells. Cells were cultured for 24 h on uncoated (Plastic) or Col 1, FN1, or Matrigel glass coverslips, fixed and stained with β-catenin antibody or with phalloïdin (filamentous actin). Bar: 20 μm. $N = 3$.

Supplementary Figure 3 | Effect of the different ECM components on the phenotype of Caki-2 cells. Cells were cultured for 24 h on uncoated (Plastic) or Col 1, FN1, or Matrigel glass coverslips, fixed and stained with β-catenin antibody or with phalloïdin (filamentous actin). Bar: 20 μm. $N = 3$.

Supplementary Figure 4 | Effect of the different ECM components on heparanase mRNA expression. Relative mRNA levels for heparanase were assessed by RT-qPCR after 24 h of RCC cells cultured on plastic, Col 1, FN1, or Matrigel. No heparanase mRNA were detected in Renca cells. $N = 4$.

Supplementary Figure 5 | Effect of the different ECM components on the expression of Zeb1 and 2, two transcription factors implicated in EMT. Relative mRNA levels for Zeb1 **(A)** and Zeb2 **(B)** were assessed by RT-qPCR after 24 h of RCC cells cultured on plastic, Col 1, FN1, or Matrigel. 786-O cells: $N = 4$. Caki-2 cells: $N = 5$.

Supplementary Figure 6 | Effect of the different ECM components on the expression of Snail 1 and 2, two transcription factors implicated in EMT. Relative mRNA levels for Snail 1 **(A)** and Snail 2 **(B)** were assessed by RT-qPCR after 24 h of RCC cells cultured on plastic, Col 1, FN1 or Matrigel. Renca cells, $N = 7$. 786-O cells: $N = 4$.

REFERENCES

1. Mancini V, Battaglia M, Ditonno P, Palazzo S, Lastilla G, Montironi R, et al. Current insights in renal cell cancer pathology. *Urol Oncol.* (2008) 26:225–38. doi: 10.1016/j.urolonc.2007.05.017
2. Mikami S, Oya M, Mizuno R, Kosaka T, Ishida M, Kuroda N, et al. Recent advances in renal cell carcinoma from a pathological point of view. *Pathol Int.* (2016) 66:481–90. doi: 10.1111/pin.12433
3. Muglia VF, Prando A. Renal cell carcinoma: histological classification and correlation with imaging findings. *Radiol Bras.* (2015) 48:166–74. doi: 10.1590/0100-3984.2013.1927
4. Lopez-Beltran A, Carrasco JC, Cheng L, Scarpelli M, Kirkali Z, Montironi R. 2009 update on the classification of renal epithelial tumors in adults. *Int J Urol.* (2009) 16:432–43. doi: 10.1111/j.1442-2042.2009.02302.x
5. Meléndez-Rodríguez F, Roche O, Sanchez-Prieto R, Aragones J. Hypoxia-inducible factor 2-dependent pathways driving von hippel-lindau-deficient renal cancer. *Front Oncol.* (2018) 8:214. doi: 10.3389/fonc.2018.00214
6. Kim JS, Song KS, Yu IJ. Multiwall carbon nanotube-induced DNA damage and cytotoxicity in male human peripheral blood lymphocytes. *Int J Toxicol.* (2015) 35:27–37. doi: 10.1177/1091581815598749
7. Delahunt B, Eble JN. Papillary renal cell carcinoma: a clinicopathologic and immunohistochemical study of 105 tumors. *Mod Pathol.* (1997) 10:537–44.
8. Fuhrman SA, Lasky LC, Limas C. Prognostic significance of morphologic parameters in renal cell carcinoma. *Am J Surg Pathol.* (1982) 6:655–63. doi: 10.1097/00000478-198210000-00007
9. Bretheau D, Lechevallier E, de Fromont M, Sault MC, Rampal M, Coulange C. Prognostic value of nuclear grade of renal cell carcinoma. *Cancer.* (1995) 76:2543–9. doi: 10.1002/1097-0142(19951215)76:12<2543::AID-CNCR2820761221>3.0.CO;2-S
10. Delahunt B, Eble JN, Egevad L, Samaratunga H. Grading of renal cell carcinoma. *Histopathology.* (2019) 74:4–17. doi: 10.1111/his.13735
11. Bæk Møller N, Budolfsen C, Grimm D, Krüger M, Infanger M, Wehland M, et al. Drug-induced hypertension caused by multikinase inhibitors (Sorafenib, Sunitinib, Lenvatinib and Axitinib) in renal cell carcinoma treatment. *Int J Mol Sci.* (2019) 20:4712. doi: 10.3390/ijms20194712
12. Hanahan D, Weinberg RA. Hallmarks of cancer: the next generation. *Cell.* (2011) 144:646–74. doi: 10.1016/j.cell.2011.02.013
13. Roma-Rodrigues C, Mendes R, Baptista PV, Fernandes AR. Targeting tumor microenvironment for cancer therapy. *Int J Mol Sci.* (2019) 20:840. doi: 10.3390/ijms20040840
14. Lohi J, Leivo I, Oivula J, Lehto VP, Virtanen I. Extracellular matrix in renal cell carcinomas. *Histol Histopathol.* (1998) 13:785–96.
15. Droz D, Patey N, Paraf F, Chrétien Y, Gogusev J. Composition of extracellular matrix and distribution of cell adhesion molecules in renal cell tumors. *Lab Invest.* (1994) 71:710–8.
16. Boguslawska J, Kedzierska H, Poplawski P, Rybicka B, Tanski Z, Piekielko-Witkowska A. Expression of genes involved in cellular adhesion and extracellular matrix remodeling correlates with poor survival of patients with renal cancer. *J Urol.* (2016) 195:1892–902. doi: 10.1016/j.juro.2015.11.050
17. Best SL, Liu Y, Keikhosravi A, Drifka CR, Woo KM, Mehta GS, et al. Collagen organization of renal cell carcinoma differs between low and high grade tumors. *BMC Cancer.* (2019) 19:490. doi: 10.1186/s12885-019-5708-z
18. Ou YC, Li JR, Wang JD, Chang CY, Wu CC, Chen WY, et al. Fibronectin promotes cell growth and migration in human renal cell carcinoma cells. *Int J Mol Sci.* (2019) 20:2792. doi: 10.3390/ijms20112792
19. Bakhtyar N, Wong N, Kapoor A, Cutz JC, Hill B, Ghert M, et al. Clear cell renal cell carcinoma induces fibroblast-mediated production of stromal periostin. *Eur J Cancer.* (2013) 49:3537–46. doi: 10.1016/j.ejca.2013.06.032
20. Lohi J, Korhonen M, Leivo I, Kangas L, Tani T, Kalluri R, et al. Expression of type IV collagen α1(IV)-α6(IV) polypeptides in normal and developing human kidney and in renal cell carcinomas and oncocytomas. *Int J Cancer.* (1997) 72:43–9. doi: 10.1002/(SICI)1097-0215(19970703)72:1<43::AID-IJC6>3.0.CO;2-4
21. Lohi J, Tani T, Leivo I, Linnala A, Kangas L, Burgeson RE, et al. Expression of laminin in renal-cell carcinomas, renal-cell carcinoma cell lines and xenografts in nude mice. *Int J Cancer.* (1996) 68:364–71. doi: 10.1002/(SICI)1097-0215(19961104)68:3<364::AID-IJC15>3.0.CO;2-8
22. Winer A, Adams S, Mignatti P. Matrix metalloproteinase inhibitors in cancer therapy: turning past failures into future successes. *Mol Cancer Ther.* (2018) 17:1147–55. doi: 10.1158/1535-7163.MCT-17-0646
23. Masola V, Zaza G, Gambaro G, Franchi M, Onisto M. Role of heparanase in tumor progression: molecular aspects and therapeutic options. *Semin Cancer Biol.* (2019) 62:86–98. doi: 10.1016/j.semcancer.2019.07.014
24. Uhlen M, Zhang C, Lee S, Sjöstedt E, Fagerberg L, Bidkhori G, et al. A pathology atlas of the human cancer transcriptome. *Science.* (2017) 357:660. doi: 10.1126/science.aan2507
25. Iliopoulos O, Kibel A, Gray S, Kaelin WG. Tumour suppression by the human von Hippel-Lindau gene product. *Nat Med.* (1995) 1:822–6. doi: 10.1038/nm0895-822
26. Shinojima T, Oya M, Takayanagi A, Mizuno R, Shimizu N, Murai M. Renal cancer cells lacking hypoxia inducible factor (HIF)-1alpha expression maintain vascular endothelial growth factor expression through HIF-2alpha. *Carcinogenesis.* (2007) 28:529–36. doi: 10.1093/carcin/bgl143
27. Brodaczewska KK, Szczylik C, Fiedorowicz M, Porta C, Czarnecka AM. Choosing the right cell line for renal cell cancer research. *Mol Cancer.* (2016) 15:83. doi: 10.1186/s12943-016-0565-8
28. Schokrpur S, Hu J, Moughon DL, Liu P, Lin LC, Hermann K, et al. CRISPR-mediated VHL knockout generates an improved model for metastatic renal cell carcinoma. *Sci Rep.* (2016) 6:29032. doi: 10.1038/srep29032
29. Croissant C, Tuariihionoa A, Bacou M, Souleyreau W, Sala M, Henriet E, et al. DDR1 and DDR2 physical interaction leads to signaling interconnection but with possible distinct functions. *Cell Adh Migr.* (2018) 12:324–34. doi: 10.1080/19336918.2018.1460012
30. Bachmann M, Kukkurainen S, Hytönen VP, Wehrle-Haller B. Cell Adhesion by Integrins. *Physiol Rev.* (2019) 99:1655–99. doi: 10.1152/physrev.00036.2018
31. Toth M, Chvyrkova I, Bernardo MM, Hernandez-Barrantes S, Fridman R. Pro-MMP-9 activation by the MT1-MMP/MMP-2 axis and MMP-3: role of TIMP-2 and plasma membranes. *Biochem Biophys Res Commun.* (2003) 308:386–95. doi: 10.1016/S0006-291X(03)01405-0

32. Hernandez-Barrantes S, Toth M, Bernardo MM, Yurkova M, Gervasi DC, Raz Y, et al. Binding of active (57 kDa) membrane type 1-matrix metalloproteinase (MT1-MMP) to tissue inhibitor of metalloproteinase (TIMP)-2 regulates MT1-MMP processing and pro-MMP-2 activation. *J Biol Chem.* (2000) 275:12080–9. doi: 10.1074/jbc.275.16.12080
33. Xu S, Xu H, Wang W, Li S, Li H, Li T, etal. The role of collagen in cancer: from bench to bedside. *J Transl Med.* (2019) 17:309. doi: 10.1186/s12967-019-2058-1
34. Wolfenson H, Yang B, Sheetz MP. Steps in mechanotransduction pathways that control cell morphology. In: Nelson MT, Walsh K, editors. *Annual Review of Physiology,* Vol. 81. Palo Alto, CA: Annual Reviews (2019). p. 585–605. doi: 10.1146/annurev-physiol-021317-121245
35. Pastushenko I, Blanpain C. EMT transition states during tumor progression and metastasis. *Trends Cell Biol.* (2019) 29:212–26. doi: 10.1016/j.tcb.2018.12.001
36. Lamouille S, Xu J, Derynck R. Molecular mechanisms of epithelial-mesenchymal transition. *Nat Rev Mol Cell Biol.* (2014) 15:178–96. doi: 10.1038/nrm3758
37. Valiathan RR, Marco M, Leitinger B, Kleer CG, Fridman R. Discoidin domain receptor tyrosine kinases: new players in cancer progression. *Cancer Metastasis Rev.* (2012) 31:295–321. doi: 10.1007/s10555-012-9346-z
38. Shintani Y, Maeda M, Chaika N, Johnson KR, Wheelock MJ. Collagen I promotes epithelial-to-mesenchymal transition in lung cancer cells via transforming growth factor-beta signaling. *Am J Respir Cell Mol Biol.* (2008) 38:95–104. doi: 10.1165/rcmb.2007-0071OC
39. Humphries JD, Byron A, Humphries MJ. Integrin ligands at a glance. *J Cell Sci.* (2006) 119:3901–3. doi: 10.1242/jcs.03098
40. Eikesdal HP, Sugimoto H, Birrane G, Maeshima Y, Cooke VG, Kieran M, et al. Identification of amino acids essential for the antiangiogenic activity of tumstatin and its use in combination antitumor activity. *Proc Natl Acad Sci USA.* (2008) 105:15040–5. doi: 10.1073/pnas.0807055105
41. Mikami S, Oya M, Shimoda M, Mizuno R, Ishida M, Kosaka T, et al. Expression of heparanase in renal cell carcinomas: implications for tumor invasion and prognosis. *Clin Cancer Res.* (2008) 14:6055–61. doi: 10.1158/1078-0432.CCR-08-0750
42. Ilan N, Elkin M, Vlodavsky I. Regulation, function and clinical significance of heparanase in cancer metastasis and angiogenesis. *Int J Biochem Cell Biol.* (2006) 38:2018–39. doi: 10.1016/j.biocel.2006.06.004
43. Fleming JM, Yeyeodu ST, McLaughlin A, Schuman D, Taylor DK. *In situ* drug delivery to breast cancer-associated extracellular matrix. *ACS Chem Biol.* (2018) 13:2825–40. doi: 10.1021/acschembio.8b00396

Conflict of Interest: The authors declare that the research was conducted in the absence of any commercial or financial relationships that could be construed as a potential conflict of interest.

Copyright © 2020 Majo, Courtois, Souleyreau, Bikfalvi and Auguste. This is an open-access article distributed under the terms of the Creative Commons Attribution License (CC BY). The use, distribution or reproduction in other forums is permitted, provided the original author(s) and the copyright owner(s) are credited and that the original publication in this journal is cited, in accordance with accepted academic practice. No use, distribution or reproduction is permitted which does not comply with these terms.

frontiers in Oncology

REVIEW
published: 30 April 2020
doi: 10.3389/fonc.2020.00641

Shaping Up the Tumor Microenvironment With Cellular Fibronectin

Georgios Efthymiou[1], *Angélique Saint*[1,2†], *Michaël Ruff*[1†], *Zeinab Rekad*[1], *Delphine Ciais*[1] *and Ellen Van Obberghen-Schilling*[1,2*]

[1] Université Côte d'Azur, CNRS, INSERM, iBV, Nice, France, [2] Centre Antoine Lacassagne, Nice, France

Normal tissue homeostasis and architecture restrain tumor growth. Thus, for a tumor to develop and spread, malignant cells must overcome growth-repressive inputs from surrounding tissue and escape immune surveillance mechanisms that curb cancer progression. This is achieved by promoting the conversion of a physiological microenvironment to a pro-tumoral state and it requires a constant dialog between malignant cells and ostensibly normal cells of adjacent tissue. Pro-tumoral reprogramming of the stroma is accompanied by an upregulation of certain extracellular matrix (ECM) proteins and their cognate receptors. Fibronectin (FN) is one such component of the tumor matrisome. This large multidomain glycoprotein dimer expressed over a wide range of human cancers is assembled by cell-driven forces into a fibrillar array that provides an obligate scaffold for the deposition of other matrix proteins and binding sites for functionalization by soluble factors in the tumor microenvironment. Encoded by a single gene, FN regulates the proliferation, motile behavior and fate of multiple cell types, largely through mechanisms that involve integrin-mediated signaling. These processes are coordinated by distinct isoforms of FN, collectively known as cellular FN (as opposed to circulating plasma FN) that arise through alternative splicing of the *FN1* gene. Cellular FN isoforms differ in their solubility, receptor binding ability and spatiotemporal expression, and functions that have yet to be fully defined. FN induction at tumor sites constitutes an important step in the acquisition of biological capabilities required for several cancer hallmarks such as sustaining proliferative signaling, promoting angiogenesis, facilitating invasion and metastasis, modulating growth suppressor activity and regulating anti-tumoral immunity. In this review, we will first provide an overview of ECM reprogramming through tumor-stroma crosstalk, then focus on the role of cellular FN in tumor progression with respect to these hallmarks. Last, we will discuss the impact of dysregulated ECM on clinical efficacy of classical (radio-/chemo-) therapies and emerging treatments that target immune checkpoints and explore how our expanding knowledge of the tumor ECM and the central role of FN can be leveraged for therapeutic benefit.

Keywords: tumor, extracellular matrix, fibronectin, oncofetal variants, cancer hallmarks

OPEN ACCESS

Edited by:
Vasiliki Gkretsi,
European University Cyprus, Cyprus

Reviewed by:
Oliver Kepp,
Institut Gustave Roussy, France
Giuseppina Comito,
University of Florence, Italy

***Correspondence:**
Ellen Van Obberghen-Schilling
vanobber@unice.fr

† These authors have contributed equally to this work

Specialty section:
This article was submitted to Molecular and Cellular Oncology, a section of the journal Frontiers in Oncology

Received: *24 February 2020*
Accepted: *06 April 2020*
Published: *30 April 2020*

Citation:
Efthymiou G, Saint A, Ruff M, Rekad Z, Ciais D and Van Obberghen-Schilling E (2020) Shaping Up the Tumor Microenvironment With Cellular Fibronectin. Front. Oncol. 10:641. doi: 10.3389/fonc.2020.00641

INTRODUCTION

Historically, studies addressing the genesis and progression of cancer have focused on the genotype of tumor cells. In the case of carcinomas, nascently transformed epithelial cells progress to an invasive phenotype by the accumulation of mutations. However, this is only part of the story, as schematized in **Figure 1**. Tumor progression and expansion are accompanied by major changes in the tissue immediately adjacent to premalignant lesions and require reciprocal interactions between malignant epithelial cells and stromal cells. Tumor-induced alterations in the reactive stroma involving modifications in ECM composition, organization, and physical properties, have drawn increasing attention over the past few years as a more holistic view of tumor progression, complexity and heterogeneity of tumor microenvironment (TME) is being embraced and scrutinized for the discovery of novel, clinically relevant therapeutic opportunities.

The ECM proteins induced in tumor tissue are often development- and disease-specific isoforms generated by alternative splicing events. Such is the case with fibronectin (FN), as described below. Before focusing on FN and its multi-faceted role in the tumor setting, we will briefly discuss important notions and emerging themes regarding the production, organization and remodeling of ECM in tumor tissue. Numerous outstanding reviews are cited in this section to provide a more comprehensive picture of these themes.

STROMAL REPROGRAMMING THROUGH TUMOR-STROMA CROSSTALK

Tumor Matrisome

Gene expression screens have revealed that many genes encoding ECM components are dysregulated during tumor progression (3, 4). As the ECM is composed of large insoluble components, its protein composition has been detailed only recently. In an effort led by the laboratory of Richard Hynes, proteomics-based methods coupled with bioinformatics were used to define the "matrisome" of several normal and diseased tissues, including multiple tumor types (5). The computationally

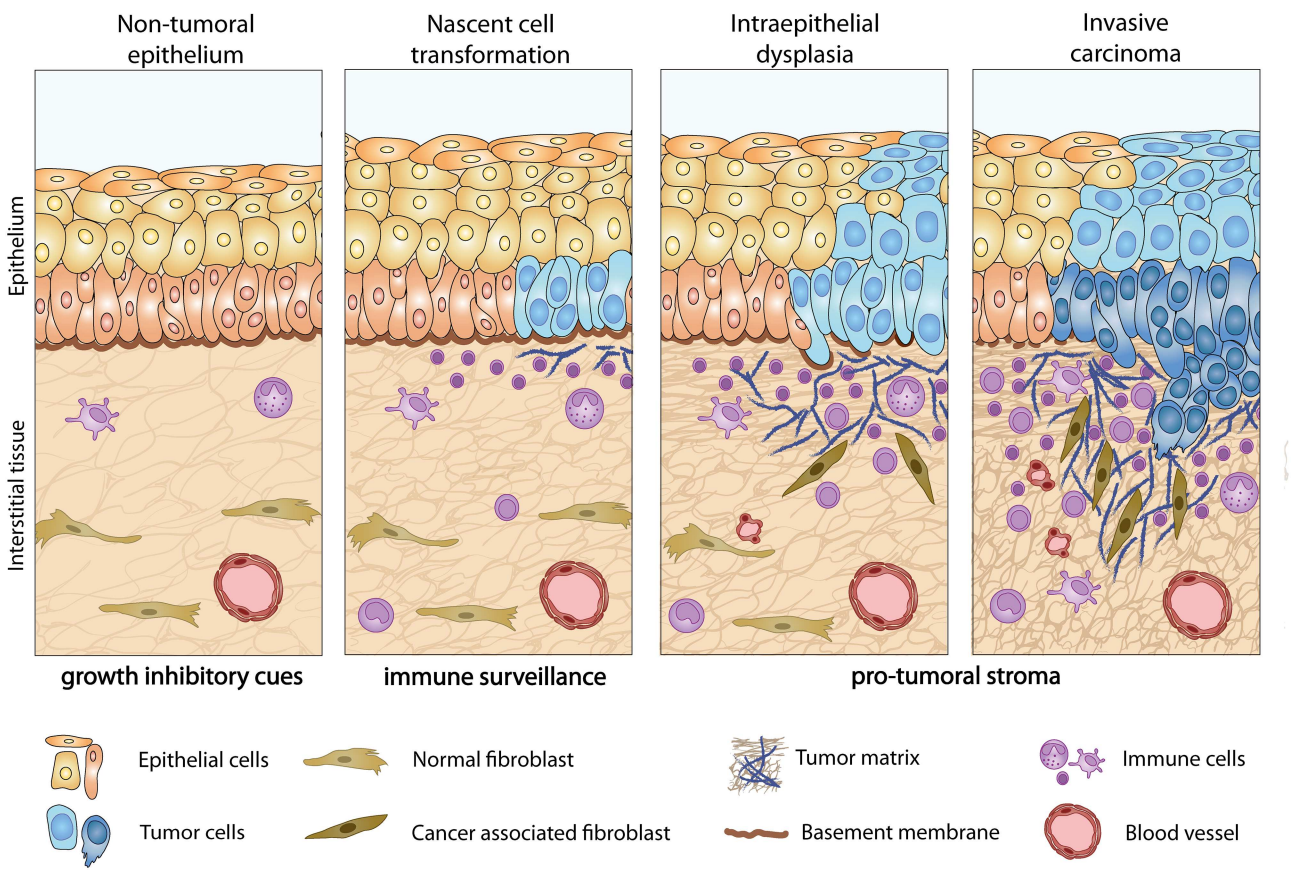

FIGURE 1 | Tumor-induced stromagenic reprogramming during carcinoma progression. In normal epithelial tissue (left) homeostatic processes and the presence of an intact basement membrane restrain tumor growth. During early stages of tumor development, nascently transformed cells release pro-inflammatory cues that recruit immune cells to the dermal-epidermal interface and stimulate a wound healing response characterized by fibroblast activation and recruitment of angiogenic blood vessels. Activated stromal cells in turn promote the invasive phenotype of tumor cells through direct and indirect mechanisms. This tumor-stroma interplay is accompanied by the upregulation of a specific set of ECM components (1) and their receptors (2), in both tumor and stromal cells.

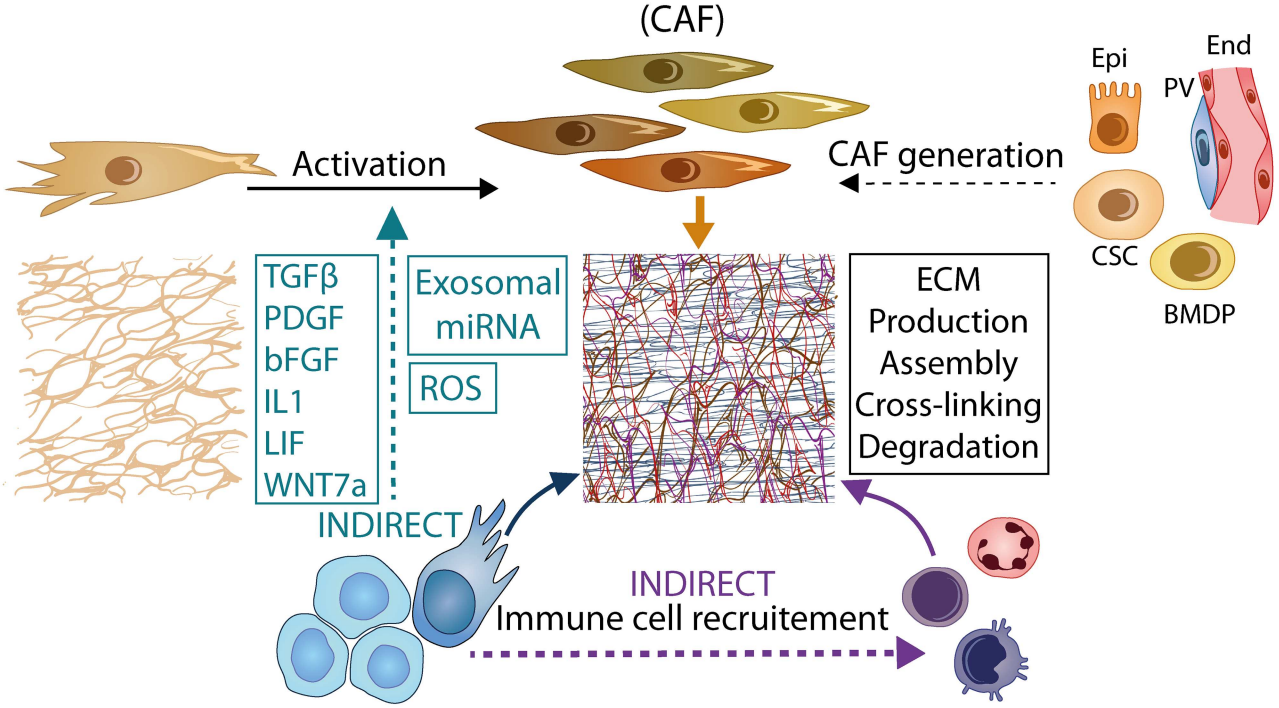

FIGURE 2 | Tumor-CAF crosstalk and molecular mediators of ECM reprogramming. Tumor cells promote the generation of CAFs from resident fibroblasts or cells of different origin through the secretion of cytokines (e.g., TGF-β, PDGF, bFGF, IL1, LIF, WNT7A), the production of ROS, and exosomal delivery of miRNA. CAFs remodel the ECM by producing, assembling, cross-linking, and degrading ECM components. Tumor cells and infiltrating immune cells are also important proponents of ECM remodeling. The complex crosstalk between tumor and stromal cells leads to a global increase in ECM abundance and stiffness which in turn amplifies CAF activation via a positive feedback loop. Epi, epithelial cells; End, endothelial cells; PV, peri-vascular cells; CSC, cancer stem cells; BMDP, bone marrow derived precursor cells.

predicted matrisome corresponds to over 1,000 genes encoding a set of 278 core components and 753 matrisome-associated proteins, of which 86% of the core matrisome proteins and 58% of the matrisome-associated components have been detected in tissues using ECM-focused proteomics strategies [see (6) for the latest Matrisome database]. Examples of upregulated ECM components in cancer include collagens, non-collagen glycoproteins (FN, tenascin C, periostin), proteoglycans (biglycan, decorin), ECM regulators (cathepsin B, LOXL), and secreted factors (TGF-β1) [reviewed in (7)], to name only a few.

Source of Tumor ECM

Fibroblasts are considered to be the major source of ECM in tumor tissue as they are abundant, highly secretory and competent for ECM assembly [reviewed in (8)]. Other stromal cells, including vascular and immune cells, contribute to tumor ECM production as well. *In vitro* and *in vivo* studies have established that matrix proteins expressed by malignant cells also become directly incorporated in the matrix. Sets of tumor cell-derived ECM proteins were elegantly identified using xenograft models in which human tumor cells were grafted in murine hosts (5, 9–11). Interestingly, in these models the ECM composition was found to differ depending on the metastatic potential of the malignant cells, their tissue of origin, and whether they were derived from primary tumors or metastases. The multicellular origin of the neoplastic ECM holds true for human tumors as well. In a single-cell transcriptomic analysis of oral squamous cell carcinomas, ECM genes that are often linked with EMT (e.g., TGFBI, LAMC2, tenascin C) were found to be upregulated in carcinoma cells. Interestingly, their expression was enhanced in a subset of tumor cells displaying a partial EMT phenotype and located in close apposition to surrounding stroma, as determined by immunohistochemistry (12). These results indicate that paracrine signals from the stromal compartment trigger ECM gene expression in leading-edge cancer cells and they suggest a role for the upregulated matrix proteins in tumor invasion. Just as stromal mediators can trigger ECM gene expression in malignant cells, malignant cells can increase matrix production in the stromal compartment by promoting the activation of normal fibroblasts, of various origins, to carcinoma-associated fibroblasts (CAFs) as schematized in **Figure 2**. In addition to reprogramming CAF precursors, cancer cells recruit immune cells to the TME, such as tumor-associated macrophages (TAMs), neutrophils, dendritic cells, natural killer cells, T and B lymphocytes (13, 14). All of these cells represent a potential source of ECM components. This has been shown for TAMs which are extremely abundant in several tumor pathologies [as

reviewed in (15, 16)]. TAMs also "enrich" the tumor matrix by secreting high levels of ECM-binding cytokines and growth factors that stimulate fibroblast activation (17).

CAF Heterogeneity

The tumor-promoting effects of CAFs have been widely investigated and include the enhancement of cell proliferation, survival, migration/invasion, angiogenesis, chemoresistance, and immunosuppression, as detailed in recent reviews (18–20). Their activity is mediated through the secretion of a plethora of growth factors, cytokines and exosomes, but also through the production and remodeling of the ECM. CAFs have been equated to myofibroblasts, or activated fibroblasts linked to wound healing and contracture (21), because they often express α-smooth muscle actin (αSMA). However, it is now clear that CAFs exist as a heterogeneous population with distinct, yet overlapping, functions. Precise characterization of CAFs has been difficult as no marker is exclusive or absolute. Various combinations of markers including but not limited to αSMA, FAP, FSP1, CAV1, IL6, VIM, ITGB1, PDGFRα/β have been used to identify CAF subtypes in different tumor tissues using flow cytometry (22, 23) and single cell transcriptomics (12, 24). However, the distinct functions of these CAF subtypes and their associated ECM are not well-characterized to date.

CAFs arise from several different cell types including resident fibroblasts, bone marrow-derived precursor cells, vascular smooth muscle cells, pericytes, cancer stem cells, as well as endothelial and certain epithelial cells via endothelial- and epithelial-to-mesenchymal transition, respectively (25–28). CAF heterogeneity is thus due in part to their diverse origin, which is still under intense investigation and undoubtedly depends on the tumor (sub)type and anatomical localization. In addition, extracellular signals from the microenvironment, in particular mediators from other cells, drive CAF heterogeneity and dynamic changes in biomarker expression. Moreover, the positioning of CAFs in time and space, with respect to tumor cells, is an important determinant underlying the generation of CAF subtypes (23, 29–31).

CAF Generation

Until recently, the activation states of CAFs have been oversimplified and reduced to normal fibroblasts and activated fibroblasts, determined by αSMA expression. However, as indicated above, the activation state of CAFs cannot be solely defined by αSMA expression since certain CAF populations display only minimal αSMA levels (30, 32, 33).

Most inducers of CAF-like phenotypes (**Figure 2**) are also involved in fibroblast conversion to myofibroblasts during fibrosis, such as TGF-β. TGF-β is a master regulator of myofibroblast and CAF generation (34, 35) and a powerful inducer of several ECM components including collagen of type I, II, III, IV, and V, FN, thrombospondin, osteopontin, tenascin C, TGFBI, periostin, elastin, hyaluronic acid, osteonectin/SPARC, as well as chondroitin/dermatan sulfate proteoglycans, such as biglycan and decorin (36–38). TGF-β not only activates resident fibroblasts but also promotes the differentiation of CAF precursors including adipose tissue-derived stem cells, endothelial cells, and bone marrow-derived mesenchymal stem cells (39).

Similar to TGF-β, platelet-derived growth factor (PDGF) and fibroblast growth factor 2 (bFGF/FGF2) play critical roles in myofibroblast activation and fibrosis (40–42). In cancer, they were found to regulate CAF activation and αSMA expression as well, although their effects varied depending on the cell types examined (32, 43–46).

Reactive oxygen species (ROS) generated by cancer cells were shown to promote the fibroblast-to-myofibroblast transition by a mechanism involving TGF-β, PDGF, and CXCL12 signaling (47). Certain cytokines are important activators of fibroblasts, such as IL1α, which triggers fibroblast differentiation in inflammatory CAFs by inducing LIF, a cytokine of the IL6 family that activates JAK/STAT signaling (29). Apart from growth factors and cytokines, cancer cells also produce extracellular vesicles containing miRNA (e.g., miR-9, miR-155, miR-211) and proteins (TGF-β, BMP, and tetraspanins) that induce fibroblast activation or CAF generation from mesenchymal stem cells [reviewed in (48)].

ECM Organization and Remodeling

In addition to the stimulation of ECM protein expression, tumor-fibroblast crosstalk profoundly impacts matrix assembly, cross-linking and remodeling. The assembly of matrix macromolecules into a 3D structure is a dynamic process largely carried out in the tumor stroma by CAFs. Fibrillar collagens are the major components of the tumor ECM and collagen architecture is severely altered in tumor tissue [see (49, 50)]. In breast cancer, distinct patterns of fibrillar collagen organization, termed "tumor-associated collagen signatures" (TACS 1–3), have been defined to classify the changes in collagen arrangement that accompany carcinoma progression (51). TACS 3, characterized by straightened and aligned collagen fibers oriented perpendicular to the tumor boundary, was found to be an independent prognostic indicator of poor survival (52). For the present review, it is important to note the interdependence of collagen and FN networks. Fibrillar assembly of FN is required for collagen fibrillogenesis (53–56). Indeed, FN is a provisional matrix molecule (57) that provides a template for deposition of not only collagen, but for several ECM components including LTBP1, fibulin, and thrombospondin [(58) and references therein] as well.

CELLULAR "ONCOFETAL" FIBRONECTIN: A KEY MULTI-REGULATORY COMPONENT OF THE TUMOR ECM

FN is a major core component of the tumor matrisome. Initially discovered as a "contaminant" in one of the steps of fibrinogen isolation more than 70 years ago (59), it is now one of the most extensively studied proteins, in terms of structural analysis and functional aspects.

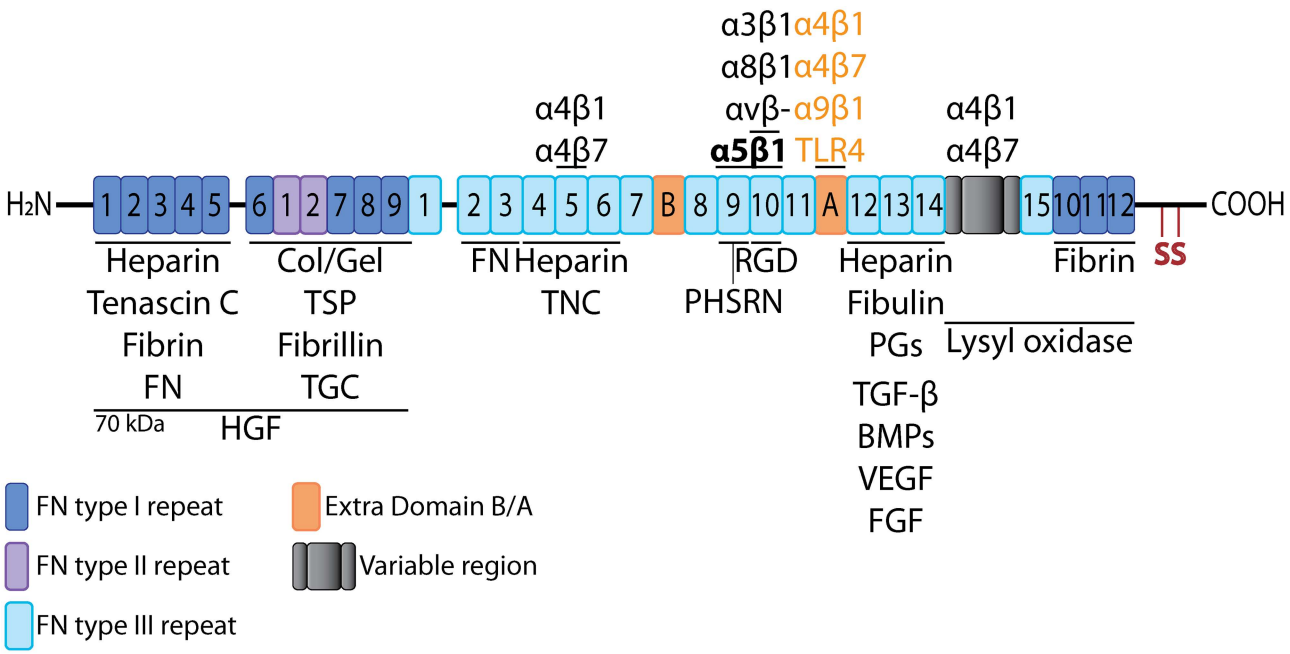

FIGURE 3 | Fibronectin linear structure. Schematic representation of the linear structure of FN molecule, showing the different types of repeats and multiple binding sites for cells and other molecules. Adapted from Xu and Mosher (62) and Van Obberghen-Schilling et al. (63). TSP, thrombospondin; Col/Gel, collagen/gelatin; PGs, proteoglycans; TGC, tissue transglutaminase.

Fibronectin Structure

FN is a high molecular weight glycoprotein composed of two similar subunits of 220–250 kDa (60, 61), linked together via disulfide bonding between two carboxy-terminal cysteine residues per subunit. FN is secreted in a soluble form by hepatocytes into the bloodstream (plasma FN, pFN), or expressed in tissues by fibroblasts and other cell types (cellular FN, cFN) forming an insoluble mesh. The primary structure of a FN subunit is characterized by the presence of three distinct types of repeats [reviewed in (62)], as schematized in **Figure 3**. There are 12 type I repeats (FNI_{1-12}), two type II repeats ($FNII_{1-2}$), and 15 (up to 17, see below) type III repeats [$FNIII_{1-15}$ (64)]. Apart from the repetitive domains, there is also a variable region (V or IIICS, type III connecting segment) that lies between $FNIII_{14}$ and $FNIII_{15}$. The V region is not addressed in this review. The reader is invited to see other works, such as Xu et al. (62), Schwarzbauer and DeSimone (65), and references therein.

FNI and FNII repeats are composed of 45 and 60 amino acids, respectively, and they contain cysteine residues that form intra-domain disulfide bonds (66, 67). By contrast, FNIII repeats are composed of 90 amino acids, they contain no cysteines, and are organized in two antiparallel β-sheets folded in a sandwich-like conformation with a hydrophobic core (68–71). This structure results in a compact form that can be extended when strain is applied (72). There are 15 FNIII domains present in every FN monomer, and two additional domains termed Extra Domains (EDB and EDA) that are only included in cFN via alternative splicing, as described below.

Fibronectin Interactions and Function

The modular structure of FN and its multiple post-translational modifications result in numerous interactions with a variety of molecules that mediate cell attachment, ECM assembly, cell motility, cytoskeleton contractility, and host-pathogen interactions, to name just a few. Integrins represent the major family of cellular receptors through which FN exerts multiple functions in health and disease (73).

Integrin α5β1 is the "classic" FN receptor, that recognizes the tripeptide cell-binding site Arg-Gly-Asp (RGD) located in the $FNIII_{10}$ repeat (71, 74–76). This interaction is facilitated and further stabilized by the synergistic effect of the PHSRN site located in $FNIII_9$ (75). Binding of FN to α5β1 results in activation of the integrin, subsequently leading in Rho-mediated acto-myosin contractility that in turn promotes assembly of fibronectin into a fibrillar matrix (77–80). Integrin αvβ3 also binds the RGD site, as do α3β1, α8β1, αIIbβ3, and other αv-based integrins [reviewed in (62)], while α4β1 and α4β7 bind to specific sequences in $FNIII_5$ (81), $FNIII_{14}$ (76), and in the V region (82–84).

Apart from cell receptors, FN also interacts with ECM components via distinct sites in the FN molecule. Through the 70 kDa region (see **Figure 3**), FN binds collagen and gelatin, as well as fibrillin, and thrombospondin (85). This results in the enrichment of the provisional FN mesh with additional components of the matrisome, contributing to ECM maturation, which in turn promotes cell adhesion *in vivo*, and blood vessel morphogenesis during embryonic development and pathological angiogenesis [reviewed in (62, 63)]. The formation of the

provisional meshwork lies on the ability of FN to self-associate at three distinct regions [reviewed in (86)], promoting polymeric assembly and mediating FN fibrillogenesis (87).

FN fibrillogenesis is a multistep process that involves the modular structure of FN, interactions of FN with other molecules, and cytoskeletal rearrangements in cells that assemble it [reviewed in (80)]. In brief, FN in a compact conformation is presented to the cell surface in an autocrine or paracrine manner. FN binding to α5β1 triggers integrin activation, clustering and the recruitment of cytoplasmic partners, including ILK, PINCH, parvin, and tensin. This intracellular machinery drives Rho-mediated stress fiber formation. Cell-generated acto-myosin contractility applies strain on the FN molecule resulting in its switch from a compact to a stretched state, thereby allowing intermolecular interactions required for FN incorporation into fibrils (72, 88, 89). Furthermore, integrin clustering and formation of complexes with additional cell receptors, like syndecan-4 [reviewed in (90)] or urokinase plasminogen activator receptor [uPAR (91)], can enhance FN assembly and strengthen FN-integrin binding (91–93). Finally, longitudinal and lateral association of FN molecules to existing fibrils results in FN polymerization, probably mediated by the protein-disulfide isomerase activity of FN, located in the FNI_{12} (94).

On this polymerized FN network, many other ECM associated components are assembled, such as heparin sulfate proteoglycans via their respective binding sites (64, 95–98), enhancing adhesion and spreading (92, 99). Similarly, TNC binds to FN and fine tunes cell adhesion and motility during angiogenesis and tumor progression [reviewed in (63)]. Finally, FN acts as a scaffold upon which the bioavailability and activity of several growth factors is orchestrated (100). Interaction of FN with growth factors (e.g., members of the TGF-β superfamily, PDGF, HGF, VEGF, FGF) may impact cell migration, cell proliferation, survival signals, and angiogenesis, as downstream outcomes of their activation through mechanical or enzymatic activation (101).

Fibronectin Splicing: The Oncofetal Fibronectin Variants

The 75 kbp long human *FN1* gene is composed of 46 exons, and produces up to 20 distinct isoforms via alternative splicing [(102) and reviewed in (76)]. The first alternatively spliced region identified was the Extra Domain A (EDA, EIIIA, EDI), a FNIII repeat lying between $FNIII_{11}$ and $FNIII_{12}$, followed by the discovery of Extra Domain B (EDB, EIIIB, EDII) between $FNIII_7$ and $FNIII_8$ (103–106). Extra Domains are encoded by a single exon each, and they are only present in the cFN. Conversely, pFN lacks both Extra Domains.

Regulation of FN splicing depends strictly on tissue type and developmental stage, and it is tightly coupled to the activity of members of the SR protein family [(e.g., SRSF3, SRSF5) reviewed in (107)]. pFN is expressed throughout the entire lifespan of the organism, though declining with age (108–110). In contrast, cFN expression is elevated during embryonic development but diminishes significantly after birth (111–113). Intriguingly, cFN is re-expressed during the adult life under certain conditions that involve TGF-β signaling. Such conditions include tissue repair, fibrosis, angiogenesis, and cancer (114–117). Accordingly, increased SRSF3 and SRSF5 expression correlates with certain types of cancers [i.e., oral squamous cell carcinoma (118, 119)] and TGF-β signaling has been shown to regulate their expression (120), similar to that of cFNs (121–123). In light of the restricted expression of Extra Domain-containing FN, the hypernym "oncofetal FN" was used in the early 1980s to collectively describe these FN variants.

Functional Roles of the Extra Domains

Despite extensive research, the precise functional properties of EDB and EDA have yet to be fully deciphered. Non-exhaustive lists of *in vitro* and *in vivo* studies regarding EDB and EDA functions can be found in Muro et al. (124) and To and Midwood (125).

A series of elegant approaches have shed light in the functions of EDB and EDA. In two independent *in vivo* studies, mice expressing FN with constitutively included or excluded EDA were generated. All animals were viable and developed normally. However, mice lacking EDA displayed abnormal and delayed skin wound healing, and decreased motor coordination abilities, while mice constitutively expressing EDA showed a pronounced decrease in the level of FN in all tissues and decreased locomotory activity (126, 127). Interestingly, both mouse strains had shorter lifespans compared to control littermates (126). By contrast, deletion of EDB displayed no significant phenotype in mouse development and fertility, but fibroblasts extracted from EDB-null mice grew more slowly *in vitro*, and were less efficient at depositing and assembling FN (128). Most importantly, absence of both Extra Domains was deleterious for the organism due to severe cardiovascular defects (e.g., vascular leakage, defective angiogenesis) (129) suggesting that the Extra Domains have overlapping functions during embryonic development, and at least one of the two is necessary for normal body growth.

In disease-challenged situations in the adult, when cFN expression reappears, both Extra Domains have been correlated with a pro-fibrotic tissue landscape. More specifically, increased expression of FN-EDA resulted in differentiation of normal lipocytes to myofibroblast-like cells (115) and this phenotype was mediated by TGF-β1 (130). Furthermore, absence of EDA-containing FN in an idiopathic pulmonary lung fibrosis mouse model resulted in less collagen deposition and fewer α-SMA expressing myofibroblasts. This effect correlated with diminished activation of TGF-β suggesting that EDA is implicated in latent TGF-β activation (124). Most importantly, the presence of EDA highly correlated with enhanced matrix remodeling, matrix metalloproteinase (MMP) expression, and re-organization of the actin cytoskeleton (131), pointing toward a pro-fibrotic role for EDA. Similar findings were obtained in a tumoral context when tumor sections were found to be enriched in FN-EDB and FN-EDA in newly formed blood vessels of the tumor (132, 133). Reinforcing the potential tumorigenic role of cFN, EDA-containing FN induced G1-S phase transition by increasing the expression of Cyclin D1 and upregulation of integrin-mediated mitogenic signal transduction (134).

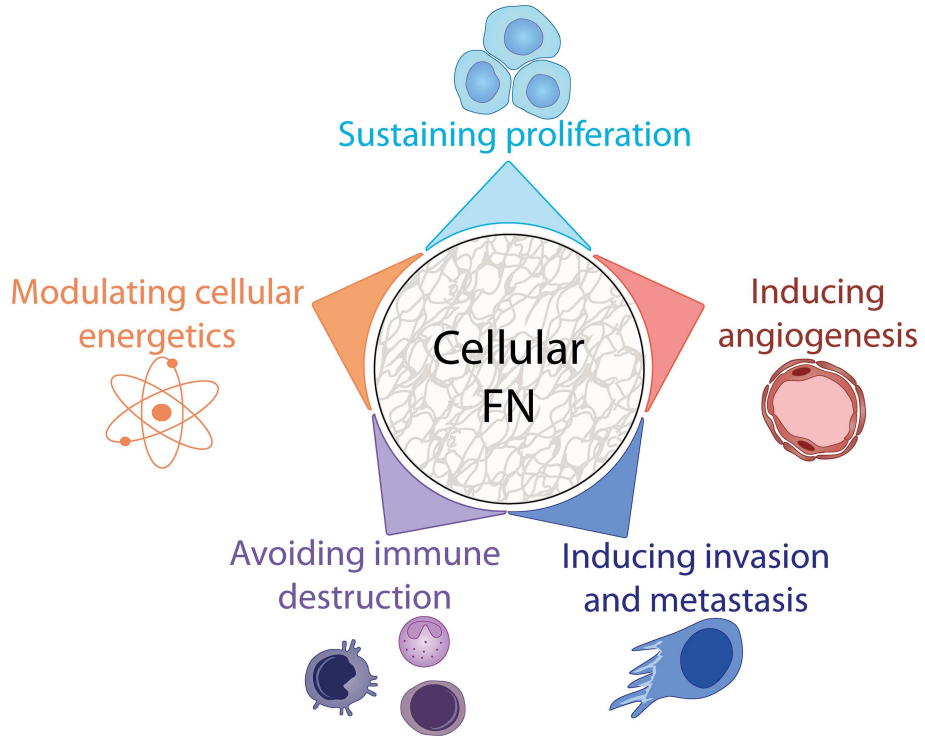

FIGURE 4 | Involvement of cFN in cancer hallmarks. FN participates in tumor progression by impacting several enabling hallmarks of cancer, see text for details.

The aforementioned effects may be due in part to the increased cell receptor repertoire of cFN compared to pFN. More specifically, EDA contains an EDHIGEL sequence that has been identified as a binding site for integrins α4β1, α4β7, and α9β1 (135, 136). Furthermore, EDA is a ligand and activator of toll-like receptor 4 (TLR4) (137), thus triggering immune responses, described in subsequent sections. Conversely, no receptor has been identified so far for EDB, though a role has been suggested for EDB in osteoblast differentiation involving a β1-containing integrin (138).

cFN AND THE HALLMARKS OF CANCER

A major finding during the early days of FN research was that surface fibroblast antigen (SFA), as FN was named at the time, was significantly reduced in quantity upon malignant transformation of chicken and human fibroblasts infected with Rous Sarcoma Virus (RSV) (139, 140). However, it is now widely acknowledged that FN is strongly upregulated in several different tumor types. As the "malignant cell-centric" view of tumors shifted in recent years to a more inclusive view that encompasses their microenvironment, reports of the tumor suppressive functions of FN have been replaced by reports of its positive role in tumor growth and metastasis [reviewed in (86)]. This can be at least partly explained by the role of FN as a provisional matrix component promoting the formation of a primed TME that sustains cancer cell survival, stimulates proliferation, migration, angiogenesis and immune modulation (**Figure 4**). In this section, we will comment on the implication of cFN in these processes and highlight how cFN induction at tumor sites regulates various cellular responses that characterize the cancer hallmarks defined by Hanahan and Weinberg in 2001 (141) and amended in 2011 (142).

Sustaining Proliferative Signaling and Evading Growth Suppression

Several lines of evidence have brought FN under the spotlight for its role in cell proliferation. Developmental processes, such as the establishment of antero-posterior polarity, the formation of the neural tube and mesodermally derived tissues are thought to be regulated by FN-mediated cell proliferation (143). Regarding tissue homeostasis, FN choreographs the proliferative phase of wound healing by bringing together different cells and components (144). In cancer, FN is a basic component of the tumor niche that has been shown to facilitate cancer cell proliferation and survival. *In vitro* studies have underlined the role of FN in promoting cancer cell growth, survival, and invasion in glioma (145), renal cell carcinoma (146), and gall bladder carcinoma (147). *In vivo*, it was shown that tumor cells injected in mice lacking circulating FN grew more slowly and apoptosis was increased (148). Similarly, tissue-specific depletion of FN resulted in lower tumor cell proliferation and invasion in the bone marrow (148).

One of the earliest studies on cFN variants highlighted the potency of EDA-containing FN to induce expression of cyclin D1, hyperphosphorylation of pRb and activation of ERK2 resulting in cell cycle progression (134). Similar results were obtained 10 years later when Kohan and colleagues described that recombinant EDA-containing peptides were able to induce MAPK-ERK1/2 activation and fibroblast differentiation through α4β7 binding and FAK activation (149). In a 3D cell culture system, blocking of FN-α5β1 interaction induced apoptosis in breast cancer cells via a mechanism that involves Akt, suggesting a protective role of FN for tumor cells (150). Though the authors did not directly assess the anti-apoptotic role of EDA *per se*, they hypothesized that it is the EDA-mediated strengthening of FN-α5β1 interactions (151) that results in the protective effect of FN against cell death. Finally, in two human tumor cell lines it was shown utilizing CRISPR/Cas9 technology that exclusion of EDA resulted in a pronounced decrease in cell proliferation (152).

In vivo, ovarian cancer cells displayed decreased proliferation and metastasis in mice bearing a tissue-specific deletion of *Fn1* in the lining of the peritoneal cavity. The effects were attributed to a tumor-stroma crosstalk and the participation of TGF-β signaling (153). The splicing pattern of the FN produced in control mice was not identified, but given its cellular nature, and the implication of TGF-β in Extra Domain inclusion (see previous section), addressing how normal cells residing in the TME influence tumor cells by cFN expression is a question worth-addressing.

In contrast to EDA, the role of EDB in tumor cell proliferation is largely unknown, in spite of its increased presence in the TME. In vascular endothelial cells, EDB-containing peptides were found to stimulate proliferation (154), while EDB knock-down impaired cell growth (154, 155).

Inducing Angiogenesis

FN clearly occupies a central note in the "angiome," the global protein connectivity network of genes associated with angiogenesis (156). The importance of FN in angiogenesis was first revealed by genetic studies in the mouse demonstrating that invalidation of the FN gene induces embryonic lethality (around E9.5) with cardiovascular and angiogenesis defects (143). Intriguingly, specific ablation of cFN (including both EDB and EDA domains) in mice that still express pFN also triggered defective angiogenesis leading to hemorrhagic vessels and embryonic lethality at E10.5 (129), attesting to a critical role for these cFN exons in developmental angiogenesis. The source of the cFN is also critical for its role in vascular development. In the neonatal retina, angiogenesis is regulated by endothelium-derived FN in an autocrine manner (157). This is an important notion, as FN production in endothelial cells is tightly coupled to its assembly (155), and assembly of cFN into a three-dimensional fibrillar meshwork is essential for neovessel formation (158).

Concerning the role of FN in tumor angiogenesis, results from animal models (e.g., inducible deletion, tumor xenografts) are less clear. Post-natal deletion of endothelial cFN in a spontaneous RIPTag-driven model of carcinogenesis fails to inhibit tumor angiogenesis (159, 160), suggesting a complex functional role of FN in tumor angiogenesis and partially explaining the disappointing results of targeting FN-binding integrins in the clinic, as discussed below. Nonetheless, cFN has been recognized for quite some time to be a useful marker of cancer-associated vessels (133, 161, 162). Expression of cFN is also upregulated in malignant cells of certain tumors with mesenchymal phenotypes. This is the case for glioblastoma multiforme (GBM) (163), a devastating malignancy in which cFN was shown to be expressed in both blood vessels and tumor cells (164). In addition to cell-autonomous effects of cFN on the invasive behavior of tumor cells, paracrine effects of GBM cell-derived FN enhance the recruitment of blood vessels through integrin-dependent binding to endothelial cells.

Effects of FN on endothelial cell adhesion, spreading and migration have been extensively studied *in vitro*. However, it is important to consider that beyond its role as ligand for signaling receptors on endothelial cells, FN in perivascular matrices constitutes an obligate scaffold for organization of the vessel-associated ECM and a repository for pro-angiogenic factors [reviewed in (63)]. FN can bind directly to (165) and modulate the function of VEGF (166), one of the most potent angiogenic factors. Moreover, it has been demonstrated that astrocytic derived FN promotes retinal angiogenesis by dual integrin-dependent and -independent functions on endothelial retinal cells, promoting filopodia adhesion or VEGF-induced directional tip cell migration, respectively (167). Thus, there is still much work to be done on several fronts to fully grasp the role of FN in tumor angiogenesis and how this is linked to tumor expansion, as discussed below.

Activating Invasion and Metastasis

Elevated FN expression is associated with invasive tumors and poor prognosis in many cancers [as reviewed in (55, 150, 163, 168–172), to cite a few]. However, this is not the case in all tumor pathologies and the role of FN in tumor invasion and metastasis has been controversial [(86) and references therein]. Lin and colleagues recently analyzed 72 studies published over the past four decades that address the role of cancer cell-derived FN (termed cancerous FN) and stromal FN in tumor progression (86). Interestingly, a tumor-suppressive function for cancerous FN was reported in 57.7% of the articles prior to 2000, yet only 15% since that date. Conversely, reports of a tumor- and metastasis-promoting role for cancerous FN increased from 11.5% before 2000 to 25% after 2000. Publications describing the implication of stromal FN in early tumor progression, but not late metastasis, remained constant at 30%.

These results raise the question of how FN came to be pro-tumoral. The increase in tumor-promoting effects of FN observed over the past several years is likely due to improved biological tools and approaches as well as a more holistic view of cancer. Indeed, since 2000 the field has evolved from the study of 2D cultured tumor lines and xenografts in immunocompromised mice models, to multimodal analysis of human tumors in their tissue context. The emergence of single cell transcriptomics (vs. transcriptomic studies that measure tumors in bulk) has refined the molecular signatures of tumor cells and different stromal cell populations thus providing a closer look at FN expression and function in different cell types, and across cancer types.

Moreover, former studies on tumors were largely centered on malignant cells. However, in most carcinomas FN is produced and assembled by stromal cells (173). Indeed, recent studies have shown that stromal FN participates not only in the early steps of tumor formation but also in the promotion of tumor cell motility and invasive behavior. Remodeling the matrix by CAFs is a key feature of cancer cell invasion (174). The ability of fibroblasts to induce cancer cell invasion was found to depend on the amount of FN that they produce and assemble (175). Assembly of the protein is required, as addition of soluble FN failed to promote invasion of the cancer cells through collagen gels. Once aligned by CAFs, linear arrays of FN fibers can promote directional migration of carcinoma cells (55, 176). In the case of head and neck squamous cell carcinomas, migration of tumor cell cohorts on fibroblast-derived matrices involves the cFN-binding integrin αvβ6 and is associated with the activation of latent TGF-β at the tumor-stroma interface (55, 177). Treatment of lung tumor cells with soluble FN stimulated migration and invasion via FAK/Src/PI3K/ERK as well as activation of MMP expression (178). Thus, FN can act both as a physical scaffold laying the path for tumor cell invasion, a platform for latent TGF-β activation and a ligand for activation of intra-cellular signaling pathways and subsequent induction of matrix-degrading proteases. Finally, given that FN is an exquisitely extensible molecule, tensile forces and FN-dependent mechano-signaling in the TME play a decisive role in invasion and metastasis. The topic of ECM stiffness and tissue mechanics is excellently reviewed in (89).

More Than a Marker of Epithelial to Mesenchymal Transition (EMT)

FN is a mesenchymal marker par excellence. In mesenchymal-like tumors, such as glioblastomas, FN expression and assembly by tumor cells has been shown to facilitate intercellular cohesion and collective invasion through a basement membrane-like ECM (164). FN knock-down in glioma xenografts reduced tumor growth and improved survival of implanted animals (164, 179). In epithelial tumors its expression is often used to detect mesenchymal transition (180). EMT is a complex program whereby epithelial cells loose polarity and cell-cell adhesion to acquire a mesenchymal phenotype and invasive properties [reviewed in (25, 180, 181)]. Early studies described the role of FN in EMT during chick embryo gastrulation and neurulation (182). Later, FN was associated with EMT during tumorigenesis. However, it is more than just a marker of EMT. FN can contribute to mesenchymal transition by providing a platform for integrin-dependent activation of latent TGF-β (183). Thus, at the leading edge of invasive tumors paracrine interactions between CAFs and malignant epithelial cells can promote a so-called partial EMT (pEMT) phenotype characterized by the expression of EMT-related genes in tumor cells that retain their epithelial phenotype (12). This is the case for leading edge tumor cells that express αvβ6, a cellular receptor for EDA-containing cFN. In ovarian cancer, TGF-β produced by tumor cells stimulates mesenchymal transition in mesothelial cells resulting in the upregulation of FN in the ECM of mesothelial cells which increases adhesion and invasion of the sub-mesothelial basement membrane by ovarian carcinoma cells (153).

FN in Metastasis

Circulating FN also contributes to tumor angiogenesis and metastatic spread of malignant cells. In pFN-deficient mice, obtained by conditional KO of the *Fn1* gene in the liver, von Au and colleagues showed that a decrease in pFN reduces tumor angiogenesis, tumor growth and bone metastasis through an apparent feed forward upregulation of its own production and by modulating the response to VEGF (148). Plasma FN is one of the most abundant adhesion proteins in the blood. However, it is functionally invisible to the apical surface of endothelial cells in mature blood vessels. Following injury or angiogenic stimulation, endothelial cells upregulate cFN production and become responsive to the pro-adhesive and integrin-mediated angiogenic functions of FN. In a study by Barbazan et al., FN deposits were detected on the luminal side of hepatic blood vessels in human colorectal cancer patients (184). Using a mouse model of intestinal tumor metastasis, they demonstrated that FN deposits in the hepatic vasculature facilitate the arrest of circulating tumor cells and extravasation via a mechanism involving talin-dependent integrin signaling in the tumor cells. pFN can also promote lung metastasis by forming pFN-fibrin clots that retain circulating tumor cells via integrin αvβ3 (177).

The final step of cancer progression is colonization of secondary organs. This highly rate-limiting step is critically affected by the matrix microenvironment (185). For making a hospitable home, cancer cells need to prepare the local microenvironment before they arrive at the distant secondary site referred to as the pre-metastatic niche (186). Pioneering studies from David Lyden's lab revealed the importance of bone marrow-derived cells (BMDC) in the establishment of a pre-metastatic niche for tumor cell metastasis (187). In response to soluble factors, such as VEGF or PDGF, VEGFR1-positive BMDCs are mobilized to colonize sites of future metastasis, prior to the arrival of tumor cells, by interacting with tumor-induced EDA-containing FN through α4β1 integrin. In turn, VEGFR1-positive BMDCs secrete chemokines, such as SDF1 to attract $CXCR4^+$ tumor cells to the newly formed metastatic niche. EDA-containing FN, together with tenascin C, versican and periostin have also been found in other secondary sites prior to tumor cell arrival, and may be important for recruitment of stromal cells as well as for circulating tumor cells to the pre-metastatic niche (153, 188–190).

Avoiding Immune Destruction

Tumor Promoting Inflammation

The acquisition of functional capabilities allowing survival, proliferation and spread of cancer cells, defined as hallmarks most recently by Hanahan and Weinberg (142), are rendered possible by so-called enabling characteristics. One important enabling feature that has drawn much attention over the past 20 years is the inflammatory state of tumor lesions. Chronic inflammation driven by infiltrating immune cells can empower multiple cancer hallmarks.

ECM remodeling in the tumor stroma is associated to the release of proteolytic fragments, termed "matrikines," into the microenvironment. Some of these ECM domains retain secondary structure and can display bioactivity (191)

as Damage-Associated Molecular Pattern (DAMP) molecules, endogenous activators of innate immunity (192). Toll-like receptor 4 (TLR4), a DAMP receptor initially thought to be restricted to immune cells, is present and functional on a variety of non-immune normal cells and tumor cells. TLR4 has been implicated in the development of several types of cancer and fibrosis (193, 194). As part of the anti-tumor immune response, DAMP-induced TLR4 activation triggers the production of pro-inflammatory cytokines, chemokines, and effector molecules. However, continuous TLR4 signaling results in chronic inflammation. Recombinant fragments of FN containing the EDA domain, but not the full length (soluble) protein were shown to bind and activate the TLR4 (137). Binding of EDA results in TLR4-mediated NF-κB pathway activation and subsequent production of pro-inflammatory, pro-fibrotic cytokines and MMPs (137, 195, 196).

In mesenchymal cells, TLR4 signaling leads to the stimulation of a pro-fibrotic gene program with augmented expression of tissue repair, wound healing and ECM remodeling genes, while induction of inflammatory genes is relatively weak (193). A second FN Type III domain, FNIII-1c, was shown to activate TLR4-mediated inflammatory cytokine release in human fibroblasts in synergy with the EDA domain (197). Type III domains of FN can be released from the matrix by proteolysis, or become exposed in response to mechanical forces (198). Therefore, the presence of EDA-containing cFN fragments or mechanically strained fibers in the tumor matrix landscape can trigger and sustain innate immunity, inflammation, and myofibroblast generation driven by one or more EDA-dependent inflammatory feedback loops (199).

Regulation of Anti-tumoral Immunity

The immune system is an important barrier against tumor progression. How tumor cells develop immune system-evading mechanisms and how the different immune cells interact with tumor cells is a field of intense research. In general, the presence of tumor infiltrating CD8-expressing lymphocytes in the TME is associated with an improved prognosis and a better response to therapy in a broad range of tumor types (200–205). However, the presence of immune cells with inhibitory function, such as myeloid-derived suppressor cells and regulatory T cells (Tregs) that dampen the immune control of cancer, can be associated with worse outcome [(204) and references therein]. Analysis of histological sections of tumor samples led to the segregation of cancer immune phenotypes into three distinct profiles: immune-inflamed, immune-dessert and immune-excluded (206). Immune-inflamed and immune-dessert phenotypes are generally characterized by an abundant or sparse immune infiltrate, respectively. In immune-inflamed tumors, the immune cells are positioned in proximity to the tumor cells. Immune-excluded tumors also display an abundant infiltrate but the immune cells fail to effectively penetrate the tumor parenchyma and they remain in the stroma surrounding tumor cell nests. This immune phenotype is characterized by an excessive deposition of ECM components, including dense aligned bundles of collagen and FN around tumor islets. Live-cell imaging studies on patient-derived lung tumor tissue sections revealed active T cell motility in regions of loose FN and collagen I, whereas T cells migrated poorly in dense matrix areas surrounding tumor nests (207, 208). Thus, the ECM can promote tumor evasion from the immune system by limiting the anti-tumor activity of T cells, either directly by inhibiting the contact of infiltrating immune cells with cancer cell nests (207, 209) or indirectly through the recruitment of TAMs that cause lymphocyte retention in the stroma (210). The latter mechanism, using live imaging techniques in a mouse model and on fresh human carcinoma slices, demonstrated that TAMs impede CD8-expressing T cells from reaching tumor cells by lymphocyte trapping in the stroma and consequently limit the efficacy of immune check point inhibitor (anti-PD-1) treatment. TAMs are key components of the tumor ECM microenvironment directly affecting its production and remodeling. TAMs isolated from human ovarian carcinomas (15) and from an orthotopic colorectal cancer model (16) display a gene expression profile in which matrix glycoproteins, including FN, are highly upregulated (211). Clearly, the ECM is emerging as an important component of stromal-based immunomodulatory mechanisms that alter the trafficking, maturation and function of immune cells through multiple mechanisms, many of which have yet to be uncovered. cFN is a prominent component as a provider of DAMPs, by virtue of its obligate role in activation of ECM-tethered latent TGF-β and its function as a mechanically-tuned repository of immunomodulatory cytokines and growth factors, as discussed in previous sections.

Deregulating Cellular Energetics

The metabolic shift toward aerobic glycolysis in cancer cells is a well-established phenomenon that is currently used in tumor diagnosis. During the past decade, numerous studies underlined a potential metabolic crosstalk between normal and transformed cells in the tumor niche (212). The link between the ECM and cell metabolic activity presents an emerging, compelling field of scientific research. Recently, several groups have provided evidence pinpointing toward shifts in cell metabolic processes mediated by matrix composition, stiffness, and remodeling (213–215). Moreover, physical properties of the TME, like pH regulation, are shaped by increased expression of pumps and transporters, and their transportation to the plasma membrane [reviewed in (216)]. Thus, the tumor landscape is sculpted and primed in order to promote cancer cell growth, motility and invasion. To our knowledge, no EDB- or EDA-oriented studies regarding cellular energetics have been reported. The handful of studies describing the role of FN Extra Domains in regulating metabolic processes has only been performed in non-tumoral contexts, thus whether the presence of the Extra Domains reflects reprogramming of cell energetics is an open question.

In an *in vivo* study, investigators used a diabetes-impaired endothelial vasodilation mouse model to study the effect of EDA-containing FN. Mice constitutively excluding EDA displayed increased endothelial dysfunction, and the underlying mechanism involved increased superoxide anion levels, NADPH oxidase (NOX4) expression, and TGF-β, suggesting a protective role of FN-EDA against vascular oxidative stress (217). Conversely, overexpression of FN-EDA or pFN in a mouse

monocyte macrophage cell line, dysregulated the endogenous sterol response pathway through ER stress response, though no difference was observed between cells expressing the different isoforms (218). EDB was not included in the study, and its potential involvement is thought provoking and constitutes an interesting perspective.

TARGETING THE DYSREGULATED TUMOR ECM

Potential Therapeutic Implications of FN

The striking implication of tumor ECM components and their cellular receptors in tumor progression and response to conventional and emerging therapies has led to the quest for novel TME-directed therapeutic strategies. Different approaches have been employed to target FN, or its receptors (219). The first approach pioneered by Neri et al. is based on antibody-mediated delivery of therapeutic agents to cFN isoforms present in the TME. Both EDA and EDB domains have been used for specific delivery of cytokines, cytotoxic agents, chemotherapy drugs and imaging agents to tumors expressing cFN variants [reviewed in (161, 220)]. The tumor-targeting immunocytokine L19-IL2 is a good example. It is composed of the human scFv antibody fragment (L19), specific to the EDB domain of FN, fused to recombinant human IL2. Following extensive preclinical studies, L19-IL2 immunocytokine has demonstrated therapeutic activity in advanced solid cancer (221). In combination with darcabazine, it displayed encouraging clinical activity in patients with metastatic melanoma in a phase I and II studies (222, 223). A randomized Phase IIb study was completed but not yet reported (NCT01055522). L19-IL2 was also tested in combination with radiotherapy. In a preclinical study, that combination enhance the radiotherapy-induced antitumor immune reaction and provided a long-lasting antitumor effect dependent on EDB expression and infiltration of cytotoxic T cells (224). A Phase I clinical study combining L19-IL2 with Stereotactic Ablative Body Radiotherapy (SABR) in oligometastic tumors (NCT02086721) was completed but results are not published. Additional clinical trials involving L19-derived targeting agents (L19-IL2, L19-TNF) alone or combined with other therapies are ongoing in several tumor types (see the NIH website identifier: https://clinicaltrials.gov).

EDA and EDB based vaccines appear to be promising for the treatment and prevention of cancer. Regarding the EDA domain, a fusion protein between streptavidin and the endogenous TLR4 ligand EDA showed the capacity to target biotinylated antigens to dendritic cells and induce T cell responses *in vivo* (225). As EDA is known to activate the NF-κB pathway leading to the activation of innate immune system and release of inflammatory cytokines, it has been explored as a cancer vaccine adjuvant in mouse models (195, 226, 227). Immunological activity of EDA depends upon its local intramolecular context within the FN chain. Immobilizing EDA-containing FN fragments within a fibrin matrix model along with antigenic peptides stimulates cytotoxic $CD8^+$ T cell responses in two murine cancer models (228). Thus, delivering ECM-bound FN EDA fragments in combination with antigens could be an attractive option for anti-tumoral immunotherapies.

The second approach consists of directly interrupting the pro-tumoral effects of FN by using antibodies and small-molecule inhibitors that interrupt interactions between FN and its integrin partners. Integrins as therapeutic targets have been a focus of drug development for over 3 decades, with some successes in preclinical studies in cancer. Developments in integrin-directed therapeutics in cancer and other pathologies have been reviewed in Raab-Westphal et al. (2). Integrin α5β1, the "prototype" FN receptor, is implicated in different aspects of tumor progression, and it appears particularly overexpressed in the most aggressive tumor grades. It is a pertinent therapeutic target in solid tumors and appears safe for the patients in a phase I clinical study (229). Unfortunately, in a phase II clinical study, anti-α5β1 integrin antibody volociximab tested as monotherapy in patients with platinum-resistant advanced epithelial ovarian or primary peritoneal cancer, showed insufficient clinical activity (230). In patients with refractory or relapsed metastatic clear cell renal carcinoma, volociximab led to stable decrease in 80% of patients but no randomized controlled trial has been reported so far. Integrin α4β1, a FN receptor that binds to the EDA domain and variable region of the protein, promotes the homing of monocytes to tumors, and is essential for the participation of myeloid cells in angiogenesis and tumor growth. Specific antagonists of integrin α4β1 prevented monocyte stimulation of angiogenesis *in vivo*, macrophage colonization of tumors, and tumor angiogenesis (231). However, whereas suppression of myeloid cell homing to tumors using α4β1 antagonists appears to be an effective approach to impede tumor angiogenesis and growth, depletion of the integrin in a mouse model of colon adenocarcinoma resulted in an age-dependent effect and accelerated tumor growth in mature mice (232). These findings support a central role for α4β1 in tumor growth control but call for more in depth studies of its cellular expression pattern and function in the TME prior to its use as a pharmacological target.

The αv integrins represent an interesting class of adhesion receptors that recognize RGD-containing ligands, including FN, and have multiple roles in cancer hallmarks (e.g., angiogenesis, growth and dissemination, and immunomodulation) (233). αv-based integrins are overexpressed in several tumor pathologies and their expression can be found on both tumor cells and stromal cells. In addition to being promiscuous receptors, with FN being only one of numerous ligands, the αv-based integrins have been linked to local TGF-β activation, which compounds the complexity of their effects in the TME (234).

Impact of FN on Treatment Response

Integrin-mediated cell-ECM and in particular cell-FN interactions confer resistance to chemotherapy as well as to ionizing radiation (235–241). In an *in vitro* and *in vivo* model of human non-small lung cancer, cetuximab promoted FN expression via p38-MAPK-ATF2 signaling (237). Cell adhesion to FN enhanced tumor cell resistance to radiotherapy, and attenuated the cytotoxic and radiosensitizing

effects of cetuximab (237). More recently, chemotherapy resistance in esophageal cancer cell lines increased in cells growing in a three-dimensional environment enriched in collagen and FN (242). These results illustrate that FN plays a key role in the response of cancer cells to treatment. Conversely, anti-tumor therapies modify the tumor ECM environment, as exemplified by radiation-induced fibrosis (243).

CONCLUDING REMARKS

Our understanding of stromal reprogramming in the TME has advanced at a rapid pace in recent years, driven by technological advances and the integration of massive amounts of information from different fields, spanning multiple scales. As illustrated above, cFN is recurrently a central component of the tumor stroma that contributes to several cancer hallmarks and enabling characteristics. Further understanding of cFN production, assembly and remodeling in primary tumor beds, draining lymph nodes and at metastatic sites is needed to grasp the full complexity of tumor progression and metastatic spread. This knowledge should provide valuable insights into cell-ECM interactions and the physical and functional interplay between different cellular components of the TME. Elucidating the role of cFN variants in modulation of immune cell trafficking, phenotype and functional maturation is of particular importance for improving the current armatorium of immunomodulatory agents and for providing therapeutic alternatives that target the stroma.

AUTHOR CONTRIBUTIONS

All authors listed have made a substantial, direct and intellectual contribution to the work, and approved it for publication.

ACKNOWLEDGMENTS

The pioneering and insightful scientists whose biochemical, molecular, and genetic studies laid the foundation for the enormous corpus of work on FN were gratefully acknowledged. We also extend our apologies to colleagues whose original contributions could not be cited due to space limitations. EV acknowledges funding from the French National Agency for Research (ANR-16-CE93-0005-01), the Fondation ARC (PJA20151203207, fellowship GE), The Fondation Recherche Médicale (fellowship AS), the Ligue National Contre le Cancer (LNCC/EVO Programme Priorité Tabac), the LabEx SIGNALIFE program (ANR-11-LABX-0028-01), the Fédération Hospitalo-Universitaire OncoAge and the 3IA Côte d'Azur (ANR-19-P3IA-0002).

REFERENCES

1. Lu P, Weaver VM, Werb Z. The extracellular matrix: a dynamic niche in cancer progression. *J Cell Biol.* (2012) 196:395–406. doi: 10.1083/jcb.201102147
2. Raab-Westphal S, Marshall J, Goodman S. Integrins as therapeutic targets: successes and cancers. *Cancers.* (2017) 9:110. doi: 10.3390/cancers9090110
3. Eckhardt BL, Parker BS, Laar RK van, Restall CM, Natoli AL, Tavaria MD, et al. Genomic analysis of a spontaneous model of breast cancer metastasis to bone reveals a role for the extracellular matrix. *Mol Cancer Res.* (2005) 3:1–13.
4. Ramaswamy S, Ross KN, Lander ES, Golub TR. A molecular signature of metastasis in primary solid tumors. *Nat Genet.* (2003) 33:49–54. doi: 10.1038/ng1060
5. Naba A, Clauser KR, Hoersch S, Carr SA, Hynes RO. The matrisome: *in silico* definition and *in vivo* characterization by proteomics of normal and tumor extracellular matrices. *Mol Cell Proteomics.* (2012) 11:M111.014647. doi: 10.1074/mcp.M111.014647
6. Shao X, Taha IN, Clauser KR, Gao Y (Tom), Naba A. MatrisomeDB: the ECM-protein knowledge database. *Nucleic Acids Res.* (2020) 48:D1136–44. doi: 10.1093/nar/gkz849
7. Xiong G-F, Xu R. Function of cancer cell-derived extracellular matrix in tumor progression. *JCMT.* (2016) 2:357. doi: 10.20517/2394-4722.2016.08
8. Karagiannis GS, Poutahidis T, Erdman SE, Kirsch R, Riddell RH, Diamandis EP. Cancer-associated fibroblasts drive the progression of metastasis through both paracrine and mechanical pressure on cancer tissue. *Mol Cancer Res.* (2012) 10:1403–18. doi: 10.1158/1541-7786.MCR-12-0307
9. Naba A, Clauser KR, Lamar JM, Carr SA, Hynes RO. Extracellular matrix signatures of human mammary carcinoma identify novel metastasis promoters. *eLife.* (2014) 3:e01308. doi: 10.7554/eLife.01308
10. Naba A, Clauser KR, Whittaker CA, Carr SA, Tanabe KK, Hynes RO. Extracellular matrix signatures of human primary metastatic colon cancers and their metastases to liver. *BMC Cancer.* (2014) 14:518. doi: 10.1186/1471-2407-14-518
11. Tian C, Clauser KR, Öhlund D, Rickelt S, Huang Y, Gupta M, et al. Proteomic analyses of ECM during pancreatic ductal adenocarcinoma progression reveal different contributions by tumor and stromal cells. *Proc Natl Acad Sci USA.* (2019) 116:19609–18. doi: 10.1073/pnas.1908626116
12. Puram SV, Tirosh I, Parikh AS, Patel AP, Yizhak K, Gillespie S, et al. Single-cell transcriptomic analysis of primary and metastatic tumor ecosystems in head and neck cancer. *Cell.* (2017) 171:1611–24.e24. doi: 10.1016/j.cell.2017.10.044
13. Hill BS, Sarnella A, D'Avino G, Zannetti A. Recruitment of stromal cells into tumour microenvironment promote the metastatic spread of breast cancer. *Semin Cancer Biol.* (2019) 60:202–13. doi: 10.1016/j.semcancer.2019.07.028
14. Binnewies M, Roberts EW, Kersten K, Chan V, Fearon DF, Merad M, et al. Understanding the tumor immune microenvironment (TIME) for effective therapy. *Nat Med.* (2018) 24:541–50. doi: 10.1038/s41591-018-0014-x
15. Liguori M, Solinas G, Germano G, Mantovani A, Allavena P. Tumor-associated macrophages as incessant builders and destroyers of the cancer stroma. *Cancers (Basel).* (2011) 3:3740–61. doi: 10.3390/cancers3043740
16. Afik R, Zigmond E, Vugman M, Klepfish M, Shimshoni E, Pasmanik-Chor M, et al. Tumor macrophages are pivotal constructors of tumor collagenous matrix. *J Exp Med.* (2016) 213:2315–31. doi: 10.1084/jem.20151193
17. Ireland LV, Mielgo A. Macrophages and fibroblasts, key players in cancer chemoresistance. *Front Cell Dev Biol.* (2018) 6:131. doi: 10.3389/fcell.2018.00131
18. LeBleu VS, Kalluri R. A peek into cancer-associated fibroblasts: origins, functions and translational impact. *Dis Models Mech.* (2018) 11:dmm029447. doi: 10.1242/dmm.029447
19. De Jaeghere EA, Denys HG, De Wever O. Fibroblasts fuel immune escape in the tumor microenvironment. *Trends Cancer.* (2019) 5:704–23. doi: 10.1016/j.trecan.2019.09.009
20. Monteran L, Erez N. The dark side of fibroblasts: cancer-associated fibroblasts as mediators of immunosuppression in the tumor microenvironment. *Front Immunol.* (2019) 10:1835. doi: 10.3389/fimmu.2019.01835

21. Rockey DC, Weymouth N, Shi Z. Smooth muscle α actin (Acta2) and myofibroblast function during hepatic wound healing. *PLoS ONE.* (2013) 8:e77166. doi: 10.1371/journal.pone.0077166
22. Costa A, Kieffer Y, Scholer-Dahirel A, Pelon F, Bourachot B, Cardon M, et al. Fibroblast heterogeneity and immunosuppressive environment in human breast cancer. *Cancer Cell.* (2018) 33:463–79.e10. doi: 10.1016/j.ccell.2018.01.011
23. Givel A-M, Kieffer Y, Scholer-Dahirel A, Sirven P, Cardon M, Pelon F, et al. miR200-regulated CXCL12β promotes fibroblast heterogeneity and immunosuppression in ovarian cancers. *Nat Commun.* (2018) 9:1056. doi: 10.1038/s41467-018-03348-z
24. Bernard V, Semaan A, Huang J, San Lucas FA, Mulu FC, Stephens BM, et al. Single-cell transcriptomics of pancreatic cancer precursors demonstrates epithelial and microenvironmental heterogeneity as an early event in neoplastic progression. *Clin Cancer Res.* (2019) 25:2194–205. doi: 10.1158/1078-0432.CCR-18-1955
25. Kalluri R, Weinberg RA. The basics of epithelial-mesenchymal transition. *J Clin Invest.* (2009) 119:1420–8. doi: 10.1172/JCI39104
26. Nair N, Calle AS, Zahra MH, Prieto-Vila M, Oo AKK, Hurley L, et al. A cancer stem cell model as the point of origin of cancer-associated fibroblasts in tumor microenvironment. *Sci Rep.* (2017) 7:6838. doi: 10.1038/s41598-017-07144-5
27. Rønnov-Jessen L, Petersen OW, Koteliansky VE, Bissell MJ. The origin of the myofibroblasts in breast cancer. Recapitulation of tumor environment in culture unravels diversity and implicates converted fibroblasts and recruited smooth muscle cells. *J Clin Invest.* (1995) 95:859–73. doi: 10.1172/JCI117736
28. Zeisberg EM, Potenta S, Xie L, Zeisberg M, Kalluri R. Discovery of endothelial to mesenchymal transition as a source for carcinoma-associated fibroblasts. *Cancer Res.* (2007) 67:10123–8. doi: 10.1158/0008-5472.CAN-07-3127
29. Biffi G, Oni TE, Spielman B, Hao Y, Elyada E, Park Y, et al. IL-1-induced JAK/STAT signaling is antagonized by TGF-beta to shape CAF heterogeneity in pancreatic ductal adenocarcinoma. *Cancer Discov.* (2018) CD-18-0710. doi: 10.1158/2159-8290.CD-18-0710
30. Öhlund D, Handly-Santana A, Biffi G, Elyada E, Almeida AS, Ponz-Sarvise M, et al. Distinct populations of inflammatory fibroblasts and myofibroblasts in pancreatic cancer. *J Exp Med.* (2017) 214:579–96. doi: 10.1084/jem.20162024
31. Ligorio M, Sil S, Malagon-Lopez J, Nieman LT, Misale S, Di Pilato M, et al. Stromal microenvironment shapes the intratumoral architecture of pancreatic cancer. *Cell.* (2019) 178:160–75.e27. doi: 10.1016/j.cell.2019.05.012
32. Bordignon P, Bottoni G, Xu X, Popescu AS, Truan Z, Guenova E, et al. Dualism of FGF and TGF-β signaling in heterogeneous cancer-associated fibroblast activation with ETV1 as a critical determinant. *Cell Rep.* (2019) 28:2358–72.e6. doi: 10.1016/j.celrep.2019.07.092
33. Sugimoto H, Mundel TM, Kieran MW, Kalluri R. Identification of fibroblast heterogeneity in the tumor microenvironment. *Cancer Biol Ther.* (2006) 5:1640–6. doi: 10.4161/cbt.5.12.3354
34. Löhr M, Schmidt C, Ringel J, Kluth M, Müller P, Nizze H, et al. Transforming growth factor-β1 induces desmoplasia in an experimental model of human pancreatic carcinoma. *Cancer Res.* (2001) 61:550–5.
35. Meng X-M, Nikolic-Paterson DJ, Lan HY. TGF-β: the master regulator of fibrosis. *Nat Rev Nephrol.* (2016) 12:325–38. doi: 10.1038/nrneph.2016.48
36. Poltavets V, Kochetkova M, Pitson SM, Samuel MS. The role of the extracellular matrix and its molecular and cellular regulators in cancer cell plasticity. *Front Oncol.* (2018) 8:431. doi: 10.3389/fonc.2018.00431
37. Roberts AB, McCune BK, Sporn MB. TGF-β: regulation of extracellular matrix. *Kidney Int.* (1992) 41:557–9. doi: 10.1038/ki.1992.81
38. Qin X, Yan M, Zhang J, Wang X, Shen Z, Lv Z, et al. TGFβ3-mediated induction of periostin facilitates head and neck cancer growth and is associated with metastasis. *Sci Rep.* (2016) 6:20587. doi: 10.1038/srep20587
39. Calon A, Tauriello DVF, Batlle E. TGF-beta in CAF-mediated tumor growth and metastasis. *Semin Cancer Biol.* (2014) 25:15–22. doi: 10.1016/j.semcancer.2013.12.008
40. Shao Z-M, Nguyen M, Barsky SH. Human breast carcinoma desmoplasia is PDGF initiated. *Oncogene.* (2000) 19:4337–45. doi: 10.1038/sj.onc.1203785
41. Bishen KA, Radhakrishnan R, Satyamoorthy K. The role of basic fibroblast growth factor in oral submucous fibrosis pathogenesis. *J Oral Pathol Med.* (2008) 37:402–11. doi: 10.1111/j.1600-0714.2008.00649.x
42. Strutz F, Zeisberg M, Ziyadeh FN, Yang C-Q, Kalluri R, Müller GA, et al. Role of basic fibroblast growth factor-2 in epithelial-mesenchymal transformation. *Kidney Int.* (2002) 61:1714–28. doi: 10.1046/j.1523-1755.2002.00333.x
43. Ishiguro S, Akasaka Y, Kiguchi H, Suzuki T, Imaizumi R, Ishikawa Y, et al. Basic fibroblast growth factor induces down-regulation of α-smooth muscle actin and reduction of myofibroblast areas in open skin wounds. *Wound Repair Regen.* (2009) 17:617–25. doi: 10.1111/j.1524-475X.2009.00511.x
44. Procopio M-G, Laszlo C, Al Labban D, Kim DE, Bordignon P, Jo S-H, et al. Combined CSL and p53 downregulation promotes cancer-associated fibroblast activation. *Nat Cell Biol.* (2015) 17:1193–204. doi: 10.1038/ncb3228
45. Kartha VK, Stawski L, Han R, Haines P, Gallagher G, Noonan V, et al. PDGFRβ is a novel marker of stromal activation in oral squamous cell carcinomas. *PLoS ONE.* (2016) 11:e0154645. doi: 10.1371/journal.pone.0154645
46. Siedlecki J, Asani B, Wertheimer C, Hillenmayer A, Ohlmann A, Priglinger C, et al. Combined VEGF/PDGF inhibition using axitinib induces αSMA expression and a pro-fibrotic phenotype in human pericytes. *Graefes Arch Clin Exp Ophthalmol.* (2018) 256:1141–9. doi: 10.1007/s00417-018-3987-8
47. Costa A, Scholer-Dahirel A, Mechta-Grigoriou F. The role of reactive oxygen species and metabolism on cancer cells and their microenvironment. *Semin Cancer Biol.* (2014) 25:23–32. doi: 10.1016/j.semcancer.2013.12.007
48. Yang X, Li Y, Zou L, Zhu Z. Role of exosomes in crosstalk between cancer-associated fibroblasts and cancer cells. *Front Oncol.* (2019) 9:356. doi: 10.3389/fonc.2019.00356
49. Egeblad M, Rasch MG, Weaver VM. Dynamic interplay between the collagen scaffold and tumor evolution. *Curr Opin Cell Biol.* (2010) 22:697–706. doi: 10.1016/j.ceb.2010.08.015
50. Malik R, Lelkes PI, Cukierman E. Biomechanical and biochemical remodeling of stromal extracellular matrix in cancer. *Trends Biotechnol.* (2015) 33:230–6. doi: 10.1016/j.tibtech.2015.01.004
51. Provenzano PP, Eliceiri KW, Campbell JM, Inman DR, White JG, Keely PJ. Collagen reorganization at the tumor-stromal interface facilitates local invasion. *BMC Med.* (2006) 4:38. doi: 10.1186/1741-7015-4-38
52. Conklin MW, Eickhoff JC, Riching KM, Pehlke CA, Eliceiri KW, Provenzano PP, et al. Aligned collagen is a prognostic signature for survival in human breast carcinoma. *Am J Pathol.* (2011) 178:1221–32. doi: 10.1016/j.ajpath.2010.11.076
53. Sottile J, Hocking DC. Fibronectin polymerization regulates the composition and stability of extracellular matrix fibrils and cell-matrix adhesions. *MBoC.* (2002) 13:3546–59. doi: 10.1091/mbc.e02-01-0048
54. Velling T, Risteli J, Wennerberg K, Mosher DF, Johansson S. Polymerization of type I and III collagens is dependent on fibronectin and enhanced by integrins α11β1 and α2β1. *J Biol Chem.* (2002) 277:37377–81. doi: 10.1074/jbc.M206286200
55. Gopal S, Veracini L, Grall D, Butori C, Schaub S, Audebert S, et al. Fibronectin-guided migration of carcinoma collectives. *Nat Commun.* (2017) 8:14105. doi: 10.1038/ncomms14105
56. Lu Y, Kamel-El Sayed SA, Wang K, Tiede-Lewis LM, Grillo MA, Veno PA, et al. Live imaging of type I collagen assembly dynamics in osteoblasts stably expressing GFP and mCherry-tagged collagen constructs: live imaging of type I collagen assembly. *J Bone Miner Res.* (2018) 33:1166–82. doi: 10.1002/jbmr.3409
57. Barker TH, Engler AJ. The provisional matrix: setting the stage for tissue repair outcomes. *Matrix Biol.* (2017) 60–61:1–4. doi: 10.1016/j.matbio.2017.04.003
58. Dallas SL, Sivakumar P, Jones CJP, Chen Q, Peters DM, Mosher DF, et al. Fibronectin regulates latent transforming growth factor-β (TGFβ) by controlling matrix assembly of latent TGFβ-binding protein-1. *J Biol Chem.* (2005) 280:18871–80. doi: 10.1074/jbc.M410762200
59. Morrison PR, Edsall JT, Miller SG. Preparation and properties of serum and plasma proteins. XVIII. The separation of purified fibrinogen from fraction I of human plasma. *J Am Chem Soc.* (1948) 70:3103–8. doi: 10.1021/ja01189a080

60. Engel J, Odermatt E, Engel A, Madri JA, Furthmayr H, Rohde H, et al. Shapes, domain organizations and flexibility of laminin and fibronectin, two multifunctional proteins of the extracellular matrix. *J Mol Biol.* (1981) 150:97–120. doi: 10.1016/0022-2836(81)90326-0
61. Erickson HP, Carrell N, McDonagh J. Fibronectin molecule visualized in electron microscopy: a long, thin, flexible strand. *J Cell Biol.* (1981) 91:673–8. doi: 10.1083/jcb.91.3.673
62. Xu J, Mosher D. Fibronectin and other adhesive glycoproteins. In: Mecham RP, editor. *The Extracellular Matrix: An Overview*. Berlin; Heidelberg: Springer Berlin Heidelberg (2011). p. 41–75. doi: 10.1007/978-3-642-16555-9_2
63. Van Obberghen-Schilling E, Tucker RP, Saupe F, Gasser I, Cseh B, Orend G. Fibronectin and tenascin-C: accomplices in vascular morphogenesis during development and tumor growth. *Int J Dev Biol.* (2011) 55:511–25. doi: 10.1387/ijdb.103243eo
64. Hynes RO. *Fibronectins*. New York, NY: Springer New York (1990). doi: 10.1007/978-1-4612-3264-3
65. Schwarzbauer JE, DeSimone DW. Fibronectins, their fibrillogenesis, and *in vivo* functions. *Cold Spring Harbor Perspect Biol.* (2011) 3:a005041. doi: 10.1101/cshperspect.a005041
66. Baron M, Norman D, Willis A, Campbell ID. Structure of the fibronectin type 1 module. *Nature.* (1990) 345:642–6. doi: 10.1038/345642a0
67. Potts JR, Bright JR, Bolton D, Pickford AR, Campbell ID. Solution structure of the N-terminal F1 module pair from human fibronectin. *Biochemistry.* (1999) 38:8304–12. doi: 10.1021/bi990202b
68. Dickinson CD, Veerapandian B, Dai X-P, Hamlin RC, Xuong N, Ruoslahti E, et al. Crystal structure of the tenth type III cell adhesion module of human fibronectin. *J Mol Biol.* (1994) 236:1079–92. doi: 10.1016/0022-2836(94)90013-2
69. Dickinson CD, Gay DA, Parello J, Ruoslahti E, Ely KR. Crystals of the cell-binding module of fibronectin obtained from a series of recombinant fragments differing in length. *J Mol Biol.* (1994) 238:123–7. doi: 10.1006/jmbi.1994.1272
70. Leahy DJ, Aukhil I, Erickson HP. 2.0 Å crystal structure of a four-domain segment of human fibronectin encompassing the RGD loop and synergy region. *Cell.* (1996) 84:155–64. doi: 10.1016/S0092-8674(00)81002-8
71. Main AL, Harvey TS, Baron M, Boyd J, Campbell ID. The three-dimensional structure of the tenth type III module of fibronectin: An insight into RGD-mediated interactions. *Cell.* (1992) 71:671–8. doi: 10.1016/0092-8674(92)90600-H
72. Krammer A, Lu H, Isralewitz B, Schulten K, Vogel V. Forced unfolding of the fibronectin type III module reveals a tensile molecular recognition switch. *Proc Natl Acad Sci USA.* (1999) 96:1351–6. doi: 10.1073/pnas.96.4.1351
73. Hynes RO. Integrins bidirectional, allosteric signaling machines. *Cell.* (2002) 110:673–87. doi: 10.1016/S0092-8674(02)00971-6
74. Pytela R, Pierschbacher MD, Ruoslahti E. Identification and isolation of a 140 kd cell surface glycoprotein with properties expected of a fibronectin receptor. *Cell.* (1985) 40:191–8. doi: 10.1016/0092-8674(85)90322-8
75. Pierschbacher MD, Ruoslahti E. Cell attachment activity of fibronectin can be duplicated by small synthetic fragments of the molecule. *Nature.* (1984) 309:30–3. doi: 10.1038/309030a0
76. Pankov R, Yamada KM. Fibronectin at a glance. *J Cell Sci.* (2002) 115:3861–3. doi: 10.1242/jcs.00059
77. Danen EHJ, Sonneveld P, Brakebusch C, Fässler R, Sonnenberg A. The fibronectin-binding integrins α5β1 and αvβ3 differentially modulate RhoA-GTP loading, organization of cell matrix adhesions, and fibronectin fibrillogenesis. *J Cell Biol.* (2002) 159:1071–86. doi: 10.1083/jcb.200205014
78. Zhong C, Chrzanowska-Wodnicka M, Brown J, Shaub A, Belkin AM, Burridge K. Rho-mediated contractility exposes a cryptic site in fibronectin and induces fibronectin matrix assembly. *J Cell Biol.* (1998) 141:539–51. doi: 10.1083/jcb.141.2.539
79. Wennerberg K, Lohikangas L, Gullberg D, Pfaff M, Johansson S, Fiissler R. 31 Integrin-dependent and -independent polymerization of fibronectin. *J Cell Biol.* (1996) 132:12. doi: 10.1083/jcb.132.1.227
80. Mao Y, Schwarzbauer JE. Fibronectin fibrillogenesis, a cell-mediated matrix assembly process. *Matrix Biol.* (2005) 24:389–99. doi: 10.1016/j.matbio.2005.06.008
81. Moyano JV, Carnemolla B, Dominguez-Jimenez C, Garcia-Gila M, Albar JP, Sanchez-Aparicio P, et al. Fibronectin type III5 repeat contains a novel cell adhesion sequence, KLDAPT, which binds activated α4β1 and α4β7 integrins. *J Biol Chem.* (1997) 272:24832–6. doi: 10.1074/jbc.272.40.24832
82. Komoriya A, Green L, Mervic M, Yamada SS, Yamada KM, Humphries MJ. The minimal essential sequence for a major cell type-specific adhesion site (CS1)within the alternatively spliced type I11 connecting segment domain of fibronectiins leucine-aspartic acid- valine. *J Biol Chem.* (1991) 266:15075–9.
83. Mould AP, Komoriya A, Yamada KM, Humphries MJ. The CS5 peptide is a second site in the IIICS region of fibronectin recognized by the integrin alpha 4 beta 1. Inhibition of alpha 4 beta 1 function by RGD peptide homologues. *J Biol Chem.* (1991) 266:3579–85.
84. Humphries JD. Integrin ligands at a glance. *J Cell Sci.* (2006) 119:3901–3. doi: 10.1242/jcs.03098
85. Dallas SL, Chen Q, Sivakumar P. Dynamics of assembly and reorganization of extracellular matrix proteins. In: *Current Topics in Developmental Biology*. Elsevier (2006). p. 1–24. Available online at: https://linkinghub.elsevier.com/retrieve/pii/S0070215306750013
86. Lin T-C, Yang C-H, Cheng L-H, Chang W-T, Lin Y-R, Cheng H-C. Fibronectin in cancer: friend or foe. *Cells.* (2019) 9:27. doi: 10.3390/cells9010027
87. Aguirre KM, McCormick R, Schwarzbauer JE. Fibronectin self-association is mediated by complementary sites within the amino-terminal one-third of the molecule. *J Biol Chem.* (1994) 269:27863–8.
88. Baneyx G, Baugh L, Vogel V. Fibronectin extension and unfolding within cell matrix fibrils controlled by cytoskeletal tension. *Proc Natl Acad Sci USA.* (2002) 99:5139–43. doi: 10.1073/pnas.072650799
89. Vogel V. Unraveling the mechanobiology of extracellular matrix. *Annu Rev Physiol.* (2018) 80:353–87. doi: 10.1146/annurev-physiol-021317-121312
90. Morgan MR, Humphries MJ, Bass MD. Synergistic control of cell adhesion by integrins and syndecans. *Nat Rev Mol Cell Biol.* (2007) 8:957–69. doi: 10.1038/nrm2289
91. Monaghan E, Gueorguiev V, Wilkins-Port C, McKeown-Longo PJ. The receptor for urokinase-type plasminogen activator regulates fibronectin matrix assembly in human skin fibroblasts. *J Biol Chem.* (2004) 279:1400–7. doi: 10.1074/jbc.M310374200
92. Saoncella S, Echtermeyer F, Denhez F, Nowlen JK, Mosher DF, Robinson SD, et al. Syndecan-4 signals cooperatively with integrins in a rhodependent manner in the assembly of focal adhesions and actin stress fibers. *Proc Natl Acad Sci USA.* (1999) 96:2805–10. doi: 10.1073/pnas.96.6.2805
93. Wilcox-Adelman SA, Denhez F, Goetinck PF. Syndecan-4 modulates focal adhesion kinase phosphorylation. *J Biol Chem.* (2002) 277:32970–7. doi: 10.1074/jbc.M201283200
94. Langenbach KJ, Sottile J. Identification of protein-disulfide isomerase activity in fibronectin. *J Biol Chem.* (1999) 274:7032–8. doi: 10.1074/jbc.274.11.7032
95. Yamada KM, Kennedy DW, Kimata K, Pratt RM. Characterization of fibronectin interactions with glycosaminoglycans and identification of active proteolytic fragments. *J Biol Chem.* (1980) 255:6055–63.
96. Barkalow FJB, Schwarzbauer JE. Localization of the major heparin-binding site in fibronectin. *J Biol Chem.* (1991) 266:7812–8.
97. Moyano JV, Carnemolla B, Albar JP, Leprini A, Gaggero B, Zardi L, et al. Identification of a novel heparin and cell binding sequence in repeat III5. *J Biol Chem.* (1999) 274:135–42. doi: 10.1074/jbc.274.1.135
98. Mostafavi-Pour Z, Askari JA, Whittard JD, Humphries MJ. Identification of a novel heparin-binding site in the alternatively spliced IIICS region of fibronectin: roles of integrins and proteoglycans in cell adhesion to fibronectin splice variants. *Matrix Biol.* (2001) 20:63–73. doi: 10.1016/S0945-053X(00)00131-1
99. Woods A. Syndecans: transmembrane modulators of adhesion and matrix assembly. *J Clin Invest.* (2001) 107:935–41. doi: 10.1172/JCI12802
100. Frantz C, Stewart KM, Weaver VM. The extracellular matrix at a glance. *J Cell Sci.* (2010) 123:4195–200. doi: 10.1242/jcs.023820
101. Hynes RO. The extracellular matrix: not just pretty fibrils. *Science.* (2009) 326:1216–9. doi: 10.1126/science.1176009
102. Umezawa K, Kornblihtt AR, Baralle FE. Isolation and characterization of cDNA clones for human liver fibronectin. *FEBS Lett.* (1985) 186:31–4. doi: 10.1016/0014-5793(85)81333-8

103. Schwarzbauer JE, Tamkun JW, Lemischka IR, Hynes RO. Three different fibronectin mRNAs arise by alternative splicing within the coding region. *Cell.* (1983) 35:421–31. doi: 10.1016/0092-8674(83)90175-7
104. Kornblihtt AR, Vibe-Pedersen K, Baralle FE. Human fibronectin: molecular cloning evidence for two mRNA species differing by an internal segment coding for a structural domain. *EMBO J.* (1984) 3:221–6. doi: 10.1002/j.1460-2075.1984.tb01787.x
105. Gutman A, Kornblihtt AR. Identification of a third region of cell-specific alternative splicing in human fibronectin mRNA. *Proc Natl Acad Sci USA.* (1987) 84:7179–82. doi: 10.1073/pnas.84.20.7179
106. Schwarzbauer JE, Patel RS, Fonda D, Hynes RO. Multiple sites of alternative splicing of the rat fibronectin gene transcript. *EMBO J.* (1987) 6:2573–80. doi: 10.1002/j.1460-2075.1987.tb02547.x
107. White E, Baralle F, Muro A. New insights into form and function of fibronectin splice variants. *J Pathol.* (2008) 216:1–14. doi: 10.1002/path.2388
108. Mamuya W, Chobanian A, Brecher P. Age-related changes in fibronectin expression in spontaneously hypertensive, Wistar-Kyoto, and Wistar rat hearts. *Circ Res.* (1992) 71:1341–50. doi: 10.1161/01.RES.71.6.1341
109. Wang J, Yin L, Chen Z. New insights into the altered fibronectin matrix and extrasynaptic transmission in the aging brain. *J Clin Gerontol Geriatr.* (2011) 2:35–41. doi: 10.1016/j.jcgg.2010.12.002
110. Negishi H, Yamada H, Okuyama K, Sagawa T, Makinoda S, Fujimoto S. Fetal fibronectin concentration in amniotic fluid decreases with advancing gestational age. *Int J Gynecol Obstet.* (1995) 49:17–20. doi: 10.1016/0020-7292(95)02341-9
111. Chauhan AK, Iaconcig A, Baralle FE, Muro AF. Alternative splicing of fibronectin: a mouse model demonstrates the identity of *in vitro* and *in vivo* systems and the processing autonomy of regulated exons in adult mice. *Gene.* (2004) 324:55–63. doi: 10.1016/j.gene.2003.09.026
112. Pagani F. Tissue-specific splicing pattern of fibronectin messenger RNA precursor during development and aging in rat. *J Cell Biol.* (1991) 113:1223–9. doi: 10.1083/jcb.113.5.1223
113. Magnuson VL, Young M, Schattenberg DG, Mancini MA, Chen D, Steffensen B, et al. The alternative splicing of fibronectin pre-mRNAIs altered during aging andin response to growth factors. *J Biol Chem.* (1991) 266:14654–62.
114. Ffrench-Constant C. Reappearance of an embryonic pattern of fibronectin splicing during wound healing in the adult rat. *J Cell Biol.* (1989) 109:903–14. doi: 10.1083/jcb.109.2.903
115. Jarnagin WR. Expression of variant fibronectins in wound healing: cellular source and biological activity of the EIIIA segment in rat hepatic fibrogenesis. *J Cell Biol.* (1994) 127:2037–48. doi: 10.1083/jcb.127.6.2037
116. Du K, Peng Y, Greenbaum LE, Haber BA, Taub R. HRS/SRp40-mediated inclusion of the fibronectin EIIIB exon, a possible cause of increased EIIIB expression in proliferating liver. *Mol Cell Biol.* (1997) 17:4096–104. doi: 10.1128/MCB.17.7.4096
117. Ffrench-Constant C. Alternative splicing of fibronectin–many different proteins but few different functions. *Exp Cell Res.* (1995) 221:261–71. doi: 10.1006/excr.1995.1374
118. Chen Y, Huang Q, Liu W, Zhu Q, Cui C-P, Xu L, et al. Mutually exclusive acetylation and ubiquitylation of the splicing factor SRSF5 control tumor growth. *Nat Commun.* (2018) 9:2464. doi: 10.1038/s41467-018-04815-3
119. Yang S, Jia R, Bian Z. SRSF5 functions as a novel oncogenic splicing factor and is upregulated by oncogene SRSF3 in oral squamous cell carcinoma. *Biochim Biophys Acta.* (2018) 1865:1161–72. doi: 10.1016/j.bbamcr.2018.05.017
120. Hallgren O, Malmström J, Malmström L, Andersson-Sjöland A, Wildt M, Tufvesson E, et al. Splicosomal and serine and arginine-rich splicing factors as targets for TGF-β. *Fibrogen Tissue Repair.* (2012) 5:6. doi: 10.1186/1755-1536-5-6
121. Balza E, Borsi L, Allemanni G, Zardi L. Transforming growth factor β regulates the levels of different fibronectin isoforms in normal human cultured fibroblasts. *FEBS Lett.* (1988) 228:42–4. doi: 10.1016/0014-5793(88)80580-5
122. Borsi L, Castellani P, Risso AM, Leprini A, Zardi L. Transforming growth factor-β regulates the splicing pattern of fibronectin messenger RNA precursor. FEBS Letters. (1990) 261:175-8. doi: 10.1016/0014-5793(90)80664-5
123. Viedt C, Bürger A, Hänsch GM. Fibronectin synthesis in tubular epithelial cells: up-regulation of the EDA splice variant by transforming growth factor β. *Kidney Int.* (1995) 48:1810–7. doi: 10.1038/ki.1995.479
124. Muro AF, Moretti FA, Moore BB, Yan M, Atrasz RG, Wilke CA, et al. An essential role for fibronectin extra type III domain A in pulmonary fibrosis. *Am J Respir Crit Care Med.* (2008) 177:638–45. doi: 10.1164/rccm.200708-1291OC
125. To WS, Midwood KS. Plasma and cellular fibronectin: distinct and independent functions during tissue repair. *Fibrogen Tissue Repair.* (2011) 4:21. doi: 10.1186/1755-1536-4-21
126. Muro AF, Chauhan AK, Gajovic S, Iaconcig A, Porro F, Stanta G, et al. Regulated splicing of the fibronectin EDA exon is essential for proper skin wound healing and normal lifespan. *J Cell Biol.* (2003) 162:149–60. doi: 10.1083/jcb.200212079
127. Chauhan AK, Moretti FA, Iaconcig A, Baralle FE, Muro AF. Impaired motor coordination in mice lacking the EDA exon of the fibronectin gene. *Behav Brain Res.* (2005) 161:31–8. doi: 10.1016/j.bbr.2005.02.020
128. Fukuda T, Yoshida N, Kataoka Y, Manabe R, Mizuno-Horikawa Y, Sato M, et al. Mice lacking the EDB segment of fibronectin develop normally but exhibit reduced cell growth and fibronectin matrix assembly *in vitro*. *Cancer Res.* (2002) 62:5603–10.
129. Astrof S, Crowley D, Hynes RO. Multiple cardiovascular defects caused by the absence of alternatively spliced segments of fibronectin. *Dev Biol.* (2007) 311:11–24. doi: 10.1016/j.ydbio.2007.07.005
130. Serini G, Bochaton-Piallat M-L, Ropraz P, Geinoz A, Borsi L, Zardi L, et al. The fibronectin domain ED-A is crucial for myofibroblastic phenotype induction by transforming growth factor-β1. *J Cell Biol.* (1998) 142:9. doi: 10.1083/jcb.142.3.873
131. Saito S, Yamaji N, Yasunaga K, Saito T, Matsumoto S, Katoh M, et al. The fibronectin extra domain A activates matrix metalloproteinase gene expression by an interleukin-1-dependent mechanism. *J Biol Chem.* (1999) 274:30756–63. doi: 10.1074/jbc.274.43.30756
132. Glukhova MA, Frid MG, Shekhonin BV, Vasilevskaya TD, Grunwald J, Saginati M, et al. Expression of extra domain A fibronectin sequence in vascular smooth muscle cells is phenotype dependent. *J Cell Biol.* (1989) 109:357–66. doi: 10.1083/jcb.109.1.357
133. Castellani P, Viale G, Dorcaratto A, Nicolo G, Kaczmarek J, Querze G, et al. The fibronectin isoform containing the ED-B oncofetal domain: a marker of angiogenesis. *Int J Cancer.* (1994) 59:612–8. doi: 10.1002/ijc.2910590507
134. Manabe R, Oh-e N, Sekiguchi K. Alternatively spliced EDA segment regulates fibronectin-dependent cell cycle progression and mitogenic signal transduction. *J Biol Chem.* (1999) 274:5919–24. doi: 10.1074/jbc.274.9.5919
135. Liao YF, Gotwals PJ, Koteliansky VE, Sheppard D, Van De Water L. The EIIIA segment of fibronectin is a ligand for integrins α9β1 and α4β1 providing a novel mechanism for regulating cell adhesion by alternative splicing. *J Biol Chem.* (2002) 277:14467–74. doi: 10.1074/jbc.M201100200
136. Shinde AV, Bystroff C, Wang C, Vogelezang MG, Vincent PA, Hynes RO, et al. Identification of the peptide sequences within the EIIIA (EDA) segment of fibronectin that mediate integrin α9β1-dependent cellular activities. *J Biol Chem.* (2008) 283:2858–70. doi: 10.1074/jbc.M708306200
137. Okamura Y, Watari M, Jerud ES, Young DW, Ishizaka ST, Rose J, et al. The extra domain A of fibronectin activates toll-like receptor 4. *J Biol Chem.* (2001) 276:10229–33. doi: 10.1074/jbc.M100099200
138. Sens C, Huck K, Pettera S, Uebel S, Wabnitz G, Moser M, et al. Fibronectins containing extradomain A or B enhance osteoblast differentiation via distinct integrins. *J Biol Chem.* (2017) 292:7745–60. doi: 10.1074/jbc.M116.739987
139. Ruoslahti E, Vaheri A. Novel human serum protein from fibroblast plasma membrane. *Nature.* (1974) 248:789–91. doi: 10.1038/248789a0
140. Keski-Oja J, Vaheri A, Ruoslahti E. Fibroblast surface antigen (SF): THE external glycoprotein lost in proteolytic stimulation and malignant transformation. *Int J Cancer.* (1976) 17:261–9. doi: 10.1002/ijc.2910170215
141. Hanahan D, Weinberg RA. The hallmarks of cancer. *Cell.* (2000) 100:57–70. doi: 10.1016/S0092-8674(00)81683-9
142. Hanahan D, Weinberg RA. Hallmarks of cancer: the next generation. *Cell.* (2011) 144:646–74. doi: 10.1016/j.cell.2011.02.013
143. George EL, Georges-Labouesse EN, Patel-King RS, Rayburn H, Hynes RO. Defects in mesoderm, neural tube and vascular development in mouse embryos lacking fibronectin. *Development.* (1993) 119:1079–91.

144. Lenselink EA. Role of fibronectin in normal wound healing: role of fibronectin in normal wound healing. *Int Wound J.* (2015) 12:313–6. doi: 10.1111/iwj.12109
145. Liao Y-X, Zhang Z-P, Zhao J, Liu J-P. Effects of fibronectin 1 on cell proliferation, senescence and apoptosis of human glioma cells through the PI3K/AKT signaling pathway. *Cell Physiol Biochem.* (2018) 48:1382–96. doi: 10.1159/000492096
146. Ou Y-C, Li J-R, Wang J-D, Chang C-Y, Wu C-C, Chen W-Y, et al. Fibronectin promotes cell growth and migration in human renal cell carcinoma cells. *IJMS.* (2019) 20:2792. doi: 10.3390/ijms20112792
147. Cao Y, Liu X, Lu W, Chen Y, Wu X, Li M, et al. Fibronectin promotes cell proliferation and invasion through mTOR signaling pathway activation in gallbladder cancer. *Cancer Lett.* (2015) 360:141–50. doi: 10.1016/j.canlet.2015.01.041
148. von Au A, Vasel M, Kraft S, Sens C, Hackl N, Marx A, et al. Circulating fibronectin controls tumor growth. *Neoplasia.* (2013) 15:925–38. doi: 10.1593/neo.13762
149. Kohan M, Muro AF, White ES, Berkman N. EDA-containing cellular fibronectin induces fibroblast differentiation through binding to α 4 β 7 integrin receptor and MAPK/Erk 1/2-dependent signaling. *FASEB J.* (2010) 24:4503–12. doi: 10.1096/fj.10-154435
150. Nam J-M, Onodera Y, Bissell MJ, Park CC. Breast cancer cells in three-dimensional culture display an enhanced radioresponse after coordinate targeting of integrin alpha5beta1 and fibronectin. *Cancer Res.* (2010) 70:5238–48. doi: 10.1158/0008-5472.CAN-09-2319
151. Manabe R, Oh-e N, Maeda T, Fukuda T, Sekiguchi K. Modulation of cell-adhesive activity of fibronectin by the alternatively spliced EDA segment. *J Cell Biol.* (1997) 139:295–307. doi: 10.1083/jcb.139.1.295
152. Lv W-Q, Wang H-C, Peng J, Wang Y-X, Jiang J-H, Li C-Y. Gene editing of the extra domain A positive fibronectin in various tumors, amplified the effects of CRISPR/Cas system on the inhibition of tumor progression. *Oncotarget.* (2017) 8:105020–36. doi: 10.18632/oncotarget.21136
153. Kenny HA, Chiang C-Y, White EA, Schryver EM, Habis M, Romero IL, et al. Mesothelial cells promote early ovarian cancer metastasis through fibronectin secretion. *J Clin Invest.* (2014) 124:4614–28. doi: 10.1172/JCI74778
154. Khan ZA, Chan BM, Uniyal S, Barbin YP, Farhangkhoee H, Chen S, et al. EDB fibronectin and angiogenesis–a novel mechanistic pathway. *Angiogenesis.* (2005) 8:183–96. doi: 10.1007/s10456-005-9017-6
155. Cseh B, Fernandez-Sauze S, Grall D, Schaub S, Doma E, Van Obberghen-Schilling E. Autocrine fibronectin directs matrix assembly and crosstalk between cell-matrix and cell-cell adhesion in vascular endothelial cells. *J Cell Sci.* (2010) 123:3989–99. doi: 10.1242/jcs.073346
156. Chu L-H, Rivera CG, Popel AS, Bader JS. Constructing the angiome: a global angiogenesis protein interaction network. *Physiol Genom.* (2012) 44:915–24. doi: 10.1152/physiolgenomics.00181.2011
157. Turner CJ, Badu-Nkansah K, Hynes RO. Endothelium-derived fibronectin regulates neonatal vascular morphogenesis in an autocrine fashion. *Angiogenesis.* (2017) 20:519–31. doi: 10.1007/s10456-017-9563-8
158. Zhou X, Rowe RG, Hiraoka N, George JP, Wirtz D, Mosher DF, et al. Fibronectin fibrillogenesis regulates three-dimensional neovessel formation. *Genes Dev.* (2008) 22:1231–43. doi: 10.1101/gad.1643308
159. Murphy PA, Begum S, Hynes RO. Tumor angiogenesis in the absence of fibronectin or its cognate integrin receptors. *PLoS ONE.* (2015) 10:e0120872. doi: 10.1371/journal.pone.0120872
160. van der Flier A, Badu-Nkansah K, Whittaker CA, Crowley D, Bronson RT, Lacy-Hulbert A, et al. Endothelial 5 and v integrins cooperate in remodeling of the vasculature during development. *Development.* (2010) 137:2439–49. doi: 10.1242/dev.049551
161. Kaspar M, Zardi L, Neri D. Fibronectin as target for tumor therapy. *Int J Cancer.* (2006) 118:1331–9. doi: 10.1002/ijc.21677
162. Rybak J-N, Roesli C, Kaspar M, Villa A, Neri D. The extra-domain A of fibronectin is a vascular marker of solid tumors and metastases. *Cancer Res.* (2007) 67:10948–57. doi: 10.1158/0008-5472.CAN-07-1436
163. Colin C, Baeza N, Bartoli C, Fina F, Eudes N, Nanni I, et al. Identification of genes differentially expressed in glioblastoma versus pilocytic astrocytoma using suppression subtractive hybridization. *Oncogene.* (2006) 25:2818–26. doi: 10.1038/sj.onc.1209305
164. Serres E, Debarbieux F, Stanchi F, Maggiorella L, Grall D, Turchi L, et al. Fibronectin expression in glioblastomas promotes cell cohesion, collective invasion of basement membrane *in vitro* and orthotopic tumor growth in mice. *Oncogene.* (2014) 33:3451–62. doi: 10.1038/onc.2013.305
165. Wijelath ES, Murray J, Rahman S, Patel Y, Ishida A, Strand K, et al. Novel vascular endothelial growth factor binding domains of fibronectin enhance vascular endothelial growth factor biological activity. *Circ Res.* (2002) 91:25–31. doi: 10.1161/01.RES.0000026420.22406.79
166. Wijelath ES, Rahman S, Namekata M, Murray J, Nishimura T, Mostafavi-Pour Z, et al. Heparin-II domain of fibronectin is a vascular endothelial growth factor-binding domain: enhancement of vegf biological activity by a singular growth factor/matrix protein synergism. *Circ Res.* (2006) 99:853–60. doi: 10.1161/01.RES.0000246849.17887.66
167. Stenzel D, Lundkvist A, Sauvaget D, Busse M, Graupera M, van der Flier A, et al. Integrin-dependent and -independent functions of astrocytic fibronectin in retinal angiogenesis. *Development.* (2011) 138:4451–63. doi: 10.1242/dev.071381
168. Franke FE, Von Georgi R, Zygmunt M, Münstedt K. Association between fibronectin expression and prognosis in ovarian carcinoma. *Anticancer Res.* (2003) 23:4261–7.
169. Shi K, Wang S-L, Shen B, Yu F-Q, Weng D-F, Lin J-H. Clinicopathological and prognostic values of fibronectin and integrin αvβ3 expression in primary osteosarcoma. *World J Surg Oncol.* (2019) 17:23. doi: 10.1186/s12957-019-1566-z
170. Wang JP, Hielscher A. Fibronectin: how its aberrant expression in tumors may improve therapeutic targeting. *J Cancer.* (2017) 8:674–82. doi: 10.7150/jca.16901
171. Yi W, Xiao E, Ding R, Luo P, Yang Y. High expression of fibronectin is associated with poor prognosis, cell proliferation and malignancy via the NF-κB/p53-apoptosis signaling pathway in colorectal cancer. *Oncol Rep.* (2016) 36:3145–53. doi: 10.3892/or.2016.5177
172. Richter P, Junker K, Franz M, Berndt A, Geyer C, Gajda M, et al. IIICS de novo glycosylated fibronectin as a marker for invasiveness in urothelial carcinoma of the urinary bladder (UBC). *J Cancer Res Clin Oncol.* (2008) 134:1059–65. doi: 10.1007/s00432-008-0390-6
173. Stenman S, Vaheri A. Fibronectin in human solid tumors. *Int J Cancer.* (1981) 27:427–35. doi: 10.1002/ijc.2910270403
174. Attieh Y, Vignjevic DM. The hallmarks of CAFs in cancer invasion. *Eur J Cell Biol.* (2016) 95:493–502. doi: 10.1016/j.ejcb.2016.07.004
175. Attieh Y, Clark AG, Grass C, Richon S, Pocard M, Mariani P, et al. Cancer-associated fibroblasts lead tumor invasion through integrin-β3-dependent fibronectin assembly. *J Cell Biol.* (2017) 216:3509–20. doi: 10.1083/jcb.201702033
176. Erdogan B, Ao M, White LM, Means AL, Brewer BM, Yang L, et al. Cancer-associated fibroblasts promote directional cancer cell migration by aligning fibronectin. *J Cell Biol.* (2017) 216:3799–816. doi: 10.1083/jcb.201704053
177. Malik G, Knowles LM, Dhir R, Xu S, Yang S, Ruoslahti E, et al. Plasma fibronectin promotes lung metastasis by contributions to fibrin clots and tumor cell invasion. *Cancer Res.* (2010) 70:4327–34. doi: 10.1158/0008-5472.CAN-09-3312
178. Meng XN, Jin Y, Yu Y, Bai J, Liu GY, Zhu J, et al. Characterisation of fibronectin-mediated FAK signalling pathways in lung cancer cell migration and invasion. *Br J Cancer.* (2009) 101:327–34. doi: 10.1038/sj.bjc.6605154
179. Sengupta S, Nandi S, Hindi ES, Wainwright DA, Han Y, Lesniak MS. Short hairpin RNA-mediated fibronectin knockdown delays tumor growth in a mouse glioma model. *Neoplasia.* (2010) 12:837–47. doi: 10.1593/neo.10662
180. Dongre A, Weinberg RA. New insights into the mechanisms of epithelial-mesenchymal transition and implications for cancer. *Nat Rev Mol Cell Biol.* (2019) 20:69–84. doi: 10.1038/s41580-018-0080-4
181. Thiery JP. Epithelial-mesenchymal transitions in tumour progression. *Nat Rev Cancer.* (2002) 2:442–54. doi: 10.1038/nrc822
182. Duband JL, Thiery JP. Appearance and distribution of fibronectin during chick embryo gastrulation and neurulation. *Dev Biol.* (1982) 94:337–50. doi: 10.1016/0012-1606(82)90352-9
183. Fontana L, Chen Y, Prijatelj P, Sakai T, Fässler R, Sakai LY, et al. Fibronectin is required for integrin αvβ6-mediated activation of latent TGF-β complexes containing LTBP-1. *FASEB J.* (2005) 19:1798–808. doi: 10.1096/fj.05-4134com

184. Barbazán J, Alonso-Alconada L, Elkhatib N, Geraldo S, Gurchenkov V, Glentis A, et al. Liver metastasis is facilitated by the adherence of circulating tumor cells to vascular fibronectin deposits. *Cancer Res.* (2017) 77:3431–41. doi: 10.1158/0008-5472.CAN-16-1917
185. Kai F, Drain AP, Weaver VM. The extracellular matrix modulates the metastatic journey. *Dev Cell.* (2019) 49:332–46. doi: 10.1016/j.devcel.2019.03.026
186. Liu Y, Cao X. Characteristics and significance of the pre-metastatic niche. *Cancer Cell.* (2016) 30:668–81. doi: 10.1016/j.ccell.2016.09.011
187. Kaplan RN, Riba RD, Zacharoulis S, Bramley AH, Vincent L, Costa C, et al. VEGFR1-positive haematopoietic bone marrow progenitors initiate the pre-metastatic niche. *Nature.* (2005) 438:820–7. doi: 10.1038/nature04186
188. Costa-Silva B, Aiello NM, Ocean AJ, Singh S, Zhang H, Thakur BK, et al. Pancreatic cancer exosomes initiate pre-metastatic niche formation in the liver. *Nat Cell Biol.* (2015) 17:816–26. doi: 10.1038/ncb3169
189. Erler JT, Bennewith KL, Cox TR, Lang G, Bird D, Koong A, et al. Hypoxia-induced lysyl oxidase is a critical mediator of bone marrow cell recruitment to form the premetastatic niche. *Cancer Cell.* (2009) 15:35–44. doi: 10.1016/j.ccr.2008.11.012
190. Wang Y, Sun Y, Li D, Zhang L, Wang K, Zuo Y, et al. Platelet P2Y12 is involved in murine pulmonary metastasis. *PLoS ONE.* (2013) 8:e80780. doi: 10.1371/journal.pone.0080780
191. Maquart F-X, Pasco S, Ramont L, Hornebeck W, Monboisse J-C. An introduction to matrikines: extracellular matrix-derived peptides which regulate cell activity. *Crit Rev Oncol Hematol.* (2004) 49:199–202. doi: 10.1016/j.critrevonc.2003.06.007
192. Kelsh RM, McKeown-Longo PJ. Topographical changes in extracellular matrix: activation of TLR4 signaling and solid tumor progression. *Trends Cancer Res.* (2013) 9:1–13.
193. Bhattacharyya S, Varga J. Endogenous ligands of TLR4 promote unresolving tissue fibrosis: Implications for systemic sclerosis and its targeted therapy. *Immunol Lett.* (2018) 195:9–17. doi: 10.1016/j.imlet.2017.09.011
194. Mishra S, Kundu K. Synthesis, characterization and applications of polyacrylamide grafted fenugreek gum (FG-g-PAM) as flocculant: microwave vs thermal synthesis approach. *Int J Biol Macromol.* (2019) 141:792–808. doi: 10.1016/j.ijbiomac.2019.09.033
195. Lasarte JJ, Casares N, Gorraiz M, Hervás-Stubbs S, Arribillaga L, Mansilla C, et al. The extra domain a from fibronectin targets antigens to TLR4-expressing cells and induces cytotoxic T cell responses *in vivo*. *J Immunol.* (2007) 178:748–56. doi: 10.4049/jimmunol.178.2.748
196. Malara A, Gruppi C, Abbonante V, Cattaneo D, De Marco L, Massa M, et al. EDA fibronectin-TLR4 axis sustains megakaryocyte expansion and inflammation in bone marrow fibrosis. *J Exp Med.* (2019) 216:587–604. doi: 10.1084/jem.20181074
197. Kelsh R, You R, Horzempa C, Zheng M, McKeown-Longo PJ. Regulation of the innate immune response by fibronectin: synergism between the III-1 and EDA domains. *PLoS ONE.* (2014) 9:e102974. doi: 10.1371/journal.pone.0102974
198. Smith ML, Gourdon D, Little WC, Kubow KE, Eguiluz RA, Luna-Morris S, et al. Force-induced unfolding of fibronectin in the extracellular matrix of living cells. *PLoS Biol.* (2007) 5:e268. doi: 10.1371/journal.pbio.0050268
199. McFadden JP, Basketter DA, Dearman RJ, Kimber IR. Extra domain A-positive fibronectin-positive feedback loops and their association with cutaneous inflammatory disease. *Clin Dermatol.* (2011) 29:257–65. doi: 10.1016/j.clindermatol.2010.11.003
200. Galon J. Type, density, and location of immune cells within human colorectal tumors predict clinical outcome. *Science.* (2006) 313:1960–4. doi: 10.1126/science.1129139
201. Mlecnik B, Tosolini M, Kirilovsky A, Berger A, Bindea G, Meatchi T, et al. Histopathologic-based prognostic factors of colorectal cancers are associated with the state of the local immune reaction. *JCO.* (2011) 29:610–8. doi: 10.1200/JCO.2010.30.5425
202. Zhang L, Conejo-Garcia JR, Katsaros D, Gimotty PA, Massobrio M, Regnani G, et al. Intratumoral T cells, recurrence, and survival in epithelial ovarian cancer. *N Engl J Med.* (2003) 348:203–13. doi: 10.1056/NEJMoa020177
203. Fridman WH, Pagès F, Sautès-Fridman C, Galon J. The immune contexture in human tumours: impact on clinical outcome. *Nat Rev Cancer.* (2012) 12:298–306. doi: 10.1038/nrc3245
204. Barnes TA, Amir E. HYPE or HOPE: the prognostic value of infiltrating immune cells in cancer. *Br J Cancer.* (2017) 117:451–60. doi: 10.1038/bjc.2017.220
205. Garner H, de Visser K. Immune crosstalk in cancer progression and metastatic spread: a complex conversation. *Nat Rev Immunol.* (in press). doi: 10.1038/s41577-019-0271-z
206. Chen DS, Mellman I. Elements of cancer immunity and the cancer-immune set point. *Nature.* (2017) 541:321–30. doi: 10.1038/nature21349
207. Salmon H, Franciszkiewicz K, Damotte D, Dieu-Nosjean M-C, Validire P, Trautmann A, et al. Matrix architecture defines the preferential localization and migration of T cells into the stroma of human lung tumors. *J Clin Invest.* (2012) 122:899–910. doi: 10.1172/JCI45817
208. Joyce JA, Fearon DT. T cell exclusion, immune privilege, and the tumor microenvironment. *Science.* (2015) 348:74–80. doi: 10.1126/science.aaa6204
209. Peranzoni E, Rivas-Caicedo A, Bougherara H, Salmon H, Donnadieu E. Positive and negative influence of the matrix architecture on antitumor immune surveillance. *Cell Mol Life Sci.* (2013) 70:4431–48. doi: 10.1007/s00018-013-1339-8
210. Peranzoni E, Lemoine J, Vimeux L, Feuillet V, Barrin S, Kantari-Mimoun C, et al. Macrophages impede CD8 T cells from reaching tumor cells and limit the efficacy of anti-PD-1 treatment. *Proc Natl Acad Sci USA.* (2018) 115:E4041–50. doi: 10.1073/pnas.1720948115
211. Varol C, Sagi I. Phagocyte-extracellular matrix crosstalk empowers tumor development and dissemination. *FEBS J.* (2018) 285:734–51. doi: 10.1111/febs.14317
212. Pavlides S, Whitaker-Menezes D, Castello-Cros R, Flomenberg N, Witkiewicz AK, Frank PG, et al. The reverse Warburg effect: aerobic glycolysis in cancer associated fibroblasts and the tumor stroma. *Cell Cycle.* (2009) 8:3984–4001. doi: 10.4161/cc.8.23.10238
213. Sullivan WJ, Mullen PJ, Schmid EW, Flores A, Momcilovic M, Sharpley MS, et al. Extracellular matrix remodeling regulates glucose metabolism through TXNIP destabilization. *Cell.* (2018) 175:117–32.e21. doi: 10.1016/j.cell.2018.08.017
214. Morris BA, Burkel B, Ponik SM, Fan J, Condeelis JS, Aguirre-Ghiso JA, et al. Collagen matrix density drives the metabolic shift in breast cancer cells. *EBio Med.* (2016) 13:146–56. doi: 10.1016/j.ebiom.2016.10.012
215. Xu S, Xu H, Wang W, Li S, Li H, Li T, et al. The role of collagen in cancer: from bench to bedside. *J Transl Med.* (2019) 17:309. doi: 10.1186/s12967-019-2058-1
216. Kato Y, Ozawa S, Miyamoto C, Maehata Y, Suzuki A, Maeda T, et al. Acidic extracellular microenvironment and cancer. *Cancer Cell Int.* (2013) 13:89. doi: 10.1186/1475-2867-13-89
217. Gortan Cappellari G, Barazzoni R, Cattin L, Muro AF, Zanetti M. Lack of fibronectin extra domain A alternative splicing exacerbates endothelial dysfunction in diabetes. *Sci Rep.* (2016) 6:37965. doi: 10.1038/srep 37965
218. Du H, Wang Y, Zhang Z, Yang J, Zhang J, Zhang Y. Fibronectin overexpression modulates formation of macrophage foam cells by activating SREBP2 involved in endoplasmic reticulum stress. *Cell Physiol Biochem.* (2015) 36:1821–34. doi: 10.1159/000430153
219. Rick JW, Chandra A, Dalle Ore C, Nguyen AT, Yagnik G, Aghi MK. Fibronectin in malignancy: cancer-specific alterations, protumoral effects, and therapeutic implications. *Semin Oncol.* (2019) 46:284–90. doi: 10.1053/j.seminoncol.2019.08.002
220. Kumra H, Reinhardt DP. Fibronectin-targeted drug delivery in cancer. *Adv Drug Deliv Rev.* (2016) 97:101–10. doi: 10.1016/j.addr.2015.11.014
221. Johannsen M, Spitaleri G, Curigliano G, Roigas J, Weikert S, Kempkensteffen C, et al. The tumour-targeting human L19-IL2 immunocytokine: preclinical safety studies, phase I clinical trial in patients with solid tumours and expansion into patients with advanced renal cell carcinoma. *Eur J Cancer.* (2010) 46:2926–35. doi: 10.1016/j.ejca.2010.07.033
222. Eigentler TK, Weide B, de Braud F, Spitaleri G, Romanini A, Pflugfelder A, et al. A dose-escalation and signal-generating study of the immunocytokine L19-IL2 in combination with dacarbazine for the therapy of patients with metastatic melanoma. *Clin Cancer Res.* (2011) 17:7732–42. doi: 10.1158/1078-0432.CCR-11-1203
223. Weide B, Eigentler T, Catania C, Ascierto PA, Cascinu S, Becker JC, et al. A phase II study of the L19IL2 immunocytokine in combination with

dacarbazine in advanced metastatic melanoma patients. *Cancer Immunol Immunother.* (2019) 68:1547–59. doi: 10.1007/s00262-019-02383-z

224. Rekers NH, Zegers CM, Germeraad WT, Dubois L, Lambin P. Long-lasting antitumor effects provided by radiotherapy combined with the immunocytokine L19-IL2. *Oncoimmunology.* (2015) 4:e1021541. doi: 10.1080/2162402X.2015.1021541
225. Arribillaga L, Durantez M, Lozano T, Rudilla F, Rehberger F, Casares N, et al. A fusion protein between streptavidin and the endogenous TLR4 ligand EDA targets biotinylated antigens to dendritic cells and induces T cell responses *in vivo*. *BioMed Res Int.* (2013) 2013:1–9. doi: 10.1155/2013/864720
226. Mansilla C, Berraondo P, Durantez M, Martínez M, Casares N, Arribillaga L, et al. Eradication of large tumors expressing human papillomavirus E7 protein by therapeutic vaccination with E7 fused to the extra domain a from fibronectin. *Int J Cancer.* (2012) 131:641–51. doi: 10.1002/ijc.26412
227. Rudilla F, Fayolle C, Casares N, Durantez M, Arribillaga L, Lozano T, et al. Combination of a TLR4 ligand and anaphylatoxin C5a for the induction of antigen-specific cytotoxic T cell responses. *Vaccine.* (2012) 30:2848–58. doi: 10.1016/j.vaccine.2012.02.052
228. Julier Z, Martino MM, de Titta A, Jeanbart L, Hubbell JA. The TLR4 agonist fibronectin extra domain A is cryptic, exposed by elastase-2; use in a fibrin matrix cancer vaccine. *Sci Rep.* (2015) 5:8569. doi: 10.1038/srep08569
229. Schaffner F, Ray A, Dontenwill M. Integrin α5β1, the fibronectin receptor, as a pertinent therapeutic target in solid tumors. *Cancers.* (2013) 5:27–47. doi: 10.3390/cancers5010027
230. Bell-McGuinn KM, Matthews CM, Ho SN, Barve M, Gilbert L, Penson RT, et al. A phase II, single-arm study of the anti-α5β1 integrin antibody volociximab as monotherapy in patients with platinum-resistant advanced epithelial ovarian or primary peritoneal cancer. *Gynecol Oncol.* (2011) 121:273–9. doi: 10.1016/j.ygyno.2010.12.362
231. Jin H, Su J, Garmy-Susini B, Kleeman J, Varner J. Integrin α4β1 promotes monocyte trafficking and angiogenesis in tumors. *Cancer Res.* (2006) 66:2146–52. doi: 10.1158/0008-5472.CAN-05-2704
232. Oh J, Magnuson A, Benoist C, Pittet MJ, Weissleder R. Age-related tumor growth in mice is related to integrin α4 in $CD8^+$ T cells. *JCI Insight.* (2018) 3:e122961. doi: 10.1172/jci.insight.122961
233. Desgrosellier JS, Cheresh DA. Integrins in cancer: biological implications and therapeutic opportunities. *Nat Rev Cancer.* (2010) 10:9–22. doi: 10.1038/nrc2748
234. Batlle E, Massagué J. Transforming Growth factor-β signaling in immunity and cancer. *Immunity.* (2019) 50:924–40. doi: 10.1016/j.immuni.2019.03.024
235. Sethi T, Rintoul RC, Moore SM, MacKinnon AC, Salter D, Choo C, et al. Extracellular matrix proteins protect small cell lung cancer cells against apoptosis: a mechanism for small cell lung cancer growth and drug resistance *in vivo*. *Nat Med.* (1999) 5:662–8. doi: 10.1038/9511
236. Hazlehurst L, Damiano J, Buyuksal I, Pledger W, Dalton W. Adhesion to fibronectin via β1 integrins regulates p27kip1 levels and contributes to cell adhesion mediated drug resistance (CAM-DR). *Oncogene.* (2000) 19:4319–27. doi: 10.1038/sj.onc.1203782
237. Eke I, Storch K, Krause M, Cordes N. Cetuximab attenuates its cytotoxic and radiosensitizing potential by inducing fibronectin biosynthesis. *Cancer Res.* (2013) 73:5869–79. doi: 10.1158/0008-5472.CAN-13-0344
238. Matsunaga T, Takemoto N, Sato T, Takimoto R, Tanaka I, Fujimi A, et al. Interaction between leukemic-cell VLA-4 and stromal fibronectin is a decisive factor for minimal residual disease of acute myelogenous leukemia. *Nat Med.* (2003) 9:1158–65. doi: 10.1038/nm909
239. Eke I, Sandfort V, Storch K, Baumann M, Röper B, Cordes N. Pharmacological inhibition of EGFR tyrosine kinase affects ILK-mediated cellular radiosensitization *in vitro*. *Int J Radiat Biol.* (2007) 83:793–802. doi: 10.1080/09553000701727549
240. Hehlgans S, Haase M, Cordes N. Signalling via integrins: Implications for cell survival and anticancer strategies. *Biochim Biophys Acta.* (2007) 1775:163–80. doi: 10.1016/j.bbcan.2006.09.001
241. Estrugo D, Fischer A, Hess F, Scherthan H, Belka C, Cordes N. Ligand bound β1 integrins inhibit procaspase-8 for mediating cell adhesion-mediated drug and radiation resistance in human leukemia cells. *PLoS ONE.* (2007) 2:e269. doi: 10.1371/journal.pone.0000269
242. Senthebane D, Jonker T, Rowe A, Thomford N, Munro D, Dandara C, et al. The role of tumor microenvironment in chemoresistance: 3D extracellular matrices as accomplices. *IJMS.* (2018) 19:2861. doi: 10.3390/ijms19102861
243. Straub JM, New J, Hamilton CD, Lominska C, Shnayder Y, Thomas SM. Radiation-induced fibrosis: mechanisms and implications for therapy. *J Cancer Res Clin Oncol.* (2015) 141:1985–94. doi: 10.1007/s00432-015-1974-6

Conflict of Interest: The authors declare that the research was conducted in the absence of any commercial or financial relationships that could be construed as a potential conflict of interest.

Copyright © 2020 Efthymiou, Saint, Ruff, Rekad, Ciais and Van Obberghen-Schilling. This is an open-access article distributed under the terms of the Creative Commons Attribution License (CC BY). The use, distribution or reproduction in other forums is permitted, provided the original author(s) and the copyright owner(s) are credited and that the original publication in this journal is cited, in accordance with accepted academic practice. No use, distribution or reproduction is permitted which does not comply with these terms.

frontiers in Oncology

MINI REVIEW
published: 30 April 2020
doi: 10.3389/fonc.2020.00527

Functional Interplay Between Collagen Network and Cell Behavior Within Tumor Microenvironment in Colorectal Cancer

Cuong Cao Le [1,2,3], Amar Bennasroune [1,2], Benoit Langlois [1,2], Stéphanie Salesse [1,2], Camille Boulagnon-Rombi [1,2,4], Hamid Morjani [1,3], Stéphane Dedieu [1,2†] and Aline Appert-Collin [1,2†]*

[1] Université de Reims Champagne-Ardenne, Reims, France, [2] CNRS UMR 7369, Matrice Extracellulaire et Dynamique Cellulaire, MEDyC, Reims, France, [3] Unité BioSpecT, EA7506, Reims, France, [4] Laboratoire de Biopathologie, Centre Hospitalier Universitaire et Faculté de Médecine, Reims, France

OPEN ACCESS

Edited by:
Vasiliki Gkretsi, European University Cyprus, Cyprus

Reviewed by:
Elvira Olaso, University of the Basque Country, Spain
Gunjan Agarwal, The Ohio State University, United States

***Correspondence:**
Aline Appert-Collin
aline.bennasroune@univ-reims.fr

† These authors have contributed equally to this work and share co-senior authors

Specialty section:
This article was submitted to Molecular and Cellular Oncology, a section of the journal Frontiers in Oncology

Received: *18 January 2020*
Accepted: *24 March 2020*
Published: *30 April 2020*

Citation:
Le CC, Bennasroune A, Langlois B, Salesse S, Boulagnon-Rombi C, Morjani H, Dedieu S and Appert-Collin A (2020) Functional Interplay Between Collagen Network and Cell Behavior Within Tumor Microenvironment in Colorectal Cancer. Front. Oncol. 10:527. doi: 10.3389/fonc.2020.00527

Colorectal cancer is the second most common cancer diagnosed in men and the third most commonly occurring in women worldwide. Interactions between cells and the surrounding extracellular matrix (ECM) are involved in tumor development and progression of many types of cancer. The organization of the ECM molecules provides not only physical scaffoldings and dynamic network into which cells are embedded but also allows the control of many cellular behaviors including proliferation, migration, differentiation, and survival leading to homeostasis and morphogenesis regulation. Modifications of ECM composition and mechanical properties during carcinogenesis are critical for tumor initiation and progression. The core matrisome consists of five classes of macromolecules, which are collagens, laminins, fibronectin, proteoglycans, and hyaluronans. In most tissues, fibrillar collagen is the major component of ECM. Cells embedded into fibrillar collagen interact with it through their surface receptors, such as integrins and discoidin domain receptors (DDRs). On the one hand, cells incorporate signals from ECM that modify their functionalities and behaviors. On the other hand, all cells within tumor environment (cancer cells, cancer-associated fibroblasts, endothelial cells, and immune cells) synthesize and secrete matrix macromolecules under the control of multiple extracellular signals. This cell-ECM dialog participates in a dynamic way in ECM formation and its biophysical and biochemical properties. Here, we will review the functional interplay between cells and collagen network within the tumor microenvironment during colorectal cancer progression.

Keywords: colorectal cancer, collagen, cancer-associated fibroblast, tumor cell, endothelial cell, *in vitro* model

COLLAGEN AND COLORECTAL CANCER: STATE OF PLAY

In recent decades, several works have underlined the importance of the microenvironment in colon cancer progression (1). In the tumor microenvironment (TME), extracellular matrix (ECM) plays a key role in this process. Among ECM adhesive components, type I collagen is one of the important factors regulating cancer-related events at different tumorigenesis stages (2). After effacement of the basement membrane, paracrine signals from the nascent tumor lead to profound reorganizations

of submucosal ECM that include deposition of fibrillar collagens together with growth factors and ECM-modifying enzymes that stimulate active vascular remodeling. Some recent studies based on global transcriptomic or proteomic approaches shed new light on the specific markers that are dysregulated during early steps of colon carcinogenesis, but also in locally advanced or metastatic colorectal cancer (CRC) (3–5). Interestingly, proteomic analysis of detergent insoluble fractions of paired primary colon tumors and liver metastasis compared with adjacent non-tumorous tissues illustrated the pathological samples' specific enrichment in core matrisome and several collagen-modifying enzymes such as MMPs, ADAMs, and LOXL1 (5). Desmoplasia and collagen deposition constitute a hallmark of CRC and various collagens including type I, VI, VII, VIII, X, XI, and XVIII were found accumulated in CRC samples (6–12). A recent study showed an increase of type I collagen in tumor tissues compared to normal tissue (13). Moreover, type I collagen mRNAs were also reported as increased in blood of CRC patients compared to healthy individuals (13, 14). Consistently, second harmonic generation imaging of fibrillar collagen contents has shown clinical efficacy to stratify high-grade tumors and relevance to predict CRC patient outcome (7, 15).

The most studied type I collagen receptors are integrins α1β1, α2β1, α10β1, and α11β1 (16). These receptors can be activated by several ligands such as type I collagen after recognition of its GFOGER sequence (17). α1β1 dimer was considered as the most expressed receptor in colon carcinoma (18). β1-integrin expression in tumors was correlated with reduced overall survival and reduced disease-free survival in a large cohort of CRC patients (19). Notably, β1 integrin is detected in CRC patients' serum and its level of expression appears to correlate with aggressiveness and presence of micrometastasis (20). β1 integrin overexpression is also associated with CRC progression and colorectal liver metastasis (20, 21). *In vitro*, β1 integrin expression is down-regulated in response to 3D type I collagen (22, 23). However, although β1 integrin seems to contribute to metastasis development, β1 integrin targeted therapy is not successful in CRC management. In fact, simultaneous inhibition of β1 integrin and EGFR in CRC does not improve radiotherapy efficiency (24).

Collagen also signals to cells through the receptor tyrosine kinases discoidin domain receptors DDR1 and DDR2; both of them have also been reported to interact with type I collagen (25) and to play a role in tumor progression (23). These receptors, which harbor a tyrosine kinase activity, recognize GVMGFO sequence of type I collagen (26) and exhibit a relatively late and prolonged activation (27). DDR1 is expressed in colon carcinoma and promote metastasis in invasive colon carcinoma (28–30). Concerning DDR2, a high expression was associated with higher frequencies of T4, lymph node metastasis, peritoneal spread, and worse prognosis, suggesting that DDR2 expression might be an effective therapeutic target (31).

This growing data set supports a key role of collagens and their partners during tumorigenesis processes and as potential biomarkers of CRC. The following parts aim to highlight current evidence regarding the functional interplay between cells within the TME and collagen network during CRC progression. The main data are presented in **Figure 1**.

THE RELATIONSHIP BETWEEN COLLAGEN AND CANCER CELLS

Analysis of ECM signatures in patients' colon tumors has revealed that type I collagen is highly expressed (5). Accordingly, high density of type I collagen constitutes a poor prognosis factor in colon carcinoma and type I collagen-rich environment is able to induce mesenchymal gene expression and invasion (32). Beside the density, collagen topology (fiber alignment) and elasticity (stiffness) appear to be also associated to colon tumorigenesis. Brauchle et al. have demonstrated that the alignment of collagen fibers is increased in colon carcinoma tissues when compared to normal tissues and associated with increased stiffness (33). Biophysical investigations have also shown different molecular fingerprints for collagen fibers in colon carcinoma tissues when compared to normal tissues (33). Another study has shown that density and collagen fiber alignment were higher in tumor invasion front than in primary tumor and normal tissue (34). Of note, hypoxia, which is associated with collagen density and organization, has an impact on colon cancer carcinoma migration and invasion through promotion of epithelial-to-mesenchymal transition (35).

Concerning the role of type I collagen receptors in tumor progression, Roche's group has elegantly recently shown that DDR1 plays a crucial role in the invasion function of metastatic colon carcinoma (28, 29). They have particularly demonstrated that pharmacological inhibition of DDR1-BCR signaling axis decreased invasion and metastatic processes in colon carcinoma, suggesting that DDR1 targeting could be an efficient co-treatment strategy in colon carcinoma (28, 29). More recently, NSD2 circular RNA has been shown to promote DDR1 expression and CRC metastasis by targeting miR-199b-5p (36). For integrins, Wu and co-workers have lately reported that type I collagen is able to support colon carcinoma cell stemness, invasion, and metastasis through activation of α2β1 integrin heterodimer and PI3K/AKT/Snail signaling pathway (37).

Regarding the role of type I collagen in the cancer cell sensitivity to targeted therapies, a recent study has demonstrated that 3D type I collagen may protect colon carcinoma against the anti-EGFR cetuximab therapy by increasing tyrosine phosphorylation of MET and RON (32). The effect of 3D type I collagen on the sensitivity to vemurafenib of colon carcinoma, carrying the $BRAF^{V600E}$ mutation has also been investigated. At the opposite of the general concept describing type I collagen as a shield of colon carcinoma cells against therapies, authors have demonstrated that cells seeded in 3D type I collagen were 10-fold more sensitive to the vemurafenib targeted drug. On the contrary, 3D matrix was able to protect tumor cells against the cytotoxic effect of the fluorouracil chemotherapeutic agent (38). However, another one carried out on resistance to chemotherapy and the ATP binding cassette transporter P-glycoprotein, which

Abbreviations: CAF. cancer-associated fibroblast; CRC, colorectal cancer; DDR, discoidin domain receptor; ECM, extracellular matrix; FAP, fibroblast activation protein; SHG, second harmonic generation; TME, tumor microenvironment.

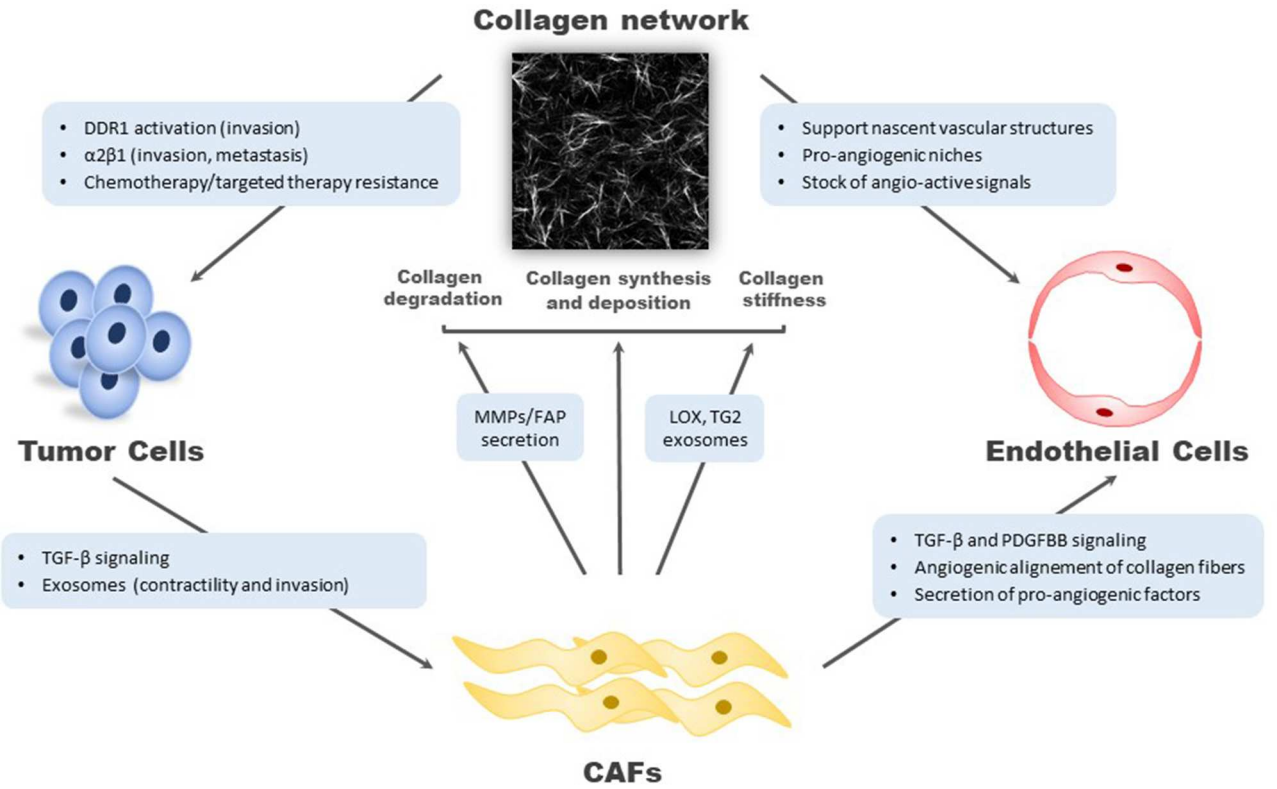

FIGURE 1 | Relationship between type I collagen network and cells in tumor microenvironment. On the one hand, cancer cells, cancer-associated fibroblasts, and endothelial cells influence collagen structure and composition. On the other hand, type I collagen participates to tumor progression. DDR1, discoidin domain receptor I; FAP, fibroblast activation protein; LOX, lysyl oxidase; MMP, metalloproteinase; PDGFBB, platelet-derived growth factor BB; TG2, transglutaminase 2; TGF-β, transforming growth factor-β.

is encoded by *ABCB1* gene, has shown that 3D ECM is able to increase sensitivity of primary colon carcinoma cells to chemotherapy by affecting the cell polarity and consequently the polarization of P-glycoprotein expression at the cell surface (39). Interestingly, the expression of *ABCB1* gene appears to be regulated in colon carcinoma. In fact, the overexpression of the caudal-related homeobox transcription factor (Cdx2) has been reported to upregulate the expression of *ABCB1*/gene and consequently P-glycoprotein in highly resistant colon carcinoma to chemotherapy (40).

However, Cdx2 has also been described to play a role as a tumor suppressor (41). In fact, Cdx2 expression has been shown to be lower in colon carcinoma with the highest grades (42). In agreement with the role of ECM in colon carcinoma progression, type I collagen has been shown to promote tumorigenesis by downregulating Cdx2 expression (43). Brummer's group has demonstrated a few years ago a positive correlation between BRAF mutation and low level of Cdx2 expression in colon carcinoma. Type I collagen at high density has also been reported to suppress HNF4α when inducing mesenchymal gene expression *in vitro* and in patient-derived colon tumors (32). Consistently, invalidation or inhibition of HNF4α promotes colon carcinogenesis, whereas its enforced expression is able to inhibit cell growth in colon carcinoma (44, 45).

THE RELATIONSHIP BETWEEN COLLAGEN AND CANCER-ASSOCIATED FIBROBLASTS

Cancer-associated fibroblasts (CAFs) are the most abundant cell type in TME; they are an activated type of fibroblast that plays a major role in tumorigenesis and metastatic processes (46). CAFs demonstrate a functional heterogeneity in CRC that may arise from different cellular origins and can affect the clinical course of colon cancer patients (47). In CRC, an abundance of CAFs in the TME has been associated with poor outcomes and transcriptomic studies linked CAF signature with poor prognosis and highly aggressive CRC molecular subtypes. CAFs are not only associated with advanced CRC but also found in early stages (48). Several studies identified CAFs as potential prognosis and recurrence markers in patients with colon cancer (49–52). Histologic evaluations of CRC patient samples and organotypic 3D co-culture models demonstrated that CAFs are the primary drivers of collagen synthesis and remodeling in the highly desmoplastic environment found in CRC (53, 54). Interestingly, a significant heterogeneity was observed within CAF population related to collagen remodeling (55). Transcriptome and proteome profiling identified CRC CAFs as the main source for connective tissue components of the

ECM, such as collagens, thus altering the molecular composition of the matrix by increasing the deposition of new matrix components (56, 57). Another way for CAFs to remodel ECM is to degrade it by using MMPs and formation of degradative protrusions. Genes induced in CRC CAFs, compared to normal colonic fibroblasts, include several tumor-promoting MMPs and TGF-β1 increased Collagen I and various proteases expression by CAFs (56–58). In CAFs, formation of invadopodia that remodel collagen fibers is dependent on twist1 and palladin (isoform 4). Twist1-expressing fibroblasts acquired CAF properties such as collagen contraction and alignment, and palladin and collagen α1(VI) were identified as two major mediators of these Twist1 effects. Interestingly, Twist1, palladin, and collagen α1(VI) are overexpressed in purified colon CAFs as compared with their normal counterparts and associate with poor prognosis in CRC (59). In addition to MMPs, CAFs also express other proteases such as the fibroblast activation protein (FAP), a collagenase and gelatinase (60). Stromal FAP expression in human colon cancer samples is a marker of early stage in cancer development and correlated with poor patient outcome (61). FAP-α activity has a strong impact on fibroblast secretome composition, including matrix processing enzymes, and influence morphology and collagen contraction capacity of immortalized CRC CAFs. Recent studies established a direct link between CAFs and the modifications of ECM organization and stiffness described in colon cancer. LOXL2, a collagen cross-linker, was reported as highly expressed in CAFs and is associated with poor CRC survival (62). Hic-5, a non-enzymatic adaptor protein, was described as a novel factor responsible for the development of CRC, by promoting in CAFs the production of collagen I and LOX that lead to stiffness of cancer tissues (63). More recently, in a collagen gel co-culture system, with fibroblasts and CRC cells, Delaine-Smith's group demonstrated that fibroblast-derived TG2 (transglutaminase-2), a protein cross-linking enzyme, induced gel stiffening by formation of thicker collagen fibers and proposed a regulatory link between TG2 and LOX. In addition, stiffness is further increased by fibroblast/CRC cross-talk and a potential role for extracellular vesicles in mediating this tumor-driven fibroblast response is suggested by authors (64). Another study reported that fibroblasts activated by late-stage CRC cell-derived exosomes became specialized in type I collagen and physical remodeling of ECM through cytoskeletal re-organization, membrane protrusion formation, and secretion of matrix-remodeling proteins (65).

THE RELATIONSHIP BETWEEN COLLAGEN AND ENDOTHELIAL CELLS

Angiogenesis exerts crucial functions during major steps of CRC progression (1, 3, 66). Stimulation of CRC cells by oncogenic drivers such as EGF or stabilization of hypoxia-inducible factors (HIFs) was involved in the secretion of angiogenic diffusible factors and ECM structural compounds in the TME (67). Moreover, collagen supports nascent vascular structures during intussusceptive angiogenesis in CRC (68). A nine-gene signature including collagen I, X, and XI was specifically enriched in angiogenic and hypoxic CRC gene sets (4). Another study identified a matrisomal signature of 110 genes induced during the angiogenic switch of the standard RIP1-Tag2 murine model of tumor angiogenesis (3). The expression of this set of genes, which includes collagens I, VI, VIII, and X and various ECM regulators was positively correlated with that of endothelial cell markers and increased with CRC progression. This signature was also specifically induced in hepatic metastasis suggesting a functional contribution to both early events and metastatic cascade. It is now well-established that tumor and stromal cells synergize to activate pro-angiogenic signals in the TME (3, 61, 66, 69, 70). CAFs and tumor-associated macrophages (TAM) are both involved in TGF-β signaling activation during the angiogenic switch (3). Stromal activation of this pathway promotes both tumor initiation and early metastatic events (66) and was specifically associated to consensus molecular subtypes CMS4 of CRC that express various angiogenesis markers and present the worst overall survival (71). Several reports illustrated the contributions of tumor-resident or infiltrated stromal cells to ECM-modifying events that accommodate endothelial cells' fitness and provide angiogenic cues (61, 69, 72). Although a clear scenario is sometimes difficult to draw on the angiogenic consequences of collagen deposition, emerging angio-active parameters include types of collagens (network, fibrils-anchoring or fibrillar collagens that convey different angiogenic signals), topology, and stiffness. Post-translational modifications such as proteolytic degradation or cross-linking can modulate the biophysical properties of collagen-rich scaffolds (11, 70, 72, 73). FAP-α expression and activity were linked to the secretion of pro-angiogenic factors such as angiopoietin-1 and VEGF-C by colon patient-derived CAFs (61). Gain- and loss-of-function experiments illustrated that FAP-α-dependent CAF secretome can stimulate 3D endothelial spheroids sprouting. *In vivo*, targeting of FAP-α into an immune-competent murine model of colon cancer decreased blood vessel density and induced fibrillar collagen accumulation (69). The activity of SNAI1 and PDGFBB contributes to CAF ability to assemble aligned collagen fibers that promote endothelial cell proliferation and morphogenesis in a 3D model of CAF-derived matrices (72). SNAI1 expression by fibroblasts was also associated with the abundance of CD34-positive endothelial cells in an *in vivo* model of CRC. A pro-tumoral action of TAM could be explained by their ability to assemble collagenous ECM enriched with type I, VI, and XIV collagens (70). These fibers were deposited, cross-linked, and linearized at areas of tumor invasiveness demonstrating the crucial importance of TAM in organizing collagenous ECM niches. Co-culture of TAM with CRC cells can potentiate the production of tumor-derived MMP2 and MMP9 (74). Recruitment of collagenolytic enzyme-expressing immune cells in the CRC TME might influence the bioavailability of ECM-immobilized angiogenic factors such as VEGF, as reported in other tumor context (75, 76). Collagen-enriched niches emerge as biomarkers of desmoplastic and angiogenic CRC microenvironment (77, 78). High expression of collagens I and IV, with tumor endothelial marker-1 (TEM-1, endosialin), especially when distributed around tumor vessels, allows stratification of CRC patients according to their poor

prognosis (77). Collagen-enriched niches might also account for the adaptive response of the TME to anti-angiogenic therapies (78, 79). Collagen IV empty sleeves resulting from tumor vessel pruning triggered by VEGFR2 can promote a rapid vascular regrowth after treatment withdrawal (79). VEGFR2 blocking in a CRC model normalized tumor vessels, decreasing diameter while ameliorating collagen IV perivascular coverage (78). Endostatin, a collagen XVIII-derived fragment, is an inflammatory marker detected around blood vessels and in the plasma of advanced CRC patients (12). This molecule, efficient to inhibit both lymphangiogenesis and hemangiogenesis (80), is considered as a valuable tool to control metastatic CRC growth since several studies reported its moderate toxicity without observing the increased metastatic dissemination encountered in response to the anti-VEGF antibody bevacizumab (30).

IN VITRO TME MODELS USING COLLAGEN

Two-dimensional (2D) collagen-coated systems' routine use has largely shown their limitations to summarize the complexity of tumor initiation and progression processes. It is absolutely necessary to include some major extracellular components to mimic properties of the TME such as the spatial configuration (81) and the addition of supporting materials with mechanical properties close to the ECM encountered during disease progression (82). The use of *in vitro* 3D models should fill the gap between traditional 2D cell culture and animal models, by mimicking the cancer micro- and macro-environment potentially able to integrate multiple cell types in a controlled environment, and should allow one to better characterize CRC drivers and develop new therapeutic strategies in constantly upgraded models of growing complexity. One possible approach is to develop spheroids of cancer cells seeded on low-attachment tissue culture plates. Whereas, this type of culture allows cancer cells to communicate with one another and to release low levels of intrinsic collagen (83), substantial aspects of TME are still missing. More complex models using biological scaffolds such as collagen are therefore added to create an ECM to obtain biomimicry and study cancer progression by recreating the TME. Patient-derived xenograft models are an important tool for preclinical and clinical research, especially when orthotopically transplanted. However, in this model, the principal limit is that TME cannot be properly reconstituted owing to important stromal cells such as cancer-associated fibroblasts and endothelial cells, which are not derived from the tumor samples and can be late recruited (84). New 3D models of cancer using a collagen matrix can promote the crosstalk between cancer and stromal cell. Co-cultures of different CRC cell lines with fibroblasts and endothelial cells in 3D spheroids have been elaborated to test drug dose response and compared with results in 2D and homotypic 3D cultures. The results suggest that 3D co-cultures are more relevant, providing a higher level of translational information that should help to define patient-specific treatment options (85).

Pape and colleagues developed a CRC model using high-density type I monomeric collagen, termed tumoroids (86). This model consists of a central cancer mass containing either the highly invasive HCT116 or less invasive HT29 cells embedded in collagen type I hydrogels to mimic the TME *in situ* (87). The stromal compartment in this model is easily manipulated and ECM components and stromal cell types can be added accordingly. Furthermore, on-chip biomimetic microenvironments using microfluidic technologies are being developed to better reproduce the complexity of *in vivo* restrictions. In this model, human colonic microvascular endothelial cells cultivated in a 3D vessel-mimetic device are attached to the wall of the lateral channels of the microfluidic chip whereas HCT-116 cells are embedded in collagen IV-enriched Matrigel in the central chamber (88).

Considering the feature of tumor heterogeneity, the main limitation of these models is the presence of a single CRC cell type exhibiting a unique genetic pattern. The development of more realistic preclinical models is absolutely required and is a major challenge for the coming years, especially for improving drug screening. The use of patient-derived 3D tumor models may provide a solution to overcome the oversimplified 2D cell cultures and the limitations of *in vivo* models (89). These new designs are not intended to completely supplant but rather complete and expand the currently available techniques.

AUTHOR CONTRIBUTIONS

All authors listed have made a substantial, direct and intellectual contribution to the work, and approved it for publication.

FUNDING

Financial support was received from CNRS, URCA and la Structure Fédérative de Recherche Cap Santé.

REFERENCES

1. Crotti S, Piccoli M, Rizzolio F, Giordano A, Nitti D, Agostini M. Extracellular matrix and colorectal cancer: how surrounding microenvironment affects cancer cell behavior? *J Cell Physiol.* (2017) 232:967–75. doi: 10.1002/jcp.25658
2. Xu R, Won J-Y, Kim C-H, Kim D-E, Yim H. Roles of the phosphorylation of transcriptional factors in epithelial-mesenchymal transition. *J Oncol.* (2019) 2019:11. doi: 10.1155/2019/5810465
3. Langlois B, Saupe F, Rupp T, Arnold C, van der Heyden M, Orend G, et al. AngioMatrix, a signature of the tumor angiogenic switch-specific matrisome, correlates with poor prognosis for glioma and colorectal cancer patients. *Oncotarget.* (2014) 5:10529–45. doi: 10.18632/oncotarget.2470
4. Yuzhalin AE, Urbonas T, Silva MA, Muschel RJ, Gordon-Weeks AN. A core matrisome gene signature predicts cancer outcome. *Br J Cancer.* (2018) 118:435–40. doi: 10.1038/bjc.2017.458
5. Naba A, Clauser KR, Whittaker CA, Carr SA, Tanabe KK, Hynes RO. Extracellular matrix signatures of human primary metastatic

colon cancers and their metastases to liver. *BMC Cancer*. (2014) 14:518. doi: 10.1186/1471-2407-14-518
6. Skovbjerg H, Anthonsen D, Lothe IM, Tveit KM, Kure EH, Vogel LK. Collagen mRNA levels changes during colorectal cancer carcinogenesis. *BMC Cancer*. (2009) 9:136. doi: 10.1186/1471-2407-9-136
7. Burke K, Smid M, Dawes RP, Timmermans MA, Salzman P, van Deurzen CH, et al. Using second harmonic generation to predict patient outcome in solid tumors. *BMC Cancer*. (2015) 15:929. doi: 10.1186/s12885-015-1911-8
8. Qiao J, Fang CY, Chen SX, Wang XQ, Cui SJ, Liu XH, et al. Stroma derived COL6A3 is a potential prognosis marker of colorectal carcinoma revealed by quantitative proteomics. *Oncotarget*. (2015) 6:29929–46. doi: 10.18632/oncotarget.4966
9. Shang J, Wang F, Chen P, Wang X, Ding F, Liu S, et al. Co-expression network analysis identified COL8A1 is associated with the progression and prognosis in human colon adenocarcinoma. *Dig Dis Sci*. (2018) 63:1219–28. doi: 10.1007/s10620-018-4996-5
10. Sole X, Crous-Bou M, Cordero D, Olivares D, Guino E, Sanz-Pamplona R, et al. Discovery and validation of new potential biomarkers for early detection of colon cancer. *PLoS ONE*. (2014) 9:e106748. doi: 10.1371/journal.pone.0106748
11. Yuzhalin AE, Gordon-Weeks AN, Tognoli ML, Jones K, Markelc B, Konietzny R, et al. Colorectal cancer liver metastatic growth depends on PAD4-driven citrullination of the extracellular matrix. *Nat Commun*. (2018) 9:4783. doi: 10.1038/s41467-018-07306-7
12. Kantola T, Vayrynen JP, Klintrup K, Makela J, Karppinen SM, Pihlajaniemi T, et al. Serum endostatin levels are elevated in colorectal cancer and correlate with invasion and systemic inflammatory markers. *Br J Cancer*. (2014) 111:1605–13. doi: 10.1038/bjc.2014.456
13. Zou X, Feng B, Dong T, Yan G, Tan B, Shen H, et al. Up-regulation of type I collagen during tumorigenesis of colorectal cancer revealed by quantitative proteomic analysis. *J Proteomics*. (2013) 94:473–85. doi: 10.1016/j.jprot.2013.10.020
14. Rodia MT, Ugolini G, Mattei G, Montroni I, Zattoni D, Ghignone F, et al. Systematic large-scale meta-analysis identifies a panel of two mRNAs as blood biomarkers for colorectal cancer detection. *Oncotarget*. (2016) 7:30295–306. doi: 10.18632/oncotarget.8108
15. Birk JW, Tadros M, Moezardalan K, Nadyarnykh O, Forouhar F, Anderson J, et al. Second harmonic generation imaging distinguishes both high-grade dysplasia and cancer from normal colonic mucosa. *Dig Dis Sci*. (2014) 59:1529–4. doi: 10.1007/s10620-014-3121-7
16. Barczyk M, Carracedo S, Gullberg D. Integrins. *Cell Tissue Res*. (2009) 339:269. doi: 10.1007/s00441-009-0834-6
17. Knight CG, Morton LF, Peachey AR, Tuckwell DS, Farndale RW, Barnes MJ. The collagen-binding A-domains of integrins alpha(1)beta(1) and alpha(2)beta(1) recognize the same specific amino acid sequence, GFOGER, in native (triple-helical) collagens. *J Biol Chem*. (2000) 275:35–40. doi: 10.1074/jbc.275.1.35
18. Boudjadi S, Carrier JC, Beaulieu J-F. Integrin α1 subunit is up-regulated in colorectal cancer. *Biomark Res*. (2013) 1:16. doi: 10.1186/2050-7771-1-16
19. Liu QZ, Gao XH, Chang WJ, Gong HF, Fu CG, Zhang W, et al. *Expression of ITGB1 predicts prognosis in colorectal cancer: a large prospective study based on tissue microarray*. Int J Clin Exp Pathol. (2015) 8:12802-10.
20. Oh BY, Kim KH, Chung SS, Hong KS, Lee RA. Role of beta1-integrin in colorectal cancer: case-control study. *Ann Coloproctol*. (2014) 30:61–70. doi: 10.3393/ac.2014.30.2.61
21. Sun C, Zargham R, Shao Q, Gui X, Marcus V, Lazaris A, et al. Association of CD98, integrin beta1, integrin beta3 and Fak with the progression and liver metastases of colorectal cancer. *Pathol Res Pract*. (2014) 210:668–74. doi: 10.1016/j.prp.2014.06.016
22. Assent D, Bourgot I, Hennuy B, Geurts P, Noel A, Foidart JM, et al. A membrane-type-1 matrix metalloproteinase (MT1-MMP)-discoidin domain receptor 1 axis regulates collagen-induced apoptosis in breast cancer cells. *PLoS ONE*. (2015) 10:e0116006. doi: 10.1371/journal.pone.0116006
23. Saby C, Buache E, Brassart-Pasco S, El Btaouri H, Courageot MP, Van Gulick L, et al. Type I collagen aging impairs discoidin domain receptor 2-mediated tumor cell growth suppression. *Oncotarget*. (2016) 7:24908–27. doi: 10.18632/oncotarget.8795
24. Poschau M, Dickreuter E, Singh-Muller J, Zscheppang K, Eke I, Liersch T, et al. EGFR and beta1-integrin targeting differentially affect colorectal carcinoma cell radiosensitivity and invasion. *Radiother Oncol*. (2015) 116:510–6. doi: 10.1016/j.radonc.2015.06.005
25. Rammal H, Saby C, Magnien K, Van-Gulick L, Garnotel R, Buache E, et al. Discoidin domain receptors: potential actors and targets in cancer. *Front Pharmacol*. (2016) 7:55. doi: 10.3389/fphar.2016.00055
26. Konitsiotis AD, Raynal N, Bihan D, Hohenester E, Farndale RW, Leitinger B. Characterization of high affinity binding motifs for the discoidin domain receptor DDR2 in collagen. *J Biol Chem*. (2008) 283:6861–8. doi: 10.1074/jbc.M709290200
27. Vogel W, Gish GD, Alves F, Pawson T. The discoidin domain receptor tyrosine kinases are activated by collagen. *Mol Cell*. (1997) 1:13–23. doi: 10.1016/S1097-2765(00)80003-9
28. Jeitany M, Leroy C, Tosti P, Lafitte M, Le Guet J, Simon V, et al. Inhibition of DDR1-BCR signalling by nilotinib as a new therapeutic strategy for metastatic colorectal cancer. *EMBO Mol Med*. (2018) 10:e7918. doi: 10.15252/emmm.201707918
29. Sirvent A, Lafitte M. DDR1 inhibition as a new therapeutic strategy for colorectal cancer. *Mol Cell Oncol*. (2018) 5:e1465882. doi: 10.1080/23723556.2018.1465882
30. Chen CT, Yamaguchi H, Lee HJ, Du Y, Lee HH, Xia W, et al. Dual targeting of tumor angiogenesis and chemotherapy by endostatin-cytosine deaminase-uracil phosphoribosyltransferase. *Mol Cancer Ther*. (2011) 10:1327–36. doi: 10.1158/1535-7163.MCT-10-1117
31. Sasaki S, Ueda M, Iguchi T, Kaneko M, Nakayama H, Watanabe T, et al. DDR2 expression is associated with a high frequency of peritoneal dissemination and poor prognosis in colorectal cancer. *Anticancer Res*. (2017) 37:2587–91. doi: 10.21873/anticanres.11603
32. Vellinga TT, den Uil S, Rinkes IH, Marvin D, Ponsioen B, Alvarez-Varela A, et al. Collagen-rich stroma in aggressive colon tumors induces mesenchymal gene expression and tumor cell invasion. *Oncogene*. (2016) 35:5263–71. doi: 10.1038/onc.2016.60
33. Brauchle E, Kasper J, Daum R, Schierbaum N, Falch C, Kirschniak A, et al. Biomechanical and biomolecular characterization of extracellular matrix structures in human colon carcinomas. *Matrix Biol*. (2018) 68–9:180–93. doi: 10.1016/j.matbio.2018.03.016
34. Blockhuys S, Agarwal NR, Hildesjo C, Jarlsfelt I, Wittung-Stafshede P, Sun XF. Second harmonic generation for collagen I characterization in rectal cancer patients with and without preoperative radiotherapy. *J Biomed Opt*. (2017) 22:1–6. doi: 10.1117/1.JBO.22.10.106006
35. Hongo K, Tsuno NH, Kawai K, Sasaki K, Kaneko M, Hiyoshi M, et al. Hypoxia enhances colon cancer migration and invasion through promotion of epithelial-mesenchymal transition. *J Surg Res*. (2013) 182:75–84. doi: 10.1016/j.jss.2012.08.034
36. Chen LY, Zhi Z, Wang L, Zhao YY, Deng M, Liu YH, et al. NSD2 circular RNA promotes metastasis of colorectal cancer by targeting miR-199b-5p-mediated DDR1 and JAG1 signalling. *J Pathol*. (2019) 248:103–15. doi: 10.1002/path.5238
37. Wu X, Cai J, Zuo Z, Li J. Collagen facilitates the colorectal cancer stemness and metastasis through an integrin/PI3K/AKT/Snail signaling pathway. *Biomed Pharmacother*. (2019) 114:108708. doi: 10.1016/j.biopha.2019.108708
38. Kikuchi K, Hoshino D. Sensitization of HT29 colorectal cancer cells to vemurafenib in three-dimensional collagen cultures. *Cell Biol Int*. (2019) 44:621–9. doi: 10.1002/cbin.11262
39. Ashley N, Ouaret D, Bodmer WF. Cellular polarity modulates drug resistance in primary colorectal cancers via orientation of the multidrug resistance protein ABCB1. *J Pathol*. (2019) 247:293–304. doi: 10.1002/path.5179
40. Takakura Y, Hinoi T, Oue N, Sasada T, Kawaguchi Y, Okajima M, et al. CDX2 regulates multidrug resistance 1 gene expression in malignant intestinal epithelium. *Cancer Res*. (2010) 70:6767–78. doi: 10.1158/0008-5472.CAN-09-4701
41. Bonhomme C, Duluc I, Martin E, Chawengsaksophak K, Chenard MP, Kedinger M, et al. The Cdx2 homeobox gene has a tumour suppressor function in the distal colon in addition to a homeotic role during gut development. *Gut*. (2003) 52:1465–71. doi: 10.1136/gut.52.10.1465

42. Asgari-Karchekani S, Karimian M, Mazoochi T, Taheri MA, Khamehchian T. CDX2 protein expression in colorectal cancer and its correlation with clinical and pathological characteristics, prognosis, and survival rate of patients. *J Gastrointest Cancer*. (2019). doi: 10.1007/s12029-019-00314-w
43. Brabletz T, Spaderna S, Kolb J, Hlubek F, Faller G, Bruns CJ, et al. Down-regulation of the homeodomain factor Cdx2 in colorectal cancer by collagen type I: an active role for the tumor environment in malignant tumor progression. *Cancer Res*. (2004) 64:6973–7. doi: 10.1158/0008-5472.CAN-04-1132
44. Tanaka T, Jiang S, Hotta H, Takano K, Iwanari H, Sumi K, et al. Dysregulated expression of P1 and P2 promoter-driven hepatocyte nuclear factor-4alpha in the pathogenesis of human cancer. *J Pathol*. (2006) 208:662–72. doi: 10.1002/path.1928
45. Chellappa K, Robertson GR, Sladek FM. HNF4α: a new biomarker in colon cancer? *Biomarkers Med*. (2012) 6:297–300. doi: 10.2217/bmm.12.23
46. Kalluri R. The biology and function of fibroblasts in cancer. *Nat Rev Cancer*. (2016) 16:582–98. doi: 10.1038/nrc.2016.73
47. Herrera M, Islam AB, Herrera A, Martin P, Garcia V, Silva J, et al. Functional heterogeneity of cancer-associated fibroblasts from human colon tumors shows specific prognostic gene expression signature. *Clin Cancer Res*. (2013) 19:5914–26. doi: 10.1158/1078-0432.CCR-13-0694
48. Herrera M, Herrera A, Dominguez G, Silva J, Garcia V, Garcia JM, et al. Cancer-associated fibroblast and M2 macrophage markers together predict outcome in colorectal cancer patients. *Cancer Sci*. (2013) 104:437–44. doi: 10.1111/cas.12096
49. Tsujino T, Seshimo I, Yamamoto H, Ngan CY, Ezumi K, Takemasa I, et al. Stromal myofibroblasts predict disease recurrence for colorectal cancer. *Clin Cancer Res*. (2007) 13:2082–90. doi: 10.1158/1078-0432.CCR-06-2191
50. Berdiel-Acer M, Cuadras D, Diaz-Maroto NG, Sanjuan X, Serrano T, Berenguer A, et al. A monotonic and prognostic genomic signature from fibroblasts for colorectal cancer initiation, progression, and metastasis. *Mol Cancer Res*. (2014) 12:1254–66. doi: 10.1158/1541-7786.MCR-14-0121
51. Calon A, Lonardo E, Berenguer-Llergo A, Espinet E, Hernando-Momblona X, Iglesias M, et al. Stromal gene expression defines poor-prognosis subtypes in colorectal cancer. *Nat Genet*. (2015) 47:320–9. doi: 10.1038/ng.3225
52. Mukaida N, Sasaki S. Fibroblasts, an inconspicuous but essential player in colon cancer development and progression. *World J Gastroenterol*. (2016) 22:5301–5316. doi: 10.3748/wjg.v22.i23.5301
53. Coulson-Thomas VJ, Coulson-Thomas YM, Gesteira TF, de Paula CA, Mader AM, Waisberg J, et al. Colorectal cancer desmoplastic reaction up-regulates collagen synthesis and restricts cancer cell invasion. *Cell Tissue Res*. (2011) 346:223–36. doi: 10.1007/s00441-011-1254-y
54. Shin N, Son GM, Shin DH, Kwon MS, Park BS, Kim HS, et al. Cancer-associated fibroblasts and desmoplastic reactions related to cancer invasiveness in patients with colorectal cancer. *Ann Coloproctol*. (2019) 35:36–46. doi: 10.3393/ac.2018.09.10
55. Hanley CJ, Noble F, Ward M, Bullock M, Drifka C, Mellone M, et al. A subset of myofibroblastic cancer-associated fibroblasts regulate collagen fiber elongation, which is prognostic in multiple cancers. *Oncotarget*. (2016) 7:6159–74. doi: 10.18632/oncotarget.6740
56. Torres S, Bartolome RA, Mendes M, Barderas R, Fernandez-Acenero MJ, Pelaez-Garcia A, et al. Proteome profiling of cancer-associated fibroblasts identifies novel proinflammatory signatures and prognostic markers for colorectal cancer. *Clin Cancer Res*. (2013) 19:6006–19. doi: 10.1158/1078-0432.CCR-13-1130
57. Rupp C, Scherzer M, Rudisch A, Unger C, Haslinger C, Schweifer N, et al. IGFBP7, a novel tumor stroma marker, with growth-promoting effects in colon cancer through a paracrine tumor-stroma interaction. *Oncogene*. (2015) 34:815–25. doi: 10.1038/onc.2014.18
58. Tommelein J, Verset L, Boterberg T, Demetter P, Bracke M, De Wever O. Cancer-associated fibroblasts connect metastasis-promoting communication in colorectal cancer. *Front Oncol*. (2015) 5:63. doi: 10.3389/fonc.2015.00063
59. Garcia-Palmero I, Torres S, Bartolome RA, Pelaez-Garcia A, Larriba MJ, Lopez-Lucendo M, et al. Twist1-induced activation of human fibroblasts promotes matrix stiffness by upregulating palladin and collagen alpha1(VI). *Oncogene*. (2016) 35:5224–36. doi: 10.1038/onc.2016.57
60. Brokopp CE, Schoenauer R, Richards P, Bauer S, Lohmann C, Emmert MY, et al. Fibroblast activation protein is induced by inflammation and degrades type I collagen in thin-cap fibroatheromata. *Eur Heart J*. (2011) 32:2713–22. doi: 10.1093/eurheartj/ehq519
61. Koczorowska MM, Tholen S, Bucher F, Lutz L, Kizhakkedathu JN, De Wever O, et al. Fibroblast activation protein-alpha, a stromal cell surface protease, shapes key features of cancer associated fibroblasts through proteome and degradome alterations. *Mol Oncol*. (2016) 10:40–58. doi: 10.1016/j.molonc.2015.08.001
62. Torres S, Garcia-Palmero I, Herrera M, Bartolome RA, Pena C, Fernandez-Acenero MJ, et al. LOXL2 is highly expressed in cancer-associated fibroblasts and associates to poor colon cancer survival. *Clin Cancer Res*. (2015) 21:4892–902. doi: 10.1158/1078-0432.CCR-14-3096
63. Omoto T, Kim-Kaneyama JR, Lei XF, Orimo A, Ohnishi K, Yoshihara K, et al. The impact of stromal Hic-5 on the tumorigenesis of colorectal cancer through lysyl oxidase induction and stromal remodeling. *Oncogene*. (2018) 37:1205–19. doi: 10.1038/s41388-017-0033-y
64. Delaine-Smith R, Wright N, Hanley C, Hanwell R, Bhome R, Bullock M, et al. Transglutaminase-2 mediates the biomechanical properties of the colorectal cancer tissue microenvironment that contribute to disease progression. *Cancers*. (2019) 11:701. doi: 10.3390/cancers11050701
65. Rai A, Greening DW, Chen M, Xu R, Ji H, Simpson RJ. Exosomes derived from human primary and metastatic colorectal cancer cells contribute to functional heterogeneity of activated fibroblasts by reprogramming their proteome. *Proteomics*. (2019) 19:e1800148. doi: 10.1002/pmic.201800148
66. Calon A, Espinet E, Palomo-Ponce S, Tauriello DV, Iglesias M, Cespedes MV, et al. Dependency of colorectal cancer on a TGF-beta-driven program in stromal cells for metastasis initiation. *Cancer Cell*. (2012) 22:571–84. doi: 10.1016/j.ccr.2012.08.013
67. Khong TL, Thairu N, Larsen H, Dawson PM, Kiriakidis S, Paleolog EM. Identification of the angiogenic gene signature induced by EGF and hypoxia in colorectal cancer. *BMC Cancer*. (2013) 13:518. doi: 10.1186/1471-2407-13-518
68. Paku S, Dezso K, Bugyik E, Tovari J, Timar J, Nagy P, et al. A new mechanism for pillar formation during tumor-induced intussusceptive angiogenesis: inverse sprouting. *Am J Pathol*. (2011) 179:1573–85. doi: 10.1016/j.ajpath.2011.05.033
69. Santos AM, Jung J, Aziz N, Kissil JL, Pure E. Targeting fibroblast activation protein inhibits tumor stromagenesis and growth in mice. *J Clin Invest*. (2009) 119:3613–25. doi: 10.1172/JCI38988
70. Afik R, Zigmond E, Vugman M, Klepfish M, Shimshoni E, Pasmanik-Chor M, et al. Tumor macrophages are pivotal constructors of tumor collagenous matrix. *J Exp Med*. (2016) 213:2315–31. doi: 10.1084/jem.20151193
71. Guinney J, Dienstmann R, Wang X, de Reynies A, Schlicker A, Soneson C, et al. The consensus molecular subtypes of colorectal cancer. *Nat Med*. (2015) 21:1350–6. doi: 10.1038/nm.3967
72. Herrera A, Herrera M, Guerra-Perez N, Galindo-Pumarino C, Larriba MJ, Garcia-Barberan V, et al. Endothelial cell activation on 3D-matrices derived from PDGF-BB-stimulated fibroblasts is mediated by Snail1. *Oncogenesis*. (2018) 7:76. doi: 10.1038/s41389-018-0085-z
73. Olof Olsson P, Gustafsson R, Salnikov AV, Gothe M, Zeller KS, Friman T, et al. Inhibition of integrin alphaVbeta6 changes fibril thickness of stromal collagen in experimental carcinomas. *Cell Commun Signal*. (2018) 16:36. doi: 10.1186/s12964-018-0249-7
74. Kang JC, Chen JS, Lee CH, Chang JJ, Shieh YS. Intratumoral macrophage counts correlate with tumor progression in colorectal cancer. *J Surg Oncol*. (2010) 102:242–8. doi: 10.1002/jso.21617
75. Cavdar Z, Canda AE, Terzi C, Sarioglu S, Fuzun M, Oktay G. Role of gelatinases (matrix metalloproteinases 2 and 9), vascular endothelial growth factor and endostatin on clinicopathological behaviour of rectal cancer. *Colorectal Dis*. (2011) 13:154–60. doi: 10.1111/j.1463-1318.2009.02105.x
76. Nozawa H, Chiu C, Hanahan D. Infiltrating neutrophils mediate the initial angiogenic switch in a mouse model of multistage carcinogenesis. *Proc Natl Acad Sci USA*. (2006) 103:12493–8. doi: 10.1073/pnas.0601807103
77. O'Shannessy DJ, Somers EB, Chandrasekaran LK, Nicolaides NC, Bordeaux J, Gustavson MD. Influence of tumor microenvironment on prognosis in colorectal cancer: Tissue architecture-dependent signature of endosialin (TEM-1) and associated proteins. *Oncotarget*. (2014) 5:3983–95. doi: 10.18632/oncotarget.2108

78. Tong RT, Boucher Y, Kozin SV, Winkler F, Hicklin DJ, Jain RK. Vascular normalization by vascular endothelial growth factor receptor 2 blockade induces a pressure gradient across the vasculature and improves drug penetration in tumors. *Cancer Res.* (2004) 64:3731–6. doi: 10.1158/0008-5472.CAN-04-0074
79. Mancuso MR, Davis R, Norberg SM, O'Brien S, Sennino B, Nakahara T, et al. Rapid vascular regrowth in tumors after reversal of VEGF inhibition. *J Clin Invest*. (2006) 116:2610–21. doi: 10.1172/JCI24612
80. Jia Y, Liu M, Huang W, Wang Z, He Y, Wu J, et al. Recombinant human endostatin endostar inhibits tumor growth and metastasis in a mouse xenograft model of colon cancer. *Pathol Oncol Res*. (2012) 18:315–23. doi: 10.1007/s12253-011-9447-y
81. Stock K, Estrada MF, Vidic S, Gjerde K, Rudisch A, Santo VE, et al. Capturing tumor complexity *in vitro*: comparative analysis of 2D and 3D tumor models for drug discovery. *Sci Rep*. (2016) 6:28951. doi: 10.1038/srep 28951
82. Mierke CT. The fundamental role of mechanical properties in the progression of cancer disease and inflammation. *Rep Prog Phys*. (2014) 77:076602. doi: 10.1088/0034-4885/77/7/076602
83. De Angelis ML, Bruselles A, Francescangeli F, Pucilli F, Vitale S, Zeuner A, et al. Colorectal cancer spheroid biobanks: multi-level approaches to drug sensitivity studies. (2018) 34:459–69. doi: 10.1007/s10565-018-9423-3
84. Yada E, Wada S, Yoshida S, Sasada T. Use of patient-derived xenograft mouse models in cancer research and treatment. *Future Sci OA*. (2017) 4:FSO271. doi: 10.4155/fsoa-2017-0136
85. Zoetemelk M, Rausch M, Colin DJ, Dormond O, Nowak-Sliwinska P. Short-term 3D culture systems of various complexity for treatment optimization of colorectal carcinoma. *Sci Rep*. (2019) 9:7103. doi: 10.1038/s41598-019-42836-0
86. Pape J, Magdeldin T, Ali M, Walsh C, Lythgoe M, Emberton M, et al. Cancer invasion regulates vascular complexity in a three-dimensional biomimetic model. *Eur J Cancer*. (2019) 119:179–93. doi: 10.1016/j.ejca.2019.07.005
87. Magdeldin T, Lopez-Davila V, Pape J, Cameron GW, Emberton M, Loizidou M, et al. Engineering a vascularised 3D *in vitro* model of cancer progression. *Sci Rep*. (2017) 7:44045. doi: 10.1038/srep44045
88. Carvalho MR, Barata D. Colorectal tumor-on-a-chip system: A 3D tool for precision onco-nanomedicine. *Sci Adv*. (2019) 5:eaaw1317. doi: 10.1126/sciadv.aaw1317
89. Piccoli M, D'Angelo E, Crotti S, Sensi F, Urbani L, Maghin E, et al. Decellularized colorectal cancer matrix as bioactive microenvironment for *in vitro* 3D cancer research. *J Cell Physiol*. (2018) 233:5937–48. doi: 10.1002/jcp.26403

Conflict of Interest: The authors declare that the research was conducted in the absence of any commercial or financial relationships that could be construed as a potential conflict of interest.

Copyright © 2020 Le, Bennasroune, Langlois, Salesse, Boulagnon-Rombi, Morjani, Dedieu and Appert-Collin. This is an open-access article distributed under the terms of the Creative Commons Attribution License (CC BY). The use, distribution or reproduction in other forums is permitted, provided the original author(s) and the copyright owner(s) are credited and that the original publication in this journal is cited, in accordance with accepted academic practice. No use, distribution or reproduction is permitted which does not comply with these terms.

frontiers in Cell and Developmental Biology

ORIGINAL RESEARCH
published: 12 May 2020
doi: 10.3389/fcell.2020.00320

Label-Free Infrared Spectral Histology of Skin Tissue Part I: Impact of Lumican on Extracellular Matrix Integrity

Lise Nannan[1,2], Valérie Untereiner[3], Isabelle Proult[1,2], Camille Boulagnon-Rombi[1,2,4], Charlie Colin-Pierre[1,2,5], Ganesh D. Sockalingum[6] and Stéphane Brézillon[1,2]*

[1] Université de Reims Champagne-Ardenne, Laboratoire de Biochimie Médicale et Biologie Moléculaire, Reims, France, [2] CNRS UMR 7369, Matrice Extracellulaire et Dynamique Cellulaire, Reims, France, [3] Université de Reims Champagne-Ardenne, Cellular and Tissue Imaging Platform, Reims, France, [4] Laboratoire de Pathologie, Centre Hospitalier Universitaire de Reims, Reims, France, [5] BASF Beauty Care Solutions France SAS, Pulnoy, France, [6] Université de Reims Champagne-Ardenne, BioSpecT-BioSpectroscopie Translationnelle, EA7506, UFR de Pharmacie, Reims, France

Proteoglycans (PG) play an important role in maintaining the extracellular matrix (ECM) integrity. Lumican, a small leucine rich PG, is one such actor capable of regulating such properties. In this study, the integrity of the dermis of lumican-deleted $Lum^{-/-}$ vs. wild-type mice was investigated by conventional histology and by infrared spectral histology (IRSH). Infrared spectroscopy is a non-invasive, rapid, label-free and sensitive technique that allows to probe molecular vibrations of biomolecules present in a tissue. Our IRSH results obtained on control (WT, $n = 3$) and $Lum^{-/-}$ ($n = 3$) mice showed that different histological structures were identified by using K-means clustering and validated by hematoxylin eosin saffron (HES) staining. Furthermore, an important increase of the dermis thickness was observed in $Lum^{-/-}$ compared to WT mice. In terms of structural information, analysis of the spectral images also revealed an intra-group homogeneity and inter-group heterogeneity. In addition, type I collagen contribution was evaluated by HES and picrosirius red staining as well as with IRSH. Both techniques showed a strong remodeling of the ECM in $Lum^{-/-}$ mice due to the looseness of collagen fibers in the increased dermis space. These results confirmed the impact of lumican on the ECM integrity. The loss of collagen fibers organization due to the absence of lumican can potentially increase the accessibility of anti-cancer drugs to the tumor. These results are qualitatively interesting and would need further structural characterization of type I collagen fibers in terms of size, organization, and orientation.

Keywords: lumican, extracellular matrix, skin remodeling, infrared imaging, histology

OPEN ACCESS

Edited by:
Erik Maquoi, University of Liège, Belgium

Reviewed by:
Dragana Nikitovic, University of Crete, Greece
George N. Tzanakakis, University of Crete, Greece

****Correspondence:***
Ganesh D. Sockalingum
ganesh.sockalingum@univ-reims.fr

Specialty section:
This article was submitted to Molecular and Cellular Oncology, a section of the journal Frontiers in Cell and Developmental Biology

Received: *17 January 2020*
Accepted: *15 April 2020*
Published: *12 May 2020*

Citation:
Nannan L, Untereiner V, Proult I, Boulagnon-Rombi C, Colin-Pierre C, Sockalingum GD and Brézillon S (2020) Label-Free Infrared Spectral Histology of Skin Tissue Part I: Impact of Lumican on Extracellular Matrix Integrity. Front. Cell Dev. Biol. 8:320. doi: 10.3389/fcell.2020.00320

INTRODUCTION

Skin is the largest organ of the human body. It constitutes a physiological and physical barrier and has different functions of protection, thermoregulation, sensitization, excretion, and absorption. However, it is prone to numerous pathologies such as cutaneous skin cancers including melanoma. It is mainly composed of three layers with the epidermis, the dermis, and the hypodermis

(Dréno, 2009). The epidermis is a squamous keratinized stratified epithelium. It constitutes the superficial layer of the skin and has a protective function. It is separated from the dermis by a basal lamina: the dermal–epidermal junction itself is involved in the wound healing process. The dermis is a fibrous connective tissue, elastic and highly vascularized. It consists of papillary dermis, reticular dermis and appendages of the skin such as sweat glands and sebaceous glands as well as hair follicles. The papillary dermis is superficial and loose and consists of fine collagen fibers intertwined perpendicular to the epidermis. It also contains elastic fibers. Small blood vessels from the vascular plexus constitute a place of nutritive exchange with the deep layers of the epidermis. The papillary dermis is located above the reticular dermis. The latter is deep and consists of fibers intertwined collagen, in large irregular bundles, horizontally (Ueda et al., 2019). It also contains thick elastin fibers, blood vessels, nerves as well as nerve endings. The hypodermis constitutes the last and deepest layer of the skin. It is composed of subcutaneous white adipose tissue, an energy pool based on a muscular layer. Fibroblasts are the place of synthesis of macromolecules of the extracellular matrix (ECM) including proteoglycans (PGs; Postlethwaite and Kang, 1998). Extracellular matrix of the dermis is mainly constituted of type I and III collagens and PGs.

Lumican belongs to the family of small leucine-rich proteoglycans (SLRP). In the skin, it is a glycoprotein of 57 kDa but in the cornea, it is a PG with glycosaminoglycan (GAG) chains of keratan sulfate. Other major members of the SLRP family are decorin, biglycan and fibromodulin. The papillary dermis is rich in fibroblasts, the principal place of synthesis of SLRP including lumican. The latter is associated with collagen fibrils and especially with type I collagen. Homozygous mice deleted for Lumican gene were generated by Chakravarti et al. (1995, 1998). These mice exhibit a particular phenotype characterized by a fragile and elastic skin and an opacified cornea. This particular phenotype is explained by the abnormal organization of collagen fibers. They have larger diameters and interfibrillar space, demonstrating the architectural role of lumican in maintaining ECM integrity. Together, PGs and lumican regulate the assembly of collagen fibrils in many tissues. In humans, these phenotypic characteristics are comparable to those observed in the case Ehlers-Danlos syndrome. In addition, lumican has been shown to exhibit anti-tumoral activity in melanoma (Brézillon et al., 2007). Furthermore, the involvement of α2β1 integrin has been demonstrated in the modulation of lumican related cell invasion (D'Onofrio et al., 2008; Zeltz et al., 2010). Thus, during the adhesion of the tumor cells to a coating of lumican, a reorganization of the cytoskeleton is observed (Radwanska et al., 2008).

Classically the architectural modification of the dermis matrix is evaluated by conventional histology, biochemical analysis, and immunohistochemistry (Chakravarti et al., 1995, 1998). In this study, we present a novel approach based on infrared spectral imaging (IRSI) to assess morphological and chemical changes in the dermis. Infrared spectroscopy is a vibrational spectroscopy method that is used to characterize simple samples in different forms (solid, liquid, or gas) but also more complex systems such as cells or tissues based on the principle of interaction between light and matter. It is non-invasive and does not require any special preparation. Moreover, it is rapid, label-free, easy to use, and very sensitive (Mainreck et al., 2012). Spectral signatures are related to vibrations of molecular bonds that allow to characterize and determine molecular structure and composition. Coupled with a microscope, it gives maps/spectral images that enable to associate each pixel element to an entire IR spectrum. Infrared spectral imaging (IRSI) is a fast-growing technique and is intensively developed today for cell (spectral cytology) and tissue (spectral histology, IRSH) characterization (Draux et al., 2009; Baker et al., 2014). Spectral information can be used to identify specific biomarkers for disease diagnosis. For example, it has been used for differentiating between spinocellular cancer (SCC) and basocellular cancer (BCC) skin cancers and for demarcating the peritumoral area of melanoma (Ly et al., 2008). It has been successful in discriminating between healthy and cancerous tissues in colon cancer (Nallala et al., 2012).

In this report, the role of lumican on the organization the dermis matrix was undertaken. In parallel to the conventional histology, infrared spectral imaging was applied on skin tissue sections from control wild type (WT) $Lum^{+/+}$ and Lumican-deleted $Lum^{-/-}$ mice to better characterize the dermis remodeling.

MATERIALS AND METHODS

Animal Care

$Lum^{-/-}$ mouse line was generated by targeted mutation and fixed to the C57BL/6J genetic background (B6.129S-Lumtm1Chak/J; Chakravarti et al., 1995). This study was performed in compliance with "The French Animal Welfare Act" and following "The French Board for Animal Experiments." Experiments were conducted under approval of the French "Ministère de l'Enseignement Supérieur et de la Recherche" (ethics committee n°C2EA-56) in compliance with the "Directive 2010/63/UE."

Preparation of Tissue Samples

Skin samples were taken from the ventral flanks of C57BL/6J mice aged 2 to 3 months of control $Lum^{+/+}$ (WT) and homozygous mice deleted for Lumican gene $Lum^{-/-}$ (KO) with 3 mice per group, respectively. Skin samples were fixed in 4% formalin solution and paraffin embedded (FFPE). Three serial sections of 5 μm thick were cut from the blocks for conventional histology [Hematoxylin eosin saffron (HES)], picrosirius red (PSR), and IRSH. The first section was stained by HES to observe skin histology. Eosin being acidic stains the cytoplasm in pink while the basic hematoxylin stains the nucleus in purple. Saffron dye makes it possible to differentiate between connective tissue and muscle which is not the case for HE. The second section was placed on a 1 mm thick calcium fluoride (CaF_2) window for IRSI analysis. It can be noted that the IRSI method does not require any staining as structural features are revealed by the intrinsic biomolecular information. The third one was stained with PSR to observe type I collagen fibers (see workflow in **Figure 1**). Picrosirius

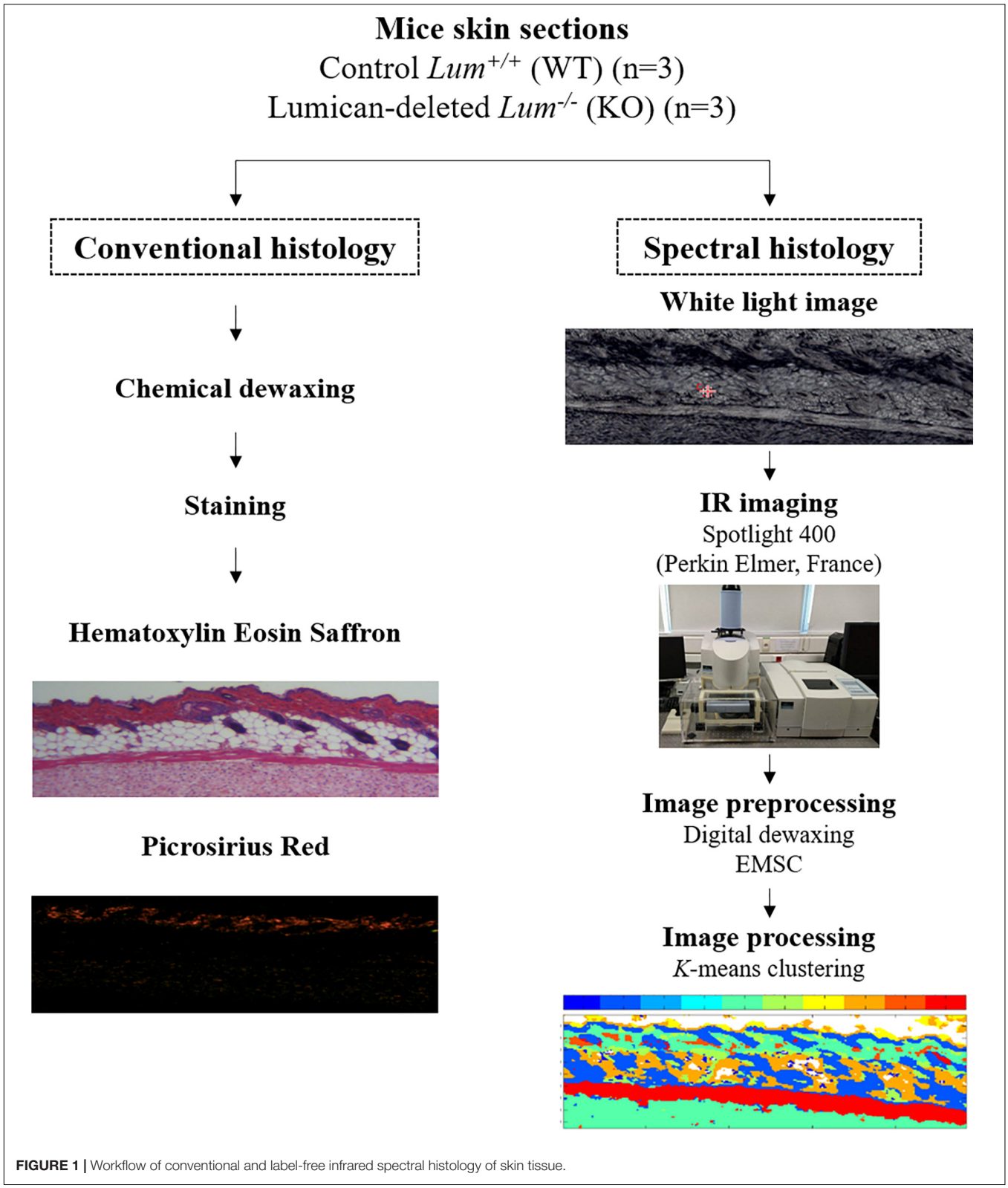

FIGURE 1 | Workflow of conventional and label-free infrared spectral histology of skin tissue.

red is one of the best understood histochemical techniques able to selectively highlight collagen networks. The collagen fibers are specifically appraised with polarized light detection. Indeed, the special dye PSR has the ability to enhance the natural birefringence of the collagen when exposed to polarized light.

Microscopic Observations

HES stained sections were imaged with the Olympus IX70 microscope with a 5x objective. Picrosirius red stained sections were imaged with a Zeiss Axiovert 200 M microscope equipped with a 4x objective in polarized illumination to highlight type I collagen fibers. All microscopy images were digitized using a iScan Coreo (Roche Ventana, Meilhan, France).

IR Spectral Imaging of Mice Skin Sections

All tissue sections $Lum^{+/+}$ and $Lum^{-/-}$ were imaged in transmission mode using the Spotlight 400 infrared imaging system at a spatial resolution of 6.25 μm/pixel (see workflow in **Figure 1**). The acquisition parameters were: spectral range from 4000 to 750 cm^{-1}, spectral resolution of 4 cm^{-1} and 8 scans/pixel. Calcium fluoride was used because it is transparent in the mid-infrared. The region of interest of the sample was first chosen using the white light image from the infrared microscope and then the IRSI acquisition was started. Prior to this, a background spectrum was measured in a blank area of the CaF_2 which was then automatically subtracted from each pixel spectrum of the sample.

IR Image Preprocessing

Since FFPE tissues were used and no chemical deparaffinisation was performed, a mathematical approach of digital dewaxing developed in-house in Matlab software (The Mathworks, Natick, MA; Ly et al., 2008) was carried out as paraffin gives strong FTIR peaks (Ly et al., 2008). Prior to this, all IR images underwent an atmospheric correction using the Spectrum Image 6.4 software (Perkin-Elmer). This step reduces the absorption of molecules present in the sample environment such as carbon dioxide or water vapor. The digital dewaxing procedure included the acquisition of a paraffin image under the same conditions as the sample. This image was used as a target in the Extended Multiplicative Signal Correction (EMSC) algorithm digital dewaxing model. It was used to estimate the contribution of the paraffin in each pixel of the image and therefore only the tissue variability was considered in the processing step such as clustering analysis. The EMSC algorithm also included correction of the baseline and variations related to the difference in sample thickness. Indeed, this step allowed the removal of spectral and spatial artifacts that can influence the spectral image analysis. All spectral images were preprocessed and processed in the reduced spectral region from 1800 to 800 cm^{-1}.

IR Image Processing

Spectral image analysis was based on the *K*-means clustering algorithm. This unsupervised and non-hierarchical technique allows to group pixel spectra into distinct classes (clusters) based on the spectral distance (similarity). Hence, similar data will be grouped in a same cluster and a pixel can be attributed to only one cluster. Each pixel is found associated with a class; a *K*-class. The number of classes is chosen by the user. Each class has a centroid which is chosen randomly at the beginning of the process. Each pixel spectrum is compared to the centroids and regrouped according to the closest similarity. This procedure is iterated until all the pixel spectra are attributed to a given class and until all centroids reached convergence, i.e., are stabilized. Finally, each class is represented by a color and the cluster image is reconstituted as a false color map. In order to compare different skin section images from $Lum^{+/+}$ and $Lum^{-/-}$ a common *K*-means was employed using 5 and 10 classes.

Correlation of IR Spectral Images With Type I Collagen Spectrum

The correlation of skin section spectral images with type I collagen spectrum was performed using the Spectrum Image 6.4 software (Perkin-Elmer). To do so, a spectrum of type I collagen was recorded from a 5 μm thick section of FFPE rat-tail tendon and correlated pixel by pixel with an atmospheric-corrected image of skin tissue section. The result was given as a correlated image with a correlation scale ranging from 0 (dark color) to 1 (white color).

Statistical Analysis

Statistical analyses were performed using Student's *t*-test and the results were expressed as the mean ± SEM using Prism 8.2.1 (GraphPad Software, La Jolla, CA, United States). The results were considered statistically significant when $^{**}p < 0.01$.

RESULTS

Comparison Between Conventional and Label-Free Infrared Spectral Histology in Skin Tissue From Mice Control $Lum^{+/+}$ (WT) vs. Lumican-Deleted $Lum^{-/-}$ (KO)

The HES stained sections (**Figures 2A,B**) highlight the different skin structures. The epidermis is stained in purple and characterized by a thin outer lining. The dermis appears in pink below the epidermis and is characterized by the presence of hair bulbs. The papillary dermis and the reticular dermis are not distinguishable at low magnification. The hypodermis (in white) is highlighted by the presence of adipose tissue. Underneath the hypodermis, the dark pink layer is composed of muscle fibers recognizable by their elongated shape. The subcutaneous fat is present under the muscle fiber layer. By comparing **Figures 2A,B**, it can be noticed that $Lum^{+/+}$ skin section appears more compact and its dermis is about 2 times thinner compared to $Lum^{-/-}$ mice. In addition, the layer of adipose tissue is reduced resulting in a thinner hypodermis in $Lum^{-/-}$ compared to $Lum^{+/+}$ skin tissue sections. This histological comparison is highlighted with a higher magnification in **Supplementary Figure 1**. The HES stained sections (**Figures 2A,B**) and the white light images (**Figures 2C,D**) are used as reference images for comparison with IRSH obtained by the common *K*-means classification with 5 (**Figures 2E,F**) and 10 classes (**Figures 2G,H**). The spectral images equally show different histological structures of the skin such as the epidermis, dermis, hypodermis, muscle fibers, subcutaneous fat and hair bulbs (see legend **Figures 2A,B**). It is

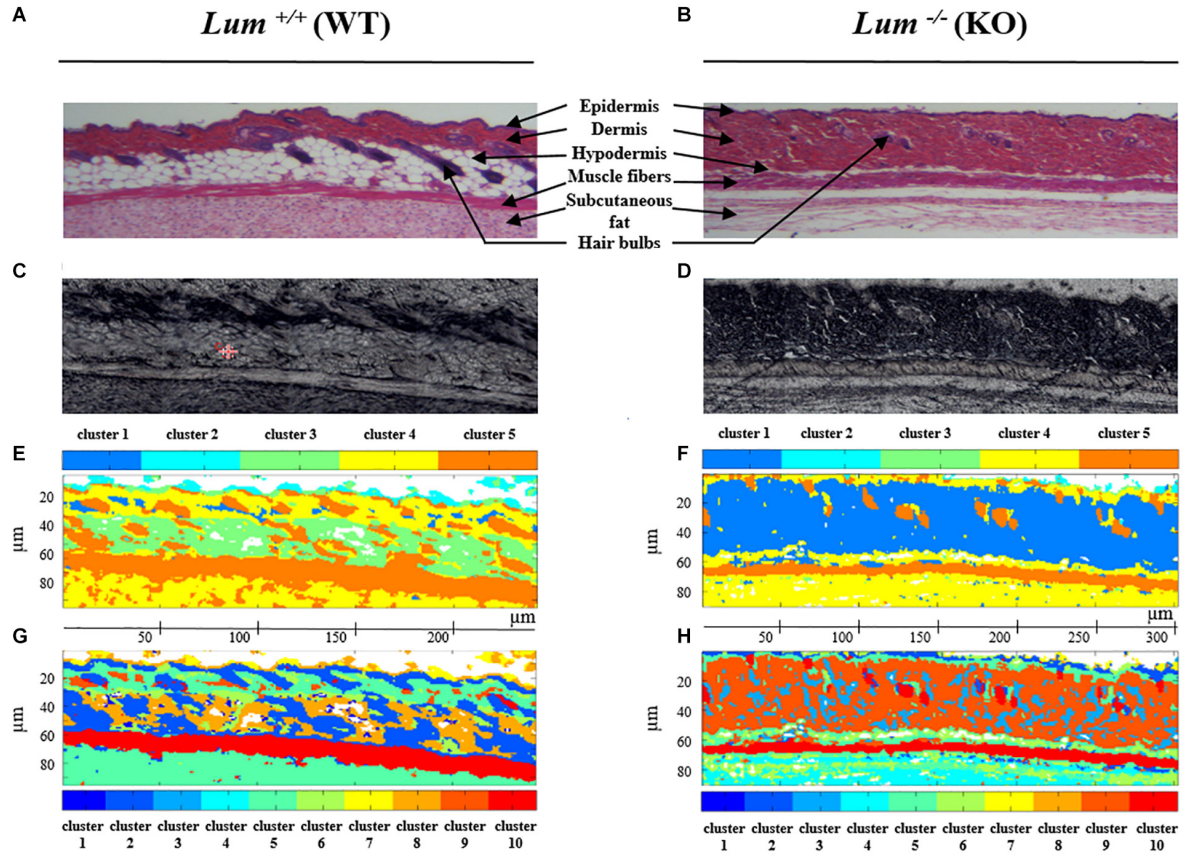

FIGURE 2 | Comparison between conventional and label-free infrared spectral histology of skin tissue from control $Lum^{+/+}$ and Lumican-deleted $Lum^{-/-}$ mice. **(A,B)** HES staining of skin sections. **(C,D)** Corresponding white light images on CaF_2 window. **(E,F)** Representative color-coded *K*-means clustering images with 5 classes using the entire mid-infrared spectral range (1800–800 cm^{-1}). **(G,H)** Representative color-coded *K*-means clustering images with 10 classes using the entire mid-infrared spectral range (1800–800 cm^{-1}).

possible to distinguish these different structures with the pseudo-colors obtained by the common *K*-means classification in the spectral images. In the case of the clustering with k = 5 classes, the dermis in $Lum^{+/+}$ skin tissue sections (**Figure 2E**), is mainly represented by cluster 4 (yellow) while in $Lum^{-/-}$ skin tissue sections (**Figure 2F**), it is mainly represented by cluster 1 (dark blue). In both cases, the hair bulbs are identified by cluster 5 (orange). In the case of the clustering with k = 10 classes, the dermis is mainly represented by cluster 5 (blue green) in $Lum^{+/+}$ skin tissue sections (**Figure 2G**) and by cluster 9 (dark orange) in $Lum^{-/-}$ mice (**Figure 2H**). The common *K*-means clustering results obtained with 10 classes show a higher heterogeneity in the whole tissue section while keeping the correspondence with conventional histology.

Reproducible Remodeling of the Dermis Architecture Revealed by Infrared Imaging in Different Groups $Lum^{+/+}$ (WT) *vs* $Lum^{-/-}$ (KO)

In order to verify the above hypothesis, the measurements were repeated on three independent mice skin sections in each group using the common *K*-means clustering with 10 classes. As shown in **Figure 3A**, all three $Lum^{+/+}$ skin sections exhibit a thin dermis and similar spectral images with a homogeneity of pseudo-colors and tissue structures. In contrast, all three $Lum^{-/-}$ skin sections (**Figure 3B**) are characterized by a thicker dermis and exhibit similar pseudo-colors within this group. In addition, the comparison of the two mice groups, shows a loss of the integrity of the skin dermis in the $Lum^{-/-}$ group and an intergroup heterogeneity suggesting a remodeling of the dermis architecture in the $Lum^{-/-}$ group.

These qualitative observations enable to determine two specific clusters in relation with the dermis structure: clusters 1 and 9 for K-means with 5 and 10 classes, respectively. Differences in the percentage distribution of clusters between the two groups of mice are represented in the form of a histogram. The percentage of cluster 9 (in orange) corresponding to dermis is the only one to increase significantly by 5.3-fold ($^{**}p < 0.01$) in the $Lum^{-/-}$ group compared with $Lum^{+/+}$ control group (**Figure 3C** and **Supplementary Table 1**). Similar results have been obtained by common *K*-means with 5 classes (**Supplementary Figure 2**) where an intragroup homogeneity

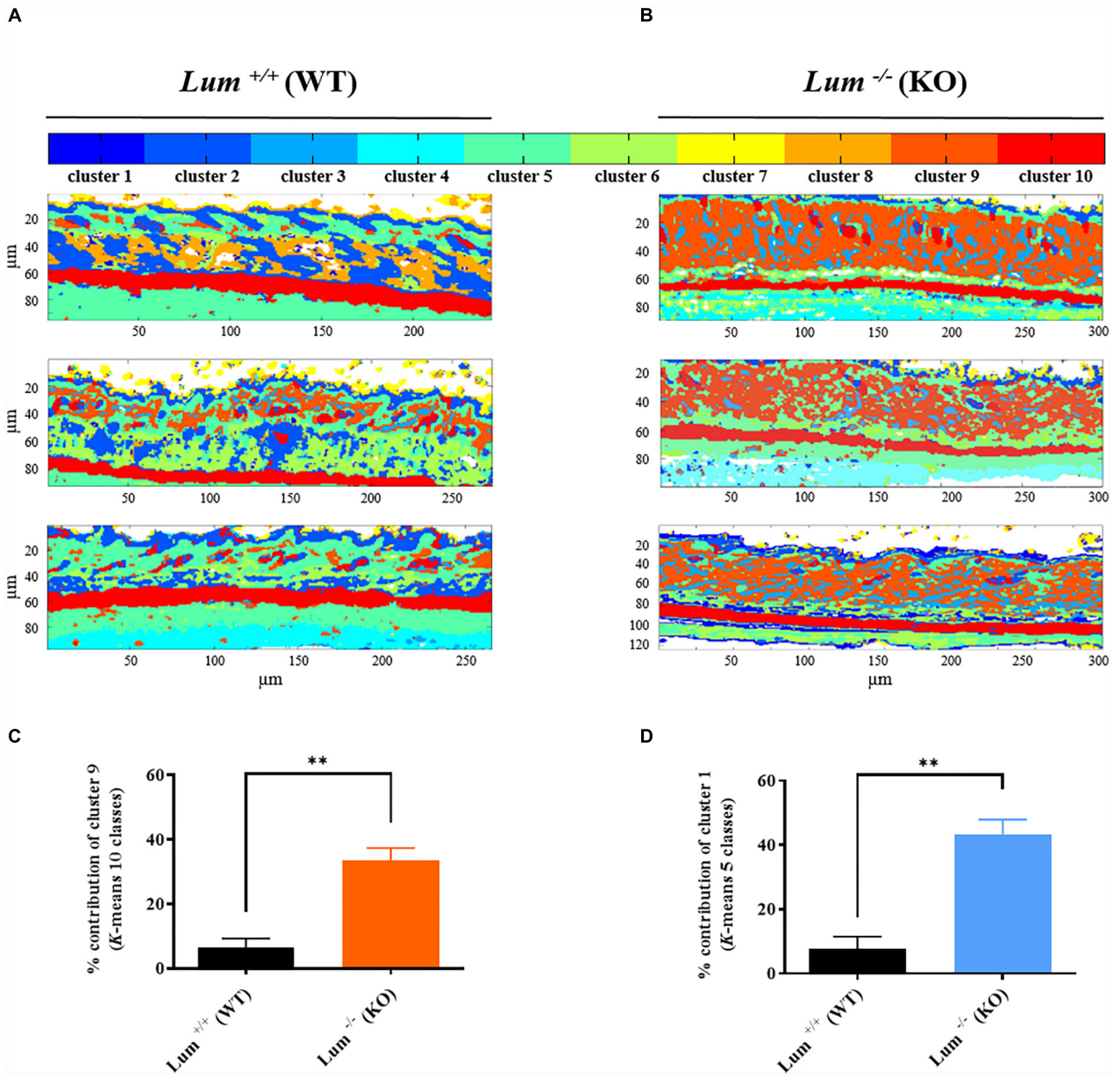

FIGURE 3 | Infrared spectral imaging reveals dermis remodeling from different groups control $Lum^{+/+}$ and Lumican-deleted $Lum^{-/-}$ mice. **(A,B)** Representative color-coded *K*-means clustering images with 10 classes using the entire mid-infrared spectral range (1800–800 cm^{-1}). **(C)** Histogram showing results from statistical analysis of relative contribution of cluster 9 after *K*-means clustering with 10 classes (mean ± SEM, *t* test, $^{**}p < 0.01$). **(D)** Histogram showing results from statistical analysis of relative contribution of cluster 1 after *K*-means clustering with 5 classes (mean ± SEM, *t* test, $^{**}p < 0.01$).

is observed. The intergroup comparison reveals for cluster 1 (blue) a significant 5.6-fold increase ($^{**}p < 0.01$) in the $Lum^{-/-}$ group compared to $Lum^{+/+}$ control group (**Figure 3D** and **Supplementary Table 2**). However, the classification with 10 classes appears better as it improves the differentiation of histological structures and reveals more molecular signatures that were represented by only one cluster in the clustering with 5 classes. In this classification, cluster 9 is associated with the dermis and the observed increase correlates with that obtained for cluster 1 using a *K*-means classification with 5 classes.

Infrared Spectral Correlation of Type I Collagen With Skin Tissue Remodeling

In order to compare the contribution of type I collagen in the skin tissue of both mice groups ($Lum^{+/+}$ and $Lum^{-/-}$), we performed HES staining (**Figures 4A,B**), picrosirius red staining (**Figures 4C,D**) and IRSH (**Figures 4E,F**). HES staining confirmed the higher dermis thickness in $Lum^{-/-}$ compared to $Lum^{+/+}$, which is explained by a disorganization of type I collagen fibers as revealed by picrosirius red staining.

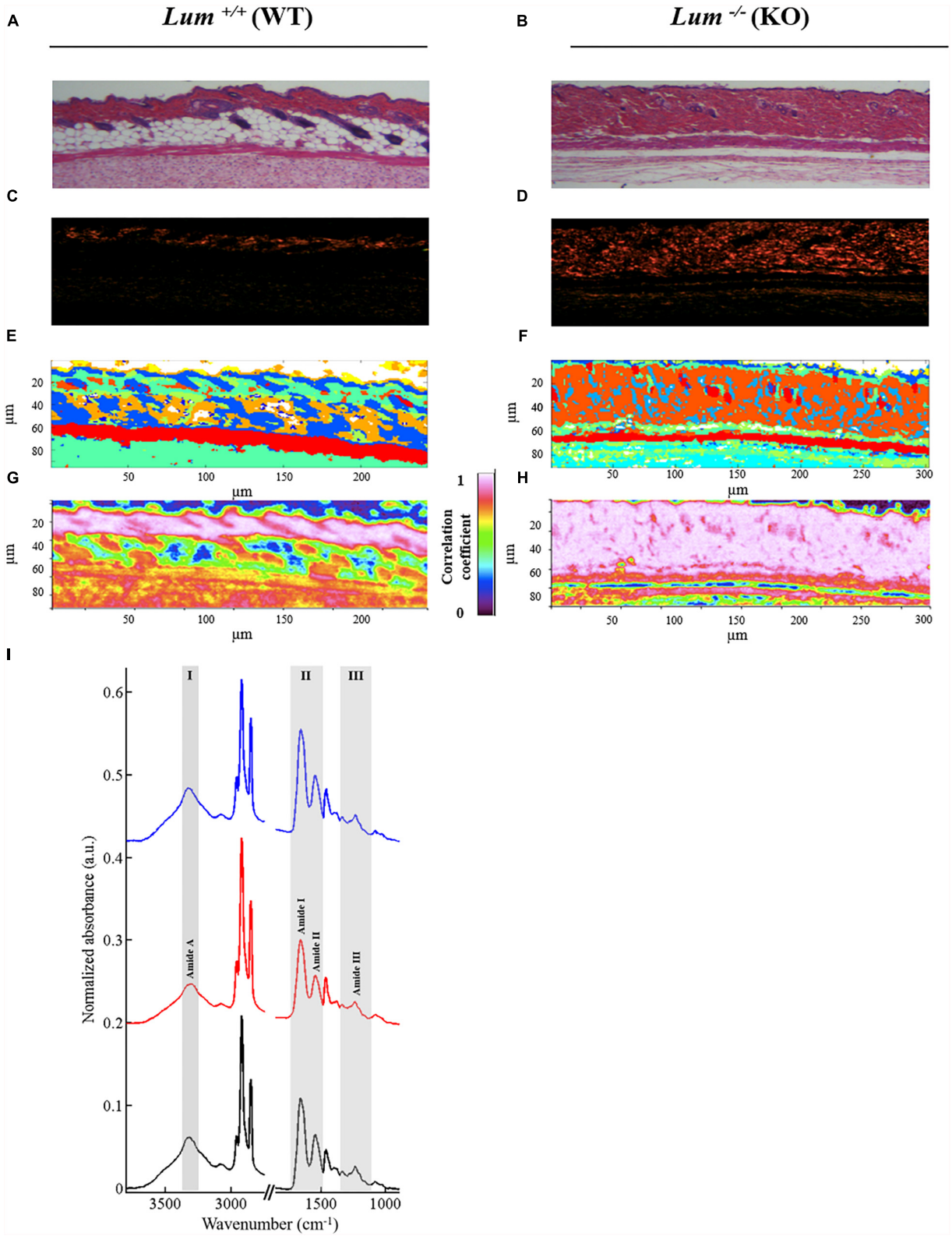

FIGURE 4 | Correlation of the type I collagen spectral signature with skin dermis by infrared imaging. **(A,B)** HES staining and **(C,D)** picrosirius red staining of skin sections (objective 63x). **(E,F)** Representative color-coded *K*-means clustering images with 10 classes using the entire mid-infrared spectral range (1800–800 cm^{-1}). **(G,H)** IR correlation maps using reference spectrum from type I collagen of rat tail tendon. **(I)** Comparison between type I collagen reference spectrum (black line) with spectrum taken randomly from the dermis of ($Lum^{+/+}$) (red line) and ($Lum^{-/-}$) (blue line) mice skin tissues.

Comparison of HES, picrosirius red stainings with the IRSH strongly suggests that cluster 9 (in orange) mainly corresponds to type I collagen fibers (stained in red). In order to better observe the contribution of type I collagen in spectral images, a correlation image (**Figures 4G,H**) was computed with a representative spectrum of type I collagen obtained from a rat-tail tendon included in paraffin.

Figure 4I shows the comparison of a representative spectrum of type I collagen obtained from a paraffin-embedded rat-tail tendon with a representative spectrum taken from the dermis of $Lum^{+/+}$ and $Lum^{-/-}$ mice. Three characteristic spectral zones of collagen bands are highlighted in gray between 3600–3200 cm^{-1} (zone I: amide A), 1700–1500 cm^{-1} (zone II: amides I and II), and 1330–1204 cm^{-1} (zone III: amide III). The latter is composed of a triplet 1330, 1280, and 1204 cm^{-1}. The other peaks are assigned to paraffin. These spectra allow identifying by IRSH the presence of collagen in the dermis. The correlation images are shown in **Figures 4G,H** with a color scale which varies from 0 (low correlation) to 1 (high correlation). A strong correlation coefficient of 0.973 and 0.980 is observed in the dermis respectively for the $Lum^{+/+}$ and $Lum^{-/-}$ mice groups. These correlation images demonstrate a strong contribution of type I collagen in the dermis in both groups of mice with however a thicker dermis in $Lum^{-/-}$ compared to $Lum^{+/+}$ mice as previously described. These results corroborate with those obtained by staining with picrosirius red.

DISCUSSION

This work reports on the role of lumican on the organization of the dermis matrix in WT $Lum^{+/+}$ and Lumican-deleted $Lum^{-/-}$ mice. Lumican plays an important role in maintaining the ECM integrity (Chakravarti et al., 1995). Different approaches combining conventional histology and IRSH have been undertaken to characterize the skin tissue remodeling. In order to compare spectral images with conventional histology, it is necessary to apply multivariate data analysis, here for instance *K*-means clustering, to extract morphological and chemical features. *K*-means clustering is an unsupervised method that minimizes intra-cluster variation and allows to compare several images together to show inter- and intra-group structural modifications (Sebiskveradze et al., 2018). In a first approach comparing HES staining and IRSH of the skin of mice $Lum^{+/+}$ and $Lum^{-/-}$ shows a good correspondence of different histological skin structures from the epidermis to the subcutaneous fat. An important increase in the dermis is observed in $Lum^{-/-}$ mice. Chakravarti and collaborators showed in the same skin model structural differences and suggests a disorganized and loose dermis in Lumican-deleted mice (Chakravarti et al., 1995). Similarly, in other organs like the heart, lumican was shown to be important for survival, cardiac remodeling and fibrosis in response to pressure-overload (Mohammadzadeh et al., 2019, 2020). Our results demonstrate that IRSH can identify such structural changes in a label-free manner. Interestingly, these observations were reproducible in the dermis of all $Lum^{-/-}$ mice. Furthermore, IRSI of $Lum^{+/+}$ and $Lum^{-/-}$ mice skin sections obtained after common *K*-means classification with 5 and 10 classes, allowed to highlight specific clusters of the dermis able to discriminate WT and Lumican-deleted mice (clusters 1 and 9, respectively).

Finally, the contribution of collagen type I was evaluated by HES and picrosirius red staining and correlating each pixel of the spectral images with a representative spectrum of type I collagen. The overall results show a very strong correlation of type I collagen in the dermis by both conventional histology and IRSH. Lumican-deleted $Lum^{-/-}$ mice exhibit a loosening of the intertwining of collagen fibers and an increase in interfibrillar space. The difference of dermis size is explained by an increase in interfibrillar space and diameter of type I collagen fibers in the absence of lumican as previously described by Chakravarti and collaborators (Chakravarti et al., 1995, 1998). However, in the present report, spectral analysis of collagen by correlation remains qualitative and requires further investigation to evaluate its properties such as fiber size and orientation (Jeanne et al., 2017) as well as its quantitative contribution and mechanical characteristics (Aziz et al., 2018; Peñuela et al., 2018). It is important to note that IRSH can not only distinguish different structures of the skin but can also specifically target ECM macromolecules such as collagen. From a therapeutic point of view, for example in the context of tumor progression such as melanoma, it will be important to study the drug delivery potential taking into account the role of lumican in ECM integrity. Indeed, an absence of Lumican can potentially increase the intra- and peri-tumoral accessibility of anti-cancer drugs, as described by Jeanne and collaborators (Jeanne et al., 2017).

CONCLUSION

We demonstrate here in this study that IRSH represents an interesting approach to identify tissue structures. It is complementary to conventional histology and moreover exhibits some interesting advantages. It avoids the use of different chemicals employed for staining and does not require any labeling. Furthermore, it can be directly applied to paraffin embedded tissues. It allows to visualize the remodeling of the skin tissue in the absence of lumican. Moreover, it can reveal specific histological features in a single analysis without the use of different stainings. It would be interesting to develop a quantitative numerical analysis to evaluate the amount of collagen in the spectral image and compare it with the polarized image with the picrosirius red. Perspectively, it would be interesting to study the impact of lumican in skin tissue by polarized IR spectroscopy, nano-IR spectroscopy and second harmonic generation (SHG) to gain more insight into the organization of collagen fibers.

DATA AVAILABILITY STATEMENT

All datasets generated for this study are included in the article/**Supplementary Material**.

ETHICS STATEMENT

This study was performed in compliance with "The French Animal Welfare Act" and following "The French Board for Animal Experiments". Experiments were conducted under approval of the French "Ministère de l'Enseignement Supérieur et de la Recherche" (ethics committee n°C2EA-56) in compliance with the "Directive 2010/63/UE".

AUTHOR CONTRIBUTIONS

SB and GS contributed to the study conception and design. LN, VU, IP, and SB performed experiments. LN, VU, CB-R, CC-P, SB, and GS contributed to data analysis and interpretation. All authors contributed to the manuscript writing and revision.

ACKNOWLEDGMENTS

The authors acknowledge Prof. Shukti Chakravarti (University of New York) for kindly providing us with the $Lum^{-/-}$ mouse line. The authors thank the URCA-PICT and URCAnim Technological Platforms for technological support.

SUPPLEMENTARY MATERIAL

The Supplementary Material for this article can be found online at: https://www.frontiersin.org/articles/10.3389/fcell.2020.00320/full#supplementary-material

REFERENCES

Aziz, J., Ahmad, M. F., Rahman, M. T., Yahya, N. A., Czernuszka, J., and Radzi, Z. (2018). AFM analysis of collagen fibrils in expanded scalp tissue after anisotropic tissue expansion. *Int. J. Biol. Macromol.* 107, 1030–1038. doi: 10.1016/j.ijbiomac.2017.09.066

Baker, M. J., Trevisan, J., Bassan, P., Bhargava, R., Butler, H. J., Dorling, K. M., et al. (2014). Using Fourier transform IR spectroscopy to analyze biological materials. *Nat. Protocol.* 9, 1771–1791. doi: 10.1038/nprot.2014.110

Brézillon, S., Venteo, L., Ramont, L., D'Onofrio, M. F., Perreau, C., Pluot, M., et al. (2007). Expression of Lumican, a small leucine-rich proteoglycan with antitumour activity, in human malignant melanoma. *Clin. Exp. Dermatol.* 32, 405–416. doi: 10.1111/j.1365-2230.2007.02437.x

Chakravarti, S., Magnuson, T., Lass, J. H., Jepsen, K. J., LaMantia, C., and Carroll, H. (1998). Luminican regulates collagen fibril assembly: skin fragility and corneal opacity in the absence of Lumican. *J. Cell Biol.* 141, 1277–1286. doi: 10.1083/jcb.141.5.1277

Chakravarti, S., Stallings, R. L., SundarRaj, N., Cornuet, P. K., and Hassell, J. R. (1995). Primary structure of human lumican (keratan sulfate proteoglycan) and localization of the gene (LUM) to chromosome 12q21.3-q22. *Genomics* 27, 481–488. doi: 10.1006/geno.1995.1080

D'Onofrio, M. F., Brézillon, S., Baranek, T., Perreau, T., Roughley, P. J., Maquart, F. X., et al. (2008). Identification of beta1 as mediator of melanoma cell adhesion to Lumican. *Biochem. Biophys. Res. Commun.* 365, 266–272. doi: 10.1016/j.bbrc.2007.10.155

Draux, F., Jeannesson, P., Gobinet, C., Sule-Suso, J., Sandt, C., Dumas, P., et al. (2009). IR spectroscopy reveals effect of non-cytotoxic doses of anti-tumour drug on cancer cells. *Anal. Bioanal.* 395, 2293–2301. doi: 10.1007/s00216-009-3140-y

Dréno, B. (2009). Anatomy and physiology of skin and cutaneous annexes. *Ann. Dermatol. Venereol.* 136, S247–S251. doi: 10.1016/S0151-9638(09)72527-X

Jeanne, A., Untereiner, V., Perreau, C., Proult, I., Gobinet, C., Boulagnon-Rombi, C., et al. (2017). Lumican delays melanoma growth in mice and drives tumor molecular assembly as well as response to matrix-targeted TAX2 therapeutic peptide. *Sci. Rep.* 9:7700. doi: 10.1038/s41598-017-07043-9

Ly, E., Piot, O., Wolthuis, R., Durlach, A., Bernard, P., and Manfait, M. (2008). Combination of FTIR spectral imaging and chemometrics for tumour detection from paraffin-embedded biopsies. *Analyst* 133, 197–205. doi: 10.1039/b715924b

Mainreck, N., Brézillon, S., Sockalingum, G. D., Maquart, F. X., Manfait, M., and Wegrowski, Y. (2012). Characterization of glycosaminoglycans by tandem vibrational microspectroscopy and multivariate data analysis. *Methods Mol. Biol.* 836, 117–130. doi: 10.1007/978-1-61779-498-8_8

Mohammadzadeh, N., Lunde, I. G., Andenaes, K., Strand, M. E., Aronsen, J. M., Skrbic, B., et al. (2019). The extracellular matrix proteoglycan lumican improves survival and counteracts cardiac dilatation and failure in mice subjected to pressure overload. *Sci. Rep.* 9:9206. doi: 10.1038/s41598-019-45651-9

Mohammadzadeh, N., Melleby, A. O., Palmero, S., Sjaastad, I., Chakravarti, S., Engebretsen, K. V. T., et al. (2020). Moderate loss of the extracellular matrix proteoglycan lumican attenuates cardiac fibrosis in mice subjected to pressure overload. *Cardiology* 22, 1–12. doi: 10.1159/000505318

Nallala, J., Gobinet, C., Diebold, M. D., Untereiner, V., Bouché, O., Manfait, M., et al. (2012). Infrared spectral imaging as a novel approach for histopathological recognition in colon cancer diagnosis. *J. Biomed. Opt.* 17:116013. doi: 10.1117/1.JBO.17.11.116013

Peñuela, L., Negro, C., Massa, M., Repaci, E., Cozzani, E., Parodi, A., et al. (2018). Atomic force microscopy for biomechanical and structural analysis of human dermis: a complementary tool for medical diagnosis and therapy monitoring. *Exp. Dermatol.* 27, 150–155. doi: 10.1111/exd.13468

Postlethwaite, A. E., and Kang, A. H. (1998). "Fibroblasts and matrix proteins," in *Inflammation: Basic Principles and Clinical Correlates*, ed. J. I. Gallin (Philadelphia, FL: Lippincotte Williams and Wilkins), 227–257.

Radwanska, A., Bacynska, D., Nowak, D., Brézillon, S., Popow, A., Maquart, F. X., et al. (2008). Lumican affects actin cytoskeletal organization in human melanoma A375 cells. *Life Sci.* 83, 651–660. doi: 10.1016/j.lfs.2008.09.008

Sebiskveradze, D., Bertino, B., Gaydou, V., Dugaret, A. S., Roquet, M., Zugaj, D. E., et al. (2018). Mid-infrared spectral microimaging of inflammatory skin lesions. *J. Biophotonics* 11:e201700380. doi: 10.1002/jbio.201700380

Ueda, M., Saito, S., Murata, T., Hirano, T., Bise, R., Kabashima, K., et al. (2019). Combined multiphoton imaging and biaxial tissue extension for quantitative analysis of geometric fiber organization in human reticular dermis. *Sci. Rep.* 9:10644. doi: 10.1038/s41598-019-47213-47215

Zeltz, C., Brézillon, S., Käpylä, J., Eble, J. A., Bobichon, H., Terryn, C., et al. (2010). Lumican inhibits cell migration through α2β1 intregin. *Exp. Cell Res.* 316, 2922–2931. doi: 10.1016/j.yexcr.2010.08.002

Conflict of Interest: The authors declare that the research was conducted in the absence of any commercial or financial relationships that could be construed as a potential conflict of interest.

Copyright © 2020 Nannan, Untereiner, Proult, Boulagnon-Rombi, Colin-Pierre, Sockalingum and Brézillon. This is an open-access article distributed under the terms of the Creative Commons Attribution License (CC BY). The use, distribution or reproduction in other forums is permitted, provided the original author(s) and the copyright owner(s) are credited and that the original publication in this journal is cited, in accordance with accepted academic practice. No use, distribution or reproduction is permitted which does not comply with these terms.

frontiers in Oncology

ORIGINAL RESEARCH
published: 14 May 2020
doi: 10.3389/fonc.2020.00774

Syndecan-1-Dependent Regulation of Heparanase Affects Invasiveness, Stem Cell Properties, and Therapeutic Resistance of Caco2 Colon Cancer Cells

Sampath Kumar Katakam[1], Paride Pelucchi[2], Cinzia Cocola[2], Rolland Reinbold[2], Israel Vlodavsky[3], Burkhard Greve[4] and Martin Götte[1]**

[1] Department of Gynecology and Obstetrics, Münster University Hospital, Münster, Germany, [2] Institute of Biomedical Technologies, National Research Council, Milan, Italy, [3] The Rappaport Faculty of Medicine, Technion Integrated Cancer Center (TICC), Haifa, Israel, [4] Department of Radiotherapy-Radiooncology, Münster University Hospital, Münster, Germany

OPEN ACCESS

Edited by:
Hamid Morjani, Université de Reims Champagne-Ardenne, France

Reviewed by:
Ivan Fernande Vega, Araba University Hospital, Spain
Tünde Szatmári, National Public Health Institute (OKI), Hungary

***Correspondence:**
Burkhard Greve
greveb@uni-muenster.de
Martin Götte
mgotte@uni-muenster.de

Specialty section:
This article was submitted to Molecular and Cellular Oncology, a section of the journal Frontiers in Oncology

Received: *05 February 2020*
Accepted: *21 April 2020*
Published: *14 May 2020*

Citation:
Katakam SK, Pelucchi P, Cocola C, Reinbold R, Vlodavsky I, Greve B and Götte M (2020) Syndecan-1-Dependent Regulation of Heparanase Affects Invasiveness, Stem Cell Properties, and Therapeutic Resistance of Caco2 Colon Cancer Cells. Front. Oncol. 10:774. doi: 10.3389/fonc.2020.00774

The heparan sulfate proteoglycan Syndecan-1 binds cytokines, morphogens and extracellular matrix components, regulating cancer stem cell properties and invasiveness. Syndecan-1 is modulated by the heparan sulfate-degrading enzyme heparanase, but the underlying regulatory mechanisms are only poorly understood. In colon cancer pathogenesis, complex changes occur in the expression pattern of Syndecan-1 and heparanase during progression from well-differentiated to undifferentiated tumors. Loss of Syndecan-1 and increased expression of heparanase are associated with a change in phenotypic plasticity and an increase in invasiveness, metastasis and dedifferentiation. Here we investigated the regulatory and functional interplay of Syndecan-1 and heparanase employing siRNA-mediated silencing and plasmid-based overexpression approaches in the human colon cancer cell line Caco2. Heparanase expression and activity were upregulated in Syndecan-1 depleted cells. This increase was linked to an upregulation of the transcription factor Egr1, which regulates heparanase at the promoter level. Inhibitor experiments demonstrated an impact of focal adhesion kinase, Wnt and ROCK-dependent signaling on this process. siRNA-depletion of Syndecan-1, and upregulation of heparanase increased the colon cancer stem cell phenotype based on sphere formation assays and phenotypic marker analysis (Side-population, NANOG, KLF4, NOTCH, Wnt, and TCF4 expression). Syndecan-1 depletion increased invasiveness of Caco2 cells *in vitro* in a heparanase-dependent manner. Finally, upregulated expression of heparanase resulted in increased resistance to radiotherapy, whereas high expression of enzymatically inactive heparanase promoted chemoresistance to paclitaxel and cisplatin. Our findings provide a new avenue to target a stemness-associated signaling axis as a therapeutic strategy to reduce metastatic spread and cancer recurrence.

Keywords: heparanase, syndecan, colon cancer, cancer stem cells, heparan sulfate, proteoglycan

INTRODUCTION

In the tumor microenvironment (TME), repopulation of cells after radiotherapy and chemotherapy represents a mechanism of resistance and tumor recurrence (1). Abnormal changes in extracellular matrix (ECM) components and their degradative enzymes causes an imbalance between tissue homeostasis and cancer, resulting in changes in cell plasticity associated with increased invasion, metastasis and dedifferentiation (2). The "metastatic niche" is regulated by the "cancer stem cell niche" with abnormal changes in ECM dynamics (2–4). For example, heparanase (HPSE), matrix metalloproteinases, and sulfatases, are highly expressed in many cancers, whereas some heparan sulfate sulfotransferases are silenced (5–7). Indeed, proteoglycan-degrading enzymes such as HPSE, the only mammalian endoglycosidase capable of cleaving heparan sulfate, regulate ECM dynamics that are under the tight homeostatic control of several signaling pathways (7, 8). Recent studies indicate that the interplay between the cell surface proteoglycan Syndecan-1 (Sdc-1) and HPSE have important functional connections in the progression of colorectal cancer and myeloma. For example, in colon cancer progression, there is a gradual increase in the expression of HPSE (9) and a decrease in Sdc-1 (10) expression during progression from well-differentiated to poorly differentiated colon carcinoma. Differences in the mRNA and protein expression of Sdc-1 have been noted, as Sdc-1 mRNA was strongly overexpressed in metastatic colon tumors, whereas using immunohistochemistry, metastatic tumors showed a dramatic decrease in staining, while labeling was still strong in the adjacent normal mucosa (11, 12). Moreover, in metastatic tumors HPSE mRNA levels were reduced in 40% of patients, whereas overexpression was observed in 20% of patients, indicating considerable heterogeneity (11). Deeply invading colon carcinoma cells showed decreased expression of Sdc-1 (13) and increased expression of HPSE (14, 15). Consistent with these findings, the malignant transformation of Caco2 colon carcinoma cells resulted in a decrease in the Sdc-1 expression (15) which might also regulate HPSE activity. Transcriptional studies show that loss of Sdc-1 (13, 16) and enhanced expression of HPSE (17–19) correlate with tumor growth, invasion, metastatic potential, and reduced postoperative survival of cancer patients (20). In colitis and the associated tumorigenic models, the transcriptional regulator early growth response 1 (EGR1) acts as a potent inducer of HPSE in colonic epithelial tumor cells (17, 21, 22). While Sdc-1 expression maintains epithelial integrity, loss of expression results in high HPSE expression, changes in epithelial morphology and polarity, thereby promoting epithelial-mesenchymal transition (EMT) (23). Thus, Sdc-1 and HPSE work together to enhance cell invasiveness via EMT pathways, which may further enhance stem cell-like pluripotency signatures (24, 25). As EMT regulates metastasis (26–28), high expression of HPSE may further enhance metastasis based on the concept of migrating cancer stem cells (CSCs). Data in different tumor entities have revealed further pathogenetic mechanisms for the functional interplay of Sdc-1 and HPSE. For example, in multiple myeloma, high HPSE expression is linked to poor prognosis, and contributes to disease pathogenesis by inducing Sdc-1 shedding from the tumor cell membrane (29), which promotes sequestering of shed Sdc-1 bound growth factors in the tumor microenvironment (30). Additional molecular mechanisms linked to HPSE overexpression include activation of the Erk signaling pathway, the reduction of nuclear Sdc-1 leading to increased acetylated histone H3 and subsequent upregulation of vascular endothelial growth factor (VEGF) and matrix metalloproteinase (MMP)-9 (30). Finally, both HPSE and Sdc-1 regulate the activity of pathways relevant to cancer progression, such as the stemness-associated Wnt pathway (3, 31, 32) and metastasis-related focal adhesion kinase (FAK) signaling (3, 33, 34).

Although high HPSE expression in various solid tumors confers resistance to stress and chemo/radiotherapy (35–37), its role in promoting tumor initiation via the expression of CSC-like signatures has not been elucidated. Owing to the role of Sdc-1 and HPSE in tumor growth, invasion and metastasis we aimed at investigating the underlying molecular interplay between Sdc-1 and HPSE and the possible signaling routes in the well-established colon cancer cell line Caco2, applying both stable overexpression and transient siRNA knockdown methods. Our results report for the first time the dynamic interplay between Sdc-1 and HPSE in stemness-associated colon cancer via a signaling axis involving early growth response protein 1 (EGR1), FAK, and Wnt. Our findings could form a conceptual framework for establishing novel therapeutic possibilities and recognize the long-term driven functions of Sdc-1 and HPSE in colon cancer.

MATERIALS AND METHODS

Materials

Tissue culture supplies were from Gibco BRL (Karlsruhe, Germany). Unless stated otherwise, all chemicals were from Sigma Aldrich (Deisenhofen, Germany).

Cell Culture

The human colon carcinoma cell line Caco2 (German Collection of Microorganisms and Cell Cultures, Department of Human and Animal Cell Cultures, Braunschweig, Germany) was stably transfected with a pcDNA3.1 control plasmid (Invitrogen), or plasmids overexpressing Syndecan-1 cDNA (38), native HPSE, or enzymatically inactive HPSE double mutated in Glu225 and Glu343 (39). Stable clones were selected using 800 μg/ml G418. Caco2 cells were maintained in RPMI media containing 10% fetal calf serum (FCS), 1% glutamine, 1% penicillin/streptomycin and 800 μg/ml G418 in a humidified atmosphere of 5% CO_2 at 37°C. Successful transfection was confirmed by qPCR.

siRNA Knockdown of Syndecan-1 and Egr1 Expression

siRNA knockdown was performed using pre-validated siRNAs #12634 and # 4537 (Ambion, Cambridgeshire, UK) targeting the coding regions of Syndecan-1, and EGR1, respectively, and a negative control siRNA (negative control #1, Ambion). In preliminary experiments, we optimized conditions for the efficient transfection of Caco2 cells. Fresh medium was added 16 h after transfection, and experiments were conducted

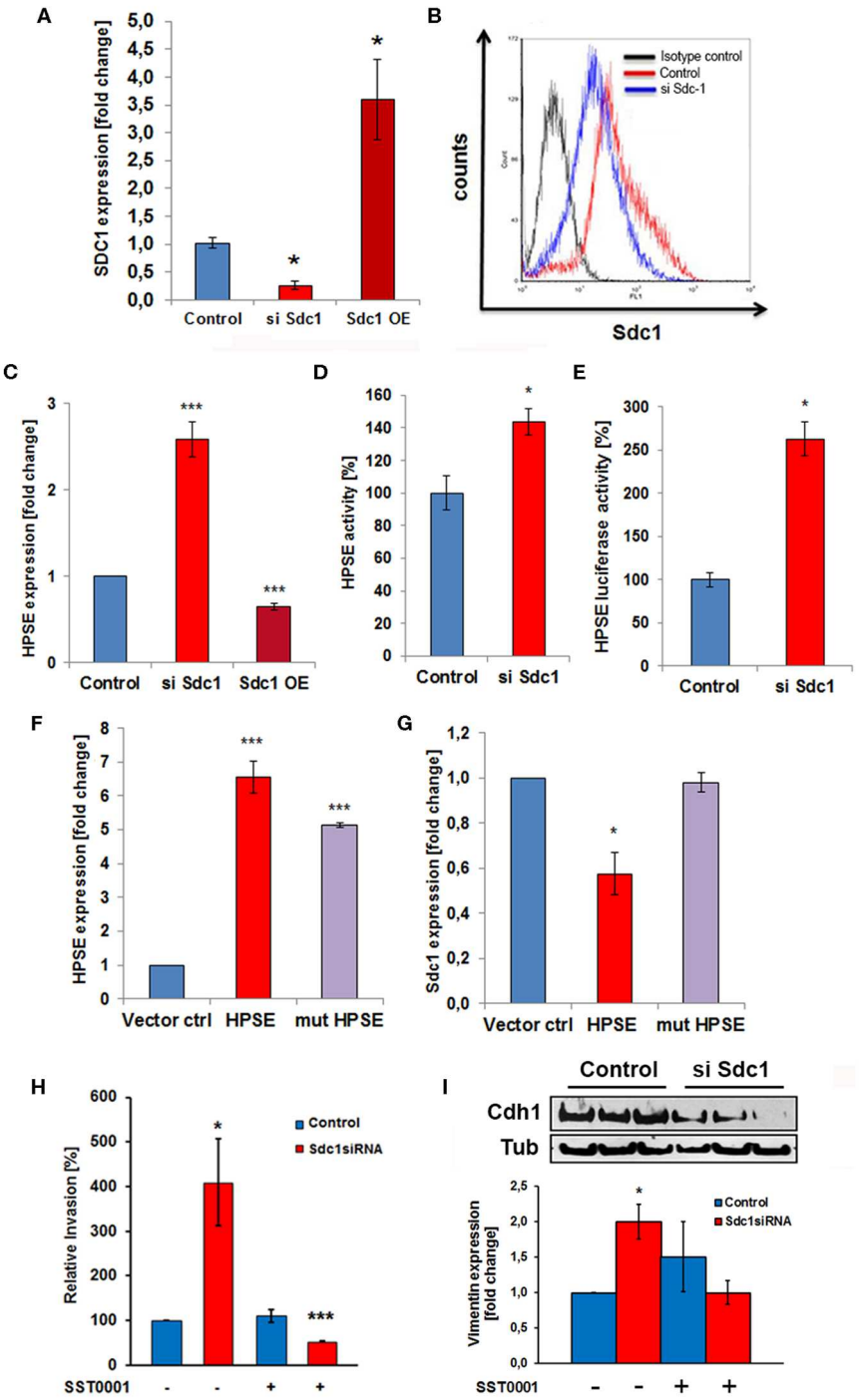

FIGURE 1 | The heparan sulfate proteoglycan Syndecan-1 regulates Caco2 cell invasiveness in a heparanase-dependent manner. **(A)** Confirmation of Sdc-1 siRNA knockdown and overexpression by qPCR. *$p < 0.05$ vs. all groups. **(B)** Confirmation of Sdc-1 siRNA knockdown by flow cytometry. **(C)** siRNA knockdown (siSdc1) or plasmid-mediated overexpression (OE) of Sdc-1 leads to up-or downregulation of HPSE expression, respectively (qPCR). ***$p < 0.001$ vs. all groups. **(D,E)** Sdc-1 knockdown results in an upregulation of HPSE enzymatic activity **(D)** and a substantial 3-fold activation of HPSE promoter activity (**E**, luciferase reporter assay). *$p <$ 0.05 vs. control. **(F,G)** Plasmid-mediated overexpression of enzymatically active HPSE (HPSE) results in a decrease of Sdc-1 expression (qPCR). Overexpression of an enzymatically inactive HPSE variant (mut-HPSE) did not affect Sdc-1 expression. ***$p < 0.01$ vs. control. **(H)** Caco2 cell invasion is stimulated in response to Sdc-1silencing. The HPSE inhibitor SST0001 abolishes the increased Matrigel invasiveness of Sdc-1 siRNA-treated Caco2 cells. *p<0.05 vs. control. **(I)** Sdc-1 siRNA knockdown affects the expression of the EMT markers E-cadherin and vimentin. Upper panel: Western blotting demonstrates downregulation of the epithelial marker E-cadherin (Cdh1) upon Sdc-1 silencing. Tubulin (Tub) = loading control. Representative picture of three independent experiments. Lower panel: qPCR analysis reveals upregulation of the mesenchymal marker vimentin upon Sdc-1-silencing, which could be reversed by the HPSE inhibitor SST0001. *$p < 0.05$ vs. untreated control and treated Sdc1 siRNA. All panels $N \geq 3$. Error bars = SEM.

48 h after transfection. Target downregulation was confirmed by qPCR.

Cell viability and Chemosensitivity Assay

Cell viability was evaluated by MTT (3-(4,5-dimethylthiazol-2-yl)-2,5-diphenyltetrazolium bromide) assay exactly as previously described (6). To test chemosensitivity, the MTT assay was performed in the presence of titrated concentrations of Paclitaxel (10 pM−1 μM), and cis-diamineplatinum II dichloride (50 nM−5 mM), which were added 24 h after initial cell plating.

Invasion Assay

BioCoat Matrigel Invasion Chamber (BD Biosciences, Heidelberg, Germany) assays are based on the chemotaxis-driven invasion of porous filter membranes coated with a basement membrane-like matrix. Assays were performed exactly as previously described (6) using an invasion time of 4 days. For inhibitor studies, SST0001 (1 μg/ml; = Roneparstat) (40, 41) was added to both compartments 24 h after cell plating. Relative invasiveness was expressed as percentage of the cell number on compound-treated inserts compared with control inserts. The invasion experiments were performed and analyzed by two different researchers (SKK, BP).

Quantitative Real-Time PCR

Total cellular RNA was isolated using rna-OLS (OMNI Life Science, Hamburg, Germany) and reverse transcribed (Advantage First strand cDNA synthesis kit; Fermentas, St. Leon-Rot, Germany). qPCR and melting curve analysis were performed using Qiagen QuantiTect SYBR Green PCR kit in a LightCycler (Roche, IN). Expression of additional mRNAs was analyzed using the following TaqMan probes on an ABI PRISM 7300 Sequence Detection System, as described previously (42): 18S rRNA Hs99999901_s1, KLF4 Hs00358836_m1, SDC1 Hs00174579_m1, HPSE Hs00180737_m1. The $2^{-\Delta\Delta Ct}$ method was used to determine relative gene transcript levels after normalization to 18S rRNA. PF-562271 (Sigma-Aldrich) was used for 24 h at 10 μg/ml in some experiments.

Western Blot and Immunoprecipitation

Immunoblotting was performed exactly as previously described (6, 42), using the following primary antibodies (1:1,000): rabbit polyclonal anti-phospho FAK Y925 (Cell Signaling, Beverly, MA, USA), rabbit polyclonal anti-FAK (Cell Signaling), rabbit monoclonal anti-human TCF4 (Cell Signaling), mouse anti-E-cadherin (1:2,000; BD Biosciences), mouse anti-human α-Tubulin (Sigma-Aldrich) and appropriate secondary antibodies (diluted 1:5,000): HRP-conjugated goat-anti-mouse or goat-anti-rabbit IgG (Merck-Millipore, Darmstadt, Germany). For immunoprecipitation, cell lysates of Caco2 cells were prepared 72 h after transfection with control or Sdc-1 siRNA as described previously (42). 0.5 mg protein was incubated with 1:50 dilution of primary antibody (rabbit monoclonal anti-human EGR1, Cell Signaling) at 4°C on a rocker platform overnight. Afterward, the mixture was incubated analogously with 20 μl resuspended protein A/G-PLUS-Agarose. Immunoprecipitates were pelleted by centrifugation (1,000 g, 5 min, 4°C), washed four times with RIPA buffer and boiled in 40 μl SDS sample buffer (5 min). SDS-PAGE, Western blotting, stripping and reprobing were performed as described previously (6) using 30–60 μg of protein/lane on 7.5– 12% gels.

Side Population Analysis

Side population (SP) analysis was performed using the Hoechst 33342 dye exclusion technique as previously described (43). In this assay, a putative CSC population is identified based on the dye efflux properties of ATP-binding cassette (ABC) transporters, which are highly expressed in these cells (44). In some experiments, the inhibitors IWP-2 (10 μM) and SST0001 (10 μg/ml) were used for 1 h prior to SP analysis. 1×10^6 cells were incubated in DMEM containing 2% (v/v) FCS for 90 min at 37°C either with 5 μg/ml Hoechst 33342 (Sigma-Aldrich) or in the presence of 50 μM verapamil (Sigma-Aldrich). Finally, 2 μg/ml propidium iodide was added for cell death discrimination, and cells were stored on ice until analysis. Cells were analyzed on a CyFlow Space (Sysmex/Partec) using a 16 mW 375 nm UV laser for excitation, emission was measured at 475 nm (BP 455/50) and at 665 nm (LP 665 nm). Signals were slivered by a dichroic mirror of 610 nm to measure Hoechst signal intensity in both channels. All cells with a low Hoechst fluorescence and which were not visible in the verapamil control were gated (R2) as SP cells. Data acquisition and processing were done by using FloMax software (Quantum Analysis, Münster, Germany).

Sphere Culture of Caco2 Cells

Sphere suspension cultures of Caco2 cells were performed in a serum-free medium (RPMI, High Glucose, GlutaMAX™Gibco®), supplemented with B27 (Gibco®), 20 ng/ml EGF (Sigma) and 20 ng/ml basic fibroblast growth factor (bFGF, Immunotools) at a density of 1 x 10^3 cells/ml. Sphere cultures were performed and analyzed by three independent researchers (PP, CC, RR).

Irradiation

Irradiation was performed at room temperature with a linear accelerator using a dose rate of 4.8 Gy min^{-1} and a dose of 2 Gy was applied. To measure the colony-forming ability after irradiation, 1 x 10^3 cells were resuspended in 1 ml culture medium, plated into 3.5 cm Petri dishes with a 2.5 mm grid (Nunc, Langenselbold, Germany) and incubated for about 6 days in a CO_2 incubator at 37°C. Cell colonies with more than 50 cells were counted using a microscope (Olympus, Hamburg, Germany). The survival fraction was calculated as follows: plating efficiency treated/plating efficiency control. Radiation resistance was analyzed by two independent researchers (SKK, AvD).

Promoter Reporter Assay

The 1.9-kb human heparanase promoter region [HPSE (-1791/+109)-LUC] was subcloned upstream of the LUC gene in a pGL2 basic reporter plasmid (Promega, Madison, WI, USA) (45, 46). 24 h after siRNA transfection, cells were replaced with serum-free media for 6 h and co-transfected with a reporter construct at 1 μg/well (6 well) using FuGENE 6 reagent

(Promega) according to the standard protocol. Control cells were transfected with basic pGL2 plasmid containing LUC gene alone (without promoter). 46 h after transfection, luciferase assay was done using the Luciferase Reporter Assay system. (Promega-E1500). The relative light units were determined in each sample with a luminometer and results were normalized against beta-galactosidase activity measured by a colorimetric assay. Data are presented as the means of quadruplicates ± s.d., and all experiments were repeated at least three times with similar results.

HPSE Activity Assay

HPSE activity of 1×10^6 cells was measured using a commercial heparan sulfate degrading enzyme assay kit (Takara.Mirus.Bio, Madison, WI) which is based on the measurement of HPSE-induced degradation of biotinylated-HS (b-HS) fragments, according to the manufacturer's protocol.

Statistical Analysis

Unless indicated otherwise, data were analyzed using the unpaired two-tailed Student's *t*-test. A $P < 0.05$ was considered statistically significant. All experiments were performed at least three times on independent biological replicates.

RESULTS

Syndecan-1 Regulates Heparanase Expression and Caco2 Cell Invasiveness

Based on the deregulated expression of Sdc-1 and HPSE in colon cancer and the role of Sdc-1 as a signaling co-receptor, we hypothesized that loss of Sdc-1 may regulate HPSE expression. To test our hypothesis, we manipulated Sdc-1 levels via siRNA knockdown in the human colon cancer cell line Caco2. Sdc-1 knockdown (**Figures 1A,B**) resulted in a substantial increase in HPSE mRNA expression (**Figure 1C**), HPSE activity (**Figure 1D**) and HPSE promoter activity (**Figure 1E**). Consistently, plasmid-based Sdc-1 overexpression was associated with HPSE downregulation (**Figures 1A,C**). Conversely, plasmid-based overexpression of HPSE induced a reduction of Sdc-1 expression, whereas upregulation of an enzymatically inactive form of HPSE had no effect (**Figures 1F,G**). At the functional level, Sdc-1 knockdown resulted in increased invasiveness of Caco2 cells through Matrigel (**Figure 1H**), which could be blocked by the HPSE inhibitor SST0001 (Roneparstat), a glycol-split heparin (40) (**Figure 1H**), suggesting a mechanistic role for HPSE upregulation in Sdc-1 deficient cells in this process. Sdc-1 depletion resulted in a downregulation of the epithelial cell adhesion molecule E-cadherin and an upregulation of the mesenchymal marker vimentin (**Figure 1I**), suggesting a possible involvement of EMT in this process. Notably, the Sdc-1-dependent upregulation of vimentin could be abolished by the HPSE inhibitor SST0001, consistent with its inhibitory effect in the invasion assay (**Figures 1H,I**). To analyze the interdependence of Sdc-1 and HPSE expression, we tested the impact of Sdc-1 depletion on expression of the transcription factor Egr1, a known regulator of HPSE expression (21, 41). qPCR and Western blot analysis revealed an upregulation of Egr1 in Sdc-1-depleted cells (**Figures 2A,B**). Notably, siRNA depletion of EGR1 abolished the upregulation of HPSE mRNA expression (**Figure 2C**) and dampened HPSE promoter activation (**Figure 2D**) in Sdc-1-depleted cells. Notably, the increased activity of FAK in Sdc-1-depleted cells was abolished by EGR1 siRNA knockdown (**Figure 2E**), whereas application of a FAK inhibitor resulted in an inhibition of Sdc-1-dependent EGR1 and HPSE expression (**Figures 2F,G**), indicating a mechanistic involvement of this pathway.

Heparanase Regulates the Cancer Stem Cell Phenotype of Caco2 Cells

Altered Sdc-1 expression has been linked to aberrant CSC function, a phenotype linked to therapeutic resistance and cancer recurrence (3, 47). To test a possible involvement of the Sdc-1-HPSE axis in this phenotype, we analyzed several readouts of stem cell activity in our cells. Sdc-1 knockdown enhanced the CSC-associated side population (SP) phenotype (**Figure 3A**). Notably, the HPSE inhibitor SST0001 abolished this effect (**Figure 3A**) and inhibited the formation of colonospheres in wild-type cells (**Figure 3B**). While upregulation of both enzymatically active and inactive HPSE forms massively increased the SP phenotype (**Figures 3C,D**), upregulation of the stemness-associated transcription factors Krüppel-like factor 4 (KLF4) and transcription factor 4 (TCF4) was more pronounced in cells overexpressing native HPSE (**Figures 3E,F**). Expression of NANOG was upregulated by both forms of HPSE, whereas NOTCH1 expression was differentially affected by the catalytically active and inactive forms of HPSE (**Figure 3E**). Application of the Wnt-pathway inhibitor IWP2 reduced the effect of HPSE expression on the side population phenotype (**Figure 3G**). Overall, these data suggest that HPSE regulates CSC properties by affecting multiple stemness-associated signaling pathways. As CSC function has been linked to therapeutic resistance (3), we finally tested the influence of HPSE overexpression on resistance to irradiation and chemotherapy. The Caco2 colony formation capacity under control conditions was reduced by HPSE overexpression compared to vector controls. However, upon radiation with a therapeutically relevant dose of 2 Gy, HPSE overexpressing cells showed no significant decrease in colony formation capacity, whereas colony formation was significantly decreased in control cells (**Figure 4A**). Chemosensitivity assays revealed an increased resistance of cells overexpressing enzymatically inactive HPSE to paclitaxel and cisplatin, whereas upregulation of enzymatically active HPSE has either no effect (cisplatin) or a mixed, dose-dependent effect (paclitaxel) (**Figures 4B,C**). Taken together, our data suggest that HPSE overexpression is associated with changes in the resistance of colon cancer cells to chemo- and radiotherapy, involving a differential role for the enzymatic activity of HPSE.

DISCUSSION

The cell surface proteoglycan Sdc-1 acts as an ECM adhesion receptor and co-receptor for numerous signaling pathways with

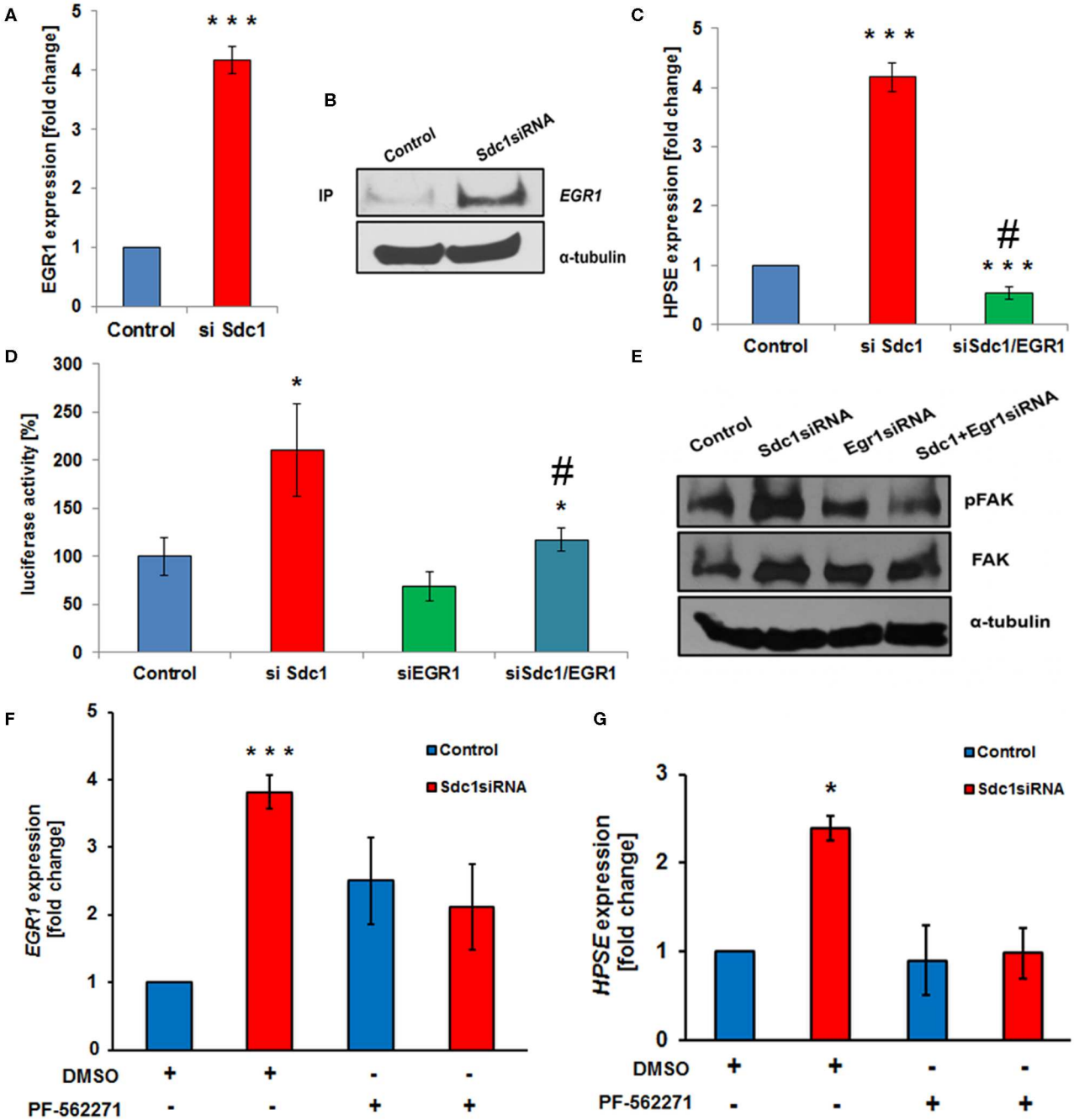

FIGURE 2 | Syndecan-1 regulates HPSE expression in Caco2 cells in an Egr1 and focal adhesion kinase (FAK)-dependent manner. **(A,B)** Sdc1 siRNA knockdown results in a substantial upregulation of the transcriptional regulator Egr1, as demonstrated by qPCR **(A)** and Western blotting **(B)**. ***$p < 0.001$ vs. control. **(C,D)** Egr1 siRNA knockdown abolishes the Sdc1 siRNA-induced upregulation of HPSE as demonstrated by qPCR **(C)** and HPSE-promoter-based luciferase reporter assays **(D)**. **(C)** ***$p < 0.001$ vs. control, #$p < 0.001$ vs. si Sdc-1. **(D)** ***$p < 0.001$ vs. control, #$p = 0.06$ vs. si Sdc-1. **(E)** Egr1 siRNA depletion inhibits the activation of FAK phosphorylation induced by Sdc-1 siRNA knockdown (Western blot). **(F,G)** The FAK inhibitor PF-562271 prevents the Sdc-1-knockdown-induced upregulation of Egr1 **(F)** and HPSE **(G)** (qPCR). **(E)** ***$p < 0.001$ vs. control, **(F)** *$p < 0.05$ vs. all groups. All panels: $N \geq 3$. Error bars = SEM.

relevance to tumor progression (23, 48). The Sdc-1 heparan sulfate chains serve as substrates for HPSE, and this degradative process modulates tumor angiogenesis, growth factor-dependent tumor cell proliferation and metastatic behavior in a variety of tumor entities (8). Notably, a decrease in Sdc-1 and increase in HPSE expression has been observed in several cancers particularly in colon cancer enhancing tumorigenesis, invasion, and metastasis (7–15). The molecular mechanism underlying this

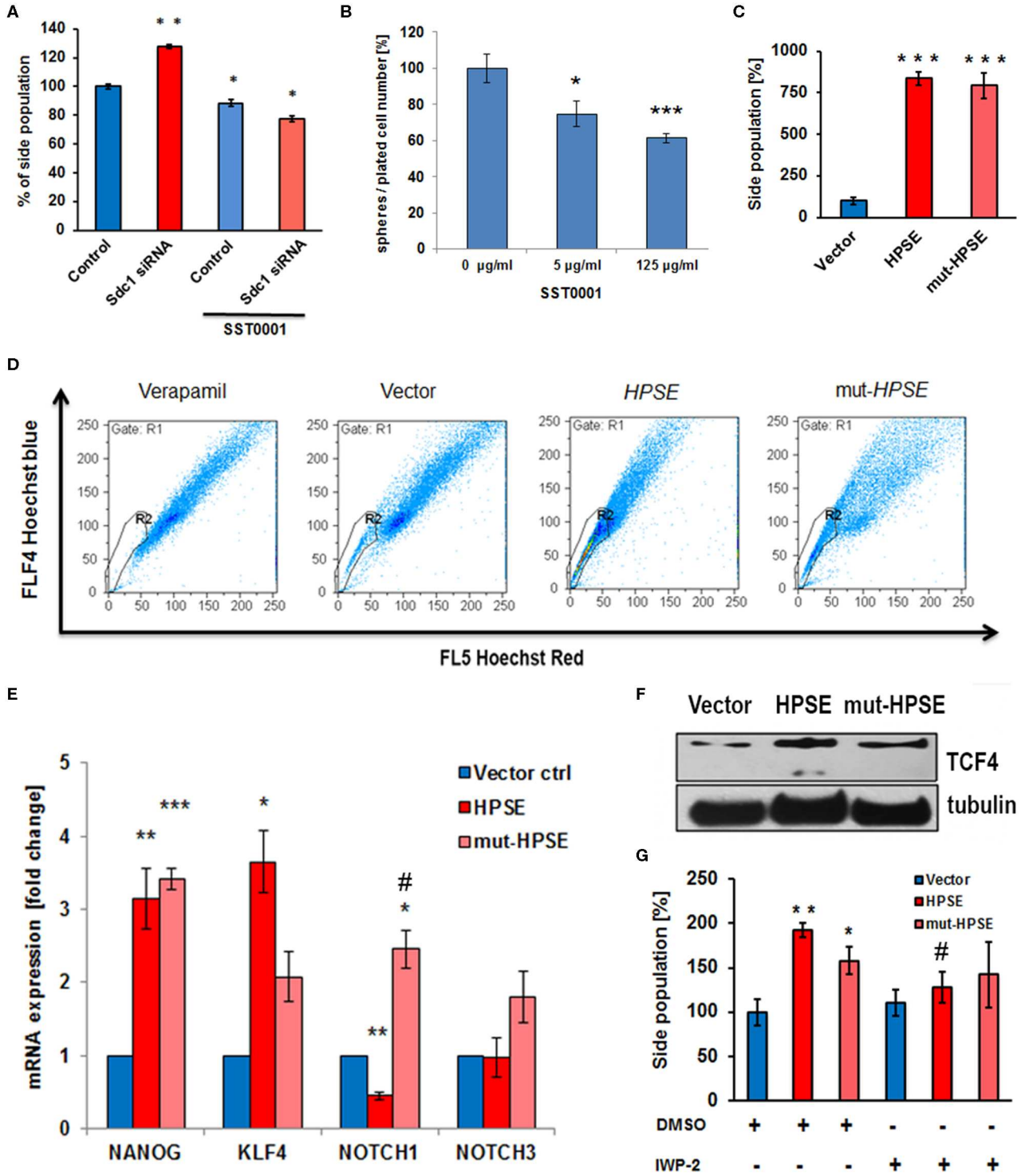

FIGURE 3 | Heparanase regulates the cancer stem cell phenotype of Caco2 cells. **(A)** Sdc-1 siRNA knockdown and heparanase inhibition by SST0001 affect the stem cell marker side population in opposite directions. $^{**}p < 0.01$ vs. all groups. $^{*}p < 0.05$ vs. untreated control. **(B)** The HPSE inhibitor SST0001 (10 µg/ml) reduces sphere formation as a readout of stem cell acivity. $^{***}p < 0.001$, $^{*}p < 0.05$ vs. untreated control. **(C,D)** Overexpression of native and enzymatically inactive forms of HPSE markedly increases the Caco2 side population. $^{***}p < 0.001$ vs. vector control. **(C)** Quantification of flow cytometric data. **(D)** representative flow cytometric measurements. Verapamil = inhibitor control. **(E,F)** Overexpression of native and enzymatically inactive forms of HPSE differentially affect the expression of the stem cell markers NANOG, KLF4, NOTCH1, NOTCH3, and TCF4. **(E)** qPCR, $^{***}p < 0.001$, $^{**}p < 0.01$, $^{*}p < 0.05$ vs. vector control, $\#p < 0.05$ vs. HPSE. **(F)** Western-Blot. **(G)** The Wnt pathway inhibitor IWP2 reduces the enhancing effect of HPSE overexpression on the side population phenotype. $^{**}p < 0.01$, $^{*}p < 0.05$ vs. control, $\#p < 0.05$ vs. untreated HPSE. All panels $N \geq 3$. Error bars = SEM. **(D,F)** representative example of three independent experiments.

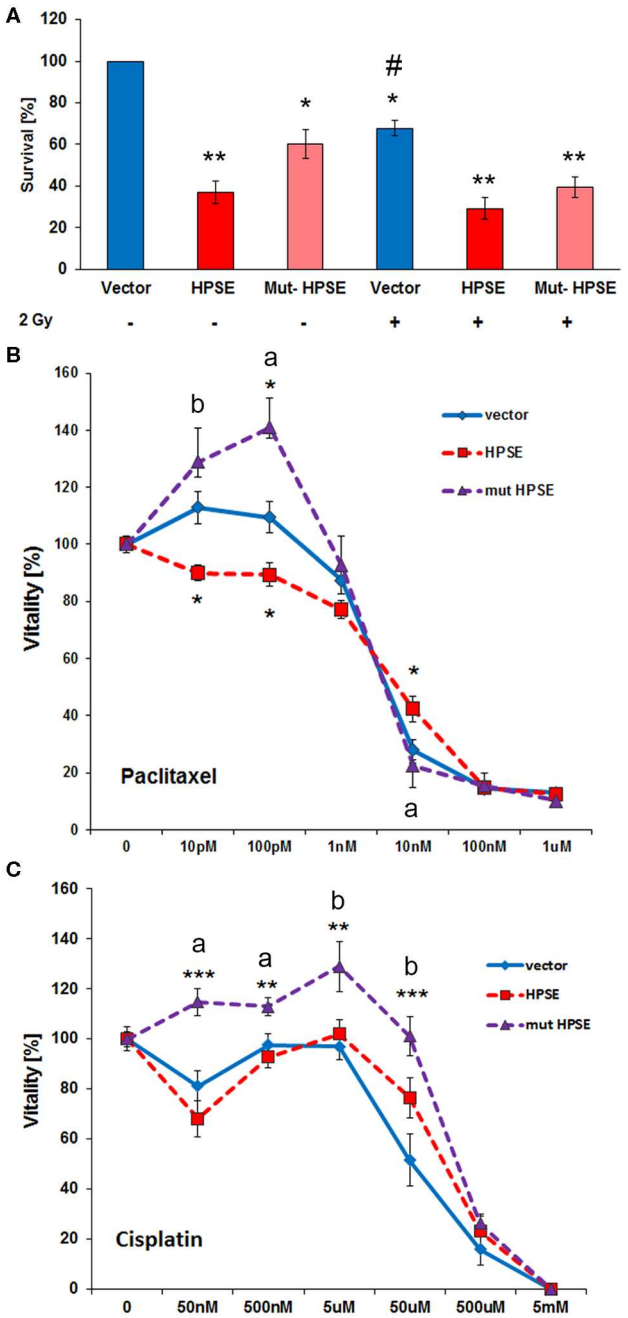

FIGURE 4 | Enzymatically active and inactive forms of heparanase differentially affect the resistance of Caco2 cells to chemotherapeutics and radiation treatment. **(A)** Vector control and HPSE / mutant HPSE overexpressing Caco2 cells were subjected to irradiation with 2 Gy and then to a colony formation assay as a readout of cell survival. Compared to controls, HPSE overexpressing cells showed reduced colony formation. Only control cells showed a significant radiation-induced reduction in colony formation. **(B)** Overexpression of enzymatically inactive HPSE increases Caco2 resistance to Paclitaxel chemotherapy, whereas HPSE reduces resistance at low treatment doses. MTT cell viability assay. **(C)** Overexpression of enzymatically inactive HPSE increases Caco2 resistance to Cisplatin chemotherapy. MTT cell viability assay. All panels $N \geq 3$. Error bars = SEM, $^{***}p < 0.001$, $^{**}p < 0.01$, $^{*}p < 0.05$ vs. control. $^{a}p < 0.01$ vs. HPSE, $^{b}p < 0.05$ vs. HPSE. $\#p < 0.05$ vs. unirradiated control within the same treatment group.

regulation has not been resolved. Our results demonstrate that (i) loss of Sdc-1 enhances transcriptional regulation of HPSE and vice versa, (ii) increased Sdc-1-dependent HPSE expression increases invasiveness and can be reversed by HPSE inhibition, (iii) molecular cross-talk between EGR1 and activation of FAK upon loss of Sdc-1 collectively drive HPSE expression, (iv) this expression boosts colon CSC properties, and (v) these processes are associated with alterations in the resistance of Caco2 cells to radio- and chemotherapy *in vitro*.

Increased expression of EGR1, an early growth response gene mediated by Sdc-1 downregulation, correlated with the increase in HPSE expression. Mutagenesis and trans-activation studies have previously shown that EGR1 binds to the HPSE promoter and up-regulates HPSE transcription in colon cancer cells (21). Our results further support that EGR1 directly regulates HPSE transcription. Data in fibrosarcoma cells suggest that the nuclear localization of Sdc-1 is a critical factor in regulating EGR1 expression, as expression of Sdc-1 lacking its nuclear localization signal resulted in upregulation of EGR1 (49). Therefore, the upregulation of EGR1 observed in Sdc-1-depleted Caco2 cells in our study may have been due to the reduction in nuclear, Sdc-1. Increased invasion of Sdc-1-depleted cells may be due to the degradation of HS chains, which impairs cell-cell contact and cell-matrix adhesion interactions. HPSE controls cell barrier function attributed to its HS degradative and Sdc-1 sheddase activity (8), suggesting that cleavage of Sdc-1 at the cell membrane will favor proinvasive conditions. Several pharmacodynamic studies have demonstrated that the HPSE inhibitor SST0001, has anti-tumor activity in different cancer models (40). Given that HPSE has multiple functions in the tumor microenvironment it is conceivable that SST0001 decreases the invasion of Sdc-1 depleted cells through HPSE-mediated signaling events (50, 51), or via direct inhibition of its basement-membrane degrading properties. Due to the loss of heparan sulfate, epithelial cells lose their cell polarity and gain migratory and invasive properties via the process of epithelial to mesenchymal transition (EMT). Indeed, in our experimental system, Sdc-1-depletion resulted in a downreguation of the antimetastatic epithelial cell adhesion molecule E-cadherin, and an upregulation of the mesenchymal marker vimentin. Although the underlying molecular processes remain poorly understood, it was reported that Sdc-1 depletion enhances formation of lamellipodia associated with an increase in invasive capabilities (42). It is well-documented that HSPG bind several EMT-inducing factors, such as FGF, hepatocyte growth factor and transforming growth factor-β. Therefore, enhanced HPSE expression may liberate these bound factors and thereby further enhancing EMT-like conditions (52). Moreover, we could show that HPSE inhibition could revert the upregulation of mesenchymal vimentin observed in Sdc-1-depleted cells. Also, a shift of Sdc-1 from epithelial to stromal cells might attenuate the antimetastatic effect of Sdc-1 at the cancer cell surface where loss of its expression can promote EMT (53).

A mountain of evidence shows that EMT-like conditions promote proliferation, metastasis, chemo-, immune- and radiotherapy resistance, all of which are relevant to cancer stem cell properties (26–28, 54). In breast cancer, enhanced activation

of integrins caused by Sdc-1 downregulation results in increased FAK activation (33). We, therefore, hypothesized that FAK might be involved in HPSE regulation. Indeed, blocking FAK autophosphorylation decreased HPSE expression in the absence of Sdc-1 (**Figure 2G**). It was previously reported that a putative HPSE receptor activates the phosphoinositide 3-kinase-protein kinase B (AKT) pathway (51), but it is not clear whether phosphorylated FAK activates this receptor. However, PF562271 effectively abolished heparanase-induced AKT activation (51), consistent with our results, where FAK inhibitor attenuated HPSE expression. It was reported that integrin/epidermal growth factor receptor cross-talk dependent adhesion signals regulate EGR1 expression (55). It is conceivable that upon Sdc-1 loss, the beta1 integrin complex on the plasma membrane may trigger the expression of EGR1 through adhesion-dependent signals, which would further lead to the activation of FAK. Overall, these data demonstrate that upon Sdc-1 loss, an EGR1/pFAK cross-talk is required for expression of HPSE through a novel regulatory signaling cascade, opening new strategies for therapeutic intervention.

Previous data from our group have indicated a role for Sdc-1 in CSC function (3, 31, 47), including an impact on the side population. Here, we demonstrate that basal sphere formation of our Caco2 model cell line and the Sdc-1 knockdown-induced increase in the SP can be blocked by HPSE inhibition, whereas upregulation of HPSE results in a substantial increase of this surrogate stem cell marker, independent of HPSE enzymatic activity. These results ascribe, for the first time, a role for HPSE in regulating CSC properties, and an impact of the HPSE inhibitor SST0001 on SP levels. As SST0001 profoundly decreased invasion of Sdc-1 depleted cells, it is conceivable that genes involved in cell invasion may also further regulate SP and/or that SST0001 is directly acting on genes associated with stemness. The significant increase in the SP as a result of HPSE overexpression provides further evidence for the multifunctional roles of HPSE in the tumor microenvironment. At the mRNA level, we saw a high increase in the expression of NANOG and KLF4 in cells expressing either native or mutant HPSE. Indeed there are indications for cell adhesion-dependent functions of enzymatically inactive HPSE (56, 57). The increase in NOTCH1 and NOTCH3 in mutant HPSE expressing cells could explain the increase in the SP seen in dominant negative clones (47, 58). During progression of the primary tumor, HPSE, by promoting autocrine and paracrine signaling functions, appears to initiate non-stem cell epithelial cells to develop into tumor-initiating cells via the re-expression of stem cell markers, including pluripotency-associated transcription factors (9). A range of signals were shown to regulate the tumor-initiating stem cell capacities of colon cancer, including the Wnt pathway (59). We observed a high expression of TCF4 in HPSE-overexpressing clones. Our results furthermore showed a decrease in the SP upon incubation with IWAP2 that inhibits the palmitylation of Wnt proteins and thereby blocks Wnt secretion and activity (60).

CSCs have been implicated in resistance to irradiation and chemotherapy due to increased expression of MDR proteins and highly efficient DNA repair mechanisms (3, 7). Irradiated HPSE overexpressing cells showed partial radioresistance compared to untreated controls. In addition, we observed increased chemoresistance in cells expressing mutant HPSE. The mutant inactive form of heparanase is involved in adhesion-dependent signaling which in turn may promote chemoresistance of cancer cells by increasing the side population (8, 57). It is also important to consider that the SP is controlled by several additional factors including, genetic alterations, the ECM niche microenvironment, micro RNA's, stem cells and their quiescent vs. active state (61). Altogether, the nature of drug resistance of tumor-initiating cells is multifactorial, with various signaling pathways and complex mechanisms that could fine-tune chemosensitivity.

To summarize, we have shown for the first time the involvement of HPSE in colon cancer stem cell properties and observed an increase in cell invasiveness linked to the regulatory interplay of Sdc-1 and HPSE. Moreover, we identified relevant signaling pathways (FAK, Wnt, Notch) and transcription factors (Egr1, TCF4), as constituents of this regulatory circuit, which paves the way for a more efficient combinatorial targeting of colon cancer in the context of therapeutic resistance.

DATA AVAILABILITY STATEMENT

All datasets generated for this study are included in the article/supplementary material.

AUTHOR CONTRIBUTIONS

SK performed the majority of experiments, analyzed data, drafted figures, and the initial version of the manuscript. PP performed molecular biology and stem cell culture experiments. CC performed stem cell culture experiments. RR supervised and performed molecular biology and stem cell culture experiments, analyzed data, and designed experiments. IV provided essential reagents and expertise on HPSE, revised the manuscript. BG assisted with, and analyzed flow cytometric and irradiation experiments, designed experiments, cosupervised the study, drafted figures. MG conceived and supervised the study, analyzed data drafted the final figures, and wrote the manuscript. All authors have read, revised, and approved the final version of the manuscript.

FUNDING

Funding was provided by deutsche Forschungsgemeinschaft DFG IRTG Molecular and Cellular GlycoSciences; Grant number: GRK 1549, and German-Israel Research Foundation (GIF) grant No. I-1004-202.15/2008 (to MG and IV). IV is a Research Professor of the Israel Cancer Research Fund (ICRF).

ACKNOWLEDGMENTS

The work presented in this manuscript is part of the Ph.D. thesis of SK (62). We thank Birgit Pers and Annette van Dülmen for expert technical assistance, Valeria Tria and Stefano Molgara for help with molecular cell biology experiments, Prof. Ludwig Kiesel for general support and Dr. Alessandro Noseda for the gift of SST0001.

REFERENCES

1. Barker HE, Paget JT, Khan AA, Harrington KJ. The tumour microenvironment after radiotherapy: mechanisms of resistance and recurrence. *Nat Rev Cancer*. (2015) 15:409–25. doi: 10.1038/nrc3958
2. Gialeli C, Theocharis AD, Karamanos NK. Roles of matrix metalloproteinases in cancer progression and their pharmacological targeting. *FEBS J*. (2011) 278:16–27. doi: 10.1111/j.1742-4658.2010.07919.x
3. Vitale D, Kumar Katakam S, Greve B, Jang B, Oh ES, Alaniz L, et al. Proteoglycans and glycosaminoglycans as regulators of cancer stem cell function and therapeutic resistance. *FEBS J*. (2019) 286:2870–82. doi: 10.1111/febs.14967
4. Filatova A, Acker T, Garvalov BK. The cancer stem cell niche(s): the crosstalk between glioma stem cells and their microenvironment. *Biochim Biophys Acta*. (2013) 1830:2496–508. doi: 10.1016/j.bbagen.2012.10.008
5. Ibrahim SA, Hassan H, Götte M. MicroRNA regulation of proteoglycan function in cancer. *FEBS J*. (2014) 281:5009–22. doi: 10.1111/febs.13026
6. Vijaya Kumar A, Salem Gassar E, Spillmann D, Stock C, Sen YP, Zhang T, et al. HS3ST2 modulates breast cancer cell invasiveness via MAP kinase-and Tcf4(Tcf7l2)- dependent regulation of protease and cadherin expression. *Int J Cancer*. (2014) 135:2579–92. doi: 10.1002/ijc.28921
7. Götte M, Yip GW. Heparanase, hyaluronan, and CD44 in cancers: a breast carcinoma perspective. *Cancer Res*. (2006) 66:10233–7. doi: 10.1158/0008-5472.CAN-06-1464
8. Vlodavs.ky I, Singh P, Boyango I, Gutter-Kapon L, Elkin M, Sanderson RD, et al. Heparanase: from basic research to therapeutic applications in cancer and inflammation. *Drug Resist Updat*. (2016) 29:54–75. doi: 10.1016/j.drup.2016.10.001
9. Friedmann Y, Vlodavs.ky I, Aingorn H, Aviv A, Peretz T, Pecker I, et al. Expression of heparanase in normal, dysplastic, and neoplastic human colonic mucosa and stroma. Evidence for its role in colonic tumorigenesis. *Am J Pathol*. (2000) 157:1167–75. doi: 10.1016/S0002-9440(10)64632-9
10. Hashimoto Y, Skacel M, Adams JC. Association of loss of epithelial syndecan-1 with stage and local metastasis of colorectal adenocarcinomas: an immunohistochemical study of clinically annotated tumors. *BMC Cancer*. (2008) 8:185. doi: 10.1186/1471-2407-8-185
11. Fernández-Vega I, García-Suárez O, García B, Crespo A, Astudillo A, Quirós LM. Heparan sulfate proteoglycans undergo differential expression alterations in right sided colorectal cancer, depending on their metastatic character. *BMC Cancer*. (2015) 15:742. doi: 10.1186/s12885-015-1724-9
12. Crespo A, García-Suárez O, Fernández-Vega I, Solis-Hernandez MP, García B, Castañón S, et al. Heparan sulfate proteoglycans undergo differential expression alterations in left sided colorectal cancer, depending on their metastatic character. *BMC Cancer*. (2018) 18:687. doi: 10.1186/s12885-018-4597-x
13. Fujiya M, Watari J, Ashida T, Honda M, Tanabe H, Fujiki T, et al. Reduced expression of syndecan-1 affects metastatic potential and clinical outcome in patients with colorectal cancer. *Jpn J Cancer Res*. (2001) 92:1074–81. doi: 10.1111/j.1349-7006.2001.tb01062.x
14. Takaoka M, Naomoto Y, Ohkawa T, Uetsuka H, Shirakawa Y, Uno F, et al. Heparanase expression correlates with invasion and poor prognosis in gastric cancers. *Lab Invest*. (2003) 83:613–22. doi: 10.1097/01.LAB.0000067482.84946.BD
15. Levy P, Munier A, Baron-Delage S, Di Gioia Y, Gespach C, Capeau J, et al. Syndecan-1 alterations during the tumorigenic progression of human colonic Caco-2 cells induced by human Ha-ras or polyoma middle T oncogenes. *Br J Cancer*. (1996) 74:423–31. doi: 10.1038/bjc.1996.376
16. Lundin M, Nordling S, Lundin J, Isola J, Wiksten JP, Haglund C. Epithelial syndecan-1 expression is associated with stage and grade in colorectal cancer. *Oncology*. (2005) 68:306–13. doi: 10.1159/000086969
17. Lerner I, Hermano E, Zcharia E, Rodkin D, Bulvik R, Doviner V, et al. Heparanase powers a chronic inflammatory circuit that promotes colitis-associated tumorigenesis in mice. *J Clin Invest*. (2011) 121:1709–21. doi: 10.1172/JCI43792
18. Doviner V, Maly B, Kaplan V, Gingis-Velitski S, Ilan N, Vlodavs.ky I, et al. Spatial and temporal heparanase expression in colon mucosa throughout the adenoma-carcinoma sequence. *Mod Pathol*. (2006) 19:878–88. doi: 10.1038/modpathol.3800603
19. Nobuhisa T, Naomoto Y, Ohkawa T, Takaoka M, Ono R, Murata T, et al. Heparanase expression correlates with malignant potential in human colon cancer. *J Cancer Res Clin Oncol*. (2005) 131:229–37. doi: 10.1007/s00432-004-0644-x
20. Mikami S, Ohashi K, Usui Y, Nemoto T, Katsube K, Yanagishita M, et al. Loss of syndecan-1 and increased expression of heparanase in invasive esophageal carcinomas. *Jpn J Cancer Res*. (2001) 92:1062–73. doi: 10.1111/j.1349-7006.2001.tb01061.x
21. de Mestre AM, Rao S, Hornby JR, Soe-Htwe T, Khachigian LM, Hulett MD. Early growth response gene 1 (EGR1) regulates heparanase gene transcription in tumor cells. *J Biol Chem*. (2005) 280:35136–47. doi: 10.1074/jbc.M503414200
22. Ilan N, Elkin M, Vlodavs.ky I. Regulation, function and clinical significance of heparanase in cancer metastasis and angiogenesis. *Int J Biochem Cell Biol*. (2006) 38:2018–39. doi: 10.1016/j.biocel.2006.06.004
23. Götte M, Kovalszky I. Extracellular matrix functions in lung cancer. *Matrix Biol*. (2018) 73:105–21. doi: 10.1016/j.matbio.2018.02.018
24. Visvader JE, Lindeman GJ. Cancer stem cells in solid tumours: accumulating evidence and unresolved questions. *Nat Rev Cancer*. (2008) 8:755–68. doi: 10.1038/nrc2499
25. Brabletz T, Jung A, Spaderna S, Hlubek F, Kirchner T. Opinion: migrating cancer stem cells - an integrated concept of malignant tumour progression. *Nat Rev Cancer*. (2005) 5:744–9. doi: 10.1038/nrc1694
26. Mani SA, Guo W, Liao MJ, Eaton EN, Ayyanan A, Zhou AY, et al. The epithelial-mesenchymal transition generates cells with properties of stem cells. *Cell*. (2008) 133:704–15. doi: 10.1016/j.cell.2008.03.027
27. Aktas B, Tewes M, Fehm T, Hauch S, Kimmig R, Kasimir-Bauer S. Stem cell and epithelial-mesenchymal transition markers are frequently overexpressed in circulating tumor cells of metastatic breast cancer patients. *Breast Cancer Res*. (2009) 11:R46. doi: 10.1186/bcr2333
28. Piperigkou Z, Franchi M, Riethmüller C, Götte M, Karamanos NK. miR-200b restrains EMT and aggressiveness and regulates matrix composition depending on ER status and signaling in mammary cancer. *Matrix Biol Plus*. (in press). doi: 10.1016/j.mbplus.2020.100024
29. Mahtouk K, Hose D, Raynaud P, Hundemer M, Jourdan M, Jourdan E, et al. Heparanase influences expression and shedding of syndecan-1, and its expression by the bone marrow environment is a bad prognostic factor in multiple myeloma. *Blood*. (2007) 109:4914–23. doi: 10.1182/blood-2006-08-043232
30. Ramani VC, Purushothaman A, Stewart MD, Thompson CA, Vlodavs.ky I, Au JL, et al.The heparanase/syndecan-1 axis in cancer: mechanisms and therapies. *FEBS J*. (2013) 280:2294–306. doi: 10.1111/febs.12168
31. Ibrahim SA, Hassan H, Vilardo L, Kumar SK, Kumar AV, Kelsch R, et al. Syndecan-1 (CD138) modulates triple-negative breast cancer stem cell properties via regulation of LRP-6 and IL-6-mediated STAT3 signaling. *PLoS ONE*. (2013) 8:e85737. doi: 10.1371/journal.pone.0085737
32. Ridgway LD, Wetzel MD, Marchetti D. Heparanase modulates Shh and Wnt3a signaling in human medulloblastoma cells. *Exp Ther Med*. (2011) 2:229–38. doi: 10.3892/etm.2010.189
33. Hassan H, Greve B, Pavao MS, Kiesel L, Ibrahim SA, Götte M. Syndecan-1 modulates β-integrin-dependent and interleukin-6-dependent functions in breast cancer cell adhesion, migration, and resistance to irradiation. *FEBS J*. (2013) 280:2216–27. doi: 10.1111/febs.12111
34. Spyrou A, Kundu S, Haseeb L, Yu D, Olofsson T, Dredge K, et al. Inhibition of heparanase in pediatric brain tumor cells attenuates their proliferation, invasive capacity, and *in vivo* tumor growth. *Mol Cancer Ther*. (2017) 16:1705–16. doi: 10.1158/1535-7163.MCT-16-0900
35. Xing Y, Cui D, Wang S, Wang P, Xing X, Li H. Oleuropein represses the radiation resistance of ovarian cancer by inhibiting hypoxia and microRNA-299-targetted heparanase expression. *Food Funct*. (2017) 8:2857–64. doi: 10.1039/C7FO00552K
36. Davidson B, Shafat I, Risberg B, Ilan N, Trope' CG, Vlodavs.ky I, et al. Heparanase expression correlates with poor survival in metastatic ovarian carcinoma. *Gynecol Oncol*. (2007) 104:311–9. doi: 10.1016/j.ygyno.2006.08.045

37. Shteingauz A, Boyango I, Naroditsky I, Hammond E, Gruber M, Doweck I, et al. Heparanase enhances tumor growth and chemoresistance by promoting autophagy. *Cancer Res*. (2015) 75:3946–57. doi: 10.1158/0008-5472.CAN-15-0037
38. Wang Z, Götte M, Bernfield M, Reizes O. Constitutive and accelerated shedding of murine syndecan-1 is mediated by cleavage of its core protein at a specific juxtamembrane site. *Biochemistry*. (2005) 44:12355–61. doi: 10.1021/bi050620i
39. Hulett MD, Hornby JR, Ohms SJ, Zuegg J, Freeman C, Gready JE, et al. Identification of active-site residues of the pro-metastatic endoglycosidase heparanase. *Biochemistry*. (2000) 39:15659–67. doi: 10.1021/bi002080p
40. Lanzi C, Zaffaroni N, Cassinelli G. Targeting heparan sulfate proteoglycans and their modifying enzymes to enhance anticancer chemotherapy efficacy and overcome drug resistance. *Curr Med Chem*. (2017) 24:2860–86. doi: 10.2174/0929867324666170216114248
41. Meirovitz A, Hermano E, Lerner I, Zcharia E, Pisano C, Peretz T, et al. Role of heparanase in radiation-enhanced invasiveness of pancreatic carcinoma. *Cancer Res*. (2011) 71:2772–80. doi: 10.1158/0008-5472.CAN-10-3402
42. Ibrahim SA, Yip GW, Stock C, Pan JW, Neubauer C, Poeter M, et al. Targeting of syndecan-1 by microRNA miR-10b promotes breast cancer cell motility and invasiveness via a Rho-GTPase- and E-cadherin-dependent mechanism. *Int J Cancer*. (2012) 131:E884–96. doi: 10.1002/ijc.27629
43. Götte M, Greve B, Kelsch R, Müller-Uthoff H, Weiss K, Kharabi Masouleh B, et al. The adult stem cell marker musashi-1 modulates endometrial carcinoma cell cycle progression and apoptosis via notch-1 and p21(WAF1/CIP1). *Int J Cancer*. (2011) 129:2042–49. doi: 10.1002/ijc.25856
44. Greve B, Kelsch R, Spaniol K, Eich HT, Götte M. Flow cytometry in cancer stem cell analysis and separation. *Cytometry A*. (2012) 81:284–93. doi: 10.1002/cyto.a.22022
45. Elkin M, Cohen I, Zcharia E, Orgel A, Guatta-Rangini Z, Peretz T, et al. Regulation of heparanase gene expression by estrogen in breast cancer. *Cancer Res*. (2003) 63:8821–6.
46. Zcharia E, Zilka R, Yaar A, Yacoby-Zeevi O, Zetser A, Metzger S, et al. Heparanase accelerates wound angiogenesis and wound healing in mouse and rat models. *FASEB J*. (2005) 19:211–21. doi: 10.1096/fj.04-1970com
47. Ibrahim SA, Gadalla R, El-Ghonaimy EA, Samir O, Mohamed HT, Hassan H, et al. Syndecan-1 is a novel molecular marker for triple negative inflammatory breast cancer and modulates the cancer stem cell phenotype via the IL-6/STAT3, notch and EGFR signaling pathways. *Mol Cancer*. (2017) 16:57. doi: 10.1186/s12943-017-0621-z
48. Espinoza-Sánchez NA, Götte M. Role of cell surface proteoglycans in cancer immunotherapy. *Semin Cancer Biol*. (2019) 62:48–67. doi: 10.1016/j.semcancer.2019.07.012
49. Szatmári T, Mundt F, Kumar-Singh A, Möbus L, Ötvös R, Hjerpe A, Dobra K. Molecular targets and signaling pathways regulated by nuclear translocation of syndecan-1. *BMC Cell Biol*. (2017) 18:34. doi: 10.1186/s12860-017-0150-z
50. Cassinelli G, Lanzi C, Tortoreto M, Cominetti D, Petrangolini G, Favini E, et al. Antitumor efficacy of the heparanase inhibitor SST0001 alone and in combination with antiangiogenic agents in the treatment of human pediatric sarcoma models. *Biochem Pharmacol*. (2013) 85:1424–32. doi: 10.1016/j.bcp.2013.02.023
51. Riaz A, Ilan N, Vlodavs.ky I, Li JP, Johansson S. Characterization of heparanase-induced phosphatidylinositol 3-kinase-AKT activation and its integrin dependence. *J Biol Chem*. (2013) 288:12366–75. doi: 10.1074/jbc.M112.435172
52. Kirkbride KC, Ray BN, Blobe GC. Cell-surface co-receptors: emerging roles in signaling and human disease. *Trends Biochem Sci*. (2005) 30:611–21. doi: 10.1016/j.tibs.2005.09.003
53. Mennerich D, Vogel A, Klaman I, Dahl E, Lichtner RB, Rosenthal A, et al. Shift of syndecan-1 expression from epithelial to stromal cells during progression of solid tumours. *Eur J Cancer*. (2004) 40:1373–82. doi: 10.1016/j.ejca.2004.01.038
54. Nieto MA, Cano A. The epithelial-mesenchymal transition under control: global programs to regulate epithelial plasticity. *Semin Cancer Biol*. (2012) 22:361–8. doi: 10.1016/j.semcancer.2012.05.003
55. Cabodi S, Morello V, Masi A, Cicchi R, Broggio C, Distefano P, et al. Convergence of integrins and EGF receptor signaling via PI3K/Akt/FoxO pathway in early gene Egr-1 expression. *J Cell Physiol*. (2009) 218:294–303. doi: 10.1002/jcp.21603
56. Goldshmidt O, Zcharia E, Cohen M, Aingorn H, Cohen I, Nadav L, et al. Heparanase mediates cell adhesion independent of its enzymatic activity. *FASEB J*. (2003) 17:1015–25. doi: 10.1096/fj.02-0773com
57. Levy-Adam F, Ilan N, Vlodavs.ky I. Tumorigenic and adhesive properties of heparanase. *Semin Cancer Biol*. (2010) 20:153–60. doi: 10.1016/j.semcancer.2010.06.005
58. Shibue T, Brooks MW, Weinberg RA. An integrin-linked machinery of cytoskeletal regulation that enables experimental tumor initiation and metastatic colonization. *Cancer Cell*. (2013) 24:481–98. doi: 10.1016/j.ccr.2013.08.012
59. Yamada T, Takaoka AS, Naishiro Y, Hayashi R, Maruyama K, Maesawa C, et al. Transactivation of the multidrug resistance 1 gene by T-cell factor 4/beta-catenin complex in early colorectal carcinogenesis. *Cancer Res*. (2000) 60:4761–6.
60. Chikazawa N, Tanaka H, Tasaka T, Nakamura M, Tanaka M, Onishi H, et al. Inhibition of Wnt signaling pathway decreases chemotherapy-resistant side-population colon cancer cells. *Anticancer Res*. (2010) 30: 2041–8.
61. Richard V, Nair MG, Santhosh Kumar TR, Pillai MR. Side population cells as prototype of chemoresistant, tumor-initiating cells. *Biomed Res Int*. (2013) 2013:517237. doi: 10.1155/2013/517237
62. Kumar Katakam S. *Syndecan-1 and heparanase as novel regulators of colon cancer stem cell function* (Ph.D. thesis). Faculty of Biology, Westfälische-Wilhelms-Universität Münster, Münster, Germany (2015).

Conflict of Interest: The authors declare that the research was conducted in the absence of any commercial or financial relationships that could be construed as a potential conflict of interest.

Copyright © 2020 Katakam, Pelucchi, Cocola, Reinbold, Vlodavsky, Greve and Götte. This is an open-access article distributed under the terms of the Creative Commons Attribution License (CC BY). The use, distribution or reproduction in other forums is permitted, provided the original author(s) and the copyright owner(s) are credited and that the original publication in this journal is cited, in accordance with accepted academic practice. No use, distribution or reproduction is permitted which does not comply with these terms.

frontiers in Cell and Developmental Biology

ORIGINAL RESEARCH
published: 29 May 2020
doi: 10.3389/fcell.2020.00377

Label-Free Infrared Spectral Histology of Skin Tissue Part II: Impact of a Lumican-Derived Peptide on Melanoma Growth

Stéphane Brézillon[1,2]*, *Valérie Untereiner*[3], *Hossam Taha Mohamed*[1,2,4,5], *Estelle Ahallal*[1,2], *Isabelle Proult*[1,2], *Pierre Nizet*[1,2], *Camille Boulagnon-Rombi*[2,6] and *Ganesh. D. Sockalingum*[7]

[1] Université de Reims Champagne-Ardenne, Laboratoire de Biochimie Médicale et Biologie Moléculaire, Reims, France, [2] CNRS UMR 7369, Matrice Extracellulaire et Dynamique Cellulaire - MEDyC, Reims, France, [3] Université de Reims Champagne-Ardenne, PICT, Reims, France, [4] Zoology Department, Faculty of Science, Cairo University, Giza, Egypt, [5] Faculty of Biotechnology, October University for Modern Sciences and Arts, Giza, Egypt, [6] CHU de Reims, Laboratoire Central d'Anatomie et de Cytologie Pathologique, Reims, France, [7] Université de Reims Champagne-Ardenne, BioSpecT-EA7506, Reims, France

OPEN ACCESS

Edited by:
Rafael Fridman, Wayne State University, United States

Reviewed by:
Dragana Nikitovic, University of Crete, Greece
Oliver Kepp, Institut Gustave Roussy, France

***Correspondence:**
Stéphane Brézillon
stephane.brezillon@univ-reims.fr

Specialty section:
This article was submitted to Molecular and Cellular Oncology, a section of the journal Frontiers in Cell and Developmental Biology

Received: *11 February 2020*
Accepted: *27 April 2020*
Published: *29 May 2020*

Citation:
Brézillon S, Untereiner V, Mohamed HT, Ahallal E, Proult I, Nizet P, Boulagnon-Rombi C and Sockalingum GD (2020) Label-Free Infrared Spectral Histology of Skin Tissue Part II: Impact of a Lumican-Derived Peptide on Melanoma Growth. Front. Cell Dev. Biol. 8:377. doi: 10.3389/fcell.2020.00377

Melanoma is the most aggressive type of cutaneous malignancies. In addition to its role as a regulator of extracellular matrix (ECM) integrity, lumican, a small leucine-rich proteoglycan, also exhibits anti-tumor properties in melanoma. This work focuses on the use of infrared spectral imaging (IRSI) and histopathology (IRSH) to study the effect of lumican-derived peptide (L9Mc) on B16F1 melanoma primary tumor growth. Female C57BL/6 mice were injected with B16F1 cells treated with L9Mc ($n = 10$) or its scrambled peptide ($n = 8$), and without peptide (control, $n = 9$). The melanoma primary tumors were subjected to histological and IR imaging analysis. In addition, immunohistochemical staining was performed using anti-Ki-67 and anti-cleaved caspase-3 antibodies. The IR images were analyzed by common K-means clustering to obtain high-contrast IRSH that allowed identifying different ECM tissue regions from the epidermis to the tumor area, which correlated well with H&E staining. Furthermore, IRSH showed good correlation with immunostaining data obtained with anti-Ki-67 and anti-cleaved caspase-3 antibodies, whereby the L9Mc peptide inhibited cell proliferation and increased strongly apoptosis of B16F1 cells in this mouse model of melanoma primary tumors.

Keywords: melanoma, lumican-derived peptides, B16F1, infrared histology, immunohistochemistry

INTRODUCTION

Melanoma is the most aggressive and deadliest form of skin cancers representing 80% of deaths in cutaneous malignancies (Miller and Mihm, 2006; Hodi et al., 2010). The early stages of melanoma can be cured *via* surgery. In contrast, treatment of metastatic melanoma is a health issue due to resistance to most available therapies and low survival rates (Soengas and Lowe, 2003; Gray-Schopfer et al., 2007; Greene and Sobin, 2008). The biological changes occurring in the primary tumor that lead to metastatic tumors including loss of adherent junctions, extracellular matrix (ECM) degradation, increased carcinoma cells motility and resistance to apoptosis, are now better understood. In addition, the important role of stromal and infiltrating immune cells in tumor

progression and patient's outcome has been reported in several studies (Pages et al., 2010; Hanahan and Weinberg, 2011; Galon et al., 2012). Thus, anticancer strategies developed over the last years, focused on understanding the cross-talk between malignant cells (Valkenburg et al., 2018; Liu et al., 2019) and the tumor microenvironment including both stromal cells and ECM (Belotti et al., 2011; Venning et al., 2015) such as targeting matricellular proteins, that regulate the communication between ECM and cancer cells (Wong and Rustgi, 2013).

Lumican belongs to the small leucine-rich proteoglycans (SLRP) family (McEwan et al., 2006) and was shown to control the assembly of collagen fibers in the ECM (Chakravarti et al., 1998; Iozzo and Schaefer, 2015). Proteoglycans play a major role in the control of tumor progression. Lumican is expressed in various tumor tissues but both positive and negative correlations with tumor aggressiveness have been reported (Brézillon et al., 2013; Nikitovic et al., 2014). Brézillon et al., revealed that the downregulation of lumican expression in melanoma is associated with increased invasion (Brézillon et al., 2007). They have also shown that lumican inhibits melanoma cell migration (Brézillon et al., 2009; Stasiak et al., 2016), while promoting their adhesion (D'Onofrio et al., 2008). Moreover, previous studies showed the ability of lumican (and its derived peptides), in contrast to decorin, to inhibit MMP-14 activity in melanoma cells, where lumican directly interacts with MMP-14 and inhibits its activity (Pietraszek et al., 2013, 2014). Thus, lumican is able to inhibit the remodeling of the skin ECM by inhibiting MMPs activity, and consequently melanoma progression. Furthermore, lumican is highly expressed within the stroma surrounded several solid tumors such as prostate cancer (Coulson-Thomas et al., 2013) and lung adenocarcinoma (Cappellesso et al., 2015). Another study reported that extracellular lumican enhances the cytotoxicity of chemotherapy in pancreatic ductal adenocarcinoma cells by autophagy inhibition (Li et al., 2016). Recently, optical imaging techniques such as Second Harmonic Generation (SHG) and FTIR were used to validate that lumican disorganizes ECM and more specifically collagen fibers orientation (Jeanne et al., 2017).

IR spectroscopy is a promising rapid, non-destructive, reagent and label-free technique that is used for structural and compositional analysis due to its ability to give a complete "molecular fingerprint" of the studied sample (Baker et al., 2014). It is highly sensitive to the structure, composition, and environment of the molecules constituting the studied specimen. It has been successfully used to characterize, differentiate, and classify types and subtypes of glycosaminoglycans (GAGs) despite their close molecular structures (Mainreck et al., 2011; Mohamed et al., 2017) and to perform cell phenotyping (Brézillon et al., 2014, 2017; Mohamed et al., 2017, 2018).

At the tissue level, FTIR imaging combined with multivariate statistical analysis has shown its capability to discriminate between inflammatory and non-inflammatory breast cancer tissues (Mohamed et al., 2018). Wald et al., demonstrated that FTIR imaging histopathology was able to discriminate between non-metastatic and metastatic lymph nodes from melanoma patients and to distinguish between infiltrating lymphocytic cell subpopulations, thus predicting if they originated from normal or metastatic lymph nodes (Wald et al., 2016a). However, they did not find any significant differences between primary and metastatic melanoma cells or any significant correlation between the infrared spectra of melanoma cells and the percentage of proliferative cells (Wald and Goormaghtigh, 2015).

In the present report, we conducted an investigation combining IR spectral histopathology (IRSH), conventional histology and immunohistochemistry to study the effect of lumican-derived peptide (L9Mc) on tumor progression in melanoma primary tumors.

MATERIALS AND METHODS

Cell Culture

Murine melanoma cell line B16F1 (ATCC®CRL-6323™) was cultured in DMEM medium with 10% fetal bovine serum, 1% of penicillin/streptomycin antibiotic mixture and 50 mg/mL geneticin at 37°C and 5% CO_2.

In vivo Studies

A total of 27 female C57BL/6 mice were purchased from Harlan-France (Gannat, France) for enrolment in this study. Mice were individually caged in a room with fixed level of humidity and temperature. For mice nutrition, we used standard food and water. All mice were adapted for 7 days before starting the experiments. B16F1 cells at 80% confluency were detached using trypsin/EDTA solution, then the cell suspension was centrifuged at 300 g for 3 min. The collected cell pellet was resuspended in basal medium at the concentration of 2.50×10^6 cells/mL in absence or presence of 100 μM lumican-derived peptide L9Mc, or its scrambled peptide (L9Mc SCR). At day 0, 25×10^4 B16F1 cells (mixed or not with the peptides, 2 mg/mL) were injected in the right flank of 27 mice ($n = 9$ for control, $n = 8$ for L9Mc SCR and $n = 10$ for L9Mc). In addition, 200 μg of peptides at 2 mg/mL were injected at days 6, 9, and 13 to the corresponding groups. At day 19, mice were sacrificed and the primary tumors were collected and formalin-fixed paraffin-embedded (FFPE) for conventional histology, immunohistochemistry, and IRSH. All experiments were performed according to the instructions of the Center National de la Recherche Scientifique. This study was performed in compliance with the French Animal Welfare Act and following the French Board for Animal Experiments. Experiments were conducted under approval of the French "Ministère de l'Enseignement Supérieur et de la Recherche" (Ethics Committee C2EA-56) in accordance with the directive "2010/63/UE."

Histopathological Examination of Skin Tissue Samples

Three 5 μm thick serial sections were obtained from the FFPE tumor tissues. The first and third sections were chemically dewaxed and stained with standard Hematoxylin and Eosin solution (H&E) that respectively highlights the nucleus in purple and the cytoplasm in pink. These sections underwent histopathological examination by a confirmed pathologist from the Pathology Department of the Reims University Hospital to annotate the different tissue structures.

Immunohistochemistry

Immunohistochemical (IHC) staining was performed after chemical dewaxing of two 3 μm thick sections using antibodies against Ki-67 (SP6) (Abcam, Cambridge, UK) and cleaved caspase-3 (Cell Signaling, Danvers, MA, USA). Ki-67 and cleaved caspase-3 stainings are indicators for proliferation and apoptosis indexes, respectively. IHC staining was carried out by adding 100 μL of DAB+chromogen diluted at 1:50 in substrate buffer [EnVision+ Dual Link System-HRP (DAB+)] for 10 min. Finally, tissue specimens were washed in phosphate buffer saline (PBS), the nuclei counterstained with hematoxylin and mounted using Eukitt® for microscopic examination. Positively stained melanoma cells, in which Ki-67 and cleaved caspase-3 highlight in brown the nucleus and the cytoplasm respectively, were quantified using ImageJ software (National Institutes of Health, Bethesda, MD, USA).

Infrared Spectral Imaging of Formalin Fixed Paraffin Embedded Tissues

The second 5 μm thick tissue section was placed on a 1 mm thick calcium fluoride (CaF_2) window (Crystran, Dorset, UK) for IRSH analysis without any particular preparation such as chemical dewaxing or staining. FTIR images were acquired in transmission mode using the Spotlight™ 400 imaging system (PerkinElmer, Villebon-sur-Yvette, France) at a pixel size of 6.25 μm, a spectral resolution of 4 cm^{-1} and 16 scans in the spectral range of 800–4,000 cm^{-1}. Prior to this, a visible image of the tissue section is acquired using the IR microscope and the region of interest selected with the help of the H&E stained tissue. Further, a background spectrum was recorded in a blank area of the window that was automatically subtracted from each pixel spectrum of the image.

Spectral Image Preprocessing

The recorded FTIR hyperspectral images of FFPE melanoma tissues exhibit both tissue biochemical information and paraffin bands (1,378 and 1,467 cm^{-1}) in the 900–1,800 cm^{-1} spectral region. To avoid chemical dewaxing, images were digitally corrected for paraffin spectral contribution. This is achieved *via* an automated data processing method based on Extended Multiplicative Signal Correction (EMSC) as reported before (Ly et al., 2008). To obtain IRSH images, an unsupervised common K-means clustering method was applied to the tissue spectra (Nguyen et al., 2016). In this method, each spectrum belongs to a unique cluster and spectral images can be reconstructed based on pixel spectral similarity for a rapid and simple visual analysis of clustering results. Both EMSC and K-means clustering algorithms were implemented in Matlab Statistics Toolbox software. In addition to the cluster images, a dendrogram obtained by Hierarchical Cluster Analysis (HCA) and based on spectral distance calculation between different cluster centroids, was also obtained. Each centroid spectrum can be assigned to a different tissue component. All processed IRSH images were compared with adjacent H&E and IHC stained sections. The workflow for histopathological, immunohistochemical, and IRSH analyses is illustrated in **Figure 1**.

Statistical Analysis

All data are presented as the mean ± standard deviation (SD). One-way ANOVA was used in the three groups comparison analysis of melanoma primary tumors data. In addition, Student's *t*-test was used in a pairwise comparison analysis of melanoma primary tumors data. A $P < 0.05$ was considered significant with $^{*}P < 0.05$ and $^{**}P < 0.01$.

RESULTS

Infrared Spectral Histology Correlates Well With Conventional Histology of Melanoma

Five control, five L9Mc SCR-treated and five L9Mc-treated melanoma primary tumor sections were examined by both conventional and infrared spectral histologies. H&E staining of representative sections of each group are shown in **Figures 2A**, **3A,F**, respectively, and at a higher magnification (2.5x, 10x, and 15x) in **Supplementary Figure 1** with the corresponding Crosscope links. In the case of L9Mc-treated melanoma, there is a clear evidence that the volume of the tumor is 3–4-fold reduced ($n = 10$, mean volume: 0.31 ± 0.26 cm^3) compared to the control ($n = 9$, mean volume: 1.02 ± 0.97 cm^3) and L9Mc SCR-treated ($n = 8$, mean volume: 1.25 ± 1.80 cm^3) groups (data not shown). The regions of interest (ROI) analyzed by FTIR are represented by rectangles. In the case of control tissue, the ROI is highlighted in **Figure 2B**. The melanoma tumor is easily recognized by a purple staining, while peritumoral area appears in light pink staining. In addition, the muscle fibers are characterized by an intense pink color. Hair bulbs can be identified by their dark pink staining in the dermis. The highlighted zone of L9Mc SCR sections is shown in **Figure 3B**. Tumor cells are clearly visible in purple while necrotic area appears in light purple. Moreover, the external thin layer of the epidermis is characterized by a dark pink color, and the dermis appears in intense pink. The hypodermis layer is mainly characterized by a light pink staining. The highlighted zone of L9Mc sections is shown in **Figure 3G**. Similar histological structures can be assigned to this tissue. However, the ECM remodeling is less marked than in the case of control and L9Mc SCR-treated tumors.

After digital dewaxing of the FTIR images of melanoma primary tumor tissue sections, a common K-means clustering was performed using 9 clusters. The common K-means is used here so that the same histological feature is assigned the same pseudo-color in all images. The reconstructed color-coded cluster images enabled the recovery of different histological features that allowed to precisely localize melanoma from other tissue components. These are depicted in **Figures 2C**, **3C,H** for control, L9Mc SCR-treated and L9Mc-treated, respectively. The centroid spectra of the 9 clusters are displayed in **Figure 4A**. These centroid spectra allowed generating a hierarchical classification based on spectral distance (**Figure 4B**) and to visualize the similarities or differences between the different tissue components. Annotation of each generated cluster was then performed with the help of a confirmed pathologist resulting in the following precise tissue characterization: melanoma tissues

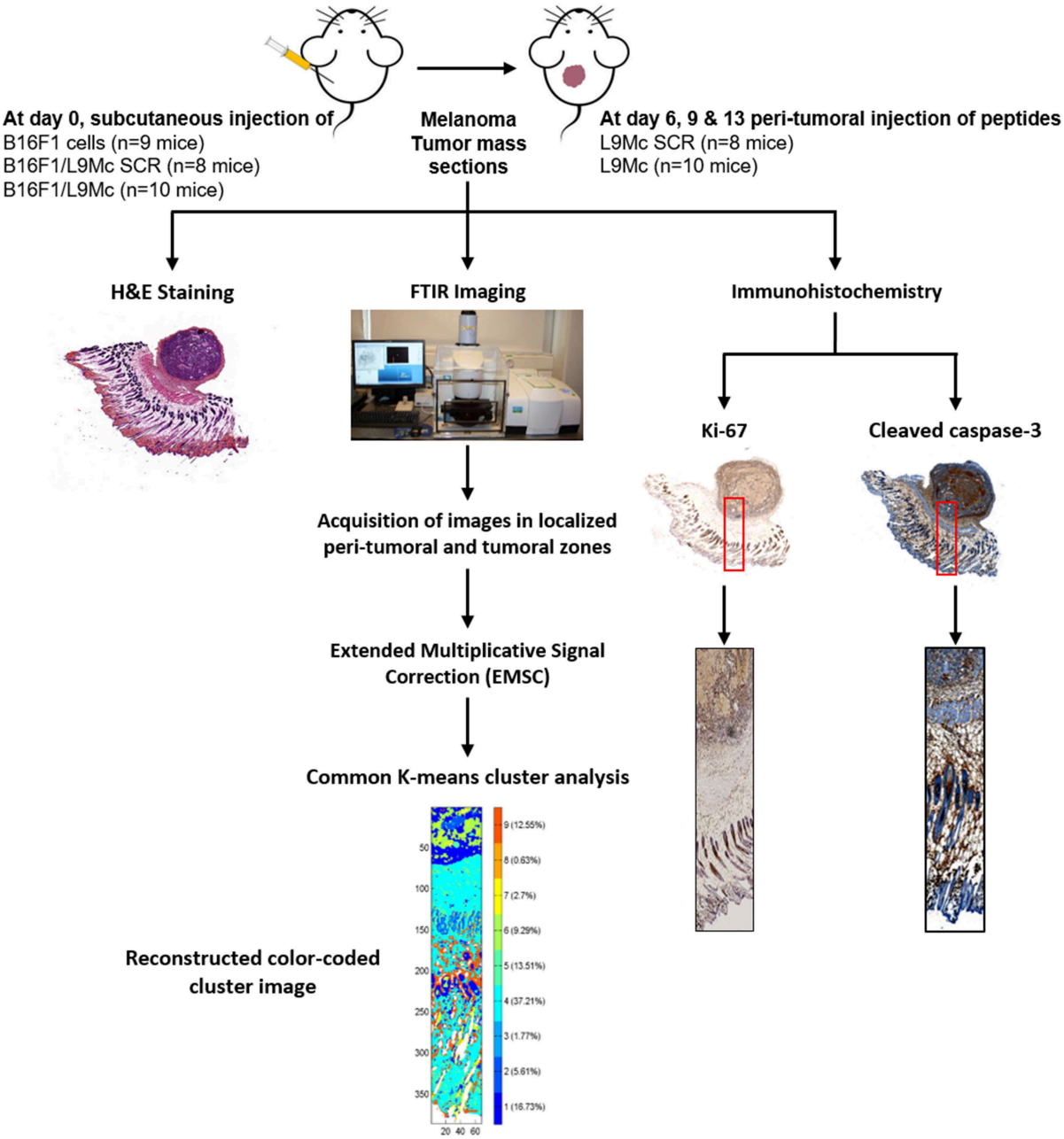

FIGURE 1 | Workflow showing the histology, FTIR imaging analysis, and immunohistochemistry of FFPE melanoma sections, and analysis of FTIR images with common K-means clustering.

were represented by cluster 3, necrotic tissues by cluster 4, epidermis by cluster 8, dermis with hair bulb by cluster 2, hypodermis and subcutaneous fats by clusters 6 and 7, respectively, and dermal muscle fibers by clusters 1, 5, and 9.

Further, we focused on clusters 3 and 4 (representing melanoma tissues and necrotic tissues, respectively) to evaluate the effect of the L9Mc peptide on tumor growth, as they seem to represent good qualitative spectral markers of melanoma tumors. The percentage of contribution of these 2 clusters in each spectral image was assessed for the 3 groups of mice and is shown in **Figure 4C**. Our data show that, in presence of L9Mc, melanoma tissue tends to decrease, while necrotic tissue tends to increase.

L9Mc Decreases Proliferation and Increases Apoptosis of B16F1 Cells *in vivo*

The histological characterization of melanoma was further investigated by immunohistochemistry analysis for Ki-67 staining (control, $n = 6$; L9Mc SCR, $n = 4$; L9Mc, $n = 4$) and

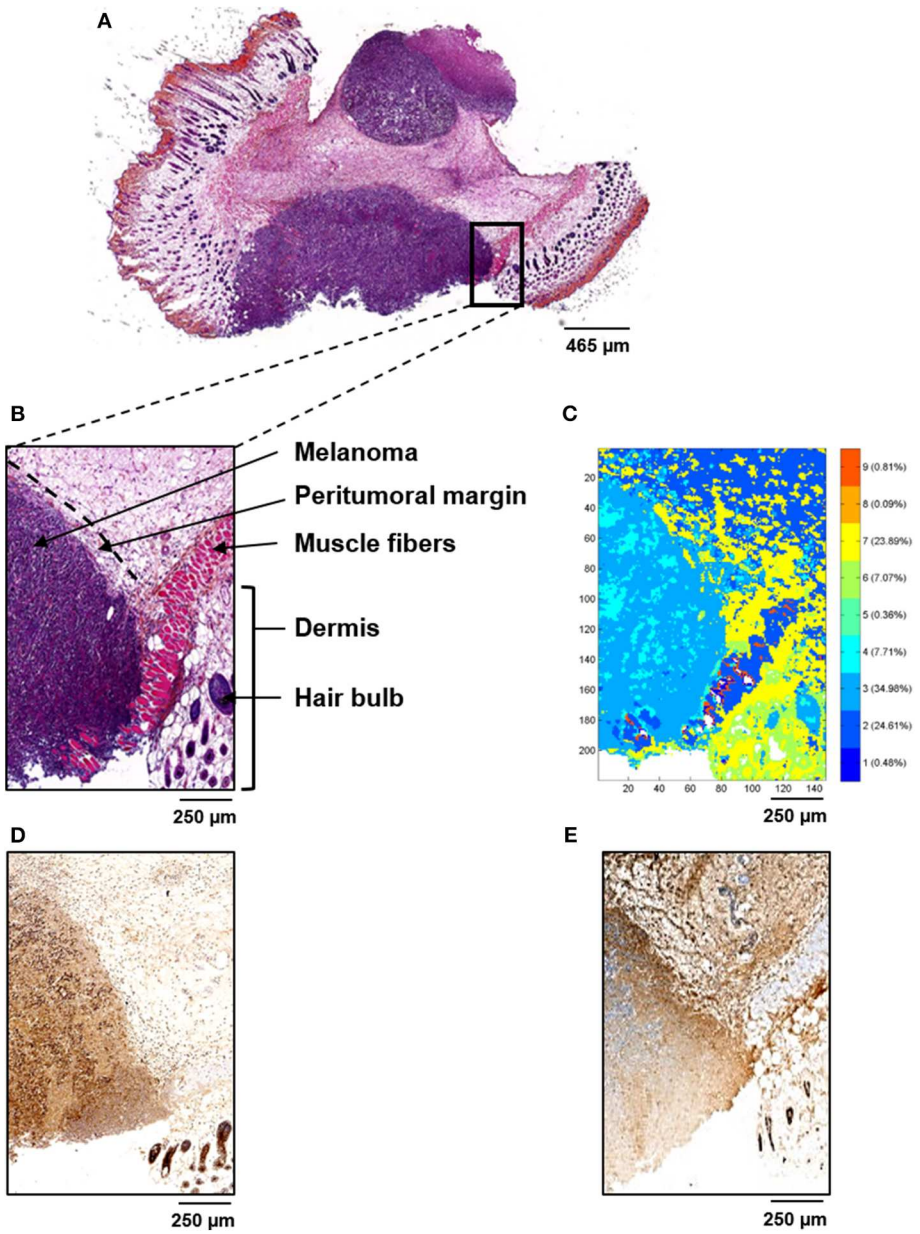

FIGURE 2 | Conventional and spectral histologies of control melanoma primary tumor tissues. **(A)** H&E staining of the whole tissue sample. **(B)** Selected ROI (represented by a black rectangle in **(A)** used for FTIR imaging. **(C)** Common K-means FTIR reconstructed image using 9 classes revealing histological features identified in **(B)**. **(D,E)** Immunostaining of Ki-67 and cleaved caspase-3, respectively, in the same ROI.

for cleaved caspase-3 staining (control, $n = 6$; L9Mc SCR, $n = 5$; L9Mc, $n = 5$). Ki-67 immunostaining for proliferation of B16F1 cells are shown in **Figures 2D**, **3D,I** for control, L9Mc SCR and L9Mc, respectively, and at higher magnification (40x) in **Supplementary Figure 2**. Cleaved caspase-3 immunostaining for apoptosis of B16F1 cells are shown in **Figures 2E**, **3E,J** for control, L9Mc SCR and L9Mc, respectively, and at higher magnification (40x) in **Supplementary Figure 2**.

Interestingly, the inhibitory effect of L9Mc on primary melanoma tumor volume is associated with a significant decrease in Ki-67 proliferation marker expression (59.44 ± 13.83% of positive cells) and increase in cleaved caspase-3 apoptosis marker (220.54 ± 59.87% of positive cells) while in the control and L9Mc SCR groups, the Ki-67 expression of positive cells were 100% and 93.75 ± 24.87% and the cleaved caspase-3 marker were 100% and 100.33 ± 39.58% of positive cells, respectively (**Figure 4D**). All data from statistical analyses are not shown here but we give below an example as an illustration.

Immunostaining results of melanoma primary tumor from control B16F1 cells showed high percentage of Ki-67 positive

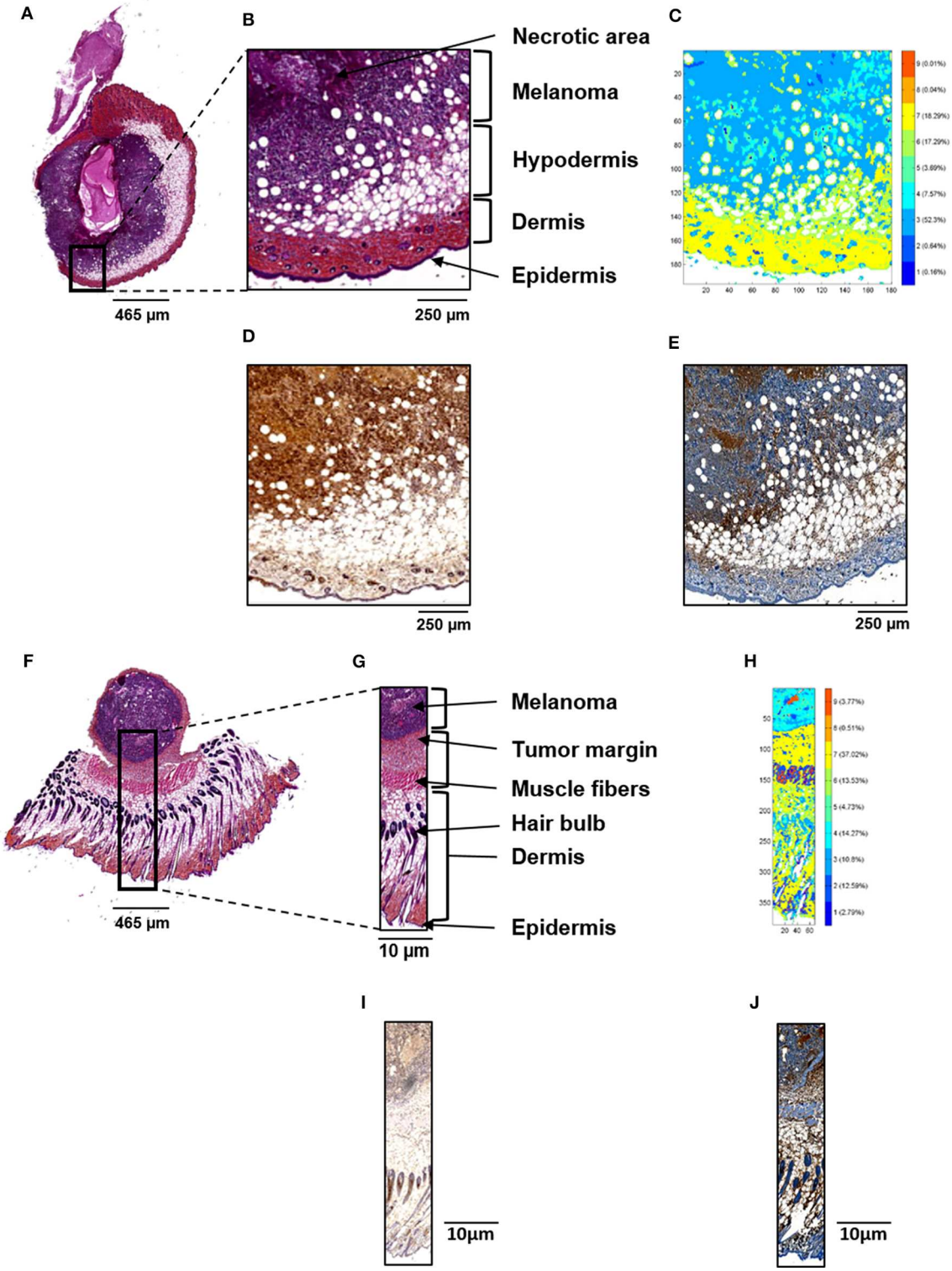

FIGURE 3 | Conventional and spectral histologies of L9Mc SCR **(A–E)** and L9Mc-treated **(F–J)** melanoma primary tumor tissues. H&E staining **(A,F)** of the whole tissue sample. **(B,G)** Selected ROI (represented by a black rectangle in **A** and **F**, respectively) used for FTIR imaging. **(C,H)** Common K-means FTIR reconstructed image using 9 classes revealing histological features identified in **(B,G)**, respectively. Immunostaining of Ki-67 **(D,I)** and cleaved caspase-3 **(E,J)** in the same ROI.

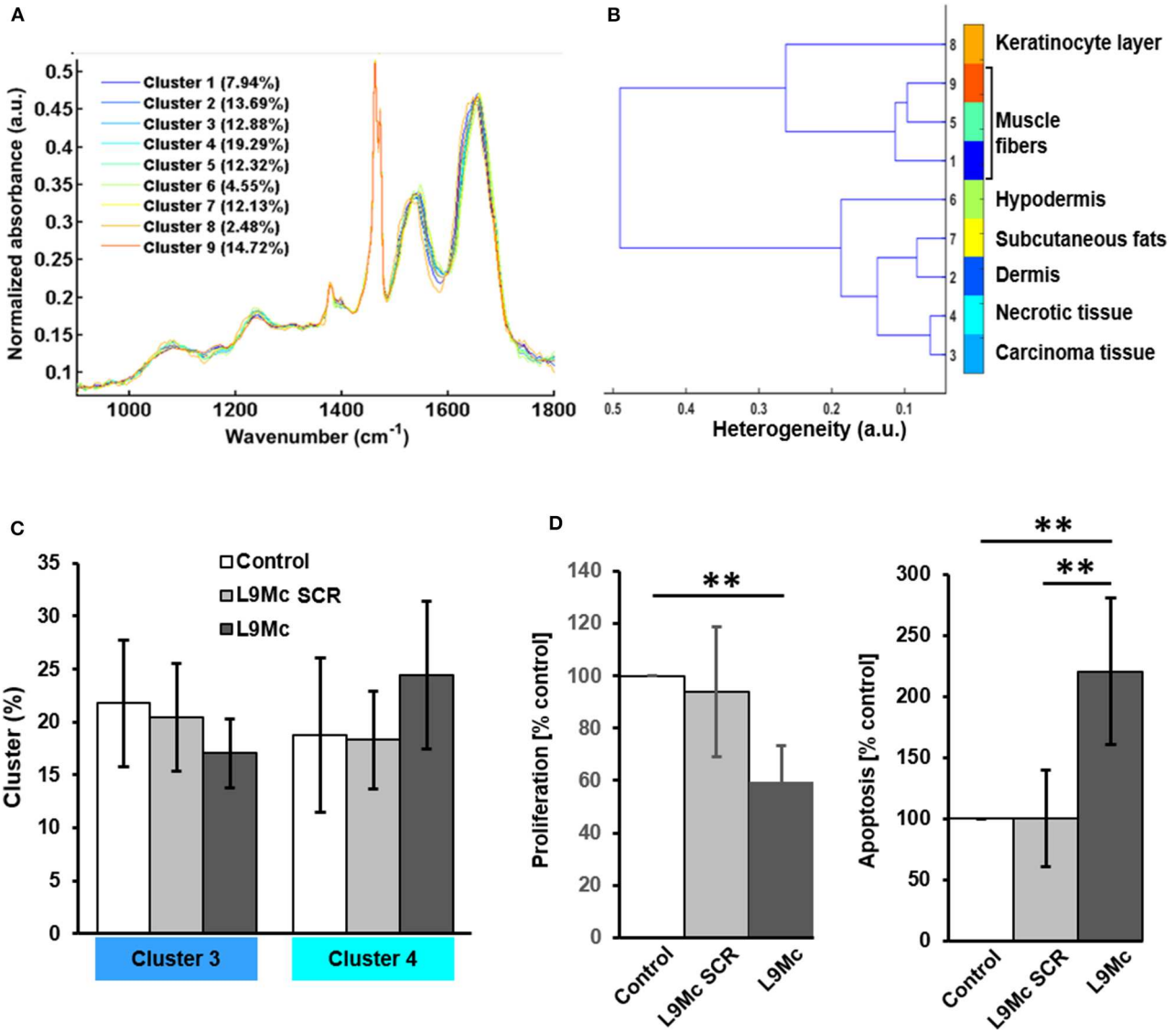

FIGURE 4 | Centroid spectra **(A)** and dendrogram **(B)** resulting from common K-means analysis using 9 classes, each corresponding to different skin and carcinoma histological features. **(C)** Histogram showing the percentage contribution of clusters 3 (carcinoma tissue) and 4 (necrotic tissue) after L9Mc treatment, compared to L9Mc SCR treatment and control melanoma. Data represent the mean ± SE. **(D)** Histogram showing the percentage of positive cells for Ki-67 and cleaved caspase-3 by immunohistochemistry after L9Mc treatment, compared to L9Mc SCR treatment and control melanoma. Data represent the mean ± SD. A $P < 0.05$ was considered significant with $^{**}P < 0.01$ as determined by the Student's *t*–test.

cells (82%) and low percentage of cleaved caspase-3 (3%) positive cells (**Figures 2D,E**, respectively). The K-means cluster image shown in **Figure 2C** correlates quite well with both histological and immunohistochemical data. Immunostaining results of melanoma primary tumor from L9Mc SCR and L9Mc showed 66 and 56% of Ki-67 positive cells (**Figures 3D,I**) and 1 and 40% of cleaved caspase-3 (**Figures 3E,J**), respectively. In a similar way as above, the K-means cluster images shown in **Figures 3C,H** correlate quite well with both histological and immunohistochemical data showing the advantage of label-free spectral histology.

DISCUSSION

Cancer diagnosis is mainly based on microscopic examination of stained tissue sections by an expert pathologist. This pathological examination depends on the cell morphology and tissue architecture. However, an accurate diagnosis of the cancer and its staging can be challenging (Kumar et al., 2018). There is an ongoing quest for an accurate, rapid, sensitive, and inexpensive method for cancer diagnosis. FTIR imaging can be a potential approach as it exhibits such characteristics and is moreover a label-free technique. It has proved to be useful to probe

skin pathophysiological changes. For example, modifications of dermal collagen during chronological aging can be monitored by polarized FTIR imaging (Nguyen et al., 2014; Eklouh-Molinier et al., 2015). Pathological processes in skin can be characterized by FTIR imaging by identifying melanoma cells and tissues (Wald and Goormaghtigh, 2015; Wald et al., 2016b), discriminating between nevus and melanoma (Hammody et al., 2005; Tfayli et al., 2005), primary cutaneous melanoma (Ly et al., 2010), different metastatic forms (Andleeb et al., 2018) and different types of inflammatory skin lesions (Sebiskveradze et al., 2018). In combination with pattern recognition techniques, FTIR imaging was able to investigate tumor heterogeneity (Sebiskveradze et al., 2011) and differential diagnosis (Ly et al., 2009) in skin carcinoma. All these and other studies have clearly demonstrated the potential of IRSI as a non-invasive and non-destructive approach to investigate skin pathologies. The approach has also shown its potential for investigating other organs than skin. Using a robust prediction model, it has successfully differentiated normal and malignant colonic features without *a priori* histopathological information. The obtained IRSH images not only revealed common histology features, but also highlighted additional features like tumor budding and tumor- associated stroma (Nallala et al., 2014). Kuepper et al. studied UICC-Stage II and III colorectal cancers on 110 cases and reported very high sensitivity and specificity (Kuepper et al., 2018). In breast cancer it has shown its capability to delineate between non-inflammatory and inflammatory biopsies, the latter having a poor prognosis because of the lack of specific biomarkers (Mohamed et al., 2018). Using prostate tissue microarrays, Kwak et al. have reported area under ROC curve as high as 0.95 with a blind testing (Kwak et al., 2011). The potential of IRSH was taken a step further in a recent study where a score of tumor aggressiveness could be associated to preneoplastic lesions and squamous cell lung carcinomas. The score correlated quite well with the aggressiveness score calculated using histopathological criteria (Gaydou et al., 2018).

We have previously shown that melanoma progression was downregulated by lumican (Brézillon et al., 2013) and its derived peptides (Pietraszek et al., 2013). However, the role of lumican in cancer is controversial and in many cases it actually facilitates cancer growth. As an example of positive correlation, in lung adenocarcinomas the expression level of lumican in cancer cells correlated with pleural invasion and larger tumor size (Matsuda et al., 2008). Similarly, lumican overexpression in pancreatic cancer increased cell invasiveness and proliferation (Williams et al., 2010; Yamamoto et al., 2012; Sharma et al., 2013). In contrast, lumican was reported to decrease cell proliferation in osteosarcoma (Nikitovic et al., 2008). Lumican present in the ECM has restrictive role on invasion in prostate cancer (Coulson-Thomas et al., 2013), in melanoma (Stasiak et al., 2016), and in breast cancer (Troup et al., 2003; Karamanou et al., 2017, 2020).

In this report, our aim was to assess by FTIR imaging the effect of antitumoral effectors, such as the L9Mc lumican-derived peptide on primary melanoma development. In addition to its properties of melanoma tumor growth inhibition (Stasiak et al., 2016), lumican was previously described as a key actor in tumor matrix assembly *in vivo* (Jeanne et al., 2017). Thus, lumican was able to modulate the response of a therapeutic peptide targeting the extracellular matrix by specific inhibition of thrombospondin-1, playing a substantial role in maintaining tumor microenvironment integrity (Jeanne et al., 2017). In addition, lumican has been shown to inhibit lung metastasis by decreasing cell proliferation and by stimulating cell apoptosis of melanoma nodules (Brézillon et al., 2009). Moreover, the effect of lumican-derived peptides on growth and migration of melanoma cells was previously demonstrated *in vitro*. Lumcorin and L9M peptides, which contain the same LRR9 core sequence as L9Mc, have been described to inhibit melanoma cell migration in a mechanism including focal adhesion kinase (FAK) dephosphorylation and matrix metalloproteinase-14 (MMP-14) inhibition. Furthermore, these two peptides were shown to significantly decrease proliferation of melanoma cells and their ability to form colonies in soft agar assay (Pietraszek et al., 2013).

After initiating melanoma primary tumors via injecting control, L9Mc SCR and L9Mc peptides treated B16F1 melanoma cells, the obtained melanoma tissues underwent FTIR imaging analysis. Using common K-means cluster analysis with 9 clusters, melanoma, and normal skin tissue structures were clearly distinguished *via* the obtained color-encoded images. This is also evidenced by the dendrogram obtained after hierarchical cluster analysis of the centroid spectra, based on similarity evaluation using Ward's algorithm. This correlates well with the results obtained by H&E staining, highlighting the potential of spectral histology in tissue characterization.

Comparison of cluster percentages between control, L9Mc SCR- and L9Mc-treated melanoma tumors showed no significant statistical differences. However, a decrease trend in the contribution of cluster 3 (melanoma tissues) was observed in presence of L9Mc compared to control and L9Mc SCR. In a similar manner, we observed an increase trend for cluster 4 (necrotic tissues) in L9Mc-treated melanoma tissues compared to control and L9Mc SCR-treated melanoma tissues.

In order to understand and complement these observed spectral trends, IHC analysis was performed using Ki-67 proliferation and cleaved caspase-3 apoptotic markers. The percentage of positive cells for Ki-67 staining was significantly decreased in L9Mc-treated melanoma tumors compared to the control melanoma tissues, showing the anti-proliferative activity of this peptide. Interestingly, the L9M peptide was shown to inhibit melanoma cell proliferation (Pietraszek et al., 2013). This is in accordance with the melanoma *in vivo* model used in this present study, highlighting L9Mc as having a similar biological effect as lumcorin and L9M. On the other hand, the percentage of positive cells for cleaved caspase-3 showed a significant increase in the L9Mc-treated melanoma tumors compared to the control and L9Mc SCR-treated melanoma tissues, highlighting the pro-apoptotic effect of this peptide. Interestingly, lumican was previously shown to reduce melanoma tumor growth through the induction of apoptosis (Vuillermoz et al., 2004). Proliferation and apoptosis mechanisms of action of lumican were elucidated by the characterization of lumican-deficient mice. In lumican knockout $Lum^{-/-}$ mice, apoptosis of stromal cells was down-regulated. The function of FasL on intra-ocular tumors was determined by the microenvironment

in conjunction with the form and level of FasL expressed (Gregory et al., 2002). The $Lum^{-/-}$ fibroblasts exhibited a decreased p21WAF/CIP1 expression, an universal inhibitor of cyclin-dependent kinases, and consequently increased cyclins A, D1, and E. The tumor suppressor p53, an upstream regulator of p21, is down-regulated in $Lum^{-/-}$ fibroblasts. Thus, the regulation of p21 by lumican is a p53-dependent pathway (Vij et al., 2004). Lumican overexpression was shown to suppress tumorigenic transformation of rat fibroblasts induced by v-src and v-K-*ras* (Yoshioka et al., 2000). Lumican overexpression decreases subcutaneous primary melanoma tumor growth *in vivo,* with a concomitant decrease of cyclin D1 expression (Vuillermoz et al., 2004) as well as a decrease in the number of lung metastatic nodules in which an increase of tumor cell apoptosis was observed.

Lumican and its derived peptides were also demonstrated to inhibit melanoma cell proliferation *in vitro* (D'Onofrio et al., 2008; Zeltz et al., 2009; Brézillon et al., 2013; Pietraszek et al., 2013; Stasiak et al., 2016; Jeanne et al., 2017).

Based on these immunohistochemistry results, clusters 3 and 4 could be identified as potential spectral markers to study the effect of anti-tumor peptides on proliferation and apoptosis.

In the context of this study, the IRSH images were performed at 6.25 μm/pixel available with our instrumentation. It may be argued that this can be a limitation to correctly perform digital histopathology. This is indeed not a limitation to the technique because it has been previously shown that optics upgrade allows imaging with an effective geometric pixel size of $\sim 1 \times 1$ μm^2 (Findlay et al., 2015) and high contrast stain-free digital histopathology has been reported with smaller pixel size of 0.32×0.32 μm^2 (Schnell et al., 2020). One shortcoming impeding the clinical translation of conventional IRSH has been the fact that it is too time-consuming for consideration as a clinical tool. This can now be circumvented due to recent instrumental development based on infrared quantum cascade lasers (QCL). In this context, IRSH is able to provide highly resolved diagnostic images with short acquisition times, in the time-frame equivalent to frozen sample handling by the pathologist (Yeh et al., 2015; Kuepper et al., 2018). On a clinical ground, it does not mean that the technique will replace conventional histology but an all-digital histopathology could be of an aid to pathologists for rapid screening of biopsies. Thus, a trained system with a good database and machine learning approaches is able to correctly and objectively identify histological features and perform digital IRSH with high sensitivity and specificity (AUC $\geq$0.95). This has been demonstrated in several studies (Kwak et al., 2011; Kuepper et al., 2018).

CONCLUSION

Melanoma is one of the most lethal and fatal forms of skin cancer with a higher incidence of metastasis. Understanding these pathological conditions is crucial for patient therapy and management. In this study, we show that FTIR imaging is a potential tool to investigate changes occurring in melanoma tissues treated with peptide-based anti-tumor molecules. Therefore, such a novel approach based on spectral analysis can complement conventional histology and immunohistochemistry techniques with the advantage of being rapid, non-destructive, reagent-, and label-free.

DATA AVAILABILITY STATEMENT

All datasets generated for this study are included in the article/**Supplementary Material**.

ETHICS STATEMENT

All experiments were performed according to the instructions of the Center National de la Recherche Scientifique. This study was performed in compliance with the French Animal Welfare Act and following the French Board for Animal Experiments. Experiments were conducted under approval of the French Ministère de l'Enseignement Supérieur et de la Recherche (Ethics Committee C2EA-56) in accordance with the directive 2010/63/UE.

AUTHOR CONTRIBUTIONS

SB and GS contributed to study conception and design. CB-R, SB, VU, PN, HM, and GS contributed to manuscript writing and revision. EA, HM, VU, IP, and SB performed experiments. CB-R, SB, VU, HM, and GS contributed to data analysis and interpretation.

FUNDING

Financial support from the European Commission, H2020-MSCA-RISE-2014, funding scheme Marie Sklodovska-Curie, Research of Innovation Staff Exchange (RISE), GLYCANC ID 645756 was gratefully acknowledged. HTM is a recipient of this funding scheme.

ACKNOWLEDGMENTS

The authors thank the URCA-PICT Technological Platform for technological support.

SUPPLEMENTARY MATERIAL

The Supplementary Material for this article can be found online at: https://www.frontiersin.org/articles/10.3389/fcell.2020.00377/full#supplementary-material

Supplementary Figure 1 | Highlight on skin histological structures. H&E stained sections (2.5x, 10x, and 15x) of B16F1 primary melanoma tumors are shown for control, L9Mc SCR and L9Mc treated mice, respectively. Hematoxylin and Eosin solution highlights the nucleus in purple and the cytoplasm in pink, respectively. The stained sections are available via the following Crosscope links:
- Control https://accounts.crosscope.com/quorum/4d05469771f2506a7b3d5277f87e97a3
- L9M SRC https://accounts.crosscope.com/quorum/eb1abb0ea6a108bc3844eeb00b091070
- L9Mc https://accounts.crosscope.com/quorum/af01e8c842752f8b2572bfed6ea7eb3f.

Supplementary Figure 2 | Cleaved caspase-3 and Ki-67 immunostaining. Representative immunostaining (40x) of cleaved caspase-3 (top row) and Ki-67 (bottom row) of B16F1 cells are shown for control (left column), L9Mc SCR (middle column) and L9Mc treated mice (right column), respectively. Cleaved caspase-3, marker of apoptosis, and Ki-67, marker of proliferation, are detected in brown in the nucleus and in the cytoplasm, respectively. As compared to both control groups, an increased apoptosis and a decreased proliferation are observed in L9Mc treated mice.

REFERENCES

Andleeb, F., Atiq, A., Atiq, M., and Malik, S. (2018). Attenuated total reflectance spectroscopy to diagnose skin cancer and to distinguish different metastatic potential of melanoma cell. *Cancer Biomark.* 23, 373–380. doi: 10.3233/CBM-181393

Baker, M. J., Trevisan, J., Bassan, P., Bhargava, R., Butler, H. J., Dorling, K. M., et al. (2014). Using Fourier transform IR spectroscopy to analyze biological materials. *Nat. Protoc.* 9, 1771–1791. doi: 10.1038/nprot.2014.110

Belotti, D., Foglieni, C., Resovi, A., Giavazzi, R., and Taraboletti, G. (2011). Targeting angiogenesis with compounds from the extracellular matrix. *Int. J. Biochem. Cell Biol.* 43, 1674–1685. doi: 10.1016/j.biocel.2011.08.012

Brézillon, S., Pietraszek, K., Maquart, F. X., and Wegrowski, Y. (2013). Lumican effects in the control of tumour progression and their links with metalloproteinases and integrins. *FEBS J.* 280, 2369–2381. doi: 10.1111/febs.12210

Brézillon, S., Untereiner, V., Lovergne, L., Tadeo, I., Noguera, R., Maquart, F. X., et al. (2014). Glycosaminoglycan profiling in different cell types using infrared spectroscopy and imaging. *Anal. Bioanal. Chem.* 406, 5795–5803. doi: 10.1007/s00216-014-7994-2

Brézillon, S., Untereiner, V., Mohamed, H. T., Hodin, J., Chatron-Colliet, A., Maquart, F. X., et al. (2017). Probing glycosaminoglycan spectral signatures in live cells and their conditioned media by raman microspectroscopy. *Analyst* 142, 1333–1341. doi: 10.1039/C6AN01951J

Brézillon, S., Venteo, L., Ramont, L., D'Onofrio, M. F., Perreau, C., Pluot, M., et al. (2007). Expression of lumican, a small leucine-rich proteoglycan with antitumour activity, in human malignant melanoma. *Clin. Exp. Dermatol.* 32, 405–416. doi: 10.1111/j.1365-2230.2007.02437.x

Brézillon, S., Zeltz, C., Schneider, L., Terryn, C., Vuillermoz, B., Ramont, L., et al. (2009). Lumican inhibits B16F1 melanoma cell lung metastasis. *J. Physiol. Pharmacol.* 60, 15–22.

Cappellesso, R., Millioni, R., Arrigoni, G., Simonato, F., Caroccia, B., Iori, E., et al. (2015). Lumican is overexpressed in lung adenocarcinoma pleural effusions. *PLoS ONE* 10:e0126458. doi: 10.1371/journal.pone.0126458

Chakravarti, S., Magnuson, T., Lass, J. H., Jepsen, K. J., LaMantia, C., and Carroll, H. (1998). Lumican regulates collagen fibril assembly: skin fragility and corneal opacity in the absence of lumican. *J. Cell Biol.* 141, 1277–1286. doi: 10.1083/jcb.141.5.1277

Coulson-Thomas, V. J., Coulson-Thomas, Y. M., Gesteira, T. F., Andrade de Paula, C. A., Carneiro, C. R., Ortiz, V., et al. (2013). Lumican expression, localization and antitumor activity in prostate cancer. *Exp. Cell Res.* 319:967–981. doi: 10.1016/j.yexcr.2013.01.023

D'Onofrio, M. F., Brezillon, S., Baranek, T., Perreau, C., Roughley, P. J., Maquart, F. X., et al. (2008). Identification of beta1 integrin as mediator of melanoma cell adhesion to lumican. *Biochem. Biophys. Res. Commun.* 365, 266–272. doi: 10.1016/j.bbrc.2007.10.155

Eklouh-Molinier, C., Happillon, T., Bouland, N., Fichel, C., Diébold, M. D., Angiboust, J. F., et al. (2015). Investigating the relationship between changes in collagen fiber orientation during skin aging and collagen/water interactions by polarized-FTIR microimaging. *Analyst* 140, 6260–6268. doi: 10.1039/C5AN00278H

Findlay, C. R., Wiens, R., Rak, M., Sedlmair, J., Hirschmugl, C. J., Morrison, J., et al. (2015). Rapid biodiagnostic *ex vivo* imaging at 1 μm pixel resolution with thermal source FTIR FP. *Analyst* 140, 2493–2503. doi: 10.1039/C4AN01982B

Galon, J., Pages, F., Marincola, F. M., Thurin, M., Trinchieri, G., Fox, B. A., et al. (2012). The immune score as a new possible approach for the classification of cancer. *J. Transl. Med.* 10:1. doi: 10.1186/1479-5876-10-1

Gaydou, V., Polette, M., Gobinet, C., Kileztky, C., Angiboust, J. F., Birembaut, P., et al. (2018). New insights into spectral histopathology: infrared-based scoring of tumour aggressiveness of squamous cell lung carcinomas. *Chem. Sci.* 10, 4246–4258. doi: 10.1039/C8SC04320E

Gray-Schopfer, V., Wellbrock, C., and Marais, R. (2007). Melanoma biology and new targeted therapy. *Nature* 445, 851–857. doi: 10.1038/nature05661

Greene, F. L., and Sobin, L. H. (2008). The staging of cancer: a retrospective and prospective appraisal. *CA Cancer J. Clin.* 58, 180–190. doi: 10.3322/CA.2008.0001

Gregory, M. S., Repp, A. C., Holhbaum, A. M., Saff, R. R., Marshak-Rothstein, A., and Ksander, B. R. (2002). Membrane Fas ligand activates innate immunity and terminates ocular immune privilege. *J. Immunol.* 169, 2727–2735. doi: 10.4049/jimmunol.169.5.2727

Hammody, Z., Sahu, R. K., Mordechai, S., Cagnano, E., and Argov, S. (2005). Characterization of malignant melanoma using vibrational spectroscopy. *ScientificWorldJournal* 5, 173–182. doi: 10.1100/tsw.2005.1

Hanahan, D., and Weinberg, R. A. (2011). Hallmarks of cancer: the next generation. *Cell* 144, 646–674. doi: 10.1016/j.cell.2011.02.013

Hodi, F. S., O'Day, S. J., McDermott, D. F., Weber, R. W., Sosman, J. A., Haanen, J. B., et al. (2010). Improved survival with ipilimumab in patients with metastatic melanoma. *N. Engl. J. Med.* 363, 711–723. doi: 10.1056/NEJMoa1003466

Iozzo, R. V., and Schaefer, L. (2015). Proteoglycan form and function: a comprehensive nomenclature of proteoglycans. *Matrix Biol.* 42, 11–55. doi: 10.1016/j.matbio.2015.02.003

Jeanne, A., Untereiner, V., Perreau, C., Proult, I., Gobinet, C., Boulagnon-Rombi, C., et al. (2017). Lumican delays melanoma growth in mice and drives tumor molecular assembly as well as response to matrix-targeted TAX2 therapeutic peptide. *Sci. Rep.* 7:7700. doi: 10.1038/s41598-017-07043-9

Karamanou, K., Franchi, M., Onisto, M., Passi, A., Vynios, D. H., and Brézillon, S. (2020). Evaluation of lumican effects on morphology of invading breast cancer cells, expression of integrins and downstream signaling. *FEBS J.* doi: 10.1111/febs.15289. [Epub ahead of print].

Karamanou, K., Franchi, M., Piperigkou, Z., Perreau, C., Maquart, F. X., Vynios, D. H., et al. (2017). Lumican effectively regulates the estrogen receptors-associated functional properties of breast cancer cells, expression of matrix effectors and epithelial-to-mesenchymal transition. *Sci. Rep.* 7:45138. doi: 10.1038/srep45138

Kuepper, C., Kallenbach-Thieltges, A., Juette, H., Tannapfel, A., Grosserueschkamp, F., and Gerwert, K. (2018). Quantum cascade laser-based infrared microscopy for label-free and automated cancer classification in tissue sections. *Sci. Rep.* 8, 1–10. doi: 10.1038/s41598-018-26098-w

Kumar, S., Srinivasan, A., and Nikolajeff, F. (2018). Role of infrared spectroscopy and imaging in cancer diagnosis. *Curr. Med. Chem.* 25, 1055–1072. doi: 10.2174/0929867324666170523121314

Kwak, J. T., Hewitt, S. M., Sinha, S., and Bhargava, R. (2011). Multimodal microscopy for automated histologic analysis of prostate cancer. *BMC Cancer* 11:62. doi: 10.1186/1471-2407-11-62

Li, X., Roife, D., Kang, Y., Dai, B., Pratt, M., and Fleming, J. B. (2016). Extracellular lumican augments cytotoxicity of chemotherapy in pancreatic ductal adenocarcinoma cells via autophagy inhibition. *Oncogene* 35, 4881–4890. doi: 10.1038/onc.2016.20

Liu, T., Han, C., Wang, S., Fang, P., Ma, Z., Xu, L., et al. (2019). Cancer-associated fibroblasts: an emerging target of anti-cancer immunotherapy. *J. Hematol. Oncol.* 12:86. doi: 10.1186/s13045-019-0770-1

Ly, E., Cardot-Leccia, N., Ortonne, J., Benchetrit, M., Michiels, J., Manfait, M., et al. (2010). Histopathological characterization of primary cutaneous melanoma using infrared microimaging: a proof-of-concept study. *Br. J. Dermatol.* 162, 1316–1323. doi: 10.1111/j.1365-2133.2010.09762.x

Ly, E., Piot, O., Durlach, A., Bernard, P., and Manfait, M. (2009). Differential diagnosis of cutaneous carcinomas by infrared spectral micro-imaging combined with pattern recognition. *Analyst* 134, 1208–1214. doi: 10.1039/b820998g

Ly, E., Piot, O., Wolthuis, R., Durlach, A., Bernard, P., and Manfait, M. (2008). Combination of FTIR spectral imaging and chemometrics for tumour detection from paraffin-embedded biopsies. *Analyst* 133, 197–205. doi: 10.1039/B715924B

Mainreck, N., Brezillon, S., Sockalingum, G. D., Maquart, F. X., Manfait, M., and Wegrowski, Y. (2011). Rapid characterization of glycosaminoglycans using a combined approach by infrared and Raman microspectroscopies. *J. Pharm. Sci.* 100, 441–450. doi: 10.1002/jps.22288

Matsuda, Y., Yamamoto, T., Kudo, M., Kawahara, K., Kawamoto, M., Nakajima, Y., et al. (2008). Expression and roles of lumican in lung adenocarcinoma and squamous cell carcinoma. *Int. J. Oncol.* 33, 1177–1185. doi: 10.3892/ijo_00000107

McEwan, P. A., Scott, P. G., Bishop, P. N., and Bella, J. (2006). Structural correlations in the family of small leucine-rich repeat proteins and proteoglycans. *J. Struct. Biol.* 155, 294–305. doi: 10.1016/j.jsb.2006.01.016

Miller, A. J., and Mihm, M. C. Jr. (2006). Melanoma. *N. Engl. J. Med.* 355, 51–65. doi: 10.1056/NEJMra052166

Mohamed, H. T., Untereiner, V., Proult, I., Ibrahim, S. A., Gotte, M., El-Shinawi, M., et al. (2018). Characterization of inflammatory breast cancer: a vibrational microspectroscopy and imaging approach at the cellular and tissue level. *Analyst* 143, 6103–6112. doi: 10.1039/C8AN01292J

Mohamed, H. T., Untereiner, V., Sockalingum, G. D., and Brézillon, S. (2017). Implementation of infrared and raman modalities for glycosaminoglycan characterization in complex systems. *Glycoconj. J.* 34, 309–323. doi: 10.1007/s10719-016-9743-6

Nallala, J., Diebold, M. D., Gobinet, C., Bouch,é, O., Sockalingum, G. D., Piot, O., et al. (2014). Infrared spectral histopathology for cancer diagnosis: a novel approach for automated pattern recognition of colon adenocarcinoma. *Analyst* 139, 4005–4015. doi: 10.1039/C3AN01022H

Nguyen, T., Eklouh-Molinier, C., Sebiskveradze, D., Feru, J., Terryn, C., Manfait, M., et al. (2014). Changes of skin collagen orientation associated with chronological aging as probed by polarized-FTIR micro-imaging. *Analyst* 139, 2482–2488. doi: 10.1039/c3an00353a

Nguyen, T. N., Jeannesson, P., Groh, A., Piot, O., Guenot, D., and Gobinet, C. (2016). Fully unsupervised inter-individual IR spectral histology of paraffinized tissue sections of normal colon. *J. Biophotonics* 9, 521–532. doi: 10.1002/jbio.201500285

Nikitovic, D., Berdiaki, A., Zafiropoulos, A., Katonis, P., Tsatsakis, A., Karamanos, N. K., et al. (2008). Lumican expression is positively correlated with the differentiation and negatively with the growth of human osteosarcoma cells. *FEBS J.* 275, 350–361. doi: 10.1111/j.1742-4658.2007.06205.x

Nikitovic, D., Papoutsidakis, A., Karamanos, N. K., and Tzanakakis, G. N. (2014). Lumican affects tumor cell functions, tumor-ECM interactions, angiogenesis and inflammatory response. *Matrix Biol.* 35, 206–214. doi: 10.1016/j.matbio.2013.09.003

Pages, F., Galon, J., Dieu-Nosjean, M. C., Tartour, E., Sautes-Fridman, C., and Fridman, W. H. (2010). Immune infiltration in human tumors: a prognostic factor that should not be ignored. *Oncogene* 29, 1093–1102. doi: 10.1038/onc.2009.416

Pietraszek, K., Brézillon, S., Perreau, C., Malicka-Blaszkiewicz, M., Maquart, F. X., and Wegrowski, Y. (2013). Lumican-derived peptides inhibit melanoma cell growth and migration. *PLoS ONE* 8:e76232. doi: 10.1371/journal.pone.0076232

Pietraszek, K., Chatron-Colliet, A., Brezillon, S., Perreau, C., Jakubiak-Augustyn, A., Krotkiewski, H., et al. (2014). Lumican: a new inhibitor of matrix metalloproteinase-14 activity. *FEBS Lett.* 588, 4319–4324. doi: 10.1016/j.febslet.2014.09.040

Schnell, M., Mittal, S., Falahkheirkhah, K., Mittal, A., Yeh, K., Kenkel, S., et al. (2020). All-digital histopathology by infrared-optical hybrid microscopy. *Proc. Natl. Acad. Sci. U.S.A.* 117, 3388–3396. doi: 10.1073/pnas.1912400117

Sebiskveradze, D., Bertino, B., Gaydou, V., Dugaret, A. S., Roquet, M., Zugaj, D. E., et al. (2018). Mid-infrared spectral microimaging of inflammatory skin lesions. *J. Biophotonics* 11:e201700380. doi: 10.1002/jbio.201700380

Sebiskveradze, D., Vrabie, V., Gobinet, C., Durlach, A., Bernard, P., Ly, E., et al. (2011). Automation of an algorithm based on fuzzy clustering for analyzing tumoral heterogeneity in human skin carcinoma tissue sections. *Lab. Invest* 91, 799–811. doi: 10.1038/labinvest.2011.13

Sharma, B., Ramus, M. D., Kirkwood, C. T., Sperry, E. E., Chu, P. H., Kao, W. W., et al. (2013). Lumican exhibits anti-angiogenic activity in a context specific manner. *Cancer Microenviron.* 6, 263–271. doi: 10.1007/s12307-013-0134-2

Soengas, M. S., and Lowe, S. W. (2003). Apoptosis and melanoma chemoresistance. *Oncogene* 22, 3138–3151. doi: 10.1038/sj.onc.1206454

Stasiak, M., Boncela, J., Perreau, C., Karamanou, K., Chatron-Colliet, A., Proult, I., et al. (2016). Lumican inhibits SNAIL-induced melanoma cell migration specifically by blocking MMP-14 activity. *PLoS ONE* 11:e0150226. doi: 10.1371/journal.pone.0150226

Tfayli, A., Piot, O., Durlach, A., Bernard, P., and Manfait, M. (2005). Discriminating nevus and melanoma on paraffin-embedded skin biopsies using FTIR microspectroscopy. *Biochim. Biophys. Acta* 1724, 262–269. doi: 10.1016/j.bbagen.2005.04.020

Troup, S., Njue, C., Kliewer, E. V., Parisien, M., Roskelley, C., Chakravarti, S., et al. (2003). Reduced expression of the small leucine-rich proteoglycans, lumican, and decorin is associated with poor outcome in node-negative invasive breast cancer. *Clin. Cancer Res.* 9, 207–214.

Valkenburg, K. C., de Groot, A. E., and Pienta, K. J. (2018). Targeting the tumour stroma to improve cancer therapy. *Nat. Rev. Clin. Oncol.* 15, 366–381. doi: 10.1038/s41571-018-0007-1

Venning, F. A., Wullkopf, L., and Erler, J. T. (2015). Targeting ECM disrupts cancer progression. *Front. Oncol.* 5:224. doi: 10.3389/fonc.2015.00224

Vij, N., Roberts, L., Joyce, S., and Chakravarti, S. (2004). Lumican suppresses cell proliferation and aids fas-fas ligand mediated apoptosis: implications in the cornea. *Exp. Eye Res.* 78, 957–971. doi: 10.1016/j.exer.2003.12.006

Vuillermoz, B., Khoruzhenko, A., D'Onofrio, M. F., Ramont, L., Venteo, L., Perreau, C., et al. (2004). The small leucine-rich proteoglycan lumican inhibits melanoma progression. *Exp. Cell Res.* 296, 294–306. doi: 10.1016/j.yexcr.2004.02.005

Wald, N., Bordry, N., Foukas, P. G., Speiser, D. E., and Goormaghtigh, E. (2016a). Identification of melanoma cells and lymphocyte subpopulations in lymph node metastases by FTIR imaging histopathology. *Biochim. Biophys. Acta* 1862, 202–212. doi: 10.1016/j.bbadis.2015.11.008

Wald, N., and Goormaghtigh, E. (2015). Infrared imaging of primary melanomas reveals hints of regional and distant metastases. *Analyst* 140, 2144–2155. doi: 10.1039/C4AN01831A

Wald, N., Le Corre, Y., Martin, L., Mathieu, V., and Goormaghtigh, E. (2016b). Infrared spectra of primary melanomas can predict response to chemotherapy: the example of dacarbazine. *Biochim. Biophys. Acta* 1862, 174–181. doi: 10.1016/j.bbadis.2015.10.030

Williams, K. E., Fulford, L. A., and Albig, A. R. (2010). Lumican reduces tumor growth via induction of fas-mediated endothelial cell apoptosis. *Cancer Microenviron.* 4, 115–126. doi: 10.1007/s12307-010-0056-1

Wong, G. S., and Rustgi, A. K. (2013). Matricellular proteins: priming the tumour microenvironment for cancer development and metastasis. *Br. Cancer J.* 108, 755–761. doi: 10.1038/bjc.2012.592

Yamamoto, T., Matsuda, Y., Kawahara, K., Ishiwata, T., and Naito, Z. (2012). Secreted 70 kDa lumican stimulates growth and inhibits invasion of human pancreatic cancer. *Cancer Lett.* 320, 31–39. doi: 10.1016/j.canlet.2012.01.023

Yeh, K., Kenkel, S., Liu, J. N., and Bhargava, R. (2015). Fast infrared chemical imaging with a quantum cascade laser. *Anal. Chem.* 87, 485–493. doi: 10.1021/ac5027513

Yoshioka, N., Inoue, H., Nakanishi, K., Oka, K., Yutsudo, M., Yamashita, A., et al. (2000). Isolation of transformation suppressor genes by cDNA subtraction: lumican suppresses transformation induced by v-src and vK-ras. *J. Virol.* 74, 1008–1013. doi: 10.1128/JVI.74.2.1008-1013.2000

Zeltz, C., Brézillon, S., Perreau, C., Ramont, L., Maquart, F. X., and Wegrowski, Y. (2009). Lumcorin: a leucine-rich repeat 9-derived peptide from human lumican inhibiting melanoma cell migration. *FEBS Lett.* 583, 3027–3032. doi: 10.1016/j.febslet.2009.08.012

Conflict of Interest: The authors declare that the research was conducted in the absence of any commercial or financial relationships that could be construed as a potential conflict of interest.

Copyright © 2020 Brézillon, Untereiner, Mohamed, Ahallal, Proult, Nizet, Boulagnon-Rombi and Sockalingum. This is an open-access article distributed under the terms of the Creative Commons Attribution License (CC BY). The use, distribution or reproduction in other forums is permitted, provided the original author(s) and the copyright owner(s) are credited and that the original publication in this journal is cited, in accordance with accepted academic practice. No use, distribution or reproduction is permitted which does not comply with these terms.

frontiers in Cell and Developmental Biology

ORIGINAL RESEARCH
published: 03 June 2020
doi: 10.3389/fcell.2020.00412

LRP-1 Promotes Colon Cancer Cell Proliferation in 3D Collagen Matrices by Mediating DDR1 Endocytosis

Cao Cuong Le[1,2,3], Amar Bennasroune[1,2], Guillaume Collin[1,3], Cathy Hachet[1,2], Véronique Lehrter[1,3], Damien Rioult[4], Stéphane Dedieu[1,2†], Hamid Morjani[1,3†] and Aline Appert-Collin[1,2†]*

[1] Université de Reims Champagne-Ardenne, Reims, France, [2] CNRS UMR 7369, Matrice Extracellulaire et Dynamique Cellulaire, MEDyC, Reims, France, [3] Unité BioSpecT, EA7506, Reims, France, [4] Plateau Technique Mobile de Cytométrie Environnementale MOBICYTE, URCA/INERIS, Reims Champagne-Ardenne University (URCA), Reims, France

Low density lipoprotein receptor related protein-1 (LRP-1) is a large ubiquitous endocytic receptor mediating the clearance of various molecules from the extracellular matrix. Several studies have shown that LRP-1 plays crucial roles during tumorigenesis functioning as a main signal pathway regulator, especially by interacting with other cell-surface receptors. Discoïdin Domain Receptors (DDRs), type I collagen receptors with tyrosine kinase activity, have previously been associated with tumor invasion and aggressiveness in diverse tumor environments. Here, we addressed whether it could exist functional interplays between LRP-1 and DDR1 to control colon carcinoma cell behavior in three-dimensional (3D) collagen matrices. We found that LRP-1 established tight molecular connections with DDR1 at the plasma membrane in colon cancer cells. In this tumor context, we provide evidence that LRP-1 regulates by endocytosis the cell surface levels of DDR1 expression. The LRP-1 mediated endocytosis of DDR1 increased cell proliferation by promoting cell cycle progression into S phase and decreasing apoptosis. In this study, we identified a new molecular way that controls the cell-surface expression of DDR1 and consequently the colon carcinoma cell proliferation and apoptosis and highlighted an additional mechanism by which LRP-1 carries out its sensor activity of the tumor microenvironment.

Keywords: LRP-1, DDR1, colon cancer cell, proliferation, 3D collagen matrix

OPEN ACCESS

Edited by:
Luisa Lanfrancone, European Institute of Oncology (IEO), Italy

Reviewed by:
Veronica Vella, University of Catania, Italy
Malgorzata Wygrecka, University of Giessen, Germany

***Correspondence:**
Aline Appert-Collin
aline.bennasroune@univ-reims.fr

† These authors have contributed equally to this work

Specialty section:
This article was submitted to Molecular and Cellular Oncology, a section of the journal Frontiers in Cell and Developmental Biology

Received: *03 February 2020*
Accepted: *04 May 2020*
Published: *03 June 2020*

Citation:
Le CC, Bennasroune A, Collin G, Hachet C, Lehrter V, Rioult D, Dedieu S, Morjani H and Appert-Collin A (2020) LRP-1 Promotes Colon Cancer Cell Proliferation in 3D Collagen Matrices by Mediating DDR1 Endocytosis. Front. Cell Dev. Biol. 8:412. doi: 10.3389/fcell.2020.00412

INTRODUCTION

The low-density lipoprotein (LDL) receptor-related protein (LRP) superfamily contains twelve transmembrane proteins participating in a wide range of physiopathological processes (Emonard et al., 2014; Pohlkamp et al., 2017). Belonging to this family, LRP-1 is widely expressed in a large variety of tissues and exhibits functionalities in controlling key biological processes such as pericellular protease activities and extracellular matrix (ECM) function. This protein consists of a large functional endocytic receptor firstly synthesized as a 600-kDa precursor cleaved to an extracellular ligand-binding subunit of 515 kDa and a transmembrane 85 kDa part containing a 100 amino acids cytosolic tail. LRP-1-mediated endocytosis is tightly coupled to regulation of signaling pathways (Muratoglu et al., 2010; Mantuano et al., 2013; Kang et al., 2014). LRP-1

can indeed regulate mitogen-activated protein kinases (MAPK) as well as the survival-associated PI3K/Akt signaling pathway (Fuentealba et al., 2009; Langlois et al., 2010; Roura et al., 2014). LRP-1-dependent endocytosis and signaling-related events have been shown to play critical roles in severe pathologies including both Parkinson's and Alzheimer's diseases, metabolism dysfunction and cancer. Regarding tumor growth and metastasis, the molecular contribution of LRP-1 remains misunderstood and be highly dependent of the tumor microenvironment. Although LRP-1 expression and its role in cancer hallmarks are now well referenced in glioma (Boyé et al., 2017), melanoma (Salama et al., 2019), thyroid (Perrot et al., 2012; Appert-Collin et al., 2017; Theret et al., 2017), and breast carcinoma (Beaujouin et al., 2010; Tian et al., 2019), little is known about LRP-1 functionalities in colorectal carcinoma (CRC). LRP-1B, a member of LDL-R family highly homologous to LRP-1, is downregulated in the colon cancer tissues and inhibits the growth, migration and metastasis of colon cancer cells (Wang et al., 2017). Previous studies based on few colon adenocarcinoma samples have shown a frequent loss of LRP-1 immunohistochemical expression in adenocarcinomatous cells (Obermeyer et al., 2007; Toquet et al., 2007). A recent clinical study from our team demonstrated that LRP-1 expression was significantly lower in colon adenocarcinoma cells compared to colon epithelial cells and stromal cells and that this decrease in LRP-1 expression is associated with worse patient outcomes (Boulagnon-Rombi et al., 2018). Moreover, LRP-1 mutations have been reported in patients with liver metastasis (Wu et al., 2019). In the light of these data, the role of LRP-1 in CRC remains poorly understood and deserves to be further studied, especially to gain molecular insights.

Type I collagen is one of the main components of the cellular microenvironment in many mammalian tissues and plays a crucial role in tumor progression in several solid tumors, particularly in CRC (Brabletz et al., 2004). This protein is highly expressed in CRC with infiltrative growth phenotype (Oku et al., 2008). Two cellular groups of membrane receptors can interact with type I collagen, β1 integrin heterodimers and discoidin domain receptors (DDRs). DDR1 and DDR2 are the only receptors of collagen harboring a tyrosine kinase function (Leitinger, 2003; Abdulhussein et al., 2004; Rammal et al., 2016). DDR1 is activated by most collagen types, including I and IV, whereas DDR2 is only activated by fibrillary collagens. Upon collagen binding, activation of DDR1 and DDR2 are associated with a slow and sustained self-phosphorylation in comparison to other tyrosine kinase receptors (Shrivastava et al., 1997; Vogel et al., 1997). Indeed, tyrosine residues of DDR receptors are phosphorylated after 2 h and can be maintained for several hours. DDR1 expression has been associated with an increase in tumor invasion and aggressiveness of many human tumors, including esophageal cancer (Nemoto et al., 1997), gastric cancer (Xie et al., 2016), glioma (Yamanaka et al., 2006), breast cancer (Malaguarnera et al., 2015), and lung cancer (Xiao et al., 2015). The role of DDR1 in the regulation of tumor cell proliferation and apoptosis remains poorly documented and somewhat controversial. In breast cancer, DDR1 activates the insulin-like growth factor I receptor (IGF-1R) to support several IGF-1R-mediated biological responses such as cell proliferation (Malaguarnera et al., 2015). In lung cancer cells, DDR1 knockdown has been reported to decrease ERK and Akt phosphorylation leading to a downregulation of cell proliferation suggesting a role of DDR1 autophosphorylation triggered by collagen IV binding in lung cancer progression (Xiao et al., 2015). However, other studies have demonstrated that, in breast carcinomas, DDR1 promotes apoptosis through induction of pro-apoptotic protein BIK1 (Assent et al., 2015; Saby et al., 2018, 2019). In the case of CRC, recent studies have shown that nilotinib, a specific inhibitor of DDR1 phosphorylation, strongly reduced DDR1-mediated CRC cell invasion and metastasis in mouse models (Jeitany et al., 2018), and that the use of antibody-drug conjugates targeting DDR1 exhibits antitumor effects in a mouse model of CRC (Tao et al., 2019). These works have been carried out on CRC cells harboring invasive-like phenotype. Concerning the non-invasive epithelial-like carcinoma cells, a previous study reported a down-regulation of cell proliferation using 3D matrix, but the role of DDR1 in such a process was not explored (Luca et al., 2013).

In the present work, we investigated whether LRP-1 may control DDR1 expression at the plasma membrane in non-invasive CRC and influence its ability to regulate tumor cell proliferation upon its activation by type I collagen. Our data demonstrate for the first time that LRP-1 can induce endocytosis of DDR1 in CRC, thus decreasing the ability of the 3D collagen matrix/DDR1 axis to inhibit tumor cell proliferation.

MATERIALS AND METHODS

Cell Lines

LS174T (Duke's type B), HT-29 and RKO cell lines were purchased from American Type Culture Collection (ATCC, Rockville, MD, United States). LS174T, HT-29 and RKO cells were grown in Eagle's Minimum Essential Medium (EMEM) (ATCC 30-2003) or in Dulbecco's Modified Eagle Medium (DMEM) with high glucose (4.5 g/L) (Thermo scientific), respectively. Culture media were supplemented with 10% (v/v) fetal bovine serum (FBS) (Dutscher, France) and 1% penicillin-streptomycin (v/v, Invitrogen, Cergy-Pontoise, France). Cultures were maintained at 37°C in a humidified atmosphere containing 5% CO2 (v/v). Cells were routinely passaged at preconfluency using 0.05% trypsin, 0.53 mM EDTA (Invitrogen, 25300) and screened for the absence of mycoplasma using PCR methods.

Vectors, Transfection and Infection

DDR1-GFP overexpression was performed using pLVX-CMV-DDR1-GFP construct which was a generous gift from Frederic Saltel (INSERM, UMR1053, BaRITOn Bordeaux Research in Translational Oncology, Bordeaux, France). DDR1-GFP lentiviral particles were generated by transient co-transfection of 293T with pCMV ΔR8.91 (gag-pol) and phCMVG-VSVG (env) expression constructs using the FuGene 6 transfection reagent (Promega) according to manufacturer's recommendations. Three days after transfection, the supernatant containing lentiviruses

was collected, filtered through 0.45 μm filter, mixed with fresh medium (1 of 4) and hexadimethrine bromide at 8 μg/ml (Sigma) and used to infect HT-29 recipient cells. GFP control cells were processed in the same way. Infected cells were selected using puromycin (Invitrogen) at 3 μg/ml. LRP-1 knock-down was achieved using shRNA sequences previously described (Dedieu et al., 2008) that were purchased from Sigma. shRNA LRP-1 lentiviral particles were produced in 293T cells using FuGene 6 transfection reagent (Promega) and used to infect HT-29 recipient cells as described above. HT-29 cells expressing control shRNA were generated in the same way. Infected cells were selected using puromycin (Invitrogen) at 3 μg/ml.

2D and 3D Cell Culture

Fibrillar native type I collagen was extracted from tail tendons of 2-month-old rats and prepared as already described (Saby et al., 2016). For 2D cell cultures, each well was coated with 5 $\mu g/cm^2$ of collagen solubilized in 0.018 M acetic acid. Coated substrates were dried overnight at room temperature (RT) under sterile conditions. Thereafter, wells were washed two times with PBS (Invitrogen) before cell plating. In cell proliferation studies, cells were seeded on the coated surfaces at a density of 15×10^3 cells/well or 5×10^3 cells/0.33 cm^2 (24 well plates). In other studies, cell density was adjusted depending on the confluence. To quantify cell proliferation, after 5 days, cells were detached by trypsin and counted by phase-contrast microscopy (multiple-repeated counting for each condition). Each condition was done in triplicate and repeated in at least three biological experiments. For 3D culture, cells were seeded at a final density of 15×10^3 cells/mL. For that, 3×10^4 cells were resuspended in 100 μl of FBS and mixed with a solution containing 100 μl of 10X DMEM culture medium for HT-29 cells or EMEM for LS174T cells, 100 μl NaHCO3 (0.44 M), 90 μl NaOH 0.1 M, 10 μl sodium pyruvate, 10 μL Ampicillin + Streptomycin, (and 10 μl glutamine 200 mM for MEM culture medium), the premix is adjusted to 500 μl with sterile ultrapure water. After that, the mix containing cells is gently homogenized with 500 μl of collagen 3 mg/ml to finalize the collagen-based medium. Then, 1 ml/well of this pre-solidified medium was deposited in 24-well plates, and collagen gel solidification was performed at 37°C during 30 min. Finally, 1 ml of complete culture medium was added on top of each gel and the plates were incubated at 37°C. Covering medium is changed every 2 days. After 3 or 5 days, the covering medium was removed, and gels were digested with 2 mg/ml collagenase P (Roche). After collecting the cells from digested gel, cells were dissociated by tryspin and viable cell number was determined by phase contrast microscopy using Kova Glasstic Slides (Kova International Inc., Garden Grove, CA, United States).

Antibodies and Recombinant Proteins

Anti-LRP1 β-chain antibody (clone EPR3724) was purchased from Abcam (Cambridge, United Kingdom). Rabbit monoclonal antibodies against DDR1 (D1G6), phospho-DDR1 (Tyr792, 4G10), GFP (D5.1), and GAPDH (14C10) were purchased from cell signaling. Rabbit monoclonal antibodies against DDR2 were purchased from R&D systems (Lille, France). IgGs used as a negative control for immunoprecipitation and cell treatments were purchased from Santa Cruz Biotechnology (Heidelberg, Germany). Blocking LRP-1 polyclonal antibody (R2629) was a generous gift from Dr. D. K. Strickland (Department of Surgery, University of Maryland School of Medicine, Baltimore, MD, United States) (Mikhailenko et al., 2001). Histidine-tagged RAP (Receptor-associated protein) was purified as previously described (Dedieu et al., 2008).

RNA Isolation and qPCR

Total mRNAs were extracted using TRIzol reagent (Thermofisher), isolated from other cellular materials by chloroform/isoamyl alcohol (24:1) precipitation before centrifugation (12,000 × *g*, 4°C, 15 min), as previously described (Theret et al., 2017). 250 ng total mRNAs were reverse-transcribed using VERSO cDNA kit (Thermofisher) according to the manufacturer instructions. Real-time PCR was then performed using an Absolute SYBR Green Rox mix (Thermofisher) and a CFX 96 real time PCR detection system (Bio-Rad, Hercules, CA, United States). The cycle threshold (Ct) values were recorded using Bio-Rad CFX Manager 3.0 software (Bio-Rad) (Le Cigne et al., 2016). Results are expressed as 1/DCt. DCt corresponds to the difference between Ct of the sequence of interest and Ct of our reference sequences (RS18 and RPL32) (Scandolera et al., 2015). PCR primers were synthesized by Eurogentec (Liege, Belgium) as follow (5′-3′): for LRP1: GCTATCGACGCCCCTAAGAC and CGCCAGCCCTTTGAGATACA; for DDR1: ACTTTGGCAT GAGCCGGAAC and ACGTCACTCGCAGTCGTGAAC; for RS18: GCAGAATCCACGCCAGTACAA and GCCAGTGGTC TTGGTGTGCT; for RPL32: CATTGGTTATGGAAG CAACAAA and TTCTTGGAGGAAACATTGTGAG.

Total Protein Extraction and Immunoblotting

Cells were seeded in 3D type I collagen matrix for 5 days, then were harvested from digested matrices using collagenase P (2 mg/ml), washed twice with PBS, and lysed. The cells were then pelleted by centrifuging at 1000 rpm for 5 min. Whole-cell extracts were lysed in RIPA buffer (Thermofisher), sonicated and then incubated on ice. Cell lysates were collected after a centrifugation at 14000 rpm and 4°C for 15 min. Protein concentration was quantified by BCA assay (Thermofisher). Proteins were separated by sodium dodecyl sulfate-polyacrylamide gel electrophoresis (SDS-PAGE) and transferred onto a nitrocellulose membrane (Amersham Biosciences, Little Chalfont, United Kingdom). Membranes were blocked with 5% skimmed milk (m/v) in Tris buffered saline (0.02 M Tris–HCl, 0.137 M NaCl, pH 7.4), supplemented with 1% Tween 20 (v/v) at RT for 1 h. Blocked membranes were incubated with antibodies against LRP-1 β-chain (EPR3724), DDR1 (D1G6) and GAPDH (14C10) overnight at 4°C under gentle agitation. Finally, membranes were incubated with corresponding peroxidase conjugated secondary antibody at RT. Chemiluminescent reactions were revealed by using ECL Prime Kit (GE Healthcare, Orsay, France), signal was detected by the Odyssey-FC system (Licor, Lincoln, NE, United States).

Cell Surface Protein Isolation

The cells were treated with or without 500 nM RAP for 1 h, washed twice with PBS before suffering a biotinylation with 0.5 μg/mL of EZ-Link sulfo-NHS-LC-biotin (Thermofisher) in cold PBS. After three washes, biotinylated cells were incubated with 100 mM glycine at 4°C during 30 min to limit nonspecific binding. Cells were washed three times with PBS before protein extraction. Cells were scrapped in cold lysis buffer (10 mM Tris HCl, pH 7.5, 150 mM NaCl, 2 mM Na3VO4, 5 mM EDTA, 1% Triton X-100, supplemented with protease inhibitor cocktail), followed by a quick sonication on ice. Cell extracts were pelleted at 10,000 g (20 min, 4°C) before protein quantification. Solubilized biotinylated proteins (200 μg) were then affinity purified using 40 μL of streptavidin-agarose beads (GE Healthcare), overnight at 4°C under gentle agitation. After washes with lysis buffer, Laemmli buffer was added and samples were heated at 100°C for 5 min and resolved by SDS-PAGE followed by immunoblotting analysis.

Endocytosis Assay

Endocytosis assays were adjusted from validated method (Theret et al., 2017). Cell-surface proteins were labeled using 0.5 μg/mL of EZ-Link sulfo-NHS-LC-biotin (Thermofisher) in cold PBS at 4°C for 30 min. After washes with PBS, cells were incubated with 100 mM glycine at 4°C for 15 min. Nonspecific binding and free biotin were discarded by warm PBS washes before addition of warm medium supplemented with 10% FBS. Cells were treated with 500 nM RAP at 37°C for 1 h to antagonize endocytosis function of LRP-1. Cells were then quickly placed on ice to block internalization activities. After three washes with PBS, cells were incubated with 50 mM glutathione in cold buffer (75 mM NaCl, 75 mM NaOH, 1 mM MgCl2, 0.1 mM CaCl2, 10 mM EDTA, pH 8.6) at 4°C for 30 min to remove remaining biotin at the cell surface. To evaluate the total amount of surface biotinylation, one culture dish was kept on ice after biotin labeling and preserved from glutathione treatment. The efficiency of glutathione efficacy at the cell surface was controlled to be over 90%. Whole-cells extracts were prepared as described above. Internalized DDR1 was determined from 350 μg of cell lysate by adding 40 μL of streptavidin-agarose beads (GE Healthcare), incubating overnight at 4°C under gentle agitation and using DDR1 antibody through immunoblotting, as described above.

Immunoprecipitation

Whole cell extracts from HT-29$^{DDR1-GFP}$ were performed as described in a previous study (Theret et al., 2017). Whole cell lysates were subjected to immunoprecipitation using anti-LRP-1 (EPR3724), anti-DDR1 (D1G6) antibodies or nonspecific IgGs at 4°C for 12 h, bound to protein G sepharose beads (GE Healthcare) at 4°C for 2 h and finally washed three times with cold lysis buffer followed by a protein denaturation step at 100°C for 5 min. After that, the samples were centrifuged at 10000 rpm for 1 min, supernatants were then subjected to a western blot analysis using anti-LRP-1 β-chain (clone EFR3724), anti-DDR1 (D1D6), and anti-GFP antibodies.

DDR1 Phosphorylation Analysis

HT-29 and HT-29 overexpressing DDR1-GFP (HT-29$^{DDR1-GFP}$) cells were cultured in 3D type I collagen matrices with or without 50 nM nilotinib treatment for 16 h. Matrices were digested before undergoing a standard procedure for total protein extraction in 3D (Saby et al., 2016). Then, 300 μg of whole-cell extracts were immunoprecipitated with anti-DDR1 (D1D6), as described above. The proteins were separated by SDS-PAGE and the immunoprecipitates were blotted with anti-phosphotyrosine antibody, clone 4G10 (Millipore, 05-321). The blots were then stripped using a stripping buffer (200 mM glycine, 1% SDS, 0.02% sodium azide, pH 2.5) and re-probed with anti-DDR1 antibody.

Cell Cycle

Double thymidine block procedure was adapted from an established protocol (Chen and Deng, 2018). Specifically, HT-29 and HT-29$^{DDR1-GFP}$ cells were cultured in medium supplemented with 2 mM thymidine for 18 h then switched to thymidine-free medium for 9 h. After two washes with PBS, cells were cultured again in medium supplemented with 2 mM thymidine for 15 h. Cells were released by washing twice with PBS before trypsinization. The synchronized cells were then seeded into 3D type I collagen matrices with or without 1 μM RAP treatment for 24 h. Collagen matrices were further digested to harvest cultured cells. Lastly, cells were washed twice with PBS and stained with nuclear isolation medium-4,6-diamidino-2-phenylindole dihydrochloride named NIM-DAPI (NPE Systems, Pembroke Pines, FL, United States) at RT for 5 min. The samples were analyzed with an Accuri-C6 Special Order Product (BD Bioscience) by acquisition of 20000 events. Analysis was performed with an excitation wavelength of 375 nm and fluorescence detection at 427 ± 10 nm.

Apoptosis Assay

HT-29 and HT-29$^{DDR1-GFP}$ cells were cultured in 3D type I collagen matrices with or without 1 μM RAP treatment for 3 days. The culture medium was replaced every 2 days by fresh complete DMEM medium with or without 1 μM RAP. After 5 days, cells were harvested as described above. Harvested cells were washed with PBS before suffering a quick trypsinization. The single cells were then incubated with Annexin V-iFluor 647 Apoptosis solution (Abcam, United Kingdom), supplemented with propidium iodide (Sigma-Aldrich). The incubation was carried out at RT for 30 min. Apoptosis assays were performed using flow cytometer, FL4 channel (BD Biosciences, San Jose, CA, United States).

Immunofluorescence

HT-29$^{DDR1-GFP}$ cells were seeded onto collagen-coated glass slides for 48 h at 37°C and then fixed in PBS containing 4% paraformaldehyde for 15 min at RT. After three washes with PBS, cells were incubated for 30 min in PBS containing 1% bovine serum albumin and then incubated overnight at 4°C with GFP primary antibodies. Then, after five washes with PBS, cells were incubated with secondary antibodies conjugated to Alexa Fluor 488 (1/1000) during 1 h at RT. DAPI was added

during washes. Slides were incubated with mounting medium. Immunofluorescence-labeled cell preparations were analyzed using a Zeiss LSM 710 confocal laser scanning microscope with the 63× oil-immersion objective Zeiss operating system (Carl Zeiss MicroImaging GmbH, Deutschland).

Data Analysis

All statistical results were analyzed from at least three independent experiments. Data were represented as the standard deviation (SD) using Graphpad Prism software. Student's *t*-test and ANOVA test were used for statistical analysis. Immunoblotting images were analyzed by ImageJ software.

RESULTS

LRP-1 Inhibition Decreases Colon Carcinoma Cell Proliferation Only in 3D Collagen Matrices

To study the involvement of LRP-1 and DDR1 in the regulation of colon tumor cell proliferation by 3D collagen matrix, the endogenous expression level of LRP-1 and DDR1 were analyzed by both RT-qPCR and immunoblotting in LS174T and HT-29 cells (**Figure 1**). Results showed that the expression of the two receptors at the mRNA and protein levels in HT-29 cells are higher than in LS174T cells. It should be noted that DDR2 is not expressed in these two cells lines (data not shown).

We then examined the effect of LRP-1 inhibition on HT-29 and LS174T cell proliferation in 2D and in 3D collagen matrices. For this purpose, we compared the cell proliferation after 5 days of culture in the presence or absence of RAP (receptor associated protein), the LRP-1 antagonist, or its blocking antibody (R2629). As shown in **Figures 2A,B**, in both cell lines, treatment by RAP or R2629 did not modify cell proliferation in 2D collagen coating. By contrast, 3D-cell proliferation was decreased by about 50% in each cell line when using RAP or R2629 treatment whereas IgG treatment has no effect (**Supplementary Figure S1**). To focus on the role of LRP-1 in the regulation of cell proliferation in 3D collagen matrices, an RNA interference strategy against LRP-1 was performed in HT-29 cells. Two different cell lines that stably overexpressed a specific shRNA for LRP-1 [shLRP-$1_{(a)}$ and shLRP-$1_{(b)}$] were selected, and a control cell line was established after infection with control shRNA (shCTRL). The endogenous level of LRP-1 was assessed by both RT-qPCR and immunoblotting (**Figure 2C**, left panel). As expected, infection with lentiviruses expressing shCTRL had no effect on the LRP-1 expression level while LRP-1-specific shRNA was able to efficiently knock-down the expression of LRP-1 at the mRNA level (data not shown) as well as at the protein level by about 90%. The same inhibition was observed for both shLRP-1 cell lines (**Figure 2C**, left panel). As shown in **Figure 2C** (right panel), proliferation of LRP-1-silenced cancer cells was decreased by about 50% in 3D collagen matrices, whereas no effect of LRP-1 silencing was observed in 2D (data not shown). Taken together, these data indicate that LRP-1 sustains colon cancer cell proliferation, and that this process occurs only in a 3D collagen environment. Similar study on cell proliferation have been conducted using RKO colon carcinoma cells that do not express DDR1 (**Supplementary Figure S2A**). Results demonstrated that LRP-1 inhibition by RAP did not modify RKO cell proliferation both in 2D and in 3D matrices, suggesting that LRP-1 supports CRC proliferation in a DDR1 dependent manner (**Supplementary Figure S2B**).

LRP-1 and DDR1 Coexist Within the Same Molecular Complexes

Since LRP-1 had a positive effect on cell proliferation only in 3D collagen environment by LRP-1, we hypothesized that LRP-1 could interact with DDR1, one of the key collagen membrane receptors, to induce its endocytosis. To validate this hypothesis, we first evaluated whether LRP-1 may influence the DDR1 amount at the plasma membrane of HT-29 cells. After cell-surface protein labeling with the membrane-impermeable biotinylation reagent sulfo-NHS-LC-biotin, biotinylated proteins were selectively recovered from cell extracts by streptavidin affinity precipitation, and DDR1 was detected in the affinity precipitates by immunoblot analysis. After RAP treatment, DDR1 was found to accumulate at the plasma membrane fraction (**Figure 3A**), suggesting that LRP-1 mediates DDR1 internalization. Thus, we investigated DDR1 uptake by using a previously validated endocytosis assay (Theret et al., 2017). This method requires labeling of cell surface proteins using the non-membrane permeating sulfo-NHS-LC-biotin at 4°C, then moving to a permissive temperature for endocytosis (37°C). Cell surface protein biotinylation as well as efficiency of biotin stripping with glutathione were controlled (**Figure 3B**, left panel). As shown in **Figure 3B** (right panel), DDR1 internalization was decreased by about 40% when LRP-1-mediated endocytosis was antagonized by RAP treatment. To test whether LRP-1 and DDR1 may participate in a common biomolecular complex, coimmunoprecipitation experiments were carried out in DDR1 overexpressing HT-29 cells (HT-$29^{DDR1-GFP}$). As shown in **Figure 3C**, HT-$29^{DDR1-GFP}$ expressed a high level of recombinant DDR1-GFP. Our data clearly demonstrated that DDR1 was coimmunoprecipitated with LRP-1. Reverse immunoprecipitation experiments with anti-DDR1 were also performed using the same cell lysates and confirmed that LRP-1 and DDR1 were detected in the same molecular complexes in colon carcinomas (**Figure 3D**).

LRP-1 Promotes HT-29 Proliferation in a DDR1 Dependent Fashion

Previous reports demonstrated that cancer cell growth was downregulated by 3D type I collagen matrix in epithelial-like breast carcinoma cells and that this was dependent on activation of DDR1 by collagen (Assent et al., 2015; Saby et al., 2018). Considering that LRP-1 induced HT29 cell proliferation in 3D collagen matrices (**Figure 2**) and drives endocytosis of DDR1 (**Figure 3**), we assume that the cell-surface expression level of DDR1 may constitute a key parameter to control growth and survival of colon cancer cells. To address this hypothesis, we compared the cell proliferation of HT-$29^{DDR1-GFP}$ and

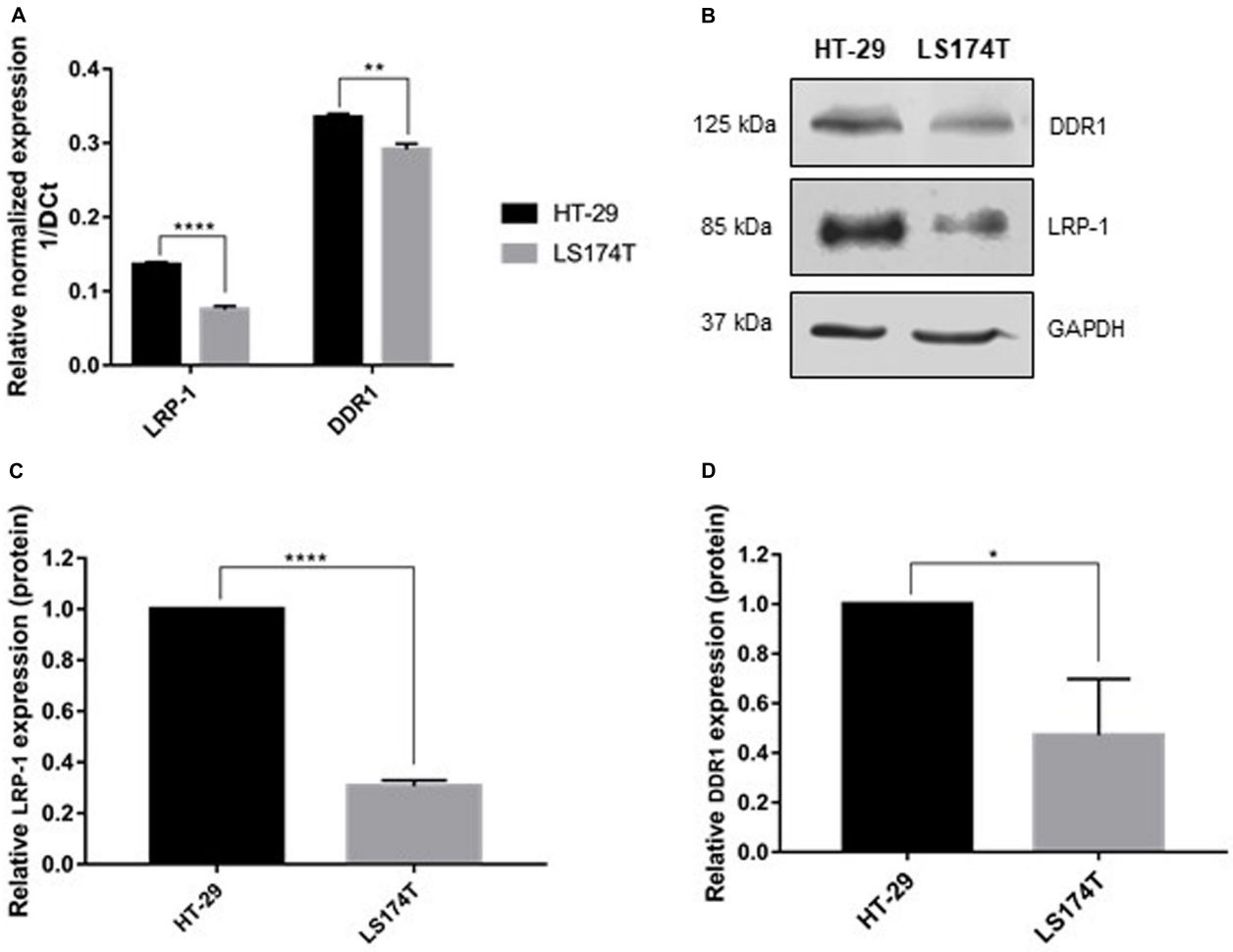

FIGURE 1 | Molecular characterization of colorectal carcinoma cell lines. **(A)** Transcriptional level of LRP-1 and DDR1 were assessed using RTqPCR. LRP-1 and DDR1 mRNA expression levels in HT-29 (black boxes) and LS174T (gray boxes) were normalized with both RPL32 and RS18 mRNA expression. **(B)** Whole cell extracts from HT-29 and LS174T cells were analyzed by SDS PAGE followed by western blotting using anti-DDR1, anti-LRP-1 and anti-GAPDH antibodies. Graphical representations of LRP-1 **(C)** and DDR1 **(D)** expression at protein level as normalized with GAPDH. All experiments were performed in three biological replicates. Plots are presented as the mean SD, $^{**}p < 0.01$; $^{****}p < 0.0001$, $n = 3$, two sample t-test. $^{*}p = 0.01$.

control counterparts. As expected, overexpression of DDR1 led to decreased cell proliferation in collagen 3D matrices by about 40%, compared to control cells (**Figure 4A**). Furthermore, cell proliferation in collagen 3D matrices was decreased by about 60% under RAP or R2629 antibody treatments in HT-29 cells overexpressing DDR1-GFP (**Figure 4B**). Interestingly, the proliferative inhibition under LRP-1 antagonization was more important when DDR1 was overexpressed.

DDR1 Activity Is Necessary to Induce Cell Proliferation in HT-29$^{DDR1-GFP}$ Cells

Since DDR1 phosphorylation could be responsible of growth inhibition (Saby et al., 2018), we evaluated the impact of nilotinib (50 nM), a receptor tyrosine kinase inhibitor with high potency against DDR1, on colon carcinoma cell proliferation using both control (**Figure 4C**) and HT-29$^{DDR1-GFP}$ (**Figure 4D**) cells. Nilotinib treatment had no effect on cell proliferation in control cells (**Figure 4C**, right panel) whereas carcinoma cell proliferation in DDR1-overexpressing cells was increased after nilotinib treatment (**Figure 4D**, right panel). Consistently, DDR1 phosphorylation was drastically inhibited upon nilotinib treatment in HT-29$^{DDR1-GFP}$ cells (**Figure 4D**, left panel). Taken together, these data suggest that collagen-induced cell growth inhibition relies on DDR1 phosphorylation.

LRP-1 Inhibition Induces Cells Cycle Arrest in the G0/G1 Phase

To further characterize the role of LRP-1 in the regulation of cancer cell proliferation, we investigated whether RAP treatment affects the cell cycle of HT-29 colon carcinomas. First, HT-29 and HT-29$^{DDR1-GFP}$ cells were synchronized in G0/G1-phase by double thymidine blocking. The cells were then seeded in 3D collagen matrix to allow their re-entry into the cell cycle. The results of flow cytometric

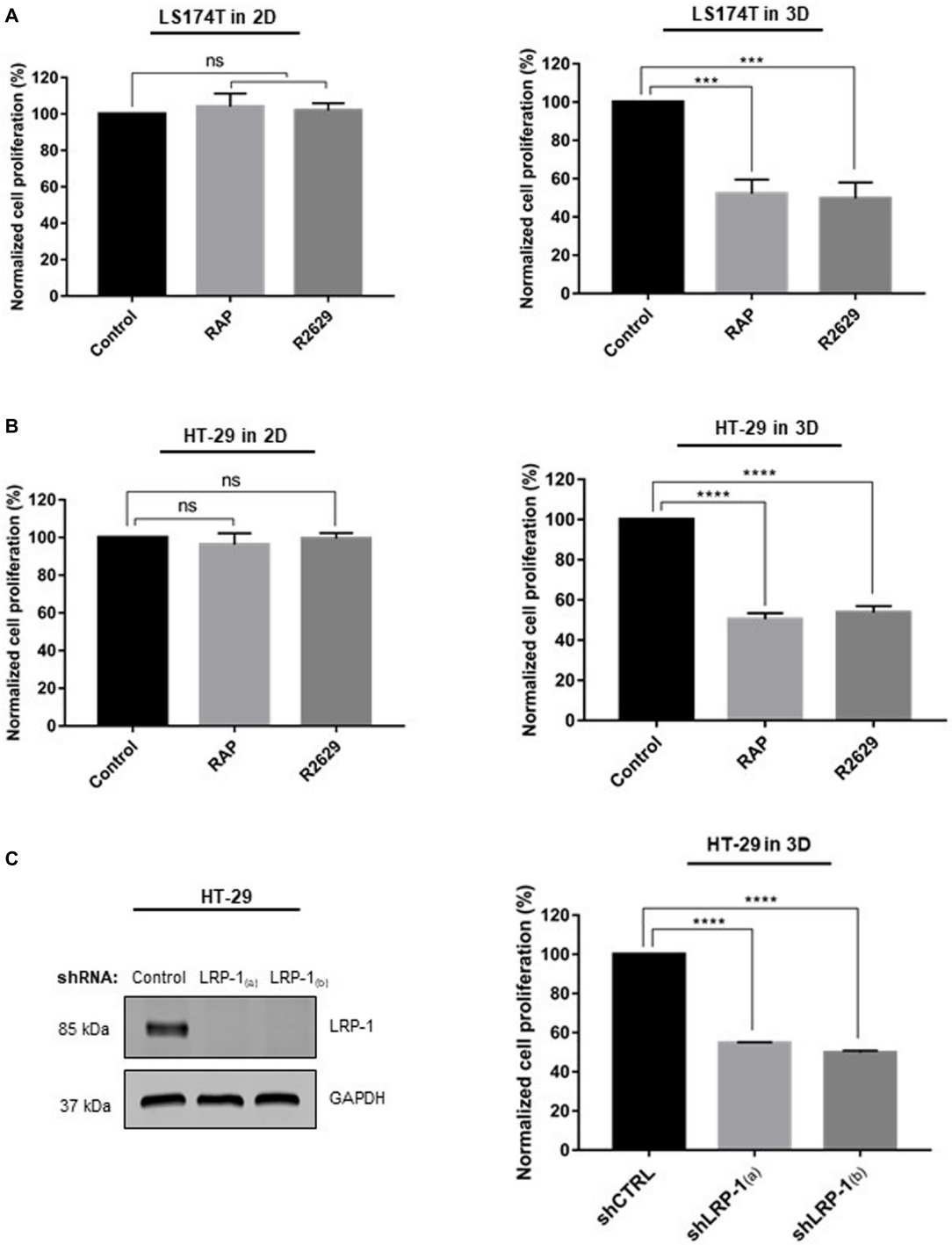

FIGURE 2 | Effect of LRP-1 antagonists and LRP-1 knockdown on colorectal cancer cell proliferation. LS174T **(A)** and HT-29 **(B)** cells were cultured in 2D type I collagen coating (left panels) or 3D type I collagen matrices (right panels) without (black boxes) or with RAP (500 nM, light gray boxes) or R2629 (2.5 μg/mL, dark gray boxes) treatment. After 5 days of culture, cell growth indices were assessed using at least three separate sets of culture, all conditions were repeated at least three times. **(C)** HT-29 cells were transduced with lentivirus encoding non-silencing shRNA (shCTRL) or shRNA targeting LRP-1 [shLRP1$_{(a)}$ and shLRP1$_{(b)}$] (right panel). Whole-cell extracts from each clonal cell were submitted to immunoblot analysis using anti-LRP-1 antibody (5A6). GAPDH expression level served as a loading control. shCTRL (black boxes) and shLRP-1$_{(a)}$ or shLRP-1$_{(b)}$ (gray boxes) HT-29 cells were seeded in 3D type I collagen matrix (left panel) during 5 days with or without RAP and R2629 treatment. Cell growth was evaluated by at least three separate experiments, each done in triplicate. The data are presented as the mean SD. ***$p < 0.001$; ****$p = 0.0001$; ns: not significant, One-way ANOVA test using Dunnett's multiple comparisons.

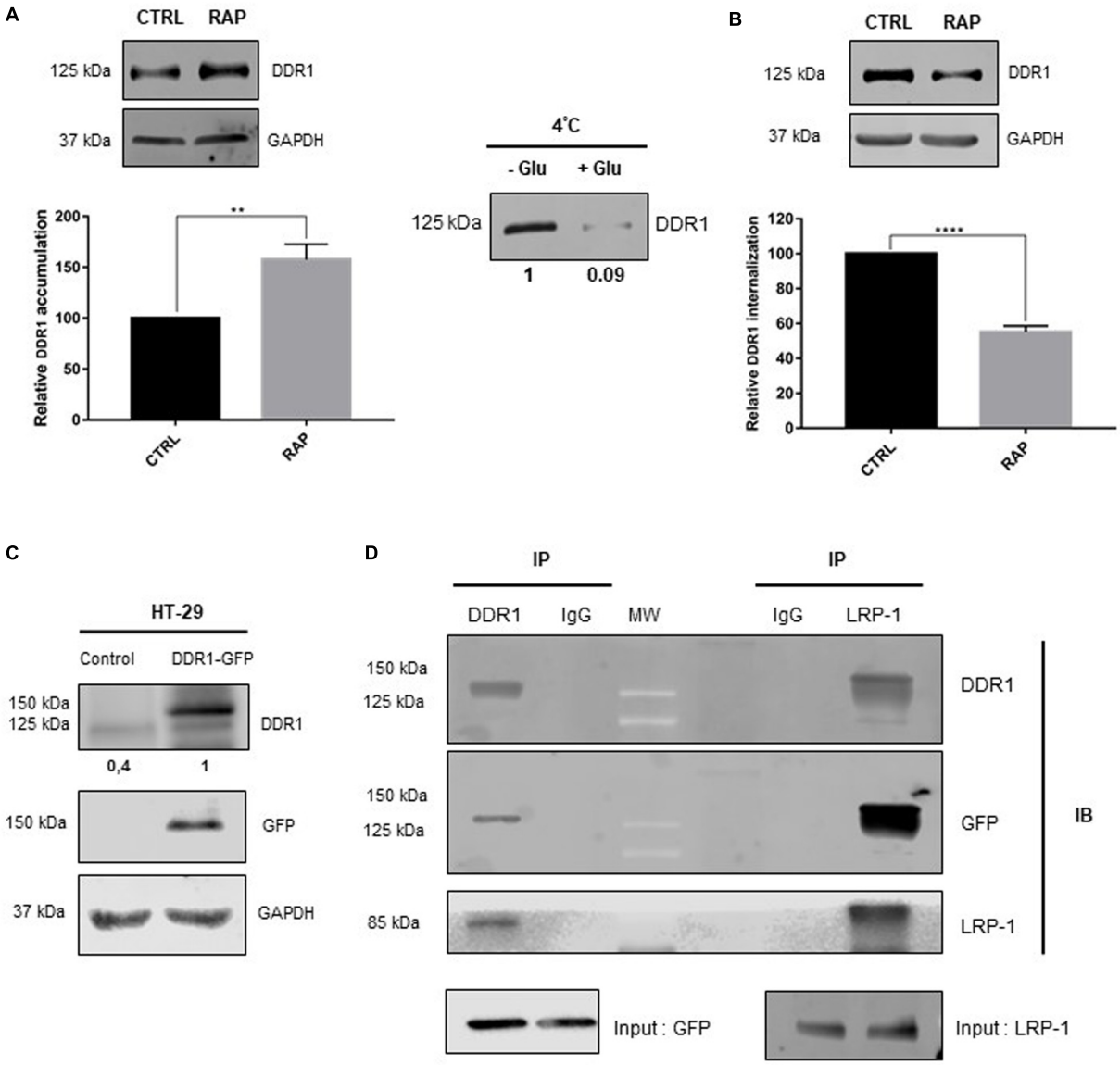

FIGURE 3 | RAP treatment inhibits DDR1 endocytosis and led to its accumulation at the plasma membrane. **(A)** Plasma membrane extracts from cell surface biotinylated proteins were obtained from HT-29 cells treated or not with RAP (1 μM, 1 h). Immunoblot analysis was performed using anti-DDR1 antibodies. Expression level of GAPDH in the intracellular fraction served as a loading control and for normalization. Three independent experiments were conducted, the data is represented as the mean SD. $^{**}p < 0.005$, two sample *t*-test. **(B)** HT-29 cells were treated with/without RAP (1 μM) for 1 h. Plasma membrane proteins were biotinylated and endocytosis assay was carried out as reported in the experimental procedure section. DDR1 internalization was quantified by immunoblotting using DDR1 antibody (right panels including graph, $^{****}p < 0.0001$, two sample *t*-test). Left panel (4°C) serves to control DDR1 binding to the cell surface (-Glut, without glutathione) and glutathione efficacy for biotin stripping (+ glut, with glutathione). **(C)** Whole-cell extracts were obtained from HT-29 cells overexpressing GFP (control) or DDR1-GFP. Immunoblot analysis was performed using anti-DDR1 and anti-GFP antibodies and GAPDH served as a loading control. LRP-1 **(D)** or DDR1 containing complexes were immunoprecipitated (IP) from DDR1-GFP overexpressing HT-29 cells whole-cell extracts by using anti-LRP-1 (clone EPR3724) or anti-DDR1 (D1G6) monoclonal antibody, respectively. Immunocomplexes were then subjected to SDS-PAGE and immunoblotted (IB) by using specific antibodies for LRP-1, DDR1, and GFP.

analysis revealed that HT-29 cells treated by RAP displayed an increased cell proportion in G1-phase (35% vs. 19%) and a decreased cell proportion in (S+G2-M)-phase (60% vs. 75%), compared to non-treated cells (**Figure 5A**). Moreover, the effect of RAP treatment on G1 and (S+G2-M)-phases was higher in HT-29$^{DDR1-GFP}$ (54 and 48%, respectively) (**Figure 5B**). To confirm whether LRP-1 inhibition affects the G1/S transition, HT-29 and HT-29$^{DDR1-GFP}$ were treated with the R2629 blocking antibody (**Figures 5C,D**). R2629 treatment has confirmed the obtained data wherein cells were treated with RAP. In fact, R2629-treated cells displayed also an increase in the proportion of cells in G1-phase and a

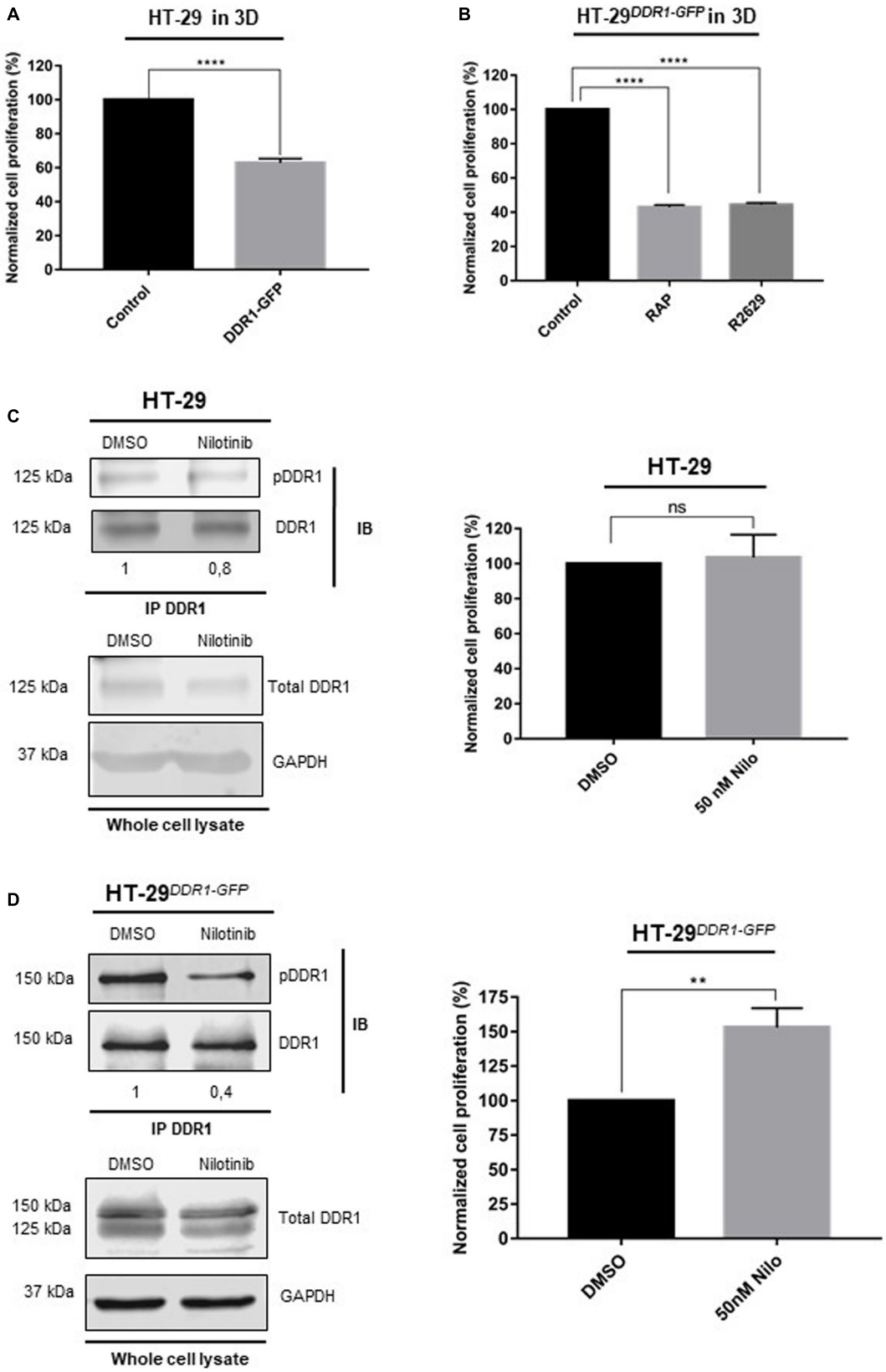

FIGURE 4 | Continued

FIGURE 4 | DDR1 down-regulates colorectal cancer cell proliferation in 3D collagen matrix. **(A)** Wild-type HT-29 were cultured in 3D type I collagen matrix for 5 days, then cell proliferation was evaluated by three independent experiments. The data are represented as the mean SD, $^{****}p < 0.0001$, two sample *t*-test. **(B)** HT-29$^{DDR1-GFP}$ cells were seeded in 3D type I collagen matrix during 5 days with/without RAP or LRP-1 blocking antibodies (R2629). Cell proliferation was then evaluated by at least 3 separate sets of culture, the data are presented as the mean SD and compared to untreated cells. $^{****}p = 0.0001$, One-way ANOVA test using Dunnett's multiple comparisons. HT-29 **(C)** and HT-29$^{DDR1-GFP}$ cells **(D)** were seeded in 3D type I collagen matrix and cultured with 50 nM nilotinib or DMSO (that served as a control) for 5 days. Left panels: DDR1 containing complexes were immunoprecipitated (IP) whole-cell extracts by using an anti-DDR1 monoclonal antibody (D1G6). Immunocomplexes were then subjected to SDS-PAGE and immunoblotted (IB) by using anti-DDR1 (D1G6) and anti-phospho-DDR1 (Tyr792, 4G10). Numbers under the immunoblots indicate the fold change ratio (pDDR1/DDR1), as compared to DMSO-treated cells that serve as the reference ($n = 3$). The bottom panel indicates the expression of DDR1 and GAPDH in whole cell lysates and served as a control. Right panels: cell proliferation was evaluated by three independent experiments, the data are presented as the mean SD. $^{**}p < 0.005$; ns: not significant, two sample *t*-test.

decrease in S-phase cell population, compared to non-treated cells (**Figures 5C,D**).

LRP-1 Counteracts the DDR1-Dependant Promotion of Apoptosis in Colon Carcinomas

The inhibition of breast cancer cell growth induced by type I collagen 3D matrices has been previously attributed to a strong DDR1-dependent induced apoptosis (Assent et al., 2015; Saby et al., 2018). To evaluate whether type I collagen/DDR1 axis can induce apoptosis in colon carcinoma, the apoptosis assay was performed using Annexin V staining and flow cytometry. As shown in **Figures 6A,B**, LRP-1 antagonization by RAP resulted in an increase in the proportion of apoptotic and necrotic cells in 3D collagen environment. Interestingly, this effect was higher in HT-29$^{DDR1-GFP}$ cells (15.0% of apoptotic cells), compared to HT-29 cells (5.9% of apoptotic cells). The ability of DDR1 to increase apoptosis of colon carcinomas was confirmed in **Figure 6C**. These results were corroborated by immunofluorescence experiments. As shows in **Figure 6D**, the assay consistently shown the increased presence of nuclear condensation and DNA fragmentation upon LRP-1 inhibition.

DISCUSSION

The findings of this study have highlighted the first ever molecular association between LRP-1 and DDR1 in colon carcinoma. Indeed, we showed that the endocytic receptor LRP-1 established tight molecular connections with DDR1 at the plasma membrane of colon cancer cells. In this tumor context, we provide evidence that LRP-1 promotes cell proliferation through regulating the levels of membrane DDR1 in 3D collagen matrices. The LRP-1 mediated endocytosis of DDR1 supports colon carcinoma cell proliferation by promoting the entry of cell cycle to the S phase and decreasing apoptosis.

LRP-1 is considered as a key integrator of signals from the ECM and a multifunctional regulator of cancer-related events. Its overall function remains nevertheless extremely complex to decipher especially because the deregulation degree of its expression is highly variable depending on the type of tumors and the stage of cancer progression. In malignant diseases, the current trend seems to correlate LRP-1 overexpression with poor prognostic, increased cell proliferation, invasiveness and tumor recurrence (Catasus et al., 2011; Gheysarzadeh et al., 2019; Tian et al., 2019). To date, few studies have examined the contribution of LRP-1 in the field of CRC despite obvious clinical interest. We have recently highlighted that low LRP-1 immunohistochemistry score in malignant colon adenocarcinoma cells is a strong prognosis marker (Boulagnon-Rombi et al., 2018). We especially reported that in patients with metastases, LRP-1 expression predicts a shorter overall survival, especially when patients were treated by anti-VEGF therapies. The lower expression of LRP-1 in malignant cells is partly explained by LRP-1 gene mutation through the hypermutator type of CRC. In the present study conducted using relevant 3D collagen matrices, we showed in a surprising way that LRP-1 inhibition decreased colon carcinoma cell proliferation. Although these results seem to be conflicting with the previous data (Boulagnon-Rombi et al., 2018), it could be explained by the fact that the studied cell lines in this work are non-invasive cells in which LRP-1 expression is not modified and cell-surface DDR1 expression remains quite low due to the LRP-1-mediated internalization process, thus leading to high proliferation. In contrast, during metastasis development, we supposed that LRP-1 expression is down-regulated after cleavage by sheddases leading to a higher expression of DDR1 at the cell surface and then an increased tumor invasion. Although it is well documented that LRP-1 may activate crucial downstream signaling pathways such as Ras, c-Myc, MAPK, and Akt/PI3K, which are widely known as oncogenic pathways, especially in cell proliferation and survival processes (Van Gool et al., 2015), very few data have previously involved LRP-1 during cancer cell proliferation steps. Salama and collaborators reported the involvement of LRP-1:tPA pathway in promoting melanoma cell migration and proliferation (Salama et al., 2019). Their results, using loss- and gain-of-function strategy demonstrated a model wherein LRP-1 drives melanoma growth and metastases by enhancing ERK activation resulting in increased proteolytic events and in changing the cellular content within the tumor. Data from Beaujouin et al. (2010) also revealed that secreted pro-cath-D binds to LRP-1 promoting human mammary fibroblast outgrowth.

Interestingly, our findings stressed that LRP-1 displays a pro-proliferative effect on colon cancer cells only in 3D type I collagen matrices. During tumor progression, especially after degradation of the basement membrane, type I collagen is a key component of the stroma at the invasion front of human colorectal cancer (Brabletz et al., 2004). In addition to its properties as a scaffold protein, type

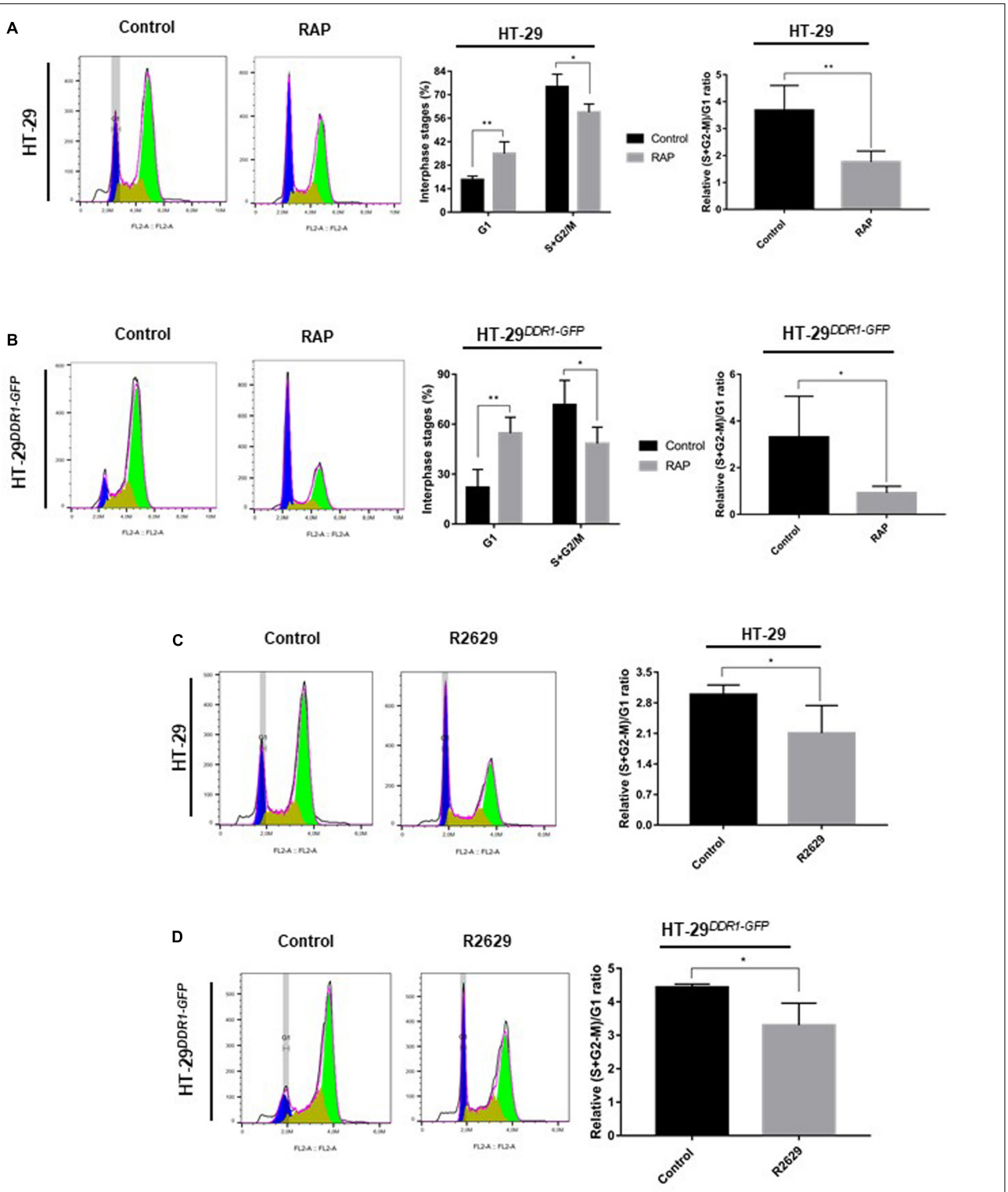

FIGURE 5 | Inhibition of LRP-1-mediated endocytosis induces cell cycle arrest at G1 phase. HT-29 **(A,C)** and HT-29$^{DDR1-GFP}$ **(B,D)** cells were grown on plastic surface and synchronized by double thymidine block. Synchronized cells were then seeded in 3D type I collagen matrix with or without 1 μM RAP **(A,B)** or LRP-1-blocking antibodies (R2629, 30 μg/mL) **(C,D)** for 24 h, followed by a cell cycle analysis. After nuclear staining with DAPI, 20.000 events were acquired and analyzed by flow cytometry. On the left colored panels, cell cycle distributions of HT-29 **(A,C)** and HT-29$^{DDR1-GFP}$ **(B,D)** cells treated with or without RAP or R2629 for 24 h are shown as histogram plots of the FL3 fluorescence channel. On the right panels, histograms represent the percentage of interphase stages (G1, S+G2/M) and the relative (S+G2-M)/G1 ratio of HT-29 **(A,C)** or HT-29$^{DDR1-GFP}$ **(B,D)** cells treated with (gray boxes) or without (black boxes) RAP or R2629. The data are presented as the mean SD. *$p < 0.05$; **$p = 0.01$, two samples *t*-test. Cell cycle assays were performed in four separate biological experiments for RAP treatment **(A,B)** and two separate experiments, each conducted in double triplicates for R2629 treatment **(C,D)**.

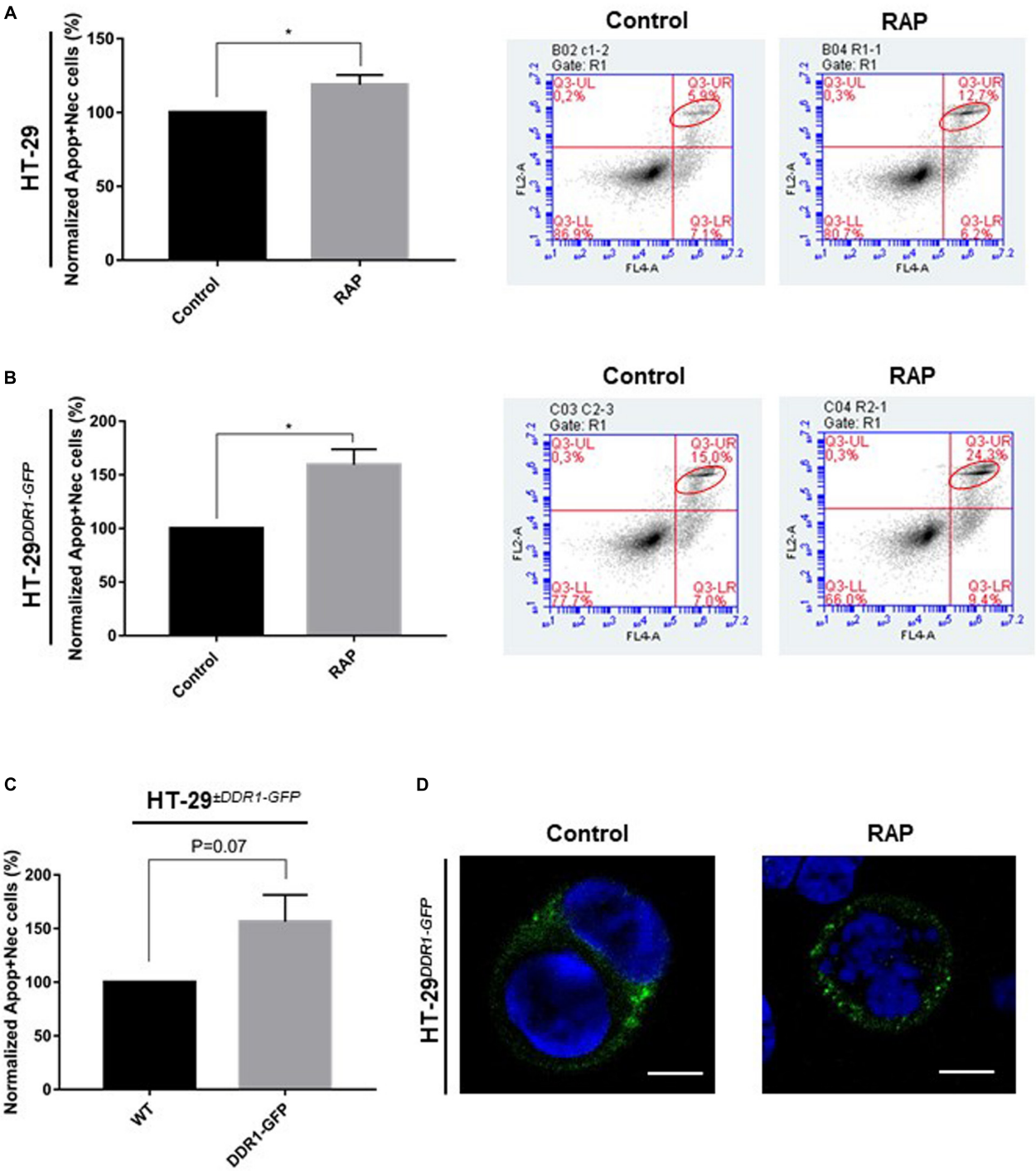

FIGURE 6 | Inhibition of LRP-1 results in an increase in apoptosis. HT-29 **(A)** and, gray boxes HT-29$^{DDR1-GFP}$ cells **(B)** were seeded in 3D type I collagen matrix and were treated without (black boxes) or with RAP (1 μM) for 3 days. The cells were then collected from digested matrix and suffered a rapid trypsinization before underwent an apoptotic assay. Apoptotic cells were stained with Annexin V and histogram (left panel), showed the percent of apoptotic. The values of treated samples were normalized to their controls, the data are represented as the mean SD, $*p < 0.05$, two sample *t*-test. **(C)** The plot represents the apoptotic indices of wild-type HT-29 overexpressing GFP (black boxes) and HT-29$^{DDR1-GFP}$ (gray boxes) cells seeded in 3D collagen matrix. The apoptosis assays were performed in two distinct experiments, each done in double triplicates. **(D)** Immunostaining of recombinant DDR1 (green) in untreated (left picture) or RAP-treated (right picture) HT-29$^{DDR1-GFP}$ cells. DNA is stained with DAPI. Scale bar: 5 μm.

I collagen can induce different cellular signaling pathways, which regulate several functions of tumor cells (Leitinger, 2011). Accumulating evidence suggest that DDR plays a key role in cancer progression by regulating the interactions of cells with the stromal collagen (Valiathan et al., 2012; Toy et al., 2015; Gao et al., 2016; Jeitany et al., 2018). Data obtained on HT-29 cells demonstrated that inhibition of LRP-1-dependent endocytosis by either RAP or R2629 antibodies led to membrane DDR1 accumulation in the same extent. We then demonstrated that LRP-1 and DDR1 are tightly associated in the same biomolecular complexes at the plasma membrane of colon carcinoma to constitute a new endocytosis complex. These results are even more interesting, as so far, little information is available concerning the regulation of DDR1 expression at the cell membrane. It is nevertheless known that activated DDR1 undergoes aggregation followed by cytoplasmic internalization and incorporation into early endosomes (Mihai et al., 2009). In mouse fibroblasts, DDR1 was reported to be internalized alone or complexed with other receptor tyrosine kinases (RTKs). Indeed, IGF-I receptor can phosphorylate DDR1 in breast carcinoma thus inducing co-internalization of the receptors and incorporation into early endosomes (Malaguarnera et al., 2015). Internalized RTKs can recycle back to the plasma membranes, be degraded, or undergo an endosome/Golgi/endoplasmic reticulum retrograde pathway. Interestingly, a novel mechanism whereby activated DDR1 plays a role of transcription factor has been demonstrated in injured human and mouse kidney proximal tubules (Chiusa et al., 2019).

Our findings showed that LRP-1 exerts its proliferative effects by down-regulating the amount of DDR1 at the plasma membrane. Indeed, by inducing the endocytosis of DDR1, LRP-1 counteracts the negative effect of DDR1 on cancer cell proliferation. Antagonization of LRP-1 by RAP or blocking antibodies indeed induced a significant cell cycle arrest in G1 phase, and this is magnified under DDR1 overexpression. Moreover, inhibition of LRP-1 by RAP treatment increases apoptosis of wild-type HT-29 cells and more importantly of HT-29$^{DDR1-GFP}$. In a coherent way, overexpression of DDR1 in HT-29 cells favors cell cycle arrest and apoptosis of colon carcinoma in 3D environment. These data are consistent with those previously obtained by Erik Maquoi's group demonstrating that MCF-7 and ZR-75-1 breast carcinoma cell growth was reduced in 3D type I collagen gels, but not when the cells were plated on a 2D matrix (Maquoi et al., 2012; Assent et al., 2015). Moreover, type I collagen was able to induce apoptosis in these cells. In fact, type I collagen can activate DDR1 to induce the expression of BIK, a pro-apoptotic member of the BCL-2 protein family, thereby triggering apoptotic cell death in these breast cancer cell lines (Assent et al., 2015). In addition, our group already demonstrated that young collagen inhibited cell proliferation and induced apoptosis when compared to the old one, due to a higher level of DDR1 phosphorylation (Assent et al., 2015; Saby et al., 2018). Furthermore, DDR2 is able to inhibit proliferation of human melanoma and fibrosarcoma cells by inducing a growth arrest in the G0/G1 phase of the cell cycle when the cells were plated on fibrillar collagen. This process was shown to be induced through p15INK4b cyclin-dependent kinase inhibitor, suggesting that this protein could be a downstream target of DDR2 signaling (Henriet et al., 2000; Wall et al., 2005, 2007). Moreover, DDR2, upon activation by 3D collagen, was able to target the cell cycle by increasing the expression of the cyclin-dependent kinase inhibitor p21^{CIP1} and thus inhibiting cell proliferation in a fibrosarcoma model (Saby et al., 2016). In contrast, DDR1 activation can also induce pro-survival signals (Ongusaha et al., 2003). In colon carcinoma cells, DDR1 regulates the cleavage of Notch 1 by a γ-secretase and the subsequent release and translocation of its intracellular domain to the nucleus to stimulate pro-survival genes (Kim et al., 2011). The collective findings suggest that DDR1 can induce survival as well as apoptosis, highly depending on experimental settings.

Finally, we identified a new molecular way that controls the cell-surface expression of DDR1 and suggested an additional role of LRP-1 as a key sensor of the tumor microenvironment.

DATA AVAILABILITY STATEMENT

All datasets generated for this study are included in the article/**Supplementary Material**.

AUTHOR CONTRIBUTIONS

CL was responsible for the execution of experiments, data analysis, and preparation of the manuscript. CH, GC, AB, and VL supported the experimental work and data analysis. AB contributed to the interpretation of the results and the writing of the manuscript. AA-C, HM, and SD designed, supervised the study, and wrote the manuscript. All authors critically commented on and approved the final submitted version of the manuscript.

FUNDING

The work was supported by the Structure Fédérative de Recherche Cap Santé (SFR Cap Santé), the Centre National de la Recherche Scientifique (CNRS), the Université de Reims Champagne-Ardenne, and the University of Science and Technology of Hanoi (Fellowship of CL).

ACKNOWLEDGMENTS

We thank Dr. Frederic Saltel (INSERM U1053, Bordeaux) for the gift of the lentivirus encoding DDR1-GFP and Dr. Dudley K. Strickland (University of Maryland School of Medicine, Baltimore, MD, United States) for the gift of R2629 antibody. We also thank Dr. Christine Terryn from the Image Core Facility (PICT) of the University of Reims Champagne-Ardenne for its excellent technical assistance and Mrs. Laurence Van-Gullick for her valuable technical assistance.

SUPPLEMENTARY MATERIAL

The Supplementary Material for this article can be found online at: https://www.frontiersin.org/articles/10.3389/fcell.2020.00412/full#supplementary-material

FIGURE S1 | No effect of IgG control on colorectal cancer cell proliferation n 3D matrix. Colorectal carcinomas were cultured in 3D type I collagen matrices without (black boxes) or with non-reactive IgG (light gray boxes) treatment. After 5 days of culture, cell growth indices were assessed using at least three separate sets of culture, all conditions were repeated at least three times. ns: not significant.

FIGURE S2 | Effect of LRP-1 antagonist on RKO cell proliferation. **(A)** Whole cell extracts from RKO cells were analyzed by SDS PAGE followed by western blotting using anti-DDR1 antibodies. **(B)** RKO cells were cultured in 2D type I collagen coating (left panel) or 3D type I collagen matrices (right panel) without (black boxes) or with RAP (500 nM, light gray boxes) treatment. After 5 days of culture, cell growth indices were assessed using at least three separate sets of culture, all conditions were repeated at least three times. ns: not significant.

REFERENCES

Abdulhussein, R., McFadden, C., Fuentes-Prior, P., and Vogel, W. F. (2004). Exploring the collagen-binding site of the DDR1 tyrosine kinase receptor. *J. Biol. Chem.* 279, 31462–31470. doi: 10.1074/jbc.M400651200

Appert-Collin, A., Bennasroune, A., Jeannesson, P., Terryn, C., Fuhrmann, G., Morjani, H., et al. (2017). Role of LRP-1 in cancer cell migration in 3-dimensional collagen matrix. *Cell Adh. Migr.* 11, 316–326. doi: 10.1080/19336918.2016.1215788

Assent, D., Bourgot, I., Hennuy, B., Geurts, P., Noel, A., Foidart, J. M., et al. (2015). A membrane-type-1 matrix metalloproteinase (MT1-MMP)-discoidin domain receptor 1 axis regulates collagen-induced apoptosis in breast cancer cells. *PLoS One* 10:e0116006. doi: 10.1371/journal.pone.0116006

Beaujouin, M., Prebois, C., Derocq, D., Laurent-Matha, V., Masson, O., Pattingre, S., et al. (2010). Pro-cathepsin D interacts with the extracellular domain of the beta chain of LRP1 and promotes LRP1-dependent fibroblast outgrowth. *J. Cell. Sci.* 123(Pt 19), 3336–3346. doi: 10.1242/jcs.070938

Boulagnon-Rombi, C., Schneider, C., Leandri, C., Jeanne, A., Grybek, V., Bressenot, A. M., et al. (2018). LRP1 expression in colon cancer predicts clinical outcome. *Oncotarget* 9, 8849–8869. doi: 10.18632/oncotarget.24225

Boyé, K., Pujol, N. I, Alves, D., Chen, Y.-P., Daubon, T., Lee, Y.-Z., et al. (2017). The role of CXCR3/LRP1 cross-talk in the invasion of primary brain tumors. *Nat. Commun.* 8:1571. doi: 10.1038/s41467-017-01686-y

Brabletz, T., Spaderna, S., Kolb, J., Hlubek, F., Faller, G., Bruns, C. J., et al. (2004). Down-regulation of the homeodomain factor Cdx2 in colorectal cancer by collagen type I: an active role for the tumor environment in malignant tumor progression. *Cancer Res.* 64, 6973–6977. doi: 10.1158/0008-5472.CAN-04-1132

Catasus, L., Llorente-Cortes, V., Cuatrecasas, M., Pons, C., Espinosa, I., and Prat, J. (2011). Low-density lipoprotein receptor-related protein 1 (LRP-1) is associated with highgrade, advanced stage and p53 and p16 alterations in endometrial carcinomas. *Histopathology* 59, 567–571. doi: 10.1111/j.1365-2559.2011.03942.x

Chen, G., and Deng, X. (2018). Cell synchronization by double thymidine block. *Bio Protoc.* 8:e2994. doi: 10.21769/BioProtoc.2994

Chiusa, M., Hu, W., Liao, H.-J., Su, Y., Borza, C. M., de Caestecker, M. P., et al. (2019). The extracellular matrix receptor discoidin domain receptor 1 regulates collagen transcription by translocating to the nucleus. *J. Am. Soc. Nephrol.* 30, 1605–1624. doi: 10.1681/ASN.2018111160

Dedieu, S., Langlois, B., Devy, J., Sid, B., Henriet, P., Sartelet, H., et al. (2008). LRP-1 silencing prevents malignant cell invasion despite increased pericellular proteolytic activities. *Mol. Cell. Biol.* 28, 2980–2995. doi: 10.1128/MCB.02238-07

Emonard, H., Theret, L., Bennasroune, A. H., and Dedieu, S. (2014). Regulation of LRP-1 expression: make the point. *Pathol. Biol.* 62, 84–90. doi: 10.1016/j.patbio.2014.02.002

Fuentealba, R. A., Liu, Q., Kanekiyo, T., Zhang, J., and Bu, G. (2009). Low density lipoprotein receptor-related protein 1 promotes anti-apoptotic signaling in neurons by activating Akt survival pathway. *J. Biol. Chem.* 284, 34045–34053. doi: 10.1074/jbc.M109.021030

Gao, H., Chakraborty, G., Zhang, Z., Akalay, I., Gadiya, M., Gao, Y., et al. (2016). Multi-organ site metastatic reactivation mediated by non-canonical discoidin domain receptor 1 signaling. *Cell* 166, 47–62. doi: 10.1016/j.cell.2016.06.009

Gheysarzadeh, A., Ansari, A., Emami, M. H., Razavi, A. E., and Mofid, M. R. (2019). Over-expression of low-density lipoprotein receptor-related Protein-1 is associated with poor prognosis and invasion in pancreatic ductal adenocarcinoma. *Pancreatology* 19, 429–435. doi: 10.1016/j.pan.2019.02.012

Henriet, P., Zhong, Z. D., Brooks, P. C., Weinberg, K. I., and DeClerck, Y. A. (2000). Contact with fibrillar collagen inhibits melanoma cell proliferation by up-regulating p27KIP1. *Proc. Natl. Acad. Sci. U.S.A.* 97, 10026–10031. doi: 10.1073/pnas.170290997

Jeitany, M., Leroy, C., Tosti, P., Lafitte, M., Guet, J. Le, Simon, V., et al. (2018). Inhibition of DDR1-BCR signalling by nilotinib as a new therapeutic strategy for metastatic colorectal cancer. *EMBO Mol. Med.* 10:e7918. doi: 10.15252/emmm.201707918

Kang, H. S., Kim, J., Lee, H. J., Kwon, B. M., Lee, D. K., and Hong, S. H. (2014). LRP1-dependent pepsin clearance induced by 2'-hydroxycinnamaldehyde attenuates breast cancer cell invasion. *Int. J. Biochem. Cell. Biol.* 53, 15–23. doi: 10.1016/j.biocel.2014.04.021

Kim, H. G., Hwang, S. Y., Aaronson, S. A., Mandinova, A., and Lee, S. W. (2011). DDR1 receptor tyrosine kinase promotes prosurvival pathway through Notch1 activation. *J. Biol. Chem.* 286, 17672–17681. doi: 10.1074/jbc.M111.236612

Langlois, B., Perrot, G., Schneider, C., Henriet, P., Emonard, H., Martiny, L., et al. (2010). LRP-1 promotes cancer cell invasion by supporting ERK and inhibiting JNK signaling pathways. *PLoS One* 5:e11584. doi: 10.1371/journal.pone.0011584

Le Cigne, A., Chieze, L., Beaussart, A., El-Kirat-Chatel, S., Dufrene, Y. F., Dedieu, S., et al. (2016). Analysis of the effect of LRP-1 silencing on the invasive potential of cancer cells by nanomechanical probing and adhesion force measurements using atomic force microscopy. *Nanoscale* 8, 7144–7154. doi: 10.1039/c5nr08649c

Leitinger, B. (2003). Molecular analysis of collagen binding by the human discoidin domain receptors, DDR1 and DDR2. Identification of collagen binding sites in DDR2. *J. Biol. Chem.* 278, 16761–16769. doi: 10.1074/jbc.M301370200

Leitinger, B. (2011). Transmembrane collagen receptors. *Annu. Rev. Cell Dev. Biol.* 27, 265–290. doi: 10.1146/annurev-cellbio-092910-154013

Luca, A. C., Mersch, S., Deenen, R., Schmidt, S., Messner, I., Schäfer, K. L., et al. (2013). Impact of the 3D microenvironment on phenotype, gene expression, and EGFR inhibition of colorectal cancer cell lines. *PLoS One* 8:e59689. doi: 10.1371/journal.pone.0059689

Malaguarnera, R., Nicolosi, M. L., Sacco, A., Morcavallo, A., Vella, V., Voci, C., et al. (2015). Novel cross talk between IGF-IR and DDR1 regulates IGF-IR trafficking, signaling and biological responses. *Oncotarget* 6, 16084–16105. doi: 10.18632/oncotarget.3177

Mantuano, E., Lam, M. S., and Gonias, S. L. (2013). LRP1 assembles unique co-receptor systems to initiate cell signaling in response to tissue-type plasminogen activator and myelin-associated glycoprotein. *J. Biol. Chem.* 288, 34009–34018. doi: 10.1074/jbc.M113.509133

Maquoi, E., Assent, D., Detilleux, J., Pequeux, C., Foidart, J. M., and Noel, A. (2012). MT1-MMP protects breast carcinoma cells against type I collagen-induced apoptosis. *Oncogene* 31, 480–493. doi: 10.1038/onc.2011.249

Mihai, C., Chotani, M., Elton, T. S., and Agarwal, G. (2009). Mapping of DDR1 distribution and oligomerization on the cell surface by FRET microscopy. *J. Mol. Biol.* 385, 432–445. doi: 10.1016/j.jmb.2008.10.067

Mikhailenko, I., Battey, F. D., Migliorini, M., Ruiz, J. F., Argraves, K., Moayeri, M., et al. (2001). Recognition of alpha 2-macroglobulin by the low density lipoprotein receptor-related protein requires the cooperation of two ligand binding cluster regions. *J. Biol. Chem.* 276, 39484–39491. doi: 10.1074/jbc.M104382200

Muratoglu, S. C., Mikhailenko, I., Newton, C., Migliorini, M., and Strickland, D. K. (2010). Low density lipoprotein receptor-related protein 1 (LRP1) forms a signaling complex with platelet-derived growth factor receptor-beta in

endosomes and regulates activation of the MAPK pathway. *J. Biol. Chem.* 285, 14308–14317. doi: 10.1074/jbc.M109.046672

Nemoto, T., Ohashi, K., Akashi, T., Johnson, J. D., and Hirokawa, K. (1997). Overexpression of protein tyrosine kinases in human esophageal cancer. *Pathobiology* 65, 195–203. doi: 10.1159/000164123

Obermeyer, K., Krueger, S., Peters, B., Falkenberg, B., Roessner, A., and Rocken, C. (2007). The expression of low density lipoprotein receptor-related protein in colorectal carcinoma. *Oncol. Rep.* 17, 361–367.

Oku, Y., Shimoji, T., Takifuji, K., Hotta, T., Yokoyama, S., Matsuda, K., et al. (2008). Identification of the molecular mechanisms for dedifferentiation at the invasion front of colorectal cancer by a gene expression analysis. *Clin. Cancer Res.* 14, 7215–7222. doi: 10.1158/1078-0432.CCR-08-0370

Ongusaha, P. P., Kim, J. I., Fang, L., Wong, T. W., Yancopoulos, G. D., Aaronson, S. A., et al. (2003). p53 induction and activation of DDR1 kinase counteract p53-mediated apoptosis and influence p53 regulation through a positive feedback loop. *EMBO J.* 22, 1289–1301. doi: 10.1093/emboj/cdg129

Perrot, G., Langlois, B., Devy, J., Jeanne, A., Verzeaux, L., Almagro, S., et al. (2012). LRP-1–CD44, a new cell surface complex regulating tumor cell adhesion. *Mol. Cell. Biol.* 32, 3293–3307. doi: 10.1128/MCB.00228-12

Pohlkamp, T., Wasser, C. R., and Herz, J. (2017). Functional roles of the interaction of APP and lipoprotein receptors. *Front. Mol. Neurosci.* 10:54. doi: 10.3389/fnmol.2017.00054

Rammal, H., Saby, C., Magnien, K., Van-Gulick, L., Garnotel, R., Buache, E., et al. (2016). Discoidin domain receptors: potential actors and targets in cancer. *Front. Pharmacol.* 7:55. doi: 10.3389/fphar.2016.00055

Roura, S., Cal, R., Galvez-Monton, C., Revuelta-Lopez, E., Nasarre, L., Badimon, L., et al. (2014). Inverse relationship between raft LRP1 localization and non-raft ERK1,2/MMP9 activation in idiopathic dilated cardiomyopathy: potential impact in ventricular remodeling. *Int. J. Cardiol.* 176, 805–814. doi: 10.1016/j.ijcard.2014.07.270

Saby, C., Buache, E., Brassart-Pasco, S., El Btaouri, H., Courageot, M. P., Van Gulick, L., et al. (2016). Type I collagen aging impairs discoidin domain receptor 2-mediated tumor cell growth suppression. *Oncotarget* 7, 24908–24927. doi: 10.18632/oncotarget.8795

Saby, C., Collin, G., Sinane, M., Buache, E., Van Gulick, L., Saltel, F., et al. (2019). DDR1 and MT1-MMP expression levels are determinant for triggering BIK-mediated apoptosis by 3D type I collagen matrix in invasive basal-like breast carcinoma cells. *Front. Pharmacol.* 10:462. doi: 10.3389/fphar.2019.00462

Saby, C., Rammal, H., Magnien, K., Buache, E., Brassart-Pasco, S., Van-Gulick, L., et al. (2018). Age-related modifications of type I collagen impair DDR1-induced apoptosis in non-invasive breast carcinoma cells. *Cell Adh. Migr.* 12, 335–347. doi: 10.1080/19336918.2018.1472182

Salama, Y., Lin, S. Y., Dhahri, D., Hattori, K., and Heissig, B. (2019). The fibrinolytic factor tPA drives LRP1-mediated melanoma growth and metastasis. *FASEB J.* 33, 3465–3480. doi: 10.1096/fj.201801339RRR

Scandolera, A., Rabenoelina, F., Chaintreuil, C., Rusciani, A., Maurice, P., Blaise, S., et al. (2015). Uncoupling of elastin complex receptor during in vitro aging is related to modifications in its intrinsic sialidase activity and the subsequent lactosylceramide production. *PLoS One* 10:e0129994. doi: 10.1371/journal.pone.0129994

Shrivastava, A., Radziejewski, C., Campbell, E., Kovac, L., McGlynn, M., Ryan, T. E., et al. (1997). An orphan receptor tyrosine kinase family whose members serve as nonintegrin collagen receptors. *Mol. Cell.* 1, 25–34. doi: 10.1016/s1097-2765(00)80004-0

Tao, Y., Wang, R., Lai, Q., Wu, M., Wang, Y., Jiang, X., et al. (2019). Targeting of DDR1 with antibody-drug conjugates has antitumor effects in a mouse model of colon carcinoma. *Mol. Oncol.* 13, 1855–1873. doi: 10.1002/1878-0261.12520

Theret, L., Jeanne, A., Langlois, B., Hachet, C., David, M., Khrestchatisky, M., et al. (2017). Identification of LRP-1 as an endocytosis and recycling receptor for β1-integrin in thyroid cancer cells. *Oncotarget* 8, 78614–78632. doi: 10.18632/oncotarget.20201

Tian, Y., Wang, C., Chen, S., Liu, J., Fu, Y., and Luo, Y. (2019). Extracellular Hsp90α and clusterin synergistically promote breast cancer epithelial-to-mesenchymal transition and metastasis via LRP1. *J. Cell Sci.* 132:jcs228213. doi: 10.1242/jcs.228213

Toquet, C., Jarry, A., Bou-Hanna, C., Bach, K., Denis, M. G., Mosnier, J. F., et al. (2007). Altered Calreticulin expression in human colon cancer: maintenance of Calreticulin expression is associated with mucinous differentiation. *Oncol. Rep.* 17, 1101–1107. doi: 10.3892/or.17.5.1101

Toy, K. A., Valiathan, R. R., Núñez, F., Kidwell, K. M., Gonzalez, M. E., Fridman, R., et al. (2015). Tyrosine kinase discoidin domain receptors DDR1 and DDR2 are coordinately deregulated in triple-negative breast cancer. *Breast Cancer Res. Treat.* 150, 9–18. doi: 10.1007/s10549-015-3285-7

Valiathan, R. R., Marco, M., Leitinger, B., Kleer, C. G., and Fridman, R. (2012). Discoidin domain receptor tyrosine kinases: new players in cancer progression. *Cancer Metastasis Rev.* 31, 295–321. doi: 10.1007/s10555-012-9346-z

Van Gool, B., Dedieu, S., Emonard, H., and Roebroek, A. J. M. (2015). The matricellular receptor LRP1 forms an interface for signaling and endocytosis in modulation of the extracellular tumor environment. *Front. Pharmacol.* 6:271. doi: 10.3389/fphar.2015.00271

Vogel, W., Gish, G. D., Alves, F., and Pawson, T. (1997). The discoidin domain receptor tyrosine kinases are activated by collagen. *Mol. Cell.* 1, 13–23. doi: 10.1016/s1097-2765(00)80003-9

Wall, S. J., Werner, E., Werb, Z., and DeClerck, Y. A. (2005). Discoidin domain receptor 2 mediates tumor cell cycle arrest induced by fibrillar collagen. *J. Biol. Chem.* 280, 40187–40194. doi: 10.1074/jbc.M508226200

Wall, S. J., Zhong, Z. D., and DeClerck, Y. A. (2007). The cyclin-dependent kinase inhibitors p15INK4B and p21CIP1 are critical regulators of fibrillar collagen-induced tumor cell cycle arrest. *J. Biol. Chem.* 282, 24471–24476. doi: 10.1074/jbc.M702697200

Wang, Z., Sun, P., Gao, C., Chen, J., Li, J., Chen, Z., et al. (2017). Down-regulation of LRP1B in colon cancer promoted the growth and migration of cancer cells. *Exp. Cell. Res.* 357, 1–8. doi: 10.1016/j.yexcr.2017.04.010

Wu, J. B., Sarmiento, A. L., Fiset, P. O., Lazaris, A., Metrakos, P., Petrillo, S., et al. (2019). Histologic features and genomic alterations of primary colorectal adenocarcinoma predict growth patterns of liver metastasis. *World J. Gastroenterol.* 25, 3408–3425. doi: 10.3748/wjg.v25.i26.3408

Xiao, Q., Jiang, Y., Liu, Q., Yue, J., Liu, C., Zhao, X., et al. (2015). Minor Type IV Collagen α5 Chain promotes cancer progression through discoidin domain receptor-1. *PLoS Genet.* 11:e1005249. doi: 10.1371/journal.pgen.1005249

Xie, R., Wang, X., Qi, G., Wu, Z., Wei, R., Li, P., et al. (2016). DDR1 enhances invasion and metastasis of gastric cancer via epithelial-mesenchymal transition. *Tumor Biol.* 37, 12049–12059. doi: 10.1007/s13277-016-5070-6

Yamanaka, R., Arao, T., Yajima, N., Tsuchiya, N., Homma, J., Tanaka, R., et al. (2006). Identification of expressed genes characterizing long-term survival in malignant glioma patients. *Oncogene* 25, 5994–6002. doi: 10.1038/sj.onc.1209585

Conflict of Interest: The authors declare that the research was conducted in the absence of any commercial or financial relationships that could be construed as a potential conflict of interest.

Copyright © 2020 Le, Bennasroune, Collin, Hachet, Lehrter, Rioult, Dedieu, Morjani and Appert-Collin. This is an open-access article distributed under the terms of the Creative Commons Attribution License (CC BY). The use, distribution or reproduction in other forums is permitted, provided the original author(s) and the copyright owner(s) are credited and that the original publication in this journal is cited, in accordance with accepted academic practice. No use, distribution or reproduction is permitted which does not comply with these terms.

frontiers in Cell and Developmental Biology

ORIGINAL RESEARCH
published: 03 July 2020
doi: 10.3389/fcell.2020.00522

Cell Derived Matrix Fibulin-1 Associates With Epidermal Growth Factor Receptor to Inhibit Its Activation, Localization and Function in Lung Cancer Calu-1 Cells

Keerthi Harikrishnan, Omkar Joshi, Saili Madangirikar and Nagaraj Balasubramanian**

Indian Institute of Science Education and Research, Pune, India

OPEN ACCESS

Edited by:
Sophie Tartare-Deckert, INSERM U1065 Centre Mediterraneien de Meidecine Moleiculaire, France

Reviewed by:
Maria Francesca Baietti, VIB KU Leuven Center for Cancer Biology, Belgium
Ute Jungwirth, University of Bath, United Kingdom

***Correspondence:**
Keerthi Harikrishnan
keerthivikram@gmail.com
Nagaraj Balasubramanian
nagaraj@iiserpune.ac.in

Specialty section:
This article was submitted to Molecular and Cellular Oncology, a section of the journal Frontiers in Cell and Developmental Biology

Received: *05 March 2020*
Accepted: *02 June 2020*
Published: *03 July 2020*

Citation:
Harikrishnan K, Joshi O, Madangirikar S and Balasubramanian N (2020) Cell Derived Matrix Fibulin-1 Associates With Epidermal Growth Factor Receptor to Inhibit Its Activation, Localization and Function in Lung Cancer Calu-1 Cells. Front. Cell Dev. Biol. 8:522. doi: 10.3389/fcell.2020.00522

Epidermal Growth Factor Receptor (EGFR) is a known promoter of tumor progression and is overexpressed in lung cancers. Growth factor receptors (including EGFR) are known to interact with extracellular matrix (ECM) proteins, which regulate their activation and function. Fibulin-1 (FBLN1) is a major component of the ECM in lung tissue, and its levels are known to be downregulated in non-small cell lung cancers (NSCLC). To test the possible role FBLN1 isoforms could have in regulating EGFR signaling and function in lung cancer, we performed siRNA mediated knockdown of FBLN1C and FBLN1D in NSCLC Calu-1 cells. Their loss significantly increased basal (with serum) and EGF (Epidermal Growth Factor) mediated EGFR activation without affecting net EGFR levels. Overexpression of FBLN1C and FBLN1D also inhibits EGFR activation confirming their regulatory crosstalk. Loss of FBLN1C and FBLN1D promotes EGFR-dependent cell migration, inhibited upon Erlotinib treatment. Mechanistically, both FBLN1 isoforms interact with EGFR, their association not dependent on its activation. Notably, cell-derived matrix (CDM) enriched FBLN1 binds EGFR. Calu-1 cells plated on CDM derived from FBLN1C and FBLN1D knockdown cells show a significant increase in EGF mediated EGFR activation. This promotes cell adhesion and spreading with active EGFR enriched at membrane ruffles. Both adhesion and spreading on CDMs is significantly reduced by Erlotinib treatment. Together, these findings show FBLN1C/1D, as part of the ECM, can bind and regulate EGFR activation and function in NSCLC Calu-1 cells. They further highlight the role tumor ECM composition could have in influencing EGFR dependent lung cancers.

Keywords: FBLN1, EGFR, ECM, cell derived matrix, matrix microenvironment, lung cancer

HIGHLIGHTS

- FBLN1C/1D suppress EGFR activation and EGFR dependent migration of Calu-1 cells.
- FBLN1C /1D isoforms bind EGFR, independent of its activation.
- Cell derived matrix FBLN1 associates with EGFR in Calu-1 cells.
- Cell derived matrix FBLN1C and FBLN1D regulate EGFR activation and localization to regulate cell adhesion, spreading in Calu-1 cells.

INTRODUCTION

Lung cancer is the leading cause of cancer related deaths worldwide. Non-small cell lung cancer (NSCLC) accounts for 85% of the cases (Chen et al., 2014). Epidermal growth factor receptor (EGFR) is a protein that is expressed on the cell surface and influences cell growth, survival and motility (Normanno et al., 2006). EGFR is overexpressed in lung cancer (Sharma et al., 2007; Malik and Raina, 2015) and is associated with poor prognosis (Gridelli et al., 2003; Scagliotti et al., 2004). Tumors that are initially responsive to EGFR targeted therapies can also acquire drug resistance rendering their treatment ineffective (Gridelli et al., 2003; Wheeler et al., 2010). The extracellular matrix (ECM), as a vital regulatory player in the tumor microenvironment not only provides structural support but also regulates downstream signaling to control cell growth, survival, differentiation and motility (Lu et al., 2012; Pickup et al., 2014). Crosstalk between the tumor ECM and growth factor receptors (like EGFR) has been further shown to play an important functional role in mediating tumor progression and metastasis (Wu et al., 2004; Reticker-Flynn et al., 2012; Du et al., 2013; Kim et al., 2014; Stevens et al., 2017). In the lungs, proteomic analysis shows ECM proteins to be a major component of the cellular microenvironment (Burgstaller et al., 2017). FBLN1 is prominently expressed in lung ECM, significantly more than other FBLN isoforms (Consortium, 2015; Burgstaller et al., 2017; Krasny et al., 2018). Although a large number of matrix proteins are altered in lung cancers, the functional role of some of the major lung ECM proteins like Fibulin-1, Elastin, Nephronectin, Agrin, Laminin remain poorly documented (Burgstaller et al., 2017; Gocheva et al., 2017).

Fibulins are a family of secreted glycoproteins that consist of a series of epidermal growth factor (EGF) like repeats followed by a C terminal fibulin type module (Argraves et al., 1990). Fibulin-1 is the prototypic member of this family of proteins, and is highly expressed in blood vessels, skin, heart, and lung (Argraves et al., 2003; Chu and Tsuda, 2004; Lau et al., 2010). Alternative splicing of FBLN1 produces two splice variants in mice (FBLN1C/FBLN1D) and four splice variants in humans (FBLN1A/B/C/D) (Argraves et al., 2003). Human FBLN1A/1B are known to be restricted to the placenta making human FBLN1C/1D the prevalent isoforms in human tissues (Tran et al., 1997). FBLN1 has a diverse array of ligands and has been shown to interact with other ECM proteins including Versican (Aspberg et al., 1999), Aggrecan (Aspberg et al., 1999), Laminin (Sasaki et al., 1995; Timpl et al., 2000; Ogawa et al., 2007), Tropoelastin (Sasaki et al., 1999), Nidogen (Sasaki et al., 1995), and Fibronectin (Balbona et al., 1992). FBLN1 also interacts with growth factors including heparin-binding epidermal growth factor (HB-EGF) (Brooke et al., 2002), connective tissue growth factor (CCN2) and CCN3 (Notch ligand) (Perbal et al., 1999). The significance of these interactions in regulating cellular processes is only beginning to be understood. FBLN1C and FBLN1D isoforms also have distinct biological roles based on their differential affinity and localization with other matrix proteins (Sasaki et al., 1995; Perbal et al., 1999; Brooke et al., 2002; Muriel et al., 2006).

Fibulin-1 is seen to exhibit both pro-oncogenic as well as tumor suppressive effects (Gallagher et al., 2005). FBLN1 is upregulated in breast and ovarian cancers where FBLN1C is expressed at higher levels than FBLN1D (Moll et al., 2002; Bardin et al., 2005). As a tumor suppressor FBLN1 levels are downregulated in epithelial cancers including melanoma (Wu et al., 2014), squamous cell carcinoma (Zhang et al., 2013), renal cell carcinoma (Xiao et al., 2013), hepatocellular carcinoma (Kanda et al., 2011), gastric carcinoma (Cheng et al., 2008), prostate carcinoma (Wlazlinski et al., 2007), colorectal carcinoma (Pesson et al., 2014), and lung adenocarcinoma (LUAD) (Cui et al., 2015). Further, overexpression of FBLN1D in fibrosarcoma cells is seen to inhibit tumor growth *in vivo* (Qing et al., 1997), with purified placental FBLN1 seen to inhibit adhesion, spreading, motility and invasion of breast cancer cells (Twal et al., 2001). Recent studies show that FBLN1 levels are downregulated in patients with NSCLC and is associated with poor prognosis (Yue et al., 2009; Cui et al., 2015).

Extracellular matrix proteins have been known to sequester growth factors (Grahovac and Wells, 2014; Hastings et al., 2019) and growth factor receptors to regulate their function (Kim et al., 2011; Grahovac and Wells, 2014). An important example of this is Fibronectin binding to VEGF and its regulation of angiogenesis (Zhu and Clark, 2014). In cancers, ECM proteins like Perlecan, Versican, Aggrecan, Decorin and Biglycan all bind growth factors to support pro-tumorigenic as well as anti-tumorigenic effects (Hynes and Naba, 2012; Grahovac and Wells, 2014). ECM proteins Laminin-5 (Schenk et al., 2003), Tenascin-C (Iyer et al., 2008), and Decorin (Iozzo et al., 1999) bind EGFR to regulate its activation and function in cancers (Grahovac and Wells, 2014).

Epidermal growth factor receptor activation is a vital regulator of oncogenic signaling in cancer cell invasion and metastasis (Normanno et al., 2006). EGFR is overexpressed in a variety of epithelial carcinomas, including neuronal, breast, and lung (Normanno et al., 2006; Bakker et al., 2017). It is subject to multiple regulatory cues including the ECM (Kim et al., 2011; Stevens et al., 2017). ECM composition is altered dynamically during cancer progression (Lu et al., 2012; Pickup et al., 2014), making the regulation of EGFR signaling by matrix proteins in cancers of direct interest. When compared across tissues, FBLN1 expression levels are seen to be prominent in the Lung (Consortium, 2015). Lung tissue matrisome studies have also confirmed FBLN1 to be significantly enriched (Krasny et al., 2018) making it an important candidate in ECM function. ECM-mediated EGFR signaling has been shown to regulate cell adhesion and motility (Alexi et al., 2011; Bakker et al., 2017) supporting tumorigenesis (Grahovac and Wells, 2014). Tenascin-C mediated EGFR activation drives cell migration and invasion in melanomas (Shao et al., 2015). Versican, Thrombospondin -1 and SPARC can all regulate EGFR activation, though their direct association is not known (Grahovac and Wells, 2014). FBLN3 binds EGFR through its EGF like repeats inhibiting its activation and function in lung and brain cancer cells (Kim et al., 2014; Wang et al., 2017).

Changes in lung tumor ECM have been shown to affect growth factor signaling pathways regulating EMT, cell proliferation, survival and migration to drive oncogenic transformation

(Rintoul and Sethi, 2001; Pirinen et al., 2005; Lim et al., 2017). Cell-derived matrices (CDM) in better representing the tumor ECM composition elicit a more physiological tumor cell response (Scherzer et al., 2015; Kaukonen et al., 2017). This study reveals the role FBLN1 isoforms FBLN1C and FBLN1D as part of the CDM have in regulating EGFR activation and function in lung cancer cells.

RESULTS

Fibulin-1 Levels Are Significantly Downregulated in Lung Cancer

To test the expression of FBLN1 in lung cancers we first evaluated the TCGA lung cancer dataset (Campbell et al., 2016) and detected ∼ 2.41 fold decrease in FBLN1 transcript levels in lung cancer samples relative to normal lung (**Figure 1A**). NSCLC account for 85% of all lung cancers (Chen et al., 2014), with lung adenocarcinoma (LUAD) and lung squamous cell carcinoma (LUSC) being the most common pathological NSCLC subtypes. We hence looked at the LUAD and LUSC datasets in TCGA which showed a ∼2.75 and ∼2.04 fold decrease in the expression of FBLN1 relative to normal lung tissue (**Figure 1A**). Two LUAD datasets from Oncomine (Okayama et al., 2012; Selamat et al., 2012) also showed a ∼2.8 and ∼4.04 fold decrease in FBLN1 expression relative to normal lung tissue (**Figure 1B**). Together these findings confirm that FBLN1 levels are downregulated in NSCLC. The relative levels and the contribution of FBLN1C and FBLN1D isoforms in NSCLC remain untested. With EGFR overexpression in lung cancers known to be correlated with poor prognosis (Chen et al., 2014), a significant increase in EGFR transcript levels was seen in the TCGA pan lung cancer (∼1.3 fold) and LUSC (∼1.7 fold) [datasets (**Figure 1C**)]. The TCGA LUAD dataset showed EGFR expression to be comparable, though both the Oncomine LUAD datasets show EGFR to be overexpressed relative to normal lung tissues (∼1.89 fold) (∼2.99 fold) (**Figure 1D**), (Okayama et al., 2012; Selamat et al., 2012). FBLN1 and EGFR gene expression data from the TCGA Pan Lung cancer, LUAD and LUSC datasets were also compared using cBioPortal and did not show significant mutual exclusivity or co-occurrence. While such a correlation would support the presence of a functional association between FBLN1 and EGFR, the lack thereof does not preclude existence of the same.

Fibulin-1 Isoforms Inhibit EGFR Activation and Function in Lung Cancer Calu-1 Cells

Of the four known FBLN1 isoforms relative expression of FBLN1C and 1D, known to be ubiquitously expressed, were tested across a panel of cancer cell lines by quantitative RTPCR and were found to be comparable (**Figure 1E**). EGFR expression did, however, vary significantly across these cell lines (**Figure 1E**), (Rusnak et al., 2007). NSCLC cell lines Calu-1 and A549 with comparable FBLN1C and FBLN1D expression and moderate EGFR expression were used to evaluate role of FBLN1 isoforms and their possible crosstalk with EGFR. With no commercial siRNA available for specifically targeting human FBLN1C and FBLN1D we designed siRNA to target a unique 415 bp region (EXON 18, 19, 20) in FBLN1D and 350 bp region (EXON16) in FBLN1C (**Supplementary Figure 1A**). This limited the number of individual siRNA sequences that showed specificity *in silico*, which were then tested *in vivo*. siRNA-mediated knockdown of FBLN1C and FBLN1D in Calu-1 cells (**Supplementary Figures 1B,C**) showed loss of FBLN1C did not affect FBLN1D levels significantly, and vice versa (**Supplementary Figures 1B,C**). The same was tested for by western blot using a total FBLN1 antibody in conditioned culture media (CCM), whole cell lysates (WCL), and cell derived matrix (CDM). FBLN1C and FBLN1D isoforms have a predicted molecular weight (MW) of ∼74 kD and ∼77 kD, respectively, but run closer to ∼100 kDa on SDS PAGE, as reported earlier (Argraves et al., 1990; Hanada and Sasaki, 2018). This could further be affected by their differential glycosylation (Argraves et al., 1990; Aspberg et al., 1999). Isoform specific siRNA mediated knockdown (**Figure 1F** and **Supplementary Figures 1B,C**) shows FBLN1D to run marginally higher on a 10% SDS PAGE as compared to FBLN1C, in CCM, WCL, and CDM (**Figure 1F** and **Supplementary Figures 1B,C**). This differential mobility of FBLN1C and 1D is further confirmed on their overexpression discussed below (**Figure 1I** and **Supplementary Figure 1E**).

We further tested if and how both Fibulin-1 isoforms regulate EGFR activation in Calu-1 cells on sustained serum growth factor stimulation. Loss of FBLN1C and FBLN1D significantly increased EGFR activation (**Figure 1G** and **Supplementary Figure 1B**) without affecting its expression (**Supplementary Figure 1D**). Rapid EGF stimulation (100 ng/ml) of serum deprived Calu-1 cells significantly promoted EGFR activation on loss of FBLN1C and FBLN1D (**Figure 1H** and **Supplementary Figure 1C**). Effect of FBLN1C and FBLN1D on EGFR activation was comparable (**Figures 1G,H**). Overexpression of untagged human FBLN1C and FBLN1D in Calu-1 cells was accordingly seen to significantly suppress EGFR activation (**Figure 1I**). FBLN1C overexpression had a marginally, but significantly, better effect than FBLN1D on EGFR activation. Overexpressed FBLN1 ran at ∼100 kD on 10% SDS PAGE, FBLN1D running marginally higher than FBLN1C (**Figure 1I**), as was seen in knockdown studies above (**Figure 1F** and **Supplementary Figure 1E**).

The effect FBLN1C/1D mediated activation of EGFR has on the migration of Calu-1 cells was tested (Normanno et al., 2006). Wound-healing assays in the presence of serum growth factors showed loss of FBLN1C and FBLN1D (**Supplementary Figure 1C**) to both significantly promote Calu-1 cell migration (**Figure 1J** and **Supplementary Figure 1C**). FBLN1C knockdown (as in overexpression studies) was seen to marginally better promote migration than FBLN1D, Erlotinib treatment (**Supplementary Figure 1F**) significantly inhibiting both their effects. Marginal differences in the relative effects of FBLN1 isoforms on EGFR activation and function could reflect their regulation to be context dependent, possibly mediated by their relative association.

We further wanted to evaluate this FBLN1-EGFR crosstalk in an additional NSCLC cell line and optimized the FBLN1C and FBLN1D knockdown in A549 cells. Quantitative RT-PCR

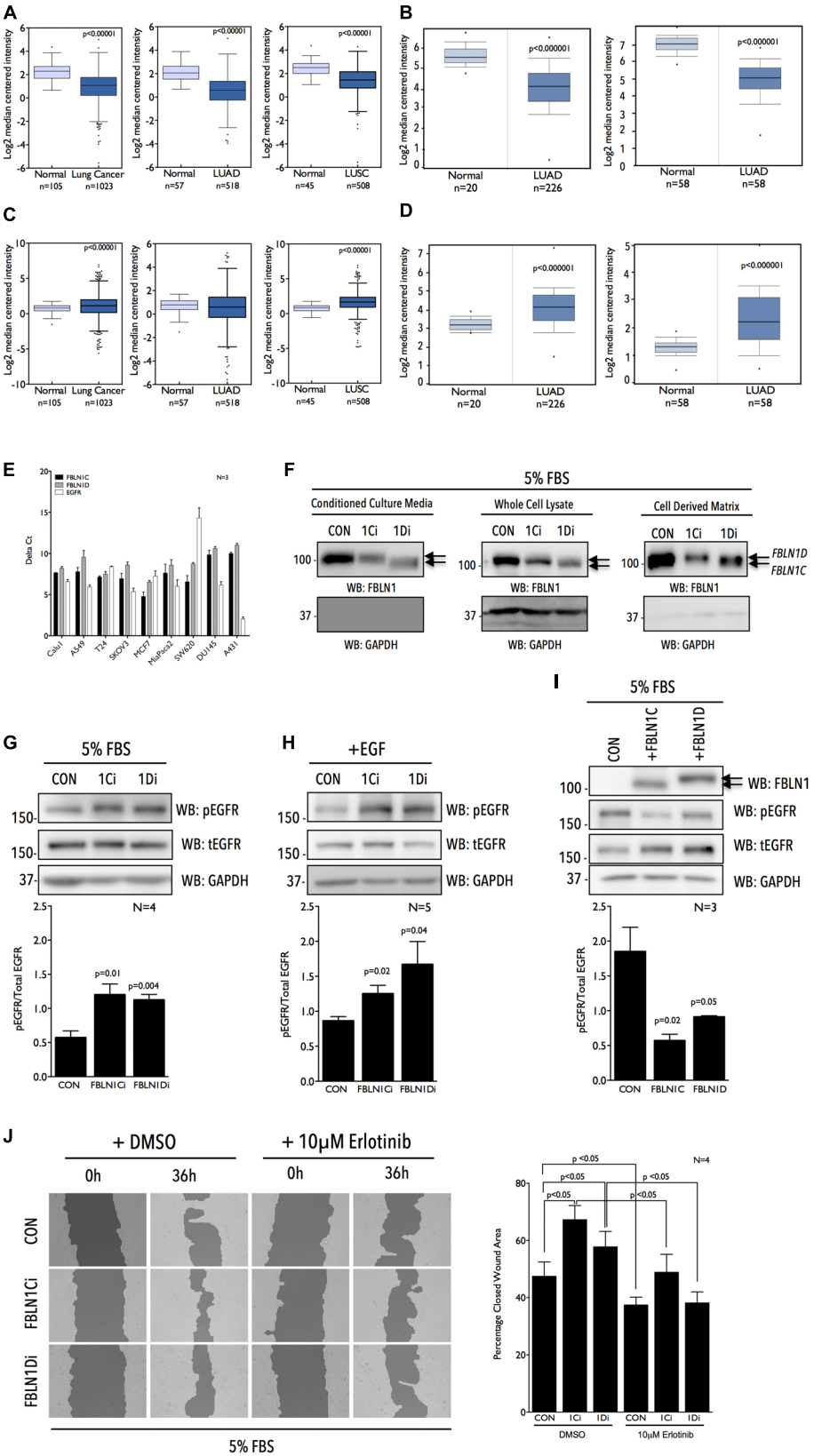

FIGURE 1 | Continued

FIGURE 1 | Fibulin-1 is a negative regulator of EGFR activation and function in Calu-1 cells. Graphs represent transcript levels of FBLN1 **(A,B)** and EGFR **(C,D)** in normal lung and pan lung cancer, lung adenocarcinoma (LUAD) and lung squamous cell carcinoma (LUSC) tissues from TCGA database **(A,C)** and normal lung and lung adenocarcinoma (LUAD) tissues (Okayama et al., 2012 Cancer Research and Selamat et al., 2012 Genome Research) from Oncomine database **(B,D)**. **(E)** RTPCR analysis evaluates FBLN1C (Black bar), FBLN1D (Gray bar), and EGFR (White bar) expression in a panel of cancer cell lines listed. Graph represents mean ± SE of Delta Ct values from three independent experiments. **(F)** Western blot was used to detect Fibulin-1 (WB: FBLN1) and GAPDH (WB: GAPDH) in conditioned culture media, whole cell lysate and cell derived matrix from FBLN1C (1Ci), FBLN1D (1Di) knockdown and control (CON) Calu-1 cells grown with 5% FBS. Arrows mark the position of FBLN1C and FBLN1D isoforms in the representative blots. Blot is best representative of three independent experiments. **(G–I)** Western blot detection of EGFR phosphorylated on tyrosine1173 (WB: pEGFR), total EGFR (WB: tEGFR), and GAPDH (WB: GAPDH) in lysates from Calu-1 cells **(G)** in the presence of serum growth factors (5% FBS), **(H)** on stimulation with EGF (100 ng/ml) for 5 min (+EGF) in serum deprived control (CON), FBLN1C (1Ci), FBLN1D (1Di) knockdown cells and **(I)** in the presence of serum growth factors (5% FBS) in Calu-1 cells overexpressing untagged FBLN1C or FBLN1D. Overexpression of Fibulin-1C (+FBLN1C) and Fibulin-1D (+FBLN1D) was confirmed by western blot (WB: FBLN1). Arrows mark the position of FBLN1C and FBLN1D isoforms in the representative blots. **(G–I)** Bar graphs represents mean ± SE of pEGFR to total EGFR ratio from 3 to 5 independent experiments as indicated in each graph. Statistical analysis of the data was done using the students *t*-test and *p* values are as shown. **(J)** Representative images of wound healing assay done in the presence of serum growth factor (5% FBS) in Control (CON) vs. FBLN1C (1Ci) vs. FBLN1D (1Di) knockdown Calu-1 cells at 0 h and 36 h in the presence of DMSO or 10 μM Erlotinib. Images were analyzed using T-Scratch software and the percent closed wound area calculated. Graph represents mean ± SE from four independent experiments. Statistical analysis of the data was done using two-way ANOVA and *p* values are as shown.

results showed that while FBLN1C knockdown was specific (**Supplementary Figure 1G**), knockdown of FBLN1D was not and affected FBLN1C levels as well (**Supplementary Figure 1G**). We further overexpressed FBLN1C and FBLN1D to evaluate its effect on EGFR activation. Like with Calu-1 cells (**Figure 1G**), FBLN1C overexpression significantly inhibited EGFR activation, while FBLN1D overexpression showed a similar trend (**Supplementary Figure 1H**). This coupled with further studies evaluating the association of FBLN1 and EGFR in A549 cells (**Supplementary Figures 3C–E**) suggests this regulatory crosstalk could be conserved across NSCLC cells, though this needs further evaluation.

Fibulin-1C and Fibulin-1D Bind EGFR, Independent of Its Activation

The association of FBLN1 and EGFR could regulate its activation and function in cells, and was tested by immunoprecipitation studies. HEK293T cells overexpressing untagged FBLN1C/FBLN1D and EGFR were used to immunoprecipitate FBLN1 using anti-FBLN1 antibody and EGFR was seen to be co-immunoprecipitated (**Figures 2A,C**). Similarly, overexpressed EGFR immunoprecipitated with an anti-EGFR antibody co-immunoprecipitated FBLN1 (**Figures 2B,D**). This FBLN1-EGFR association could be direct or indirect, mediated through other proteins. Lack of FBLN1C or FBLN1D specific antibodies did not allow for the testing of their relative association with EGFR. We next tested if EGF mediated EGFR activation affects its association with FBLN1C/1D. HEK293T cells over expressing EGFR when stimulated with EGF (100 ng/ml for 5 min) increased EGFR activation (**Supplementary Figures 2A,B**), but did not affect its association with FBLN1C or FBLN1D (**Figures 2E,F**). Quantitation of EGFR intensity in FBLN1 pulldown confirms the same (**Figures 2E,F**). This suggests that while FBLN1 can bind and regulate EGFR activation (**Figures 1G–I**) its activation status does not affect their association (**Figures 2E,F**).

Matrix Fibulin-1 Associates With EGFR in Calu-1 Cells

We further tested if this association is detectable for endogenous FBLN1C/1D and EGFR in Calu-1 cells, where our studies show them to be functionally related (**Figures 1G–J**). Immunoprecipitation of endogenous FBLN1 using anti-FBLN1 antibody from WCL, failed to detect any association with EGFR (**Figure 3A** and **Supplementary Figure 3A**). This could reflect the fact that only a small fraction of the endogenous proteins bind each other or their association could be spatially or temporally regulated making it challenging to detect in whole cell lysate IP studies. FBLN1 is likely to be enriched in the matrix (Krasny et al., 2018), which could support its association and regulation of EGFR. To test this, we used a detergent free decellularization protocol to isolate cell-derived matrix (CDM). We compared equal protein from CDM and whole cell lysate of Calu-1 cells and confirmed a 11 fold enrichment of FBLN1 in the CDM (**Figure 3B**). Immunostaining of this CDM, further confirmed the presence of FBLN1 (**Figure 3C**), with decellularization confirmed by the absence of any detectable staining with phalloidin (**Figure 3C** and **Supplementary Figure 3B**). EGFR levels while much less were detected in these CDM preparations (**Figure 3B**) allowing us to test for its association with FBLN1. Immunoprecipitation of FBLN1 from the CDM does detect the co-immunoprecipitation of matrix associated EGFR (**Figure 3D**), unlike in WCL (**Figure 3A**). We also evaluated the association of matrix FBLN1 and EGFR in NSCLC A549 cells. A549 cells are known deposit less matrix as compared to Calu-1 cells (Andriani et al., 2016; Peixoto et al., 2019). FBLN1 levels in A549 CDMs were hence not as enriched (**Supplementary Figure 3C**) when compared to Calu-1 CDMs (**Figure 3B**). Immunoprecipitation of FBLN1 from WCL (**Supplementary Figure 3D**) and CDM (**Supplementary Figure 3E**) of A549 cells could detect FBLN1 association with EGFR only in the CDM (**Supplementary Figure 3E**), similar to that of Calu-1 cells. Together these findings confirm the association of endogenous FBLN1 with EGFR to be prominent in the CDM.

Matrix Derived Fibulin-1 Regulates EGFR Activation and Localization to Control Cell Adhesion and Spreading

The ECM has been known to act as a reservoir for growth factors and growth factor receptors to modulate cellular behavior (Grahovac and Wells, 2014; Zhu and Clark, 2014; Hastings et al., 2019). To determine if matrix derived FBLN1, seen to

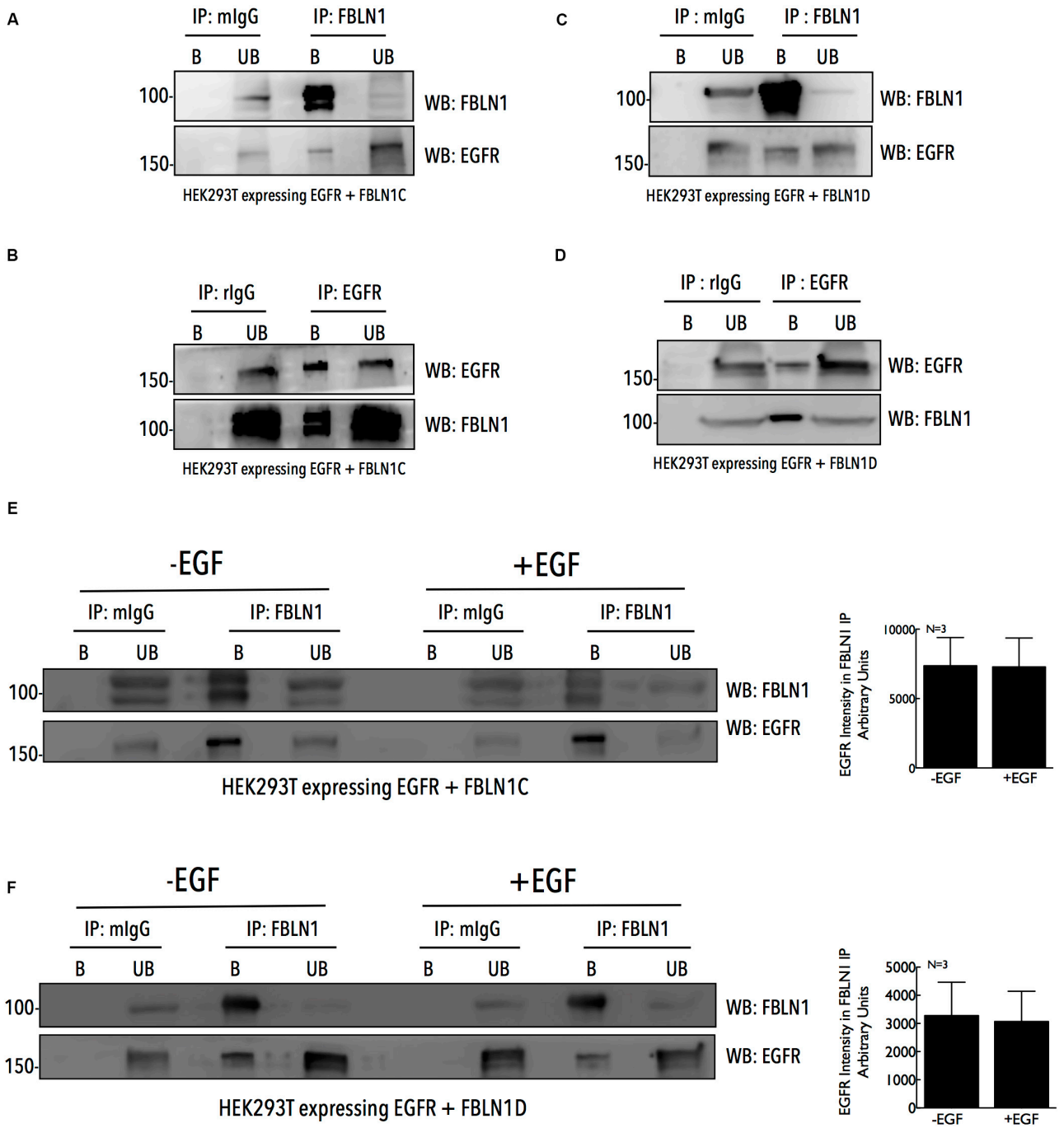

FIGURE 2 | Fibulin-1C and Fibulin-1D co-immunoprecipitate EGFR, independent of its activation. Immunoprecipitated Fibulin-1 **(A,C,E,F)** (IP: FBLN1) and EGFR **(B,D)** (IP: EGFR) from HEK 293T cells, expressing EGFR-GFP **(B,D)** and untagged Fibulin-1C **(A,B)** or untagged Fibulin-1D **(C,D)** were compared to mouse IgG **(A,C,E,F)** (IP : mIgG) and rabbit IgG **(B,D)** (IP: rIgG), respectively. Immunoprecipitation of Fibulin-1 (WB: FBLN1) and EGFR (WB: EGFR) along with their co-precipitation was detected by western blot. The immunoprecipitated (bound) protein eluted and un-bound fractions (B vs. UB) were also compared by western blot. The results are representative of three independent experiments. **(E,F)** HEK 293T cells expressing untagged FBLN1C or FBLN1D and EGFR-GFP were serum starved, stimulated with EGF (100 ng/ml) for 5 min and Fibulin-1C **(E)** and Fibulin1D **(F)** immunoprecipitated. These were probed by western blot for Fibulin-1 (WB: FBLN1) (to confirm IP) and EGFR (WB: EGFR) (to detect Co-IP). The results are representative of three independent experiments that gave similar results. Bar graphs on the right represent mean ± SE of EGFR intensity detected in the FBLN1 IP with (+EGF) and without (–EGF) EGF treatment from three independent experiments as indicated.

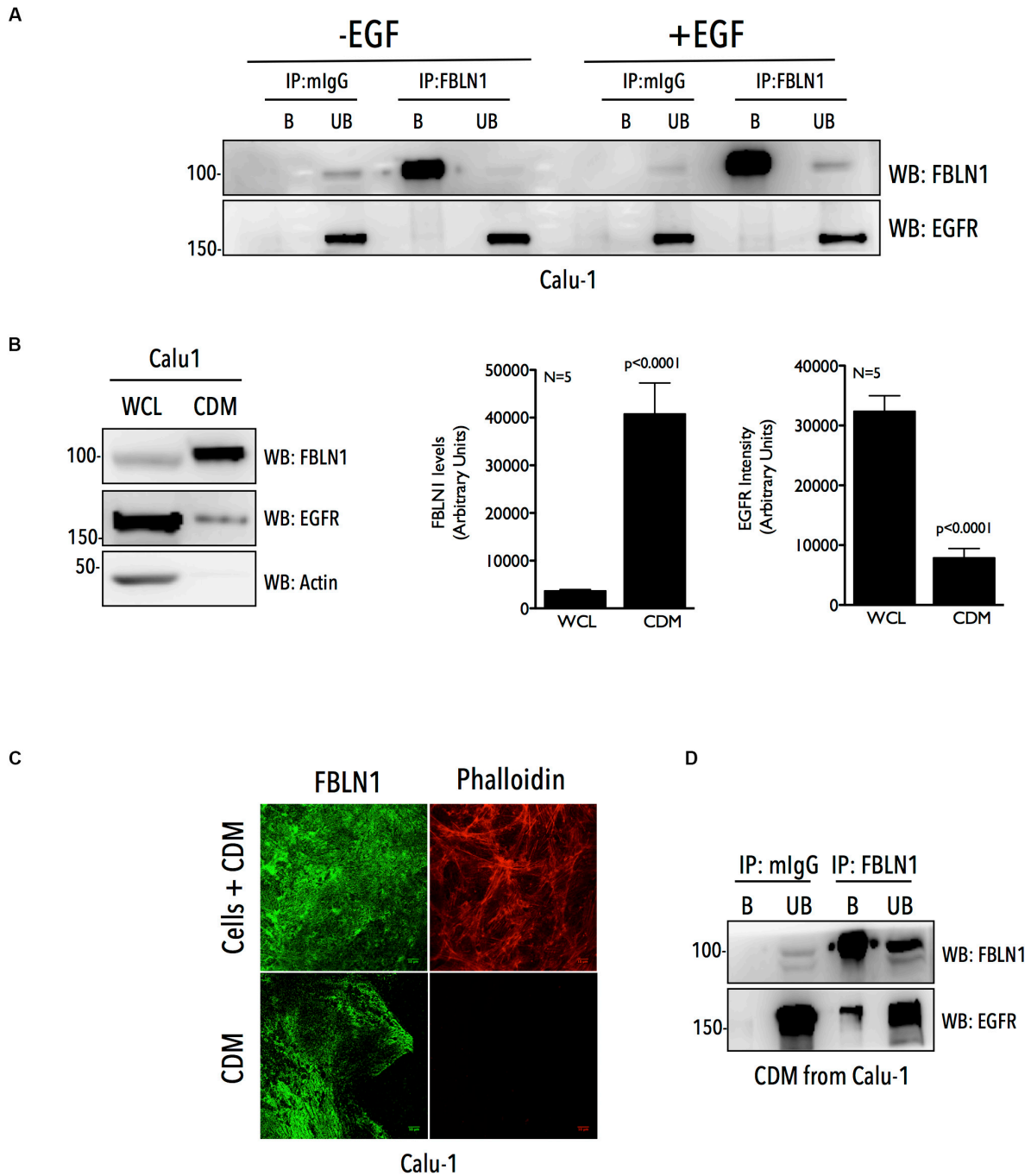

FIGURE 3 | Cell derived matrix Fibulin-1 co-immunoprecipitates EGFR in Calu-1 cells. **(A)** Calu-1 cells serum starved for 12 h were stimulated with EGF (100 ng/ml) for 5 min and endogenous Fibulin-1 (IP: FBLN1) was immunoprecipitated and compared to mouse IgG (IP: mIgG). Immunoprecipitation of Fibulin-1 (WB: FBLN1) and co-precipitation of EGFR (WB: EGFR) was tested by western blot. The immunoprecipitated (bound) protein eluted and un-bound fractions (B vs. UB) were also compared by western blot. The results are representative of three independent experiments. **(B)** 10 μg of whole cell lysate (WCL) and cell derived matrix (CDM) from Calu-1 cells were probed for Fibulin-1 (WB: FBLN1), EGFR (WB: EGFR), and Actin (WB: Actin) by western blot. Bar graphs represent mean ± SE of Fibulin-1 and EGFR band intensities in CDM and WCL from five independent experiments. Statistical analysis of the data was done using the student's *t* test and *p* values are as shown. **(C)** Calu-1 cells and CDM made from these cells were fixed and immunostained to detect FBLN1 and Actin (phalloidin alexa-594). Representative confocal images for each are shown. Scale bar represents 10 μm. Data is representative of three independent experiments with similar results. **(D)** Endogenous Fibulin-1 from CDM of Calu-1 cells was immunoprecipitated (IP: FBLN1) and compared to mouse IgG (IP: mIgG). Immunoprecipitation of Fibulin-1 (WB: FBLN1) and co-precipitation of EGFR (WB: EGFR) was tested by western blot. The immunoprecipitated (bound) protein eluted and un-bound fractions (B vs. UB) were also compared by western blot. The results are representative of three independent experiments.

bind EGFR (**Figure 3D**), can regulate its activation and function in Calu-1 cells, we isolated CDM from control, FBLN1C and FBLN1D knockdown cells and tested their role in regulating EGFR activation and migration in replated Calu-1 cells. siRNA mediated knockdown of FBNL1C and FBLN1D in WCL of Calu-1 cells is specific (**Figure 1F**) which is reflected in their CDMs (**Figures 1F**, **4A** and **Supplementary Figure 4A**). Western blot detection of FBLN1 in knockdown CDMs from Calu-1 cells grown with serum showed FBLN1C/1D isoforms to retain their differential mobility as reported earlier (**Figures 4A**, 1F). The protein content of CDMs made by similar number of control vs. knockdown cells was largely comparable (**Supplementary Figures 4B,C**). CDMs thus derived from control and knockdown Calu-1 cells were used to replate untreated Calu-1 cells and their function compared (**Figure 4A**). Re-plating of Calu-1 cells on knockdown CDMs for 18 h did not visibly affect FBLN1 levels (**Figure 4A** right panel). We hence tested the migration of individual Calu-1 cells replated on CDMs in the presence of serum growth factors. This revealed no significant difference in the distance, velocity and directionality of Calu-1 cells (**Figures 4B,C**) on control vs. FBLN1C vs. FBLN1D knockdown CDMs (**Supplementary Figure 4D**). We hence tested the EGFR activation status in Calu-1 cells replated on CDMs for 18 h in the presence of serum and noted no change in the EGFR activation on knockdown CDMs, relative to control (**Figure 4D** and **Supplementary Figure 4E**).

Since this reflected a more sustained growth factor mediated activation of EGFR on knockdown CDMs, we asked if a more rapid and robust activation by externally added EGF (5 min stimulation) can change the cellular response. Indeed, on EGF stimulation EGFR activation was significantly better in cells plated on FBLN1C (∼1.5 fold) and FBLN1D knockdown (∼2.0 fold) CDMs, relative to control CDM (**Figure 4E** and **Supplementary Figure 4F**). This is comparable to results seen on EGF stimulation of FBLN1 KD Calu-1 cells (**Figure 1H**), suggesting matrix associated Fibulin-1 to be a major mediator of this regulatory crosstalk. Such a rapid activation of EGFR is reported on re-adhesion of cells to ECM promoting cell binding and spreading (Normanno et al., 2006; Guo et al., 2015). We hence tested the possible impact Fibulin-1 in the CDM could have in mediating re-adherent Calu-1 cell adhesion and spreading. Cells were detached and replated on control vs. FBLN1 knockdown CDMs for 20 min to trigger integrin signaling and EGFR activation to drive adhesion and cell spreading (Su and Besner, 2014; Lopez-Luque et al., 2019). Cells replated on FBLN1C knockdown and FBLN1D knockdown derived CDMs attached and spread significantly better than control CDMs, which was significantly reduced by Erlotinib mediated inhibition of EGFR (**Figures 5A,B** and **Supplementary Figure 5A**). We further looked at the localization of activated EGFR (pEGFR) in spreading cells and found it to be enriched at membrane ruffles in cells replated on FBLN1C knockdown CDM and FBLN1D knockdown CDM, relative to control CDM (**Figure 5C** and **Supplementary Figure 5B**). Since EGFR has been known to be transactivated in a ligand independent manner via integrin binding to Fibronectin (Guo et al., 2015), we tested the levels of Fibronectin (FN) in Calu-1 cells upon FBLN1C and FBLN1D knockdown and did not see any differences (**Supplementary Figure 5C**). Taken together these studies identify a role for matrix bound FBLN1 to spatially regulate EGFR activation in Calu-1 cells to regulate cell function.

DISCUSSION

As part of the tumor microenvironment the ECM not only provides structural support but through the biophysical and biochemical cues creates a dynamic microenvironment that helps cancer cells evade growth suppression, acquire resistance to apoptosis and initiate metastasis (Lu et al., 2012; Pickup et al., 2014; Walker et al., 2018). ECM molecules like Fibulin-3, Tenascin-C and Emilin-2 have been known to associate with growth factor receptors like EGFR to regulate its activation and function during cancer progression (Iyer et al., 2008; Grahovac and Wells, 2014; Kim et al., 2014; Paulitti et al., 2018). Fibulins as part of the ECM are seen to interact with various basement membrane proteins and elastic fibers (Argraves et al., 2003; Chu and Tsuda, 2004). FBLN2, FBLN3, and FBLN5 have been shown to regulate Notch (Baird et al., 2013), Insulin Growth Factor receptor (IGF1R) (Kim et al., 2014), EGFR signaling pathways, respectively, in glioma (Hu et al., 2009), lung (Yue et al., 2009; Kim et al., 2014; Wang et al., 2017), and pancreatic cancers (Camaj et al., 2009). Both FBLN1, FBLN3 are highly expressed in normal adult lung and downregulated in lung cancer cells (NSCLC) (Yue et al., 2009; Kim et al., 2014; Cui et al., 2015). FBLN3 is also shown to directly bind EGFR (Camaj et al., 2009) and affects its activation in NSCLC, though its effect on EGFR mediated tumor progression is marginal (Kim et al., 2014). TCGA and Oncomine data both show FBLN1 (and FBLN3–data not shown) to be downregulated in NSCLC, with significant overexpression of EGFR (**Figures 1A–D**; Okayama et al., 2012; Selamat et al., 2012; Campbell et al., 2016). This study in identifying a role for matrix FBLN1 in regulating EGFR activation in NSCLC Calu-1 cells further adds to our understanding of this regulatory crosstalk in lung cancers. Our results show that FBLN1 suppresses EGFR activation, and that loss of FBLN1C/FBLN1D (as seen in lung cancers) can promote EGFR dependent cellular function.

Structurally, Fibulin-1 comprises of several EGF like modules that could be important for its association with EGFR, as seen for other matrix proteins (Argraves et al., 1990; Timpl et al., 2003; Grahovac and Wells, 2014). FBLN1 has also been shown to interact with other EGFR interacting proteins like Versican, Fibronectin and HB-EGF, which could indirectly mediate the association of FBLN1 with EGFR. It would also be interesting to determine whether FBLN1C and FBLN1D also bind EGFR ligands (i.e., EGF and HB-EGF) differentially and the impact that has on this regulation. Such a regulation could also contribute to the differential effects seen in wound healing assays, possibly occurring as a result of increased HB-EGF shedding which could have an effect on EGFR activation and cell migration (Brooke et al., 2002; Yin et al., 2007) as seen in **Figure 1H**. Both the FBLN1 isoforms, FBLN1C and FBLN1D bind EGFR (**Figures 2A–D**), and the enrichment of FBLN1 in CDM allows the detection of

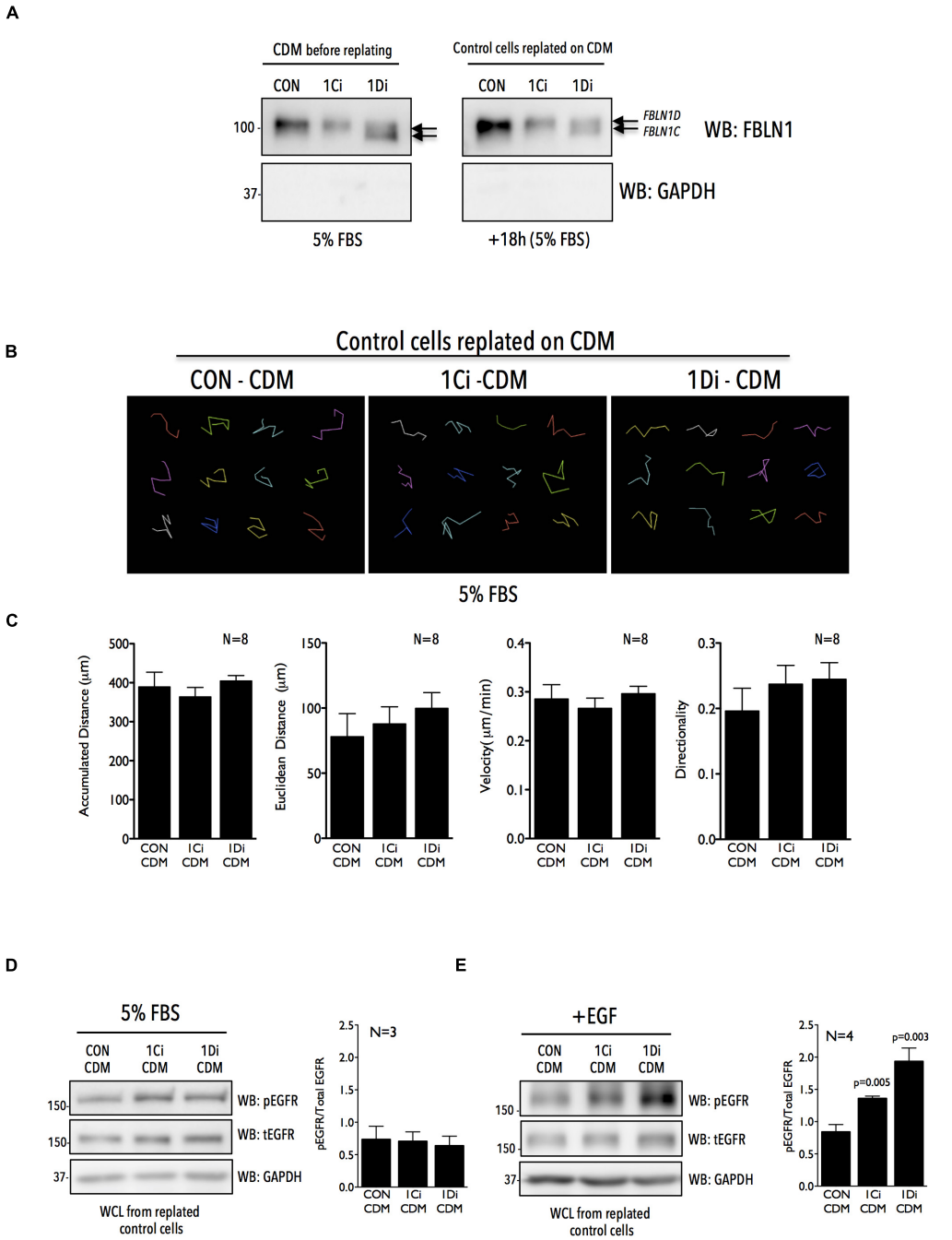

FIGURE 4 | Matrix Fibulin-1 regulates EGF dependent EGFR activation in Calu-1 cells. **(A)** Endogenous Fibulin-1 (WB: FBLN1) and GAPDH (WB: GAPDH) were detected by western blot in cell derived matrix (CDM before replating) made from control (CON), FBLN1C (1Ci) and FBLN1D (1Di) knockdown Calu-1 cells, grown with serum (5% FBS) for 72 h. Calu-1 cells were replated on this CDM and grown for 18 h with serum [+18 h (5% FBS)] and levels of Fibulin-1 (WB: FBLN1) and GAPDH (WB: GAPDH) detected by western blot in cell derived matrix (CDM after replating) and compared to those seen in CDM before replating. FBLN1C and FBLN1D isoforms detected in blots of knockdown lysates are marked by arrows. Blot is best representative of three independent experiments that gave similar results. **(B)** Representative individual migration tracks of Calu-1 cells adherent in the presence of serum growth factors (5% FBS) on CDM (made as detailed above) from control (CON-CDM), FBLN1C (1Ci-CDM), and FBLN1D (1Di-CDM) knockdown Calu-1 cells. **(C)** Accumulated distance, euclidean distance, velocity and directionality of 100 migrating cells (per experiment) and represented in the bar graphs as mean ± SE from eight independent experiments. *p* values were calculated using one-way ANOVA and Tukey's *post hoc* test and represented if found to be significant. **(D,E)** Western blot detection of EGFR phosphorylated on tyrosine 1173 (WB: pEGFR), total EGFR (WB: tEGFR) and GAPDH (WB: GAPDH) in Calu-1 plated on CDM (made as detailed above) from control (CON-CDM), FBLN1C (1Ci-CDM) and FBLN1D (1Di-CDM) knockdown cells **(D)** in the presence of serum growth factors (5% FBS) **(E)** on stimulation with EGF (100 ng/ml) for 5 min (+EGF) in serum deprived Calu-1 cells. Bar graphs represents mean ± SE of pEGFR to total EGFR ratio from 3 or 4 independent experiments as indicated. Statistical analysis of the data was done using the students *t*-test and *p* values are as shown.

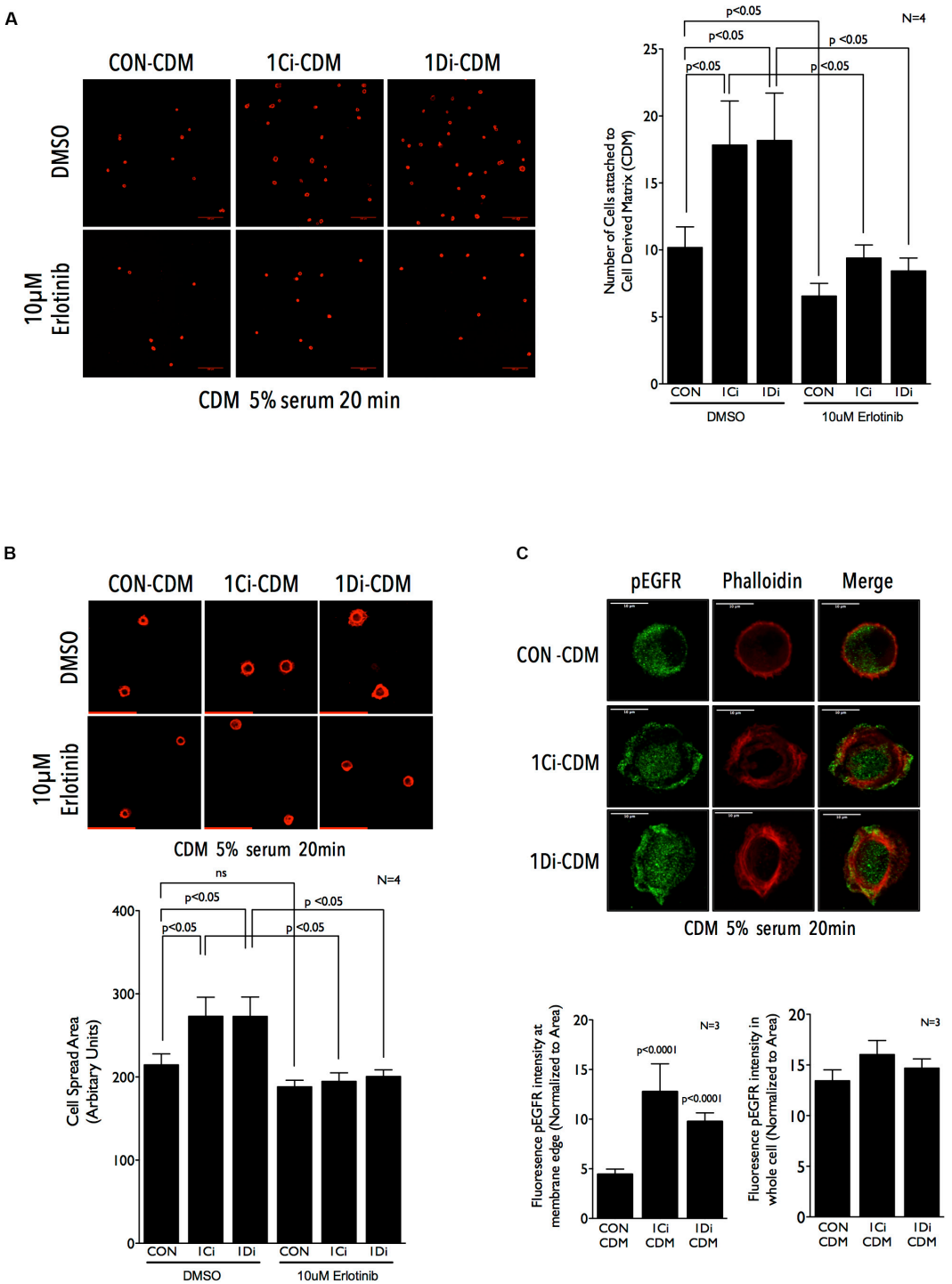

FIGURE 5 | Matrix Fibulin-1 regulates EGFR-dependent adhesion and spreading in re-adherent Calu-1 cells. **(A,B)** Representative images of Calu-1 cells re-adherent for 20 min in the presence of serum growth factors (5% FBS) with DMSO or 10 μm Erlotinib on CDM from control (CON-CDM), FBLN1C (1Ci-CDM) and FBLN1D (1Di-CDM) knockdown Calu-1 cells. Bar graph represent mean ± SE of **(A)** number of cells attached **(B)** cell spread area, from 10 or more frames each in four independent experiments. Statistical analysis of the data was done using two-way ANOVA and *p* values are as shown. **(C)** Representative images of Calu-1 cells replated for 20 min in the presence of on CDM from control (CON-CDM), FBLN1C (1Ci-CDM) and FBLN1D (1Di-CDM) knockdown Calu-1 cells shows the localization of EGFR phosphorylated on tyrosine1173 (pEGFR) and actin cytoskeleton (phalloidin), with merged images. Scale bar represents 10 μm. The intensity of pEGFR in region of 0.5 μm from the cell edge was measured and normalized to its area (left graph). The same was done for the entire cell as well (right graph) and compared between control (CON), FBLN1C (1Ci-CDM) and FBLN1D (1Di-CDM) knockdown Calu-1 cells. The bar graph represents mean ± SE of these from three independent experiments. Statistical analysis of the data was done using two-way ANOVA and *p* values are as shown.

its association with EGFR (**Figure 3D**). Similar to other ECM proteins that bind EGFR, FBLN1 mediated tethering of EGFR to the ECM can limit its availability for ligand binding on the cell surface via steric hindrance (Santra et al., 2002; Camaj et al., 2009), this by affecting its clustering and dimerization can also regulate its activation (Ferguson et al., 2003; Tsai and Nussinov, 2019). Further, the stability, internalization and degradation of EGFR could also be affected by matrix FBLN1 to regulate its cellular function. EGFR activation does not affect its association with FBLN1C or 1D, which is distinctly different from FBLN3 (Camaj et al., 2009; Hu et al., 2014). This could further drive the impact FBLN1 downregulation has on EGFR dependent lung cancer cells (NSCLC) (Yue et al., 2009; Kim et al., 2014; Cui et al., 2015).

Fibulin-1 isoforms in Calu-1 cells show a distinct difference in their mobility on SDS PAGE, reflecting possible changes in their post-translational modification (Argraves et al., 1990; Aspberg et al., 1999), which is retained in the FBLN1 secreted in the conditioned culture medium and matrix bound FBLN1 (**Figure 1F**). This is further evident in isoform specific knockdowns of FBLN1C/1D (**Figure 1F**) and their overexpression (**Figure 1I**). Fibulin-1 isoforms differ marginally in their relative effects on EGFR activation, suggesting their regulation of its activation and function could possibly be context dependent. One of the regulating factors could be the nature of EGF stimulation. In response to sustained growth factor mediated EGF stimulation (5% FBS) FBLN1C and FBLN1D comparably affect EGFR activation in Calu-1 cells (**Figure 1G**). Rapid and robust activation of EGFR by stimulation with EGF (100 ng/ml for 5 min) revealed a more pronounced and differential regulation by FBLN1 isoforms, with FBLN1D seemingly a more potent regulator (**Figures 1H**, **4E**). This effect is seen in Calu-1 cells lacking FBLN1D (**Figure 1H**) and Calu-1 cells plated on FBLN1D knockdown CDMs (**Figure 4E**).

The differential stimulation of EGFR on FBLN1 mediated cell function is further evident in the effect FBLN1C, FBLN1D knockdown has on migration in the wound healing versus single cell migration of Calu-1 cells re-plated on knockdown CDMs. With FBLN1 enriched in CDM we expect the behavior of Calu-1 cells in both these conditions to be comparable. However, in wound healing assays, loss of FBLN1C and 1D promotes Calu-1 cell migration, while this effect is not seen in single cell migration when control Calu-1 cells are re-plated on FBLN1C and 1D knockdown CDMs in the presence of 5% FBS. Calu-1 cells plated on FBLN1 knockdown CDMs in the presence of 5% FBS show no differential EGFR activation (**Figure 4D**), unless cells are rapidly stimulated with externally added EGF (**Figure 4E**). This suggests that the nature of EGFR stimulation (Serum vs. EGF) could affect the impact FBLN1 has on cellular function. In wound healing assays, cellular damage by the scratch releases ATP, which stimulates the shedding of HB-EGF mediating the transactivation of EGFR (Yin et al., 2007) could drive the differential migration of FBLN1 knockdown cells. Studies have shown FBLN1C binds HB-EGF (Brooke et al., 2002), which is a prominently overexpressed ligand for EGFR in NSCLC (Hsieh et al., 2017; Yotsumoto et al., 2017). This could in part contribute to the differential effect FBLN1C has relative to FBLN1D in EGFR dependent migration and wound closure.

Epidermal growth factor receptor has been known to play a major role in mediating cell adhesion (Andl et al., 2003; Abu-Ali et al., 2008; Ungewiss et al., 2018) and cell spreading (Marcoux and Vuori, 2003; Abu-Ali et al., 2008; Balanis et al., 2011; Morello et al., 2011). EGFR mediated activation of PKC is known to regulate cell matrix adhesion in breast and brain cancers (Sun et al., 2005; Micallef et al., 2009). Integrin mediated adhesion is seen to regulate EGFR activation by recruiting Vav2 (GEF for Rac) via PI3 kinase to promote cell spreading (Thalappilly et al., 2010). EGFR also binds FAK via SRC-3Δ4 adaptor molecule and phosphorylates it at Y925 to promote cancer cell migration and invasion (Long et al., 2010). Inhibition of EGFR disrupts cell spreading on fibronectin, with reduced membrane ruffles (Thalappilly et al., 2010). CDM mediated rapid stimulation of EGFR in Calu-1 cells regulates cell adhesion and its localization at lamellopodial ruffles and cell spreading (**Figure 5**). Matrix Fibulin-1 levels by affecting ECM composition and architecture could influence the integrin-EGFR crosstalk in these cells. Although, no differences in the levels of Fibronectin are seen upon FBLN1 knockdown in Calu-1 cells (**Supplementary Figure 5C**), further studies are required to evaluate the effects loss of Fibulin-1 has on Fibronectin polymerization and its incorporation into the ECM. With the known role EGFR activation and localization to the mitochondria has in lung cancer cells (Che et al., 2015), evaluating the impact matrix Fibulin-1 could have in mediating mitochondrial function would be of much interest.

Cancer cell secreted matrix proteins and growth factors are known to support tumor invasion (Walker et al., 2018; Hoshiba, 2019). Studies have shown CDM from cancer cells drive cell adhesion, migration, invasion, angiogenesis and chemo resistance (Senthebane et al., 2017; Hoshiba, 2019; Nallanthighal et al., 2019). Changes in the composition of the cancer CDM can hence affect neighboring cancer and normal cells influencing tumor organization and progression (Attieh et al., 2017; Erdogan et al., 2017; Paolillo and Schinelli, 2019). Non-small-cell lung cancers (NSCLCs) have diverse pathological features, that are a result of genetic and cellular heterogeneity (Chen et al., 2014). Several components including origin of cells, genetic alterations and microenvironmental factors all contribute to the lineage identity of lung tumors (Fong et al., 2003; Sharma et al., 2007; Chen et al., 2014; Malik and Raina, 2015). Cell-derived matrix from FBLN1C/FBLN1D knockdown Calu-1 cells regulating EGFR and its function (cell adhesion and spreading) mimics the loss of FBLN1 phenotype in Calu-1 cells. The possible overlap and differences in the role FBLN1C/1D on EGFR function could extend the impact tumor microenvironments could have in regulating cell signaling and behavior in heterogenous lung tumors.

MATERIALS AND METHODS

Cell Culture

Calu-1 cells (ECACC), A549 (ECACC), and HEK293T (Obtained from Dr. Aurnab Ghose, IISER Pune) cells were cultured in Dulbecco's Modified Eagles Medium (DMEM) High, supplemented with 5% v/v FBS (Invitrogen), and

1% v/v Penicillin/Streptomycin (Invitrogen). Media was changed every 3 days and cells were passaged at 70–80% confluency with Trypsin (Invitrogen). Cell lines were grown at 37°C under 5% CO_2. All cell lines were routinely tested for mycoplasma contamination.

Plasmids and siRNAs

Untagged FBLN1C and FBLN1D constructs were obtained from Dr. Marion Cooley (Augusta University, Augusta, GA, United States). GFP tagged EGFR construct was bought from Addgene. Sequences of all the constructs were verified before use. FBLN1C and FBLN1D siRNAs were designed using Dharmacon Design Center and synthesized in duplex form from Sigma with [dT] overhangs under standard desalting conditions. The siRNA's were reconstituted with nuclease free water and stored at −20°C until further use.

Transfections and Knockdowns

Cells were transfected using Polyethanolamine (PEI) (Sigma) according to the manufacturer's protocol. Transfections were done in 6-well plates or 10-cm dishes with complete medium using 2 μg or 10 μg DNA, respectively, for 48 h (for all constructs used). At 48 h after transfection, cells were serum deprived for 12 h in low-serum DMEM (containing 0.2% FBS) and then used for immunoprecipitation (IP) experiments. Calu-1 and A549 cells transfected with FBLN1C or FBLN1D were subjected to cell lysis at the end of 48 h post transfection.

siRNA mediated knockdown was performed using RNAiMAX (Invitrogen). Cells were plated for 6 h at a density of 2.4×10^5 per well in a six well plate followed by first shot of FBLN1C (5 picomoles) and FBLN1D siRNA knockdown (5 picomoles). Media was changed 24 h post knockdown along with a second shot of knockdown. Media was changed 24 h post second shot knockdown and the cells were trypsinized, counted and replated for assays as described below.

Preparation of Conditioned Culture Media (CCM)

Control, FBLN1C and FBLN1D knockdown Calu-1 cells (2.5×10^5 cells/well) were grown for 72 h (upon replating) in six well plates without media change. At then end of 72 h, 500 ul of the CCM from the CON, FBLN1C and FBLN1D knockdown Calu-1 cells was collected. CCM was then centrifuged at 1000 rpm for 5 min at room temperature (RT) to remove any cell debris. 400 ul of this supernatant CCM was collected and 100 ul of 5X laemmli added, boiled at 95°C, cooled and used for SDS PAGE.

RNA Extraction and qRT-PCR

RNA was isolated using TRIzol (Invitrogen) and cDNA was prepared from total RNA using iScript cDNA synthesis kit (Bio-Rad) according to the manufacturer's specifications. Undiluted cDNA was used in 5 μl quantitative PCR (qRT-PCR) reaction with SYBR FAST qPCR master mix (Kapa Biosystems) in a Bio-Rad CFX96 Real Time System using the following human primer sequences. FBLN1C 5′ caactgctccatcaacgaga 3′ (Forward), 5′ attctcagaggcagcttgga 3′ (Reverse), FBLN1D 5′ cgagtgccctgagaactacc 3′ (Forward), 5′ gagatgacggtgtgggagat 3′ (Reverse), EGFR 5′ gatacccaggaccaagccac 3′ (Forward), 5′ ggaatgcaacttccaaaatgtg 3′ (Reverse), Actin 5′ ctcctgagcgcaagtactcc 3′ (Forward), 5′ ccggactcgtcatactcctg 3′ (Reverse). All samples were amplified in triplicates. Fold change in gene expression relative to control was calculated using the delta delta Ct.

Antibodies and Reagents

The following antibodies were used for western blotting: mouse anti-FBLN1 (Santa Cruz Biotechnology SC25281) at 1:1000 dilution, mouse anti-Fibronectin (DSHBS1-1634) at 1:250 dilution, rabbit anti-EGFR (Cell Signaling 2232S) at 1: 1000 dilution, rabbit anti-phospho-EGFR Y1173 (R&D systems AF1095) at 1:1000 dilution, mouse anti- βActin (Abcam Clone ACTN05 (C4) Ab3280) at 1:2000 dilution and rabbit anti-GAPDH (G9545 Sigma Aldrich) at 1:5000 dilution. Horseradish Peroxidase conjugated secondary antibodies (Anti-Mouse and Anti-Rabbit) were used at a dilution of 1:10,000 and were purchased from Jackson Immuno Research.

Opti-MEM was purchased from Invitrogen (cat. no. 22600-050). Ammonium Hydroxide (NH_4OH, 05002-1L), DMSO (D2438) and EGF was purchased from Sigma (E9644). Erlotinib Hydrochloride was purchased from Santa Cruz Biotechnology (CAS- 183319-69-9). Protein A Sepharose beads (GE 17-0780-01) were purchased from Sigma Aldrich. Mouse IgG (Millipore 12-371) and Rabbit IgG (Millipore 12-370) were also purchased from Sigma Aldrich.

Alexa Fluor 488/594 conjugated to Phalloidin (Invitrogen, cat. no. A12379 and A12381) was used at a dilution of 1:400. Secondary antibodies conjugated to Goat anti-mouse IgG Alexa Fluor 488, Goat anti-Rabbit IgG Alexa Fluor 488 were used at a dilution of 1:500 and was purchased from Invitrogen Molecular Probes (cat. no. A-11029 and A-11008). Fluoromount-G (cat. no. 0100-01) was purchased from Southern Biotech.

Immunofluorescence Staining for Fibulin-1 and Phosphorylated EGFR (Y1173)

Calu-1 Cells or CDM on coverslips were fixed with 3.5% paraformaldehyde (PFA) in phosphate buffered saline (PBS) for 15 min at RT. Cells were permeabilized with PBS containing 5% bovine serum albumin (BSA) and 0.05% Triton X-100 for 15 min at RT. Blocking was done with 5% BSA in PBS for 60 min at RT followed by incubation with anti-Fibulin-1 (1:100, 90 min incubation at RT) or anti-phosphorylated EGFR (Y1173) antibody (1:100, 180 min incubation at RT) diluted in 1% BSA in PBS. The coverslips were then washed three times for 5 min each with 0.1% BSA in PBS. Coverslips were then incubated with anti-mouse Alexa Flour 488 (1:500) and Alexa Flour 594 Phalloidin (1:500) in 1% BSA in PBS for 1 h at RT. The coverslips were then washed three times for 5 min each with 0.1% BSA in PBS and mounted using Fluoromount-G and left to dry for 24 h followed by imaging using a confocal microscope.

Preparation of Cell Derived Matrix (CDM)

Control CDM for Western Blotting and Immunoprecipitation Experiments

Calu-1 cells were plated at a density of 4×10^5 cells in a 100 mm dish and cultured for 5 days. Cells reached 100% confluency at the end of day 5. On day 6, media was aspirated followed by a gentle PBS wash. The cells were then treated with 20 mM NH_4OH (made with Distilled Water) for 4 min followed by three washes with distilled water (2 min each). Decellularization was confirmed when the cells were no longer visible when visualized under the microscope. CDM left back on the plate was lysed and the lysates were protein estimated and subjected to Immunoprecipitation (IP) and western blotting.

FBLN1C, FBLN1D Knockdown CDM for Cell Adhesion, Cell Spreading and pEGFR Immunostaining

Calu-1 cells which were subjected to FBLN1C, FBLN1D knockdown were used to make CDM on coverslips. Briefly, 24 h post second shot knockdown (KD) as described in the section "Transfections and Knockdowns," cells were trypsinized and replated on coverslips in a six well plate at a density of 2.5×10^5 cells per well and grown for 72 h. CDM was made from FBLN1C and FBLN1D knockdown cells by decellularization using 20 mM NH_4OH (made with sterile distilled water) for 4 min followed by two washes (2 min each) of sterile distilled water. The coverslips were then washed with sterile PBS and blocked for 30 min with 5% serum containing medium (with and without Erlotinib) to be used for further experiments.

Cell Adhesion and Spreading Assay

Calu-1 cells were plated at a density of 4×10^5 cells in a 60 mm dish and cultured for 24 h. Cells treated with DMSO or Erlotinib (10 μM) for 6 h were replated at a density of 4×10^4/well in a six well plate on control CDM, FBLN1C knockdown CDM and FBLN1D knockdown CDM for 20 min. Erlotinib was maintained in the media during all steps of processing. Cells were then fixed with 3.5% PFA at RT followed by Phalloidin staining. Confocal images of cells attached to CDM were analyzed using Image J software (NIH). Number of cells attached to the CDM in each frame was counted using cell count tool in Image J. For calculating cell spread area, thresholding was done to select the entire cell and the tracing tool was used to select the edge of the cell. Wand tool was used to measure the area of the cell within the mapped edge. 10 images per group were used to calculate number of cells attached to CDM. For calculating cell-spread area, at least 75 cells per group in each experiment were used for analysis.

Co-immunoprecipitation Experiments

HEK 293T Cells

HEK293T cells transfected with 5 μg of FBLN1C or 5 μg of FBLN1D and 5 μg of EGFR-GFP with PEI for 48 h. For experiments with and without EGF stimulation, cells were serum starved with 0.2% serum containing media for 12 h followed by a 5 min treatment with 100 ng/ml of EGF. Cells were lysed with 20 mM HEPES 7.8, 120 mM NaCl, 10% Glycerol, 1% NP40, 5 mM EDTA, 1 mM MgCl2, 5 mM NaF, 4 mM Vanadate, 1 mM PMSF and 1X PIC) for 30 min on ice followed by centrifugation at 12,000 rpm for 30 min at 4°C. Supernatant was collected and the lysate was protein estimated using BCA kit. Lysates were precleared with 20 μl of protein A sepharose beads in end to end rotor for 1 h at 4°C. 500 μg of lysate used for each IP reaction was incubated for 1 h at 4°C on end to end rotor with anti-EGFR (2 μl) or FBLN1 antibodies (1 μg) and their respective Ms IgG/Rb IgG (1 μg) controls. Lysates with the antibodies were incubated with 40 μl of Protein A sepharose bead slurry for 2 h at 4°C on end to end rotor. Antibody coupled beads were washed thrice with lysis buffer to remove unbound fractions. Beads containing the immunecomplexes were transferred to a different tube after third wash and eluted using 40 μl of 1X Laemmli buffer and boiled at 95°C for 10 min on thermomixer (500 rpm). Bound and unbound fractions subjected to SDS-PAGE electrophoresis were probed with anti-FBLN1 and anti-EGFR antibodies and blots were developed using the LAS4000 detection system (Fujifilm-GE).

Calu-1 Cells

Calu-1 cells were plated at a density of 4×10^5 cells in a 100 mm dish and cultured for 5 days. Cells reached 100% confluency at the end of day 5. At the end of day 5 cells were serum starved with 0.2% serum containing media for 12 h followed by a 5 min treatment with 100 ng/ml of EGF. Cell lysates were prepared and subjected to IP using anti-FBLN1 antibody as stated above.

Calu-1 and A549 CDM

Calu-1 cells were plated at a density of 4×10^5 cells in a 100 mm dish and cultured for 5 days. Cells reached 100% confluency at the end of day 5. On day 6, media was aspirated followed by a gentle PBS wash. The cells were then treated with 20 mM Ammonium Hydroxide (made with Distilled Water) for 4 min followed by three washes with distilled water (2 min each). CDM was lysed as mentioned above and the protein estimation was done using MicroBCA kit. CDM samples were diluted using dilution buffer (20 mM HEPES 7.8, 120 mM NaCl, 1% Glycerol, 1% NP40, 5 mM EDTA, and 1 mM $MgCl_2$) to make it compatible with the MicroBCA kit. CDM was precleared with 20 μl of protein A sepharose beads in end to end rotor for 1 h at 4°C. 100 μg of lysate used for each IP reaction was incubated for 1 h at 4°C on end to end rotor with anti-FBLN1 antibody (1 μg) or Ms IgG (1 μg) controls. CDM containing the immunecomplexes was then incubated with 40 ul of Protein A sepharose bead slurry for 3 h at 4°C on end to end rotor. Antibody coupled beads were washed thrice with lysis buffer to remove unbound fractions. Beads containing the immunecomplexes were transferred to a different tube after third wash and eluted using 40 ul of 1X Laemmli buffer and boiled at 95°C for 10 min on thermomixer (500 rpm). Bound and unbound fractions subjected to SDS-PAGE electrophoresis were probed with anti-FBLN1 and anti-EGFR antibodies and blots were developed using the LAS4000 detection system (Fujifilm-GE).

Wound Healing Migration Assay

Wound healing assay was used to determine the collective cell migration of Calu-1 cells upon FBLN1C and FBLN1D knockdown. FBLN1C/FBLN1D knockdown in Calu-1 cells was performed as described above in the "Transfections and Knockdowns." Twenty fours post second shot knockdown, cells were plated at 2×10^5 cells/ well in a 24 well plate and cultured overnight. Cells were treated with DMSO or Erlotinib (10 μM) for 6 h in 5% serum containing media. Cells were then treated with Mitomycin C (10 μg/ml) for 1 h to inhibit cell proliferation and scratch was performed with a 10 μl sterile pipette tip. Cells were washed with PBS to remove cell wounded cells and debris. Fresh media was added to the cells and 5 images at different locations in the scratch were taken per group at 0 h, 12 h, 24 h, and 36 h, respectively. Percentage closed wound area was calculated using T-Scratch software.

Single Cell Migration Assay on CDM

Upon second shot knockdown, cells were plated at 5×10^4 cells/ well in a 24 well plate and cultured for 72 h. CDM from FBLN1C, FBLN1D knockdown cells were prepared as described in the section "FBLN1C, FBLN1D Knockdown CDM for Cell Adhesion, Cell Spreading and pEGFR Immunostaining." Untreated Calu-1 cells were plated at 2×10^4 cells/ well in a 24 well plate and allowed to attach for 3 h. Images were taken every 90 min for 12 h. Cells were manually tracked using MTrack plugin in Image J software (NIH). Distance, Velocity and Persistence was calculated using Chemotaxis and Migration tool in Image J software.

Quantitation of Fluorescent Phosphorylated EGFR in Cell Edge and Whole Cells

Confocal cross section images were shot at the plane the cells are most spread and the used for this analysis. To calculate enrichment of active phosphorylated EGFR (pEGFR) in Calu-1 cell edges cells replated on cell derived matrices from control, FBLN1C and FBLN1D knockdown cells were imaged using a laser confocal. The cell spread area (Area 1) was defined by thresholding of the Phalloidin stained cell image using Image J. This was used to define a mask for the perimeter of the cell. The area that this mask measures is called Area 1. This mask was stored in the ROI (Region of Interest) manager. This ROI was then shrunk evenly by 0.5 μm using the Enlarge option (by entering a negative 0.5 μm value). The area that this shrunk mask now measures is called Area 2. pEGFR intensity in Area 1 and Area 2 were measured and intensity in Area1 minus Area2 was calculated and normalized to the area of this region. This effectively gives us the intensity of pEGFR (active EGFR)/Area in 0.5 μm of the cell edge in the actively spreading cells.

TCGA/ONCOMINE Analysis

Analysis of FBLN1, EGFR transcript levels from TCGA datasets was done using the normalized RNA-Seq expression data. The following datasets were downloaded from the UCSC Xena browser[1]: TCGA Lung Cancer (LUNG) (15 datasets, n = 1129, version 2017-09-08), TCGA LUAD (23 datasets, n = 576, version 2017-10-13), and TCGA LUSC (24 datasets, n = 553, version 2017-10-13). FBLN1 and EGFR expression in LUAD datasets was determined using the online ONCOMINE database. The following datasets that were used for this analysis were from these studies Okayama et al. (2012) Cancer Research 2012 and Selamat et al. (2012) Genome Research 2012.

Statistical Analysis

Statistical analysis of data was done using the unpaired two-tailed Student's t-test for analyzing two groups and two tailed single sample t test was used for datasets normalized to respective controls. In experiments with more than three groups, two-way ANOVA was used to calculate p values. All analysis was done using GraphPad PRISM software.

DATA AVAILABILITY STATEMENT

All datasets generated for this study are included in the article/**Supplementary Material**.

AUTHOR CONTRIBUTIONS

KH and NB conceptualized the study based on preliminary results and wrote the manuscript. KH designed and executed all the experiments in the manuscript. OJ performed the Fibronectin experiments. SM conducted the Fibulin-1 in CDM experiments. All authors provided comments and feedback on the manuscript and approved the final draft.

FUNDING

Funding to NB lab was generously provided by the Wellcome Trust-DBT India Alliance grant (30711059). KH received funding from the IISER Pune Postdoctoral Fellowship Program and Department of Science and Technology, India – Women Scientist Division-A (SR/WOS-A/LS-158/2017) division. OJ was funded by Indian Institute of Science – KVPY program (SB-1612068).

ACKNOWLEDGMENTS

We would like to thank Scott Argraves (Medical University of South Carolina, Charleston, SC, United States) where some of the preliminary studies were carried out. We thank IISER Pune Leica Micro Imaging Center Inauguration and Super Resolution Imaging facility for the Confocal Microscopy imaging. We also thank NB lab members for their valuable feedback and comments on the manuscript.

[1] https://xenabrowser.net/datapages/

SUPPLEMENTARY MATERIAL

The Supplementary Material for this article can be found online at: https://www.frontiersin.org/articles/10.3389/fcell.2020.00522/full#supplementary-material

FIGURE S1 | (A) Supplementary Table S1 lists custom designed siRNA sequences against FBLN1C and FBLN1D used for the knockdown experiments. **(B)** RTPCR analysis of FBLN1C (gray bar) and FBLN1D (white bar) transcript levels in siRNA-mediated knockdown of FBLN1C (FBLN1Ci) and FBLN1D (FBLN1Di) in Calu-1 cells compared to their control (CON) (black bar) **(Figures 1F,G)**. Delta Delta Ct calculated relative to control was used to determine gene expression. Graph represents mean ± SE of relative gene expression from four independent experiments. **(C,D)** RTPCR analysis of FBLN1C (gray bar) **(B)**, FBLN1D (white bar) **(B)** and EGFR (black bar) **(C)** in siRNA-mediated knockdown of FBLN1C (FBLN1Ci) and FBLN1D (FBLN1Di) in Calu-1 cells compared to their control (CON) (black bar) **(Figures 1H,I)**. Delta Delta Ct calculated relative to control (CON) was used to determine fold change in gene expression. Graph represents mean ± SE of relative gene expression from nine independent experiments. **(E)** Comparison of western blots for the detection of FBLN1 (WB: FBLN1) in conditioned culture medium of Control (CON), FBLN1C (Ci) and FBLN1D (Di) knockdown cells (adapted from **Figure 1F**) and whole cell lysates of Calu-1 cells overexpressing FBLN1C (+1C) and FBLN1D (+1D) in the presence of serum (5% FBS) (adapted from **Figure 1I**). Blue and red arrows mark FBLN1C and FBLN1D, respectively. Images are representative of four independent experiments. **(F)** Western blot detection of EGFR phosphorylated on tyrosine 1173 (WB: pEGFR), total EGFR (WB: tEGFR) and GAPDH (WB: GAPDH) in Calu-1 cells grown with serum growth factors (5% FBS) and treated with DMSO or 10 μM Erlotinib. Bar graphs represents mean ± SE of pEGFR to total EGFR ratio from three independent experiments. Statistical analysis of the data was done using the one sample *t*-test and *p* values are as shown. **(G)** RTPCR analysis of FBLN1C (gray bar) and FBLN1D (white bar) transcript levels in siRNA-mediated knockdown of FBLN1C (FBLN1Ci) and FBLN1D (FBLN1Di) compared to control (CON) (black bar) A549 cells. Delta Delta Ct calculated relative to control was used to determine gene expression. Graph represents mean ± SE of relative gene expression from four independent experiments. **(H)** Western blot detection of EGFR phosphorylated on tyrosine1173 (WB: pEGFR), total EGFR (WB: tEGFR) and GAPDH (WB: GAPDH) in lysates from A549 cells grown in the presence of serum growth factors (5% FBS) overexpressing untagged Fibulin-1C (+FBLN1C) and Fibulin-1D (+FBLN1D). Overexpression of FBLN1C and FBLN1D was confirmed by western blot (WB: FBLN1) and their relative positions marked by arrows. Bar graphs represents mean ± SE of pEGFR to total EGFR ratio from five independent experiments. Statistical analysis of the data was done using the students *t*-test and *p* values are as shown.

FIGURE S2 | (A,B) Western blot detection of EGFR phosphorylated on tyrosine1173 (WB: pEGFR), total EGFR (WB: tEGFR), Fibulin-1 (WB: FBLN1), and Actin (WB: Actin) in lysates from serum deprived HEK293T cells **(A)** overexpressing EGFR-GFP and untagged FBLN1C or **(B)** EGFR-GFP and untagged FBLN1D and treated without (-EGF) or with stimulation using EGF (100 ng/ml) for 5 min (+EGF). Data is representative of three independent experiments with similar results.

FIGURE S3 | (A) Western blot detection of EGFR phosphorylated on tyrosine1173 (WB: pEGFR), total EGFR (WB: tEGFR), Fibulin-1 (WB: FBLN1) and GAPDH (WB: GAPDH) in lysates from serum deprived Calu-1 cells without (-EGF) on with stimulation using EGF (100 ng/ml) for 5 min (+EGF). Data is representative of three independent experiments with similar results. **(B)** CDM from Calu-1 cells fixed and immunostained using Alexa 488 conjugated mouse IgG (MsIgG) and phalloidin alexa-594 (Phalloidin). Representative confocal images are representative of three independent experiments with similar results. Scale bar represents 10 μm. **(C)** 10 μg of whole cell lysate (WCL) and cell derived matrix (CDM) from A549 cells were probed for Fibulin-1 (WB: FBLN1), EGFR (WB: EGFR), and Actin (WB: Actin) by western blot. The results are representative of three independent experiments. **(D,E)** Endogenous Fibulin-1 from **(D)** WCL, Fibulin-1 from CDM **(E)** of A549 cells was immunoprecipitated (IP: FBLN1) and compared to mouse IgG (IP: mIgG). Immunoprecipitation of Fibulin-1 (WB: FBLN1) and co-precipitation of EGFR (WB: EGFR) was tested by western blot. The immunoprecipitated (bound) protein eluted and un-bound fractions (B vs. UB) were also compared by western blot. The results are representative of three independent experiments which gave similar results.

FIGURE S4 | (A) Bar graphs represent mean ± SE of FBLN1 levels in CDM from 4 independent experiments normalized to control (CON). Statistical analysis of the data was done using the single sample *t*-test and *p* values are as shown. **(B)** RTPCR analysis of FBLN1C (gray bar) and FBLN1D (white bar) transcript levels in siRNA-mediated knockdown of FBLN1C (FBLN1Ci) and FBLN1D (FBLN1Di) in Calu-1 cells compared to their control (CON) (black bar). Delta Delta Ct calculated relative to control was used to determine gene expression. Graph represents mean ± SE of relative gene expression from four independent experiments as indicated. **(C)** Bar graphs represent mean ± SE of protein concentration in CDM quantified using BCA from four independent experiments as indicated. **(D–F)** RTPCR analysis of FBLN1C (gray bar) and FBLN1D (white bar) transcript levels in siRNA-mediated knockdown of FBLN1C (FBLN1Ci) and FBLN1D (FBLN1Di) in Calu-1 cells compared to their control (CON) (black bar) **(D)** in single cell migration (**Figure 4C**) **(E)** in EGFR activation studies with serum growth factors (**Figure 4D**) and **(F)** without serum growth factors (**Figure 4E**). Graph represents mean ± SE of relative gene expression from 4 to 8 independent experiments as indicated.

FIGURE S5 | (A,B) RTPCR analysis of FBLN1C (gray bar) and FBLN1D (white bar) transcript levels in siRNA-mediated knockdown of FBLN1C (FBLN1Ci) and FBLN1D (FBLN1Di) in Calu-1 cells compared to their control (CON) (black bar) **(A)** cell adhesion and spreading (**Figures 5A,B**) **(B)** phosphorylated EGFR localization studies with serum growth factors (**Figure 5C**). Graph represents mean ± SE of relative gene expression from 3 to 4 independent experiments as indicated. **(C)** Western blot detection of Fibulin-1 (WB: FBLN1), Fibronectin (WB: FN), and GAPDH (WB: GAPDH) in lysates from Calu-1 cells in the presence of serum growth factors (5% FBS) in control (CON), FBLN1C (1Ci), FBLN1D (1Di) knockdown Calu-1 cells. Bar graphs represents mean ± SE of FBLN1/GAPDH and FN/GAPDH ratio from four independent experiments, normalized to respective control (CON). Statistical analysis of the data was done using the single sample *t*-test and *p* values are as shown.

REFERENCES

Abu-Ali, S., Fotovati, A., and Shirasuna, K. (2008). Tyrosine-kinase inhibition results in EGFR clustering at focal adhesions and consequent exocytosis in uPAR down-regulated cells of head and neck cancers. *Mol. Cancer* 7:47. doi: 10.1186/1476-4598-7-47

Alexi, X., Berditchevski, F., and Odintsova, E. (2011). The effect of cell-ECM adhesion on signalling via the ErbB family of growth factor receptors. *Biochem. Soc. Trans.* 39, 568–573. doi: 10.1042/bst0390568

Andl, C. D., Mizushima, T., Nakagawa, H., Oyama, K., Harada, H., Chruma, K., et al. (2003). Epidermal growth factor receptor mediates increased cell proliferation, migration, and aggregation in esophageal keratinocytes in vitro and in vivo. *J. Biol. Chem.* 278, 1824–1830. doi: 10.1074/jbc.m209148200

Andriani, F., Bertolini, G., Facchinetti, F., Baldoli, E., Moro, M., Casalini, P., et al. (2016). Conversion to stem-cell state in response to microenvironmental cues is regulated by balance between epithelial and mesenchymal features in lung cancer cells. *Mol. Oncol.* 10, 253–271. doi: 10.1016/j.molonc.2015.10.002

Argraves, W. S., Greene, L. M., Cooley, M. A., and Gallagher, W. M. (2003). Fibulins: physiological and disease perspectives. *EMBO Rep.* 4, 1127–1131. doi: 10.1038/sj.embor.7400033

Argraves, W. S., Tran, H., Burgess, W. H., and Dickerson, K. (1990). Fibulin is an extracellular matrix and plasma glycoprotein with repeated domain structure. *J. Cell Biol.* 111, 3155–3164. doi: 10.1083/jcb.111.6.3155

Aspberg, A., Adam, S., Kostka, G., Timpl, R., and Heinegard, D. (1999). Fibulin-1 is a ligand for the C-type lectin domains of aggrecan and versican. *J. Biol. Chem.* 274, 20444–20449. doi: 10.1074/jbc.274.29.20444

Attieh, Y., Clark, A. G., Grass, C., Richon, S., Pocard, M., Mariani, P., et al. (2017). Cancer-associated fibroblasts lead tumor invasion through integrin-beta3-dependent fibronectin assembly. *J. Cell Biol.* 216, 3509–3520. doi: 10.1083/jcb.201702033

Baird, B. N., Schliekelman, M. J., Ahn, Y. H., Chen, Y., Roybal, J. D., Gill, B. J., et al. (2013). Fibulin-2 is a driver of malignant progression in lung adenocarcinoma. *PLoS One* 8:e67054. doi: 10.1371/journal.pone.0067054

Bakker, J., Spits, M., Neefjes, J., and Berlin, I. (2017). The EGFR odyssey – from activation to destruction in space and time. *J. Cell Sci.* 130, 4087–4096. doi: 10.1242/jcs.209197

Balanis, N., Yoshigi, M., Wendt, M. K., Schiemann, W. P., and Carlin, C. R. (2011). beta3 integrin-EGF receptor cross-talk activates p190RhoGAP in mouse mammary gland epithelial cells. *Mol. Biol. Cell* 22, 4288–4301. doi: 10.1091/mbc.e10-08-0700

Balbona, K., Tran, H., Godyna, S., Ingham, K. C., Strickland, D. K., and Argraves, W. S. (1992). Fibulin binds to itself and to the carboxyl-terminal heparin-binding region of fibronectin. *J. Biol. Chem.* 267, 20120–20125.

Bardin, A., Moll, F., Margueron, R., Delfour, C., Chu, M. L., Maudelonde, T., et al. (2005). Transcriptional and posttranscriptional regulation of fibulin-1 by estrogens leads to differential induction of messenger ribonucleic acid variants in ovarian and breast cancer cells. *Endocrinology* 146, 760–768. doi: 10.1210/en.2004-1239

Brooke, J. S., Cha, J. H., and Eidels, L. (2002). Latent transforming growth factor beta-binding protein-3 and fibulin-1C interact with the extracellular domain of the heparin-binding EGF-like growth factor precursor. *BMC Cell Biol.* 3:2. doi: 10.1186/1471-2121-3-2

Burgstaller, G., Oehrle, B., Gerckens, M., White, E. S., Schiller, H. B., and Eickelberg, O. (2017). The instructive extracellular matrix of the lung: basic composition and alterations in chronic lung disease. *Eur. Respir. J.* 50:1601805. doi: 10.1183/13993003.01805-2016

Camaj, P., Seeliger, H., Ischenko, I., Krebs, S., Blum, H., Toni, E.N. De, et al. (2009). EFEMP1 binds the EGF receptor and activates MAPK and Akt pathways in pancreatic carcinoma cells. *Biol. Chem.* 390, 1293–1302.

Campbell, J. D., Alexandrov, A., Kim, J., Wala, J., Berger, A. H., Pedamallu, C. S., et al. (2016). Distinct patterns of somatic genome alterations in lung adenocarcinomas and squamous cell carcinomas. *Nat. Genet.* 48, 607–616. doi: 10.1038/ng.3564

Che, T. F., Lin, C. W., Wu, Y. Y., Chen, Y. J., Han, C. L., Chang, Y. L., et al. (2015). Mitochondrial translocation of EGFR regulates mitochondria dynamics and promotes metastasis in NSCLC. *Oncotarget* 6, 37349–37366. doi: 10.18632/oncotarget.5736

Chen, Z., Fillmore, C. M., Hammerman, P. S., Kim, C. F., and Wong, K. K. (2014). Non-small-cell lung cancers: a heterogeneous set of diseases. *Nat. Rev. Cancer* 14, 535–546. doi: 10.1038/nrc3775

Cheng, Y. Y., Jin, H., Liu, X., Siu, J. M., Wong, Y. P., Ng, E. K., et al. (2008). Fibulin 1 is downregulated through promoter hypermethylation in gastric cancer. *Br. J. Cancer* 99, 2083–2087. doi: 10.1038/sj.bjc.6604760

Chu, M. L., and Tsuda, T. (2004). Fibulins in development and heritable disease. *Birth Defects Res. C Embryo. Today* 72, 25–36. doi: 10.1002/bdrc.20003

Consortium, G. T. (2015). Human genomics. The genotype-tissue expression (GTEx) pilot analysis: multitissue gene regulation in humans. *Science* 348, 648–660.

Cui, Y., Liu, J., Yin, H. B., Liu, Y. F., and Liu, J. H. (2015). Fibulin-1 functions as a prognostic factor in lung adenocarcinoma. *Jpn. J. Clin. Oncol.* 45, 854–859. doi: 10.1093/jjco/hyv094

Du, W. W., Fang, L., Yang, X., Sheng, W., Yang, B. L., Seth, A., et al. (2013). The role of versican in modulating breast cancer cell self-renewal. *Mol. Cancer. Res.* 11, 443–455. doi: 10.1158/1541-7786.mcr-12-0461

Erdogan, B., Ao, M., White, L. M., Means, A. L., Brewer, B. M., Yang, L., et al. (2017). Cancer-associated fibroblasts promote directional cancer cell migration by aligning fibronectin. *J. Cell Biol.* 216, 3799–3816. doi: 10.1083/jcb.201704053

Ferguson, K. M., Berger, M. B., Mendrola, J. M., Cho, H. S., Leahy, D. J., and Lemmon, M. A. (2003). EGF activates its receptor by removing interactions that autoinhibit ectodomain dimerization. *Mol. Cell* 11, 507–517. doi: 10.1016/s1097-2765(03)00047-9

Fong, K. M., Sekido, Y., Gazdar, A. F., and Minna, J. D. (2003). Lung cancer. 9: molecular biology of lung cancer: clinical implications. *Thorax* 58, 892–900. doi: 10.1136/thorax.58.10.892

Gallagher, W. M., Currid, C. A., and Whelan, L. C. (2005). Fibulins and cancer: friend or foe? *Trends Mol. Med.* 11, 336–340. doi: 10.1016/j.molmed.2005.06.001

Gocheva, V., Naba, A., Bhutkar, A., Guardia, T., Miller, K. M., Li, C. M., et al. (2017). Quantitative proteomics identify Tenascin-C as a promoter of lung cancer progression and contributor to a signature prognostic of patient survival. *Proc. Natl. Acad. Sci. U.S.A.* 114, E5625–E5634.

Grahovac, J., and Wells, A. (2014). Matrikine and matricellular regulators of EGF receptor signaling on cancer cell migration and invasion. *Lab. Invest.* 94, 31–40. doi: 10.1038/labinvest.2013.132

Gridelli, C., Rossi, A., and Maione, P. (2003). Treatment of non-small-cell lung cancer: state of the art and development of new biologic agents. *Oncogene* 22, 6629–6638. doi: 10.1038/sj.onc.1206957

Guo, G., Gong, K., Wohlfeld, B., Hatanpaa, K. J., Zhao, D., and Habib, A. A. (2015). Ligand-independent EGFR signaling. *Cancer Res.* 75, 3436–3441. doi: 10.1158/0008-5472.can-15-0989

Hanada, K., and Sasaki, T. (2018). Expression and purification of recombinant fibulins in mammalian cells. *Methods Cell Biol.* 143, 247–259. doi: 10.1016/bs.mcb.2017.08.014

Hastings, J. F., Skhinas, J. N., Fey, D., Croucher, D. R., and Cox, T. R. (2019). The extracellular matrix as a key regulator of intracellular signalling networks. *Br. J. Pharmacol.* 176, 82–92. doi: 10.1111/bph.14195

Hoshiba, T. (2019). Decellularized extracellular matrix for cancer research. *Materials (Basel)* 12:1311. doi: 10.3390/ma12081311

Hsieh, C. H., Chou, Y. T., Kuo, M. H., Tsai, H. P., Chang, J. L., and Wu, C. W. (2017). A targetable HB-EGF-CITED4 axis controls oncogenesis in lung cancer. *Oncogene* 36, 2946–2956. doi: 10.1038/onc.2016.465

Hu, B., Thirtamara-Rajamani, K. K., Sim, H., and Viapiano, M. S. (2009). Fibulin-3 is uniquely upregulated in malignant gliomas and promotes tumor cell motility and invasion. *Mol. Cancer Res.* 7, 1756–1770. doi: 10.1158/1541-7786.mcr-09-0207

Hu, Y., Gao, H., Vo, C., Ke, C., Pan, F., Yu, L., et al. (2014). Anti-EGFR function of EFEMP1 in glioma cells and patient prognosis. *Oncoscience* 1, 205–215.

Hynes, R. O., and Naba, A. (2012). Overview of the matrisome–an inventory of extracellular matrix constituents and functions. *Cold Spring Harb. Perspect. Biol.* 4:a004903. doi: 10.1101/cshperspect.a004903

Iozzo, R. V., Moscatello, D. K., McQuillan, D. J., and Eichstetter, I. (1999). Decorin is a biological ligand for the epidermal growth factor receptor. *J. Biol. Chem.* 274, 4489–4492. doi: 10.1074/jbc.274.8.4489

Iyer, A. K., Tran, K. T., Griffith, L., and Wells, A. (2008). Cell surface restriction of EGFR by a tenascin cytotactin-encoded EGF-like repeat is preferential for motility-related signaling. *J. Cell Physiol.* 214, 504–512. doi: 10.1002/jcp.21232

Kanda, M., Nomoto, S., Okamura, Y., Hayashi, M., Hishida, M., Fujii, T., et al. (2011). Promoter hypermethylation of fibulin 1 gene is associated with tumor progression in hepatocellular carcinoma. *Mol. Carcinogen.* 50, 571–579. doi: 10.1002/mc.20735

Kaukonen, R., Jacquemet, G., Hamidi, H., and Ivaska, J. (2017). Cell-derived matrices for studying cell proliferation and directional migration in a complex 3D microenvironment. *Nat. Protoc.* 12, 2376–2390. doi: 10.1038/nprot.2017.107

Kim, I. G., Kim, S. Y., Choi, S. I., Lee, J. H., Kim, K. C., and Cho, E. W. (2014). Fibulin-3-mediated inhibition of epithelial-to-mesenchymal transition and self-renewal of ALDH+ lung cancer stem cells through IGF1R signaling. *Oncogene* 33, 3908–3917. doi: 10.1038/onc.2013.373

Kim, S. H., Turnbull, J., and Guimond, S. (2011). Extracellular matrix and cell signalling: the dynamic cooperation of integrin, proteoglycan and growth factor receptor. *J. Endocrinol.* 209, 139–151. doi: 10.1530/joe-10-0377

Krasny, L., Bland, P., Kogata, N., Wai, P., Howard, B. A., Natrajan, R. C., et al. (2018). SWATH mass spectrometry as a tool for quantitative profiling of the matrisome. *J. Proteomics* 189, 11–22. doi: 10.1016/j.jprot.2018.02.026

Lau, J. Y., Oliver, B. G., Baraket, M., Beckett, E. L., Hansbro, N. G., Moir, L. M., et al. (2010). Fibulin-1 is increased in asthma–a novel mediator of airway remodeling? *PLoS One* 5:e13360. doi: 10.1371/journal.pone.0013360

Lim, S. B., Tan, S. J., Lim, W. T., and Lim, C. T. (2017). An extracellular matrix-related prognostic and predictive indicator for early-stage non-small cell lung cancer. *Nat. Commun.* 8:1734.

Long, W., Yi, P., Amazit, L., LaMarca, H. L., Ashcroft, F., Kumar, R., et al. (2010). SRC-3Delta4 mediates the interaction of EGFR with FAK to promote cell migration. *Mol. Cell* 37, 321–332. doi: 10.1016/j.molcel.2010.01.004

Lopez-Luque, J., Bertran, E., Crosas-Molist, E., Maiques, O., Malfettone, A., Caja, L., et al. (2019). Downregulation of epidermal growth factor receptor in

hepatocellular carcinoma facilitates transforming growth factor-beta-induced epithelial to amoeboid transition. *Cancer Lett.* 464, 15–24. doi: 10.1016/j.canlet.2019.08.011

Lu, P., Weaver, V. M., and Werb, Z. (2012). The extracellular matrix: a dynamic niche in cancer progression. *J. Cell Biol.* 196, 395–406. doi: 10.1083/jcb.201102147

Malik, P. S., and Raina, V. (2015). Lung cancer: prevalent trends & emerging concepts. *Indian J. Med. Res.* 141, 5–7.

Marcoux, N., and Vuori, K. (2003). EGF receptor mediates adhesion-dependent activation of the Rac GTPase: a role for phosphatidylinositol 3-kinase and Vav2. *Oncogene* 22, 6100–6106. doi: 10.1038/sj.onc.1206712

Micallef, J., Taccone, M., Mukherjee, J., Croul, S., Busby, J., Moran, M. F., et al. (2009). Epidermal growth factor receptor variant III-induced glioma invasion is mediated through myristoylated alanine-rich protein kinase C substrate overexpression. *Cancer Res.* 69, 7548–7556. doi: 10.1158/0008-5472.can-08-4783

Moll, F., Katsaros, D., Lazennec, G., Hellio, N., Roger, P., Giacalone, P. L., et al. (2002). Estrogen induction and overexpression of fibulin-1C mRNA in ovarian cancer cells. *Oncogene* 21, 1097–1107. doi: 10.1038/sj.onc.1205171

Morello, V., Cabodi, S., Sigismund, S., Camacho-Leal, M. P., Repetto, D., Volante, M., et al. (2011). beta1 integrin controls EGFR signaling and tumorigenic properties of lung cancer cells. *Oncogene* 30, 4087–4096. doi: 10.1038/onc.2011.107

Muriel, J. M., Xu, X., Kramer, J. M., and Vogel, B. E. (2006). Selective assembly of fibulin-1 splice variants reveals distinct extracellular matrix networks and novel functions for perlecan/UNC-52 splice variants. *Dev. Dyn.* 235, 2632–2640. doi: 10.1002/dvdy.20888

Nallanthighal, S., Heiserman, J. P., and Cheon, D. J. (2019). The role of the extracellular matrix in cancer stemness. *Front. Cell Dev. Biol.* 7:86. doi: 10.3389/fcell.2019.00086

Normanno, N., De Luca, A., Bianco, C., Strizzi, L., Mancino, M., Maiello, M. R., et al. (2006). Epidermal growth factor receptor (EGFR) signaling in cancer. *Gene* 366, 2–16.

Ogawa, T., Tsubota, Y., Hashimoto, J., Kariya, Y., and Miyazaki, K. (2007). The short arm of laminin gamma2 chain of laminin-5 (laminin-332) binds syndecan-1 and regulates cellular adhesion and migration by suppressing phosphorylation of integrin beta4 chain. *Mol. Biol. Cell* 18, 1621–1633. doi: 10.1091/mbc.e06-09-0806

Okayama, H., Kohno, T., Ishii, Y., Shimada, Y., Shiraishi, K., Iwakawa, R., et al. (2012). Identification of genes upregulated in ALK-positive and EGFR/KRAS/ALK-negative lung adenocarcinomas. *Cancer Res.* 72, 100–111. doi: 10.1158/0008-5472.can-11-1403

Paolillo, M., and Schinelli, S. (2019). Extracellular matrix alterations in metastatic processes. *Int. J. Mol. Sci.* 20:4947. doi: 10.3390/ijms20194947

Paulitti, A., Andreuzzi, E., Bizzotto, D., Pellicani, R., Tarticchio, G., Marastoni, S., et al. (2018). The ablation of the matricellular protein EMILIN2 causes defective vascularization due to impaired EGFR-dependent IL-8 production affecting tumor growth. *Oncogene* 37, 3399–3414. doi: 10.1038/s41388-017-0107-x

Peixoto, P., Etcheverry, A., Aubry, M., Missey, A., Lachat, C., Perrard, J., et al. (2019). EMT is associated with an epigenetic signature of ECM remodeling genes. *Cell Death Dis.* 10:205.

Perbal, B., Martinerie, C., Sainson, R., Werner, M., He, B., and Roizman, B. (1999). The C-terminal domain of the regulatory protein NOVH is sufficient to promote interaction with fibulin 1C: a clue for a role of NOVH in cell-adhesion signaling. *Proc. Natl. Acad. Sci. U.S.A.* 96, 869–874. doi: 10.1073/pnas.96.3.869

Pesson, M., Volant, A., Uguen, A., Trillet, K., De La Grange, P., Aubry, M., et al. (2014). A gene expression and Pre-mRNA splicing signature that marks the adenoma-adenocarcinoma progression in colorectal cancer. *PLoS One* 9:e87761. doi: 10.1371/journal.pone.0087761

Pickup, M. W., Mouw, J. K., and Weaver, V. M. (2014). The extracellular matrix modulates the hallmarks of cancer. *EMBO Rep.* 15, 1243–1253. doi: 10.15252/embr.201439246

Pirinen, R., Leinonen, T., Bohm, J., Johansson, R., Ropponen, K., Kumpulainen, E., et al. (2005). Versican in nonsmall cell lung cancer: relation to hyaluronan, clinicopathologic factors, and prognosis. *Hum. Pathol.* 36, 44–50. doi: 10.1016/j.humpath.2004.10.010

Qing, J., Maher, V. M., Tran, H., Argraves, W. S., Dunstan, R. W., and McCormick, J. J. (1997). Suppression of anchorage-independent growth and matrigel invasion and delayed tumor formation by elevated expression of fibulin-1D in human fibrosarcoma-derived cell lines. *Oncogene* 15, 2159–2168. doi: 10.1038/sj.onc.1201385

Reticker-Flynn, N. E., Malta, D. F., Winslow, M. M., Lamar, J. M., Xu, M. J., Underhill, G. H., et al. (2012). A combinatorial extracellular matrix platform identifies cell-extracellular matrix interactions that correlate with metastasis. *Nat. Commun.* 3:1122.

Rintoul, R. C., and Sethi, T. (2001). The role of extracellular matrix in small-cell lung cancer. *Lancet Oncol.* 2, 437–442. doi: 10.1016/s1470-2045(00)00421-6

Rusnak, D. W., Alligood, K. J., Mullin, R. J., Spehar, G. M., Arenas-Elliott, C., Martin, A. M., et al. (2007). Assessment of epidermal growth factor receptor (EGFR, ErbB1) and HER2 (ErbB2) protein expression levels and response to lapatinib (Tykerb, GW572016) in an expanded panel of human normal and tumour cell lines. *Cell Prolif.* 40, 580–594. doi: 10.1111/j.1365-2184.2007.00455.x

Santra, M., Reed, C. C., and Iozzo, R. V. (2002). Decorin binds to a narrow region of the epidermal growth factor (EGF) receptor, partially overlapping but distinct from the EGF-binding epitope. *J. Biol. Chem.* 277, 35671–35681. doi: 10.1074/jbc.m205317200

Sasaki, T., Gohring, W., Miosge, N., Abrams, W. R., Rosenbloom, J., and Timpl, R. (1999). Tropoelastin binding to fibulins, nidogen-2 and other extracellular matrix proteins. *FEBS Lett.* 460, 280–284. doi: 10.1016/s0014-5793(99)01362-9

Sasaki, T., Kostka, G., Gohring, W., Wiedemann, H., Mann, K., Chu, M. L., et al. (1995). Structural characterization of two variants of fibulin-1 that differ in nidogen affinity. *J. Mol. Biol.* 245, 241–250. doi: 10.1006/jmbi.1994.0020

Scagliotti, G. V., Selvaggi, G., Novello, S., and Hirsch, F. R. (2004). The biology of epidermal growth factor receptor in lung cancer. *Clin. Cancer Res.* 10, 4227s–4232s.

Schenk, S., Hintermann, E., Bilban, M., Koshikawa, N., Hojilla, C., Khokha, R., et al. (2003). Binding to EGF receptor of a laminin-5 EGF-like fragment liberated during MMP-dependent mammary gland involution. *J. Cell Biol.* 161, 197–209. doi: 10.1083/jcb.200208145

Scherzer, M. T., Waigel, S., Donninger, H., Arumugam, V., Zacharias, W., Clark, G., et al. (2015). Fibroblast-derived extracellular matrices: an alternative cell culture system that increases metastatic cellular properties. *PLoS One* 10:e0138065. doi: 10.1371/journal.pone.0138065

Selamat, S. A., Chung, B. S., Girard, L., Zhang, W., Zhang, Y., Campan, M., et al. (2012). Genome-scale analysis of DNA methylation in lung adenocarcinoma and integration with mRNA expression. *Genome Res.* 22, 1197–1211. doi: 10.1101/gr.132662.111

Senthebane, D. A., Rowe, A., Thomford, N. E., Shipanga, H., Munro, D., Mazeedi, M., et al. (2017). The role of tumor microenvironment in chemoresistance: to survive, keep your enemies closer. *Int. J. Mol. Sci.* 18:1586. doi: 10.3390/ijms18071586

Shao, H., Kirkwood, J. M., and Wells, A. (2015). Tenascin-C Signaling in melanoma. *Cell Adh. Migr.* 9, 125–130. doi: 10.4161/19336918.2014.972781

Sharma, S. V., Bell, D. W., Settleman, J., and Haber, D. A. (2007). Epidermal growth factor receptor mutations in lung cancer. *Nat. Rev. Cancer.* 7, 169–181.

Stevens, L. E., Cheung, W. K. C., Adua, S. J., Arnal-Estape, A., Zhao, M., Liu, Z., et al. (2017). Extracellular matrix receptor expression in subtypes of lung adenocarcinoma potentiates outgrowth of micrometastases. *Cancer Res.* 77, 1905–1917. doi: 10.1158/0008-5472.can-16-1978

Su, Y., and Besner, G. E. (2014). Heparin-binding EGF-like growth factor (HB-EGF) promotes cell migration and adhesion via focal adhesion kinase. *J. Surg. Res.* 189, 222–231. doi: 10.1016/j.jss.2014.02.055

Sun, R., Gao, P., Chen, L., Ma, D., Wang, J., Oppenheim, J. J., et al. (2005). Protein kinase C zeta is required for epidermal growth factor-induced chemotaxis of human breast cancer cells. *Cancer Res.* 65, 1433–1441. doi: 10.1158/0008-5472.can-04-1163

Thalappilly, S., Soubeyran, P., Iovanna, J. L., and Dusetti, N. J. (2010). VAV2 regulates epidermal growth factor receptor endocytosis and degradation. *Oncogene* 29, 2528–2539. doi: 10.1038/onc.2010.1

Timpl, R., Sasaki, T., Kostka, G., and Chu, M. L. (2003). Fibulins: a versatile family of extracellular matrix proteins. *Nat. Rev. Mol. Cell Biol.* 4, 479–489. doi: 10.1038/nrm1130

Timpl, R., Tisi, D., Talts, J. F., Andac, Z., Sasaki, T., and Hohenester, E. (2000). Structure and function of laminin LG modules. *Matrix Biol.* 19, 309–317. doi: 10.1016/s0945-053x(00)00072-x

Tran, H., Mattei, M., Godyna, S., and Argraves, W. S. (1997). Human fibulin-1D: molecular cloning, expression and similarity with S1-5 protein, a new member of the fibulin gene family. *Matrix Biol.* 15, 479–493. doi: 10.1016/s0945-053x(97)90021-4

Tsai, C. J., and Nussinov, R. (2019). Emerging allosteric mechanism of EGFR activation in physiological and pathological contexts. *Biophys. J.* 117, 5–13. doi: 10.1016/j.bpj.2019.05.021

Twal, W. O., Czirok, A., Hegedus, B., Knaak, C., Chintalapudi, M. R., Okagawa, H., et al. (2001). Fibulin-1 suppression of fibronectin-regulated cell adhesion and motility. *J. Cell Sci.* 114, 4587–4598.

Ungewiss, H., Rotzer, V., Meir, M., Fey, C., Diefenbacher, M., Schlegel, N., et al. (2018). Dsg2 via Src-mediated transactivation shapes EGFR signaling towards cell adhesion. *Cell Mol. Life Sci.* 75, 4251–4268. doi: 10.1007/s00018-018-2869-x

Walker, C., Mojares, E., and Del Rio Hernandez, A. (2018). Role of extracellular matrix in development and cancer progression. *Int. J. Mol. Sci.* 19:3028. doi: 10.3390/ijms19103028

Wang, S., Zhang, D., Han, S., Gao, P., Liu, C., Li, J., et al. (2017). Fibulin-3 promotes osteosarcoma invasion and metastasis by inducing epithelial to mesenchymal transition and activating the Wnt/beta-catenin signaling pathway. *Sci. Rep.* 7:6215.

Wheeler, D. L., Dunn, E. F., and Harari, P. M. (2010). Understanding resistance to EGFR inhibitors-impact on future treatment strategies. *Nat. Rev. Clin. Oncol.* 7, 493–507. doi: 10.1038/nrclinonc.2010.97

Wlazlinski, A., Engers, R., Hoffmann, M. J., Hader, C., Jung, V., Muller, M., et al. (2007). Downregulation of several fibulin genes in prostate cancer. *Prostate* 67, 1770–1780. doi: 10.1002/pros.20667

Wu, B. J., Zhou, Z. P., Li, W. P., Ding, W., Wu, Y. Z., Zhou, Z. W., et al. (2014). Abnormal hypermethylation and clinicopathological significance of FBLN1 gene in cutaneous melanoma. *Tumour Biol.* 35, 123–127. doi: 10.1007/s13277-013-1015-5

Wu, Y., Chen, L., Cao, L., Sheng, W., and Yang, B. B. (2004). Overexpression of the C-terminal PG-M/versican domain impairs growth of tumor cells by intervening in the interaction between epidermal growth factor receptor and beta1-integrin. *J. Cell Sci.* 117, 2227–2237. doi: 10.1242/jcs.01057

Xiao, W., Wang, J., Li, H., Guan, W., Xia, D., Yu, G., et al. (2013). Fibulin-1 is down-regulated through promoter hypermethylation and suppresses renal cell carcinoma progression. *J. Urol.* 190, 291–301. doi: 10.1016/j.juro.2013.01.098

Yin, J., Xu, K., Zhang, J., Kumar, A., and Yu, F. S. (2007). Wound-induced ATP release and EGF receptor activation in epithelial cells. *J. Cell Sci.* 120, 815–825. doi: 10.1242/jcs.03389

Yotsumoto, F., Fukagawa, S., Miyata, K., Nam, S. O., Katsuda, T., Miyahara, D., et al. (2017). HB-EGF is a promising therapeutic target for lung cancer with secondary mutation of EGFR(T790M). *Anticancer Res.* 37, 3825–3831.

Yue, W., Sun, Q., Landreneau, R., Wu, C., Siegfried, J. M., Yu, J., et al. (2009). Fibulin-5 suppresses lung cancer invasion by inhibiting matrix metalloproteinase-7 expression. *Cancer Res.* 69, 6339–6346. doi: 10.1158/0008-5472.can-09-0398

Zhang, S., Feng, X. L., Shi, L., Gong, C. J., He, Z. J., Wu, H. J., et al. (2013). Genome-wide analysis of DNA methylation in tongue squamous cell carcinoma. *Oncol. Rep.* 29, 1819–1826. doi: 10.3892/or.2013.2309

Zhu, J., and Clark, R. A. F. (2014). Fibronectin at select sites binds multiple growth factors and enhances their activity: expansion of the collaborative ECM-GF paradigm. *J. Invest. Dermatol.* 134, 895–901. doi: 10.1038/jid.2013.484

Conflict of Interest: The authors declare that the research was conducted in the absence of any commercial or financial relationships that could be construed as a potential conflict of interest.

Copyright © 2020 Harikrishnan, Joshi, Madangirikar and Balasubramanian. This is an open-access article distributed under the terms of the Creative Commons Attribution License (CC BY). The use, distribution or reproduction in other forums is permitted, provided the original author(s) and the copyright owner(s) are credited and that the original publication in this journal is cited, in accordance with accepted academic practice. No use, distribution or reproduction is permitted which does not comply with these terms.

frontiers in Cell and Developmental Biology

ORIGINAL RESEARCH
published: 08 July 2020
doi: 10.3389/fcell.2020.00549

TRPM7/RPSA Complex Regulates Pancreatic Cancer Cell Migration

Thibaut Lefebvre[1], Pierre Rybarczyk[1,2], Clara Bretaudeau[3], Alison Vanlaeys[1], Rémi Cousin[3], Sylvie Brassart-Pasco[3], Denis Chatelain[2], Isabelle Dhennin-Duthille[1], Halima Ouadid-Ahidouch[1], Bertrand Brassart[3†] and Mathieu Gautier[1†]*

[1] Laboratoire de Physiologie Cellulaire et Moléculaire – UR-UPJV 4667, UFR Sciences, Université de Picardie Jules Verne (UPJV), Amiens, France, [2] Service d'Anatomie et Cytologie Pathologiques, CHU Amiens-Picardie, Amiens, France, [3] UMR CNRS 7369 Matrice Extracellulaire et Dynamique Cellulaire (MEDyC), Université de Reims Champagne Ardenne (URCA), Reims, France

OPEN ACCESS

Edited by:
Erik Maquoi,
University of Liège, Belgium

Reviewed by:
Ivana Novak,
University of Copenhagen, Denmark
Ildikò Szabò,
University of Padua, Italy

***Correspondence:**
Mathieu Gautier
mathieu.gautier@u-picardie.fr

[†] These authors share senior authorship

Specialty section:
This article was submitted to Molecular and Cellular Oncology, a section of the journal Frontiers in Cell and Developmental Biology

Received: 10 March 2020
Accepted: 10 June 2020
Published: 08 July 2020

Citation:
Lefebvre T, Rybarczyk P, Bretaudeau C, Vanlaeys A, Cousin R, Brassart-Pasco S, Chatelain D, Dhennin-Duthille I, Ouadid-Ahidouch H, Brassart B and Gautier M (2020) TRPM7/RPSA Complex Regulates Pancreatic Cancer Cell Migration. Front. Cell Dev. Biol. 8:549. doi: 10.3389/fcell.2020.00549

Pancreatic ductal adenocarcinoma (PDAC) is a malignancy with a very poor prognosis due to highly metastatic profile. Cell migration is an essential step of the metastatic cascade allowing cancer cells to spread toward target tissues. Recent studies strongly suggest that bioactive elastin peptides, also named elastokines or elastin-derived peptides (EDPs), are released in the extracellular microenvironment during tumoral remodeling of the stroma. EDPs stimulate cancer cell migration by interacting with their membrane receptor, ribosomal protein SA (RPSA). Others membrane proteins like ion channels are also involved in cancer cell migration. It has been recently shown that the transient receptor potential melastatin-related 7 (TRPM7) channel regulates PDAC cell migration and invasion. The objective of this work was to study the effect of EDPs on TRPM7 channel in human pancreatic cancer cells. We showed that EDPs promote MIA PaCa-2 cell migration using Boyden chamber assay. Cells transfected with a siRNA targeting TRPM7 were not able to migrate in response to EDPs indicating that TRPM7 regulated cell migration induced by these peptides. Moreover, EDPs were able to stimulate TRPM7 currents recorded by Patch-Clamp. Finally, we showed that TRPM7 channels and RPSA receptors are colocalized at the plasma membrane of human pancreatic cancer cells. Taken together, our data suggest that TRPM7/RPSA complex regulated human pancreatic cancer cell migration. This complex may be a promising therapeutic target in PDAC.

Keywords: pancreatic ductal adenocarcinoma, elastin-derived peptides, transient receptor potential melastatin-related 7, ribosomal protein SA, cell migration

INTRODUCTION

Pancreatic ductal adenocarcinoma (PDAC) represents 85–90% of all pancreatic cancer types. The incidence of PDAC is continuously increasing in such a way that PDAC is expected to be the second cancer in term of mortality in 2030 (Rahib et al., 2014). PDAC is characterized by an abundant desmoplastic stroma that participates to the formation of metastasis and chemoresistance. This remodeled stroma is a complex structure composed of extracellular matrix (ECM) proteins and various cell types. Cancer development is influenced by ECM components. ECM/cell interactions

involve cell adhesion to extracellular macromolecules through cell surface receptors and lead to ECM degradation and bioactive ECM macromolecule fragments release, called matrikines. Elastin is the major component of elastic fibers, particularly abundant in elastic tissues such as arteries and lung. Its proteolysis by elastase-type proteinases (metalloproteinases, pancreatic elastase, leucocyte elastase) is linked to the genesis of several diseases affecting elastin-rich organs (Lohmann et al., 1994; Houghton et al., 2011). This degradation is known to unmask cryptic sites within the ECM and to release matrikines, termed elastin-derived peptides (EDPs) or elastokines. These EDPs display a wide range of biological activities, influencing cell migration (Senior et al., 1980; Da Silva et al., 2018), differentiation (Betre et al., 2006), proliferation, chemotaxis (Long et al., 1988; Da Silva et al., 2018), survival, tumor progression (Huet et al., 2002; Toupance et al., 2012; Donet et al., 2014; Brassart et al., 2019), angiogenesis (Robinet et al., 2005), aneurysm formation, and atherogenesis. Among all the EDPs described in the literature, two categories of EDPs were listed: VGVAPG, VAPG, VGVPG, VGAPG, (VGVAPG)n, and PGAIPG with the xGxxPG consensus sequence, and, AGVPGLGVG, AGVPGFGVG, GLGVGVAPG, and GFGVGAGVP with the xGxPGxGxG consensus sequence. *In vivo* study showed that xGxPGxGxG peptides like AG-9 promote tumor progression to a greater extent than do xGxxPG peptides like VG-6. These results were confirmed by *in vitro* studies in proliferation assays, migration assays, adhesion assays, proteinase secretion studies, and pseudotube formation assays to investigate angiogenesis (Da Silva et al., 2018). The set of these biological properties regulated by AG-9 and VG-6 peptides involves a lactose-insensitive receptor, the ribosomal protein SA (RPSA) (Brassart et al., 2019). Mecham et al. (1989) were the first to report the 37/67-kDa laminin receptor to bind elastin. The 37/67-kDa laminin receptor, RPSA, also known as 37LRP, 67LR, ICAS, LAMBR, LAMR1, LBP, LBP/p40, LRP, LRP/LR, NEM/1CHD4, SA, lamR, and p40, is ubiquitously expressed. It provides cellular adhesion to the basement membrane. The major forms described for RPSA were 37-, 53-, and 67-kDa forms but several groups have reported the presence of additional high-molecular-weight (HMW) forms of 32, 37, 45, 53, 55, 67, 80, and >110-kDa. The nature of conversion of the 37-kDa form to higher molecular weight species remains poorly understood (DiGiacomo and Meruelo, 2016). The RPSA receptor is located in the nucleus [association with nucleolar pre-40S ribosomes, small nucleolar ribonucleoproteins (snoRNPs), chromatin, histones], in the cytosol (ribosomal component; co-localize with actin and cytoskeletal stress fibers) and at the cell surface. It mediates cell proliferation, adhesion, and differentiation. It was reported to enhance tumor cell invasion and adhesion as well as angiogenesis, key steps in tumor progression. Recent findings have shown that RPSA is involved in the maintenance of cell viability through apoptotic evasion, allowing tumor progression (Vania et al., 2019). The green-tea-derived polyphenol, (−)-epigallocatechin-3-gallate (EGCG), is a small molecule that was reported to affect cell behavior through RPSA binding and cytoskeletal alterations. EGCG inhibitory effect appears to be blocked by RPSA antibodies, which do not trigger the same effects, indicating that the polyphenol may act agonistically or allosterically (DiGiacomo and Meruelo, 2016). The functional domain responsible for the anti-cancer activity of EGCG may be located in the 10 amino acid sequence of RPSA, IPCNNKGAHS (Fujimura et al., 2012).

The RPSA has been very recently shown to be overexpressed in PDAC tissues in relation-enhanced cell invasion, metastasis, and poor prognosis (Wu et al., 2019). We recently showed that PDAC cell migration and invasion are regulated by the transient receptor potential melastatin-related 7 (TRPM7) channel expression (Rybarczyk et al., 2012, 2017). TRPM7 expression is also increased in PDAC tissues in relation with poor prognosis (Rybarczyk et al., 2012; Yee et al., 2015). TRPM7 is a non-selective cation channel fused with a kinase domain at its C-terminus (Nadler et al., 2001; Runnels et al., 2001). As both RPSA and TRPM7 are overexpressed and regulate cancer cell migration, it is tempting to speculate that these two biomarkers could interact in PDAC. The aim of this study is to determine how TRPM7 and RPSA regulate enhanced PDAC cell migration induced by EDPs.

MATERIALS AND METHODS

Cell Culture

Human pancreatic cancer cell line MIA PaCa-2 (ATCC CRL-1420) was used for this study. This cell line was derived from a poorly differentiated tumor which corresponds to a grade 3 PDAC (Deer et al., 2010). MIA PaCa-2 cells were cultured in Dulbecco's modified Eagle's medium (Gibco) supplemented with 10% FCS (Lonza). Cells were trypsinized once a week using trypsin-EDTA (Sigma-Aldrich) and incubated at +37°C in a humidified atmosphere with 5% CO_2.

Elastin Peptides

VG-6 and AG-9 peptides were purchased from Proteogenix (Schiltigheim, France). EGCG was purchased from Enzo Life Sciences. Rabbit anti-TRPM7 and anti-RPSA antibodies were purchased from Abcam.

Cell Migration

Migration tests were performed in 8-μm pore size polyethylene terephthalate membrane cell culture inserts (BD FALCONTM Cell Culture Inserts, BD Biosciences). The upper compartment was seeded with 4.10^4 cells in FCS-free growth medium with or without different synthetic elastin peptide concentration (10^{-9} to 10^{-7} M) for 24 h at +37°C. The lower compartment was also filled with FCS-free growth medium. Thus, migration assays were performed without addition of chemoattractant. After incubation, cells were washed by phosphate buffered saline (PBS), fixed by methanol and stained by hematoxylin (HHSM, Accustain, Sigma-Aldrich) for 5 min. The remaining cells were removed from the upper side of the membrane by scrubbing. Quantification of the migration assay was performed by counting the number of cells at the lower surface of the filters (20 different fields per condition).

Cell Viability

Cell viability was assessed by using 3-(4,5-dimethyl-2-thiazolyl)-2,5-diphenyl-2H-tetrazolium bromide (MTT, Sigma-Aldrich, Inc.). MTT was solubilized in culture media without FCS at the final concentration of 0.5 mg/mL. Cells were incubated with MTT for 50 min at +37°C in the dark. The purple formazan crystals produced by viable cells were dissolved by DMSO and the absorbance was quantified at 550 nm with an Infinite® 200 Pro reader (Tecan Trading AG).

Electrophysiology

Magnesium Inhibited Cation (MIC) currents were recorded using the whole-cell patch-clamp technique as previously published (Rybarczyk et al., 2017). The composition of the extracellular solution was (in mM): Na-gluconate 150; K-gluconate 5; Mg-gluconate 2; Ca-gluconate 2; HEPES 10; glucose 5; TEA-Cl 5; pH adjusted to 7.4 with NaOH. The composition of intrapipette solution was (in mM): Na-gluconate 8; Cs-methanesulfonate 145; EGTA 10; HEPES 10; pH adjusted to 7.2 with CsOH. Membrane potential was held at −40 mV and currents were elicited by a ramp depolarization from −100 mV to +100 mV for 350 ms at the frequency of 0.1 Hz. Signals were filtered at 1 kHz and digitized at 5 kHz using an Axopatch 200B patch-clamp amplifier (Molecular Devices, Sunnyvale, CA, United States) combined with a 1322A digidata (Molecular Devices, Sunnyvale, CA, United States). MIC currents developed during the dialysis of the intracellular media by a free Mg intrapipette solution (Prakriya and Lewis, 2002). Membrane currents were expressed as current densities in pA/pF. All experiments were performed at room temperature.

Cell Transfection

Cell transfections with siRNA were performed as previously described (Rybarczyk et al., 2012). The TRPM7 siRNA used in the current study (5′-GTCTTGCCATGAAATACTC-3′) targets the mRNA sequence coding for the 170–188th N-terminal region of TRPM7 and was previously proved to be an effective target for TRPM7 silencing (Hanano et al., 2004; Vanlaeys et al., 2020). SiRNA were transfected in pancreatic cancer cells by nucleofection using a NucleofectorTM II device (Lonza, Bâle, Switzerland). Cells (10^6 cells) were transfected with 2 μg siRNA (corresponding to a final concentration of 1.5 μM) according to the optimized protocol recommended by Lonza. All the experiments were performed 48 h after the nucleofection. In parallel, cells were transfected with a non-targeting siRNA (siControl). Non-targeting and TRPM7-targeting siRNA were both provided by Dharmacon Research Inc., United States.

Quantitative RT-PCR

Total RNA isolation, reverse transcription and real-time PCR analysis were performed as previously described (Rybarczyk et al., 2017).

Western Blotting

Cells were lysed 30 min on ice in RIPA assay buffer (1% Triton X-100, 1% Na deoxycholate, 150 mM NaCl, 10 mM PO4Na2/K, pH 7.2) supplemented with Sigma P8340 inhibitors cocktail, 2 mM EDTA, and 5 mM orthovanadate. After centrifugation at 13000 rpm, the proteins in the supernatant were quantified using the BCA method (BioRad). Equal amounts of each protein sample (50 μg) were separated by electrophoresis on sodium dodecyl sulfate (SDS) polyacrylamide gel electrophoresis and blotted onto nitrocellulose membrane (Amersham). Blots were incubated with antibodies raised against TRPM7 (1/1000, ab109438, Abcam) and GAPDH (1/4000, ab8245, Abcam). Blots were developed with the enhanced chemiluminescence system using specific peroxidase-conjugated anti-IgG secondary antibodies.

Confocal Microscopy

Cells were plated on glass slides and incubated in 10% serum-containing medium for 16 h. AG-9 synthetic elastin peptides (10^{-7} M) were then added to serum-free culture medium supplemented or not with EGCG 10 μM and cells were incubated at +37°C for 24°C. After several washes, cells were fixed for 5 min with 4% paraformaldehyde. The slides were washed with PBS-T and saturated in PBS-T with 5% BSA. Cells were then incubated for 1 h at room temperature with the first antibodies diluted 1/400 in PBS-T with 1% BSA. Slides were washed in PBS-T and cells were incubated for 30 min with the Alexa-488 or Alexa-568-conjugated secondary antibodies diluted 1/1000 in PBS-T with 1% BSA. Cells were then washed with PBS-T. Control preparations were incubated with omission of the first antibody. Immunofluorescence-labeled cell preparations were studied using a Zeiss LSM 710® NLO confocal laser scanning microscope (Carl ZEISS SAS, Marly-le-Roi, France) with the 63× oil-immersion objective (ON 1.4) coupled with CHAMELEON femtosecond Titanium-Sapphire Laser (Coherent, Santa Clara, CA, United States). Alexa 488 and 568 were sequentially excited by 488 nm line of Argon laser and diode laser 561 nm. Emitted signals were, respectively, collected with 493–560 nm and 570–700 bandpass filters. Image acquisitions were performed with ZEN Software (Carl ZEISS SAS, Marly-le-Roi, France) and all acquisition settings were constant between specimens. Colocalization analyses were made with ImageJ software (Colocalization Analysis plugin).

Immunohistochemistry

Human tissues samples from PDAC (n = 8) were used with the agreement of patients treated by surgery in the University Hospital of Amiens (Picardie, France). Experiments on human tissues were approved by the Comité Consultatif de Protection des Personnes dans la Recherche Biomédicale de Picardie (Amiens, France). Immunohistochemistry was performed on human tissues using the indirect immune-peroxidase staining technique on the paraffin-embedded material with a Ventana XT instrument (Ventana Medical Systems, Roche Diagnostics). Tissue sections were obtained from 8 patients undergoing a surgery of PDAC at Amiens hospital, France. The 8 cases of PDAC were diagnosed as moderately differentiated by confirmed pathologists.

Each selected section contained both tumoral and non-tumoral adjacent pancreatic tissues. Sections were incubated with

anti-RPSA Rabbit polyclonal antibody (ab99484 from Abcam), and negative controls were performed after deparaffinization with xylene and dehydration with a serial ethanol gradient. Antigens were retrieved by heating slides in citrate buffer (pH 6.0) for 8 min at +95°C. Samples were incubated for further 56 min with Ultra CC2 (cell conditioning, pH 6.0) and anti-RPSA antibody (diluted 1/2000) was applied for 32 min. Negative control was realized by omitting the primary antibodies. Analysis of tissue section was done after counter-coloration by light microscopy by confirmed pathologists (PR and DC).

Statistical Analysis

Data are presented as mean ± SEM and n refers to the number of independent repeat of experiment. Statistical analyses were made using Student's *t*-tests or Mann-Whitney rank sum test depending on sample normality or paired Wilcoxon signed rank test using Sigma-Stat 3.0 (Systat Software, Inc.). When more than two conditions were compared, a Kruskal–Wallis one-way ANOVA was used followed by *post hoc* Dunn's Method tests. Results were considered significant when $^{*}P < 0.05$, $^{**}P < 0.01$, and $^{***}P < 0.001$.

RESULTS

Chronic Treatment With AG-9 and VG-6 Increases Pancreatic Cancer Cell Migration Through TRPM7 Expression

MIA PaCa-2 cells were incubated with AG-9 or VG-6 at 10^{-7} M for 24 h. Cell migration was increased by 72.8 ± 16.5% for AG-9 ($n = 4$) and by 57.6 ± 12.5% for VG-6 ($n = 4$) ($P < 0.001$; **Figure 1A**). Cell viability was assessed during 96 h and no effect of EDPs was observed (**Figure 1B**). These results showed that EDPs increased PDAC cell migration without changing the cell viability. We previously showed that PDAC cell migration is dependent of TRPM7 expression (Rybarczyk et al., 2012, 2017). We confirmed that TRPM7 was implicated in MIA PaCa-2 basal migration since cell migration was reduced in cells transfected with a siTRPM7 ($n = 4$; $P < 0.001$; **Figures 1C,E**). AG-9 and VG-6 had still a pro-migratory effect in cells transfected with a scrambled siRNA but they had no effect in siTRPM7 cells ($n = 4$; $P > 0.05$; **Figures 1C,E**). MTT assays were also performed to control that the effects observed for cell migration were not due to modifications of cell viability. AG-9 treatment slightly increased cell viability by 21.33 ± 3.05% only in cells transfected with a siRNA targeting TRPM7 ($n = 4$; $P < 0.05$; **Figure 1D**). On the other hand, VG-6 treatment had no effect on cell viability ($n = 3$; $P < 0.05$; **Figure 1F**). Taken together, our results show that EDPs increased PDAC cell migration in a TRPM7 dependent manner.

AG-9 Stimulates TRPM7 Currents in Pancreatic Cancer Cells

Firstly, TRPM7 expression was assessed by quantitative RT-PCR following the treatment with AG-9 or VG-6 for 24 h. TRPM7 expression was not modified by EDP treatment ($n = 4$; $P < 0.05$; **Figure 2A**) while TRPM7 silencing decreased TRPM7 expression by 90.2 ± 0.1% at mRNA level ($n = 4$; $P < 0.01$; **Figure 2B**), and by 30 ± 7% at protein level ($n = 4$; $P < 0.05$; **Figures 2C,D**) when compared to siControl. We previously showed that Magnesium-Inhibited Cation (MIC) currents are mainly due to TRPM7 channel activity in MIA PaCa-2 cells (Rybarczyk et al., 2017). MIC currents were recorded by using the conventional technique of patch-clamp in whole-cell configuration. Maximal MIC current intensity was reached after almost 15 min of intracellular media dialysis with EGTA (data not shown, see Rybarczyk et al., 2017). A typical example of AG-9 acute perfusion effect on MIC currents is displayed in the **Figures 2E,F**. AG-9 increased outward (recorded at +100 mV) in a sustained and reversible manner (representative trace of 5 experiments, **Figure 2E**). I-V relationships showed that AG-9 increased the outward rectification (representative trace of 5 experiments, **Figure 2F**). We further built the I-V relationships of AG-9 sensitive currents by subtracting the basal MIC current from that recorded during AG-9 perfusion. AG-9-sensitive currents had inward component at negative membrane potentials, strong outward rectification at positive potential and a reversal membrane potential close to 0 mV ($n = 5$; **Figure 2G**). Interestingly, the AG-9-sensitive currents seem more linear than the typical MCI currents. TRPM7 silencing fully abolished the AG-9-sensitive currents indicating that AG-9 activated TRPM7 channels in PDAC cells ($n = 4$; $P < 0.05$; **Figures 2G,H**).

TRPM7 and RPSA Colocalize in Pancreatic Cancer Cells

We previously showed that EGCG treatment prevents AG-9-induced blebbing by RPSA inhibition (Brassart et al., 2019). As demonstrated above, AG-9 activates TRPM7 channels. We have previously shown that AG-9 interacts with cancer cells through RPSA binding. We were interesting in the possible relation between RPSA and TRPM7. EGCG was previously reported to bind RPSA and to prevent AG-9/RPSA interaction. For this reason, MIA PaCa-2 pancreatic cancer cells were pre-incubated with EGCG (10 μM) for 1 h, then incubated with or without AG-9 (10^{-7} M) for 24 h before fixation with paraformaldehyde and labeling with anti-TRPM7 and RPSA antibodies. Immunocytofluorescence microscopy analysis on optical sections showed TRPM7/RPSA colocalization in absence of effectors. In presence of AG-9 peptide, TRPM7/RPSA colocalization increases by 269 ± 61% ($n = 3$; $P < 0.001$; **Figures 3A,B**). TRPM7/RPSA colocalization was not significantly modified by EGCG treatment in comparison with untreated MIA PaCa-2 cells. Co-treatment with AG-9 and EGCG significantly decreased TRPM7/RPSA colocalization by 71.7 ± 1.4% ($n = 3$; $P < 0.001$; **Figures 3A,B**). These data demonstrated that AG-9 peptide influences the colocalization of TRPM7 and RPSA in pancreatic cancer cells.

RPSA Is Overexpressed in Human PDAC Tissues

The expression of RPSA in human PDAC tissues was studied using IHC and demonstrated a higher expression in tumoral cells compared to non-tumoral duct cells (**Figure 4**). In the

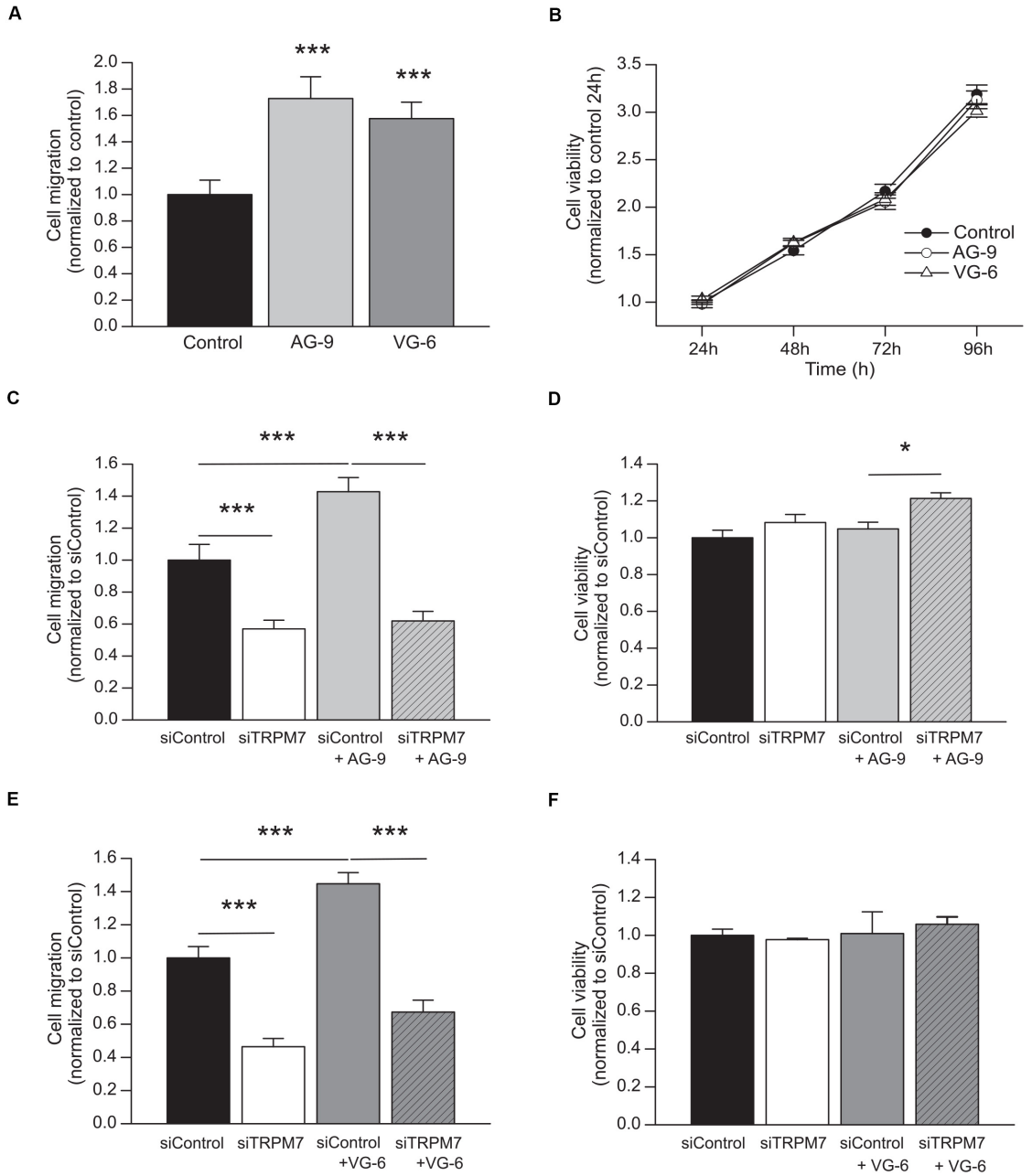

FIGURE 1 | EDPs enhance MIA PaCa-2 migration through TRPM7 expression. **(A)** Effect of 24 h incubation with 10^{-7} M AG-9 and VG-6 EDPs on the MIA PaCa-2 cell migration assessed by Boyden chamber assay. **(B)** Effect of EDPs on cell viability assessed by MTT assay. **(C)** Effect of TRPM7 silencing on AG-9 enhanced cell migration. **(D)** Effect of TRPM7 silencing and AG-9 treatment on cell viability. **(E)** Effect of TRPM7 silencing on VG-6 enhanced cell migration. **(F)** Effect of TRPM7 silencing and VG-6 treatment on cell viability. All results are shown as means ± SEM. *$P < 0.05$; ***$P < 0.001$ by ANOVA followed by *post hoc* Dunn's tests.

8 selected patients suffering of a moderately differentiated PDAC, a strongest staining was recorded in tumoral tissues compared to non-tumoral pancreatic ducts (**Figures 4A,C**). For each case, the staining was localized into the cytoplasm with little variation dependent of the characteristic of tumoral cells (hypersecretion, microvacuoles in the cytoplasm). In non-tumoral tissues into ducts, the staining was also cytoplasmic and RPSA seems to be ubiquitously expressed (**Figure 4A**). Indeed, other cell types like inflammatory, stromal and acinar cells showed a specific staining. Importantly, no unspecific staining was observed, especially in extracellular matrix fibers like collagen (**Figure 4B**).

Focusing on pancreatic ducts, an overexpression of RPSA was observed in tumoral cells. Anti-RPSA staining was stronger in tumoral cells (**Figure 4D**) compared to the non-tumoral duct cells (**Figure 4C**).

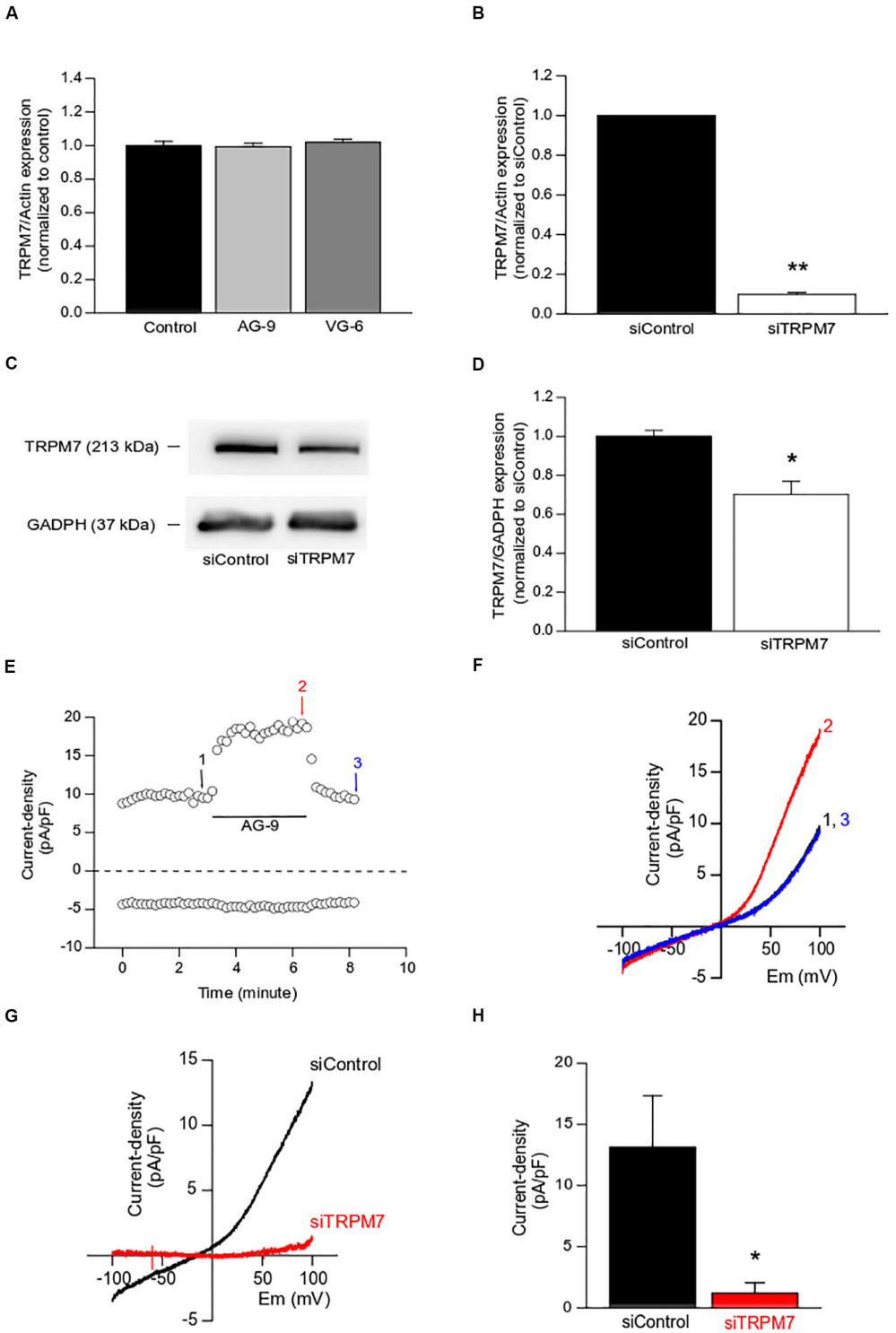

FIGURE 2 | Functional modulation of TRPM7 channels by EDPs. **(A)** Effect of EDPs incubation on TRPM7 expression assessed by qRT-PCR in MIA PaCa-2 cells. **(B)** Effect of TRPM7 silencing on TRPM7 expression assessed by qRT-PCR. **(C)** Typical example of lysates from MIA PaCa-2 cells transfected with a scrambled siRNA (siControl) or targeting TRPM7 (siTRPM7) and immunoblotted with anti-TRPM7 and anti-GADPH antibodies. **(D)** Quantification of immunoblotting normalized to siControl. **(E)** Typical example of MIC current recorded at +100 mV (outward current) and at −100 mV (inward current) before (1), during (2), and after (3) the application of AG-9 (10^{-7} M). **(F)** Current–voltage relationships corresponding to the traces recorded in **(C)**. **(G)** Averaged current–voltage relationship of AG-9-activated currents recorded in cells transfected with a non-targeting siRNA (siControl, black traces) and in cells transfected with a siRNA targeting TRPM7 (siTRPM7, red traces). **(H)** Current densities of AG-9-activated currents recorded at +100 mV. *$P < 0.05$ and **$P < 0.01$ by Mann-Whitney rank sum tests.

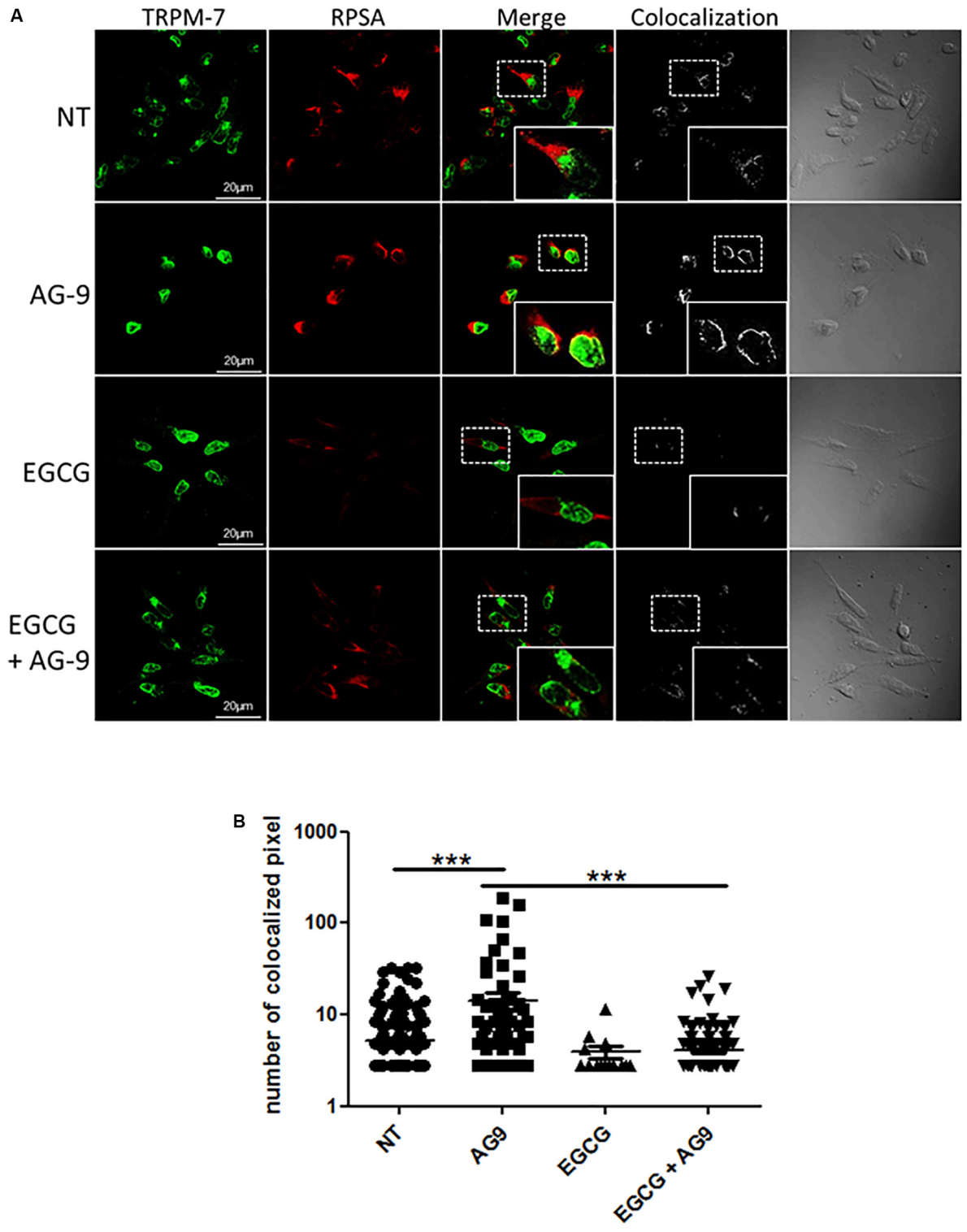

FIGURE 3 | Cellular distribution of TRPM7 and RPSA. **(A)** MIA PaCa-2 cells were pre-incubated with or without EGCG (10 μM) for 1 h and then with or without AG-9 (10^{-7} M) for 24 h at +37°C and analyzed by confocal microscopy for TRPM7 and RPSA protein cellular distribution. Colocalization was studied with the Colocalization plugin of ImageJ. Inserts: 2.25× magnification. Scale bar: 20 μm. **(B)** Quantification of TRPM7/RPSA colocalization pixels in confocal optical sections of MIA PaCa-2 cells in the presence or not of AG-9 (10^{-7} M) and EGCG (10 μM). Data from one experiment, representative of three independent experiments, are shown. ***$P < 0.001$ by Mann-Whitney rank sum tests.

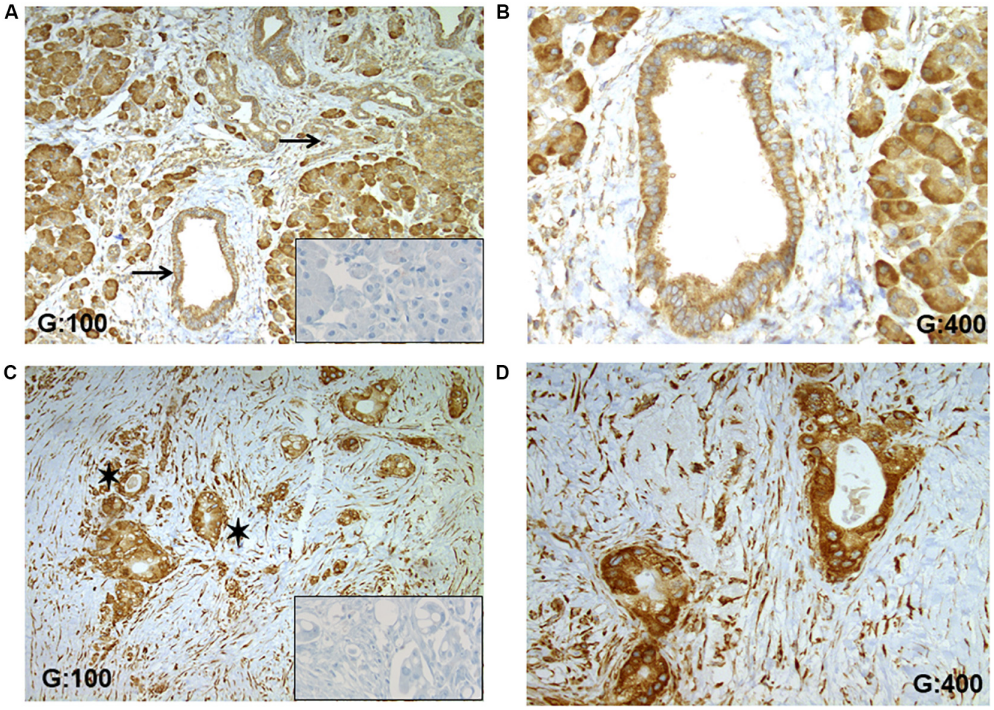

FIGURE 4 | RPSA expression in human PDAC. **(A)** RPSA is ubiquitously expressed in the normal pancreatic tissue (pancreatic duct and acinar cells, inflammatory, and stromal cells) but no unspecific staining was seen in collagen fibers, black arrows focus on healthy pancreatic ducts. **(B)** At high magnification, a weak and cytosolic staining was observed in normal duct cells. **(C)** In PDAC tissue, a high staining was observed in all tumoral cells, and black stars show tumoral glandular structures. **(D)** At high magnification, a high and cytosolic staining was always observed in tumoral cells. Inserts: RPSA staining was not apparent in the absence of the primary antibody.

DISCUSSION

In the present study, we showed that TRPM7 is involved in the MIA PaCa-2 cell migration stimulated by elastin-derived peptides (EDPs) AG-9 and VG-6 and that EDPs treatment lead to TRPM7 / RPSA interaction in PDAC cells.

These results confirm that EDPs exert protumor activities by increasing cell migration as previously shown by Da Silva et al. (2018) in HT-29 colon adenocarcinoma cell line. Pancreatic adenocarcinoma (PDAC) is characterized by an abundant desmoplastic stroma composed by extracellular matrix (ECM) proteins and various cell types. The ECM represents up to 90% of the PDAC tumor mass. For instance, it has been shown that collagen I and IV promote PDAC cell proliferation and migration (Lafaro and Melstrom, 2019). Thus, our results provide new insights into the regulation of PDAC cell migration by ECM. To our knowledge, the role of EDPs had not yet been described in PDAC. Our work suggests that EDPs could participate to the stimulation of PDAC cell migration and invasion induced by the interaction with the desmoplastic stroma.

EDP-stimulated cell migration was prevented by TRPM7 silencing indicating that this protein is required for this mechanism. TRPM7 is overexpressed in numerous malignancies including PDAC (Rybarczyk et al., 2012; Yee et al., 2015). *In vitro*, TRPM7 silencing reduced basal (non-stimulated) migration (Rybarczyk et al., 2012) and basal or FBS-stimulated PDAC cell invasion (Yee et al., 2015; Rybarczyk et al., 2017). EDP treatment did not modify TRPM7 expression but acute application of EDP induced the generation of a large TRPM7-like membrane current in MIA PaCa-2 cells. TRPM7 channels are essential for Ca^{2+}, Mg^{2+}, and Zn^{2+} cellular influx (Mittermeier et al., 2019). It has been shown that EDPs increases cytosolic calcium levels in human fibrosarcoma cells (Brassart et al., 2019). Surprisingly, we did not observe any effect of chronic nor acute application of EDPs on cation influx recorded by manganese-induced quenching of fura-2 fluorescence (data not shown). These results suggest that EDPs activated TRPM7 channels without inducing a large increase of divalent cation influx in the cytosol. However, we cannot exclude that EDPs induced variation of divalent cation concentration into highly localized nanodomains. For example, TRPM7 channels are linked to high-calcium microdomains, also called calcium flickers or sparks, promoting directional migration in human lung fibroblasts (Wei et al., 2009) and also invadosome formation in mouse neuroblastoma cells (Visser et al., 2013). TRPM7 is a non-selective cation channel fused with a functional kinase domain at its c-terminus (Nadler et al., 2001; Runnels et al., 2001). Several studies also showed a role of TRPM7 kinase domain in cancer cell migration (Middelbeek et al., 2012; Guilbert et al., 2013; Song et al., 2017). Interestingly, the AG-9 sensitive currents seem more linear than the typical MIC currents. Kozak et al. (2002) described that external Mg^{2+} blocked monovalent cation current in a fast,

reversible and voltage-dependent manner. Our data suggest that AG-9 only increased the monovalent component of TRPM7 current and particularly the outwardly rectifying one. It is tempting to speculate that AG-9 interferes with external Mg^{2+} to change TRPM7 permeation. Taken together, these data strongly suggest that AG-9 modifies monovalent but not divalent currents through TRPM7. However, this is only descriptive and further experiments are needed to better understand how AG-9 acts with TRPM7 channels to enhance pancreatic cancer cell migration.

We recently showed that EDPs induced cancer cell blebbing and shedding of extracellular vesicles through binding to RPSA (Brassart et al., 2019). Here, we further showed that EDPs treatment induced the colocalization of TRPM7 and RPSA in MIA PaCa-2 cells. This colocalization was prevented by co-treatment with AG-9 and EGCG, an inhibitor of RPSA. Taken together, our results show that EDPs stimulate PDAC cell migration and TRPM7/RPSA colocalization. Interestingly, it has been shown that RPSA interacts with integrin alpha 6 (ITGA6) and regulates PDAC cell invasion through MAPK signaling pathways (Wu et al., 2019). TRPM7 silencing reduced the phosphorylation level of MAPK signal molecules (P38, ERK, and JNK) in metastatic breast cancer cells and decreased their migration and invasion (Meng et al., 2013). Based on our results and the literature, we can hypothesize that EDP release in the desmoplastic stroma during pancreatic carcinogenesis may induce formation of TRPM7/RPSA complexes in PDAC cells. It is tempting to speculate that such complexes may activate oncogenic signaling pathways leading to enhanced cell migration but this hypothesis needs further investigations. Moreover, our results confirm that RPSA is overexpressed in human pancreatic tumor tissues compared to their adjacent non-tumor counterparts (Wu et al., 2019). RPSA is ubiquitously expressed and IHC staining was observed in number cell types without any unspecific staining. This ubiquitous expression need to focus on non-tumoral ducts cells and to compare them to the tumoral cells. Wu et al. (2019) described the same overexpression of RPSA in PDAC tissues by using different antibodies. Interestingly, we previously showed a similar overexpression of TRPM7 in PDAC primary tumor (Rybarczyk et al., 2012) as well as in lymph node (Rybarczyk et al., 2017). Further investigations are needed to increase the number of patients and the diversification of tumor status (grading, metastatic status, . . .). Thus, targeting of TRPM7/RPSA complexes could be a promising strategy to reduce cancer cell migration in the neoplastic pancreas.

DATA AVAILABILITY STATEMENT

The raw data supporting the conclusions of this article will be made available by the authors, without undue reservation, to any qualified researcher.

ETHICS STATEMENT

The studies involving human participants were reviewed and approved by human tissue samples from PDAC ($n = 8$) and were used with the agreement of patients treated by surgery in the University Hospital of Amiens (Picardie, France). Experiments on human tissues were approved by the Comité Consultatif de Protection des Personnes dans la Recherche Biomédicale de Picardie (Amiens, France). The patients/participants provided their written informed consent to participate in this study.

AUTHOR CONTRIBUTIONS

TL did the experiments (cell culture, treatments, cell migration, and proliferation assays). PR and DC did the experiments (IHC in patient tissues). AV did the experiments (Western-Blots). CB and RC helped for the cell treatment. SB-P and ID-D helped to design the experiments (confocal microscopy for SB-P and IHC for ID-D). HO-A helped to design the experiments and correct the manuscript. BB and MG designed the study, wrote the manuscript, and did the experiments (confocal microscopy for BB and patch-clamp for MG). All authors contributed to the article and approved the submitted version.

ACKNOWLEDGMENTS

We thank Aurélie Dupont-Deshorgues, Marie-Pierre Mabille, and Louis-Victor Gaudet for their technical help. This work was supported by L'Université de Picardie Jules Verne (UPJV), L'Université de Reims Champagne-Ardenne (URCA), Le CHU Amiens-Picardie, Le Centre National de la Recherche Scientifique (UMR 7369), La Ligue Contre le Cancer (Comité du Septentrion), and Le Cancéropôle Nord-Ouest (CNO).

REFERENCES

Betre, H., Ong, S. R., Guilak, F., Chilkoti, A., Fermor, B., and Setton, L. A. (2006). Chondrocytic differentiation of human adipose-derived adult stem cells in elastin-like polypeptide. *Biomaterials* 27, 91–99. doi: 10.1016/j.biomaterials.2005.05.071

Brassart, B., Da Silva, J., Donet, M., Seurat, E., Hague, F., Terryn, C., et al. (2019). Tumour cell blebbing and extracellular vesicle shedding: key role of matrikines and ribosomal protein SA. *Br. J. Cancer* 120, 453–465. doi: 10.1038/s41416-019-0382-0

Da Silva, J., Lameiras, P., Beljebbar, A., Berquand, A., Villemin, M., Ramont, L., et al. (2018). Structural characterization and in vivo pro-tumor properties of a highly conserved matrikine. *Oncotarget* 9, 17839–17857. doi: 10.18632/oncotarget.24894

Deer, E. L., Gonzalez-Hernandez, J., Coursen, J. D., Shea, J. E., Ngatia, J., Scaife, C. L., et al. (2010). Phenotype and genotype of pancreatic cancer cell lines. *Pancreas* 39, 425–435. doi: 10.1097/MPA.0b013e3181c15963

DiGiacomo, V., and Meruelo, D. (2016). Looking into laminin receptor: critical discussion regarding the non-integrin 37/67-kDa laminin receptor/RPSA protein. *Biol. Rev. Camb. Philos. Soc.* 91, 288–310. doi: 10.1111/brv.12170

Donet, M., Brassart-Pasco, S., Salesse, S., Maquart, F. X., and Brassart, B. (2014). Elastin peptides regulate HT-1080 fibrosarcoma cell migration and invasion through an Hsp90-dependent mechanism. *Br. J. Cancer* 111, 139–148. doi: 10.1038/bjc.2014.239 bjc2014239

Fujimura, Y., Sumida, M., Sugihara, K., Tsukamoto, S., Yamada, K., and Tachibana, H. (2012). Green tea polyphenol EGCG sensing motif on the 67-kDa laminin receptor. *PLoS One* 7:e37942. doi: 10.1371/journal.pone.0037942

Guilbert, A., Gautier, M., Dhennin-Duthille, I., Rybarczyk, P., Sahni, J., Sevestre, H., et al. (2013). Transient receptor potential melastatin 7 is involved in oestrogen receptor-negative metastatic breast cancer cells migration through its kinase domain. *Eur. J. Cancer* 49, 3694–3707. doi: 10.1016/j.ejca.2013.07.008

Hanano, T., Hara, Y., Shi, J., Morita, H., Umebayashi, C., Mori, E., et al. (2004). Involvement of TRPM7 in cell growth as a spontaneously activated Ca2+ entry pathway in human retinoblastoma cells. *J. Pharmacol. Sci.* 95, 403–419. doi: 10.1254/jphs.fp0040273

Houghton, A. M., Mouded, M., and Shapiro, S. D. (2011). "Consequences of elastolysis," in *Extracellular Matrix Degradation*, eds W. Parks and R. Mecham (Berlin: Springer), 217–249. doi: 10.1007/978-3-642-16861-1_9

Huet, E., Brassart, B., Cauchard, J. H., Debelle, L., Birembaut, P., Wallach, J., et al. (2002). Cumulative influence of elastin peptides and plasminogen on matrix metalloproteinase activation and type I collagen invasion by HT-1080 fibrosarcoma cells. *Clin. Exp. Metastasis* 19, 107–117. doi: 10.1023/a:1014547324918

Kozak, J. A., Kerschbaum, H. H., and Cahalan, M. D. (2002). Distinct properties of CRAC and MIC channels in RBL cells. *J. Gen. Physiol.* 120, 221–235. doi: 10.1085/jgp.20028601

Lafaro, K. J., and Melstrom, L. G. (2019). The paradoxical web of pancreatic cancer tumor microenvironment. *Am. J. Pathol.* 189, 44–57. doi: 10.1016/j.ajpath.2018.09.009

Lohmann, W., Schill, W. B., Bucher, D., Peters, T., Nilles, M., Schulz, A., et al. (1994). Elastosis and cancer. *Z. Naturforsch. C J. Biosci.* 49, 223–229. doi: 10.1515/znc-1994-3-410

Long, M. M., King, V. J., Prasad, K. U., and Urry, D. W. (1988). Chemotaxis of fibroblasts toward nonapeptide of elastin. *Biochim. Biophys. Acta* 968, 300–311. doi: 10.1016/0167-4889(88)90021-3

Mecham, R. P., Hinek, A., Griffin, G. L., Senior, R. M., and Liotta, L. A. (1989). The elastin receptor shows structural and functional similarities to the 67-kDa tumor cell laminin receptor. *J. Biol. Chem.* 264, 16652–16657.

Meng, X., Cai, C., Wu, J., Cai, S., Ye, C., Chen, H., et al. (2013). TRPM7 mediates breast cancer cell migration and invasion through the MAPK pathway. *Cancer Lett.* 333, 96–102. doi: 10.1016/j.canlet.2013.01.031

Middelbeek, J., Kuipers, A. J., Henneman, L., Visser, D., Eidhof, I., van Horssen, R., et al. (2012). TRPM7 is required for breast tumor cell metastasis. *Cancer Res.* 72, 4250–4261. doi: 10.1158/0008-5472.can-11-3863

Mittermeier, L., Demirkhanyan, L., Stadlbauer, B., Breit, A., Recordati, C., Hilgendorff, A., et al. (2019). TRPM7 is the central gatekeeper of intestinal mineral absorption essential for postnatal survival. *Proc. Natl. Acad. Sci. U.S.A.* 116, 4706–4715. doi: 10.1073/pnas.1810633116

Nadler, M. J., Hermosura, M. C., Inabe, K., Perraud, A. L., Zhu, Q., Stokes, A. J., et al. (2001). LTRPC7 is a Mg.ATP-regulated divalent cation channel required for cell viability. *Nature* 411, 590–595. doi: 10.1038/35079092

Prakriya, M., and Lewis, R. S. (2002). Separation and characterization of currents through store-operated CRAC channels and Mg2+-inhibited cation (MIC) channels. *J. Gen. Physiol.* 119, 487–507.

Rahib, L., Smith, B. D., Aizenberg, R., Rosenzweig, A. B., Fleshman, J. M., and Matrisian, L. M. (2014). Projecting cancer incidence and deaths to 2030: the unexpected burden of thyroid, liver, and pancreas cancers in the United States. *Cancer Res.* 74, 2913–2921. doi: 10.1158/0008-5472.CAN-14-0155

Robinet, A., Fahem, A., Cauchard, J. H., Huet, E., Vincent, L., Lorimier, S., et al. (2005). Elastin-derived peptides enhance angiogenesis by promoting endothelial cell migration and tubulogenesis through upregulation of MT1-MMP. *J. Cell Sci.* 118(Pt 2), 343–356. doi: 10.1242/jcs.01613

Runnels, L. W., Yue, L., and Clapham, D. E. (2001). TRP-PLIK, a bifunctional protein with kinase and ion channel activities. *Science* 291, 1043–1047. doi: 10.1126/science.1058519 1058519

Rybarczyk, P., Gautier, M., Hague, F., Dhennin-Duthille, I., Chatelain, D., Kerr-Conte, J., et al. (2012). Transient receptor potential melastatin-related 7 channel is overexpressed in human pancreatic ductal adenocarcinomas and regulates human pancreatic cancer cell migration. *Int. J. Cancer* 131, E851–E861. doi: 10.1002/ijc.27487

Rybarczyk, P., Vanlaeys, A., Brassart, B., Dhennin-Duthille, I., Chatelain, D., Sevestre, H., et al. (2017). The transient receptor potential melastatin 7 channel regulates pancreatic cancer cell invasion through the Hsp90alpha/uPA/MMP2 pathway. *Neoplasia* 19, 288–300. doi: 10.1016/j.neo.2017.01.004

Senior, R. M., Griffin, G. L., and Mecham, R. P. (1980). Chemotactic activity of elastin-derived peptides. *J. Clin. Invest.* 66, 859–862. doi: 10.1172/JCI109926

Song, C., Bae, Y., Jun, J., Lee, H., Kim, N. D., Lee, K. B., et al. (2017). Identification of TG100-115 as a new and potent TRPM7 kinase inhibitor, which suppresses breast cancer cell migration and invasion. *Biochim. Biophys. Acta* 1861, 947–957. doi: 10.1016/j.bbagen.2017.01.034

Toupance, S., Brassart, B., Rabenoelina, F., Ghoneim, C., Vallar, L., Polette, M., et al. (2012). Elastin-derived peptides increase invasive capacities of lung cancer cells by post-transcriptional regulation of MMP-2 and uPA. *Clin. Exp. Metastasis* 29, 511–522. doi: 10.1007/s10585-012-9467-3

Vania, L., Morris, G., Otgaar, T. C., Bignoux, M. J., Bernert, M., Burns, J., et al. (2019). Patented therapeutic approaches targeting LRP/LR for cancer treatment. *Exp. Opin. Ther. Pat.* 29, 987–1009. doi: 10.1080/13543776.2019.1693543

Vanlaeys, A., Fouquet, G., Kischel, P., Hague, F., Pasco-Brassart, S., Lefebvre, T., et al. (2020). Cadmium exposure enhances cell migration and invasion through modulated TRPM7 channel expression. *Arch. Toxicol.* 94, 735–747. doi: 10.1007/s00204-020-02674-w

Visser, D., Langeslag, M., Kedziora, K. M., Klarenbeek, J., Kamermans, A., Horgen, F. D., et al. (2013). TRPM7 triggers Ca2+ sparks and invadosome formation in neuroblastoma cells. *Cell Calcium* 54, 404–415. doi: 10.1016/j.ceca.2013.09.003

Wei, C., Wang, X., Chen, M., Ouyang, K., Song, L. S., and Cheng, H. (2009). Calcium flickers steer cell migration. *Nature* 457, 901–905. doi: 10.1038/nature07577

Wu, Y., Tan, X., Liu, P., Yang, Y., Huang, Y., Liu, X., et al. (2019). ITGA6 and RPSA synergistically promote pancreatic cancer invasion and metastasis via PI3K and MAPK signaling pathways. *Exp. Cell Res.* 379, 30–47. doi: 10.1016/j.yexcr.2019.03.022

Yee, N. S., Kazi, A. A., Li, Q., Yang, Z., Berg, A., and Yee, R. K. (2015). Aberrant over-expression of TRPM7 ion channels in pancreatic cancer: required for cancer cell invasion and implicated in tumor growth and metastasis. *Biol. Open* 4, 507–514. doi: 10.1242/bio.20137088

Conflict of Interest: The authors declare that the research was conducted in the absence of any commercial or financial relationships that could be construed as a potential conflict of interest.

The handling editor declared a past co-authorship with one of the authors SB-P.

Copyright © 2020 Lefebvre, Rybarczyk, Bretaudeau, Vanlaeys, Cousin, Brassart-Pasco, Chatelain, Dhennin-Duthille, Ouadid-Ahidouch, Brassart and Gautier. This is an open-access article distributed under the terms of the Creative Commons Attribution License (CC BY). The use, distribution or reproduction in other forums is permitted, provided the original author(s) and the copyright owner(s) are credited and that the original publication in this journal is cited, in accordance with accepted academic practice. No use, distribution or reproduction is permitted which does not comply with these terms.

frontiers in Oncology

MINI REVIEW
published: 22 July 2020
doi: 10.3389/fonc.2020.01231

Targeting the Extra-Cellular Matrix—Tumor Cell Crosstalk for Anti-Cancer Therapy: Emerging Alternatives to Integrin Inhibitors

Girieca Lorusso[1], *Curzio Rüegg*[1] *and François Kuonen*[2]*

[1] *Experimental and Translational Oncology, Department of Oncology Microbiology and Immunology, Faculty of Science and Medicine, University of Fribourg, Fribourg, Switzerland,* [2] *Department of Dermatology and Venereology, Hôpital de Beaumont, Lausanne University Hospital Center, Lausanne, Switzerland*

The extracellular matrix (ECM) is a complex network composed of a multitude of different macromolecules. ECM components typically provide a supportive structure to the tissue and engender positional information and crosstalk with neighboring cells in a dynamic reciprocal manner, thereby regulating tissue development and homeostasis. During tumor progression, tumor cells commonly modify and hijack the surrounding ECM to sustain anchorage-dependent growth and survival, guide migration, store pro-tumorigenic cell-derived molecules and present them to enhance receptor activation. Thereby, ECM potentially supports tumor progression at various steps from initiation, to local growth, invasion, and systemic dissemination and ECM-tumor cells interactions have long been considered promising targets for cancer therapy. Integrins represent key surface receptors for the tumor cell to sense and interact with the ECM. Yet, attempts to therapeutically impinge on these interactions using integrin inhibitors have failed to deliver anticipated results, and integrin inhibitors are still missing in the emerging arsenal of drugs for targeted therapies. This paradox situation should urge the field to reconsider the role of integrins in cancer and their targeting, but also to envisage alternative strategies. Here, we review the therapeutic targets implicated in tumor cell adhesion to the ECM, whose inhibitors are currently in clinical trials and may offer alternatives to integrin inhibition.

Keywords: extracellular matrix, tumor, progression, crosstalk, clinical perspectives

OPEN ACCESS

Edited by:
Nils Cordes, Technische Universität Dresden, Germany

Reviewed by:
Elisa Giannoni, University of Florence, Italy
Priyanka Gupta, University of Alabama at Birmingham, United States

***Correspondence:**
François Kuonen
francois.kuonen@chuv.ch

Specialty section:
This article was submitted to Molecular and Cellular Oncology, a section of the journal Frontiers in Oncology

Received: *10 January 2020*
Accepted: *16 June 2020*
Published: *22 July 2020*

Citation:
Lorusso G, Rüegg C and Kuonen F (2020) Targeting the Extra-Cellular Matrix—Tumor Cell Crosstalk for Anti-Cancer Therapy: Emerging Alternatives to Integrin Inhibitors. Front. Oncol. 10:1231. doi: 10.3389/fonc.2020.01231

INTRODUCTION: TARGETING THE ECM-TUMOR CELL CROSSTALK

The extra-cellular matrix (ECM) is a dynamic niche continuously undergoing quantitative and qualitative remodeling by renewed synthesis and proteolytic modifications. During ECM remodeling, changes to its physical structure and organization occur, leading to a dysregulation in fiber composition, tissue architecture, and stiffness contributing to cancer progression and fibrosis (1). The cell can sense the surrounding ECM fibers by transmembrane surface molecules, such as integrins or other glycoproteins, acting as cellular mechano-chemical sensors. The relevance of the finely tuned integration and crosstalk between the ECM molecules, the cellular cytoskeleton, and the downstream signaling pathways, has been widely recognized and studied (2, 3). Their complex dynamic bi-directional interactions and mechano-transduction control have

been associated to fundamental physiological processes such as branching tissues morphogenesis and angiogenesis during development and homeostasis. These interactions are also relevant to pathological conditions including cancer, from initial malignant transformation to the disruption of tissue polarity and promotion of invasiveness toward dissemination and metastasis development (4, 5). Integrins represent the key cell surface receptors for the cell to sense the ECM, triggering signaling pathways that determine cell fate and evolution toward a malignant phenotype and resistance to therapy (6, 7). Numerous experimental and preclinical studies conducted over the past decades highlighted the central role of integrins in affecting different steps of tumorigenesis, by controlling tumor cell adhesion, proliferation, migration, invasion, and survival (6). This made integrins appealing therapeutic targets leading to the development of integrin inhibitors and their clinical testing in cancer trials. Unfortunately and unexpectedly, integrin inhibitors failed to deliver any tangible therapeutic benefits for cancer patients (8–10). This failure may be due to the intrinsic complexity of integrin signaling that we still do not fully understand. But they also question the pharmacokinetic/pharmacodynamics properties of the integrin inhibitors developed, the integrin subunit and the associated biological process targeted, the preclinical models used as well as the design of the clinical trials performed (7, 8). Addressing those yet unanswered questions is likely to pave the road toward successful introduction of a novel generation of integrin inhibitors in clinical practice. In the meantime, long-ago discovered non-integrin ECM receptors as well as intra-cellular downstream effectors of the ECM-tumor cell crosstalk (signaling molecules) taking part in several key aspects of tumor progression, were largely neglected. Considering the clinical failure of integrin inhibitors, these ECM-tumor crosstalk targets are potential candidates that may be therapeutically exploited in alternative to integrin inhibitors. Here we review those currently tested in anti-cancer clinical trials, and portray their biology and activity in promoting tumor evolution.

NON-INTEGRIN TUMOR CELL RECEPTORS TO THE ECM

CD44

CD44 is a non-kinase transmembrane glycoprotein expressed in various cancer types (11). CD44 extracellular domain contains binding sites for various ECM proteins such as collagen, laminin, and fibronectin (12, 13), while hyaluronic acid (HA) produced both by tumor cells and tumor stroma is the main and most specific CD44 ligand (14, 15) (**Figure 1**). CD44 functions are modulated by both glycosylation and alternative splicing (16–18). Unlike the standard CD44 (CD44s), variant CD44 isoforms (CD44v) contain exons with specific post-translational modifications allowing binding of tumor-promoting cytokines like osteopontin (OPN), hepatocyte growth factor (HGF), vascular endothelial growth factor (VEGF), and basic fibroblast growth factor (bFGF) (19–23). Upon HA binding, CD44 proteins change conformation, oligomerize, and redistribute in glycolipid-enriched domains (GEMs) at the cell membrane (24, 25). There, activated CD44 preferentially interacts with activated receptor tyrosine kinases (RTKs) (26), various adaptor proteins such as ankyrin or the ERM (ezrin, radixin, and meosin), ultimately leading to cytoskeletal changes (spectrin, F-actin) (27, 28), Src family kinases (SFK) members accumulation (29), and activation of downstream pathways, such as Rho-GTPases (30–33), PI3K/AKT, or Ras/MAPK (34, 35) (**Figure 1**). Since the seminal discovery of their role in metastasis (36), CD44s and CD44v have been implicated in various steps of tumor progression. In particular, HA-induced CD44 conformational changes and subsequent cytoskeletal modifications promote tumor cell migration, invasion, and epithelial-to-mesenchymal transition (EMT) (27, 28, 30, 37–45). In glioma cells, HA-CD44 interactions were shown to occur specifically at the leading edge of migrating cells upon regulation by activated protein kinase C (PKC) (46). Upon HA binding, various proteases cleave CD44 allowing dynamic cytoskeletal changes, filopodia formation and ultimately CD44-mediated migration (47–50). Recently, non-catalytic MMP-9–mediated activation of CD44 was shown to promote tumor cell amoeboid migration (51). Since mesenchymal migration is based on integrin—ECM interactions, it is tempting to hypothesize that CD44 may support migration plasticity and escape to integrin inhibition (52–54). Further along tumor progression, circulating tumor cells (CTC) need to extravasate at distant organs. CD44 expressed on CTC was shown to interact with the HA coat produced by endothelial cells and initiate the process of tumor cell extravasation (55), particularly to the bone marrow, as shown in various tumor models through *in vitro* studies (56, 57). Importantly, both Cathepsin K, a potent collagenase typically expressed by osteoclasts during osteolysis, and MMP-9 were reported to be induced upon HA-mediated CD44 activation in prostate and breast cancer cells, suggesting their role in the colonization of metastatic osteolytic prostate and/or breast cancer cells (58–60). CD44 alternative splicing was reported to promote lung colonization by metastatic cancer cells (61). Recent studies implicated HA-CD44 interaction in tumor cell resistance to chemotherapy, by inducing multi-drug resistance 1 gene (MDR1) expression (62), ABC drug transporters (63), ankyrin-induced drug fluxes (62), and tumor cell survival pathways like ErbB2 signaling and PI3K/AKT pathway (64). Alternatively, HA-CD44 interactions may provide chemo-resistance through decreased apoptosis/cell death pathways by inducing anti-apoptotic proteins like inhibitors of the apoptosis family members (IAPs) (65–68), reducing pro-apoptotic proteins (69) or modulating autophagy (70).

Altogether, CD44 is involved at multiple steps of tumor progression and its inhibition appears as a promising alternative for tumor-ECM targeting therapies. Low molecular mass HA, soluble CD44, CD44 blocking antibodies, CD44 blocking peptides/aptamers, CD44-targeting sh/siRNA or silibinin (a plant-derived inhibitor of CD44 expression) have all been used successfully to interfere with CD44 function in preclinical

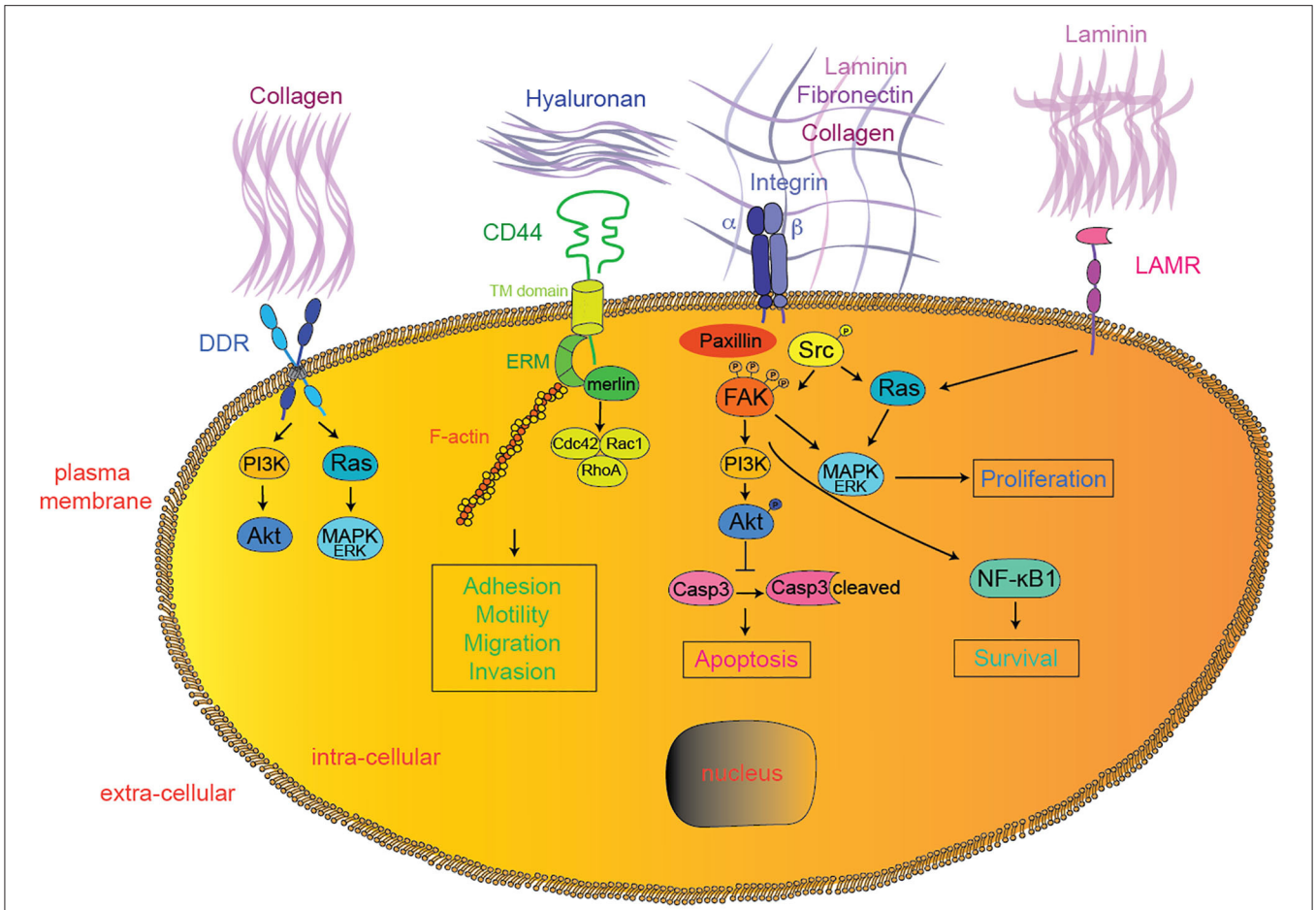

FIGURE 1 | Extracellular matrix—tumor cell interactions. In addition to integrins, DDR, CD44, LAMRs, FAK, and SFK represent emerging therapeutic targets currently tested in clinical trials for solid tumors. Downstream effectors interactions were simplified for clarity reasons. DDR, discoidin domain receptor; LAMR, 36/67 kDa laminin receptors; FAK, focal adhesion kinase; PI3K, phosphoinositide-3-kinase; MAPK, mitogen-activated protein kinases; Casp3, caspase 3; NF-κB1, nuclear factor-kappa B1.

models of solid tumor progression (**Table 1**). The CD44-blocking antibody RO5429083 was tested in a phase I, dose-escalation clinical study in metastatic or locally advanced, CD44-positive malignant solid tumors (NCT01358903) as well as in a phase I clinical study, alone or in combination with cytarabine, for acute myelogenous leukemia (NCT01641250). Alternatively, CD44 targeting may serve to specifically deliver cytotoxic drugs or radioisotopes to tumor cells. Bivatuzumab-mertansine, a CD44v6-specific targeting antibody linked to the cytotoxic drug mertansine, was tested in phase I dose-escalation clinical studies for CD44v6-positive recurrent or metastatic breast cancers (NCT02254031, NCT02254005) and advanced squamous cell carcinoma of the head and neck (NCT02254044, NCT02254018). The ^{186}Re-labeled bivatuzumab was tested in phase I biodistribution studies for non-small cell lung cancers (NCT02204059) and adenocarcinoma of the breast (NCT02204046). Although preliminary, these results encourage further clinical assessment of CD44-targeting therapies, either alone or in combination.

Discoidin Domain Receptors (DDR)

DDR1 and DDR2 belong to the family of the transmembrane receptor tyrosine kinase (RTK) with an extracellular discoidin domain binding to collagen in its native triple-helical conformation (227, 228) (**Figure 1**). DDR1 and DDR2 bind to various collagen isoforms with different affinities. DDR1 typically binds to collagens I-VI and VIII, while DDR2 preferentially binds to collagens I-III and X (228–231). Upon collagen binding, DDRs cluster and get activated through auto-phosphorylation at multiple tyrosine residues within the cytosolic part of the protein (232, 233), leading to the recruitment of adaptor or signaling proteins like ShcA, SHP-2, SFKs, the proline-rich tyrosine kinase 2 (Pyk2), and the non-muscle myosin heavy chain (NMHC) IIA (234, 235). In cancer cells, DDR activation was reported to induce Ras/MAPK (236), PI3K/AKT (236), Notch (237), NF-κB (238), PKCα/JAK/Stat (239), and p130CS/JNK pathways (234), thereby participating in various steps of tumor progression (**Figure 1**). Both DDR1 and DDR2 were shown to promote tumor cell proliferation, survival (236, 238, 240, 241), and migration

TABLE 1 | *In vivo* preclinical studies for solid tumors.

	Molecule	Combination	Tumor model	Biological process	References
Targeting CD44	Low molecular mass HA	–	Ovary, peripheral nerve	Tumor growth/metastasis	(71–73)
	soluble CD44	–	Melanoma, breast	Tumor growth	(74–76)
	CD44 blocking antibody	–	Breast, colon, pancreas, liver	Tumor growth, metastasis	(77–81)
	CD44v6 blocking antibody	–	Pancreas	Metastasis	(80, 82, 83)
	CD44 peptide	–	Melanoma, gastric	Tumor growth/metastasis	(81, 83–85)
	CD44v3 peptide	–	Glioblastoma	Tumor growth	(71–73, 84, 86)
	CD44v6 si/shRNA	–	Colon, gastric	Tumor growth	(82)
	CD44/Epcam aptamer		Ovary	Tumor growth	(82, 85)
	Silibinin	–	Prostate	Tumor growth	(86)
Targeting DDR	DDR1 blocking antibody	–	Breast	Tumor growth	(87)
	7rh (DDR1 inhibitor)	–	Gastric, pancreas	Tumor growth	(88, 89)
	WRG-28 (DDR2 inhibitor)	–	Breast	Metastasis	(90)
	Dasatinib (multikinase inhibitor)	–	Lung	Tumor growth	(91)
	Nilotinib (multikinase inhibitor)	–	Colon	Metastasis	(92)
	7rh (DDR1 inhibitor)	Dasatinib	Nasopharyngeal carcinoma	Tumor growth	(93)
	7rh (DDR1 inhibitor)	LY-411575 (Notch inhibitor)	Lung	Tumor growth	(91)
	DDR1-IN1 (DDR1 inhibitor)	Temzolomide/radiotherapy	Glioblastoma	Tumor growth	(94)
	Dasatinib (multikinase inhibitor)	JQ1 (BET inhibitor)	Lung	Tumor growth	(95)
	LAMR small molecule inhibitor	–	Breast	Metastasis	(96)
Targeting LAMR	LAMR^{37} blocking antibody	–	Fibrosarcoma	Metastasis	(97)
	OFA/iLRP-blocking antibody	–	Melanoma	Metastasis	(98–100)
	OFA/iLRP-based immunotherapy	–	Fibrosarcoma, sarcoma	Tumor growth/metastasis	(99, 100)
	FAK C-terminal domain	–	Fibroblasts, breast	Tumor growth/metastasis	(101, 102)
Targeting FAK	TAE-226	–	Glioma, ovary	Tumor growth	(103)
	VS-6062 (FAK/Pyk2 inhibitor)	–	Prostate, pancreas, melanoma, basal cell carcinoma	Tumor growth/metastasis	(104–107)
	VS-4718	–	Breast, ovary	Tumor growth/metastasis	(108, 109)
	VS-6063	–	Ovary	Tumor growth	(110)
	Compounds 14, Y15, Y11	–	Breast, pancreas, colon	Tumor growth	(111–114)
	Compounds C4, INT2-31, M13, R2 (FAK scaffold inhibitors)	–	Breast, pancreas, neuroblastoma, melanoma, colon	Tumor growth	(115–121)
	BI853520	–	Breast, mesothelioma	Tumor growth	(122, 123)
	NVP-TAE-226	–	Ewing sarcoma	Tumor growth/metastasis	(124)
	NVP-TAE-226	Docetaxel	Ovary	Tumor growth	(125)
	VS-6062 (FAK/Pyk2 inhibitor)	Sunitinib	Liver	Tumor growth	(126)
	VS-6062 (FAK/Pyk2 inhibitor)	Vemurafenib	Colon	Tumor growth	(127)
	Compound Y15	5-FU	Colon	Tumor growth	(113)
	Compound Y15	Gemcitabine	Pancreas	Tumor growth	(112, 128)
	Compound C4 (FAK scaffold inhibitor)	Temzolomide	Glioblastoma	Tumor growth	(128)
		Doxorubicin	Breast	Tumor growth	(115)
	Compound R2 (FAK scaffold inhibitor)	Doxorubicin, 5-FU	Colon	Tumor growth	(121)
	PF5735228	WZ811 (CXCR4 inhibitor)	Lung	Tumor growth	(129)
	VS-4718	HDAC inhibitors	Lung, Esophagus	Tumor growth	(130)
	VS-4718	PD-1 antagonist, T cell immunotherapy	Pancreas	Tumor growth	(131)

(Continued)

TABLE 1 | Continued

	Molecule	Combination	Tumor model	Biological process	References
	VS-6063	Docetaxel	Prostate	Tumor growth	(132)
	FAKsi nanoparticles	Paclitaxel nanoparticles	Ovary	Tumor growth	(133)
	Bosutinib (multikinase inhibitor)	–	Neuroblastoma, thyroid, prostate, pancreas, colon	Tumor growth/metastasis	(134–139)
Targeting SFK	Dasatinib (multikinase inhibitor)	–	Prostate, pancreas, colon	Tumor growth/metastasis	(140–142)
	Saracatinib (multikinase inhibitor)	–	Pancreas, prostate, head and neck, liver, gastric, biliary, sarcoma, colon, skin	Tumor growth/metastasis	(143–153)
	Ponatinib (multikinase inhibitor)	–	Glioblastoma, neuroblastoma, endometrial, gastric, breast, lung, bladder, colon, rhabdomyosarcoma, GIST	Tumor growth	(154–159)
	Vandetanib (multikinase inhibitor)	–	Breast, thyroid, glioblastoma, lung, liver, prostate, head and neck, vulva, ovary, gastric, pancreas, kidneys, colon	Tumor growth/metastasis	(160–185)
	Dasatinib (multikinase inhibitor)	Cetuximab	Colon	Tumor growth	(186)
	Dasatinib (multikinase inhibitor)	Erlotinib/gemcitabine	Pancreas	Tumor growth	(187)
	Saracatinib (multikinase inhibitor)	Axitinib/erlotinib	Colon	Tumor growth	(188)
		Trastuzumab	Breast	Tumor growth	(189)
		Trametinib	NSCLC	Tumor growth	(190)
		Bevacizumab	Glioma	Tumor growth	(191)
		Rapamycin	Liver	Tumor growth	(192)
		Paclitaxel	Breast, ovary	Tumor growth	(193, 194)
		Cisplatin	Bladder	Tumor growth	(195)
		Oxaliplatin	Colon	Tumor growth	(194, 196)
		Gemcitabine	Urothelial	Tumor growth	(197)
		Vincristine	Breast	Metastasis	(198)
		MCL-1 inhibitor	Breast	Tumor growth	(199)
		CYT997	Prostate	Tumor growth/metastasis	(200)
		Caffeic acid phenetyl	Glioma	Tumor growth	(201)
		Dendritic cell vaccine	Breast	Tumor growth/metastasis	(202)
		Anti-CTLA-4	Head and neck	Tumor growth	(203)
		Cetuximab	NSCLC	Tumor growth	(204)
	Saracatinib (multikinase inhibitor) Vandetanib (multikinase inhibitor)	Cabozantinib	Schwannoma	Tumor growth	(205)
		Capivasertib	Head and neck	Tumor growth	(206)
		Trastuzumab	Breast, gastric	Tumor growth	(207, 208)
		Anastrozole	Breast	Tumor growth	(209)
		Fulvestrant	Ovary, breast	Tumor growth	(210, 211)
		5-FU	Gastric	Tumor growth	(212)
		Celecoxib	Osteosarcoma	Tumor growth	(213)
	Vandetanib (multikinase inhibitor)	Tamoxifen	Breast	Tumor growth	(214)
		Paclitaxel	Ovary, colon	Tumor growth/metastasis	(215, 216)
		Cisplatin	Neuroblastoma	Tumor growth	(217)
		Oxiplatin	Colon	Tumor growth	(218)
		Temozolomide	NSCLC, glioblastoma	Tumor growth	(219–221)
		Radiotherapy	Head and neck, lung	Tumor growth	(222)
		Radiotherapy/gemcitabine	Pancreas	Tumor growth	(223)
		Radiotherapy/irinotecan	Colon	Tumor growth	(224)
		Radiotherapy/cisplatin	Head and neck	Tumor growth	(225)
		L19m-TNFalpha	Esophagus	Tumor growth	(226)

(242–245). Interestingly, EMT was reported to rely on the switch from DDR1 (epithelial) to DDR2 (mesenchymal) expression (246), although various reports implicate both DDR1 and DDR2 in EMT-mediated tumor cell invasion (234, 247). More recently, DDRs were implicated in the late stages of metastatic tumor progression (244, 248). Typically, DDR1 drives site-specific metastasis of lung cancer cells to bone (248). Additionally, the collagen-dependent interaction between Transmembrane 4 L6 Family Member 1 (TM4SF1) and DDR1 regulates dormancy vs. growth at the metastatic site (239). Finally, both DDR1 and DDR2 promote resistance to radio- and chemo-therapy in various preclinical models (94, 236–238, 249). However, despite these converging evidences implicating DDRs in tumor progression, one should consider that DDR-mediated effects are highly versatile and cell-dependent. For example, DDR1 was shown to either support or prevent integrin α2β1-mediated cell migration in different experimental models (234, 250, 251). Moreover, the dynamic regulation of DDR expression during tumor progression will determine the consequences of DDR inhibition (231). Thus, the complex regulation of DDR activity in tumor cells may stand for the controversy concerning their contribution to cancer progression (243, 248, 252–254) and affect the potential efficacy of DDR targeting in cancer. Still, the recent identification of activating mutations in the cytoplasmic signaling portions of DDR affecting intracellular signaling (240, 255–257) opens new perspectives in the identification of patients who might benefit the most from DDR inhibition.

DDR1 and DDR2 kinases are efficiently inhibited by multikinase inhibitors like ponatinib, imatinib, dasatinib, and nilotinib (258). Dasatinib, nilotinib, a DDR1 blocking antibody, the selective DDR1 inhibitors 7rh and DDR1-IN-1 and the selective allosteric DDR2 inhibitor WRG-28 were shown to efficiently prevent DDR-mediated tumor progression in preclinical models (**Table 1**). Driven by these encouraging results, dasatinib was tested in a phase II clinical trial for patients with advanced non-small cell lung cancers harboring a DDR2 mutation (NCT01514864). Unfortunately, it was abandoned because of lack of efficacy and slow enrollment. Currently, nilotinib is being assessed in a phase II clinical trial for malignant locally advanced or metastatic solid neoplasms presenting DDR1 or DDR2 mutations (NCT02029001). Importantly, non-canonical activation of DDR1 was shown to promote metastasis through tyrosine kinase-independent signaling in preclinical models (239), warranting cautious assessment of RTK inhibitors to target DDR. Further efforts should aim at the development of specific DDR1 and DDR2 inhibitors targeting canonical and non-canonical activation routes, the identification of the patients who may benefit the most from DDR inhibition and their use in combination therapies.

36/67 kDa Laminin Receptors (LAMR)

The 67 kDa ($LAMR^{67}$) laminin receptor was first identified as a receptor for laminin 1 (259–261) (**Figure 1**). It is currently hypothesized that $LAMR^{67}$ arises from post-translational modifications of the precursor 37 kDa laminin receptor ($LAMR^{37}$), although the precise mechanisms (like sumoylation) are still to be resolved (262–264). LAMRs harbor multiple cellular localizations, as assessed by the wide range of cellular processes they are implicated in: ribosomal biogenesis (265), protein translation (266–268), pre-rRNA processing (269), cellular adhesion and migration (267, 270), invasion (271), cellular proliferation (272, 273), cytoskeletal modulation (267, 274), and chromatin and histone modifications (275). Both $LAMR^{37}$ and $LAMR^{67}$ were identified at the cell membrane where they potentially bind to laminins, associate with integrins (276, 277) and get phosphorylated (278, 279). Although the downstream signaling mechanisms are still unelucidated, various authors reported modifications of Ras/MAPK and JNK/p38 signaling upon laminin-binding to LAMRs (280), possibly through interactions with FAK and paxillin (267, 281) (**Figure 1**). Given their various implications in cellular regulation, it is not surprising to find elevated LAMR expression in various cancers (282–288) and their involvement in tumor cell growth, migration, invasion, and aggressiveness (266, 282, 289). Importantly, laminin 1—LAMR interaction was shown to be implicated in tumor cell adhesion (271, 290) and invasion (291, 292) and LAMR down-regulation was shown to promote tumor cell apoptosis (293–296). Whether this is mediated by laminin 1-dependent activation of LAMR remains unknown. Recent data suggest that LAMR interaction with FAK may depend on laminin 1—LAMR interaction and promote Ras/MAPK and/or PI3K/AKT-mediated survival (297, 298). However, LAMR was found to promote tumor progression through various laminin 1-independent manners, such as regulation of telomerases (299), reviewed in (300).

Despite various emerging strategies aimed to target LAMR (300), *in vivo* preclinical studies assessing the feasibility and efficiency of targeting LAMR are still scant. Both a $LAMR^{37}$ blocking antibody and a small molecule inhibitor preventing laminin-LAMR interaction were shown to impede metastatic progression (**Table 1**). The green tea-derived epigallocatechin-3-gallate (EGCG) is a small molecule affecting a large number of cellular targets, including $LAMR^{67}$ (301) and $LAMR^{37}$ (302). EGCG is currently assessed in a phase I study for chemopreventive effect in patients with curative-intent resections of colorectal cancer (NCT02891538). Interestingly, the immunogenic LAMR tumor-associated antigen, referred as oncofoetal antigen immature laminin receptor protein (OFA-iLRP), has been successfully used as a tumor antigen for vaccine-based therapies in preclinical studies (**Table 1**). Cellular immunotherapy using autologous dendritic cell loaded with OFA-iLRP was tested in a phase I-II clinical study for metastatic breast cancers (NCT00879489). Altogether, LAMR targeting appears promising for cancer therapy, although major efforts should aim at the development of specific inhibitors and acquisition of stronger preclinical data prior to further clinical trial.

DOWNSTREAM EFFECTORS OF INTEGRIN-MEDIATED TUMOR CELL ADHESION TO THE ECM

Focal Adhesion Kinase (FAK)

Focal adhesion kinase (FAK) is a cytoplasmic non-receptor protein tyrosine kinase. It is an important cell signaling

hub highly phosphorylated upon integrin activation, and has long been recognized as promoting cancer cell migration, proliferation, and survival/chemoresistance through downstream activation of Rho-GEF, talin, cortactin, SFKs, PI3K/AKT, Ras/MAPK, or NF-κB pathways (303, 304) (**Figure 1**). More recent studies have described that besides its classical localization at the plasma membrane of tumor cells, FAK can also translocate to the nucleus and act as a transcription factor driving the expression of cytokines and chemokines favoring tumor immune evasion, independently of integrin signaling (305). In pancreatic cancer, FAK inhibition increases the immune infiltrate within the tumor environment, thereby sensitizing tumors to immune-checkpoint blockade (306). In addition, FAK inhibition also affect stromal cells. By targeting carcinoma-associated endothelial cells, FAK inhibition enhances vascular permeability, drug delivery, and overcomes chemo-resistance to DNA-damaging agents (307). Altogether, these data largely support the potential for therapeutic benefits of FAK inhibitors, used alone or in combination therapies, in the arsenal of anti-cancer strategies, illustrated by their success in various preclinical models (**Table 1**). FAK inhibition mostly relies on small molecule inhibitors working through various mechanisms: ATP competitive kinase inhibition (TAE-226, VS-4718, VS-6062, VS-6063, GSK-2256098, PF-573228), FAK scaffold inhibition (compounds 14, Y11, Y15, C4, INT2-31, M13, R2), or more recently ATP competitive non-kinase inhibition (BI853520) (**Table 1**). In combination, FAK inhibition was reported to improve the efficacy of chemotherapeutic agents (docetaxel, paclitaxel, temzolomide, 5-FU, gemcitabine, doxorubicin), targeted therapies (EGFR inhibitor, Src inhibitor, sunitinib, BRAF inhibitor, CXCR4 inhibitor, HDAC inhibitor), or immunotherapy (PD1 antagonists, T cell immunotherapy) (**Table 1**). Acceptable safety profiles were obtained in phase I clinical trials for VS-6062 (104, 308), GSK-2256098 (309–311), VS-6063 (312, 313), VS-4718 and BI853520 (314–316), with VS-6062, GSK-2256098, and VS-6063 showing stabilization of disease in patients with various advanced solid tumors. Both GSK-2256098, in combination with trametinib, and VS-6063, however, failed to show efficacy in phase II clinical trials for pancreatic adenocarcinoma and malignant mesothelioma, respectively [NCT02428270, (317)]. This unexpected failure may have been prevented by the stratification of the patients based on FAK amplification/activity in order to select for the best responders. VS-6063 is currently tested in multiple clinical trials: (i) a phase II clinical trial in a pre-operative setting for malignant mesothelioma (NCT02004028); (ii) a phase II clinical trial in association with the PD-1 inhibitor pembrolizumab for advanced solid tumors (NCT02758587, NCT03727880); (iii) a phase I clinical trial in association with the RAF/MEK inhibitor RO5126766 for advanced solid tumors (NCT03875820); (iv) a phase I clinical trial in association with the anti-PDL1 antibody avelumab for epithelial ovarian cancer (NCT02943317); (v) a phase I clinical trial in association with pembrolizumab and gemcitabine for advanced solid tumors (NCT02546531). The results of these ongoing clinical trials will be decisive to shape the future development of FAK inhibitors in clinical practice.

Src Family Kinases (SFK)

The SFK, composed of c-Src, Fyn, Yes, Lck, Lyn, Hck, Fgr, and Blk, are cytoplasmic non-receptor protein tyrosine kinases. Their prominent functions are mediated by their SH2 and SH3 domains interacting with various RTKs (such as EGF-R, HER2, IGF-R, HGF-R, and PDGF-R), thereby participating in integration and regulation of RTK signaling. But SFK also participate in ECM-mediated signaling. Through phosphorylation of FAK, SFK activation stabilizes focal adhesion complexes enhancing cell adhesion to the ECM (318) (**Figure 1**). Altogether, SFK are implicated in many steps of tumorigenesis, including proliferation, migration, invasion, survival in the circulation and at distant metastatic sites (319–324), achieved through modulation of various downstream effectors as PI3K/AKT, Ras/MAPK, or Stat3 (325, 326). Additionally, SFK activation confers therapeutic resistance to targeted RTK therapies (e.g., Trastuzumab/Herceptin for HER2), to hormone-receptor endocrine therapies (e.g., Tamoxifen for Estrogen Receptor), as well as to traditional chemo- and radiotherapies (327). Given their central role in tumor cell signaling and pleiotropic functions in cancer, SFK represent a promising target for anti-cancer therapies. SFK are currently most efficiently targeted using non-specific ATP-competitive multikinase inhibitors, such as dasatinib, bosutinib, saracatinib, ponatinib, and vandetanib, targeting many different tyrosine kinases (such as BCR-ABL, Kit, PDGFR, EGFR, RET, VEGFR) in addition to SFK members (328). With the exception of vandetanib, approved for the treatment of thyroid medullary carcinoma, dasatinib, ponatinib, and bosetanib have been approved by the FDA for hematological malignancies only, based on their BCR/Abl inhibitory capacity (328). *In vivo* preclinical data, however, suggest their potential efficacy in solid tumors as well, alone or in combination, although not necessarily through SFK inhibition (**Table 1**). Up to date, the results of phase II clinical trials with SKF inhibitors in monotherapy have been disappointing, as they showed only modest or no efficacy (326, 329). Such failure may be largely attributed to the current lack of biomarkers for the identification patients with aberrant SFK, the lack of specificity of SFK inhibitors, and the sometimes opposing effects of SFK members at various steps of tumor progression (330, 331). The interpretation of the numerous ongoing clinical trials (http://www.clinicaltrials.gov/) as well as the design of future successful clinical trials testing SFK inhibitors for solid tumors will largely depend on our capacity to overcome these important issues.

CONCLUSION

Despite huge expectations based on preclinical studies, integrin inhibitors failed to deliver anticipated results and have not entered the clinical practice yet. Understanding and surmounting the pitfalls of integrin inhibition will be crucial to further sustain the targeting of tumor cell–ECM interactions as an anticancer strategy. Yet, other long-time discovered molecules at the interface between tumor cell and ECM as CD44, DDR, LAMR, FAK, and SFK, are emerging as alternative

therapeutic targets in clinical trials. Alike integrin inhibitors, their therapeutic relevance will depend on the specificity and pharmacokinetic/dynamic properties of the inhibitors developed, on the adequacy of the preclinical models used for validation, on the biological process targeted, on the biomarkers used for the identification of best responders and on the combination strategies applied in clinical trials. Importantly, our growing knowledge of the biology of ECM—tumor cell interactions will be instrumental in overcoming these important pitfalls and extend the arsenal of clinically valuable inhibitors targeting the ECM—tumor cells crosstalk in the near future.

AUTHOR CONTRIBUTIONS

GL wrote the review and edited the manuscript. CR edited the manuscript. FK planned the outline, wrote the review, and edited the manuscript. All authors read and approved the submitted version of the manuscript.

FUNDING

Work in our laboratories was supported by the Swiss National Science Foundation grants PZ00P3_185926 (to FK) and 31003A_179248 (to CR).

REFERENCES

1. Lu P, Weaver VM, Werb Z. The extracellular matrix: a dynamic niche in cancer progression. *J Cell Biol.* (2012) 196:395–406. doi: 10.1083/jcb.201102147
2. Hynes RO. The extracellular matrix: not just pretty fibrils. *Science.* (2009) 326:1216–9. doi: 10.1126/science.1176009
3. Hynes RO. Stretching the boundaries of extracellular matrix research. *Nat Rev Mol Cell Biol.* (2014) 15:761–3. doi: 10.1038/nrm3908
4. Bonnans C, Chou J, Werb Z. Remodelling the extracellular matrix in development and disease. *Nat Rev Mol Cell Biol.* (2014) 15:786–801. doi: 10.1038/nrm3904
5. Ringer P, Colo G, Fassler R, Grashoff C. Sensing the mechano-chemical properties of the extracellular matrix. *Matrix Biol.* (2017) 64:6–16. doi: 10.1016/j.matbio.2017.03.004
6. Cooper J, Giancotti FG. Integrin signaling in cancer: mechanotransduction, stemness, epithelial plasticity, and therapeutic resistance. *Cancer Cell.* (2019) 35:347–67. doi: 10.1016/j.ccell.2019.01.007
7. Hamidi H, Ivaska J. Every step of the way: integrins in cancer progression and metastasis. *Nat Rev Cancer.* (2018) 18:533–48. doi: 10.1038/s41568-018-0038-z
8. Alday-Parejo B, Stupp R, Ruegg C. Are integrins still practicable targets for anti-cancer therapy? *Cancers.* (2019) 11:978. doi: 10.3390/cancers11070978
9. Kapp TG, Rechenmacher F, Sobahi TR, Kessler H. Integrin modulators: a patent review. *Expert Opin Ther Pat.* (2013) 23:1273–95. doi: 10.1517/13543776.2013.818133
10. Vicente-Manzanares M, Sanchez-Madrid F. Targeting the integrin interactome in human disease. *Curr Opin Cell Biol.* (2018) 55:17–23. doi: 10.1016/j.ceb.2018.05.010
11. Yin T, Wang G, He S, Liu Q, Sun J, Wang Y. Human cancer cells with stem cell-like phenotype exhibit enhanced sensitivity to the cytotoxicity of IL-2 and IL-15 activated natural killer cells. *Cell Immunol.* (2016) 300:41–5. doi: 10.1016/j.cellimm.2015.11.009
12. Ishii S, Ford R, Thomas P, Nachman A, Steele G Jr, Jessup JM. CD44 participates in the adhesion of human colorectal carcinoma cells to laminin and type IV collagen. *Surg Oncol.* (1993) 2:255–64. doi: 10.1016/0960-7404(93)90015-Q
13. Jalkanen S, Jalkanen M. Lymphocyte CD44 binds the COOH-terminal heparin-binding domain of fibronectin. *J Cell Biol.* (1992) 116:817–25. doi: 10.1083/jcb.116.3.817
14. Aruffo A, Stamenkovic I, Melnick M, Underhill CB, Seed B. CD44 is the principal cell surface receptor for hyaluronate. *Cell.* (1990) 61:1303–13. doi: 10.1016/0092-8674(90)90694-A
15. Banerji S, Wright AJ, Noble M, Mahoney DJ, Campbell ID, Day AJ, et al. Structures of the Cd44-hyaluronan complex provide insight into a fundamental carbohydrate-protein interaction. *Nat Struct Mol Biol.* (2007) 14:234–9. doi: 10.1038/nsmb1201
16. Stamenkovic I, Amiot M, Pesando JM, Seed B. A lymphocyte molecule implicated in lymph node homing is a member of the cartilage link protein family. *Cell.* (1989) 56:1057–62. doi: 10.1016/0092-8674(89)90638-7
17. Goldstein LA, Zhou DF, Picker LJ, Minty CN, Bargatze RF, Ding JF, et al. A human lymphocyte homing receptor, the hermes antigen, is related to cartilage proteoglycan core and link proteins. *Cell.* (1989) 56:1063–72. doi: 10.1016/0092-8674(89)90639-9
18. Idzerda RL, Carter WG, Nottenburg C, Wayner EA, Gallatin WM, St John T. Isolation and DNA sequence of a cDNA clone encoding a lymphocyte adhesion receptor for high endothelium. *Proc Natl Acad Sci USA.* (1989) 86:4659–63. doi: 10.1073/pnas.86.12.4659
19. Bennett KL, Jackson DG, Simon JC, Tanczos E, Peach R, Modrell B, et al. CD44 isoforms containing exon V3 are responsible for the presentation of heparin-binding growth factor. *J Cell Biol.* (1995) 128:687–98. doi: 10.1083/jcb.128.4.687
20. Tremmel M, Matzke A, Albrecht I, Laib AM, Olaku V, Ballmer-Hofer K, et al. A CD44v6 peptide reveals a role of CD44 in VEGFR-2 signaling and angiogenesis. *Blood.* (2009) 114:5236–44. doi: 10.1182/blood-2009-04-219204
21. Todaro M, Gaggianesi M, Catalano V, Benfante A, Iovino F, Biffoni M, et al. CD44v6 is a marker of constitutive and reprogrammed cancer stem cells driving colon cancer metastasis. *Cell Stem Cell.* (2014) 14:342–56. doi: 10.1016/j.stem.2014.01.009
22. Megaptche AP, Erb U, Buchler MW, Zoller M. CD44v10, osteopontin and lymphoma growth retardation by a CD44v10-specific antibody. *Immunol Cell Biol.* (2014) 92:709–20. doi: 10.1038/icb.2014.47
23. Weber GF, Ashkar S, Glimcher MJ, Cantor H. Receptor-ligand interaction between CD44 and osteopontin (Eta-1). *Science.* (1996) 271:509–12. doi: 10.1126/science.271.5248.509
24. Lesley J, Hyman R, Kincade PW. CD44 and its interaction with extracellular matrix. *Adv Immunol.* (1993) 54:271–335. doi: 10.1016/S0065-2776(08)60537-4
25. Liu D, Sy MS. Phorbol myristate acetate stimulates the dimerization of CD44 involving a cysteine in the transmembrane domain. *J Immunol.* (1997) 159:2702–11.
26. Misra S, Toole BP, Ghatak S. Hyaluronan constitutively regulates activation of multiple receptor tyrosine kinases in epithelial and carcinoma cells. *J Biol Chem.* (2006) 281:34936–41. doi: 10.1074/jbc.C600138200
27. Fehon RG, McClatchey AI, Bretscher A. Organizing the cell cortex: the role of ERM proteins. *Nat Rev Mol Cell Biol.* (2010) 11:276–87. doi: 10.1038/nrm2866
28. Lokeshwar VB, Fregien N, Bourguignon LY. Ankyrin-binding domain of CD44(GP85) is required for the expression of hyaluronic acid-mediated adhesion function. *J Cell Biol.* (1994) 126:1099–109. doi: 10.1083/jcb.126.4.1099
29. Foger N, Marhaba R, Zoller M. Involvement of CD44 in cytoskeleton rearrangement and raft reorganization in T cells. *J Cell Sci.* (2001) 114:1169–78.
30. Bourguignon LY, Zhu H, Zhou B, Diedrich F, Singleton PA, Hung MC. Hyaluronan promotes CD44v3-Vav2 interaction with Grb2-p185(HER2) and induces Rac1 and Ras signaling during ovarian tumor cell migration and growth. *J Biol Chem.* (2001) 276:48679–92. doi: 10.1074/jbc.M106759200

31. Ponta H, Sherman L, Herrlich PA. CD44: from adhesion molecules to signalling regulators. *Nat Rev Mol Cell Biol.* (2003) 4:33–45. doi: 10.1038/nrm1004
32. Bourguignon LY. Hyaluronan-mediated CD44 activation of RhoGTPase signaling and cytoskeleton function promotes tumor progression. *Semin Cancer Biol.* (2008) 18:251–9. doi: 10.1016/j.semcancer.2008.03.007
33. Bourguignon LY, Singleton PA, Zhu H, Diedrich F. Hyaluronan-mediated CD44 interaction with RhoGEF and Rho kinase promotes Grb2-associated binder-1 phosphorylation and phosphatidylinositol 3-kinase signaling leading to cytokine (macrophage-colony stimulating factor) production and breast tumor progression. *J Biol Chem.* (2003) 278:29420–34. doi: 10.1074/jbc.M301885200
34. Orian-Rousseau V, Morrison H, Matzke A, Kastilan T, Pace G, Herrlich P, et al. Hepatocyte growth factor-induced Ras activation requires ERM proteins linked to both CD44v6 and F-actin. *Mol Biol Cell.* (2007) 18:76–83. doi: 10.1091/mbc.e06-08-0674
35. Weber GF. Molecular mechanisms of metastasis. *Cancer Lett.* (2008) 270:181–90. doi: 10.1016/j.canlet.2008.04.030
36. Gunthert U, Hofmann M, Rudy W, Reber S, Zoller M, Haussmann I, et al. A new variant of glycoprotein CD44 confers metastatic potential to rat carcinoma cells. *Cell.* (1991) 65:13–24. doi: 10.1016/0092-8674(91)90403-L
37. Bourguignon LY, Singleton PA, Zhu H, Zhou B. Hyaluronan promotes signaling interaction between CD44 and the transforming growth factor beta receptor I in metastatic breast tumor cells. *J Biol Chem.* (2002) 277:39703–12. doi: 10.1074/jbc.M204320200
38. Bourguignon LY, Wong G, Earle CA, Xia W. Interaction of low molecular weight hyaluronan with CD44 and toll-like receptors promotes the actin filament-associated protein 110-actin binding and MyD88-NFkappaB signaling leading to proinflammatory cytokine/chemokine production and breast tumor invasion. *Cytoskeleton.* (2011) 68:671–93. doi: 10.1002/cm.20544
39. Bourguignon LY, Wong G, Earle C, Krueger K, Spevak CC. Hyaluronan-CD44 interaction promotes c-Src-mediated twist signaling, microRNA-10b expression, and RhoA/RhoC up-regulation, leading to Rho-kinase-associated cytoskeleton activation and breast tumor cell invasion. *J Biol Chem.* (2010) 285:36721–35. doi: 10.1074/jbc.M110.162305
40. Zhao S, Chen C, Chang K, Karnad A, Jagirdar J, Kumar AP, et al. CD44 expression level and isoform contributes to pancreatic cancer cell plasticity, invasiveness, and response to therapy. *Clin Cancer Res.* (2016) 22:5592–604. doi: 10.1158/1078-0432.CCR-15-3115
41. Bellerby R, Smith C, Kyme S, Gee J, Gunthert U, Green A, et al. Overexpression of specific CD44 isoforms is associated with aggressive cell features in acquired endocrine resistance. *Front Oncol.* (2016) 6:145. doi: 10.3389/fonc.2016.00145
42. Cho SH, Park YS, Kim HJ, Kim CH, Lim SW, Huh JW, et al. CD44 enhances the epithelial-mesenchymal transition in association with colon cancer invasion. *Int J Oncol.* (2012) 41:211–8. doi: 10.3892/ijo.2012.1453
43. Brown RL, Reinke LM, Damerow MS, Perez D, Chodosh LA, Yang J, et al. CD44 splice isoform switching in human and mouse epithelium is essential for epithelial-mesenchymal transition and breast cancer progression. *J Clin Invest.* (2011) 121:1064–74. doi: 10.1172/JCI44540
44. Ni J, Cozzi PJ, Hao JL, Beretov J, Chang L, Duan W, et al. CD44 variant 6 is associated with prostate cancer metastasis and chemo-/radioresistance. *Prostate.* (2014) 74:602–17. doi: 10.1002/pros.22775
45. Thomas L, Byers HR, Vink J, Stamenkovic I. CD44H regulates tumor cell migration on hyaluronate-coated substrate. *J Cell Biol.* (1992) 118:971–7. doi: 10.1083/jcb.118.4.971
46. Lamontagne CA, Grandbois M. PKC-induced stiffening of hyaluronan/CD44 linkage; local force measurements on glioma cells. *Exp Cell Res.* (2008) 314:227–36. doi: 10.1016/j.yexcr.2007.07.013
47. Nagano O, Saya H. Mechanism and biological significance of CD44 cleavage. *Cancer Sci.* (2004) 95:930–5. doi: 10.1111/j.1349-7006.2004.tb03179.x
48. Nagano O, Murakami D, Hartmann D, De Strooper B, Saftig P, Iwatsubo T, et al. Cell-matrix interaction via CD44 is independently regulated by different metalloproteinases activated in response to extracellular Ca(2+) influx and PKC activation. *J Cell Biol.* (2004) 165:893–902. doi: 10.1083/jcb.200310024
49. Nakamura H, Suenaga N, Taniwaki K, Matsuki H, Yonezawa K, Fujii M, et al. Constitutive and induced CD44 shedding by ADAM-like proteases and membrane-type 1 matrix metalloproteinase. *Cancer Res.* (2004) 64:876–82. doi: 10.1158/0008-5472.CAN-03-3502
50. Sugahara KN, Hirata T, Tanaka T, Ogino S, Takeda M, Terasawa H, et al. Chondroitin sulfate E fragments enhance CD44 cleavage and CD44-dependent motility in tumor cells. *Cancer Res.* (2008) 68:7191–9. doi: 10.1158/0008-5472.CAN-07-6198
51. Orgaz JL, Pandya P, Dalmeida R, Karagiannis P, Sanchez-Laorden B, Viros A, et al. Diverse matrix metalloproteinase functions regulate cancer amoeboid migration. *Nat Commun.* (2014) 5:4255. doi: 10.1038/ncomms5255
52. Friedl P, Alexander S. Cancer invasion and the microenvironment: plasticity and reciprocity. *Cell.* (2011) 147:992–1009. doi: 10.1016/j.cell.2011.11.016
53. Te Boekhorst V, Preziosi L, Friedl P. Plasticity of cell migration *in vivo* and *in silico*. *Annu Rev Cell Dev Biol.* (2016) 32:491–526. doi: 10.1146/annurev-cellbio-111315-125201
54. Schmidt S, Friedl P. Interstitial cell migration: integrin-dependent and alternative adhesion mechanisms. *Cell Tissue Res.* (2010) 339:83–92. doi: 10.1007/s00441-009-0892-9
55. Siegelman MH, Stanescu D, Estess P. The CD44-initiated pathway of T-cell extravasation uses VLA-4 but not LFA-1 for firm adhesion. *J Clin Invest.* (2000) 105:683–91. doi: 10.1172/JCI8692
56. Okado T, Hawley RG. Adhesion molecules involved in the binding of murine myeloma cells to bone marrow stromal elements. *Int J Cancer.* (1995) 63:823–30. doi: 10.1002/ijc.2910630613
57. Draffin JE, McFarlane S, Hill A, Johnston PG, Waugh DJ. CD44 potentiates the adherence of metastatic prostate and breast cancer cells to bone marrow endothelial cells. *Cancer Res.* (2004) 64:5702–11. doi: 10.1158/0008-5472.CAN-04-0389
58. Lark MW, Stroup GB, James IE, Dodds RA, Hwang SM, Blake SM, et al. A potent small molecule, nonpeptide inhibitor of cathepsin K (SB 331750) prevents bone matrix resorption in the ovariectomized rat. *Bone.* (2002) 30:746–53. doi: 10.1016/S8756-3282(02)00675-0
59. Corey E, Brown LG, Quinn JE, Poot M, Roudier MP, Higano CS, et al. Zoledronic acid exhibits inhibitory effects on osteoblastic and osteolytic metastases of prostate cancer. *Clin Cancer Res.* (2003) 9:295–306.
60. Littlewood-Evans AJ, Bilbe G, Bowler WB, Farley D, Wlodarski B, Kokubo T, et al. The osteoclast-associated protease cathepsin K is expressed in human breast carcinoma. *Cancer Res.* (1997) 57:5386–90.
61. Yae T, Tsuchihashi K, Ishimoto T, Motohara T, Yoshikawa M, Yoshida GJ, et al. Alternative splicing of CD44 mRNA by ESRP1 enhances lung colonization of metastatic cancer cell. *Nat Commun.* (2012) 3:883. doi: 10.1038/ncomms1892
62. Bourguignon LY, Peyrollier K, Xia W, Gilad E. Hyaluronan-CD44 interaction activates stem cell marker Nanog, Stat-3-mediated MDR1 gene expression, and ankyrin-regulated multidrug efflux in breast and ovarian tumor cells. *J Biol Chem.* (2008) 283:17635–51. doi: 10.1074/jbc.M800109200
63. Ricciardelli C, Ween MP, Lokman NA, Tan IA, Pyragius CE, Oehler MK. Chemotherapy-induced hyaluronan production: a novel chemoresistance mechanism in ovarian cancer. *BMC Cancer.* (2013) 13:476. doi: 10.1186/1471-2407-13-476
64. Misra S, Ghatak S, Zoltan-Jones A, Toole BP. Regulation of multidrug resistance in cancer cells by hyaluronan. *J Biol Chem.* (2003) 278:25285–8. doi: 10.1074/jbc.C300173200
65. Bourguignon LY, Earle C, Wong G, Spevak CC, Krueger K. Stem cell marker (Nanog) and Stat-3 signaling promote MicroRNA-21 expression and chemoresistance in hyaluronan/CD44-activated head and neck squamous cell carcinoma cells. *Oncogene.* (2012) 31:149–60. doi: 10.1038/onc.2011.222
66. Chen L, Bourguignon LY. Hyaluronan-CD44 interaction promotes c-Jun signaling and miRNA21 expression leading to Bcl-2 expression and chemoresistance in breast cancer cells. *Mol Cancer.* (2014) 13:52. doi: 10.1186/1476-4598-13-52
67. Bourguignon LY, Wong G, Earle C, Chen L. Hyaluronan-CD44v3 interaction with Oct4-Sox2-Nanog promotes miR-302 expression leading to self-renewal, clonal formation, and cisplatin resistance in cancer stem cells from head and neck squamous cell carcinoma. *J Biol Chem.* (2012) 287:32800–24. doi: 10.1074/jbc.M111.308528

68. Fedorchenko O, Stiefelhagen M, Peer-Zada AA, Barthel R, Mayer P, Eckei L, et al. CD44 regulates the apoptotic response and promotes disease development in chronic lymphocytic leukemia. *Blood.* (2013) 121:4126–36. doi: 10.1182/blood-2012-11-466250
69. Park YS, Huh JW, Lee JH, Kim HR. shRNA against CD44 inhibits cell proliferation, invasion and migration, and promotes apoptosis of colon carcinoma cells. *Oncol Rep.* (2012) 27:339–46. doi: 10.3892/ijo.2016.3801
70. Lv L, Liu HG, Dong SY, Yang F, Wang QX, Guo GL, et al. Upregulation of CD44v6 contributes to acquired chemoresistance via the modulation of autophagy in colon cancer SW480 cells. *Tumour Biol.* (2016) 37:8811–24. doi: 10.1007/s13277-015-4755-6
71. Slomiany MG, Dai L, Tolliver LB, Grass GD, Zeng Y, Toole BP. Inhibition of functional hyaluronan-CD44 interactions in CD133-positive primary human ovarian carcinoma cells by small hyaluronan oligosaccharides. *Clin Cancer Res.* (2009) 15:7593–601. doi: 10.1158/1078-0432.CCR-09-2317
72. Ween MP, Hummitzsch K, Rodgers RJ, Oehler MK, Ricciardelli C. Versican induces a pro-metastatic ovarian cancer cell behavior which can be inhibited by small hyaluronan oligosaccharides. *Clin Exp Metastasis.* (2011) 28:113–25. doi: 10.1007/s10585-010-9363-7
73. Slomiany MG, Dai L, Bomar PA, Knackstedt TJ, Kranc DA, Tolliver L, et al. Abrogating drug resistance in malignant peripheral nerve sheath tumors by disrupting hyaluronan-CD44 interactions with small hyaluronan oligosaccharides. *Cancer Res.* (2009) 69:4992–8. doi: 10.1158/0008-5472.CAN-09-0143
74. Ahrens T, Sleeman JP, Schempp CM, Howells N, Hofmann M, Ponta H, et al. Soluble CD44 inhibits melanoma tumor growth by blocking cell surface CD44 binding to hyaluronic acid. *Oncogene.* (2001) 20:3399–408. doi: 10.1038/sj.onc.1204435
75. Xu XM, Chen Y, Chen J, Yang S, Gao F, Underhill CB, et al. A peptide with three hyaluronan binding motifs inhibits tumor growth and induces apoptosis. *Cancer Res.* (2003) 63:5685–90.
76. Yu Q, Toole BP, Stamenkovic I. Induction of apoptosis of metastatic mammary carcinoma cells *in vivo* by disruption of tumor cell surface CD44 function. *J Exp Med.* (1997) 186:1985–96. doi: 10.1084/jem.186.12.1985
77. Ghatak S, Misra S, Toole BP. Hyaluronan oligosaccharides inhibit anchorage-independent growth of tumor cells by suppressing the phosphoinositide 3-kinase/Akt cell survival pathway. *J Biol Chem.* (2002) 277:38013–20. doi: 10.1074/jbc.M202404200
78. Li L, Hao X, Qin J, Tang W, He F, Smith A, et al. Antibody against CD44s inhibits pancreatic tumor initiation and postradiation recurrence in mice. *Gastroenterology.* (2014) 146:1108–18. doi: 10.1053/j.gastro.2013.12.035
79. Weigand S, Herting F, Maisel D, Nopora A, Voss E, Schaab C, et al. Global quantitative phosphoproteome analysis of human tumor xenografts treated with a CD44 antagonist. *Cancer Res.* (2012) 72:4329–39. doi: 10.1158/0008-5472.CAN-12-0136
80. Seiter S, Arch R, Reber S, Komitowski D, Hofmann M, Ponta H, et al. Prevention of tumor metastasis formation by anti-variant CD44. *J Exp Med.* (1993) 177:443–55. doi: 10.1084/jem.177.2.443
81. Hibino S, Shibuya M, Engbring JA, Mochizuki M, Nomizu M, Kleinman HK. Identification of an active site on the laminin alpha5 chain globular domain that binds to CD44 and inhibits malignancy. *Cancer Res.* (2004) 64:4810–6. doi: 10.1158/0008-5472.CAN-04-0129
82. Misra S, Hascall VC, De Giovanni C, Markwald RR, Ghatak S. Delivery of CD44 shRNA/nanoparticles within cancer cells: perturbation of hyaluronan/CD44v6 interactions and reduction in adenoma growth in Apc Min/+ MICE. *J Biol Chem.* (2009) 284:12432–46. doi: 10.1074/jbc.M806772200
83. Khurana SS, Riehl TE, Moore BD, Fassan M, Rugge M, Romero-Gallo J, et al. The hyaluronic acid receptor CD44 coordinates normal and metaplastic gastric epithelial progenitor cell proliferation. *J Biol Chem.* (2013) 288:16085–97. doi: 10.1074/jbc.M112.445551
84. Xu Y, Stamenkovic I, Yu Q. CD44 attenuates activation of the hippo signaling pathway and is a prime therapeutic target for glioblastoma. *Cancer Res.* (2010) 70:2455–64. doi: 10.1158/0008-5472.CAN-09-2505
85. Zheng J, Zhao S, Yu X, Huang S, Liu HY. Simultaneous targeting of CD44 and EpCAM with a bispecific aptamer effectively inhibits intraperitoneal ovarian cancer growth. *Theranostics.* (2017) 7:1373–88. doi: 10.7150/thno.17826
86. Nambiar D, Prajapati V, Agarwal R, Singh RP. *In vitro* and *in vivo* anticancer efficacy of silibinin against human pancreatic cancer BxPC-3 and PANC-1 cells. *Cancer Lett.* (2013) 334:109–17. doi: 10.1016/j.canlet.2012.09.004
87. Zhong X, Zhang W, Sun T. DDR1 promotes breast tumor growth by suppressing antitumor immunity. *Oncol Rep.* (2019) 42:2844–54. doi: 10.3892/or.2019.7338
88. Jin H, Ham IH, Oh HJ, Bae CA, Lee D, Kim YB, et al. Inhibition of discoidin domain receptor 1 prevents stroma-induced peritoneal metastasis in gastric carcinoma. *Mol Cancer Res.* (2018) 16:1590–600. doi: 10.1158/1541-7786.MCR-17-0710
89. Aguilera KY, Huang H, Du W, Hagopian MM, Wang Z, Hinz S, et al. Inhibition of discoidin domain receptor 1 reduces collagen-mediated tumorigenicity in pancreatic ductal adenocarcinoma. *Mol Cancer Ther.* (2017) 16:2473–85. doi: 10.1158/1535-7163.MCT-16-0834
90. Grither WR, Longmore GD. Inhibition of tumor-microenvironment interaction and tumor invasion by small-molecule allosteric inhibitor of DDR2 extracellular domain. *Proc Natl Acad Sci USA.* (2018) 115:E7786–94. doi: 10.1073/pnas.1805020115
91. Ambrogio C, Gomez-Lopez G, Falcone M, Vidal A, Nadal E, Crosetto N, et al. Combined inhibition of DDR1 and notch signaling is a therapeutic strategy for KRAS-driven lung adenocarcinoma. *Nat Med.* (2016) 22:270–7. doi: 10.1038/nm.4041
92. Jeitany M, Leroy C, Tosti P, Lafitte M, Le Guet J, Simon V, et al. Inhibition of DDR1-BCR signalling by nilotinib as a new therapeutic strategy for metastatic colorectal cancer. *EMBO Mol Med.* (2018) 10:e7918. doi: 10.15252/emmm.201707918
93. Lu QP, Chen WD, Peng JR, Xu YD, Cai Q, Feng GK, et al. Antitumor activity of 7RH, a discoidin domain receptor 1 inhibitor, alone or in combination with dasatinib exhibits antitumor effects in nasopharyngeal carcinoma cells. *Oncol Lett.* (2016) 12:3598–608. doi: 10.3892/ol.2016.5088
94. Vehlow A, Klapproth E, Jin S, Hannen R, Hauswald M, Bartsch JW, et al. Interaction of discoidin domain receptor 1 with a 14-3-3-Beclin-1-akt1 complex modulates glioblastoma therapy sensitivity. *Cell Rep.* (2019) 26:3672–83.e7. doi: 10.1016/j.celrep.2019.02.096
95. Xu C, Buczkowski KA, Zhang Y, Asahina H, Beauchamp EM, Terai H, et al. NSCLC driven by DDR2 mutation is sensitive to dasatinib and JQ1 combination therapy. *Mol Cancer Ther.* (2015) 14:2382–9. doi: 10.1158/1535-7163.MCT-15-0077
96. Kim DG, Lee JY, Kwon NH, Fang P, Zhang Q, Wang J, et al. Chemical inhibition of prometastatic lysyl-tRNA synthetase-laminin receptor interaction. *Nat Chem Biol.* (2014) 10:29–34. doi: 10.1038/nchembio.1381
97. Narumi K, Inoue A, Tanaka M, Isemura M, Shimo-Oka T, Abe T, et al. Inhibition of experimental metastasis of human fibrosarcoma cells by anti-recombinant 37-kDa laminin binding protein antibody. *Jpn J Cancer Res.* (1999) 90:425–31. doi: 10.1111/j.1349-7006.1999.tb00765.x
98. McClintock SD, Warner RL, Ali S, Chekuri A, Dame MK, Attili D, et al. Monoclonal antibodies specific for oncofetal antigen–immature laminin receptor protein: effects on tumor growth and spread in two murine models. *Cancer Biol Ther.* (2015) 16:724–32. doi: 10.1080/15384047.2015.1026484
99. Barsoum AL, Liu B, Rohrer JW, Coggin JH Jr, Tucker JA, Pannell LK, et al. Production, safety and antitumor efficacy of recombinant oncofetal antigen/immature laminin receptor protein. *Biomaterials.* (2009) 30:3091–9. doi: 10.1016/j.biomaterials.2009.02.022
100. Rohrer JW, Barsoum AL, Coggin JH Jr. Identification of oncofetal antigen/immature laminin receptor protein epitopes that activate BALB/c mouse OFA/iLRP-specific effector and regulatory T cell clones. *J Immunol.* (2006). 176:2844–56. doi: 10.4049/jimmunol.176.5.2844
101. Hauck CR, Hsia DA, Puente XS, Cheresh DA, Schlaepfer DD. FRNK blocks v-Src-stimulated invasion and experimental metastases without effects on cell motility or growth. *EMBO J.* (2002) 21:6289–302. doi: 10.1093/emboj/cdf631
102. Mitra SK, Mikolon D, Molina JE, Hsia DA, Hanson DA, Chi A, et al. Intrinsic FAK activity and Y925 phosphorylation facilitate an angiogenic switch in tumors. *Oncogene.* (2006) 25:5969–84. doi: 10.1038/sj.onc.1209588
103. Liu TJ, LaFortune T, Honda T, Ohmori O, Hatakeyama S, Meyer T, et al. Inhibition of both focal adhesion kinase and insulin-like growth factor-I receptor kinase suppresses glioma proliferation *in vitro* and *in vivo*. *Mol Cancer Ther.* (2007) 6:1357–67. doi: 10.1158/1535-7163.MCT-06-0476

104. Roberts WG, Ung E, Whalen P, Cooper B, Hulford C, Autry C, et al. Antitumor activity and pharmacology of a selective focal adhesion kinase inhibitor, PF-562,271. *Cancer Res.* (2008) 68:1935–44. doi: 10.1158/0008-5472.CAN-07-5155
105. Stokes JB, Adair SJ, Slack-Davis JK, Walters DM, Tilghman RW, Hershey ED, et al. Inhibition of focal adhesion kinase by PF-562,271 inhibits the growth and metastasis of pancreatic cancer concomitant with altering the tumor microenvironment. *Mol Cancer Ther.* (2011) 10:2135–45. doi: 10.1158/1535-7163.MCT-11-0261
106. Jeong K, Murphy JM, Rodriguez YAR, Kim JS, Ahn EE, Lim SS. FAK inhibition reduces metastasis of alpha4 integrin-expressing melanoma to lymph nodes by targeting lymphatic VCAM-1 expression. *Biochem Biophys Res Commun.* (2019) 509:1034–40. doi: 10.1016/j.bbrc.2019.01.050
107. Kuonen F, Surbeck I, Sarin KY, Dontenwill M, Ruegg C, Gilliet M, et al. TGFbeta, fibronectin and integrin alpha5beta1 promote invasion in basal cell carcinoma. *J Invest Dermatol.* (2018) 138:2432–42. doi: 10.1016/j.jid.2018.04.029
108. Tanjoni I, Walsh C, Uryu S, Tomar A, Nam JO, Mielgo A, et al. PND-1186 FAK inhibitor selectively promotes tumor cell apoptosis in three-dimensional environments. *Cancer Biol Ther.* (2010) 9:764–77. doi: 10.4161/cbt.9.10.11434
109. Walsh C, Tanjoni I, Uryu S, Tomar A, Nam JO, Luo H, et al. Oral delivery of PND-1186 FAK inhibitor decreases tumor growth and spontaneous breast to lung metastasis in pre-clinical models. *Cancer Biol Ther.* (2010) 9:778–90. doi: 10.4161/cbt.9.10.11433
110. Kang Y, Hu W, Ivan C, Dalton HJ, Miyake T, Pecot CV, et al. Role of focal adhesion kinase in regulating YB-1-mediated paclitaxel resistance in ovarian cancer. *J Natl Cancer Inst.* (2013) 105:1485–95. doi: 10.1093/jnci/djt210
111. Golubovskaya VM, Nyberg C, Zheng M, Kweh F, Magis A, Ostrov D, et al. A small molecule inhibitor, 1,2,4,5-benzenetetraamine tetrahydrochloride, targeting the y397 site of focal adhesion kinase decreases tumor growth. *J Med Chem.* (2008) 51:7405–16. doi: 10.1021/jm800483v
112. Hochwald SN, Nyberg C, Zheng M, Zheng D, Wood C, Massoll NA, et al. A novel small molecule inhibitor of FAK decreases growth of human pancreatic cancer. *Cell Cycle.* (2009) 8:2435–43. doi: 10.4161/cc.8.15.9145
113. Heffler M, Golubovskaya VM, Dunn KM, Cance W. Focal adhesion kinase autophosphorylation inhibition decreases colon cancer cell growth and enhances the efficacy of chemotherapy. *Cancer Biol Ther.* (2013) 14:761–72. doi: 10.4161/cbt.25185
114. Golubovskaya VM, Figel S, Ho BT, Johnson CP, Yemma M, Huang G, et al. A small molecule focal adhesion kinase (FAK) inhibitor, targeting Y397 site: 1-(2-hydroxyethyl)-3, 5, 7-triaza-1-azoniatricyclo [3.3.1.1(3,7)]decane; bromide effectively inhibits FAK autophosphorylation activity and decreases cancer cell viability, clonogenicity and tumor growth *in vivo*. *Carcinogenesis.* (2012) 33:1004–13. doi: 10.1093/carcin/bgs120
115. Kurenova EV, Hunt DL, He D, Magis AT, Ostrov DA, Cance WG. Small molecule chloropyramine hydrochloride (C4) targets the binding site of focal adhesion kinase and vascular endothelial growth factor receptor 3 and suppresses breast cancer growth *in vivo*. *J Med Chem.* (2009) 52:4716–24. doi: 10.1021/jm900159g
116. Kurenova E, Liao J, He DH, Hunt D, Yemma M, Bshara W, et al. The FAK scaffold inhibitor C4 disrupts FAK-VEGFR-3 signaling and inhibits pancreatic cancer growth. *Oncotarget.* (2013) 4:1632–46. doi: 10.18632/oncotarget.1365
117. Stewart JE, Ma X, Megison M, Nabers H, Cance WG, Kurenova EV, et al. Inhibition of FAK and VEGFR-3 binding decreases tumorigenicity in neuroblastoma. *Mol Carcinog.* (2015) 54:9–23. doi: 10.1002/mc.22070
118. Ucar DA, Kurenova E, Garrett TJ, Cance WG, Nyberg C, Cox A, et al. Disruption of the protein interaction between FAK and IGF-1R inhibits melanoma tumor growth. *Cell Cycle.* (2012) 11:3250–9. doi: 10.4161/cc.21611
119. Ucar DA, Magis AT, He DH, Lawrence NJ, Sebti SM, Kurenova E, et al. Inhibiting the interaction of cMET and IGF-1R with FAK effectively reduces growth of pancreatic cancer cells *in vitro* and *in vivo*. *Anticancer Agents Med Chem.* (2013) 13:595–602. doi: 10.2174/1871520611313040009
120. Golubovskaya VM, Palma NL, Zheng M, Ho B, Magis A, Ostrov D, et al. A small-molecule inhibitor, 5'-O-tritylthymidine, targets FAK and Mdm-2 interaction, and blocks breast and colon tumorigenesis *in vivo*. *Anticancer Agents Med Chem.* (2013) 13:532–45. doi: 10.2174/1871520611313040002
121. Golubovskaya VM, Ho B, Zheng M, Magis A, Ostrov D, Morrison C, et al. Disruption of focal adhesion kinase and p53 interaction with small molecule compound R2 reactivated p53 and blocked tumor growth. *BMC Cancer.* (2013) 13:342. doi: 10.1186/1471-2407-13-342
122. Tiede S, Meyer-Schaller N, Kalathur RKR, Ivanek R, Fagiani E, Schmassmann P, et al. The FAK inhibitor BI 853520 exerts anti-tumor effects in breast cancer. *Oncogenesis.* (2018) 7:73. doi: 10.1038/s41389-018-0083-1
123. Laszlo V, Valko Z, Ozsvar J, Kovacs I, Garay T, Hoda MA, et al. The FAK inhibitor BI 853520 inhibits spheroid formation and orthotopic tumor growth in malignant pleural mesothelioma. *J Mol Med.* (2019) 97:231–42. doi: 10.1007/s00109-018-1725-7
124. Moritake H, Saito Y, Sawa D, Sameshima N, Yamada A, Kinoshita M, et al. TAE226, a dual inhibitor of focal adhesion kinase and insulin-like growth factor-I receptor, is effective for Ewing sarcoma. *Cancer Med.* (2019) 8:7809–21. doi: 10.1002/cam4.2647
125. Halder J, Lin YG, Merritt WM, Spannuth WA, Nick AM, Honda T, et al. Therapeutic efficacy of a novel focal adhesion kinase inhibitor TAE226 in ovarian carcinoma. *Cancer Res.* (2007) 67:10976–83. doi: 10.1158/0008-5472.CAN-07-2667
126. Bagi CM, Christensen J, Cohen DP, Roberts WG, Wilkie D, Swanson T, et al. Sunitinib and PF-562,271 (FAK/Pyk2 inhibitor) effectively block growth and recovery of human hepatocellular carcinoma in a rat xenograft model. *Cancer Biol Ther.* (2009) 8:856–65. doi: 10.4161/cbt.8.9.8246
127. Chen G, Gao C, Gao X, Zhang DH, Kuan SF, Burns TF, et al. Wnt/beta-Catenin pathway activation mediates adaptive resistance to BRAF inhibition in colorectal cancer. *Mol Cancer Ther.* (2018) 17:806–13. doi: 10.1158/1535-7163.MCT-17-0561
128. Golubovskaya VM, Huang G, Ho B, Yemma M, Morrison CD, Lee J, et al. Pharmacologic blockade of FAK autophosphorylation decreases human glioblastoma tumor growth and synergizes with temozolomide. *Mol Cancer Ther.* (2013) 12:162–72. doi: 10.1158/1535-7163.MCT-12-0701
129. Dragoj M, Bankovic J, Sereti E, Stojanov SJ, Dimas K, Pesic M, et al. Anti-invasive effects of CXCR4 and FAK inhibitors in non-small cell lung carcinomas with mutually inactivated p53 and PTEN tumor suppressors. *Invest New Drugs.* (2017) 35:718–32. doi: 10.1007/s10637-017-0494-4
130. Dawson JC, Serrels B, Byron A, Muir MT, Makda A, Garcia-Munoz A, et al. A synergistic anti-cancer FAK and HDAC inhibitor combination discovered by a novel chemical-genetic high-content phenotypic screen. *Mol Cancer Ther.* (2019) 19:637–49. doi: 10.1101/590802
131. Jiang H, Hegde S, Knolhoff BL, Zhu Y, Herndon JM, Meyer MA, et al. Targeting focal adhesion kinase renders pancreatic cancers responsive to checkpoint immunotherapy. *Nat Med.* (2016) 22:851–60. doi: 10.1038/nm.4123
132. Lin HM, Lee BY, Castillo L, Spielman C, Grogan J, Yeung NK, et al. Effect of FAK inhibitor VS-6063 (defactinib) on docetaxel efficacy in prostate cancer. *Prostate.* (2018) 78:308–17. doi: 10.1002/pros.23476
133. Byeon Y, Lee JW, Choi WS, Won JE, Kim GH, Kim MG, et al. CD44-Targeting PLGA nanoparticles incorporating paclitaxel and FAK siRNA Overcome chemoresistance in epithelial ovarian cancer. *Cancer Res.* (2018) 78:6247–56. doi: 10.1158/0008-5472.CAN-17-3871
134. Bieerkehazhi S, Chen Z, Zhao Y, Yu Y, Zhang H, Vasudevan SA, et al. Novel Src/Abl tyrosine kinase inhibitor bosutinib suppresses neuroblastoma growth via inhibiting Src/Abl signaling. *Oncotarget.* (2017) 8:1469–80. doi: 10.18632/oncotarget.13643
135. Kim WG, Guigon CJ, Fozzatti L, Park JW, Lu C, Willingham MC, et al. SKI-606, an Src inhibitor, reduces tumor growth, invasion, and distant metastasis in a mouse model of thyroid cancer. *Clin Cancer Res.* (2012) 18:1281–90. doi: 10.1158/1078-0432.CCR-11-2892
136. Rabbani SA, Valentino ML, Arakelian A, Ali S, Boschelli F. SKI-606 (Bosutinib) blocks prostate cancer invasion, growth, and metastasis *in vitro* and *in vivo* through regulation of genes involved in cancer growth and skeletal metastasis. *Mol Cancer Ther.* (2010) 9:1147–57. doi: 10.1158/1535-7163.MCT-09-0962
137. Messersmith WA, Rajeshkumar NV, Tan AC, Wang XF, Diesl V, Choe SE, et al. Efficacy and pharmacodynamic effects of bosutinib (SKI-606), a

Src/Abl inhibitor, in freshly generated human pancreas cancer xenografts. *Mol Cancer Ther.* (2009) 8:1484–93. doi: 10.1158/1535-7163.MCT-09-0075
138. Jallal H, Valentino ML, Chen G, Boschelli F, Ali S, Rabbani SA. A Src/Abl kinase inhibitor, SKI-606, blocks breast cancer invasion, growth, and metastasis *in vitro* and *in vivo*. *Cancer Res.* (2007) 67:1580–8. doi: 10.1158/0008-5472.CAN-06-2027
139. Golas JM, Lucas J, Etienne C, Golas J, Discafani C, Sridharan L, et al. SKI-606, a Src/Abl inhibitor with *in vivo* activity in colon tumor xenograft models. *Cancer Res.* (2005) 65:5358–64. doi: 10.1158/0008-5472.CAN-04-2484
140. Park SI, Zhang J, Phillips KA, Araujo JC, Najjar AM, Volgin AY, et al. Targeting SRC family kinases inhibits growth and lymph node metastases of prostate cancer in an orthotopic nude mouse model. *Cancer Res.* (2008) 68:3323–33. doi: 10.1158/0008-5472.CAN-07-2997
141. Trevino JG, Summy JM, Lesslie DP, Parikh NU, Hong DS, Lee FY, et al. Inhibition of SRC expression and activity inhibits tumor progression and metastasis of human pancreatic adenocarcinoma cells in an orthotopic nude mouse model. *Am J Pathol.* (2006) 168:962–72. doi: 10.2353/ajpath.2006.050570
142. Scott AJ, Song EK, Bagby S, Purkey A, McCarter M, Gajdos C, et al. Evaluation of the efficacy of dasatinib, a Src/Abl inhibitor, in colorectal cancer cell lines and explant mouse model. *PLoS ONE.* (2017) 12:e0187173. doi: 10.1371/journal.pone.0187173
143. Rajeshkumar NV, Tan AC, De Oliveira E, Womack C, Wombwell H, Morgan S, et al. Antitumor effects and biomarkers of activity of AZD0530, a src inhibitor, in pancreatic cancer. *Clin Cancer Res.* (2009) 15:4138–46. doi: 10.1158/1078-0432.CCR-08-3021
144. Yang JC, Ok JH, Busby JE, Borowsky AD, Kung HJ, Evans CP. Aberrant activation of androgen receptor in a new neuropeptide-autocrine model of androgen-insensitive prostate cancer. *Cancer Res.* (2009) 69:151–60. doi: 10.1158/0008-5472.CAN-08-0442
145. Lang L, Shay C, Xiong Y, Thakkar P, Chemmalakuzhy R, Wang X, et al. Combating head and neck cancer metastases by targeting Src using multifunctional nanoparticle-based saracatinib. *J Hematol Oncol.* (2018) 11:85. doi: 10.1186/s13045-018-0623-3
146. Xiong J, Wu JS, Mao SS, Yu XN, Huang XX. Effect of saracatinib on pulmonary metastases from hepatocellular carcinoma. *Oncol Rep.* (2016) 36:1483–90. doi: 10.3892/or.2016.4968
147. Yamaguchi H, Takanashi M, Yoshida N, Ito Y, Kamata R, Fukami K, et al. Saracatinib impairs the peritoneal dissemination of diffuse-type gastric carcinoma cells resistant to Met and fibroblast growth factor receptor inhibitors. *Cancer Sci.* (2014) 105:528–36. doi: 10.1111/cas.12387
148. Cavalloni G, Peraldo-Neia C, Sarotto I, Gammaitoni L, Migliardi G, Soster M, et al. Antitumor activity of Src inhibitor saracatinib (AZD-0530) in preclinical models of biliary tract carcinomas. *Mol Cancer Ther.* (2012) 11:1528–38. doi: 10.1158/1535-7163.MCT-11-1020
149. Dong M, Rice L, Lepler S, Pampo C, Siemann DW. Impact of the Src inhibitor saracatinib on the metastatic phenotype of a fibrosarcoma (KHT) tumor model. *Anticancer Res.* (2010) 30:4405–13.
150. Arcaroli JJ, Touban BM, Tan AC, Varella-Garcia M, Powell RW, Eckhardt SG, et al. Gene array and fluorescence *in situ* hybridization biomarkers of activity of saracatinib (AZD0530), a Src inhibitor, in a preclinical model of colorectal cancer. *Clin Cancer Res.* (2010) 16:4165–77. doi: 10.1158/1078-0432.CCR-10-0066
151. Bertotti A, Bracco C, Girolami F, Torti D, Gastaldi S, Galimi F, et al. Inhibition of Src impairs the growth of met-addicted gastric tumors. *Clin Cancer Res.* (2010) 16:3933–43. doi: 10.1158/1078-0432.CCR-10-0106
152. Serrels B, Serrels A, Mason SM, Baldeschi C, Ashton GH, Canel M, et al. A novel Src kinase inhibitor reduces tumour formation in a skin carcinogenesis model. *Carcinogenesis.* (2009) 30:249–57. doi: 10.1093/carcin/bgn278
153. Chang YM, Bai L, Liu S, Yang JC, Kung HJ, Evans CP. Src family kinase oncogenic potential and pathways in prostate cancer as revealed by AZD0530. *Oncogene.* (2008) 27:6365–75. doi: 10.1038/onc.2008.250
154. Zhang J, Zhou Q, Gao G, Wang Y, Fang Z, Li G, et al. The effects of ponatinib, a multi-targeted tyrosine kinase inhibitor, against human U87 malignant glioblastoma cells. *Onco Targets Ther.* (2014) 7:2013–9. doi: 10.2147/OTT.S67556
155. Laramy JK, Kim M, Gupta SK, Parrish KE, Zhang S, Bakken KK, et al. Heterogeneous binding and central nervous system distribution of the multitargeted kinase inhibitor ponatinib restrict orthotopic efficacy in a patient-derived xenograft model of glioblastoma. *J Pharmacol Exp Ther.* (2017) 363:136–47. doi: 10.1124/jpet.117.243477
156. Whittle SB, Patel K, Zhang L, Woodfield SE, Du M, Smith V, et al. The novel kinase inhibitor ponatinib is an effective anti-angiogenic agent against neuroblastoma. *Invest New Drugs.* (2016) 34:685–92. doi: 10.1007/s10637-016-0387-y
157. Gozgit JM, Wong MJ, Moran L, Wardwell S, Mohemmad QK, Narasimhan NI, et al. Ponatinib (AP24534), a multitargeted pan-FGFR inhibitor with activity in multiple FGFR-amplified or mutated cancer models. *Mol Cancer Ther.* (2012) 11:690–9. doi: 10.1158/1535-7163.MCT-11-0450
158. Li SQ, Cheuk AT, Shern JF, Song YK, Hurd L, Liao H, et al. Targeting wild-type and mutationally activated FGFR4 in rhabdomyosarcoma with the inhibitor ponatinib (AP24534). *PLoS ONE.* (2013) 8:e76551. doi: 10.1371/journal.pone.0076551
159. Garner AP, Gozgit JM, Anjum R, Vodala S, Schrock A, Zhou T, et al. Ponatinib inhibits polyclonal drug-resistant KIT oncoproteins and shows therapeutic potential in heavily pretreated gastrointestinal stromal tumor (GIST) patients. *Clin Cancer Res.* (2014) 20:5745–55. doi: 10.1158/1078-0432.CCR-14-1397
160. Li L, Yu J, Jiao S, Wang W, Zhang F, Sun S. Vandetanib (ZD6474) induces antiangiogenesis through mTOR-HIF-1 alpha-VEGF signaling axis in breast cancer cells. *Onco Targets Ther.* (2018) 11:8543–53. doi: 10.2147/OTT.S175578
161. Ferrari SM, Bocci G, Di Desidero T, Ruffilli I, Elia G, Ragusa F, et al. Vandetanib has antineoplastic activity in anaplastic thyroid cancer, *in vitro* and *in vivo*. *Oncol Rep.* (2018) 39:2306–14. doi: 10.3892/or.2018.6305
162. Wang X, Qiu Y, Yu Q, Li H, Chen X, Li M, et al. Enhanced glioma therapy by synergistic inhibition of autophagy and tyrosine kinase activity. *Int J Pharm.* (2018) 536:1–10. doi: 10.1016/j.ijpharm.2017.09.007
163. Cascone T, Xu L, Lin HY, Liu W, Tran HT, Liu Y, et al. The HGF/c-MET pathway is a driver and biomarker of VEGFR-inhibitor resistance and vascular remodeling in non-small cell lung cancer. *Clin Cancer Res.* (2017) 23:5489–501. doi: 10.1158/1078-0432.CCR-16-3216
164. Starenki D, Hong SK, Wu PK, Park JI. Vandetanib and cabozantinib potentiate mitochondria-targeted agents to suppress medullary thyroid carcinoma cells. *Cancer Biol Ther.* (2017) 18:473–83. doi: 10.1080/15384047.2017.1323594
165. De Andrade JP, Park JM, Gu VW, Woodfield GW, Kulak MV, Lorenzen AW, et al. EGFR is regulated by TFAP2C in luminal breast cancer and is a target for vandetanib. *Mol Cancer Ther.* (2016) 15:503–11. doi: 10.1158/1535-7163.MCT-15-0548-T
166. Hatem R, Labiod D, Chateau-Joubert S, de Plater L, El Botty R, Vacher S, et al. Vandetanib as a potential new treatment for estrogen receptor-negative breast cancers. *Int J Cancer.* (2016) 138:2510–21. doi: 10.1002/ijc.29974
167. Saito M, Ishigame T, Tsuta K, Kumamoto K, Imai T, Kohno T. A mouse model of KIF5B-RET fusion-dependent lung tumorigenesis. *Carcinogenesis.* (2014) 35:2452–6. doi: 10.1093/carcin/bgu158
168. Wunderlich A, Khoruzhyk M, Roth S, Ramaswamy A, Greene BH, Doll D, et al. Pretherapeutic drug evaluation by tumor xenografting in anaplastic thyroid cancer. *J Surg Res.* (2013) 185:676–83. doi: 10.1016/j.jss.2013.06.017
169. Takeda H, Takigawa N, Ohashi K, Minami D, Kataoka I, Ichihara E, et al. Vandetanib is effective in EGFR-mutant lung cancer cells with PTEN deficiency. *Exp Cell Res.* (2013) 319:417–23. doi: 10.1016/j.yexcr.2012.12.018
170. Inoue K, Torimura T, Nakamura T, Iwamoto H, Masuda H, Abe M, et al. Vandetanib, an inhibitor of VEGF receptor-2 and EGF receptor, suppresses tumor development and improves prognosis of liver cancer in mice. *Clin Cancer Res.* (2012) 18:3924–33. doi: 10.1158/1078-0432.CCR-11-2041
171. Guerin O, Etienne-Grimaldi MC, Monteverde M, Sudaka A, Brunstein MC, Formento P, et al. Contrasted effects of the multitarget TKi vandetanib on docetaxel-sensitive and docetaxel-resistant prostate cancer cell lines. *Urol Oncol.* (2013) 31:1567–75. doi: 10.1016/j.urolonc.2012.03.003
172. Klein JD, Christopoulos A, Ahn SM, Gooding WE, Grandis JR, Kim S. Antitumor effect of vandetanib through EGFR inhibition in head and neck squamous cell carcinoma. *Head Neck.* (2012) 34:1269–76. doi: 10.1002/hed.21917
173. Navis AC, Hamans BC, Claes A, Heerschap A, Jeuken JW, Wesseling P, et al. Effects of targeting the VEGF and PDGF pathways in diffuse

orthotopic glioma models. *J Pathol.* (2011) 223:626–34. doi: 10.1002/path.2836
174. Gule MK, Chen Y, Sano D, Frederick MJ, Zhou G, Zhao M, et al. Targeted therapy of VEGFR2 and EGFR significantly inhibits growth of anaplastic thyroid cancer in an orthotopic murine model. *Clin Cancer Res.* (2011) 17:2281–91. doi: 10.1158/1078-0432.CCR-10-2762
175. Wachsberger PR, Lawrence YR, Liu Y, Daroczi B, Xu X, Dicker AP. Epidermal growth factor receptor expression modulates antitumor efficacy of vandetanib or cediranib combined with radiotherapy in human glioblastoma xenografts. *Int J Radiat Oncol Biol Phys.* (2012) 82:483–91. doi: 10.1016/j.ijrobp.2010.09.019
176. Sano D, Fooshee DR, Zhao M, Andrews GA, Frederick MJ, Galer C, et al. Targeted molecular therapy of head and neck squamous cell carcinoma with the tyrosine kinase inhibitor vandetanib in a mouse model. *Head Neck.* (2011) 33:349–58. doi: 10.1002/hed.21455
177. Ichihara E, Ohashi K, Takigawa N, Osawa M, Ogino A, Tanimoto M, et al. Effects of vandetanib on lung adenocarcinoma cells harboring epidermal growth factor receptor T790M mutation *in vivo*. *Cancer Res.* (2009) 69:5091–8. doi: 10.1158/0008-5472.CAN-08-4204
178. Naumov GN, Nilsson MB, Cascone T, Briggs A, Straume O, Akslen LA, et al. Combined vascular endothelial growth factor receptor and epidermal growth factor receptor (EGFR) blockade inhibits tumor growth in xenograft models of EGFR inhibitor resistance. *Clin Cancer Res.* (2009) 15:3484–94. doi: 10.1158/1078-0432.CCR-08-2904
179. Wedge SR, Ogilvie DJ, Dukes M, Kendrew J, Chester R, Jackson JA, et al. ZD6474 inhibits vascular endothelial growth factor signaling, angiogenesis, and tumor growth following oral administration. *Cancer Res.* (2002) 62:4645—55.
180. McCarty MF, Wey J, Stoeltzing O, Liu W, Fan F, Bucana C, et al. ZD6474, a vascular endothelial growth factor receptor tyrosine kinase inhibitor with additional activity against epidermal growth factor receptor tyrosine kinase, inhibits orthotopic growth and angiogenesis of gastric cancer. *Mol Cancer Ther.* (2004) 3:1041–8.
181. Conrad C, Ischenko I, Kohl G, Wiegand U, Guba M, Yezhelyev M, et al. Antiangiogenic and antitumor activity of a novel vascular endothelial growth factor receptor-2 tyrosine kinase inhibitor ZD6474 in a metastatic human pancreatic tumor model. *Anticancer Drugs.* (2007) 18:569–79. doi: 10.1097/CAD.0b013e3280147d13
182. Drevs J, Konerding MA, Wolloscheck T, Wedge SR, Ryan AJ, Ogilvie DJ, et al. The VEGF receptor tyrosine kinase inhibitor, ZD6474, inhibits angiogenesis and affects microvascular architecture within an orthotopically implanted renal cell carcinoma. *Angiogenesis.* (2004) 7:347–54. doi: 10.1007/s10456-005-1394-3
183. Wu W, Onn A, Isobe T, Itasaka S, Langley RR, Shitani T, et al. Targeted therapy of orthotopic human lung cancer by combined vascular endothelial growth factor and epidermal growth factor receptor signaling blockade. *Mol Cancer Ther.* (2007) 6:471–83. doi: 10.1158/1535-7163.MCT-06-0416
184. Ciardiello F, Bianco R, Caputo R, Caputo R, Damiano V, Troiani T, et al. Antitumor activity of ZD6474, a vascular endothelial growth factor receptor tyrosine kinase inhibitor, in human cancer cells with acquired resistance to antiepidermal growth factor receptor therapy. *Clin Cancer Res.* (2004) 10:784–93. doi: 10.1158/1078-0432.CCR-1100-03
185. Taguchi F, Koh Y, Koizumi F, Tamura T, Saijo N, Nishio K. Anticancer effects of ZD6474, a VEGF receptor tyrosine kinase inhibitor, in gefitinib ("Iressa")-sensitive and resistant xenograft models. *Cancer Sci.* (2004) 95:984–9. doi: 10.1111/j.1349-7006.2004.tb03187.x
186. Dunn EF, Iida M, Myers RA, Campbell DA, Hintz KA, Armstrong EA, et al. Dasatinib sensitizes KRAS mutant colorectal tumors to cetuximab. *Oncogene.* (2011) 30:561–74. doi: 10.1038/onc.2010.430
187. Nagaraj NS, Washington MK, Merchant NB. Combined blockade of Src kinase and epidermal growth factor receptor with gemcitabine overcomes STAT3-mediated resistance of inhibition of pancreatic tumor growth. *Clin Cancer Res.* (2011) 17:483–93. doi: 10.1158/1078-0432.CCR-10-1670
188. Berndsen RH, Swier N, van Beijnum JR, Nowak-Sliwinska P. Colorectal cancer growth retardation through induction of apoptosis, using an optimized synergistic cocktail of axitinib, erlotinib, and dasatinib. *Cancers.* (2019) 11:1878. doi: 10.3390/cancers11121878
189. Seoane S, Montero JC, Ocana A, Pandiella A. Effect of multikinase inhibitors on caspase-independent cell death and DNA damage in HER2-overexpressing breast cancer cells. *J Natl Cancer Inst.* (2010) 102:1432–46. doi: 10.1093/jnci/djq315
190. Rao G, Kim IK, Conforti F, Liu J, Zhang YW, Giaccone G. Dasatinib sensitises KRAS-mutant cancer cells to mitogen-activated protein kinase kinase inhibitor via inhibition of TAZ activity. *Eur J Cancer.* (2018) 99:37–48. doi: 10.1016/j.ejca.2018.05.013
191. Huveldt D, Lewis-Tuffin LJ, Carlson BL, Schroeder MA, Rodriguez F, Giannini C, et al. Targeting Src family kinases inhibits bevacizumab-induced glioma cell invasion. *PLoS ONE.* (2013) 8:e56505. doi: 10.1371/journal.pone.0056505
192. Walker S, Wankell M, Ho V, White R, Deo N, Devine C, et al. Targeting mTOR and Src restricts hepatocellular carcinoma growth in a novel murine liver cancer model. *PLoS ONE.* (2019) 14:e0212860. doi: 10.1371/journal.pone.0212860
193. Tian J, Raffa FA, Dai M, Moamer A, Khadang B, Hachim IY, et al. Dasatinib sensitises triple negative breast cancer cells to chemotherapy by targeting breast cancer stem cells. *Br J Cancer.* (2018) 119:1495–507. doi: 10.1038/s41416-018-0287-3
194. Xiao J, Xu M, Hou T, Huang Y, Yang C, Li J. Dasatinib enhances antitumor activity of paclitaxel in ovarian cancer through Src signaling. *Mol Med Rep.* (2015) 12:3249–56. doi: 10.3892/mmr.2015.3784
195. Levitt JM, Yamashita H, Jian W, Lerner SP, Sonpavde G. Dasatinib is preclinically active against Src-overexpressing human transitional cell carcinoma of the urothelium with activated Src signaling. *Mol Cancer Ther.* (2010) 9:1128–35. doi: 10.1158/1535-7163.MCT-10-0096
196. Perez M, Lucena-Cacace A, Marin-Gomez LM, Padillo-Ruiz J, Robles-Frias MJ, Saez C, et al. Dasatinib, a Src inhibitor, sensitizes liver metastatic colorectal carcinoma to oxaliplatin in tumors with high levels of phospho-Src. *Oncotarget.* (2016) 7:33111–24. doi: 10.18632/oncotarget.8880
197. Vallo S, Michaelis M, Gust KM, Black PC, Rothweiler F, Kvasnicka HM, et al. Dasatinib enhances tumor growth in gemcitabine-resistant orthotopic bladder cancer xenografts. *BMC Res Notes.* (2016) 9:454. doi: 10.1186/s13104-016-2256-3
198. Zeng F, Ju RJ, Liu L, Xie HJ, Mu LM, Lu WL. Efficacy in treating lung metastasis of invasive breast cancer with functional vincristine plus dasatinib liposomes. *Pharmacology.* (2018) 101:43–53. doi: 10.1159/000480737
199. Young AI, Law AM, Castillo L, Chong S, Cullen HD, Koehler M, et al. MCL-1 inhibition provides a new way to suppress breast cancer metastasis and increase sensitivity to dasatinib. *Breast Cancer Res.* (2016) 18:125. doi: 10.1186/s13058-016-0781-6
200. Teng Y, Cai Y, Pi W, Gao L, Shay C. Augmentation of the anticancer activity of CYT997 in human prostate cancer by inhibiting Src activity. *J Hematol Oncol.* (2017) 10:118. doi: 10.1186/s13045-017-0485-0
201. Balkhi HM, Haq E, Gul T, Sana S. Anti-glioma effects of caffeic acid phenethyl ester and dasatinib combination therapy in an *in vivo* rat glioma model. *Anticancer Agents Med Chem.* (2018) 18:1729–35. doi: 10.2174/1871520618666180515144835
202. Song N, Guo H, Ren J, Hao S, Wang X. Synergistic anti-tumor effects of dasatinib and dendritic cell vaccine on metastatic breast cancer in a mouse model. *Oncol Lett.* (2018) 15:6831–8. doi: 10.3892/ol.2018.8188
203. Yu GT, Mao L, Wu L, Deng WW, Bu LL, Liu JF, et al. Inhibition of SRC family kinases facilitates anti-CTLA4 immunotherapy in head and neck squamous cell carcinoma. *Cell Mol Life Sci.* (2018) 75:4223–34. doi: 10.1007/s00018-018-2863-3
204. Formisano L, D'Amato V, Servetto A, Brillante S, Raimondo L, Di Mauro C, et al. Src inhibitors act through different mechanisms in non-small cell lung cancer models depending on EGFR and RAS mutational status. *Oncotarget.* (2015) 6:26090–103. doi: 10.18632/oncotarget.4636
205. Fuse MA, Plati SK, Burns SS, Dinh CT, Bracho O, Yan D, et al. Combination therapy with c-met and Src inhibitors induces caspase-dependent apoptosis of merlin-deficient schwann cells and suppresses growth of schwannoma cells. *Mol Cancer Ther.* (2017) 16:2387–98. doi: 10.1158/1535-7163.MCT-17-0417
206. Lang L, Shay C, Zhao X, Xiong Y, Wang X, Teng Y. Simultaneously inactivating Src and AKT by saracatinib/capivasertib co-delivery nanoparticles to improve the efficacy of anti-Src therapy in head

and neck squamous cell carcinoma. *J Hematol Oncol.* (2019) 12:132. doi: 10.1186/s13045-019-0827-1

207. Wang L, Yu X, Dong J, Meng Y, Yang Y, Wang H, et al. Combined SRC inhibitor saracatinib and anti-ErbB2 antibody H2-18 produces a synergistic antitumor effect on trastuzumab-resistant breast cancer. *Biochem Biophys Res Commun.* (2016) 479:563–70. doi: 10.1016/j.bbrc.2016.09.111
208. Han S, Meng Y, Tong Q, Li G, Zhang X, Chen Y, et al. The ErbB2-targeting antibody trastuzumab and the small-molecule SRC inhibitor saracatinib synergistically inhibit ErbB2-overexpressing gastric cancer. *MAbs.* (2014) 6:403–8. doi: 10.4161/mabs.27443
209. Chen Y, Guggisberg N, Jorda M, Gonzalez-Angulo A, Hennessy B, Mills GB, et al. Combined Src and aromatase inhibition impairs human breast cancer growth *in vivo* and bypass pathways are activated in AZD0530-resistant tumors. *Clin Cancer Res.* (2009) 15:3396–405. doi: 10.1158/1078-0432.CCR-08-3127
210. Simpkins F, Hevia-Paez P, Sun J, Ullmer W, Gilbert CA, da Silva T, et al. Src inhibition with saracatinib reverses fulvestrant resistance in ER-positive ovarian cancer models *in vitro* and *in vivo*. *Clin Cancer Res.* (2012) 18:5911–23. doi: 10.1158/1078-0432.CCR-12-1257
211. Chen Y, Alvarez EA, Azzam D, Wander SA, Guggisberg N, Jorda M, et al. Combined Src and ER blockade impairs human breast cancer proliferation *in vitro* and *in vivo*. *Breast Cancer Res Treat.* (2011) 128:69–78. doi: 10.1007/s10549-010-1024-7
212. Nam HJ, Im SA, Oh DY, Elvin P, Kim HP, Yoon YK, et al. Antitumor activity of saracatinib (AZD0530), a c-Src/Abl kinase inhibitor, alone or in combination with chemotherapeutic agents in gastric cancer. *Mol Cancer Ther.* (2013) 12:16–26. doi: 10.1158/1535-7163.MCT-12-0109
213. Liu J, Wu J, Zhou L, Pan C, Zhou Y, Du W, et al. ZD6474, a new treatment strategy for human osteosarcoma, and its potential synergistic effect with celecoxib. *Oncotarget.* (2015) 6:21341–52. doi: 10.18632/oncotarget.4179
214. Spanheimer PM, Park JM, Askeland RW, Kulak MV, Woodfield GW, De Andrade JP, et al. Inhibition of RET increases the efficacy of antiestrogen and is a novel treatment strategy for luminal breast cancer. *Clin Cancer Res.* (2014) 20:2115–25. doi: 10.1158/1078-0432.CCR-13-2221
215. Cesca M, Frapolli R, Berndt A, Scarlato V, Richter P, Kosmehl H, et al. The effects of vandetanib on paclitaxel tumor distribution and antitumor activity in a xenograft model of human ovarian carcinoma. *Neoplasia.* (2009) 11:1155–64. doi: 10.1593/neo.09866
216. Ciardiello F, Caputo R, Damiano V, Caputo R, Troiani T, Vitagliano D, et al. Antitumor effects of ZD6474, a small molecule vascular endothelial growth factor receptor tyrosine kinase inhibitor, with additional activity against epidermal growth factor receptor tyrosine kinase. *Clin Cancer Res.* (2003) 9:1546–56.
217. Li C, Yang C, Wei G. Vandetanib inhibits cisplatinresistant neuroblastoma tumor growth and invasion. *Oncol Rep.* (2018) 39:1757–64. doi: 10.3892/or.2018.6255
218. Troiani T, Lockerbie O, Morrow M, Ciardiello F, Eckhardt SG. Sequence-dependent inhibition of human colon cancer cell growth and of prosurvival pathways by oxaliplatin in combination with ZD6474 (Zactima), an inhibitor of VEGFR and EGFR tyrosine kinases. *Mol Cancer Ther.* (2006) 5:1883–94. doi: 10.1158/1535-7163.MCT-06-0055
219. Klinge CM. Inhibition of non-small-cell lung cancer growth by combined fulvestrant and vandetanib. *Future Oncol.* (2012) 8:529–33. doi: 10.2217/fon.12.42
220. Siegfried JM, Gubish CT, Rothstein ME, Henry C, Stabile LP. Combining the multitargeted tyrosine kinase inhibitor vandetanib with the antiestrogen fulvestrant enhances its antitumor effect in non-small cell lung cancer. *J Thorac Oncol.* (2012) 7:485–95. doi: 10.1097/JTO.0b013e31824177ea
221. Jo MY, Kim YG, Kim Y, Lee SJ, Kim MH, Joo KM, et al. Combined therapy of temozolomide and ZD6474 (vandetanib) effectively reduces glioblastoma tumor volume through anti-angiogenic and anti-proliferative mechanisms. *Mol Med Rep.* (2012) 6:88–92. doi: 10.3892/mmr.2012.868
222. Hoang T, Huang S, Armstrong E, Eickhoff JC, Harari PM. Augmentation of radiation response with the vascular targeting agent ZD6126. *Int J Radiat Oncol Biol Phys.* (2006) 64:1458–65. doi: 10.1016/j.ijrobp.2005.11.017
223. Bianco C, Giovannetti E, Ciardiello F, Mey V, Nannizzi S, Tortora G, et al. Synergistic antitumor activity of ZD6474, an inhibitor of vascular endothelial growth factor receptor and epidermal growth factor receptor signaling, with gemcitabine and ionizing radiation against pancreatic cancer. *Clin Cancer Res.* (2006) 12:7099–107. doi: 10.1158/1078-0432.CCR-06-0833
224. Wachsberger P, Burd R, Ryan A, Daskalakis C, Dicker AP. Combination of vandetanib, radiotherapy, and irinotecan in the LoVo human colorectal cancer xenograft model. *Int J Radiat Oncol Biol Phys.* (2009) 75:854–61. doi: 10.1016/j.ijrobp.2009.06.016
225. Sano D, Matsumoto F, Valdecanas DR, Zhao M, Molkentine DP, Takahashi Y, et al. Vandetanib restores head and neck squamous cell carcinoma cells' sensitivity to cisplatin and radiation *in vivo* and *in vitro*. *Clin Cancer Res.* (2011) 17:1815–27. doi: 10.1158/1078-0432.CCR-10-2120
226. Crescenzi M, Persano L, Esposito G, Zulato E, Borsi L, Balza E, et al. Vandetanib improves anti-tumor effects of L19mTNFalpha in xenograft models of esophageal cancer. *Clin Cancer Res.* (2011) 17:447–58. doi: 10.1158/1078-0432.CCR-10-1420
227. Leitinger B. Transmembrane collagen receptors. *Annu Rev Cell Dev Biol.* (2011) 27:265–90. doi: 10.1146/annurev-cellbio-092910-154013
228. Vogel W, Gish GD, Alves F, Pawson T. The discoidin domain receptor tyrosine kinases are activated by collagen. *Mol Cell.* (1997) 1:13–23. doi: 10.1016/S1097-2765(00)80003-9
229. Shrivastava A, Radziejewski C, Campbell E, Kovac L, McGlynn M, Ryan TE, et al. An orphan receptor tyrosine kinase family whose members serve as nonintegrin collagen receptors. *Mol Cell.* (1997) 1:25–34. doi: 10.1016/S1097-2765(00)80004-0
230. Leitinger B, Kwan AP. The discoidin domain receptor DDR2 is a receptor for type X collagen. *Matrix Biol.* (2006) 25:355–64. doi: 10.1016/j.matbio.2006.05.006
231. Valiathan RR, Marco M, Leitinger B, Kleer CG, Fridman R. Discoidin domain receptor tyrosine kinases: new players in cancer progression. *Cancer Metastasis Rev.* (2012) 31:295–321. doi: 10.1007/s10555-012-9346-z
232. Juskaite V, Corcoran DS, Leitinger B. Collagen induces activation of DDR1 through lateral dimer association and phosphorylation between dimers. *Elife.* (2017) 6:e25716. doi: 10.7554/eLife.25716
233. Lemmon MA, Schlessinger J. Cell signaling by receptor tyrosine kinases. *Cell.* (2010) 141:1117–34. doi: 10.1016/j.cell.2010.06.011
234. Shintani Y, Fukumoto Y, Chaika N, Svoboda R, Wheelock MJ, Johnson KR. Collagen I-mediated up-regulation of N-cadherin requires cooperative signals from integrins and discoidin domain receptor 1. *J Cell Biol.* (2008) 180:1277–89. doi: 10.1083/jcb.200708137
235. Dejmek J, Dib K, Jonsson M, Andersson T. Wnt-5a and G-protein signaling are required for collagen-induced DDR1 receptor activation and normal mammary cell adhesion. *Int J Cancer.* (2003) 103:344–51. doi: 10.1002/ijc.10752
236. Ongusaha PP, Kim JI, Fang L, Wong TW, Yancopoulos GD, Aaronson SA, et al. p53 induction and activation of DDR1 kinase counteract p53-mediated apoptosis and influence p53 regulation through a positive feedback loop. *EMBO J.* (2003) 22:1289–301. doi: 10.1093/emboj/cdg129
237. Kim HG, Hwang SY, Aaronson SA, Mandinova A, Lee SW. DDR1 receptor tyrosine kinase promotes prosurvival pathway through Notch1 activation. *J Biol Chem.* (2011) 286:17672–81. doi: 10.1074/jbc.M111.236612
238. Das S, Ongusaha PP, Yang YS, Park JM, Aaronson SA, Lee SW. Discoidin domain receptor 1 receptor tyrosine kinase induces cyclooxygenase-2 and promotes chemoresistance through nuclear factor-kappaB pathway activation. *Cancer Res.* (2006) 66:8123–30. doi: 10.1158/0008-5472.CAN-06-1215
239. Gao H, Chakraborty G, Zhang Z, Akalay I, Gadiya M, Gao Y, et al. Multi-organ site metastatic reactivation mediated by non-canonical discoidin domain receptor 1 signaling. *Cell.* (2016) 166:47–62. doi: 10.1016/j.cell.2016.06.009
240. Hammerman PS, Sos ML, Ramos AH, Xu C, Dutt A, Zhou W, et al. Mutations in the DDR2 kinase gene identify a novel therapeutic target in squamous cell lung cancer. *Cancer Discov.* (2011) 1:78–89. doi: 10.1158/2159-8274.CD-11-0005
241. Badaoui M, Mimsy-Julienne C, Saby C, Van Gulick L, Peretti M, Jeannesson P, et al. Collagen type 1 promotes survival of human breast cancer cells by overexpressing Kv10.1 potassium and Orai1 calcium channels through DDR1-dependent pathway. *Oncotarget.* (2018) 9:24653–71. doi: 10.18632/oncotarget.19065

242. Ram R, Lorente G, Nikolich K, Urfer R, Foehr E, Nagavarapu U. Discoidin domain receptor-1a (DDR1a) promotes glioma cell invasion and adhesion in association with matrix metalloproteinase-2. *J Neuro-Oncol.* (2006) 76:239–48. doi: 10.1007/s11060-005-6874-1
243. Neuhaus B, Buhren S, Bock B, Alves F, Vogel WF, Kiefer F. Migration inhibition of mammary epithelial cells by Syk is blocked in the presence of DDR1 receptors. *Cell Mol Life Sci.* (2011) 68:3757–70. doi: 10.1007/s00018-011-0676-8
244. Badiola I, Villace P, Basaldua I, Olaso E. Downregulation of discoidin domain receptor 2 in A375 human melanoma cells reduces its experimental liver metastasis ability. *Oncol Rep.* (2011) 26:971–8. doi: 10.3892/or.2011.1356
245. Dejmek J, Leandersson K, Manjer J, Bjartell A, Emdin SO, Vogel WF, et al. Expression and signaling activity of Wnt-5a/discoidin domain receptor-1 and Syk plays distinct but decisive roles in breast cancer patient survival. *Clin Cancer Res.* (2005) 11:520–8.
246. Maeyama M, Koga H, Selvendiran K, Yanagimoto C, Hanada S, Taniguchi E, et al. Switching in discoid domain receptor expressions in SLUG-induced epithelial-mesenchymal transition. *Cancer.* (2008) 113:2823–31. doi: 10.1002/cncr.23900
247. Walsh LA, Nawshad A, Medici D. Discoidin domain receptor 2 is a critical regulator of epithelial-mesenchymal transition. *Matrix Biol.* (2011) 30:243–7. doi: 10.1016/j.matbio.2011.03.007
248. Valencia K, Ormazabal C, Zandueta C, Luis-Ravelo D, Anton I, Pajares MJ, et al. Inhibition of collagen receptor discoidin domain receptor-1 (DDR1) reduces cell survival, homing, and colonization in lung cancer bone metastasis. *Clin Cancer Res.* (2012) 18:969–80. doi: 10.1158/1078-0432.CCR-11-1686
249. Vehlow A, Cordes N. DDR1 (discoidin domain receptor tyrosine kinase 1) drives glioblastoma therapy resistance by modulating autophagy. *Autophagy.* (2019) 15:1487–8. doi: 10.1080/15548627.2019.1618540
250. Wang CZ, Su HW, Hsu YC, Shen MR, Tang MJ. A discoidin domain receptor 1/SHP-2 signaling complex inhibits alpha2beta1-integrin-mediated signal transducers and activators of transcription 1/3 activation and cell migration. *Mol Biol Cell.* (2006) 17:2839–52. doi: 10.1091/mbc.e05-11-1068
251. Yeh YC, Wang CZ, Tang MJ. Discoidin domain receptor 1 activation suppresses alpha2beta1 integrin-dependent cell spreading through inhibition of Cdc42 activity. *J Cell Physiol.* (2009) 218:146–56. doi: 10.1002/jcp.21578
252. Ford CE, Lau SK, Zhu CQ, Andersson T, Tsao MS, Vogel WF. Expression and mutation analysis of the discoidin domain receptors 1 and 2 in non-small cell lung carcinoma. *Br J Cancer.* (2007) 96:808–14. doi: 10.1038/sj.bjc.6603614
253. Yang SH, Baek HA, Lee HJ, Park HS, Jang KY, Kang MJ, et al. Discoidin domain receptor 1 is associated with poor prognosis of non-small cell lung carcinomas. *Oncol Rep.* (2010) 24:311–9. doi: 10.3892/or_00000861
254. Barker KT, Martindale JE, Mitchell PJ, Kamalati T, Page MJ, Phippard DJ, et al. Expression patterns of the novel receptor-like tyrosine kinase, DDR, in human breast tumours. *Oncogene.* (1995) 10:569–75.
255. Davies H, Hunter C, Smith R, Stephens P, Greenman C, Bignell G, et al. Somatic mutations of the protein kinase gene family in human lung cancer. *Cancer Res.* (2005) 65:7591–5. doi: 10.1158/0008-5472.CAN-05-1855
256. Ding L, Getz G, Wheeler DA, Mardis ER, McLellan MD, Cibulskis K, et al. Somatic mutations affect key pathways in lung adenocarcinoma. *Nature.* (2008) 455:1069–75. doi: 10.1038/nature07423
257. Jing H, Song J, Zheng J. Discoidin domain receptor 1: new star in cancer-targeted therapy and its complex role in breast carcinoma. *Oncol Lett.* (2018) 15:3403–8. doi: 10.3892/ol.2018.7795
258. Kothiwale S, Borza CM, Lowe EW Jr, Pozzi A, Meiler J. Discoidin domain receptor 1 (DDR1) kinase as target for structure-based drug discovery. *Drug Discov Today.* (2015) 20:255–61. doi: 10.1016/j.drudis.2014.09.025
259. Lesot H, Kuhl U, Mark K. Isolation of a laminin-binding protein from muscle cell membranes. *EMBO J.* (1983) 2:861–5. doi: 10.1002/j.1460-2075.1983.tb01514.x
260. Malinoff HL, Wicha MS. Isolation of a cell surface receptor protein for laminin from murine fibrosarcoma cells. *J Cell Biol.* (1983) 96:1475–9. doi: 10.1083/jcb.96.5.1475
261. Rao NC, Barsky SH, Terranova VP, Liotta LA. Isolation of a tumor cell laminin receptor. *Biochem Biophys Res Commun.* (1983) 111:804–8. doi: 10.1016/0006-291X(83)91370-0
262. Rao CN, Castronovo V, Schmitt MC, Wewer UM, Claysmith AP, Liotta LA, et al. Evidence for a precursor of the high-affinity metastasis-associated murine laminin receptor. *Biochemistry.* (1989) 28:7476–86. doi: 10.1021/bi00444a047
263. Ren J, Gao X, Jin C, Zhu M, Wang X, Shaw A, et al. Systematic study of protein sumoylation: Development of a site-specific predictor of SUMOsp 2.0. *Proteomics.* (2009) 9:3409–12. doi: 10.1002/pmic.200800646
264. DiGiacomo V, Meruelo D. Looking into laminin receptor: critical discussion regarding the non-integrin 37/67-kDa laminin receptor/RPSA protein. *Biol Rev Camb Philos Soc.* (2016) 91:288–310. doi: 10.1111/brv.12170
265. Ford CL, Randal-Whitis L, Ellis SR. Yeast proteins related to the p40/laminin receptor precursor are required for 20S ribosomal RNA processing and the maturation of 40S ribosomal subunits. *Cancer Res.* (1999) 59:704–10.
266. Scheiman J, Tseng JC, Zheng Y, Meruelo D. Multiple functions of the 37/67-kd laminin receptor make it a suitable target for novel cancer gene therapy. *Mol Ther.* (2010) 18:63–74. doi: 10.1038/mt.2009.199
267. Venticinque L, Jamieson KV, Meruelo D. Interactions between laminin receptor and the cytoskeleton during translation and cell motility. *PLoS ONE.* (2011) 6:e15895. doi: 10.1371/journal.pone.0015895
268. O'Donohue MF, Choesmel V, Faubladier M, Fichant G, Gleizes PE. Functional dichotomy of ribosomal proteins during the synthesis of mammalian 40S ribosomal subunits. *J Cell Biol.* (2010) 190:853–66. doi: 10.1083/jcb.201005117
269. Venticinque L, Meruelo D. Comprehensive proteomic analysis of nonintegrin laminin receptor interacting proteins. *J Proteome Res.* (2012) 11:4863–72. doi: 10.1021/pr300307h
270. Poon SL, Klausen C, Hammond GL, Leung PC. 37-kDa laminin receptor precursor mediates GnRH-II-induced MMP-2 expression and invasiveness in ovarian cancer cells. *Mol Endocrinol.* (2011). 25:327–38. doi: 10.1210/me.2010-0334
271. Omar A, Reusch U, Knackmuss S, Little M, Weiss SF. Anti-LRP/LR-specific antibody IgG1-iS18 significantly reduces adhesion and invasion of metastatic lung, cervix, colon and prostate cancer cells. *J Mol Biol.* (2012) 419:102–9. doi: 10.1016/j.jmb.2012.02.035
272. Satoh K, Narumi K, Abe T, Sakai T, Kikuchi T, Tanaka M, et al. Diminution of 37-kDa laminin binding protein expression reduces tumour formation of murine lung cancer cells. *Br J Cancer.* (1999) 80:1115–22. doi: 10.1038/sj.bjc.6690474
273. Scheiman J, Jamieson KV, Ziello J, Tseng JC, Meruelo D. Extraribosomal functions associated with the C terminus of the 37/67 kDa laminin receptor are required for maintaining cell viability. *Cell Death Dis.* (2010) 1:e42. doi: 10.1038/cddis.2010.19
274. Guirguis R, Margulies I, Taraboletti G, Schiffmann E, Liotta L. Cytokine-induced pseudopodial protrusion is coupled to tumour cell migration. *Nature.* (1987) 329:261–3. doi: 10.1038/329261a0
275. Kinoshita K, Kaneda Y, Sato M, Saeki Y, Wataya-Kaneda M, Hoffmann A. LBP-p40 binds DNA tightly through associations with histones H2A, H2B, and H4. *Biochem Biophys Res Commun.* (1998) 253:277–82. doi: 10.1006/bbrc.1998.9699
276. Ardini E, Tagliabue E, Magnifico A, Buto S, Castronovo V, Colnaghi MI, et al. Co-regulation and physical association of the 67-kDa monomeric laminin receptor and the alpha6beta4 integrin. *J Biol Chem.* (1997) 272:2342–5. doi: 10.1074/jbc.272.4.2342
277. Romanov V, Sobel ME, pinto da Silva P, Menard S, Castronovo V. Cell localization and redistribution of the 67 kD laminin receptor and alpha 6 beta 1 integrin subunits in response to laminin stimulation: an immunogold electron microscopy study. *Cell Adhes Commun.* (1994) 2:201–9. doi: 10.3109/15419069409004438
278. Rush J, Moritz A, Lee KA, Guo A, Goss VL, Spek EJ, et al. Immunoaffinity profiling of tyrosine phosphorylation in cancer cells. *Nat Biotechnol.* (2005) 23:94–101. doi: 10.1038/nbt1046
279. Davis CM, Papadopoulos V, Jia MC, Yamada Y, Kleinman HK, Dym M. Identification and partial characterization of laminin binding proteins in immature rat sertoli cells. *Exp Cell Res.* (1991) 193:262–73. doi: 10.1016/0014-4827(91)90095-C
280. Givant-Horwitz V, Davidson B, Reich R. Laminin-induced signaling in tumor cells: the role of the M(r) 67,000 laminin receptor. *Cancer Res.* (2004) 64:3572–9. doi: 10.1158/0008-5472.CAN-03-3424

281. Kim KJ, Chung JW, Kim KS. 67-kDa laminin receptor promotes internalization of cytotoxic necrotizing factor 1-expressing Escherichia coli K1 into human brain microvascular endothelial cells. *J Biol Chem.* (2005). 280:1360–8. doi: 10.1074/jbc.M410176200
282. Berno V, Porrini D, Castiglioni F, Campiglio M, Casalini P, Pupa SM, et al. The 67 kDa laminin receptor increases tumor aggressiveness by remodeling laminin-1. *Endocr Relat Cancer.* (2005) 12:393–406. doi: 10.1677/erc.1.00870
283. Carbone A, Gloghini A, Colombatti A, Castronovo V, Menard S. Expression of the monomeric 67-kd laminin-binding protein in human lymphomas as defined by MLuC5 monoclonal antibody and paraffin section immunohistochemistry. *Hum Pathol.* (1995) 26:541–6. doi: 10.1016/0046-8177(95)90251-1
284. Colnaghi MI. The simultaneous expression of c-erbB-2 oncoprotein and laminin receptor on primary breast tumors has a predicting potential analogous to that of the lymph node status. *Adv Exp Med Biol.* (1994) 353:149–54. doi: 10.1007/978-1-4615-2443-4_14
285. Martignone S, Menard S, Bufalino R, Cascinelli N, Pellegrini R, Tagliabue E, et al. Prognostic significance of the 67-kilodalton laminin receptor expression in human breast carcinomas. *J Natl Cancer Inst.* (1993) 85:398–402. doi: 10.1093/jnci/85.5.398
286. Sanjuan X, Fernandez PL, Miquel R, Munoz J, Castronovo V, Menard S, et al. Overexpression of the 67-kD laminin receptor correlates with tumour progression in human colorectal carcinoma. *J Pathol.* (1996) 179:376–80. doi: 10.1002/(SICI)1096-9896(199608)179:4<376::AID-PATH591>3.0.CO;2-V
287. Tagliabue E, Pastorino U. Re: killing of laminin receptor-positive human lung cancers by tumor-infiltrating lymphocytes bearing gamma delta + T-cell receptors. *J Natl Cancer Inst.* (1996) 88:1241–2. doi: 10.1093/jnci/88.17.1241
288. Viacava P, Naccarato AG, Collecchi P, Menard S, Castronovo V, Bevilacqua G. The spectrum of 67-kD laminin receptor expression in breast carcinoma progression. *J Pathol.* (1997) 182:36–44. doi: 10.1002/(SICI)1096-9896(199705)182:1<36::AID-PATH802>3.0.CO;2-W
289. Wewer UM, Taraboletti G, Sobel ME, Albrechtsen R, Liotta LA. Role of laminin receptor in tumor cell migration. *Cancer Res.* (1987) 47:5691–8.
290. Khumalo T, Reusch U, Knackmuss S, Little M, Veale RB, Weiss SF. Adhesion and invasion of breast and oesophageal cancer cells are impeded by anti-LRP/LR-specific antibody IgG1-iS18. *PLoS ONE.* (2013) 8:e66297. doi: 10.1371/journal.pone.0066297
291. Rebelo TM, Chetty CJ, Ferreira E, Weiss SF. Anti-LRP/LR-specific antibody IgG1-iS18 impedes adhesion and invasion of pancreatic cancer and neuroblastoma cells. *BMC Cancer.* (2016) 16:917. doi: 10.1186/s12885-016-2953-2
292. Chetty C, Khumalo T, Da Costa Dias B, Reusch U, Knackmuss S, Little M, et al. Anti-LRP/LR specific antibody IgG1-iS18 impedes adhesion and invasion of liver cancer cells. *PLoS ONE.* (2014) 9:e96268. doi: 10.1371/journal.pone.0096268
293. Rebelo TM, Vania L, Ferreira E, Weiss SFT. siRNA - mediated LRP/LR knock-down reduces cellular viability of malignant melanoma cells through the activation of apoptotic caspases. *Exp Cell Res.* (2018) 368:1–12. doi: 10.1016/j.yexcr.2018.04.003
294. Chetty CJ, Ferreira E, Jovanovic K, Weiss SFT. Knockdown of LRP/LR induces apoptosis in pancreatic cancer and neuroblastoma cells through activation of caspases. *Exp Cell Res.* (2017) 360:264–72. doi: 10.1016/j.yexcr.2017.09.016
295. Khumalo T, Ferreira E, Jovanovic K, Veale RB, Weiss SF. Knockdown of LRP/LR Induces apoptosis in breast and oesophageal cancer cells. *PLoS ONE.* (2015) 10:e0139584. doi: 10.1371/journal.pone.0139584
296. Vania L, Rebelo TM, Ferreira E, Weiss SFT. Knock-down of LRP/LR promotes apoptosis in early and late stage colorectal carcinoma cells via caspase activation. *BMC Cancer.* (2018) 18:602. doi: 10.1186/s12885-018-4531-2
297. Lu CL, Xu J, Yao HJ, Luo KL, Li JM, Wu T, et al. Inhibition of human 67-kDa laminin receptor sensitizes multidrug resistance colon cancer cell line SW480 for apoptosis induction. *Tumour Biol.* (2016) 37:1319–25. doi: 10.1007/s13277-015-3873-5
298. Sun L, Liu L, Liu X, Wang Y, Li M, Yao L, et al. MGr1-Ag/37LRP induces cell adhesion-mediated drug resistance through FAK/PI3K and MAPK pathway in gastric cancer. *Cancer Sci.* (2014) 105:651–9. doi: 10.1111/cas.12414
299. Naidoo K, Malindisa ST, Otgaar TC, Bernert M, Da Costa Dias B, Ferreira E, et al. Knock-Down of the 37kDa/67kDa Laminin Receptor LRP/LR impedes telomerase activity. *PLoS ONE.* (2015) 10:e0141618. doi: 10.1371/journal.pone.0141618
300. Vania L, Morris G, Otgaar TC, Bignoux MJ, Bernert M, Burns J, et al. Patented therapeutic approaches targeting LRP/LR for cancer treatment. *Expert Opin Ther Pat.* (2019) 29:987–1009. doi: 10.1080/13543776.2019.1693543
301. Tachibana H, Koga K, Fujimura Y, Yamada K. A receptor for green tea polyphenol EGCG. *Nat Struct Mol Biol.* (2004) 11:380–1. doi: 10.1038/nsmb743
302. Zidane N, Ould-Abeih MB, Petit-Topin I, Bedouelle H. The folded and disordered domains of human ribosomal protein SA have both idiosyncratic and shared functions as membrane receptors. *Biosci Rep.* (2012) 33:113–24. doi: 10.1042/BSR20120103
303. Sulzmaier FJ, Jean C, Schlaepfer DD. FAK in cancer: mechanistic findings and clinical applications. *Nat Rev Cancer.* (2014) 14:598–610. doi: 10.1038/nrc3792
304. Alanko J, Mai A, Jacquemet G, Schauer K, Kaukonen R, Saari M, et al. Integrin endosomal signalling suppresses anoikis. *Nat Cell Biol.* (2015) 17:1412–21. doi: 10.1038/ncb3250
305. Zhou J, Yi Q, Tang L. The roles of nuclear focal adhesion kinase (FAK) on cancer: a focused review. *J Exp Clin Cancer Res.* (2019) 38:250. doi: 10.1186/s13046-019-1265-1
306. Golubovskaya VM. Targeting FAK in human cancer: from finding to first clinical trials. *Front Biosci.* (2014) 19:687–706. doi: 10.2741/4236
307. Roy-Luzarraga M, Hodivala-Dilke K. Molecular pathways: endothelial cell FAK-a target for cancer treatment. *Clin Cancer Res.* (2016) 22:3718–24. doi: 10.1158/1078-0432.CCR-14-2021
308. Infante JR, Camidge DR, Mileshkin LR, Chen EX, Hicks RJ, Rischin D, et al. Safety, pharmacokinetic, and pharmacodynamic phase I dose-escalation trial of PF-00562271, an inhibitor of focal adhesion kinase, in advanced solid tumors. *J Clin Oncol.* (2012) 30:1527–33. doi: 10.1200/JCO.2011.38.9346
309. Mak G, Soria JC, Blagden SP, Plummer R, Fleming RA, Nebot N, et al. A phase Ib dose-finding, pharmacokinetic study of the focal adhesion kinase inhibitor GSK2256098 and trametinib in patients with advanced solid tumours. *Br J Cancer.* (2019) 120:975–81. doi: 10.1038/s41416-019-0452-3
310. Soria JC, Gan HK, Blagden SP, Plummer R, Arkenau HT, Ranson M, et al. A phase I, pharmacokinetic and pharmacodynamic study of GSK2256098, a focal adhesion kinase inhibitor, in patients with advanced solid tumors. *Ann Oncol.* (2016) 27:2268–74. doi: 10.1093/annonc/mdw427
311. Brown NF, Williams M, Arkenau HT, Fleming RA, Tolson J, Yan L, et al. A study of the focal adhesion kinase inhibitor GSK2256098 in patients with recurrent glioblastoma with evaluation of tumor penetration of [11C]GSK2256098. *Neuro Oncol.* (2018) 20:1634–42. doi: 10.1093/neuonc/noy078
312. Jones SF, Siu LL, Bendell JC, Cleary JM, Razak AR, Infante JR, et al. A phase I study of VS-6063, a second-generation focal adhesion kinase inhibitor, in patients with advanced solid tumors. *Invest New Drugs.* (2015) 33:1100–7. doi: 10.1007/s10637-015-0282-y
313. Shimizu T, Fukuoka K, Takeda M, Iwasa T, Yoshida T, Horobin J, et al. A first-in-Asian phase 1 study to evaluate safety, pharmacokinetics and clinical activity of VS-6063, a focal adhesion kinase (FAK) inhibitor in Japanese patients with advanced solid tumors. *Cancer Chemother Pharmacol.* (2016) 77:997–1003. doi: 10.1007/s00280-016-3010-1
314. Doi T, Yang JC, Shitara K, Naito Y, Cheng AL, Sarashina A, et al. Phase I study of the focal adhesion kinase inhibitor BI 853520 in Japanese and Taiwanese patients with advanced or metastatic solid tumors. *Target Oncol.* (2019) 14:57–65. doi: 10.1007/s11523-019-0 0620-0
315. de Jonge MJA, Steeghs N, Lolkema MP, Hotte SJ, Hirte HW, van der Biessen DAJ, et al. Phase I study of BI 853520, an inhibitor of focal adhesion kinase, in patients with advanced or metastatic nonhematologic malignancies. *Target Oncol.* (2019) 14:43–55. doi: 10.1007/s11523-018-00617-1
316. Verheijen RB, van der Biessen DAJ, Hotte SJ, Siu LL, Spreafico A, de Jonge MJA, et al. Randomized, open-label, crossover studies evaluating the effect of food and liquid formulation on the pharmacokinetics of the novel focal adhesion kinase (FAK) inhibitor BI 853520. *Target Oncol.* (2019) 14:67–74. doi: 10.1007/s11523-018-00618-0

317. Fennell DA, Baas P, Taylor P, Nowak AK, Gilligan D, Nakano T, et al. Maintenance defactinib versus placebo after first-line chemotherapy in patients with merlin-stratified pleural mesothelioma: COMMAND-A double-blind, randomized, phase II study. *J Clin Oncol.* (2019) 37:790–8. doi: 10.1200/JCO.2018.79.0543
318. Brunton VG, Frame MC. Src and focal adhesion kinase as therapeutic targets in cancer. *Curr Opin Pharmacol.* (2008) 8:427–32. doi: 10.1016/j.coph.2008.06.012
319. Eckert MA, Lwin TM, Chang AT, Kim J, Danis E, Ohno-Machado L, et al. Twist1-induced invadopodia formation promotes tumor metastasis. *Cancer Cell.* (2011) 19:372–86. doi: 10.1016/j.ccr.2011.01.036
320. Pichot CS, Hartig SM, Xia L, Arvanitis C, Monisvais D, Lee FY, et al. Dasatinib synergizes with doxorubicin to block growth, migration, and invasion of breast cancer cells. *Br J Cancer.* (2009) 101:38–47. doi: 10.1038/sj.bjc.6605101
321. Zhang XH, Wang Q, Gerald W, Hudis CA, Norton L, Smid M, et al. Latent bone metastasis in breast cancer tied to Src-dependent survival signals. *Cancer Cell.* (2009) 16:67–78. doi: 10.1016/j.ccr.2009.05.017
322. Barkan D, El Touny LH, Michalowski AM, Smith JA, Chu I, Davis AS, et al. Metastatic growth from dormant cells induced by a col-I-enriched fibrotic environment. *Cancer Res.* (2010) 70:5706–16. doi: 10.1158/0008-5472.CAN-09-2356
323. Sakuma Y, Tsunezumi J, Nakamura Y, Yoshihara M, Matsukuma S, Koizume S, et al. ABT-263, a Bcl-2 inhibitor, enhances the susceptibility of lung adenocarcinoma cells treated with Src inhibitors to anoikis. *Oncol Rep.* (2011) 25:661–7. doi: 10.3892/or.2010.1123
324. Zhu P, Tan MJ, Huang RL, Tan CK, Chong HC, Pal M, et al. Angiopoietin-like 4 protein elevates the prosurvival intracellular O2(-):H2O2 ratio and confers anoikis resistance to tumors. *Cancer Cell.* (2011) 19:401–15. doi: 10.1016/j.ccr.2011.01.018
325. Desgrosellier JS, Barnes LA, Shields DJ, Huang M, Lau SK, Prevost N, et al. An integrin alpha(v)beta(3)-c-Src oncogenic unit promotes anchorage-independence and tumor progression. *Nat Med.* (2009) 15:1163–9. doi: 10.1038/nm.2009
326. Zhang S, Yu D. Targeting Src family kinases in anti-cancer therapies: turning promise into triumph. *Trends Pharmacol Sci.* (2012) 33:122–8. doi: 10.1016/j.tips.2011.11.002
327. Kanda R, Kawahara A, Watari K, Murakami Y, Sonoda K, Maeda M, et al. Erlotinib resistance in lung cancer cells mediated by integrin beta1/Src/Akt-driven bypass signaling. *Cancer Res.* (2013) 73:6243–53. doi: 10.1158/0008-5472.CAN-12-4502
328. Roskoski R Jr. Src protein-tyrosine kinase structure, mechanism, and small molecule inhibitors. *Pharmacol Res.* (2015). 94:9–25. doi: 10.1016/j.phrs.2015.01.003
329. Mayer EL, Krop IE. Advances in targeting SRC in the treatment of breast cancer and other solid malignancies. *Clin Cancer Res.* (2010) 16:3526–32. doi: 10.1158/1078-0432.CCR-09-1834
330. Elias D, Vever H, Laenkholm AV, Gjerstorff MF, Yde CW, Lykkesfeldt AE, et al. Gene expression profiling identifies FYN as an important molecule in tamoxifen resistance and a predictor of early recurrence in patients treated with endocrine therapy. *Oncogene.* (2015) 34:1919–27. doi: 10.1038/onc.2014.138
331. Tabaries S, Annis MG, Hsu BE, Tam CE, Savage P, Park M, et al. Lyn modulates Claudin-2 expression and is a therapeutic target for breast cancer liver metastasis. *Oncotarget.* (2015) 6:9476–87. doi: 10.18632/oncotarget.3269

Conflict of Interest: The authors declare that the research was conducted in the absence of any commercial or financial relationships that could be construed as a potential conflict of interest.

Copyright © 2020 Lorusso, Rüegg and Kuonen. This is an open-access article distributed under the terms of the Creative Commons Attribution License (CC BY). The use, distribution or reproduction in other forums is permitted, provided the original author(s) and the copyright owner(s) are credited and that the original publication in this journal is cited, in accordance with accepted academic practice. No use, distribution or reproduction is permitted which does not comply with these terms.

frontiers in Oncology

MINI REVIEW
published: 30 July 2020
doi: 10.3389/fonc.2020.00882

Contribution of the Low-Density Lipoprotein Receptor Family to Breast Cancer Progression

Océane Campion[1,2†], *Tesnim Al Khalifa*[1,2†], *Benoit Langlois*[1,2], *Jessica Thevenard-Devy*[1,2], *Stéphanie Salesse*[1,2], *Katia Savary*[1,2], *Christophe Schneider*[1,2], *Nicolas Etique*[1,2], *Stéphane Dedieu*[1,2‡] *and Jérôme Devy*[1,2*‡]

[1] *Université de Reims Champagne-Ardenne (URCA), Reims, France,* [2] *CNRS UMR 7369, Matrice Extracellulaire et Dynamique Cellulaire, MEDyC, Reims, France*

The low-density lipoprotein receptor (LDLR) family comprises 14 single-transmembrane receptors sharing structural homology and common repeats. These receptors specifically recognize and internalize various extracellular ligands either alone or complexed with membrane-spanning co-receptors that are then sorted for lysosomal degradation or cell-surface recovery. As multifunctional endocytic receptors, some LDLR members from the core family were first considered as potential tumor suppressors due to their clearance activity against extracellular matrix-degrading enzymes. LDLRs are also involved in pleiotropic functions including growth factor signaling, matricellular proteins, and cell matrix adhesion turnover and chemoattraction, thereby affecting both tumor cells and their surrounding microenvironment. Therefore, their roles could appear controversial and dependent on the malignancy state. In this review, recent advances highlighting the contribution of LDLR members to breast cancer progression are discussed with focus on (1) specific expression patterns of these receptors in primary cancers or distant metastasis and (2) emerging mechanisms and signaling pathways. In addition, potential diagnosis and therapeutic options are proposed.

Keywords: LDLR, breast cancer, microenvironment, biomarker, therapeutic targets

OPEN ACCESS

Edited by:
Frederic Saltel, INSERM U1053 Bordeaux Recherche en Oncologie Translationnelle, France

Reviewed by:
Concepción Vicenta Llorente, Instituto de Investigaciones Biomédicas de Barcelona (IIBB), Spain
Alessandra Ghigo, University of Turin, Italy

****Correspondence:***
Jérôme Devy
jerome.devy@univ-reims.fr

†These authors share first authorship

‡These authors share senior authorship

Specialty section:
This article was submitted to Molecular and Cellular Oncology, a section of the journal Frontiers in Oncology

Received: *02 March 2020*
Accepted: *05 May 2020*
Published: *30 July 2020*

Citation:
Campion O, Al Khalifa T, Langlois B, Thevenard-Devy J, Salesse S, Savary K, Schneider C, Etique N, Dedieu S and Devy J (2020) Contribution of the Low-Density Lipoprotein Receptor Family to Breast Cancer Progression. Front. Oncol. 10:882. doi: 10.3389/fonc.2020.00882

THE LOW-DENSITY LIPOPROTEIN RECEPTOR FAMILY AND BREAST CANCER: A STATE OF ART

The low-density lipoprotein receptor (LDLR) gene family encodes single-spanning transmembrane receptors usually referred to as LDLR-related proteins (LRPs). The 14 described members are LDLR, VLDLR, LRP1/CD91/A2MR, LRP1B, LRP2/megalin/GP330, LRP3, LRP4/MEGF7, LRP5, LRP6, LRP8/ApoER2, LRP10/LRP9, LRP11/SorLA LRP12/ST7, and LRAD3 (see **Table 1**). Despite various homology levels, most members are clustered type I receptors sharing structural motifs (e.g., cysteine-rich complement-type repeats), involved in specific recognition of extracellular ligands, EGF-precursor homologous and β-propeller domains critical for protein folding, and pH-dependent lysosomal release of ligands. The short intracellular tail encompasses motifs allowing the recruitment of scaffolds driving the endocytic machinery and intracellular signaling. The LDLR founding member was first identified as a frequently mutated etiological factor of familial hypercholesterolemia. LDLR functions were then extended to numerous physiopathological contexts such as vascular integrity, neurobiology, and cancer development due to their peculiar

ability to control membrane compartmentalization of receptors and clearance of various classes of extracellular ligands. Some LRPs were thus implicated in the specific recognition of above 50 extracellular factors, among which several growth- or migration-regulatory molecules located in the tumor microenvironment (TME) of various cancers, including mammary cancers.

Breast cancer (BC) is one of the most diagnosed cancers among women worldwide and is the second-leading cause of cancer death. Based on their histological features, breast tumors are divided into two subtypes, *in situ* breast carcinoma and invasive breast carcinoma. The first subtype is sub-classified as either ductal (DCIS) or lobular carcinoma *in situ* (LCIS). Invasive carcinomas are further categorized into several histological subtypes, such as infiltrating ductal, invasive lobular, ductal/lobular, mucinous (colloid), tubular, medullary, and papillary carcinomas. Classification of BC based on molecular components is more useful for treatment planning and development of targeted therapies. In this classification, BC is mainly divided into hormone-receptor positive (ER^+/PR^+), human epidermal growth factor receptor-2 overexpressing ($HER2^+$), and triple negative (TNBC). Over the past decades, breakthroughs have been made in BC treatment including surgery, radiotherapy, chemotherapy, endocrine therapy, targeted therapy, and immunotherapy. Despite all these therapeutic options, TNBC remains associated with poor outcomes and a historical lack of targeted therapies. Regarding metastases from BC, the most common first site of distant spread is bone (41%), followed by lung (22%), brain (7%), and liver (7%). The remaining 20% of patients have multiple metastatic sites (21). In this review, our focus will be on the role played by the members of the LDLR family in BC by examining specifically their implications within the tumor microenvironment. The clinical relevance of targeting these receptors for developing new targeted therapies will also be discussed.

LRPS AND BREAST CANCER CELLS: A CLOSE AND COMPLEX RELATIONSHIP

Obesity and hypercholesterolemia are risk factors for BC that negatively impact therapeutic efficacy (22, 23). Higher levels of plasmatic cholesterol, LDL (low-density lipoprotein), and triglycerides and low circulating levels of HDL are frequently found in patients with BC (24). Interestingly, LDL was reported to affect the sensitivity of tumor cells to radiotherapy in inflammatory BC (25). LDL could affect the adhesion of BC cells involved in cell migration and proliferation and a difference in the quantity and type of lipid synthesis and storage has been demonstrated in basal-like ER^- compared to luminal ER^+ BC cells (26). Patients with BC usually exhibit elevated serum levels of oxidized LDL, reported to induce structural DNA alterations, a decrease in DNA repair, and pro-oncogenic signaling pathways (1).

In mammary tumor tissues, LDLR expression is higher and cholesteryl ester accumulation is associated with an increase of Ki67 expression and poor clinical outcome (27, 28). BC cells express higher LRP1 and LDLR, allowing a better uptake of LDL-C from the blood (29). Cholesterol may also generate 27-hydroxycholesterol, an estrogen mimetic involved in epithelial-to-mesenchymal transition (EMT) in ER^+ BC cells (30, 31). In addition, LDLR and acyl-CoA:cholesterol acyltransferase-1 are increased in HER2-positive and triple-negative tumors compared to luminal A tumors (1).

Among LDLR, the giant receptors are represented by LRP1, LRP1B, and LRP2, sharing strong structure homologies but showing discrepancies in terms of endocytic kinetics and expression pattern (32). LRP2/Megalin is required for the internalization of vitamin D and its activation to 1,25-OH vitamin D. A reduced expression was found in some BC, leading to a decrease of its nuclear receptor VDR activation, which plays an important anti-proliferative role (33). *LRP2* mRNA was also detected at fairly high levels in invasive BC but with extremely high variability (11).

LRP1B, a close homolog of LRP1, is among the top 10 significantly mutated genes in human cancer (34, 35). LRP1B is mutated in circulating tumor cells from BC and may participate in human mammary gland carcinogenesis (12). The nuclear localization of its intracellular domain is significantly related to poor prognosis in patients with invasive ductal breast carcinoma and to a significant decrease of both disease-free and overall survival in patients with luminal A type breast carcinoma (10).

LRP1 was initially identified as a tumor suppressor controlling, by endocytic clearance, the extracellular matrix-degrading enzymes in the microenvironment of various invasive tumors (36). In BC models, α2-macroglobulin/LRP1-dependent uptake of pepsin is involved in the control of the invasive potential of luminal and TNBC cells (37). However, other studies support a more complex view of LRP1 functions in tumor cells. The serine protease inhibitor PN-1/SerpinE2, which is highly expressed in ER^- and high-grade BC, stimulates lung metastasis of mammary tumor cells through LRP1-dependent secretion of MMP-9 (38). By contrast, SerpinE2 and LRP1 were identified among the genes induced by ZEB-1, an EMT driver that limits the expression of LRP1-targeting miRNAs, thereby triggering tumor cell autocrine factors that predict poor survival in early stage of BC (39). LRP1 can exert a dramatic control of tumor cell plasticity and migratory capacities. Its silencing in TNBC cells increased cellular rigidity, decreased cellular protrusions, and finally impaired migration (8). Converging data illustrate the important role of Hsp90α binding to LRP1 during EMT-related events in BC (40–43). Hypoxia leads to HIF1-α-dependent secretion of Hsp90α by TNBC cells. Its specific binding to LRP1 stimulates tumor development and metastatic lung colonization (42). This interaction and subsequent pro-metastatic signals are reinforced by clusterin in both luminal and TNBC models (43). Interestingly, within extracellular space, Hsp90α is absent from the normal microenvironment, suggesting promising

Abbreviations: BBB, blood–brain barrier; BC, breast cancer; DCIS, Ductal carcinoma *in situ*; ECM, extracellular matrix; EMT, epithelial-to-mesenchymal transition; ER, estrogen receptor; HDL, high-density lipoprotein; HER2, human epidermal growth factor receptor-2; LCIS , lobular carcinoma *in situ*; LDL, low-density lipoprotein; LDLR, low-density lipoprotein receptor; LRP, LDL receptor-related protein; PR, progesterone receptor; TME, tumor microenvironment; TNBC, triple-negative breast cancer; VDR, vitamin D receptor; VLDL, very low density lipoprotein.

TABLE 1 | The 14 members of the low-density lipoprotein receptor family and their involvement in breast cancer.

LRP isotype	Alternative name	MW (kDa)	Tissue distribution	How involved in breast cancer
LDLR		120-160	Ubiquitous	• Overexpressed in HER2$^+$ and TNBC (MDA-MB-231) (1) • Overexpression accelerates LDL cholesterol-mediated BC growth in mouse models of hyperlipidemia (2)
VLDL-R *(type II)*		96	Abundant in heart, skeletal muscle, ovary and kidney	• Up-regulated expression correlates with BC metastasis (3) • Promotes BC cell migration by up-regulating VEGF, MMP2 and MMP7 (4) • Survival factor in TNBC (5, 6)
LRAD3	Ldlrad3	50	Neurons	None
LRP1	α2MR APOER CD91	600	Ubiquitous (liver, brain, adipose tissue, fibroblasts and tissue stroma)	• Overexpressed in aggressive HER2$^+$ and TNBC and associated with increased invasion (7) • Stimulates TNBC migration (8) • C766T polymorphism is suspected to increase risk of BC development (9)
LRP1B	LRP-DIT	515	Especially in brain, thyroid, skeletal muscles, testis, ovary, colon	• Considered as tumor suppressor in several cancer types but not in BC • Intracellular nuclear localization correlates with poor prognosis in invasive ductal BC (10)
LRP2	Megalin GP330	517/600	Placenta, kidney, mammary epithelial cells	• High mRNA levels in invasive BC (11) • Mutated in circulating tumor cells from BC (12) • Upregulated in T-47D (13)
LRP3	hLRP105	105	Widely expressed (ovary, heart, brain, liver, pancreas, prostate and small intestine, skeletal muscle)	ND
LRP4	MEGF7	212	Bone, cartilage, muscle, brain	ND
LRP5	LR3 LRP7	216	Widely expressed (including in mammary epithelium) with high expression in liver	• Overexpressed in TNBC and basal-like BC (14, 15) • Stimulates STK40 expression and cell viability in TNBC (15) • Regulates glucose uptake in mammary epithelial cells (16)
LRP6		180	Co-expressed with LRP5 during embryogenesis and in adult tissues	• Overexpressed in TNBC and basal-like BC (14) • Role in TNBC cell migration and invasion (MDA-MB-231 and BT549) (15) • Increases the pool of stem cells in TNBC (17)
LRP8	APOER2	106	Brain, placenta, platelets	• Overexpressed in TNBC and ER$^-$ BC (18, 19) • Positive regulator of BC stem cells in TNBC, supports chemoresistance and metastasis (18) • Suggested as novel therapeutic target in TNBC (6)
LRP10	LRP9 in mouse	76	Ubiquitous (Leukocyte, lung, placenta, small intestine, liver, kidney, spleen, thymus, colon, skeletal muscle, heart)	ND
LRP11	sorLA LR11	53	Substantial levels in kidney, testis, ovary, lymph nodes, vascular smooth muscle cells and nervous system	• Drives resistance to anti-HER2 therapy (20)
LRP12	ST7	94	Heart, skeletal muscle, brain, lung, placenta and pancreas	ND

The family core members are underlined in green, the structurally distant members are in blue, and the most distant members are in orange. ND: not determined.

opportunities for targeted therapy (42). These studies underline the versatility of LRP1 functions in breast TME and support ongoing research to identify the specific molecular interfaces mobilized by the receptor that could be targeted to control aggressive behavior of tumor cells. A less characterized member of LRPs, SorLA/LRP11, was recently involved in the endocytic trafficking of HER2 (20). The depletion of SorLA was reported to affect lysosomal function and sensitize HER2-overexpressing cells resistant to targeted therapy. Its targeting could therefore affect compartmentalized pools of oncogenic receptors and restore efficacy of conventional treatments.

LRP5 and LRP6, as co-receptors of the Wnt/β-catenin pathway, are directly involved in breast tumorigenesis. Wnt ligands such as frizzled homolog 7 and LRP6 are overexpressed in TNBC (44), whereas Wnt antagonists are frequently silenced by methylation in BC (45). Blockade or silencing of LRP6 in SUM1315 basal BC cells results in a re-expression of epithelial markers and a decreased capacity to self-renew and metastasize (46). Similarly, LRP6 downregulation in MDA-MB-231 decreases the pool of BC stem cells (17). These effects are more pronounced on TNBC cell migration and invasion (47). The use of benzimidazole compounds on TNBC cells exerts anticancer activity by inhibiting the Wnt/β-catenin pathway. Prodigiosin and other compounds decrease the phosphorylation of LRP6 (active form), and inhibit the activation of mTORC and Wnt/βcatenin signaling (48–52). The disruption of lipid rafts in TNBC cells is associated with a decrease of LRP6 and β-catenin expression, cell proliferation, and migration (53). Besides this Wnt/βcatenin canonical pathway, LRP5 was also reported to be involved in the uptake of glucose in mammary epithelial cells, through Apolipoprotein E (ApoE) binding. The glucose uptake is essential for regulating the growth rate of these cells (16). A soluble LRP6 ectodomain can prevent tumor progression, by inhibiting cell migration and metastasis, by limiting the Frz-mediated non-canonical pathway activation in breast tumor cells (54).

The function of LRP8/ApoER2, strongly expressed in ER negative breast tumors was recently described in breast tumor initiating cells, which constitute a clinical challenge of the pathology (18). Interestingly, its depletion impairs TNBC cell proliferation and promotes apoptosis (19). LRP8 depletion also leads to Wnt/β-catenin signaling inhibition, decreases the pool of BC cells, limits their tumorigenic potential in murine xenografts, and finally restores TNBC cell sensitivity to chemotherapy (18). An overview of the complex and multiple LRPs-mediated signaling pathways is shown in **Figure 1**.

FUNCTIONAL INTERPLAY BETWEEN LRPS AND CELLS WITHIN THE TUMOR MICROENVIRONMENT

The breast TME encompasses multiple cell types including fibroblasts, immune cells, adipocytes, and endothelial cells (55). In human breast tumors, fibroblasts are the most abundant stromal cells and high levels of LRP1 expression was reported (56). In fibroblasts, LRP1 binds to CTGF, PDGF, and TGFβ and interacts with their respective receptors, thereby modulating their mitogenic or contractile capacities (57–61). Similarly, to LRP1, LRP6 interacts closely with PDGFRβ and TGF-βRI in pericytes and is involved in their trans-differentiation into myofibroblasts in response to TGFβ or CTGF. Therefore, it stimulates the PDGF-BB-dependent proliferation of established myofibroblasts via β-catenin-independent mechanisms (62). Likewise, Wnt7a secreted by aggressive breast tumor cells promotes the activation of stromal fibroblasts through TGFβ signaling (63). In cancer-associated fibroblast from mammary tumors, the stabilization of LRP6 at cell surface by DKK3 stimulates β-catenin and YAP/TAZ signals, promoting pro-tumorigenic functions such as ECM stiffening (64). Interestingly, pro-cath-D hypersecreted by cancer cells in the breast TME stimulates fibroblast outgrowth by inhibiting the release of LRP1β (intracellular domain), which is able to regulate gene transcription (65).

Adipocytes are mainly engaged during BC progression through a metabolic crosstalk with adjacent tumor cells and adopt a modified phenotype called cancer-associated adipocytes (66). Resulting dysfunctional adipocytes overexpressed fatty acid, cholesterol, triglycerides, hormones, but also adipokines, inflammatory cytokines, and proteases that are linked to cancer progression (66). LRP-1 is highly expressed in preadipocytes and is involved in adipocyte differentiation, especially through its regulation of peroxisome proliferator-activated receptor γ (67). LRP1 has also been demonstrated to be upregulated in obese mouse adipocytes and obese human adipose tissues (67) and to regulate insulin receptor and GLUT4 trafficking and activation (68, 69). Through modulation of Wnt5a signaling, LRP1 controls cholesterol storage and fatty acid synthesis during adipocyte differentiation (70). An attenuated endocytosis of apoA5 by adipocytes was demonstrated in both adipose tissue from obese patients and insulin-resistant adipocytes. The mechanism underlying this phenomenon might be related to a reduced endocytic activity of LRP1 and/or an attenuated insulin-dependent movement of LRP1 from intracellular structures to the cell surface (71). These mechanisms may lead to excessive augmentation of triglyceride storage and abnormal metabolism of adipocytes, hence promoting the development of obesity and obesity-associated disorders such as BC.

LRP1 is also abundantly expressed by various immune cells and its function in HSP-mediated antigen presentation and subsequent innate immune response is well described in macrophages and dendritic cells (72). LRP1 also inhibits macrophage-driven inflammation by decreasing cell-surface abundance of the TNF receptor-1 and Iκ-B kinase/NF-κB intracellular activation (73). By contrast, production of sLRP1 (shed or soluble LRP1) by macrophages induces pro-inflammatory factor synthesis such as IL-10, TNF-α, and MCP-1 (74). Macrophage inflammatory protein-1a/CCL3, known to amplify inflammation, is overproduced in the absence of LRP1 in myeloid cells, leading to enhanced CCR5-expressing monocyte recruitment to tumors and cancer angiogenesis (75).

Recent studies have demonstrated the crucial angio-modulatory actions of LRP family members in various solid tumors, including BCs (39, 51, 76–79). LDL and VLDL (very low density lipoprotein) are involved in the secretion of diffusible

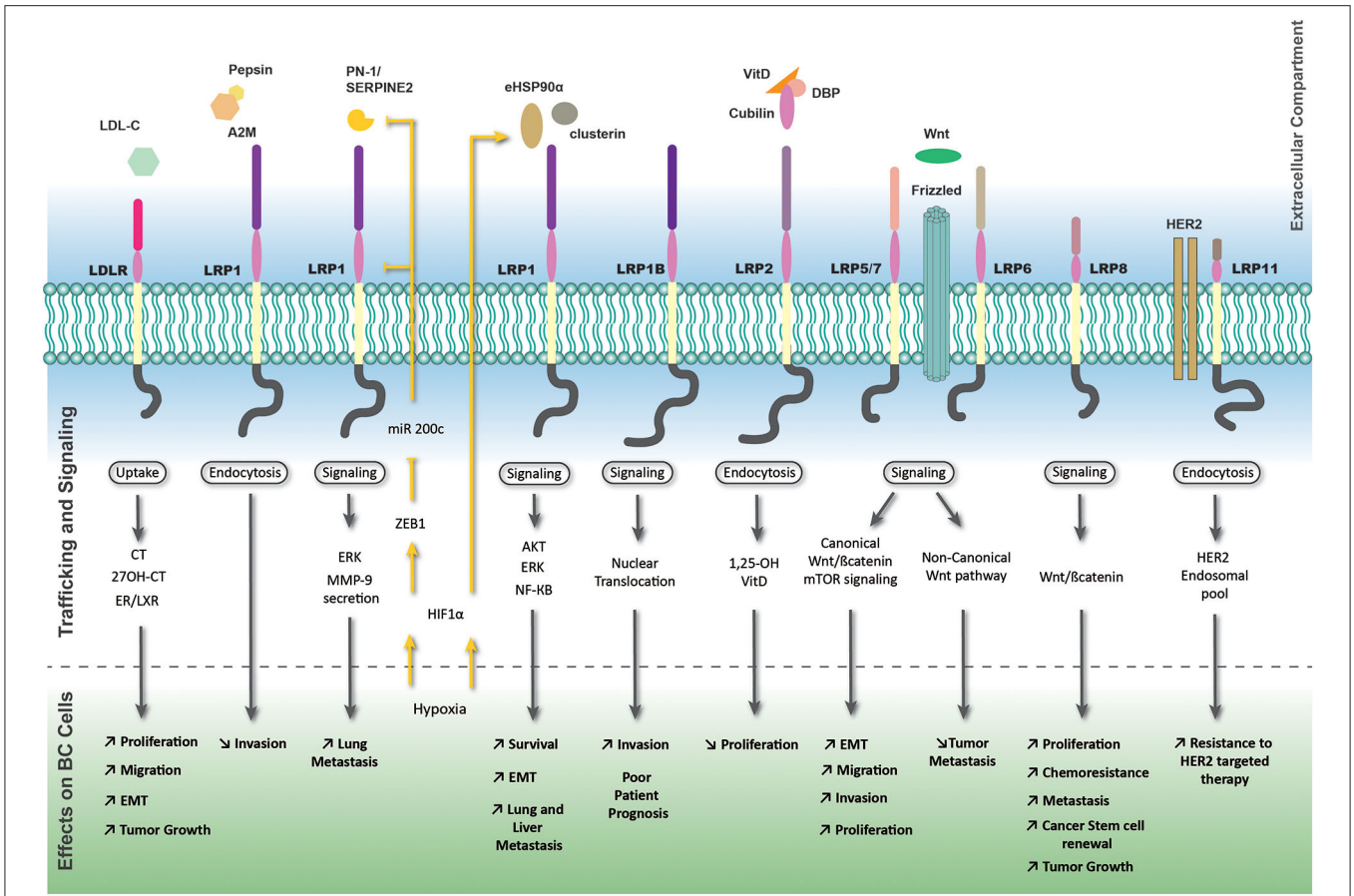

FIGURE 1 | LRP-mediated signaling pathways and trafficking in breast tumor cells. The most important members of the LDLR family exhibiting effects on breast cancer cells are represented with their associated extracellular ligands. Outside-in and inside-out pathways are represented by black and yellow arrows or lines, respectively. The yellow strikethrough line indicates an inhibition. A2M, alpha-2 macroglobulin; CT, cholesterol; ER, estrogen receptor; LXR, liver X receptor; VitD, vitamin D.

angiogenic factors by BC cells, such as amphiregulin (79). Moreover, the binding of Wnt3a to LRP6 stimulates VEGF production by TNBC cells (51). The stoichiometry of Wnt ligands and their secreted regulators such as Dickkopfs (DKK) seems instrumental to fine-tune LRP5/6 functions in the TME. DKK1 was indeed described as anti-angiogenic, whereas DKK2 binding to LRP6 triggers potent induction of endothelial cell sprouting (80). LRP1 is widely expressed in various endothelial cells and its specific binding to tPA alone or complexed with uPA/PAI-1 induces vascular permeability in the blood–brain barrier (BBB) or in lung microvasculature, two major sites of BC cell metastatic homing (81, 82). LRP1 controls multiple aspects of endothelial cell metabolism (83) and participates to the control of intercellular junctionality, morphogenesis, and proliferation (81, 84, 85). Interestingly and as stated above, during epithelial-to-mesenchymal transition in breast tumors, LRP1 expression was derepressed through ZEB-1-dependent inhibition of LRP1-targeting miRNAs, thereby contributing to vascular mimicry of breast tumor cells (39). The induction of this endocytic receptor could thus reinforce endothelial interface of breast tumor cells and facilitate their metastatic dissemination.

CLINICAL SIGNIFICANCE OF LRPS AS BIOMARKER IN THE CONTEXT OF BREAST TUMORS

A large-scale study conducted on solid tumors indicates that mostly LDLR mRNA are overexpressed in breast invasive carcinomas with *LRP2* mRNA being the most expressed, but no correlation with patient survival was observed (11). Only a few studies are focused on LRP1 expression in BC patient samples. LRP1 was first immunohistochemically studied in fresh frozen tissue from primary invasive breast carcinomas, ductal *in situ* carcinomas, and auxiliary lymph-node metastases in 1996 (56). LRP1 staining appeared intense in all stromal fibroblasts both outside and within the tumor tissue and scattered in macrophages and mast cells. Interestingly, epithelial cells, endothelial cells, and lymphocytes appeared negative for LRP1. A more recent immunohistochemistry study of LRP1 expression, performed on infiltrating ductal breast carcinomas, brought different results as cytoplasmic LRP1 overexpression was identified in tumor cells in addition to non-neoplastic stromal cells, whereas normal ductal cells were always negative (7). Concerning *LRP1* polymorphism,

although C766T mutation was firstly reported as significantly higher in patients with BC (9), the increased risk of BC development associated to LRP1 polymorphism is not definitely established. Of note, neoadjuvant chemotherapy in BC did not impair LRP1 expression (28).

A BETTER UNDERSTANDING OF LRP FUNCTIONALITIES MAY LEAD TO EFFICIENT THERAPEUTIC STRATEGIES

Therapeutic approaches involving LRPs developed in oncology, particularly in BC, aim to address the endocytic properties of these receptors as vectorization tools. One of the remaining therapeutic concerns for BC patients is related to metastases. Brain metastases occur in about 15–30% of women with stage IV BC. The targeting of the BBB, formed by endothelial cells, astrocytes, and pericytes embedded in the capillary basement membrane, remains critical for treating brain metastases. As LRP1 transports ligands such as β-Amyloid or tPA across the BBB and is expressed at high levels in this tissue (86), it appears as a promising candidate for targeted therapy against metastatic BC cells. In this context, the main therapeutic approaches use the Angiopep-2, an LRP1 binding peptide first identified by Demeule and colleagues (87). Combined with three paclitaxel residues, this molecule (namely, GRN1005, formerly known as ANG1005) binds to LRP1, crosses the BBB, and allows a better drug delivery in the brain compartment (78, 87). Phase I/II clinical trials with ANG1005/GRN1005 show that treatment is safe and brings clinical benefit for both peripheral metastatic BC and brain metastasis, even if the tumor had previously developed resistance to conventional taxanes. Interestingly, an open-label Phase III study will start in 2020 to investigate whether ANG1005 can prolong patient survival in HER2-negative BC patients with newly diagnosed leptomeningeal disease and previously treated brain metastases (NCT03613181). Angiopep-2 can also be useful to target BC cells overexpressing LRP1. For instance, Angiopep-2 was used to decorate nanoparticules combined with doxycycline (Angio-DOX-DGL-GNP) in TNBC to facilitate the drug penetration and accumulation in BC cells (88).

The endocytic properties of LRP2 have also been used to improve the effectiveness of anticancer drugs in resistant BC cells (89). In this context, lipid-polyethylenimine hybrid nanocarriers decorated with apolipoprotein E (Ap-LPN) were developed for improving siRNA delivery against clusterin in MCF7 BC cells, leading to increased cell chemosensitization toward paclitaxel.

Another strategy of tumor targeting was used with the NT4 peptide, a tetrabranched peptide from the human neurotensin, capable of binding LRP1 and LRP6 by mimicking ApoE and midkine heparin binding site (90). Depau and collaborators showed that methotrexate conjugated with NT4 can overcome drug resistance in methotrexate-resistant human BC cells (91). NT4 conjugated with other drugs (NT4-paclitaxel, NT4-5FdU) were tested in various animal models of human cancer, including an orthotopic mouse model of human BC, leading to improved drug activity as compared to unconjugated counterpart (92–94).

More recently, some LRPs have been identified as direct molecular targets for BC. LRP6 is probably the most promising target in the TNBC with its overexpression leading to Wnt signaling pathway activation together with tumorigenesis promotion (5). Several drugs such as salinomycin, prodigiosin, and niclosamide indeed induce LRP6 phosphorylation and degradation leading to decreased tumor growth (49, 50, 95). Ren and collaborators have suggested that soluble LRP6 ectodomain could also be used as an innovative anti-metastatic drug (54).

CONCLUSION AND SUBJECTIVE POINTS OF VIEW

Receptors from the LDLR family are increasingly emerging as key relevant biomarkers in oncology and potential therapeutic targets. Their multiple implications within the TME, variable expression related to tumor stages, together with molecular versatility, constitute the main challenges to better understand their functionalities. In breast cancer, scientific evidence is fragmented, sometimes contradictory, and only a few clinical data are available. Potential prognostic value of these receptors is still unclear, thus preventing from demonstrating clinical benefits. Additional studies will be necessary to establish a link between LRPs and some events promoting obesity or metabolic diseases, particularly to improve the treatment of BC in post-menopausal patients. LRP1 is likely to be the most promising receptor because it constitutes an efficient drug carrier within tumor cells. Very promising trials are ongoing in HER2-negative BC patients with metastasis. In addition, LRP1 could also be considered as an attractive therapeutic target in TNBC. However, its high molecular weight, intricate regulation, and sub-cellular localization together with its ability to bind multiple extracellular ligands within the same clusters, make current research extremely complex and can lead to contradictory conclusions. The use of more advanced *in vitro* multi-cellular and 3D tumor-based systems (tumoroïds) with patient-derived cells will be key to deeper understand the functionality of this receptor. In the coming years and in order to consider LRP1 as an innovative vectorization tool, the approach should be focused on the endocytic properties of overexpressed LRP1 rather than on the modulation (e.g., inhibition or reduction) of LRP1 expression.

AUTHOR CONTRIBUTIONS

All authors listed have made a substantial, direct and intellectual contribution to the work, and approved it for publication.

ACKNOWLEDGMENTS

We acknowledge Arlette Thomachot and Dr. Laetitia Devy for editorial assistance.

REFERENCES

1. Cedo L, Reddy ST, Mato E, Blanco-Vaca F, Escola-Gil JC. HDL and lDL: potential new players in breast cancer development. *J Clin Med.* (2019) 8:853. doi: 10.3390/jcm8060853
2. Gallagher EJ, Zelenko Z, Neel BA, Antoniou IM, Rajan L, Kase N, et al. Elevated tumor lDLR expression accelerates lDL cholesterol-mediated breast cancer growth in mouse models of hyperlipidemia. *Oncogene.* (2017) 36:6462–6471. doi: 10.1038/onc.2017.247
3. He L, Lu Y, Wang P, Zhang J, Yin C, Qu S. Up-regulated expression of type iI very low density lipoprotein receptor correlates with cancer metastasis and has a potential link to β-catenin in different cancers. *BMC cancer.* (2010) 10:601. doi: 10.1186/1471-2407-10-601
4. He L, Lu Y, Guo J. Type iI vLDLR promotes cell migration by up-regulation of vEGF, mMP2 and mMP7 in breast cancer cells. *Chin Germ J Clin Oncol.* (2013) 12:374–8. doi: 10.1007/s10330-013-1218-7
5. Roslan Z, Muhamad M, Selvaratnam L, Ab-Rahim S. The roles of low-Density lipoprotein receptor-Related proteins 5, 6, and 8 in cancer: a Review. *J Oncol.* (2019) 2019:4536302. doi: 10.1155/2019/4536302
6. Arun B, Bayraktar S, Shiang C, Qi Y, Wang B, Angelica GB, et al. High throughput siRNA screen identifies LRP8 as druggable metabolic regulator in TripleNegative breast cancer. *SM J Hematol Oncol.* (2016) 1:1003.
7. Catasus L, Gallardo A, Llorente-Cortes V, Escuin D, Munoz J, Tibau A, et al. Low-density lipoprotein receptor-related protein 1 is associated with proliferation and invasiveness in her-2/neu and triple-negative breast carcinomas. *Hum Pathol.* (2011) 42:1581–8. doi: 10.1016/j.humpath.2011.01.011
8. Berquand A, Meunier M, Thevenard-Devy J, Ivaldi C, Campion O, Dedieu S, et al. A gentle approach to investigate the influence of lRP-1 silencing on the migratory behavior of breast cancer cells by atomic force microscopy and dynamic cell studies. *Nanomedicine.* (2019) 18:359–70. doi: 10.1016/j.nano.2018.10.012
9. Benes P, Jurajda M, Zaloudik J, Izakovicova-Holla L, Vacha J. C766T low-density lipoprotein receptor-related protein 1 (LRP1) gene polymorphism and susceptibility to breast cancer. *Breast Cancer Res.* (2003) 5:R77–81. doi: 10.1186/bcr591
10. Asano Y, Takeuchi T, Okubo H, Saigo C, Kito Y, Iwata Y, et al. Nuclear localization of lDL receptor-related protein 1B in mammary gland carcinogenesis. *J Mol Med (Berl).* (2019) 97:257–68. doi: 10.1007/s00109-018-01732-2
11. Gonias SL, Karimi-Mostowfi N, Murray SS, Mantuano E, Gilder AS. Expression of lDL receptor-related proteins (LRPs) in common solid malignancies correlates with patient survival. *PLoS ONE.* (2017) 12:e0186649. doi: 10.1371/journal.pone.0186649
12. Wang Y, Guo L, Feng L, Zhang W, Xiao T, Di X, et al. Single nucleotide variant profiles of viable single circulating tumour cells reveal cTC behaviours in breast cancer. *Oncol Rep.* (2018) 39:2147–2159. doi: 10.3892/or.2018.6325
13. Chlon TM, Taffany DA, Welsh J, Rowling MJ. Retinoids modulate expression of the endocytic partners megalin, cubilin, and disabled-2 and uptake of vitamin d-binding protein in human mammary cells. *J Nutr.* (2008) 138:1323–8. doi: 10.1093/jn/138.7.1323
14. Lindvall C, Zylstra CR, Evans N, West RA, Dykema K, Furge KA, et al. The wnt co-receptor lrp6 is required for normal mouse mammary gland development. *PLoS ONE.* (2009) 4:e5813. doi: 10.1371/journal.pone.0005813
15. Maubant S, Tahtouh T, Brisson A, Maire V, Némati F, Tesson B, et al. LRP5 regulates the expression of sTK40, a new potential target in triple-negative breast cancers. *Oncotarget.* (2018) 9:22586. doi: 10.18632/oncotarget.25187
16. Chin EN, Martin JA, Kim S, Fakhraldeen SA, Alexander CM. Lrp5 has a wnt-Independent role in glucose uptake and growth for mammary epithelial cells. *Mol Cell Biol.* (2015) 36:871–85. doi: 10.1128/MCB.00800-15
17. Ibrahim SA, Hassan H, Vilardo L, Kumar SK, Kumar AV, Kelsch R, et al. Syndecan-1 (CD138) modulates triple-negative breast cancer stem cell properties via regulation of lRP-6 and iL-6-mediated sTAT3 signaling. *PLoS ONE.* (2013) 8:e85737. doi: 10.1371/journal.pone.0085737
18. Lin CC, Lo MC, Moody R, Jiang H, Harouaka R, Stevers N, et al. Targeting lRP8 inhibits breast cancer stem cells in triple-negative breast cancer. *Cancer Lett.* (2018) 438:165–73. doi: 10.1016/j.canlet.2018.09.022
19. Maire V, Mahmood F, Rigaill G, Ye M, Brisson A, Nemati F, et al. LRP8 is overexpressed in estrogen-negative breast cancers and a potential target for these tumors. *Cancer Med.* (2019) 8:325–36. doi: 10.1002/cam4.1923
20. Pietila M, Sahgal P, Peuhu E, Jantti NZ, Paatero I, Narva E, et al. SORLA regulates endosomal trafficking and oncogenic fitness of hER2. *Nat Commun.* (2019) 10:2340. doi: 10.1038/s41467-019-10275-0
21. Berman AT, Thukral AD, Hwang WT, Solin LJ, Vapiwala N. Incidence and patterns of distant metastases for patients with early-stage breast cancer after breast conservation treatment. *Clin Breast Cancer.* (2013) 13:88–94. doi: 10.1016/j.clbc.2012.11.001
22. Liu J, Xu A, Lam KS, Wong NS, Chen J, Shepherd PR, et al. Cholesterol-induced mammary tumorigenesis is enhanced by adiponectin deficiency: role of lDL receptor upregulation. *Oncotarget.* (2013) 4:1804–18. doi: 10.18632/oncotarget.1364
23. Lee K, Kruper L, Dieli-Conwright CM, Mortimer JE. The impact of obesity on breast cancer diagnosis and treatment. *Curr Oncol Rep.* (2019) 21:41. doi: 10.1007/s11912-019-0787-1
24. Li X, Liu ZL, Wu YT, Wu H, Dai W, Arshad B, et al. Status of lipid and lipoprotein in female breast cancer patients at initial diagnosis and during chemotherapy. *Lipids Health Dis.* (2018) 17:91. doi: 10.1186/s12944-018-0745-1
25. Wolfe AR, Atkinson RL, Reddy JP, Debeb BG, Larson R, Li L, et al. High-density and very-low-density lipoprotein have opposing roles in regulating tumor-initiating cells and sensitivity to radiation in inflammatory breast cancer. *Int J Radi Oncol.* (2015) 91:1072–80. doi: 10.1016/j.ijrobp.2014.12.039
26. Guan X, Liu Z, Zhao Z, Zhang X, Tao S, Yuan B, et al. Emerging roles of low-density lipoprotein in the development and treatment of breast cancer. *Lipids Health Dis.* (2019) 18:137. doi: 10.1186/s12944-019-1075-7
27. de Gonzalo-Calvo D, Lopez-Vilaro L, Nasarre L, Perez-Olabarria M, Vazquez T, Escuin D, et al. Intratumor cholesteryl ester accumulation is associated with human breast cancer proliferation and aggressive potential: a molecular and clinicopathological study. *BMC Cancer.* (2015) 15:460. doi: 10.1186/s12885-015-1469-5
28. Pires LA, Hegg R, Freitas FR, Tavares ER, Almeida CP, Baracat EC, et al. Effect of neoadjuvant chemotherapy on low-density lipoprotein (LDL) receptor and lDL receptor-related protein 1 (LRP-1) receptor in locally advanced breast cancer. *Braz J Med Biol Res.* (2012) 45:557–64. doi: 10.1590/S0100-879X2012007500068
29. dos Santos CR, Domingues G, Matias I, Matos J, Fonseca I, de Almeida JM, et al. LDL-cholesterol signaling induces breast cancer proliferation and invasion. *Lipids Health Dis.* (2014) 13:16. doi: 10.1186/1476-511X-13-16
30. Torres CG, Ramirez ME, Cruz P, Epunan MJ, Valladares LE, SierraltaWD. 27-hydroxycholesterol induces the transition of MCF7 cells into a mesenchymal phenotype. *Oncol Rep.* (2011) 26:389–97. doi: 10.3892/or.2011.1284
31. Cruz P, Torres C, Ramirez ME, Epunan MJ, Valladares LE, Sierralta WD. Proliferation of human mammary cancer cells exposed to 27-hydroxycholesterol. *Exp Ther Med.* (2010) 1:531–6. doi: 10.3892/etm_00000084
32. Liu CX, Li Y, Obermoeller-McCormick LM, Schwartz AL, Bu G. The putative tumor suppressor lRP1B, a novel member of the low density lipoprotein (LDL) receptor family, exhibits both overlapping and distinct properties with the lDL receptor-related protein. *J Biol Chem.* (2001) 276:28889–96. doi: 10.1074/jbc.M102727200
33. Cabezas F, Farfan P, Marzolo MP. Participation of the sMAD2/3 signalling pathway in the down regulation of megalin/LRP2 by transforming growth factor beta (TGF-ss1). *PLoS One.* (2019) 14:e0213127. doi: 10.1371/journal.pone.0213127
34. Knisely JM, Li Y, Griffith JM, Geuze HJ, Schwartz AL, Bu G. Slow endocytosis of the lDL receptor-related protein 1B: implications for a novel cytoplasmic tail conformation. *Exp Cell Res.* (2007) 313:3298–307. doi: 10.1016/j.yexcr.2007.05.026
35. Chen H, Chong W, Wu Q, Yao Y, Mao M, Wang X. Association of lRP1B mutation with tumor mutation burden and outcomes in melanoma and non-small cell lung cancer patients treated with immune check-Point blockades. *Front Immunol.* (2019) 10:1113. doi: 10.3389/fimmu.2019.01523
36. Dedieu S, Langlois B. LRP-1: a new modulator of cytoskeleton dynamics and adhesive complex turnover in cancer cells. *Cell Adh Migr.* (2008) 2:77–80. doi: 10.4161/cam.2.2.6374

37. Kang HS, Kim J, Lee HJ, Kwon BM, Lee DK, Hong SH. LRP1-dependent pepsin clearance induced by 2'-hydroxycinnamaldehyde attenuates breast cancer cell invasion. *Int J Biochem Cell Biol.* (2014) 53:15–23. doi: 10.1016/j.biocel.2014.04.021
38. Fayard B, Bianchi F, Dey J, Moreno E, Djaffer S, Hynes NE, et al. The serine protease inhibitor protease nexin-1 controls mammary cancer metastasis through lRP-1-mediated mMP-9 expression. *Cancer Res.* (2009) 69:5690–8. doi: 10.1158/0008-5472.CAN-08-4573
39. Langer EM, Kendsersky ND, Daniel CJ, Kuziel GM, Pelz C, Murphy KM, et al. ZEB1-repressed microRNAs inhibit autocrine signaling that promotes vascular mimicry of breast cancer cells. *Oncogene.* (2018) 37:1005–019. doi: 10.1038/onc.2017.356
40. Boel NM, Hunter MC, Edkins AL. LRP1 is required for novobiocin-mediated fibronectin turnover. *Sci Rep.* (2018) 8:11438. doi: 10.1038/s41598-018-29531-2
41. Dong H, Zou M, Bhatia A, Jayaprakash P, Hofman F, Ying Q, et al. Breast cancer mDA-MB-231 cells use secreted heat shock protein-90alpha (Hsp90alpha) to survive a hostile hypoxic environment. *Sci Rep.* (2016) 6:20605. doi: 10.1038/srep20605
42. Sahu D, Zhao Z, Tsen F, Cheng CF, Park R, Situ AJ, et al. A potentially common peptide target in secreted heat shock protein-90alpha for hypoxia-inducible factor-1alpha-positive tumors. *Mol Biol Cell.* (2012) 23:602–13. doi: 10.1091/mbc.e11-06-0575
43. Tian Y, Wang C, Chen S, Liu J, Fu Y, Luo Y. Extracellular hsp90alpha and clusterin synergistically promote breast cancer epithelial-to-mesenchymal transition and metastasis via lRP1. *J Cell Sci.* (2019) 132:228213. doi: 10.1242/jcs.228213
44. Yang L, Wu X, Wang Y, Zhang K, Wu J, Yuan YC, et al. FZD7 has a critical role in cell proliferation in triple negative breast cancer. *Oncogene.* (2011) 30:4437–46. doi: 10.1038/onc.2011.145
45. Suzuki H, Toyota M, Carraway H, Gabrielson E, Ohmura T, Fujikane T, et al. Frequent epigenetic inactivation of wnt antagonist genes in breast cancer. *Br J Cancer.* (2008) 98:1147–56. doi: 10.1038/sj.bjc.6604259
46. DiMeo TA, Anderson K, Phadke P, Fan C, Perou CM, Naber S, et al. A novel lung metastasis signature links wnt signaling with cancer cell self-renewal and epithelial-mesenchymal transition in basal-like breast cancer. *Cancer Res.* (2009) 69:5364–73. doi: 10.1158/0008-5472.CAN-08-4135
47. Ma J, Lu W, Chen D, Xu B, Li Y. Role of wnt co-Receptor lRP6 in triple negative breast cancer cell migration and invasion. *J Cell Biochem.* (2017) 118:2968–76. doi: 10.1002/jcb.25956
48. Gangrade A, Pathak V, Augelli-Szafran CE, Wei HX, Oliver P, Suto M, et al. Preferential inhibition of wnt/beta-Catenin signaling by novel benzimidazole compounds in triple-negative breast cancer. *Int J Mol Sci.* (2018) 19:1524. doi: 10.3390/ijms19051524
49. Wang Z, Li B, Zhou L, Yu S, Su Z, Song J, et al. Prodigiosin inhibits wnt/beta-catenin signaling and exerts anticancer activity in breast cancer cells. *Proc Natl Acad Sci USA.* (2016) 113:13150–5. doi: 10.1073/pnas.1616336113
50. Lu W, Li Y. Salinomycin suppresses lRP6 expression and inhibits both wnt/beta-catenin and mTORC1 signaling in breast and prostate cancer cells. *J Cell Biochem.* (2014) 115:1799–807. doi: 10.1002/jcb.24850
51. Zhang J, Yang Z, Li P, Bledsoe G, Chao L, Chao J. Kallistatin antagonizes wnt/beta-catenin signaling and cancer cell motility via binding to low-density lipoprotein receptor-related protein 6. *Mol Cell Biochem.* (2013) 379:295–301. doi: 10.1007/s11010-013-1654-2
52. Lu W, Lin C, Li Y. Rottlerin induces wnt co-receptor lRP6 degradation and suppresses both wnt/beta-catenin and mTORC1 signaling in prostate and breast cancer cells. *Cell Signal.* (2014) 26:1303–9. doi: 10.1016/j.cellsig.2014.02.018
53. Badana AK, Chintala M, Gavara MM, Naik S, Kumari S, Kappala VR, et al. Lipid rafts disruption induces apoptosis by attenuating expression of lRP6 and survivin in triple negative breast cancer. *Biomed Pharmacother.* (2018) 97:359–68. doi: 10.1016/j.biopha.2017.10.045
54. Ren DN, Chen J, Li Z, Yan H, Yin Y, Wo D, et al. LRP5/6 directly bind to frizzled and prevent frizzled-regulated tumour metastasis. *Nat Commun.* (2015) 6:6906. doi: 10.1038/ncomms7906
55. Soysal SD, Tzankov A, Muenst SE. Role of the tumor microenvironment in breast cancer. *Pathobiology.* (2015) 82:142–52. doi: 10.1159/000430499
56. Christensen L, Wiborg Simonsen AC, Heegaard CW, Moestrup SK, Andersen JA, Andreasen PA. Immunohistochemical localization of urokinase-type plasminogen activator, type-1 plasminogen-activator inhibitor, urokinase receptor and alpha(2)-macroglobulin receptor in human breast carcinomas. *Int J Cancer.* (1996) 66:441–52. doi: 10.1002/(SICI)1097-0215(19960516)66:4<441::AID-IJC6>3.0.CO;2-W
57. Newton CS, Loukinova E, Mikhailenko I, Ranganathan S, Gao Y, Haudenschild C, et al. Platelet-derived growth factor receptor-beta (PDGFR-beta) activation promotes its association with the low density lipoprotein receptor-related protein (LRP). Evidence for co-receptor function. *J Biol Chem.* (2005) 280:27872–8. doi: 10.1074/jbc.M505410200
58. Yang M, Huang H, Li J, Li D, Wang H. Tyrosine phosphorylation of the lDL receptor-related protein (LRP) and activation of the eRK pathway are required for connective tissue growth factor to potentiate myofibroblast differentiation. *FASEB J.* (2004) 18:1920–1. doi: 10.1096/fj.04-2357fje
59. Muratoglu SC, Mikhailenko I, Newton C, Migliorini M, Strickland DK. Low density lipoprotein receptor-related protein 1 (LRP1) forms a signaling complex with platelet-derived growth factor receptor-beta in endosomes and regulates activation of the mAPK pathway. *J Biol Chem.* (2010) 285:14308–17. doi: 10.1074/jbc.M109.046672
60. Schnieder J, Mamazhakypov A, Birnhuber A, Wilhelm J, Kwapiszewska G, Ruppert C, et al. Loss of lRP1 promotes acquisition of contractile-myofibroblast phenotype and release of active tGF-beta1 from eCM stores. *Matrix Biol.* (2020) 88:69–88. doi: 10.1016/j.matbio.2019.12.001
61. Hu K, Wu C, Mars WM, Liu Y. Tissue-type plasminogen activator promotes murine myofibroblast activation through lDL receptor-related protein 1-mediated integrin signaling. *J Clin Invest.* (2007) 117:3821–32. doi: 10.1172/JCI32301
62. Ren S, Johnson BG, Kida Y, Ip C, Davidson KC, Lin SL, et al. LRP-6 is a coreceptor for multiple fibrogenic signaling pathways in pericytes and myofibroblasts that are inhibited by dKK-1. *Proc Natl Acad Sci USA.* (2013) 110:1440–5. doi: 10.1073/pnas.1211179110
63. Avgustinova A, Iravani M, Robertson D, Fearns A, Gao Q, Klingbeil P, et al. Tumour cell-derived wnt7a recruits and activates fibroblasts to promote tumour aggressiveness. *Nat Commun.* (2016) 7:10305. doi: 10.1038/ncomms10305
64. Ferrari N, Ranftl R, Chicherova I, Slaven ND, Moeendarbary E, Farrugia AJ, et al. Dickkopf-3 links hSF1 and yAP/TAZ signalling to control aggressive behaviours in cancer-associated fibroblasts. *Nat Commun.* (2019) 10:130. doi: 10.1038/s41467-018-07987-0
65. Derocq D, Prebois C, Beaujouin M, Laurent-Matha V, Pattingre S, Smith GK, et al. Cathepsin d is partly endocytosed by the lRP1 receptor and inhibits lRP1-regulated intramembrane proteolysis. *Oncogene.* (2012) 31:3202–12. doi: 10.1038/onc.2011.501
66. Choi J, Cha YJ, Koo JS. Adipocyte biology in breast cancer: from silent bystander to active facilitator. *Prog Lipid Res.* (2018) 69:11–20. doi: 10.1016/j.plipres.2017.11.002
67. Masson O, Chavey C, Dray C, Meulle A, Daviaud D, Quilliot D, et al. LRP1 receptor controls adipogenesis and is up-regulated in human and mouse obese adipose tissue. *PLoS ONE.* (2009) 4:e7422. doi: 10.1371/journal.pone.0007422
68. Jedrychowski MP, Gartner CA, Gygi SP, Zhou L, Herz J, Kandror KV, et al. Proteomic analysis of gLUT4 storage vesicles reveals lRP1 to be an important vesicle component and target of insulin signaling. *J Biol Chem.* (2010) 285:104–14. doi: 10.1074/jbc.M109.040428
69. Actis Dato V, Chiabrando GA. The role of low-density lipoprotein receptor-related protein 1 in lipid metabolism, glucose homeostasis and inflammation. *Int J Mol Sci.* (2018) 19:1780. doi: 10.3390/ijms19061780
70. El Asmar A, El Rassi Z. Hepatoblastoma in childhood, long term survival achieved: 2 case reports and literature review. *Int J Surg Case Rep.* (2016) 21:55–8. doi: 10.1016/j.ijscr.2016.02.019
71. Zheng XY, Yu BL, Xie YF, Zhao SP, Wu CL. Apolipoprotein a5 regulates intracellular triglyceride metabolism in adipocytes. *Mol Med Rep.* (2017) 16:6771–9. doi: 10.3892/mmr.2017.7461
72. Pawaria S, Binder RJ. CD91-dependent programming of t-helper cell responses following heat shock protein immunization. *Nat Commun.* (2011) 2:521. doi: 10.1038/ncomms1524

73. Mantuano E, Brifault C, Lam MS, Azmoon P, Gilder AS, Gonias SL. LDL receptor-related protein-1 regulates nFkappaB and microRNA-155 in macrophages to control the inflammatory response. *Proc Natl Acad Sci USA*. (2016) 113:1369–74. doi: 10.1073/pnas.1515480113
74. Gorovoy M, Gaultier A, Campana WM, Firestein GS, Gonias SL. Inflammatory mediators promote production of shed lRP1/CD91, which regulates cell signaling and cytokine expression by macrophages. *J Leukoc Biol.* (2010) 88:769–78. doi: 10.1189/jlb.0410220
75. Staudt ND, Jo M, Hu J, Bristow JM, Pizzo DP, Gaultier A, et al. Myeloid cell receptor lRP1/CD91 regulates monocyte recruitment and angiogenesis in tumors. *Cancer Res.* (2013) 73:3902–12. doi: 10.1158/0008-5472.CAN-12-4233
76. Njah K, Chakraborty S, Qiu B, Arumugam S, Raju A, Pobbati AV, et al. A role of agrin in maintaining the stability of vascular endothelial growth factor receptor-2 during tumor angiogenesis. *Cell Rep.* (2019) 28:949–65 e7. doi: 10.1016/j.celrep.2019.06.036
77. Pencheva N, Tran H, Buss C, Huh D, Drobnjak M, Busam K, et al. Convergent multi-miRNA targeting of apoE drives lRP1/LRP8-dependent melanoma metastasis and angiogenesis. *Cell.* (2012) 151:1068–82. doi: 10.1016/j.cell.2012.10.028
78. Li F, Tang SC. Targeting metastatic breast cancer with aNG1005, a novel peptide-paclitaxel conjugate that crosses the blood-brain-barrier (BBB). *Genes Dis.* (2017) 4:1–3. doi: 10.1016/j.gendis.2017.01.004
79. Lu CW, Lo YH, Chen CH, Lin CY, Tsai CH, Chen PJ, et al. VLDL and lDL, but not hDL, promote breast cancer cell proliferation, metastasis and angiogenesis. *Cancer Lett.* (2017) 388:130–8. doi: 10.1016/j.canlet.2016.11.033
80. Min JK, Park H, Choi HJ, Kim Y, Pyun BJ, Agrawal V, et al. The wNT antagonist dickkopf2 promotes angiogenesis in rodent and human endothelial cells. *J Clin Invest.* (2011) 121:1882–93. doi: 10.1172/JCI42556
81. Makarova AM, Lebedeva TV, Nassar T, Higazi AA, Xue J, Carinato ME, et al. Urokinase-type plasminogen activator (uPA) induces pulmonary microvascular endothelial permeability through low density lipoprotein receptor-related protein (LRP)-dependent activation of endothelial nitric-oxide synthase. *J Biol Chem.* (2011) 286:23044–53. doi: 10.1074/jbc.M110.210195
82. Wang X, Lee SR, Arai K, Lee SR, Tsuji K, Rebeck GW, et al. Lipoprotein receptor-mediated induction of matrix metalloproteinase by tissue plasminogen activator. *Nat Med.* (2003) 9:1313–7. doi: 10.1038/nm926
83. Mao H, Xie L, Pi X. Low-Density lipoprotein receptor-Related protein-1 signaling in angiogenesis. *Front Cardiovasc Med.* (2017) 4:34. doi: 10.3389/fcvm.2017.00034
84. Mao H, Lockyer P, Townley-Tilson WH, Xie L, Pi X. LRP1 regulates retinal angiogenesis by inhibiting pARP-1 activity and endothelial cell proliferation. *Arterioscler Thromb Vasc Biol.* (2016) 36:350–60. doi: 10.1161/ATVBAHA.115.306713
85. Vezina A, Charfi C, Zgheib A, Annabi B. Cerebrovascular angiogenic reprogramming upon lRP1 repression: impact on sphingosine-1-Phosphate-Mediated signaling in brain endothelial cell chemotactism. *Mol Neurobiol.* (2018) 55:3551–63. doi: 10.1007/s12035-017-0614-3
86. Zhao Y, Li D, Zhao J, Song J, Zhao Y. The role of the low-density lipoprotein receptor-related protein 1 (LRP-1) in regulating blood-brain barrier integrity. *Rev Neurosci.* (2016) 27:623–34. doi: 10.1515/revneuro-2015-0069
87. Thomas FC, Taskar K, Rudraraju V, Goda S, Thorsheim HR, Gaasch JA, et al. Uptake of aNG1005, a novel paclitaxel derivative, through the blood-brain barrier into brain and experimental brain metastases of breast cancer. *Pharm Res.* (2009) 26:2486–94. doi: 10.1007/s11095-009-9964-5
88. Hu G, Chun X, Wang Y, He Q, Gao H. Peptide mediated active targeting and intelligent particle size reduction-mediated enhanced penetrating of fabricated nanoparticles for triple-negative breast cancer treatment. *Oncotarget.* (2015) 6:41258–74. doi: 10.18632/oncotarget.5692
89. Xue HY, Wong HL. Targeting megalin to enhance delivery of anti-clusterin small-interfering rNA nanomedicine to chemo-treated breast cancer. *Eur J Pharm Biopharm.* (2012) 81:24–32. doi: 10.1016/j.ejpb.2012.02.005
90. Falciani C, Brunetti J, Lelli B, Ravenni N, Lozzi L, Depau L, et al. Cancer selectivity of tetrabranched neurotensin peptides is generated by simultaneous binding to sulfated glycosaminoglycans and protein receptors. *J Med Chem.* (2013) 56:5009–18. doi: 10.1021/jm400329p
91. Depau L, Brunetti J, Falciani C, Scali S, Riolo G, Mandarini E, et al. Coupling to a cancer-selective heparan-sulfate-targeted branched peptide can by-pass breast cancer cell resistance to methotrexate. *Oncotarget.* (2017) 8:76141–152. doi: 10.18632/oncotarget.19056
92. Falciani C, Fabbrini M, Pini A, Lozzi L, Lelli B, Pileri S, et al. Synthesis and biological activity of stable branched neurotensin peptides for tumor targeting. *Mol Cancer Ther.* (2007) 6:2441–8. doi: 10.1158/1535-7163.MCT-07-0164
93. Falciani C, Brunetti J, Pagliuca C, Menichetti S, Vitellozzi L, Lelli B, et al. Design and in vitro evaluation of branched peptide conjugates: turning nonspecific cytotoxic drugs into tumor-selective agents. *ChemMedChem.* (2010) 5:567–74. doi: 10.1002/cmdc.200900527
94. Brunetti J, Pillozzi S, Falciani C, Depau L, Tenori E, Scali S, et al. Tumor-selective peptide-carrier delivery of paclitaxel increases in vivo activity of the drug. *Sci Rep.* (2015) 5:17736. doi: 10.1038/srep17736
95. Lu W, Lin C, Roberts MJ, Waud WR, Piazza GA, Li Y. Niclosamide suppresses cancer cell growth by inducing wnt co-receptor lRP6 degradation and inhibiting the wnt/beta-catenin pathway. *PLoS ONE.* (2011) 6:e29290. doi: 10.1371/journal.pone.0029290

Conflict of Interest: The authors declare that the research was conducted in the absence of any commercial or financial relationships that could be construed as a potential conflict of interest.

Copyright © 2020 Campion, Al Khalifa, Langlois, Thevenard-Devy, Salesse, Savary, Schneider, Etique, Dedieu and Devy. This is an open-access article distributed under the terms of the Creative Commons Attribution License (CC BY). The use, distribution or reproduction in other forums is permitted, provided the original author(s) and the copyright owner(s) are credited and that the original publication in this journal is cited, in accordance with accepted academic practice. No use, distribution or reproduction is permitted which does not comply with these terms.

frontiers in Oncology

REVIEW
published: 18 August 2020
doi: 10.3389/fonc.2020.01488

Reciprocal Interplay Between Fibrillar Collagens and Collagen-Binding Integrins: Implications in Cancer Progression and Metastasis

Isabelle Bourgot†, *Irina Primac*†, *Thomas Louis, Agnès Noël and Erik Maquoi**

Laboratory of Tumor and Development Biology, GIGA-Cancer, University of Liège, Liège, Belgium

Cancers are complex ecosystems composed of malignant cells embedded in an intricate microenvironment made of different non-transformed cell types and extracellular matrix (ECM) components. The tumor microenvironment is governed by constantly evolving cell-cell and cell-ECM interactions, which are now recognized as key actors in the genesis, progression and treatment of cancer lesions. The ECM is composed of a multitude of fibrous proteins, matricellular-associated proteins, and proteoglycans. This complex structure plays critical roles in cancer progression: it functions as the scaffold for tissues organization and provides biochemical and biomechanical signals that regulate key cancer hallmarks including cell growth, survival, migration, differentiation, angiogenesis, and immune response. Cells sense the biochemical and mechanical properties of the ECM through specialized transmembrane receptors that include integrins, discoidin domain receptors, and syndecans. Advanced stages of several carcinomas are characterized by a desmoplastic reaction characterized by an extensive deposition of fibrillar collagens in the microenvironment. This compact network of fibrillar collagens promotes cancer progression and metastasis, and is associated with low survival rates for cancer patients. In this review, we highlight how fibrillar collagens and their corresponding integrin receptors are modulated during cancer progression. We describe how the deposition and alignment of collagen fibers influence the tumor microenvironment and how fibrillar collagen-binding integrins expressed by cancer and stromal cells critically contribute in cancer hallmarks.

Keywords: fibrillar collagens, extracellular matrix, integrins, cancer, metastasis

OPEN ACCESS

Edited by:
Serge Roche,
Institut National de la Santé et de la Recherche Médicale (INSERM), France

Reviewed by:
Birgit Leitinger,
Imperial College London, United Kingdom
Olivier Destaing,
INSERM U1209 Institut pour l'Avancée des Biosciences (IAB), France

***Correspondence:**
Erik Maquoi
erik.maquoi@uliege.be

†*These authors share first authorship*

Specialty section:
This article was submitted to Molecular and Cellular Oncology, a section of the journal Frontiers in Oncology

Received: *13 February 2020*
Accepted: *13 July 2020*
Published: *18 August 2020*

Citation:
Bourgot I, Primac I, Louis T, Noël A and Maquoi E (2020) Reciprocal Interplay Between Fibrillar Collagens and Collagen-Binding Integrins: Implications in Cancer Progression and Metastasis. Front. Oncol. 10:1488. doi: 10.3389/fonc.2020.01488

INTRODUCTION

Cancer progression is a highly dynamic process implicating distinct features responsible for tumor growth and metastatic dissemination. These features comprise sustained proliferative signals, evading growth suppression, resisting cell death, stimulating angiogenesis, activating invasion and metastasis, deregulating cell metabolism and avoiding immune destruction (1). These hallmarks are obtained through reciprocal interactions between cellular and non-cellular components of tumors, which define the tumor microenvironment (TME). The critical role of the TME in cancer progression has been initially recognized in 1863 by Virchow, who first described that malignancies occurred at sites of chronic inflammation (2). In 1889, the

"seed and soil" hypothesis was proposed by Paget suggesting that the TME was important for tumor progression (3). Solid tumors are very heterogeneous and resemble a complicated organ whose complexity approaches and may even exceed that of normal healthy tissues (4). These tumors contain a complex mixture of non-cancerous cellular elements including blood and lymphatic vessels, pericytes, cancer-associated fibroblasts (CAFs), mesenchymal cells, immune/inflammatory cells and nervous network. Non-soluble or semi-soluble substances, such as the extracellular matrix (ECM), and soluble substances, such as interstitial fluids, cytokines, chemokines, growth factors, and metabolites constitute the acellular components of the TME (5–7). Physico-chemical parameters including interstitial pressures, oxygen level, and pH/redox potential represent additional critical characteristics of the TME. It is important to note that the TME is relatively abundant in comparison to cancer cells, with a proportional ratio nearly always in favor of the TME. In solid tumors, including breast and pancreatic tumors, the TME constitute up to 90% of the tumor mass (8–10). The TME is also characterized by a compositional and spatial heterogeneity, which varies greatly across tumor types, amongst patients with a given cancer type, and across distinct lesions in a given patient.

The ECM, which provides architectural support and anchorage for the cells, is composed of a complex meshwork of highly cross-linked components, including fibrous proteins, glycoproteins, proteoglycans, and polysaccharides (11–13). The biomechanical and biochemical properties of the ECM regulate cell survival, proliferation, differentiation and motility by ligating specific cell surface receptors including integrins, discoidin receptors and syndecans (14, 15). Besides these signaling properties, the ECM also play essential roles in tissue function by providing a structural and mechanical support for tissue integrity. It also influences the availability of cytokines and growth factors and maintains the hydration of the microenvironment. The structure of the ECM is highly dynamic and continuously remodeled through ECM deposition, degradation, or modification (16). Collagens are the most abundant components of the ECM, however, their structure and composition differ across various tissue types (17, 18). For example, the basement membrane, a well-structured matrix underlining epithelial and endothelial cells and separating them from the interstitial stroma, mainly consists of collagens type IV and VIII, while the interstitial stroma is mostly composed of fibrillar collagens type I, II, and III (19, 20).

Abnormal deposition and crosslinking of fibrillar collagens has serious repercussion on tissue homeostasis. Solid tumor's ECM is typically more rigid than normal tissue as a result of the overexpression of several ECM components, including collagens I, II, III, V, IX, XI, and heparan sulfate proteoglycans as well as ECM-crosslinking enzymes such as lysyl oxidases (21, 22). This accumulation generates a stroma characterized by a dense meshwork of fibrillar proteins (**Figure 1**), which progressively causes tissue stiffening, a hallmark of many cancers, such as breast, pancreatic and prostate cancers (23, 24). Stiffened ECM increases integrin-mediated mechanotransduction related signals, thereby promoting cancer cell survival, proliferation, and invasion (25–27). In epithelial cancers, the transition from an *in situ* to an invasive carcinoma with associated high mortality is characterized by the focal degradation of the basement membrane (28). The breaching of the basement membrane by malignant cells is significantly influenced by the stiffness of the associated interstitial ECM (29). Tumor cell invasion through the basement membrane exposes malignant cells to a completely different microenvironment mostly dominated by the fibrillar collagens of the interstitial stroma (**Figure 1**). This new microenvironment rewires tumor cells by altering gene expression, cell proliferation, apoptosis, migration and survival, thereby directly affecting the hallmarks of cancer (30–33).

In this review, we describe the different fibrillar collagens and highlight how these proteins and their corresponding integrin receptors are modulated during cancer progression. We describe how the deposition and alignment of collagen fibers influence the TME and how integrin binding fibrillar collagen expressed by cancer and stromal cells represent critical players in cancer hallmarks. A brief overview of the different imaging techniques used to visualize and analyze fibrillar collagens is also provided.

COLLAGENS

Collagens, which constitutes up to 30% of the total protein mass in the human body, represent the most abundant proteins in mammals and are characteristic of the metazoan family (34, 35). In the human genome, 44 collagen genes code for polypeptidic chains and are combined in diverse ways to form 28 collagen types, numbered with roman numerals in vertebrates (I–XXVIII) (36, 37).

The term "collagen" is commonly used to refer to homotrimeric and heterotrimeric proteins formed by three polypeptide chains (α-chains). A characteristic feature of all collagens is the presence of a tight right-handed triple helix composed of three polypeptides α-chains forming a functional collagen molecule (**Figure 2**) (36, 39, 40). The triple helix motif can represent up to 96% of the collagen structure (for collagen I) to <10% (collagen XII) (41). Collagen molecules are made up of a tight right-handed helix composed of three α-chains, each of which contains one or more regions characterized by the repeating amino acid motif $(Gly\text{-}X\text{-}Y)_n$, with proline and 4-hydroxyproline amino acids often found at the X and Y positions, respectively (42). The presence of a glycine residue in every third position is required for the assembly into a triple helix. Indeed, the tight packing of the three α-chains near the common axis induces steric constraints on every third amino acid position and only glycine, the smallest amino acid can accommodate without any chain deformation. Consequently, the glycine residues are positioned in the center of the triple helix, where they stabilize the structure (42–44). Some collagen molecules assemble as homotrimers, whereas others assemble as heterotrimers composed of two or three distinct α-chain types. For example, type I collagen contains two identical α1 chains and one α2 chain, $[\alpha1(I)]_2$ α2(I). Each α-chain forms an extended left-handed helix with a pitch of 18 amino acid per turn (45).

All members of the collagen family present diverse supramolecular assemblies in the ECM and the capacity to bind

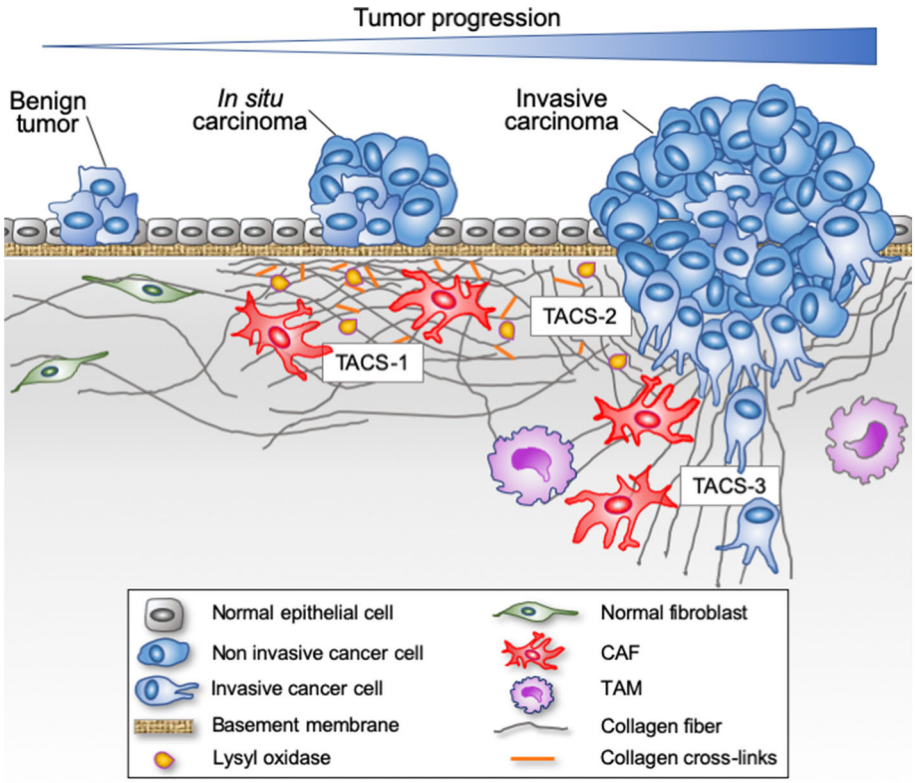

FIGURE 1 | Evolution of fibrillar collagen organization during tumor progression. The transition from a benign tumor to an *in situ* carcinoma is associated with a progressive reorganization of the tumor microenvironment. Epithelial cells are separated from the stroma by a continuous basement membrane. Tumor-derived paracrine signals promote a desmoplasic reaction characterized by the activation of the resident fibroblasts into cancer-associated fibroblasts (CAFs) able to secrete and reorganize the collagen fibers (cross-linking), thereby increasing the stiffness of the stroma. Tumor-associated macrophages (TAMs) are also recruited and contribute to collagen remodeling. When invasive cancer cells have breached the basement membrane, they become confronted with the collagen-rich desmoplasic stroma. The collagen fibers located in the vicinity of the invading cancer cells can be organized parallel to the tumor border (Tumor Associated Collagen Signature—TACS-2) or linearized and oriented perpendicular to the tumor border (TACS-3), thereby promoting the migration of invading cancer cells.

to cell surface receptors or other protein glycosaminoglycans (GAGs) (41). Their size, function and tissue distribution may vary considerably from networks to fibrils. The existence of several α-chains, different supramolecular structures for each collagen type, diverse molecular isoforms as well as the use of alternative promoters and alternative splicing highlight the complexity and diversity of the collagen family (46, 47). Based on this variability, vertebrate collagens have been classified into different families. The most abundant collagen family, with about 90% of the total collagens, is represented by the fibrillar collagens (**Table 1**). In human, the main fibrillar collagens include types I, II and III (major fibrillar collagens), V and XI (minor fibrillar collagens), and the more recently discovered types XXIV and XXVII (49, 50). Fibrillar collagens are characterized by the presence of uninterrupted triple-helical domains of about 300 nm, forming large extracellular fibrils. Type I collagen represents the archetypal fibrillar collagen due to the presence of a trimeric structure and the absence of imperfection in the triple helix. This molecular organization contrasts with that of other collagen families, which present interruptions in the triple helix or do not assemble into fibrils (**Figure 3**). Network-forming collagens and anchoring fibril (ex: type IV and type VII collagens) have extended triple helices (>350 nm) with imperfections in the Gly-X-Y repeat sequences. Types VI, VIII, and X collagen are characterized by the presence of short continuous triple-helical domains. Type VI belongs to beaded filament (51), while types VIII and X form hexagonal networks (40). FACITs (Fibril-Associated Collagens with Interrupted Triple helices) are referred to as fibril-associated molecular bridges. They include collagen IX, XII, XIV, XVI, XIX, XX, XXI, XXII, and XXVI, which are associated to the surface of different collagen fibrils (**Figures 2**, **3**) (40, 52). Collagens type XIII, XVII, XXIII, and XXV represent the MACIT, Membrane-Associated Collagens with Interrupted Triple helices, and function as cell surface molecules with a transmembrane domain. Finally, the multiplexin family (collagens XV and XVIII) is characterized by the presence of multiple triple helix domains interrupted by non-collagenous domains (36).

In this review, we will focus on the fibrillar and fibrillar-associated collagens. For further information on non-fibrillar collagens, the reader is referred to other publications (18, 41, 53, 54).

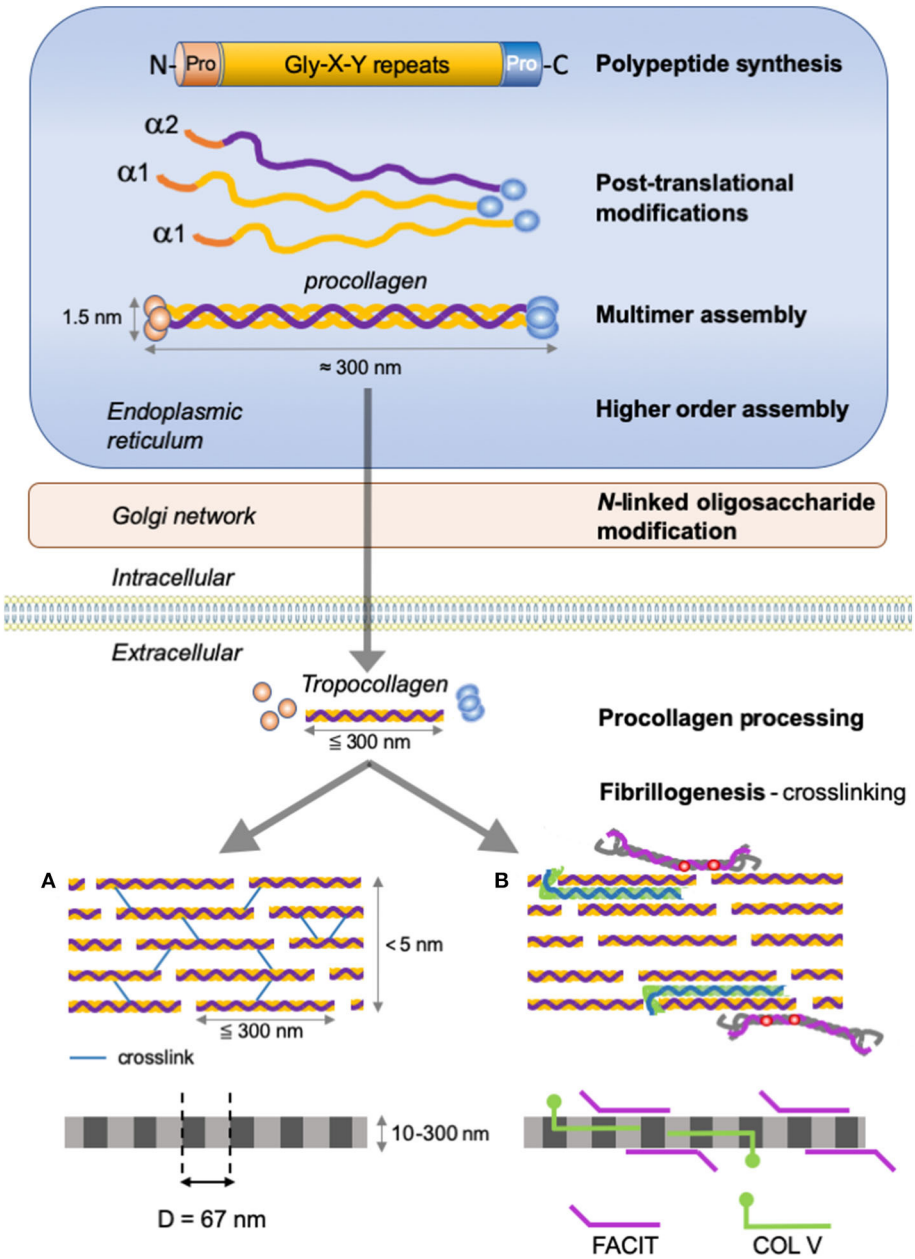

FIGURE 2 | Type I collagen supramolecular assembly pathway. The standard fibrillar collagen molecule is characterized by N- and C-terminal propeptide sequences, which flank a series of Gly-X-Y repeats (where X and Y represent any amino acids but are frequently proline and hydroxyproline). These form the central triple helical structure of procollagen and collagen. Three precursor α-chains (two α1 and one α2) are co-translationally translocated into the endoplasmic reticulum lumen, where specific post-translational modifications occur. Three collagen α-chains associate specifically via their C-terminal domains to form heterotrimers. The helical collagens are trafficked via the Golgi network to the plasma membrane, and secreted into the extracellular space as precursor forms, called procollagens, with N- and C-terminal non-collagenous domains. These domains are removed by the action of specific proteases, and the collagens are assembled into dense fibrils with a characteristic D-periodicity of about 67 nm **(A)**. The fibril is stabilized by covalent lysine- and hydroxylysine-derived crosslinks. In addition to fibrillar collagen, other collagens, such as type V and FACIT collagens, are incorporated into the fibril structure **(B)**. Type V collagen is inserted between strands of the microfibril, and FACIT collagens cling to the surface of the microfibril and work to stabilize higher order structures. Adapted from (38).

FIBRILLAR COLLAGENS

A key characteristic of fibrillar collagens is their ability to assemble and to form highly orientated supramolecular aggregates. Type I collagen represents 90% of the total collagen. It constitutes the major collagen of the skin, tendons, ligaments, cornea, and other interstitial connective tissues. Type I collagen is mostly incorporated into a composite containing either type

TABLE 1 | Molecular chain compositions of human fibrillar and FACIT collagens.

Classes	Type	Molecular composition	Remarks
Fibrillar collagen	I	$[1\alpha(I)]_2\alpha2(I)$	Fibrils composed of uninterrupted triple helical domains that are primarily found in skin, bone, tendons and ligaments, cartilage, cornea
	II	$[\alpha1(II)]_3$	
	III	$[\alpha1(III)]_3$	
	V	$[\alpha1(V)]_2$, α2(V); $[\alpha1(V)]_3$; α1(XI)α2(V)α3(XI)	
	XI	α1(XI)α2(XI)α3(XI)	
	XXIV	$[\alpha1(XXIV)]_3$	
	XXVII	$[\alpha1(XXVII)]_3$	
FACIT collagen	IX	[α1(IX), α2(IX), α3(IX)]	Fibril-associated collagens with interrupted triple helices: forming molecular bridges to the surface of collagen fibrils (e.g., IX, XII, XIV, XVI, XIX, XX, XXI)
	XII	$[\alpha1(XII)]_3$	
	XIV	$[\alpha1(XIV)]_3$	
	XVI	$[\alpha1(XVI)]_3$	
	XIX	$[\alpha1(XIX)]_3$	
	XX	$[\alpha1(XX)]_3$	
	XXI	$[\alpha1(XXI)]_3$	
	XXII	$[\alpha1(XXII)]_3$	

Adapted from (41, 48).

III collagen in skin and reticular fibers (55) or type V collagen in bone (56). The biomechanical properties of these composites (e.g., torsional stability, tensile strength, torsional stiffness) ensure the stability and integrity of these tissues (57, 58). The production of fibrillar collagens requires several intracellular and extracellular post-translational steps, which lead to the formation of elongated, cable-like striated fibril structures that are capable of withstanding tensile forces. This illustrates the close relationship between the three-dimensional protein structure and the role of the resultant ECM.

BIOSYNTHESIS AND ARRANGEMENT IN SUPERSTRUCTURE

Collagen biosynthesis is a complex multistep process starting with the synthesis of long α-chains precursors called *procollagens* (**Figure 2**). The growing peptide chains are co-translationally transported into the rough endoplasmic reticulum where multiple co- and post-translational modifications take place prior to the formation of the triple-helical procollagen.

The fibrillar collagen precursor is synthetized as a multidomain precursor constituted by a long triple helical COL1 domain (about 300 nm in length) flanked by two non-collagenous domains: a specific trimeric C-terminal NC1 domain (C-telopeptide and a C-propeptide) and a N-terminal NC2 domain (a short, non-helical, N-telopeptide and an N-terminal propeptide) (**Figure 2**). These non-collagenous domains represent important structural components: the C-propeptide plays an essential function in the initiation of triple helix formation and the N-propeptide is implicated in the regulation of primary fibril diameters (38).

Extensive post-translational modifications, including hydroxylation of proline and lysine residues, glycosylation of lysine and hydroxylysine residues, occur prior to the formation of the triple helix (36). These modifications are stopped by the formation of the triple helix. Hydroxylation of proline and lysine residues are catalyzed by prolyl 3-hydroxylase, collagen prolyl 4-hydroxylase (C-P4Hs), and lysyl hydroxylase, respectively. These proline and hydroxyproline amino acids can comprise up to 20% of the molecule. Prolyl hydroxylation (in Y position) is essential for intramolecular hydrogen bonding and to increase the thermal stability of the triple helix. In fibril forming collagens ∼50% of prolines are 4-hydroxylated; the extent of these hydroxylations varies between tissues and collagen types (59). Finally, glucosyl and galactosyl residues are added to the hydroxyl groups of hydroxylysine residues by the hydroxylysyl galactosyltransferase and galactosylhydroxylysyl-glucosyltransferase, respectively. Thus, the three α-chains are maintained together by intramolecular hydrogen bonds (high proline and 4-hydroxyproline content-dependent) and electrostatic interactions involving lysine and aspartate (42, 60–62). Highly ordered hydration networks surround the triple helices allowing a close packaging along the central axis of the molecule. Following hydroxylation and glycosylation processes, C-propeptide domains have an essential function (as nucleus) in the initiation and folding of the triple helix (43, 44, 63, 64). These domains allow the proper selection and alignment of collagen α-chains via intrachain disulfide bonds between the C-terminal propeptides of three procollagens sequences. The central portions of the chains zipper from C- to N-terminus to form the triple helix (65).

Many chaperone proteins including the heat shock protein 47 (HSP47) may influence and guide the formation of the triple helix during procollagen assembly (66). The binding of HSP47 enables the effective assembly and folding of the procollagen chains and facilitates the stabilization of procollagen triple helix at body temperature.

Once assembled in the endoplasmic reticulum, procollagen molecules are packaged in the Golgi for export into the ECM. Once released in the extracellular space, the procollagen is cleaved to form the mature triple-helical collagen or tropocollagen. Cleavage of N- and C-propeptides allows spontaneous fibrillogenesis in the extracellular environment. During or following exocytosis, extracellular proteinases, the procollagen N-proteinases (identified as the ADAMTS-2, -3, -14) and procollagen C-proteinases (identified as the BMP-1/tolloid proteinases) remove the N- and C-terminal propeptides (67–74). The removal of these propeptides exposes the telopeptides (short non-triple helical extensions of the polypeptide chains), which become binding sites for further covalent crosslinking during fibrillogenesis (75). The complete removal of the propeptides from collagen I, II and III fibrils allows fibrillogenesis in the extracellular space (76). In some cases, propeptides terminal-ends remain attached or partially attached, thereby affecting the solubility of the procollagen in the extracellular space, inhibiting premature fibril assembly or influencing fibril shape and diameter. For example, the uncleaved N-propeptides of collagen type V and XI influence fibril growth by sterically limiting lateral molecule addition (77).

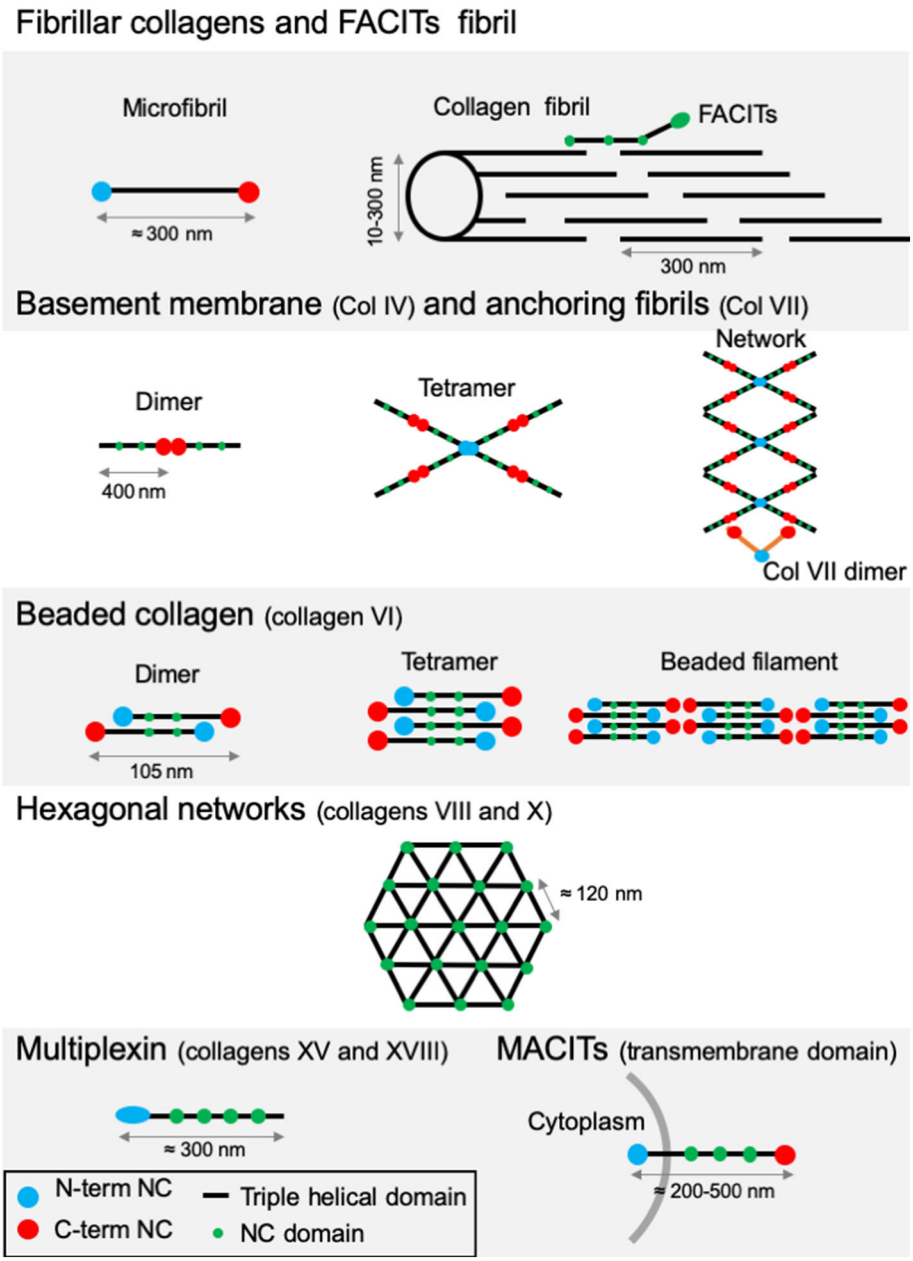

FIGURE 3 | Supramolecular structures formed by some archetypal collagens. *Fibrillar collagens and FACITs fibrils*: the association of mature protomers together leads to the formation of microfibrils which in turn assemble into fibrils. FACITs protomers attach at the surface of fibers with the C-terminal part protruding and regulate fibrillogenesis. *Basement membrane and anchoring fibrils*: formation of type IV collagen dimer occurs by the association of two protomers through their globular NC C-terminal domain. Dimers interact together through their N-terminal domains to constitute tetramers. Networks are the result of the two first steps linked to additional lateral interactions between the molecules. Dimers of type VII collagen interact with the network of type IV collagen. *Beaded collagen*: an association between the type VI collagen dimer and tetramer takes place inside the cells. Connection of tetramers leads to the formation of long filaments called "beaded filaments" according to their appearance in electron microscopy. *Hexagonal networks*: collagens VIII and X form hexagonal networks in Descemet's membrane and in hypertrophic cartilage, respectively. *Multiplexin*: collagens XVIII and XV are found in basement membrane. *MACITs*: transmembrane collagens (XIII, XVII, XXIII, and XXV). The N-terminal NC domain (N-terminal NC) is located inside the cell, whereas the triple helix region is extracellular. NC, non-collagenous domain. Adapted from (41).

After processing, the mature protein (*tropocollagen)*, consists almost entirely of a triple-stranded helix and is considered as the building block for higher order fibrils and fibers. The self-assembly of tropocollagen monomers (300 nm long, 1.4 nm diameter) results in the formation of collagen microfibrils with a quarter-stagger axial D periodicity of 67 nm long repeats to create the characteristic striation observed in collagen-containing tissues (69, 78). The staggered arrangement

optimizes electrostatic and hydrophobic interactions and allows the formation of covalent intermolecular cross-links between lysine/hydroxylysine residues of helical and neighboring non-helical regions thereby stabilizing the collagen fibrils (75, 79, 80). This process is initiated by the oxidative deamination of lysyl and hydroxylsyl residues in the N- and C-terminal telopeptide regions catalyzed by enzymes of the lysyl oxidase family (LOX) (81). The newly generated aldehyde group forms crosslinks with the (hydroxy)lysines in the triple-helical region of neighboring molecules. These links are crucial to confer the mechanical characteristics of collagen-containing tissues (82–84).

The short primary fibrils are unilaterally elongated via a multistage process including nucleation and organization to form intermediate-sized microfibrils. Once assembled, collagen microfibrils grow into fibrils through longitudinal and axial increase (77, 85). The assembly can also be regulated by many collagen binding proteins such as the FACITs (**Figure 2**), which integrate into the fibrils, selectively altering the surface properties of the collagen fibril as well as the interactions with accessory ECM molecules including the small leucine-rich repeat proteoglycans (78, 86).

IMPLICATIONS OF FIBRILLAR COLLAGENS IN CANCER PROGRESSION

In 1986, Dvorak reported an association between the TME and wound healing, suggesting that tumors behave as wounds that do not heal (87). In agreement with this concept, a fibro-inflammatory microenvironment has been shown to play critical roles in supporting tumor progression (88). Indeed, compelling studies suggest that a normal microenvironment prevents premalignant cells from progressing into cancer, whereas an abnormal or wound repair–associated microenvironment can be tumor-promoting (88). Reacting to a disruption in tissue homeostasis, resident fibroblasts are progressively activated into CAFs, which represent the most frequent cell type in the TME of many carcinomas, including pancreas, breast, and hepatic carcinomas (89, 90). During cancer progression, fibroblast activation and expansion is induced (**Figure 1**), such that low-grade premalignant lesions are already surrounded by areas of fibrosis (91). As these CAFs coevolve with the advancing cancer, they take on diverse functions that support tumor progression (92). In that context, CAFs represent key players in tumor fibrosis (also called desmoplasia), which is defined as a fibrotic state characterized by an excessive synthesis, deposition and remodeling of fibrillar collagens in the surroundings of the tumor (22, 93). Increasing evidence suggests heterogeneity among CAFs. Single-cell RNA-seq analyses of different mouse and human tumors highlighted the existence of at least three CAF populations (92, 94, 95). Among these, a population of CAFs has been coined myofibroblastic CAFs or matrix CAFs (mCAFs) and abundantly produces a wide variety of ECM components including type I and type III fibrillar collagens, matrix-modifying enzymes such as LOX as well as a contractile phenotype. Consistent with its role as a key regulator of fibrogenic gene expression and the myofibroblast state, TGF-β signaling promotes the mCAF phenotype (96, 97).

By exerting contraction forces on collagen fibers, CAFs induce the reorientation and alignment of fibrillar proteins. The dense collagen network is also crosslinked, thereby increasing matrix stiffness.

Atomic force microscopy analysis of a murine model of spontaneous breast cancer (MMTV-PyMT mice) revealed that while the elastic modulus of the normal mammary gland was about 400 Pa, it increased to 1,200 and 3,000 Pa in pre-malignant and malignant tumors, respectively (98). In human breast, the stiffness of the normal and non-invasive stroma is around 400 Pa. In sharp contrast, the invasive regions of aggressive tumors were much stiffer (>5 kPa). Interestingly, the tumor invasion front appears stiffer than the tumor core tissue (99).

This desmoplasia-associated collagen remodeling elicits biochemical and biophysical cues which influence stromal and tumor cell properties, providing crucial physical guidance facilitating cell migration, invasion, and metastasis through reciprocal interactions between the cells and the ECM (21, 26, 100–105).

Several key biophysical parameters of type I collagen matrix play a role in cancer cell migration, in particular the mechanical properties, the pore size, the density and orientation of cell adhesion sites presented by the collagen fibers, and the local direction of the fibers (106).

Collagen fiber diameter and pore size play key roles in cell force generation and migration (107, 108), with larger fiber diameter and pore size promoting cell force generation and migration (21).

During migration, cancer cells follow the path of least resistance, they recognize and use open pores within the matrix. A correlation between cell-migration speed and pore size has been shown (107, 109). Cancer-cell migration is also positively correlated with the stiffness of the tumor and associated stromal matrix (110, 111). However, fiber alignment appears as the best predictor of cell speed in collagen matrix.

The mode of cell migration is also dictated by the microstructure of the matrix. At low collagen densities, when the matrix pore size is larger than the nucleus of the migrating cell, matrix cleavage is not critical and cells move rapidly using pseudopodial protrusions in an amoeboid mode of migration (107, 112). Increased deposition of fibrillar collagens may lead to decreased porosity near the tumor. At high collagen densities, when the pore size is significantly smaller than the nucleus of the cell, cell movements rely more extensively on the cleavage of collagen fibers by secreted and cell membrane-associated collagenolytic enzymes including matrix metalloproteinases (MMPs), cathepsins, and serine proteinases. In this case, tumor cells undergo a more mesenchymal mode of migration: they use proteinase-assisted invadopodia to open the pore to the necessary size and move through them by transmitting forces via adhesion. However, some cells are able to migrate through small pores in the absence of matrix remodeling by disrupting and subsequently repairing their nuclei (113).

The proteinase-assisted migration generates channel-like tracks (3–30 μm in diameter and 100–600 μm in length) in the

matrix (114). These migration tracks opened by path-finding cells can subsequently be used by several following cancer cells (109, 115).

CAFs also play an active role in promoting cancer cell infiltration into the tumor stroma by taking the lead and forming tracks in which tumor cells follow (116). The remodeling of fibrillar collagens by CAFs and/or cancer cells may lead to heterogeneities in density and network organization.

The alignment of the fibrillar components of the ECM has a strong influence on the direction and speed of migrating cells (16, 117). Experimental models have demonstrated that cancer cells invade more efficiently through *in vitro* engineered lattices of linear type I collagen than through disorganized lattices (105, 106, 118). *In vivo*, local tumor cell invasion was oriented along radially aligned collagen fibers. These reorganized collagen fibers are called tumor-associated collagen signatures (TACS, **Figure 1**). Three TACS corresponding to different levels of collagen fibers reorganization have been described and represent novel markers to locate and characterize tumors (103, 119–121). In TACS-1 stage, a localized increase in the deposition of collagen without obvious alignment is observed near the tumor. In TACS-2 stage (pre-invasive tissue), the collagen fibers are aligned in parallel to the tumor border. In TACS-3 stage (metastatic stage), the collagen fibers are bundled and aligned perpendicular to the tumor border. Collagen linearization is therefore considered as a key feature of metastatic carcinomas and predictive of poor prognosis in breast carcinoma and *in situ* breast ductal carcinoma (121–123). The aligned collagen fibers provide tracks not only for cancer cells but also for macrophages, thereby promoting their migration into the TME (124). Recently, WISP1, a matricellular protein secreted by cancer cells, was shown to induce collagen linearization by binding directly type I collagen, thereby promoting its linearization, independently of cell-derived mechanical tensions (125). Moreover, fibroblast activation protein (FAP), another important ECM-associated proteinase, promotes the formation *in vitro* of desmoplastic-like aligned matrices (126) and its overexpression has been associated with a poor patient outcome.

The accumulation of cross-linked collagens and the subsequent stiffening of the matrix also lead to elevated interstitial fluid pressure in the desmoplastic TME inducing resistance to treatment by decreasing chemotherapy and immunotherapy drug delivery (127).

In addition to their biomechanical contribution to cancer progression, CAF-derived collagen-rich ECMs also indirectly fuel cancer cells with amino acids. Indeed, collagen uptake and catabolism, with subsequent proline catabolism, has been shown to support cancer cell proliferation (128).

Even if CAFs are usually considered as the key ECM remodelers in the TME, both epithelial and immune cells also contribute to the synthesis and secretion of fibrillar ECM components (129). Indeed, epithelial cells are able to secrete ECM components (including type I collagen) (130–133). In colorectal cancer, tumor associated macrophages (TAMs) could even play a more important role in collagen deposition, cross-linking, and linearization than CAFs (134).

The desmoplastic reaction has been frequently associated with a poor survival of cancer patients (135–140). According to clinical data, tumor collagen content, alignment and distribution have been considered as prognostic factors related to cancer differentiation, invasion and clinical outcome in different cancers (141–143). However, the implications of fibrillar collagens during cancer progression are not restricted to the primary tumors. Despite the successful treatment of a primary tumor, dormant disseminated tumor cells may be reactivated to form actively proliferating metastatic lesions (144, 145). This reactivation is associated with the induction of fibrosis characterized by the deposition of fibrillar collagens in the metastatic microenvironment (146).

Beside the above described functions in desmoplasia, fibrillar collagens are extremely important in major steps of cancer progression. Specific chains of these collagens and procollagens act as effectors and allow modulation of key processes in cancer progression (e.g., proliferation, apoptosis, angiogenesis, invasion, and metastasis). Some studies reveal that these effects can be either pro- or anti-tumorigenic and are collagen type-dependent (147, 148). A non-exhaustive overview of the contribution of each fibrillar collagens in cancer progression is presented in **Table 2**.

In order to complete this overview of the roles of fibrillar collagens in cancer, we explored *in silico,* whether the mRNA level of the different fibrillar collagens were connected with clinical outcome in human cancers. Patients were divided into two groups (low and high expression groups) according to the gene expression level in tumor tissue. Kaplan-Meier log rank analysis showed that a high expression level of a few collagens was associated with a significantly longer overall survival period in some cancers (e.g., COL2A1 in pancreatic ductal adenocarcinoma—**Figure 4A**). However, for most fibrillar collagens, high expression levels were linked with significantly shorter overall survival periods (e.g., COL5A1 in kidney renal papillary cell carcinomas—**Figure 4B**). The complete analysis of the prognostic value of the expression level of 11 fibrillar collagens on the survival of patients suffering from 13 different cancers is summarized in **Figure 4C**.

FIBRILLAR COLLAGENS, AGING AND CANCER: A DANGEROUS TRIO

The incidence of most cancers strongly increases with age and cancer represents the primary cause of death in population aged 60–79 years. The risk of having an invasive cancer in patients over 60 is more than 2-fold that of younger patients (183).

Many studies have shown that aging affects the normal cells of the TME. Among these stromal cells, fibroblasts and immune cells, which represent key actors in tumor progression and metastasis, are notably susceptible to this age-related impact (184). ECM integrity decreases substantially as we age. Age-related alterations in the physical features of the ECM comprise decreases in collagen density (185–187), ECM fiber thickness and area (188, 189).

TABLE 2 | Influence of fibrillar collagen expression on cancer properties.

Type	Subtype	Cancers	Implications	References
COL I	COL1A1	Hepatocellular	Clonogenicity, motility, invasiveness and stemness	(149)
		Bladder	Proliferation, migration, and invasion	(150)
		Malignant astrocytoma	Invasion	(151)
		Breast	Migration	(152)
		Colorectal	Migration	(153)
		Oral squamous cell carcinoma	Proliferation and migration	(154)
		Gastric	Proliferation, migration, and invasion	(155)
COL II	COL2A1	Ovarian	Prognostic value	(156)
		Gastric	Prognostic value	(157)
			Biomarker	(158)
COL III	COL3A1	Ovarian	Lymphovascular metastasis	(159)
			Patient survival	(160)
			Drug resistance	(161)
		Bladder	Patient survival	(162)
		Glioblastoma	Patient survival	(163)
		Colorectal	Patient survival	(164)
			Proliferation	(164)
COL V	COL5A1	Ovarian	Lymphovascular metastasis	(159)
		Breast	Viability and migration	(165)
			Patient survival	(165)
		Lung	Proliferation, apoptosis, invasion	(166)
			Patient survival	(166)
		Renal	Proliferation, apoptosis, migration, invasion	(167)
			Patient survival	(167)
		Tongue squamous cell carcinoma	Patient survival and metastasis	(168)
		Breast	Prognostic value	(169)
	COL5A2	Ovarian	Lymphovascular metastasis	(159)
		Tongue squamous cell carcinoma	Patient survival	(168)
		Bladder	Patient survival	(170)
	COL5A3	Breast	Proliferation	(171)
COL XI	COL11A1	Ovarian	Patient survival	(172)
			Invasion	(172)
			Drug resistance	(173)
		Non-small cell lung carcinoma	Proliferation, migration, invasion, drug resistance	(174)
		Pan-cancer	Marker of activated CAF	(175)
		Gastric	Proliferation, migration, invasion	(176)
		Esophageal squamous cell carcinoma	Prognostic value	(177)
		Pancreas	Prognostic value	(178)
		Breast	Prognostic value	(179)
COL XXIV	COL24A1	Head and neck	Prognostic value	(180)
		Hepatocellular carcinoma	Prognostic value	(181)

Because of their long half-life, fibrillar collagens are subjected to post-translational changes during biological aging. These modifications include mineralization, accumulation of advanced glycation end-products (AGEs) (190), an increase in crosslinks level (191), and the reduction of glycosaminoglycans (GAGs), which impact fiber stability. These biochemical alterations change the structural organization of type I collagen (192–194). Such changes in structural properties of type I collagen affect its susceptibility to matrix metalloproteinases (MMPs)-mediated degradation (185, 195), and lead to a tissues stiffening. These structural alterations also influence the recognition of the collagen fibers by cell surface receptors such as discoidin domain receptors (DDR), which are sensitive to the structural organization of the collagen. *In vitro* studies have shown that aged type I collagen upregulates the proliferation of fibrosarcoma cells (196) and presents a reduced pro-apoptotic potential toward luminal breast cancer cells (197).

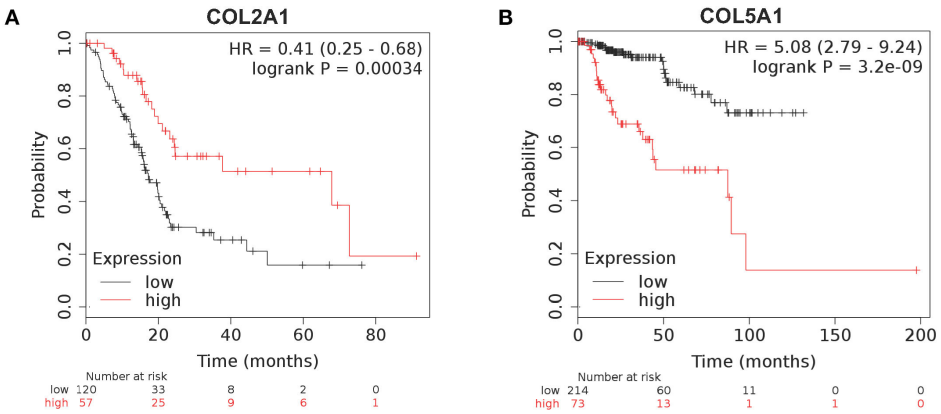

C

	COL1 A1	COL1 A2	COL2 A1	COL3 A1	COL5 A1	COL5 A2	COL5 A3	COL11 A1	COL11 A2	COL24 A1	COL27 A1
Bladder carcinoma (n=404)	**1.56** *0.028*	**1.57** *0.003*	1.33 *0.085*	**1.54** *0.0072*	**1.59** *0.0018*	**1.66** *0.0007 9*	**2.26** *7.7x10^{-5}*	**1.43** *0.022*	0.74 *0.083*	0.8 *0.15*	0.77 *0.11*
Breast cancer (n=1089)	1.26 *0.16*	1.26 *0.17*	0.75 *0.078*	**1.29** *0.013*	1.35 *0.079*	1.38 *0.069*	**1.28** *0.016*	**1.64** *0.0027*	1.14 *0.45*	1.22 *0.24*	**0.73** *0.048*
Cervical squamous cell carcinoma (n=304)	**2.19** *0.0057*	1.61 *0.09*	1.46 *0.12*	**1.69** *0.036*	**1.86** *0.01*	**1.93** *0.0064*	**1.76** *0.019*	**2.21** *0.0006*	0.62 *0.12*	1.31 *0.31*	0.81 *0.39*
Esophagal adeno-carcinoma (n=78)	**1.66** *0.12*	1.45 *0.25*	1.91 *0.055*	**1.95** *0.011*	1.79 *0.075*	1.59 *0.15*	1.47 *0.25*	**2.33** *0.017*	0.78 *0.45*	1.3 *0.45*	0.64 *0.21*
Esophagal squamous cell carcinoma (n=81)	**0.59** *0.2*	**0.55** *0.25*	**0.47** *0.064*	**0.57** *0.028*	**0.69** *0.37*	**0.54** *0.12*	1.67 *0.27*	**0.58** *0.23*	**0.44** *0.051*	**0.63** *0.27*	**0.59** *0.2*
Head-neck squamous cell carcinoma (n=499)	**1.2** *0.22*	**0.85** *0.25*	**1.26** *0.11*	**1.2** *0.02*	**1.27** *0.083*	**1.26** *0.11*	**1.15** *0.35*	**1.327** *0.047*	**0.82** *0.16*	**1.21** *0.16*	**1.13** *0.45*
Kidney renal clear cell carcinoma (n=530)	**1.73** *0.0004*	**1.55** *0.0098*	**1.65** *0.0015*	1.35 *0.061*	**1.77** *0.0002*	1.33 *0.083*	**1.61** *0.0018*	**1.92** *1.7x10^{-5}*	**1.65** *0.0023*	**1.72** *0.0003*	1.33 *0.06*
Kidney renal papillary cell carcinoma (n=287)	**4.63** *2.9x10^{-8}*	**4.03** *6.5x10^{-7}*	**3.39** *0.0032*	**4.95** *8.2x10^{-9}*	**5.08** *8.2x10^{-9}*	**4.84** *1.2x10^{-8}*	**4.35** *2.5x10^{-7}*	**4.67** *3.9x10^{-8}*	**2.77** *0.0005 9*	**3.64** *5.6x10^{-6}*	**0.47** *0.016*
Liver hepatocellular carcinoma (n=370)	1.41 *0.059*	1.51 *0.051*	**1.62** *0.022*	1.38 *0.069*	1.4 *0.081*	1.4 *0.067*	1.37 *0.077*	**1.62** *0.006*	**0.65** *0.017*	**2.01** *8.7x10^{-5}*	0.77 *0.14*
Lung adeno-carcinoma (n=504)	**1.63** *0.0013*	**1.38** *0.029*	0.77 *0.094*	1.35 *0.063*	**1.46** *0.011*	**1.5** *0.019*	**1.43** *0.038*	**1.91** *0.0002 5*	0.88 *0.41*	**0.65** *0.0048*	0.75 *0.063*
Lung squamous cell carcinoma (n=495)	**1.33** *0.038*	1.28 *0.075*	1.26 *0.16*	**1.4** *0.022*	**1.35** *0.031*	**1.36** *0.031*	1.27 *0.079*	0.87 *0.31*	**1.36** *0.04*	1.35 *0.077*	1.19 *0.21*
Ovarian cancer (n=373)	**1.38** *0.019*	**1.38** *0.019*	1.41 *0.02*	**1.37** *0.026*	**1.48** *0.005*	1.3 *0.065*	1.19 *0.21*	1.23 *0.13*	**1.31** *0.045*	1.31 *0.052*	1.21 *0.17*
Pancreatic ductal adeno-carcinoma (n=177)	1.4 *0.11*	1.43 *0.09*	**0.41** *0.0003*	1.6 *0.075*	1.56 *0.09*	1.45 *0.077*	**1.62** *0.046*	**1.74** *0.011*	0.71 *0.11*	**1.55** *0.039*	**0.49** *0.0015*

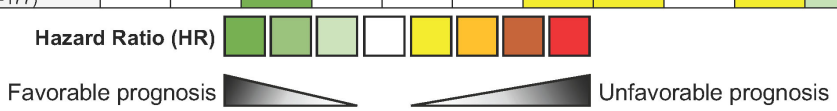

FIGURE 4 | Influence of 11 fibrillar collagen gene expression on patient prognosis outcome in 13 different cancers. Hazard ratio (HR) and log-rank *p*-values were calculated using the pan-cancer RNA-seq Kaplan-Meier plotter (182). **(A)** Kaplan-Meier plot showing that patients with a high COL2A1 gene expression (red lines) have a higher overall survival than those with a low gene expression (black lines). **(B)** Kaplan-Meier plot showing that patients with a high COL5A1 gene expression (red lines) have a lower overall survival than those with a low gene expression (black lines). HR and 95% confidence interval are shown. Log-rank $P < 0.05$ was considered to indicate statistical significance. **(C)** Summary of HR (**bold**) and log-rank *p*-values (*italic*) for 11 fibrillar collagen genes in 13 different cancers. Collagen genes whose mRNA levels were significantly associated with patient's overall survival in a specific cancer were color coded according to the log-rank *p*-values and HR (unfavorable prognosis: yellow to red; favorable prognosis: light to dark green).

IMAGING FIBRILLAR COLLAGENS

Several techniques can be used to image the architecture of collagen networks depending on the experimental conditions and the studied features. Histochemical (van Gieson staining, Picro-Sirius red, etc.) and immunohistochemical techniques are routinely used to stain fibrillar collagens (198–200). These techniques require additional fixation and preparation steps, which can alter the collagen structure of the samples, and hence are limited to *ex vivo* materials. Images of stained samples are obtained using bright-field, polarized and fluorescence microscopy techniques (199, 200). Laser scanning microscopes or multiphoton laser scanning microscopes have also been used to visualize stained tissues in three dimensions (198).

Transmission electron microscopy (TEM) and scanning electron microscopy (SEM) also allow to visualize collagens *ex vivo* and *in vitro*. The analyzed tissues must previously be washed, dehydrated, dried and sputter coated before imaging (103, 201, 202). While SEM and TEM provide highly detailed information on microstructure and nanostructure of collagens, respectively, the preparation steps may greatly alter the samples. SEM can be used to image morphology and arrangement of the collagen fibers but its three-dimensional imaging capability is limited (103). Besides these methods requiring a preparative step, non-disruptive techniques are also available. Among these techniques, confocal reflection microscopy (CRM) is a high resolution technique for imaging specimens which differ in refractive index from their surroundings or which possess a high reflectance (203). It is widely used to visualize polymers and biomaterials. A laser-scanning confocal microscope in reflection is able to detect variations of backscattered light intensity at the collagen-to-media interface for each sequential focal plane, resulting in the reconstruction of a three-dimensional image of the sample (204). CRM is readily applicable to dynamically follow living specimens. This technique can be combined with fluorescence confocal imaging without modifying the microscope hardware (76). While this visualization technique is mostly used *in vitro* to study the interactions between cells and ECM components (76, 194, 201, 203, 204), it also enables the *in vivo* visualization of epidermis and superficial dermis in real time, providing a tool for imaging skin lesions and helping skin cancer diagnosis (205–207). Excitation wavelength is proportional to the minimal resolution but decreasing it reduces the penetration depth (204). Hence, simultaneous excitation at 488 and 567 nm leads to better imaging than individual 488 and 567 nm excitations. In practice, a penetration depth of up to 100 μm is achieved for CRM on 3D collagen scaffolds, while resolution strongly declines after 30 μm.

Second harmonic generation (SHG) microscopy is a highly specific optical method of direct visualization of fibrillar collagens that can be carried out using most two-photon fluorescence microscopes (208). It allows the non-invasive assessment of the abundance and structure of fibrillar collagens with a high resolution and specificity. For those reasons, it represents the most widely used technique for the *in vivo* imaging of fibrillar collagens.

SHG occurs when two photons interact with optically non-linear material and merge to generate a new photon with twice the energy and half the wavelength of the initial photons. Fibrillar collagen non-linear optical response, which results in a strong SHG signal, originates from its non-centrosymmetric triple helical molecular assemblies, which exhibit large hyperpolarizabilities (209, 210). This process is sensitive to the microscopic structure of the scattering material. Therefore, SHG emission directionality is influenced by the diameter of the collagen fibrils that are bundled into fibers, their spacing within the fiber, and the disorder in their packing (209, 211, 212). Among the different collagens, type I collagen has the most ordered structure and, hence, produces the strongest SHG signal (213). Maximum SHG resolution is higher than what is obtained using linear optical microscopy techniques and enables to image collagen fibrils (209, 214). SHG signal intensity is dependent of the fibril/fiber orientation (210). In particular, fibers which are perpendicular to the laser light polarization axis will result in a weak signal. SHG is also very low with fibers perpendicular to the imaging plane (due to the centrosymmetric structure of fiber cross section). It should also be emphasized that, due to resolution limitations, collagen fibrils with a diameter lower than 100 μm will not be detected. The SHG optical sectioning capability enables tissue imaging in three dimensions (215). SHG imaging is therefore a label-free, non-destructive, high resolution, sensitive and specific modality for visualizing the spatial distribution of fibrillar collagens *in vitro*, *ex vivo* (**Figure 5**), and *in vivo*. SHG images can be subsequently analyzed with specific image analysis tools such as CT-FIRE which can extract individual collagen fibers from images for a quantitative assessment of fiber metrics including fiber angle, fiber length, fiber straightness, and fiber width (216). In the context of cancer, SHG measurement has been used as an independent prognostic indicator of metastatic outcome in patients with estrogen receptor positive, lymph node-negative breast cancer as well as in stage I colon adenocarcinomas (217).

Other techniques can be performed to directly monitor collagen fibers. Small angle X-ray scattering (SAXS) characterizes collagen fibril structure and organization into fibers of whole samples (218, 219). It represents an efficient way for observing and investigating the structural organization of collagen fibrils including their orientation. Collagen fibril orientation can then be used to derive the collagen fiber orientation. When used in combination with Fourier transformed infrared (FTIR) microspectroscopy, which gives chemical information on submolecular bounds and functional groups, and unsupervised hierarchical cluster analysis, it can characterize, classify and map cell clusters in *ex vivo* tissue samples (219). Magnetic resonance imaging (MRI) can be used to study *ex vivo* and *in vivo* the three-dimensional organization and density of collagens (220, 221). Finally, real-time collagen imaging in *in vivo* models can also be achieved by using transgenic lines expressing fluorescent protein-tagged fibrillar collagen (222).

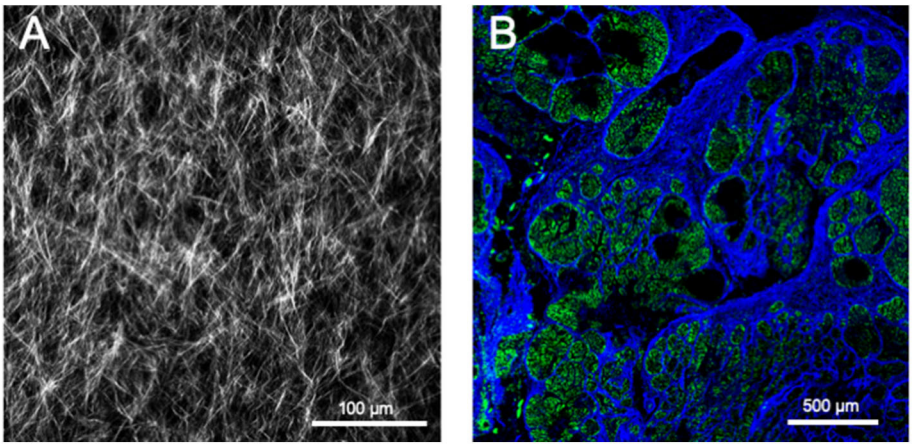

FIGURE 5 | Second harmonic generation (SHG) image of fibrillar collagens. **(A)** SHG image of *in vitro* polymerized collagen I. **(B)** SHG of a mouse mammary PyMT tumor section. Collagen fibers appear in blue, while the cellular structures appear in green due to the autofluorescence of the sample.

STRUCTURAL AND FUNCTIONAL FEATURES OF COLLAGEN-BINDING INTEGRINS

Fibrillar collagen receptors include different classes of molecules such as DDRs, mannose receptors, leucocyte receptor complex, as well as proteolytic enzymes. DDRs (DDR1 and DDR2) are tyrosine kinase receptors that become specifically activated by the native triple helix of fibrillar collagens I–III, followed by tyrosine autophosphorylation, receptor internalization and signaling (223, 224). Leucocyte receptor complex members like OSCAR (osteoclast associated receptor) and GPVI (glycoprotein VI) have been also shown to act as fibrillar collagen receptors and mediate processes such as osteoclastogenesis (225) and platelet activation and aggregation, respectively (226). The uPARAP/Endo180 mannose receptor has been shown to recognize fibrillar collagens such as collagen I, II, and V and acts as an endocytic receptor by modulating the collagen fragment internalization and its lysosomal degradation, playing a role in the fibrillar collagen turnover (227). In this context, proteolytic enzymes such as MMPs and cathepsins also recognize fibrillar collagens and mediate collagen degradation in the extracellular compartment (228). These different non-integrin collagen receptors have been shown to play key roles in specific hallmarks of cancer, including among others proliferation, apoptosis, drug resistance, inflammation, neo-angiogenesis and metastasis (227, 229).

Integrins comprise a large family of matricellular receptors involved in the transduction of the bidirectional signaling between cells and the surrounding ECM. Each integrin consists of a cell surface heterodimer of α and β subunits non-covalently associated and composed by a large ectodomain, a transmembrane domain and a short cytoplasmic tail (**Figure 6**). The ECM ligand specificity of integrins is ascribed to the large ectodomain, while the cytoplasmic tail is known to bind several intracellular regulatory and cytoskeletal molecules. Integrin α and β subunits heterodimerize in the endoplasmic reticulum, undergo posttranslational modifications such as glycosylation in Golgi, and are subsequently transported in an inactive form at the cell surface where activated to interact with specific ECM ligands. Recognition of different ECM ligands by specific integrins triggers distinct intracellular signals, enabling cells to regulate their behavior in response to microenvironmental changes.

Among the 24 different integrin heterodimers (18 α subunits and 8 β subunits), collagen binding integrins include four different α subunits bound to a common β1 subunit: α1β1, α2β1, α10β1, and α11β1. Other classes of integrins include integrins presenting a Arg-Gly-Asp (RGD) motif, laminin binding integrins and leucocyte receptors. The members of collagen binding integrin subgroup recognize their fibrillar ligands either directly by using an inserted domain in their α subunit (αI domain) (230) or indirectly by a class of non-collagen bridging molecules—COLINBRI" (COLlagen INtegrin BRIdging) (231) (**Figure 6**).

Specific collagenous motifs are recognized by integrin αI domains, the major functional motif being the GFOGER (O = 4-hydroxyproline) sequence in the triple-helical conformation. The binding of this motif occurs in a metal-dependent manner via a Metal Ion-Dependent Adhesion Site (MIDAS) which coordinates a divalent cation Mg^{2+} and is highly conserved in all four collagen binding integrins (232). Other motifs with a GxOGER sequence (x = hydrophobic residue) include GROGER, GLOGER, GMOGER, and occur at specific loci within the D-periods of fibrillary collagens. A description of all known integrin recognition motifs for fibrillar collagens has been previously addressed by Hamaia and Farndale (233). Previous studies reported that α1 and α10 integrins poorly bind to the fibrillar form of collagens, when compared to their α2 and α11 counterparts, and rather favor the binding to the native monomeric form of other types of collagens such as network-forming (collagen IV and VI) or FACIT collagens (collagen IX) (231). It has been demonstrated that integrin α1 prefers to bind to the monomeric form of collagen I rather than to its mature

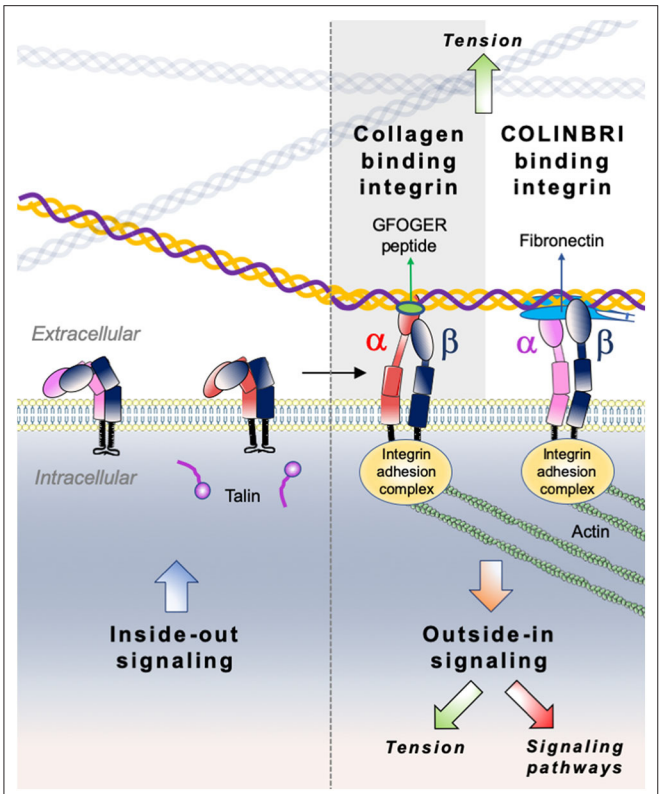

FIGURE 6 | Illustration of direct (collagen-binding integrin-mediated) and indirect (COLINBRI-mediated) integrin heterodimers binding to collagen fibrils. Inactive integrins adopt a compact conformation in which the α- (red/purple) and β-subunit (black) are closely associated. Intracellular signals, culminating in the binding of talin to the β-subunit tail, lead to conformational changes that result in increased affinity for extracellular ligands. The primed integrin binds ligand, which represents the end-point of inside-out signaling. The binding of talin and ligand initiate focal contact formation. As the cytoskeleton matures, tension (green arrows) is generated on the integrin receptor across the cell membrane. The force applied to the integrin strengthens receptor-ligand binding and allows the formation of stable focal adhesions and the initiation of intracellular signaling cascades (red arrow), the end-point of outside-in signaling. In the direct cell-binding mechanism, collagen-binding integrins directly interact with the GFOGER sequence of fibrillar collagen to provide cell adhesion. In the indirect way, cell binding involves COLINBRIs like fibronectin represented here in blue. The COLINBRI molecule is anchored to collagen and provides cell attachment by interaction with the COLINBRI-binding integrins.

fibrillar form (234) and also binds with a higher affinity to the collagen IV (a basement membrane collagen) (235). Likewise, integrin α10 displays a higher affinity for network-forming collagen IV and VI when compared to the fibrillar collagens I-III (236). Higher fibrillar collagen specificity was however demonstrated for the α2 and α11 integrin I domains. These integrins prefer the binding of mature fibrillar collagen forms mostly through the GFOGER motif. Along with the binding of collagenous ligands, these integrins show also specificity for other ECM components such as laminins, proteoglycans, and tenascins. A detailed ligand specificity of collagen binding integrins is described in **Table 3**.

Most of the functional motifs in the collagen triple helix contain hydroxylated proline residues. Along with its critical role in the stabilization of the collagen triple helix and fibril formation, hydroxylation of proline in position Y of the collagen triplet sequence -G-X-Y- has also an important role in the recognition of functional sites by the collagen receptors. It has been reported that α2 integrin binding to the GFPGER motif (P = 4-proline) is weaker than its binding to the consensus GFOGER motif, suggesting a higher avidity of integrin receptors for hydroxyproline-containing motifs of collagens (244). Furthermore, a recent study reported that absence of hydroxyproline residues in the GFOGER motif strongly impairs the avidity of α1 and α11 integrins for the collagen molecule and with a less prominent difference for the α2 integrin (245). This study revealed that absence of proline hydroxylation in collagen can affect integrin binding not only by the structural destabilization of the triple helix, but also by a direct mechanism, in which the residue Arg-218 in the α1I integrin domain directly interacts with the hydroxyproline residue in the integrin-binding motif of collagen.

Indirect binding of fibrillar collagens may involve collagen-binding integrins but also RGD integrins or leucocyte receptors. COLINBRIs have been described as prototypical ECM molecules being able to bridge between integrins and fibrillar collagens. Such molecules include among others fibronectin, vitronectin, periostin, and small leucine-rich proteoglycan/protein (SLRP) family members (231). These proteins show binding sites for specific fibrillar collagens, as well as several integrin-recognizing sites. They also play a role in collagen fibrillogenesis, deposition, and modulation of integrin affinity for collagenous ligands. An example of such a COLINBRI molecule is fibronectin, which displays a binding domain for the collagen Iα1 chain in its N-terminal part and several binding sites for RGD-binding integrins (α5β1 or αvβ3 integrins) and leucocyte receptors (α4β1 or α4β7 integrins). Previous studies have reported the reciprocal mechanoregulation between the two ECM molecules and the active role of fibronectin in the collagen initial fibril-formation and assembly (246). In this context, collagen-binding integrins have also been reported to interact with COLINBRI-like molecules, particularly with SLRPs. Decorin interacts with α2β1 integrin and allosterically modulates its collagen I-binding activity in angiogenic endothelial cells, but not quiescent cells, thus promoting a migratory phenotype (247). Conversely, lumican, another SLRP involved in collagen type I fibrillogenesis, displays an inhibitory effect on melanoma cell migration modulated by the interaction of its proteic core with the activated I domain of the α2 integrin subunit (248). For a detailed comparison of integrin and non-integrin collagen receptor binding sites, we refer the reader to Zeltz et al. (231) and Zhu et al. (249).

MECHANISTIC INSIGHTS INTO COLLAGEN-BINDING INTEGRIN SIGNALING

Collagen-binding integrins, similarly to the other type of integrins operate as bidirectional signaling receptors upon a biochemical or mechanical activation. The two directions

TABLE 3 | Specificity of collagen-binding integrins.

Integrin subunit	Collagen specificity	Motifs	Other ECM ligands	References
α1	Collagen I, II, III, IV, V, VI, IX, XVI and XVIII Highest affinity for collagen IV	GFOGER (collagen I, II, IV) GVOGEA (collagen II) GLOGEN (collagen III)	Laminins, galectins, arresten and semaphorin 7A	(231–233, 237, 238)
α2	Collagen I, II, III, IV, V and XI	GFOGER (collagen I, II, IV) GMOGER	Laminins, Tenascin C, decorin, endorepellin, perlecan, and chondroadherin	(231–233, 239, 240)
α10	Collagen I, II, IV, VI Highest affinity for collagen IV and VI	GFOGER (Collagen I, II, IV)	ND	(233, 236, 241)
α11	Collagen I, IV, V, IX Highest for collagen I	GFOGER (Collagen I, II, IV)	ND	(231, 232, 242, 243)

of integrin signaling have different biological consequences and involve distinct conformational states. In the traditional "**outside-in**" signaling, integrins act as membrane receptors in transmitting information from the surrounding environment into cells (**Figure 6**). This signaling refers to multivalent integrin-ligand binding, integrin conformational switch from an inactive low avidity state to a high avidity state, subsequent clustering and association with actin cytoskeleton (250). During "**inside–out**" signaling, talin, an intracellular activator, binds to the cytoplasmic tail of integrin β-subunit, inducing conformational changes that increase the affinity for extracellular ligands (251). Although conceptually different, the "outside-in" and "inside-out" integrin signaling processes are often complementary and closely linked both leading to regulation of cell polarity and cytoskeleton assembly, of gene expression, cell survival and motility. It is worth noting, that most of the previously described mechanistic studies on integrin signaling were performed on RGD binding integrins, as well as on α1β1 and α2β1 collagen-binding integrins, while integrin α10β1 and α11β1 signaling is still poorly explored. Furthermore, the specificity of integrin signaling relies on multiple factors, including heterodimer subtype, cellular context, ECM organization and ligand recognition. Analogously to other integrin subtypes, the signaling responses of collagen binding integrins are mostly mediated by the common β1 subunit and are not specific to the αβ heterodimer. Only a few studies reported the implication of the α cytoplasmic domain in the cellular signaling of collagen binding integrins. We therefore described below a general integrin signaling pathway applied to most integrins and highlight relevant studies which describe distinct signaling events for collagen binding integrins.

Integrin signaling requires the assembly of a dynamic multiprotein machinery around their cytoplasmic tails, called "adhesome." It was reported that integrin adhesome comprises a network of at least 156 components linked via 690 different interactions (252). These components are classified into several functional groups, which comprise 25 adaptor proteins, 24 cytoskeletal molecules, nine actin-binding proteins, 18 tyrosine and serine/threonine kinases, 12 tyrosine and serine/threonine protein phosphatases, seven transmembrane receptors, six adhesion proteins, eight GTPase-activating proteins (GAPs), eight guanine nucleotide exchange factors (GEFs), five GTPases, and 32 other components (252). Integrin connection to the cytoskeletal machinery is mediated by integrin adhesion complexes (IACs)—macromolecular complexes which transduce biochemical and mechanical signals from the microenvironment into biological responses (253). The formation of several major types of IACs has been reported, including focal complexes, focal adhesions and fibrillar adhesions, which play a central role in cell adhesion and migration (253). Most of the IAC proteomic analyses were performed on complexes isolated from fibronectin-attached cells, while still little is known about the adhesome complexes related to collagen binding integrins. These studies identified around 60 core proteins within IACs which constitute the cell adhesion machinery and link integrins bound to their ECM ligands to the cytoskeleton (254). It is plausible to assume that IACs associated to collagen binding integrins share a great similarity with those derived from fibronectin-attached integrins, as their have a common β1 subunit.

Integrin clustering refers to the interaction of integrin αβ heterodimers to form hetero-oligomers at cell surface. This event is relevant for "outside-in" signaling of integrins, including mechano-transduction processes and integrin recycling (251, 255). Upon clustering, integrins associate with a cytoskeletal signaling complex that promotes the assembly of actin filaments into large stress fibers (251). The resulting intracellular structures formed by integrins and cytoskeletal proteins are known as "focal adhesions" and "focal complexes." Early steps of integrin signaling involve interactions with tyrosine kinases such as focal adhesion kinase (FAK), Src-kinases, abelson murine leukemia viral oncogene homolog 1 (Abl) and integrin-linked kinase (ILK), scaffold molecules such as p130CRK-associated substrate (p130CAS) and cytoskeletal proteins such as talin and kindlin. In the canonical integrin pathway, the active FAK/Src complex interacts with p130CAS and paxillin that in turn recruit Crk adaptor molecule leading to activation of several downstream molecules, including ras-related C3 botulinum toxin substrate 1 (Rac1), serine/threonine-protein kinase PAK 1, and c-Jun N-terminal kinase (JNK). The FAK/Src complex can also recruit other adaptor molecules leading to activation of major signaling pathways such as PI3K, RhoGTP-ases, p38, Erk, and phospholipase gamma (PLCG) pathways (256). Several studies have reported the implication of collagen binding integrins in multiple pathways mentioned above and mainly for α1β1 and α2β1 integrins. For example, binding of collagen type I by

integrin α1β1 has been shown to sustain mesangial cell spreading via the activation of Erk1/2 pathway (257). Collagen binding of integrin α2β1 through the GFOGER motif has been shown to mediate an "outside-in" signaling and to promote platelet spreading via activation of Src, FAK, and PLCG2 pathways (258). Similarly, integrin α2β1-mediated adhesion of platelets to type I collagen or GFOGER peptide has been shown to induce a downstream Pyk2 activation and PI3Kβ and Akt phosphorylation (259). Platelets adhesion to the monomeric collagen type I via α2β1 integrin was also shown to trigger the activation of PLCγ2 downstream signaling via Src kinases and Rac GTPases (260). Interestingly, both α1 and α2 collagen binding integrins have been shown to be involved in the production of reactive oxygen species (ROS), either by negatively regulating Rac1 activation and collagen synthesis through a crosstalk with the epidermal growth factor receptor (EGFR) (261), or by p38 MAPK phosphorylation and regulation of cell cycle (262). Furthermore, α11β1 integrin has been also shown to be required for an efficient collagen remodeling in wound healing via the non-canonical TGF-β1-dependent JNK signaling (263).

"Inside-out" signaling of integrins involves interactions with intracellular molecules at the cytoplasmic tails, which regulate integrin conformation. These interactions mainly occur at the cytoplasmic domain of the β integrin subunit. Talins and kindlins play a key role in this process. The binding of adaptor protein talin to the cytoplasmic tail of integrin β-subunit is a critical event in affinity activation of integrins (264). Talin association triggers integrin activation through the disruption of inhibitory interactions between α- and β-subunit cytoplasmic tails with subsequent transition from the bent to the extended conformation and increase in integrin affinity for extracellular ligands (255). Another major regulator of inside-out signaling, kindlin binds to the cytoplasmic tail of integrin β-subunit, supports integrin activation and recruits paxillin to the nascent focal adhesions, which in turn promotes the formation of membrane protrusions and therefore cell migration (265). In this context, talin was shown to be required for α2β1 integrin-mediated platelet adhesion to collagen type I and to promote platelet aggregation (266). Interestingly, another study reported that the interaction between integrin α2β1 in a non-activated conformation and collagen type I results in the activation of FAK in a talin-independent manner and requires the protein kinase C (267). While most of these interactions involve the β1 cytoplasmic tail, some studies also reported the role of α1 and α2 subunits in the integrin downstream signaling. Notably, SHARPIN, an inactivator of talin and kindlin recruitment to β subunits, has been found to bind α1 and α2 tails, rather than β1 cytoplasmic domain (268). The T-cell protein tyrosine phosphatase (TCPTP) has been also found to bind the cytoplasmic tail of α1 integrin upon cell adhesion to collagen and to negatively regulate EGFR signaling (269). Similarly, it has also been reported that α2 cytoplasmic tail is involved in the downstream activation of p38 signaling and upregulation of collagen gene transcription (270). The distinct signaling events induced by the different collagen binding integrin α subunits is remarkably highlighted by the opposite effect that these subunits have on collagen synthesis. Indeed, while α1β1 integrin is a known repressor of collagen type I synthesis (271), α2β1 integrin promotes its expression (270). Additionally, several studies have reported a link between the ligand-induced activation of collagen binding integrins and the production of collagen remodeling proteinases such as MMPs (272–274).

Collagen-binding integrins have been also reported to crosstalk with receptor tyrosine kinases (RTKs) and mediate many cellular functions, including signaling, ligand recognition, and RTK endocytosis and trafficking. Multiple studies have reported the spatial coexistence between integrins and RTKs at cell surface with a synergistic signaling between the two receptors mainly related to the "outside-in" signaling of integrins (275). The interaction between the two partners was reported to be ligand-dependent or independent. A detailed description of these interactions was addressed by previous reviews (275–277). In the context of collagen binding integrins, a crosstalk between EGFR and α1β1 or α2β1 integrins has been reported to regulate the downstream signaling and trafficking of this tyrosine kinase receptor (269, 278). The cooperation between HGFR and α2β1 integrin has been shown to regulate the innate immune response upon mast cell adhesion to collagen type I (279). Furthermore, we have recently shown that integrin α11 associates to PDGFRβ in cancer associated fibroblasts and activates its JNK downstream signaling (280).

DDRs can also positively and negatively regulate collagen-binding integrin-mediated signal transduction and cell adhesion: DDR-mediated signaling can directly affect the activity of integrins but it can also converge with integrin-triggered pathways to regulate cellular functions, whereby each receptor engages its own downstream pathway (281).

COLLAGEN-BINDING INTEGRINS IN CANCER

Integrin expression patterns undergo major changes during tumor progression and metastasis leading to significant alterations in the phenotype of both cancer and stromal cells. In cancer cells, integrins have a key role in sustaining cell proliferation and invasion, evading tumor suppressors and cell death and promoting the EMT (282). Stromal integrins, on the other hand, are implicated in processes such as tumor angiogenesis, desmoplastic reaction and metastasis by modulating cell adhesion and invasion, and ECM remodeling. In view of their bidirectional signaling, integrins provide spatially restricted communication between cells and the surrounding microenvironment and act as key mechanosensing elements and RTK co-partners to modulate biological processes essential for tumor cell survival. Normal cells rely on integrin-mediated cell adhesion to ECM components to proliferate and survive. Defects in cell ability to attach to ECM are associated with impaired pro-survival integrin-dependent signaling pathways including PI3K/Akt, MAPK, FAK, NF-κB, leading to anoikis (283). Integrins modulate all steps of the metastatic process, from invasion from the primary tumor and intravasation into the bloodstream, to colonization of the secondary sites. Distinct integrin-ligand binding combinations act as drivers

of organ-specificity colonization of tumor cells and the subsequent cell survival and adaptation to the newly acquired microenvironment. The desmoplastic reaction has been linked to high expression levels of integrins in metastatic cancers (284). Being key modulators of ECM, tumor and stromal integrins regulate matrix composition in order to control cell adhesion and invasion. Along with the aforementioned processes, integrins also contribute to tumor regulation through angiogenesis, metabolic reprogramming, evasion of immune destruction and acquisition of drug resistance.

Several mechanisms have been found to be involved in collagen-binding integrin regulation of tumor growth and metastasis. In the following section, we will discuss each of the four collagen-binding integrins, their expression profile and implication in pathological conditions with a special focus on cancer disease.

α1β1 integrin is widely expressed in normal tissues, particularly in the mesenchyme, vascular and immune system with limited expression in the epithelium (285). As illustrated in **Table 3**, this integrin can bind many types of collagens, including collagen I, II, III, IV, V, VI, IX, XVI, and XVIII, as well as laminins, galectins, arresten, and semaphorin 7A (232). As previously mentioned, α1β1 integrin is mostly detected in connective tissues and it exhibits a higher affinity for collagen IV when compared to collagen I (235). Integrin α1β1 functions include cell adhesion and survival, collagen synthesis and MMP secretion. This receptor has been associated with pathological conditions such as osteoporosis, renal injury, rheumatoid arthritis, psoriasis, as well as cancer (285). Integrin α1 mutant mice are viable and fertile with no marked phenotype (286). Integrin α1 adult mice exhibit however a mild decrease in body weight, hypocellular dermis (287) and aged animals display different phenotypes, including osteoarthritis (288), and retinal degeneration (289). *In vitro*, integrin α1-deficient cells display adhesion alteration when cultured on collagen I and IV, as well as failure to recruit and activate Shc adaptor molecule with consequent reduction in cell proliferation and survival (287). When challenged to different pathological conditions, α1-mutant mice present reduced psoriasis (290), accelerated aging-dependent osteoarthritis (288), diminished bone fracture healing (291), severe hepatic insulin resistance and lower hepatic fat accumulation upon a high fat diet (292), and increased glomerulosclerosis in diabetic mice (293) (**Table 4**).

In the context of cancer, integrin α1β1 is still poorly explored. Only a few studies reported its role in tumor progression and metastasis, mostly in non-small cell lung carcinoma and colorectal cancer. In an orthotopic model of non-small cell lung carcinoma in α1-null mice with increased MMP9 levels, a decreased number, size and vascularization of primary tumors and metastases was observed, highlighting the proangiogenic features of this integrin (294). Similarly, in another study of a spontaneous non-small cell lung carcinoma mouse model in KrasLA2/α1-null mice, tumors appeared smaller, less angiogenic, with reduced proliferation and increased apoptosis (295). Overexpression of α1β1 integrin has been reported in 65% of colorectal cancers and correlates for more than 70% with Myc oncogene expression (336, 337). Furthermore, in a xenograft model of colorectal cancers, α1-deficient tumors displayed extensive necrosis, low mitotic index and reduced angiogenesis (296). Reduced angiogenesis in absence of α1β1 integrin was also reported in an experimental breast cancer model (297). Some melanoma studies also reported a link between high expression of α1β1 integrin and a poor patient outcome (298, 299). Oral squamous cell carcinomas, broncho-alveolar and gastric carcinomas were also reported to display a gain of α1β1 integrin expression (300–302).

α2β1 integrin is mostly expressed by normal epithelial cells, fibroblasts and platelets/megakaryocytes, and depending on the differentiation state also in T lymphocytes and endothelial cells (239). It preferentially binds to fibrillar collagen types I, II, III, V, and XI. It also binds to non-collagenous ligands such as laminins, tenascin C, decorin, endorepellin, and chondroadherin (232). One of the main functions of integrin α2β1 is the adhesion-mediated survival particularly in platelets, where this integrin constitutes the most abundant collagen receptor. It is also a major regulator of cell motility, mainly via p38 MAPK pathway activation (239). Genetic alteration of integrin α2β1 expression has been detected in pathological conditions such as hemostasis, thrombosis, fibrosis, and immune response. The mutant mice for integrin α2 integrin subunit present a mild phenotype in the mammary gland branching morphogenesis defect (305, 306) adhesion defects for platelets, fibroblasts and keratinocytes when tested for collagen I (307), and a reduced age-related bone deterioration (308). Pathologically challenged mice display, reduced wound healing with increased neovascularization (309), defects in age related bone degradation due to the over-expression of collagen I (308), decreased innate immune response to Listera infection and reduced thrombi formation (239), decreased glomerulosclerosis and collagen deposition after renal injury (310), and reduced joint inflammation and cartilage destruction in rheumatoid arthritis (311).

In cancer, α2β1 integrin was extensively studied in the context of angiogenesis. In the MMTV-neu spontaneous mouse model of breast cancer, α2β1 integrin acts as a metastasis suppressor by inhibiting tumor cell intravasation without altering tumor development or growth (312). The same study provided evidence for a correlation between α2β1 integrin expression and estrogen positivity in breast cancer patients and that the decreased α2β1 integrin levels predict metastasis and decreased survival in prostate and breast cancer patients. Conversely, in another recent study of a xenograft model of MCF-7 cells interacting with platelets, α2 downregulation prevented breast cancer metastasis (313). In an experimental model of breast cancer metastasis, the MMP13 expression observed in MDA-MB-231 metastasizing cells to the bones was induced by collagen type I through integrin α1β1 and α2β1-mediated p38 MAPK pathway (314). The implication of α2β1 integrin, as well as α1β1 integrin was further emphasized by a melanoma xenograft model in a double knockout model, in which absence of both integrins impaired tumor angiogenesis (66). In another melanoma study, α2β1 integrin co-localized with E-cadherin and N-cadherin at tumor cell-cell contacts in both primary and metastatic samples (315). Disturbance of these adhesive networks impaired tumor growth in a xenograft model and N-cadherin downregulation prevented

TABLE 4 | Phenotypical consequences of collagen-binding integrin knockouts in mice.

Integrin subunit	Expression	Knockout phenotype	Pathologically challenged knockout phenotype	Cancer phenotype
α1	Endothelial cells, fibroblasts, pericytes, mesangial cells, bone marrow mesenchymal stem cells, hepatic stellate cells, chondrocytes, neural cells, Schwann cells, immune cells (285, 286)	No pronounced phenotype (286) moderate decrease in body weight, hypocellular dermis (287) aged-related osteoarthritis (288), retinal degeneration (289)	Reduced psoriasis (290) and inflammation (129), accelerated aging-dependent osteoarthritis (288), reduced bone fracture healing (291), increased glomerulosclerosis in diabetic mice (293), hepatic insulin resistance and decreased hepatic fat accumulation on a high fat diet (292)	Reduced tumor number and size, reduced angiogenesis and proliferation, increased apoptosis in models of non-small cell lung carcinoma α1-null mice (294, 295); overexpression in colorectal cancers and correlation with Myc oncogene; reduced angiogenesis, increased necrosis and low mitotic index in a xenograft model of colorectal cancers (296); reduced angiogenesis in an experimental breast cancer model (297); correlation with a poor patient outcome in melanoma (298, 299); gain of expression in oral squamous cell carcinomas, broncho-alveolar and gastric carcinomas (300–302)
α2	Epithelial cells, platelets/megakaryocytes, endothelial cells fibroblasts (303, 304)	Moderate phenotype in mammary gland morphogenesis (305, 306), adhesion defects for isolated platelets on collagen I (307), reduced age-related osteoporosis (308)	Increased neovascularization in wound healing (309), defects in age-related bone loss (308), decreased immune response to peritoneal Listera infection and reduced thrombi formation (239), decreased glomerulosclerosis upon renal injury (310), reduced inflammation and cartilage deterioration in rheumatoid arthritis (311), reduced inflammatory bowel disease (65)	Metastasis suppressor in the MMTV-neu mouse breast cancer model and correlation with patient outcome in breast and prostate cancers (312); impaired breast cancer metastasis in a xenograft model of MCF-7 cells interacting with platelets (313); reduced MMP13 expression by metastasizing cells to the bones in an experimental model of MDA-MB-231 breast cancer cells (314); impaired tumor angiogenesis in a melanoma xenograft model in a double knockout model (66); co-localization with E-cadherin and N-cadherin at tumor cell-cell contacts in primary and metastatic samples of melanoma (315); selective metastasis to the bones in prostate cancer (316); implication in doxorubicin-induced drug resistance in leukemia (317, 318); implication in other types of cancers, including pancreatic, colorectal, gastric and lung cancers, oral squamous cell carcinoma and T-cell acute lymphoblastic leukemia (319)
α10	Chondrocytes, mesenchymal stem cells, junctional fibroblasts (241, 320)	Mild chondrodysplasia (321), canine chondrodysplasia and limb dwarfism (322)	ND	Upregulation in malignant melanoma (323); overexpression in glioblastoma (324); high expression correlated with disease-specific death and distant metastasis in high-grade myxofibrosarcoma (325)
α11	Fibroblasts (cancer associated fibroblasts, myofibroblasts), mesenchymal stem cells (326–328)	Dwarfism, altered incisor tooth eruption, increased mortality and decreased IGF-1 serum levels (327, 329, 330)	Reduced wound strength and deposition of granulation tissue in wound healing (263), reduced cardiac fibrosis and left ventricular hypertrophy (331)	Decreased tumorigenicity of cancer cells (328) and matrix stiffness (332) in a challenged xenograft model of lung cancer; correlation with tumor progression and postoperative recurrence in non-small cell lung cancer (333); association with a pro-tumorigenic PDGFRβ-positive subset of cancer associated fibroblasts and correlation with a poor clinical outcome in breast cancer (280); correlation with aggressive phenotypes of breast cancer (334); decreased intratumoral interstitial fluid pressure and collagen structure in a challenged mouse tumor model (335)

α2β1 integrin-mediated tumor cell invasion on collagen type I matrix. In prostate cancer, α2β1 integrin contributes to a selective metastasis to the bone, rather than to other sites in patient samples and downregulation of this integrin impairs the adhesion and migration of prostate cancer cells toward collagen type I within the bone (316). Implication of α2β1 integrin in tumor progression and metastasis was reported in several other types of cancers, including pancreatic, colorectal, gastric and lung cancers, oral squamous cell carcinoma and T-cell acute lymphoblastic leukemia, which were previously reviewed

in (319). Lastly, it has been reported that α2β1 integrin and collagen I participate to doxorubicin-induced drug resistance in leukemia by either protecting leukemia cells from apoptosis through MAPK/ERK pathway activation (317), or by decreasing the DNA damage through the inhibition of Rac1 activation (318).

α10β1 integrin expression is mostly restricted to the cartilaginous tissue and this integrin is considered as a phenotypic marker for chondrocyte differentiation. Integrin α10β1 is a receptor for fibril-forming collagen type II, for network-forming collagen IV and beaded-filaments forming VI (321). It has a lower affinity for other types of fibrillar collagens. Integrin α10β1 is implicated in chondrocyte differentiation potency and is associated to an increase of collagen type II synthesis (338). The major physiological role of α10β1 integrin concerns the skeletal development, as this receptor is mainly expressed in the cartilage. Indeed, α10β1 integrin ablation in mouse models results in mild chondrodysplasia with altered chondrocyte functionality (321). Integrin α10-deficiency is associated to changes in chondrocyte morphology, increased apoptosis and reduced proliferation, resulting in a mild growth retardation (339). Furthermore, a previous study reported that canine chondrodysplasia is associated with a naturally occurring mutation of α10β1 integrin gene, and the observed limb dwarfism resembled the phenotype detected in the α1-null mouse model (322). The implication of this integrin in other pathological conditions is poorly documented.

In cancer, the role of α10β1 integrin remains poorly explored. A previous study reported the upregulation of α10β1 integrin in malignant melanoma when compared to primary melanocytes (323). In a recent study, this integrin emerged as a potential therapeutic target for treatment of glioblastoma (324). This study revealed that α10β1 integrin is overexpressed in glioblastoma patient tissues and cells when compared to normal brain tissues, and high α10 expression was associated to increased proliferation and migration. Interestingly, α10β1 integrin was correlated to disease-specific death and distant metastasis in a cohort of 64 primary high-grade myxofibrosarcomas (325). The authors demonstrated that α10β1 integrin promotes tumor cell survival through activation of TRIO-RAC-RICTOR-mTOR signaling, and that this pathway constitutes a promising targeted therapeutic strategy for patients with high-risk myxofibrosarcoma.

α11β1 integrin expression is primarily confined to mesenchymal-like cells during pathological conditions including fibrosis, wound healing and cancer. Integrin α11 is the latest integrin family member to be identified. α11β1 integrin binds with high affinity collagen type I and contains the I domain, which recognizes the triple-helical GFOGER motif sequence (340). The highest α11 transcript levels were detected in embryos and human adult uterus, heart and periodontal ligament. A complete characterization of α11 expression in human adult tissues has not yet been performed. While the other collagen binding integrins α1 and α2 are expressed in a several cell types, α11 expression appears to be restricted to distinct cell subsets of mesenchymal origin. Generally, it is considered that α11 integrin is expressed *in vitro* by mesenchymal derived cells, and *in vivo* by fibroblasts at sites of highly organized collagen structures (230). Integrin α11 expression is promoted by TGFβ (341) and by the mechanical stiffness of the environment in a mechanism involving an autocrine loop of Activin (326). Integrin α11 is a major collagen receptor on fibroblastic cells and *in vitro* studies revealed that this integrin plays a key role in the adhesion and motility of these cells (242). Additionally, α11 integrin plays a critical role in collagen reorganization and remodeling. Several studies reported that *in vitro* integrin α11-deficiency impacts contraction of collagen matrices (273, 329). Furthermore, integrin α11 was also reported to be also implicated in TGFβ-induced myofibroblast differentiation (326). Interestingly, a recent study investigated the contribution of α11 integrin cytoplasmic tail to cell proliferation and invasion via a FAK/ERK-dependent activation (342).

The α11-deficient mice are viable and fertile but display the following defects: dwarfism, altered teeth, increased mortality, and decreased IGF-1 serum levels (327, 329). Dwarfism of α11-deficient mice does not seem to be related to structural defects in forming cartilage or bone, but it is rather due to the tooth alteration and IGF-1 serum levels in these mice. Indeed, a strong malnutrition of α11-deficient mice was observed due to a late incisor eruption and altered tooth shape (327). However, further investigations revealed that α11-deficient mice are already smaller at birth, before the incisor eruption effect could impact the body size, suggesting that other mechanisms could be involved in the acquired phenotype. Accordingly, IGF1 is a growth factor with a crucial role in growth control and bone mineralization. Indeed, low hepatic IGF1 production was detected in α11-deficient mice, implying that dwarfism observed in these mice may also be induced by the severely diminished IGF1 serum levels (330).

Only a limited number of studies have investigated the function of integrin α11 in pathological conditions. In wound healing, it has been reported that upregulated integrin α11 promotes wound strength and deposition of granulation tissue through a TGFβ-dependent JNK signaling (263). Overexpression of integrin α11 has been also linked to left ventricular hypertrophy and cardiac fibrosis, as a result of soluble factor secretion and increase collagen deposition in the heart (331). Recent studies have extensively investigated integrin α11 in the context of cancer associated fibroblasts. In lung cancer, stromal integrin α11 increases the tumorigenicity of cancer cells in xenograft models by modulating both IGF-2 production (328) and matrix stiffness (332). Likewise, another study reported integrin α11 association with tumor progression and postoperative recurrence in non-small cell lung cancer (333). We have recently demonstrated that integrin α11 identifies a PDGFRβ-positive subset of cancer associated fibroblasts displaying pro-tumorigenic features in breast cancer. Our study revealed that high stromal integrin α11/PDGFRβ expression is correlated with a poorer clinical outcome in breast cancer patients and that this integrin harnesses the PDGFRβ/JNK signaling pathway to promote the invasion of cancer cells (280). The implication of stromal α11β1 integrin in breast cancer was further investigated in another recent study, which emphasized the correlation of this integrin expression with aggressive phenotypes of breast cancer (334). Furthermore, an additional report highlighted the contribution of integrin α11 to breast

cancer progression by regulating the intratumoral interstitial fluid pressure and collagen structure (335). Interestingly, a recent study analyzed the expression of α11β1 integrin in a panel of 14 different types of cancers and identified that this integrin is expressed by subset of non-pericyte-derived cancer associated fibroblasts and constitutes an important receptor for collagen remodeling. Integrin α11 contribution to other neoplastic malignancies and metastatic dissemination has not been yet documented. Its restricted expression, confined to a distinct mesenchymal cell subset, makes integrin α11 a good candidate for targeting the stromal compartment in cancer.

CONCLUSIONS AND PERSPECTIVES

Even if the hallmarks of cancer are driven by oncogenic mutations, most of them are modulated by the biochemical and biomechanical properties of the ECM that surrounds the tumor. By using different cell surface receptors, including integrins, cancer, and stromal cells are able to both impact and be impacted by ECM components in general and, more specifically, fibrillar collagens. In agreement with this concept, collagen fibers should no longer be viewed as passive scaffolds but as complex and constantly evolving signaling hubs that modulate a multitude of cellular functions.

It is now well-accepted that cancer should be viewed as a disease affecting the entire tissue rather than single cells. Indeed, tumors evolve in complex, dynamic, and functionally diverse TMEs. The diversity of TMEs depends on several factors including among others the tissue wherein the tumor develops, the stage of tumor evolution, the age of the patient. In contrast to cancer cells, the different cell populations which compose the TME are genetically stable, making them attractive targets for the development of innovative therapies with a low risk of development of treatment resistance. Furthermore, the efficacy of several standard chemotherapies and targeted agents is modulated by the TME, supporting the relevance of combining cancer cell-targeting agents with TME-directed therapies. However, issues related to cancer cell heterogeneity hold true for the TME. In that respect, a high degree of variability has been observed in ECM deposition and stiffness in a single tumor (343). Heterogeneity of the ECM could unravel the lack of success of the clinical trials of therapeutics targeting this feature of tumor development (343). We should also keep in mind that specific ECM components might have opposing roles during tumor progression in different cancers, suggesting that the impact of the ECM on the hallmarks of cancer cannot be broadly extrapolated to all cancer types.

It is worth noting that fibrillar collagens-derived proteolytic fragments are released in the blood stream where they represent easily accessible biomarkers to monitor cancer progression (140, 344–346).

While many questions related to how the biochemical and biomechanical properties of fibrillar collagens determine tumor progression remain unanswered, the potential for these ECM components to be effective markers and/or targets in treating cancer patients remains very promising.

AUTHOR CONTRIBUTIONS

IB, IP, TL, AN, and EM drafted the first version of the manuscript and IB, IP, and EM the figures and tables. All authors have critically reviewed and approved the manuscript.

FUNDING

This work was supported by: grants from the Fonds de la Recherche Scientifique - FNRS (F.R.S.-FNRS, Belgium), the Fondation contre le Cancer (foundation of public interest, Belgium), the Fonds spéciaux de la Recherche (University of Liège), the Fondation Hospitalo Universitaire Léon Fredericq (FHULF, University of Liège), the Direction Générale Opérationnelle de l'Economie, de l'Emploi et de la Recherche from the Service Public de Wallonie (SPW, Belgium), the Walloon Region through the FRFS-WELBIO strategic research programme, the Wallonia-Brussels Federation (grant for Concerted Research Actions). TL was the recipient of a FNRS-Télévie grant. EM was a Research Associate from the Fund for Scientific Research—FNRS (Belgium).

ACKNOWLEDGMENTS

We apologize to authors whose work could not be discussed here because of space limitations.

REFERENCES

1. Hanahan D, Weinberg RA. Hallmarks of cancer: the next generation. *Cell.* (2011) 144:646–74. doi: 10.1016/j.cell.2011.02.013
2. Balkwill F, Mantovani A. Inflammation and cancer: back to virchow? *Lancet.* (2001) 357:539–45. doi: 10.1016/S0140-6736(00)04046-0
3. Paget S. The distribution of secondary growths in cancer of the breast. *Lancet.* (1889) 133:571–3. doi: 10.1016/S0140-6736(00)49915-0
4. Egeblad M, Nakasone ES, Werb Z. Tumors as organs: complex tissues that interface with the entire organism. *Dev Cell.* (2010) 18:884–901. doi: 10.1016/j.devcel.2010.05.012
5. Chen F, Zhuang X, Lin L, Yu P, Wang Y, Shi Y, et al. New horizons in tumor microenvironment biology: challenges and opportunities. *BMC Med.* (2015) 13:14–45. doi: 10.1186/s12916-015-0278-7
6. Patel H, Nilendu P, Jahagirdar D, Pal JK, Sharma NK. Modulating secreted components of tumor microenvironment: a masterstroke in tumor therapeutics. *Cancer Biol Ther.* (2018) 19:3–12. doi: 10.1080/15384047.2017.1394538
7. Denton AE, Roberts EW, Fearon DT. Stromal cells in the tumor microenvironment BT - stromal immunology. In: Owens B, Lakins M, editors. *Stromal Immunology*. Cham: Springer (2018). p. 99–114.
8. Neesse A, Bauer CA, Öhlund D, Lauth M, Buchholz M, Michl P, et al. Stromal biology and therapy in pancreatic cancer: ready for clinical translation? *Gut*. (2018) 68:159–71. doi: 10.1136/gutjnl-2018-316451
9. Polyak K, Kalluri R. The role of the microenvironment in mammary gland development and cancer. *Cold Spring Harb Perspect Biol.* (2010) 2:a003244. doi: 10.1101/cshperspect.a003244

10. Conklin MW, Keely PJ. Why the stroma matters in breast cancer. *Cell Adhes Migr.* (2012) 6:249–60. doi: 10.4161/cam.20567
11. Hynes RO. The extracellular matrix: not just pretty fibrils. *Science.* (2009) 326:1216–19. doi: 10.1126/science.1176009
12. Hynes RO, Naba A. Overview of the matrisome–an inventory of extracellular matrix constituents and functions. *Cold Spring Harb Perspect Biol.* (2012) 4:a004903. doi: 10.1101/cshperspect.a004903
13. Oskarsson T. Extracellular matrix components in breast cancer progression and metastasis. *Breast.* (2013) 22(Suppl. 2):S66–72. doi: 10.1016/j.breast.2013.07.012
14. Leitinger B, Hohenester E. Mammalian collagen receptors. *Matrix Biol.* (2007) 26:146–55. doi: 10.1016/j.matbio.2006.10.007
15. Xian X, Gopal S, Couchman JR. Syndecans as receptors and organizers of the extracellular matrix. *Cell Tissue Res.* (2010) 339:31–46. doi: 10.1007/s00441-009-0829-3
16. Walker C, Mojares E, del Río Hernández A. Role of extracellular matrix in development and cancer progression. *Int J Mol Sci.* (2018) 19:3028–31. doi: 10.3390/ijms19103028
17. Yue B. Biology of the extracellular matrix: an overview. *J Glaucoma.* (2014) 23:S20–3. doi: 10.1097/IJG.0000000000000108
18. Mouw JK, Ou G, Weaver VM. Extracellular matrix assembly: a multiscale deconstruction. *Nat Publ Gr.* (2014) 15:771–85. doi: 10.1038/nrm3902
19. Theocharis AD, Manou D, Karamanos NK. The extracellular matrix as a multitasking player in disease. *FEBS J.* (2019) 286:2830–69. doi: 10.1111/febs.14818
20. Frantz C, Stewart KM, Weaver VM. The extracellular matrix at a glance. *J Cell Sci.* (2010) 123:4195–200. doi: 10.1242/jcs.023820
21. Levental KR, Yu H, Kass L, Lakins JN, Egeblad M, Erler JT, et al. Matrix crosslinking forces tumor progression by enhancing integrin signaling. *Cell.* (2009) 139:891–906. doi: 10.1016/j.cell.2009.10.027
22. Venning FA, Wullkopf L, Erler JT. Targeting ECM disrupts cancer progression. *Front Oncol.* (2015) 5:224. doi: 10.3389/fonc.2015.00224
23. Gkretsi V, Stylianopoulos T. Cell adhesion and matrix stiffness: coordinating cancer cell invasion and metastasis. *Front Oncol.* (2018) 8:145. doi: 10.3389/fonc.2018.00145
24. Jinka R, Kapoor R, Sistla PG, Raj TA, Pande G. Alterations in cell-extracellular matrix interactions during progression of cancers. *Int J Cell Biol.* (2012) 2012:219196–8. doi: 10.1155/2012/219196
25. Paszek MJ, Zahir N, Johnson KR, Lakins JN, Rozenberg GI, Gefen A, et al. Tensional homeostasis and the malignant phenotype. *Cancer Cell.* (2005) 8:241–54. doi: 10.1016/j.ccr.2005.08.010
26. Butcher DT, Alliston T, Weaver VM. A tense situation: forcing tumour progression. *Nat Rev Cancer.* (2009) 9:108–22. doi: 10.1038/nrc2544
27. Sulzmaier FJ, Jean C, Schlaepfer DD. FAK in cancer: mechanistic findings and clinical applications. *Nat Rev Cancer.* (2014) 14:598–610. doi: 10.1038/nrc3792
28. Hanahan D, Weinberg RA. The hallmarks of cancer. *Cell.* (2000) 100:57–70. doi: 10.1016/S0092-8674(00)81683-9
29. Chang TT, Thakar D, Weaver VM. Force-dependent breaching of the basement membrane. *Matrix Biol.* (2017) 57–58:178–89. doi: 10.1016/j.matbio.2016.12.005
30. Pickup MW, Mouw JK, Weaver VM. The extracellular matrix modulates the hallmarks of cancer. *EMBO Rep.* (2014) 15:1243–53. doi: 10.15252/embr.201439246
31. Assent D, Bourgot I, Hennuy B, Geurts P, Noël A, Foidart J-M, et al. A membrane-type-1 matrix metalloproteinase (MT1-MMP) - discoidin domain receptor 1 axis regulates collagen-induced apoptosis in breast cancer cells. *PLoS ONE.* (2015) 10:e0116006. doi: 10.1371/journal.pone.0116006
32. Maquoi E, Assent D, Detilleux J, Pequeux C, Foidart J-M, Noël A. MT1-MMP protects breast carcinoma cells against type i collagen-induced apoptosis. *Oncogene.* (2012) 31:480–93. doi: 10.1038/onc.2011.249
33. Saby C, Collin G, Sinane M, Buache E, Van Gulick L, Saltel F, et al. DDR1 and MT1-MMP expression levels are determinant for triggering BIK-mediated apoptosis by 3D type I collagen matrix in invasive basal-like breast carcinoma cells. *Front Pharmacol.* (2019) 10:462. doi: 10.3389/fphar.2019.00462
34. Exposito J-Y, Valcourt U, Cluzel C, Lethias C. The fibrillar collagen family. *Int J Mol Sci.* (2010) 11:407–26. doi: 10.3390/ijms11020407
35. Exposito J-Y, Cluzel C, Garrone R, Lethias C. Evolution of collagens. *Anat Rec.* (2002) 268:302–16. doi: 10.1002/ar.10162
36. Myllyharju J, Kivirikko KI. Collagens, modifying enzymes and their mutations in humans, flies and worms. *Trends Genet.* (2004) 20:33–43. doi: 10.1016/j.tig.2003.11.004
37. Ricard-Blum S, Ruggiero F. The collagen superfamily: from the extracellular matrix to the cell membrane. *Pathol Biol.* (2005) 53:430–42. doi: 10.1016/j.patbio.2004.12.024
38. Bateman JF, Boot-Handford RP, Lamandé SR. Genetic diseases of connective tissues: cellular and extracellular effects of ECM mutations. *Nat Rev Genet.* (2009) 10:173–83. doi: 10.1038/nrg2520
39. Mayne R, Burgeson RE. *Structure and function of collagen types.* Orlando: Academic Press (1987).
40. Van der Rest M, Garrone R. Collagen family of proteins. *FASEB J.* (1991) 5:2814–23. doi: 10.1096/fasebj.5.13.1916105
41. Ricard-Blum S. The collagen family. *Cold Spring Harb Perspect Biol.* (2011) 3:a004978. doi: 10.1101/cshperspect.a004978
42. Brodsky B, Persikov AV. Molecular structure of the collagen triple helix. *Adv Protein Chem.* (2005) 70:301–39. doi: 10.1016/S0065-3233(05)70009-7
43. Hulmes DJS. Collagen diversity, synthesis and assembly BT – collagen. In: Fratzl P, editor. *Collagen.* Boston, MA: Springer (2008). p. 15–47.
44. Lees JF, Tasab M, Bulleid NJ. Identification of the molecular recognition sequence which determines the type-specific assembly of procollagen. *EMBO J.* (1997) 65:908–16. doi: 10.1093/emboj/16.5.908
45. Hofmann H, Fietzek PP, Kuhn K. The role of polar and hydrophobic interactions for the molecular packing of type I collagen: a three-dimensional evaluation of the amino acid sequence. *J Mol Biol.* (1978) 125:137–65. doi: 10.1016/0022-2836(78)90342-X
46. Hoffman GG, Branam AM, Huang G, Pelegri F, Cole WG, Wenstrup RM, et al. Characterization of the six zebrafish clade B fibrillar procollagen genes, with evidence for evolutionarily conserved alternative splicing within the pro-α1(V) C-propeptide. *Matrix Biol.* (2010) 29:261–75. doi: 10.1016/j.matbio.2010.01.006
47. Fang M, Jacob R, McDougal O, Oxford JT. Minor fibrillar collagens, variable regions alternative splicing, intrinsic disorder, and tyrosine sulfation. *Protein Cell.* (2012) 3:419–33. doi: 10.1007/s13238-012-2917-5
48. Eyre DR, Weis MA, Wu J-J. Articular cartilage collagen: an irreplaceable framework? *Eur Cells Mater.* (2006) 12:57–63. doi: 10.22203/eCM.v012a07
49. Boot-Handford RP, Tuckwell DS, Plumb DA, Rock CF, Poulsom R. A novel and highly conserved collagen (pro(alpha)1(XXVII)) with a unique expression pattern and unusual molecular characteristics establishes a new clade within the vertebrate fibrillar collagen family. *J Biol Chem.* (2003) 278:31067–77. doi: 10.1074/jbc.M212889200
50. Koch M, Schulze J, Hansen U, Ashwodt T, Keene DR, Brunken WJ, et al. A novel marker of tissue junctions, collagen XXII. *J Biol Chem.* (2004) 279:22514–21. doi: 10.1074/jbc.M400536200
51. von der Mark H, Aumailley M, Wick G, Fleischmajer R, Timpl R. Immunochemistry, genuine size tissue localization of collagen VI. *Eur J Biochem.* (1984) 142:493–502. doi: 10.1111/j.1432-1033.1984.tb08313.x
52. Shaw LM, Olsen BR. FACIT collagens: diverse molecular bridges in extracellular matrices. *Trends Biochem Sci.* (1991) 16:191–4. doi: 10.1016/0968-0004(91)90074-6
53. Kadler KE, Baldock C, Bella J, Boot-Handford RP. Collagens at a glance. *J Cell Sci.* (2007) 120:1955–8. doi: 10.1242/jcs.03453
54. Gelse K. Collagens—structure, function, and biosynthesis. *Adv Drug Deliv Rev.* (2003) 55:1531–46. doi: 10.1016/j.addr.2003.08.002
55. Fleischmajer R, Perlish JS, Burgeson RE, Bahai FS, Timpl R. Type I and Type III collagen interactions during fibrillogenesisa. *Ann N Y Acad Sci.* (1990) 580:161–75. doi: 10.1111/j.1749-6632.1990.tb17927.x
56. Niyibizi C, Eyre DR. Bone Type V collagen: chain composition and location of a trypsin cleavage site. *Connect Tissue Res.* (2009) 20:247–50. doi: 10.3109/03008208909023894
57. Mayne R. Cartilage collagens. what is their function, and are they involved in articular disease? *Arthritis Rheum.* (1989) 32:241–6. doi: 10.1002/anr.1780320302
58. von der Mark K, Schöber S, Goodman SL. Integrins in cell migration BT - integrin Protocols. In: Howlett A, editor. *Integrin Protocols.* NJ: Humana Press (1999). p. 219–230.

59. Kivirikko KI, Kishida Y, Sakakibara S, Prockop DJ. Hydroxylation of (X-Pro-Gly)n by protocollagen proline hydroxylase effect of chain length, helical conformation and amino acid sequence in the substrate. *Biochim Biophys Acta Protein Struct.* (1972) 271:347–56. doi: 10.1016/0005-2795(72)90209-7
60. Persikov AV, Ramshaw JAM, Kirkpatrick A, Brodsky B. Electrostatic interactions involving lysine make major contributions to collagen triple-helix stability. *Biochemistry.* (2005) 44:1414–22. doi: 10.1021/bi048216r
61. Fallas JA, Gauba V, Hartgerink JD. Solution structure of an ABC collagen heterotrimer reveals a single-register helix stabilized by electrostatic interactions. *J Biol Chem.* (2009) 284:26851–9. doi: 10.2210/pdb2klw/pdb
62. Bella J, Eaton M, Brodsky B, Berman HM. Crystal and molecular structure of a collagen-like peptide at 1.9 A resolution. *Science.* (1994) 266:75–81. doi: 10.1126/science.7695699
63. Bourhis J-M, Mariano N, Zhao Y, Harlos K, Exposito J-Y, Jones EY, et al. Structural basis of fibrillar collagen trimerization and related genetic disorders. *Nat Struct Mol Biol.* (2012) 19:1031–6. doi: 10.1038/nsmb.2389
64. McLaughlin SH, Bulleid NJ. Molecular recognition in procollagen chain assembly. *Matrix Biol.* (1998) 16:369–77. doi: 10.1016/S0945-053X(98)90010-5
65. Gillberg L, Berg S, de Verdier PJ, Lindbom L, Werr J, Hellstrom PM. Effective treatment of mouse experimental colitis by alpha 2 integrin antibody: comparison with alpha 4 antibody and conventional therapy. *Acta Physiol.* (2013) 207:326–36. doi: 10.1111/apha.12017
66. Ghatak S, Niland S, Schulz JN, Wang F, Eble JA, Leitges M, et al. Role of integrins α1β1 and α2β1 in wound and tumor angiogenesis in mice. *Am J Pathol.* (2016) 186:3011–27. doi: 10.1016/j.ajpath.2016.06.021
67. Bekhouche M, Colige A. The procollagen N-proteinases ADAMTS2, 3 and 14 in pathophysiology. *Matrix Biol.* (2015) 44–46:46–53. doi: 10.1016/j.matbio.2015.04.001
68. Vadon-Le Goff S, Hulmes DJS, Moali C. BMP-1/tolloid-like proteinases synchronize matrix assembly with growth factor activation to promote morphogenesis and tissue remodeling. *Matrix Biol.* (2015) 44–46:14–23. doi: 10.1016/j.matbio.2015.02.006
69. Hulmes DJS. Building collagen molecules, fibrils, and suprafibrillar structures. *J Struct Biol.* (2002) 137:2–10. doi: 10.1006/jsbi.2002.4450
70. Porter S, Clark IM, Kevorkian L, Edwards DR. The ADAMTS metalloproteinases. *Biochem J.* (2005) 386:15–27. doi: 10.1042/BJ20040424
71. Hopkins DR, Keles S, Greenspan DS. The bone morphogenetic protein 1/Tolloid-like metalloproteinases. *Matrix Biol.* (2007) 26:508–23. doi: 10.1016/j.matbio.2007.05.004
72. Colige A, Ruggiero F, Vandenberghe I, Dubail J, Kesteloot F, Van Beeumen J, et al. Domains and maturation processes that regulate the activity of ADAMTS-2, a metalloproteinase cleaving the aminopropeptide of fibrillar procollagens types I–III and V. *J Biol Chem.* (2005) 280:34397–408. doi: 10.1074/jbc.M506458200
73. Le Goff C, Somerville RPT, Kesteloot F, Powell K, Birk DE, Colige AC, et al. Regulation of procollagen amino-propeptide processing during mouse embryogenesis by specialization of homologous ADAMTS proteases: insights on collagen biosynthesis and dermatosparaxis. *Development.* (2006) 133:1587–96. doi: 10.1242/dev.02308
74. Prockop DJ, Sieron AL, Li S-W. Procollagen N-proteinase and procollagen C-proteinase. Two unusual metalloproteinases that are essential for procollagen processing probably have important roles in development and cell signaling. *Matrix Biol.* (1998) 16:399–408. doi: 10.1016/S0945-053X(98)90013-0
75. Prockop DJ, Fertala A. Inhibition of the self-assembly of collagen I into fibrils with synthetic peptides. Demonstration that assembly is driven by specific binding sites on the monomers. *J Biol Chem.* (1998) 273:15598–604. doi: 10.1074/jbc.273.25.15598
76. Artym VV, Matsumoto K. Imaging cells in three-dimensional collagen matrix. *Curr Protoc Cell Biol.* (2010) 48:10.18.1-10.18.20. doi: 10.1002/0471143030.cb1018s48
77. Wenstrup RJ, Florer JB, Brunskill EW, Bell SM, Chervoneva I, Birk DE. Type V collagen controls the initiation of collagen fibril assembly. *J Biol Chem.* (2004) 279:53331–7. doi: 10.1074/jbc.M409622200
78. Kadler KE, Holmes DF, Trotter JA, Chapman JA. Collagen fibril formation. *Biochem J.* (1996) 316:1–11. doi: 10.1042/bj3160001
79. Yamauchi M, Sricholpech M. Lysine post-translational modifications of collagen. *Essays Biochem.* (2012) 52:113–33. doi: 10.1042/bse0520113
80. Trackman PC. Enzymatic and non-enzymatic functions of the lysyl oxidase family in bone. *Matrix Biol.* (2016) 52–54:7–18. doi: 10.1016/j.matbio.2016.01.001
81. Mäki JM. Lysyl oxidases in mammalian development and certain pathological conditions. *Histol Histopathol.* (2009) 24:651–60. doi: 10.14670/HH-24.651
82. Lucero HA, Kagan HM. Lysyl oxidase: an oxidative enzyme and effector of cell function. *Cell Mol Life Sci.* (2006) 63:2304–16. doi: 10.1007/s00018-006-6149-9
83. Rucker RB, Murray J. Cross-linking amino acids in collagen and elastin. *Am J Clin Nutr.* (1978) 31:1221–36. doi: 10.1093/ajcn/31.7.1221
84. Orgel JP, Wess TJ, Miller A. The *in situ* conformation and axial location of the intermolecular cross-linked non-helical telopeptides of type I collagen. *Structure.* (2000) 8:137–42. doi: 10.1016/S0969-2126(00)00089-7
85. Bruckner P. Suprastructures of extracellular matrices: paradigms of functions controlled by aggregates rather than molecules. *Cell Tissue Res.* (2009) 339:7–18. doi: 10.1007/s00441-009-0864-0
86. Molnar J, Fong KSK, He QP, Hayashi K, Kim Y, Fong SFT, et al. Structural and functional diversity of lysyl oxidase and the LOX-like proteins. *Biochim Biophys Acta Proteins Proteomics.* (2003) 1647:220–24. doi: 10.1016/S1570-9639(03)00053-0
87. Dvorak HF. Tumors: wounds that do not heal. Similarities between tumor stroma generation and wound healing. *N Engl J Med.* (1986) 315:1650–9. doi: 10.1056/NEJM198612253152606
88. Hanahan D, Coussens LM. Accessories to the crime: functions of cells recruited to the tumor microenvironment. *Cancer Cell.* (2012) 21:309–22. doi: 10.1016/j.ccr.2012.02.022
89. Bissell MJ, Hines WC. Why don't we get more cancer? A proposed role of the microenvironment in restraining cancer progression. *Nat Med.* (2011) 17:320–29. doi: 10.1038/nm.2328
90. Pietras K, Östman A. Hallmarks of cancer: interactions with the tumor stroma. *Exp Cell Res.* (2010) 316:1324–31. doi: 10.1016/j.yexcr.2010.02.045
91. Collins MA, Bednar F, Zhang Y, Brisset J-C, Galbán S, Galbán CJ, et al. Oncogenic Kras is required for both the initiation and maintenance of pancreatic cancer in mice. *J Clin Invest.* (2012) 122:639–53. doi: 10.1172/JCI59227
92. Helms E, Onate MK, Sherman MH. Fibroblast heterogeneity in the pancreatic tumor microenvironment. *Cancer Discov.* (2020) 10:648–56. doi: 10.1158/2159-8290.CD-19-1353
93. Pankova D, Chen Y, Terajima M, Schliekelman MJ, Baird BN, Fahrenholtz M, et al. Cancer-associated fibroblasts induce a collagen cross-link switch in tumor stroma. *Mol Cancer Res.* (2016) 14:287–95. doi: 10.1158/1541-7786.MCR-15-0307
94. Costa A, Kieffer Y, Scholer-Dahirel A, Pelon F, Bourachot B, Cardon M, et al. Fibroblast heterogeneity and immunosuppressive environment in human breast cancer. *Cancer Cell.* (2018) 33:463–79.e10. doi: 10.1016/j.ccell.2018.01.011
95. Bartoschek M, Oskolkov N, Bocci M, Lövrot J, Larsson C, Sommarin M, et al. Spatially and functionally distinct subclasses of breast cancer-associated fibroblasts revealed by single cell RNA sequencing. *Nat Commun.* (2018) 9:5150. doi: 10.1038/s41467-018-07582-3
96. Evans RA, Tian YC, Steadman R, Phillips AO. TGF-β1-mediated fibroblast–myofibroblast terminal differentiation—the role of smad proteins. *Exp Cell Res.* (2003) 282:90–100. doi: 10.1016/S0014-4827(02)00015-0
97. Vaughan MB, Howard EW, Tomasek JJ. Transforming growth factor-β1 promotes the morphological and functional differentiation of the myofibroblast. *Exp Cell Res.* (2000) 257:180–89. doi: 10.1006/excr.2000.4869
98. Lopez JI, Kang I, You W-K, McDonald DM, Weaver VM. *In situ* force mapping of mammary gland transformation. *Integr Biol.* (2011) 3:910–21. doi: 10.1039/c1ib00043h
99. Acerbi I, Cassereau L, Dean I, Shi Q, Au A, Park C, et al. Human breast cancer invasion and aggression correlates with ECM stiffening and immune cell infiltration. *Integr Biol.* (2015) 7:1120–34. doi: 10.1039/c5ib00040h
100. Cox TR, Erler JT. Remodeling and homeostasis of the extracellular matrix: implications for fibrotic diseases and cancer. *Dis Model Mech.* (2011) 4:165–78. doi: 10.1242/dmm.004077

101. Friedl P, Wolf K. Tube travel: the role of proteases in individual and collective cancer cell invasion. *Cancer Res.* (2008) 68:7247–9. doi: 10.1158/0008-5472.CAN-08-0784
102. Gritsenko PG, Ilina O, Friedl P. Interstitial guidance of cancer invasion. *J Pathol.* (2012) 226:185–99. doi: 10.1002/path.3031
103. Provenzano PP, Eliceiri KW, Campbell JM, Inman DR, White JG, Keely PJ. Collagen reorganization at the tumor-stromal interface facilitates local invasion. *BMC Med.* (2006) 4:215–23. doi: 10.1186/1741-7015-4-38
104. Condeelis J, Segall JE. Intravital imaging of cell movement in tumours. *Nat Rev Cancer.* (2003) 3:921–30. doi: 10.1038/nrc1231
105. Kraning-Rush CM, Carey SP, Lampi MC, Reinhart-King CA. Microfabricated collagen tracks facilitate single cell metastatic invasion in 3D. *Integr Biol.* (2013) 5:606–16. doi: 10.1039/c3ib20196a
106. Riching KM, Cox BL, Salick MR, Pehlke C, Riching AS, Ponik SM, et al. 3D collagen alignment limits protrusions to enhance breast cancer cell persistence. *Biophys J.* (2014) 107:2546–58. doi: 10.1016/j.bpj.2014.10.035
107. Wolf K, te Lindert M, Krause M, Alexander S, te Riet J, Willis AL, et al. Physical limits of cell migration: control by ECM space and nuclear deformation and tuning by proteolysis and traction force. *J Cell Biol.* (2013) 201:1069–84. doi: 10.1083/jcb.201210152
108. Pathak A, Kumar S. Independent regulation of tumor cell migration by matrix stiffness and confinement. *Proc Natl Acad Sci USA.* (2012) 109:10334–9. doi: 10.1073/pnas.1118073109
109. Doyle AD, Petrie RJ, Kutys ML, Yamada KM. Dimensions in cell migration. *Curr Opin Cell Biol.* (2013) 25:642–9. doi: 10.1016/j.ceb.2013.06.004
110. Fenner J, Stacer AC, Winterroth F, Johnson TD, Luker KE, Luker GD. Macroscopic stiffness of breast tumors predicts metastasis. *Sci Rep.* (2014) 4:5512. doi: 10.1038/srep05512
111. Reid SE, Kay EJ, Neilson LJ, Henze AT, Serneels J, McGhee EJ, et al. Tumor matrix stiffness promotes metastatic cancer cell interaction with the endothelium. *EMBO J.* (2017) 36:2373–89. doi: 10.15252/embj.201694912
112. Harada T, Swift J, Irianto J, Shin J-W, Spinler KR, Athirasala A, et al. Nuclear lamin stiffness is a barrier to 3D migration, but softness can limit survival. *J Cell Biol.* (2014) 204:669–82. doi: 10.1083/jcb.201308029
113. Denais CM, Gilbert RM, Isermann P, McGregor AL, te Lindert M, Weigelin B, et al. Nuclear envelope rupture and repair during cancer cell migration. *Science.* (2016) 352:353–8. doi: 10.1126/science.aad7297
114. Paul CD, Mistriotis P, Konstantopoulos K. Cancer cell motility: lessons from migration in confined spaces. *Nat Rev Cancer.* (2017) 17:131–40. doi: 10.1038/nrc.2016.123
115. Petrie RJ, Yamada KM. Multiple mechanisms of 3D migration: the origins of plasticity. *Curr Opin Cell Biol.* (2016) 42:7–12. doi: 10.1016/j.ceb.2016.03.025
116. Gaggioli C, Hooper S, Hidalgo-Carcedo C, Grosse R, Marshall JF, Harrington K, et al. Fibroblast-led collective invasion of carcinoma cells with differing roles for RhoGTPases in leading and following cells. *Nat Cell Biol.* (2007) 9:1392–400. doi: 10.1038/ncb1658
117. Sharma P, Ng C, Jana A, Padhi A, Szymanski P, Lee JSH, et al. Aligned fibers direct collective cell migration to engineer closing and nonclosing wound gaps. *Mol Biol Cell.* (2017) 28:2579–88. doi: 10.1091/mbc.e17-05-0305
118. Ray A, Slama ZM, Morford RK, Madden SA, Provenzano PP. Enhanced directional migration of cancer stem cells in 3D aligned collagen matrices. *Biophys J.* (2017) 112:1023–36. doi: 10.1016/j.bpj.2017.01.007
119. Malik R, Lelkes PI, Cukierman E. Biomechanical and biochemical remodeling of stromal extracellular matrix in cancer. *Trends Biotechnol.* (2015) 33:230–6. doi: 10.1016/j.tibtech.2015.01.004
120. Beacham DA, Cukierman E. Stromagenesis: the changing face of fibroblastic microenvironments during tumor progression. *Semin Cancer Biol.* (2005) 15:329–41. doi: 10.1016/j.semcancer.2005.05.003
121. Conklin MW, Eickhoff JC, Riching KM, Pehlke CA, Eliceiri KW, Provenzano PP, et al. Aligned collagen is a prognostic signature for survival in human breast carcinoma. *AJPA.* (2011) 178:1221–32. doi: 10.1016/j.ajpath.2010.11.076
122. Conklin MW, Gangnon RE, Sprague BL, Van Gemert L, Hampton JM, Eliceiri KW, et al. Collagen alignment as a predictor of recurrence after ductal carcinoma *in situ*. *Cancer Epidemiol Prev Biomarkers.* (2018) 27:138–45. doi: 10.1158/1055-9965.EPI-17-0720
123. Colpaert C, Vermeulen P, Jeuris W, van Beest P, Goovaerts G, Weyler J, et al. Early distant relapse in 'node-negative' breast cancer patients is not predicted by occult axillary lymph node metastases, but by the features of the primary tumour. *J Pathol.* (2001) 193:442–9. doi: 10.1002/path.829
124. Ford AJ, Orbach SM, Rajagopalan P. Fibroblasts stimulate macrophage migration in interconnected extracellular matrices through tunnel formation and fiber alignment. *Biomaterials.* (2019) 209:88–102. doi: 10.1016/j.biomaterials.2019.03.044
125. Jia H, Janjanam J, Wu SC, Wang R, Pano G, Celestine M, et al. The tumor cell-secreted matricellular protein WISP1 drives pro-metastatic collagen linearization. *EMBO J.* (2019) 38:315–55. doi: 10.15252/embj.201801302
126. Lee H-O, Mullins SR, Franco-Barraza J, Valianou M, Cukierman E, Cheng JD. FAP-overexpressing fibroblasts produce an extracellular matrix that enhances invasive velocity and directionality of pancreatic cancer cells. *BMC Cancer.* (2011) 11:245. doi: 10.1186/1471-2407-11-245
127. Heldin C-H, Rubin K, Pietras K, Östman A. High interstitial fluid pressure — an obstacle in cancer therapy. *Nat Rev Cancer.* (2004) 4:806–13. doi: 10.1038/nrc1456
128. Olivares O, Mayers JR, Gouirand V, Torrence ME, Gicquel T, Borge L, et al. Collagen-derived proline promotes pancreatic ductal adenocarcinoma cell survival under nutrient limited conditions. *Nat Commun.* (2017) 8:16014–31. doi: 10.1038/ncomms16031
129. de Fougerolles AR, Sprague AG, Nickerson-Nutter CL, Chi-Rosso G, Rennert PD, Gardner H, et al. Regulation of inflammation by collagen-binding integrins alpha1beta1 and alpha2beta1 in models of hypersensitivity and arthritis. *J Clin Invest.* (2000) 105:721–9. doi: 10.1172/JCI7911
130. Naba A, Clauser KR, Hoersch S, Liu H, Carr SA, Hynes RO. The matrisome: *in silico* definition and *in vivo* characterization by proteomics of normal and tumor extracellular matrices. *Mol Cell Proteomics.* (2012) 11:M111.014647. doi: 10.1074/mcp.M111.014647
131. Naba A, Clauser KR, Lamar JM, Carr SA, Hynes RO. Extracellular matrix signatures of human mammary carcinoma identify novel metastasis promoters. *Elife.* (2014) 3:e01308. doi: 10.7554/eLife.01308
132. Zahir N, Weaver VM. Death in the third dimension: apoptosis regulation and tissue architecture. *Curr Opin Genet Dev.* (2004) 14:71–80. doi: 10.1016/j.gde.2003.12.005
133. Jenkins MH, Croteau W, Mullins DW, Brinckerhoff CE. The BRAFV600E inhibitor, PLX4032, increases type I collagen synthesis in melanoma cells. *Matrix Biol.* (2015) 48:66–77. doi: 10.1016/j.matbio.2015.05.007
134. Afik R, Zigmond E, Vugman M, Klepfish M, Shimshoni E, Pasmanik-Chor M, et al. Tumor macrophages are pivotal constructors of tumor collagenous matrix. *J Exp Med.* (2016) 213:2315–31. doi: 10.1084/jem.20151193
135. Drifka CR, Loeffler AG, Mathewson K, Keikhosravi A, Eickhoff JC, Liu Y, et al. Highly aligned stromal collagen is a negative prognostic factor following pancreatic ductal adenocarcinoma resection. *Oncotarget.* (2016) 7:76197–213. doi: 10.18632/oncotarget.12772
136. Hanley CJ, Noble F, Ward M, Bullock M, Drifka C, Mellone M, et al. A subset of myofibroblastic cancer-associated fibroblasts regulate collagen fiber elongation, which is prognostic in multiple cancers. *Oncotarget.* (2016) 7:6159–74. doi: 10.18632/oncotarget.6740
137. Kehlet SN, Sanz-Pamplona R, Brix S, Leeming DJ, Karsdal MA, Moreno V. Excessive collagen turnover products are released during colorectal cancer progression and elevated in serum from metastatic colorectal cancer patients. *Sci Rep.* (2016) 6:30599. doi: 10.1038/srep30599
138. Willumsen N, Bager CL, Leeming DJ, Smith V, Christiansen C, Karsdal MA, et al. Serum biomarkers reflecting specific tumor tissue remodeling processes are valuable diagnostic tools for lung cancer. *Cancer Med.* (2014) 3:1136–45. doi: 10.1002/cam4.303
139. Lu P, Weaver VM, Werb Z. The extracellular matrix: a dynamic niche in cancer progression. *J Cell Biol.* (2012) 196:395–406. doi: 10.1083/jcb.201102147
140. Bager CL, Willumsen N, Leeming DJ, Smith V, Karsdal MA, Dornan D, et al. Collagen degradation products measured in serum can separate ovarian and breast cancer patients from healthy controls: a preliminary study. *Cancer Biomark.* (2015) 15:783–8. doi: 10.3233/CBM-150520
141. Mammoto T, Jiang A, Jiang E, Panigrahy D, Kieran MW, Mammoto A. Role of collagen matrix in tumor angiogenesis and glioblastoma multiforme progression. *Am J Pathol.* (2013) 183:1293–305. doi: 10.1016/j.ajpath.2013.06.026

142. Thangavelu PU, Krenács T, Dray E, Duijf PHG. In epithelial cancers, aberrant COL17A1 promoter methylation predicts its misexpression and increased invasion. *Clin Epigenetics.* (2016) 8:120. doi: 10.1186/s13148-016-0290-6
143. Matte BF, Kumar A, Placone JK, Zanella VG, Martins MD, Engler AJ, et al. Matrix stiffness mechanically conditions EMT and migratory behavior of oral squamous cell carcinoma. *J Cell Sci.* (2019) 132:jcs224360. doi: 10.1242/jcs.224360
144. Townson JL, Chambers AF. Dormancy of solitary metastatic cells. *Cell Cycle.* (2006) 5:1744–50. doi: 10.4161/cc.5.16.2864
145. Wikman H, Vessella R, Pantel K. Cancer micrometastasis and tumour dormancy. *APMIS.* (2008) 116:754–70. doi: 10.1111/j.1600-0463.2008.01033.x
146. Barkan D, El Touny LH, Michalowski AM, Smith JA, Chu I, Davis AS, et al. Metastatic growth from dormant cells induced by a col-I-enriched fibrotic environment. *Cancer Res.* (2010) 70:5706–16. doi: 10.1158/0008-5472.CAN-09-2356
147. Brisson BK, Mauldin EA, Lei W, Vogel LK, Power AM, Lo A, et al. Type III collagen directs stromal organization and limits metastasis in a murine model of breast cancer. *Am J Pathol.* (2015) 185:1471–86. doi: 10.1016/j.ajpath.2015.01.029
148. Chintala SK, Sawaya R, Gokaslan ZL, Rao JS. The effect of type III collagen on migration and invasion of human glioblastoma cell lines *in vitro*. *Cancer Lett.* (1996) 102:57–63. doi: 10.1016/0304-3835(96)04163-8
149. Ma H-P, Chang H-L, Bamodu OA, Yadav VK, Huang T-Y, Wu ATH, et al. Collagen 1A1 (COL1A1) is a reliable biomarker and putative therapeutic target for hepatocellular carcinogenesis and metastasis. *Cancers.* (2019) 11:786. doi: 10.3390/cancers11060786
150. Zhu H, Chen H, Wang J, Zhou L, Liu S. Collagen stiffness promoted non-muscle-invasive bladder cancer progression to muscle-invasive bladder cancer. *Onco Targets Ther.* (2019) 12:3441–57. doi: 10.2147/OTT.S194568
151. Sun S, Wang Y, Wu Y, Gao Y, Li Q, Abdulrahman AA, et al. Identification of COL1A1 as an invasion-related gene in malignant astrocytoma. *Int J Oncol.* (2018) 53:2542–54. doi: 10.3892/ijo.2018.4568
152. Liu J, Shen J-X, Wu H-T, Li X-L, Wen X-F, Du C-W, et al. Collagen 1A1 (COL1A1) promotes metastasis of breast cancer and is a potential therapeutic target. *Discov Med.* (2018) 25:211–23.
153. Zhang Z, Wang Y, Zhang J, Zhong J, Yang R. COL1A1 promotes metastasis in colorectal cancer by regulating the WNT/PCP pathway. *Mol Med Rep.* (2018) 17:5037–42. doi: 10.3892/mmr.2018.8533
154. He B, Lin X, Tian F, Yu W, Qiao B. MiR-133a-3p inhibits oral squamous cell carcinoma (OSCC) proliferation and invasion by suppressing COL1A1. *J Cell Biochem.* (2018) 119:338–46. doi: 10.1002/jcb.26182
155. Wang Q, Yu J. MiR-129-5p suppresses gastric cancer cell invasion and proliferation by inhibiting COL1A1. *Biochem Cell Biol.* (2018) 96:19–25. doi: 10.1139/bcb-2016-0254
156. Ji J, Zhao L, Budhu A, Forgues M, Jia H-L, Qin L-X, et al. Let-7g targets collagen type I alpha2 and inhibits cell migration in hepatocellular carcinoma. *J Hepatol.* (2010) 52:690–7. doi: 10.1016/j.jhep.2009.12.025
157. Wang J, Gao P, Song Y, Sun J, Chen X, Yu H, et al. Prognostic value of gastric cancer-associated gene signatures: evidence based on a meta-analysis using integrated bioinformatics methods. *J Cell Mol Med.* (2018) 22:5743–7. doi: 10.1111/jcmm.13823
158. Yan Z, Xu W, Xiong Y, Cheng Y, Xu H, Wang Z, et al. Highly accurate two-gene signature for gastric cancer. *Med Oncol.* (2013) 30:584. doi: 10.1007/s12032-013-0584-x
159. Yue H, Wang J, Chen R, Hou X, Li J, Lu X. Gene signature characteristic of elevated stromal infiltration and activation is associated with increased risk of hematogenous and lymphatic metastasis in serous ovarian cancer. *BMC Cancer.* (2019) 19:1266. doi: 10.1186/s12885-019-6470-y
160. Engqvist H, Parris TZ, Kovács A, Nemes S, Werner Rönnerman E, De Lara S, et al. Immunohistochemical validation of COL3A1, GPR158 and PITHD1 as prognostic biomarkers in early-stage ovarian carcinomas. *BMC Cancer.* (2019) 19:912–28. doi: 10.1186/s12885-019-6084-4
161. Januchowski R, Swierczewska M, Sterzynska K, Wojtowicz K, Nowicki M, Zabel M. Increased expression of several collagen genes is associated with drug resistance in ovarian cancer cell lines. *J Cancer.* (2016) 7:1295–310. doi: 10.7150/jca.15371
162. Yuan L, Shu B, Chen L, Qian K, Wang Y, Qian G, et al. Overexpression of COL3A1 confers a poor prognosis in human bladder cancer identified by co-expression analysis. *Oncotarget.* (2017) 8:70508–20. doi: 10.18632/oncotarget.19733
163. Gao Y-F, Mao X-Y, Zhu T, Mao C-X, Liu Z-X, Wang Z-B, et al. COL3A1 and SNAP91: novel glioblastoma markers with diagnostic and prognostic value. *Oncotarget.* (2016) 7:70494–503. doi: 10.18632/oncotarget.12038
164. Wang X-Q, Tang Z-X, Yu D, Cui S-J, Jiang Y-H, Zhang Q, et al. Epithelial but not stromal expression of collagen alpha-1(III) is a diagnostic and prognostic indicator of colorectal carcinoma. *Oncotarget.* (2016) 7:8823–38. doi: 10.18632/oncotarget.6815
165. Ren W, Zhang Y, Zhang L, Lin Q, Zhang J, Xu G. Overexpression of collagen type V α1 chain in human breast invasive ductal carcinoma is mediated by TGF-β1. *Int J Oncol.* (2018) 52:1694–704. doi: 10.3892/ijo.2018.4317
166. Liu W, Wei H, Gao Z, Chen G, Liu Y, Gao X, et al. COL5A1 may contribute the metastasis of lung adenocarcinoma. *Gene.* (2018) 665:57–66. doi: 10.1016/j.gene.2018.04.066
167. Feng G, Ma H-M, Huang H-B, Li Y-W, Zhang P, Huang J-J, et al. Overexpression of COL5A1 promotes tumor progression and metastasis and correlates with poor survival of patients with clear cell renal cell carcinoma. *Cancer Manag Res.* (2019) 11:1263–74. doi: 10.2147/CMAR.S188216
168. Chen H-C, Tseng Y-K, Shu C-W, Weng T-J, Liou H-H, Yen L-M, et al. Differential clinical significance of COL5A1 and COL5A2 in tongue squamous cell carcinoma. *J Oral Pathol Med.* (2019) 48:468–76. doi: 10.1111/jop.12861
169. Wu M, Sun Q, Mo C-H, Pang J-S, Hou J-Y, Pang L-L, et al. Prospective molecular mechanism of COL5A1 in breast cancer based on a microarray, RNA sequencing and immunohistochemistry. *Oncol Rep.* (2019) 42:151–75. doi: 10.3892/or.2019.7147
170. Zeng X-T, Liu X-P, Liu T-Z, Wang X-H. The clinical significance of COL5A2 in patients with bladder cancer: a retrospective analysis of bladder cancer gene expression data. *Medicine.* (2018) 97:e0091. doi: 10.1097/MD.0000000000010091
171. Huang G, Ge G, Izzi V, Greenspan DS. α3 chains of type V collagen regulate breast tumour growth via glypican-1. *Nat Commun.* (2017) 8:14351. doi: 10.1038/ncomms14351
172. Wu YH, Chang TH, Huang YF, Huang HD, Chou C-Y. COL11A1 promotes tumor progression and predicts poor clinical outcome in ovarian cancer. *Oncogene.* (2014) 33:3432–40. doi: 10.1038/onc.2013.307
173. Wu Y-H, Chang T-H, Huang Y-F, Chen C-C, Chou C-Y. COL11A1 confers chemoresistance on ovarian cancer cells through the activation of Akt/c/EBPβ pathway and PDK1 stabilization. *Oncotarget.* (2015) 6:23748–63. doi: 10.18632/oncotarget.4250
174. Shen L, Yang M, Lin Q, Zhang Z, Zhu B, Miao C. COL11A1 is overexpressed in recurrent non-small cell lung cancer and promotes cell proliferation, migration, invasion and drug resistance. *Oncol Rep.* (2016) 36:877–85. doi: 10.3892/or.2016.4869
175. Jia D, Liu Z, Deng N, Tan TZ, Huang RY-J, Taylor-Harding B, et al. A COL11A1-correlated pan-cancer gene signature of activated fibroblasts for the prioritization of therapeutic targets. *Cancer Lett.* (2016) 382:203–14. doi: 10.1016/j.canlet.2016.09.001
176. Li A, Li J, Lin J, Zhuo W, Si J. COL11A1 is overexpressed in gastric cancer tissues and regulates proliferation, migration and invasion of HGC-27 gastric cancer cells *in vitro*. *Oncol Rep.* (2017) 37:333–40. doi: 10.3892/or.2016.5276
177. Zhang B, Zhang C, Yang X, Chen Y, Zhang H, Liu J, et al. Cytoplasmic collagen XIαI as a prognostic biomarker in esophageal squamous cell carcinoma. *Cancer Biol Ther.* (2018) 19:364–72. doi: 10.1080/15384047.2018.1423915
178. Sun D, Jin H, Zhang J, Tan X. Integrated whole genome microarray analysis and immunohistochemical assay identifies COL11A1, GJB2 and CTRL as predictive biomarkers for pancreatic cancer. *Cancer Cell Int.* (2018) 18:174–11. doi: 10.1186/s12935-018-0669-x
179. Toss MS, Miligy IM, Gorringe KL, Aleskandarany MA, Alkawaz A, Mittal K, et al. Collagen (XI) alpha-1 chain is an independent prognostic factor in breast ductal carcinoma *in situ*. *Mod Pathol.* (2019) 32:1460–72. doi: 10.1038/s41379-019-0286-9
180. Misawa K, Kanazawa T, Imai A, Endo S, Mochizuki D, Fukushima H, et al. Prognostic value of type XXII and XXIV collagen mRNA

expression in head and neck cancer patients. *Mol Clin Oncol.* (2014) 2:285–91. doi: 10.3892/mco.2013.233
181. Wang F, Dong J, Zhang Y, Yue S, Guo H, Liang P, et al. Identification of novel diagnostic and prognostic biomarkers for hepatocellular carcinoma. *Oncol Rep*. (2019) 43:87–98. doi: 10.3892/or.2019.7415
182. Nagy Á, Lánczky A, Menyhárt O, Gyorffy B. Validation of miRNA prognostic power in hepatocellular carcinoma using expression data of independent datasets. *Sci Rep.* (2018) 8:9227–9. doi: 10.1038/s41598-018-29514-3
183. Siegel RL, Miller KD, Jemal A. Cancer statistics, 2018. *CA Cancer J Clin.* (2018) 68:7–30. doi: 10.3322/caac.21442
184. Fane M, Weeraratna AT. How the ageing microenvironment influences tumour progression. *Nat Rev Cancer.* (2019) 20:89–106. doi: 10.1038/s41568-019-0222-9
185. Panwar P, Lamour G, Mackenzie NCW, Yang H, Ko F, Li H, et al. Changes in structural-mechanical properties and degradability of collagen during aging-associated modifications. *J Biol Chem.* (2015) 290:23291–306. doi: 10.1074/jbc.M115.644310
186. Diridollou S, Vabre V, Berson M, Vaillant L, Black D, Lagarde JM, et al. Skin ageing: changes of physical properties of human skin *in vivo*. *Int J Cosmet Sci.* (2001) 23:353–62. doi: 10.1046/j.0412-5463.2001.00105.x
187. Fisher GJ, Kang S, Varani J, Bata-Csorgo Z, Wan Y, Datta S, et al. Mechanisms of photoaging and chronological skin aging. *Arch Dermatol.* (2002) 138:1462–70. doi: 10.1001/archderm.138.11.1462
188. Oh J-H, Kim YK, Jung J-Y, Shin J, Kim KH, Cho KH, et al. Intrinsic aging- and photoaging-dependent level changes of glycosaminoglycans and their correlation with water content in human skin. *J Dermatol Sci.* (2011) 62:192–201. doi: 10.1016/j.jdermsci.2011.02.007
189. Marcos-Garcés V, Molina Aguilar P, Bea Serrano C, García Bustos V, Benavent Seguí J, Ferrández Izquierdo A, et al. Age-related dermal collagen changes during development, maturation and ageing - a morphometric and comparative study. *J Anat.* (2014) 225:98–108. doi: 10.1111/joa.12186
190. Simm A, Müller B, Nass N, Hofmann B, Bushnaq H, Silber R-E, et al. Protein glycation - between tissue aging and protection. *Exp Gerontol.* (2015) 68:71–75. doi: 10.1016/j.exger.2014.12.013
191. Monnier VM, Mustata GT, Biemel KL, Reihl O, Lederer MO, Zhenyu D, et al. Cross-linking of the extracellular matrix by the maillard reaction in aging and diabetes: an update on 'a puzzle nearing resolution'. *Ann N Y Acad Sci.* (2005) 1043:533–44. doi: 10.1196/annals.1333.061
192. Aït-Belkacem D, Guilbert M, Roche M, Duboisset J, Ferrand P, Sockalingum G, et al. Microscopic structural study of collagen aging in isolated fibrils using polarized second harmonic generation. *J Biomed Opt.* (2012) 17:80501–6. doi: 10.1117/1.JBO.17.8.080506
193. Wilson SL, Guilbert M, Sulé-Suso J, Torbet J, Jeannesson P, Sockalingum GD, et al. A microscopic and macroscopic study of aging collagen on its molecular structure, mechanical properties, and cellular response. *FASEB J.* (2014) 28:14–25. doi: 10.1096/fj.13-227579
194. Guilbert M, Roig B, Terryn C, Garnotel R, Jeannesson P, Sockalingum GD, et al. Highlighting the impact of aging on type I collagen: label-free investigation using confocal reflectance microscopy and diffuse reflectance spectroscopy in 3D matrix model. *Oncotarget.* (2016) 7:8546–55. doi: 10.18632/oncotarget.7385
195. Panwar P, Butler GS, Jamroz A, Azizi P, Overall CM, Brömme D. Aging-associated modifications of collagen affect its degradation by matrix metalloproteinases. *Matrix Biol.* (2018) 65:30–44. doi: 10.1016/j.matbio.2017.06.004
196. Saby C, Buache E, Brassart-Pasco S, El Btaouri H, Courageot M-P, Van Gulick L, et al. Type I collagen aging impairs discoidin domain receptor 2-mediated tumor cell growth suppression. *Oncotarget.* (2016) 7:24908–27. doi: 10.18632/oncotarget.8795
197. Saby C, Rammal H, Magnien K, Buache E, Brassart-Pasco S, Van-Gulick L, et al. Age-related modifications of type I collagen impair DDR1-induced apoptosis in non-invasive breast carcinoma cells. *Cell Adhes Migr.* (2018) 12:335–47. doi: 10.1080/19336918.2018.1472182
198. Alcaraz J, Carrasco JL, Millares L, Luis I-C, Fernández-Porras FJ, Martínez-Romero A, et al. Stromal markers of activated tumor associated fibroblasts predict poor survival and are associated with necrosis in non-small cell lung cancer. *Lung Cancer.* (2019) 135:151–60. doi: 10.1016/j.lungcan.2019.07.020
199. Mayorca-Guiliani AE, Willacy O, Madsen CD, Rafaeva M, Heumüller SE, Bock F, et al. Decellularization and antibody staining of mouse tissues to map native extracellular matrix structures in 3D. *Nat Protoc.* (2019) 14:3395–425. doi: 10.1038/s41596-019-0225-8
200. Rich L, Whittaker P. Collagen and picrosirius red staining: a polarized light assessment of fibrillar hue and spatial distribution. *Braz J Morphol Sci.* (2005) 22:97–104.
201. Friedl P, Maaser K, Klein CE, Niggemann B, Krohne G, Zänker KS. Migration of highly aggressive MV3 melanoma cells in 3-dimensional collagen lattices results in local matrix reorganization and shedding of alpha2 and beta1 integrins and CD44. *Cancer Res.* (1997) 57:2061–70.
202. Choi S, Friedrichs J, Song YH, Werner C, Estroff LA, Fischbach C. Intrafibrillar, bone-mimetic collagen mineralization regulates breast cancer cell adhesion and migration. *Biomaterials.* (2019) 198:95–106. doi: 10.1016/j.biomaterials.2018.05.002
203. Brightman AO, Rajwa BP, Sturgis JE, McCallister ME, Robinson JP, Harbin SLV. Time-lapse confocal reflection microscopy of collagen fibrillogenesis and extracellular matrix assembly *in vitro*. *Biopolymers.* (2000) 54:222–34. doi: 10.1002/1097-0282(200009)54:3<222::AID-BIP80>3.0.CO;2-K
204. Friedl P. Dynamic imaging of cellular interactions with extracellular matrix. *Histochem Cell Biol.* (2004) 122:183–90. doi: 10.1007/s00418-004-0682-0
205. Wielowieyska-Szybinska D, Białek-Galas K, Podolec K, Wojas-Pelc A. The use of reflectance confocal microscopy for examination of benign and malignant skin tumors. *Postepy Dermatol Alergol.* (2014) 31:380–7. doi: 10.5114/pdia.2014.40961
206. Bozkurt A, Kose K, Alessi-Fox C, Dy JG, Brooks DH, Rajadhyaksha M. Unsupervised delineation of stratum corneum using reflectance confocal microscopy and spectral clustering. *Skin Res Technol.* (2017) 23:176–85. doi: 10.1111/srt.12316
207. Ahlgrimm-Siess V, Laimer M, Rabinovitz HS, Oliviero M, Hofmann-Wellenhof R, Marghoob AA, et al. Confocal microscopy in skin cancer. *Curr Dermatol Rep.* (2018) 7:105–18. doi: 10.1007/s13671-018-0218-9
208. Abraham T, Hogg J. Lung alveolar wall disruption in three-dimensional space identified using second-harmonic generation multiphoton excitation fluorescence In: Vo-Dinh T, Grundfest WS, Mahadevan-Jansen A, editors. *Advanced Biomedical Clinical Diagnostic Systems VIII*. San Francisco, CA: International Society for Optics and Photonics (2010). 75550X.
209. Williams RM, Zipfel WR, Webb WW. Interpreting second-harmonic generation images of collagen I fibrils. *Biophys J.* (2005) 88:1377–86. doi: 10.1529/biophysj.104.047308
210. Mostaço-Guidolin L, Rosin NL, Hackett T-L. Imaging collagen in scar tissue: developments in second harmonic generation microscopy for biomedical applications. *Int J Mol Sci.* (2017) 18:1772. doi: 10.3390/ijms18081772
211. Han X, Burke RM, Zettel ML, Tang P, Brown EB. Second harmonic properties of tumor collagen: determining the structural relationship between reactive stroma and healthy stroma. *Opt Express.* (2008) 16:1846–59. doi: 10.1364/OE.16.001846
212. Lacomb R, Nadiarnykh O, Townsend SS, Campagnola PJ. Phase matching considerations in second harmonic generation from tissues: effects on emission directionality, conversion efficiency and observed morphology. *Opt Commun.* (2008) 281:1823–32. doi: 10.1016/j.optcom.2007.10.040
213. Roth S, Freund I. Optical second-harmonic scattering in rat-tail tendon. *Biopolymers.* (1981) 20:1271–90. doi: 10.1002/bip.1981.360200613
214. Zipfel WR, Williams RM, Webb WW. Nonlinear magic: multiphoton microscopy in the biosciences. *Nat Biotechnol.* (2003) 21:1369–77. doi: 10.1038/nbt899
215. Gailhouste L, Le Grand Y, Odin C, Guyader D, Turlin B, Ezan F, et al. Fibrillar collagen scoring by second harmonic microscopy: a new tool in the assessment of liver fibrosis. *J Hepatol.* (2010) 52:398–406. doi: 10.1016/j.jhep.2009.12.009
216. Bredfeldt JS, Liu Y, Pehlke CA, Conklin MW, Szulczewski JM, Inman DR, et al. Computational segmentation of collagen fibers from second-harmonic generation images of breast cancer. *J Biomed Opt*. (2014) 19:16007. doi: 10.1117/1.JBO.19.1.016007
217. Burke K. Using second harmonic generation to predict patient outcome in solid tumors. *BMC Cancer.* (2015) 15:929. doi: 10.1186/s12885-015-1911-8
218. Suhonen H, Fernández M, Serimaa R, Suortti P. Simulation of small-angle x-ray scattering from collagen fibrils and

comparison with experimental patterns. *Phys Med Biol.* (2005) 50:5401–16. doi: 10.1088/0031-9155/50/22/012
219. Ooi GJ, Fox J, Siu K, Lewis R, Bambery KR, McNaughton D, et al. Fourier transform infrared imaging and small angle x-ray scattering as a combined biomolecular approach to diagnosis of breast cancer. *Med Phys.* (2008) 35:2151–61. doi: 10.1118/1.2890391
220. Nissi MJ, Töyräs J, Laasanen MS, Rieppo J, Saarakkala S, Lappalainen R, et al. Proteoglycan and collagen sensitive MRI evaluation of normal and degenerated articular cartilage. *J Orthop Res.* (2004) 22:557–64. doi: 10.1016/j.orthres.2003.09.008
221. Egnell L, Vidić I, Jerome NP, Bofin AM, Bathen TF, Goa PE. Stromal collagen content in breast tumors correlates with *in vivo* diffusion-weighted imaging: a comparison of multi B-value DWI with histologic specimen from benign and malignant breast lesions. *J Magn Reson Imaging.* (2019) 51:1868–87. doi: 10.1002/jmri.27018
222. Morris JL, Cross SJ, Lu Y, Kadler KE, Lu Y, Dallas SL, et al. Live imaging of collagen deposition during skin development and repair in a collagen I – GFP fusion transgenic zebrafish line. *Dev Biol.* (2018) 441:4–11. doi: 10.1016/j.ydbio.2018.06.001
223. Vogel W, Gish GD, Alves F, Pawson T. The discoidin domain receptor tyrosine kinases are activated by collagen. *Mol Cell.* (1997) 1:13–23. doi: 10.1016/S1097-2765(00)80003-9
224. Fu HL, Valiathan RR, Arkwright R, Sohail A, Mihai C, Kumarasiri M, et al. Discoidin domain receptors: unique receptor tyrosine kinases in collagen-mediated signaling. *J Biol Chem.* (2013) 288:7430–37. doi: 10.1074/jbc.R112.444158
225. Barrow AD, Raynal N, Andersen TL, Slatter DA, Bihan D, Pugh N, et al. OSCAR is a collagen receptor that costimulates osteoclastogenesis in DAP12-deficient humans and mice. *J Clin Invest.* (2011) 121:3505–16. doi: 10.1172/JCI45913
226. Nieswandt B, Watson SP. Platelet-collagen interaction: is GPVI the central receptor? *Blood.* (2003) 102:449–61. doi: 10.1182/blood-2002-12-3882
227. Melander MC, Jurgensen HJ, Madsen DH, Engelholm LH, Behrendt N. The collagen receptor uPARAP/Endo180 in tissue degradation and cancer. *Int J Oncol.* (2015) 47:1177–88. doi: 10.3892/ijo.2015.3120
228. Sprangers S, Everts V. Molecular pathways of cell-mediated degradation of fibrillar collagen. *Matrix Biol.* (2019) 75–76:190–200. doi: 10.1016/j.matbio.2017.11.008
229. Henriet E, Sala M, Abou Hammoud A, Tuariihionoa A, Di Martino J, Ros M, et al. Multitasking discoidin domain receptors are involved in several and specific hallmarks of cancer. *Cell Adhes Migr.* (2018) 12:363–77. doi: 10.1080/19336918.2018.1465156
230. Gullberg D. *I Domain Integrins.* Dordrecht: Springer (2014).
231. Zeltz C, Orgel J, Gullberg D. Molecular composition and function of integrin-based collagen glues-introducing COLINBRIs. *Biochim Biophys Acta.* (2014) 1840:2533–48. doi: 10.1016/j.bbagen.2013.12.022
232. Heino J. Cellular signaling by collagen-binding integrins. *Adv Exp Med Biol.* (2014) 819:143–55. doi: 10.1007/978-94-017-9153-3_10
233. Hamaia S, Farndale RW. Integrin recognition motifs in the human collagens. *Adv Exp Med Biol.* (2014) 819:127–42. doi: 10.1007/978-94-017-9153-3_9
234. Jokinen J, Dadu E, Nykvist P, Käpylä J, White DJ, Ivaska J, et al. Integrin-mediated cell adhesion to type I collagen fibrils. *J Biol Chem.* (2004) 279:31956–63. doi: 10.1074/jbc.M401409200
235. Eble JA, Golbik R, Mann K, Kuhn K. The alpha 1 beta 1 integrin recognition site of the basement membrane collagen molecule [alpha 1(IV)]2 alpha 2(IV). *EMBO J.* (1993) 12:4795–802. doi: 10.1002/j.1460-2075.1993.tb06168.x
236. Tulla M, Pentikainen OT, Viitasalo T, Kapyla J, Impola U, Nykvist P, et al. Selective binding of collagen subtypes by integrin alpha 1I, alpha 2I, and alpha 10I domains. *J Biol Chem.* (2001) 276:48206–12. doi: 10.1074/jbc.M104058200
237. Hamaia SW, Pugh N, Raynal N, Nemoz B, Stone R, Gullberg D, et al. Mapping of potent and specific binding motifs, GLOGEN and GVOGEA, for integrin alpha1beta1 using collagen toolkits II and III. *J Biol Chem.* (2012) 287:26019–28. doi: 10.1074/jbc.M112.353144
238. Kapyla J, Jaalinoja J, Tulla M, Ylostalo J, Nissinen L, Viitasalo T, et al. The fibril-associated collagen IX provides a novel mechanism for cell adhesion to cartilaginous matrix. *J Biol Chem.* (2004) 279:51677–87. doi: 10.1074/jbc.M409412200
239. Madamanchi A, Santoro SA, Zutter MM. Alpha2beta1 integrin. *Adv Exp Med Biol.* (2014) 819:41–60. doi: 10.1007/978-94-017-9153-3_3
240. Carafoli F, Hamaia SW, Bihan D, Hohenester E, Farndale RW. An activating mutation reveals a second binding mode of the integrin alpha2 I domain to the GFOGER motif in collagens. *PLoS ONE.* (2013) 8:e69833. doi: 10.1371/journal.pone.0069833
241. Camper L, Hellman U, Lundgren-Akerlund E. Isolation, cloning, and sequence analysis of the integrin subunit alpha10, a beta1-associated collagen binding integrin expressed on chondrocytes. *J Biol Chem.* (1998) 273:20383–9. doi: 10.1074/jbc.273.32.20383
242. Tiger CF, Fougerousse F, Grundstrom G, Velling T, Gullberg D. α110β1 integrin is a receptor for interstitial collagens involved in cell migration and collagen reorganization on mesenchymal nonmuscle cells. *Dev Biol.* (2001) 237:116–29. doi: 10.1006/dbio.2001.0363
243. Zhang WM, Kapyla J, Puranen JS, Knight CG, Tiger CF, Pentikainen OT, et al. α 11β 1 integrin recognizes the GFOGER sequence in interstitial collagens. *J Biol Chem.* (2003) 278:7270–7. doi: 10.1074/jbc.M210313200
244. Knight CG, Morton LF, Peachey AR, Tuckwell DS, Farndale RW, Barnes MJ. The collagen-binding A-domains of integrins alpha(1)beta(1) and alpha(2)beta(1) recognize the same specific amino acid sequence, GFOGER, in native (triple-helical) collagens. *J Biol Chem.* (2000) 275:35–40. doi: 10.1074/jbc.275.1.35
245. Sipilä KH, Drushinin K, Rappu P, Jokinen J, Salminen TA, Salo AM, et al. Proline hydroxylation in collagen supports integrin binding by two distinct mechanisms. *J Biol Chem.* 293:7645–58. doi: 10.1074/jbc.RA118.002200
246. Kubow KE, Vukmirovic R, Zhe L, Klotzsch E, Smith ML, Gourdon D, et al. Mechanical forces regulate the interactions of fibronectin and collagen I in extracellular matrix. *Nat Commun.* (2015) 6:8026. doi: 10.1038/ncomms9026
247. Fiedler LR, Schonherr E, Waddington R, Niland S, Seidler DG, Aeschlimann D, et al. Decorin regulates endothelial cell motility on collagen I through activation of insulin-like growth factor I receptor and modulation of alpha2beta1 integrin activity. *J Biol Chem.* (2008) 283:17406–15. doi: 10.1074/jbc.M710025200
248. Zeltz C, Brezillon S, Kapyla J, Eble JA, Bobichon H, Terryn C, et al. Lumican inhibits cell migration through alpha2beta1 integrin. *Exp Cell Res.* (2010) 316:2922–31. doi: 10.1016/j.yexcr.2010.08.002
249. Zhu J, Madhurapantula RS, Kalyanasundaram A, Sabharwal T, Antipova O, Bishnoi SW, et al. Ultrastructural location and interactions of the immunoglobulin receptor binding sequence within fibrillar type I collagen. *Int J Mol Sci.* (2020) 21:4166. doi: 10.3390/ijms21114166
250. Seguin L, Desgrosellier JS, Weis SM, Cheresh DA. Integrins and cancer: regulators of cancer stemness, metastasis, and drug resistance. *Trends Cell Biol.* (2015) 25:234–40. doi: 10.1016/j.tcb.2014.12.006
251. Hamidi H, Ivaska J. Every step of the way: integrins in cancer progression and metastasis. *Nat Rev Cancer.* (2018) 18:533–48. doi: 10.1038/s41568-018-0038-z
252. Zaidel-Bar R, Itzkovitz S, Ma'ayan A, Iyengar R, Geiger B. Functional atlas of the integrin adhesome. *Nat Cell Biol.* (2007) 9:858–67. doi: 10.1038/ncb0807-858
253. Humphries JD, Chastney MR, Askari JA, Humphries MJ. Signal transduction via integrin adhesion complexes. *Curr Opin Cell Biol.* (2019) 56:14–21. doi: 10.1016/j.ceb.2018.08.004
254. Horton ER, Byron A, Askari JA, Ng DHJ, Millon-Fremillon A, Robertson J, et al. Definition of a consensus integrin adhesome and its dynamics during adhesion complex assembly and disassembly. *Nat Cell Biol.* (2015) 17:1577–87. doi: 10.1038/ncb3257
255. Shattil SJ, Kim C, Ginsberg MH. The final steps of integrin activation: the end game. *Nat Rev Mol Cell Biol.* (2010) 11:288–300. doi: 10.1038/nrm2871
256. Kechagia JZ, Ivaska J, Roca-Cusachs P. Integrins as biomechanical sensors of the microenvironment. *Nat Rev Mol Cell Biol.* 20:1–17. doi: 10.1038/s41580-019-0134-2
257. Kagami S, Urushihara M, Kondo S, Loster K, Reutter W, Tamaki T, et al. Requirement for tyrosine kinase-ERK1/2 signaling in alpha 1 beta 1 integrin-mediated collagen matrix remodeling by rat mesangial cells. *Exp Cell Res.* (2001) 268:274–83. doi: 10.1006/excr.2001.5279

258. Inoue O, Suzuki-Inoue K, Dean WL, Frampton J, Watson SP. Integrin alpha2beta1 mediates outside-in regulation of platelet spreading on collagen through activation of Src kinases and PLCgamma2. *J Cell Biol.* (2003) 160:769–80. doi: 10.1083/jcb.200208043
259. Consonni A, Cipolla L, Guidetti G, Canobbio I, Ciraolo E, Hirsch E, et al. Role and regulation of phosphatidylinositol 3-kinase β in platelet integrin α2β1 signaling. *Blood.* (2012) 119:847–56. doi: 10.1182/blood-2011-07-364992
260. Guidetti GF, Bernardi B, Consonni A, Rizzo P, Gruppi C, Balduini C, et al. Integrin alpha2beta1 induces phosphorylation-dependent and phosphorylation-independent activation of phospholipase Cgamma2 in platelets: role of Src kinase and Rac GTPase. *J Thromb Haemost.* (2009) 7:1200–6. doi: 10.1111/j.1538-7836.2009.03444.x
261. Chen X, Abair TD, Ibanez MR, Su Y, Frey MR, Dise RS, et al. Integrin alpha1beta1 controls reactive oxygen species synthesis by negatively regulating epidermal growth factor receptor-mediated Rac activation. *Mol Cell Biol.* (2007) 27:3313–26. doi: 10.1128/MCB.01476-06
262. Honoré S, Kovacic H, Pichard V, Briand C, Rognoni J-B. Alpha2beta1-integrin signaling by itself controls G1/S transition in a human adenocarcinoma cell line ($Caco_2$): implication of NADPH oxidase-dependent production of ROS. *Exp Cell Res.* (2003) 285:59–71. doi: 10.1016/S0014-4827(02)00038-1
263. Schulz JN, Zeltz C, Sorensen IW, Barczyk M, Carracedo S, Hallinger R, et al. Reduced granulation tissue and wound strength in the absence of alpha11beta1 integrin. *J Invest Dermatol.* (2015) 135:1435–44. doi: 10.1038/jid.2015.24
264. Harburger DS, Calderwood DA. Integrin signalling at a glance. *J Cell Sci.* (2009) 122:159–63. doi: 10.1242/jcs.018093
265. Bottcher RT, Veelders M, Rombaut P, Faix J, Theodosiou M, Stradal TE, et al. Kindlin-2 recruits paxillin and Arp2/3 to promote membrane protrusions during initial cell spreading. *J Cell Biol.* (2017) 216:3785–98. doi: 10.1083/jcb.201701176
266. Petrich BG, Marchese P, Ruggeri ZM, Spiess S, Weichert RA, Ye F, et al. Talin is required for integrin-mediated platelet function in hemostasis and thrombosis. *J Exp Med.* (2007) 204:3103–11. doi: 10.1084/jem.20071800
267. Salmela M, Jokinen J, Tiitta S, Rappu P, Cheng RH, Heino J. Integrin alpha2beta1 in nonactivated conformation can induce focal adhesion kinase signaling. *Sci Rep.* (2017) 7:3414. doi: 10.1038/s41598-017-03640-w
268. Rantala JK, Pouwels J, Pellinen T, Veltel S, Laasola P, Mattila E, et al. SHARPIN is an endogenous inhibitor of β1-integrin activation. *Nat Cell Biol.* (2011) 13:1315–24. doi: 10.1038/ncb2340
269. Mattila E, Pellinen T, Nevo J, Vuoriluoto K, Arjonen A, Ivaska J. Negative regulation of EGFR signalling through integrin-alpha1beta1-mediated activation of protein tyrosine phosphatase TCPTP. *Nat Cell Biol.* (2005) 7:78–85. doi: 10.1038/ncb1209
270. Ivaska J, Reunanen H, Westermarck J, Koivisto L, Kähäri VM, Heino J. Integrin alpha2beta1 mediates isoform-specific activation of p38 and upregulation of collagen gene transcription by a mechanism involving the alpha2 cytoplasmic tail. *J Cell Biol.* (1999) 147:401–16. doi: 10.1083/jcb.147.2.401
271. Langholz O, Röckel D, Mauch C, Kozlowska E, Bank I, Krieg T, et al. Collagen and collagenase gene expression in three-dimensional collagen lattices are differentially regulated by alpha 1 beta 1 and alpha 2 beta 1 integrins. *J Cell Biol.* (1995) 131:1903–15. doi: 10.1083/jcb.131.6.1903
272. Ravanti L, Heino J, López-Otín C, Kähäri VM. Induction of collagenase-3 (MMP-13) expression in human skin fibroblasts by three-dimensional collagen is mediated by p38 mitogen-activated protein kinase. *J Biol Chem.* (1999) 274:2446–55. doi: 10.1074/jbc.274.4.2446
273. Barczyk MM, Lu N, Popova SN, Bolstad AI, Gullberg D. alpha11beta1 integrin-mediated MMP-13-dependent collagen lattice contraction by fibroblasts: evidence for integrin-coordinated collagen proteolysis. *J Cell Physiol.* (2013) 228:1108–19. doi: 10.1002/jcp.24261
274. Lochter A, Navre M, Werb Z, Bissell MJ. alpha1 and alpha2 integrins mediate invasive activity of mouse mammary carcinoma cells through regulation of stromelysin-1 expression. *Mol Biol Cell.* (1999) 10:271–82. doi: 10.1091/mbc.10.2.271
275. Yamada KM, Even-Ram S. Integrin regulation of growth factor receptors. *Nat Cell Biol.* (2002) 4:E75–6. doi: 10.1038/ncb0402-e75
276. Ivaska J, Heino J. Cooperation between integrins and growth factor receptors in signaling and endocytosis. *Annu Rev Cell Dev Biol.* (2011) 27:291–320. doi: 10.1146/annurev-cellbio-092910-154017
277. Schnittert J, Bansal R, Storm G, Prakash J. Integrins in wound healing, fibrosis and tumor stroma: high potential targets for therapeutics and drug delivery. *Adv Drug Deliv Rev.* (2018) 129:37–53. doi: 10.1016/j.addr.2018.01.020
278. Guha D, Saha T, Bose S, Chakraborty S, Dhar S, Khan P, et al. Integrin-EGFR interaction regulates anoikis resistance in colon cancer cells. *Apoptosis.* (2019) 24:958–71. doi: 10.1007/s10495-019-01573-5
279. McCall-Culbreath KD, Li Z, Zutter MM. Crosstalk between the alpha2beta1 integrin and c-met/HGF-R regulates innate immunity. *Blood.* (2008) 111:3562–70. doi: 10.1182/blood-2007-08-107664
280. Primac I, Maquoi E, Blacher S, Heljasvaara R, Van Deun J, Smeland HY, et al. Stromal integrin alpha11 regulates PDGFR-beta signaling and promotes breast cancer progression. *J Clin Invest.* (2019) 130:4609–28. doi: 10.1172/JCI125890
281. Leitinger B. Discoidin domain receptor functions in physiological and pathological conditions. *Int Rev Cell Mol Biol.* (2014) 310:39–87. doi: 10.1016/B978-0-12-800180-6.00002-5
282. Danen EHJ. Integrin signaling as a cancer drug target. *ISRN Cell Biol.* (2013) 201:14. doi: 10.1155/2013/135164
283. Vachon PH. Integrin signaling, cell survival, and anoikis: distinctions, differences, and differentiation. *J Signal Transduct.* (2011) 2011:738137. doi: 10.1155/2011/738137
284. Conti JA, Kendall TJ, Bateman A, Armstrong TA, Papa-Adams A, Xu Q, et al. The desmoplastic reaction surrounding hepatic colorectal adenocarcinoma metastases aids tumor growth and survival via alphav integrin ligation. *Clin Cancer Res.* (2008) 14:6405–13. doi: 10.1158/1078-0432.CCR-08-0816
285. Gardner H. Integrin alpha1beta1. *Adv Exp Med Biol.* (2014) 819:21–39. doi: 10.1007/978-94-017-9153-3_2
286. Gardner H, Kreidberg J, Koteliansky V, Jaenisch R. Deletion of integrin alpha 1 by homologous recombination permits normal murine development but gives rise to a specific deficit in cell adhesion. *Dev Biol.* (1996) 175:301–13. doi: 10.1006/dbio.1996.0116
287. Pozzi A, Wary KK, Giancotti FG, Gardner HA. Integrin alpha1beta1 mediates a unique collagen-dependent proliferation pathway *in vivo*. *J Cell Biol.* (1998) 142:587–94. doi: 10.1083/jcb.142.2.587
288. Zemmyo M, Meharra EJ, Kuhn K, Creighton-Achermann L, Lotz M. Accelerated, aging-dependent development of osteoarthritis in alpha1 integrin-deficient mice. *Arthritis Rheum.* (2003) 48:2873–80. doi: 10.1002/art.11246
289. Peng YW, Zallocchi M, Meehan DT, Delimont D, Chang B, Hawes N, et al. Progressive morphological and functional defects in retinas from alpha1 integrin-null mice. *Invest Ophthalmol Vis Sci.* (2008) 49:4647–54. doi: 10.1167/iovs.08-2011
290. Conrad C, Boyman O, Tonel G, Tun-Kyi A, Laggner U, de Fougerolles A, et al. Alpha1beta1 integrin is crucial for accumulation of epidermal T cells and the development of psoriasis. *Nat Med.* (2007) 13:836–42. doi: 10.1038/nm1605
291. Ekholm E, Hankenson KD, Uusitalo H, Hiltunen A, Gardner H, Heino J, et al. Diminished callus size and cartilage synthesis in alpha 1 beta 1 integrin-deficient mice during bone fracture healing. *AJPA.* (2002) 160:1779–85. doi: 10.1016/S0002-9440(10)61124-8
292. Williams AS, Kang L, Zheng J, Grueter C, Bracy DP, James FD, et al. Integrin alpha1-null mice exhibit improved fatty liver when fed a high fat diet despite severe hepatic insulin resistance. *J Biol Chem.* (2015) 290:6546–57. doi: 10.1074/jbc.M114.615716
293. Zent R, Yan X, Su Y, Hudson BG, Borza DB, Moeckel GW, et al. Glomerular injury is exacerbated in diabetic integrin alpha1-null mice. *Kidney Int.* (2006) 70:460–70. doi: 10.1038/sj.ki.5000359
294. Chen X, Su Y, Fingleton B, Acuff H, Matrisian LM, Zent R, et al. An orthotopic model of lung cancer to analyze primary and metastatic NSCLC growth in integrin alpha1-null mice. *Clin Exp Metastasis.* (2005) 22:185–93. doi: 10.1007/s10585-005-7453-8
295. Macias-Perez I, Borza C, Chen X, Yan X, Ibanez R, Mernaugh G, et al. Loss of integrin alpha1beta1 ameliorates Kras-induced lung cancer. *Cancer Res.* (2008) 68:6127–35. doi: 10.1158/0008-5472.CAN-08-1395

296. Boudjadi S, Bernatchez G, Senicourt B, Beausejour M, Vachon PH, Carrier JC, et al. Involvement of the integrin alpha1beta1 in the progression of colorectal cancer. *Cancers.* (2017) 9:96. doi: 10.3390/cancers9080096
297. Pozzi A, Moberg PE, Miles LA, Wagner S, Soloway P, Gardner HA. Elevated matrix metalloprotease and angiostatin levels in integrin alpha 1 knockout mice cause reduced tumor vascularization. *Proc Natl Acad Sci USA.* (2000) 97:2202–7. doi: 10.1073/pnas.040378497
298. Schadendorf D, Fichtner I, Makki A, Alijagic S, Kupper M, Mrowietz U, et al. Metastatic potential of human melanoma cells in nude mice–characterisation of phenotype, cytokine secretion and tumour-associated antigens. *Br J Cancer.* (1996) 74:194–9. doi: 10.1038/bjc.1996.337
299. Schadendorf D, Gawlik C, Haney U, Ostmeier H, Suter L, Czarnetzki BM. Tumour progression and metastatic behaviour *in vivo* correlates with integrin expression on melanocytic tumours. *J Pathol.* (1993) 170:429–34. doi: 10.1002/path.1711700405
300. Ratzinger S, Grassel S, Dowejko A, Reichert TE, Bauer RJ. Induction of type XVI collagen expression facilitates proliferation of oral cancer cells. *Matrix Biol.* (2011) 30:118–25. doi: 10.1016/j.matbio.2011.01.001
301. Koukoulis GK, Warren WH, Virtanen I, Gould VE. Immunolocalization of integrins in the normal lung and in pulmonary carcinomas. *Hum Pathol.* (1997) 28:1018–25. doi: 10.1016/S0046-8177(97)90054-X
302. Fukuda K, Saikawa Y, Yagi H, Wada N, Takahashi T, Kitagawa Y. Role of integrin alpha1 subunits in gastric cancer patients with peritoneal dissemination. *Mol Med Rep.* (2012) 5:336–40. doi: 10.3892/mmr.2011.642
303. Wu JE, Santoro SA. Complex patterns of expression suggest extensive roles for the alpha 2 beta 1 integrin in murine development. *Dev Dyn.* (1994) 199:292–314. doi: 10.1002/aja.1001990405
304. Zutter MM, Santoro SA. Widespread histologic distribution of the alpha 2 beta 1 integrin cell-surface collagen receptor. *AJPA.* (1990) 137:113–20.
305. Holtkotter O, Nieswandt B, Smyth N, Muller W, Hafner M, Schulte V, et al. Integrin alpha 2-deficient mice develop normally, are fertile, but display partially defective platelet interaction with collagen. *J Biol Chem.* (2002) 277:10789–94. doi: 10.1074/jbc.M112307200
306. Chen J, Diacovo TG, Grenache DG, Santoro SA, Zutter MM. The alpha(2) integrin subunit-deficient mouse: a multifaceted phenotype including defects of branching morphogenesis and hemostasis. *AJPA.* (2002) 161:337–44. doi: 10.1016/S0002-9440(10)64185-5
307. Barczyk M, Carracedo S, Gullberg D. Integrins. *Cell Tissue Res.* (2010) 339:269–80. doi: 10.1007/s00441-009-0834-6
308. Stange R, Kronenberg D, Timmen M, Everding J, Hidding H, Eckes B, et al. Age-related bone deterioration is diminished by disrupted collagen sensing in integrin alpha2beta1 deficient mice. *Bone.* (2013) 56:48–54. doi: 10.1016/j.bone.2013.05.003
309. Zweers MC, Davidson JM, Pozzi A, Hallinger R, Janz K, Quondamatteo F, et al. Integrin alpha2beta1 is required for regulation of murine wound angiogenesis but is dispensable for reepithelialization. *J Invest Dermatol.* (2007) 127:467–78. doi: 10.1038/sj.jid.5700546
310. Borza CM, Su Y, Chen X, Yu L, Mont S, Chetyrkin S, et al. Inhibition of integrin alpha2beta1 ameliorates glomerular injury. *J Am Soc Nephrol.* (2012) 23:1027–38. doi: 10.1681/ASN.2011040367
311. Peters MA, Wendholt D, Strietholt S, Frank S, Pundt N, Korb-Pap A, et al. The loss of alpha2beta1 integrin suppresses joint inflammation and cartilage destruction in mouse models of rheumatoid arthritis. *Arthritis Rheum.* (2012) 64:1359–68. doi: 10.1002/art.33487
312. Ramirez NE, Zhang Z, Madamanchi A, Boyd KL, O'Rear LD, Nashabi A, et al. The $alpha_2beta_1$ integrin is a metastasis suppressor in mouse models and human cancer. *J Clin Invest.* (2011) 121:226–37. doi: 10.1172/JCI42328
313. Zuo XX, Yang Y, Zhang Y, Zhang ZG, Wang XF, Shi YG. Platelets promote breast cancer cell MCF-7 metastasis by direct interaction: surface integrin alpha2beta1-contacting-mediated activation of Wnt-beta-catenin pathway. *Cell Commun Signal.* (2019) 17:142. doi: 10.1186/s12964-019-0464-x
314. Ibaragi S, Shimo T, Hassan NM, Isowa S, Kurio N, Mandai H, et al. Induction of MMP-13 expression in bone-metastasizing cancer cells by type I collagen through integrin alpha1beta1 and alpha2beta1-p38 MAPK signaling. *Anticancer Res.* (2011) 31:1307–13.
315. Siret C, Terciolo C, Dobric A, Habib MC, Germain S, Bonnier R, et al. Interplay between cadherins and alpha2beta1 integrin differentially regulates melanoma cell invasion. *Br J Cancer.* (2015) 113:1445–53. doi: 10.1038/bjc.2015.358
316. Sottnik JL, Daignault-Newton S, Zhang X, Morrissey C, Hussain MH, Keller ET, et al. Integrin alpha2beta 1 (alpha2beta1) promotes prostate cancer skeletal metastasis. *Clin Exp Metastasis.* (2013) 30:569–78. doi: 10.1007/s10585-012-9561-6
317. Naci D, El Azreq MA, Chetoui N, Lauden L, Sigaux F, Charron D, et al. $\alpha2\beta1$ integrin promotes chemoresistance against doxorubicin in cancer cells through extracellular signal-regulated kinase (ERK). *J Biol Chem.* (2012) 287:17065–76. doi: 10.1074/jbc.M112.349365
318. Naci D, Berrazouane S, Barabe F, Aoudjit F. Cell adhesion to collagen promotes leukemia resistance to doxorubicin by reducing DNA damage through the inhibition of Rac1 activation. *Sci Rep.* (2019) 9:19455. doi: 10.1038/s41598-019-55934-w
319. Naci D, Vuori K, Aoudjit F. Alpha2beta1 integrin in cancer development and chemoresistance. *Semin Cancer Biol.* (2015) 35:145–53. doi: 10.1016/j.semcancer.2015.08.004
320. Varas L, Ohlsson LB, Honeth G, Olsson A, Bengtsson T, Wiberg C, et al. Alpha10 integrin expression is up-regulated on fibroblast growth factor-2-treated mesenchymal stem cells with improved chondrogenic differentiation potential. *Stem Cells Dev.* (2007) 16:965–78. doi: 10.1089/scd.2007.0049
321. Lundgren-Akerlund E, Aszodi A. Integrin alpha10beta1: a collagen receptor critical in skeletal development. *Adv Exp Med Biol.* (2014) 819:61–71. doi: 10.1007/978-94-017-9153-3_4
322. Kyostila K, Lappalainen AK, Lohi H. Canine chondrodysplasia caused by a truncating mutation in collagen-binding integrin alpha subunit 10. *PLoS ONE.* (2013) 8:e75621. doi: 10.1371/journal.pone.0075621
323. Wenke AK, Kjellman C, Lundgren-Akerlund E, Uhlmann C, Haass NK, Herlyn M, et al. Expression of integrin alpha10 is induced in malignant melanoma. *Cell Oncol.* (2007) 29:373–86. doi: 10.1097/00008390-200609001-00192
324. Munksgaard Thoren M, Chmielarska Masoumi K, Krona C, Huang X, Kundu S, Schmidt L, et al. Integrin α10, a novel therapeutic target in glioblastoma, regulates cell migration, proliferation, and survival. *Cancers.* (2019) 11:587. doi: 10.3390/cancers11040587
325. Okada T, Lee AY, Qin LX, Agaram N, Mimae T, Shen Y, et al. Integrin-alpha10 dependency identifies RAC and RICTOR as therapeutic targets in high-grade myxofibrosarcoma. *Cancer Discov.* (2016) 6:1148–65. doi: 10.1158/2159-8290.CD-15-1481
326. Carracedo S, Lu N, Popova SN, Jonsson R, Eckes B, Gullberg D. The fibroblast integrin alpha11beta1 is induced in a mechanosensitive manner involving activin A and regulates myofibroblast differentiation. *J Biol Chem.* (2010) 285:10434–45. doi: 10.1074/jbc.M109.078766
327. Popova SN, Rodriguez-Sanchez B, Liden A, Betsholtz C, Van Den Bos T, Gullberg D. The mesenchymal alpha11beta1 integrin attenuates PDGF-BB-stimulated chemotaxis of embryonic fibroblasts on collagens. *Dev Biol.* (2004) 270:427–42. doi: 10.1016/j.ydbio.2004.03.006
328. Zhu C-Q, Popova SN, Brown ER, Barsyte-Lovejoy D, Navab R, Shih W, et al. Integrin alpha 11 regulates IGF2 expression in fibroblasts to enhance tumorigenicity of human non-small-cell lung cancer cells. *Proc Natl Acad Sci USA.* (2007) 104:11754–9. doi: 10.1073/pnas.0703040104
329. Popova SN, Barczyk M, Tiger CF, Beertsen W, Zigrino P, Aszodi A, et al. Alpha11 beta1 integrin-dependent regulation of periodontal ligament function in the erupting mouse incisor. *Mol Cell Biol.* (2007) 27:4306–16. doi: 10.1128/MCB.00041-07
330. Blumbach K, Niehoff A, Belgardt BF, Ehlen HW, Schmitz M, Hallinger R, et al. Dwarfism in mice lacking collagen-binding integrins alpha2beta1 and alpha11beta1 is caused by severely diminished IGF-1 levels. *J Biol Chem.* (2012) 287:6431–40. doi: 10.1074/jbc.M111.283119
331. Romaine A, Sorensen IW, Zeltz C, Lu N, Erusappan PM, Melleby AO, et al. Overexpression of integrin α11 induces cardiac fibrosis in mice. *Acta Physiol.* (2018) 222. doi: 10.1111/apha.12932
332. Navab R, Strumpf D, To C, Pasko E, Kim KS, Park CJ, et al. Integrin alpha11beta1 regulates cancer stromal stiffness and promotes tumorigenicity and metastasis in non-small cell lung cancer. *Oncogene.* (2016) 35:1899–908. doi: 10.1038/onc.2015.254
333. Ando T, Kage H, Matsumoto Y, Zokumasu K, Yotsumoto T, Maemura K, et al. Integrin alpha11 in non-small cell lung cancer is associated

with tumor progression and postoperative recurrence. *Cancer Sci.* (2020) 111:200–8. doi: 10.1111/cas.14257

334. Smeland HY, Askeland C, Wik E, Knutsvik G, Molven A, Edelmann RJ, et al. Integrin alpha11beta1 is expressed in breast cancer stroma and associates with aggressive tumor phenotypes. *J Pathol Clin Res.* (2019) 6:69–82. doi: 10.1002/cjp2.148
335. Smeland HY, Lu N, Karlsen T V, Salvesen G, Reed RK, Stuhr L. Stromal integrin alpha11-deficiency reduces interstitial fluid pressure and perturbs collagen structure in triple-negative breast xenograft tumors. *BMC Cancer.* (2019) 19:234. doi: 10.1186/s12885-019-5449-z
336. Boudjadi S, Carrier JC, Beaulieu JF. Integrin alpha1 subunit is up-regulated in colorectal cancer. *Biomark Res.* (2013) 1:16. doi: 10.1186/2050-7771-1-16
337. Boudjadi S, Carrier JC, Groulx JF, Beaulieu JF. Integrin alpha1beta1 expression is controlled by c-MYC in colorectal cancer cells. *Oncogene.* (2016) 35:1671–8. doi: 10.1038/onc.2015.231
338. Benya PD, Padilla SR. Modulation of the rabbit chondrocyte phenotype by retinoic acid terminates type II collagen synthesis without inducing type I collagen: the modulated phenotype differs from that produced by subculture. *Dev Biol.* (1986) 118:296–305. doi: 10.1016/0012-1606(86)90096-5
339. Bengtsson T, Aszodi A, Nicolae C, Hunziker EB, Lundgren-Akerlund E, Fassler R. Loss of alpha10beta1 integrin expression leads to moderate dysfunction of growth plate chondrocytes. *J Cell Sci.* (2005) 118:929–36. doi: 10.1242/jcs.01678
340. Velling T, Kusche-Gullberg M, Sejersen T, Gullberg D. cDNA cloning and chromosomal localization of human alpha(11) integrin. A collagen-binding, I domain-containing, beta(1)-associated integrin alpha-chain present in muscle tissues. *J Biol Chem.* (1999) 274:25735–42. doi: 10.1074/jbc.274.36.25735
341. Lu N, Carracedo S, Ranta J, Heuchel R, Soininen R, Gullberg D. The human alpha11 integrin promoter drives fibroblast-restricted expression *in vivo* and is regulated by TGF-beta1 in a Smad- and Sp1-dependent manner. *Matrix Biol.* (2010) 29:166–76. doi: 10.1016/j.matbio.2009.11.003
342. Erusappan P, Alam J, Lu N, Zeltz C, Gullberg D. Integrin alpha11 cytoplasmic tail is required for FAK activation to initiate 3D cell invasion and ERK-mediated cell proliferation. *Sci Rep.* (2019) 9:15283. doi: 10.1038/s41598-019-51689-6
343. Rombouts K, Carloni V. The fibrotic microenvironment as a heterogeneity facet of hepatocellular carcinoma. *Fibrogenes Tissue Repair.* (2013) 6 :17. doi: 10.1186/1755-1536-6-17
344. Banys-Paluchowski M, Loibl S, Witzel I, Mundhenke C, Lederer B, Solbach C, et al. Clinical relevance of collagen protein degradation markers C3M and C4M in the serum of breast cancer patients treated with neoadjuvant therapy in the geparquinto trial. *Cancers.* (2019) 11:1186. doi: 10.1055/s-0039-1687939
345. Willumsen N, Ali SM, Leitzel K, Drabick JJ, Yee N, Polimera HV, et al. Collagen fragments quantified in serum as measures of desmoplasia associate with survival outcome in patients with advanced pancreatic cancer. *Sci Rep.* (2019) 9:19761. doi: 10.1038/s41598-019-56268-3
346. Lipton A, Leitzel K, Ali SM, Polimera H V., Nagabhairu V, Marks E, et al. High turnover of extracellular matrix reflected by specific protein fragments measured in serum is associated with poor outcomes in two metastatic breast cancer cohorts. *Int J Cancer.* (2018) 143:3027–34. doi: 10.1002/ijc.31627

Conflict of Interest: The authors declare that the research was conducted in the absence of any commercial or financial relationships that could be construed as a potential conflict of interest.

Copyright © 2020 Bourgot, Primac, Louis, Noël and Maquoi. This is an open-access article distributed under the terms of the Creative Commons Attribution License (CC BY). The use, distribution or reproduction in other forums is permitted, provided the original author(s) and the copyright owner(s) are credited and that the original publication in this journal is cited, in accordance with accepted academic practice. No use, distribution or reproduction is permitted which does not comply with these terms.

frontiers in Oncology

MINI REVIEW
published: 19 August 2020
doi: 10.3389/fonc.2020.01456

Extracellular Vesicle-Dependent Cross-Talk in Cancer—Focus on Pancreatic Cancer

Lise Nannan[1,2,3†], *Jean-Baptiste Oudart*[1,2,4†], *Jean Claude Monboisse*[1,2,4], *Laurent Ramont*[1,2,4], *Sylvie Brassart-Pasco*[1,2] *and Bertrand Brassart*[1,2*]

[1] Université de Reims Champagne Ardenne, SFR CAP-Santé (FED 4231), Laboratoire de Biochimie Médicale et Biologie Moléculaire, Reims, France, [2] CNRS UMR 7369, Matrice Extracellulaire et Dynamique Cellulaire–MEDyC, Reims, France, [3] Biomedical MRI Group, Department of Imaging and Pathology, KU Leuven, Leuven, Belgium, [4] CHU Reims, Service de Biochimie–Pharmacologie–Toxicologie, Reims, France

Extracellular vesicles (EVs) like exosomes and shed microvesicles are generated by many different cells. However, among all the cells, cancer cells are now recognized to secrete more EVs than healthy cells. Tumor-derived EVs can be isolated from biofluids such as blood, urine, ascitic fluid, and saliva. Their numerous components (nucleic acids, proteins, and lipids) possess many pleiotropic functions involved in cancer progression. The tumor-derived EVs generated under the influence of tumor microenvironment play distant roles and promote cellular communication by directly interacting with different cells. Moreover, they modulate extracellular matrix remodeling and tumor progression. Tumor-derived EVs are involved in pre-metastatic niche formation, dependent on the EV-associated protein receptors, and in cancer chemoresistance as they transfer drug-resistance-related genes to recipient cells. Recent advances in preclinical and clinical fields suggest their potential use as biomarkers for diagnosis and prognosis as well as for drug delivery in cancer. In this Review, we discuss EV characteristics and pro-tumor capacities, and highlight the future crucial impact of tumor-derived EVs in pancreatic cancer diagnosis and prognosis.

Keywords: extracellular vesicle (EV), pancreatic cancer, biomarkers, imaging *in vivo*, bioactivities

OPEN ACCESS

Edited by:
Erik Maquoi,
University of Liège, Belgium

Reviewed by:
Stefano Fais,
Istituto Superiore di Sanità (ISS), Italy
Sonia A. Melo,
Universidade Do Porto, Portugal

***Correspondence:**
Bertrand Brassart
bertrand.brassart@univ-reims.fr

[†] *These authors have contributed equally to this work*

Specialty section:
This article was submitted to Molecular and Cellular Oncology, a section of the journal Frontiers in Oncology

Received: *16 January 2020*
Accepted: *09 July 2020*
Published: *19 August 2020*

Citation:
Nannan L, Oudart J-B, Monboisse JC, Ramont L, Brassart-Pasco S and Brassart B (2020) Extracellular Vesicle-Dependent Cross-Talk in Cancer—Focus on Pancreatic Cancer. Front. Oncol. 10:1456. doi: 10.3389/fonc.2020.01456

INTRODUCTION

Intercellular communication is essential to cell development and maintenance of homeostasis in multicellular organisms. Naturally produced and released into the extracellular microenvironment by most cell types and belonging multiple distinct classes depending on their origin, EVs are predominantly described in intercellular communication although their functions are not limited to this aspect (1). These cell-to-cell communications occur locally or at distance. Distant intercellular communication is achieved via EVs. Among all EVs, two major EV classes are relatively well-described: exosomes (50–150-nm diameter, membranous vesicles of endocytic origin) and microvesicles (large membranous vesicles of 100–1,000-nm diameter directly shed from the plasma membrane) (2). Since the 1990's with the first evidence on EV roles in cell-to-cell communication and more especially during the past 10 years, considerable progress have been made to understand EV functions (3–5) and potential applications in clinical domains (6–9). Numerous studies have shown the biological roles of EVs in physio-pathological processes, such as immune and microbiological regulation, stem cell biology, cardiovascular diseases,

neurodegenerative diseases, metabolic disorders, and cancer progression (10–13). The regulation of a broad range of cellular activities and biological responses is due to their biogenesis and probably to the extracellular environment and constraints. EVs are specifically loaded with cell-specific proteins, lipids, mRNAs, and miRNAs, corresponding to EV membrane's or cargo's "molecular signature," which reflect activity/status of the parent cancer cells (2). Kahlert et al. demonstrated that pancreatic cancer cell-derived EVs contain fragments of genomic DNA (14). The deregulation of EV biogenesis in different pathologies, especially cancer, was also evidenced furthering tumor cell immune escape, therapy resistance, tumor growing, invasion, and metastasis (15).

Practically, most studies are focused on EVs that measure 1 μm or less, corresponding mostly to exosomes. To date, few articles are based on microvesicles larger than 1 μm like large oncosome (16–19). In 2014, The International Society for Extracellular Vesicles (ISEV) proposed Minimal Information for Studies of Extracellular Vesicles ("MISEV") guidelines for EV isolation and purification. Among the different EV isolation methods, such as membrane filtration, affinity isolation, or size exclusion chromatography from conditioned cell culture media and body fluids (plasma, serum, and urine), the must employed method is the ultracentrifugation (20). According to the MISEV2014, EV detection and characterization must be realized by transmission electron microscopy and EV marker immunodetection by western-blotting or flow cytometry. Specific exosome markers correspond to tetraspanins (CD9, CD63, and CD81), ESCRT-associated proteins like tumor susceptibility gene 101 (TSG101) and apoptosis-linked gene 2-interacting protein X (ALIX), heat shock proteins (Hsp70 and Hsp90), integrins, and membrane transport and fusion proteins (annexins). To date, microvesicle characterization is less obvious due to the absence of specific markers. Recently, following the increase in studies focusing on EVs, many critics have emerged. EV nomenclature, collection, pre-processing, separation, and concentration methods, quantification and characterization are now required. The MISEV2018 guideline harmonizes these aspects and avoids misunderstandings such as the presence of potential contaminant in EV preparations (21).

BIOGENESIS OF EVs

Classification in microvesicle or exosome depends on EV biogenesis mode. However, depending on the cell source, exosome, and microvesicle biogenesis can share similarities. Exosome and microvesicle biogenesis share common molecular components and biogenesis mechanisms at the plasma membrane or at the endosomal membrane (1). EV biogenesis mechanisms have only recently started to be uncovered. Tumor microenvironmental modifications appear to play a crucial role in EV release. Ionic homeostasis changes were reported to influence EV biogenesis. Intracellular Ca^{2+} increase induces the collapse of plasma membrane phospholipid asymmetry, the destabilization of plasma membrane-cytoskeletal anchorage and finally the release of EVs (18–22). Microenvironmental acidosis promotes tumor progression by stimulating invasion and metastasis and was reported to stimulate EV shedding (23–25). Extracellular matrix (ECM) degradation and bioactive peptide release, such as elastin-derived peptides, increase EV release by cancer cells (18). To date, independent pathways have been shown to be involved in EV biogenesis: the endosomal sorting complex required for the transport (ESCRT) dependent pathway, the asymmetry lipid involvement required for the budding formation and release, the tetraspanin-dependent pathway responsible for selecting cargoes for exosomes, the syndecan and syntenin pathways required for budding (2, 26–28). The intracellular trafficking involved in exosome and EV secretion is mediated by Rab GTPase proteins (Rab proteins and SNARE proteins) that control intracellular vesicle trafficking, exosome release and the fusion of lipid bilayer at the plasma membrane. The cytoskeletal components play a crucial role in the budding and the release of EVs (29). Actomyosin cytoskeleton reorganization is necessary to microvesicle formation and probably to exosome release at the plasma membrane.

BIOACTIVITIES OF PANCREATIC DUCTAL ADENOCARCINOMA (PDAC) EVs

Like in many cancer, the PDAC microenvironment is complex. It results from communications between PDAC cells, stromal cells such as fibroblasts, myofibroblasts, stellate cells, vascular endothelial cells, immune cells, all embedded in an abundant ECM (30). Cancer-associated fibroblasts (CAFs) promote ECM remodeling and tumor growth. Immune cells have a highly immunosuppressive activity and further contribute to immune evasion. Interactions between cellular and acellular components of the PDAC-tumor microenvironment promote tumor progression, contribute to metabolism alterations, cancer cell proliferation, tumor metastasis, and abnormal tumor-associated immunity (31). In this environment, EVs play a crucial role (32–34). Stromal EVs promote invasive behavior and upregulate drug resistance and immune escape pathways in cancer cells. PDAC EVs induce stromal cell phenotype changes, from fibroblasts to CAFs for example, promote tumor cell proliferation, invasion, and metastasis; they also modulate tumor-associated immunity (35). Pancreatic exosomes were also reported to induce cell death and to inhibit Notch-1 pathway (36). Microvesicules derived from human pancreas carcinoma cells were reported to induce IL-10 synthesis in human classical monocytes *via* hyaluronan, which in turn activates the PI3K/Akt/mTOR pathway (37).

Whatever the nature of the EV/cell interaction, EVs play cargo molecule function, and protect their contents from degradative enzymes like RNases and proteinases due to their double lipid membrane (1). After their release in the extracellular microenvironment, EVs target recipient cells and deliver their content that induce functional responses and modulate phenotypic changes with physiological and pathological consequences. This EV-dependent cell-to-cell communication requires receptor-related events like docking at the cell membrane, activation of cell surface receptors, and intracellular signaling, vesicle endocytosis, or membrane fusion

with target cell (1). These aspects of the EV-derived intercellular communication are not fully understood. Due to different factors (EV origin and type, identity and origin of the targeting cells), these processes are complex and determine downstream effects and processes. Current studies mainly focused on membrane interaction, receptor/ligand identification, and intercellular fate of EV pools. The mechanisms of EV uptake and cargo delivery into the target cells are still incompletely characterized. Depending on the EV origin and the target cell type, this step may be either very specific (ligand-receptor interactions: integrins/ICAM interaction, lectin/proteoglycan interaction, lipid-binding protein/phosphatidylserine interaction) or very general (micropinocytosis, phagocytosis, caveolae-, or clathrin-dependent mechanisms, membrane fusion) (1, 2). EVs may transfer informations to target cells by acting at the cell surface as cargo of ligand to cell membrane receptor, without delivery of their content. The presence of a specific protein on EV surface can lead to positive- or negative-election mechanisms. The CD47 integrin-associated protein is often present at the EV surface and increases the time of EV circulation in the blood by preventing their phagocytosis by macrophages and monocytes (38). This results in an increased EV uptake by pancreatic cells. All these biological activities, associated with the increased production of EV in PDAC, are consistent with a potential role of EVs as biomarkers of PDAC.

EVs AS BIOMARKERS FOR DIAGNOSIS AND PROGNOSIS IN PANCREATIC CANCER

EVs, especially exosomes, are considered a future potent tool for both diagnostic, prognostic, and therapeutic applications, being a natural way for efficient biodelivery. EVs of defined cell types may serve as novel tools for various therapeutic approaches, including anti-tumor therapy, pathogen vaccination, immune-modulatory, and regenerative therapies or drug delivery (6). The emerging field of basic and applied EV research will significantly influence the biomedicinal landscape in the future. EVs contain specific molecules of originate cells, display stability, and abundance in various biofluids, that may largely increase sensitivity and specificity in PDAC diagnosis. Many clinical trials show increased number of biofluid exosomes in cancer patients compared to healthy people (39–42), suggesting that the measure of the levels of circulating exosomes could represent a disease marker *per se* (43). This may be the case of pancreatic cancer as well. In this section, we will focus on the impact of the EVs on the diagnosis and prognosis of PDAC. The continuing increase in PDAC incidence leads it to be the second leading cause of cancer mortality in 2030 (44). The dismal prognosis of PDAC is mainly attributed to poor detection rates at early stages, rapid progression, and disappointing surgical resection outcomes. Most patients with PDAC lack diagnostic symptoms during early stages, and existing early screening biomarker lack (35). Diagnosis mainly relies on medical imaging and pathological confirmation on tissue sample analysis (45). The identification of blood markers remains an important challenge in daily practice, since the tumor marker CA19-9 showed a lack of sensitivity and specificity in non-advanced PDAC. To increase pathological diagnosis performance, different biomarkers have been studied in order to differentiate PDAC from benign lesions. Molecular markers such as exosomal DNA mutation or exosomal miR expression and exosomal surface biomarkers such as integrins or glypican1 (GPC1) remains the most promising exosomal biomarkers of PDAC.

EV Proteins as Potential Biomarkers of PDAC

Differences in composition between exosomes from human non-malignant epithelial and pancreatic cancer cells were analyzed by Emmanouilidi et al. (46). Proteomic analysis reveals the selective enrichment of known exosome markers and also signaling proteins involved in pancreatic cancer progression (KRAS, CD44, and EGFR) in oncogenic exosomes compared to exosomes from non-malignant cells. Moreover, oncogenic exosomes contain factors known to regulate the pre-metastatic niche (S100A4, F3, ITGβ5, and ANXA1), clinically-relevant proteins which correlate with poor prognosis (CLDN1, MUC1) as well as protein networks involved in various cancer hallmarks including proliferation (CLU, CAV1), invasion (PODXL, ITGA3), metastasis (LAMP1, ST14) and immune surveillance escape (B2M). This study highlights the modification of exosome protein content during tumorigenesis and suggests putative components as prognostic and diagnostic biomarkers in pancreatic cancer (46).

To date, only described in prostate cancer, the microenvironmental pressure induces a preferential expression of known tumor markers like Prostate Specific Antigen (PSA) on the released exosomes. Increased exosomal PSA expression has been shown to represent a valuable biomarker for both screening and secondary prevention of prostate cancer in clinical studies (47). Up to now, PDAC exosome researches do not provide such a promising tumor-specific biomarker.

However, different cell surface biomarkers were assessed for the diagnosis or prognosis of PDAC. Among these potential biomarkers, integrins and GPC1 are of particular interest. The implication of integrins in the determination of organotropic metastasis was investigated by Hoshino et al. in 2015 (48). They showed that the capture of tumor-derived exosomes by organ-specific cells prepares the pre-metastatic niche. Proteomic analysis revealed that tumor-derived exosomes harbored specific integrin patterns associated with the organ-specific metastases. Exosomal $\alpha_6\beta_4$ and $\alpha_6\beta_1$ integrins were associated with lung metastasis, whereas $\alpha_v\beta_5$ integrin was related to liver metastasis. Moreover, exosomal integrin patterns could also modulate the interaction between exosomes and ECM components in specific organs. Interestingly, $\alpha_v\beta_5$ integrin mainly expressed in BxPC-3-LiT pancreatic cell line derived exosomes co-localized with liver macrophages in fibronectin-rich microenvironments. Accumulating evidence showed that exosomes are not only protein or nucleic acid cargos. Recent proteomic studies showed that the amount of α_6, α_v, and β_1 integrin-subunits in tumor-derived exosomes was correlated with tumor stages in different

epithelial cancer cells and could be considered as a putative circulating biomarker of some primary tumors (49). As well, the detection of exosomal $\alpha_v\beta_3$ integrin in prostate cancer patients could be a clinically useful biomarker of prostate cancer progression (50).

GPC1 is a cell surface heparan sulfate proteoglycan, barely expressed in normal pancreatic tissue. Its transcript is silenced in non-tumoral tissue whereas it is re-expressed in PDAC due to potential epigenetic variation of promotor methylation (51). Immunochemistry analysis of PDAC tissues showed that highly positive expression is associated with shorter overall survival (OS) and could be considered as a diagnostic and prognostic marker of PDAC (52). On the other hand ELISA based assay of serum GPC1 do not allow to distinguish PDAC patients from controls and cannot be used as a diagnostic biomarker of PDAC patients. Nevertheless, GPC1 appeared specifically enriched in circulating pancreatic cancer cell-derived exosomes (53, 54). Using flow cytometry analysis of serum, Melo et al. reported that GPC1 positive exosomes allowed to distinct healthy subjects or benign pancreatic disease patients from pancreatic cancer patients. Moreover, exosomal GPC1 level correlates with tumor burden and patient survival (53, 54). GPC1 was also suggested as an early diagnostic and prognostic marker as well as a therapeutic target for PDAC by Haizhen et al. (51). By contrast, a recent study showed that GPC1 positive EVs do not allow to distinct PDAC from benign pancreatic diseases (55). Despite these conflicting results, exosomal GPC1 remains a potential biomarker of interest in the diagnosis or prognosis of PDAC but needs further investigations to be validated in daily practice.

Cytoskeleton-associated protein 4 (CKAP4), a novel Dickkopf WNT Signaling Pathway Inhibitor 1 (DKK1) receptor was highly detected in the serum of PDAC patients, whereas it was barely detectable in serum from postoperative patients. Exosomal CKAP4 may represent a PDAC biomarker and anti-CKAP4 mAbs can contribute to the development of novel diagnostic methods and therapeutics (56).

Large extracellular vesicles, specifically AnnexinV$^+$ EpCAM$^+$ CD147$^+$ tumor-associated microparticles were reported to facilitate the detection of pancreas carcinoma (57).

Venous thrombo-embolic event (VTE) biomarkers including D-dimers and microvesicle-tissue factor (MV-TF) were reported to be related to cancer process and dissemination. D-dimers and MV-TF activity are associated to future VTE in PDAC patients and could help to identify patients who could benefit from thromboprophylaxis (58).

KRAS Mutation in Circulating EVs as a Biomarker of PDAC

Up to 80% of PDAC cells harbored *KRAS* mutations. *KRAS* analyses can be performed either on tissue or plasma samples. However, circulating tumor DNA (ctDNA) can only be detected in 30–68% of resectable tumors and in 70–80% of advanced PDAC. This may be explained by a limited amount of ctDNA released by tumor cells at early stages of the disease or by the degradation of ctDNA by DNases (59). Nevertheless, detection of ctDNA seems to be correlated with the prognosis of PDAC. For example, Lin et al. showed that ctDNA was detected in 29.2% of PDAC patients and its detection of ctDNA was associated with a significantly shorter overall survival (OS) (60). Kalluri et al. showed that exosomes contained double stranded DNA (61). Exosomal DNA seems to be protected from blood DNAse degradation which potentially allows the identification of a higher rate of mutations. As reported in plasma samples, circulating exosomal DNA analyses allow the detection of *KRAS* mutation in PDAC. Yang et al. reported 39.6% of *KRAS* c.35G>A (p.Gly12Asp) mutation in 48 PDAC derived exosomal plasma samples. Moreover, *KRAS* mutations have also been isolated in non-tumoral samples (i.e., chronic pancreatitis) and more surprisingly in three of 114 (2.6%) healthy subject samples (62). *KRAS* mutations in presumed healthy subject were also identified in different studies both in ctDNA and exosomal DNA (26, 63). Moreover, *KRAS* mutation allele frequency (MAF) from exosomal DNA is significantly associated with disease progression after neoadjuvant chemotherapy in a prospective cohort of potentially resectable pancreatic tumor. In addition, exosomal *KRAS* MAF>5% is associated with shorter progression free survival (PFS) and OS in treatment-naïve metastatic patients (64). Blood molecular analyses are not currently used in daily practice for the management of PDAC despite the very high proportion of *KRAS* mutated tumors. Other studies are needed to confirm these results but circulating exosomal DNA analysis may be considered as a potential screening, diagnosis, or prognosis tool for PDAC management. Castillo et al. performed exosomal proteomic analysis on the "surfaceome" on different human PDAC cell lines, which revealed protein specific expression pattern on exosomal surface (i.e., CLDN4, EpCAM, CD151, LGALS3BP, HIST2H2BE, and HIST2H2BF) (65). This protein panel could be used as a capture assay to enrich pancreatic cancer-specific exosomal cargo, which may improve detection of molecular alterations such as *KRAS* mutations.

Exosomal miRNA in PDAC EVs

Kumar et al. indicated the presence of a wide variety of RNAs including mRNA, miRNA, lncRNA, tRNA, and piRNA in exosomes in serum of healthy subjects, as well as intraductal papillary mucosal neoplasms and PDAC (66). Exosomes from cancer cells or stromal cells like stellate cells, endothelial cells, or immune cells, carrying miRNAs, participate in tumor pathogenesis and progression by modulating microenvironment and cell phenotypes (1). Ali et al. suggested a crosstalk between pancreatic stellate cells/CAF cells and PDAC cells, resulting in a miR-21/miR-221 over-expression which contributes to aggressiveness to PDAC (67). Takikawa et al. demonstrated that pancreatic stellate cell-derived exosomes contained a variety of miRNAs including miR-21-5p, some of them such as miR-451a were enriched in exosomes compared to stellate cell origin (68). These pancreatic stellate cell-derived exosomes stimulated PDAC cell proliferation, migration, and chemokine (C—X—C motif) ligands 1 and 2 mRNA expression. Yin et al. investigated the role of the exosome-derived tumor-associated macrophage miR-501-3p in the progression of PDAC (69). M2 macrophage-derived exosomal miR-501-3p inhibits tumor suppressor *TGFBR3* gene

and facilitates the development of PDAC by activating the TGF-β signaling pathway. Exosomal miRNA involvement in PDAC could provide novel targets for the prevention of tumor progression and/or for the treatment of PDAC.

Detection of exosomal miRNAs in biofluids like serum, plasma, or saliva, being sensitive, non-invasive, and easy to obtain, has a great potential to become a novel screening method for PDAC patients. Despite a lack of standardization in exosomal isolation and measurement, exosomal miR expression seems to be a promising circulating biomarker in PDAC diagnosis or prognosis (70). Lai et al. compared exosomal GPC1 levels to a miR signature for the diagnosis of PDAC. Interestingly, exosomal miR signature (miR-10b, miR-17-5p, miR-21, miR-30c, miR-181a, and let7a) could differentiate PDAC from normal tissue whereas GPC1 did not (70–72). Numerous studies compared the expression of miR in PDAC vs. control group and concluded that miR were highly enriched in pancreatic cancer exosomes (73). Xu et al. found that miR-196a was enriched in PDAC derived exosomes compared with healthy subjects, whereas miR-1246, miR-3976, miR-4306, and miR-4644 expression were significantly increased compared with control groups (74). Interestingly, these miR were also elevated in exosome-depleted serum, but at a low level (75). Zhou et al. identified six exosomal miRNA signatures (miR-122-5p, miR-125b-5p, miR-192-5p, miR-193b-3p, miR-221-3p, and miR-27b-3p) in plasma of pancreatic cancer patients vs. healthy patients (76). These miRNAs could modulate several molecular pathways closely related with pancreatic cancer like p53 and TGF-β signaling pathways. Among these exosomal miRNAs, down-regulation of plasma miR-125b-5p concentration might act as an independent biomarker in predicting OS of pancreatic patients. Zou et al. identified a six-miRNA (let-7b-5p, miR-192-5p, miR-19a-3p, miR-19b-3p, miR-223-3p, and miR-25-3p) panel in serum for pancreatic cancer early and non-invasive diagnosis (77). Their analysis shows significant miR-192-5p, miR-19a-3p, and miR-19b-3p over-expression in both pancreatic tissue and serum-derived exosomes samples. In the same way, exosomal miR-21, miR-191, and miR-451a were also enriched in pancreatic cancer derived exosomes vs. controls. In addition, a high exosomal miR-21 expression was associated with poor OS in pancreatic cancer patients (median OS of 344 vs. 846 days for low expression) (78). These results are consistent with Karasek et al. results which concluded that plasma levels of miR-21 were significantly higher in PDAC compared to healthy controls and associated with poor OS in PDAC (79).

To date, no exosomal biomarkers are used in clinical practice. Exosome isolation from liquid biopsy varies between studies. Further large prospective studies are needed to clarify the potential use of exosomal biomarkers in cancer diagnosis and prognosis.

EV IMAGING *IN VIVO* AND POTENTIAL APPLICATION IN PDAC METASTASIS STUDY

PDAC diagnosis mainly relies on medical imaging and pathological confirmation on tissue sample analysis. EV tracking *in vivo* using multimodal imaging should provide crucial informations in PDAC development. In a context of translational research, a multitude of non-invasive imaging modalities is available both in a preclinical and clinical setting. Multimodal imaging is useful in cancer disease to follow tumor growth, anatomical imaging process, and composition of tumor by contrast or metabolism (80). Non-invasive imaging modalities may provide better understanding of the *in vivo* kinetics of EV release and dissemination during cancer progression. Molecular imaging implies two main methods: direct and indirect EV labeling. During the last decade, the *in vivo* multimodal imaging of small animals, which includes a multitude of techniques, was used in preclinical research. Imaging technology is essential to understand the biodistribution of EVs and their therapeutic implication in pathologies, at the level of intercellular communication between EVs from donor vesicles to receptor cells or distant organs. Thus, it is possible to understand how EVs derived from tumor and/or stromal cells could affect their environment. Currently, multimodal imaging relies on optical imaging, nuclear imaging or Positron Emission Tomography (PET), and Magnetic Resonance Imaging (MRI) (81).

Optical Imaging for PDAC EV Tracking Analysis

Optical imaging tools and particularly bioluminescence imaging is an indirect cell labeling technique using reporter genes. It is a useful imaging modality considering the easy translation from *in vitro* to *in vivo*. Bioluminescence signal is generated by conversion of chemical energy into visible light due to luciferase enzymes and their substrates in living animals such as *Gaussia* luciferase (GLuc), *Renilla* luciferase (RLuc), *Firefly* luciferase (FLuc), or bacterial luciferase (82–86). In living animals, spatio-temporally real-time non-invasive biological process is a useful for the evaluation of biodistribution, survival, and proliferation of administered cells (87). During last decade, a new optical imaging reporter was used to demonstrate the specific targeting after systemic injection of EVs into the original tumor sites in a thyroid cancer model and for loading anticancer drugs into mesenchymal stem cell-derived exosome mimetics for cancer therapy using *Renilla* Luciferase (Rluc) and *Firefly* Luciferase (Fluc) (88, 89). However, this technique needs to take into consideration the toxicity and half-life of the substrates (e.g., coelenterazine), the poor spatial resolution, limitation of penetration depth, and low quantification accuracy in tissues *in vivo*. Fluorescence imaging is a direct labeling used to observe the initial spatio-temporal biodistribution, localization, and migration of administrated cells. Nonetheless, the using for long-term monitoring cannot be used due to signal dilution by mitotic division of labeled cells and enduring signals from labeled cells (90). However, it is conceivable to image exogenous EV expressing recombinant labeled cell surface biomarkers within the body after a systemic injection and also allows the visualization of intercellular communication through microscopic analysis. Fluorescence measure is achievable thanks to recombinant protein labeling with GFP or RFP. CD63 is commonly used as a marker of exosome (91). Organic fluorescent

dyes are also used in direct imaging technique; they are easy to use, their fluorescent signal is stable over time and do not imply genetic engineering of the cells (92, 93). The most commonly used dyes to label cell membrane for imaging are DiR, cy7, DiD, DiL, and PKL. However, labeling with lipophilic dyes promotes clumping of EV. It is important to avoid artifacts by performing many washes prior to injection and/or incubation. EV organotropism could be influenced by EV labeling with lipophilic dye. Optical imaging and its weaknesses make visualization of inner organs impossible and exclude clinical translation.

Nuclear Imaging for PDAC EV Tracking Analysis

Nuclear imaging or PET allows to visualize *in vivo* three-dimensional measurement of metabolic and molecular processes with a high sensitivity for preclinical and clinical imaging. For cancer imaging the most commonly used tracer is 2-[^{18}F] fluoro-2-deoxy-D-glucose ([^{18}F]-FDG) (94). In fact, it is possible to visualize the accumulation of radioactive tracers associated with EVs in organs after *in vivo* administration. Combined with other advanced imaging techniques such as MRI or single photon emission computed tomography (SPECT), it is possible to track EVs in tissues and overcome the limitation of tissue penetration of optical imaging. In the study of EVs, this technique uses direct labeling methods and radionuclides like ^{111}In-oxine or ^{99m}Tc-hexamethylpropyleneamineoxin (HMPAO) (95–97). Nuclear imaging allows much greater penetration in tissues than optical imaging. However, this technique is very expensive and depends on the regulatory policies of radioactive molecules.

MRI for PDAC EV Tracking Analysis

MRI is a preclinical imaging technique using anatomical modalities which provides high anatomical resolution images with an excellent two- and three-dimensional spatial resolution and no depth limitation. MRI gives an excellent tissue contrast using specialized and personalized protocol like T_2-weighted imaged and diffusivity of water molecules with Apparent Diffusion Coefficient (98, 99). The combination of MRI and PET imaging modalities into a single scanner correlates to anatomical findings, morphological information, molecular aspects, and metabolic alterations of cancer diseases (100).

Ultra-small super magnetic particles such as iron oxide or ultra-small super-paramagnetic iron oxide (USPIO) are tracers that allow T_2-weighted to study the EV location in the body (61, 101, 102). These USPIOs can be incorporated by electroporation into EVs or by directly adding them directly into the cell culture medium *in vitro* (102). This technique may be complementary to bioluminescence optical imaging, giving robust, and reliable data. However, before injection, it requires a large amount of labeled EVs to quantify MRI scans. Nonetheless, despite a high-resolution images, the sensitivity with EV-USPIO is lower compared to optical imaging and nuclear imaging (103).

Recent studies have shown the bio-pathological role of EVs in tumor progression, disease diagnosis, and drug-delivery for therapeutic purposes (93, 104). Each imaging modality presents advantages and disadvantages but considering all these different techniques is essential to select the most appropriate one (61). Improving multimodal imaging techniques may benefit to EV future applications including diagnostic and therapeutic approaches in various diseases (38).

Application in PDAC Metastatic Studies?

PDAC is highly metastatic with poor prognosis, mainly due to delayed detection. Intercellular communication is critical for metastatic progression. PDAC-derived exosomes induce liver pre-metastatic niche formation in naïve mice and consequently increase liver metastatic burden (15). EV tracking *in vivo* using multimodal imaging should provide crucial informations in PDAC development. EVs may also be used as vehicles for drug-delivery and *in vivo* imaging will allow to study their biodistribution (105). A standard operating procedure was established by Mendt et al. to generate engineered exosomes with the ability to target oncogenic KRAS (iExosomes). The clinical-grade iExosomes were tested in multiple *in vitro* and *in vivo* studies to confirm suppression of oncogenic KRAS and an increase in the survival of several mouse models with pancreatic cancer (106, 107).

CONCLUSION

EVs present different origins and therefore different contents. By their differences, their contribution in the cross-talk between many cell types is not anecdotal. EV domain is of growing interest. However, EV studies must overcome some difficulties such as the homogenization of the standardization of methodological approaches in EV isolation and a strict respect in the EV characterization. *In vivo* studies by different approaches will contribute to better understand EV impacts in physio-pathological conditions and principally in cancers such as PDAC. EVs may also contribute in patient diagnosis or prognosis. Strategies to promote the therapeutic application of EVs in future clinical studies are more and more considered. EVs of defined cell types could serve as innovative tools for different therapeutic approaches, including anti-tumor therapy, immune-modulatory, and regenerative therapies and drug delivery.

AUTHOR CONTRIBUTIONS

BB, SB-P, LN, and J-BO: conception, design, and manuscript writing. All authors: revision and final approval of the manuscript.

FUNDING

This work was supported by grants from the Centre National de la Recherche Scientifique (UMR 7369), the University of Reims Champagne-Ardenne and the Region Champagne-Ardenne.

REFERENCES

1. van Niel G, D'Angelo G, Raposo G. Shedding light on the cell biology of extracellular vesicles. *Nat Rev Mol Cell Biol.* (2018) 213–28. doi: 10.1038/nrm.2017.125
2. Mathieu M, Martin-Jaular L, Lavieu G, Théry C. Specificities of secretion and uptake of exosomes and other extracellular vesicles for cell-to-cell communication. *Nat Cell Biol.* (2019) 21:9–17. doi: 10.1038/s41556-018-0250-9
3. Yáñez-Mó M, Siljander PRM, Andreu Z, Zavec AB, Borràs FE, Buzas EI, et al. Biological properties of extracellular vesicles and their physiological functions. *J Extracell Vesicles.* (2015) 4:27066. doi: 10.3402/jev.v4.27066
4. Wolf P. The nature and significance of platelet products in human plasma. *Br J Haematol.* (1967) 13:269–88. doi: 10.1111/j.1365-2141.1967.tb08741.x
5. Chargaff E, West R. The biological significance of the thromboplastic protein of blood. *J Biol Chem.* (1946) 166:189–97.
6. Lener T, Gimona M, Aigner L, Börger V, Buzas E, Camussi G, et al. Applying extracellular vesicles based therapeutics in clinical trials - an ISEV position paper. *J Extracell Vesicles.* (2015) 4:30087. doi: 10.3402/jev.v4.30087
7. Fais S, O'Driscoll L, Borras FE, Buzas E, Camussi G, Cappello F, et al. Evidence-based clinical use of nanoscale extracellular vesicles in nanomedicine. *ACS Nano.* (2016) 10:3886–99. doi: 10.1021/acsnano.5b08015
8. Keller S, Ridinger J, Rupp AK, Janssen JWG, Altevogt P. Body fluid derived exosomes as a novel template for clinical diagnostics. *J Transl Med.* (2011) 9:86. doi: 10.1186/1479-5876-9-86
9. Piccin A, Murphy WG, Smith OP. Circulating microparticles: pathophysiology and clinical implications. *Blood Rev.* (2007) 21:157–71. doi: 10.1016/j.blre.2006.09.001
10. Taylor DD, Gerçel-Taylor C. Tumour-derived exosomes and their role in cancer-associated T-cell signalling defects. *Br J Cancer.* (2005) 92:305–11. doi: 10.1038/sj.bjc.6602316
11. Raposo G, Stoorvogel W. Extracellular vesicles: exosomes, microvesicles, and friends. *J Cell Biol.* (2013) 200:373–83. doi: 10.1083/jcb.201211138
12. Al-Nedawi K, Meehan B, Micallef J, Lhotak V, May L, Guha A, et al. Intercellular transfer of the oncogenic receptor EGFRvIII by microvesicles derived from tumour cells. *Nat Cell Biol.* (2008) 10:619–24. doi: 10.1038/ncb1725
13. Zaborowski MP, Balaj L, Breakefield XO, Lai CP. Extracellular vesicles: composition, biological relevance, and methods of study. *Bioscience.* (2015) 65:783–97. doi: 10.1093/biosci/biv084
14. Kahlert C, Melo SA, Protopopov A, Tang J, Seth S, Koch O, et al. Identification of doublestranded genomic dna spanning all chromosomes with mutated KRAS and P53 DNA in the serum exosomes of patients with pancreatic cancer. *J Biol Chem.* (2014) 289:3869–75. doi: 10.1074/jbc.C113.532267
15. Costa-Silva B, Aiello NM, Ocean AJ, Singh S, Zhang H, Thakur BK, et al. Pancreatic cancer exosomes initiate pre-metastatic niche formation in the liver. *Nat Cell Biol.* (2015) 17:816–26. doi: 10.1038/ncb3169
16. Stone L. Sending a signal through oncosomes. *Nat Rev Urol.* (2017) 4:259. doi: 10.1038/nrurol.2017.41
17. Bertolini I, Terrasi A, Martelli C, Gaudioso G, Di Cristofori A, Storaci AM, et al. A GBM-like V-ATPase signature directs cell-cell tumor signaling and reprogramming via large oncosomes. *EBioMedicine.* (2019) 41:225–35. doi: 10.1016/j.ebiom.2019.01.051
18. Brassart B, Da Silva J, Donet M, Seurat E, Hague F, Terryn C, et al. Tumour cell blebbing and extracellular vesicle shedding: key role of matrikines and ribosomal protein SA. *Br J Cancer.* (2019) 120:453–65. doi: 10.1038/s41416-019-0382-0
19. Minciacchi VR, Spinelli C, Reis-Sobreiro M, Cavallini L, You S, Zandian M, et al. MYC mediates large oncosome-induced fibroblast reprogramming in prostate cancer. *Cancer Res.* (2017) 77:2306–17. doi: 10.1158/0008-5472.CAN-16-2942
20. Lötvall J, Hill AF, Hochberg F, Buzás EI, Di Vizio D, Gardiner C, et al. Minimal experimental requirements for definition of extracellular vesicles and their functions: a position statement from the International society for extracellular vesicles. *J Extracell Vesicles.* (2014) 3:26913. doi: 10.3402/jev.v3.26913
21. Théry C, Witwer KW, Aikawa E, Alcaraz MJ, Anderson JD, Andriantsitohaina R, et al. Minimal information for studies of extracellular vesicles 2018 (MISEV2018): a position statement of the International society for extracellular vesicles and update of the MISEV2014 guidelines. *J Extracell Vesicles.* (2018) 7:1535750. doi: 10.1080/20013078.2018.1461450
22. Sanderson MP, Keller S, Alonso A, Riedle S, Dempsey PJ, Altevogt P. Generation of novel, secreted epidermal growth factor receptor (EGFR/ErbB1) isoforms via metalloprotease-dependent ectodomain shedding and exosome secretion. *J Cell Biochem.* (2008) 103:1783–97. doi: 10.1002/jcb.21569
23. Gillies RJ, Pilot C, Marunaka Y, Fais S. Targeting acidity in cancer and diabetes. *Biochim Biophys Acta Rev Cancer.* (2019) 1871:273–80. doi: 10.1016/j.bbcan.2019.01.003
24. Logozzi M, Spugnini E, Mizzoni D, Di Raimo R, Fais S. Extracellular acidity and increased exosome release as key phenotypes of malignant tumors. *Cancer Metastasis Rev.* (2019) 38:93–101. doi: 10.1007/s10555-019-09783-8
25. Pillai SR, Damaghi M, Marunaka Y, Spugnini EP, Fais S, Gillies RJ. Causes, consequences, and therapy of tumors acidosis. *Cancer Metastasis Rev.* (2019) 38:205–22. doi: 10.1007/s10555-019-09792-7
26. Allenson K, Castillo J, San Lucas FA, Scelo G, Kim DU, Bernard V, et al. High prevalence of mutant KRAS in circulating exosome-derived DNA from early-stage pancreatic cancer patients. *Ann Oncol.* (2017) 28:741–7. doi: 10.1093/annonc/mdx004
27. Aires V, Brassart B, Carlier A, Scagliarini A, Mandard S, Limagne E, et al. A role for peroxisome proliferator-activated receptor gamma in resveratrol-induced colon cancer cell apoptosis. *Mol Nutr Food Res.* (2014) 58:1785–94. doi: 10.1002/mnfr.201300962
28. Gagliano N, Sommariva M, Moscheni C, Liguori E, Cazzaniga F, Sartori P, et al. Extracellular matrix components affect cell migration and invasive potential of cultured human pancreatic ductal adenocarcinoma cells. *Ital J Anat Embryol.* (2017) 122:97.
29. Ostrowski M, Carmo NB, Krumeich S, Fanget I, Raposo G, Savina A, et al. Rab27a and Rab27b control different steps of the exosome secretion pathway. *Nat Cell Biol.* (2010) 12:19–30. doi: 10.1038/ncb2000
30. Procacci P, Moscheni C, Sartori P, Sommariva M, Gagliano N. Tumor–stroma cross-talk in human pancreatic ductal adenocarcinoma: a focus on the effect of the extracellular matrix on tumor cell phenotype and invasive potential. *Cells.* (2018) 7:158. doi: 10.3390/cells7100158
31. Mahadevan D, Von Hoff DD. Tumor-stroma interactions in pancreatic ductal adenocarcinoma. *Mol Cancer Ther.* (2007) 6:1186–97. doi: 10.1158/1535-7163.MCT-06-0686
32. Lucien F, Leong HS. The role of extracellular vesicles in cancer microenvironment and metastasis: myths and challenges. *Biochem Soc Trans.* (2019) 47:273–280. doi: 10.1042/BST20180253
33. Massoumi RL, Hines OJ, Eibl G, King JC. Emerging evidence for the clinical relevance of pancreatic cancer exosomes. *Pancreas.* (2019) 48:1–8. doi: 10.1097/MPA.0000000000001203
34. Von Ahrens D, Bhagat TD, Nagrath D, Maitra A, Verma A. The role of stromal cancer-associated fibroblasts in pancreatic cancer. *J Hematol Oncol.* (2017) 10:76. doi: 10.1186/s13045-017-0448-5
35. Qiu J, Yang G, Feng M, Zheng S, Cao Z, You L, et al. Extracellular vesicles as mediators of the progression and chemoresistance of pancreatic cancer and their potential clinical applications. *Mol Cancer.* (2018) 17:2. doi: 10.1186/s12943-017-0755-z
36. Beloribi S, Ristorcelli E, Breuzard G, Silvy F, Bertrand-Michel J, Beraud E, et al. Exosomal lipids impact notch signaling and induce death of human pancreatic tumoral SOJ-6 cells. *PLoS ONE.* (2012) 7:e47480. doi: 10.1371/journal.pone.0047480
37. Lenart M, Rutkowska-Zapala M, Baj-Krzyworzeka M, Szatanek R, Weglarczyk K, Smallie T, et al. Hyaluronan carried by tumor-derived microvesicles induces IL-10 production in classical (CD14++CD16–) monocytes via PI3K/Akt/mTOR-dependent signalling pathway. *Immunobiology.* (2017) 222:1–10. doi: 10.1016/j.imbio.2015.06.019
38. Syn NL, Wang L, Chow EKH, Lim CT, Goh BC. Exosomes in cancer nanomedicine and immunotherapy: prospects and challenges. *Trends Biotechnol.* (2017) 35:665–76. doi: 10.1016/j.tibtech.2017.03.004
39. Kanwar SS, Dunlay CJ, Simeone DM, Nagrath S. Microfluidic device (ExoChip) for on-chip isolation, quantification and

characterization of circulating exosomes. *Lab Chip.* (2014) 14:1891–900. doi: 10.1039/C4LC00136B
40. Logozzi M, de Milito A, Lugini L, Borghi M, Calabrò L, Spada M, et al. High levels of exosomes expressing CD63 and caveolin-1 in plasma of melanoma patients. *PLoS ONE.* (2009) 4:e5219. doi: 10.1371/journal.pone.0005219
41. Osti D, Del BM, Rappa G, Santos M, Matafora V, Richichi C, et al. Clinical significance of extracellular vesicles in plasma from glioblastoma patients. *Clin Cancer Res.* (2019) 25:266–276. doi: 10.1158/1078-0432.CCR-18-1941
42. Zorrilla SR, Pérez-Sayans M, Fais S, Logozzi M, Torreira MG, García AG. A pilot clinical study on the prognostic relevance of plasmatic exosomes levels in oral squamous cell carcinoma patients. *Cancers.* (2019) 11:429. doi: 10.3390/cancers11030429
43. Cappello F, Logozzi M, Campanella C, Bavisotto CC, Marcilla A, Properzi F, et al. Exosome levels in human body fluids: a tumor marker by themselves? *Eur J Pharm Sci.* (2017) 96:93–8. doi: 10.1016/j.ejps.2016.09.010
44. Rahib L, Smith BD, Aizenberg R, Rosenzweig AB, Fleshman JM, Matrisian LM. Projecting cancer incidence and deaths to 2030: the unexpected burden of thyroid, liver, and pancreas cancers in the united states. *Cancer Res.* (2014) 74:2913–21. doi: 10.1158/0008-5472.CAN-14-0155
45. Moravec R, Divi R, Verma M. Detecting circulating tumor material and digital pathology imaging during pancreatic cancer progression. *World J Gastrointest Oncol.* (2017) 9:235–50. doi: 10.4251/wjgo.v9.i6.235
46. Emmanouilidi A, Paladin D, Greening DW, Falasca M. Oncogenic and non-malignant pancreatic exosome cargo reveal distinct expression of oncogenic and prognostic factors involved in tumor invasion and metastasis. *Proteomics.* (2019) 19:e1800158. doi: 10.1002/pmic.201800158
47. Logozzi M, Angelini DF, Giuliani A, Mizzoni D, Raimo R Di, Maggi M, et al. Increased plasmatic levels of psa-expressing exosomes distinguish prostate cancer patients from benign prostatic hyperplasia: a prospective study. *Cancers.* (2019) 11:1449. doi: 10.3390/cancers11101449
48. Hoshino A, Costa-Silva B, Shen TL, Rodrigues G, Hashimoto A, Tesic Mark M, et al. Tumour exosome integrins determine organotropic metastasis. *Nature.* (2015) 527:329–35. doi: 10.1038/nature15756
49. Hurwitz SN, Meckes DG. Extracellular vesicle integrins distinguish unique cancers. *Proteomes.* (2019) 7:14. doi: 10.20944/preprints201904.0052.v1
50. Krishn SR, Singh A, Bowler N, Duffy AN, Friedman A, Fedele C, et al. Prostate cancer sheds the αvβ3 integrin *in vivo* through exosomes. *Matrix Biol.* (2019) 77:41–57. doi: 10.1016/j.matbio.2018.08.004
51. Lu H, Niu F, Liu F, Gao J, Sun Y, Zhao X. Elevated glypican-1 expression is associated with an unfavorable prognosis in pancreatic ductal adenocarcinoma. *Cancer Med.* (2017) 6:1181–91. doi: 10.1002/cam4.1064
52. Zhou CY, Dong YP, Sun X, Sui X, Zhu H, Zhao YQ, et al. High levels of serum glypican-1 indicate poor prognosis in pancreatic ductal adenocarcinoma. *Cancer Med.* (2018) 7:5525–33. doi: 10.1002/cam4.1833
53. Frampton AE, Prado MM, López-Jiménez E, Fajardo-Puerta AB, Jawad ZAR, Lawton P, et al. Glypican-1 is enriched in circulating-exosomes in pancreatic cancer and correlates with tumor burden. *Oncotarget.* (2018) 9:19006–13. doi: 10.18632/oncotarget.24873
54. Melo SA, Luecke LB, Kahlert C, Fernandez AF, Gammon ST, Kaye J, et al. Glypican-1 identifies cancer exosomes and detects early pancreatic cancer. *Nature.* (2015) 523:177–82. doi: 10.1038/nature14581
55. Lucien F, Lac V, Billadeau DD, Borgida A, Gallinger S, Leong HS. Glypican-1 and glycoprotein 2 bearing extracellular vesicles do not discern pancreatic cancer from benign pancreatic diseases. *Oncotarget.* (2019) 10:1045–55. doi: 10.18632/oncotarget.26620
56. Kimura H, Yamamoto H, Harada T, Fumoto K, Osugi Y, Sada R, et al. CKAP4, a DKK1 receptor, is a biomarker in exosomes derived from pancreatic cancer and a molecular target for therapy. *Clin Cancer Res.* (2019) 25:1936–47. doi: 10.1158/1078-0432.CCR-18-2124
57. Julich-Haertel H, Urban SK, Krawczyk M, Willms A, Jankowski K, Patkowski W, et al. Cancer-associated circulating large extracellular vesicles in cholangiocarcinoma and hepatocellular carcinoma. *J Hepatol.* (2017) 67:282–92. doi: 10.1016/j.jhep.2017.02.024
58. Faille D, Bourrienne MC, de Raucourt E, de Chaisemartin L, Granger V, Lacroix R, et al. Biomarkers for the risk of thrombosis in pancreatic adenocarcinoma are related to cancer process. *Oncotarget.* (2018) 9:26453–65. doi: 10.18632/oncotarget.25458
59. Buscail E, Maulat C, Muscari F, Chiche L, Cordelier P, Dabernat S, et al. Liquid biopsy approach for pancreatic ductal adenocarcinoma. *Cancers.* (2019) 11:852. doi: 10.3390/cancers11060852
60. Lin M, Alnaggar M, Liang S, Chen J, Xu K, Dong S, et al. Circulating tumor DNA as a sensitive marker in patients undergoing irreversible electroporation for pancreatic cancer. *Cell Physiol Biochem.* (2018) 47:1556–64. doi: 10.1159/000490874
61. Kalluri R, Lebleu VS. Discovery of double-stranded genomic DNA in circulating exosomes. *Cold Spring Harb Symp Quant Biol.* (2016) 81:275–80. doi: 10.1101/sqb.2016.81.030932
62. Yang S, Che SPY, Kurywchak P, Tavormina JL, Gansmo LB, Correa de Sampaio P, et al. Detection of mutant KRAS and TP53 DNA in circulating exosomes from healthy individuals and patients with pancreatic cancer. *Cancer Biol Ther.* (2017) 18:158–65. doi: 10.1080/15384047.2017.1281499
63. Cohen JD, Javed AA, Thoburn C, Wong F, Tie J, Gibbs P, et al. Combined circulating tumor DNA and protein biomarker-based liquid biopsy for the earlier detection of pancreatic cancers. *Proc Natl Acad Sci USA.* (2017) 114:10202–7. doi: 10.1073/pnas.1704961114
64. Bernard V, Kim DU, San Lucas FA, Castillo J, Allenson K, Mulu FC, et al. Circulating nucleic acids are associated with outcomes of patients with pancreatic cancer. *Gastroenterology.* (2019) 156:108–18. doi: 10.1053/j.gastro.2018.09.022
65. Castillo J, Bernard V, San Lucas FA, Allenson K, Capello M, Kim DU, et al. Surfaceome profiling enables isolation of cancerspecific exosomal cargo in liquid biopsies from pancreatic cancer patients. *Ann Oncol.* (2018) 29:223–9. doi: 10.1093/annonc/mdx542
66. Kumar SR, Kimchi ET, Manjunath Y, Gajagowni S, Stuckel AJ. RNA cargos in extracellular vesicles derived from blood serum in pancreas associated conditions. *Sci Rep.* (2020) 10:2800. doi: 10.1038/s41598-020-59523-0
67. Ali S, Suresh R, Banerjee S, Bao B, Xu Z, Wilson J, et al. Contribution of microRNAs in understanding the pancreatic tumor microenvironment involving cancer associated stellate and fibroblast cells. *Am J Cancer Res.* (2015) 5:1251–64.
68. Takikawa T, Masamune A, Yoshida N, Hamada S, Kogure T, Shimosegawa T. Exosomes derived from pancreatic stellate cells: microRNA signature and effects on pancreatic cancer cells. *Pancreas.* (2017) 46:19–27. doi: 10.1097/MPA.0000000000000722
69. Yin Z, Ma T, Huang B, Lin L, Zhou Y, Yan J, et al. Macrophage-derived exosomal microRNA-501-3p promotes progression of pancreatic ductal adenocarcinoma through the TGFBR3-mediated TGF-β signaling pathway. *J Exp Clin Cancer Res.* (2019) 38:310. doi: 10.1186/s13046-019-1313-x
70. An T, Qin S, Xu Y, Tang Y, Huang Y, Situ B, et al. Exosomes serve as tumour markers for personalized diagnostics owing to their important role in cancer metastasis. *J Extracell Vesicles.* (2015) 4:27522. doi: 10.3402/jev.v4.27522
71. Lai X, Wang M, McElyea SD, Sherman S, House M, Korc M. A microRNA signature in circulating exosomes is superior to exosomal glypican-1 levels for diagnosing pancreatic cancer. *Cancer Lett.* (2017) 393:86–93. doi: 10.1016/j.canlet.2017.02.019
72. Que R, Ding G, Chen J, Cao L. Analysis of serum exosomal microRNAs and clinicopathologic features of patients with pancreatic adenocarcinoma. *World J Surg Oncol.* (2013) 11:219. doi: 10.1186/1477-7819-11-219
73. Gao Z, Jiang W, Zhang S, Li P. The state of the art on blood microRNAs in pancreatic ductal adenocarcinoma. *Anal Cell Pathol.* (2019) 2019:9419072. doi: 10.1155/2019/9419072
74. Xu YF, Hannafon BN, Zhao YD, Postier RG, Ding WQ. Plasma exosome miR-196a and miR-1246 are potential indicators of localized pancreatic cancer. *Oncotarget.* (2017) 8:77028–40. doi: 10.18632/oncotarget.20332
75. Madhavan B, Yue S, Galli U, Rana S, Gross W, Müller M, et al. Combined evaluation of a panel of protein and miRNA serum-exosome biomarkers for pancreatic cancer diagnosis increases sensitivity and specificity. *Int J Cancer.* (2015) 136:2616–27. doi: 10.1002/ijc.29324
76. Zhou X, Lu Z, Wang T, Huang Z, Zhu W, Miao Y. Plasma miRNAs in diagnosis and prognosis of pancreatic cancer: a miRNA expression analysis. *Gene.* (2018) 673:181–93. doi: 10.1016/j.gene.2018.06.037
77. Zou X, Wei J, Huang Z, Zhou X, Lu Z, Zhu W, et al. Identification of a six-miRNA panel in serum benefiting pancreatic cancer diagnosis. *Cancer Med.* (2019) 8:2810–22. doi: 10.1002/cam4.2145

78. Goto T, Fujiya M, Konishi H, Sasajima J, Fujibayashi S, Hayashi A, et al. An elevated expression of serum exosomal microRNA-191, - 21,−451a of pancreatic neoplasm is considered to be efficient diagnostic marker. *BMC Cancer.* (2018) 18:116. doi: 10.1186/s12885-018-4006-5
79. Karasek P, Gablo N, Hlavsa J, Kiss I, Vychytilova-Faltejskova P, Hermanova M, et al. Pre-operative plasma miR-21-5p is a sensitive biomarker and independent prognostic factor in patients with pancreatic ductal adenocarcinoma undergoing surgical resection. *Cancer Genomics Proteomics.* (2018) 15:321–7. doi: 10.21873/cgp.20090
80. Abadjian MCZ, Edwards WB, Anderson CJ. Imaging the tumor microenvironment. *Adv Exp Med Biol.* (2017) 1036:229–57. doi: 10.1007/978-3-319-67577-0_15
81. Gangadaran P, Hong CM, Ahn BC. Current perspectives on *in vivo* noninvasive tracking of extracellular vesicles with molecular imaging. *Biomed Res Int.* (2017) 2017:9158319. doi: 10.1155/2017/9158319
82. Keyaerts M, Caveliers V, Lahoutte T. Bioluminescence imaging: looking beyond the light. *Trends Mol Med.* (2012) 18:164–72. doi: 10.1016/j.molmed.2012.01.005
83. Verhaegent M, Christopoulos TK. Recombinant Gaussia luciferase: overexpression, purification, and analytical application of a bioluminescent reporter for DNA hybridization. *Anal Chem.* (2002) 74:4378–85. doi: 10.1021/ac025742k
84. Lorenz WW. Expression of the Renilla reniformis luciferase gene in mammalian cells. *J Biolumin Chemilumin.* (1996) 11:31–7.doi: 10.1002/SICI1099-127119960111:1<31::AID-BIO398>3.0.CO;2-M
85. Nealson KH, Hastings JW. Bacterial bioluminescence: its control and ecological significance. *Microbiol Rev.* (1979) 43:496–518. doi: 10.1128/MMBR.43.4.496-518.1979
86. Fraga H. Firefly luminescence: a historical perspective and recent developments. *Photochem Photobiol Sci.* (2008) 7:146–58. doi: 10.1039/b719181b
87. Kim JE, Kalimuthu S, Ahn BC. *In vivo* cell tracking with bioluminescence imaging. *Nucl Med Mol Imaging.* (2015) 49:3–10. doi: 10.1007/s13139-014-0309-x
88. Kalimuthu S, Gangadaran P, Rajendran RL, Zhu L, Oh JM, Lee HW, et al. A new approach for loading anticancer drugs into mesenchymal stem cell-derived exosome mimetics for cancer therapy. *Front Pharmacol.* (2018) 9:1116. doi: 10.3389/fphar.2018.01116
89. Gangadaran P, Li XJ, Kalimuthu S kumar, Min OJ, Hong CM, Rajendran RL, et al. New optical imaging reporter-labeled anaplastic thyroid cancer-derived extracellular vesicles as a platform for *in vivo* tumor targeting in a mouse model. *Sci Rep.* (2018) 8:13509. doi: 10.1038/s41598-018-31998-y
90. Kraitchman DL, Bulte JWM. *In vivo* imaging of stem cells and beta cells using direct cell labeling and reporter gene methods. *Arterioscler Thromb Vasc Biol.* (2009) 29:1025–30. doi: 10.1161/ATVBAHA.108.165571
91. Mittelbrunn M, Gutiérrez-Vázquez C, Villarroya-Beltri C, González S, Sánchez-Cabo F, González MÁ, et al. Unidirectional transfer of microRNA-loaded exosomes from T cells to antigen-presenting cells. *Nat Commun.* (2011) 2:282. doi: 10.1038/ncomms1285
92. Grange C, Tapparo M, Bruno S, Chatterjee D, Quesenberry PJ, Tetta C, et al. Biodistribution of mesenchymal stem cell-derived extracellular vesicles in a model of acute kidney injury monitored by optical imaging. *Int J Mol Med.* (2014) 33:1055–63. doi: 10.3892/ijmm.2014.1663
93. Wiklander OPB, Nordin JZ, O'Loughlin A, Gustafsson Y, Corso G, Mäger I, et al. Extracellular vesicle in vivo biodistribution is determined by cell source, route of administration and targeting. *J Extracell Vesicles.* (2015) 4:26316. doi: 10.3402/jev.v4.26316
94. Rigo P, Paulus P, Kaschten BJ, Hustinx R, Bury T, Jerusalem G, et al. Oncological applications of positron emission tomography with fluorine-18 fluorodeoxyglucose. *Eur J Nucl Med Mol Imaging.* (1996) 23:1641–74. doi: 10.1007/BF01249629
95. Hwang DW, Choi H, Jang SC, Yoo MY, Park JY, Choi NE, et al. Noninvasive imaging of radiolabeled exosome-mimetic nanovesicle using 99m Tc-HMPAO. *Sci Rep.* (2015) 5:15636. doi: 10.1038/srep15636
96. Smyth T, Kullberg M, Malik N, Smith-Jones P, Graner MW, Anchordoquy TJ. Biodistribution and delivery efficiency of unmodified tumor-derived exosomes. *J Control Release.* (2015) 199:145–55. doi: 10.1016/j.jconrel.2014.12.013
97. Varga Z, Gyurkó I, Pálóczi K, Buzás EI, Horváth I, Hegedus N, et al. Radiolabeling of extracellular vesicles with 99mTc for quantitative *in vivo* imaging studies. *Cancer Biother Radiopharm.* (2016) 31:168–73. doi: 10.1089/cbr.2016.2009
98. Koh DM, Padhani AR. Diffussion-weighted MRI: a new functional clinical technique for tumour imaging. *Br J Radiol.* (2006) 79:633–5. doi: 10.1259/bjr/29739265
99. Koh DM, Collins DJ. Diffusion-weighted MRI in the body: applications and challenges in oncology. *Am J Roentgenol.* (2007) 188:1622–35. doi: 10.2214/AJR.06.1403
100. Seemann MD. Whole-body PET/MRI: the future in oncological imaging. *Technol Cancer Res Treat.* (2005) 4:577–82. doi: 10.1177/153303460500400512
101. Chuo STY, Chien JCY, Lai CPK. Imaging extracellular vesicles: current and emerging methods. *J Biomed Sci.* (2018) 25:91. doi: 10.1186/s12929-018-0494-5
102. Busato A, Bonafede R, Bontempi P, Scambi I, Schiaffino L, Benati D, et al. Magnetic resonance imaging of ultrasmall superparamagnetic iron oxide-labeled exosomes from stem cells: a new method to obtain labeled exosomes. *Int J Nanomed.* (2016) 11:2481–90. doi: 10.2147/IJN.S104152
103. Ahn BC. Requisites for successful theranostics with radionuclide-based reporter gene imaging. *J Drug Target.* (2014) 22:295–303. doi: 10.3109/1061186X.2013.878940
104. El Andaloussi S, Mäger I, Breakefield XO, Wood MJA. Extracellular vesicles: biology and emerging therapeutic opportunities. *Nat Rev Drug Discov.* (2013) 12:347–57. doi: 10.1038/nrd3978
105. Villa F, Quarto R, Tasso R. Extracellular vesicles as natural, safe and efficient drug delivery systems. *Pharmaceutics.* (2019) 11:557. doi: 10.3390/pharmaceutics11110557
106. Kamerkar S, Lebleu VS, Sugimoto H, Yang S, Ruivo CF, Melo SA, et al. Exosomes facilitate therapeutic targeting of oncogenic KRAS in pancreatic cancer. *Nature.* (2017) 546:498–503. doi: 10.1038/nature22341
107. Mendt M, Kamerkar S, Sugimoto H, McAndrews KM, Wu CC, Gagea M, et al. Generation and testing of clinical-grade exosomes for pancreatic cancer. *JCI Insight.* (2018) 3:e99263. doi: 10.1172/jci.insight.99263

Conflict of Interest: The authors declare that the research was conducted in the absence of any commercial or financial relationships that could be construed as a potential conflict of interest.

The handling editor declared a past co-authorship with one of the authors SB-P.

Copyright © 2020 Nannan, Oudart, Monboisse, Ramont, Brassart-Pasco and Brassart. This is an open-access article distributed under the terms of the Creative Commons Attribution License (CC BY). The use, distribution or reproduction in other forums is permitted, provided the original author(s) and the copyright owner(s) are credited and that the original publication in this journal is cited, in accordance with accepted academic practice. No use, distribution or reproduction is permitted which does not comply with these terms.

frontiers in Oncology

MINI REVIEW
published: 28 August 2020
doi: 10.3389/fonc.2020.01620

A Complex and Evolutive Character: Two Face Aspects of ECM in Tumor Progression

*Margaux Sala†, Manon Ros† and Frédéric Saltel**

Univ. Bordeaux, INSERM, BaRITOn, U1053, Bordeaux, France

Tumor microenvironment, including extracellular matrix (ECM) and stromal cells, is a key player during tumor development, from initiation, growth and progression to metastasis. During all of these steps, remodeling of matrix components occurs, changing its biochemical and physical properties. The global and basic cancer ECM model is that tumors are surrounded by activated stromal cells, that remodel physiological ECM to evolve into a stiffer and more crosslinked ECM than in normal conditions, thereby increasing invasive capacities of cancer cells. In this review, we show that this too simple model does not consider the complexity, specificity and heterogeneity of each organ and tumor. First, we describe the general ECM in context of cancer. Then, we go through five invasive and most frequent cancers from different origins (breast, liver, pancreas, colon, and skin), and show that each cancer has its own specific matrix, with different stromal cells, ECM components, biochemical properties and activated signaling pathways. Furthermore, in these five cancers, we describe the dual role of tumor ECM: as a protective barrier against tumor cell proliferation and invasion, and as a major player in tumor progression. Indeed, crosstalk between tumor and stromal cells induce changes in matrix organization by remodeling ECM through invadosome formation in order to degrade it, promoting tumor progression and cell invasion. To sum up, in this review, we highlight the specificities of matrix composition in five cancers and the necessity not to consider the ECM as one general and simple entity, but one complex, dynamic and specific entity for each cancer type and subtype.

Keywords: extracellular matrix, invasion, invadosome, CAFs, matrix protective role, matrix promoting role

OPEN ACCESS

Edited by:
Vasiliki Gkretsi,
European University Cyprus, Cyprus

Reviewed by:
Kideok Jin,
Albany College of Pharmacy and Health Sciences, United States
Daniele Vergara,
University of Salento, Italy

***Correspondence:**
Frédéric Saltel
frederic.saltel@inserm.fr

†These authors have contributed equally to this work

Specialty section:
This article was submitted to Molecular and Cellular Oncology, a section of the journal Frontiers in Oncology

Received: *12 February 2020*
Accepted: *27 July 2020*
Published: *28 August 2020*

Citation:
Sala M, Ros M and Saltel F (2020) A Complex and Evolutive Character: Two Face Aspects of ECM in Tumor Progression. Front. Oncol. 10:1620. doi: 10.3389/fonc.2020.01620

INTRODUCTION

In 2012, Hanahan et al. reviewed the hallmarks of cancer by including the tumor microenvironment (1). This concept postulates that cancer cells are not able to promote the disease alone but they could recruit and modulate resident and normal cell types in order to establish cooperation to promote tumor progression (2). The tumor microenvironment is a complex and dynamic network composed of cancer cells, stromal tissue (stromal cells such as fibroblasts, macrophages, immune cells, cytokines, and vascular tissue), as well as the extracellular matrix (ECM) (3). ECM plays key roles during tumor development, from initiation, growth and progression to metastasis (2).

Remodeling of matrix components occurs during all of these steps. The role of the ECM in this journey is still not emphasized enough with the exception of some studies (4–7).

The ECM is the acellular component, secreted by the cells, that forms a tissue. It has a supporting role for normal cells, as well as a role in maintaining tissue homeostasis. In addition, the ECM is also involved in the establishment, separation and maintenance of differentiated tissues and organs (8). Structurally, ECM proteins notably form the basement membrane (BM), which separate the epithelium or endothelium from the stroma and the interstitial matrix involved in tissue resistance (9). The ECM composition can be very different according to the tissue, due to the wide variety of proteins involved in its composition. ECM is composed of hydrated gel-forming macromolecules [hyaluronic acid (HA), proteoglycans], fibrillar proteins (collagen) and structural proteins (elastin and fibronectin). These macromolecules can assemble together to form three dimensional supramolecular structures with distinct biochemical and biophysical properties (10). Cells can interact with the ECM through expression of receptors at their cell surface, in order to maintain physiological signaling such as homeostasis, adhesion and migration.

In addition to its structural role, the ECM has a reservoir role for bioactive molecules such as cytokines and growth factors. ECM is then involved in cell growth, proliferation, survival, differentiation, migration and invasion (9). ECM is a dynamic environment which is constantly remodeled to adapt and maintain tissue homeostasis (11). This remodeling process is deregulated during cancer, with abnormal ECM deposition and stiffness, leading to tumor progression (12). In order to sense, remodel and degrade the ECM, matrix receptors such as CD44, integrins or discoidin domain receptors contribute to formation of invasive structures called invadosomes (or invadopodia), allowing invasion of cancer cells and metastasis formation (13, 14). However, this classical model of ECM remodeling with increased crosslinking, stiffness and tumor-promoting signaling pathway activation does not apply to all stages of all cancers. This model does not consider ECM heterogeneity, complexity and specificity of each organ and each tumor. Indeed, each organ possesses its own ECM with unique architecture, composition and biological and physical properties associated with organ specific roles (9). Most of the studies still consider the model of tumor ECM as one entity without discriminating each cancer type. Indeed, studies are usually performed on a 2-dimensional (2D) matrix made of only one matrix element, vitronectin, laminin and quite often, collagen I. Moreover, those matrix elements are not in their physiological organization. For example, type I collagen is used as monomers and not in its physiological triple helix form, which does not reflect the *in vivo* ECM. It will be interesting to study and compare all tumors and associated extracellular matrices, in order to create more complex and relevant ECM networks to work with.

The ECM is also the interface between tumor cells and normal tissues. This interface evolves over time, in parallel with the tumor. Initially, the ECM forms a physical barrier, preventing the proliferation and invasion of tumor cells and then, plays a protective role (15). We could hypothesize that stresses, such as hypoxia, oxidative or metabolic stresses, proliferation of tumor cells or ECM accumulation could lower protective nature of the matrix and favor tumor progression. Consequently, dialogue between tumor cells and surrounding ECM is a key element in the tumor progression process by promoting tumor cell invasion (9, 12). So far, there have been no studies on the ECM's protective barrier role, and as such, this molecular mechanism needs further investigations. The basic scheme of tumor associated matrix is that ECM remodeling process is abnormally deregulated during cancer, with an increase in ECM deposition and degradation, promoting tumor invasion.

In this review, we describe the main molecular components of the ECM and associated biomechanical properties. We describe the ECM composition and its role in five cancers (breast, liver, pancreas, colon cancer, and melanoma), highlight their similarities and differences, show that each cancer possesses its own specific matrix associated with physical and biochemical properties. Furthermore, in these five cancers, we evaluate the protective and the pro-invasive role of the ECM.

To sum up, in order to go beyond the classical and reducing scheme of the tumor-associated ECM, the originality of this review is that we highlight the complexity and the specificity of the matrix related to the organ and cancer. Then, we do not only describe a pro-tumor role for ECM but also a protective role, which is less investigated.

ECM COMPOSITION AND ITS EVOLUTIVE ROLE DURING CANCER PROGRESSION

Components and Deposition of the Physiological ECM

The ECM and, more globally, the matrisome are dynamic structures composed of thousands of proteins including glycoproteins (such as fibronectin and laminin) and fibrous proteins such as collagens (7). The ECM form structures such as the BM and the interstitial matrix (9). The main role of BM is to act as a physical barrier between the epithelial cells and the stroma of an organ. The BM is more compact than interstitial matrix; it is composed of laminins, heparan sulfate proteoglycans, collagen IV and proteins synthetized and secreted by epithelial cells, endothelial cells and myofibroblasts (9).

The interstitial ECM is mainly composed of collagens I and III, fibronectin, and proteoglycans. The ECM is mainly secreted by fibroblasts, but in different specialized tissues such as cartilage or bones, ECM could be secreted by chondroblasts or osteoblasts, respectively. This physiological ECM is very heterogenous between the organs. For instance, fibroblasts are able to synthetize and secrete collagens I or III, elastic fibers, reticular fibers and proteoglycans, whereas, chondroblasts synthesize and secrete extracellular matrix of cartilage composed of collagen II, elastic fibers and glycosaminoglycans. Osteoblasts synthesize and secrete extracellular matrix of bones principally composed of type I collagen. Specific to blood vessels, different studies showed that pericytes, vascular smooth muscle cells

and fibroblasts are able to produce ECM such as collagen IV, fibronectin, and laminin (16). The different origins of these ECM-secreting cells contribute to heterogeneity and complexity of the physiological ECM.

Physiological ECM is constantly remodeled. Indeed, its components are secreted, modified and degraded, in order to adapt and maintain tissue homeostasis. This process is important to maintain physical properties of the different matrix, and also participate in the physiology of the tissue. This remodeling process is deregulated and occurs abundantly during cancer. The ECM in cancer participate in cancer cells epithelial to mesenchymal transition (EMT), BM degradation, migration into the stroma and invasion through the interstitial ECM (17). ECM in cancer is also the interface between tumor cells and normal tissues and could have two opposite roles: protective and pro-tumor.

Extracellular Matrix Evolution in Cancer

ECM Protective Role

The ECM could act as a physical barrier actor in order to inhibit tumor progression. In different cancers, myoepithelial cells or cancer-associated fibroblasts (CAFs) surround the tumor and secrete growth factors, protease inhibitors, angiogenic inhibitors or several tumor suppressors in order to prevent tumor growth, invasion and metastasis. Furthermore, different ECM elements, such as collagen IV or collagen I, could also participate in restraining tumor growth and could first act as a protective barrier by inhibiting cell proliferation. We describe these different elements in detail later in this review.

Very little is known about the protective role of the ECM and how this protective barrier becomes pro-invasive and requires further investigation. Some cancers do not even appear to have any protective effect induced by the ECM or stromal cells. We could hypothesize that when stromal cells are overactivated into stromal cancer cells, they induce an upregulation of ECM component secretion. First, in some cancers, collagen secretion could act as a protective barrier around the tumor cells. Subsequently, cancer cell proliferation and alterations increase over time, the pressure and the stiffness become too high, inducing a stress on tumor cells. To overcome these stresses, tumor cells evolve to pursue proliferation and tumor progression.

Tumor-Promoting Role of the ECM

Tumor cells can cause activation of stromal cells into stromal cancer cells that can remodel the ECM to create a pro-tumor environment. We propose to name this matrix promoting tumor progression: Tumor Associated Extracellular Matrix (TAEM). Collagen I is the main component and most studied ECM element, therefore, we focus on this element in this review. Even if the most abundant element of the TAEM is collagen I, ECM is highly complex and heterogenous, and most of the studies of cancers are still mainly performed on only one type of matrix. It is important to study the full matrisome of each cancer and cancer subtype and study the interaction between the different TAEM elements. This would allow better understanding of what role can have each specific molecule. Thus, we could focus on the ones that can have a protective role and could become therapeutic targets.

One general feature during cancer is that type I collagen is overexpressed (18, 19), crosslinked and continuously remodeled, although the process varies between different cancers.

Next, we describe the remodeling of TAEM: (i) its deposition and (ii) its degradation by invadopodia formation (20) through (iii) matrix receptors, leading to loss of ECM homeostasis (19) and change of biomechanical properties of the ECM.

ECM deposition

Cancer cells, through activation of normal cells into stromal cells, or by themselves, can remodel physiological ECM into TAEM. Fibroblasts are the most abundant cells of the tumor stroma and are involved in several biological processes. Some fibroblasts can be recruited, activated and transformed into CAFs by different secreted factors from tumor cells in the microenvironment such as TGF-β, PDGF or FGF (21, 22). CAFs can result from the activation of fibroblasts near the tumor, mesenchymal stem cells, but also from cells that have undergone EMT (21–26). Once activated, owing to their different origins, CAFs possess a variety of tumor promoting functions, adding another step in the complexity and heterogeneity of the stroma.

One of their functions is to secrete various ECM elements including collagen I, fibronectin and hyaluronan, growth factors (HFG, PDGF, and CTGF), chemokines, cytokines, interleukines (IL-6 and IL-8) and proteases in order to promote tumor cell proliferation, angiogenesis and invasion (3, 27). Moreover, during remodeling in cancer, ECM undergoes drastic structural changes due to chemical and physical restructuration, leading to TAEM. Many studies have shown an increased ECM deposition, inducing a stiffer stroma; in addition, morphological changes that occur are characterized by more aligned collagens at the tumor front (28). Tissue stiffness can be increased by enzymes such as lysyl oxidases (LOX), which can crosslink collagen. These enzymes can be secreted either by stromal or tumor cells, inducing increased crosslinks and, thus, an accumulation of collagen I, fibrosis and promoting metastasis (29–31).

Different studies showed mechano-regulatory mechanisms wherein ECM rigidity perturbs epithelial morphogenesis and tissue polarity (28, 32–34). For example, Weaver et al. have shown that this mechanism will enhance ERK activation and increase cancer cell malignant phenotype (28). CAFs can also mechanically remodel the ECM, through compaction and CAF contractility, in order to create paths to increase cancer cell migration and invasion (35).

Invadosome formation leads to ECM degradation

The other way to remodel the ECM into TAEM is by degradation. This ECM degradation can be achieved by cancer cells and all cells present in the tumor microenvironment, all of them can form invasive and degradative structures called invadosomes. Invadosomes are membrane protrusions that can be found on normal cells (named podosomes) as well as in tumor cells (where they are named invadopodia). Contrary to other actin-based structures such as filopodia, focal adhesions or lamellipodia, invadosomes not only possess adhesive, mechanosensitive capacities but also proteolytic activity by recruiting, secreting and activating matrix metalloproteinases (MMPs), allowing them

to degrade the ECM. They also present their own translational machinery to maintain their structure and function (36).

Invadosomes are plastic structures, with the ability to adapt to the available ECM receptors as well as to the microenvironment. Invadosomes are complex and highly dynamic structures composed of a F-actin core surrounded by a ring of scaffold and adaptor proteins in 2D. Actin-regulating proteins, kinases and small GTPases regulate actin machinery within the invadosomes (37, 38). Key molecular players for functional invadosomes have already been identified, including the adaptor protein Tks5, Cdc42 (36, 39), the actin regulators cortactin and N-WASP, as well as the transmembrane protein MT1-MMP (37).

Even though invadosomes share a common molecular signature, they exist in different organizations, depending on the cell type and on the microenvironment. Cells can form invadosomes as dots (such as MDA-MB-231 cells), as rosettes (such as NIH3T3-Src cells) or as aggregates (such as macrophages and osteoclasts). All of them can reorganize their actin cytoskeleton to form another class of invadosomes, called linear invadosomes, when seeded on type I collagen (40, 41).

This last linear organization is induced by physiological fibrillar collagen I and form specifically along fibrils. Even if cells can form invadosomes to degrade the BM, this suggests that when cancer cells are in direct contact with collagen I after BM degradation, TAEM promotes invadosome formation. The collagen receptor discoidin domain receptor 1 (DDR1) is responsible for linear invadosome formation and their degradation function. Indeed, DDR1 activates the RhoGTPase Cdc42 and its guanine exchange factor Tuba, inducing their localization in linear invadosomes (42).

Moreover, other collagen receptors such as integrins or CD44, that can also be found on stromal cells as well as cancer cells, have also been shown to be involved in invadosome formation (43–45). Most cells possess the ability to form invadosomes that are dependent on various stimuli like growth factors (VEGF, TGF-β. . .), genome alteration or microenvironment (40, 45, 46), allowing TAEM degradation.

We can hypothesize that cell cooperation between cancer cells and stromal cells could promote invadosome formation: indeed, stromal cancer cell activation by tumor cells induce ECM deposition and secretion. This will, in turn, promote invadosome formation by the binding of ECM elements (such as collagen I) to cancer cell receptors. Different studies have shown that increased ECM rigidity promotes invadosome formation and activation. Some studies already demonstrated a cooperation between tumor cells and CAFs or macrophages in order to secrete ECM-degrading enzymes (47–50), but no study clearly demonstrated cell cooperation to directly promote invadosome formation. However, we could imagine that stromal cells around the tumor, such as fibroblasts or endothelial cells, could secrete many soluble factors such as TGF-β or TNF-α in order to promote invadosome formation by cancer cells. This would lead to an invasive loop, inducing TAEM degradation, at the same time as tumor cell proliferation and angiogenesis.

To sum up, both stromal and cancer cells are able to create TAEM by secreting ECM and degrading it to promote tumor growth, invasion and metastasis. To create TAEM, a crosstalk between stromal and cancer cells is needed. This TAEM will, in turn, serves for communication between stromal and cancer cells. In order to mediate the interaction with the TAEM, stromal and tumor cells will bind with different matrix elements via the presence of receptor panels on their surface, each cell expressing different receptors modulated during tumor progression, contributing to tumor heterogeneity.

ECM receptor expressions in cancer cells and in CAFs

Even though many receptors are able to bind the ECM, three are mainly described in tumor progression (CD44, integrins and DDRs). Due to prominent interest in cancer cells, rather than in stromal cells and ECM, a large number of well-described reviews focus on these matrix receptors in cancer cells (14, 51–53). Indeed, we describe, the role of CD44, integrins and DDRs - notably in invadosomes and metastasis formation - in cancer cells and CAFs.

CD44 is a transmembrane glycoprotein receptor which is an adhesion molecule that is upregulated following tissue injury, and is implicated in many chronic inflammatory diseases such as atherosclerosis or autoimmune diseases. It can interact with its extracellular domain with different ligands like HA, osteopontin, fibronectin, collagen, MMPs and different growth factors such as HGF, bFGF and VEGF. This receptor is overexpressed in CAFs (54) and in a large number of cancer cells [pancreatic cancer, breast cancer, prostate cancer, head and neck squamous cell carcinoma (HNSCC), and gastrointestinal cancer] where it is involved in several steps of tumor progression such as tumor invasion, EMT, metastasis formation and resistance to chemotherapy (52). High expression of CD44 in cancer cells is also associated with cancer stem cell (CSC) properties and is used as a CSC marker. $CD44^+$ cancer cells show an increase in EMT and in invasion, correlated with poor prognosis (55–58).

Integrins are transmembrane heterodimers which consist of α-subunit associated with a β-subunit in a non-covalent manner. Integrins are able to bind different elements of ECM such as vitronectin, fibronectin, laminin or collagens. Only four integrins are able to bind collagen I: α1β1, α2β1, α10β1, and α11β1 (59). Integrins are overexpressed in a large number of cancers in both stromal and tumor cells where they can promote survival, proliferation, motility, invasion, and ECM modulation (53). Moreover, various studies have shown that integrin α11 is expressed in CAFs in a large number of cancers, like non-small cell lung cancer (NSCLC) or HNSCC. In these cancers, α11β1 expression is involved in migration, tumorigenicity and invasion of tumor cells (60–63). Furthermore, in NSCLC, α11β1 expressed in CAF induces collagen reorganization and tissue stiffness, promoting tumor growth and metastatic potential of tumor cells (63). Thus, α11β1 seems to be an important receptor for collagen remodeling and CAF migration in the tumor microenvironment.

DDRs are members of the tyrosine kinase receptor family and are composed by two members, DDR1 and DDR2 (64). These transmembrane receptors are activated by collagens in their native triple helix form (65–67). Moreover, DDRs are involved in several physiological functions such as embryogenesis and wound healing and are overexpressed in a large number of cancer subtypes, where they are associated with cell proliferation, invasion, migration and drug resistance (51).

DDR1 and DDR2 play an important role in the tumor microenvironment which is involved in the dissemination of tumor cells. These receptors could be expressed both by cancer cells and CAFs in order to promote tumorigenesis. For instance, Jin et al. have shown that CAFs promote the secretion of cytokine IL-6 which activates the JAK/STAT3 pathway in gastric carcinoma cells, inducing DDR1 upregulation, promoting peritoneal tumorigenesis (68). Thus, inhibition of DDR1 is an interesting strategy for the treatment of peritoneal metastasis of gastric cancer.

To sum up this part, tumor cells are able to activate fibroblasts into CAFs by factor secretion and CAFs are in turn able to secrete TAEM in order to promote tumor cell invasion, proliferation, migration and metastasis. To our knowledge, little is known about the effect of these collagen receptor expressions in other stromal cells such as immune cells or adipocytes and on the crosstalk with tumor cells.

However, these collagen receptors are known to be involved in invadosome formation, allowing tumor cells to remodel and degrade the ECM in order to migrate, invade and form metastasis. Those receptors are also able to interact together (DDRs/integrins and integrins/CD44) (64, 69, 70). It will be important to study if these three receptors cooperate together in tumorigenesis and if there is any compensation in their functions.

Although the remodeling of the matrix is an important step, this classical model of ECM remodeling does not apply to all cancers. Indeed, this model of an increased ECM deposition, stiffness and increased activated stromal cells, neither considers the complexity of the organ, the heterogeneity of the tumor nor the specificity of its own ECM. Moreover, most studies focus on the pro-tumor role of ECM whereas initially, in certain cancers, it could play a protective role, making it possible to restrict tumor progression. Then, the dynamic of the microenvironment causes the protective side of the matrix to become pro-tumor. This will in turn induce ECM rigidity, remodeling and degradation which will then promote tumor cell invasion (9, 12).

To illustrate this point, we next describe the composition and evolution of the ECM in five cancers: breast cancer, liver cancer, pancreas cancer, colon cancer and melanoma as well as the dual role of their ECM in cancer progression.

BREAST CANCER

ECM Composition and Function

Healthy breast epithelium forms a ductal network surrounded by adipose tissue. This network connects mammary lobes to nipples. The normal breast tissue is made of two compartments: the epithelium and the stroma. The epithelium of the ducts and of the lobule of the mammary gland is made of luminal cells, which express hormone receptors, and myoepithelial cells. Both cell types are surrounded by a BM. The mammary gland goes through several cycles of changes such as differentiation, development and apoptosis during physiological adult life, including during puberty and pregnancy (71–73). These cycles are highly regulated, but the disruption of the tissue homeostasis, tissue organization and cell function can lead to cancer.

The most common breast cancer is ductal carcinoma. It is thought to arise after cellular abnormalities, inducing abnormal proliferation in the terminal duct lobular units. Then, a multistep transformation of epithelial cells and accumulation of abnormalities induce hyperplasia, premalignancy, *in situ* carcinoma, and finally, invasive carcinoma (71, 72). Breast cancers are highly heterogenous and are divided into six subtypes, depending on their histology, epidemiology and molecular signatures: luminal A, luminal B, Her2-positive, claudin-low triple negative (also called basal-like), and normal-like (73). Their diversity induces more or less invasive forms with different clinical outcomes.

The tumor microenvironment of breast cancer is far from homogenous and can evolve during tumor progression in the same tumor (**Figure 1**). From primary tumor growth to extravasation and metastasis formation, the ECM is constantly changing. For example, even when a ductal carcinoma *in situ* (DCIS) becomes an invasive carcinoma, the microenvironment is different, due to a differential gene expression of all the cell types between these two cancer steps (74). The ECM is highly dynamic and is now known to be a major player in tumor progression (75).

The ECM in breast shows similarities to tissues undergoing wound healing (76, 77) or breast tissue going back to homeostasis through remodeling after pregnancy, with overexpression of fibrillar collagens, fibronectin and ECM remodeling enzymes (78). This change in ECM has also been associated with increased risk of breast cancer after pregnancy (78, 79).

During breast cancer, one main change in the ECM is the collagen abundance (**Figure 1**). Collagen I, III and V are accumulated while collagen IV is decreased, due to degradation of the BM (75). Collagen crosslinking is increased too, inducing a change in collagen organization (shaping it more aligned), and an increased ECM stiffness. Both characteristics are associated with tumor progression. The crosslinking is facilitated by LOX enzymes, which are also overexpressed in breast cancer (29, 80, 81).

Collagen fibril formation is induced by fibronectin (82), changing collagens into scaffold for tumor cells to migrate and invade (48). Fibronectin is also overexpressed during breast cancer (by CAFs and cancer cells) and is associated with poor prognosis, notably because it promotes metastasis (83, 84). Hyaluronan as well as versican also accumulate in the breast cancer ECM and are associated with poor prognosis (85, 86). Indeed, hyaluronan helps creating a pro-tumor microenvironment (87), while versican promotes breast cancer cell self-renewal and migration (88, 89). Several matricellular proteins, such as osteopontin, tenascin C or periostin, are also overexpressed during breast cancer and are associated with increased migration, invasion, and a poor outcome (90).

Extracellular matrix modifications do not only come from matrix components, but also from remodeling enzymes: from proteases such as MMPs (MMP-2, -3, -9, and -14) to crosslinking enzymes such as LOX. These enzymes are often overexpressed in breast cancer, and promote cancer development and metastasis (76). However, these two families of enzymes can be differentially expressed depending on cancer subtypes. For example, LOX, LOXL2, LOXL3, and LOXL4 are overexpressed in more

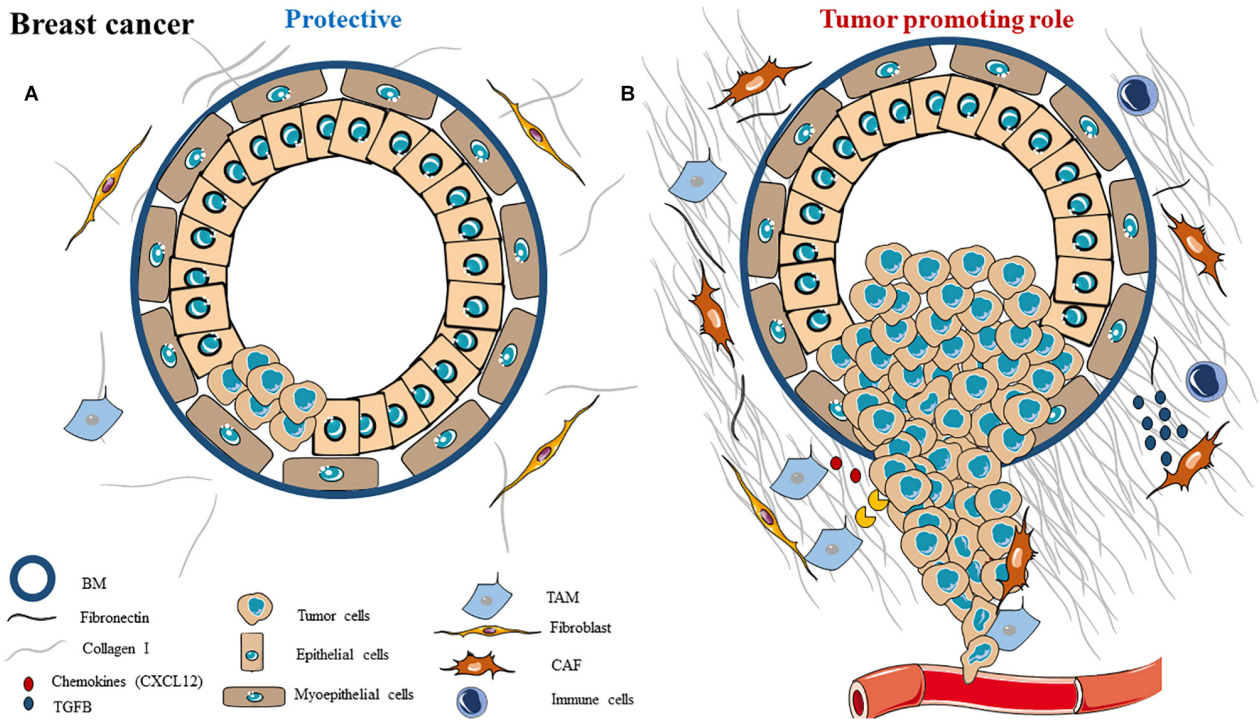

FIGURE 1 | Schematic representation of ECM composition and ECM dual role as a **(A)** protective barrier or as a **(B)** tumor promoting role in breast cancer.

invasive cancers, such as triple negative breast cancers, inducing cancer cell invasion and metastasis (91, 92). Similarly, MMP-9 overexpression is higher in high-grade and more invasive breast cancers (such as triple negative and Her2-positive), where it is associated with metastasis and relapse (93).

ECM Evolution During Cancer

Protective Role

Several components of the ECM can first have protective roles in order to inhibit tumor progression (**Figure 1A**). For example, myoepithelial cells can be considered as the main natural tumor suppressor in breast cancer, and their disruption seems to be a key step in tumor progression. Indeed, the myoepithelial cells are located between the stroma and the luminal cells (from which cancer arises), creating a separating sheet between the epithelium and the stroma. They have an important role during lactation as well as protective roles during tumorigenesis, as they form a physical barrier around luminal cells (94–96). Myoepithelial cells can act on tumor cells and on fibroblasts to reduce MMP-2, MMP-9, and MT1-MMP gene expression, decreasing cancer cells invasive capacities (97). They also express some proteinase inhibitors, such as the MMP inhibitor TIMP-1, and angiogenic inhibitors such as thrombospondin-1 and bFGF receptors (98), allowing them to inhibit angiogenesis (99). They can secrete several tumor suppressors such as maspin, cytokeratins, relaxin and activin in order to prevent tumor growth, invasion and metastasis (96). The myoepithelial cells also participate in accumulating ECM and basement membrane instead of degrading it. To do so, these cells express high levels of collagen, fibronectin and laminin (100, 101). All of these show that these specific cells can have several positive roles in preventing tumorigenesis.

Moreover, some studies also suggest a protective role for CAFs in breast cancer. CAFs can secrete factors such as caveolin-1 and podoplanin, which are associated with decreased metastasis (102). CAFs can also inhibit PI3K and TGF-β signaling through secretion of SLIT2 and asporin, respectively, inducing a decrease in EMT, invasion and metastasis (103).

Proteoglycans are proteins that are heavily glycosylated and can bind ECM components like collagens. Decorin, a member of the proteoglycan family, is also known to have anti-tumor roles (104). Indeed, reduced expression of decorin is associated with poor prognosis and may promote tumorigenesis and invasion (105), while its overexpression is associated with better prognosis and leads to tumor growth and metastasis inhibitions (through ERbB2 inhibition) (106–108).

This suggests that several cell types and ECM elements may have protective roles in breast cancer, but some of them may not be elucidated yet, and it needs further investigation. However, there is not enough information to understand at what stages stromal cells are activated and when the protective role becomes pro-tumor. It would be important to understand this time frame in order to block this transition to inhibit tumor progression.

Tumor Promoting Role

Many ECM components (cellular as well as matrix) play a role in favoring breast cancer progression (**Figure 1B**). For example,

CAFs are the most abundant cell types in breast cancer stroma, they can derive from resident fibroblast or myoepithelial cell activation (103). CAFs can secrete ECM components (such as type I collagen or fibrin) and several soluble factors, such as growth factors (EGF, HGF, TGF-β), metalloproteinases (MMP-1, -2, -9) or chemokines (CXCL12), to promote tumor growth and metastasis (74, 95). Macrophages (also known as tumor-associated macrophages, TAMs) are also involved: they can secrete VEGF, cytokines or TGF-β to promote cancer cell survival, angiogenesis and invasion (109, 110). Finally, tumor-infiltrating lymphocytes help tumorigenesis by blocking anti-tumor response and suppressing immune cells (111).

Several studies showed that myoepithelial cells from normal or cancer tissues strongly differ in their gene expression. The cells isolated from normal tissue express high levels of interstitial ECM, such as laminin, tenascin or tropomyosin, while the cells isolated from DCIS overexpress proteases (such as MMP-2), protease inhibitors (such as TIMP3 or thrombospondin-2), chemokines, cytokines and collagens (74). They are also deficient in production of laminin, showing that they tend to degrade the normal ECM instead of depositing it as in physiological conditions (72). Another study by Hu et al. showed that myoepithelial cell differentiation must be maintained in order to avoid invasive phenotype of breast cancer. Loss of myoepithelial cells, through inhibition of TGF-β, Hedgehog, p63 or cell adhesion signaling by tumor cells induces the transition from DCIS into invasive carcinomas, suggesting that loss of myoepithelial cells is a prerequisite for tumor invasion (112).

Moreover, increasing invasion and metastasis can also be promoted through a crosstalk between different cell types. For example, Condeelis et al. have shown, using intravital imaging, that tumor microenvironment plays a key role in invasion and metastasis by creating an essential paracrine loop between tumor cells and macrophages with direct interaction of the two cell types. This induces a specific microenvironment, dependent on macrophages and EGF and CFS-1 signaling, which is essential for intravasation of cancer cells (48).

Extracellular matrix binding receptors are also involved in this tumor-promoting role. Indeed, CD44, integrins and DDRs are overexpressed in breast cancer and promote tumor progression (51–53, 64). For example, CD44 standard isoform (CD44s) is positively correlated with CSC gene signature in breast cancer, notably through PDGFRβ/Stat3 activation (113). CD44 can also activate several signaling pathways such as MAPK, PI3K/Akt to induce migration, survival and invasion (114).

Integrins are also key players in breast cancer, notably in the metastatic cascade. Indeed, they promote migration, MMP expression, secretion and location at invadosome in order to facilitate invasion (115). They also directly control invadosome formation and can be found localized in these structures (116). Moreover, one study demonstrated that collagen binding integrin α11 expressed by CAFs activates PDGFRβ/JNK signaling in breast cancer cells to promote tumor cell invasion (117).

Concerning DDRs, Corsa et al. demonstrated that in CAF, DDR2 is critical for ECM production and the organization of collagen fiber (118). They also showed, in these cells, that DDR2 is involved in breast cancer cells metastasis in the lungs, by affecting collective cell migration. Furthermore, this team demonstrated that DDR2, when expressed by stromal cells, promotes the metastatic spread of breast cancer cells. DDR1 has also been shown to be involved in many steps of breast cancer, including invasion (through its interaction with collagen I and invadosome formation), proliferation, migration (both through its association with the insulin-like growth factor-I receptor) and resistance to treatment (through its interaction with collagen IV and NFκB activation) (42, 51).

Concerning the matrix components (secreted by cancer cells as well as stromal cells), fibronectin overexpression can modulate cancer cell signaling in order to promote tumorigenesis, for example, by inducing EMT via ERK (119) or STAT3 (120) activation. Laminins are also involved: laminin-5 can promote survival through NFκB activation in activated B cells (121) and invasion and migration through integrin interaction (122), and laminin-511 promotes metastasis (123). Versican can also increase tumorigenesis by inducing cancer-cell self-renewal through EGRF signaling (89) and by inducing cell survival, tumor growth and metastasis (124, 125).

Collagen is also described as a key player in tumor development. The increased ECM stiffness during cancer induces a change in biochemical signaling and in cell behavior, promoting tumor progression in several ways. For example, increased stiffness in mammary epithelial cells induces MAPK activation and proliferation (126). This mechano-regulatory mechanism could also induce aggressive phenotype in tumors (28). Increased stiffness of ECM also promotes transcriptional coactivator with a PDZ-binding motif (TAZ) activity (leading to an increase of CSC properties) (127) as well as PI3K activity (leading to invasion) (80). Studies have shown that, to increase invasion, matrix density can also promote invadosome formation and ECM degradation (128). Invadosome formation can also be induced by the ECM itself, via collagen: type I collagen is an inducer or linear invadosome formation and matrix degradation (41, 42). Indeed, breast cancer cells seeded on type I collagen tend to have an increased matrix degradation capacity than on gelatin.

Extracellular matrix degradation is mediated by proteases. In cancer, MMPs are key players in ECM remodeling and degradation. Some of them, such as MMP-2, MMP-9 and MMP-14 are overexpressed in breast cancer, inducing collagen degradation and promoting metastasis (129, 130). Heparanase, another ECM remodeling enzyme, has been shown to be involved in breast cancer progression. Its overexpression induces mammary tumor growth, survival and cell spreading (131–134). Similarly, the inhibition of cathepsins, which are lysosomal proteases, was shown to inhibit breast cancer metastasis (135, 136).

To sum up, in breast cancer, many ECM players are involved in tumor progression, creating stroma that are either pro-invasive or protective. However, studies we reviewed did not specify differences between breast cancer subtypes, because they are mostly performed with the same types of samples (MDA-MB-231 or MCF-7 cells *in vitro,* and comparing normal breast and DCIS *in vivo*). There is a real need to find new matrix to work on (not only collagen matrix), and to work in 3D using

organoids, adapted to each cancer type and subtype, to be more representative of what is happening for real *in vivo*.

LIVER CANCER

ECM Composition and Function

Liver is structured in highly organized units of hexagonal shape called lobules, whose size is about 1 mm. The prominent cell type (50–60% in cell number) is hepatocytes (parenchymal cells), which carry out the main functions such as detoxification, synthesis of plasma proteins, lipids, glycogen, and activation of inflammatory or immune responses. However, about 40% of the liver cells are non-parenchymal (NP), including sinusoidal endothelial cells (LSEC, serve as a filtration barrier), Kupffer cells (KC, function as *in situ* macrophages), hepatic stellate cells (HSC, fat-storing cells; play a major role in the progression of fibrosis) and a small fraction of biliary epithelial cells (cholangiocytes) and liver-associated lymphocytes and leukocytes.

Besides this diversity in cell types, the population of hepatocytes is itself heterogeneous: hepatocytes are functionally different depending on their location within the lobule, dictated by the unique vasculature of the liver. Perivenous (or centrolobular) hepatocytes are exposed to lower oxygen tension as well as nutrient and hormone levels. In other words, the oxygen gradient through the lobule translates into a gradient of metabolic functions, which leads to the so-called zonation of the liver (137). In adults, normal liver ECM is mainly composed by collagen (60%), non-collagenous proteins and proteoglycans. Collagen I (COL1A1 and COL1A2) is predominant, but other collagens such as COL2A1, COL21A1, COL23A1, COL5A3, and COL26A1 are present. Collagen fibers were found in the portal tracts, whereas the normal parenchyma contains only few collagen fibers (138). An originality of liver microvasculature is the presence of a very fine and partial basal membrane associated with fenestrated endothelial cells to facilitate exchange between blood and hepatocytes.

Liver cancers are the fourth most lethal cancers worldwide (139). Hepatocellular Carcinoma (HCC) is the most common form of primary liver cancer. Intra- and extra-hepatic metastases are usual complication in HCC. Due to frequent late diagnosis, the prognosis for HCC is poor. In most cases, HCC develops upon chronic liver disease caused by various factors such as viral hepatitis B/C, alcohol or metabolic syndrome (Non-Alcoholic SteatoHepatitis). Persistent hepatic injury and associated regeneration could produce a stressful environment leading to inflammation and hypoxia, which are features of HCC microenvironment.

In most cases (70%), HCC occurs on a cirrhotic liver. Cirrhosis is characterized by formation of regenerative nodules of liver parenchyma that are separated by fibrotic septa. Activation of hepatic stellate cells (HSCs) into myofibroblasts, mostly characterized by Smooth Muscle Actin (SMA) expression are the principal source of secrete matrix playing an important role in the initiation of liver fibrosis, cirrhosis development and cancer emergence. In normal liver, HSCs are quiescent cells found in the perisinusoidal space of Disse. Chronic liver injuries promote a complete cell transdifferentiation into proliferative myofibroblasts. In this context, the microenvironment is very specific, associated with type I and type II collagens and elastin accumulation corresponding to the pathological evolution of liver fibrosis.

Nevertheless, in some cases, HCC is observed in non-pathological liver. Consequently, the matrix microenvironment varies a lot between the different HCCs in terms of etiology and the presence of cirrhosis or not. Here, we describe the role of ECM on HCC progression and invasion.

Some ECM elements are deregulated during cirrhosis and HCC. Those ECM elements can be secreted by different cell types such as tumor cells and myofibroblasts or CAFs. Several matrix elements such as type I and type III collagens are upregulated during fibrosis and cirrhosis. In HCC, other matrix elements such as type IV collagen, tenascin, osteopontin and laminin are upregulated (**Figure 2**). In normal liver, heparan sulfate is the main glycosaminoglycan component, whereas chondroitin sulfate is prevalent in HCC.

Various proteoglycans (PGs) are involved in HCC progression, at cell surface (such as syndecan-1 or Glypican 3), in the pericellular space (such as agrin or collagen XVIII/endostatin) and in the extracellular space (for instance versican, decorin). Most of these PGs are overexpressed in HCC and can serve as biomarkers (140).

ECM Evolution During Cancer

Protective Role

In a significant proportion (40 to 60%), HCC can be surrounded by a fibrous capsule, whose thickness varies from 0.13 to 3 mm (141), presenting a trabecular pattern (**Figure 2A**). This encapsulation is present in small ($\leq$5 cm), as well as in large HCC (>5 cm) (142). There is no link between the presence of a capsule and the presence of cirrhosis. It is important to note that several studies have shown that this fibrous capsule is associated with a better prognosis than non-encapsulated tumors, suggesting a protective effect of this capsule (142). On the contrary, the presence of an invaded capsule corresponds to a bad survival prognosis, a recurrence and a non-transplantation criteria (143).

This capsule is composed of several matrix elements, including type I and III collagens (144) and the presence of an inflammatory infiltrate is not systematic. To date, there are only few studies on the molecular mechanisms that control the formation of this capsule and the cellular origin of the elements that compose it. A study by Ishizaki et al. demonstrated the presence of positive α-SMA cells, which is a marker of CAF, associated with the presence of procollagen I and III in the capsule (145). The origins of CAFs can be multiple, contributing to the heterogeneity of the tumor. They could participate in the secretion of this fibrous capsule in collaboration with myofibroblasts.

Most analyses of this capsule are based on the immunohistochemistry technique. New global studies could allow further the knowledge of the composition of this structure and determine molecular mechanisms and ECM elements associated with the protective effect of the capsule.

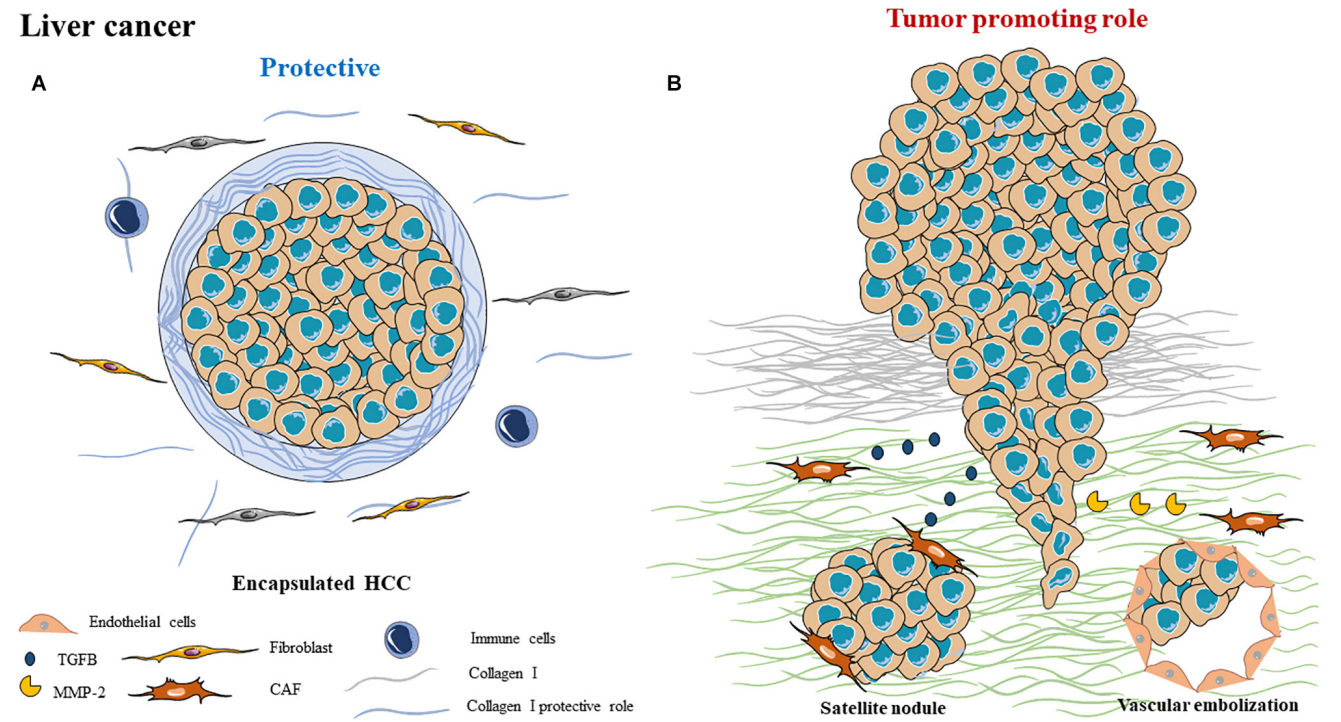

FIGURE 2 | Schematic representation of ECM composition and ECM dual role as a **(A)** protective barrier or as a **(B)** tumor promoting role in liver cancer.

Tumor Promoting Role

In presence or absence of a capsule, HCC is a highly invasive tumor (**Figure 2B**). HCC invasion criteria correspond to satellite nodules, vascular embolization and are hallmarks of HCC progression. Intra-liver metastasis formation contributes to the very high HCC mortality rate as they cause liver failure. Presence of these invasive features is a non-transplantation criterion, which is the only way to treat advanced HCC.

Hepatocellular Carcinoma tumors often occur in cirrhosis context where the number of activated fibroblasts is very high. Several studies have shown the importance of crosstalk between cancer cells and fibroblasts in HCC. Cytokines secreted by cancer cells, such as transforming growth factor-β (TGF-β), stimulate myofibroblasts, leading to their activation. Growth factors and inflammatory cytokines such as PDGF, TGF-β, TNF-α, IL-6, and IL-1β, expressed by cancer cells during HCC, activate and transform quiescent fibroblasts into myofibroblasts and then into CAFs (146). Several studies demonstrate the role of CAFs during HCC progression. A positive correlation exists between the frequency of CAFs around HCC nodules and the tumor size. Moreover, these cells secrete the hepatocyte growth factor (HGF), fibroblast growth factor (FGF), TGF-β, CCL-2, -5, -7 and CXCL16, promoting tumor cell proliferation and invasion, respectively (147).

Increased expression of MMPs was detected at the nodule periphery; metalloproteinases such as MMP-9, MMP-2 and MT1-MMP are probably involved in HCC invasion. Indeed, TGF-β is overexpressed and overactivated during HCC, inducing an increase in ECM deposition (such as type I collagen) and EMT (148). LOXL2 is also a very important element in HCC, its expression is controlled by hypoxia and TGF-β. LOXL2 modulates matrix rigidity, increasing collagen crosslinking and promoting invasion (149). Matrix accumulation and crosslinking increase stiffness, inducing HCC cell proliferation and invasion (150). Physical parameters seem to be crucial to promote HCC progression. Indeed, if the fibrous capsule plays first a protective role, its rigidity could then promote an invasive switch. To illustrate this point, an invaded capsule corresponds to a very aggressive feature associated with a very poor prognosis.

Hepatocellular Carcinoma invasion can be increased by different ways. Indeed, EMT, MMPs secretion and matrix stiffness are elements that control invadopodia formation. Several studies have demonstrated the ability of HCC cells to form invadopodia and to degrade ECM. Keratin 19, MMP-2, TIMP2, Mena, Agrin, Src, and TGF-β are notably described to participate in invadopodia formation in HCC cells (151–154). For example, TGF-β stimulates type I collagen, DDR1 and LOXL2 expression, modulating ECM organization and inducing invadopodia formation (155).

Accumulation and overexpression of various ECM elements also promote cell proliferation, provide survival signals and induce tumor invasion. In parallel, associated receptors must be present and are involved in signaling pathways. In fact, in HCC, a large number of ECM receptors are overexpressed such as integrins, CD44, DDRs. For example, β1 integrin induces a pro-survival signal through MAPK pathway in HCC cells (156). CD44 plays an important role in tumor cell initiation, proliferation, invasion and CSC properties (157). CD44 is required for Mdm2

nuclear translocation and AKT activation leading to tumor progression (157).

Discoidin domain receptor 1 and DDR2 are also overexpressed in HCC. Both participate in tumor cell proliferation, EMT and invasion processes through ERK signalization, SNAIL1 stabilization and MMPs activation, respectively (155, 158, 159).

To conclude, a large number of studies demonstrate a real impact of the ECM on the development and evolution of HCC. However, many questions remain. Moreover, this notion of protection or, on the contrary, pro-invasive role of the ECM is not yet considered in the clinic, neither in the diagnosis nor in the management of the patients. This aspect is obscured not only by the lack of knowledge but also by the lack of adapted therapeutic solutions. At the research level, *in vivo* and *in vitro* models do not reflect the complexity and dynamics of the interface between the tumor and the ECM.

PANCREATIC CANCER

ECM Composition and Function

In physiological conditions of pancreas, BMs predominate, occurring around each acinar cell of the exocrine pancreas, surrounding blood vessels and encasing each pancreatic islet (160, 161). The interstitial matrix confers tensile strength and elasticity to tissues, mainly due to the presence of fibrillar collagens. The interstitial matrix is limited in the pancreas and appears as a thin layer immediately subjacent and external to the peri-islet BM and surrounding large ducts and blood vessels. One specificity of the pancreas ECM it is that there is no hyaluronan, but it is composed of hyaladherins such as versican, inter-alpha-inhibitor (IαI), and tumor necrosis factor-stimulated gene-6 (TSG-6) (162). The human peri-islet BM is mainly composed of collagen type IV, agrin, perlecan, nidogen-1 and -2 and laminin isoforms (160, 161). In normal pancreatic tissue, resident fibroblasts, pancreatic stellate cells (PSCs), immune cells, and vascular cells play a critical role in tissue repair and wound healing (163) (**Figure 3A**). In physiological conditions, quiescent PSCs reside at the basolateral aspect of pancreatic acinar cells and could synthesize ECM proteins and ECM degrading enzymes (164). Following pancreatic injury or tissue damages, injured acinar cells produce and secrete inflammatory cytokines and pro-angiogenic growth factors that increase recruitment and activation of immune cells, promoting angiogenesis. This also leads to increased PSC-mediated deposition of ECM to restore normal pancreatic function. PSCs regulate ECM by maintaining the balance between ECM synthesis and degradation (165, 166).

Pancreatic ductal adenocarcinoma (PDAC) is the most common type of pancreatic cancer. In PDAC, disruption of BM integrity leads to a decrease of collagen IV, altered epithelial cells become cancer cells and activate PSCs to create a permissive microenvironment for cancer progression (167). Once PSCs are activated, the equilibrium shifts, that causes ECM proteins such as collagen I to accumulate (164, 168). This abundant amounts of ECM corresponds to a desmoplastic reaction which exerts mechanical and biochemical effects of PDAC cells by promoting tumor progression (168). The PDAC fibrotic stroma is composed of connective tissues which are rich in collagens I (mainly) and III, fibronectin, CAFs [most of them are pancreatic stellate cells (168)], vascular and immune cells as well as cytokines and growth factors (169–173) (**Figure 3B**).

ECM Evolution During Cancer

Protective Role

The vast majority of patients with PDAC present metastatic disease whereas, normally, deposition of huge amounts of collagen around PDAC cells might inhibit invasion and metastasis. Indeed, PDAC cells have mechanisms that help them overcome this fibrotic barrier and ECM here provides a protective effect in PDAC. Therefore, to our knowledge, there is no physical barrier mediated by the ECM or stromal cells that could constrain tumor progression. However, some matrix elements could be involved in a protective role and are described as better prognosis in PDAC. Indeed, overexpression of some components of the ECM such as collagen XV could act as a tumor suppressor in the BM zone by reducing migratory ability of PDAC cells (174). Proteoglycans can be expressed by tumor cells as well as stellate cells and could play anti-tumor role. For example, biglycan expression is inversely correlated to poor prognosis (175). For instance, lumican expression is associated with an increased survival in patients. It is expressed in both the tumor and the stromal compartments and could directly interact with tumor cells, turning PDAC cells into quiescent cells in G0/G1 arrest (176).

Tumor Promoting Role

The ECM is essential in PDAC development, from the initiation to tumor progression (**Figure 3**). The fibrotic ECM tumor stroma is mainly composed by CAFs and most of them are pancreatic stellate cells (168). PDAC cells secrete Sonic Hedgehog signaling molecule and TGF-β to attract and activate PSCs. Activated PSCs produce pro-inflammatory growth factors and chemokines which could act as a feedback loop to maintain their activity and then promote the synthesis of ECM proteins such as collagen (177–179). Subsequently, activated PSCs promote tumor growth and local invasion of PDAC cells (180).

Pancreatic ductal adenocarcinoma cell properties could also be altered by tissue stiffness of the ECM, which reduces tissue polarity, inhibits adherent junctions, promotes tumor cell proliferation and EMT, by altering expression of vimentin and E-cadherin in PDAC cells (181). Inhibition of PDAC cell contractility decreases MMP activity, suggesting that PDAC cells also influence the ECM properties (182). Crosslinking of collagen I in PDAC could be mediated by LOX and tissue transglutaminase 2 (TG2) (31, 183, 184). TG2 is weakly expressed in normal pancreatic tissue, but its expression and secretion in ECM are increased in PDAC cells (56). Crosslinked collagen activates Yes-associated protein (YAP) and TAZ and promotes proliferation and EMT of PDAC cells (56). ECM degradation is mediated by proteases. For instance, in PDAC, MMPs are key players in ECM remodeling and degradation, as well as in proliferation of Panc-1 cells (185). One study

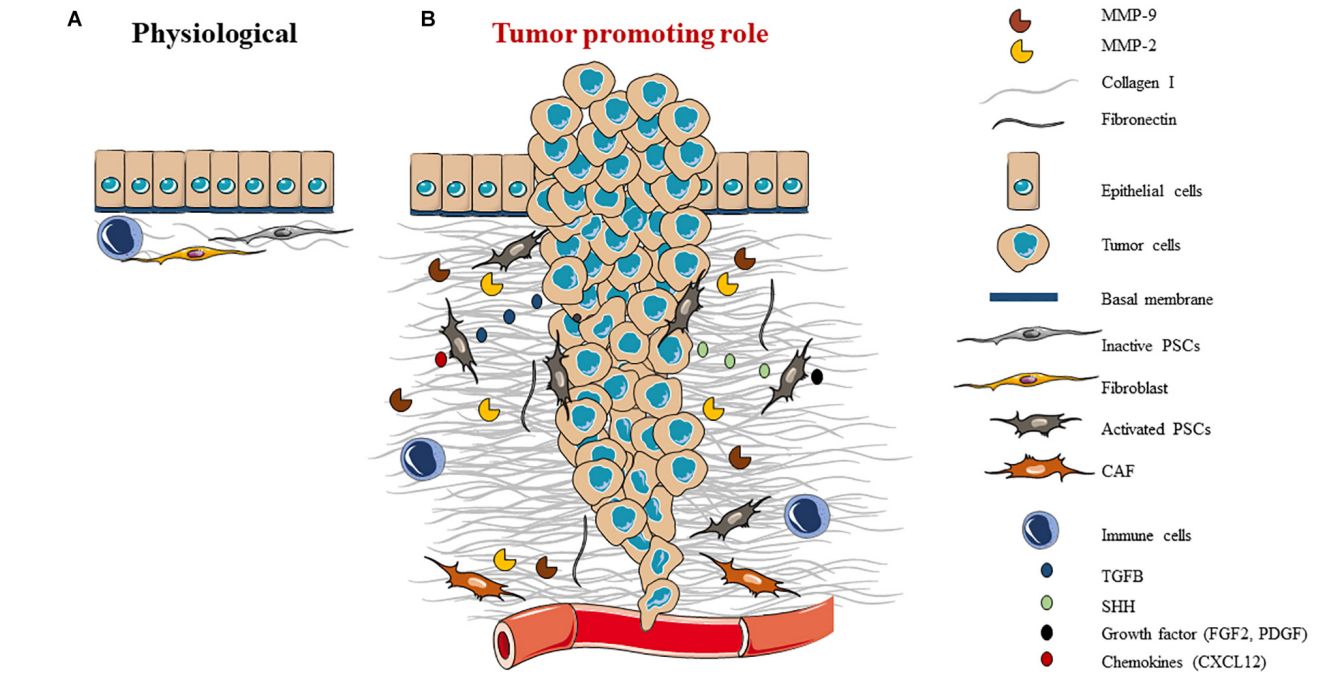

FIGURE 3 | Schematic representation of ECM composition **(A)** and ECM role as a **(B)** tumor promoting role in pancreas.

showed that ROCK1 and ROCK2 promote expression of MMP-10 and -13, enhancing collagen degradation and thus local invasion (186).

Some other matrix components play a crucial role in promoting tumor progression. In patients with PDAC, a level of laminin inferior to 25% in BM (due to BM disruption) or an increase of circulating collagen IV are associated with bad prognosis (187, 188). In PDAC, fibronectin shares similarities with collagen: it can also bind to integrins (such as α5β1) leading to FAK activation (189). Fibronectin acts as a major pro-tumor actor in PDAC, promoting resistance to radiotherapy, proliferation and production of reactive oxygen species (190, 191). Fibronectin also plays an important role in amplifying ECM synthesis by PSCs. By binding to the latent TGF-β binding protein, fibronectin allows the release of active TGF-β, which in turn activates PSCs (192). Similar to fibronectin, vitronectin is a major glycoprotein that binds to both integrins (α5β3) and collagens (193). In physiological conditions, vitronectin is involved in wound healing and homeostasis whereas in PDAC, vitronectin is overexpressed and binds to collagen I, promoting cancer cell migration. It also stimulates secretion of interleukin 8 and promotes proliferation of PDAC cells (194, 195). Proteoglycans such as Glypican-1 is overexpressed in PDAC tumor cells and involved in tumorigenicity (196). Another proteoglycan, SPOCK-1, is able to remodel the ECM, and allows tumor cells to become more invasive (197). HA, which can bind to proteoglycans, is important to promote cell survival, proliferation, and invasion through its binding to CD44 and to the receptor for HA-mediated motility (RHAMM). HA is required, with the help of collagen, to induce an increase in tissue pressure (198).

Extracellular matrix binding receptors also are key players in tumor progression. Collagen I is the most abundant and well characterized component of interstitial matrix in PDAC. Collagen binds to integrins or DDR1 located on PDAC cells, inducing important downstream signaling pathways. Binding of collagen I to integrin on PDAC cells promotes proliferation, migration and inhibits apoptosis of tumor cells through an autocrine loop (199). Collagen I-Integrin signaling also promotes migration of PANC-1 and UlaPaCa cells through activation of FAK (200). FAK activation by this complex could lead to disruption of E-cadherin, promote Wnt activation and thereby regulate EMT (201, 202). The binding of collagen I to DDR1 activates FAK-related protein tyrosine kinase (PYK2), resulting in the expression of the EMT marker N-cadherin (203). Furthermore, binding of collagen I to DDR1 together with transmembrane-4-L-sox-family member 1 (TM4SF1) promotes invadosome formation, induces cell migration and promotes MMP-2 and -9 expressions (204, 205). Another study showed that high levels of palladin expression in PCSs enhance their ability to remodel the ECM by regulating the activity of Cdc42, which promotes invadosome formation as dots or rosettes in PSCs and tumor cell invasion (206). However, it has been reported in PDAC that PSCs can regulate matrix degradation by the activity of the large GTPase Dynamin 2 promoting tumor invasion, independent of invadopodia formation (207). Indeed, PSCs are able to promote tumor cell invasion by degradation of the matrix, dependent or independent of invadosome formation.

Finally, PSCs can directly interact with cancer cells, promote local tumor growth, and co-migrate with cancer cells to distant metastatic sites, establishing stromal abundant tumors beyond the pancreas. Additionally, activated PSCs and cancer cells produce pro-angiogenic factors, which promote neo-angiogenesis and support cancer cell growth and survival under a hypoxic tumor-microenvironment (208, 209).

To conclude, ECM in PDAC is one of the hallmarks of cancer and promotes PDAC progression. Little is known about the protective role of ECM in PDAC and needs further investigation. We could hypothesize that the aggressiveness of this cancer could be due to the absence of a protective role of the ECM or stromal cells compared to other cancers.

COLORECTAL CANCER

ECM Composition and Function

In colon, in physiological conditions, colonic epithelial cells are anchored to the BM and act as a physical barrier with absorptive and exocrine functions (**Figure 4A**). BM is synthetized and secreted by epithelial and mesenchymal cells and separates the colon mucosa from its submucosa (210, 211). BM is composed of collagen IV, proteoglycan perlecan and glycoproteins such as laminin, fibronectin and nidogen (212). Stromal ECM is composed of similar components, but collagen IV is substituted by collagen I produced by resident fibroblasts.

Colorectal cancer (CRC) is the third most common cancer worldwide. An orderly ECM confers unique biomechanical properties in order to assure the regulation of cell proliferation and tissue homeostasis. During cancer, after BM degradation, abnormal ECM deposition and stiffness are observed, which correspond to desmoplastic reaction, promoting tumor progression (12).

Desmoplasia defines the abundant collagenous stroma surrounding parenchymal cells that is deposited after BM degradation. Fibroblasts are activated into myofibroblasts and become the primary producers of ECM in response to desmoplasia, leading to dramatic tissue remodeling (213). ECM of the CRC desmoplastic reaction is composed by collagen types I, III, IV, and V, proteoglycans (biglycan, fibromodulin, perlecan and versican) and small leucine-rich proteoglycans (SLRPs) decorin (214). Desmoplastic reaction prognosis is controverted in colorectal cancer: some studies report that it has a pro-tumor role but most of the studies describe a protective role, which is associated to good prognosis (214, 215) (**Figure 4B**). Therefore, it is important to study which ECM elements involved in the desmoplastic reaction are protectors or promoters of tumor progression.

ECM Evolution During Cancer

Protective Role

In a study from 2011, Coulson-Thomas et al., showed that co-culture systems with colorectal cancer cell lines and fibroblasts promote an increase in ECM density which could inhibit the migration and invasion of CRC tumors. The desmoplastic collagen fibers were thicker than in normal tissue and arranged into parallel bundles with an altered orientation. This study demonstrated a protective role of CRC desmoplastic reaction by forming a barrier which can restrain tumor growth by creating an increased pressure, preventing tumor invasion of the surrounding tissue (214) (**Figure 4B**). A clinical study showed that desmoplasia is a protective factor for survival in patients with CRC. Thus, desmoplasia could prevent cancer cell invasion by building a barrier around the tumor (215).

However, for now, no study analyzes how and how long the protective barrier of desmoplasia needs to become pro-invasive and requires investigating. It could be due to collagen up-regulation as well as other ECM components such as fibromodulin, biglycan and fibronectin surrounding CRC. We could hypothesize that these components could first act as a protective barrier around the tumor cells; the pressure and stiffness then become too high in tumor cells which continue to proliferate which leads to the disruption of the protective barrier, allowing invasion and migration of tumor cells.

Tumor Promoting Role

Basement membrane disruption participates in tumor progression by releasing angiogenic, growth stimuli and chemotactic factors in order to promote tumor angiogenesis, growth and cell proliferation. For example, laminin 332 degradation promotes EGFR activation, causing a decrease of cell matrix adhesion enhancing migration (216). In CRC, loss of BM integrity is correlated to metastatic potential.

During cancer, the newly deposited collagen I replaces the proteolytically degraded ECM proteins by secreted proteases. This change can cause cellular migration which is predominantly oriented along radially aligned collagen fibers, promoting invasion. In physiological conditions, collagen fibers are disposed in the epithelium stroma with an angle of 10°, whereas in CRC, collagen fibers are thicker and present an angle of 50° (217). Furthermore, it has been demonstrated that ordered collagen fibers and an increase in collagen density are associated with CRC, demonstrating the main role played by collagen in malignant tissue transformation (218) (**Figure 4C**). In CRC, ECM elasticity ranges from soft and compliant to stiff and rigid. As mentioned before, tissue stiffness can be increased by enzymes such as LOX, which can crosslink collagen. In CRC cells, LOX is upregulated leading to increased tissue stiffness and activation of Src/FAK pathway promoting proliferation, invasion and metastasis (219, 220). Furthermore, at clinical level, LOX upregulation is associated with poor prognosis of CRC (221). Crosslinked collagen activates YAP and TAZ, promoting malignancy of CRCs.

A recent study analyzes the changes of the ECM at different stages of CRC and their effect on proliferation of cancer cells. It was shown that expression of MMP-2 and type I collagen are positively correlated to the stages in CRC. Collagen I expression is the highest in stage III and stage IV and lowest in normal tissue and stage I. The expression of MMP-9 is also higher in CRC, mainly in stage III. As regards collagen IV and TIMP-3, their expression is inversely correlated to CRC stages (221).

The binding of ECM elements to ECM receptors promotes tumorigenesis. Binding of collagen I to DDR1 promotes local

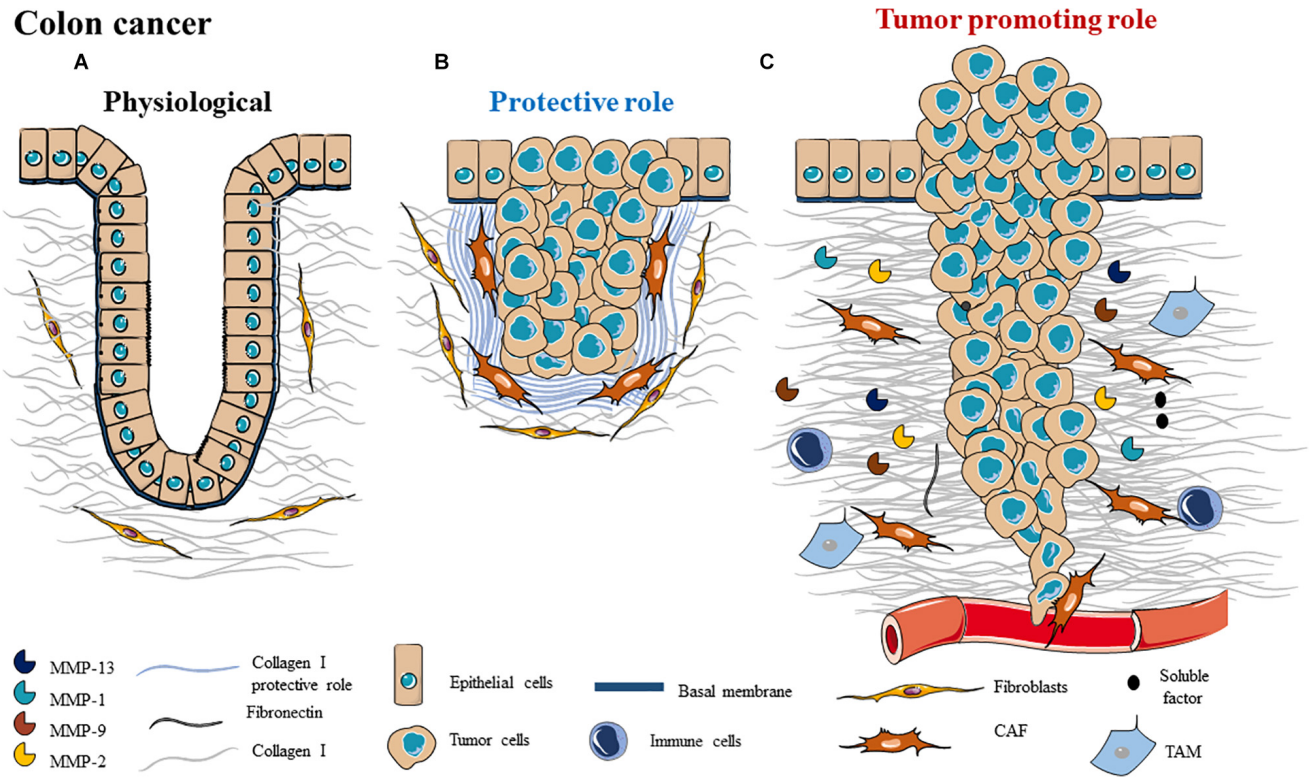

FIGURE 4 | Schematic representation of ECM composition **(A)** and ECM dual role as a **(B)** protective barrier or as a **(C)** tumor promoting role in colon cancer.

invasion of primary CRC cells and promotes their dissemination. DDR1 overexpression is associated with poor prognosis in CRC patients (222). Binding of collagen I to DDR2 promotes cell proliferation, migration, invasion and peritoneal dissemination of colon cancer cells (223). Binding of collagen I to α2β1 integrin activates the pro-survival PI3K/AKT signaling pathway; resulting in the tumor promotion in CRC cells. This complex allows activation of transcription factor SNAIL; which in turn downregulates the expression of E-cadherin, inducing EMT and distant metastasis (224). Overexpression of CD44 is associated with poor prognosis of CRCs. The binding of HA to CD44v6 improves cancer cell proliferation, invasion, metastasis and resistance in colon cancer. The binding of osteopontin to CD44v6 also improves proliferation, invasion and metastasis of CRC cells (225). CAFs also improve the adhesion and migration of CRC through upregulation of CD44 in cancer cells (226). One study demonstrated that CD44 expression in CAFs maintains stem-cell properties of CRC cells but the exact molecular mechanism is not known. Furthermore, CD44 expressed by CAFs may interact with CRC cells to support cancer cell survival in hypovascular areas but it needs further investigations (54).

Besides collagen I, other proteins are deregulated in ECM of CRC. A downregulation of proteins such as keratin or collagen IV has been found in CRC tissues compared to normal tissues (227). During tumor invasion and metastasis, tumor cells directly secrete degradative enzymes and induce CAFs, inflammatory cells and the endothelial cells to produce proteolytic enzymes to degrade ECM. In CRC, MMP-1 and MMP-13 collagenases and MMP-2 and MMP-9 (two gelatinases) expression correlates to advanced CRC stage and poor prognosis (228). Different co-culture of CRC cell lines and TAM cell lines cause the upregulation of tumor cell-derived MMP-2 and MMP-9 expression and secretion, with increased tumor invasiveness and migration (229). Proteases such as ADAM9, ADAM10, TSLI and MMP-1, -2, -9, -11, and -12 have been found in colon primary tumor but not in metastasis, suggesting their role in migration of primary tumor cells (230). Myofibroblasts also promote CRC invasion by secreting soluble factors such as HGF and SPARC or by remodeling the ECM (231, 232). Myofibroblasts may interact directly with tumor cells by leading collective tumor cell invasion, through a process dependent on the Rho-GTPase effector ROCK (233).

Colorectal cancer cells are able to form invadosomes organized in dots in order to invade (234–236). Invadopodia formation could be mediated through activation of ROCK-II, modulating MMP-2 and -13 expressions and activities and by Smad 4-independent BMP signaling in CRC cells. Src activation could also induce Nox A1 phosphorylation, this will; in turn; lead to reactive oxygen species (ROS) generation promoting invadopodia formation (235–237). However, no study analyzes if these cancer cells are able to form linear invadosomes when they are seeded on collagen I. As expected, proteases were peculiar of primary colon tumor: ADAM 9, 10, TSL1 and MMP1, 2, 9, 11, and 12 have been found solely in colon tumor (230) and

not in the metastasis, suggesting their role in the migration process. In another paper, the paired biopsies from tumor and its normal counterpart were obtained from 13 patients. Fifty-six proteins have been identified in the insoluble tissue fraction, after the extraction of lipids and soluble proteins. The digested peptides from ECM fraction were analyzed using a nano-ESI source by means of label-free quantitation approach (e.g., solely based on measurements of observed peptide ion peak intensities). The obtained data for Beside collagens, other ECM proteins are deregulated in CRC. One study report that MAGP2 (Microfibrial-associated glycoprotein 2), which is ECM component, is upregulated in CRC tissues compared to adjacent tissue, promoting proliferation, migration and invasion of cancer cells and the increase in it promoted malignant phenotypes of CRC cells including proliferation, migration, and invasion. Microfibrial-associated glycoprotein 2 can increase expression of the downstream genes of Notch, including HES1, Slug, Snail, matrix metalloproteinase (MMP) 2, MMP9, whereas its decrease Kruppel-like factor 4 (KLF4) expression. In this study they hypothesized that MAGP2 could be secreted by cancer cells or by CAF (238).

Furthermore, it has recently been shown that citrullined ECM proteins are characteristic of colon cell metastasis in the liver, suggesting that this process is important for the metastatic journey. Citrullination is the deamination of arginine residues to form peptides containing the non-coding amino acid citrulline. This process is a well-recognized characteristic of chronic inflammation, as demonstrates in autoimmunity where ECM proteins are extensively citrullinated. In CRC, citrullination is catalyzed by PAD4 which is produced by tumor cells, then PAD4 is delivered to the liver metastatic ECM by extracellular vesicles (239). ECM citrullination is a driver of human CRC liver metastasis.

To sum up, ECM of CRC evolves during tumor progression. The ECM first acts as a protective barrier to restrain tumor growth to local area and subsequently becoming a key player in tumor progression. Desmoplasia seems to act as a protective barrier and is a good prognostic in patient with colon cancer. It seems that the same element in colon ECM could have both a protective or a tumor promoting role. However, it would be interesting to study how the microenvironment dynamic influences this switch from protective to tumor promoting role.

MELANOMA

ECM Composition and Function

Mammalian skin is composed of a multi-layered epithelium (**Figure 5**). The outer surface of the skin, the epidermis, consists of a keratinized stratified squamous epithelium. The epithelium rests on a layer of nourishing fibroelastic connective tissue called the dermis, which mainly consists of type I collagen. The dermis is connected to the underlying tissue by a layer of loose connective tissue, the hypodermis or subcutaneous layer, which contains varying amounts of fat tissue. Skin is composed of cells such as fibroblasts, endothelial cells, keratinocytes and ECM (240).

The separation between the epidermis and the dermis is a BM (**Figure 5**). In skin, BMs are composed of laminin, type IV collagen, nidogen, and perlecan, a heparan sulfate proteoglycan (241). In contrast, the tensile strength and elasticity in the dermis underneath is determined by ECM, composed of collagen types I (80%), III (15%), and type V (5%), microfibrils, elastic fibers, proteoglycans, glycosaminoglycans and water (242). In normal dermis, collagen fibers exhibit a random, "basket-weave" structure (243). The cutaneous ECM is constantly remodeled throughout the lifespan, for example during wound-healing or aging (243).

Melanoma is a cancer that arises from melanocytes. This very aggressive skin cancer develops in very rich in fibrillar type I collagen environment (**Figure 5**). In physiological conditions, keratinocytes modulate behavior of melanocyte population and the dermally located fibroblasts synthesize the ECM. During the initiation of melanomagenesis, melanocytes accumulate sufficient mutations to degenerate, notably through the aberrant activation of an oncogene such as the *BRAF V600E* mutation. Melanoma cells, therefore, hyper-proliferate on the surface of the skin during radial growth. Subsequently, the cells deeply invade the deep layers of the skin, after having degraded the BM separating the epidermis from the dermis. The transition from radial to vertical growth phase in melanoma is associated with loss of E-cadherin expression, increased N-cadherin expression and increased expression of αvβ3 integrin, leading to secretion of the antiapoptotic factor bcl-2 and MMP-2, an endopeptidase that degrades collagen IV at the BM (244–246). Additionally, the shift from E-cadherin to N-cadherin expression allows melanoma cells to interact with fibroblasts and vascular endothelial cells to better facilitate migration and intravasation (247). The fibroblasts also become activated, resulting in increased growth factor production leading to a hyperproliferative microenvironment that supports growth of many cell types and collagen I synthesis (248). Finally, the tumor is fully competent to invade and metastasize to distant organs. Once metastasis to distant organs has occurred, the tumor enters its final stage and is termed metastatic melanoma.

ECM Evolution During Cancer

Protective Role

The ECM can first act as a protective barrier against melanoma progression (**Figure 5**). In the dermis, the major component of the extracellular matrix is type I collagen, which is synthesized mainly by fibroblasts. It has been established that collagen I acts as a protective barrier in tumor progression and proliferation (249). In the same study, they showed that contact with fibrillar collagen inhibits the proliferation of malignant and highly metastatic M24met cells. Inhibition of proliferation is due to the binding of collagen to α2β1 integrin which induces an increase in p27KIP1 mRNA and protein, promoting growth arrest in the G1/S transition and inhibition of cyclin E-associated kinase activity (249).

During the early phase of melanomagenesis such as Radial Growth Phase (RGP), co-culture of fibroblasts with RGP melanoma cells represses tumor growth; whereas advanced

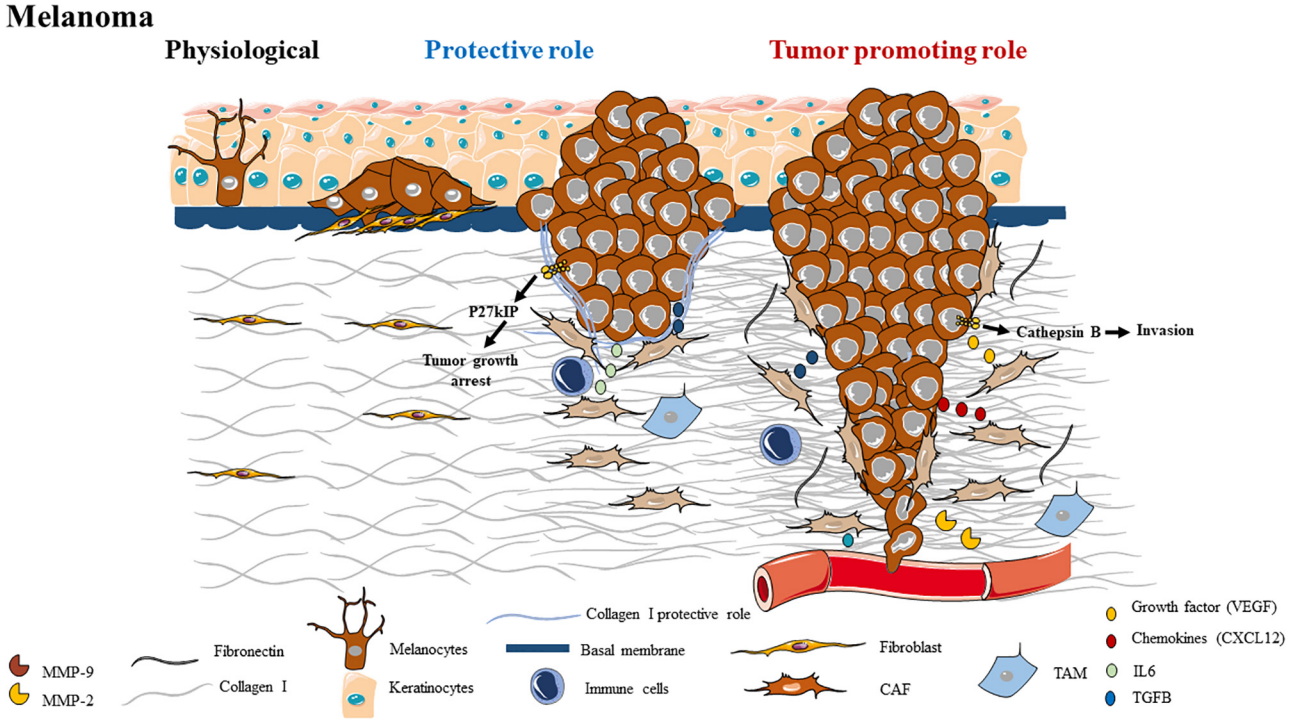

FIGURE 5 | Schematic representation of ECM composition and ECM dual role as a protective barrier or as a tumor promoting role in melanoma.

melanoma cells acquire an ability to escape such control mechanisms (250). It is possible that dermal fibroblasts form a physical barrier that blocks melanoma cells to migrate and invade the surrounding tissues. Another hypothesis, regarding the inhibitory effect of dermal fibroblasts, is that dermal fibroblasts could recruit immune cells by secreting interleukin-6 (IL-6) (251).

Tumor Promoting Role

Cancer-associated fibroblasts at the level of the primary tumor are called melanoma associated fibroblast (MAFs) and are involved in melanoma progression (**Figure 5**). Fibroblasts can be activated by chemical factors secreted by melanoma cells, inducing fibroblasts to migrate toward, surround, and then infiltrate the tumor mass. For example, in melanoma, the secretion of TGF-β by tumor cells allows the activation of MAFs (252), which are able to synthesize and deposit ECM proteins such as collagen, fibronectin and tenascin (253, 254).

PDGF and bFGF could increase the production of glycosaminoglycan (GAG) from MAFs (255). Oxidative stress induced by hypoxia in the melanoma as well as factors secreted by melanoma cells stimulate MAFs to secrete cytokines and growth factors such as VEGF, stromal derivative factor-1 (SDF-1 or CXCL12) and IL-6 thus promoting invasion into the melanoma (256, 257).

Melanoma associated fibroblast are also able to remodel the ECM by MMP-1, MMP-2, MMP-13, and MT1-MMP (MMP-14) secretion, which could influence the motility and invasiveness of melanoma cells (205, 258–261). In primary and metastatic melanoma, it has been shown that up-regulation of FAP-α expression (an active serine protease which could degrade type I collagen) enhances ECM remodeling, tumor cell growth and migration (262, 263).

Collagen I receptors are also involved in tumor progression. CD44 expression is associated with poor prognosis of melanoma, and different studies have shown that binding of collagen I or HA to CD44 promote tumor progression (264, 265). The binding of collagen I to α2β1 integrin promoting cathepsin B-mediated invasiveness was associated with secreted acidic and cysteine-rich proteins in melanoma (266). The binding of collagen I to DDR1 enhances invasion and the binding of collagen I to DDR2 induces MMP-2 and MMP-9 expressions as well as Erk/NF-κB signaling pathways to promote invasion (267). Despite the abundance of collagen I, melanoma progression is characterized by the increase of other matrix proteins such as tenascin-C and fibronectin. These two proteins could affect the organization of collagen fibers. It has been shown that MAFs facilitate tumor invasion through αVβ3 integrin-dependent fibronectin secretion, which induces mechanical changes in the ECM through the contraction of collagen fibers (268). It has been previously demonstrated that biglycan expression is involved in matrix contraction and increased in matrix stiffness which induce β1 integrin expression, promoting invasion of melanoma cells (269). However, most of the studies focus on ECM stiffness and its protective role during resistance to the treatment. It has been shown that an increase in ECM stiffness upon exposure of BRAF inhibitor promotes a protective matrix environment during resistance to treatment (270, 271). This increasing stiffness leads to the re-organization of

β1 integrin into focal adhesions and elevated pFAK levels (271). The binding of fibronectin to α4β1or αVβ3 integrins promote melanoma cell invasion (268, 272).

Tks4 and Tks5 adaptor proteins are key players in melanoma growth and metastasis *in vitro* and *in vivo*, promoting invadopodia formation by MT1-MMP regulation (273). Another study showed that, invadopodia formation in melanoma cells could be regulated by crosstalk between receptor tyrosine kinases AXL and ERBB3 (274). Our data report that when melanoma cells are seeded on collagen I matrix, there is invadosome reorganization into linear invadosomes (51).

Finally, MAFs expresses a lot of proteins which are key players for melanoma cell metastasis. MAFs secrete tenascin C and periostin, which are required for the development of a CSC phenotype and the formation of metastatic sites. MAFs are also able to secrete the matricellular protein CCN2, which is required for melanoma metastasis (275, 276). Furthermore, different crosstalk between MAFs and melanoma cells are involved in metastasis of melanoma cells. For example, CXCR4 (CXC chemokine receptor-4) is expressed on the surface of melanoma cells, while its ligand CXCL12 is released by MAFs in the tumor microenvironment, promoting the migration and metastasis of melanoma cells to distal metastatic sites through interaction with CXCR4 expressed on tumor cells (277–279). Besides, HGF secreted by MAFs induce fibronectin expression and associated matrix assembly, which promotes melanoma cell metastasis (280).

Extracellular matrix in melanoma firstly acts as a protective barrier to avoid tumor progression. Then, ECM becomes an essential partner in order to facilitate migration, invasion, metastasis and resistance in the melanoma. It could be important to study the crosstalk between cancer cells and stromal cell in the promotion of ECM remodeling, degradation and invasion, in a physiological matrix model, in different skin acellular models that exist (262, 281).

SIMILARITIES AND DIFFERENCES BETWEEN THE ECM OF THE FIVE CANCERS

We note that these five cancers share similarities (**Table 1**). First, a crosstalk between cancer and stromal cells, where cancer cells could activate stromal cells into stromal cancer cells, promoting enhancement of ECM deposition. The stromal cancer cells in turn are able to secrete growth factors and cytokines to promote the invasion of tumor cells. Second, these 5 cancers also share some similarities in their ECM composition: after BM disruption, collagens I, III, and V, proteoglycans, glycosaminoglycans and elastic fibers accumulate. Whereas after BM disruption there generally is a decrease of collagen IV, we note that liver cancer ECM showed an upregulation of collagen IV. Furthermore, at late stages of tumor progression, biomechanical properties of the matrix, such as the alignment of ECM constituents have been correlated to cell invasion and poor prognosis. Moreover, a recent paper showed the importance of crosstalk between stromal cells and ECM to promote breast cancer cell migration (282). Indeed, CAFs, through cell collision guidance, induce their own alignment, which in turn, promote ECM alignment. This increased ECM alignment promotes tumor cell invasion, suggesting that the cancer ECM anisotropy is a key characteristic to take into consideration while studying cancer.

Despite similarities in these different types of matrix, we also note major differences (**Table 1**). For instance, collagen crosslinking is mediated by LOX only in breast and colon cancers, whereas in pancreas, crosslinking could be also mediated by transglutaminase 2 (30, 32, 81, 82, 184, 221). In liver cancer, collagen crosslinking is mediated by LOXL2 only. Regarding melanoma, tenascin C and fibronectin affect the organization of collagen fibers and biglycan is involved in matrix contraction and increased matrix stiffness (175, 268). To our knowledge, no study reports the role of LOX in collagen crosslinking in melanoma.

One other major difference is that TAEM in breast, liver, colon and melanoma cancer has an anti-tumor role to restrict tumor growth at the primary site, whereas this is not observed in pancreatic cancer. ECM in breast cancer is the most studied and described. One of the specificities of breast cancer is that myoepithelial cells act as a protective barrier around the tumor cells and are able to decrease the secretion of MMP-2, MMP-9, and MT1-MMP (94–96). In addition, they can secrete protease inhibitors or angiogenic inhibitors, several tumor suppressors in order to prevent tumor growth, invasion and metastasis (81, 82, 84). CAFs are often associated with poor prognosis in cancer, whereas in liver and in breast cancer, CAFs can also participate to the protective role of ECM. In breast cancer, CAFs have been shown to secrete factors which are associated with decrease metastasis (87–89). ECM of liver cancer, colon cancer and melanoma present some similarities with regards to the protective effect. Indeed, at the early stages of tumor progression, they all show a structure like a capsule made of collagen and fibroblasts around the tumor in order to restrict tumor growth (214, 215). No study analyzes how the protective barrier of desmoplasia becomes pro-invasive, which requires further investigations. We could hypothesize that collagen secretion could first act as a physical protective barrier around the tumor cells. Then, the pressure becomes too high by tumor cells which continue to proliferate, that the protective barrier is disrupted, allowing invasion and migration of tumor cells. We could also postulate that when fibroblasts are activated into CAFs, there is an upregulation of ECM component secretion promoting pressure around the tumor, leading to the disruption of the protective barrier and then to cancer progression. Regarding pancreatic cancer, one of the most aggressive cancer, there is no collagen or fibroblast protective barrier at early stages. Thus, maybe the aggressiveness of this cancer at beginning stages could be due to the lack of the protective barrier. In all of the cancers discussed above, we could not find any study that analyzes the transition between protection and this pro-invasive effect. New epigenetic mutations in cancer cells that promote proliferation and invasion of the protective barrier - immunity or metabolic stress - could be at the origin of this transition. It would be crucial to study the elements which could induce this switch, in order to promote protective role of ECM in cancer and restrain tumor growth.

To sum up, the complexity and heterogeneity of each tumor matrix is due to the architecture and organization of each organ. In addition of this inter-tumor heterogeneity, matrix

TABLE 1 | Similarities and differences in composition and crosslinking of the tumor associated protective or tumor promoting ECM in each cancers.

	Stroma composition			
	Protective	**Pro-tumoral**		
	Composition	**Composition**	**Signaling pathways**	**Cross-linking**
Breast cancer	– Collagens I, III, V, fibronectin, laminin, decorin – Myoepithelial cells – CAFs	– Collagens I, III, V – Fibronectin, fibrin, hyaluronan, versican, osteopontin, tenascin, periostin	CD44 → PDGFRβ/Stat3 CD44 → MAPK or AKT → Invasion, migration, survival Collagen I → Integrin α11 → PDGFRβ/JNK → Invasion → DDR1 → Invadosomes formation → DDR1 + IGFRI → Proliferation and migration Collagen IV → DDR1 → NFκB → Resistance Fibronectin → Erk or Stat 3 → EMT Laminin → Integrin → Invasion and migration	LOX LOXL2 LOXL3 LOXL4
Liver cancer	– Collagens I, III – CAFs	– Collagens I, III, IV – Tenascin, osteopontin, laminin, chondroitin sulfate	Collagen I → β1 integrin → MAPK → prosurvival signal CD44 → MDM2 nuclear translocation → Akt → tumor progression TGFB → collagen I → DDR1 → LOXL2 → Invadopodia Collagen I → DDR1 → Erk → SNAIL → EMT → DDR2 → ERK → MMPs → Invasion	LOXL2
Pancreas cancer	– Byglican, lumican: associated to better prognosis	– Collagens I, III – Fibronectin, vitronectin, glypican, SPOCK1, HA	Hyaluronan → CD44 → survival, proliferation, invasion Collagen I → Integrin → FAK → migration → DDR1 → PYK2 → EMT → DDR1/TM4SF1 → invadosome formation	LOX TG2
Colon cancer	– Collagens I, III, IV, V, biglycan, fibromodulin, perlecan, versican, decorin	– Collagens I, III, V – Byglican, perlecan, versican, fibromodulin, biglycan, fibronectin	Collagen I → DDR1 → Invasion → DDR2 → Proliferation, migration, invasion → α2β1 → PI3/Akt → tumor progression → α2β1 → Snail → EMT HA → CD44v6 → proliferation, invasion, resistance Osteopontin	LOX
Melanoma	– Collagen I – Fibroblast	– Collagen I – Tenascin-C, fibronectin, periostin, osteopontin, SPARC, CCN3	Collagen I → α2β1 → Cathepsin B → invasion → DDR1 → Invasion → DDR2 → ERK/NFκB → Invasion	Fibronectin Biglycan Tenascin C

heterogeneity can also be observed at the level of the same tumor and each tumor structure could have a specific matrix.

DISCUSSION

In the last decade, the role of ECM in cancer has been widely studied and gained more and more importance. During cancer progression, ECM is constantly remodeled, and is the result of a balance between secretion and degradation. ECM evolves constantly from primary tumor to metastasis site including pre-metastatic niche. Therefore, there is modification of ECM composition and organization in the pre-metastatic niche for cancer cell to become dormant or to grow and form metastasis.

The crosstalk between tumor and stromal cells controls this balance. Tumor evolution leads to TAEM creation, which is essential in the tumor progression. In order to interact with TAEM, stromal and cancer cells need to express ECM receptors including collagen receptors promoting malignant phenotype of tumor cells such as invasion, migration and proliferation.

However, this scheme of ECM involvement in cancer progression is too simple and need to be adapted to each organ, cancer and cancer stages. We showed, in this review, that each cancer has its own matrix, with its own composition, its own molecules promoting crosslinking, therefore they present specific pro-tumor or protective effect.

The ECM is well-known and well-studied for its tumor promoting role. However, it is very important to note that, at the beginning of a large number of cancers, ECM first could serve as a protective barrier. It could be complicated to develop therapies against ECM due to its heterogeneity as well as its dual role as a pro or anti-tumor. However, there is a real need to understand the dynamics of the microenvironment, in order to determine when and how the protective barrier could became pro-tumor. This could allow development of a therapeutic strategy to enhance protective role of the ECM and control the disease by preventing or delaying the pro-tumor role of the ECM.

AUTHOR CONTRIBUTIONS

MS and MR prepared the figures and wrote and edited the manuscript. FS edited the manuscript. All authors contributed to the article and approved the submitted version.

FUNDING

This work was funded by La Fondation pour la Recherche Médicale (grant number DEQ20180839586) and Fondation de France.

REFERENCES

1. Hanahan D, Coussens LM. Accessories to the crime: functions of cells recruited to the tumor microenvironment. *Cancer Cell*. (2012) 21:309–22. doi: 10.1016/j.ccr.2012.02.022
2. Quail DF, Joyce JA. Microenvironmental regulation of tumor progression and metastasis. *Nat Med*. (2013) 19:1423–37. doi: 10.1038/nm.3394
3. Kalluri R. The biology and function of fibroblasts in cancer. *Nat Rev Cancer*. (2016) 16:582–98. doi: 10.1038/nrc.2016.73
4. Kai F, Drain AP, Weaver VM. the extracellular matrix modulates the metastatic journey. *Dev Cell*. (2019) 49:332–46. doi: 10.1016/j.devcel.2019.03.026
5. Bissell MJ, Radisky D. Putting tumours in context. *Nat Rev Cancer*. (2001) 1:46–54. doi: 10.1038/35094059
6. Boudreau A, van't Veer LJ, Bissell MJ. An "elite hacker": breast tumors exploit the normal microenvironment program to instruct their progression and biological diversity. *Cell Adh Migr*. (2012) 6:236–48. doi: 10.4161/cam.20880
7. Naba A, Clauser KR, Ding H, Whittaker CA, Carr SA, Hynes RO. The extracellular matrix: tools and insights for the "Omics" Era. *Matrix Biol*. (2016) 49:10–24. doi: 10.1016/j.matbio.2015.06.003
8. Mecham RP. Overview of extracellular matrix. *Curr Protoc Cell Biol*. (2012) Chapter 10:Unit 10.1. doi: 10.1002/0471143030.cb1001s57
9. Bonnans C, Chou J, Werb Z. Remodelling the extracellular matrix in development and disease. *Nat Rev Mol Cell Biol*. (2014) 15:786–801. doi: 10.1038/nrm3904
10. Tsang KY, Cheung MCH, Chan D, Cheah KSE. The developmental roles of the extracellular matrix: beyond structure to regulation. *Cell Tissue Res*. (2010) 339:93–110. doi: 10.1007/s00441-009-0893-8
11. Hynes RO. Extracellular matrix: not just pretty fibrils. *Science*. (2009) 326:1216–9. doi: 10.1126/science.1176009
12. Pickup MW, Mouw JK, Weaver VM. The extracellular matrix modulates the hallmarks of cancer. *EMBO Rep*. (2014) 15:1243–53. doi: 10.15252/embr.201439246
13. Harburger DS, Calderwood DA. Integrin signalling at a glance. *J Cell Sci*. (2009) 122:159–63. doi: 10.1242/jcs.018093
14. Leitinger B, Hohenester E. Mammalian collagen receptors. *Matrix Biol*. (2007) 26:146–55. doi: 10.1016/j.matbio.2006.10.007
15. Wu T-H, Yu M-C, Chen T-C, Lee C-F, Chan K-M, Wu T-J, et al. Encapsulation is a significant prognostic factor for better outcome in large hepatocellular carcinoma. *J Surg Oncol*. (2012) 105:85–90. doi: 10.1002/jso.22060
16. Kusuma S, Zhao S, Gerecht S. The extracellular matrix is a novel attribute of endothelial progenitors and of hypoxic mature endothelial cells. *FASEB J*. (2012) 26:4925–36. doi: 10.1096/fj.12-209296
17. Poltavets V, Kochetkova M, Pitson SM, Samuel MS. The role of the extracellular matrix and its molecular and cellular regulators in cancer cell plasticity. *Front Oncol*. (2018) 8:431. doi: 10.3389/fonc.2018.00431
18. Ramaswamy S, Ross KN, Lander ES, Golub TR. A molecular signature of metastasis in primary solid tumors. *Nat Genet*. (2003) 33:49–54. doi: 10.1038/ng1060
19. Fang M, Yuan J, Peng C, Li Y. Collagen as a double-edged sword in tumor progression. *Tumor Biol*. (2014) 35:2871–82. doi: 10.1007/s13277-013-1511-7
20. Xu S, Xu H, Wang W, Li S, Li H, Li T, et al. The role of collagen in cancer: from bench to bedside. *J Transl Med*. (2019) 17:309. doi: 10.1186/s12967-019-2058-1
21. Albrengues J, Bertero T, Grasset E, Bonan S, Maiel M, Bourget I, et al. Epigenetic switch drives the conversion of fibroblasts into proinvasive cancer-associated fibroblasts. *Nat Commun*. (2015) 6:10204. doi: 10.1038/ncomms10204
22. Avgustinova A, Iravani M, Robertson D, Fearns A, Gao Q, Klingbeil P, et al. Tumour cell-derived Wnt7a recruits and activates fibroblasts to promote tumour aggressiveness. *Nat Commun*. (2016) 7:10305. doi: 10.1038/ncomms10305
23. Talele NP, Fradette J, Davies JE, Kapus A, Hinz B. Expression of α-smooth muscle actin determines the fate of mesenchymal stromal cells. *Stem Cell Rep*. (2015) 4:1016–30. doi: 10.1016/j.stemcr.2015.05.004
24. Quante M, Tu SP, Tomita H, Gonda T, Wang SSW, Takashi S, et al. Bone marrow-derived myofibroblasts contribute to the mesenchymal stem cell niche and promote tumor growth. *Cancer Cell*. (2011) 19:257–72. doi: 10.1016/j.ccr.2011.01.020
25. Schulte J, Weidig M, Balzer P, Richter P, Franz M, Junker K, et al. Expression of the E-cadherin repressors Snail, Slug and Zeb1 in urothelial carcinoma of the urinary bladder: relation to stromal fibroblast activation and invasive behaviour of carcinoma cells. *Histochem Cell Biol*. (2012) 138:847–60. doi: 10.1007/s00418-012-0998-0
26. Zeisberg EM, Potenta S, Xie L, Zeisberg M, Kalluri R. Discovery of endothelial to mesenchymal transition as a source for carcinoma-associated fibroblasts. *Cancer Res*. (2007) 67:10123–8. doi: 10.1158/0008-5472.CAN-07-3127
27. Kalluri R, Zeisberg M. Fibroblasts in cancer. *Nat Rev Cancer*. (2006) 6:392–401. doi: 10.1038/nrc1877
28. Paszek MJ, Zahir N, Johnson KR, Lakins JN, Rozenberg GI, Gefen A, et al. Tensional homeostasis and the malignant phenotype. *Cancer Cell*. (2005) 8:241–54. doi: 10.1016/j.ccr.2005.08.010
29. Xiao Q, Ge G. Lysyl oxidase, extracellular matrix remodeling and cancer metastasis. *Cancer Microenviron*. (2012) 5:261–73. doi: 10.1007/s12307-012-0105-z
30. Erler JT, Bennewith KL, Cox TR, Lang G, Bird D, Koong A, et al. Hypoxia-induced lysyl oxidase is a critical mediator of bone marrow cell recruitment to form the premetastatic niche. *Cancer Cell*. (2009) 15:35–44. doi: 10.1016/j.ccr.2008.11.012
31. Cox TR, Bird D, Baker A-M, Barker HE, Ho MW-Y, Lang G, et al. Mediated collagen crosslinking is responsible for fibrosis-enhanced metastasis. *Cancer Res*. (2013) 73:1721–32. doi: 10.1158/0008-5472.CAN-12-2233
32. Scott LE, Weinberg SH, Lemmon CA. Mechanochemical signaling of the extracellular matrix in epithelial-mesenchymal transition. *Front Cell Dev Biol*. (2019) 7:135. doi: 10.3389/fcell.2019.00135
33. Stanton AE, Tong X, Yang F. Extracellular matrix type modulates mechanotransduction of stem cells. *Acta Biomater*. (2019) 96:310–20. doi: 10.1016/j.actbio.2019.06.048
34. Humphrey JD, Dufresne ER, Schwartz MA. Mechanotransduction and extracellular matrix homeostasis. *Nat Rev Mol Cell Biol*. (2014) 15:802–12. doi: 10.1038/nrm3896
35. Erdogan B, Webb DJ. Cancer-associated fibroblasts modulate growth factor signaling and extracellular matrix remodeling to regulate tumor metastasis. *Biochem Soc Trans*. (2017) 45:229–36. doi: 10.1042/BST20160387
36. Ezzoukhry Z, Henriet E, Cordelières FP, Dupuy J-W, Maître M, Gay N, et al. Combining laser capture microdissection and proteomics reveals an active translation machinery controlling invadosome formation. *Nat Commun*. (2018) 9:2031. doi: 10.1038/s41467-018-04461-9
37. Murphy DA, Courtneidge SA. The "ins" and "outs" of podosomes and invadopodia: characteristics, formation and function. *Nat Rev Mol Cell Biol*. (2011) 12:413–26. doi: 10.1038/nrm3141
38. Gimona M, Buccione R, Courtneidge SA, Linder S. Assembly and biological role of podosomes and invadopodia. *Curr Opin Cell Biol*. (2008) 20:235–41. doi: 10.1016/j.ceb.2008.01.005
39. Di Martino J, Paysan L, Gest C, Lagrée V, Juin A, Saltel F, et al. Cdc42 and Tks5: a minimal and universal molecular signature for functional invadosomes. *Cell Adh Migr*. (2014) 8:280–92. doi: 10.4161/cam.28833
40. Di Martino J, Henriet E, Ezzoukhry Z, Goetz JG, Moreau V, Saltel F. The microenvironment controls invadosome plasticity. *J Cell Sci*. (2016) 129:1759–68. doi: 10.1242/jcs.182329
41. Juin A, Billottet C, Moreau V, Destaing O, Albiges-Rizo C, Rosenbaum J, et al. Physiological type I collagen organization induces the formation of a novel class of linear invadosomes. *Mol Biol Cell*. (2012) 23:297–309. doi: 10.1091/mbc.e11-07-0594
42. Juin A, Di Martino J, Leitinger B, Henriet E, Gary A-S, Paysan L, et al. Discoidin domain receptor 1 controls linear invadosome formation via a Cdc42–Tuba pathway. *J Cell Biol*. (2014) 207:517–33. doi: 10.1083/jcb.201404079
43. Chabadel A, Wehrle-Haller B, Genot E, Jurdic P, Anton IM, Saltel F. CD44 and β3 integrin organize two functionally distinct actin-based domains in osteoclasts. *Mol Biol Cell*. (2007) 18:12.
44. Destaing O, Planus E, Bouvard D, Oddou C, Badowski C, Bossy V, et al. Organization and function. *Mol Biol Cell*. (2010) 21:12.

45. Van Goethem E, Guiet R, Balor S, Charrière GM, Poincloux R, Labrousse A, et al. Macrophage podosomes go 3D. *Eur J Cell Biol*. (2011) 90:224–36. doi: 10.1016/j.ejcb.2010.07.011
46. Eddy RJ, Weidmann MD, Sharma VP, Condeelis JS. Tumor cell invadopodia: invasive protrusions that orchestrate metastasis. *Trends Cell Biol*. (2017) 27:595–607. doi: 10.1016/j.tcb.2017.03.003
47. Theocharis AD, Manou D, Karamanos NK. The extracellular matrix as a multitasking player in disease. *FEBS J*. (2019) 286:2830–69. doi: 10.1111/febs.14818
48. Wyckoff JB, Wang Y, Lin EY, Li J -f, Goswami S, Stanley ER, et al. Direct visualization of macrophage-assisted tumor cell intravasation in mammary tumors. *Cancer Res*. (2007) 67:2649–56. doi: 10.1158/0008-5472.CAN-06-1823
49. Glentis A, Oertle P, Mariani P, Chikina A, El Marjou F, Attieh Y, et al. Cancer-associated fibroblasts induce metalloprotease-independent cancer cell invasion of the basement membrane. *Nat Commun*. (2017) 8:924. doi: 10.1038/s41467-017-00985-8
50. Carter KP, Hanna S, Genna A, Lewis D, Segall JE, Cox D. Macrophages enhance 3D invasion in a breast cancer cell line by induction of tumor cell tunneling nanotubes. *Cancer Rep*. (2019) 2:e1213. doi: 10.1002/cnr2.1213
51. Henriet E, Sala M, Abou Hammoud A, Tuariihionoa A, Di Martino J, Ros M, et al. Multitasking discoidin domain receptors are involved in several and specific hallmarks of cancer. *Cell Adh Migr*. (2018) 12:363–77. doi: 10.1080/19336918.2018.1465156
52. Chen C, Zhao S, Karnad A, Freeman JW. The biology and role of CD44 in cancer progression: therapeutic implications. *J Hematol Oncol*. (2018) 11:64. doi: 10.1186/s13045-018-0605-5
53. Desgrosellier JS, Cheresh DA. Integrins in cancer: biological implications and therapeutic opportunities. *Nat Rev Cancer*. (2010) 10:9–22. doi: 10.1038/nrc2748
54. Kinugasa Y, Matsui T, Takakura N. CD44 expressed on cancer-associated fibroblasts is a functional molecule supporting the stemness and drug resistance of malignant cancer cells in the tumor microenvironment. *Stem Cells*. (2014) 32:145–56. doi: 10.1002/stem.1556
55. Toole BP. The CD147-HYALURONAN axis in cancer. *Anat Rec*. (2019) 303:1573–83. doi: 10.1002/ar.24147
56. Shu X, Liu H, Pan Y, Sun L, Yu L, Sun L, et al. Distinct biological characterization of the CD44 and CD90 phenotypes of cancer stem cells in gastric cancer cell lines. *Mol Cell Biochem*. (2019) 459:35–47. doi: 10.1007/s11010-019-03548-1
57. Mohamed HT, Gadalla R, El-Husseiny N, Hassan H, Wang Z, Ibrahim SA, et al. Inflammatory breast cancer: activation of the aryl hydrocarbon receptor and its target CYP1B1 correlates closely with Wnt5a/b-β-catenin signalling, the stem cell phenotype and disease progression. *J Adv Res*. (2019) 16:75–86. doi: 10.1016/j.jare.2018.11.006
58. Morand GB, Morand GB, Ikenberg K, Vital DG, Cardona I, Moch H, et al. Preoperative assessment of CD44-mediated depth of invasion as predictor of occult metastases in early oral squamous cell carcinoma. *Head Neck*. (2018) 41:950–8. doi: 10.1002/hed.25532
59. Heino J. Cellular signaling by collagen-binding integrins. *Adv Exp Med Biol*. (2014) 819:143–55. doi: 10.1007/978-94-017-9153-3_10
60. Zhu C-Q, Popova SN, Brown ERS, Barsyte-Lovejoy D, Navab R, Shih W, et al. Integrin alpha 11 regulates IGF2 expression in fibroblasts to enhance tumorigenicity of human non-small-cell lung cancer cells. *Proc Natl Acad Sci USA*. (2007) 104:11754–9. doi: 10.1073/pnas.0703040104
61. Navab R, Strumpf D, To C, Pasko E, Kim KS, Park CJ, et al. Integrin α11β1 regulates cancer stromal stiffness and promotes tumorigenicity and metastasis in non-small cell lung cancer. *Oncogene*. (2016) 35:1899–908. doi: 10.1038/onc.2015.254
62. Parajuli H, Teh M-T, Abrahamsen S, Christoffersen I, Neppelberg E, Lybak S, et al. Integrin α11 is overexpressed by tumour stroma of head and neck squamous cell carcinoma and correlates positively with alpha smooth muscle actin expression. *J Oral Pathol Med*. (2017) 46:267–75. doi: 10.1111/jop.12493
63. Zeltz C, Primac I, Erusappan P, Alam J, Noel A, Gullberg D. Cancer-associated fibroblasts in desmoplastic tumors: emerging role of integrins. *Semin Cancer Biol*. (2019) 62:166–81. doi: 10.1016/j.semcancer.2019.08.004
64. Leitinger B. Discoidin domain receptor functions in physiological and pathological conditions. *Int Rev Cell Mol Biol*. (2014) 310:39–87. doi: 10.1016/B978-0-12-800180-6.00002-5
65. Leitinger B. Molecular analysis of collagen binding by the human discoidin domain receptors, DDR1 and DDR2. Identification of collagen binding sites in DDR2. *J Biol Chem*. (2003) 278:16761–9. doi: 10.1074/jbc.M301370200
66. Shrivastava A, Radziejewski C, Campbell E, Kovac L, McGlynn M, Ryan TE, et al. An orphan receptor tyrosine kinase family whose members serve as nonintegrin collagen receptors. *Mol Cell*. (1997) 1:25–34. doi: 10.1016/s1097-2765(00)80004-0
67. Vogel W, Gish GD, Alves F, Pawson T. The discoidin domain receptor tyrosine kinases are activated by collagen. *Mol Cell*. (1997) 1:13–23. doi: 10.1016/s1097-2765(00)80003-9
68. Jin H, Ham I-H, Oh HJ, Bae CA, Lee D, Kim Y-B, et al. Inhibition of discoidin domain receptor 1 prevents stroma-induced peritoneal metastasis in gastric carcinoma. *Mol Cancer Res*. (2018) 16:1590–600. doi: 10.1158/1541-7786.MCR-17-0710
69. Lundell BI, McCarthy JB, Kovach NL, Verfaillie CM. Activation of beta1 integrins on CML progenitors reveals cooperation between beta1 integrins and CD44 in the regulation of adhesion and proliferation. *Leukemia*. (1997) 11:822–9. doi: 10.1038/sj.leu.2400653
70. Katagiri YU, Sleeman J, Fujii H, Herrlich P, Hotta H, Tanaka K, et al. CD44 variants but not CD44s cooperate with beta1-containing integrins to permit cells to bind to osteopontin independently of arginine-glycine-aspartic acid, thereby stimulating cell motility and chemotaxis. *Cancer Res*. (1999) 59:219–26.
71. Hansen RK, Bissell MJ. Tissue architecture and breast cancer: the role of extracellular matrix and steroid hormones. *Endocr Relat Cancer*. (2000) 7:95–113.
72. Cichon MA, Degnim AC, Visscher DW, Radisky DC. Microenvironmental influences that drive progression from benign breast disease to invasive breast cancer. *J Mammary Gland Biol Neoplasia*. (2010) 15:389–97. doi: 10.1007/s10911-010-9195-8
73. Testa U, Castelli G, Pelosi E. Breast cancer: a molecularly heterogenous disease needing subtype-specific treatments. *Med Sci*. (2020) 8:18. doi: 10.3390/medsci8010018
74. Allinen M, Beroukhim R, Cai L, Brennan C, Lahti-Domenici J, Huang H, et al. Molecular characterization of the tumor microenvironment in breast cancer. *Cancer Cell*. (2004) 6:17–32. doi: 10.1016/j.ccr.2004.06.010
75. Insua-Rodríguez J, Oskarsson T. The extracellular matrix in breast cancer. *Adv Drug Deliv Rev*. (2016) 97:41–55. doi: 10.1016/j.addr.2015.12.017
76. Oskarsson T. Extracellular matrix components in breast cancer progression and metastasis. *Breast*. (2013) 22:S66–72. doi: 10.1016/j.breast.2013.07.012
77. Lu P, Takai K, Weaver VM, Werb Z. Extracellular matrix degradation and remodeling in development and disease. *Cold Spring Harb Perspect Biol*. (2011) 3:a005058–005058. doi: 10.1101/cshperspect.a005058
78. Schedin P, O'Brien J, Rudolph M, Stein T, Borges V. Microenvironment of the involuting mammary gland mediates mammary cancer progression. *J Mammary Gland Biol Neoplasia*. (2007) 12:71–82. doi: 10.1007/s10911-007-9039-3
79. Schedin P. Pregnancy-associated breast cancer and metastasis. *Nat Rev Cancer*. (2006) 6:281–91. doi: 10.1038/nrc1839
80. Levental KR, Yu H, Kass L, Lakins JN, Egeblad M, Erler JT, et al. Matrix crosslinking forces tumor progression by enhancing integrin signaling. *Cell*. (2009) 139:891–906. doi: 10.1016/j.cell.2009.10.027
81. Provenzano PP, Inman DR, Eliceiri KW, Knittel JG, Yan L, Rueden CT, et al. Collagen density promotes mammary tumor initiation and progression. *BMC Med*. (2008) 6:11. doi: 10.1186/1741-7015-6-11
82. Kadler KE, Hill A, Canty-Laird EG. Collagen fibrillogenesis: fibronectin, integrins, and minor collagens as organizers and nucleators. *Curr Opin Cell Biol*. (2008) 20:495–501. doi: 10.1016/j.ceb.2008.06.008
83. Fernandez-Garcia B, Eiró N, Marín L, González-Reyes S, González LO, Lamelas ML, et al. Expression and prognostic significance of fibronectin and matrix metalloproteases in breast cancer metastasis. *Histopathology*. (2014) 64:512–22. doi: 10.1111/his.12300
84. Bae YK, Kim A, Kim MK, Choi JE, Kang SH, Lee SJ. Fibronectin expression in carcinoma cells correlates with tumor aggressiveness and poor clinical

outcome in patients with invasive breast cancer. *Hum Pathol*. (2013) 44:2028–37. doi: 10.1016/j.humpath.2013.03.006
85. Kischel P, Waltregny D, Dumont B, Turtoi A, Greffe Y, Kirsch S, et al. Versican overexpression in human breast cancer lesions: known and new isoforms for stromal tumor targeting. *Int J Cancer*. (2010) 126:640–50. doi: 10.1002/ijc.24812
86. Auvinen P, Rilla K, Tumelius R, Tammi M, Sironen R, Soini Y, et al. Hyaluronan synthases (HAS1-3) in stromal and malignant cells correlate with breast cancer grade and predict patient survival. *Breast Cancer Res Treat*. (2014) 143:277–86. doi: 10.1007/s10549-013-2804-7
87. Karousou E, D'Angelo ML, Kouvidi K, Vigetti D, Viola M, Nikitovic D, et al. Collagen VI and hyaluronan: the common role in breast cancer. *Biomed Res Int*. (2014) 2014:606458. doi: 10.1155/2014/606458
88. Zhang Y, Zou X, Qian W, Weng X, Zhang L, Zhang L, et al. Enhanced PAPSS2/VCAN sulfation axis is essential for Snail-mediated breast cancer cell migration and metastasis. *Cell Death Differ*. (2019) 26:565–79. doi: 10.1038/s41418-018-0147-y
89. Du WW, Fang L, Yang X, Sheng W, Yang BL, Seth A, et al. The role of versican in modulating breast cancer cell self-renewal. *Mol Cancer Res*. (2013) 11:443–55. doi: 10.1158/1541-7786.MCR-12-0461
90. Chong HC, Tan CK, Huang R-L, Tan NS. Matricellular proteins: a sticky affair with cancers. *J Oncol*. (2012) 2012:351089. doi: 10.1155/2012/351089
91. Kirschmann DA, Seftor EA, Fong SFT, Nieva DRC, Sullivan CM, Edwards EM, et al. A molecular role for lysyl oxidase in breast cancer invasion. *Cancer Res*. (2002) 62:4478–83.
92. Chu IM, Michalowski AM, Hoenerhoff M, Szauter KM, Luger D, Sato M, et al. GATA3 inhibits lysyl oxidase-mediated metastases of human basal triple-negative breast cancer cells. *Oncogene*. (2012) 31:2017–27. doi: 10.1038/onc.2011.382
93. Yousef EM, Tahir MR, St-Pierre Y, Gaboury LA. MMP-9 expression varies according to molecular subtypes of breast cancer. *BMC Cancer*. (2014) 14:609. doi: 10.1186/1471-2407-14-609
94. Khamis ZI, Sahab ZJ, Sang Q-XA. Active roles of tumor stroma in breast cancer metastasis. *Int J Breast Cancer*. (2012) 2012:1–10. doi: 10.1155/2012/574025
95. Soysal SD, Tzankov A, Muenst SE. Role of the tumor microenvironment in breast cancer. *Pathobiology*. (2015) 82:142–52. doi: 10.1159/000430499
96. Pandey PR, Saidou J, Watabe K. Role of myoepithelial cells in breast tumor progression. *Front Biosci*. (2010) 15:226–36. doi: 10.2741/3617
97. Jones JL, Shaw JA, Pringle JH, Walker RA. Primary breast myoepithelial cells exert an invasion-suppressor effect on breast cancer cells via paracrine down-regulation of MMP expression in fibroblasts and tumour cells. *J Pathol*. (2003) 201:562–72. doi: 10.1002/path.1483
98. Barsky SH. Myoepithelial mRNA expression profiling reveals a common tumor-suppressor phenotype. *Exp Mol Pathol*. (2003) 74:113–22. doi: 10.1016/s0014-4800(03)00011-x
99. Nguyen M, Lee MC, Wang JL, Tomlinson JS, Shao ZM, Alpaugh ML, et al. The human myoepithelial cell displays a multifaceted anti-angiogenic phenotype. *Oncogene*. (2000) 19:3449–59. doi: 10.1038/sj.onc.1203677
100. Gudjonsson T, Rønnov-Jessen L, Villadsen R, Rank F, Bissell MJ, Petersen OW. Normal and tumor-derived myoepithelial cells differ in their ability to interact with luminal breast epithelial cells for polarity and basement membrane deposition. *J Cell Sci*. (2002) 115:39–50.
101. Sternlicht MD, Safarians S, Rivera SP, Barsky SH. Characterizations of the extracellular matrix and proteinase inhibitor content of human myoepithelial tumors. *Lab Invest*. (1996) 74:781–96.
102. Folgueira MAAK, Maistro S, Katayama MLH, Roela RA, Mundim FGL, Nanogaki S, et al. Markers of breast cancer stromal fibroblasts in the primary tumour site associated with lymph node metastasis: a systematic review including our case series. *Biosci Rep*. (2013) 33:e00085. doi: 10.1042/BSR20130060
103. Santi A, Kugeratski FG, Zanivan S. Cancer associated fibroblasts: the architects of stroma remodeling. *Proteomics*. (2018) 18:1700167. doi: 10.1002/pmic.201700167
104. Neill T, Schaefer L, Iozzo RV. Decorin: a guardian from the matrix. *Am J Pathol*. (2012) 181:380–7. doi: 10.1016/j.ajpath.2012.04.029
105. Oda G, Sato T, Ishikawa T, Kawachi H, Nakagawa T, Kuwayama T, et al. Significance of stromal decorin expression during the progression of breast cancer. *Oncol Rep*. (2012) 28:2003–8. doi: 10.3892/or.2012.2040
106. Santra M, Eichstetter I, Iozzo RV. An anti-oncogenic role for decorin. Down-regulation of ErbB2 leads to growth suppression and cytodifferentiation of mammary carcinoma cells. *J Biol Chem*. (2000) 275:35153–61. doi: 10.1074/jbc.M006821200
107. Goldoni S, Seidler DG, Heath J, Fassan M, Baffa R, Thakur ML, et al. An antimetastatic role for decorin in breast cancer. *Am J Pathol*. (2008) 173:844–55. doi: 10.2353/ajpath.2008.080275
108. Araki K, Wakabayashi H, Shintani K, Morikawa J, Matsumine A, Kusuzaki K, et al. Decorin suppresses bone metastasis in a breast cancer cell line. *Oncology*. (2009) 77:92–9. doi: 10.1159/000228253
109. Solinas G, Germano G, Mantovani A, Allavena P. Tumor-associated macrophages (TAM) as major players of the cancer-related inflammation. *J Leukoc Biol*. (2009) 86:1065–73. doi: 10.1189/jlb.0609385
110. Biswas SK, Allavena P, Mantovani A. Tumor-associated macrophages: functional diversity, clinical significance, and open questions. *Semin Immunopathol*. (2013) 35:585–600. doi: 10.1007/s00281-013-0367-7
111. Jiang X, Shapiro DJ. The immune system and inflammation in breast cancer. *Mol Cell Endocrinol*. (2014) 382:673–82. doi: 10.1016/j.mce.2013.06.003
112. Hu M, Yao J, Carroll DK, Weremowicz S, Chen H, Carrasco D, et al. Regulation of in situ to invasive breast carcinoma transition. *Cancer Cell*. (2008) 13:394–406. doi: 10.1016/j.ccr.2008.03.007
113. Zhang H, Brown RL, Wei Y, Zhao P, Liu S, Liu X, et al. CD44 splice isoform switching determines breast cancer stem cell state. *Genes Dev*. (2019) 33:166–79. doi: 10.1101/gad.319889.118
114. Al-Othman N, Alhendi A, Ihbaisha M, Barahmeh M, Alqaraleh M, Al-Momany BZ. Role of CD44 in breast cancer. *Breast Dis*. (2020) 39:1–13. doi: 10.3233/BD-190409
115. White DE, Muller WJ. Multifaceted roles of integrins in breast cancer metastasis. *J Mammary Gland Biol Neoplasia*. (2007) 12:135–42. doi: 10.1007/s10911-007-9045-5
116. Peláez R, Pariente A, Pérez-Sala Á, Larrayoz IM. Integrins: moonlighting proteins in invadosome formation. *Cancers*. (2019) 11:615. doi: 10.3390/cancers11050615
117. Primac I, Maquoi E, Blacher S, Heljasvaara R, Van Deun J, Smeland HY, et al. Stromal integrin α11 regulates PDGFR-β signaling and promotes breast cancer progression. *J Clin Invest*. (2019) 130:4609–28. doi: 10.1172/JCI125890
118. Corsa CAS, Brenot A, Grither WR, Van Hove S, Loza AJ, Zhang K, et al. The action of discoidin domain receptor 2 in basal tumor cells and stromal cancer-associated fibroblasts is critical for breast cancer metastasis. *Cell Rep*. (2016) 15:2510–23. doi: 10.1016/j.celrep.2016.05.033
119. Park J, Schwarzbauer JE. Mammary epithelial cell interactions with fibronectin stimulate epithelial-mesenchymal transition. *Oncogene*. (2014) 33:1649–57. doi: 10.1038/onc.2013.118
120. Balanis N, Wendt MK, Schiemann BJ, Wang Z, Schiemann WP, Carlin CR. Epithelial to mesenchymal transition promotes breast cancer progression via a fibronectin-dependent STAT3 signaling pathway. *J Biol Chem*. (2013) 288:17954–67. doi: 10.1074/jbc.M113.475277
121. Zahir N, Lakins JN, Russell A, Ming W, Chatterjee C, Rozenberg GI, et al. Autocrine laminin-5 ligates alpha6beta4 integrin and activates RAC and NFkappaB to mediate anchorage-independent survival of mammary tumors. *J Cell Biol*. (2003) 163:1397–407. doi: 10.1083/jcb.200302023
122. Carpenter PM, Dao AV, Arain ZS, Chang MK, Nguyen HP, Arain S, et al. Motility induction in breast carcinoma by mammary epithelial laminin 332 (laminin 5). *Mol Cancer Res*. (2009) 7:462–75. doi: 10.1158/1541-7786.MCR-08-0148
123. Kusuma N, Denoyer D, Eble JA, Redvers RP, Parker BS, Pelzer R, et al. Integrin-dependent response to laminin-511 regulates breast tumor cell invasion and metastasis. *Int J Cancer*. (2012) 130:555–66. doi: 10.1002/ijc.26018
124. Yee AJM, Akens M, Yang BL, Finkelstein J, Zheng P-S, Deng Z, et al. The effect of versican G3 domain on local breast cancer invasiveness and bony metastasis. *Breast Cancer Res*. (2007) 9:R47. doi: 10.1186/bcr1751
125. Dos Reis DC, Damasceno KA, de Campos CB, Veloso ES, Pêgas GRA, Kraemer LR, et al. Versican and tumor-associated macrophages promotes tumor progression and metastasis in canine and murine models of breast carcinoma. *Front Oncol*. (2019) 9:577. doi: 10.3389/fonc.2019.00577
126. Provenzano PP, Inman DR, Eliceiri KW, Keely PJ. Matrix density-induced mechanoregulation of breast cell phenotype, signaling and gene expression

through a FAK-ERK linkage. *Oncogene*. (2009) 28:4326–43. doi: 10.1038/onc.2009.299
127. Cordenonsi M, Zanconato F, Azzolin L, Forcato M, Rosato A, Frasson C, et al. The hippo transducer TAZ confers cancer stem cell-related traits on breast cancer cells. *Cell*. (2011) 147:759–72. doi: 10.1016/j.cell.2011.09.048
128. Parekh A, Ruppender NS, Branch KM, Sewell-Loftin MK, Lin J, Boyer PD, et al. Sensing and modulation of invadopodia across a wide range of rigidities. *Biophys J*. (2011) 100:573–82. doi: 10.1016/j.bpj.2010.12.3733
129. Duffy MJ, Maguire TM, Hill A, McDermott E, O'Higgins N. Metalloproteinases: role in breast carcinogenesis, invasion and metastasis. *Breast Cancer Res*. (2000) 2:252–7. doi: 10.1186/bcr65
130. Merdad A, Karim S, Schulten H-J, Dallol A, Buhmeida A, Al-Thubaity F, et al. Expression of matrix metalloproteinases (MMPs) in primary human breast cancer: MMP-9 as a potential biomarker for cancer invasion and metastasis. *Anticancer Res*. (2014) 34:1355–66.
131. Cohen I, Pappo O, Elkin M, San T, Bar-Shavit R, Hazan R, et al. Heparanase promotes growth, angiogenesis and survival of primary breast tumors. *Int J Cancer*. (2006) 118:1609–17. doi: 10.1002/ijc.21552
132. Boyango I, Barash U, Naroditsky I, Li J-P, Hammond E, Ilan N, et al. Heparanase cooperates with Ras to drive breast and skin tumorigenesis. *Cancer Res*. (2014) 74:4504–14. doi: 10.1158/0008-5472.CAN-13-2962
133. Gawthorpe S, Brown JE, Arif M, Nightingale P, Nevill A, Carmichael AR. Heparanase and COX-2 expression as predictors of lymph node metastasis in large, high-grade breast tumors. *Anticancer Res*. (2014) 34:2797–800.
134. Zcharia E, Metzger S, Chajek-Shaul T, Friedmann Y, Pappo O, Aviv A, et al. Molecular properties and involvement of heparanase in cancer progression and mammary gland morphogenesis. *J Mammary Gland Biol Neoplasia*. (2001) 6:311–22. doi: 10.1023/a:1011375624902
135. Vasiljeva O, Korovin M, Gajda M, Brodoefel H, Bojic L, Krüger A, et al. Reduced tumour cell proliferation and delayed development of high-grade mammary carcinomas in cathepsin B-deficient mice. *Oncogene*. (2008) 27:4191–9. doi: 10.1038/onc.2008.59
136. Duong LT, Wesolowski GA, Leung P, Oballa R, Pickarski M. Efficacy of a cathepsin K inhibitor in a preclinical model for prevention and treatment of breast cancer bone metastasis. *Mol Cancer Ther*. (2014) 13:2898–909. doi: 10.1158/1535-7163.MCT-14-0253
137. Kietzmann T. Metabolic zonation of the liver: the oxygen gradient revisited. *Redox Biol*. (2017) 11:622–30. doi: 10.1016/j.redox.2017.01.012
138. Baiocchini A, Montaldo C, Conigliaro A, Grimaldi A, Correani V, Mura F, et al. Extracellular matrix molecular remodeling in human liver fibrosis evolution. *PLoS One*. (2016) 11:e0151736. doi: 10.1371/journal.pone.0151736
139. Bray F, Ferlay J, Soerjomataram I, Siegel RL, Torre LA, Jemal A. Global cancer statistics 2018: GLOBOCAN estimates of incidence and mortality worldwide for 36 cancers in 185 countries. *CA Cancer J Clin*. (2018) 68:394–424. doi: 10.3322/caac.21492
140. Tanaka Y, Tateishi R, Koike K. Proteoglycans are attractive biomarkers and therapeutic targets in hepatocellular carcinoma. *Int J Mol Sci*. (2018) 19:3070. doi: 10.3390/ijms19103070
141. Ng IO, Lai EC, Ng MM, Fan ST. Tumor encapsulation in hepatocellular carcinoma. A pathologic study of 189 cases. *Cancer*. (1992) 70:45–9.
142. Iguchi T, Aishima S, Sanefuji K, Fujita N, Sugimachi K, Gion T, et al. Both fibrous capsule formation and extracapsular penetration are powerful predictors of poor survival in human hepatocellular carcinoma: a histological assessment of 365 patients in Japan. *Ann Surg Oncol*. (2009) 16:2539–46. doi: 10.1245/s10434-009-0453-1
143. Arnaoutakis DJ, Mavros MN, Shen F, Alexandrescu S, Firoozmand A, Popescu I, et al. Recurrence patterns and prognostic factors in patients with hepatocellular carcinoma in noncirrhotic liver: a multi-institutional analysis. *Ann Surg Oncol*. (2014) 21:147–54. doi: 10.1245/s10434-013-3211-3
144. Torimura T, Ueno T, Inuzuka S, Tanaka M, Abe H, Tanikawa K. Mechanism of fibrous capsule formation surrounding hepatocellular carcinoma. Immunohistochemical study. *Arch Pathol Lab Med*. (1991) 115:365–71.
145. Ishizaki M, Ashida K, Higashi T, Nakatsukasa H, Kaneyoshi T, Fujiwara K, et al. The formation of capsule and septum in human hepatocellular carcinoma. *Virchows Arch*. (2001) 438:574–80. doi: 10.1007/s004280000391
146. Kubo N, Araki K, Kuwano H, Shirabe K. Cancer-associated fibroblasts in hepatocellular carcinoma. *World J Gastroenterol*. (2016) 22:6841–50. doi: 10.3748/wjg.v22.i30.6841
147. Tahmasebi Birgani M, Carloni V. Tumor microenvironment, a paradigm in hepatocellular carcinoma progression and therapy. *Int J Mol Sci*. (2017) 18:405. doi: 10.3390/ijms18020405
148. Arrese M, Hernandez A, Astete L, Estrada L, Cabello-Verrugio C, Cabrera D. TGF-β and hepatocellular carcinoma: when a friend becomes an enemy. *Curr Protein Pept Sci*. (2018) 19:1172–9. doi: 10.2174/1389203718666171117112619
149. Wong CC, Tse AP, Huang YP, Zhu YT, Chiu DK, Lai RK, et al. Lysyl oxidase-like 2 is critical to tumor microenvironment and metastatic niche formation in hepatocellular carcinoma. *Hepatology*. (2014) 60:1645–58. doi: 10.1002/hep.27320
150. Dong Y, Zheng Q, Wang Z, Lin X, You Y, Wu S, et al. Higher matrix stiffness as an independent initiator triggers epithelial-mesenchymal transition and facilitates HCC metastasis. *J Hematol Oncol*. (2019) 12:112.
151. Chakraborty S, Lakshmanan M, Swa HLF, Chen J, Zhang X, Ong YS, et al. An oncogenic role of Agrin in regulating focal adhesion integrity in hepatocellular carcinoma. *Nat Commun*. (2015) 6:6184. doi: 10.1038/ncomms7184
152. Govaere O, Komuta M, Berkers J, Spee B, Janssen C, de Luca F, et al. Keratin 19: a key role player in the invasion of human hepatocellular carcinomas. *Gut*. (2014) 63:674–85. doi: 10.1136/gutjnl-2012-304351
153. Lin L, Yang X-M, Li J, Zhang Y-L, Qin W, Zhang Z-G. Microfilament regulatory protein MENA increases activity of RhoA and promotes metastasis of hepatocellular carcinoma. *Exp Cell Res*. (2014) 327:113–22. doi: 10.1016/j.yexcr.2014.05.010
154. Kai AK-L, Chan LK, Lo RC-L, Lee JM-F, Wong CC-L, Wong JC-M, et al. Down-regulation of TIMP2 by HIF-1α/miR-210/HIF-3α regulatory feedback circuit enhances cancer metastasis in hepatocellular carcinoma. *Hepatology*. (2016) 64:473–87. doi: 10.1002/hep.28577
155. Ezzoukhry Z, Henriet E, Piquet L, Boyé K, Bioulac-Sage P, Balabaud C, et al. TGF-β1 promotes linear invadosome formation in hepatocellular carcinoma cells, through DDR1 up-regulation and collagen I cross-linking. *Eur J Cell Biol*. (2016) 95:503–12. doi: 10.1016/j.ejcb.2016.09.003
156. Zhang H, Ozaki I, Mizuta T, Yoshimura T, Matsuhashi S, Eguchi Y, et al. Transforming growth factor-beta 1-induced apoptosis is blocked by beta 1-integrin-mediated mitogen-activated protein kinase activation in human hepatoma cells. *Cancer Sci*. (2004) 95:878–86. doi: 10.1111/j.1349-7006.2004.tb02197.x
157. Dhar D, Antonucci L, Nakagawa H, Kim JY, Glitzner E, Caruso S, et al. Liver cancer initiation requires p53 inhibition by CD44-enhanced growth factor signaling. *Cancer Cell*. (2018) 33:1061–77.e6. doi: 10.1016/j.ccell.2018.05.003
158. Park HS, Kim KR, Lee HJ, Choi HN, Kim DK, Kim BT, et al. Overexpression of discoidin domain receptor 1 increases the migration and invasion of hepatocellular carcinoma cells in association with matrix metalloproteinase. *Oncol Rep*. (2007) 18:1435–41.
159. Xie B, Lin W, Ye J, Wang X, Zhang B, Xiong S, et al. DDR2 facilitates hepatocellular carcinoma invasion and metastasis via activating ERK signaling and stabilizing SNAIL1. *J Exp Clin Cancer Res*. (2015) 34:101. doi: 10.1186/s13046-015-0218-6
160. Jiang F-X, Naselli G, Harrison LC. Distinct distribution of laminin and its integrin receptors in the pancreas. *J Histochem Cytochem*. (2002) 50:1625–32. doi: 10.1177/002215540205001206
161. Otonkoski T, Banerjee M, Korsgren O, Thornell L-E, Virtanen I. Unique basement membrane structure of human pancreatic islets: implications for beta-cell growth and differentiation. *Diabetes Obes Metab*. (2008) 10(Suppl. 4):119–27. doi: 10.1111/j.1463-1326.2008.00955.x
162. Bogdani M, Johnson PY, Potter-Perigo S, Nagy N, Day AJ, Bollyky PL, et al. Hyaluronan and hyaluronan-binding proteins accumulate in both human type 1 diabetic islets and lymphoid tissues and associate with inflammatory cells in insulitis. *Diabetes*. (2014) 63:2727–43. doi: 10.2337/db13-1658
163. Sherman MH. Stellate cells in tissue repair, inflammation, and cancer. *Annu Rev Cell Dev Biol*. (2018) 34:333–55. doi: 10.1146/annurev-cellbio-100617-062855
164. Apte MV, Pirola RC, Wilson JS. Pancreatic stellate cells: a starring role in normal and diseased pancreas. *Front Physiol*. (2012) 3:344. doi: 10.3389/fphys.2012.00344

165. Apte MV, Haber PS, Darby SJ, Rodgers SC, McCaughan GW, Korsten MA, et al. Pancreatic stellate cells are activated by proinflammatory cytokines: implications for pancreatic fibrogenesis. *Gut*. (1999) 44:534–41.
166. Bachem MG, Schneider E, Gross H, Weidenbach H, Schmid RM, Menke A, et al. Identification, culture, and characterization of pancreatic stellate cells in rats and humans. *Gastroenterology*. (1998) 115:421–32. doi: 10.1016/s0016-5085(98)70209-4
167. Feig C, Gopinathan A, Neesse A, Chan DS, Cook N, Tuveson DA. The pancreas cancer microenvironment. *Clin Cancer Res*. (2012) 18:4266–76. doi: 10.1158/1078-0432.CCR-11-3114
168. Apte MV, Park S, Phillips PA, Santucci N, Goldstein D, Kumar RK, et al. Desmoplastic reaction in pancreatic cancer: role of pancreatic stellate cells. *Pancreas*. (2004) 29:179–87.
169. Chu GC, Kimmelman AC, Hezel AF, DePinho RA. Stromal biology of pancreatic cancer. *J Cell Biochem*. (2007) 101:887–907. doi: 10.1002/jcb.21209
170. Korc M. Pancreatic cancer associated stroma production. *Am J Surg*. (2007) 194:s84–6. doi: 10.1016/j.amjsurg.2007.05.004
171. Imamura T, Iguchi H, Manabe T, Ohshio G, Yoshimura T, Wang ZH, et al. Quantitative analysis of collagen and collagen subtypes I, III, and V in human pancreatic cancer, tumor-associated chronic pancreatitis, and alcoholic chronic pancreatitis. *Pancreas*. (1995) 11:357–64. doi: 10.1097/00006676-199511000-00007
172. Mollenhauer J, Roether I, Kern HF. Distribution of extracellular matrix proteins in pancreatic ductal adenocarcinoma and its influence on tumor cell proliferation in vitro. *Pancreas*. (1987) 2:14–24. doi: 10.1097/00006676-198701000-00003
173. Linder S, Castaños-Velez E, von Rosen A, Biberfeld P. Immunohistochemical expression of extracellular matrix proteins and adhesion molecules in pancreatic carcinoma. *Hepatogastroenterology*. (2001) 48:1321–7.
174. Clementz AG, Mutolo MJ, Leir S-H, Morris KJ, Kucybala K, Harris H, et al. Collagen XV inhibits epithelial to mesenchymal transition in pancreatic adenocarcinoma cells. *PLoS One*. (2013) 8:e72250. doi: 10.1371/journal.pone.0072250
175. Weber CK, Sommer G, Michl P, Fensterer H, Weimer M, Gansauge F, et al. Biglycan is overexpressed in pancreatic cancer and induces G1-arrest in pancreatic cancer cell lines. *Gastroenterology*. (2001) 121:657–67. doi: 10.1053/gast.2001.27222
176. Li X, Kang Y, Roife D, Lee Y, Pratt M, Perez MR, et al. Prolonged exposure to extracellular lumican restrains pancreatic adenocarcinoma growth. *Oncogene*. (2017) 36:5432–8. doi: 10.1038/onc.2017.125
177. Bailey JM, Swanson BJ, Hamada T, Eggers JP, Singh PK, Caffery T, et al. Sonic hedgehog promotes desmoplasia in pancreatic cancer. *Clin Cancer Res*. (2008) 14:5995–6004. doi: 10.1158/1078-0432.CCR-08-0291
178. Löhr M, Schmidt C, Ringel J, Kluth M, Müller P, Nizze H, et al. Transforming growth factor-beta1 induces desmoplasia in an experimental model of human pancreatic carcinoma. *Cancer Res*. (2001) 61:550–5.
179. Wilson JS, Pirola RC, Apte MV. Stars and stripes in pancreatic cancer: role of stellate cells and stroma in cancer progression. *Front Physiol*. (2014) 5:52. doi: 10.3389/fphys.2014.00052
180. Apte MV, Wilson JS, Lugea A, Pandol SJ. A starring role for stellate cells in the pancreatic cancer microenvironment. *Gastroenterology*. (2013) 144:1210–9. doi: 10.1053/j.gastro.2012.11.037
181. Rice AJ, Cortes E, Lachowski D, Cheung BCH, Karim SA, Morton JP, et al. Matrix stiffness induces epithelial-mesenchymal transition and promotes chemoresistance in pancreatic cancer cells. *Oncogenesis*. (2017) 6:e352. doi: 10.1038/oncsis.2017.54
182. Haage A, Schneider IC. Cellular contractility and extracellular matrix stiffness regulate matrix metalloproteinase activity in pancreatic cancer cells. *FASEB J*. (2014) 28:3589–99. doi: 10.1096/fj.13-245613
183. Miller BW, Morton JP, Pinese M, Saturno G, Jamieson NB, McGhee E, et al. Targeting the LOX/hypoxia axis reverses many of the features that make pancreatic cancer deadly: inhibition of LOX abrogates metastasis and enhances drug efficacy. *EMBO Mol Med*. (2015) 7:1063–76. doi: 10.15252/emmm.201404827
184. Lee J, Condello S, Yakubov B, Emerson R, Caperell-Grant A, Hitomi K, et al. Tissue transglutaminase mediated tumor-stroma interaction promotes pancreatic cancer progression. *Clin Cancer Res*. (2015) 21:4482–93. doi: 10.1158/1078-0432.CCR-15-0226
185. Hotary KB, Allen ED, Brooks PC, Datta NS, Long MW, Weiss SJ. Membrane type I matrix metalloproteinase usurps tumor growth control imposed by the three-dimensional extracellular matrix. *Cell*. (2003) 114:33–45. doi: 10.1016/s0092-8674(03)00513-0
186. Rath N, Morton JP, Julian L, Helbig L, Kadir S, McGhee EJ, et al. ROCK signaling promotes collagen remodeling to facilitate invasive pancreatic ductal adenocarcinoma tumor cell growth. *EMBO Mol Med*. (2017) 9:198–218. doi: 10.15252/emmm.201606743
187. van der Zee JA, van Eijck CHJ, Hop WCJ, Biermann K, Dicheva BM, Seynhaeve ALB, et al. Tumour basement membrane laminin expression predicts outcome following curative resection of pancreatic head cancer. *Br J Cancer*. (2012) 107:1153–8.
188. Ohlund D, Lundin C, Ardnor B, Oman M, Naredi P, Sund M. Type IV collagen is a tumour stroma-derived biomarker for pancreas cancer. *Br J Cancer*. (2009) 101:91–7. doi: 10.1038/sj.bjc.6605107
189. Yao H, Zeng Z-Z, Fay KS, Veine DM, Staszewski ED, Morgan M, et al. Role of α(5)β(1) Integrin Up-regulation in radiation-induced invasion by human pancreatic cancer cells. *Transl Oncol*. (2011) 4:282–92. doi: 10.1593/tlo.11133
190. Miyamoto H, Murakami T, Tsuchida K, Sugino H, Miyake H, Tashiro S. Tumor-stroma interaction of human pancreatic cancer: acquired resistance to anticancer drugs and proliferation regulation is dependent on extracellular matrix proteins. *Pancreas*. (2004) 28:38–44. doi: 10.1097/00006676-200401000-00006
191. Edderkaoui M, Hong P, Vaquero EC, Lee JK, Fischer L, Friess H, et al. Extracellular matrix stimulates reactive oxygen species production and increases pancreatic cancer cell survival through 5-lipoxygenase and NADPH oxidase. *Am J Physiol Gastrointest Liver Physiol*. (2005) 289:G1137–47. doi: 10.1152/ajpgi.00197.2005
192. Dallas SL, Sivakumar P, Jones CJP, Chen Q, Peters DM, Mosher DF, et al. Fibronectin regulates latent transforming growth factor-beta (TGF beta) by controlling matrix assembly of latent TGF beta-binding protein-1. *J Biol Chem*. (2005) 280:18871–80. doi: 10.1074/jbc.M410762200
193. Ryschich E, Khamidjanov A, Kerkadze V, Büchler MW, Zöller M, Schmidt J. Promotion of tumor cell migration by extracellular matrix proteins in human pancreatic cancer. *Pancreas*. (2009) 38:804–10. doi: 10.1097/MPA.0b013e3181b9dfda
194. Qazi BS, Tang K, Qazi A. Recent advances in underlying pathologies provide insight into interleukin-8 expression-mediated inflammation and angiogenesis. *Int J Inflam*. (2011) 2011:908468. doi: 10.4061/2011/908468
195. Shi Q, Abbruzzese JL, Huang S, Fidler IJ, Xiong Q, Xie K. Constitutive and inducible interleukin 8 expression by hypoxia and acidosis renders human pancreatic cancer cells more tumorigenic and metastatic. *Clin Cancer Res*. (1999) 5:3711–21.
196. Kleeff J, Ishiwata T, Kumbasar A, Friess H, Büchler MW, Lander AD, et al. The cell-surface heparan sulfate proteoglycan glypican-1 regulates growth factor action in pancreatic carcinoma cells and is overexpressed in human pancreatic cancer. *J Clin Invest*. (1998) 102:1662–73. doi: 10.1172/JCI4105
197. Veenstra VL, Damhofer H, Waasdorp C, Steins A, Kocher HM, Medema JP, et al. Stromal SPOCK1 supports invasive pancreatic cancer growth. *Mol Oncol*. (2017) 11:1050–64. doi: 10.1002/1878-0261.12073
198. Abetamann V, Kern HF, Elsässer HP. Differential expression of the hyaluronan receptors CD44 and RHAMM in human pancreatic cancer cells. *Clin Cancer Res*. (1996) 2:1607–18.
199. Öhlund D, Franklin O, Lundberg E, Lundin C, Sund M. Type IV collagen stimulates pancreatic cancer cell proliferation, migration, and inhibits apoptosis through an autocrine loop. *BMC Cancer*. (2013) 13:154. doi: 10.1186/1471-2407-13-154
200. Begum A, Ewachiw T, Jung C, Huang A, Norberg KJ, Marchionni L, et al. The extracellular matrix and focal adhesion kinase signaling regulate cancer stem cell function in pancreatic ductal adenocarcinoma. *PLoS One*. (2017) 12:e0180181. doi: 10.1371/journal.pone.0180181
201. Koenig A, Mueller C, Hasel C, Adler G, Menke A. Collagen type I induces disruption of E-cadherin-mediated cell-cell contacts and promotes proliferation of pancreatic carcinoma cells. *Cancer Res*. (2006) 66:4662–71. doi: 10.1158/0008-5472.CAN-05-2804
202. Shintani Y, Fukumoto Y, Chaika N, Svoboda R, Wheelock MJ, Johnson KR. Collagen I-mediated up-regulation of N-cadherin requires cooperative signals from integrins and discoidin domain receptor 1. *J Cell Biol*. (2008) 180:1277–89. doi: 10.1083/jcb.200708137

203. Huang H, Svoboda RA, Lazenby AJ, Saowapa J, Chaika N, Ding K, et al. Up-regulation of N-cadherin by Collagen I-activated discoidin domain receptor 1 in pancreatic cancer requires the adaptor molecule Shc1. *J Biol Chem*. (2016) 291:23208–23. doi: 10.1074/jbc.M116.740605
204. Yang J-C, Zhang Y, He S-J, Li M-M, Cai X-L, Wang H, et al. TM4SF1 promotes metastasis of pancreatic cancer via regulating the expression of DDR1. *Sci Rep*. (2017) 7:45895. doi: 10.1038/srep45895
205. Gao H, Chakraborty G, Zhang Z, Akalay I, Gadiya M, Gao Y, et al. Multi-organ site metastatic reactivation mediated by non-canonical discoidin domain receptor 1 signaling. *Cell*. (2016) 166:47–62. doi: 10.1016/j.cell.2016.06.009
206. Goicoechea SM, García-Mata R, Staub J, Valdivia A, Sharek L, McCulloch CG, et al. Palladin promotes invasion of pancreatic cancer cells by enhancing invadopodia formation in cancer-associated fibroblasts. *Oncogene*. (2014) 33:1265–73. doi: 10.1038/onc.2013.68
207. Cao H, Eppinga RD, Razidlo GL, Krueger EW, Chen J, Qiang L, et al. Stromal fibroblasts facilitate cancer cell invasion by a novel invadopodia-independent matrix degradation process. *Oncogene*. (2016) 35:1099–110. doi: 10.1038/onc.2015.163
208. Xu Z, Vonlaufen A, Phillips PA, Fiala-Beer E, Zhang X, Yang L, et al. Role of pancreatic stellate cells in pancreatic cancer metastasis. *Am J Pathol*. (2010) 177:2585–96. doi: 10.2353/ajpath.2010.090899
209. Bachem MG, Schünemann M, Ramadani M, Siech M, Beger H, Buck A, et al. Pancreatic carcinoma cells induce fibrosis by stimulating proliferation and matrix synthesis of stellate cells. *Gastroenterology*. (2005) 128:907–21. doi: 10.1053/j.gastro.2004.12.036
210. Simon-Assmann P, Simo P, Bouziges F, Haffen K, Kedinger M. Synthesis of basement membrane proteins in the small intestine. *Digestion*. (1990) 46(Suppl. 2):12–21. doi: 10.1159/000200362
211. Simon-Assmann P, Kedinger M, De Arcangelis A, Rousseau V, Simo P. Extracellular matrix components in intestinal development. *Experientia*. (1995) 51:883–900. doi: 10.1007/BF01921739
212. Worthley DL, Giraud AS, Wang TC. The extracellular matrix in digestive cancer. *Cancer Microenviron*. (2010) 3:177–85. doi: 10.1007/s12307-010-0053-4
213. Kunz-Schughart LA, Knuechel R. Tumor-associated fibroblasts (part II): Functional impact on tumor tissue. *Histol Histopathol*. (2002) 17:623–37. doi: 10.14670/HH-17.623
214. Coulson-Thomas VJ, Coulson-Thomas YM, Gesteira TF, de Paula CAA, Mader AM, Waisberg J, et al. Colorectal cancer desmoplastic reaction up-regulates collagen synthesis and restricts cancer cell invasion. *Cell Tissue Res*. (2011) 346:223–36. doi: 10.1007/s00441-011-1254-y
215. Caporale A, Vestri AR, Benvenuto E, Mariotti M, Cosenza UM, Scarpini M, et al. Is desmoplasia a protective factor for survival in patients with colorectal carcinoma? *Clin Gastroenterol Hepatol*. (2005) 3:370–5. doi: 10.1016/S1542-3565(04)00674-3
216. Guess CM, Lafleur BJ, Weidow BL, Quaranta V. A decreased ratio of laminin-332 beta3 to gamma2 subunit mRNA is associated with poor prognosis in colon cancer. *Cancer Epidemiol Biomarkers Prev*. (2009) 18:1584–90. doi: 10.1158/1055-9965.EPI-08-1027
217. Adur J, Bianchi M, Pelegati VB, Viale S, Izaguirre MF, Carvalho HF, et al. Colon adenocarcinoma diagnosis in human samples by multicontrast nonlinear optical microscopy of hematoxylin and eosin stained histological sections. *J Cancer Ther*. (2014) 5:1259–69. doi: 10.4236/jct.2014.513127
218. Birk JW, Tadros M, Moezardalan K, Nadyarnykh O, Forouhar F, Anderson J, et al. Second harmonic generation imaging distinguishes both high-grade dysplasia and cancer from normal colonic mucosa. *Dig Dis Sci*. (2014) 59:1529–34. doi: 10.1007/s10620-014-3121-7
219. Baker A-M, Bird D, Lang G, Cox TR, Erler JT. Lysyl oxidase enzymatic function increases stiffness to drive colorectal cancer progression through FAK. *Oncogene*. (2013) 32:1863–8. doi: 10.1038/onc.2012.202
220. Baker A-M, Cox TR, Bird D, Lang G, Murray GI, Sun X-F, et al. The role of lysyl oxidase in SRC-dependent proliferation and metastasis of colorectal cancer. *J Natl Cancer Inst*. (2011) 103:407–24. doi: 10.1093/jnci/djq569
221. Li Z-L, Wang Z-J, Wei G-H, Yang Y, Wang X-W. Changes in extracellular matrix in different stages of colorectal cancer and their effects on proliferation of cancer cells. *World J Gastrointest Oncol*. (2020) 12:267–75. doi: 10.4251/wjgo.v12.i3.267
222. Jeitany M, Leroy C, Tosti P, Lafitte M, Le Guet J, Simon V, et al. Inhibition of DDR1-BCR signalling by nilotinib as a new therapeutic strategy for metastatic colorectal cancer. *EMBO Mol Med*. (2018) 10:e7918. doi: 10.15252/emmm.201707918
223. Kurashige J, Hasegawa T, Niida A, Sugimachi K, Deng N, Mima K, et al. Integrated molecular profiling of human gastric cancer identifies DDR2 as a potential regulator of peritoneal dissemination. *Sci Rep*. (2016) 6:22371. doi: 10.1038/srep22371
224. Wu X, Cai J, Zuo Z, Li J. Collagen facilitates the colorectal cancer stemness and metastasis through an integrin/PI3K/AKT/Snail signaling pathway. *Biomed Pharmacother*. (2019) 114:108708. doi: 10.1016/j.biopha.2019.108708
225. Ma L, Dong L, Chang P. CD44v6 engages in colorectal cancer progression. *Cell Death Dis*. (2019) 10:30.
226. Zhang R, Qi F, Shao S, Li G, Feng Y. Human colorectal cancer-derived carcinoma associated fibroblasts promote CD44-mediated adhesion of colorectal cancer cells to endothelial cells by secretion of HGF. *Cancer Cell Int*. (2019) 19:192. doi: 10.1186/s12935-019-0914-y
227. Yang H-Y, Kwon J, Park H-R, Kwon S-O, Park Y-K, Kim H-S, et al. Comparative proteomic analysis for the insoluble fractions of colorectal cancer patients. *J Proteomics*. (2012) 75:3639–53. doi: 10.1016/j.jprot.2012.04.018
228. Said AH, Raufman J-P, Xie G. The role of matrix metalloproteinases in colorectal cancer. *Cancers*. (2014) 6:366–75. doi: 10.3390/cancers6010366
229. Kang J-C, Chen J-S, Lee C-H, Chang J-J, Shieh Y-S. Intratumoral macrophage counts correlate with tumor progression in colorectal cancer. *J Surg Oncol*. (2010) 102:242–8. doi: 10.1002/jso.21617
230. Naba A, Clauser KR, Whittaker CA, Carr SA, Tanabe KK, Hynes RO. Extracellular matrix signatures of human primary metastatic colon cancers and their metastases to liver. *BMC Cancer*. (2014) 14:518. doi: 10.1186/1471-2407-14-518
231. De Wever O, Demetter P, Mareel M, Bracke M. Stromal myofibroblasts are drivers of invasive cancer growth. *Int J Cancer*. (2008) 123:2229–38. doi: 10.1002/ijc.23925
232. De Wever O, Nguyen Q-D, Van Hoorde L, Bracke M, Bruyneel E, Gespach C, et al. Tenascin-C and SF/HGF produced by myofibroblasts in vitro provide convergent pro-invasive signals to human colon cancer cells through RhoA and Rac. *FASEB J*. (2004) 18:1016–8. doi: 10.1096/fj.03-1110fje
233. Gaggioli C, Hooper S, Hidalgo-Carcedo C, Grosse R, Marshall JF, Harrington K, et al. Fibroblast-led collective invasion of carcinoma cells with differing roles for RhoGTPases in leading and following cells. *Nat Cell Biol*. (2007) 9:1392–400. doi: 10.1038/ncb1658
234. Vitale S, Avizienyte E, Brunton VG, Frame MC. Focal adhesion kinase is not required for Src-induced formation of invadopodia in KM12C colon cancer cells and can interfere with their assembly. *Eur J Cell Biol*. (2008) 87:569–79. doi: 10.1016/j.ejcb.2008.04.002
235. Vishnubhotla R, Sun S, Huq J, Bulic M, Ramesh A, Guzman G, et al. ROCK-II mediates colon cancer invasion via regulation of MMP-2 and MMP-13 at the site of invadopodia as revealed by multiphoton imaging. *Lab Invest*. (2007) 87:1149–58. doi: 10.1038/labinvest.3700674
236. Gianni D, Taulet N, DerMardirossian C, Bokoch GM. c-Src–mediated phosphorylation of NoxA1 and Tks4 induces the reactive oxygen species (ROS)–dependent formation of functional invadopodia in human colon cancer cells. *Mol Biol Cell*. (2010) 21:4287–98. doi: 10.1091/mbc.E10-08-0685
237. Voorneveld PW, Kodach LL, Jacobs RJ, Liv N, Zonnevylle AC, Hoogenboom JP, et al. Loss of SMAD4 alters BMP signaling to promote colorectal cancer cell metastasis via activation of Rho and ROCK. *Gastroenterology*. (2014) 147:196–208.e13. doi: 10.1053/j.gastro.2014.03.052
238. Feifei W, Hui G, Ruiqiang Z, Qunxiang J, Yu'an X. MAGP2, a component of extracellular matrix, is upregulated in colorectal cancer and negatively modulated by miR-200b-3p. *Technol Cancer Res Treat*. (2019) 18:1533033819870777. doi: 10.1177/1533033819870777
239. Yuzhalin AE, Gordon-Weeks AN, Tognoli ML, Jones K, Markelc B, Konietzny R, et al. Colorectal cancer liver metastatic growth depends on PAD4-driven citrullination of the extracellular matrix. *Nat Commun*. (2018) 9:4783.

240. O'Dowd G, Woodford P, Young B. *Atlas D'histologie Fonctionnelle de Wheater*. De Boeck Supérieur. (2019). Available online at: https://www.deboecksuperieur.com/ouvrage/9782807300408-atlas-d-histologie-fonctionnelle-de-wheater (accessed August 11, 2019).
241. Breitkreutz D, Koxholt I, Thiemann K, Nischt R. Skin basement membrane: the foundation of epidermal integrity–BM functions and diverse roles of bridging molecules nidogen and perlecan. *BioMed Res Int*. (2013) 2013:e179784. doi: 10.1155/2013/179784
242. Krieg T, Aumailley M. The extracellular matrix of the dermis: flexible structures with dynamic functions. *Exp Dermatol*. (2011) 20:689–95. doi: 10.1111/j.1600-0625.2011.01313.x
243. Altmeyer P, Hoffmann K, el Gammal S, Hutchinson J. *Wound Healing and Skin Physiology*. Berlin: Springer Science & Business Media. (2012).
244. Albelda SM, Mette SA, Elder DE, Stewart R, Damjanovich L, Herlyn M, et al. Integrin distribution in malignant melanoma: association of the β3 subunit with tumor progression. *Cancer Res*. (1990) 50:6757–64.
245. Brooks PC, Strömblad S, Sanders LC, von Schalscha TL, Aimes RT, Stetler-Stevenson WG, et al. Localization of matrix metalloproteinase MMP-2 to the surface of invasive cells by interaction with integrin αvβ3. *Cell*. (1996) 85:683–93. doi: 10.1016/S0092-8674(00)81235-0
246. Petitclerc E, Strömblad S, von Schalscha TL, Mitjans F, Piulats J, Montgomery AM, et al. Integrin αVβ3 promotes M21 melanoma growth in human skin by regulating tumor cell survival. *Cancer Res*. (1999) 59:2724–30.
247. Haass NK, Herlyn M. Normal human melanocyte homeostasis as a paradigm for understanding melanoma. *J Investig Dermatol Symp Proc*. (2005) 10:153–63. doi: 10.1111/j.1087-0024.2005.200407.x
248. Le Bitoux M-A, Stamenkovic I. Tumor-host interactions: the role of inflammation. *Histochem Cell Biol*. (2008) 130:1079–90. doi: 10.1007/s00418-008-0527-3
249. Henriet P, Zhong ZD, Brooks PC, Weinberg KI, DeClerck YA. Contact with fibrillar collagen inhibits melanoma cell proliferation by up-regulating p27KIP1. *Proc Natl Acad Sci USA*. (2000) 97:10026–31. doi: 10.1073/pnas.170290997
250. Cornil I, Theodorescu D, Man S, Herlyn M, Jambrosic J, Kerbel RS. Fibroblast cell interactions with human melanoma cells affect tumor cell growth as a function of tumor progression. *Proc Natl Acad Sci USA*. (1991) 88:6028–32.
251. Lu C, Vickers MF, Kerbel RS. Interleukin 6: a fibroblast-derived growth inhibitor of human melanoma cells from early but not advanced stages of tumor progression. *Proc Natl Acad Sci USA*. (1992) 89:9215–9. doi: 10.1073/pnas.89.19.9215
252. Busse A, Keilholz U. Role of TGF-β in melanoma. *Curr Pharm Biotechnol*. (2011) 12:2165–75.
253. Flach EH, Rebecca VW, Herlyn M, Smalley KSM, Anderson ARA. Fibroblasts contribute to melanoma tumor growth and drug resistance. *Mol Pharm*. (2011) 8:2039–49. doi: 10.1021/mp200421k
254. Berking C, Takemoto R, Schaider H, Showe L, Satyamoorthy K, Robbins P, et al. Transforming growth factor-β1 increases survival of human melanoma through stroma remodeling. *Cancer Res*. (2001) 61:8306–16.
255. Godden JL, Edward M, MacKie RM. Melanoma cell-derived factor stimulation of fibroblast glycosaminoglycan synthesis–the role of platelet-derived growth factor. *Eur J Cancer*. (1999) 35:473–80. doi: 10.1016/s0959-8049(98)00406-7
256. Taddei ML, Giannoni E, Raugei G, Scacco S, Sardanelli AM, Papa S, et al. Mitochondrial oxidative stress due to complex I dysfunction promotes fibroblast activation and melanoma cell invasiveness. *J Signal Transduct*. (2012) 2012:684592. doi: 10.1155/2012/684592
257. Comito G, Giannoni E, Gennaro PD, Segura CP, Gerlini G, Chiarugi P. Stromal fibroblasts synergize with hypoxic oxidative stress to enhance melanoma aggressiveness. *Cancer Lett*. (2012) 324:31–41. doi: 10.1016/j.canlet.2012.04.025
258. Meierjohann S, Hufnagel A, Wende E, Kleinschmidt MA, Wolf K, Friedl P, et al. MMP13 mediates cell cycle progression in melanocytes and melanoma cells: in vitro studies of migration and proliferation. *Mol Cancer*. (2010) 9:201. doi: 10.1186/1476-4598-9-201
259. Ntayi C, Hornebeck W, Bernard P. Influence of cultured dermal fibroblasts on human melanoma cell proliferation, matrix metalloproteinase-2 (MMP-2) expression and invasion in vitro. *Arch Dermatol Res*. (2003) 295:236–41. doi: 10.1007/s00403-003-0429-0
260. Löffek S, Zigrino P, Angel P, Anwald B, Krieg T, Mauch C. High invasive melanoma cells induce matrix metalloproteinase-1 synthesis in fibroblasts by interleukin-1alpha and basic fibroblast growth factor-mediated mechanisms. *J Invest Dermatol*. (2005) 124:638–43. doi: 10.1111/j.0022-202X.2005.23629.x
261. Wandel E, Grasshoff A, Mittag M, Haustein UF, Saalbach A. Fibroblasts surrounding melanoma express elevated levels of matrix metalloproteinase-1 (MMP-1) and intercellular adhesion molecule-1 (ICAM-1) in vitro. *Exp Dermatol*. (2000) 9:34–41. doi: 10.1034/j.1600-0625.2000.009001034.x
262. Carlson MW, Alt-Holland A, Egles C, Garlick JA. Three-dimensional tissue models of normal and diseased skin. *Curr Protoc Cell Biol*. (2008) Chapter 19:Unit 19.9. doi: 10.1002/0471143030.cb1909s41
263. Huber MA, Schubert RD, Peter RU, Kraut N, Park JE, Rettig WJ, et al. Fibroblast activation protein: differential expression and serine protease activity in reactive stromal fibroblasts of melanocytic skin tumors. *J Investig Dermatol*. (2003) 120:182–8. doi: 10.1046/j.1523-1747.2003.12035.x
264. Faassen AE, Schrager JA, Klein DJ, Oegema TR, Couchman JR, McCarthy JB. A cell surface chondroitin sulfate proteoglycan, immunologically related to CD44, is involved in type I collagen-mediated melanoma cell motility and invasion. *J Cell Biol*. (1992) 116:521–31. doi: 10.1083/jcb.116.2.521
265. Seiter S, Schadendorf D, Herrmann K, Schneider M, Rösel M, Arch R, et al. Expression of CD44 variant isoforms in malignant melanoma. *Clin Cancer Res*. (1996) 2:447–56.
266. Girotti MR, Fernández M, López JA, Camafeita E, Fernández EA, Albar JP, et al. SPARC promotes cathepsin B-mediated melanoma invasiveness through a collagen I/α2β1 integrin axis. *J Invest Dermatol*. (2011) 131:2438–47. doi: 10.1038/jid.2011.239
267. Poudel B, Lee Y-M, Kim D-K. DDR2 inhibition reduces migration and invasion of murine metastatic melanoma cells by suppressing MMP2/9 expression through ERK/NF-κB pathway. *Acta Biochim Biophys Sin*. (2015) 47:292–8. doi: 10.1093/abbs/gmv005
268. Attieh Y, Clark AG, Grass C, Richon S, Pocard M, Mariani P, et al. Cancer-associated fibroblasts lead tumor invasion through integrin-β3–dependent fibronectin assembly. *J Cell Biol*. (2017) 216:3509–20. doi: 10.1083/jcb.201702033
269. Andrlová H, Mastroianni J, Madl J, Kern JS, Melchinger W, Dierbach H, et al. Biglycan expression in the melanoma microenvironment promotes invasiveness via increased tissue stiffness inducing integrin-β1 expression. *Oncotarget*. (2017) 8:42901–16. doi: 10.18632/oncotarget.17160
270. Girard CA, Lecacheur M, Ben Jouira R, Berestjuk I, Diazzi S, Prod'homme V, et al. A feed-forward mechanosignaling loop confers resistance to therapies targeting the MAPK pathway in BRAF-mutant melanoma. *Cancer Res*. (2020) 80:1927–41. doi: 10.1158/0008-5472.CAN-19-2914
271. Hirata E, Girotti MR, Viros A, Hooper S, Spencer-Dene B, Matsuda M, et al. Intravital imaging reveals how BRAF inhibition generates drug-tolerant microenvironments with high integrin β1/FAK signaling. *Cancer Cell*. (2015) 27:574–88. doi: 10.1016/j.ccell.2015.03.008
272. Mould AP, Askari JA, Craig SE, Garratt AN, Clements J, Humphries MJ. Integrin Alpha 4 Beta 1-mediated melanoma cell adhesion and migration on vascular cell adhesion molecule-1 (VCAM-1) and the alternatively spliced IIICS region of fibronectin. *J Biol Chem*. (1994) 269:27224–30.
273. Iizuka S, Abdullah C, Buschman MD, Diaz B, Courtneidge SA. The role of Tks adaptor proteins in invadopodia formation, growth and metastasis of melanoma. *Oncotarget*. (2016) 7:78473–86. doi: 10.18632/oncotarget.12954
274. Revach O-Y, Sandler O, Samuels Y, Geiger B. Cross-talk between receptor tyrosine kinases AXL and ERBB3 regulates invadopodia formation in melanoma cells. *Cancer Res*. (2019) 79:2634–48. doi: 10.1158/0008-5472.CAN-18-2316
275. Parapuram SK, Thompson K, Tsang M, Hutchenreuther J, Bekking C, Liu S, et al. Loss of PTEN expression by mouse fibroblasts results in lung fibrosis through a CCN2-dependent mechanism. *Matrix Biol*. (2015) 43:35–41. doi: 10.1016/j.matbio.2015.01.017
276. Hutchenreuther J, Vincent KM, Carter DE, Postovit L-M, Leask A. CCN2 expression by tumor stroma is required for melanoma metastasis. *J Invest Dermatol*. (2015) 135:2805–13. doi: 10.1038/jid.2015.279

277. O'Boyle G, Swidenbank I, Marshall H, Barker CE, Armstrong J, White SA, et al. Inhibition of CXCR4–CXCL12 chemotaxis in melanoma by AMD11070. *Br J Cancer*. (2013) 108:1634–40. doi: 10.1038/bjc.2013.124
278. Scala S, Giuliano P, Ascierto PA, Ieranò C, Franco R, Napolitano M, et al. Human melanoma metastases express functional CXCR4. *Clin Cancer Res*. (2006) 12:2427–33. doi: 10.1158/1078-0432.CCR-05-1940
279. McConnell AT, Ellis R, Pathy B, Plummer R, Lovat PE, O'Boyle G. The prognostic significance and impact of the CXCR4–CXCR7–CXCL12 axis in primary cutaneous melanoma. *Br J Dermatol*. (2016) 175:1210–20.
280. Gaggioli C, Deckert M, Robert G, Abbe P, Batoz M, Ehrengruber MU, et al. HGF induces fibronectin matrix synthesis in melanoma cells through MAP kinase-dependent signaling pathway and induction of Egr-1. *Oncogene*. (2005) 24:1423–33. doi: 10.1038/sj.onc.1208318
281. Gontier E, Cario-André M, Lepreux S, Vergnes P, Bizik J, Surlève-Bazeille J-E, et al. Dermal nevus cells from congenital nevi cannot penetrate the dermis in skin reconstructs. *Pigment Cell Res*. (2002) 15:41–8. doi: 10.1034/j.1600-0749.2002.00065.x
282. Sahai E, Astsaturov I, Cukierman E, DeNardo DG, Egeblad M, Evans RM, et al. A framework for advancing our understanding of cancer-associated fibroblasts. *Nat Rev Cancer*. (2020) 20:174–89.

Conflict of Interest: The authors declare that the research was conducted in the absence of any commercial or financial relationships that could be construed as a potential conflict of interest.

Copyright © 2020 Sala, Ros and Saltel. This is an open-access article distributed under the terms of the Creative Commons Attribution License (CC BY). The use, distribution or reproduction in other forums is permitted, provided the original author(s) and the copyright owner(s) are credited and that the original publication in this journal is cited, in accordance with accepted academic practice. No use, distribution or reproduction is permitted which does not comply with these terms.

frontiers in Oncology

ORIGINAL RESEARCH
published: 10 September 2020
doi: 10.3389/fonc.2020.01593

Type I Collagen Aging Increases Expression and Activation of EGFR and Induces Resistance to Erlotinib in Lung Carcinoma in 3D Matrix Model

Thomas Sarazin[1], *Guillaume Collin*[1], *Emilie Buache*[1], *Laurence Van Gulick*[1], *Céline Charpentier*[1], *Christine Terryn*[2], *Hamid Morjani*[1†] *and Charles Saby*[1*]

[1] Université de Reims Champagne-Ardenne, Unité BioSpecT, EA7506, SFR CAP-Santé, UFR de Pharmacie, Reims, France,
[2] Université de Reims Champagne Ardenne, Plate-forme Imagerie Cellulaire et Tissulaire (PICT), Reims, France

OPEN ACCESS

Edited by:
Simona Pisanti,
University of Salerno, Italy

Reviewed by:
Luigi Fattore,
Sapienza University, Italy
Eswari Dodagatta-Marri,
University of California, United States

***Correspondence:**
Charles Saby
charles.saby@univ-reims.fr

[†]These author have contributed equally to this work and share senior authorship

Specialty section:
This article was submitted to Molecular and Cellular Oncology, a section of the journal Frontiers in Oncology

Received: 05 March 2020
Accepted: 23 July 2020
Published: 10 September 2020

Citation:
Sarazin T, Collin G, Buache E, Van Gulick L, Charpentier C, Terryn C, Morjani H and Saby C (2020) Type I Collagen Aging Increases Expression and Activation of EGFR and Induces Resistance to Erlotinib in Lung Carcinoma in 3D Matrix Model. Front. Oncol. 10:1593. doi: 10.3389/fonc.2020.01593

Type I collagen is the major structural component of lung stroma. Because of its long half-life, type I collagen undergoes post-translational modifications such as glycation during aging process. These modifications have been shown to impact the structural organization of type I collagen fibers. In the present work we evaluated the impact of collagen aging on lung carcinoma cells response to erlotinib-induced cytotoxicity and apoptosis, and on Epidermal Growth Factor Receptor (EGFR) expression and phosphorylation. To this end, experiments were performed in 2D and 3D matrix models established from type I collagen extracted from adult (10 weeks-old) and old (100 weeks-old) rat's tail tendons. Our results show that old collagen induces a significant increase in EGFR expression and phosphorylation when compared to adult collagen in 3D matrix but not in 2D coating. Such modification was associated to an increase in the IC_{50} of erlotinib in the presence of old collagen and a lower sensitivity to drug-induced apoptosis. These data suggest that collagen aging confers resistance to the cytotoxic and apoptotic effects of therapies targeting EGFR kinase function in lung carcinoma. Moreover, our data underline the importance of the 3D matrix environment in this process.

Keywords: Type I collagen, aging, EGFR, Erlotinib, resistance

INTRODUCTION

Lung cancer is one of the leading causes of cancer-related death in the world (1, 2). Among causes responsible for developing lung cancer, cigarette smoking is the most recognized risk factor (3). Importantly, risk of developing lung cancer increases considerably with age, with a peak of incidence between 50 and 65 years old. There are different lung cancer subtypes. The most frequent histologic subtype is the adenocarcinoma (4). This subtype is composed of 40% of non-small-cell lung carcinoma (NSCLC). The principal treatment for such cancer is surgery followed by radiotherapy, chemotherapy, and targeted therapies against EGFR kinase function.

EGFR is amplified in about 80% of patients with NSCLC (5). EGFR mutations can lead to constitutive activation of signaling pathways such as PI3K/Akt/mTOR, which are involved in cancer cell survival. EGFR mutations have been shown to activate constitutively anti-apoptotic

signaling pathways, thus inducing a resistance to therapies targeting EGFR kinase domain such as erlotinib. Erlotinib has shown efficacy against mutated forms of the receptor that are constitutively active (exon 19 deletion and L858R mutation on exon 21). At the opposite, the mutation T790M, which can be acquired during erlotinib treatment is observed in 50% of patients presenting failure after treatment.

To understand the mechanisms of resistance to targeted therapies like erlotinib, it is important to decipher the relationship between cancer cells and their microenvironment. It is well-known that the extracellular matrix (ECM) plays a crucial role in the regulation of tumor progression (6). In fact, ECM modulates cell proliferation, cell migration, tumor invasion, and can also promote resistance to therapies (7). The major component of ECM in several organs is type I collagen. One particularity of type I collagen is that its structural organization plays an important role in the modulation of tumor behavior. It has been shown that modifications of collagen organization (8), but also degradation (9–11) and aging (12–14) can affect several cancer hallmarks.

During chronological aging, type I collagen undergoes non-enzymatic post-translational modifications such as glycation, that results in the formation of Advanced Glycation End-product (AGE) (15). These AGEs lead to an increase in collagen cross-links (16), which have an impact on structural organization of the matrix protein (17, 18). In fact, it has been shown that these cross-links increase type I collagen fibers straightness and rigidity, whereas it decreases fibers length and width. Our team have shown that collagen aging is able to induce an increase in cell proliferation in fibrosarcoma and epithelial-like breast carcinoma (13, 14). Such process was also able to protect epithelial-like breast carcinoma against collagen-induced apoptosis (10, 14).

More recently, Chang et al. have shown that an increase of type I collagen rigidity rendered NSCLC cells A549 more resistant to erlotinib (8). It is important to note that in this work, experiments have been carried out in 2D collagen coating. Here we propose to study the effect of age-related modifications of type I collagen on A549 and transformed bronchial BZR cells sensitivity to erlotinib, in a 2D coating and 3D matrix models. We demonstrated that collagen aging confers resistance to erlotinib only in 3D matrix models. Our data suggest that resistance acquisition is associated to an increase of EGFR expression and phosphorylation in A549 and BZR cells. Moreover, our data underline the importance of the 3D environment in this process.

MATERIALS AND METHODS

Cell Culture

The human lung carcinoma cell lines A549 (CCL-185) and the bronchial transformed cell line BZR (CRL-9483) were purchased from the American Type Culture Collection (ATCC). Both cell lines were cultured in DMEM (4,5 g/l glucose) with Glutamax I (PAN-Biotech, p04-04500) supplemented with 10% fetal bovine serum (Dominique Dutscher, S1810-500) and 1% penicillin-streptomycin (Invitrogen, 15140). Cultures were maintained at 37°C in a humidified atmosphere containing 5% CO2 (v/v). Cells were routinely passaged at preconfluency using 0.05% trypsin, 0.53 mM EDTA (Invitrogen, 25300) and screened for the absence of mycoplasma using PCR methods.

Preparation and Characterization of Type I Collagen

Fibrillar native type I collagen was extracted from tail tendons of 10 weeks old (adult) and 100 weeks old (old) rats and prepared as already described (19). The animal procedure was approved by the local ethics committee in animal experimentation of Reims Champagne-Ardenne (C2EA, registration 56, France) and the experiments were performed in accordance with European directive 2010/63/UE. Briefly, type I collagen was extracted from tail tendons of Wistar rats (Janvier) using 0.5M acetic acid at 4°C, in the presence of protease inhibitors. Then type I collagen was specifically precipitated with NaCl 0.7M, and centrifuged. The precipitate was then re-suspended in 18 mM acetic acid, and salts used during the precipitation step were eliminated by dialysis against distilled water for 1 week at 4°C. Finally, the collagen was characterized as described in our previous work, before use (13, 14).

2D and 3D Cell Culture

2D and 3D cell culture experiments were performed in 24-well plates. For 2D cell cultures, each well was coated with 5 $\mu g/cm^2$ of adult or old collagens solubilized in 0.018 M acetic acid. Coated substrates were dried overnight at room temperature under sterile conditions and rinsed twice in cold PBS (Invitrogen) before cell plating. For 3D cell culture, cells were resuspended in 100 µl fetal bovine serum and mixed with a solution containing 100 µl of 10× culture medium DMEM (Gibco, 52100), 100 µl $NaHCO_3$ (0.44 M), 100 µl H_2O, 90 µl NaOH 0.1 M, 10 µl glutamine 200 mM, and 500 µl collagen 3 mg/mL. Then, 1 mL/well of this solution was deposited in 24-well-plates, and gels were polymerized at 37°C during 30 min. Finally, 1 mL of complete culture medium was added on top of each gels and the plates were incubated at 37°C. To count the cells at the end of the experiment, the covering medium was removed, and cell populated gels were digested with collagenase P (2 mg/mL—Roche, 11213873001). Viability and cellular density of this suspension were determined by phase contrast microscopy using Kova® Glasstic® Slides (Kova International Inc, 87144). In some experiments, cells were treated with EGFR pharmacological inhibitors erlotinib (Selleckchem, No.OSI-744), at 18 µM.

Laser Scanning Microscopy

Images were acquired with a laser scanning microscope LSM 710 NLO (Carl ZEISS SAS, Marly le roi, France) coupled with CHAMELEON femtosecond Titanium-Sapphire Laser (Coherent, USA) and managed with ZEN Software (Carl ZEISS SAS, Marly le roi, France) with 40x (ON: 1) objective lens. Excitation wavelength of Calcein (Invitrogen, C3100) was 488 nm Argon ion laser line, and fluorescence emission was collected using 500–560 nm bandpass filter. Second Harmonic Generation (SHG) signal was collected with 420–440 nm bandpass filter with excitation from femtosecond laser at 860 nm.

Image Analysis

Visualization of A549 cells cultured on 2D coating of type I collagen was performed using ImageJ software (U.S. National Institutes of Health, Bethesda, MD). For the visualization of A549 cells in 3D matrices of type I collagen, 3D image reconstruction was processed with Imaris software (Bitplane, UK), using Z stack from samples (Z step:0.5 μm).

EGFR Inhibition

Cell viability assay was assessed in 24-well-plates. For 2D and 3D cell cultures, 1.5×10^4 cells (A549) or 3×10^4 cells (BZR) were seeded in each well, in culture medium containing 2% fetal bovine serum. After 24 h, culture medium was replaced with fresh medium containing erlotinib, to obtain final concentration of (0; 1; 2.5; 10; 25; 100 μM)/well. After 72 h, cells were harvested and counted using phase contrast microscopy, and IC_{50} was determined for each condition.

Quantification of Apoptosis

Cells were cultured in type I collagen 3D matrices supplemented with 2% fetal bovine serum. After 36 h, 1×10^5 cells were harvested for each condition using collagenase P at 2 mg/mL, washed twice with PBS and tested for three parameters: Annexin V positive cells using Muse® Annexin V and Dead Cell Assay Kit (Millipore, MCH100105), reactive oxygen species using Muse® Oxydative Stress Kit (Millipore, MCH100111) and caspase 3 and 7 activity using Muse® Caspase-3/7 Assay Kit (Millipore, MCH100108), all according to the manufacturer's instructions.

Western Blotting

Cells were seeded at a density of 100×10^3 cellules/mL in adult and old type I collagen 3D matrices, with 2% fetal bovine serum. After 96 h, cells were harvested using collagenase P at 2 mg/mL, washed twice with PBS, and lysed with RadioImmuno Precipitation Assay (RIPA) buffer (Thermo Fisher Scientific, 89900), supplemented with Halt™ Protease and Phosphatase Inhibitor Cocktail 1× (Thermo Scientific, 78442). Cell lysates were sonicated and clarified by centrifugation at 14,000 × g at 4°C for 15 min. Then, total protein content was estimated by bicinchoninic acid (BCA) assay method (Thermo Scientific, 23227), and proteins were separated by SDS-PAGE and transferred to a nitrocellulose membrane. Membranes were blocked with Tris Buffered Saline (TBS) (0.02 M Tris-HCl, 0.137 M NaCl, pH 7.6) containing 0.1% Tween (TBS-T) and 5% Bovine Serum Albumin (BSA) at room temperature during 1 h and incubated overnight at 4°C with anti-EGFR (Cell signaling Technology, #2232) or anti-GAPDH antibodies (Cell signaling Technology, #5174). Membranes were washed with TBS-T and incubated with peroxidase conjugated anti-rabbit secondary antibody (Cell signaling Technology, #7074) at room temperature for 1 h. Chemiluminescent detection was performed by using an ECL Prime Kit (GE Healthcare, RPN2236). Electrophoretic images were analyzed with ImageJ software.

EGFR Activation

Cells were serum deprived for 10 h, then harvested and seeded at a density of 100×10^3 cellules/mL in 3D matrices of adult and old type I collagen, in presence of 2% of fetal bovine serum. After 24 h, culture medium was replaced with new medium containing 15 μM of erlotinib or DMSO for the control condition. After 72 h of treatment, cells were harvested and washed two time in DPBS. pEGFR/total EGFR ratio was determined using the Muse® EGFR-RTK activation dual detection kit Dead Cell Assay Kit (Millipore, MCH200102), according to the manufacturer's instructions.

Statistical Analysis

Data are presented as mean ± standard error of the mean (SEM) from three independent experiments. Statistical significance was assessed with Student's *t*-test, or with one-way ANOVA, followed by Tukey's multiple comparison test. *p*-values <0.05

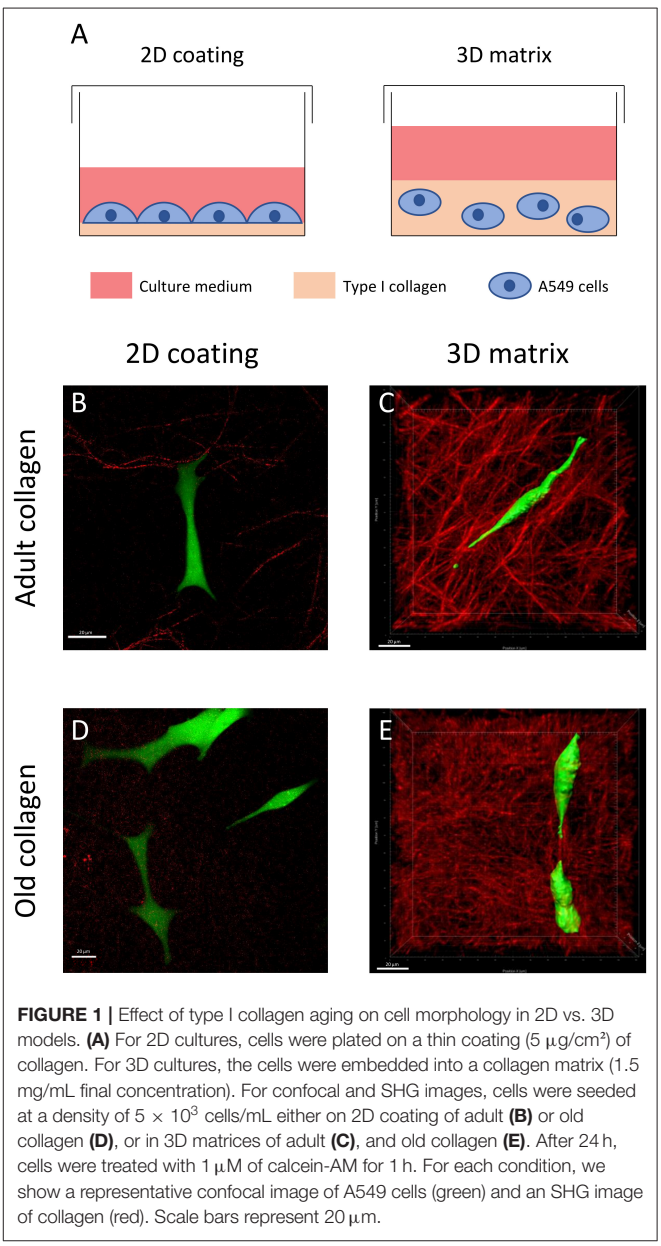

FIGURE 1 | Effect of type I collagen aging on cell morphology in 2D vs. 3D models. **(A)** For 2D cultures, cells were plated on a thin coating (5 μg/cm²) of collagen. For 3D cultures, the cells were embedded into a collagen matrix (1.5 mg/mL final concentration). For confocal and SHG images, cells were seeded at a density of 5×10^3 cells/mL either on 2D coating of adult **(B)** or old collagen **(D)**, or in 3D matrices of adult **(C)**, and old collagen **(E)**. After 24 h, cells were treated with 1 μM of calcein-AM for 1 h. For each condition, we show a representative confocal image of A549 cells (green) and an SHG image of collagen (red). Scale bars represent 20 μm.

were considered as significant ($^{*}p < 0.05$; $^{**}p < 0.01$; $^{***}p < 0.001$).

RESULTS

Collagen Aging Impacts Cell Morphology in 3D

As shown in **Figure 1**, we aimed to characterize morphology of A549 cells in adult and old type I collagen in 2D vs. 3D models. To this end, cells were plated on 2D coating or embedded in 3D type I collagen matrix for 24 h (**Figure 1A**). Type I collagen network was characterized by SHG, and images showed that adult type I collagen exhibited longer and thicker fibers than old collagen, both in 2D (**Figures 1B,D**) and 3D conditions (**Figures 1C,E**). Cell morphology was observed using confocal fluorescence microscopy. There were no significant changes in cell morphology between adult (**Figure 1B**) and old (**Figure 1D**) 2D type I collagen coating conditions. In fact, the cells exhibited in both conditions an epithelial morphology, with a large cytoplasm and several cytoplasmic protrusions. We then analyzed aged-related morphology changes in 3D matrix model. At the opposite of 2D collagen coating condition, cells cultured in 3D matrices exhibited an elongated form with less and longer protrusions (**Figures 1C,E**). Moreover, such prominent protrusions were aligned with the collagen fiber axis. Finally, when compared to 3D adult matrix (**Figure 1C**), A549 cells exhibited a less elongated form, but still with two prominent protrusions in 3D old matrix (**Figure 1E**).

Collagen Aging Promotes Lung Cancer Cells Resistance to Erlotinib

Chang et al. have shown that in a 2D collagen coating model, an increase of type I collagen rigidity rendered NSCLC cells A549 more resistant to erlotinib (8). Previous studies from our group have shown that age-related modifications of type I collagen were linked to an increase of its rigidity (17, 18), and could modulate tumor cells behavior when used in a more physiological 3D model. Since lung carcinoma cells are confronted to a collagen rich microenvironment, we decided to investigate the effect of collagen aging on the toxicity of erlotinib on A549 and BZR cells by determining the IC_{50} of erlotinib in adult and old collagen, for both cell lines. To this end, cells were treated with different concentrations of erlotinib on 2D collagen coating, and in 3D matrix models. Then, cell viability was assessed by phase contrast microscopy. **Figure 2A** shows that in 2D, the sensitivity of A549 cells (upper panel) and BZR cells (lower panel) to erlotinib was similar in both collagens, with respective erlotinib IC_{50} of 10 and 8 μM (**Figure 2C**). In 3D matrix model, old collagen was able to protect A549 cells (upper panel) and BZR cells (lower panel) against erlotinib cytotoxicity (**Figure 2B**). In fact, erlotinib IC_{50} was 18 μM in adult collagen and 26 μM in old collagen for A549 cells, and 15 μM in adult collagen and 21 μM in old

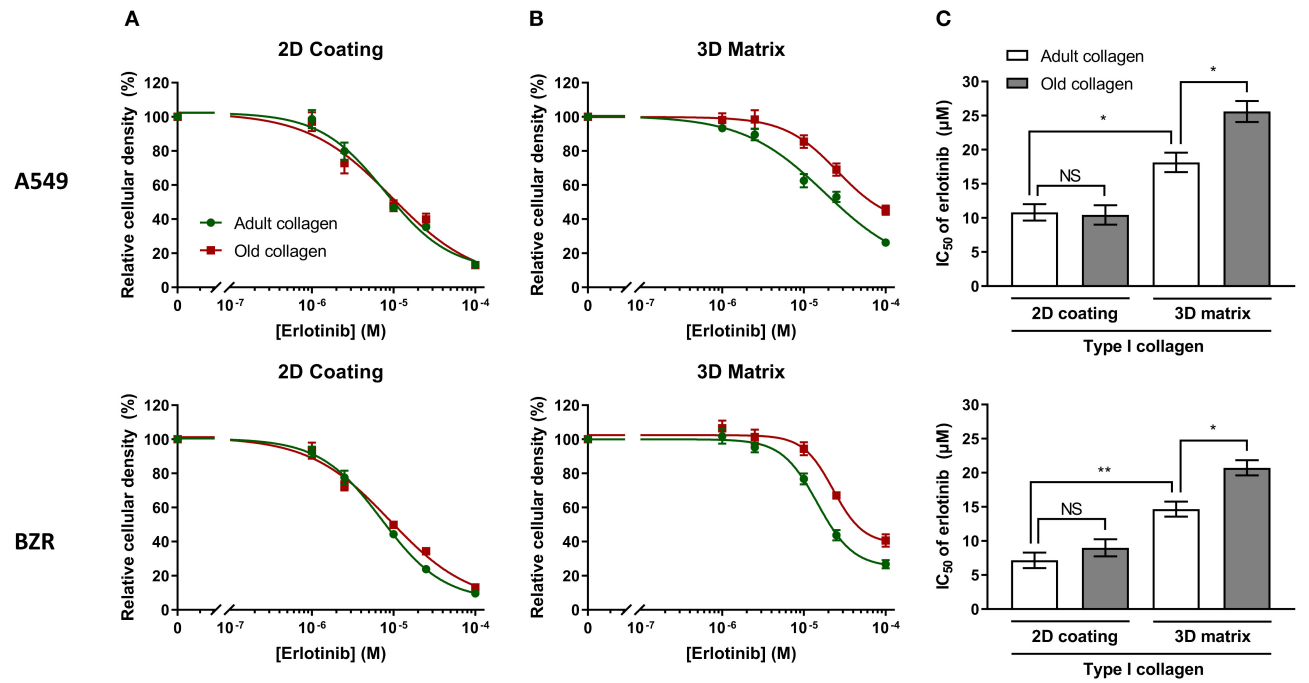

FIGURE 2 | Effect of collagen aging on erlotinib IC_{50}, in 2D vs. 3D models. A549 and BZR cell lines were seeded at a density of 1.5×10^4 cells/mL and 3×10^4 cells/mL, respectively. After 24 h, culture medium was replaced with fresh medium containing erlotinib, to obtain final concentration of (0; 1; 2.5; 10; 25; 100 μM)/well. After 72 h of culture with erlotinib, cells were harvested, and viable cell density was evaluated by phase contrast microscopy. The graphs represent erlotinib dose response curves of A549 cells (upper panel) and BZR cells (lower panel) cultured in adult and old collagen **(A)** in a 2D coating model or **(B)** in a 3D matrix model. **(C)** The histogram shows the IC_{50} of erlotinib for A549 cells (upper panel) and BZR cells (lower panel), cultured in adult vs. old collagen, in 2D vs. 3D model. Values represent the mean ± SEM ($^{*}p < 0.05$, $^{**}p < 0.01$, N.S = Not Significant).

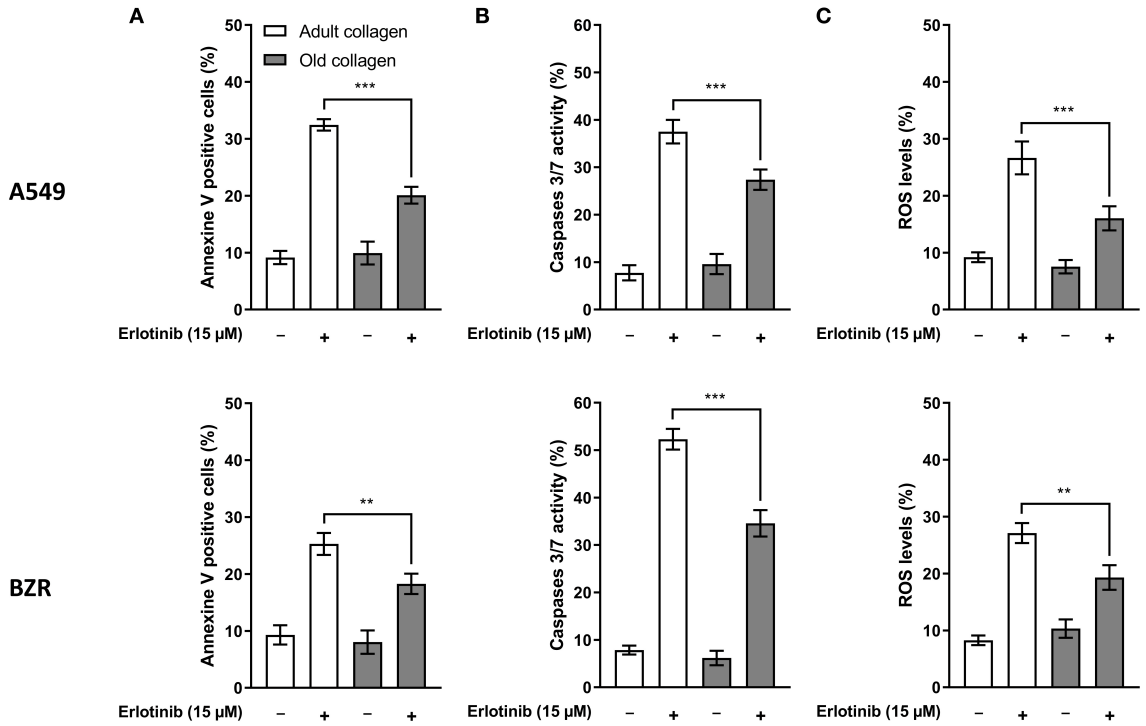

FIGURE 3 | Effect of collagen aging on erlotinib induced apoptosis in a 3D collagen model. A549 cells (upper panel) and BZR cells (lower panel) were cultured in adult and old type I collagen 3D matrices, with or without 15 µM of erlotinib. After 36 h, cells were harvested and tested for three parameters. **(A)** Annexin V positive cells, **(B)** caspase 3 and 7 activity, and **(C)** reactive oxygen species. Values represent the mean ± SEM (**$p < 0.01$, ***$p < 0.001$).

collagen for BZR cells (**Figure 2C**). We also evaluated cell growth for both cell lines in 2D and in 3D. A549 cells exhibit a higher cell growth rate in old collagen, when compared to the adult collagen in 3D but not in 2D, whereas BZR exhibit the same cell growth rate in both collagen and in both conditions (data not shown).

Collagen Aging Reduces Erlotinib Induced Apoptosis

A study from Shan et al. has shown that erlotinib was able to induce apoptosis in A549 cells (20). Here we decided to assess whether old collagen was able to decrease erlotinib-induced apoptosis in A549 and BZR cells. To this end, cells were cultured in 3D matrices of adult and old collagen in presence or not of erlotinib, and three apoptosis markers were quantified: (i) annexin V, (ii) caspases 3/7 activity, and (iii) the Reactive Oxygen Species level (ROS). As shown in **Figure 3A**, for both cell lines erlotinib induced an increase in the percentage of annexin V positive cells in both collagens, but the level observed in old collagen was significantly lower than that observed in adult collagen. In agreement with the annexin V data, **Figure 3B** shows that erlotinib induced an increase in caspase 3/7 activity in both collagens. The rate of caspase 3/7 positive cells was lower in old collagen when compared to adult collagen. Finally, **Figure 3C** shows that ROS level was increased in both collagens in the presence of erlotinib. However, the level observed in old collagen was lower than that observed in adult collagen. These data suggest that in a 3D matrix model, collagen aging protects A549, and BZR cells against erlotinib-induced apoptosis.

Collagen Aging Promotes EGFR Expression

The study reported by Chang et al. has shown that modification of collagen rigidity was able to increase EGFR expression level in A549 cells in a 2D model culture (8). Since changes occurring during collagen aging are also able to increase its rigidity (17, 18), we evaluated the effect of collagen aging on EGFR expression in A549 cells (**Figure 4A**) and in BZR cells (**Figure 4B**). While EGFR expression level was similar in both collagens in a 2D coating model, we show that in a 3D matrix model, EGFR expression level was increased by 1.5-fold for A549 and BZR, in old collagen when compared to the adult.

Collagen Aging Promotes EGFR Phosphorylation

EGFR phosphorylation level was analyzed in A549 and BZR cells cultured in 3D collagen matrix model. As shown in **Figure 5A**, EGFR phosphorylation level was 2-fold higher in old collagen than in adult collagen. However, in the presence of erlotinib, EGFR phosphorylation was significantly decreased in both collagens, but remains 2-fold higher in old collagen when compared to adult collagen. The same

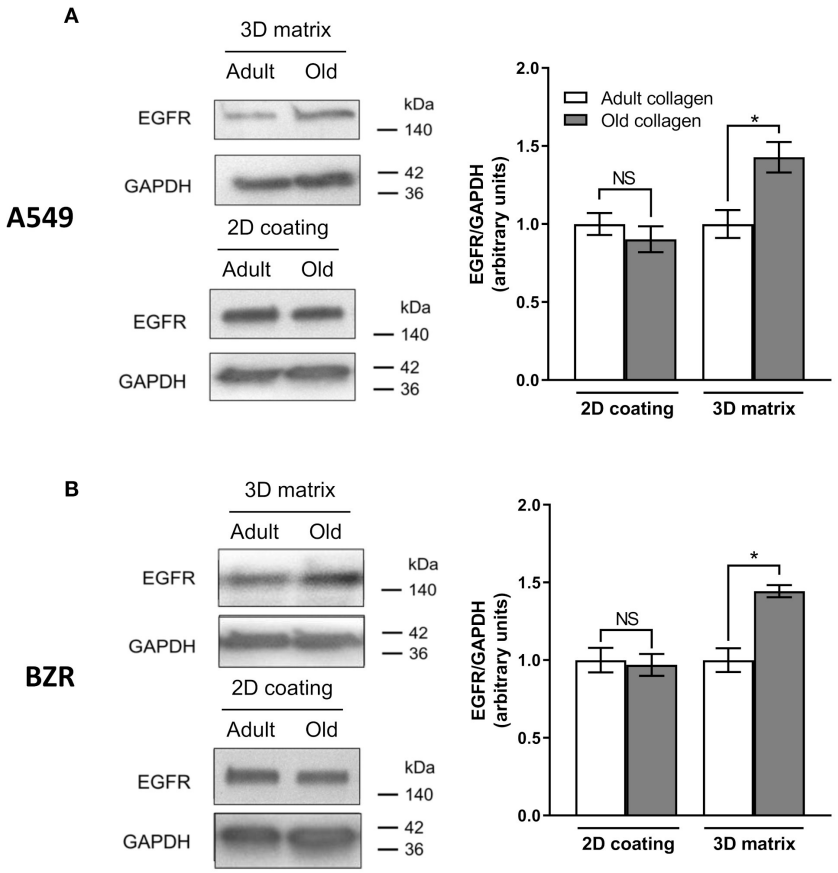

FIGURE 4 | Effect of collagen aging on EGFR expression. **(A)** A549 cells and **(B)** BZR cells were cultured 96 h in adult and old 3D collagen matrices (upper panel) and adult and old 2D collagen coatings (lower panel). Western blot analysis was performed using anti-EGFR specific antibody. GAPDH was used as a loading control. The histograms show the ratio of EGFR expression relative to GAPDH. Values represent the mean ± SEM (*$p < 0.05$, N.S = Not significant).

results were obtained for BZR cells (**Figure 5B**), with an EGFR phosphorylation level 1.5-fold higher in old collagen than in the adult one

DISCUSSION

In addition to EGFR amplification, NSCLC presenting EGFR mutations represent 10–15%. Exon 19 deletion and L858R mutations in exon 21 represent 85–90% of all mutations. Until recently, the best therapeutics for NSCLC presenting EGFR mutations were gefitinib, afatinib, and erlotinib (5). However, acquired resistance to those inhibitors are likely to occur within 10–12 months after the beginning of the treatment, mainly due to a second mutation T790M in exon 20. This mutation increases EGFR affinity for ATP and decreases treatment efficacy. New third generation inhibitors directed against this mutation have shown a better efficacy. It is the case for osimertinib, which was approved by FDA in 2016 (5). However, C797S mutation has been identified as a novel mechanism of resistance to osimertinib (21). Indeed, osimertinib has been described to bind to cysteine at position 797 of EGFR, which is replaced by serine after this secondary mutation.

Works from other groups have shown that tumor microenvironment was able to modulate sensitivity to targeted therapies and to induce drug resistance. This *de novo* resistance is called Environment-Mediated Drug Resistance (EMDR) and allow tumor cells to tolerate the effect of a therapy upon the first treatment (7). EMDR can be separated in two groups: EMDR due to soluble factors which is called Soluble Factor-Mediated Drug Resistance (SFM-DR), and EMDR due to adhesion process between the tumor cell receptors and extracellular matrix (ECM) proteins which is called Cell Adhesion-Mediated Drug Resistance (CAM-DR).

Type I collagen is the major constituent of ECM and can be found in several organs such as skin, breast, and lungs. Type I collagen plays an important role in tissues scaffolding but is also important in CAM-DR (7). In the context of lung carcinoma, Chang et al. have shown that artificial modification of type I collagen rigidity in a 2D coating model was able to increase the expression of EGFR in

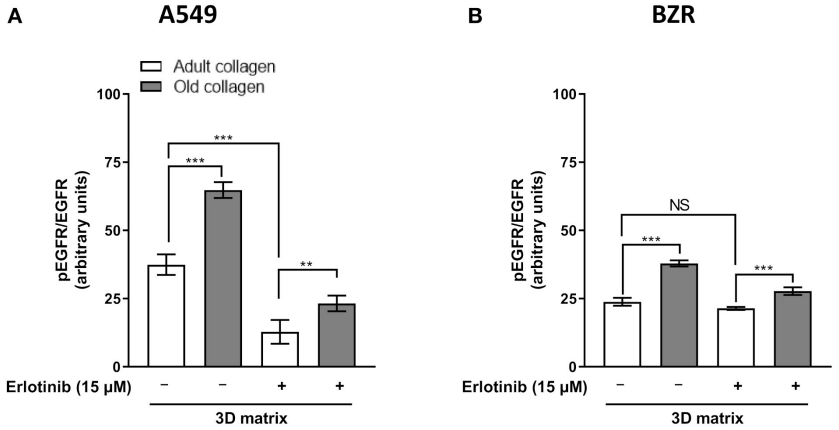

FIGURE 5 | Effect of collagen aging on EGFR activation. **(A)** A549 cells and **(B)**. BZR cells were seeded in adult and old type I collagen 3D matrices at a density of 10 × 10^4 cells/mL. After 24 h of culture, culture medium was replaced with medium containing erlotinib at a concentration of 15 µM or DMSO (vehicle), and 72 h later pEGFR/total EGFR ratio was assessed by flow cytometry. Values represent the mean ± SEM (**$p < 0.01$, ***$p < 0.001$).

A549 cells, and to induce consequently resistance to erlotinib (8).

During chronological aging, type I collagen undergoes post-translational modifications such as glycation, that leads to an increase in AGE level (15), which is associated in turn to an increase in cross-links (16) and thus to modifications of collagen organization and rigidity (17, 18). The question we address here is whether the resistance to erlotinib observed by Chang et al., in collagen 2D model by modulating collagen properties artificially, could be observed in a 3D model that better mimics tumor organization *in vivo*, and in which collagen remodeling was induced by chronological aging (22). Our data shows that collagen aging increases EGFR expression in 3D collagen matrices. Interestingly, and at the opposite to the data obtained by Chang et al. we did not observe an increase of EGFR expression in the 2D model of collagen coating. In fact, if we compare the data obtained in 2D and 3D collagen models, the differential sensitivity of cells to erlotinib was observed only in the 3D collagen model. Moreover, the IC_{50} of erlotinib were generally higher in the 3D model when compared to 2D model. Such differential sensitivity could be explained by the fact that the 3D culture model is able to confer to epithelial carcinoma cells stem-like properties, which in turn decrease their sensitivity to therapies. In fact, cancer stem cell enrichment can induce a decrease in the sensitivity of glioblastoma to kinase inhibitors (23). This has also been reported for the tumorigenic potential in breast carcinoma (24). In fact, the authors suggested that 3D collagen matrix was able to generate breast carcinoma cells with stem-like properties.

The increase in EGFR expression observed with collagen aging in 3D was correlated to an increase in EGFR phosphorylation. These data are in agreement with those reported by Bertero and Lee groups. In fact, they have shown that ECM stiffening leads to an increase in YAP expression in cancers cells (25). According to this finding, another group has shown that the increase in YAP expression leads to EGFR TKI resistance in lung adenocarcinomas (26). In the present work, Erlotinib was able to inhibit EGFR activation in both adult and old collagens. However, due to the higher level in expression and phosphorylation of EGFR in old collagen before treatment, such levels remained significantly higher in old collagen when compared to adult collagen after treatment. This differential activation of EGFR after erlotinib treatment could explain the difference observed in terms of sensitivity to erlotinib in the two collagens.

Finally, according to the WHO, the global proportion of people over 60 is expected to increase from 12 to 22% by 2050, leading to changes in patterns of morbidity and causes of death. In addition, 30% cases of cancer are diagnosed in subjects aged 75 years and over of new cases. The importance of aging has been emphasized in the oncogenic mechanisms in the majority of tumors. Aging can also be one of the causes of therapeutic failure. However, its contribution to the therapeutic response is not sufficiently taken into account today and could partly explain the failure of many therapies in the elderly patient. Non-small-cell lung carcinoma deaths occur in patients that are 60 years old or older (27). Here we show that type I collagen modifications that occurs during aging protects lung cancer cells from erlotinib-induced cytotoxicity and apoptosis. This suggests that patient's age should be taken into account in the treatment of elderly patients.

DATA AVAILABILITY STATEMENT

The datasets generated for this study are available on request to the corresponding author.

ETHICS STATEMENT

The animal procedure was approved by the local ethics committee in animal experimentation of Reims Champagne-Ardenne (C2EA, registration 56, France) and the

experiments were performed in accordance with European directive 2010/63/UE.

AUTHOR CONTRIBUTIONS

HM and CS contributed to study conception and design. TS, LV, CC, CT, and CS performed experiments. TS, GC, CT, HM, and CS contributed to data analysis and interpretation. TS, GC, EB, HM, and CS contributed to manuscript writing and revision.

FUNDING

This work was supported by grants from Ligue Contre le Cancer 2016 (16ARC035) and 2018 (18PRC063) (CCIR Grand-Est).

REFERENCES

1. Barta JA, Powell CA, Wisnivesky JP. Global epidemiology of lung cancer. *Ann Glob Health*. (2019) 85:8. doi: 10.5334/aogh.2419
2. Fitzmaurice C, Dicker D, Pain A, Hamavid H, Moradi-Lakeh M, MacIntyre MF. The Global burden of cancer 2013. *JAMA Oncol*. (2015) 4:505–27. doi: 10.1001/jamaoncol.2015.0735
3. Thun MJ, Hannan LM, Adams-Campbell LL, Boffetta P, Buring JE, Feskanich D, et al. Lung cancer occurrence in never-smokers: an analysis of 13 cohorts and 22 cancer registry studies. *PLoS Med*. (2008) 5:e185. doi: 10.1371/journal.pmed.0050185
4. Travis WD, Brambilla E, Noguchi M, Nicholson AG, Geisinger K, Yatabe Y, et al. International association for the study of lung cancer/american thoracic society/european respiratory society: international multidisciplinary classification of lung adenocarcinoma: executive summary. *Proc Am Thorac Soc*. (2011) 5:381–5. doi: 10.1513/pats.201107-042ST
5. Minari R, Bordi P, Tiseo M. Third-generation epidermal growth factor receptor-tyrosine kinase inhibitors in T790M-positive non-small cell lung cancer: review on emerged mechanisms of resistance. *Transl Lung Cancer Res*. (2016) 5:695–608. doi: 10.21037/tlcr.2016.12.02
6. Pickup MW, Mouw JK, Weaver VM. The extracellular matrix modulates the hallmarks of cancer. *EMBO Rep*. (2014) 15:1243–53. doi: 10.15252/embr.201439246
7. Meads MB, Gatenby RA, Dalton WS. Environment-mediated drug resistance: a major contributor to minimal residual disease. *Nat Rev Cancer*. (2009) 9:665–74. doi: 10.1038/nrc2714
8. Chang CC, Hsieh TL, Tiong TY, Hsiao CH, Tung-Qian Ji A, Hsu WT, et al. Regulation of metastatic ability and drug resistance in pulmonary adenocarcinoma by matrix rigidity via activating c-Met and EGFR. *Biomaterials*. (2015) 60: 141–50. doi: 10.1016/j.biomaterials.2015.04.058
9. Henriet P, Zhong ZD, Brooks PC, Weinberg KI, DeClerck YA. Contact with fibrillar collagen inhibits melanoma cell proliferation by up-regulating p27KIP1. *Proc Natl Acad Sci USA*. (2000) 18:10026–31. doi: 10.1073/pnas.170290997
10. Assent D, Bourgot I, Hennuy B, Geurts P, Noël A, Foidart JM, et al. A membrane-type-1 matrix metalloproteinase (MT1-MMP)-discoidin domain receptor 1 axis regulates collagen-induced apoptosis in breast cancer cells. *PLoS ONE*. (2015) 10:e0116006. doi: 10.1371/journal.pone.0116006
11. Saby C, Collin G, Sinane M, Buache E, Van Gulick L, Saltel F. DDR1 and MT1-MMP expression levels are determinant for triggering BIK-mediated apoptosis by 3D type I collagen matrix in invasive basal-like breast carcinoma cells. *Front Pharmacol*. (2019) 10:462. doi: 10.3389/fphar.2019.00462
12. Bartling B, Desole M, Rohrbach S, Silber RE, Simm A. Age-associated changes of extracellular matrix collagen impair lung cancer cell migration. *FASEB J*. (2009) 5:1510–20. doi: 10.1096/fj.08-122648
13. Saby C, Buache E, Brassart-Pasco S, El Btaouri H, Courageot MP, Van Gulick L, et al. Type I collagen aging impairs discoidin domain receptor 2-mediated tumor cell growth suppression. *Oncotarget*. (2016) 7:24908–27. doi: 10.18632/oncotarget.8795
14. Saby C, Rammal H, Magnien K, Buache E, Brassart-Pasco S, Van-Gulick L, et al. Age-related modifications of type I collagen impair DDR1-induced apoptosis in non-invasive breast carcinoma cells. *Cell Adhes Migr*. (2018) 12:335–47. doi: 10.1080/19336918.2018.1472182
15. Simm A, Müller B, Nass N, Hofmann B, Bushnaq H, Silber RE, et al. Protein glycation - Between tissue aging and protection. *Exp Gerontol*. (2015) 68:71–5. doi: 10.1016/j.exger.2014.12.013
16. Monnier VM, Mustata GT, Biemel KL, Reihl O, Lederer MO, Zhenyu D. Cross-linking of the extracellular matrix by the maillard reaction in aging and diabetes: an update on "a puzzle nearing resolution." *Ann N Y Acad Sci*. (2005) 1043:533–44. doi: 10.1196/annals.1333.061
17. Aït-Belkacem D, Guilbert M, Roche M, Duboisset J, Ferrand P, Sockalingum G, et al. Microscopic structural study of collagen aging in isolated fibrils using polarized second harmonic generation. *J Biomed Opt*. (2012) 17:080506–1. doi: 10.1117/1.JBO.17.8.080506
18. Van Gulick L, Saby C, Morjani H, Beljebbar A. Age-related changes in molecular organization of type I collagen in tendon as probed by polarized SHG and raman microspectroscopy. *Sci Rep*. (2019) 1:7280. doi: 10.1038/s41598-019-43636-2
19. Garnotel R, Rittie L, Poitevin S, Monboisse JC, Nguyen P, Potron G, et al. Human blood monocytes interact with type I collagen through alpha x beta 2 integrin (CD11c-CD18, gp150-95). *J Immunol*. (2000) 164:5928–34. doi: 10.4049/jimmunol.164.11.5928
20. Shan F, Shao Z, Jiang S, Cheng Z. Erlotinib induces the human non-small-cell lung cancer cells apoptosis via activating ROS-dependent JNK pathways. *Cancer Med*. (2016) 11:3166–75. doi: 10.1002/cam4.881
21. Niederst MJ, Hu H, Mulvey HE, Lockerman EL, Garcia AR, Piotrowska Z, et al. The allelic context of the C797S mutation acquired upon treatment with third-generation EGFR inhibitors impacts sensitivity to subsequent treatment strategies. *Clin Cancer Res*. (2015) 17:3924–33. doi: 10.1158/1078-0432.CCR-15-0560
22. Edmondson R, Broglie JJ, Adcock AF, Yang L. Three-dimensional cell culture systems and their applications in drug discovery and cell-based biosensors. *Assay Drug Dev Technol*. (2014) 4:207–18. doi: 10.1089/adt.2014.573
23. Fernandez-Fuente G, Mollinedo P, Grande L, Vazquez-Barquero A, Fernandez-Luna JL. Culture dimensionality influences the resistance of glioblastoma stem-like cells to multikinase inhibitors. *Mol Cancer Ther*. (2014) 13:1664–72. doi: 10.1158/1535-7163.MCT-13-0854
24. Chen L, Xiao Z, Meng Y, Zhao Y, Han J, Su G, et al. The enhancement of cancer stem cell properties of MCF-7 cells in 3D collagen scaffolds for modeling of cancer and anti-cancer drugs. *Biomaterials*. (2012) 33:1437–44. doi: 10.1016/j.biomaterials.2011.10.056
25. Bertero T, Oldham WM, Grasset EM, Bourget I, Boulter E, Pisano S, et al. Tumor-stroma mechanics coordinate amino acid availability to sustain tumor growth and malignancy. *Cell Metab*. (2019) 1:124–40.e10. doi: 10.1016/j.cmet.2018.09.012
26. Lee TF, Tseng YC, Nguyen PA, Li YC, Ho CC, Wu CW. Enhanced YAP expression leads to EGFR TKI resistance in lung adenocarcinomas. *Sci Rep*. (2018) 1:271. doi: 10.1038/s41598-017-18527-z
27. Ferlay J, Ervik M, Lam F, Colombet M, Mery L, Piñeros M, et al. *Global Cancer Observatory: Cancer Today*. (2018). Available online at: https://gco.iarc.fr/today (accessed February 20, 2020).

Conflict of Interest: The authors declare that the research was conducted in the absence of any commercial or financial relationships that could be construed as a potential conflict of interest.

Copyright © 2020 Sarazin, Collin, Buache, Van Gulick, Charpentier, Terryn, Morjani and Saby. This is an open-access article distributed under the terms of the Creative Commons Attribution License (CC BY). The use, distribution or reproduction in other forums is permitted, provided the original author(s) and the copyright owner(s) are credited and that the original publication in this journal is cited, in accordance with accepted academic practice. No use, distribution or reproduction is permitted which does not comply with these terms.

frontiers in Oncology

MINI REVIEW
published: 11 September 2020
doi: 10.3389/fonc.2020.01748

Discoidin Domain Receptors in Melanoma: Potential Therapeutic Targets to Overcome MAPK Inhibitor Resistance

*Coralie Reger de Moura[1,2], Marco Prunotto[3], Anjum Sohail[4], Maxime Battistella[2,5], Fanelie Jouenne[1,2], Daniel Marbach[6], Celeste Lebbé[2,7], Rafael Fridman[4] and Samia Mourah[1,2]**

[1] Laboratory of Pharmacogenomics, Hôpital Saint-Louis, AP-HP, Paris, France, [2] INSERM, UMR_S976, Université de Paris, Paris, France, [3] School of Pharmaceutical Sciences, University of Geneva, Geneva, Switzerland, [4] Department of Pathology, School of Medicine, Karmanos Cancer Institute, Wayne State University, Detroit, MI, United States, [5] Department of Pathology, Hôpital Saint-Louis, AP-HP, Paris, France, [6] Roche Pharmaceutical Research and Early Development, Pharmaceutical Sciences, Roche Innovation Center Basel, F. Hoffmann-La Roche Ltd., Basel, Switzerland, [7] Department of Dermatology, Hôpital Saint-Louis, AP-HP, Paris, France

OPEN ACCESS

Edited by:
Petranel T. Ferrao, South Australian Health and Medical Research Institute (SAHMRI), Australia

Reviewed by:
Luigi Fattore, Sapienza University of Rome, Italy
Alvaro Galli, Pisa Research Area, Italian National Research Council, Italy

***Correspondence:**
Samia Mourah
samia.mourah@aphp.fr

Specialty section:
This article was submitted to Molecular and Cellular Oncology, a section of the journal Frontiers in Oncology

Received: *05 March 2020*
Accepted: *04 August 2020*
Published: *11 September 2020*

Citation:
Reger de Moura C, Prunotto M, Sohail A, Battistella M, Jouenne F, Marbach D, Lebbé C, Fridman R and Mourah S (2020) Discoidin Domain Receptors in Melanoma: Potential Therapeutic Targets to Overcome MAPK Inhibitor Resistance. Front. Oncol. 10:1748. doi: 10.3389/fonc.2020.01748

Melanoma is a highly malignant skin cancer with high propensity to metastasize and develop drug resistance, making it a difficult cancer to treat. Current therapies targeting BRAF (V600) mutations are initially effective, but eventually tumors overcome drug sensitivity and reoccur. This process is accomplished in part by reactivating alternate signaling networks that reinstate melanoma proliferative and survival capacity, mostly through reprogramming of receptor tyrosine kinase (RTK) signaling. Evidence indicates that the discoidin domain receptors (DDRs), a set of RTKs that signal in response to collagen, are part of the kinome network that confer drug resistance. We previously reported that DDR1 is expressed in melanomas, where it can promote tumor malignancy in mouse models of melanoma, and thus, DDR1 could be a promising target to overcome drug resistance. In this review, we summarize the current knowledge on DDRs in melanoma and their implication for therapy, with emphasis in resistance to MAPK inhibitors.

Keywords: DDR1, melanoma, drug resistance, MAPK inhibitors, therapeutic target

DDR1, A WORSE PROGNOSTIC BIOMARKER AND AN EMERGING TARGET

Among the receptor families known to mediate the interaction of cells with collagen, the discoidin domain receptors (DDRs) constitute a major class. The DDRs are RTKs which undergo activation upon binding to collagens. There are two members in the DDR family, DDR1 and DDR2, with DDR1 comprising 5 isoforms, two of which are inactive or truncated receptors. There is only one DDR2 isoform. Structurally, full-length DDRs are multidomain type I transmembrane glycoproteins, comprising an extracellular discoidin domain, a transmembrane region, and an intracellular segment that includes a kinase domain [for structural details of DDRs see (1, 2)]. The reason for diversity in DDR1 isoforms is still unknown, but their structural differences may be necessary to activate distinct signaling pathways. The ability of DDRs to recognize collagens as

ligands places these receptors in a unique category among the RTK family because the collagen family is comprised of 28 distinct members with different structural organizations, biomechanical properties, and tissue distributions (3). To recognize and respond to the various members of the collagen superfamily under various conditions and in different tissue locations, DDRs become versatile kinases, able to interact with distinct collagen types and initiate the downstream pathway in response to alterations on collagen properties in diverse physiological and pathological conditions. DDRs undergo receptor autophosphorylation in response to both fibril- and network-forming collagens. For instance, DDR1 and DDR2 are activated by several fibrillar collagens, albeit with different efficiencies. However, both receptors are efficiently activated by the ubiquitous fibrillar collagen type I (2, 4–6). In contrast, DDRs differentially respond to the network-forming collagen IV and X, with DDR1 being activated by collagen IV while DDR2 by collagen X (6). The ability of DDRs to recognize distinct collagen types has significant implications in conditions in which cells traffic through different tissue compartments. In cancer, for instance, premalignant and fully malignant carcinoma cells can express DDR1. Thus, as cells progress from normalcy to malignancy and acquire the ability to invade basement membranes (BM) and the underlying stromal matrix, the expression of DDR1 may modulate cancer cell behavior in response to both collagen IV and collagen I, possibly by initiating ligand-specific signaling pathways. On the other hand, DDR2, which is not usually expressed in epithelial cells, has been shown to be induced during the process of epithelial-to-mesenchymal transition (EMT), a molecular and cellular program that has been associated with enhanced invasive capacity (7, 8). Thus, DDR2 together with DDR1 may contribute to the activation of signaling pathways associated with interactions of carcinoma cells with both network-forming and fibrillar collagens, as they traffic through various matrix compartments. Although DDRs are implicated in normal organ development and function (2), there is multiple evidence showing that DDRs are critical players in cancer progression, regulating multiple aspects of malignancy including cell proliferation, migration, invasion, and drug resistance (9, 10). These effects of DDRs on malignant cell behavior appear to be mediated mostly via collagen-dependent receptor phosphorylation; however, evidence has shown that DDRs can also elicit pro-malignant activities in a kinase-independent manner (11, 12). In this regard, these studies highlight the importance DDR–collagen interaction through the discoidin domain, independent of kinase activity, in mediating the functions of DDRs in cells. However, more data are needed to establish a clear distinction between collagen-independent and -dependent effects of DDRs in cancer progression. While there is consensus on the pro-malignant effects of DDR2 in cancer, this is not the case for DDR1. Indeed, evidence suggests that DDR1 can elicit either tumor-promoting or -suppressing effects on cancer in a context-dependent manner [reviewed in (13)], possibly due to the fact that DDR1 plays a role in the maintenance of normal epithelial integrity by regulating cell–BM and cell–cell interactions (14–17). On the other hand, many studies have shown that overexpression of DDR1 in several cancer types correlates with disease progression (18–20). However, it is important to note that expression analyses in tissue samples are limited because a pro-malignant role for any gene cannot be asserted without functional studies. Regardless, the emerging picture for DDR1's role in cancer progression is complex, likely involving tumor-suppressive and/or promotive effects. In this review, we will focus on DDR1 and melanoma, and its potential role in promoting malignant features and as a potential target to overcome drug resistance.

MELANOMA-TARGETED THERAPIES AND RESISTANCE

Over the past few years, numerous therapies have emerged in the management of advanced melanoma, which have profoundly transformed the therapeutic landscape and prognosis of this disease. Drug development has been driven by the unveiling of the molecular characteristics of melanomas, which provided new insights into the signaling networks that are operative in this disease (21). The mitogen-activated protein kinase (MAPK) pathway was found to be dysregulated in a significant proportion of melanomas. This dysregulation is mostly caused by the fact that the majority of melanomas harbor a mutation on the serine–threonine kinase BRAF (V600), which is part of the MAPK signaling pathway. Overall, over 90% of BRAFV600-mutated melanomas harbor a BRAFV600E mutation, 6% a BRAFV600R mutation, and 4% a BRAFV600E2, BRAFV600D, or a BRAFV600K mutation (22), and therefore mutated BRAF kinase became an attractive therapeutic target (23). As a result, several inhibitors (vemurafenib, dabrafenib, and encorafenib) were developed, which improved survival of melanoma patients when compared to conventional chemotherapy (24–26). Almost at the same time, inhibitors of MEK, a downstream signaling kinase of the MAPK pathway, were developed. These compounds (trametinib, cobimetinib, and binimetinib) also exhibited significant activity in BRAFV600-mutant melanoma (27, 28). Clinical trials evaluating the combination of BRAF inhibitors (BRAFi) with MEK inhibitors (MEKi) demonstrated significant clinical efficacy, as indicated by improved overall survival (OS) and progression-free survival (PFS). These promising results led to the approval of dabrafenib/trametinib and vemurafenib/cobimetinib combinations for patients with advanced, metastatic BRAFV600-mutant melanoma (29–31).

Despite these advances in melanoma treatment, acquired resistance to MAPK-targeted therapy is almost inescapable (32), and, as expected, resistance to BRAFi and MEKi was also found in melanoma patients. The mechanisms of resistance to MAPK inhibition are multiple and complex. In many cases, resistance is caused by reactivation of the MAPK pathway (RAS mutation, MEK and/or BRAF amplification, differential splicing leading to truncated variants of BRAF, activation of MAPKK), activation of the PI3K pathway through genetic alterations of PTEN, overexpression and activation of PDGF, IGF1, or c-Met receptors, or development of a pro-oncogenic tumor microenvironment (33–36). Another mechanism of resistance involves the action of ERBB3, a member of the EGF family of receptors, which is known

to be over-expressed in human melanoma. Evidence has shown that BRAFi and MEKi therapeutic effects on BRAFV600-treated tumors are decreased by enhanced ERBB3 signaling, suggesting that ERBB3 is implicated in adaptive resistance to BRAF and MEK inhibitors. These observation suggested that a combination of ERBB2/EGFR inhibitor, which block NRG1/ERBB3 signaling, with BRAF and MEK inhibitors could overcome resistance (37, 38). It is worth mentioning that, eventually, these multiple and distinct mechanisms of resistance to MAPK inhibitors result in ERK reactivation, demonstrating the extent to which melanoma cells are addicted to ERK signaling for proliferation and/or survival (36). Recently, characterization of tumor cell and stromal/immune transcriptomic alterations in MAPKi-treated melanomas provided insight into the responses elicited by these inhibitors, even at early stages of treatment (39). Song et al. showed that an immune-phenotypic transition due to MAPK-targeted therapies could involve a loss of T-cell inflammation leading to an anti-PD1 resistance in melanoma, even at early stages of treatment. These studies suggested that several adaptive responses in both the tumor (intrinsic) and the immune system (extrinsic) are operative, which could offer new therapeutic opportunities to overcome resistance. The studies of Yan

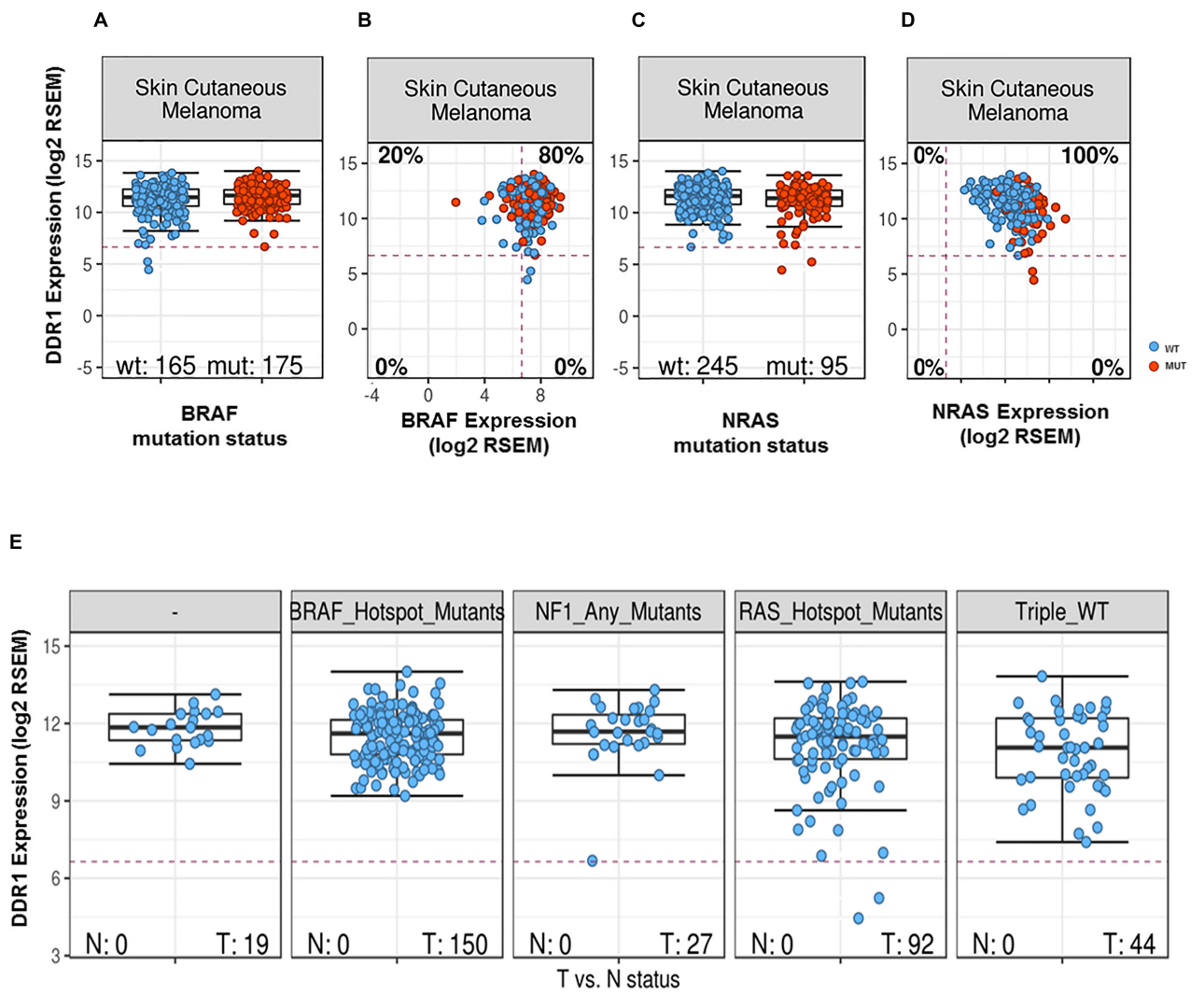

FIGURE 1 | DDR1 expression in melanoma samples as a function of expression and mutational status of *BRAF* **(A,B)** or *NRAS* **(C,D)**. Transcript abundances were quantified using RSEM (50) on a log2 scale. The red dashed lines indicate the typical cutoff for expressed genes [RSEM = log2(100)]: samples below the red lines are assumed to have no or very low expression. Classification of melanoma subtypes into mutant BRAF, mutant RAS, mutant NF1, and triple-WT (wild-type) was obtained from TCGA (51). **(A)** DDR1 expression for BRAF wild-type (left, blue) and mutated cases (right, red). **(B)** DDR1 versus BRAF expression for WT (blue) and BRAF-mutated cases (red). 80% of the samples show co-expression of DDR1 and BRAF (upper-right quadrant). **(C)** DDR1 expression for NRAS wild-type (left, blue) and mutated cases (right, red). **(D)** DDR1 versus NRAS expression for wild-type (blue) and cases with NRAS mutations (red). **(E)** DDR1 expression in melanoma molecular subtypes (BRAF, NRAS, NF1 mutated, and triple WT). There is no significant difference in the median expression of DDR1 (p-value > 0.05, Wilcoxon rank-sum test), but we note some outliers with low DDR1 expression in the NF1 mutant, RAS mutant, and triple WT cases (three left-most plots), while no outliers with low expression are observed for the BRAF mutant subtype. N, normal; T, tumor.

et al. also demonstrated that BRAF and MEK inhibitor-treated patients, showing complete responses, have preexisting tumor immunity transcriptomic signatures that are higher than those expressed in patients with progressive disease, suggesting that enriched immune infiltration improves response to BRAFi and MEKi combination (40). These observations highlight the crucial need for a better understanding of treatment effects on both the tumor and its microenvironment but also for more effective therapies aimed at overcoming or preventing drug resistance in melanoma patients. Several alternative strategies, including paradox breaker RAF inhibitors and ERK inhibitors, are currently under investigation in the BRAFi + MEKi resistance setting (41, 42). In this context, the validation of new and promising targets is the cornerstone of this challenge. Because DDRs are crucial regulators of tumor cell behavior in response to their immediate microenvironment and in light of our recent data on DDR1 in melanoma (43), we propose that DDR1 targeting in melanomas resistant to MAPK inhibitors is worth exploring.

DDR1 IN MELANOMA

Melanomas are derived from melanocytes, the melanin-producing cells in the epidermis. Melanocytes are located in the basal layer of the epidermis, making contact with the BM (44). Previous evidence demonstrated a role for DDR1, a major collagen IV receptor, in mediating the interaction of melanocytes with the BM. Adhesion of melanocytes to collagen IV, induced by overexpression of the matricellular protein CCN3, was mediated by upregulation of DDR1 protein expression, and silencing of DDR1 mRNA reduced CCN3-induced adhesion to collagen IV (45). However, whether this adhesive effect of DDR1 was mediated via its kinase activity was not determined. Regardless, CCN3-mediated DDR1 upregulation was proposed to play a major role in the adhesion of melanocytes to the BM and in the maintenance of skin homeostasis (45). While these *in vitro* studies suggested a role for DDR1 in melanocytes in normal skin, our recent immunohistochemical analyses in human skin sections demonstrated that DDR1 immunoreactivity was only detected in normal keratinocytes, albeit at relatively low levels of expression (43). Moreover, we found no detectable DDR1 expression in benign naevi in all cell types. Analyses of skin samples harboring melanoma showed a strong expression of DDR1 in the melanoma cells, which was positively correlated with invasive depth and patient survival. Our functional *in vitro* studies also showed a key role for DDR1 in melanoma cell proliferation, migration, invasion, and survival (43). Importantly, a pan-DDR inhibitor, DDR1-IN-1 (46), with higher selectivity toward DDR1 than to DDR2, decreased tumor growth in *BRAF*-mutated human melanoma xenograft models (43). Because melanoma and stromal cells also express DDR2, these preclinical studies with DDR1-IN-1 suggest that DDR1, and possibly DDR2, constitutes a potentially new target in melanoma (43). Based on these results, we posit that DDRs are promising therapeutic targets in *BRAF*-mutated melanomas.

To further examine the association between DDR1 and melanoma, we analyzed a curated set of seven non-redundant cutaneous melanoma cohorts from the cBioPortal site (47, 48). Out of a total of 667 patients, 114 (10.6%) were identified as harboring genetic alterations in DDR1. However, although the mutational burden in melanoma is higher compared to other types of cancers, no difference in survival was observed in patients harboring mutated DDR1. Analyses of TCGA database samples for DDR1 expression vs. BRAF mutational status showed DDR1 to be slightly upregulated in BRAF-mutated cancers (effect size 0.16, $p = 0.00031$; differential expression analysis of mutated vs. wild-type cases using a linear model) and with a similar tendency, but not statistically significant, between WT and mutated BRAF melanoma samples (effect size 0.27, $p = 0.061$, **Figure 1A**). However, we found that DDR1 and BRAF are co-expressed in the majority of skin melanoma samples (80%) regardless of BRAF mutational status (**Figure 1B**). Analysis of the same database for DDR1 expression vs. NRAS mutational status showed DDR1 to be slightly downregulated in all NRAS-mutated cancers (effect size -0.26, $p = 0.00053$) and with a similar tendency (effect size -0.29, $p = 0.065$, **Figure 1C**). As with BRAF, DDR1 and NRAS are co-expressed in almost all samples, regardless of NRAS mutational status (**Figure 1D**). Although not statistically significant, the analysis of the different skin melanoma subtypes showed that DDR1 expression is always high for BRAF and NF1 mutants, while there are few outliers with low DDR1 expression for RAS mutants and triple wild-type samples (**Figure 1E**).

CONCLUSION

The emerging evidence suggests that DDRs are part of the signaling networks that contribute to melanoma progression. However, more studies are warranted to dissect the molecular mechanisms by which DDR-initiated signaling influences melanoma cell behavior. Melanomas are also characterized by a stroma rich in collagen (49), which constitutes a barrier for invading tumor cells but may also actively promote disease progression through DDR signaling. We posit that a DDR/collagen axis may contribute to the resistant phenotype of BRAF-mutated melanomas and therefore a rationale target to restore therapeutic efficacy.

AUTHOR CONTRIBUTIONS

CR, MP, AS, RF, and SM contributed to development, writing, and final review of the article. MP and DM contributed to the database analysis. MB, FJ, DM, and CL contributed to the final review of the article. All authors contributed to the article and approved the submitted version.

FUNDING

This work was supported by the Institut National de la Santé et de la Recherche Medicale (INSERM), the Société Française de Dermatologie, SFD, and the Université de Paris.

REFERENCES

1. Fu H-L, Valiathan RR, Arkwright R, Sohail A, Mihai C, Kumarasiri M, et al. Discoidin domain receptors: unique receptor tyrosine kinases in collagen-mediated signaling. *J Biol Chem.* (2013) 288:7430–7. doi: 10.1074/jbc.R112.444158
2. Leitinger B. Discoidin domain receptor functions in physiological and pathological conditions. *Int Rev Cell Mol Biol.* (2014) 310:39–87. doi: 10.1016/B978-0-12-800180-6.00002-5
3. Gordon MK, Hahn RA. Collagens. *Cell Tissue Res.* (2010) 339:247–57. doi: 10.1007/s00441-009-0844-4
4. Shrivastava A, Radziejewski C, Campbell E, Kovac L, McGlynn M, Ryan TE, et al. An orphan receptor tyrosine kinase family whose members serve as nonintegrin collagen receptors. *Mol Cell.* (1997) 1:25–34. doi: 10.1016/S1097-2765(00)80004-0
5. Vogel W, Gish GD, Alves F, Pawson T. The discoidin domain receptor tyrosine kinases are activated by collagen. *Mol Cell.* (1997) 1:13–23.
6. Leitinger B, Kwan APL. The discoidin domain receptor DDR2 is a receptor for type X collagen. *Matrix Biol.* (2006) 25:355–64. doi: 10.1016/j.matbio.2006.05.006
7. Walsh LA, Nawshad A, Medici D. Discoidin domain receptor 2 is a critical regulator of epithelial-mesenchymal transition. *Matrix Biol.* (2011) 30:243–7. doi: 10.1016/j.matbio.2011.03.007
8. Zhang K, Corsa CA, Ponik SM, Prior JL, Piwnica-Worms D, Eliceiri KW, et al. The collagen receptor discoidin domain receptor 2 stabilizes SNAIL1 to facilitate breast cancer metastasis. *Nat Cell Biol.* (2013) 15:677–87. doi: 10.1038/ncb2743
9. Valiathan RR, Marco M, Leitinger B, Kleer CG, Fridman R. Discoidin domain receptor tyrosine kinases: new players in cancer progression. *Cancer Metastasis Rev.* (2012) 31:295–321. doi: 10.1007/s10555-012-9346-z
10. Henriet E, Sala M, Abou Hammoud A, Tuariihionoa A, Di Martino J, Ros M, et al. Multitasking discoidin domain receptors are involved in several and specific hallmarks of cancer. *Cell Adhes Migr.* (2018) 12:363–77. doi: 10.1080/19336918.2018.1465156
11. Gao H, Chakraborty G, Zhang Z, Akalay I, Gadiya M, Gao Y, et al. Multi-organ site metastatic reactivation mediated by non-canonical discoidin domain receptor 1 signaling. *Cell.* (2016) 166:47–62. doi: 10.1016/j.cell.2016.06.009
12. Grither WR, Longmore GD. Inhibition of tumor–microenvironment interaction and tumor invasion by small-molecule allosteric inhibitor of DDR2 extracellular domain. *Proc Natl Acad Sci USA.* (2018) 115:E7786–94. doi: 10.1073/pnas.1805020115
13. Yeh YC, Lin HH, Tang MJ. Dichotomy of the function of DDR1 in cells and disease progression. *Biochim Biophys Acta Mol Cell Res.* (2019) 1866:118473. doi: 10.1016/j.bbamcr.2019.04.003
14. Søgaard PP, Ito N, Sato N, Fujita Y, Matter K, Itoh Y. Epithelial polarization in 3D matrix requires DDR1 signaling to regulate actomyosin contractility. *Life Sci Alliance.* (2019) 2:e201800276. doi: 10.26508/lsa.201800276
15. Vogel WF, Aszodi A, Alves F, Pawson T. Discoidin domain receptor 1 tyrosine kinase has an essential role in mammary gland development. *Mol Cell Biol.* (2001) 21:2906–17. doi: 10.1128/mcb.21.8.2906-2917.2001
16. Wang CZ, Hsu YM, Tang MJ. Function of discoidin domain receptor I in HGF-induced branching tubulogenesis of MDCK cells in collagen gel. *J Cell Physiol.* (2005) 203:295–304. doi: 10.1002/jcp.20227
17. Yeh Y-C, Wu C-C, Wang Y-K, Tang M-J. DDR1 triggers epithelial cell differentiation by promoting cell adhesion through stabilization of E-cadherin. *Mol Biol Cell.* (2011) 22:940–53. doi: 10.1091/mbc.E10-08-0678
18. Rammal H, Saby C, Magnien K, Van-Gulick L, Garnotel R, Buache E, et al. Discoidin domain receptors: potential actors and targets in cancer. *Front Pharmacol.* (2016) 7:55. doi: 10.3389/fphar.2016.00055
19. Jing H, Song J, Zheng J. Discoidin domain receptor 1: new star in cancer-targeted therapy and its complex role in breast carcinoma. *Oncol Lett.* (2018) 15:3403–8. doi: 10.3892/ol.2018.7795
20. Gadiya M, Chakraborty G. Signaling by discoidin domain receptor 1 in cancer metastasis. *Cell Adhes Migr.* (2018) 12:315–23. doi: 10.1080/19336918.2018.1520556
21. Flaherty KT, Hodi FS, Bastian BC. Mutation-driven drug development in melanoma. *Curr Opin Oncol.* (2010) 22:178–83. doi: 10.1097/cco.0b013e32833888ee
22. Ascierto PA, Kirkwood JM, Grob JJ, Simeone E, Grimaldi AM, Maio M, et al. The role of BRAF V600 mutation in melanoma. *J Transl Med.* (2012) 10:85. doi: 10.1186/1479-5876-10-85
23. Davies H, Bignell GR, Cox C, Stephens P, Edkins S, Clegg S, et al. Mutations of the BRAF gene in human cancer. *Nature.* (2002) 417:949–54.
24. Sosman JA, Kim KB, Schuchter L, Gonzalez R, Pavlick AC, Weber JS, et al. Survival in BRAF V600-mutant advanced melanoma treated with vemurafenib. *N Engl J Med.* (2012) 366:707–14. doi: 10.1056/NEJMoa1112302
25. McArthur GA, Chapman PB, Robert C, Larkin J. Safety and efficacy of vemurafenib in BRAF V600E and BRAF V600K mutation-positive melanoma (BRIM-3): extended follow-up of a phase 3, randomised, open-label study HHS public access. *Lancet Oncol.* (2014) 15:323–32. doi: 10.1016/S1470-2045(14)70012-9
26. Hauschild A, Grob JJ, Demidov LV, Jouary T, Gutzmer R, Millward M, et al. Dabrafenib in BRAF-mutated metastatic melanoma: a multicentre, open-label, phase 3 randomised controlled trial. *Lancet.* (2012) 380:358–65.
27. Flaherty KT, Robert C, Hersey P, Nathan P, Garbe C, Milhem M, et al. Improved survival with MEK inhibition in BRAF-mutated melanoma. *N Engl J Med.* (2012) 367:107–14.
28. Dummer R, Ascierto PA, Gogas HJ, Arance A, Mandala M, Liszkay G, et al. Encorafenib plus binimetinib versus vemurafenib or encorafenib in patients with BRAF-mutant melanoma (COLUMBUS): a multicentre, open-label, randomised phase 3 trial. *Lancet Oncol.* (2018) 19:603–15. doi: 10.1016/S1470-2045(18)30142-6
29. Robert C, Karaszewska B, Schachter J, Rutkowski P, Mackiewicz A, Stroiakovski D, et al. Improved overall survival in melanoma with combined dabrafenib and trametinib. *N Engl J Med.* (2015) 372:30–9. doi: 10.1056/NEJMoa1412690
30. Long GV, Stroyakovskiy D, Gogas H, Levchenko E, de Braud F, Larkin J, et al. Dabrafenib and trametinib versus dabrafenib and placebo for Val600 BRAF-mutant melanoma: a multicentre, double-blind, phase 3 randomised controlled trial. *Lancet.* (2015) 386:444–51.
31. Ascierto PA, McArthur GA, Dréno B, Atkinson V, Liszkay G, Di Giacomo AM, et al. Cobimetinib combined with vemurafenib in advanced BRAF(V600)-mutant melanoma (coBRIM): updated efficacy results from a randomised, double-blind, phase 3 trial. *Lancet Oncol.* (2016) 17:1248–60. doi: 10.1016/S1470-2045(16)30122-X
32. Johnson DB, Menzies AM, Zimmer L, Eroglu Z, Ye F, Zhao S, et al. Acquired BRAF inhibitor resistance: a multicenter meta-analysis of the spectrum and frequencies, clinical behaviour, and phenotypic associations of resistance mechanisms. *Eur J Cancer.* (2015) 51:2792–9. doi: 10.1016/j.ejca.2015.08.022
33. Dummer R, Flaherty KT. Resistance patterns with tyrosine kinase inhibitors in melanoma: new insights. *Curr Opin Oncol.* (2012) 24:150–4. doi: 10.1097/CCO.0b013e32834fca92
34. Straussman R, Morikawa T, Shee K, Barzily-Rokni M, Qian ZR, Du J, et al. Tumour micro-environment elicits innate resistance to RAF inhibitors through HGF secretion. *Nature.* (2012) 487:500–4. doi: 10.1038/nature11183
35. Wilson TR, Fridlyand J, Yan Y, Penuel E, Burton L, Chan E, et al. Widespread potential for growth-factor-driven resistance to anticancer kinase inhibitors. *Nature.* (2012) 487:505–9. doi: 10.1038/nature11249
36. Little AS, Smith PD, Cook SJ. Mechanisms of acquired resistance to ERK1/2 pathway inhibitors. *Oncogene.* (2013) 32:1207–15. doi: 10.1038/onc.2012.160
37. Ruggiero CF, Malpicci D, Fattore L, Madonna G, Vanella V, Mallardo D, et al. ErbB3 phosphorylation as central event in adaptive resistance to targeted therapy in metastatic melanoma: early detection in CTCs during therapy and insights into regulation by autocrine neuregulin. *Cancers (Basel).* (2019) 11:1425. doi: 10.3390/cancers11101425
38. Abel EV, Basile KJ, Kugel CH, Witkiewicz AK, Le K, Amaravadi RK, et al. Melanoma adapts to RAF/MEK inhibitors through FOXD3-mediated upregulation of ERBB3. *J Clin Invest.* (2013) 123:2155–68. doi: 10.1172/JCI65780
39. Song C, Piva M, Sun L, Hong A, Moriceau G, Kong X, et al. Recurrent tumor cell–intrinsic and –extrinsic alterations during mapki-induced melanoma regression and early adaptation. *Cancer Discov.* (2017) 7:1248–65. doi: 10.1158/2159-8290.CD-17-0401
40. Yan Y, Wongchenko MJ, Robert C, Larkin J, Ascierto PA, Dréno B, et al. Genomic features of exceptional response in vemurafenib ± cobimetinib-treated patients with BRAF V600-mutated metastatic melanoma. Author

Manuscr Publ OnlineFirst. *Clin Cancer Res.* (2019) 25:3239–46. doi: 10.1158/1078-0432.CCR-18-0720
41. Girotti MR, Lopes F, Preece N, Niculescu-Duvaz D, Zambon A, Davies L, et al. Paradox-breaking RAF inhibitors that also target SRC are effective in drug-resistant BRAF mutant melanoma. *Cancer Cell.* (2015) 27:85–96. doi: 10.1016/j.ccell.2014.11.006
42. Xue Y, Martelotto L, Baslan T, Vides A, Solomon M, Mai TT, et al. An approach to suppress the evolution of resistance in BRAFV600E-mutant cancer. *Nat Med.* (2017) 23:929–37. doi: 10.1038/nm.4369
43. Reger de Moura C, Battistella M, Sohail A, Caudron A, Feugeas JP, Podgorniak MP, et al. Discoidin domain receptors: a promising target in melanoma. *Pigment Cell Melanoma Res.* (2019) 32:697–707. doi: 10.1111/pcmr.12809
44. Haass NK, Smalley KSM, Herlyn M. The role of altered cell-cell communication in melanoma progression. *J Mol Histol.* (2004) 35:309–18. doi: 10.1023/B:HIJO.0000032362.35354.bb
45. Fukunaga-Kalabis M, Martinez G, Liu Z-J, Kalabis J, Mrass P, Weninger W, et al. CCN3 controls 3D spatial localization of melanocytes in the human skin through DDR1. *J Cell Biol.* (2006) 175:563–9. doi: 10.1083/jcb.200602132
46. Kim H-G, Tan L, Weisberg EL, Liu F, Canning P, Choi HG, et al. Discovery of a potent and selective DDR1 receptor tyrosine kinase inhibitor. *ACS Chem Biol.* (2013) 8:2145–50. doi: 10.1021/cb400430t
47. Cerami E, Gao J, Dogrusoz U, Gross BE, Sumer SO, Aksoy BA, et al. The cBio cancer genomics portal: an open platform for exploring multidimensional cancer genomics data. *Cancer Discov.* (2012) 2:401–4. doi: 10.1158/2159-8290.CD-12-0095
48. Gao J, Aksoy BA, Dogrusoz U, Dresdner G, Gross B, Sumer SO, et al. Integrative analysis of complex cancer genomics and clinical profiles using the cBioPortal. *Sci Signal.* (2013) 6:11. doi: 10.1126/scisignal.2004088
49. Hutchenreuther J, Leask A. Why target the tumor stroma in melanoma? *J Cell Commun Signal.* (2018) 12:113–8. doi: 10.1007/s12079-017-0419-1
50. Li B, Dewey CN. RSEM: accurate transcript quantification from RNA-Seq data with or without a reference genome. *BMC Bioinformatics.* (2011) 12:323. doi: 10.1186/1471-2105-12-323
51. Akbani R, Akdemir KC, Aksoy BA, Albert M, Ally A, Amin SB, et al. Genomic classification of cutaneous melanoma. *Cell.* (2015) 161:1681–96. doi: 10.1016/j.cell.2015.05.044

Conflict of Interest: DM is employed by Roche, MP is an employee of Galapagos Ltd., at 80% employment rate, this work was performed during his 20% academic time at the University of Geneva. MB declares a consulting role for Histalim, BMS, and Innate Pharma. CL declares honoraria from Roche, advisory roles at Roche, GSK, Novartis, BMS, MSD, and Amgen and travel accommodation provided by Roche. SM declares a consulting role at Roche, Janssen, Biocartis and Novartis.

The remaining authors declare that the research was conducted in the absence of any commercial or financial relationships that could be construed as a potential conflict of interest.

Copyright © 2020 Reger de Moura, Prunotto, Sohail, Battistella, Jouenne, Marbach, Lebbé, Fridman and Mourah. This is an open-access article distributed under the terms of the Creative Commons Attribution License (CC BY). The use, distribution or reproduction in other forums is permitted, provided the original author(s) and the copyright owner(s) are credited and that the original publication in this journal is cited, in accordance with accepted academic practice. No use, distribution or reproduction is permitted which does not comply with these terms.

frontiers in Oncology

REVIEW
published: 16 October 2020
doi: 10.3389/fonc.2020.568557

Crosstalk Between Cancer Associated Fibroblasts and Cancer Cells in Scirrhous Type Gastric Cancer

Yuichiro Miki[1,2]*, *Masakazu Yashiro*[1], *Lidia Moyano-Galceran*[2], *Atsushi Sugimoto*[1], *Masaichi Ohira*[1] *and Kaisa Lehti*[2,3]

[1] Department of Gastroenterological Surgery, Osaka City University Graduate School of Medicine, Osaka, Japan, [2] Department of Microbiology, Tumor and Cell Biology, Karolinska Institutet, Stockholm, Sweden, [3] Department of Biomedical Laboratory Science, Norwegian University of Science and Technology, Trondheim, Norway

Gastric cancer (GC) is the third leading cause among all cancer deaths globally. Although the treatment outcome of GC has improved, the survival of patients with GC at stages III and IV remains unsatisfactory. Among several types of GC, scirrhous type GC (SGC) shows highly aggressive growth and invasive activity, leading to frequent peritoneal metastasis. SGC is well known to accompany abundant stromal cells that compose the tumor microenvironment (TME) along with the produced extracellular matrix (ECM) and secreted factors. One of the main stromal components is cancer associated fibroblast (CAF). In the SGC microenvironment, CAFs are a source of various secreted factors, including fibroblast growth factors (FGFs), which mediate prominent tumor-stimulating activity. In turn, cancer cells also secrete numerous factors, which can activate and educate CAFs. Current findings suggest that cancer cells and stromal cells communicate interactively *via* the soluble factors, the ECM, and likely also by exosomes. In this review, we focus on the soluble factors mediating communication between cancer cells and CAFs in SGC, and consider how they are related to the modulation of TME and the high rate of peritoneal metastasis. At last, we discuss the perspectives on targeting these communication pathways for improved future treatment.

Keywords: cancer associated fibroblast, gastric cancer, tumor microenvironment, scirrhous carcinoma of the stomach, fibroblast growth factor receptor, transforming growth factor β1

OPEN ACCESS

Edited by:
Frederic Saltel, INSERM U1053 Bordeaux Recherche en Oncologie Translationnelle, France

Reviewed by:
MinHua Zheng, Shanghai Jiao Tong University, China
Océane C. B. Martin, Université de Bordeaux, France

***Correspondence:**
Yuichiro Miki
y_miki@med.osaka-cu.ac.jp

Specialty section:
This article was submitted to Molecular and Cellular Oncology, a section of the journal Frontiers in Oncology

Received: *01 June 2020*
Accepted: *21 September 2020*
Published: *16 October 2020*

Citation:
Miki Y, Yashiro M, Moyano-Galceran L, Sugimoto A, Ohira M and Lehti K (2020) Crosstalk Between Cancer Associated Fibroblasts and Cancer Cells in Scirrhous Type Gastric Cancer. Front. Oncol. 10:568557. doi: 10.3389/fonc.2020.568557

INTRODUCTION OF SCIRRHOUS GC MICROENVIRONMENT

Gastric cancer (GC) is diagnosed with 5th frequency among all cancers and is the third-leading cause of cancer death, with one million new cases and nearly 800,000 deaths globally in 2018 (1). Although the survival outcome has been improved by early screening, optimal surgery, chemotherapy, and molecular targeted therapy, the median overall survival is reported to be only 10–16 months in patients with metastatic or unresectable GC (2–5).

Scirrhous gastric cancer (SGC), an aggressive subtype of GC, shows rapid infiltration in the gastric wall, progressive invasion into the serosal layer, and seeding to the peritoneum. GC

classification into 6 types (type 0–5) by macroscopic features, as Borrmann proposed (**Table 1**), has been used clinically. On the other hand, Laurén classified GC into two main subtypes of intestinal type (differentiated type) and diffuse type (undifferentiated type) by microscopic features (6). By using these two classifications, SGC can be defined as macroscopic Borrmann type 4 and microscopic diffuse type (**Figure 1**). The incidence of SGC was 7.5% (284/3,842) in the registry of our institute (unpublished data), which is consistent with the Japanese nation-wide registry data (6.6%) (7). The Cancer Genome Atlas (TCGA) Research Network has suggested a molecular-based classification of GC into four subtypes: 1) the Ebstein–Barr Virus positive tumors (EBV 8%), with frequent PI3KCA mutations, high DNA hypermethylation, *JAK2/PDL1* amplification and *PDL2/CDKN2A* silencing; 2) MicroSatellite Unstable tumors (MSI 22%), with high rates of mutations, including genes that encode oncogenic proteins; 3) genomically stable tumors (GS 20%), characterized by diffuse histology, mutations in CDH1/RHOA and fusions in the CLDN18 family; and 4) tumors which have chromosomal instability (CIN 50%), characterized by intestinal histology and amplification of several tyrosine-kinase receptor genes (8). Most SGCs can be classified into the GS group defined by the TCGA classification, although there is insufficient data regarding this issue (8).

The prognosis of SGC is worse than it is for the other types, and the 5-year survival rate of Japanese patients with macroscopic type 4 is reported to be 17.7%, while for all registered patients the Japanese Gastric Cancer Association (JGCA) registry reports a 5-year survival of 68.9% (9). An Italian group reported worse survival data for this sub-population of GC, and 5-year survival rate after R0 resection was reported to be only 4% (10). These unsatisfactory survival outcomes are partly because of diagnostic difficulties in early stage due to rapid growth, which leads to low percentage of curative resection for patients with SGC. Even when we perform standard treatment with curative intent, SGC often recur with peritoneal metastasis, which frequently develop resistance to

TABLE 1 | Macroscopic type of gastric cancer according to Japanese Gastric Cancer Association criteria.

Macroscopic type	Description
Type 0 (superficial)	Typical of T1 tumors.
Type 1 (mass)	Polypoid tumors, sharply demarcated from the surrounding mucosa.
Type 2 (ulcerative)	Ulcerated tumors with raised margins surrounded by a thickened gastric wall with clear margins.
Type 3 (infiltrate ulcerative)	Ulcerated tumors with raised margins surrounded by a thickened gastric wall without clear margins.
Type 4 (diffuse infiltrate)	Tumors without marked ulceration or raised margins, the gastric wall is thickened and indurated and the margin is unclear.
Type 5 (unclassifiable)	Tumors that cannot be classified into any of the above types.

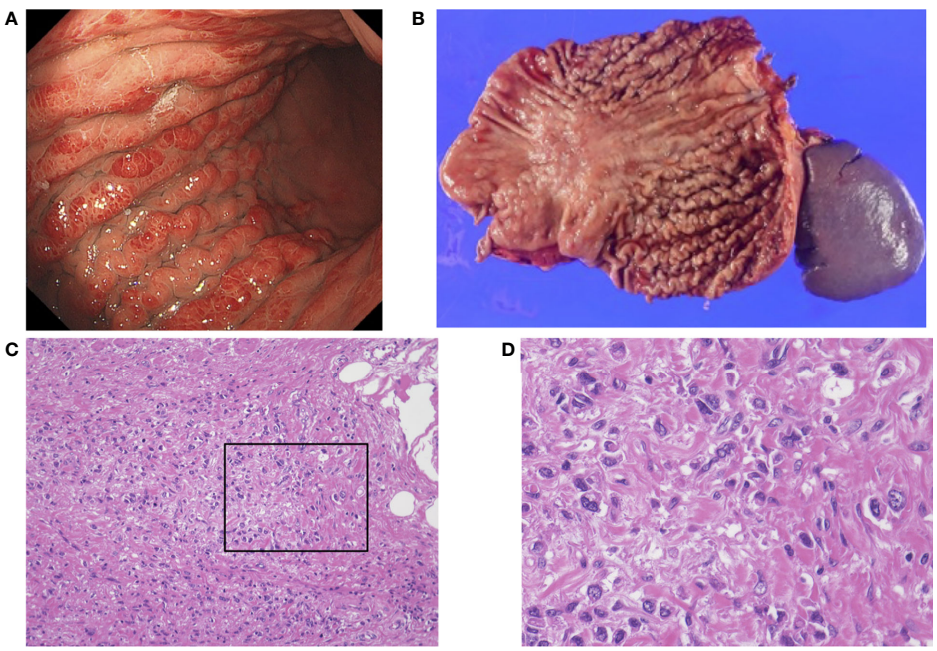

FIGURE 1 | **(A)** Endoscopic view of scirrhous type gastric cancer (SGC); **(B)** Image of resected specimens of total gastrectomy. Tumors did not have marked ulceration or raised margins, the gastric wall was thickened, showing typical macroscopic view of SGC. **(C, D)** Microscopic images from the specimen shown in **(B)**. Cancer cells are invading into the stroma containing fibroblasts and extracellular matrix.

chemotherapy as well as available molecular targeted therapy. Possibly, small cytological lesions in the peritoneum grow and generate a fibrotic microenvironment that may later interfere with drug delivery to the cancer cells.

SGC cell proliferation is coupled with remarkable fibrosis when the cancer cells enter into the submucosa composed of stromal cells. Coincidentally, the fibrosis is induced by the excessive deposition of collagen (COL), including COL1A1, COL1A2, COL3A1, COL4A1, COL4A2, COL5A1, and COL5A2 in GC (11). The unique feature of SGC, compared to the other GC types, is high expression of type IV collagen in the stroma of undifferentiated GC with desmoplastic reaction (40.4% vs 9.0%) (12). The distinctive histological findings of rapid tumor enlargement with fibrosis imply that the growth of the fibrotic tumor microenvironment (TME) can be controlled by intercellular communication between the SGC cells and the stromal cells. One of the main cellular components of SGC microenvironment is cancer associated fibroblasts (CAF). CAFs secrete various molecules, such as fibroblast growth factor (FGF), which directly stimulate cancer cells. Conversely, cancer cells also secrete factors which can activate and educate CAFs. While it has been well established that cancer cells and CAFs communicate interactively through soluble factors, the communication *via* exosomes has only been recognized more recently (13, 14). In this review, we will focus on the reciprocal communication between cancer cells and CAFs in SGC, as well as the relevance of this communication to both the remodeling of TME and the high rate of peritoneal metastasis. Finally, we will discuss the perspectives on future treatment targeting these communication pathways/mechanisms.

TME COMMUNICATIONS *VIA* SOLUBLE FACTORS

FGF-FGFR Axis

Fibroblast growth factors (FGFs) regulate various cellular processes, such as stemness, proliferation, apoptosis evasion, migration, and invasion (see **Table 2**) (15, 21, 30–32).

The FGF family includes 22 secreted factors, which are divided into seven subgroups according to their phylogenetic relation, homology, and biochemical function (33). Members of five FGF subfamilies: FGF1 (FGF1, FGF2), FGF4 (FGF4, FGF5, FGF6), FGF7 (FGF3, FGF7, FGF10, FGF22), FGF8 (FGF8, FGF17, FGF18), and FGF9 (FGF9, FGF16, FGF20) are released to function in paracrine and autocrine manner. On the other hand, the FGF15 (FGF15, FGF19, FGF21, FGF23) subfamily is produced by endocrine glands as secreted hormones for metabolic modulation with α- and β-Klotho family proteins. In contrast, FGF11, FGF12, FGF13 and FGF14 lack secretory N-terminal peptides that direct newly produced proteins to secretory pathway, and thus remain intracellular (33).

TABLE 2 | FGFs classification according to their functions in cancer progression.

Function	FGFs (reference)
Proliferation	FGF1 (15), FGF2 (16), FGF3 (15), FGF7 (17, 18), FGF10 (19)
Stemness	FGF2 (20)
Apoptosis evasion	FGF2 (21), FGF9 (22)
Migration and invasion	FGF2 (16)
Angiogenesis	FGF1 (15, 23), FGF2 (24), FGF3 (15), FGF4 (25), FGF8 (26), FGF18 (27)
Resistance to therapy	FGF1 (28), FGF2 (28), FGF3 (29), FGF4 (29), FGF19 (29)

As for the receptors of the FGF ligands, four distinct FGF receptors (FGFRs), FGFR1 (Flg), FGFR2 (K-sam), FGFR3, and FGFR4 exist, and if deregulated can function as oncogenes to drive specific cancer types including GC (17, 34–36). For example, we have previously shown that FGFR4 interaction with the membrane-type matrix metalloproteinase MT1-MMP increases both FGFR4-FRS2-Src kinase signaling and MT1-MMP-driven cancer cell invasion in a Gly388Arg SNP dependent manner (36). Canonically, FGFRs are monomers in their inactive state, and the binding of FGF ligands triggers receptor dimerization. The binding of FGF to FGFR causes activation of the receptor *via* cross-phosphorylation of the intracellular kinase domains. This leads to the recruitment of adaptor and scaffold proteins, and biochemical signals are transduced by activated FGFRs into cytosolic signaling cascades. Among four FGFRs, FGFR2 is identical to the K-*sam-II* gene, and it was originally identified in an extract from the SGC cell line KATO-III (37). We can observe this amplification of *FGFR2* in OCUM-2M, which was also established from patients with SGC (38).

Gastric cancer with *FGFR2* amplification is significantly associated with poor survival outcome. Although *FGFR2* amplification has been found in 5–10% of GC, the ratio is significantly higher in diffuse type (including SGC) (8), suggesting that *FGFR2* amplification is one of key factors in the most aggressive SGC.

FGFR2 isoforms IIIb and IIIc are mainly expressed in epithelial and mesenchymal tissues (39–41). In general, the FGFR2 IIIb isoform binds FGF3, FGF7, and FGF10 with high affinity, while the IIIc isoform has preference for FGF2, FGF4, and FGF20 (42, 43). It has also been reported that FGF10 and FGFR2-IIIb promote proliferation and patterning of the forestomach, and are involved in early epithelial growth before differentiation (44).

Despite these general findings, there are only a few studies regarding FGF-FGFR axis particularly in SGC. Yashiro et al. identified that the growth-stimulating factor from gastric fibroblasts to SGC cells is FGF7 (17). FGF7 stimulates the growth of SGC cells, but not that of well-differentiated adenocarcinoma cells. Since *FGFR2* amplification is more often observed in SGC than non-SGC, FGF-7 secreted by gastric fibroblasts is significant in the progression of SGC with *FGFR2* amplification in a paracrine manner. This was supported by the report from Huang et al., which described that FGF7/FGFR2 increase invasion and migration of GC cells through a thrombospondin 1 (THBS1)-mediated pathway. Increased expression of THBS1, an extracellular glycoprotein that has multiple roles in cell-matrix and intercellular interactions (45), significantly correlated with tumor differentiation.

Sun et al. reported that CAF-secreted and MMP7-activated FGF9 promotes apoptosis evasion and invasive ability of gastric cancer cells (22). MMP7 not only has the potential to degrade the extracellular matrix, but also promotes apoptosis evasion in cancer cells. In a Chinese GC cohort study, FGF9 was also associated with accelerated proliferation and apoptosis inhibition of GC cells in an autocrine manner (46).

TGFBR Axis

Transforming growth factor β (TGFβ) produced by fibroblasts increases the invasive capabilities of SGC cells (47) (**Figure 2**). Whole exome and RNA sequencing analyses comparing CAFs and normal fibroblasts (NF) revealed that many of the genes with upregulated expression in CAFs were associated with TGFβ1 (TGFB1) pathway (48).

In the conditioned medium from fibroblasts, TGFβ is mainly in a latent form, whereas its active form is detected in the conditioned medium from GC cells (47, 49). Proteases such as plasmin and cathepsin can activate the latent TGFβ (50). Most GC cells secrete urokinase-type plasminogen activator (uPA) which converts latent TGFβ to active TGFβ (51, 52). Our group previously reported that SGC cells derived from peritoneal metastasis (OCUM-2D) produced six times higher amounts of uPA than SGC cell line (OCUM-2M) which was established

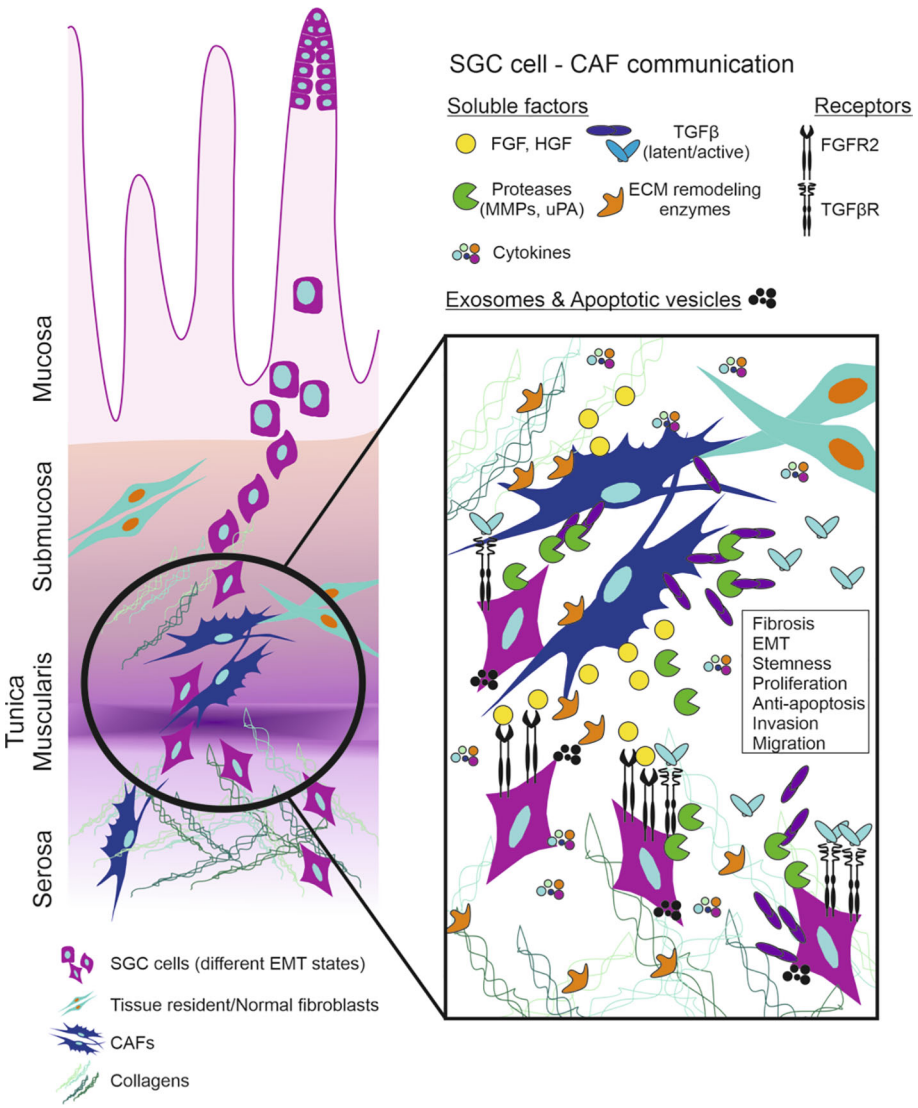

FIGURE 2 | Schematic representation of SGC cells invasion and communication with CAFs. FGF-FGFR and TGFβ-TGFβR axis are the main players in the tumor microenvironment of SGC. SGC (scirrhous gastric cancer), CAF (cancer associated fibroblasts), FGF (fibroblast growth factor), FGFR (FGF receptor), HGF (hepatocyte growth factor), MMP (matrix metalloproteinases), uPA (urokinase-type plasminogen activator), TGFβ (transforming growth factor β), TGFβR (TGFβ receptor), ECM (extracellular matrix), EMT (epithelial-to-mesenchymal transition).

from primary lesion of the same patient (53), suggesting the possible role of uPA in peritoneal metastasis of SGC. The latent TGFβ from gastric fibroblasts and SGC cells is activated by uPA from SGC cells. It has been shown that TGFβ promotes collagen synthesis not only by fibroblasts but also by cancer cells, resulting in diffuse fibrosis of SGC (54).

Although the effect of TGFβ on tumor growth is controversial, Komuro et al. used a SGC cell line (OCUM-2MLN) and showed that disruption of TGFβ signaling in SGC may accelerate tumor growth through upregulated tumor angiogenesis that is induced by decreased expression of THBS1 after inhibition of TGFβ signaling by dominant-negative TGFBR (55).

TGFβ produced by either gastric fibroblasts or cancer cells affects the invasive capabilities of SGC cells by inducing a morphologic change of the cells to a spindle shape, a process known as the epithelial-to-mesenchymal transition (EMT) (56). Cancer cells experiencing EMT develop invasive and migratory capabilities (57–59). Shinto et al. revealed that TGFβ significantly upregulates the activity of RhoA and myosin light chain-2 phosphorylation, whereas TGFβ1 decreases ZO-2 and E-cadherin in SGC cells. Moreover, the TGFBR kinase inhibitor Ki26894 inhibited both invasion and EMT in SGC cells. It has been also revealed that the combination of S-1 (Tegefur/Gimeracil/Osteracil, 5-FU derivative) and Ki26894 decreases tumor growth and lymph node metastasis more effectively than Ki26894 alone. We have confirmed that TGFβ produced by CAFs increased the migration and invasion ability of cancer cells derived from SGC (60). Our group has also shown that hypoxia stimulates EMT in SGC cells *via* autocrine TGFβ signaling (61).

Ishimoto et al. reported that CAFs express high levels of Rhomboid 5 homolog 2 (RHBDF2). Expression of RHBDF2 in fibroblasts is prompted by inflammatory cytokines secreted by SGC cells. RHBDF2 promotes cleavage of TGFBR by activating a disintegrin and metallopeptidase domain 17 (ADAM17, also called TACE) and motility of CAFs in response to TGFβ1. They reported that these CAFs with high motility can also increase the invasion of SGC cells into extracellular matrix and lymphatic vessels in nude mice (48). Kawajiri et al. revealed that A-77, another TGFβ inhibitor, decreased the invasion capability of SGC by decreasing the intercellular interaction between SGC cells and CAFs, in conjunction with decreased tumor growth and dissemination in an intraperitoneal tumor model.

In addition to the function of TGFβ in the regulation of invasiveness, CAFs regulate cancer cell stemness in SGC. Conditioned medium (CM) from CAFs can significantly increase spheroid colonies and the expression of cancer stemness markers of SGC cells. These stimulating activities by CM are significantly abolished by TGFβ inhibitors, but not by FGFR and c-Met inhibitors. Thus, TGFβ from CAFs is considered to be an important factor to sustain stemness in SGC (62).

On the other hand, TGFβ from SGC surrounding CAFs increases α-smooth muscle actin (a-SMA) expression in fibroblasts thorough SMAD pathway, suggesting that SGC cells can reprogram NFs into CAFs (63). This means that SGC cells can educate CAFs to sustain the favorable microenvironment, and TGFβ plays a critical role in this inter-cellular communication.

HGF, Matrix Metalloproteases, and Cytokines

CAFs also produce HGF, which is a known regulator of the SGC cell invasiveness. The *c-met* gene encoding the HGF receptor c-Met is amplified more frequently in SGC than in non-scirrhous gastric cancer (64). HGF is not usually detected in the CM from gastric cancer cells, thus, it can affect the invasive capabilities of SGC cells in a paracrine fashion (**Figure 2**). In diffuse-type gastric carcinoma, E-cadherin is frequently down-regulated by methylation and mutations, a phenomenon that may be related to tumor invasion (65). Additionally, another adherens junction protein, Desmoglein-2 is down-regulated in diffuse-type gastric cancer (66, 67). Sank-Uk Han reported that exposure of SNU-16 gastric cancer cells to HGF down-regulates the expression of E-cadherin, and induces morphological changes from epithelial to mesenchymal type (68). Thus, HGF could be one of the main factors which control cell-cell adhesion in SGC.

Tendo et al. reported that COX2 inhibitor in combination with S-1 (5-FU derivative) decreases the production of HGF in CAF, and suppresses tumor growth and lymph node metastasis in SGC mouse model. It has also been reported that the HGF antagonist NK4 can effectively inhibit the progression of peritoneal metastasis of SGC, revealing c-Met as a promising target candidate to halt SGC progression.

In addition to secreting growth factors, fibroblasts produce matrix metalloproteinases (MMPs) that allow cancer cells cross tissue boundaries (69, 70). In early stages, cancer cells growing at the mucosa need to invade into the submucosa beyond the muscularis mucosae. Extracellular matrix degradation and loss of cell-cell adhesion facilitate the tumor invasion. MT1-MMP on the surface of GC cells activates MMP-2 produced by fibroblasts (71). Therefore, MMP2 from the stromal cells may affect cancer progression in a paracrine manner, even though at the early stage cancer cells are separated from stromal cells by the basement membrane.

Lysyl oxidase (LOX) is produced as a 50-kDa proenzyme (pro-LOX). This pro-LOX is secreted and then cleaved by bone morphogenetic protein 1 in the extracellular space to form a 30-kDa mature enzyme and an 18-kDa pro-peptide (LOX-PP) (72, 73). LOX and LOX-like 1-4 oxidize lysine residues in collagens and elastin (74), leading to covalent cross-linking and stabilization of these ECM structural components, conferring much of the tensile strength to collagen and elastic fibers (75). Kasashima et al. reported that the expression of LOX in GC cells affects the EMT in hypoxic conditions (76). Furthermore, CAFs produce more LOXL2 than normal gastric fibroblasts, which increases the invasive capability of SGC cells in a paracrine manner (77).

Since the origin of CAFs of SGC remained uninvestigated, our group tackled the issue. Conditioned medium from SGC cells significantly increased twofold or threefold the migratory ability of bone marrow mesenchymal cells (BM-MCs) but not of

non-SGC cells. This implied that BM-MCs were preferentially recruited by a factor(s) from SGC cells. To confirm the molecules increasing the homing capability of BM-MCs, chemokines were screened using a protein array and the protein production level between diffuse type GC cells and non-diffuse type GC cells were compared. Seven out of 102 screened chemokines (CXCL1, CXCL5, lipocalin-2, CXCL8, Dkk1, CCL20, and EMMPRIN) were expressed in SGC but not in the non-SGC cell lines MKN74 and SNU16. Among them, only CXCL1 significantly increased both the invasion capacity and motility of BM-MCs. Thus, we concluded that BM-MCs are recruited to SGC TME *via* CXCL1-CXCR2 signaling (78).

EXTRACELLULAR VESICLES, miRNA

Exosomes are small vesicles with a diameter of ~30–100 nm originated from the endosomal system during formation of multivesicular bodies (79). In cancer, exosomes have been implicated in proliferation, angiogenesis, immunosuppression, and preparation of premetastatic niches in secondary organs (80). Various studies have reported that exosomes mediate local and systemic cellular communication through the transfer of information *via* microRNAs, long non-coding RNAs (lncRNAs), mRNAs, proteins, metabolites and other substances.

Although their model was not gastric cancer, Webber et al. reported that exosomal TGFβ can differentiate fibroblasts into CAFs. At the surface of exosomes, TGFβ elicits SMAD-dependent signalling (13). Thus, exosomal TGFβ may be related to the differentiation of CAFs in SGC.

Naito et al. investigated the miR-143 expression in SGC and non-SGC, and reported that miR-143 expression is significantly higher in SGC tissue than in non-SGC tissue. They also showed that miR-143 enhances the expression of collagen type III in normal gastric fibroblasts and CAFs by activation of TGFβ/SMAD signaling, suggesting that miR-143 and TGFβ signaling regulate fibrosis of SGC tissue.

Our group showed that CD9 expression is higher in CAF-secreted exosomes than in NFs exosomes, and that CAF-secreted exosomes are taken up by SGC cells, but not by the other types of GC cells. Exosomes from CAFs stimulate the migration and invasion of SGC cells, which is inhibited by antibody or siRNA against the exosomal CD9. Interestingly, MMP2 expression in SGC cells is decreased by CD9-siRNA. Thus, we concluded that CD9-positive exosomes from CAFs stimulate the MMP2 expression and migration ability of SGC cells (81).

The role of miRNA in GC has been reported in the context of FGF-FGFR signaling. FGF18 is overexpressed in genomically stable and chromosomal instable GC subtypes, where it is associated to poor patient survival. Similarly, FGF18 is upregulated in seven out of eleven (63.6%) GC cell lines. Knocking down FGF18 inhibits tumor formation capabilities, induces cell cycle arrest in G1 phase and enhances drug sensitivity. In this report, miR-590-5p was identified as a direct target of FGF18, implying that FGF18 secretion can be regulated by exosomal miRNA (82).

Exosomal miRNA from CAFs may be related to chemo-resistance of GC cells. It was recently reported that exosomal miR-522 secreted by CAFs targets ALOX15 and blocks lipid-ROS accumulation in cancer cells, inhibiting ferroptosis and resulting in decreased chemo-sensitivity (83).

Finally, we will refer to the function of apoptotic vesicles from cancer cells. Cancer cells co-invade with CAFs, and CAF invasion often precedes invasion by cancer cells, resulting in CAF-led cancer cell invasion. When cancer cells interact with CAFs by death receptor 4, caspase-8 is activated in cancer cells and leads to apoptosis. Apoptotic cancer cells conversely release apoptotic vesicles and stimulate invasion of CAFs. In CAF-led cancer invasion, cancer cells move through tunnels in the substrate made by the leading CAFs. It has also been reported that cancer cells become highly motile along collagen bundles and these bundles are used as 'highways' for efficient migration. This may be one of the mechanisms responsible for the highly invasive characteristics of SGC (84).

HIGH RATE OF PERITONEAL METASTASIS; RELATION TO EMT, NICHE FORMATION

The most frequent type of metastasis in GC is peritoneal metastasis. The peritoneum constitutes a superficial monolayer of mesothelial cells and submesothelial stromal tissue, in which cancer-stroma interactions occur (85). Fibroblasts at peritoneal metastatic sites contribute to tumor progression.

The initial step of peritoneal metastasis is the adhesion of cancer cells to the peritoneal mesothelial cells (PMCs), followed by the exfoliation of these mesothelial cells and the adhesion to the submesothelial connective tissue (**Figure 3**). The interaction between cancer cells and PMCs is mediated by the adhesion molecule CD44 expressed on the cancer cells and the hyaluronic acid expressed on PMCs surface (86). Stromal fibroblasts increase CD44 expression of GC cells through TGFβ signaling, thus stimulating the adhesion of SGC cells to the mesothelium (87). Another important step in peritoneal dissemination is the adhesion of cancer cells to the submesothelial components. The main components of the submesothelial matrix are laminin, fibronectin, type IV collagen at the basement membrane and type I collagen in the underlying interstitial matrix. Cancer cells adhere to these components *via* integrins, in particular α2β1- and α3β1-integrins (88). In the peritoneal cavity, GC cells which disseminated from the primary tumor are usually exposed to low oxygen levels (89). Experimentally, hypoxic (1% O_2) conditions increase the adhesion capability of SGC cells, compared to normoxic (21% O_2) conditions. Under hypoxia, TGFβ increases the expression of α2-, α3-, and α5-integrin in GC cells, promoting adhesion to the peritoneum. This can partially explain the high metastatic potential of SGC cells.

Upon peritoneal metastasis, a monolayer of PMCs that lines the peritoneal cavity undergoes mesothelial-to-mesenchymal transition (MMT). TGFβ from GC cells promotes morphological changes in

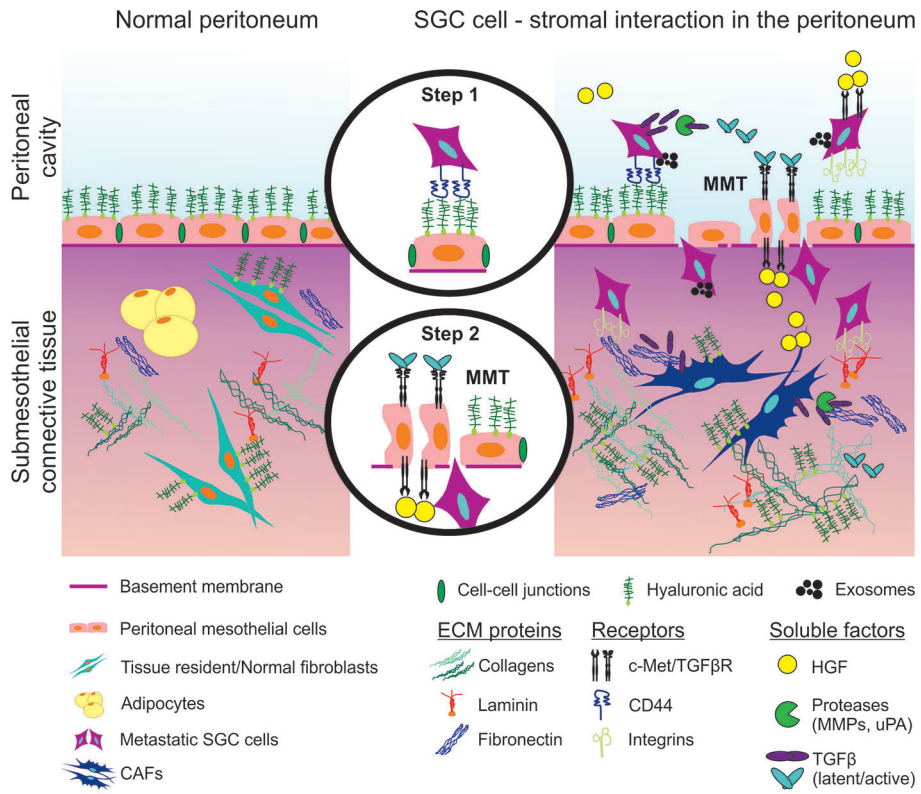

FIGURE 3 | Schematic representation of peritoneal invasion by SGC cells and communication with the stroma. Step 1: interaction between SGC cells and peritoneal mesothelial cells (PMCs). Step 2: PMCs undergo mesothelial-to-mesenchymal transition (MMT) and allow SGC cells to invade the submesothelial connective tissue. SGC (scirrhous gastric cancer), CAF (cancer associated fibroblasts), ECM (extracellular matrix), TGFβ (transforming growth factor β), TGFβR (TGFβ receptor), HGF (hepatocyte growth factor), c-Met (HGF receptor), MMP (matrix metalloproteinases), uPA (urokinase-type plasminogen activator).

mesothelial cells and thus likely associates with peritoneal dissemination (90). In fact, when mesothelial cells are exposed to fibroblasts, they become hemispherical and separated from each other, while unexposed mesothelium remains a flat monolayer. Both cancer cells and host fibroblasts stimulate morphological changes in mesothelial cells (91). HGF produced by peritoneal fibroblasts is associated with the morphology of mesothelial cells in monolayers so that the resulting microenvironment becomes suitable for the peritoneal dissemination of cancer cells (92).

Regarding exosomal communication, an investigation of exosomal miRNA profiles in peritoneal fluid showed that miR-21-5p was highly expressed in GC with serosal invasion. These findings suggest that miR-21-5p may be one candidate biomarker of peritoneal metastasis after GC resection. Exosomal miR-21-5p derived from GC cells was proven to induce MMT by activating TGFβ/SMAD pathway by alleviating the inhibitory action of SMAD7 (93).

PERSPECTIVE ON TREATMENT

FGFR2

Since previous data suggests that up-regulation of FGFR2 signaling is critical in a subset of GC patients including SGC, precision medicine approaches targeting FGFR2 by specifically designed drugs have recently emerged. Anti-FGFR2 specific monoclonal antibodies, FGF traps, and selective and non-selective FGFR inhibitors are among these drugs.

Monoclonal Antibodies, FGF Traps

There are several antibodies which have shown promise in pre-clinical studies (**Table 3**). Among trials with them, bemarituzumab (FPA144) have provided preliminary data suggesting promising efficacy in patients with GC.

Bemarituzumab is a humanized immunoglobulin G1 (IgG1) monoclonal antibody specific to FGFR2b (a splice-variant) that blocks FGF7, FGF10, and FGF22 ligand binding. In the phase I study, bemarituzumab seems to be well tolerated and demonstrates single agent activity as late-line therapy in GC patients. A phase III trial is currently evaluating Bemarituzumab in combination with chemotherapy (FOLFOX6) as front-line therapy for patients with FGFR2b-overexpressing advanced gastroesophageal cancer (FIGHT trial, Five Prime).

As FGFs are rich in gastric cancer tissues, another strategy is the use of FGF traps which can neutralize FGF and reduce cancer cell malignancy. FGF ligand traps are a fusion of an immunoglobulin Fc fragment and a soluble FGFR extracellular domain that competitively binds with FGF1, 2, 3, 7, and 10 to

TABLE 3 | Drugs targeting FGFRs.

Drug	Mechanism	Clinical data	Ongoing trial
Bemarituzumab (FPA144)	FGFR2 IIIb antibody	5 PR out of 28 patients with high FGFR2b overexpressing GEA	Phase III trial (FIGHT) (NCT03343301)
FP-1039 (GSK3052230)	FGF trap	No objective responses in phase I study for patients with advanced solid tumor	
NSC12	FGF trap	Only preclinical data	
AZD4547	FGFR1/2/3 inhibitor	*FGFR2* amplification cohort: 1PR, 4SD	SHINE trial (NCT01457846)
BGJ398	FGFR1/2/3 inhibitor	No data for GC	Phase I
E7090	FGFR1/2/3 inhibitor	Only one GC patient enrolled in the study showed PR	Phase I/II (NCT02275910)
LY2874455	Pan-FGFR inhibitor	1 PR, 12SD/29 patients	
JNI-42756493(Erdafitinib)	Pan-FGFR inhibitor	Safety profile was shown in phase I	Phase II
Lucitanib	Multi kinase inhibitor	7 responses/27 patients	Phase II
ARQ087 (Derazantinib)	Multi kinase inhibitor	3PR/18 evaluable patients with FGFR genetic alterations	
Dovitinib	Multi kinase inhibitor	1 PR, 2SD/14 evaluable patients	(NCT01719549)

FGFR, fibroblast growth factor receptor; FGF, fibroblast growth factor; PR, partial response; GEA, gastroesophageal cancer; SD, stable disease; GC, gastric cancer.

suppress ligand-dependent FGFR signaling. For example, FP-1039 (GSK3052230) is a soluble fusion of the extracellular ligand-binding domain of FGFR1 linked to a modified hinge and native Fc regions of IgG1. FP-1039 was well tolerated, even when used in combination with chemotherapy for lung cancer patients (94). Although there is no clinical data regarding FP-1039 for GC patients, it may be promising considering that FGF7 is possibly a critical player in TME of SGC.

Another FGF trap, the extracellular NSC12, can be used as an FGF antagonist in anti-angiogenic treatment with anti-vascular endothelial growth factor.

FGFR Inhibitors

According to their target specificities, FGFR kinase inhibitors can be divided to FGFR1/2/3 inhibitors, FGFR4 inhibitors, pan-FGFR inhibitors or multi- kinase FGFR inhibitors. Out of all the FGFR inhibitors, we summarize here the inhibitors which have been tested in clinical trials for gastric cancer patients or some other types of solid tumors.

AZD4547 is a selective FGFR1/2/3 inhibitor which was preclinically tested in FGFR2 amplified SNU16 and SGC083 (GC cell lines) xenograft models, showing positive results. The randomized phase II SHINE study (NCT01457846) investigated whether AZD4547 administered as second-line treatment for advanced GC patients with FGFR2 polysomy or gene amplification improved survival outcome compared to paclitaxel treatment (95). As a result, AZD4547 did not significantly improve progression-free survival (PFS) compared to paclitaxel in these patients. However, the lack of correlation between *FGFR2* amplification/polysomy and FGFR2 expression together with significant intratumor heterogeneity for FGFR2 gene amplification indicate the need for further development of predictive biomarkers.

BGJ398 is another selective FGFR1/2/3 inhibitor, which was identified from integrative analysis of the Cancer Cell Line Encyclopedia (96). Promising results were shown in phase I study for patients with advanced solid tumors, where antitumor activity was demonstrated in patients with *FGFR1*-amplified lung cancer and *FGFR3*-mutant bladder or urothelial cancer (97). However, the study did not include GC patients. *In vitro*, we have shown that BGJ398 significantly decreases the growth of SGC patient-derived OCUM-14 cells (38). Therefore, BGJ398 could be promising for SGC. A small phase I study for patients with advanced solid tumors having alterations of FGFR pathway has been completed (NCT01697605), and the result regarding SGC is awaited from the study.

E7090 is another potent FGFR1/2/3 inhibitor. *In vitro*, E7090 treatment inhibited the phosphorylation of FGFR2 as well as FRS2, ERK1/2, and AKT in SNU-16 GC cells. Moreover, E7090 also had antitumor activity in SNU-16 xenograft mouse model (98). Clinically, the phase I study showed that it has manageable safety profile in patients with advanced solid tumors (99). A phase II study for patients with cholangiocarcinoma is in progress, and the application for gastric cancer may be relevant in the future.

LY2874455 is a reversible pan-FGFR inhibitor that competes for the ATP-binding pocket the kinase domain. A phase I study to determine optimal phase II dose was performed (NCT01212107). Among 29 patients with GC enrolled in the study, one patient was reported to show partial response (PR; more than 30% reduction of the tumor size from the baseline), while 12 patients had best overall response of stable disease (SD; increase in tumor size by at least 20% from the baseline) (100). The median PFS in the GC group was 62.0 days. LY2874455 in combination with other agents should be investigated in the future.

JNI-42756493 (Erdafitinib) is another potent pan-FGFR inhibitor. The first human study reported that Erdafitinib had a manageable safety profile, although it has not been shown whether the study included GC patients (101). Another phase I study was performed in patients with advanced or refractory solid tumors in Japan, and this study includes two GC patients among 19 enrolled patients. This study concludes that Erdafitinib was well tolerated (102). The new phase II study is ongoing to evaluate the efficacy of Erdafitinib in which overall response rate [ORR; the rate of complete response (CR) and PR] is the primary outcome for participants with advanced solid tumors with FGFR mutations and gene fusions (NCT4083976).

Lucitanib is a potent, oral inhibitor of FGFR1, 2, vascular endothelial growth factor receptor types 1, 2, and 3 (VEGFR),

platelet-derived growth factor receptor types α and β (PGFRα/β). Lucitanib showed promising efficacy and a manageable profile of adverse events. Clinical benefit was shown in both FGF-aberrant and angiogenesis-sensitive patients (103). A comprehensive phase II program has been planned. Although the reported phase I study did not include GC patients, it might be a promising drug for targeting FGFR2 in a subpopulation of GC.

ARQ087 (Derazantinib) is another multi kinase inhibitor, and it works as pan-FGFR inhibitor. In phase I study, ARQ087 had manageable toxicity at the recommended phase II dose (RP2D) of 300 mg once a day, showed pharmacodynamic effects, and achieved objective responses, particularly in patients with FGFR2 genetic alterations (104). A further study for patients with intrahepatic cholangiocarcinoma is ongoing.

Dovitinib is also a potent multi-kinase inhibitor, and was evaluated in a phase I study of 35 solid tumors including two GCs (105). It was unsatisfactory that neither patient with GC had SD for more than 4 months. On the other hand, three phase II studies of Dovitinib are ongoing in GC (GASDOVI-1, NCT01719549).

Albeit according to preclinical data FGFR alterations were expected to be predictive of responsiveness to FGFR targeted therapies, FGFR alterations alone are not sufficient biomarkers for selecting patients for monotherapies using FGFR-targeted agents. Expression of FGFR mRNA or protein might be more helpful than FGFR amplification for predicting sensitivity to FGFR inhibitors in future studies.

TGFβ

TGFβ in tumor-stroma interactions favors tumor progression through mechanisms that are still unclear and controversial (106). Before cancer initiation and during the early phase of carcinogenesis, TGFβ can function as a tumor suppressor. Conversely, during the advanced stages, cancer progression and metastasis are promoted by TGFβ signaling (107). To clarify the clinical efficacy of TGFBR inhibitors on the progression of GC at both the early and advanced stages additional studies are needed.

Tranilast [N-(3,4-dimethoxycinnamoyl) anthranilic acid] is a drug which is used clinically for the treatment of excessive proliferation of fibroblasts. By blocking the interactions between fibroblasts and SGC cells, it reduces GC growth and induces cancer cell apoptosis (71). Tranilast not only inhibits fibroblast proliferation but also the release of growth-promoting factors from fibroblasts and cancer cells, and the interactions between these cells (108). In addition, Tranilast and cisplatin combinatorial treatment reduces tumor size, fibrosis, and mitosis, and increases apoptosis in SGC xenograft model (109). Furthermore, the invasion-stimulating ability of fibroblasts is suppressed by Tranilast through inhibiting the production of MMP2 and TGFβ in fibroblasts (110).

Another study also supports the hypothesis that Tranilast could be a new strategy to decrease fibrous tumor represented by peritoneal dissemination. In this study, human peritoneal mesothelial cells (HPMCs) were used to investigate the effects of Tranilast treatment on cells and a xenograft mouse model of fibrosis. TGFβ-mediated EMT-like changes in HPMCs were inhibited in a dose-dependent way by Tranilast treatment through inhibition of Smad2 phosphorylation. In the mouse model, Tranilast significantly decreased tumor size and inhibited fibrosis, compared with the control group proliferation and invasion (111).

Considering these preclinical studies, Tranilast may be a promising novel drug to decrease proliferation and invasion stimulation between fibroblasts and SGC cells (108).

In spite of many preclinical studies about TGFβ, there is still a difficulty in using TGFβ inhibitors clinically. Because TGFβ is a potent inhibitor of epithelial cell proliferation, it could be better to use TGFBR inhibitors with other chemotherapeutic drugs or molecular targeted agents in the future.

c-Met

Considering the progression mechanism of SGC, c-Met could be a targetable molecule in a subgroup of patients with SGC. Rilotumumab (monoclonal antibody for HGF) showed greater activity than placebo in phase II trial (112). However, it did not improve clinical outcomes in MET positive gastroesophageal cancer in phase III trial (113).

AMG337 is a small molecule MET inhibitor, and it showed promising efficacy in MET-amplified gastroesophageal cancer (114). The result of phase III trial is awaited.

FUTURE PERSPECTIVES

Immune checkpoint inhibitors (ICIs), such as atezolizumab, avelumab, durvalumab, nivolumab, and pembrolizumab, are monoclonal antibodies (mAbs) that block the interaction between programmed cell death protein 1 (PD-1) and its ligand PD-L1, preventing an immunosuppressive signaling cascade. Even though some subsets of patients showed a complete response to these agents (CR rate of 1.1%) (115), the ORR of unselected patients with GC who received anti-PD-1 mAbs remains approximately 10% (116).

Distinct FGFR3 alterations and FGFR3 upregulation were specifically detected in non T cell- inflamed TMEs and associated to resistance against ICIs (117). The specific FGFR inhibitor erdafitinib when administered with anti-PD-1 mAbs in mouse models of FGFR2-driven cancers showed synergistic antitumor outcomes (118), implicating that the combination of FGFR inhibitors and ICIs could be a promising strategy.

M7824 (MSB0011359C) is a novel bifunctional fusion protein formed by an anti-PD-L1 mAb fused with the extracellular domain of TGFβ receptor II, which works as a TGFβ trap (119). In phase I trial, 5 among 31 patients showed PR with manageable safety profile. The combination therapy targeting both TGFβ and ICIs can become a promising treatment strategy for SGC in future.

As described in the previous section, exosomes work as an important messenger between cancer cells and CAF. Therefore, blocking the signaling which starts from exosomes could also be a promising strategy. For example, silencing of exosomal miR-21-5p could block MMT by attenuating TGFβ/SMAD pathway. However, we should confirm which molecules, including

miRNAs, are critical players in the TME. Further pre-clinical studies will be needed in developing strategies to target exosomes.

CONCLUSION

CAFs communicate with SGC cells in a number of ways, and contribute to the progression of SGC mainly by FGF/FGFR and TGFβ/SMAD signaling axes. In this review we have collected evidence from SGC studies but also from common GC reports and thus we highlight here the need for more basic research in SGC to fully understand the mechanisms of SGC-CAF communication.

Many drugs targeting FGF/FGFR and TGFβ/SMAD signaling pathways have been tested in clinical settings. Among them, bemarituzumab (monoclonal antibody specific to the splice variant FGFR2b) showed 19.0% of ORR in patients with late-line gastroesophageal cancer with FGFR2b expression, and is the only drug being evaluated in phase III clinical trial. Considering the significant role of FGFR2 expression in SGC, a promising treatment strategy will be to use bemarituzumab for SGC cohort. Ultimately, combination therapy targeting multiple players involved in the communication between CAF and SGC cells could improve the survival outcome of patients with SGC in the future.

AUTHOR CONTRIBUTIONS

Concept, drafting: YM. Supervision: MY, MO, and KL. Figure making: YM, LM-G, and AS, editing the manuscripts: YM, MY, LM-G, and KL. All authors contributed to the article and approved the submitted version.

FUNDING

This work is supported by Swedish Cancer Society CAN 2018/858 (for KL), and Postdoctral research fellowship from the Uehara Memorial Foundation (for YM).

REFERENCES

1. Arnold M, Abnet CC, Neale RE, Vignat J, Giovannucci EL, McGlynn KA, et al. Global Burden of 5 Major Types Of Gastrointestinal Cancer. *Gastroenterology* (2020) (1):335–49. doi: 10.1053/j.gastro.2020.02.068
2. Sasako M, Sakuramoto S, Katai H, Kinoshita T, Furukawa H, Yamaguchi T, et al. Five-year outcomes of a randomized phase III trial comparing adjuvant chemotherapy with S-1 versus surgery alone in stage II or III gastric cancer. *J Clin Oncol* (2011) 29(33):4387–93. doi: 10.1200/jco.2011.36.5908
3. Noh SH, Park SR, Yang HK, Chung HC, Chung IJ, Kim SW, et al. Adjuvant capecitabine plus oxaliplatin for gastric cancer after D2 gastrectomy (CLASSIC): 5-year follow-up of an open-label, randomised phase 3 trial. *Lancet Oncol* (2014) 15(12):1389–96. doi: 10.1016/S1470-2045(14)70473-5
4. Guo X, Zhao F, Ma X, Shen G, Ren D, Zheng F, et al. A comparison between triplet and doublet chemotherapy in improving the survival of patients with advanced gastric cancer: a systematic review and meta-analysis. *BMC Cancer* (2019) 19(1):1125. doi: 10.1186/s12885-019-6294-9
5. Yasuhide Yamada NB, Mizusawa J, Iwasa S, Kadowaki S, Nakayama N, Azuma M, et al. Phase III study comparing triplet chemotherapy with S-1 and cisplatin plus docetaxel versus doublet chemotherapy with S-1 and cisplatin for advanced gastric cancer (JCOG1013). *J Clin Oncol* (2018) 36(15 suppl):4009. doi: 10.1200/JCO.2018.36.15_suppl.4009
6. Jarvi O, Lauren P. On the pathogenesis of gastric cancer. *Acta - Unio Internationalis Contra Cancrum* (1952) 8(2):393–4.
7. Katai H, Ishikawa T, Akazawa K, Isobe Y, Miyashiro I, Oda I, et al. Five-year survival analysis of surgically resected gastric cancer cases in Japan: a retrospective analysis of more than 100,000 patients from the nationwide registry of the Japanese Gastric Cancer Association (2001-2007). *Gastric Cancer* (2018) 21(1):144–54. doi: 10.1007/s10120-017-0716-7
8. Cancer Genome Atlas Research N. Comprehensive molecular characterization of gastric adenocarcinoma. *Nature* (2014) 513(7517):202–9. doi: 10.1038/nature13480
9. Nashimoto A, Akazawa K, Isobe Y, Miyashiro I, Katai H, Kodera Y, et al. Gastric cancer treated in 2002 in Japan: 2009 annual report of the JGCA nationwide registry. *Gastric Cancer* (2013) 16(1):1–27. doi: 10.1007/s10120-012-0163-4
10. Pedrazzani C, Marrelli D, Pacelli F, Di Cosmo M, Mura G, Bettarini F, et al. Gastric linitis plastica: which role for surgical resection? *Gastric Cancer* (2012) 15(1):56–60. doi: 10.1007/s10120-011-0063-z
11. Li Z, Liu Z, Shao Z, Li C, Li Y, Liu Q, et al. Identifying multiple collagen gene family members as potential gastric cancer biomarkers using integrated bioinformatics analysis. *PeerJ* (2020) 8:e9123. doi: 10.7717/peerj.9123
12. Ando H, Aihara R, Ohno T, Ogata K, Mochiki E, Kuwano H. Prognostic significance of the expression of MUC1 and collagen type IV in advanced gastric carcinoma. *Br J Surg* (2009) 96(8):901–9. doi: 10.1002/bjs.6635
13. Webber J, Steadman R, Mason MD, Tabi Z, Clayton A. Cancer exosomes trigger fibroblast to myofibroblast differentiation. *Cancer Res* (2010) 70 (23):9621–30. doi: 10.1158/0008-5472.can-10-1722
14. Luga V, Zhang L, Viloria-Petit AM, Ogunjimi AA, Inanlou MR, Chiu E, et al. Exosomes mediate stromal mobilization of autocrine Wnt-PCP signaling in breast cancer cell migration. *Cell* (2012) 151(7):1542–56. doi: 10.1016/j.cell.2012.11.024
15. Bai YP, Shang K, Chen H, Ding F, Wang Z, Liang C, et al. FGF-1/-3/FGFR4 signaling in cancer-associated fibroblasts promotes tumor progression in colon cancer through Erk and MMP-7. *Cancer Sci* (2015) 106(10):1278–87. doi: 10.1111/cas.12745
16. Coleman SJ, Chioni AM, Ghallab M, Anderson RK, Lemoine NR, Kocher HM, et al. Nuclear translocation of FGFR1 and FGF2 in pancreatic stellate cells facilitates pancreatic cancer cell invasion. *EMBO Mol Med* (2014) 6 (4):467–81. doi: 10.1002/emmm.201302698
17. Nakazawa K, Yashiro M, Hirakawa K. Keratinocyte growth factor produced by gastric fibroblasts specifically stimulates proliferation of cancer cells from scirrhous gastric carcinoma. *Cancer Res* (2003) 63(24):8848–52.
18. Pietras K, Pahler J, Bergers G, Hanahan D. Functions of paracrine PDGF signaling in the proangiogenic tumor stroma revealed by pharmacological targeting. *PloS Med* (2008) 5(1):e19. doi: 10.1371/journal.pmed.0050019
19. Lu W, Luo Y, Kan M, McKeehan WL. Fibroblast growth factor-10. A second candidate stromal to epithelial cell andromedin in prostate. *J Biol Chem* (1999) 274(18):12827–34. doi: 10.1074/jbc.274.18.12827
20. Otte J, Dizdar L, Behrens B, Goering W, Knoefel WT, Wruck W, et al. FGF Signalling in the Self-Renewal of Colon Cancer Organoids. *Sci Rep* (2019) 9 (1):17365. doi: 10.1038/s41598-019-53907-7
21. Mansukhani A, Bellosta P, Sahni M, Basilico C. Signaling by fibroblast growth factors (FGF) and fibroblast growth factor receptor 2 (FGFR2)-activating mutations blocks mineralization and induces apoptosis in osteoblasts. *J Cell Biol* (2000) 149(6):1297–308. doi: 10.1083/jcb.149.6.1297
22. Sun C, Fukui H, Hara K, Zhang X, Kitayama Y, Eda H, et al. FGF9 from cancer-associated fibroblasts is a possible mediator of invasion and anti-apoptosis of gastric cancer cells. *BMC Cancer* (2015) 15:333. doi: 10.1186/s12885-015-1353-3

23. Presta M, Dell'Era P, Mitola S, Moroni E, Ronca R, Rusnati M. Fibroblast growth factor/fibroblast growth factor receptor system in angiogenesis. *Cytokine Growth factor Rev* (2005) 16(2):159–78. doi: 10.1016/j.cytogfr.2005.01.004
24. Wang Y, Becker D. Antisense targeting of basic fibroblast growth factor and fibroblast growth factor receptor-1 in human melanomas blocks intratumoral angiogenesis and tumor growth. *Nat Med* (1997) 3(8):887–93. doi: 10.1038/nm0897-887
25. Deroanne CF, Hajitou A, Calberg-Bacq CM, Nusgens BV, Lapière CM. Angiogenesis by fibroblast growth factor 4 is mediated through an autocrine up-regulation of vascular endothelial growth factor expression. *Cancer Res* (1997) 57(24):5590–7. doi: 10.1016/S0923-1811(98)83138-1
26. Leali D, Alessi P, Coltrini D, Ronca R, Corsini M, Nardo G, et al. Long pentraxin-3 inhibits FGF8b-dependent angiogenesis and growth of steroid hormone-regulated tumors. *Mol Cancer Ther* (2011) 10(9):1600–10. doi: 10.1158/1535-7163.mct-11-0286
27. Wei W, Mok SC, Oliva E, Kim SH, Mohapatra G, Birrer MJ. FGF18 as a prognostic and therapeutic biomarker in ovarian cancer. *J Clin Invest* (2013) 123(10):4435–48. doi: 10.1172/jci70625
28. Song S, Wientjes MG, Gan Y, Au JL. Fibroblast growth factors: an epigenetic mechanism of broad spectrum resistance to anticancer drugs. *Proc Natl Acad Sci United States America* (2000) 97(15):8658–63. doi: 10.1073/pnas.140210697
29. Hanker AB, Garrett JT, Estrada MV, Moore PD, Ericsson PG, Koch JP, et al. HER2-Overexpressing Breast Cancers Amplify FGFR Signaling upon Acquisition of Resistance to Dual Therapeutic Blockade of HER2. *Clin Cancer Res* (2017) 23(15):4323–34. doi: 10.1158/1078-0432.ccr-16-2287
30. Morisaki T, Yashiro M, Kakehashi A, Inagaki A, Kinoshita H, Fukuoka T, et al. Comparative proteomics analysis of gastric cancer stem cells. *PloS One* (2014) 9(11):e110736. doi: 10.1371/journal.pone.0110736
31. Knuchel S, Anderle P, Werfelli P, Diamantis E, Rüegg C. Fibroblast surface-associated FGF-2 promotes contact-dependent colorectal cancer cell migration and invasion through FGFR-SRC signaling and integrin αvβ5-mediated adhesion. *Oncotarget* (2015) 6(16):14300–17. doi: 10.18632/oncotarget.3883
32. Yu P, Wilhelm K, Dubrac A, Tung JK, Alves TC, Fang JS, et al. FGF-dependent metabolic control of vascular development. *Nature* (2017) 545 (7653):224–8. doi: 10.1038/nature22322
33. Itoh N, Ornitz DM. Fibroblast growth factors: from molecular evolution to roles in development, metabolism and disease. *J Biochem* (2011) 149(2):121–30. doi: 10.1093/jb/mvq121
34. Turner N, Grose R. Fibroblast growth factor signalling: from development to cancer. *Nat Rev Cancer* (2010) 10(2):116–29. doi: 10.1038/nrc2780
35. Sugiyama N, Varjosalo M, Meller P, Lohi J, Chan KM, Zhou Z, et al. FGF receptor-4 (FGFR4) polymorphism acts as an activity switch of a membrane type 1 matrix metalloproteinase-FGFR4 complex. *Proc Natl Acad Sci United States America* (2010) 107(36):15786–91. doi: 10.1073/pnas.0914459107
36. Sugiyama N, Varjosalo M, Meller P, Lohi J, Hyytiainen M, Kilpinen S, et al. Fibroblast growth factor receptor 4 regulates tumor invasion by coupling fibroblast growth factor signaling to extracellular matrix degradation. *Cancer Res* (2010) 70(20):7851–61. doi: 10.1158/0008-5472.CAN-10-1223
37. Hattori Y, Odagiri H, Nakatani H, Miyagawa K, Naito K, Sakamoto H, et al. K-sam, an amplified gene in stomach cancer, is a member of the heparin-binding growth factor receptor genes. *Proc Natl Acad Sci United States America* (1990) 87(15):5983–7. doi: 10.1073/pnas.87.15.5983
38. Okuno T, Yashiro M, Masuda G, Togano S, Kuroda K, Miki Y, et al. Establishment of a New Scirrhous Gastric Cancer Cell Line with FGFR2 Overexpression, OCUM-14. *Ann Surg Oncol* (2019) 26(4):1093–102. doi: 10.1245/s10434-018-07145-2
39. Orr-Urtreger A, Bedford MT, Burakova T, Arman E, Zimmer Y, Yayon A, et al. Developmental localization of the splicing alternatives of fibroblast growth factor receptor-2 (FGFR2). *Dev Biol* (1993) 158(2):475–86. doi: 10.1006/dbio.1993.1205
40. Eswarakumar VP, Monsonego-Ornan E, Pines M, Antonopoulou I, Morriss-Kay GM, Lonai P. The IIIc alternative of Fgfr2 is a positive regulator of bone formation. *Dev (Cambridge England)* (2002) 129(16):3783–93.
41. Peters KG, Werner S, Chen G, Williams LT. Two FGF receptor genes are differentially expressed in epithelial and mesenchymal tissues during limb formation and organogenesis in the mouse. *Dev (Cambridge England)* (1992) 114(1):233–43.
42. Zhang X, Ibrahimi OA, Olsen SK, Umemori H, Mohammadi M, Ornitz DM. Receptor specificity of the fibroblast growth factor family. The complete mammalian FGF family. *J Biol Chem* (2006) 281(23):15694–700. doi: 10.1074/jbc.M601252200
43. Ornitz DM, Xu J, Colvin JS, McEwen DG, MacArthur CA, Coulier F, et al. Receptor specificity of the fibroblast growth factor family. *J Biol Chem* (1996) 271(25):15292–7. doi: 10.1074/jbc.271.25.15292
44. Nyeng P, Norgaard GA, Kobberup S, Jensen J. FGF10 signaling controls stomach morphogenesis. *Dev Biol* (2007) 303(1):295–310. doi: 10.1016/j.ydbio.2006.11.017
45. Huang T, Wang L, Liu D, Li P, Xiong H, Zhuang L, et al. FGF7/FGFR2 signal promotes invasion and migration in human gastric cancer through upregulation of thrombospondin-1. *Int J Oncol* (2017) 50(5):1501–12. doi: 10.3892/ijo.2017.3927
46. Ren C, Chen H, Han C, Fu D, Wang F, Wang D, et al. The anti-apoptotic and prognostic value of fibroblast growth factor 9 in gastric cancer. *Oncotarget* (2016) 7(24):36655–65. doi: 10.18632/oncotarget.9131
47. Inoue T, Chung YS, Yashiro M, Nishimura S, Hasuma T, Otani S, et al. Transforming growth factor-beta and hepatocyte growth factor produced by gastric fibroblasts stimulate the invasiveness of scirrhous gastric cancer cells. *Jpn J Cancer Res* (1997) 88(2):152–9. doi: 10.1111/j.1349-7006.1997.tb00360.x
48. Ishimoto T, Miyake K, Nandi T, Yashiro M, Onishi N, Huang KK, et al. Activation of Transforming Growth Factor Beta 1 Signaling in Gastric Cancer-associated Fibroblasts Increases Their Motility, via Expression of Rhomboid 5 Homolog 2, and Ability to Induce Invasiveness of Gastric Cancer Cells. *Gastroenterology* (2017) 153(1):191–204 e16. doi: 10.1053/j.gastro.2017.03.046
49. Mahara K, Kato J, Terui T, Takimoto R, Horimoto M, Murakami T, et al. Transforming growth factor beta 1 secreted from scirrhous gastric cancer cells is associated with excess collagen deposition in the tissue. *Br J Cancer* (1994) 69(4):777–83. doi: 10.1038/bjc.1994.147
50. George SJ, Johnson JL, Smith MA, Angelini GD, Jackson CL. Transforming growth factor-beta is activated by plasmin and inhibits smooth muscle cell death in human saphenous vein. *J Vasc Res* (2005) 42(3):247–54. doi: 10.1159/000085657
51. Duffy MJ, Maguire TM, McDermott EW, O'Higgins N. Urokinase plasminogen activator: a prognostic marker in multiple types of cancer. *J Surg Oncol* (1999) 71(2):130–5. doi: 10.1002/(SICI)1096-9098(199906)71:2<130::AID-JSO14>3.0.CO;2-9
52. Herszenyi L, Plebani M, Carraro P, De Paoli M, Roveroni G, Cardin R, et al. Proteases in gastrointestinal neoplastic diseases. *Clin Chim Acta* (2000) 291 (2):171–87. doi: 10.1016/S0009-8981(99)00227-2
53. Yashiro M, Chung YS, Nishimura S, Inoue T, Sowa M. Establishment of two new scirrhous gastric cancer cell lines: analysis of factors associated with disseminated metastasis. *Br J Cancer* (1995) 72(5):1200–10. doi: 10.1038/bjc.1995.486
54. Yoshida K, Yokozaki H, Niimoto M, Ito H, Ito M, Tahara E. Expression of TGF-beta and procollagen type I and type III in human gastric carcinomas. *Int J Cancer* (1989) 44(3):394–8. doi: 10.1002/ijc.2910440303
55. Komuro A, Yashiro M, Iwata C, Morishita Y, Johansson E, Matsumoto Y, et al. Diffuse-type gastric carcinoma: progression, angiogenesis, and transforming growth factor beta signaling. *J Natl Cancer Institute* (2009) 101(8):592–604. doi: 10.1093/jnci/djp058
56. Zeisberg EM, Potenta S, Xie L, Zeisberg M, Kalluri R. Discovery of endothelial to mesenchymal transition as a source for carcinoma-associated fibroblasts. *Cancer Res* (2007) 67(21):10123–8. doi: 10.1158/0008-5472.CAN-07-3127
57. Thiery JP. Epithelial-mesenchymal transitions in tumour progression. *Nat Rev Cancer* (2002) 2(6):442–54. doi: 10.1038/nrc822
58. Kalluri R, Neilson EG. Epithelial-mesenchymal transition and its implications for fibrosis. *J Clin Invest* (2003) 112(12):1776–84. doi: 10.1172/JCI200320530
59. Siegel PM, Massague J. Cytostatic and apoptotic actions of TGF-beta in homeostasis and cancer. *Nat Rev Cancer* (2003) 3(11):807–21. doi: 10.1038/nrc1208

60. Fuyuhiro Y, Yashiro M, Noda S, Matsuoka J, Hasegawa T, Kato Y, et al. Cancer-associated orthotopic myofibroblasts stimulates the motility of gastric carcinoma cells. *Cancer Sci* (2012) 103(4):797–805. doi: 10.1111/j.1349-7006.2012.02209.x
61. Matsuoka J, Yashiro M, Doi Y, Fuyuhiro Y, Kato Y, Shinto O, et al. Hypoxia stimulates the EMT of gastric cancer cells through autocrine TGFbeta signaling. *PloS One* (2013) 8(5):e62310. doi: 10.1371/journal.pone.0062310
62. Hasegawa T, Yashiro M, Nishii T, Matsuoka J, Fuyuhiro Y, Morisaki T, et al. Cancer-associated fibroblasts might sustain the stemness of scirrhous gastric cancer cells via transforming growth factor-beta signaling. *Int J Cancer* (2014) 134(8):1785–95. doi: 10.1002/ijc.28520
63. Fuyuhiro Y, Yashiro M, Noda S, Kashiwagi S, Matsuoka J, Doi Y, et al. Upregulation of cancer-associated myofibroblasts by TGF-beta from scirrhous gastric carcinoma cells. *Br J Cancer* (2011) 105(7):996–1001. doi: 10.1038/bjc.2011.330
64. Tahara E. Genetic pathways of two types of gastric cancer. *IARC Sci Publ* (2004) 157):327–49.
65. Humar B, Guilford P. Hereditary diffuse gastric cancer: a manifestation of lost cell polarity. *Cancer Sci* (2009) 100(7):1151–7. doi: 10.1111/j.1349-7006.2009.01163.x
66. Yashiro M, Nishioka N, Hirakawa K. Decreased expression of the adhesion molecule desmoglein-2 is associated with diffuse-type gastric carcinoma. *Eur J Cancer* (2006) 42(14):2397–403. doi: 10.1016/j.ejca.2006.03.024
67. Nishioka N, Yashiro M, Inoue T, Matsuoka T, Ohira M, Chung KH. A candidate tumor suppressor locus for scirrhous gastric cancer at chromosome 18q 12.2. *Int J Oncol* (2001) 18(2):317–22. doi: 10.3892/ijo.18.2.317
68. Han SU, Lee HY, Lee JH, Kim WH, Nam H, Kim H, et al. Modulation of E-cadherin by hepatocyte growth factor induces aggressiveness of gastric carcinoma. *Ann Surg* (2005) 242(5):676–83. doi: 10.1097/01.sla.0000186171.85804.fe
69. Stetler-Stevenson WG, Aznavoorian S, Liotta LA. Tumor cell interactions with the extracellular matrix during invasion and metastasis. *Annu Rev Cell Biol* (1993) 9:541–73. doi: 10.1146/annurev.cb.09.110193.002545
70. Boire A, Covic L, Agarwal A, Jacques S, Sherifi S, Kuliopulos A. PAR1 is a matrix metalloprotease-1 receptor that promotes invasion and tumorigenesis of breast cancer cells. *Cell* (2005) 120(3):303–13. doi: 10.1016/j.cell.2004.12.018
71. Yashiro M, Chung YS, Sowa M. Tranilast (N-(3,4-dimethoxycinnamoyl) anthranilic acid) down-regulates the growth of scirrhous gastric cancer. *Anticancer Res* (1997) 17(2A):895–900.
72. Panchenko MV, Stetler-Stevenson WG, Trubetskoy OV, Gacheru SN, Kagan HM. Metalloproteinase activity secreted by fibrogenic cells in the processing of prolysyl oxidase. Potential role of procollagen C-proteinase. *J Biol Chem* (1996) 271(12):7113–9. doi: 10.1074/jbc.271.12.7113
73. Uzel MI, Scott IC, Babakhanlou-Chase H, Palamakumbura AH, Pappano WN, Hong HH, et al. Multiple bone morphogenetic protein 1-related mammalian metalloproteinases process pro-lysyl oxidase at the correct physiological site and control lysyl oxidase activation in mouse embryo fibroblast cultures. *J Biol Chem* (2001) 276(25):22537–43. doi: 10.1074/jbc.M102352200
74. Borel A, Eichenberger D, Farjanel J, Kessler E, Gleyzal C, Hulmes DJ, et al. Lysyl oxidase-like protein from bovine aorta. Isolation and maturation to an active form by bone morphogenetic protein-1. *J Biol Chem* (2001) 276 (52):48944–9. doi: 10.1074/jbc.M109499200
75. Xiao Q, Ge G. Lysyl oxidase, extracellular matrix remodeling and cancer metastasis. *Cancer Microenviron Off J Int Cancer Microenviron Soc* (2012) 5 (3):261–73. doi: 10.1007/s12307-012-0105-z
76. Kasashima H, Yashiro M, Kinoshita H, Fukuoka T, Morisaki T, Masuda G, et al. Lysyl oxidase is associated with the epithelial-mesenchymal transition of gastric cancer cells in hypoxia. *Gastric Cancer* (2015) 19(2):431-42. doi: 10.1007/s10120-015-0510-3
77. Kasashima H, Yashiro M, Kinoshita H, Fukuoka T, Morisaki T, Masuda G, et al. Lysyl oxidase-like 2 (LOXL2) from stromal fibroblasts stimulates the progression of gastric cancer. *Cancer Lett* (2014) 354(2):438–46. doi: 10.1016/j.canlet.2014.08.014
78. Kasashima H, Yashiro M, Nakamae H, Kitayama K, Masuda G, Kinoshita H, et al. CXCL1-Chemokine (C-X-C Motif) Receptor 2 Signaling Stimulates the Recruitment of Bone Marrow-Derived Mesenchymal Cells into Diffuse-Type Gastric Cancer Stroma. *Am J Pathol* (2016) 186(11):3028–39. doi: 10.1016/j.ajpath.2016.07.024
79. Valadi H, Ekstrom K, Bossios A, Sjostrand M, Lee JJ, Lotvall JO. Exosome-mediated transfer of mRNAs and microRNAs is a novel mechanism of genetic exchange between cells. *Nat Cell Biol* (2007) 9(6):654–9. doi: 10.1038/ncb1596
80. Ruivo CF, Adem B, Silva M, Melo SA. The Biology of Cancer Exosomes: Insights and New Perspectives. *Cancer Res* (2017) 77(23):6480–8. doi: 10.1158/0008-5472.CAN-17-0994
81. Miki Y, Yashiro M, Okuno T, Kitayama K, Masuda G, Hirakawa K, et al. CD9-positive exosomes from cancer-associated fibroblasts stimulate the migration ability of scirrhous-type gastric cancer cells. *Br J Cancer* (2018) 118(6):867–77. doi: 10.1038/bjc.2017.487
82. Zhang J, Zhou Y, Huang T, Wu F, Pan Y, Dong Y, et al. FGF18, a prominent player in FGF signaling, promotes gastric tumorigenesis through autocrine manner and is negatively regulated by miR-590-5p. *Oncogene* (2019) 38 (1):33–46. doi: 10.1038/s41388-018-0430-x
83. Zhang H, Deng T, Liu R, Ning T, Yang H, Liu D, et al. CAF secreted miR-522 suppresses ferroptosis and promotes acquired chemo-resistance in gastric cancer. *Mol Cancer* (2020) 19(1):43. doi: 10.1186/s12943-020-01168-8
84. Itoh G, Chida S, Yanagihara K, Yashiro M, Aiba N, Tanaka M. Cancer-associated fibroblasts induce cancer cell apoptosis that regulates invasion mode of tumours. *Oncogene* (2017) 36(31):4434–44. doi: 10.1038/onc.2017.49
85. Joyce JA, Pollard JW. Microenvironmental regulation of metastasis. *Nat Rev Cancer* (2009) 9(4):239–52. doi: 10.1038/nrc2618
86. Nishimura S, Chung YS, Yashiro M, Inoue T, Sowa M. CD44H plays an important role in peritoneal dissemination of scirrhous gastric cancer cells. *Jpn J Cancer Res* (1996) 87(12):1235–44. doi: 10.1111/j.1349-7006.1996.tb03138.x
87. Koyama T, Yashiro M, Inoue T, Nishimura S, Hirakawa YSCK. TGF-beta1 secreted by gastric fibroblasts up-regulates CD44H expression and stimulates the peritoneal metastatic ability of scirrhous gastric cancer cells. *Int J Oncol* (2000) 16(2):355–62. doi: 10.3892/ijo.16.2.355
88. Nishimura S, Chung YS, Yashiro M, Inoue T, Sowa M. Role of alpha 2 beta 1-and alpha 3 beta 1-integrin in the peritoneal implantation of scirrhous gastric carcinoma. *Br J Cancer* (1996) 74(9):1406–12. doi: 10.1038/bjc.1996.556
89. Kizaka-Kondoh S, Itasaka S, Zeng L, Tanaka S, Zhao T, Takahashi Y, et al. Selective killing of hypoxia-inducible factor-1-active cells improves survival in a mouse model of invasive and metastatic pancreatic cancer. *Clin Cancer Res* (2009) 15(10):3433–41. doi: 10.1158/1078-0432.CCR-08-2267
90. Nishimura S, Hirakawa-Chung KY, Yashiro M, Inoue T, Matsuoka T, Fujihara T, et al. TGF-beta1 produced by gastric cancer cells affects mesothelial cell morphology in peritoneal dissemination. *Int J Oncol* (1998) 12(4):847–51. doi: 10.3892/ijo.12.4.847
91. Yashiro M, Chung YS, Nishimura S, Inoue T, Sowa M. Peritoneal metastatic model for human scirrhous gastric carcinoma in nude mice. *Clin Exp Metastasis* (1996) 14(1):43–54. doi: 10.1007/BF00157685
92. Yashiro M, Chung YS, Inoue T, Nishimura S, Matsuoka T, Fujihara T, et al. Hepatocyte growth factor (HGF) produced by peritoneal fibroblasts may affect mesothelial cell morphology and promote peritoneal dissemination. *Int J Cancer* (1996) 67(2):289–93. doi: 10.1002/(SICI)1097-0215(19960717)67:2<289::AID-IJC22>3.0.CO;2-5
93. Li Q, Li B, Li Q, Wei S, He Z, Huang X, et al. Exosomal miR-21-5p derived from gastric cancer promotes peritoneal metastasis via mesothelial-to-mesenchymal transition. *Cell Death Dis* (2018) 9(9):854. doi: 10.1038/s41419-018-0928-8
94. Morgensztern D, Karaseva N, Felip E, Delgado I, Burdaeva O, Domine M, et al. An open-label phase IB study to evaluate GSK3052230 in combination with paclitaxel and carboplatin, or docetaxel, in FGFR1-amplified non-small cell lung cancer. *Lung Cancer* (2019) 136:74–9. doi: 10.1016/j.lungcan.2019.08.011
95. Van Cutsem E, Bang YJ, Mansoor W, Petty RD, Chao Y, Cunningham D, et al. A randomized, open-label study of the efficacy and safety of AZD4547 monotherapy versus paclitaxel for the treatment of advanced gastric adenocarcinoma with FGFR2 polysomy or gene amplification. *Ann Oncol Off J Eur Soc Med Oncol / ESMO* (2017) 28(6):1316–24. doi: 10.1093/annonc/mdx107
96. Guagnano V, Kauffmann A, Wohrle S, Stamm C, Ito M, Barys L, et al. FGFR genetic alterations predict for sensitivity to NVP-BGJ398, a selective pan-FGFR inhibitor. *Cancer Discovery* (2012) 2(12):1118–33. doi: 10.1158/2159-8290.cd-12-0210
97. Nogova L, Sequist LV, Perez Garcia JM, Andre F, Delord JP, Hidalgo M, et al. Evaluation of BGJ398, a Fibroblast Growth Factor Receptor 1-3 Kinase

Inhibitor, in Patients With Advanced Solid Tumors Harboring Genetic Alterations in Fibroblast Growth Factor Receptors: Results of a Global Phase I, Dose-Escalation and Dose-Expansion Study. *J Clin Oncol* (2017) 35 (2):157–65. doi: 10.1200/JCO.2016.67.2048

98. Watanabe Miyano S, Yamamoto Y, Kodama K, Miyajima Y, Mikamoto M, Nakagawa T, et al. E7090, a Novel Selective Inhibitor of Fibroblast Growth Factor Receptors, Displays Potent Antitumor Activity and Prolongs Survival in Preclinical Models. *Mol Cancer Ther* (2016) 15(11):2630–9. doi: 10.1158/1535-7163.mct-16-0261
99. Koyama T, Shimizu T, Iwasa S, Fujiwara Y, Kondo S, Kitano S, et al. First-in-human phase I study of E7090, a novel selective fibroblast growth factor receptor inhibitor, in patients with advanced solid tumors. *Cancer Sci* (2020) 111(2):571–9. doi: 10.1111/cas.14265
100. Michael M, Bang YJ, Park YS, Kang YK, Kim TM, Hamid O, et al. A Phase 1 Study of LY2874455, an Oral Selective pan-FGFR Inhibitor, in Patients with Advanced Cancer. *Targeted Oncol* (2017) 12(4):463–74. doi: 10.1007/s11523-017-0502-9
101. Tabernero J, Bahleda R, Dienstmann R, Infante JR, Mita A, Italiano A, et al. Phase I Dose-Escalation Study of JNJ-42756493, an Oral Pan-Fibroblast Growth Factor Receptor Inhibitor, in Patients With Advanced Solid Tumors. *J Clin Oncol* (2015) 33(30):3401–8. doi: 10.1200/JCO.2014.60.7341
102. Nishina T, Takahashi S, Iwasawa R, Noguchi H, Aoki M, Doi T. Safety, pharmacokinetic, and pharmacodynamics of erdafitinib, a pan-fibroblast growth factor receptor (FGFR) tyrosine kinase inhibitor, in patients with advanced or refractory solid tumors. *Investigational New Drugs* (2018) 36 (3):424–34. doi: 10.1007/s10637-017-0514-4
103. Soria JC, DeBraud F, Bahleda R, Adamo B, Andre F, Dienstmann R, et al. Phase I/IIa study evaluating the safety, efficacy, pharmacokinetics, and pharmacodynamics of lucitanib in advanced solid tumors. *Ann Oncol Off J Eur Soc Med Oncol / ESMO* (2014) 25(11):2244–51. doi: 10.1093/annonc/mdu390
104. Papadopoulos KP, El-Rayes BF, Tolcher AW, Patnaik A, Rasco DW, Harvey RD, et al. A Phase 1 study of ARQ 087, an oral pan-FGFR inhibitor in patients with advanced solid tumours. *Br J Cancer* (2017) 117(11):1592–9. doi: 10.1038/bjc.2017.330
105. Sarker D, Molife R, Evans TR, Hardie M, Marriott C, Butzberger-Zimmerli P, et al. A phase I pharmacokinetic and pharmacodynamic study of TKI258, an oral, multitargeted receptor tyrosine kinase inhibitor in patients with advanced solid tumors. *Clin Cancer Res* (2008) 14(7):2075–81. doi: 10.1158/1078-0432.ccr-07-1466
106. Bierie B, Moses HL. Tumour microenvironment: TGFbeta: the molecular Jekyll and Hyde of cancer. *Nat Rev Cancer* (2006) 6(7):506–20. doi: 10.1038/nrc1926
107. Akhurst RJ. TGF-beta antagonists: why suppress a tumor suppressor? *J Clin Invest* (2002) 109(12):1533–6. doi: 10.1172/JCI0215970
108. Prud'homme GJ. Pathobiology of transforming growth factor beta in cancer, fibrosis and immunologic disease, and therapeutic considerations. *Lab Invest* (2007) 87(11):1077–91. doi: 10.1038/labinvest.3700669
109. Murahashi K, Yashiro M, Inoue T, Nishimura S, Matsuoka T, Sawada T, et al. Tranilast and cisplatin as an experimental combination therapy for scirrhous gastric cancer. *Int J Oncol* (1998) 13(6):1235–40. doi: 10.3892/ijo.13.6.1235
110. Yashiro M, Murahashi K, Matsuoka T, Nakazawa K, Tanaka H, Osaka H, et al. Tranilast (N-3,4-dimethoxycinamoyl anthranilic acid): a novel inhibitor of invasion-stimulating interaction between gastric cancer cells and orthotopic fibroblasts. *Anticancer Res* (2003) 23(5A):3899–904.
111. Saito H, Fushida S, Harada S, Miyashita T, Oyama K, Yamaguchi T, et al. Importance of human peritoneal mesothelial cells in the progression, fibrosis, and control of gastric cancer: inhibition of growth and fibrosis by tranilast. *Gastric Cancer* (2018) 21(1):55–67. doi: 10.1007/s10120-017-0726-5
112. Iveson T, Donehower RC, Davidenko I, Tjulandin S, Deptala A, Harrison M, et al. Rilotumumab in combination with epirubicin, cisplatin, and capecitabine as first-line treatment for gastric or oesophagogastric junction adenocarcinoma: an open-label, dose de-escalation phase 1b study and a double-blind, randomised phase 2 study. *Lancet Oncol* (2014) 15(9):1007–18. doi: 10.1016/s1470-2045(14)70023-3
113. Catenacci DVT, Tebbutt NC, Davidenko I, Murad AM, Al-Batran SE, Ilson DH, et al. Rilotumumab plus epirubicin, cisplatin, and capecitabine as first-line therapy in advanced MET-positive gastric or gastro-oesophageal junction cancer (RILOMET-1): a randomised, double-blind, placebo-controlled, phase 3 trial. *Lancet Oncol* (2017) 18(11):1467–82. doi: 10.1016/s1470-2045(17)30566-1
114. Van Cutsem E, Karaszewska B, Kang YK, Chung HC, Shankaran V, Siena S, et al. A Multicenter Phase II Study of AMG 337 in Patients with MET-Amplified Gastric/Gastroesophageal Junction/Esophageal Adenocarcinoma and Other MET-Amplified Solid Tumors. *Clin Cancer Res* (2019) 25 (8):2414–23. doi: 10.1158/1078-0432.ccr-18-1337
115. Chen LT, Satoh T, Ryu MH, Chao Y, Kato K, Chung HC, et al. A phase 3 study of nivolumab in previously treated advanced gastric or gastroesophageal junction cancer (ATTRACTION-2): 2-year update data. *Gastric Cancer* (2020) 23(3):510–9. doi: 10.1007/s10120-019-01034-7
116. Kang YK, Boku N, Satoh T, Ryu MH, Chao Y, Kato K, et al. Nivolumab in patients with advanced gastric or gastro-oesophageal junction cancer refractory to, or intolerant of, at least two previous chemotherapy regimens (ONO-4538-12, ATTRACTION-2): a randomised, double-blind, placebo-controlled, phase 3 trial. *Lancet* (2017) 390(10111):2461–71. doi: 10.1016/s0140-6736(17)31827-5
117. Sweis RF, Spranger S, Bao R, Paner GP, Stadler WM, Steinberg G, et al. Molecular Drivers of the Non-T-cell-Inflamed Tumor Microenvironment in Urothelial Bladder Cancer. *Cancer Immunol Res* (2016) 4(7):563–8. doi: 10.1158/2326-6066.cir-15-0274
118. Sangeetha Palakurthi MK, Zacharek S, Liu J, Bonal D, Huang W, Depeaux K, et al. Improved survival with erdafitinib (JNJ-42756493) and PD-1 blockade mediated by enhancement of anti-tumor immunity in an FGFR2-driven genetically engineered mouse model of lung cancer. *Cancer Immunol Res* (2017) 5(Suppl. 3):B27.
119. Bang TD Y-J, Kondo S, Chung HC, Muro K, Dussault I, Helwig C, et al. Updated results from a phase I trial of M7824 (MSB0011359C), a bifunctional fusion protein targeting PD-L1 and TGF-β, in patients with pretreated recurrent or refractory gastric cancer. *Ann Oncol* (2018) 29 (SUPPLEMENT 8):VIII222–VIII3. doi: 10.1093/annonc/mdy282.045

Conflict of Interest: The authors declare that the research was conducted in the absence of any commercial or financial relationships that could be construed as a potential conflict of interest.

Copyright © 2020 Miki, Yashiro, Moyano-Galceran, Sugimoto, Ohira and Lehti. This is an open-access article distributed under the terms of the Creative Commons Attribution License (CC BY). The use, distribution or reproduction in other forums is permitted, provided the original author(s) and the copyright owner(s) are credited and that the original publication in this journal is cited, in accordance with accepted academic practice. No use, distribution or reproduction is permitted which does not comply with these terms.

frontiers in Oncology

ORIGINAL RESEARCH
published: 07 December 2020
doi: 10.3389/fonc.2020.551228

Thrombospondin-1 Receptor CD47 Overexpression Contributes to P-Glycoprotein-Mediated Multidrug Resistance Against Doxorubicin in Thyroid Carcinoma FTC-133 Cells

Marie-Pierre Courageot[1], Laurent Duca[2], Laurent Martiny[2], Emmanuelle Devarenne-Charpentier[2], Hamid Morjani[1†] and Hassan El Btaouri[2†]*

[1] Laboratoire de Biospectroscopie Translationnelle (BioSpecT), UFR Pharmacie, Université de Reims Champagne Ardenne, Reims, France, [2] UMR-CNRS 7369 Matrice Extracellulaire et Dynamique Cellulaire (MEDyC), UFR Sciences Exactes et Naturelles, Université de Reims Champagne Ardenne, Moulin de la Housse, Reims, France

It is now admitted that in addition to acquired resistance, the tumor microenvironment contributes to the development of chemo-resistance and malignant progression. In a previous study, we showed that Dox induced apoptosis in FTC-133 cells by trigging JNK pathway. This process was accompanied by a decrease of thrombospondin-1 (TSP-1) expression. Moreover, exogenous TSP-1 or its C-terminal-derived peptide interact with receptor CD47 and are able to protect FTC-133 cells against Dox-induced apoptosis. Here, we investigated the involvement of TSP-1/CD47 interaction in a context of acquired multidrug resistance in FTC-133 cells. To that end, we established a Dox-resistant cell line (FTC-133R cells) which developed a resistance against Dox-induced apoptosis. Cell viability was evaluated by Uptiblue assay, nuclear Dox was measured by microspectrofluorimetry, caspase activity was measured by fluorescence of cleaved caspase-3 substrate, gene expression was evaluated by RT-PCR and protein expression was examined by western-blot. Our results showed that FTC-133R overexpressed the P-gp and were 15-fold resistant to Dox. JNK phosphorylation and Dox-induced apoptosis were reduced in FTC-133R cells. Expression of CD47 was increased in FTC-133R cells but TSP-1 expression presented similar levels in two cell lines. VPL restored Dox nuclear uptake and FTC-133R cell sensitivity to apoptosis and induced a decrease in CD47 mRNA expression. Moreover, knockdown of CD47 in FTC-133R cells induced an increase in JNK activation and sensitized FTC-133R cells to Dox. Our data suggest that CD47 is able to contribute to the protection of FTC-133R cells against Dox-induced apoptosis and/or to potentiate the acquired Dox resistance.

Keywords: chemo-resistance, doxorubicin, P-glycoprotein, TSP-1, CD47, thyroid carcinoma cells

OPEN ACCESS

Edited by:
Dong-Hua Yang,
St. John's University, United States

Reviewed by:
Shih-Wei Wang,
Mackay Medical College, Taiwan
Jih-Hwa Guh,
National Taiwan University, Taiwan

****Correspondence:***
Hassan El Btaouri
hassan.elbtaouri@univ-reims.fr

†These authors have contributed equally to this work

Specialty section:
This article was submitted to Molecular and Cellular Oncology, a section of the journal Frontiers in Oncology

Received: *12 April 2020*
Accepted: *02 November 2020*
Published: *07 December 2020*

Citation:
Courageot M-P, Duca L, Martiny L, Devarenne-Charpentier E, Morjani H and El Btaouri H (2020) Thrombospondin-1 Receptor CD47 Overexpression Contributes to P-Glycoprotein-Mediated Multidrug Resistance Against Doxorubicin in Thyroid Carcinoma FTC-133 Cells. Front. Oncol. 10:551228. doi: 10.3389/fonc.2020.551228

INTRODUCTION

Mechanisms associated with "acquired resistance" to cancer chemotherapy include decreased cellular incorporation of drugs, qualitative and/or quantitative modification of the therapeutic target, drug metabolism that decreases their effectiveness, repair of damage caused by the drug, and activation of anti-apoptotic pathways. In this case, some "predisposed" cells develop one of these mechanisms thus leading to the development of a "secondary resistant" tumor (1–3).

The main cause explaining the decrease of drug cellular incorporation is due to expression of several ATP Binding Cassette (ABC) transporters (4, 5). The first ABC transporter identified is the P-glycoprotein (P-gp) encoded by *ABCB1* gene (6, 7). The ABC proteins transport the anticancer drugs to the extracellular medium so leading to a decrease of drug concentration in the target cell nucleus. Such mechanism of resistance is called Multi-Drug Resistance (MDR). Several strategies have been developed to overcome this MDR, particularly by using small molecules able to inhibit ABC protein transport activity (8, 9). The first inhibitor described as able to inhibit P-gp and to restore sensitivity to anticancer drug is the Ca^{2+} channel inhibitor verapamil (VPL) (10–13).

However, the tumor cell escape from the drug cytotoxic effects can also involve a "*de novo* resistance". Various factors present in the tumor cell microenvironment contribute to the development of this resistance (14, 15). On the one hand, interstitial proteins of the stroma, such as collagen and fibronectin, have been identified as adhesive factors able to induce resistance to chemotherapy by interacting with specific receptors and inducing survival signaling pathways (16–18). On the other hand, stromal soluble factors can also affect cancer cell survival. This is the case for TGFβ1 which sensitize ovarian carcinoma cells to paclitaxel (19). Thrombospondin-1 (TSP-1) is able to sensitize prostate carcinoma cells to the cytotoxic effect of taxol *via* its interaction with the CD47 receptor (20).

In previous works, we have reported that TSP-1 induced FTC-133 thyroid carcinoma cell survival and protection against apoptosis. In fact, camptothecin and doxorubicin (Dox), which inhibit topoisomerases I and II respectively, induced apoptosis in FTC-133 cells through the *de novo* synthesis of ceramides (21). We have showed that both drugs activated the c-Jun N-terminal kinase/Activating transcription factor-2 (JNK/ATF-2) pathway to induce apoptosis through a *de novo* synthesis of ceramide (22). This apoptosis was accompanied by a decrease of TSP-1 expression. Addition of exogenous TSP-1 protected cells against drug-induced apoptosis (23). Moreover, the anti-apoptotic role of TSP-1 involves its C-terminus part which interacts with the CD47 membrane receptor (23, 24).

In the present study, we have investigated how TSP-1/CD47 interaction can modulate the phenotype MDR. In order to perform this study, we established a Dox-resistant FTC-133 cell line (FTC-133R cell) by stepwise increasing drug concentration. We showed that FTC-133R cells are characterized by an overexpression of the P-gp and an increase of CD47 membrane receptor and develop a resistance to Dox-induced apoptosis by inhibiting Dox nuclear accumulation and preventing JNK pathway activation. The P-gp overexpression and TSP-1/CD47 interaction contributed to the development of this resistance. In fact, inhibition of P-gp function by VPL reduced CD47 and TSP-1 expression and sensitized FTC-133R cell to Dox-induced apoptosis by activating JNK pathway. Moreover, inhibition of CD47 expression by small interfering RNA (SiRNA) bypassed P-gp-induced resistance and restored the drug cytotoxicity by activating JNK pathway in FTC-133R cells. These data confirmed that the tumor microenvironment was a key player in the development of *de novo* chemoresistance, thereby influencing the development of acquired resistance. It is therefore possible to sensitize FTC-133R to chemotherapeutic treatment-induced apoptosis by acting directly on extracellular matrix components or by activating intracellular JNK pathway.

MATERIALS AND METHODS

Materials

FTC-133 is a human follicular thyroid carcinoma derived cell line (ECACC94060901) obtained from a lymph node metastasis. Dox was obtained from Farmitalia (Italy). FTC-133R cells were selected from FTC-133 parental cells by stepwise increase of Dox concentration (from 10 to 400 nM) according to protocol of Chen et al. (25) modified. For the development FTC-133R, FTC-133 cells were incubated with 10 nM Dox and the drug concentration was doubled each time the treated cells reached the growth rate of the untreated cells, until the final concentration of 400 nM Dox was applied. Dulbecco's modified Eagle's medium/F-12, trypsin, and Lipofectamine RNAiMAX were purchased from Invitrogen (France). Foetal calf serum from Dutscher (France). TSP-1 monoclonal antibodies from ThermoFisher Scientific (France). Caspase-3, JNK, Phospho-JNK, CD47, and P-gp antibodies from Cell Signaling Technology (France). CD47 siRNA kit from Santa Cruz Biotechnology Inc (USA). ECL Western blotting detection reagents from Amersham (Germany). UptiBlue and BCA kit from Uptima (France). RNeasy® Mini kit from Qiagen (France). CaspACE assay kit, AMV reverse transcriptase and oligo(dT) primers from Promega (France). Anisomycin, VPL, β-actin antibodies, and all other reagents from Sigma (USA).

Cell Culture

FTC-133 and FTC-133R cells were cultured in 75 cm^2 flasks at 37°C containing Dulbecco's modified Eagle's medium/F-12 (1:1) supplemented with 10% (v/v) heat inactivated foetal calf serum, 100 µg/ml streptomycin and 100 IU/ml penicillin in a 5% CO_2/95% air-water saturated atmosphere [5]. After trypsinization, cells were cultured in 96-well plates for cell viability assay and in 6-well plates for flow cytometry, spectrofluorometry, western blot, mRNA extraction, cell transfection, and caspase assay.

Cell Viability Determination

Cells were seeded into 96-well plates at a density of 10^4 cells/ml for 24 h. The medium was then replaced with serum

free medium with or without different concentrations of Mitoxantrone, camptothecin, anisomycin or Dox in presence or absence of VPL 1 μM. After 24 h incubation, 10% (v/v) UptiBlue was added during an additional 3 h. The viability was then measured by spectrofluorometry (λex: 530–560 nm; λem: 590 nm). Results were calculated as percent of control as follows: (experimental absorbance/untreated control absorbance) ×100.

Nuclear Incorporation of Dox

Monitoring of the nuclear Dox incorporation was carried out using the microspectrofluorimeter M51 (Horiba Jobin Yvon France, Villeneuve d'Ascq). The cells were seeded in Petri dish 24 h prior to the measurements. After treatment with Dox 4 μM for 5 h, they were washed with PBS free of drug and placed in the medium without phenol red. To obtain fluorescence emission spectra, the 488 nm line was used with a ionized Argon laser (2065 series, SpectraPhysics, France). A nuclear spectrum of treated cells was obtained over the 500–700 nm wavelength range (26). The semi-quantification of nuclear Dox incorporation was obtained by measuring the fluorescence emission intensity of the band at 590 nm.

Western Blot

After treatment, the cells were centrifuged (3,000 g, 5 min, 4°C) then washed with ice-cold PBS and lysed in an ice cold lysis buffer containing 10 mM Tris pH 7.4, 150 mM NaCl, 5 mM EDTA, 1 mM Na_3VO_4, 1 mM dithiothreitol, 10 μg/ml leupeptin, 10 μg/ml aprotinin, 10% (v/v) glycerol, 1% (v/v) Brij. The suspension was placed on ice for 20 min and then centrifuged (14,000 g, 15 min, 4°C). Total protein concentration was determined using BCA assay kit. Equal amounts of proteins were resolved by 10% (v/v) SDS-PAGE gels, transferred to a nitrocellulose membrane and then probed with the appropriate antibodies (monoclonal anti-TSP-1: dilution 1/400; polyclonal anti-caspase-3: dilution 1/1,000; polyclonal anti-P-gp: dilution 1/1,000; polyclonal anti-PhosphoJNK: dilution 1/1,000; polyclonal anti-JNK: dilution 1/1,000; polyclonal anti-CD47: dilution 1/1,000; monoclonal anti-β-actin: dilution 1/8,000). Horseradish peroxidase-conjugated goat anti-rabbit or anti-mouse IgG were used as secondary antibodies (dilution 1/4,000 and 1/10,000 respectively) and proteins were detected using an enhanced chemiluminescence kit.

Caspase-3 Activity

After incubation, the cell were washed twice with PBS and scrapped with the ice-cold lysis buffer. Caspase-3 activity was measured by incubating 50 μg of cytosolic fraction with caspase-3 colorimetric substrate that absorbs at 405 nm following its cleavage. Absorbance was measured with a multichannel plate reader (Metertech. Inc. Σ960).

Reverse Transcription-Polymerase Chain Reaction

RT-PCR was performed on total RNA prepared by RNeasy® Mini kit (QIAGEN). One μg of total RNA was reverse transcribed using AMV reverse transcriptase and oligo(dT)15 primer. Amplification was performed using PCR Master Mix according the manufacturer's instructions. The optimal reaction conditions were: 30 cycles, 56°C for TSP-1 and 25 cycles, 50°C for S26. Specific primer pairs were for CD-47: 5'-GATCAGCT CAGCTACTAT-3' and 5'-ACAATGACAG TGATCACT-3'; for β-Actin: 5'-AGGCACCAGGGCGTGAT-3' and 5'-GCCCACAT AGGAATCCTTCTGAC-3'. The data are presented as the relative expression of target genes using the comparative threshold cycle (Ct) method (27).

Cell Transfection

FTC-133R cells were transfected with non-targeting control scRNA (scRNA-cells) or siRNA specific to CD-47 (siRNA-cells) using Lipofectamine RNAiMAX following the Santa Cruz Biotechnology Inc (USA) the manufacturer's instructions. The summary protocol: the cells were incubated in 6-well plates at 37° C in a CO_2 incubator until they were 60–80% confluent, then washed with Transfection Medium. siRNA or scRNA transfection Reagent mixture (containing 50 pmol) was added and the cells were incubated 5–7 h at 37°C in a CO_2 incubator. Cells were then washed and the efficiency of the CD47 mRNA depletion was checked out by RT-PCR after 24 h of culture period.

Statistics

Each experiment was performed at least in triplicate with three independent sets of culture. Data were expressed as mean ± SEM. The statistical significance of differences was calculated using Student's test. p values referring to corresponding control are NS, not significant; ** and $^{\times\times}$ $p < 0.01$, *** and $^{\times\times\times}$ $p < 0.001$.

RESULTS

Stepwise Selection of Multidrug Resistant-FTC-133 Cells Against Doxorubicin

To establish a Dox-resistant FTC-133 cell line (FTC-133R cell), we progressively incubated FTC-133 cells with increasing concentrations of Dox ranging from 10 to 400 nM. FTC-133 cells which gradually adapted to the higher Dox concentration were named FTC-133 resistant cells (FTC-133-R). Cell observation by phase-contrast microscopy revealed no change in the morphology of FTC-133-R compared to the parental FTC-133 cells. In addition, no significant difference between the two cell lines growth rates was observed for a 24, 48, and 72 h period (**Figure 1A**).

Implication of P-gp in FTC-133R Dox Resistance

To identify the mechanism of resistance to Dox, we first analyzed the expression of P-gp by western blot and we clearly showed a high level of P-gp expression in FTC-133R cells when compared to FTC-133 cells (**Figure 1B**). The chemo-sensitivity to Dox of resistant cells was compared to that of parental cells in the presence of increasing Dox concentrations for a period of 24 h (**Figure 1C**). As expected, Dox decreased FTC-133 cell viability in a dose-dependent manner with an

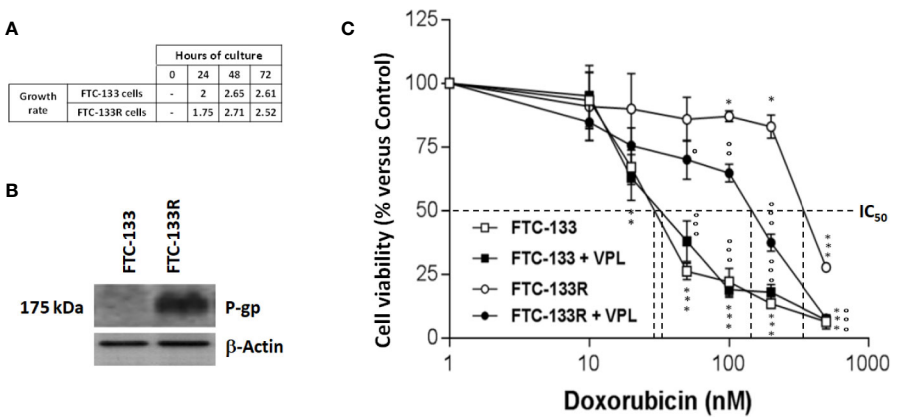

FIGURE 1 | **(A)** FTC-133 and FTC-133R cells were cultured for 24, 48, and 72 h. Cell viability was measured using UptiBlue assay. Growth rate was calculated as ratio between D_{n+1}/D_n **(B)**. FTC-133 and FTC-133R cells were cultured for 24 h. Detection of P-gp was evaluated by Western-blot. β-actin antibody was used as a control. A representative blot of three independent experiments was shown **(C)**. FTC-133 and FTC-133R cells were incubated with Dox at concentrations ranging from 10^{-9} to 10^{-6} M with or without 1 μM VPL. After 24 h, cell viability was measured using UptiBlue assay. Results were calculated as percent of control and represent mean ± standard deviation (S.D.) of at least three independent experiments. The statistical significance of differences was calculated using Student's test. *p < 0.05, **p < 0.01, ***p < 0.001 compared to untreated cells. °p < 0.05, °°p < 0.01, °°°p < 0.001 compared to Dox-treated cells.

IC_{50} = 30 nM. In contrast, FTC-133R cells exhibited a lower sensitivity to Dox, confirmed by a marked increase of IC_{50} to 580 nM. Thus, FTC-133R cells were 19-fold resistant to Dox than FTC-133 cells. Moreover, treatment of FTC-133R cells with VPL (1 μM), a standard P-gp inhibitor, induced a significant increase of Dox cytotoxicity. These results clearly established that P-gp blockade restored the FTC-133R cell sensitivity to Dox thus confirming that this process involved the P-gp transporter. In order to confirm the involvement of P-gp, cells were treated with mitoxantrone, another substrate of P-gp (28). IC_{50} of mitoxantrone was also higher in FTC-133R cells than in FTC133 cells (260 and 16 nM, respectively) (**Figure 2A**). Moreover, the analysis of camptothecin cytotoxicity, a topoisomerase I inhibitor which is not transported by P-gp, showed that IC_{50} of CPT was moderately higher in FTC-133R cells than in FTC133 cells (19 and 9.50 nM, respectively) (**Figure 2B**).

Since cytotoxic activity of Dox depends on its intracellular localization, we then measured nuclear Dox fluorescence in both parental and resistant cells (**Figure 3**). We showed that nuclear Dox fluorescence was about 3 times weaker in FTC-133R cells than in FTC-133 cells. Addition of 1 μM VPL significantly increased drug nuclear accumulation in FTC-133R cells. This result confirmed the P-gp implication in FTC-113R chemoresistance to Dox by decreasing subcellular accumulation and cytotoxicity of Dox. To investigate whether resistance to Dox cytotoxicity in FTC-133R was associated to a protection against apoptosis, we analyzed the caspase-3 activity

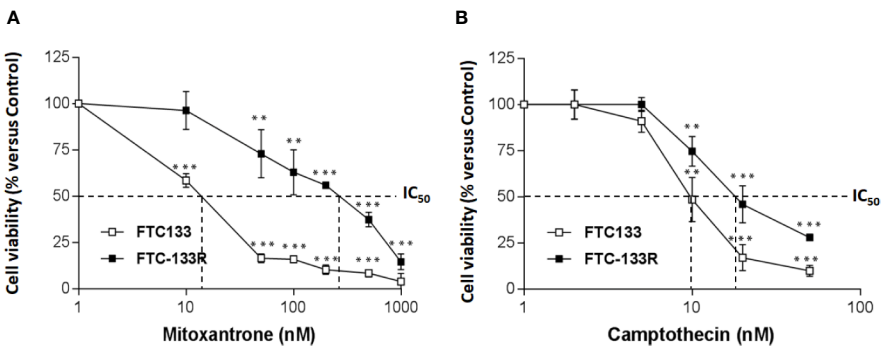

FIGURE 2 | FTC-133 and FTC-133R cells were incubated with **(A)** Mitoxantrone at concentrations ranging from 10^{-9} to 10^{-6} M **(B)**, Camptothecin at concentrations ranging from 10^{-9} to 10^{-7} M. After 24 h, cell viability was measured using UptiBlue assay. Results were calculated as percent of control and represent mean ± standard deviation (S.D.) of at least three independent experiments. The statistical significance of differences was calculated using Student's test. **p < 0.01, ***p < 0.001 compared to untreated cells.

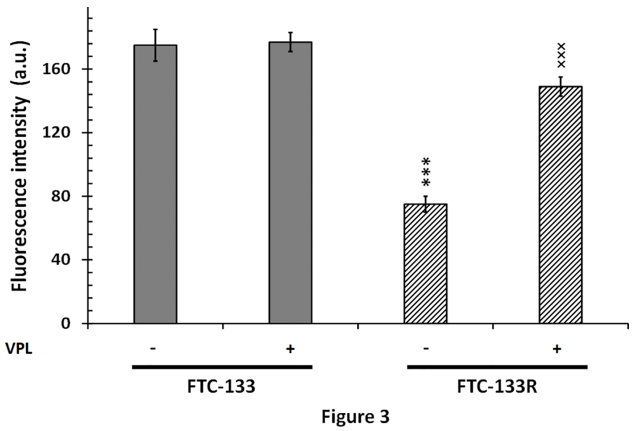

FIGURE 3 | FTC-133 and FTC-133R cells were placed in petri dishes 24 h prior to the experiments and incubated with 4 µM Dox with or without 1 µM VPL for 5 h. The cells were washed with PBS free of drugs and placed in the medium without phenol red at 4°C. The nuclear accumulation of Dox was monitored through its fluorescence emission spectra using confocal laser microspectrofluorometry. A nuclear spectrum of treated cells was obtained over the wavelength range 500–700 nm (26). The semi-quantification of nuclear Dox incorporation was obtained by measuring the fluorescence emission intensity of the band at 590 nm. Results represent mean ± standard deviation (S.D.) of at least three independent experiments. The statistical significance of differences was calculated using Student's test. ***$p < 0.001$ versus FTC-133 and $^{\times\times\times}p < 0.001$ versus FTC-133R.

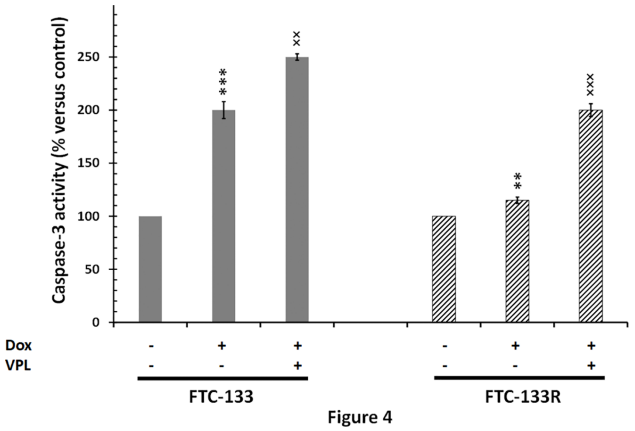

FIGURE 4 | FTC-133 and FTC-133R cells were incubated with 0.1 µM Dox in the absence or presence of 1 µM VPL for 12 h. Caspase-3 activity was measured by caspACE assay kit. Results were calculated as percent of corresponding control and represent mean ± standard deviation (S.D.) of at least three independent experiments. The statistical significance of differences was calculated using Student's test. **$p < 0.01$ and ***$p < 0.001$ versus control, $^{\times\times}p < 0.01$ and $^{\times\times\times}p < 0.001$ versus Dox treatment.

(**Figure 4**). We showed that Dox induced a very slight increase in the caspase-3 activity in FTC-133R cells when compared to FTC-133 cells. In presence of VPL, a significant increase in caspase-3 activity was observed in FTC-133R cells. This suggests that a lack in nuclear uptake of Dox in FTC-133R could be responsible for decrease of Dox cytotoxic effect and low level of caspase-3 activation.

Correlation Between P-gp and CD4/TSP-1 Expression in FTC-133 Resistant Cells

The microenvironment has emerged as a key player in the development of chemoresistance (16, 17, 29, 30). In fact, we previously reported that TSP-1/CD47 interaction could play a role in cell resistance to Dox (23, 24). So, we analyzed the expression of TSP-1 and CD47 in FTC-133R cells. PCR and western blot analysis showed that FTC-133R cells expressed similar levels of TSP-1 mRNA and protein as compared to FTC-133 cells (**Figures 5A, B**). Nevertheless, TSP-1 expression was dramatically abolished by Dox at both mRNA and protein levels in FTC-133 cells while slightly reduced in FTC-133R cells. This effect was amplified by VPL, thus suggesting that P-gp could contribute to maintain TSP-1 expression level. We then analyzed CD47 expression and we showed that CD47 mRNA and protein levels were markedly increased in FTC-133R cells as compared to FTC-133 cells (**Figures 5C, D**). In addition, following Dox treatment, CD47 mRNA and protein expression were dramatically decreased in FTC-133 cells while slightly reduced in FTC-133R cells. This effect was however amplified when Dox treatment was associated to VPL. These results suggest that CD47 overexpression in FTC-133R cells may contribute to cell protection against chemotherapy.

To confirm the role of CD47, its expression was silenced by RNA interference (siRNA) in FTC-133R cells. The efficiency of the transfection was controlled by RT-PCR and showed that CD47 expression was decreased by 83% in siRNA-CD47 transfected cells (siRNA-CD47-FTC-133R) whereas it remained unchanged in scrambled siRNA transfected cells (scRNA-FTC-133R) (**Figure 6A**). Cell viability analysis showed that silencing of CD47 mRNA sensitized FTC-133R to Dox treatment by decreasing cell viability (**Figure 6B**). Indeed, The IC_{50} of Dox was decreased from 450 nM (in scRNA-FTC-133R cells) to 320 nM (in siRNA-CD47-FTC-133R cells) (data not shown). Then, we determined whether these data could be correlated to apoptosis process by analysing caspase-3 activation. Western blot analysis showed that Dox induced an increase in pro-caspase-3 cleavage in FTC-133 cells but had no effect in scRNA-FTC-133R cells (**Figure 7A**). These results were correlated to data obtained on caspase-3 activity (**Figure 7B**). Silencing of CD47 in FTC-133R (siRNA-CD47-FTC-133R) cells restored the pro-apoptotic role of Dox through caspase-3 activation. These results confirmed the contribution of CD47 overexpression in FTC-133R cell to protection against Dox-induced apoptosis.

Anti-Apoptotic Effect of TSP-1/CD47 Interaction in FTC-133R Cells Through Blocking JNK Phosphorylation

In our previous studies, we have shown that JNK signalling pathway was involved in Dox-induced apoptosis of FTC-133 cells (23). Thus, we analyzed JNK phosphorylation in FTC-133

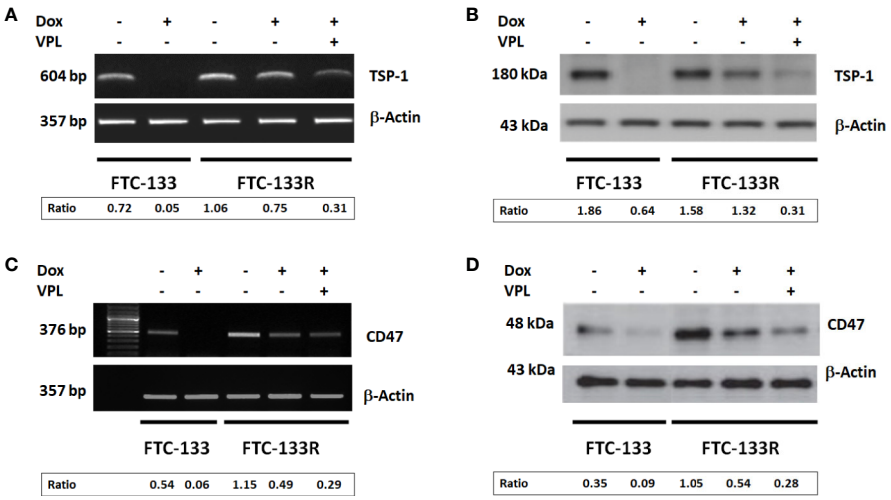

FIGURE 5 | FTC-133 and FTC-133R cells were incubated with 0.1 μM Dox in the absence or presence of 1 μM VPL for 12 h **(A)**. TSP-1 mRNA expression was evaluated by RT–PCR. The constitutively expressed β-actin gene was used as a normalizing control **(B)**. TSP-1 protein secreted in the culture medium was detected by Western blot. β-actin antibody was used as a control **(C)**. CD47 mRNA expression was evaluated by RT–PCR. The constitutively expressed β-actin gene was used as a normalizing control **(D)**. CD47 protein was detected by Western blot. A representative agarose gel electrophoresis and blot of three independent experiments was shown. The intensity of the bands was quantified by densitometry using quantity one program.

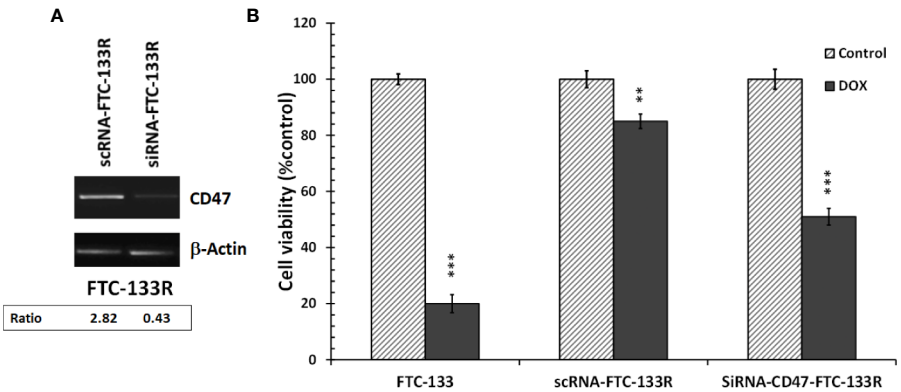

FIGURE 6 | FTC-133R cells were transfected with nontargeting control scRNA (scRNA-FTC-133R) or siRNA specific to CD47 (siRNA-CD47-FTC-133R) using Lipofectamine RNAiMAX **(A)**. CD47 mRNA levels were analyzed by RT-PCR on total RNA prepared by RNeasy® Mini kit. β-actin mRNA was used as a control. A representative agarose gel electrophoresis of three independent experiments was shown **(B)**. FTC-133, scRNA-FTC-133R and siRNA-CD47-FTC-133R cells were incubated with 0.1 μM Dox for 24 h. Cell viability was measured using UptiBlue assay. Results were calculated as percent of corresponding control and represent mean ± standard deviation (S.D.) of at least three independent experiments (**$p < 0.01$ and ***$p < 0.001$ versus control). The intensity of the bands was quantified by densitometry using quantity one program.

and FTC-133R cells (**Figure 8**). Western blot analysis showed that Dox induced JNK phosphorylation in FTC-133 cells but had not effect in FTC-133R cells (**Figure 8A**). However, Dox was able to induce JNK phosphorylation in siRNA-CD47-FTC-133R. These results suggested the implication of TSP-1/CD47 interaction in the protection against apoptosis in FTC-133R cells through blocking JNK phosphorylation. To confirm the involvement of JNK, we used the JNK agonist, anisomycin. As expected, anisomycin (1 and 2 μM) induced JNK phosphorylation in FTC-133R cells in a dose-dependent manner (**Figure 8B**). We then investigated whether JNK phosphorylation could affect FTC-133R cell resistance to the cytotoxic and apoptotic effects of Dox. As shown in **Figure 9**, anisomycin decreased FTC-133R cell viability in a dose-dependent manner and induced an increase in capsase-3 activity. These data suggest that activation of JNK pathway

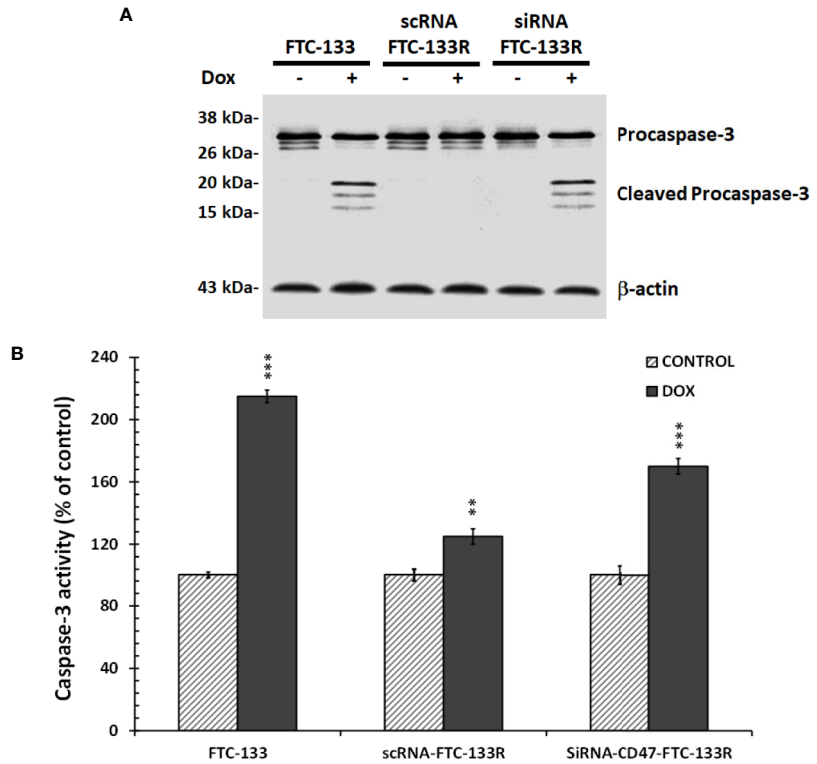

FIGURE 7 | FTC-133, scRNA-FTC-133R, and siRNA-CD47-FTC-133R cells were incubated with 0.1 μM Dox for 12 h **(A)**. Procaspase-3 and cleaved caspase-3 were detected by Western blotting. β-actin antibody was used as a control. A representative blot of three independent experiments was shown **(B)**. Caspase-3 activity was measured by caspACE assay kit. Results were calculated as percent of corresponding control and represent mean ± standard deviation (S.D.) of at least three independent experiments (**p < 0.01 and ***p < 0.001 versus control).. The intensity of the bands was quantified by densitometry using quantity one program.

allows to circumvent resistance of FTC-133R cells to the cytotoxic and apoptotic effects of Dox.

DISCUSSION

Several cellular phenomena contribute to MDR, including overexpression of drug efflux pumps, induction of cell survival pathways, and resistance to apoptosis. Drug efflux is based on the overexpression of ABC transport proteins, such as P-glycoprotein (P-gp), multidrug resistance-associated protein (MRP) and breast cancer resistance protein (BCRP) (1, 4, 5). Apart from cellular events, microenvironmental factors such as remodeling of the extracellular matrix (ECM) are implicated in MDR (31, 32). Since the last few years, several studies have shown that the tumor microenvironment modulates cell response to chemotherapy and it is clearly now admitted that this ECM-mediated effect contributes to a new form of *de novo* resistance (14, 33–35). The Dalton's group was the first to show that fibronectin was able to protect tumor cells from drug-induced apoptosis *via* the β-integrin/PI3-kinase signaling (14, 16, 17, 29, 30, 33, 36). This protective effect has also been described for vitronectin, another ECM protein (37). Conversely, some tumor stroma components are able to sensitize cancer cells to anti-cancer drugs. This is the case with the reduction of TGF in ovarian carcinoma cells treated with paclitaxel and which could be a poor prognosis for patients (19, 38).

Thrombospondin-1 (TSP-1), another ECM component composed of multiple domains, interacts with various partners leading to different effects. Indeed, TSP-1 induces apoptosis of endothelial cells *via* the CD36 receptor but also modulates tumor cell response to chemotherapy *via* the CD47 receptor (20, 39, 40).

We previously reported that Dox-induced apoptosis of human thyroid carcinoma FTC-133 cells *via* JNK/ATF-2 activation. Moreover, this effect was accompanied by a down regulation of TSP-1 expression. Addition of exogenous TSP-1 or its derived peptide 4N1 protects FTC-133 cells against Dox-induced apoptosis. This effect is mediated by TSP-1 C-terminal domain interaction with the membrane receptor CD47 in FTC-133 cells (21–23). These findings suggest that induction of apoptosis by Dox in FTC-133 cells is greatly dependent on a down-regulation of TSP-1 expression and shed new light on a possible role for TSP-1 in drug resistance. However, a link between tumor microenvironment and ABC transporterrelated MDR remains a matter of debate.

In this study, we investigated how TSP-1 contributed to FTC-133 cell *novo* resistance to Dox-induced apoptosis and thereby

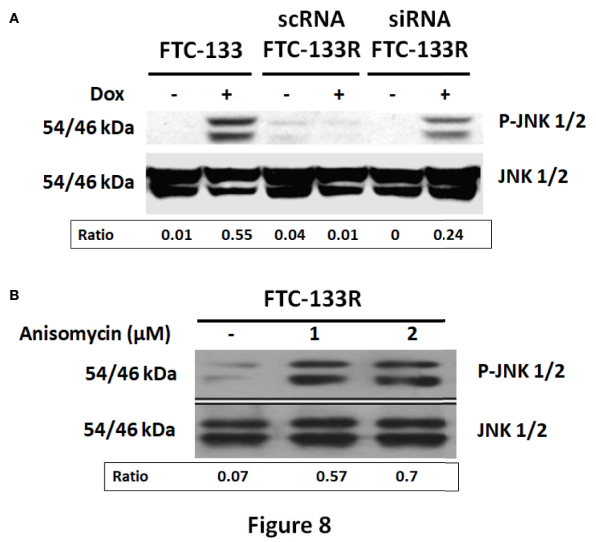

FIGURE 8 | **(A)** FTC-133, scRNA-FTC-133R, and siRNA-CD47-FTC-133R cells were incubated for 12 h with or without 0.1 μM Dox. Detection of p-JNK and JNK were evaluated by Western-blot **(B)**. FTC-133R cells were incubated with anisomycin (1 and 2 μM) for 12 h. Detection of p-JNK and JNK were evaluated by Western-blot. A representative blot of three independent experiments was shown. The intensity of the bands was quantified by densitometry using quantity one program.

affected the development of acquired drug resistance. To that end, we have selected resistant cells (FTC-133R) from the parental FTC-133 cells which overexpressed the ABC transporter P-gp and were 19-fold resistant to Dox as shown by the drug cytotoxic effect and measurement of nuclear drug uptake. Moreover, the P-gp antagonist VPL restored Dox cytotoxicity in FTC-133R cells confirming that P-gp is the predominant mechanism of acquired resistance. Indeed, it has been shown that the overexpression of P-gp in cancer was either an inherent or acquired process: the former, a reflection of its physiologic expression, and the latter, generated by the presence of anticancer drugs (41). P-gp confers resistance by preventing sufficient accumulation of anticancer drugs within the cell, thereby avoiding their cytotoxic or apoptotic effects (41).

This resistance was accompanied by a CD47 elevated expression whereas TSP-1 expression was not affected. Other studies confirmed the overexpression of integrins such as α4β1 and α5β1 in Dox-resistant 8226 myeloma cells and that integrin-mediated adhesion induced apoptosis resistance (42). In the same context, acquisition of MDR in MCF7 cells was associated with markedly decreased expression of α2β1 and αvβ3 integrin's and dramatic up-regulation of α5β1 integrin. Stimulation of β1 integrin signaling strongly sensitizes MCF-7 cells to anoikis (43). In our study, CD47 and TSP-1 expression were correlated to P-pg activity. In fact, inhibition of P-gp activity in FTC-133R cell by VPL significantly reduced both CD47 and TSP-1 expression and sensitized cells to Dox. These results corroborated our previous data reporting that TSP-1/CD47 interaction protected against Dox-induced apoptosis in FTC-133 cells (22, 23). Our studies also suggested that P-gp-overexpressed cells were able to promote the anti-apoptotic role conferred by ECM components. Moreover, prevention of TSP-1/CD47 interaction by siRNA specific to CD47 abolished the TSP-1 anti-apoptotic effect and reduced the resistance to Dox in FTC-133R. Our results clearly showed that CD47 expression was able to regulate cell resistance to Dox despite the P-gp overexpression and confirmed that the microenvironment may contribute and/or potentiate the acquired Dox resistance. Several studies showed that the tumor microenvironment disabled cytotoxic effect of some chemotherapeutic agents resulting in resistance and failure in drug response either through disturbing drug partitioning,

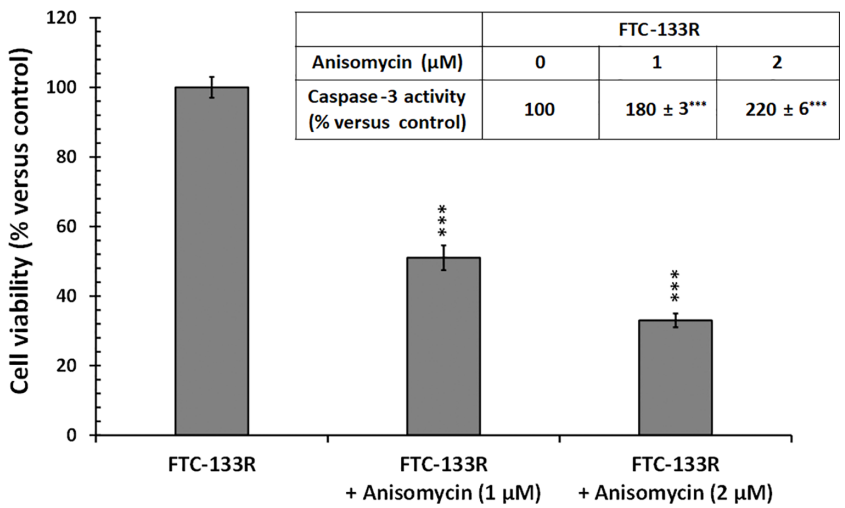

	FTC-133R		
Anisomycin (μM)	0	1	2
Caspase-3 activity (% versus control)	100	180 ± 3***	220 ± 6***

FIGURE 9 | FTC-133R cells were incubated for 24 h with or without anisomycin (1 and 2 μM), cell viability was measured using UptiBlue assay. Insert: FTC-133R cells were incubated for 12 h with or without anisomycin (1 and 2 μM). Caspase-3 activity was measured by caspACE assay kit. Results were calculated as percent of corresponding control and represent mean ± standard deviation (S.D.) of at least three independent experiments (***$p < 0.001$ versus control).

sequestering it intracellularly (31, 44), or through induction of P-gp expression (45, 46). Tatsuta et al (47). showed that ECM components modulated the P-gp expression in brain capillary endothelial cells (47). In the same perspective, Naci et al (18). confirmed that collagen/β1 integrin interaction increased MRP-1 expression in leukemic T-cells, which consequently decreased the amount of intracellular Dox and Dox-induced apoptosis (18).

Our previous data reported that the JNK/ATF-2 signaling pathway was involved in Dox-induced apoptosis in FTC-133 cells (22). Here, we showed that JNK was weakly phosphorylated following Dox treatment in FTC-133R cells. In addition, TSP-1/CD47 interaction contributed to decrease JNK activation and thus protected resistant cells from Dox-induced apoptosis. Moreover, pharmacological JNK activation bypassed resistance and restored the drug cytotoxicity in resistant cell that overexpressed P-pg. Thus, JNK signaling pathway maybe further considered as a relevant target for a novel approach to overcome chemoresistance in thyroid carcinoma. This is in agreement with other that have also reported the impact of JNK on cancer progression and therapy (48, 49).

In conclusion, our study shows that tumor cell microenvironment can modulate the response of cancer cell to chemotherapeutic treatment. Our study demonstrates an important survival role for CD47 and its ligand TSP-1 in Dox-induced apoptosis of FTC-133 cell and thus contribute to the modulation of P-gp drug resistance. Molecular characterization of acquired resistance must take into consideration the interaction of tumor cells with their microenvironment in order to identify new targets of drug resistance.

DATA AVAILABILITY STATEMENT

The original contributions presented in the study are included in the article/supplementary material. Further inquiries can be directed to the corresponding author.

AUTHOR CONTRIBUTIONS

M-PC, HM, LD, HE: performing biochemistry, cell, and molecular biology experiments. LM, ED-C, HM, HE: analysis and interpretation of data. ED-C, HM, HE: drafting of manuscript. M-PC, LM: critical revision. All authors contributed to the article and approved the submitted version.

FUNDING

This work was supported by the University of Reims Champagne Ardennes and the Centre National de la Recherche Scientifique (CNRS).

ACKNOWLEDGMENTS

We thank Marie-Line SOWA for her excellent technical assistance. We thank Sylvie Ricord for her precious assistance in proofreading the document.

REFERENCES

1. Gottesman MM. Mechanisms of cancer drug resistance. *Annu Rev Med* (2002) 53:615–27. doi: 10.1146/annurev.med.53.082901.103929
2. Holohan C, Van Schaeybroeck S, Longley DB, Johnston PG. Cancer drug resistance: an evolving paradigm. *Nat Rev Cancer* (2013) 13:714–26. doi: 10.1038/nrc3599
3. Mansoori B, Mohammadi A, Davudian S, Shirjang S, Baradaran B. The Different Mechanisms of Cancer Drug Resistance: A Brief Review. *Adv Pharm Bull* (2017) 7:339–48. doi: 10.15171/apb.2017.041
4. Gottesman MM, Fojo T, Bates SE. Multidrug resistance in cancer: role of ATP-dependent transporters. *Nat Rev Cancer* (2002) 2:48–58. doi: 10.1038/nrc706
5. Robey RW, Pluchino KM, Hall MD, Fojo AT, Bates SE, Gottesman MM. Revisiting the role of ABC transporters in multidrug-resistant cancer. *Nat Rev Cancer* (2018) 18:452–64. doi: 10.1038/s41568-018-0005-8
6. Biedler JL, Riehm H. Cellular resistance to actinomycin D in Chinese hamster cells in vitro: cross-resistance, radioautographic, and cytogenetic studies. *Cancer Res* (1970) 30:1174–84.
7. Van der Bliek AM, Baas F, Van der Velde-Koerts T, Biedler JL, Meyers MB, Ozols RF, et al. Genes amplified and overexpressed in human multidrug-resistant cell lines. *Cancer Res* (1988) 48:5927–32.
8. Morjani H, Madoulet C. Immunosuppressors as multidrug resistance reversal agents. *Methods Mol Biol* (2010) 596:433–46. doi: 10.1007/978-1-60761-416-6_19
9. Morjani H, Madoulet C. "Reversal Agents for P-Glycoprotein-Mediated Multidrug Resistance". In: *ABC Transporters and Multidrug Resistance*. Eds. Drug Discovery and Development, A Boumendjel, J Boutonnat, J Robert (John Wiley & Sons, Inc), (2009). p. 241–60.
10. Tsuruo T, Iida H, Tsukagoshi S, Sakurai Y. Overcoming of vincristine resistance in P388 leukemia in vivo and in vitro through enhanced cytotoxicity of vincristine and vinblastine by verapamil. *Cancer Res* (1981) 41:1967–72.
11. Amin ML. P-glycoprotein Inhibition for Optimal Drug Delivery. *Drug Target Insights* (2013) 7:27–34. doi: 10.4137/DTI.S12519
12. Romermann K, Wanek T, Bankstahl M, Bankstahl JP, Fedrowitz M, Muller M, et al. (R)-[(11)C]verapamil is selectively transported by murine and human P-glycoprotein at the blood-brain barrier, and not by MRP1 and BCRP. *Nucl Med Biol* (2013) 40:873–8. doi: 10.1016/j.nucmedbio.2013.05.012
13. Muller C, Bailly JD, Goubin F, Laredo J, Jaffrezou JP, Bordier C, et al. Verapamil decreases P-glycoprotein expression in multidrug-resistant human leukemic cell lines. *Int J Cancer* (1994) 56:749–54. doi: 10.1002/ijc.2910560523
14. Meads MB, Gatenby RA, Dalton WS. Environment-mediated drug resistance: a major contributor to minimal residual disease. *Nat Rev Cancer* (2009) 9:665–74. doi: 10.1038/nrc2714
15. Wang M, Zhao J, Zhang L, Wei F, Lian Y, Wu Y, et al. Role of tumor microenvironment in tumorigenesis. *J Cancer* (2017) 8:761–73. doi: 10.7150/jca.17648
16. Hazlehurst LA, Argilagos RF, Emmons M, Boulware D, Beam CA, Sullivan DM, et al. Cell adhesion to fibronectin (CAM-DR) influences acquired mitoxantrone resistance in U937 cells. *Cancer Res* (2006) 66:2338–45. doi: 10.1158/0008-5472.CAN-05-3256
17. Aoudjit F, Vuori K. Integrin signaling inhibits paclitaxel-induced apoptosis in breast cancer cells. *Oncogene* (2001) 20:4995–5004. doi: 10.1038/sj.onc.1204554
18. Naci D, El Azreq MA, Chetoui N, Lauden L, Sigaux F, Charron D, et al. alpha2beta1 integrin promotes chemoresistance against doxorubicin in cancer cells through extracellular signal-regulated kinase (ERK). *J Biol Chem* (2012) 287:17065–76. doi: 10.1074/jbc.M112.349365
19. Ahmed AA, Mills AD, Ibrahim AE, Temple J, Blenkiron C, Vias M, et al. The extracellular matrix protein TGFBI induces microtubule stabilization and sensitizes ovarian cancers to paclitaxel. *Cancer Cell* (2007) 12:514–27. doi: 10.1016/j.ccr.2007.11.014

20. Lih CJ, Wei W, Cohen SN. Txr1: a transcriptional regulator of thrombospondin-1 that modulates cellular sensitivity to taxanes. *Genes Dev* (2006) 20:2082–95. doi: 10.1101/gad.1441306
21. Rath G, Schneider C, Langlois B, Sartelet H, Morjani H, Btaouri HE, et al. De novo ceramide synthesis is responsible for the anti-tumor properties of camptothecin and doxorubicin in follicular thyroid carcinoma. *Int J Biochem Cell Biol* (2009) 41:1165–72. doi: 10.1016/j.biocel.2008.10.021
22. El Btaouri H, Morjani H, Greffe Y, Charpentier E, Martiny L. Role of JNK/ATF-2 pathway in inhibition of thrombospondin-1 (TSP-1) expression and apoptosis mediated by doxorubicin and camptothecin in FTC-133 cells. *Biochim Biophys Acta* (2011) 1813:695–703. doi: 10.1016/j.bbamcr.2011.02.004
23. Rath GM, Schneider C, Dedieu S, Rothhut B, Soula-Rothhut M, Ghoneim C, et al. The C-terminal CD47/IAP-binding domain of thrombospondin-1 prevents camptothecin- and doxorubicin-induced apoptosis in human thyroid carcinoma cells. *Biochim Biophys Acta* (2006) 1763:1125–34. doi: 10.1016/j.bbamcr.2006.08.001
24. Rath GM, Schneider C, Dedieu S, Sartelet H, Morjani H, Martiny L, et al. Thrombospondin-1 C-terminal-derived peptide protects thyroid cells from ceramide-induced apoptosis through the adenylyl cyclase pathway. *Int J Biochem Cell Biol* (2006) 38:2219–28. doi: 10.1016/j.biocel.2006.07.004
25. Chen J, Wei H, Cheng J, Xie B, Wang B, Yi J, et al.. Characteristics of doxorubicin-selected multidrug-resistant human leukemia HL-60 cells with tolerance to arsenic trioxide and contribution of leukemia stem cells. *Oncol Lett* (2018) 15:1255–62. doi: 10.3892/ol.2017.7353
26. Morjani H, Millot JM, Belhoussine R, Sebille S, Manfait M. Anthracycline subcellular distribution in human leukemic cells by microspectrofluorometry: factors contributing to drug-induced cell death and reversal of multidrug resistance. *Leukemia* (1997) 11:1170–9. doi: 10.1038/sj.leu.2400668
27. Ginzinger DG. Gene quantification using real-time quantitative PCR: an emerging technology hits the mainstream. *Exp Hematol* (2002) 30:503–12. doi: 10.1016/S0301-472X(02)00806-8
28. Fukushima T, Yamashita T, Takemura H, Suto H, Kishi S, Urasaki Y, et al. Effect of PSC 833 on the cytotoxicity and pharmacodynamics of mitoxantrone in multidrug-resistant K562 cells. *Leuk Res* (2000) 24:249–54. doi: 10.1016/S0145-2126(99)00177-0
29. Hazlehurst LA, Valkov N, Wisner L, Storey JA, Boulware D, Sullivan DM, et al. Reduction in drug-induced DNA double-strand breaks associated with beta1 integrin-mediated adhesion correlates with drug resistance in U937 cells. *Blood* (2001) 98:1897–903. doi: 10.1182/blood.V98.6.1897
30. Hazlehurst LA, Landowski TH, Dalton WS. Role of the tumor microenvironment in mediating de novo resistance to drugs and physiological mediators of cell death. *Oncogene* (2003) 22:7396–402. doi: 10.1038/sj.onc.1206943
31. Correia AL, Bissell MJ. The tumor microenvironment is a dominant force in multidrug resistance. *Drug Resist Update* (2012) 15:39–49. doi: 10.1016/j.drup.2012.01.006
32. Ji X, Lu Y, Tian H, Meng X, Wei M, Cho WC. Chemoresistance mechanisms of breast cancer and their countermeasures. *Biomed Pharmacother* (2019) 114:108800. doi: 10.1016/j.biopha.2019.108800
33. Westhoff MA, Fulda S. Adhesion-mediated apoptosis resistance in cancer. *Drug Resist Update* (2009) 12:127–36. doi: 10.1016/j.drup.2009.08.001
34. Hehlgans S, Haase M, Cordes N. Signalling via integrins: implications for cell survival and anticancer strategies. *Biochim Biophys Acta* (2007) 1775:163–80. doi: 10.1016/j.bbcan.2006.09.001
35. Nallanthighal S, Heiserman JP, Cheon DJ. The Role of the Extracellular Matrix in Cancer Stemness. *Front Cell Dev Biol* (2019) 7:86. doi: 10.3389/fcell.2019.00086
36. Meads MB, Hazlehurst LA, Dalton WS. The bone marrow microenvironment as a tumor sanctuary and contributor to drug resistance. *Clin Cancer Res* (2008) 14:2519–26. doi: 10.1158/1078-0432.CCR-07-2223
37. Uhm JH, Dooley NP, Kyritsis AP, Rao JS, Gladson CL. Vitronectin, a glioma-derived extracellular matrix protein, protects tumor cells from apoptotic death. *Clin Cancer Res* (1999) 5:1587–94.
38. Hutchinson E. Destabilizing influence. *Nat Rev Cancer* (2008) 8:1038. doi: 10.1038/nrc2316
39. de Fraipont F, Nicholson AC, Feige JJ, Van Meir EG. Thrombospondins and tumor angiogenesis. *Trends Mol Med* (2001) 7:401–7. doi: 10.1016/s1471-4914(01)02102-5
40. van Amerongen R, Berns A. TXR1-mediated thrombospondin repression: a novel mechanism of resistance to taxanes? *Genes Dev* (2006) 20:1975–81. doi: 10.1101/gad.1460806
41. Callaghan R, Luk F, Bebawy M. Inhibition of the multidrug resistance P-glycoprotein: time for a change of strategy? *Drug Metab Dispos* (2014) 42:623–31. doi: 10.1124/dmd.113.056176
42. Damiano JS, Cress AE, Hazlehurst LA, Shtil AA, Dalton WS. Cell adhesion mediated drug resistance (CAM-DR): role of integrins and resistance to apoptosis in human myeloma cell lines. *Blood* (1999) 93:1658–67.
43. Kozlova NII, Morozevich GE, Chubukina AN, Shtil AA, Berman AE. Expression of Integrins, Anchorage Dependent Apoptosis and Invasiveness of Multidrug Resistant Human Breast Carcinoma Cells. *EXCLI J* (2004) 3:68–81.
44. Gillies RJ, Raghunand N, Karczmar GS, Bhujwalla ZM. MRI of the tumor microenvironment. *J Magn Reson Imaging* (2002) 16:430–50. doi: 10.1002/jmri.10181
45. Schuetz JD, Schuetz EG. Extracellular matrix regulation of multidrug resistance in primary monolayer cultures of adult rat hepatocytes. *Cell Growth Differ* (1993) 4:31–40.
46. Ruoslahti E. Integrins. *J Clin Invest* (1991) 87:1–5. doi: 10.1172/JCI114957
47. Tatsuta T, Naito M, Mikami K, Tsuruo T. Enhanced expression by the brain matrix of P-glycoprotein in brain capillary endothelial cells. *Cell Growth Differ* (1994) 5:1145–52.
48. Dhanasekaran DN, Reddy EP. JNK-signaling: A multiplexing hub in programmed cell death. *Genes Cancer* (2017) 8:682–94. doi: 10.18632/genesandcancer.155
49. Dhanasekaran DN, Reddy EP. JNK signaling in apoptosis. *Oncogene* (2008) 27:6245–51. doi: 10.1038/onc.2008.301

Conflict of Interest: The authors declare that the research was conducted in the absence of any commercial or financial relationships that could be construed as a potential conflict of interest.

Copyright © 2020 Courageot, Duca, Martiny, Devarenne-Charpentier, Morjani and El Btaouri. This is an open-access article distributed under the terms of the Creative Commons Attribution License (CC BY). The use, distribution or reproduction in other forums is permitted, provided the original author(s) and the copyright owner(s) are credited and that the original publication in this journal is cited, in accordance with accepted academic practice. No use, distribution or reproduction is permitted which does not comply with these terms.

Advantages of publishing in Frontiers

OPEN ACCESS
Articles are free to read for greatest visibility and readership

FAST PUBLICATION
Around 90 days from submission to decision

HIGH QUALITY PEER-REVIEW
Rigorous, collaborative, and constructive peer-review

TRANSPARENT PEER-REVIEW
Editors and reviewers acknowledged by name on published articles

Frontiers
Avenue du Tribunal-Fédéral 34
1005 Lausanne | Switzerland

Visit us: www.frontiersin.org
Contact us: frontiersin.org/about/contact

REPRODUCIBILITY OF RESEARCH
Support open data and methods to enhance research reproducibility

DIGITAL PUBLISHING
Articles designed for optimal readership across devices

FOLLOW US
@frontiersin

IMPACT METRICS
Advanced article metrics track visibility across digital media

EXTENSIVE PROMOTION
Marketing and promotion of impactful research

LOOP RESEARCH NETWORK
Our network increases your article's readership